GERM CELL DEVELOPMENT AND REPRODUCTIVE AGING

EDITED BY: Miguel Angel Brieño-Enriquez, Francesca Elizabeth Duncan, Arjumand Ghazi, Michael Klutstein, Vittorio Sebastiano and Jessica Tyler

PUBLISHED IN: Frontiers in Cell and Developmental Biology

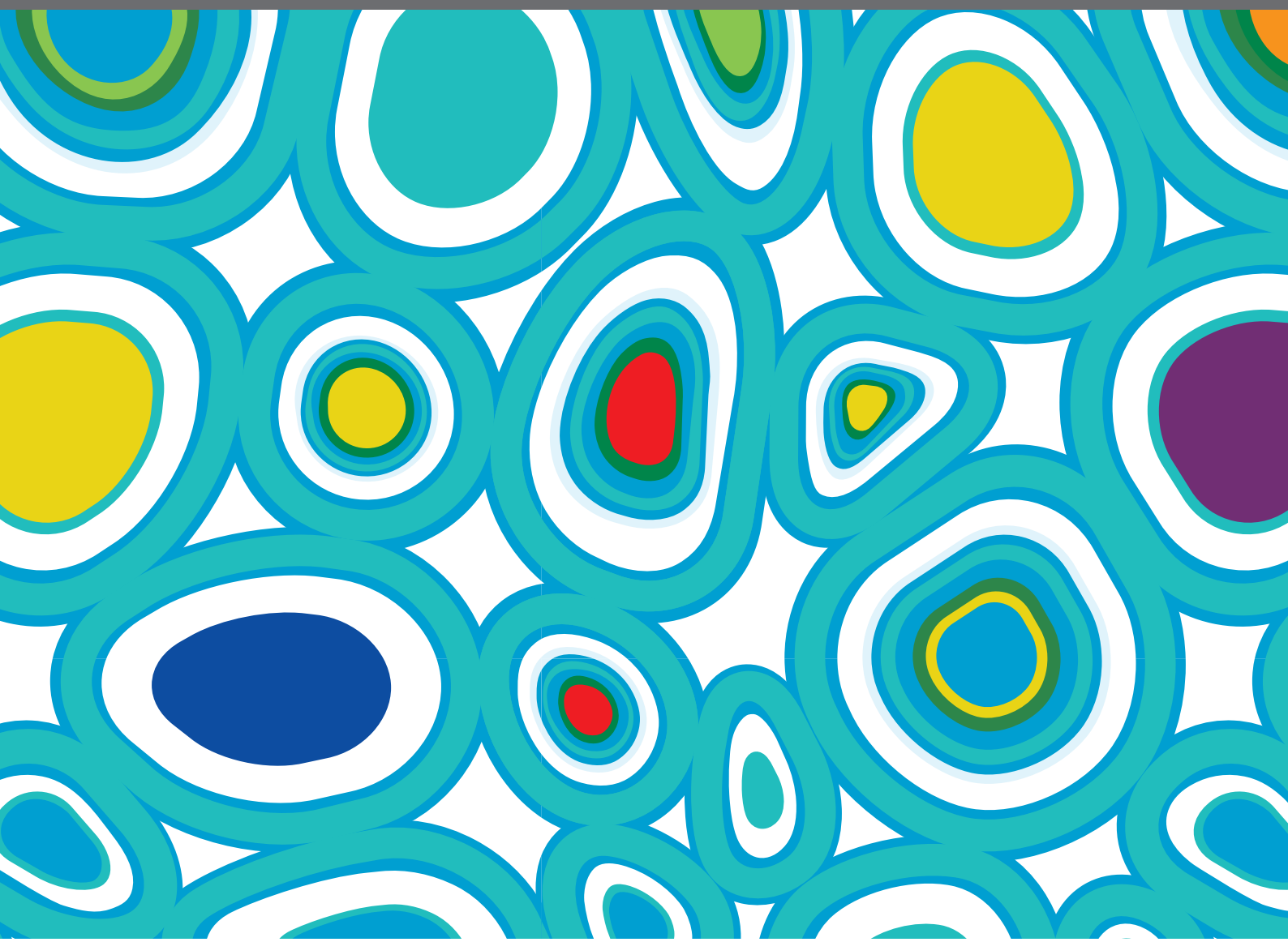

frontiers Research Topics

frontiers

ISSN 1664-8714
ISBN 978-2-88976-567-6
DOI 10.3389/978-2-88976-567-6

About Frontiers

Frontiers is more than just an open-access publisher of scholarly articles: it is a pioneering approach to the world of academia, radically improving the way scholarly research is managed. The grand vision of Frontiers is a world where all people have an equal opportunity to seek, share and generate knowledge. Frontiers provides immediate and permanent online open access to all its publications, but this alone is not enough to realize our grand goals.

Frontiers Journal Series

The Frontiers Journal Series is a multi-tier and interdisciplinary set of open-access, online journals, promising a paradigm shift from the current review, selection and dissemination processes in academic publishing. All Frontiers journals are driven by researchers for researchers; therefore, they constitute a service to the scholarly community. At the same time, the Frontiers Journal Series operates on a revolutionary invention, the tiered publishing system, initially addressing specific communities of scholars, and gradually climbing up to broader public understanding, thus serving the interests of the lay society, too.

Dedication to Quality

Each Frontiers article is a landmark of the highest quality, thanks to genuinely collaborative interactions between authors and review editors, who include some of the world's best academicians. Research must be certified by peers before entering a stream of knowledge that may eventually reach the public - and shape society; therefore, Frontiers only applies the most rigorous and unbiased reviews.
Frontiers revolutionizes research publishing by freely delivering the most outstanding research, evaluated with no bias from both the academic and social point of view. By applying the most advanced information technologies, Frontiers is catapulting scholarly publishing into a new generation.

What are Frontiers Research Topics?

Frontiers Research Topics are very popular trademarks of the Frontiers Journals Series: they are collections of at least ten articles, all centered on a particular subject. With their unique mix of varied contributions from Original Research to Review Articles, Frontiers Research Topics unify the most influential researchers, the latest key findings and historical advances in a hot research area! Find out more on how to host your own Frontiers Research Topic or contribute to one as an author by contacting the Frontiers Editorial Office: frontiersin.org/about/contact

GERM CELL DEVELOPMENT AND REPRODUCTIVE AGING

Topic Editors:
Miguel Angel Brieño-Enriquez, Magee-Womens Research Institute, United States
Francesca Elizabeth Duncan, Northwestern University, United States
Arjumand Ghazi, University of Pittsburgh, United States
Michael Klutstein, Hebrew University of Jerusalem, Israel
Vittorio Sebastiano, Stanford University, United States
Jessica Tyler, Cornell University, United States

Citation: Brieño-Enriquez, M. A., Duncan, F. E., Ghazi, A., Klutstein, M., Sebastiano, V., Tyler, J., eds. (2022). Germ Cell Development and Reproductive Aging. Lausanne: Frontiers Media SA. doi: 10.3389/978-2-88976-567-6

Table of Contents

frontiers | Frontiers in Cell and Developmental Biology

TYPE Editorial
PUBLISHED 12 October 2022
DOI 10.3389/fcell.2022.1051539

OPEN ACCESS

EDITED AND REVIEWED BY
Cecilia Giulivi,
University of California, Davis,
United States

*CORRESPONDENCE
Miguel Angel Brieño-Enriquez,
brienoenriquezma@mwri.magee.edu,
miguelbe@pitt.edu

SPECIALTY SECTION
This article was submitted to Cellular Biochemistry,
a section of the journal
Frontiers in Cell and Developmental Biology

RECEIVED 22 September 2022
ACCEPTED 30 September 2022
PUBLISHED 12 October 2022

CITATION
Brieño-Enriquez MA, Duncan FE, Ghazi A, Klutstein M, Sebastiano V and Tyler J (2022), Editorial: Germ cell development and reproductive aging. *Front. Cell Dev. Biol.* 10:1051539. doi: 10.3389/fcell.2022.1051539

Editorial: Germ cell development and reproductive aging

Miguel Angel Brieño-Enriquez[1]*, Francesca E. Duncan[2], Arjumand Ghazi[3], Michael Klutstein[4], Vittorio Sebastiano[5,6] and Jessica Tyler[7]

[1]Department of Obstetrics, Gynecology, and Reproductive Sciences, School of Medicine, Magee-Womens Research Institute, University of Pittsburgh, Pittsburgh, PA, United States, [2]Department of Obstetrics and Gynecology, Feinberg School of Medicine, Northwestern University, Chicago, IL, United States, [3]Departments of Pediatrics, Developmental Biology and Cell Biology, and Physiology, John G. Rangos Sr. Research Center, University of Pittsburgh School of Medicine, Pittsburgh, PA, United States, [4]Faculty of Dental Medicine, Institute of Biomedical and Oral Research, The Hebrew University of Jerusalem, Jerusalem, Israel, [5]Institute for Stem Cell Biology and Regenerative Medicine, Stanford University School of Medicine, Stanford, CA, United States, [6]Department of Obstetrics and Gynecology, Stanford University School of Medicine, Stanford, CA, United States, [7]Department of Pathology, Laboratory Medicine, Weill Cornell Medicine, New York, NY, United States

KEYWORDS

aging, germ cells, oocyte, sperm, primordial germ cell, reproductive aging, ovary, testis

Editorial on the Research Topic
Germ cell development and reproductive aging

Introduction

Aging and reproductive aging are influenced by environmental factors, stochastic aberrations in molecular interactions, and deterministic instructions encoded in our genome. Although no single process has been shown to be the main cause of aging, it appears that multiple processes contribute, leading to a loss of fitness and eventual death. Over the last 30 years, interest in the field of aging has exponentially increased since the pioneering discoveries of single gene mutations that double the lifespan of the nematode *Caenorhabditis elegans* (Kenyon et al., 1993). These genes and pathways have since been shown to be evolutionarily conserved and innumerable other genes and interventions that impact longevity across species have been discovered. However, these analyses have been predominantly focused on somatic tissues rather than the ovary and testis and how aging of reproductive tissues impacts somatic aging. Undoubtedly, one of the most important events in biology is the union of the sperm and egg—and their unique ability to give rise to an entirely new generation composed of billions of cells. Despite the importance and tremendous potential (immortal lineage) of these cells, the male and female gametes are not impervious to aging. In humans, prominent changes in social behavior and medical interventions have changed the landscape of reproduction, enabling a delay in childbearing and longer post-menopausal lifespan in women. All these factors have a

profound impact on the quantity, quality, and ultimate reproductive potential of germ cells. Reproductive aging is not unique to mammals but affects many other organisms, including yeast, flies, and worms. Thus, understanding the fundamental mechanisms underlying reproductive aging is essential to develop new approaches to extend reproductive lifespan, which will ultimately impact overall health. The 20 articles in this Research Topic explore critical aspects of *germ cell development and reproductive aging*. They include 10 research articles, 8 reviews, and 2 mini reviews, covering from insects to humans.

Overview

From insects to human: Convergences and divergences in reproductive aging

Reproductive aging is not exclusive to humans or laboratory model organisms but also occurs in species in the wild including large mammals. Although many mechanisms that control aging are conserved among species, there are distinct traits exhibited by different species. Comizzoli and Ottinger review the conserved mechanisms of reproductive aging and highlight the value of comparative studies addressing aging issues in conservation breeding as well as human reproductive medicine. Many of these conserved mechanisms are well known, such as depletion of the ovarian reserve or decline in testicular function, as well as phenomena observed in social insects where organismal senescence regulates aging rather than germ cell senescence. They also discuss how corals, birds, tardigrades, fish, reptiles, social insects like ants and bees and naked mole-rats do not show a decline in fertility with age and can provide knowledge that can lead to potential interventions to improve fertility in aged humans (Nisbet et al., 1999; Heinze and Schrempf, 2008; Tsujimoto et al., 2016; Place et al., 2021; Buffenstein et al., 2022).

The major determinants of reproductive aging are defects in germ cell expansion during development or premature depletion of the germline stem and progenitor pools (Antebi, 2013). On this subject, Tolkin and Hubbard review recent advances in our understanding of the role of depletion of the germline stem and progenitor cell pools in *C. elegans*. Their review dissects the role of specific molecular pathways, such as Notch and insulin/IGF like receptors, in the decline of germ cells with age. In their review, Wu et al., explore the mechanisms of vitellogenesis in insects, a critical process for egg production and embryonic development and that addresses the importance of lipids and specific germ cell proteins across species. Also, using *C. elegans* as a model, Scharf et al., performed a detailed analysis of the mechanisms involved in reproductive aging and chemical interventions that can help delay aging in nematodes. Notably, Scharf et al., also describe how reproductive aging influences birth rate affecting population dynamics. In both reviews, the authors discuss new avenues of research that can improve the effects of aging in worms and how it can be extrapolated to humans. An example of potential translation to humans is presented by Choi et al., who show that oleic acid-mediated increased reproduction can be dissociated from somatic longevity, reducing the energetic cost of reproduction.

Aging the proteome: Dynamics of mRNA translation and proteostasis

Regulation of mRNA translation is critical for the proper function of the cell. In the case of germ cells, there is accumulating evidence to suggest that changes in mRNA translation can contribute to infertility and reproductive aging in organisms from insects to humans. For this Research Topic, Mercer et al., review the dynamic regulation of mRNA translation and ribosome biogenesis in germ cells of flies, worms, and mice. The authors evaluate the conserved functions between species, their differences, and suggest potential new lines of research in this field. Changes in mRNA translation and ribosomal biology can directly affect proteostasis. Cafe et al., review the role of proteostasis in the maintenance of the germline and in reproductive health. In their review, the authors analyze proteostasis in the context of both somatic and germ cell aging, and how disruption of proteostasis leads to defects in gametes, embryogenesis, and lifespan. Intracellular communication by extracellular vesicles is key for many physiological and pathological processes and is mediated *via* cargo including nucleic acids (DNA, RNA, microRNAs, and long-non-coding RNAs) proteins and enzymes (Yanez-Mo et al., 2015). Liu et al., performed a review of the roles of extracellular vesicles in aging and their implications in reproductive diseases.

Aging is for all: Impact of aging on male germ cells

Primordial germ cells (PGCs) and spermatogonial germ cells are critical for reproduction and disruption of their proliferation or migration results in fertility defects. Aging also impacts stem cells and old spermatogonial stem cells have reduced function and ability to generate sperm (Liao et al., 2021). Defects at early stages of germ cell development are not unique to females. Zhou et al., employ a unique model, the viviparous fish black rockfish, and use different molecular approaches to trace the origin and migration of the PGCs in fish. Another powerful approach to study germ cell development is described by Xu et al., where they use mass spectrophotometry to reveal differences in protein

abundance and phosphorylation in the sperm of Yorkshire and Duroc pigs and the authors discuss the relationship between pig reproductive efficiency and fertility. Also related to male germ cell development, Zhou et al., shows that proliferation and apoptosis in human spermatogonial stem cells (SSCs) is regulated by TCF3, a member of the E-protein family of helix-loop-helix transcription factors (Slattery et al., 2008). They find that the effect of knocking down TCF3 *in vitro* produces phenotypes reminiscent of TCF3 deficient patients with non-obstructive azoospermia.

Too many avenues with a common end: Reproductive aging in females

Female reproductive aging is characterized by a loss of follicles, the functional units of the ovary consisting of oocytes surrounded by companion granulosa cells. The quality of the oocytes in the ovary also deteriorates with age. Reproductive aging is associated with adverse reproductive outcomes, including infertility, miscarriages, and birth defects (Duncan and Gerton, 2018; Gruhn et al., 2019). Moreover, reproductive aging is associated with a decline in estrogen, which is produced by growing follicles. Estrogen regulates cardiovascular, brain, immune, bone, and reproductive tissue function (Satirapod et al., 2020). In fact, menopause accelerates aging (El Khoudary et al., 2020). In this special Research Topic, 8 papers focus exclusively on different aspects of female reproductive aging. Liu et al., evaluate the role of the ten-eleven translocation (Tet) enzymes in the establishment of the ovarian reserve. They show that in the absence of Tet-1, young mice have a severe reduction in the number of follicles and become infertile by middle age. These mutants also present disruption of organelle fission, ubiquitination, autophagy, and upregulation of expression from transposable elements such as Line1. Aging not only impacts the pool of germline stem/progenitor cells, it also affects later stages of gametogenesis. One clear example is presented by Raices et al., where they demonstrate that the capacity to repair DNA damage during meiosis in the germ cell is reduced with age. Raices et al., evaluated the recruitment of the proteins RPA-1 and RAD51 that are required for homologous recombination, showing that the dynamics of early meiotic DNA damage and repair are compromised in older mothers, increasing the risk of aneuploidy and low oocyte quality.

Beyond the germ cells: Ovarian stroma, inflammation and hormones during aging

Depletion of ovarian reserve is not only regulated by the intrinsic characteristics of the germ cells, but also local environment such as the health of the stroma (Amargant et al., 2020; Umehara et al., 2022), inflammation (Foley et al., 2021; Navarro-Pando et al., 2021) and hormonal balance. Non-infectious chronic and mild inflammation is a hallmark of aging. Products of this inflammation can be detected by inflammasomes (complexes of multiple proteins that induce sterile inflammation). Regulation of inflammasomes is highly controlled by different proteins including NACHT, LRR and PYD domains-containing protein 3 (NLRP3). Liberos et al., using *Nlrp3* knockout mice, show that ablation of this gene diminished the pro-inflammatory cytokines and macrophage infiltration leading to a larger ovarian reserve. However, aging is not the only cause of inflammation in the ovary. In fact, in this Research Topic Knapik et al., review the role of T cells in ovarian physiology and disease from polycystic ovary syndrome to ovarian cancer, and how each one of these pathologies can lead to reproductive aging and infertility.

Regulation of the reproductive cycle in females is tightly regulated by hormones. In this Research Topic Björkgren et al., using mice as a model, ablate the α/β hydrolase domain-containing protein 2 (*Abhd2*). Mutant mice showed disruption of the estrus cycle rhythm. Abnormal cycles were accompanied by a phenotype that mimics the histology observed in polycystic ovaries, revealing the relevance of this gene as a non-genomic steroid regulator of the female reproductive cycle and a potential target for therapy in humans.

Protecting the quality of the egg: Is there a right time to cryopreserve the oocyte?

The quality of the oocyte is critical for fertility. In this Research Topic Beverley et al., review the impact of cohesin variants and mutations in reproductive aging, disease, and overall health. Aging is directly associated with loss of the meiosis-specific cohesion, that leads to premature segregation of sister chromatids, aneuploidy, and miscarriages. One avenue to combat oocyte aging is cryopreservation. This technique is an important option for patients that need to go through medical treatments such as chemotherapy and radiotherapy but also for females planning to delay motherhood. However, not all oocytes are equally capable of *in vitro* maturation or fertilization. Studies in this Research Topic from Kusuhara et al., and Karavani et al., in both mice and humans (respectively) identify optimal time windows for retrieving mouse and human oocytes for cryopreservation. Their findings demonstrate that younger is not always better and that oocytes harvested during the pubertal transition have a reduced competence relative to reproductively adult mice. Sirait et al., review the impact of the characteristics of the cumulus-oocyte complex, such as of the nuclear maturation,

apoptosis, extracellular matrix remodeling and steroids metabolism, as biomarkers for *in vitro* fertilization outcomes.

Conclusion

Over the past several years, significant progress has been made in our understanding of the biological functions and key events during reproductive aging. Despite the advances described above, many aspects of the biological processes involved, and treatments to improve them, remain poorly understood. Therefore, mechanistic studies are necessary to identify the molecular networks that drive reproductive aging. We need to better understand the role of other cells beyond the gametes, and the role played by the extracellular matrix, hormones, non-coding RNAs, proteostasis, and epigenetics in reproductive aging. Future identification of the molecular basis of dynamic transcriptional regulation and protein post-translational modifications in germ cells and reproductive aging remains a crucial endeavor. Understanding molecular mechanisms will allow us to develop new technologies and therapies to improve reproductive health, reproductive lifespan and organismal healthspan.

Author contributions

All authors listed have made a substantial, direct, and intellectual contribution to the work and approved it for publication.

Conflict of interest

The authors declare that the research was conducted in the absence of any commercial or financial relationships that could be construed as a potential conflict of interest.

Publisher's note

All claims expressed in this article are solely those of the authors and do not necessarily represent those of their affiliated organizations, or those of the publisher, the editors and the reviewers. Any product that may be evaluated in this article, or claim that may be made by its manufacturer, is not guaranteed or endorsed by the publisher.

References

Amargant, F., Manuel, S. L., Tu, Q., Parkes, W. S., Rivas, F., Zhou, L. T., et al. (2020). Ovarian stiffness increases with age in the mammalian ovary and depends on collagen and hyaluronan matrices. *Aging Cell* 19 (11), e13259. doi:10.1111/acel.13259

Antebi, A. (2013). Regulation of longevity by the reproductive system. *Exp. Gerontol.* 48 (7), 596–602. doi:10.1016/j.exger.2012.09.009

Buffenstein, R., Amoroso, V., Andziak, B., Avdieiev, S., Azpurua, J., Barker, A. J., et al. (2022). The naked truth: A comprehensive clarification and classification of current 'myths' in naked mole-rat biology. *Biol. Rev. Camb. Philos. Soc.* 97 (1), 115–140. doi:10.1111/brv.12791

Duncan, F. E., and Gerton, J. L. (2018). Mammalian oogenesis and female reproductive aging. *Aging (Albany NY)* 10 (2), 162–163. doi:10.18632/aging.101381

El Khoudary, S. R., Aggarwal, B., Beckie, T. M., Hodis, H. N., Johnson, A. E., Langer, R. D., et al. (2020). Menopause transition and cardiovascular disease risk: Implications for timing of early prevention: A scientific statement from the American heart association. *Circulation* 142 (25), e506–e532. doi:10.1161/CIR.0000000000000912

Foley, K. G., Pritchard, M. T., and Duncan, F. E. (2021). Macrophage-derived multinucleated giant cells: Hallmarks of the aging ovary. *Reproduction* 161 (2), V5–V9. doi:10.1530/REP-20-0489

Gruhn, J. R., Zielinska, A. P., Shukla, V., Blanshard, R., Capalbo, A., Cimadomo, D., et al. (2019). Chromosome errors in human eggs shape natural fertility over reproductive life span. *Science* 365 (6460), 1466–1469. doi:10.1126/science.aav7321

Heinze, J., and Schrempf, A. (2008). Aging and reproduction in social insects--a mini-review. *Gerontology* 54 (3), 160–167. doi:10.1159/000122472

Kenyon, C., Chang, J., Gensch, E., Rudner, A., and Tabtiang, R. (1993). A *C. elegans* mutant that lives twice as long as wild type. *Nature* 366 (6454), 461–464. doi:10.1038/366461a0

Liao, J., Suen, H. C., Luk, A. C. S., Yang, L., Lee, A. W. T., Qi, H., et al. (2021). Transcriptomic and epigenomic profiling of young and aged spermatogonial stem cells reveals molecular targets regulating differentiation. *PLoS Genet.* 17 (7), e1009369. doi:10.1371/journal.pgen.1009369

Navarro-Pando, J. M., Alcocer-Gomez, E., Castejon-Vega, B., Navarro-Villaran, E., Condes-Hervas, M., Mundi-Roldan, M., et al. (2021). Inhibition of the NLRP3 inflammasome prevents ovarian aging. *Sci. Adv.* 7 (1), eabc7409. doi:10.1126/sciadv.abc7409

Nisbet, I. C., Finch, C. E., Thompson, N., Russek-Cohen, E., Proudman, J. A., and Ottinger, M. A. (1999). Endocrine patterns during aging in the common tern (Sterna hirundo). *Gen. Comp. Endocrinol.* 114 (2), 279–286. doi:10.1006/gcen.1999.7255

Place, N. J., Prado, A. M., Faykoo-Martinez, M., Brieno-Enriquez, M. A., Albertini, D. F., and Holmes, M. M. (2021). Germ cell nests in adult ovaries and an unusually large ovarian reserve in the naked mole-rat. *Reproduction* 161 (1), 89–98. doi:10.1530/REP-20-0304

Satirapod, C., Wang, N., MacDonald, J. A., Sun, M., Woods, D. C., and Tilly, J. L. (2020). Estrogen regulation of germline stem cell differentiation as a mechanism contributing to female reproductive aging. *Aging (Albany NY)* 12 (8), 7313–7333. doi:10.18632/aging.103080

Slattery, C., Ryan, M. P., and McMorrow, T. (2008). E2A proteins: Regulators of cell phenotype in normal physiology and disease. *Int. J. Biochem. Cell Biol.* 40 (8), 1431–1436. doi:10.1016/j.biocel.2007.05.014

Tsujimoto, M., Imura, S., and Kanda, H. (2016). Recovery and reproduction of an Antarctic tardigrade retrieved from a moss sample frozen for over 30 years. *Cryobiology* 72 (1), 78–81. doi:10.1016/j.cryobiol.2015.12.003

Umehara, T., Winstanley, Y. E., Andreas, E., Morimoto, A., Williams, E. J., Smith, K. M., et al. (2022). Female reproductive life span is extended by targeted removal of fibrotic collagen from the mouse ovary. *Sci. Adv.* 8 (24), eabn4564. doi:10.1126/sciadv.abn4564

Yanez-Mo, M., Siljander, P. R., Andreu, Z., Zavec, A. B., Borras, F. E., Buzas, E. I., et al. (2015). Biological properties of extracellular vesicles and their physiological functions. *J. Extracell. Vesicles* 4, 27066. doi:10.3402/jev.v4.27066

frontiers in Cell and Developmental Biology

REVIEW
published: 17 September 2020
doi: 10.3389/fcell.2020.577084

Extracellular Vesicles: Recent Developments in Aging and Reproductive Diseases

Yu Liu, Qiuzi Shen, Ling Zhang† and Wenpei Xiang*†*

Institute of Reproductive Health and Center for Reproductive Medicine, Tongji Medical College, Huazhong University of Science and Technology, Wuhan, China

OPEN ACCESS

Edited by:
Jessica Tyler,
Cornell University, United States

Reviewed by:
Ulrike Resch,
Medical University of Vienna, Austria
Paschalia Pantazi,
Imperial College London,
United Kingdom

***Correspondence:**
Ling Zhang
Zhling312@163.com
Wenpei Xiang
wpxiang2010@gmail.com

†*These authors have contributed equally to this work*

Specialty section:
This article was submitted to Cellular Biochemistry, a section of the journal Frontiers in Cell and Developmental Biology

Received: *28 June 2020*
Accepted: *27 August 2020*
Published: *17 September 2020*

Citation:
Liu Y, Shen Q, Zhang L and Xiang W (2020) Extracellular Vesicles: Recent Developments in Aging and Reproductive Diseases. Front. Cell Dev. Biol. 8:577084. doi: 10.3389/fcell.2020.577084

Extracellular vesicles (EVs), present in cell culture media and several body fluids, play a prominent role in intercellular communication under physiological and pathological conditions. We performed a systematic literature search to review evidence regarding the existence, composition, and release of different EVs, as well as the biomarkers, cargos, and separation methods. We also reviewed the potential of EVs to transport cargos and alter the function and phenotype of recipient cells associated with aging and reproductive diseases, including polycystic ovary syndrome and endometriosis. In aging, EVs promote inflammatory reactions and offsetting the occurrence of aging. In the polycystic ovary syndrome and endometriosis, EVs and their cargos are involved in the occurrence of diseases, therapeutic strategies, and perform as non-invasive biomarkers. As the study of EVs is still in the early stages, it is not surprising that most of the current literature only describes their possible roles.

Keywords: extracellular vesicles, isolation, aging, polycystic ovary syndrome, endometriosis

INTRODUCTION

Intercellular communication has been shown to play an essential role in diverse physiological processes, including cell proliferation, development, and differentiation. Published literature in recent years has revealed a new mechanism of intercellular communication, namely via the release of extracellular vesicles (EVs). Classically, intercellular communication includes endocrine, paracrine, and autocrine or intercellular gap junctions, a kind of direct cell-cell contact, and secreted some factors. In the group of secreted factors, we will focus here on the roles of EVs. EVs secreted outside of the cell can serve as vehicles for the transport of cargo to recipient cells (Raposo and Stoorvogel, 2013). EVs display a diverse range of sizes and are present in cell culture media (under both normal and pathological conditions) and several body fluids (Caby et al., 2005; Admyre et al., 2007; Ogawa et al., 2008; Gonzales et al., 2009). The cargo of EVs contains biologically active molecules, such as nucleic acids (DNA, RNA, microRNAs and long non-coding RNAs), proteins, lipids, and nicotinamide phosphoribosyltransferase (eNAMPT) (Yoshida et al., 2019).

EVs have been shown to be involved in numerous biological functions and pathological processes (Baek et al., 2016). Meanwhile, EVs and their cargos act as non-invasive markers of

various diseases (Li et al., 2009; Mitchell et al., 2009; Choi et al., 2011; Saman et al., 2012; Ostergaard et al., 2013; Jakobsen et al., 2015). Abnormal EV levels may be one of the causes of aging and reproductive diseases (including polycystic ovary syndrome (PCOS) and endometriosis), and are closely related to the occurrence, development, and prognosis of these diseases. Moreover, EVs can alleviate aging phenotypes, and promote cell proliferation (Liu et al., 2019). Such developments offer new therapeutic strategies for the treatment of PCOS in the future. The purpose of this review is to describe the present knowledge of the role of EVs as cell-to-cell messengers in aging and reproductive diseases.

METHODS

For this review, including three strategies: literature search, study selection, and results summary. We conducted a systematic online literature search of the PubMed and Web of Science databases and searched all published articles since the database's creation to 2019. We used the following query: ('extracellular vesicles' or 'microvesicles' or 'microparticles' or 'exosomes') and ('comparison of isolation method' or 'aging' or 'polycystic ovary syndrome' or 'endometriosis'). Both animal and human studies were considered suitable for this review. Additionally, all relevant studies were identified and included. These types of EVs do not include "apoptotic bodies" and "apoptotic vesicles". Any duplicate articles were eliminated. After screening the title and/or abstracts, if the article was found to be unrelated to the study, was excluded. A total of 9072 records were retrieved from the two databases. After removing duplicates titles and other topic articles, the full-text articles of 190 articles were reviewed and 89 were considered relevant and included in this review (**Figure 1**).

EXTRACELLULAR VESICLES-IDENTIFICATION

Over the past ten years, the number of published papers on EVs has increased exponentially, which is in sharp contrast with the field of circRNA. This also proves that researchers have a growing understanding of EVs, as seen in **Figure 2**, to the extent that the 2013 Nobel Prize in Physiology or Medicine was awarded to three scientists (James E. Rothman, Randy W. Schekman, and Thomas C. Südhof) working on the transport system of vesicles inside cells. In fact, the study of EVs dates back even further. It was in 1982 when EVs were first reported in seminal plasma (Stegmayr and Ronquist, 1982). EVs were initially considered as "cellular garbage", although they are now known as important mediators of intercellular communication, participating in and activating a variety of cell signaling pathways (Raposo and Stoorvogel, 2013).

EVs are a heterogeneous population (Bobrie et al., 2012; Raposo and Stoorvogel, 2013; Kowal et al., 2016), and can be classified into three categories according to their biogenetic pathway and physical characteristics: exosomes, microvesicles (MVs), and apoptotic bodies (**Figure 3** and **Table 1**). Exosomes are small vesicles with lipid bilayers that contain cytoplasmic components of secretory cells which indirectly reflect the state and nature of the secretory cells and are biologically equivalent to the cytoplasm of the lipid bilayer. The external domains of transmembrane proteins are exposed in the extracellular space (Schorey et al., 2015). Exosomes are derived from intraluminal vesicles (ILVs) residing within multivesicular endosomes (MVEs) (van Niel et al., 2018). MVs can also be called microparticles (MPs), formerly known as 'dust', and are shed from the plasma membrane and subsequently released into the extracellular space (Mathieu et al., 2019). MVs may be released faster than exosomes, which is directly related to their production mechanism. Apoptotic bodies are released from dying cells (Colombo et al., 2014; Yanez-Mo et al., 2015). The production of EVs has been widely observed in bacteria, humans, and plants (Deatherage and Cookson, 2012; Schorey et al., 2015; Robinson et al., 2016), and demonstrates an evolutionarily conserved intercellular signaling mechanism. Exosomes are small vesicles of 40–150 nm in diameter (Jeppesen et al., 2019), although can potentially reach as large as 200 nm (Colombo et al., 2013), and therefore overlap the range of virus sizes (Gyorgy et al., 2011). MVs vary in size from 100 to 1,000 nm in diameter (Marques et al., 2013), up to 10 μm, and overlap the range of bacteria sizes (Akers et al., 2013). Apoptotic bodies are the largest vesicles (>1,000 nm) of the three classes and overlap the rang of platelet diameter (Hristov et al., 2004; Atkin-Smith et al., 2015). In fact, the diameter of vesicles does not sufficiently differentiate exosomes and MVs because in some instances their diameters may overlap with each other. Typical biomarkers for exosomes include transmembrane tetrad proteins (e.g., CD9, CD63, and CD81), Alix, TSG101, Flotillin-1, HSC70, and syntenin-1 (Mathivanan et al., 2010; Colombo et al., 2014). Discriminatory markers of MVs include annexin A1, ARF6, KIF, RACGAP, exportin-2, and chromosome segregation 1-like protein (Muralidharan-Chari et al., 2009; Xu et al., 2016; Tricarico et al., 2017; Jeppesen et al., 2019). Phosphatidylserine (PS), thrombospondin, C3b complement protein, calreticulin, and VDAC1 have been proven to be useful markers for apoptotic bodies (Takizawa et al., 1996; Fadok et al., 2001; Friedl et al., 2002; Jeppesen et al., 2014; Van Deun et al., 2014).

EXTRACELLULAR VESICLES ISOLATION METHODS

Many techniques have been established to isolate different EVs. Ultracentrifugation (UC) is one of the most commonly used methods for exosomal isolation. Extension of UC time increases the degree of pollution of non-vesicular particles (Cvjetkovic et al., 2014). Non-vesicular components are likely to be contaminating and mainly include high molecular weight proteins and protein aggregates that co-precipitate with exosomes during the UC process (Tauro et al., 2012). Moreover, UC shows the lowest recovery, but the highest protein purity of all exosomal isolation methods (Tang et al., 2017). Therefore, the UC method is the ideal option for proteomic analysis of exosomes (Alvarez et al., 2012; Rekker et al., 2014). In recent years, a series of commercial kits have been developed for the

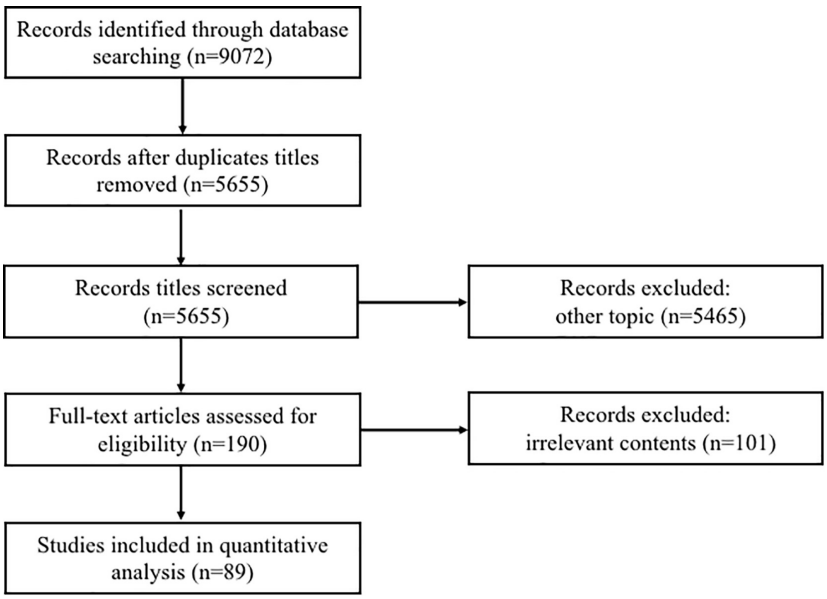

FIGURE 1 | Schematic of study selection.

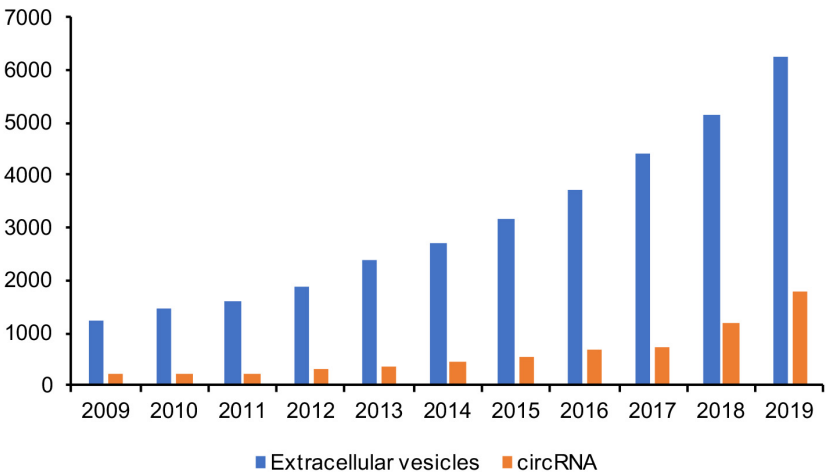

FIGURE 2 | Number of papers published in EVs research in the last decade.

isolation and extraction of exosomes (Hartman et al., 2011; da Silveira et al., 2012; Sohel et al., 2013). Compared to the UC method, commercial kits have simple methods (Helwa et al., 2017), often produce a significantly higher yield of exosomes (Helwa et al., 2017), and show a higher extraction efficiency (Tang et al., 2017). However, albumin impurities in the final extract are common. Notably, commercial kits produced the highest numbers of exosome miRNA and mRNA. Therefore, the use of commercial kits is an ideal method for subsequent RNA profiling analysis (Alvarez et al., 2012). Lastly, immunoaffinity capture is another method for separating and purifying exosomes. This method allows for the purification of high levels of exosomes and the exosome-associated proteins (Greening et al., 2015), and this is suitable for protein analysis of exosomes.

The selection of exosome isolation methods will have a substantial impact on the following RNA and protein analysis. Therefore, an appropriate exosome isolation method is essential to reveal exosomal-specific contents, and biological functions.

EXTRACELLULAR VESICLES AND AGING

Aging can be defined by a decline in multiple biological functions. There are many aging-associated disorders and chronic diseases, for example, sarcopenia (Landi et al., 2018), cancers, and cardiovascular diseases. This time-dependent process is characterized by the accumulation of cellular damage,

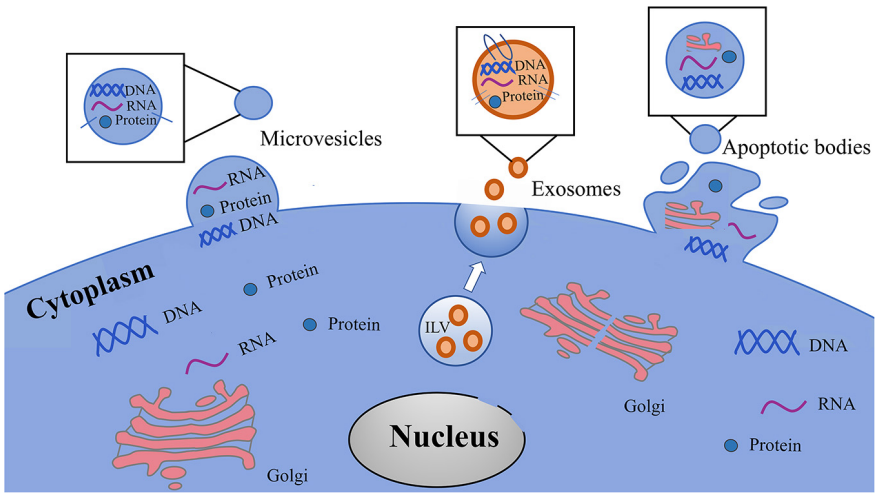

FIGURE 3 | Types of EVs in the cells culture media and body fluids. EVs are classified in three heterogeneous population, including exosomes, microvesicles and apoptotic bodies. Exosomes are originated from intraluminal vesicles (ILVs) reside within multivesicular endosomes (MVEs) that are the precursor of exosomes. Microvesicles shedding from the plasma membrane and subsequently released into the extracellular space. Apoptotic bodies are released from dying cells.

TABLE 1 | Summary of key characteristics of microvesicles, exosomes and apoptotic bodies.

	Microvesicles	Exosomes	Apoptotic bodies	References
Size (nm)	100 to 1,000/10,000 overlaps with bacteria size	40 to 150/200 overlap with virus size	>1,000 overlaps with platelet diameter	Hristov et al., 2004; Gyorgy et al., 2011; Akers et al., 2013; Colombo et al., 2013; Marques et al., 2013; Atkin-Smith et al., 2015; Jeppesen et al., 2019
Isolation procedure	Sequential centrifugation (300g/2,000g/10,000g)	Ultracentrifugation (UC), commercial kits, immunoaffinity, size exclusion, polymeric precipitation, microfluidics,	Centrifugation(300g), sequential filtering (5 and 1μm filters) and centrifugation(2,000g)	Chen et al., 2010, Hartman et al., 2011, Taylor et al., 2011; da Silveira et al., 2012; Sohel et al., 2013; Witwer et al., 2013; Boing et al., 2014; Van Deun et al., 2014; Greening et al., 2015; Xu et al., 2015
Selected protein markers	Annexin A1, ARF6, KIF, RACGAP, exportin-2 and chromosome segregation 1–like protein	Transmembrane tetrad proteins (including CD9, CD63, and CD81), Alix, TSG101, Flotillin-1, HSC70 and syntenin-1	VDAC1, PS, thrombospondin, C3b, calreticulin.	Takizawa et al., 1996; Fadok et al., 2001; Friedl et al., 2002; Muralidharan-Chari et al., 2009; Mathivanan et al., 2010; Colombo et al., 2014; Jeppesen et al., 2014, 2019; Van Deun et al., 2014; Xu et al., 2016; Tricarico et al., 2017
Biogenesis	Shedding from the plasma membrane and subsequently released into the extracellular space	Originate from intraluminal vesicles (ILVs) reside within multivesicular endosomes (MVEs) and are the precursor of exosomes	Released from dying cells	Colombo et al., 2014; Yanez-Mo et al., 2015; van Niel et al., 2018; Mathieu et al., 2019

widely recognized as a common cause of aging (Kirkwood, 2005; Gems and Partridge, 2013). A typical hallmark of senescent cells is the stability of permanent cell cycle arrest. Generally, the DNA synthesizing ability of senescent cells are typical of the G1 phase (Di Leonardo et al., 1994; Herbig et al., 2004). Aging has nine hallmarks: genomic instability, telomere shortening, epigenetic alterations, loss of proteostasis, deregulated nutrient sensing, mitochondrial dysfunction, senescence, stem cell exhaustion, and alteration in intercellular communication (Shiels et al., 2017). Cells in senescence exhibit a senescence-associated secretory phenotype (SASP), triggering the loss of DNA replication capacity (Campisi and d'Adda di Fagagna, 2007). Previous studies about aging have focused on traditional fields such as genetic alterations and epigenetics. With the development of EVs separation technology and the deepening of theoretical research, we have a new understanding of the mechanism of aging. Recently, EVs and their contents have received extensive attention in the research of aging mechanism.

EVs play a fundamental role in aging (Pusic and Kraig, 2014; Alique et al., 2017). Takasugi et al. (2017) demonstrated that EVs secreted by DNA-damaging agent doxorubicin induced senescent RPE-1 cells are important mediators of the pro-tumorigenic function of senescent cells. EVs-associated EphA2 secreted from senescent cells binds to ephrin-A1, which is highly expressed in several types of cancer cells and promotes cell proliferation through EphA2/ephrin-A1 reverse signaling. However, recent finding indicated that induced pluripotent stem cells (iPSCs) produce a large number of EVs, which could alleviate the aging-associated phenotypes of senescent mesenchymal stem cells (MSCs), promote cell proliferation, and mitigate progerin-induced senescence in premature aging cell models (Liu et al., 2019). Research into stem cells and their secreted EVs could help address the negative effects of senescent cells. This research would differ in that it requires the use of different cell sources of EVs.

At present, there are many controversies about whether EVs secretion in senescent cells is increased or decreased. In

2008, Lehmann et al. (2008) first certified that the release of EVs secretion increased during proliferative senescence in normal human diploid fibroblasts. This increase is regulated by p53 and TSAP6 (the target gene of p53). However, the exact mechanism of this regulation remains unclear. However, Eitan et al. (2017) provided an analysis of EVs in peripheral blood circulation through an epidemiologic and longitudinal study, and showed that the concentration of EVs significantly decreased with increasing age. This contrasting age-related decrease in EVs may be partly attributed to the fact that EVs from senescent individuals are easier to internalize than those from more young and healthy individuals (Eitan et al., 2017). The protein levels in EVs may be account for the age-related concentration changes and internalization activation. Recent studies revealed that the apoptosis markers such as p53, cleaved PARP, and cleaved Caspase-3 are significantly decreased, while proteins including CD151 and tetraspanin are markedly increased with cell senescence (Eitan et al., 2017). Therefore, the change of EVs levels in senescent cells needs further study.

The contents of EVs are also closely related to senescence, such as miRNA, inflammatory cargos, nicotinamide phosphoribosyltransferase, DNA and C24:1 ceramide.

TABLE 2 | EVs cargos involved in aging.

Cargos	Functions	References
miRNA	Inhibit BMSCs osteogenic differentiation and induced senescence	Davis et al., 2017
	Promote the oligodendrocyte precursor cells differentiation and improve the ability of remyelination	Pusic and Kraig, 2014
	Promote osteoclast formation and bone reabsorption, leading to the occurrence of osteoporosis	Xu et al., 2018
	Stimulate receptor cell migration and angiogenesis, preventing senescence	van Balkom et al., 2013
	Sensitivity and specificity to predict AD	Lugli et al., 2015
	A novel candidate aging biomarker	Machida et al., 2015; Bertoldi et al., 2018
Inflammatory cargos	Participate in the spread of inflammatory diseases	Boilard et al., 2010; Gomes de Andrade et al., 2018
Nicotinamide phosphoribosyltransferase (eNAMPT)	Promote the biosynthesis of systemic NAD^+ and offsets the occurrence of aging	Yoshida et al., 2019
DNA	Maintain cellular homeostasis	Ostrowski et al., 2010; Baietti et al., 2012; Takahashi et al., 2017
C24:1 ceramide	A key factor in cell death and senescence	Venable et al., 1995
	Induce senescence of bone marrow mesenchymal stem cells	Khayrullin et al., 2019

EVs: Extracellular vesicles. BMSCs: Bone marrow mesenchymal stem cells.

miRNA

Recently, a new mechanism of intercellular communication mediated by exosome-associated miRNAs has attracted widespread attention (Valadi et al., 2007). miRNAs are short non-coding RNA (ncRNA) molecules that can act as gene regulators by inhibiting translation or binding to the three primes' untranslated region (3'-UTR) of target messenger RNA (mRNA) to induce degradation of the target mRNA transcripts (Gasparello et al., 2019). miRNAs are therefore believed to be important in a range of physiological processes and the regulation of the development of many diseases. Moreover, Wei et al. (2017) recently analyzed extracellular RNA (exRNA) of EVs secreted by glioblastoma cells *in vitro* and found that ncRNA composed the majority of exRNA, instead of mRNA. This indicates that miRNAs play a significant and ever-growing role in the implementation of EVs function.

Studies have shown that exosome miRNA can be transported to surrounding tissues or cells and exert either a positive or negative impact, as summarized in **Table 2**. Several exosome-associated miRNAs are important regulators of senescence and cellular senescence. Exosomal miRNAs from senescent cells can be transported to surrounding cells and lead to aging (Smith-Vikos and Slack, 2012; Urbanelli et al., 2016). For example, Davis et al. (2017) treated bone marrow mesenchymal stem cells (BMSCs) of young mice with EVs derived from the bone marrow of aging mice and found that osteogenic differentiation was inhibited and BMSCs senescence was induced. This phenomenon can be mimicked by the transfection of miR-183-5p into BMSCs. Aging of the brain is associated with the loss of myelin, which has been shown to directly cause cognitive decline (Pusic and Kraig, 2014). In this study, serum-derived exosome miRNA in young Wistar rats promoted the differentiation of primary oligodendrocyte precursor cells (OPC) and improved the ability of remyelination in older Wistar rats. In the microenvironment of bone marrow, age-related miRNA changes can inhibit bone formation and promote bone resorption, leading to the osteoporosis. Exosomes derived from older rats BMSCs promoted the occurrence of osteoporosis and had higher levels of miR-31a-5p, compared to that of younger rats. Therefore, exosome miRNA is considered to be as an important mediator in the age-related bone marrow microenvironment (Xu et al., 2018).

However, exosomes can also suppress cellular senescence in certain contexts. Exosomes have been considered to be messengers of intercellular communication during angiogenesis. Recent studies have revealed that exosomes containing miR-214, produced by the human microvascular endothelial cell line (HMEC-1), can stimulate receptor cell migration and angiogenesis, thereby preventing the development of senescence. In contrast, the depletion of exosome miR-214 in endothelial cells failed to stimulate these processes and prevent cellular senescence (van Balkom et al., 2013). The study of miRNA in young and senescent cell EVs is helpful to reveal the new mechanisms of senescence.

Exosome miRNAs are also considered to be potential attractive biomarkers of aging (Smith et al., 2015). In a study investigating Alzheimer's disease (AD), Lugli et al. (2015) strongly suggested that plasma exosome miR-1306-5p, which targeted ADAM10, had the best sensitivity and specificity to predict AD, of all indicators examined. In salivary exosomes, miR-24-3p has been identified as a novel candidate biomarker for aging (Machida et al., 2015). The miR-183 cluster of exosomes, comprising miR-96, miR-182, and miR-183, increased during the aging process (Bertoldi et al., 2018). This suggests that the miR-183 clusters have the potential serve as biomarkers of aging.

INFLAMMATORY CARGOS

Inflammation has long been considered a defensive response to microbial agents. It is now clear that an inflammatory response can occur in the absence of infection, in a condition known as "aseptic inflammation" (Chen and Nunez, 2010). Aseptic inflammation is referred to as a chronic systemic inflammatory state during aging (Franceschi et al., 2000), in which EVs are involved (**Table 2**). EVs can trigger aseptic inflammatory responses by carrying pathogen autoantigens or damage-associated molecular patterns, and are involved in the transmission of inflammatory diseases through EV-associated cytokines, miRNAs, and lipid mediators (Buzas et al., 2014). Boilard et al. (2010) suggested that MPs originating from platelet are able to promote inflammatory reactions and stimulate cytokine responses in synovial fibroblasts via interleukin-1 (IL-1) signaling. Gomes de Andrade et al. (2018) revealed that aging could cause changes in the profiles of circulating exosomes. An age-related increase in CD63 levels was observed in exosomes from cerebrospinal fluid (CSF), and a significant decrease in IL-1β levels was observed in exosomes from the plasma of the older group of male Wistar rats (Gomes de Andrade et al., 2018). These results suggest that changes in IL-1β levels of the exosomes are significantly correlated with age-related inflammatory responses.

NICOTINAMIDE PHOSPHORIBOSYLTRANSFERASE

Nicotinamide adenine dinucleotide (NAD) is the basic chemical involved in energy metabolism in all living organisms. The expression of NAD^+, the oxidized form of NAD, in worms, various rodent tissues (fat, skeletal muscle, liver, pancreas, kidney, brain and heart), skin, and neurosensory retina is decreased with age (Braidy et al., 2011; Gomes et al., 2013; Mouchiroud et al., 2013; Khan et al., 2014; Canto et al., 2015; Verdin, 2015; Lin et al., 2018; Rajman et al., 2018; Yoshino et al., 2018). eNAMPT is an essential NAD^+ biosynthetic enzyme in mammals. In recent years, NAD^+ metabolism has become a hot topic in the field of aging (Canto et al., 2015; Rajman et al., 2018). Through the enrichment of several exosome markers, such as Flotillin-1, TSG101, CD9, CD63, and CD81, as well as the use of electron microscopy, Yoshida et al. (2019) demonstrated that both mouse and human plasma exosomes contained eNAMPT, which was internalized into target cells to directly enhance cellular NAD^+ biosynthesis. Moreover, in aging mouse plasma, exosome-containing eNAMPT content can be changed. This is a novel inter-organizational communication mechanism that maintains NAD^+ levels through exosome-mediated eNAMPT transport. eNAMPT promotes the biosynthesis of systemic NAD^+, offsets the occurrence of aging, and can be used as a new potential anti-aging intervention pathway (**Table 2**).

DNA

EVs also contain chromosomal DNA fragments. It has been reported that no matter the cause of cellular senescence, the secretion of DNA-containing exosomes increases with cell senescence (Takahashi et al., 2017). In senescent human cells, the inhibition of exosome-associated DNA secretion by knocking down Alix or Rab27, which are important molecules for the biogenesis (Baietti et al., 2012) and secretion (Ostrowski et al., 2010) of the exosomes, can provoke reactive oxygen species (ROS)-dependent DNA damage due to the accumulation of DNA in the cytoplasm and senescent cell cycle arrest or cell apoptosis. Even in non-senescent cells, the accumulation of cytoplasmic DNA can induce apoptosis. Cytoplasmic DNA has been reported as a danger signal that activates the innate immune response, including the interferon (IFN) pathway (Abe et al., 2013; Hartlova et al., 2015) and cGAS-STING-dependent signaling (Takahashi et al., 2017). Meanwhile, exosomes are actively secreted from cells in order to the remove infected adenoviral DNA (Takahashi et al., 2017). Exosomes, are therefore believed to play a critical role in senescence-associated secretory phenotypes. These results suggest that exosome secretion can maintain cellular homeostasis by removing harmful cytoplasmic DNA in senescent and non-senescent cells (**Table 2**). These findings will provide new insights into the control of cell homeostasis as well as new facets to investigate the involvement of EVs.

C24:1 CERAMIDE

Ceramide is a sphingolipid produced by the hydrolysis of sphingomyelin, catalyzed by sphingomyelinase (Wang et al., 2012), and has various of forms, such as short-, medium-, long-, and very long-chain. EVs are highly abundant in sphingolipid ceramide (Wang et al., 2012). Lipidomic analyses of serum exosomes indicated that serum exosomes from older women were highly enriched in C24:1 ceramide (Khayrullin et al., 2019). Exosome–associated ceramide has emerged as a key factor in cell death and senescence in a variety of cell types (Venable et al., 1995). Recent studies by Law et al. (2018) revealed that very long-chain ceramides with lipotoxicity can cause mitochondrial dysfunction, oxidative stress, and cell death in cardiomyocytes. *In vitro* experiments have shown that exosomes containing C24: 1 ceramide in serum could induce the senescence of BMSCs (Khayrullin et al., 2019). These results confirm that exosomes containing C24: 1 ceramide may directly lead to the involuntary senescence and apoptosis of cells (**Table 2**).

These animal and human studies provide strong evidence for the relationship between EVs, cargos, and aging. In the future studies, the relationship between other contents of EVs and senescence should be further explored to reveal the potentially unexpected role of EVs.

EXTRACELLULAR VESICLES AND REPRODUCTIVE DISEASES

It is widely accepted that normal reproductive processes, including ovulation, menstruation, implantation, and parturition, show signs of inflammation (Goswami et al., 2008). The female reproductive tract needs to solve these problems quickly to restore normal reproductive function. The dysregulation of inflammatory factors play a pivotal role in reproductive diseases (Gupta et al., 2008). As we know, EVs are involved in inflammatory state. In this review, we emphasize the involvement of EVs in PCOS and endometriosis. In view of the functions and characteristics of EVs, we focus on assessing the pathogenic role as well as diagnostic and therapeutic value of EVs in PCOS and endometriosis (**Table 3**).

EXTRACELLULAR VESICLES AND POLYCYSTIC OVARY SYNDROME

PCOS is one of the most prevalent endocrine diseases in women of reproductive age (Bozdag et al., 2016). Importantly, women with PCOS have an imbalance between procoagulant and anticoagulant factors with increased levels of proinflammatory cytokines (Repaci et al., 2011; Palomba et al., 2015; Nehir Aytan et al., 2016), which increase the risk of cardiovascular disease. Mesri and Altieri (1998) first described the role of circulating EVs in the spread of endothelial proinflammatory cascades in 1998. They demonstrated that EVs released from polymorphonuclear leukocytes by healthy volunteers could induce endothelial cells to produce cytokines and chemokines *in vitro*. In follicular fluids of PCOS women, Li et al. (2019) used a tandem mass tag quantitative proteomic approach and found that follicular fluid exosomes of both normal and PCOS samples contained S100 calcium-binding protein A9 (S100-A9). S100-A9 expression was greater in the follicular fluid exosomes of PCOS women and enhanced inflammation and disrupted steroidogenesis by activating the nuclear factor kappa B (NF-κB) signaling pathway. This activation was performed in a S100-A9 dose-dependent manner. In the follicular fluids of PCOS patients, EVs miR-132 and miR-320 are expressed at significantly lower levels than in healthy individuals (Sang et al., 2013). Moreover, these two miRNAs are also related to the production of steroidogenesis. However, the women with PCOS, miR-323-3p derived from mesenchymal stem cell exosomes alleviates PCOS by targeting PDCD4 to promote proliferation and inhibit apoptosis of cumulus cells (Zhao et al., 2019). This provides a novel therapeutic strategy for the treatment of PCOS.

MPs are also a type of EVs and play a fundamental role in the communication between source and target cells. Serum MPs' content can increase in variety of conditions, including PCOS (Willis et al., 2014; Carvalho et al., 2017b), prothrombotic states (Mooberry et al., 2016), and type 2 diabetes mellitus (Koga et al., 2005). Younger women with PCOS have increased concentrations of circulating annexin V-positive platelet MPs in plasma, compared with older women with PCOS (Willis et al., 2014). Surprisingly, in overweight women with the PCOS, plasma MPs are also higher than those in BMI-matched controls (Koiou et al., 2013). It was subsequently confirmed that elevated levels of EVs in women with PCOS are directly related to follicular counts and insulin resistance markers in the ovary (Simon et al., 2018). Interestingly, recent studies have revealed that metformin could reduce total MPs and tissue factor MPs (TFMPs) in women with PCOS (Carvalho et al., 2017a). TFMPs participate in thrombus formation and clot propagation (Nomura and Shimizu, 2015). Moreover, following

TABLE 3 | Pathogenic role and main functions of EVs in polycystic ovary syndrome and endometriosis.

Disease	Pathogenic role of EVs	Potential functions	References
PCOS	Enhance inflammation and disrupt steroidogenesis by activating the NF-κB signaling pathway		Li et al., 2019
	Alleviate PCOS by targeting PDCD4 to promote proliferation and inhibit apoptosis of cumulus cells	New therapeutic strategy	Zhao et al., 2019
		Biomarkers for predicting PCOS	Carvalho et al., 2017b
Endometriosis	Reflect the state of the inflammation and/or procoagulant system		Munros et al., 2017
	Increase total weight and impair macrophages' phagocytic ability		Sun et al., 2019
	Contribute to endometriosis by affecting inflammation, angiogenesis, and proliferation in the microenvironment of endometriotic lesions		Khalaj et al., 2019
		Prediction of successful embryo implantation	Parks et al., 2018
	Decrease of endometriosis fibrosis by reducing Collagen αI and CTGF mRNA expression		Wu et al., 2018
	Promote the occurrence of endometriosis and regulate angiogenesis		Harp et al., 2016, Qiu et al., 2019
		A non-invasive detection marker in the diagnosis of endometriosis	Muth et al., 2015

EVs: Extracellular vesicles. PCOS: Polycystic ovary syndrome. NF-κB: nuclear factor kappa B.

weight loss in a patient with PCOS, the number of MPs was significantly decreased. The relationship between MPs and the other symptoms of PCOS have not yet been established (Teede et al., 2010).

MPs may serve as useful biomarkers for predicting many diseases, including PCOS and cardiovascular disease (Carvalho et al., 2017b). The ratio of ornithine to arginine in plasma derived from PCOS patients is significantly increased (Kyselova et al., 2019). Furthermore, platelet-derived MPs are the main sources of plasma arginase (Kyselova et al., 2019). Arginase and the ratio of ornithine to arginine have also been reported to represent early biomarkers of potential cardiovascular disease in PCOS patients (Kyselova et al., 2019). Therefore, MPs can be used as potential biomarkers for disease assessment. The role of EVs in PCOS requires further study.

EXTRACELLULAR VESICLES AND ENDOMETRIOSIS

Endometriosis is a hormone-dependent, chronic, painful, and benign gynecological disorder. Although the pathogenesis of endometriosis is still unknown, Sampson's can explain the etiology of this disease through the theory of retrograde menstruation. This theory suggests that menstrual discharge returns to the peritoneal cavity through uterine contraction, adheres to the peritoneal tissue, and develops into ectopic lesions. However, of all patients with retrograde menstruation, only 5%–10% develop endometriosis (Cramer and Missmer, 2002; Giudice, 2010). Therefore, endometriosis is considered to be a dysfunctional immune response (Paul Dmowski and Braun, 2004) which promotes inflammatory responses and angiogenesis. Lately, the immune mechanism of endometriosis has received increasing attention (Ballester et al., 2011), notably due to the prevalence of EVs-related endometriosis research. Khalaj et al. (2019) suggested that in endometriosis patients, EVs could contribute to endometriosis by affecting inflammation, angiogenesis, and proliferation in the microenvironment of endometriotic lesions. Sun et al. (2019) reported that endometriosis, an inflammatory disease, possibly involves peritoneal macrophages. EVs derived from eutopic stromal cells of endometriosis could increase the total weight of mice and impair phagocytic ability of macrophages. These stromal cell-derived EVs contribute to the development of lesions. Previous studies by Munros et al. (2017) showed that in deep-infiltrating endometriosis patients, increased levels of circulating total cell-derived MPs may be reflect the state of the inflammation and procoagulant system. The increase in EVs level induces the disorder of immune function, and thus promotes the occurrence of endometriosis. Therefore, EVs have been shown to have the potential to promote endometriosis.

On the other hand, in terms of pathology, the main feature of endometriosis is ectopic tissue fibrosis, which is characterized by excessive deposition of endometriotic tissue on the extracellular matrix (Matsuzaki and Darcha, 2014; Malutan et al., 2015) and may cause scar formation or alter tissue function (Matsuzaki et al., 2010). Wu et al. (2018) reported that the increase in exosome miR-214 from endometrial stromal cells could result in the decrease of endometriosis fibrosis by reducing collagen αI and CTGF mRNA expression. Subsequently, Harp et al. (2016) proposed that exosomes released by endometriotic stromal cells could deliver specific miRNA molecules in an autocrine and paracrine manner to promote the occurrence of endometriosis and regulate angiogenesis. More recently, a study by Qiu et al. (2019) revealed that the serum exosome long non-coding RNA (lncRNA) hypoxia-inducible factor from patients with endometriosis could also promote angiogenesis. These results indicate that exosomes can promote the occurrence of endometriosis and may become an important pathogenesis for endometriosis.

Currently, the combination of laparoscopic evaluation and biopsy is the gold standard for the diagnosis of endometriosis (Gordts et al., 2015). However, both detection methods are invasive. EVs, as non-invasive detection markers, have shown to be value prospective for the diagnosis of endometriosis. Muth et al. (2015) showed that EVs from cervicovaginal lavage and vaginal swabs could be used as a novel and relatively non-invasive method to diagnose primate endometrial disease and other reproductive tract diseases.

EXTRACELLULAR VESICLES APPLICATION IN CLINICAL AND BASIC RESEARCH

The clinical application of EVs is based on four aspects (**Table 4**). First, treatment tools. EVs can increase the secretion of proinflammatory cytokines (Prado et al., 2008), and thus reducing the production or absorption of EVs may be a new strategy for the treatment of diseases. Secondly, EVs are

TABLE 4 | EVs application in clinical and basic research.

EVs application	References
Clinical	
Treat tools	Prado et al., 2008
Promising biomarkers for diagnostic diseases	Lugli et al., 2015; Machida et al., 2015; Muth et al., 2015; Carvalho et al., 2017b; Bertoldi et al., 2018; Kyselova et al., 2019
Drug delivery tools	Yoshida et al., 2019
Vaccines	Raposo et al., 1996; Zitvogel et al., 1998; Chaput and Thery, 2011
Basic research	
Function: Influence inflammation, angiogenesis, disrupting steroidogenesis and impairing macrophages' phagocytic ability. Alleviation diseases development.	Mesri and Altieri, 1998; Boilard et al., 2010; Harp et al., 2016; Munros et al., 2017; Gomes de Andrade et al., 2018; Khalaj et al., 2019; Li et al., 2019; Qiu et al., 2019; Sun et al., 2019
Mechanism: the NF-κB signaling pathway	Li et al., 2019; Zhang et al., 2019
	Wu et al., 2018; Liu et al., 2019; Mobarak et al., 2019; Yoshida et al., 2019; Zhao et al., 2019

EVs: Extracellular vesicles. NF-κB: nuclear factor kappa B.

promising biomarkers for diagnostic diseases (Lugli et al., 2015; Machida et al., 2015; Muth et al., 2015; Carvalho et al., 2017b; Bertoldi et al., 2018; Kyselova et al., 2019). EVs from bodily fluid have gained significant interest as a potential diagnostic biomarker for various diseases. Thirdly, EVs can be utilized as drug delivery tools. EVs can transport cargos to adjacent cells and be internalized into cells (Yoshida et al., 2019). Lastly, EVs may be applied to vaccinations. EVs have the potential to improve immune function (Raposo et al., 1996; Zitvogel et al., 1998; Chaput and Thery, 2011). The properties of EVs regulate the immune system, and thus give them the possibility to be involved in vaccinations.

In basic research, on the one hand, EVs contribute to disease pathophysiology. EVs and cargos include protein, miRNAs and lncRNAs that promote the development of the disease by influencing inflammation, angiogenesis, steroidogenesis and macrophage phagocytic ability (Mesri and Altieri, 1998; Boilard et al., 2010; Harp et al., 2016; Munros et al., 2017; Gomes de Andrade et al., 2018; Khalaj et al., 2019; Li et al., 2019; Qiu et al., 2019; Sun et al., 2019). This effect may be mediated by the NF-κB signaling pathway (Li et al., 2019; Zhang et al., 2019). On the other hand, EVs can also alleviate disease development (Wu et al., 2018; Liu et al., 2019; Mobarak et al., 2019; Yoshida et al., 2019; Zhao et al., 2019). It may also be a new pathway to treatment diseases.

CONCLUSION

In the recent decades, research on aging and reproductive diseases is mainly based on traditional fields such as genetic alterations and epigenetics. For this reason, many studies have focused on the development of EVs. Advances in the understanding of EVs in recent years have provided remarkable revelations. The relationship between EVs and aging as well as reproductive diseases has attention widespread attention. EVs could have the potential to be a new and non-invasive marker for assessing the condition of aging and reproductive diseases. In-depth research on the role and mechanism of EVs will provide new strategies for delaying aging and treating reproductive diseases and may eventually provide major innovations in their diagnosis and treatment. While EVs have shown potential importance and significance, stronger evidence is needed to support the possibility of EVs as clinical application. In addition, the lack of a gold standard method for EV separation and purification is a challenge and will limit the possibilities and significance of subsequent functional research.

AUTHOR CONTRIBUTIONS

YL carried out literature search, data collection and analysis, and wrote the manuscript. QS revised the manuscript. LZ carried out design and revised the manuscript. WX took part in design and revised the manuscript. All authors read and approved the manuscript.

FUNDING

This work was supported by the National Natural Science Foundation of China (NSFC 81871221).

REFERENCES

Abe, T., Harashima, A., Xia, T., Konno, H., Konno, K., Morales, A., et al. (2013). STING recognition of cytoplasmic DNA instigates cellular defense. *Mol. Cell* 50, 5–15. doi: 10.1016/j.molcel.2013.01.039

Admyre, C., Johansson, S. M., Qazi, K. R., Filen, J. J., Lahesmaa, R., Norman, M., et al. (2007). Exosomes with immune modulatory features are present in human breast milk. *J. Immunol.* 179, 1969–1978. doi: 10.4049/jimmunol.179.3.1969

Akers, J. C., Gonda, D., Kim, R., Carter, B. S., and Chen, C. C. (2013). Biogenesis of extracellular vesicles (EV): exosomes, microvesicles, retrovirus-like vesicles, and apoptotic bodies. *J. Neurooncol.* 113, 1–11. doi: 10.1007/s11060-013-1084-8

Alique, M., Ruiz-Torres, M. P., Bodega, G., Noci, M. V., Troyano, N., Bohorquez, L., et al. (2017). Microvesicles from the plasma of elderly subjects and from senescent endothelial cells promote vascular calcification. *Aging* 9, 778–789. doi: 10.18632/aging.101191

Alvarez, M. L., Khosroheidari, M., Kanchi Ravi, R., and Distefano, J. K. (2012). Comparison of protein, microRNA, and mRNA yields using different methods of urinary exosome isolation for the discovery of kidney disease biomarkers. *Kidney Int.* 82, 1024–1032. doi: 10.1038/ki.2012.256

Atkin-Smith, G. K., Tixeira, R., Paone, S., Mathivanan, S., Collins, C., Liem, M., et al. (2015). A novel mechanism of generating extracellular vesicles during apoptosis via a beads-on-a-string membrane structure. *Nat. Commun.* 6:7439.

Baek, R., Varming, K., and Jorgensen, M. M. (2016). Does smoking, age or gender affect the protein phenotype of extracellular vesicles in plasma? *Transfus. Apher. Sci.* 55, 44–52. doi: 10.1016/j.transci.2016.07.012

Baietti, M. F., Zhang, Z., Mortier, E., Melchior, A., Degeest, G., Geeraerts, A., et al. (2012). Syndecan-syntenin-ALIX regulates the biogenesis of exosomes. *Nat. Cell Biol.* 14, 677–685. doi: 10.1038/ncb2502

Ballester, M., Santulli, P., Bazot, M., Coutant, C., Rouzier, R., and Darai, E. (2011). Preoperative evaluation of posterior deep-infiltrating endometriosis demonstrates a relationship with urinary dysfunction and parametrial involvement. *J. Minim. Invasive Gynecol.* 18, 36–42. doi: 10.1016/j.jmig.2010.08.692

Bertoldi, K., Cechinel, L. R., Schallenberger, B., Corssac, G. B., Davies, S., Guerreiro, I. C. K., et al. (2018). Circulating extracellular vesicles in the aging process: impact of aerobic exercise. *Mol. Cell. Biochem.* 440, 115–125. doi: 10.1007/s11010-017-3160-4

Bobrie, A., Colombo, M., Krumeich, S., Raposo, G., and Thery, C. (2012). Diverse subpopulations of vesicles secreted by different intracellular mechanisms are present in exosome preparations obtained by differential ultracentrifugation. *J. Extracell. Vesicles* 1:18397. doi: 10.3402/jev.v1i0.18397

Boilard, E., Nigrovic, P. A., Larabee, K., Watts, G. F., Coblyn, J. S., Weinblatt, M. E., et al. (2010). Platelets amplify inflammation in arthritis via collagen-dependent microparticle production. *Science* 327, 580–583. doi: 10.1126/science.1181928

Boing, A. N., Van Der Pol, E., Grootemaat, A. E., Coumans, F. A., Sturk, A., and Nieuwland, R. (2014). Single-step isolation of extracellular vesicles by size-exclusion chromatography. *J. Extracel. Vesicles* 3:23430. doi: 10.3402/jev.v3.23430

Bozdag, G., Mumusoglu, S., Zengin, D., Karabulut, E., and Yildiz, B. O. (2016). The prevalence and phenotypic features of polycystic ovary syndrome: a systematic review and meta-analysis. *Hum. Reprod.* 31, 2841–2855. doi: 10.1093/humrep/dew218

Braidy, N., Guillemin, G. J., Mansour, H., Chan-Ling, T., Poljak, A., and Grant, R. (2011). Age related changes in NAD+ metabolism oxidative stress and Sirt1 activity in wistar rats. *PLoS One* 6:e19194. doi: 10.1371/journal.pone.0019194

Buzas, E. I., Gyorgy, B., Nagy, G., Falus, A., and Gay, S. (2014). Emerging role of extracellular vesicles in inflammatory diseases. *Nat. Rev. Rheumatol.* 10, 356–364. doi: 10.1038/nrrheum.2014.19

Caby, M. P., Lankar, D., Vincendeau-Scherrer, C., Raposo, G., and Bonnerot, C. (2005). Exosomal-like vesicles are present in human blood plasma. *Int. Immunol.* 17, 879–887. doi: 10.1093/intimm/dxh267

Campisi, J., and d'Adda di Fagagna, F. (2007). Cellular senescence: when bad things happen to good cells. *Nat. Rev. Mol. Cell Biol.* 8, 729–740. doi: 10.1038/nrm2233

Canto, C., Menzies, K. J., and Auwerx, J. (2015). NAD(+) metabolism and the control of energy homeostasis: a balancing act between mitochondria and the nucleus. *Cell Metab.* 22, 31–53. doi: 10.1016/j.cmet.2015.05.023

Carvalho, L. M. L., Ferreira, C. N., Candido, A. L., Reis, F. M., Soter, M. O., Sales, M. F., et al. (2017a). Metformin reduces total microparticles and microparticles-expressing tissue factor in women with polycystic ovary syndrome. *Arch. Gynecol. Obstet.* 296, 617–621. doi: 10.1007/s00404-017-4471-0

Carvalho, L. M. L., Ferreira, C. N., Soter, M. O., Sales, M. F., Rodrigues, K. F., Martins, S. R., et al. (2017b). Microparticles: inflammatory and haemostatic biomarkers in polycystic ovary syndrome. *Mol. Cell. Endocrinol.* 443, 155–162. doi: 10.1016/j.mce.2017.01.017

Chaput, N., and Thery, C. (2011). Exosomes: immune properties and potential clinical implementations. *Semin. Immunopathol.* 33, 419–440. doi: 10.1007/s00281-010-0233-9

Chen, X., Gao, C., Li, H., Huang, L., Sun, Q., Dong, Y., et al. (2010). Identification and characterization of microRNAs in raw milk during different periods of lactation, commercial fluid, and powdered milk products. *Cell Res.* 20, 1128–1137. doi: 10.1038/cr.2010.80

Chen, G. Y., and Nunez, G. (2010). Sterile inflammation: sensing and reacting to damage. *Nat. Rev. Immunol.* 10, 826–837. doi: 10.1038/nri2873

Choi, D. S., Park, J. O., Jang, S. C., Yoon, Y. J., Jung, J. W., Choi, D. Y., et al. (2011). Proteomic analysis of microvesicles derived from human colorectal cancer ascites. *Proteomics* 11, 2745–2751. doi: 10.1002/pmic.201100022

Colombo, M., Moita, C., Van Niel, G., Kowal, J., Vigneron, J., Benaroch, P., et al. (2013). Analysis of ESCRT functions in exosome biogenesis, composition and secretion highlights the heterogeneity of extracellular vesicles. *J. Cell Sci.* 126, 5553–5565. doi: 10.1242/jcs.128868

Colombo, M., Raposo, G., and Thery, C. (2014). Biogenesis, secretion, and intercellular interactions of exosomes and other extracellular vesicles. *Annu. Rev. Cell Dev. Biol.* 30, 255–289. doi: 10.1146/annurev-cellbio-101512-122326

Cramer, D. W., and Missmer, S. A. (2002). The epidemiology of endometriosis. *Ann. N. Y. Acad. Sci.* 955, 11–22; discussion 34–36, 396–406.

Cvjetkovic, A., Lotvall, J., and Lasser, C. (2014). The influence of rotor type and centrifugation time on the yield and purity of extracellular vesicles. *J. Extracell. Vesicles* 3:23111. doi: 10.3402/jev.v3.23111

da Silveira, J. C., Veeramachaneni, D. N., Winger, Q. A., Carnevale, E. M., and Bouma, G. J. (2012). Cell-secreted vesicles in equine ovarian follicular fluid contain miRNAs and proteins: a possible new form of cell communication within the ovarian follicle. *Biol. Reprod.* 86:71.

Davis, C., Dukes, A., Drewry, M., Helwa, I., Johnson, M. H., Isales, C. M., et al. (2017). MicroRNA-183-5p increases with age in bone-derived extracellular vesicles, suppresses bone marrow stromal (stem) cell proliferation, and induces stem cell senescence. *Tissue Eng. Part A* 23, 1231–1240. doi: 10.1089/ten.tea.2016.0525

Deatherage, B. L., and Cookson, B. T. (2012). Membrane vesicle release in bacteria, eukaryotes, and archaea: a conserved yet underappreciated aspect of microbial life. *Infect. Immun.* 80, 1948–1957. doi: 10.1128/iai.06014-11

Di Leonardo, A., Linke, S. P., Clarkin, K., and Wahl, G. M. (1994). DNA damage triggers a prolonged p53-dependent G1 arrest and long-term induction of Cip1 in normal human fibroblasts. *Genes Dev.* 8, 2540–2551. doi: 10.1101/gad.8.21.2540

Eitan, E., Green, J., Bodogai, M., Mode, N. A., Baek, R., Jorgensen, M. M., et al. (2017). Age-related changes in plasma extracellular vesicle characteristics and internalization by leukocytes. *Sci. Rep.* 7:1342.

Fadok, V. A., Bratton, D. L., and Henson, P. M. (2001). Phagocyte receptors for apoptotic cells: recognition, uptake, and consequences. *J. Clin. Invest.* 108, 957–962. doi: 10.1172/jci200114122

Franceschi, C., Bonafe, M., Valensin, S., Olivieri, F., De Luca, M., Ottaviani, E., et al. (2000). Inflamm-aging. An evolutionary perspective on immunosenescence. *Ann. N. Y. Acad. Sci.* 908, 244–254. doi: 10.1111/j.1749-6632.2000.tb06651.x

Friedl, P., Vischer, P., and Freyberg, M. A. (2002). The role of thrombospondin-1 in apoptosis. *Cell. Mol. Life Sci.* 59, 1347–1357. doi: 10.1007/s00018-002-8512-9

Gasparello, J., Lomazzi, M., Papi, C., D'aversa, E., Sansone, F., Casnati, A., et al. (2019). Efficient delivery of MicroRNA and AntimiRNA molecules using an argininocalix[4]arene macrocycle. *Mol. Ther. Nucleic Acids* 18, 748–763. doi: 10.1016/j.omtn.2019.09.029

Gems, D., and Partridge, L. (2013). Genetics of longevity in model organisms: debates and paradigm shifts. *Annu. Rev. Physiol.* 75, 621–644. doi: 10.1146/annurev-physiol-030212-183712

Giudice, L. C. (2010). Clinical practice. Endometriosis. *N. Engl. J. Med.* 362, 2389–2398.

Gomes, A. P., Price, N. L., Ling, A. J., Moslehi, J. J., Montgomery, M. K., Rajman, L., et al. (2013). Declining NAD(+) induces a pseudohypoxic state disrupting nuclear-mitochondrial communication during aging. *Cell* 155, 1624–1638. doi: 10.1016/j.cell.2013.11.037

Gomes de Andrade, G., Reck Cechinel, L., Bertoldi, K., Galvao, F., Valdeci Worm, P., and Rodrigues Siqueira, I. (2018). The aging process alters IL-1beta and CD63 levels differently in extracellular vesicles obtained from the plasma and cerebrospinal fluid. *Neuroimmunomodulation* 25, 18–22. doi: 10.1159/000488943

Gonzales, P. A., Pisitkun, T., Hoffert, J. D., Tchapyjnikov, D., Star, R. A., Kleta, R., et al. (2009). Large-scale proteomics and phosphoproteomics of urinary exosomes. *J. Am. Soc. Nephrol.* 20, 363–379. doi: 10.1681/asn.2008040406

Gordts, S., Puttemans, P., Gordts, S., and Brosens, I. (2015). Ovarian endometrioma in the adolescent: a plea for early-stage diagnosis and full surgical treatment. *Gynecol. Surg.* 12, 21–30. doi: 10.1007/s10397-014-0877-x

Goswami, B., Rajappa, M., Sharma, M., and Sharma, A. (2008). Inflammation: its role and interplay in the development of cancer, with special focus on gynecological malignancies. *Int. J. Gynecol. Cancer* 18, 591–599. doi: 10.1111/j.1525-1438.2007.01089.x

Greening, D. W., Xu, R., Ji, H., Tauro, B. J., and Simpson, R. J. (2015). A protocol for exosome isolation and characterization: evaluation of ultracentrifugation, density-gradient separation, and immunoaffinity capture methods. *Methods Mol. Biol.* 1295, 179–209. doi: 10.1007/978-1-4939-2550-6_15

Gupta, S., Goldberg, J. M., Aziz, N., Goldberg, E., Krajcir, N., and Agarwal, A. (2008). Pathogenic mechanisms in endometriosis-associated infertility. *Fertil. Steril.* 90, 247–257. doi: 10.1016/j.fertnstert.2008.02.093

Gyorgy, B., Szabo, T. G., Pasztoi, M., Pal, Z., Misjak, P., Aradi, B., et al. (2011). Membrane vesicles, current state-of-the-art: emerging role of extracellular vesicles. *Cell. Mol. Life Sci.* 68, 2667–2688. doi: 10.1007/s00018-011-0689-3

Harp, D., Driss, A., Mehrabi, S., Chowdhury, I., Xu, W., Liu, D., et al. (2016). Exosomes derived from endometriotic stromal cells have enhanced angiogenic effects in vitro. *Cell Tissue Res.* 365, 187–196. doi: 10.1007/s00441-016-2358-1

Hartlova, A., Erttmann, S. F., Raffi, F. A., Schmalz, A. M., Resch, U., Anugula, S., et al. (2015). DNA damage primes the type I interferon system via the cytosolic DNA sensor STING to promote anti-microbial innate immunity. *Immunity* 42, 332–343. doi: 10.1016/j.immuni.2015.01.012

Hartman, Z. C., Wei, J., Glass, O. K., Guo, H., Lei, G., Yang, X. Y., et al. (2011). Increasing vaccine potency through exosome antigen targeting. *Vaccine* 29, 9361–9367. doi: 10.1016/j.vaccine.2011.09.133

Helwa, I., Cai, J., Drewry, M. D., Zimmerman, A., Dinkins, M. B., Khaled, M. L., et al. (2017). A comparative study of serum exosome isolation using differential ultracentrifugation and three commercial reagents. *PLoS One* 12:e0170628. doi: 10.1371/journal.pone.0170628

Herbig, U., Jobling, W. A., Chen, B. P., Chen, D. J., and Sedivy, J. M. (2004). Telomere shortening triggers senescence of human cells through a pathway involving ATM, p53, and p21(CIP1), but not p16(INK4a). *Mol. Cell* 14, 501–513. doi: 10.1016/s1097-2765(04)00256-4

Hristov, M., Erl, W., Linder, S., and Weber, P. C. (2004). Apoptotic bodies from endothelial cells enhance the number and initiate the differentiation of human endothelial progenitor cells in vitro. *Blood* 104, 2761–2766. doi: 10.1182/blood-2003-10-3614

Jakobsen, K. R., Paulsen, B. S., Baek, R., Varming, K., Sorensen, B. S., and Jorgensen, M. M. (2015). Exosomal proteins as potential diagnostic markers in advanced non-small cell lung carcinoma. *J. Extracell. Vesicles* 4:26659. doi: 10.3402/jev.v4.26659

Jeppesen, D. K., Fenix, A. M., Franklin, J. L., Higginbotham, J. N., Zhang, Q., Zimmerman, L. J., et al. (2019). Reassessment of exosome composition. *Cell* 177, 428–445.e18.

Jeppesen, D. K., Hvam, M. L., Primdahl-Bengtson, B., Boysen, A. T., Whitehead, B., Dyrskjot, L., et al. (2014). Comparative analysis of discrete exosome fractions obtained by differential centrifugation. *J. Extracell. Vesicles* 3:25011. doi: 10.3402/jev.v3.25011

Khalaj, K., Miller, J. E., Lingegowda, H., Fazleabas, A. T., Young, S. L., Lessey, B. A., et al. (2019). Extracellular vesicles from endometriosis patients are characterized by a unique miRNA-lncRNA signature. *JCI Insight* 4:e128846.

Khan, N. A., Auranen, M., Paetau, I., Pirinen, E., Euro, L., Forsstrom, S., et al. (2014). Effective treatment of mitochondrial myopathy by nicotinamide riboside, a vitamin B3. *EMBO Mol. Med.* 6, 721–731. doi: 10.1002/emmm.201403943

Khayrullin, A., Krishnan, P., Martinez-Nater, L., Mendhe, B., Fulzele, S., Liu, Y., et al. (2019). Very long-chain C24:1 ceramide is increased in serum extracellular vesicles with aging and can induce senescence in bone-derived mesenchymal stem cells. *Cells* 8:37. doi: 10.3390/cells8010037

Kirkwood, T. B. (2005). Understanding the odd science of aging. *Cell* 120, 437–447. doi: 10.1016/j.cell.2005.01.027

Koga, H., Sugiyama, S., Kugiyama, K., Watanabe, K., Fukushima, H., Tanaka, T., et al. (2005). Elevated levels of VE-cadherin-positive endothelial microparticles in patients with type 2 diabetes mellitus and coronary artery disease. *J. Am. Coll. Cardiol.* 45, 1622–1630. doi: 10.1016/j.jacc.2005.02.047

Koiou, E., Tziomalos, K., Katsikis, I., Papadakis, E., Kandaraki, E. A., and Panidis, D. (2013). Platelet-derived microparticles in overweight/obese women with the polycystic ovary syndrome. *Gynecol. Endocrinol.* 29, 250–253. doi: 10.3109/09513590.2012.743005

Kowal, J., Arras, G., Colombo, M., Jouve, M., Morath, J. P., Primdal-Bengtson, B., et al. (2016). Proteomic comparison defines novel markers to characterize heterogeneous populations of extracellular vesicle subtypes. *Proc. Natl. Acad. Sci. U.S.A.* 113, E968–E977.

Kyselova, A., Hinrichsmeyer, H., Zukunft, S., Mann, A. W., Dornauf, I., Fleming, I., et al. (2019). Association between arginase-containing platelet-derived microparticles and altered plasma arginine metabolism in polycystic ovary syndrome. *Metabolism* 90, 16–19. doi: 10.1016/j.metabol.2018.10.008

Landi, F., Calvani, R., Cesari, M., Tosato, M., Martone, A. M., Ortolani, E., et al. (2018). Sarcopenia: an overview on current definitions, diagnosis and treatment. *Curr. Protein Pept. Sci.* 19, 633–638. doi: 10.2174/1389203718666170607113459

Law, B. A., Liao, X., Moore, K. S., Southard, A., Roddy, P., Ji, R., et al. (2018). Lipotoxic very-long-chain ceramides cause mitochondrial dysfunction, oxidative stress, and cell death in cardiomyocytes. *FASEB J.* 32, 1403–1416. doi: 10.1096/fj.201700300r

Lehmann, B. D., Paine, M. S., Brooks, A. M., Mccubrey, J. A., Renegar, R. H., Wang, R., et al. (2008). Senescence-associated exosome release from human prostate cancer cells. *Cancer Res.* 68, 7864–7871. doi: 10.1158/0008-5472.can-07-6538

Li, H., Huang, X., Chang, X., Yao, J., He, Q., Shen, Z., et al. (2019). S100-A9 protein in exosomes derived from follicular fluid promotes inflammation via activation of NF-kappaB pathway in polycystic ovary syndrome. *J. Cell. Mol. Med.* 24, 114–125. doi: 10.1111/jcmm.14642

Li, J., Sherman-Baust, C. A., Tsai-Turton, M., Bristow, R. E., Roden, R. B., and Morin, P. J. (2009). Claudin-containing exosomes in the peripheral circulation of women with ovarian cancer. *BMC Cancer* 9:244. doi: 10.1186/1471-2407-9-244

Lin, J. B., Kubota, S., Mostoslavsky, R., and Apte, R. S. (2018). Role of sirtuins in retinal function under basal conditions. *Adv. Exp. Med. Biol.* 1074, 561–567. doi: 10.1007/978-3-319-75402-4_68

Liu, S., Mahairaki, V., Bai, H., Ding, Z., Li, J., Witwer, K. W., et al. (2019). Highly purified human extracellular vesicles produced by stem cells alleviate aging cellular phenotypes of senescent human cells. *Stem Cells* 37, 779–790. doi: 10.1002/stem.2996

Lugli, G., Cohen, A. M., Bennett, D. A., Shah, R. C., Fields, C. J., Hernandez, A. G., et al. (2015). Plasma exosomal miRNAs in persons with and without Alzheimer disease: altered expression and prospects for biomarkers. *PLoS One* 10:e0139233. doi: 10.1371/journal.pone.0139233

Machida, T., Tomofuji, T., Ekuni, D., Maruyama, T., Yoneda, T., Kawabata, Y., et al. (2015). MicroRNAs in salivary exosome as potential biomarkers of aging. *Int. J. Mol. Sci.* 16, 21294–21309. doi: 10.3390/ijms160921294

Malutan, A. M., Drugan, T., Costin, N., Ciortea, R., Bucuri, C., Rada, M. P., et al. (2015). Pro-inflammatory cytokines for evaluation of inflammatory status in endometriosis. *Cent. Eur. J. Immunol.* 40, 96–102. doi: 10.5114/ceji.2015.50840

Marques, F. K., Campos, F. M., Sousa, L. P., Teixeira-Carvalho, A., Dusse, L. M., and Gomes, K. B. (2013). Association of microparticles and preeclampsia. *Mol. Biol. Rep.* 40, 4553–4559.

Mathieu, M., Martin-Jaular, L., Lavieu, G., and Thery, C. (2019). Specificities of secretion and uptake of exosomes and other extracellular vesicles for cell-to-cell communication. *Nat. Cell Biol.* 21, 9–17. doi: 10.1038/s41556-018-0250-9

Mathivanan, S., Ji, H., and Simpson, R. J. (2010). Exosomes: extracellular organelles important in intercellular communication. *J. Proteomics* 73, 1907–1920. doi: 10.1016/j.jprot.2010.06.006

Matsuzaki, S., and Darcha, C. (2014). Antifibrotic properties of epigallocatechin-3-gallate in endometriosis. *Hum. Reprod.* 29, 1677–1687. doi: 10.1093/humrep/deu123

Matsuzaki, S., Darcha, C., Maleysson, E., Canis, M., and Mage, G. (2010). Impaired down-regulation of E-cadherin and beta-catenin protein expression in endometrial epithelial cells in the mid-secretory endometrium of infertile patients with endometriosis. *J. Clin. Endocrinol. Metab.* 95, 3437–3445. doi: 10.1210/jc.2009-2713

Mesri, M., and Altieri, D. C. (1998). Endothelial cell activation by leukocyte microparticles. *J. Immunol.* 161, 4382–4387.

Mitchell, P. J., Welton, J., Staffurth, J., Court, J., Mason, M. D., Tabi, Z., et al. (2009). Can urinary exosomes act as treatment response markers in prostate cancer? *J. Transl. Med.* 7:4. doi: 10.1186/1479-5876-7-4

Mobarak, H., Heidarpour, M., Lolicato, F., Nouri, M., Rahbarghazi, R., and Mahdipour, M. (2019). Physiological impact of extracellular vesicles on female reproductive system; highlights to possible restorative effects on female age-related fertility. *Biofactors* 45, 293–303. doi: 10.1002/biof.1497

Mooberry, M. J., Bradford, R., Hobl, E. L., Lin, F. C., Jilma, B., and Key, N. S. (2016). Procoagulant microparticles promote coagulation in a factor XI-dependent manner in human endotoxemia. *J. Thromb. Haemost.* 14, 1031–1042. doi: 10.1111/jth.13285

Mouchiroud, L., Houtkooper, R. H., Moullan, N., Katsyuba, E., Ryu, D., Canto, C., et al. (2013). The NAD(+)/sirtuin pathway modulates longevity through activation of mitochondrial UPR and FOXO signaling. *Cell* 154, 430–441. doi: 10.1016/j.cell.2013.06.016

Munros, J., Martinez-Zamora, M. A., Tassies, D., Coloma, J. L., Torrente, M. A., Reverter, J. C., et al. (2017). Total circulating microparticle levels are increased in patients with deep infiltrating endometriosis. *Hum. Reprod.* 32, 325–331. doi: 10.1093/humrep/dew319

Muralidharan-Chari, V., Clancy, J., Plou, C., Romao, M., Chavrier, P., Raposo, G., et al. (2009). ARF6-regulated shedding of tumor cell-derived plasma membrane microvesicles. *Curr. Biol.* 19, 1875–1885. doi: 10.1016/j.cub.2009.09.059

Muth, D. C., Mcalexander, M. A., Ostrenga, L. J., Pate, N. M., Izzi, J. M., Adams, R. J., et al. (2015). Potential role of cervicovaginal extracellular particles in diagnosis of endometriosis. *BMC Vet. Res.* 11:187. doi: 10.1186/s12917-015-0513-7

Nehir Aytan, A., Bastu, E., Demiral, I., Bulut, H., Dogan, M., and Buyru, F. (2016). Relationship between hyperandrogenism, obesity, inflammation and polycystic ovary syndrome. *Gynecol. Endocrinol.* 32, 709–713. doi: 10.3109/09513590.2016.1155208

Nomura, S., and Shimizu, M. (2015). Clinical significance of procoagulant microparticles. *J. Intensive Care* 3:2. doi: 10.1186/s40560-014-0066-z

Ogawa, Y., Kanai-Azuma, M., Akimoto, Y., Kawakami, H., and Yanoshita, R. (2008). Exosome-like vesicles with dipeptidyl peptidase IV in human saliva. *Biol. Pharm. Bull.* 31, 1059–1062. doi: 10.1248/bpb.31.1059

Ostergaard, O., Nielsen, C. T., Iversen, L. V., Tanassi, J. T., Knudsen, S., Jacobsen, S., et al. (2013). Unique protein signature of circulating microparticles in systemic lupus erythematosus. *Arthritis Rheum.* 65, 2680–2690.

Ostrowski, M., Carmo, N. B., Krumeich, S., Fanget, I., Raposo, G., Savina, A., et al. (2010). Rab27a and Rab27b control different steps of the exosome secretion pathway. *Nat. Cell Biol.* 12, 19–30. doi: 10.1038/ncb2000

Palomba, S., Santagni, S., Falbo, A., and La Sala, G. B. (2015). Complications and challenges associated with polycystic ovary syndrome: current perspectives. *Int. J. Womens Health* 7, 745–763. doi: 10.2147/ijwh.s70314

Parks, J. C., Mccallie, B. R., Patton, A. L., Al-Safi, Z. A., Polotsky, A. J., Griffin, D. K., et al. (2018). The impact of infertility diagnosis on embryo-endometrial dialogue. *Reproduction* 155, 543–552. doi: 10.1530/REP-17-0566

Paul Dmowski, W., and Braun, D. P. (2004). Immunology of endometriosis. *Best Pract. Res. Clin. Obstet. Gynaecol.* 18, 245–263.

Prado, N., Marazuela, E. G., Segura, E., Fernandez-Garcia, H., Villalba, M., Thery, C., et al. (2008). Exosomes from bronchoalveolar fluid of tolerized mice prevent allergic reaction. *J. Immunol.* 181, 1519–1525. doi: 10.4049/jimmunol.181.2.1519

Pusic, A. D., and Kraig, R. P. (2014). Youth and environmental enrichment generate serum exosomes containing miR-219 that promote CNS myelination. *Glia* 62, 284–299. doi: 10.1002/glia.22606

Qiu, J. J., Lin, X. J., Zheng, T. T., Tang, X. Y., Zhang, Y., and Hua, K. Q. (2019). The exosomal long noncoding RNA aHIF is upregulated in serum from patients with endometriosis and promotes angiogenesis in endometriosis. *Reprod. Sci.* 26, 1590–1602. doi: 10.1177/1933719119831775

Rajman, L., Chwalek, K., and Sinclair, D. A. (2018). Therapeutic potential of NAD-boosting molecules: the in vivo evidence. *Cell Metab.* 27, 529–547. doi: 10.1016/j.cmet.2018.02.011

Raposo, G., Nijman, H. W., Stoorvogel, W., Liejendekker, R., Harding, C. V., Melief, C. J., et al. (1996). B lymphocytes secrete antigen-presenting vesicles. *J. Exp. Med.* 183, 1161–1172. doi: 10.1084/jem.183.3.1161

Raposo, G., and Stoorvogel, W. (2013). Extracellular vesicles: exosomes, microvesicles, and friends. *J. Cell Biol.* 200, 373–383. doi: 10.1083/jcb.201211138

Rekker, K., Saare, M., Roost, A. M., Kubo, A. L., Zarovni, N., Chiesi, A., et al. (2014). Comparison of serum exosome isolation methods for microRNA profiling. *Clin. Biochem.* 47, 135–138. doi: 10.1016/j.clinbiochem.2013.10.020

Repaci, A., Gambineri, A., and Pasquali, R. (2011). The role of low-grade inflammation in the polycystic ovary syndrome. *Mol. Cell. Endocrinol.* 335, 30–41. doi: 10.1016/j.mce.2010.08.002

Robinson, D. G., Ding, Y., and Jiang, L. (2016). Unconventional protein secretion in plants: a critical assessment. *Protoplasma* 253, 31–43. doi: 10.1007/s00709-015-0887-1

Saman, S., Kim, W., Raya, M., Visnick, Y., Miro, S., Saman, S., et al. (2012). Exosome-associated tau is secreted in tauopathy models and is selectively phosphorylated in cerebrospinal fluid in early Alzheimer disease. *J. Biol. Chem.* 287, 3842–3849. doi: 10.1074/jbc.m111.277061

Sang, Q., Yao, Z., Wang, H., Feng, R., Wang, H., Zhao, X., et al. (2013). Identification of microRNAs in human follicular fluid: characterization of microRNAs that govern steroidogenesis in vitro and are associated with polycystic ovary syndrome in vivo. *J. Clin. Endocrinol. Metab.* 98, 3068–3079. doi: 10.1210/jc.2013-1715

Schorey, J. S., Cheng, Y., Singh, P. P., and Smith, V. L. (2015). Exosomes and other extracellular vesicles in host-pathogen interactions. *EMBO Rep.* 16, 24–43. doi: 10.15252/embr.201439363

Shiels, P. G., Stenvinkel, P., Kooman, J. P., and Mcguinness, D. (2017). Circulating markers of ageing and allostatic load: a slow train coming. *Pract. Lab. Med.* 7, 49–54. doi: 10.1016/j.plabm.2016.04.002

Simon, C., Greening, D. W., Bolumar, D., Balaguer, N., Salamonsen, L. A., and Vilella, F. (2018). Extracellular vesicles in human reproduction in health and disease. *Endocr. Rev.* 39, 292–332. doi: 10.1210/er.2017-00229

Smith, J. A., Leonardi, T., Huang, B., Iraci, N., Vega, B., and Pluchino, S. (2015). Extracellular vesicles and their synthetic analogues in aging and age-associated brain diseases. *Biogerontology* 16, 147–185. doi: 10.1007/s10522-014-9510-7

Smith-Vikos, T., and Slack, F. J. (2012). MicroRNAs and their roles in aging. *J. Cell Sci.* 125, 7–17. doi: 10.1242/jcs.099200

Sohel, M. M., Hoelker, M., Noferesti, S. S., Salilew-Wondim, D., Tholen, E., Looft, C., et al. (2013). Exosomal and non-exosomal transport of extra-cellular microRNAs in follicular fluid: implications for bovine oocyte developmental competence. *PLoS One* 8:e78505. doi: 10.1371/journal.pone.0078505

Stegmayr, B., and Ronquist, G. (1982). Promotive effect on human sperm progressive motility by prostasomes. *Urol. Res.* 10, 253–257.

Sun, H., Li, D., Yuan, M., Li, Q., Zhen, Q., Li, N., et al. (2019). Macrophages alternatively activated by endometriosis-exosomes contribute to the development of lesions in mice. *Mol. Hum. Reprod.* 25, 5–16. doi: 10.1093/molehr/gay049

Takahashi, A., Okada, R., Nagao, K., Kawamata, Y., Hanyu, A., Yoshimoto, S., et al. (2017). Exosomes maintain cellular homeostasis by excreting harmful DNA from cells. *Nat. Commun.* 8:15287.

Takasugi, M., Okada, R., Takahashi, A., Virya Chen, D., Watanabe, S., and Hara, E. (2017). Small extracellular vesicles secreted from senescent cells promote cancer cell proliferation through EphA2. *Nat. Commun.* 8:15729.

Takizawa, F., Tsuji, S., and Nagasawa, S. (1996). Enhancement of macrophage phagocytosis upon iC3b deposition on apoptotic cells. *FEBS Lett.* 397, 269–272. doi: 10.1016/s0014-5793(96)01197-0

Tang, Y. T., Huang, Y. Y., Zheng, L., Qin, S. H., Xu, X. P., An, T. X., et al. (2017). Comparison of isolation methods of exosomes and exosomal RNA from cell culture medium and serum. *Int. J. Mol. Med.* 40, 834–844. doi: 10.3892/ijmm.2017.3080

Tauro, B. J., Greening, D. W., Mathias, R. A., Ji, H., Mathivanan, S., Scott, A. M., et al. (2012). Comparison of ultracentrifugation, density gradient separation, and immunoaffinity capture methods for isolating human colon cancer cell line LIM1863-derived exosomes. *Methods* 56, 293–304. doi: 10.1016/j.ymeth.2012.01.002

Taylor, D. D., Zacharias, W., and Gercel-Taylor, C. (2011). Exosome isolation for proteomic analyses and RNA profiling. *Methods Mol. Biol.* 728, 235–246. doi: 10.1007/978-1-61779-068-3_15

Teede, H., Deeks, A., and Moran, L. (2010). Polycystic ovary syndrome: a complex condition with psychological, reproductive and metabolic manifestations that impacts on health across the lifespan. *BMC Med.* 8:41. doi: 10.1186/1741-7015-8-41

Tricarico, C., Clancy, J., and D'souza-Schorey, C. (2017). Biology and biogenesis of shed microvesicles. *Small GTPases* 8, 220–232. doi: 10.1080/21541248.2016.1215283

Urbanelli, L., Buratta, S., Sagini, K., Tancini, B., and Emiliani, C. (2016). Extracellular vesicles as new players in cellular senescence. *Int. J. Mol. Sci.* 17:1408. doi: 10.3390/ijms17091408

Valadi, H., Ekstrom, K., Bossios, A., Sjostrand, M., Lee, J. J., and Lotvall, J. O. (2007). Exosome-mediated transfer of mRNAs and microRNAs is a novel mechanism of genetic exchange between cells. *Nat. Cell Biol.* 9, 654–659. doi: 10.1038/ncb1596

van Balkom, B. W., De Jong, O. G., Smits, M., Brummelman, J., Den Ouden, K., De Bree, P. M., et al. (2013). Endothelial cells require miR-214 to secrete exosomes that suppress senescence and induce angiogenesis in human and mouse endothelial cells. *Blood* 121, 3997–4006, S1–S15.

Van Deun, J., Mestdagh, P., Sormunen, R., Cocquyt, V., Vermaelen, K., Vandesompele, J., et al. (2014). The impact of disparate isolation methods for extracellular vesicles on downstream RNA profiling. *J. Extracell. Vesicles* 3:24858. doi: 10.3402/jev.v3.24858

van Niel, G., D'angelo, G., and Raposo, G. (2018). Shedding light on the cell biology of extracellular vesicles. *Nat. Rev. Mol. Cell Biol.* 19, 213–228. doi: 10.1038/nrm.2017.125

Venable, M. E., Lee, J. Y., Smyth, M. J., Bielawska, A., and Obeid, L. M. (1995). Role of ceramide in cellular senescence. *J. Biol. Chem.* 270, 30701–30708. doi: 10.1074/jbc.270.51.30701

Verdin, E. (2015). NAD(+) in aging, metabolism, and neurodegeneration. *Science* 350, 1208–1213. doi: 10.1126/science.aac4854

Wang, G., Dinkins, M., He, Q., Zhu, G., Poirier, C., Campbell, A., et al. (2012). Astrocytes secrete exosomes enriched with proapoptotic ceramide and prostate apoptosis response 4 (PAR-4): potential mechanism of apoptosis induction in Alzheimer disease (AD). *J. Biol. Chem.* 287, 21384–21395. doi: 10.1074/jbc.m112.340513

Wei, Z., Batagov, A. O., Schinelli, S., Wang, J., Wang, Y., El Fatimy, R., et al. (2017). Coding and noncoding landscape of extracellular RNA released by human glioma stem cells. *Nat. Commun.* 8:1145.

Willis, G. R., Connolly, K., Ladell, K., Davies, T. S., Guschina, I. A., Ramji, D., et al. (2014). Young women with polycystic ovary syndrome have raised levels of circulating annexin V-positive platelet microparticles. *Hum. Reprod.* 29, 2756–2763. doi: 10.1093/humrep/deu281

Witwer, K. W., Buzas, E. I., Bemis, L. T., Bora, A., Lasser, C., Lotvall, J., et al. (2013). Standardization of sample collection, isolation and analysis methods in extracellular vesicle research. *J. Extracell. Vesicles* 2:20360. doi: 10.3402/jev.v2i0.20360

Wu, D., Lu, P., Mi, X., and Miao, J. (2018). Exosomal miR-214 from endometrial stromal cells inhibits endometriosis fibrosis. *Mol. Hum. Reprod.* 24, 357–365.

Xu, R., Greening, D. W., Rai, A., Ji, H., and Simpson, R. J. (2015). Highly-purified exosomes and shed microvesicles isolated from the human colon cancer cell line LIM1863 by sequential centrifugal ultrafiltration are biochemically and functionally distinct. *Methods* 87, 11–25. doi: 10.1016/j.ymeth.2015.04.008

Xu, R., Greening, D. W., Zhu, H. J., Takahashi, N., and Simpson, R. J. (2016). Extracellular vesicle isolation and characterization: toward clinical application. *J. Clin. Invest.* 126, 1152–1162. doi: 10.1172/jci81129

Xu, R., Shen, X., Si, Y., Fu, Y., Zhu, W., Xiao, T., et al. (2018). MicroRNA-31a-5p from aging BMSCs links bone formation and resorption in the aged bone marrow microenvironment. *Aging Cell* 17:e12794. doi: 10.1111/acel.12794

Yanez-Mo, M., Siljander, P. R., Andreu, Z., Zavec, A. B., Borras, F. E., Buzas, E. I., et al. (2015). Biological properties of extracellular vesicles and their physiological functions. *J. Extracell. Vesicles* 4:27066.

Yoshida, M., Satoh, A., Lin, J. B., Mills, K. F., Sasaki, Y., Rensing, N., et al. (2019). Extracellular vesicle-contained eNAMPT delays aging and extends lifespan in mice. *Cell Metab.* 30, 329–342.e5.

Yoshino, J., Baur, J. A., and Imai, S. I. (2018). NAD(+) intermediates: the biology and therapeutic potential of NMN and NR. *Cell Metab.* 27, 513–528. doi: 10.1016/j.cmet.2017.11.002

Zhang, A., Wang, G., Jia, L., Su, T., and Zhang, L. (2019). Exosome-mediated microRNA-138 and vascular endothelial growth factor in endometriosis through inflammation and apoptosis via the nuclear factor-kappaB signaling pathway. *Int. J. Mol. Med.* 43, 358–370.

Zhao, Y., Tao, M., Wei, M., Du, S., Wang, H., and Wang, X. (2019). Mesenchymal stem cells derived exosomal miR-323-3p promotes proliferation and inhibits apoptosis of cumulus cells in polycystic ovary syndrome (PCOS). *Artif. Cells Nanomed. Biotechnol.* 47, 3804–3813. doi: 10.1080/21691401.2019.1669619

Zitvogel, L., Regnault, A., Lozier, A., Wolfers, J., Flament, C., Tenza, D., et al. (1998). Eradication of established murine tumors using a novel cell-free vaccine: dendritic cell-derived exosomes. *Nat. Med.* 4, 594–600. doi: 10.1038/nm0598-594

Conflict of Interest: The authors declare that the research was conducted in the absence of any commercial or financial relationships that could be construed as a potential conflict of interest.

frontiers in Cell and Developmental Biology

ORIGINAL RESEARCH
published: 28 October 2020
doi: 10.3389/fcell.2020.575788

Germline Specific Expression of a *vasa* Homologue Gene in the Viviparous Fish Black Rockfish (*Sebastes schlegelii*) and Functional Analysis of the *vasa* 3′ Untranslated Region

Li Zhou[1,2,3], Xueying Wang[1,2], Shuran Du[1,2], Yanfeng Wang[1,2], Haixia Zhao[1,2,3], Tengfei Du[1,2,3], Jiachen Yu[1,2,3], Lele Wu[1,2,3], Zongcheng Song[4], Qinghua Liu[1,2] and Jun Li[1,2]**

[1] The Key Laboratory of Experimental Marine Biology, Center for Ocean Mega-Science, Institute of Oceanology, Chinese Academy of Sciences, Qingdao, China, [2] Laboratory for Marine Biology and Biotechnology, Qingdao National Laboratory for Marine Science and Technology, Qingdao, China, [3] University of Chinese Academy of Sciences, Beijing, China, [4] Weihai Shenghang Aquatic Product Science and Technology Co., Ltd., Weihai, China

OPEN ACCESS

Edited by:
Miguel Angel Brieño-Enriquez, Magee-Womens Research Institute, United States

Reviewed by:
Mingyou Li, Shanghai Ocean University, China
Jelena Lujic, Cornell University, United States

***Correspondence:**
Qinghua Liu
qinghualiu@qdio.ac.cn
Jun Li
junli@qdio.ac.cn

Specialty section:
This article was submitted to Cellular Biochemistry, a section of the journal Frontiers in Cell and Developmental Biology

Received: *24 June 2020*
Accepted: *18 September 2020*
Published: *28 October 2020*

Citation:
Zhou L, Wang X, Du S, Wang Y, Zhao H, Du T, Yu J, Wu L, Song Z, Liu Q and Li J (2020) Germline Specific Expression of a vasa Homologue Gene in the Viviparous Fish Black Rockfish (Sebastes schlegelii) and Functional Analysis of the vasa 3′ Untranslated Region. Front. Cell Dev. Biol. 8:575788. doi: 10.3389/fcell.2020.575788

Germ cells play a key role in gonad development. As precursors, primordial germ cells (PGCs) are particularly important for germline formation. However, the origination and migration patterns of PGCs are poorly studied in marine fish, especially for viviparous economic species. The *vasa* gene has been widely used as a germ cell marker to identify a germline because *vasa* RNA is a component of germ plasm. In this study, we described the expression pattern of black rockfish (*Sebastes schlegelii*) *vasa* (*Ssvas*) in gonadal formation and development by *in situ* hybridization. The results showed that *Ssvas* failed in localization at the cleavage furrows until the late gastrula stage, when PGCs appeared and migrated to the genital ridge and formed elongated gonadal primordia at 10 days after birth. This study firstly revealed the PGCs origination and migration characteristics in viviparous marine fish. Furthermore, we microinjected chimeric mRNA containing EGFP and the 3′untranslated region (3′UTR) of *Ssvas* into zebrafish (*Danio rerio*) and marine medaka (*Oryzias melastigma*) fertilized eggs for tracing PGCs. We found that, although *Sebastes schlegelii* lacked early localization, similar to red seabream (*Pagrus major*) and marine medaka, only the 3′UTR of *Ssvas vasa* 3′UTR of black rockfish was able to label both zebrafish and marine medaka PGCs. In comparison with other three Euteleostei species, besides some basal motifs, black rockfish had three specific motifs of M10, M12, and M19 just presented in zebrafish, which might play an important role in labeling zebrafish PGCs. These results will promote germ cell manipulation technology development and facilitate artificial reproduction regulation in aquaculture.

Keywords: *vasa*, *Sebastes schlegelii*, gonad, germ cell, development, 3′UTR, localization

INTRODUCTION

As highly specialized cells, germ cells play a key role in germline development (Xu et al., 2010). In fish, the germ cells undergo a series of basic biological processes, including formation, migration, proliferation, and differentiation, and eventually develop into mature gametes (Braat et al., 1999; Nishimura and Tanaka, 2014). Healthy gonad development and gametogenesis in fish are important for aquaculture. Therefore, investigating the whole development process of germ cells facilitates the reproduction regulation in aquaculture, such as sex control, gonad maturation induction, and artificial insemination (Piferrer, 2001). At the same time, it promotes germ cell manipulations, in which the time of gonad formation can provide a reference for germ cell transplantation (Takeuchi et al., 2004; Okutsu et al., 2006).

Primordial germ cells (PGCs), the precursors of germ cells, are set aside from somatic cells early in embryogenesis (Goto-Kazeto et al., 2010). PGCs arrive in the genital ridge through a long-range cell migration, and they are covered by somatic cells to form elongated gonadal primordia. In recent years, many maternal-effect genes such as *vasa*, *dnd*, *dazl*, and *nanos* localized in germplasm have been identified and extensively used as germ cell markers to study origination and migration of PGCs in fish (Xu et al., 2007; Lindeman and Pelegri, 2010; Yoshizaki et al., 2010; Hong et al., 2016). This reveals that the PGC migration routes and gonadal formation times vary from fish species. So far, there are two classical origination and migration patterns of PGCs. One representative is the zebrafish (*Danio rerio*), in which germ plasm granules in fertilized eggs are concentrated to the distal parts of the cleavage furrows, resulting in four aggregates during the first two cleavage divisions, and these cluster cells will differentiate into PGCs at the late blastula (Yoon et al., 1997). The other representative is the medaka (*Oryzias latipes*), whose granules are distributed uniformly throughout each blastomere until the onset of epiboly, and the PGCs start to appear at late gastrulation, lacking early localization (Shinomiya et al., 2000). Once PGCs form, they migrate and concentrate on the dorsal peritoneum, under the notochord at the hatching stage. The PGCs undergo a post-hatching migration in most oviparous fish. According to histological studies, PGCs migrate from the upper part of the body cavity to the rear and settle on the dorsal side of the gut, a location that future gonad forms. The settlement time of PGCs is species specific. In ukigori (*Gymnogobius urotaenia*), PGCs reached the genital ridge at 6–8 days post-hatching (dph) (Saito et al., 2004), while in turbot (*Schophthalmus maximus*), Japanese flounder (*Paralichthys olivaceus*), and yellowtail kingfish (*Seriola lalandi*), PGCs arrived in the gonad formation location at 15–20 dph (Fernandez et al., 2015; Zhao et al., 2017; Yang et al., 2018). However, the time of primordial gonadal formation of viviparous fish has not been reported so far. After migration, the germ cells begin mitosis and meiosis, and the formed gonads differentiate into presumptive ovary or testis (Gao et al., 2009). Under the control of the endocrine regulation and the external environment, gonads gradually develop to maturity and produce sexual gametes.

The *vasa* is the first germ gene identified in fish, which encodes an ATP-dependent RNA helicase of the DEAD (Asp–Glu–Ala–Asp)-box family (Knaut et al., 2000). It has been proved to be able to fulfill potential roles in germ cell origination and migration and maintain throughout the development of germ cells in fish (Kobayashi et al., 2000; Lin et al., 2012b; Ye et al., 2016). Moreover, the function of *vasa* varied considerably in diverse species. In medaka, *vasa* knockdown led to defects in PGCs migration but not proliferation, motility, identity, and survival (Li et al., 2009), while in zebrafish, disruption of *vasa* resulted in sterility in males (Hartung et al., 2014). As a universal germ cell marker, the *vasa* gene was used to identify the fish germline in economic species such as rainbow trout (*Oncorhynchus mykiss*) (Yoshizaki et al., 2010), Dabry's sturgeon (*Acipenser dabryanus*) (Ye et al., 2016), and Atlantic cod (*Gadus morhua*) (Presslauer et al., 2012). The *vasa* mRNA has been shown to degrade rapidly in somatic cells but remain stable in PGCs, which are all mediated by the 3′untranslated region (3′UTR) (Knaut et al., 2002; Wolke et al., 2002; Mishima et al., 2006). For the inherent nature of *vasa* 3′UTR, the chimeric mRNA fused fluorescent protein-coding region to 3′UTR could be microinjected into fertilized eggs to trace PGCs (Kataoka et al., 2006; Ye et al., 2016). This is a highly efficient, fast, and specific non-transgenic method for labeling PGCs *in vivo* and has been used in a variety of fish species (Yoshizaki et al., 2005; Lin et al.,

TABLE 1 | Primers used in the study.

Primer	Sequence	Purpose
BrvasF	CTGATTTCATTGCCACTT	ISH probe for detecting *Ssvas* mRNA
BrvasR	ATTGGTGACCTTTATGGA	
BrutrF	AGGAAATATTAGAGCACA	Obtaining black rockfish and zebrafish *vasa* 3′UTRs by RT-PCR
BrutrR	GCACAAATACTTATTTAT	
ZbutrF	CTGGCCTCACACCTGTTA	
ZbutrR	CACCAGTATCCGTCTTTATT	
VeBrF	GAGCTGTACAAGTAAAGGAA ATATTAGAGCACA	Obtaining *vasa* 3′UTR fragments for Gibson assembly
VeBrR	GAATTCACTAGTGATGCACAA ATACTTATTTAT	
VeZbF	GAGCTGTACAAGTAACTGGC CTCACACCTGTTA	
VeZbR	ATTTCTGCCTATGACCACTA GCTTAAGGGCGCC	
BrvecF	ATCACTAGTGAATTCGCG	Obtaining vector fragments for Gibson assembly
BrvecR	TTACTTGTACAGCTCGTC	
ZbvecF	ATCGAATTCCCGCGGCCG	
ZbvecR	CTGCTCGACATGTTCATT	
T7	TAATACGACTCACTATAGGG	Preparation synthesis templates for chimeric mRNAs
BrutrR	GCACAAATACTTATTTAT	
SP6	ATTTAGGTGACACTATAG	
ZbutrR	CACCAGTATCCGTCTTTATT	

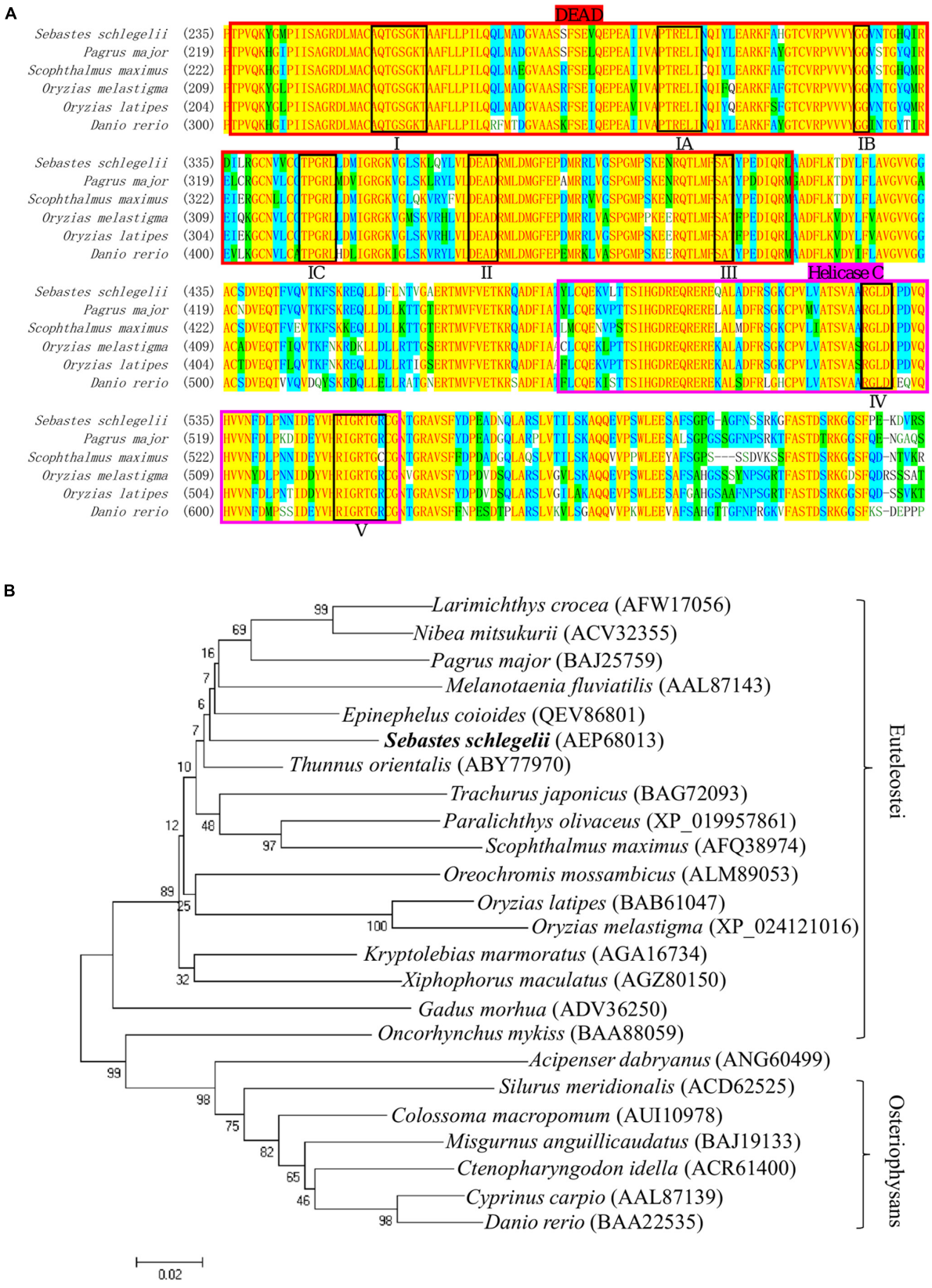

FIGURE 1 | Continued

FIGURE 1 | Multiple alignment and phylogenetic analysis of the Vasa between *Sebastes schlegelii* and other species. **(A)** Multiple alignment was carried out using the AlignX program. The eight conserved motifs are shown in block, including I domain (AQTGSGKT), IA domain (PTREL), IB domain (GG), IC domain (TPGRL), II domain (DEAD), III domain (SAT), IV domain (ARGLD), and V domain (GRTGR). The DEAD-box sequence was indicated in bright red, while Helicase C was in rose red. **(B)** The phylogenetic tree of Vasa was established by MEGA4 with neighbor-joining method. The numbers adjacent to nodes indicated bootstrap percentage value for 1000 replicates.

2012a; Zhou et al., 2019). Moreover, the chimeric mRNA from one species not only labels itself but also can successfully trace other species, even the genetic highly divergent species. For example, the chimeric mRNA (GFP-*Pmvas* 3′UTR) that contained GFP and the 3′UTR of red seabream (*Pagrus major*) could be used to trace migration of PGCs in medaka (Lin et al., 2012a). However, chimeric mRNA from one species cannot label PGCs from all species, just as the red seabream *vasa* 3′UTR failed to trace turbot PGCs, although they could label the medaka (Lin et al., 2012a; Zhou et al., 2019). This indicated that the conserved localization mechanism of *vasa* 3′UTR may relate to specific functional elements (Knaut et al., 2002; Kataoka et al., 2006; Zhou et al., 2019). For labeling ability of *vasa* 3′UTR, there may be rules to follow. However, the relevant researches in other species are limited, so it is still unclear.

Black rockfish (*Sebastes schlegelii*) is one of the most important economic rockfishes in the western North Pacific and inhabits the coastal waters of China, Japan, and Korea (Kai and Soes, 2009). As a viviparous fish, the embryos develop in female cavity for 1–2 months until birth (Liu et al., 2019). In previous research, *Sebastes schlegelii vasa* (*Ssvas*) was only detected and highly expressed in gonad during the reproductive cycle (Mu et al., 2013). There is still a lack of detailed research on germ cells during gonadal formation and development in this viviparous fish species. In this study, we aimed to describe the origination and migration pattern of *Sebastes schlegelii* PGCs in gonad formation process by *vasa* and explored the relationship between *vasa* RNA early localization and species evolution. Furthermore, we also identified the germ cells development and maturation process with *vasa*, verified the labeling ability of *Ssvas* 3′UTR in zebrafish and marine medaka (*Oryzias melastigma*), and analyzed the conservative motifs of *vasa* 3′UTR in comparison with several other species.

MATERIALS AND METHODS

Fish and Samples

Matured black rockfish used in this study were obtained from Penglai, China. Ten sexually mature individuals in November were anesthetized with a 0.05% solution of 3-aminobenzoic acid ethyl ester methanesulfonate-222 (MS-222) (Sigma–Aldrich, United States). The tissues of ovary and testis were rapidly removed. Some samples were immediately immersed in liquid nitrogen for cDNA synthesis, while others were fixed overnight with 4% paraformaldehyde in phosphate-buffered saline (PBS) and then preserved in 70% ethanol for section *in situ* hybridization (SISH). Twenty sexually mature females in April to May were also anesthetized with MS-222. Moreover, the embryos of different development stages in the ovary were removed and fixed by 4% paraformaldehyde in PBS overnight and stored at −20°C in PBS with 50% formamide for whole mount *in situ* hybridization (WISH).

One-year-old and hatching fry of black rockfish were reared at Shenghang Sci-Tech Co., Ltd. (Shandong Province, China). The testes and ovaries of six 1-year-old individuals were removed after anesthesia and fixed in 4% paraformaldehyde as above. Starting from hatching, about 20 hatched fry were fixed with 4% paraformaldehyde every day for 1 month. After 1 day of fixation, the gonadal tissue samples and fry were stored at 70% ethanol for SISH.

All experiments were performed in accordance with the relevant national and international guidelines and approved by the Institutional Animal Care and Use Committee, Institute of Oceanology, Chinese Academy of Sciences.

Sequence Analyses

A homology search of the amino acid sequence of *Ssvas* was carried out using the National Center for Biotechnology Information website[1]. The amino acid sequences were aligned using the AlignX program in Vector NTI, Suite 8 software package (Life Technologies). Phylogenetic analysis was conducted with Mega4 software using the neighbor-joining method, and the bootstrap replicates were set to 1,000 (Saitou and Nei, 1987). Some potential regulatory motifs in the 3′UTRs of teleost *vasa* were searched by MEME motif analysis (Bailey and Elkan, 1994).

In situ Hybridization

Total RNA was extracted from the ovaries of *Sebastes schlegelii* using RNA fast 200 (Fastagen, China). In accordance with the manufacturer's instructions, the first-strand cDNA was synthesized by the PrimeScript^{TM} RT reagent kit with gDNA Eraser (Takara, Japan). Then, the cDNA was stored at −20°C as a probe synthesis template.

vasa mRNA distribution was detected in embryo and tissue by *in situ* hybridization (ISH), and the protocols followed the methods described previously (Lin et al., 2012b), with a few modifications as detailed below. Briefly, the 857 bp *Ssvas* fragment (nucleotides 1,540–2,396 bp; accession no. JN634874) was inserted into pGEM-T Easy vector (Promega, Madison, WI). The primers are shown in **Table 1**. Sense and antisense RNA probes were synthesized by *in vitro* transcription from a vector under the drive of the T7 or SP6 promoter with the DIG RNA Labeling Kit (Roche, Mannheim, Germany). The RNA probes were treated with RNase-free water and purified with SigmaSpin^{TM} Sequencing

[1]http://www.ncbi.nlm.nih.gov/

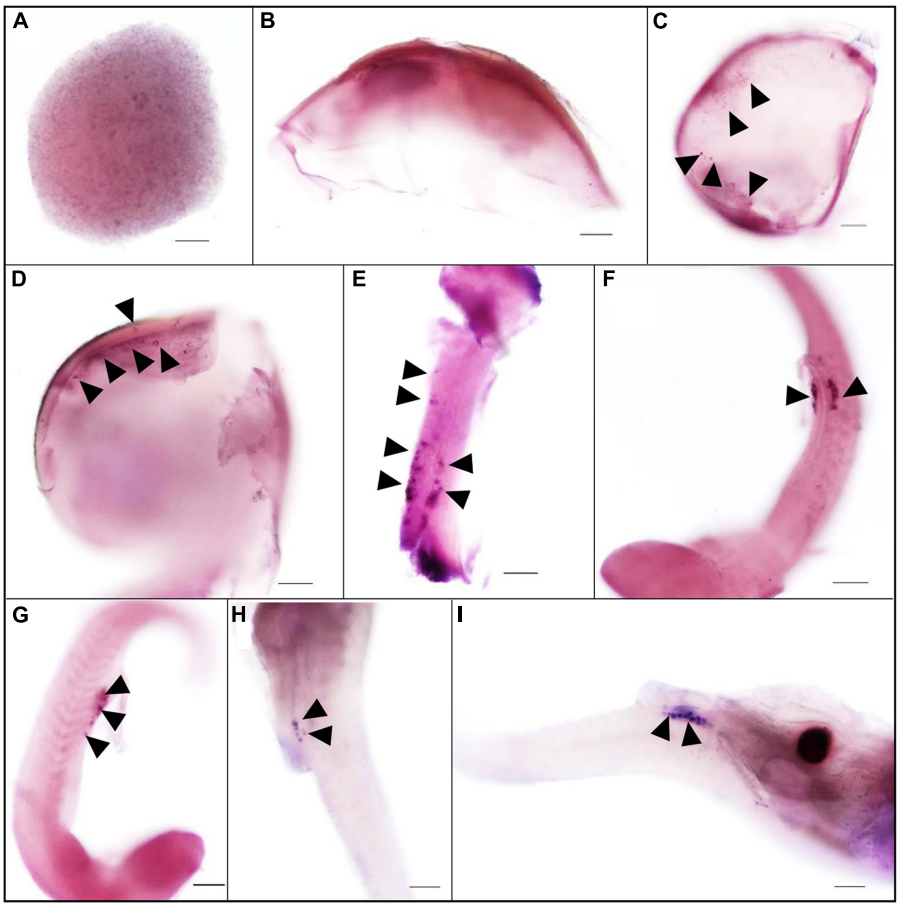

FIGURE 2 | The expression pattern of *Ssvas* during embryogenesis was analyzed with WISH. All blastomeres were strongly stained at the blastula stage **(A)**. The signal in the cell became non-uniform at the 30%-epiboly stage **(B)**. *Ssvas*-positive cells appeared at the 70% epiboly stage **(C)**. PGCs randomly aligned along the anterior of the body axes at the 90% epiboly stage–early neurula stage **(D)** and lined along the anterior–posterior axis on both sides of the embryonic body at the somite stage **(E)**. PGCs formed two clusters and aligned bilaterally on the ventral side at heart beating stage **(F,G)** and localized at the dorsal sides of the gut, ventral side of notochord at hatching Sage **(H,I)**. Black arrowheads indicated *Ssvas*-positive cells (PGCs) (stained with dark purple or blue). Scale bar, 100 μm.

Reaction Clean-Up (Sigma–Aldrich). ISH was conducted by chemical stain with BCIP/NBT substrates on whole mount and sections samples.

For WISH, embryos were dechorionated, and dehydrated and rehydrated through a graded series of methanol after being taken out from 50% formamide in PBS. The embryos were digested with proteinase K (10 μg/ml) (5–10 min for embryo < 24 h; 15–30 min for embryo > 24 h) and refixed before hybridization. For SISH, samples were dehydrated through a graded series of ethanol, embedded in paraffin wax, and cut into 5 μm-thick sections for testis and 7 μm for ovary. The sections were de-waxed using two washes of xylene and rehydrated through an ethanol gradient. After being washed with PBST, they were refixed using 4% paraformaldehyde in PBS and digested with proteinase K (10 μg/ml) for 10 min. The WISH and SISH were performed with the probes at 65°C for 14 h. Stained samples were observed and photographed through a Nikon ENi microscope, using a Nikon DS-Ri2 imaging system.

Prepare of EGFP-*Ssvasa* 3′UTR and mCherry-*Drvasa* 3′UTR mRNAs

Chimeric mRNAs which fused EGFP or mCherry to the 3′UTR of *Sebastes schlegelii* or *Danio rerio vasa* gene were synthesized by *in vitro* transcription, and the protocols followed the methods described previously (Zhou et al., 2019). The main process is as follows: firstly, template plasmids were constructed using Gibson assembly, and the 3′UTRs of EGFP-*Pmvasa* 3′UTR and mCherry-*Omvasa* 3′UTR plasmids in our lab were replaced by *vasa* 3′UTRs of black rockfish and zebrafish, respectively. Then, according to the plasmids, the transcription templates were synthesized by PCR. After purification, capped chimeric mRNAs were synthesized using mMESSAGE mMACHINE SP6/T7 kit (Ambion, United States). The primers for preparing mRNAs are also shown in **Table 1**. In the previous study, the EGFP-*Pmvasa* 3′UTR and mCherry-*Omvasa* 3′UTR mRNAs that contained red seabream and marine medaka *vasa* 3′UTRs have been synthesized in our lab (Zhou et al., 2019).

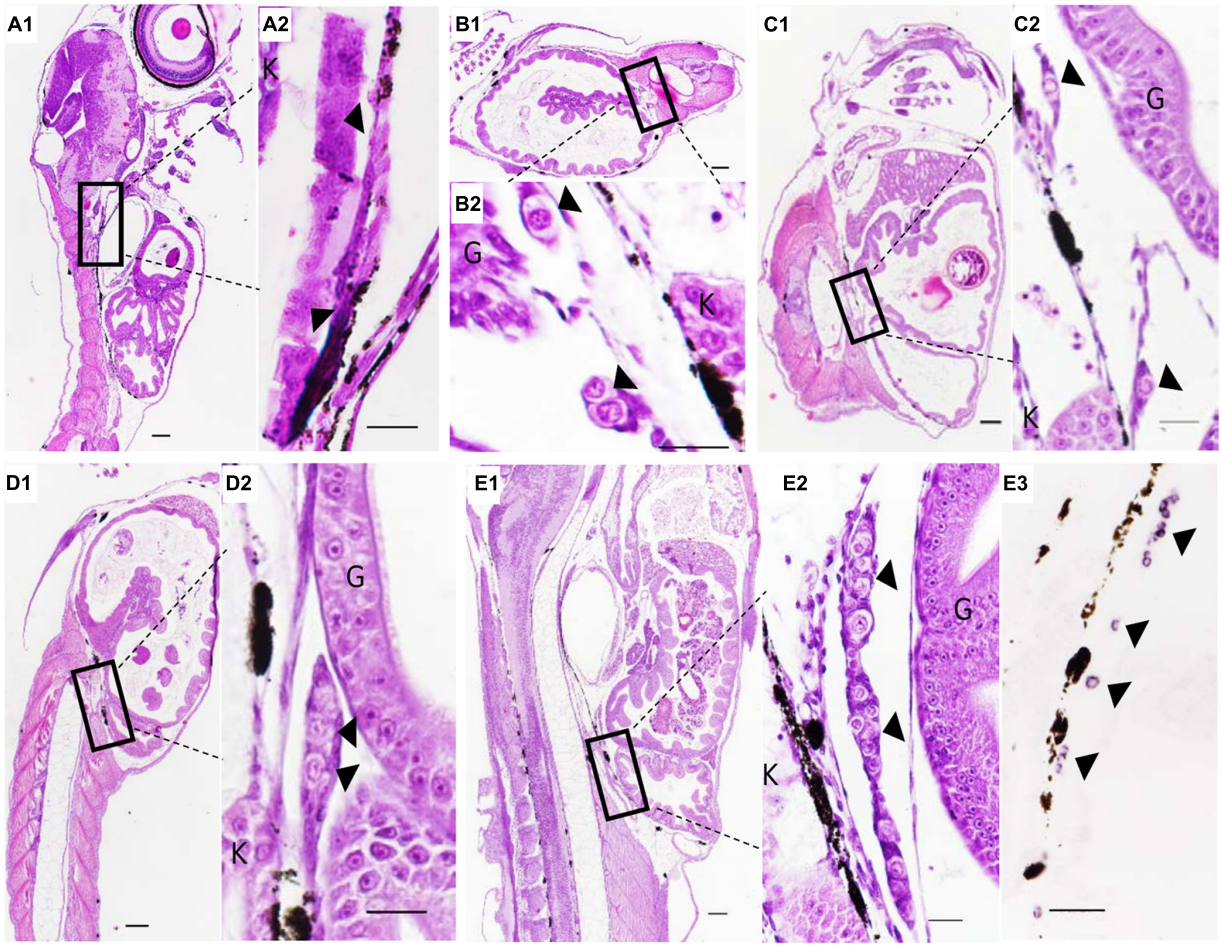

FIGURE 3 | The PGCs migration after birth of *Sebastes schlegelii*. **(A1–E2)** were tissue sections with H&E stain. **(E3)** was SISH corresponding to **(E2)**. PGCs were located in the upper part of the body cavity under the notochord at 2 dab, sagittal sections **(A1,A2)** and covered by a single-layer somatic cell at 8 dab, coronal sections **(B1,B2)**. PGCs migrated to the genital ridge at 9 dab, sagittal sections **(C1,C2)** and formed elongated gonadal primordia at 10 dab, sagittal sections **(D1,D2)**. Distinct primordial gonads were discovered in the posterior part of the body cavity **(E1,E2)**, and the PGCs were strongly stained with the *Ssvas* antisense probe by SISH at 15 dab, sagittal sections **(E3)**. Black arrowheads indicated PGCs; G and K indicated gut and kidney, respectively. Scale bar, 100 μm **(A1,B1,C1,D1,E1)**; 50 μm **(A2,B2,C2,D2,E2,E3)**.

Microinjection and Observation

Zebrafish and marine medaka were maintained at 28 ± 0.5°C (16 h light/8 h dark) at the fish facility of the Institute of Oceanology, Chinese Academy of Sciences. The marine medaka is a truly euryhaline species closely related to the medaka. Embryos were collected within 30 min after fertilization. To verify the labeling ability of *Ssvas* 3′UTR in zebrafish and marine medaka, the EGFP-*Ssvasa* 3′UTR and mCherry-*Drvasa* 3′UTR mRNAs were co-injected into zebrafish embryos at the 1–2 cell stage, and the EGFP-*Ssvasa* 3′UTR and mCherry-*Omvasa* 3′UTR mRNAs were co-injected into marine medaka embryos in the same manner. Similarly, to compare the ability of *vasa* 3′UTRs among *Sebastes schlegelii* and other teleost in marking zebrafish PGCs, the EGFP-*Pmvasa* 3′UTR and mCherry-*Omvasa* 3′UTR mRNAs were also microinjected into zebrafish embryos as above. Microinjected eggs were cultured in a biochemical incubator with 28°C for EGFP or mCherry observation and photography under fluorescent microscope (Nikon ENi, Japan) at different stages. The microscope equipped with a FITC filter or a TRITC filter and a DS-Ri2 imaging system.

RESULTS

Structure and Phylogenetic Analysis of *Sebastes schlegelii* Vasa Protein

The full-length cDNA of *Ssvas* had been isolated in the previous research. In this study, multiple alignment of different fish Vasa proteins showed that there were eight consensus motifs (I, IA, IB, IC, II, III, IV, V) in the DEAD-box protein family (**Figure 1A**). This also revealed that the DEAD domain was composed of 180 amino acids and the superfamily Helicase C-terminal (Helicase C) of 77 amino acids, which had high similarity

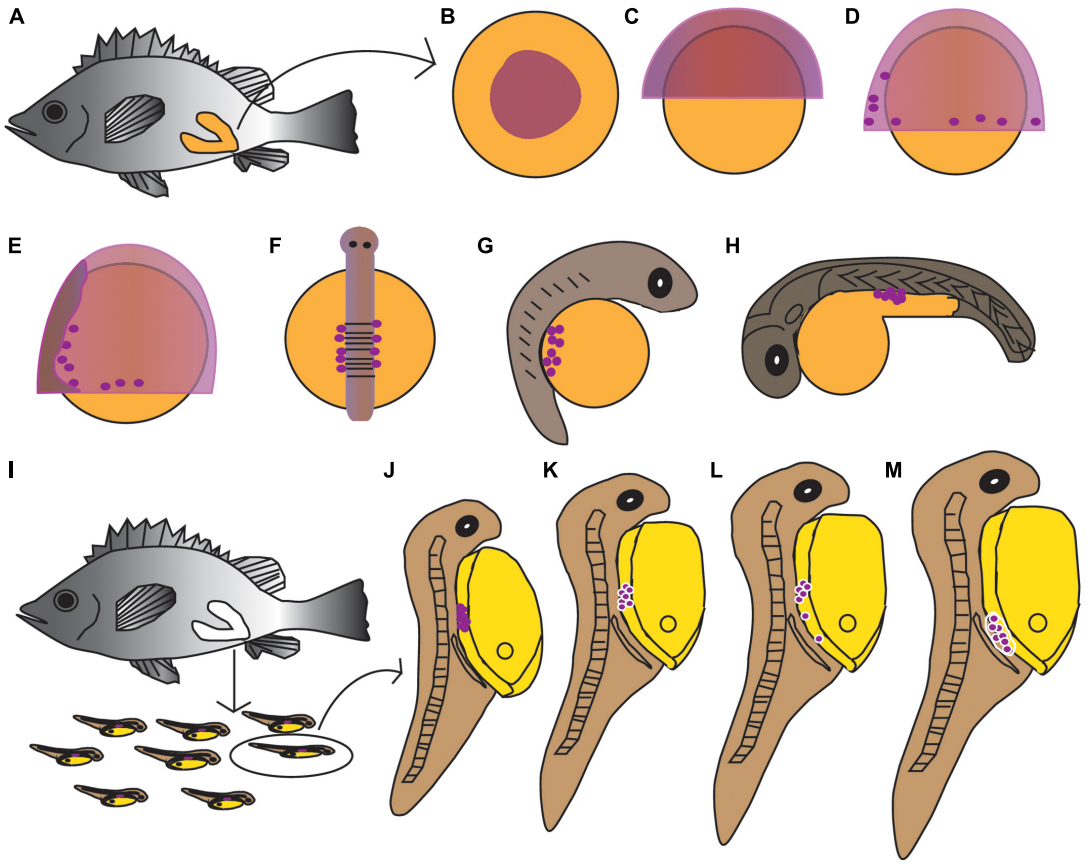

FIGURE 4 | Schematic illustration of the germline formation process in *Sebastes schlegelii*. Dark purple spots indicated PGCs signals. **(A–H)** The migration of PGCs from embryos in female fish after fertilization. **(A)** The overall appearance of the female after fertilization; **(B)** blastula stage; **(C)** 30% epiboly stage; **(D)** 70% epiboly stage; **(E)** 90% epiboly stage–early neurula stage; **(F)** somite stage; **(G)** heart beating stage; **(H)** hatching stage. **(I–M)** The migration of PGCs from larvae after birth. **(I)** The larvae were born from mature females; **(J)** 2 dab; **(K)** 8 dab; **(L)** 9 dab; and **(M)** 10–15 dab.

in teleost (**Figure 1A**). The *Sebastes schlegelii* presented Vasa typical conserved domains (**Figure 1A**). Phylogenetic analysis of Vasa protein exhibited that *Sebastes schlegelii* belonged to Euteleostei species (**Figure 1B**). In phylogeny, compared to Osteriophysans species like *Danio rerio*, *Sebastes schlegelii* was closer to some Euteleostei fish, such as *Thunnus orientalis*, *Scophthalmus maximus*, *Pagrus major*, *Oryzias latipes*, and *Oncorhynchus mykiss* (**Figure 1B**).

Spatial Localization of *Ssvas* RNA During Embryogenesis

The expression pattern of *vasa* during embryogenesis was analyzed by WISH. At the blastula stage, all blastomeres were strongly stained, without the four cell clusters like zebrafish (**Figure 2A**). In *Sebastes schlegelii*, the *Ssvas* transcripts failed in early localization during the cleavage stage. As the embryo developed, the distribution of the signal in the cell became non-uniform, and the areas of embryonic shield seemed to be darker than the rest at the 30% epiboly stage (**Figure 2B**). Until the 70% epiboly stage, some *Ssvas*-positive cells firstly appeared at the germ ring of the epiboly bottom (**Figure 2C**). According to morphology, these positive cells were early PGCs. At the 90% epiboly stage to early neurula stage, the PGCs gathered on the dorsal side of the narrow embryonic body and randomly aligned along the anterior of the body axes (**Figure 2D**). Then, they moved posterior-ward and lined along the anterior–posterior axis on both sides of the embryonic body at somite stage (**Figure 2E**). These cells formed two clusters and aligned bilaterally on the ventral side at heart beating stage (**Figures 2F,G**). Finally, the PGCs localized at the dorsal sides of the gut, ventral side of notochord at the hatching stage (**Figures 2H,I**).

The PGC Migration After Birth of *Sebastes schlegelii*

The PGCs underwent a post-birth migration in *Sebastes schlegelii*. PGCs are characterized by large cell size and obvious nuclei, which are easily distinguished with somatic cells on tissue sections. At 2 days after birth (dab), PGCs localized in the upper part of the body cavity under the notochord, around the dorsal peritoneum (**Figures 3A1,A2**). A part of PGCs were covered by a single layer somatic cell at 8 dab (**Figures 3B1,B2**). PGCs surrounded by single somatic cells were found to migrate

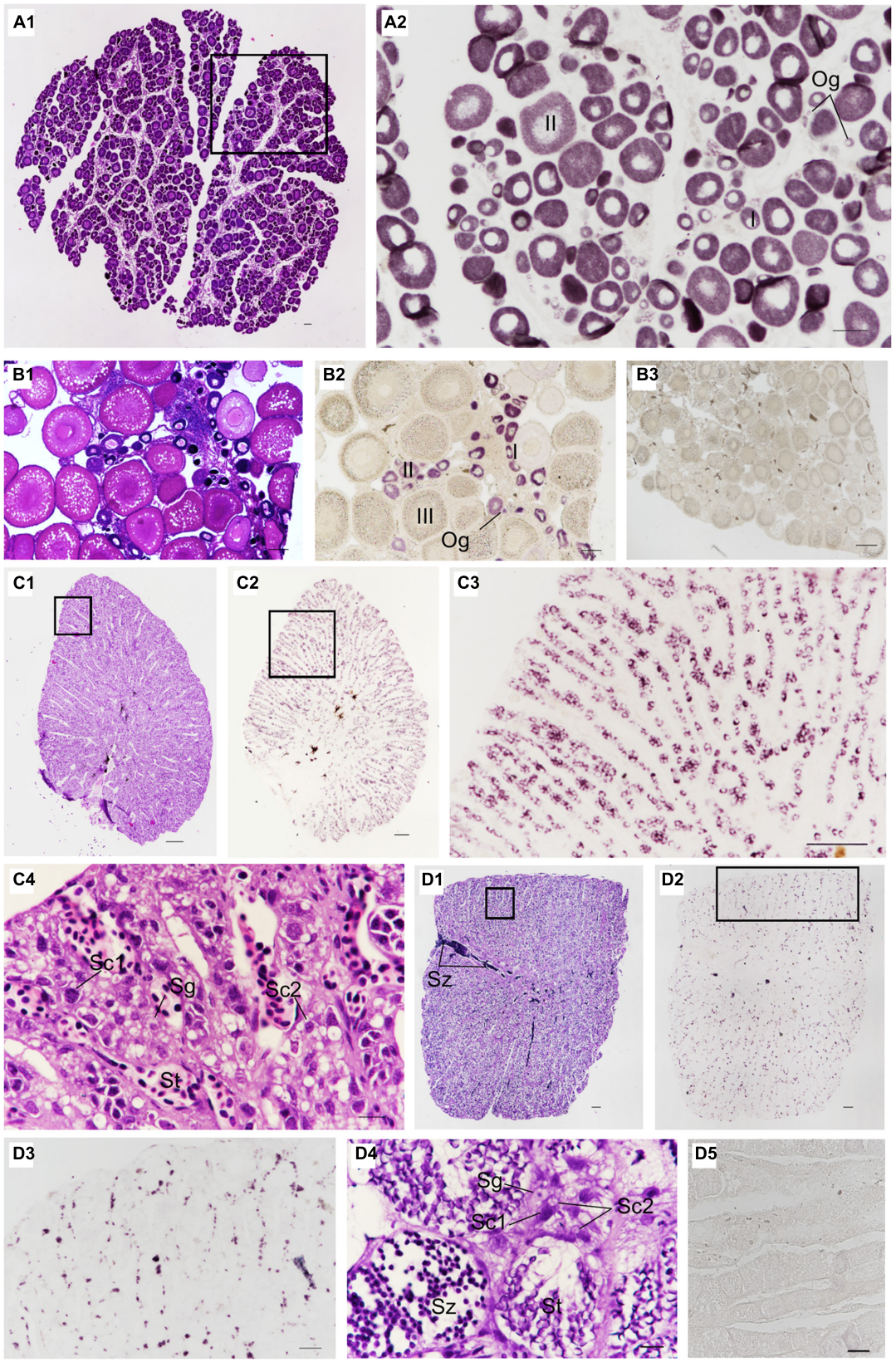

FIGURE 5 | Continued

FIGURE 5 | Distribution of *Ssvas* transcripts in gonad germ cells by SISH. Paraffin section and H&E of ovaries in 1-year-old **(A1)** and sexually mature black rockfish **(B1)**, respectively. **(A2)** Adjacent tissue section of the black box in **(A1)** was hybridized with the *Ssvas* antisense probe. **(B2)** Adjacent tissue section of **(B1)** was hybridized with the *Ssvas* antisense probe. **(B3)** The paraffin section of the ovary was hybridized with the *Ssvas* sense probe. The paraffin section and H&E of testis in 1-year-old **(C1)** and sexually mature black rockfish **(D1)**, respectively. **(C2,D2)** Adjacent tissue sections of **(C1,D1)** were hybridized with the *Ssvas* antisense probe, respectively. **(C3,D3)** The high-magnification image of the black boxes in **(C2,D2)**, respectively. **(C4–D4)** The high-magnification image of the black boxes in **(C1,D1)**, respectively. **(D5)** The paraffin section of testis was hybridized with the *Ssvas* sense probe. Og, oogonia; I, early previtellogenic phase; II, late previtellogenic phase; III, early vitellogenic phase; Sg, spermatogonia; Sc1, primary spermatocytes; Sc2, secondary spermatocytes; St, spermatids; Sz, spermatozoon. Scale bar, 100 μm **(A1–C4,D3–D5)**; 200 μm **(D1,D2)**.

to the genital ridge at 9 dab (**Figures 3C1,C2**). By 10 dab, three PGCs were completely surrounded by somatic cells and arranged in a row to form elongated gonadal primordia, which appeared under the ventral kidney and dorsal sides of the gut (**Figures 3D1,D2**). Until 15 dab, the distinct primordial gonads were discovered in the posterior part of the body cavity, and the PGCs in gonads were strongly stained with *Ssvas* antisense probe by SISH (**Figures 3E1–E3**). Through the identification of *Ssvas*, the germline formation process of *Sebastes schlegelii* was summarized, as shown in the schematic illustration (**Figure 4**).

Localization of *Ssvas* RNA in Gonads

The localization of *Ssvas* RNA was investigated in fish gonads by SISH. In accordance with adjacent histology, the stages of stained cells were identified. For 1-year-old black rockfish, in the ovary, there were mainly oogonia, early previtellogenic phase (I), and late previtellogenic phase (II) (**Figure 5A1**). *Ssvas*-specific expression was observed in all germ cells but not somatic cells (**Figure 5A2**). In oogonia, *Ssvas* mRNA was distributed evenly in the cytoplasm (**Figure 5A2**). In I–II oocytes, *Ssvas* transcripts were concentrated into several patches primarily in the perinuclear region (**Figure 5A2**). For sexually mature females, *Ssvas* transcripts were researched throughout oogenesis and showed a dynamic localization pattern in the ovary. A large number of early vitellogenesis phase (III) oocytes were present in the November individuals, but there was no *Ssvas* expression (**Figures 5B1,B2**). The tissue section hybridized with the sense probe was not stained, proving that this signal represents the expression of *Ssvas* (**Figure 5B3**).

Histological sections of the testis demonstrated that *Sebastes schlegelii* was lobular-type (**Figures 5C1**, D1). In the testis of 1-year-old black rockfish, there were spermatogonia, primary spermatocytes, secondary spermatocytes, and spermatids, without spermatozoon (**Figure 5C4**). For sexually mature males more than 3 years old, a lot of spermatozoon were found (**Figure 5D4**). The testis was composed of many testicular lobules, and the *Ssvas* signals were only present in spermatogonia and primary spermatocytes, which localized at the edge of the lobules and spread throughout the whole testis except the vas deferens (**Figures 5C2,D2**). The signals in matured testis were significantly weaker than 1-year-old testis because *Ssvas* transcripts were predominantly detected in early germ cells, such as spermatogonia and spermatocytes, and no signal was detected in spermatids and spermatozoon (**Figures 5C3,D3**). As control, the tissue section hybridized with the sense probe was not stained (**Figure 5D5**).

Visualization the PGCs of Zebrafish and Marine Medaka by *Sebastes schlegelii vasa* 3′UTR

In order to confirm that the labeling ability of *Sebastes schlegelii vasa* 3′UTR, EGFP-*Ssvasa* 3′UTR mRNA and mCherry-*Drvasa* 3′UTR mRNA were co-microinjected into zebrafish 1–2 cell stage fertilized eggs. After microinjection, mCherry and EGFP firstly expressed in the blastoderm at the 30–50% epiboly stage, and bright fluorescence accumulated in the area where the embryonic shield formed (**Figures 6A1–A3**). As embryogenesis proceeded, fluorescence concentrated on the embryonic body was more obvious, but PGCs were not distinguished from somatic cells until the early segmentation period. At the somite stage, as the fluorescence of somatic cells reduced gradually, some brighter cells moved and gathered on both sides of embryonic body (**Figures 6B1–B3**). The rounder and larger fluorescent cells were PGCs. PGCs migrated axial-ward and aggregated under the trunk at the heart beating stage (**Figures 6C1–C3**). Eventually, PGCs settled on the dorsal part of the gut at one day after hatching (**Figures 6D – D3**).

In the same way, the EGFP-*Ssvasa* 3′UTR and mCherry-*Omvasa* 3′UTR mRNAs were co-microinjected into marine medaka embryos. EGFP and mCherry firstly appeared at the 30% epiboly stage (**Figures 6E1–E3**). At the somite stage, some cells with strong fluorescence aligned on both sides of the trunk from the first somite to tail bud region (**Figures 6F1–F3**). These fluorescent cells were PGCs.

Oryzias melastigma and *Pagrus major vasa* 3′UTRs Labeling Zebrafish PGCs

To compare the labeling ability of *vasa* 3′UTRs among *Sebastes schlegelii* and other teleost in marking zebrafish PGCs, the chimeric mRNAs of EGFP-*Pmvasa* 3′UTR and mCherry-*Omvasa* 3′UTR were also microinjected into zebrafish fertilized eggs. The mCherry and EGFP fluorescence firstly appeared in blastoderm at the early gastrula stage after microinjection (**Figures 7A1–A3**). A high level of fluorescence expression was found in the zebrafish embryonic body at the early somite stage (**Figures 7B1–B3**), but PGCs were not distinguished from somatic cells during the whole embryonic development (**Figures 7C1–D3**). In order to avoid misjudgment of results, a large number of embryos at heart beating stage were observed (**Figures 7C2′**,C3′). Although some fluorescent aggregates were found in the extension of the yolk sac at heart beating stage and 1 day after hatching, PGCs could not be distinguished (**Figures 7C1–C3, D1–D3**).

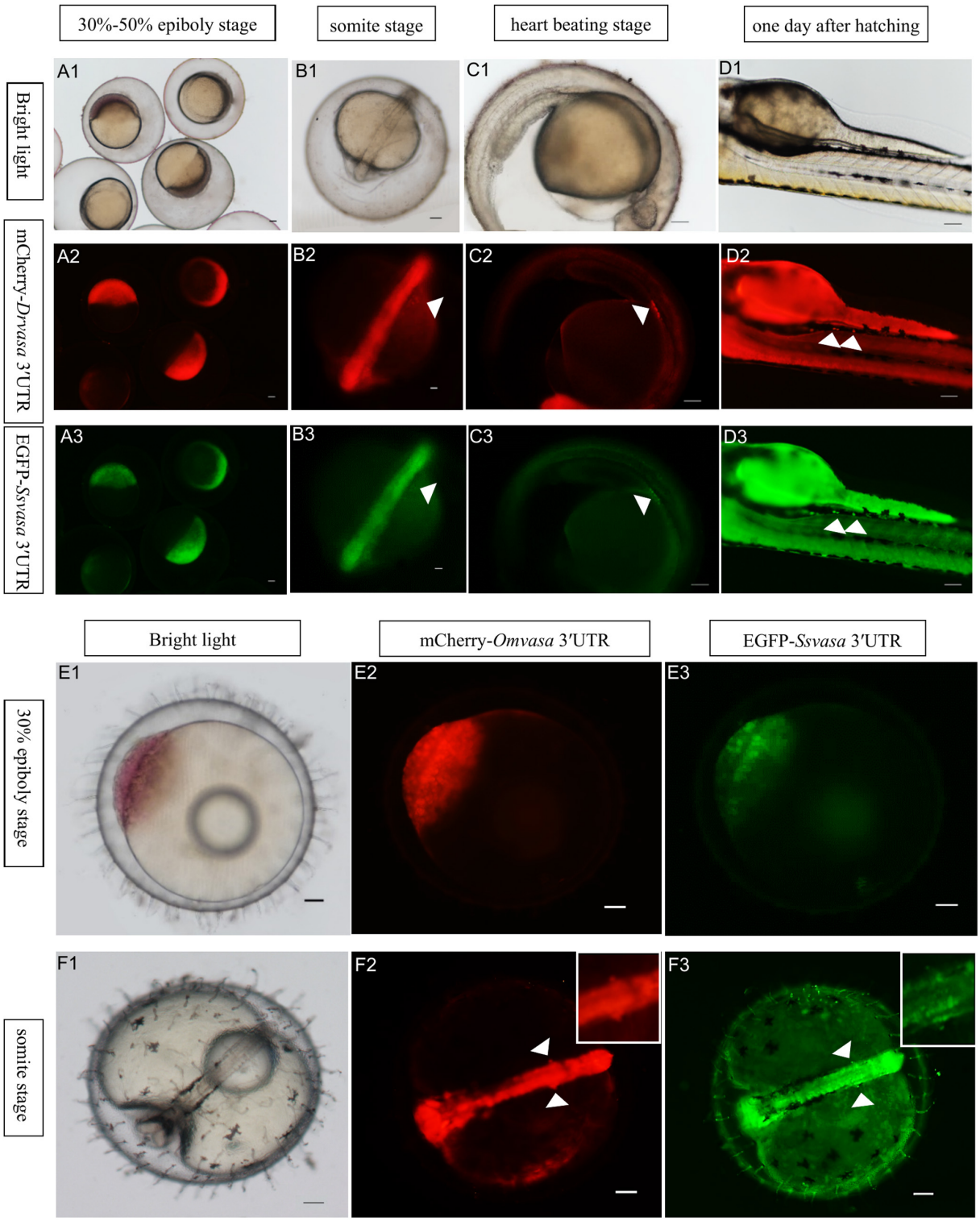

FIGURE 6 | Visualization of the PGCs of zebrafish and marine medaka by *Sebastes schlegelii vasa* 3′UTR. **(A1–D3)** Visualization of zebrafish PGCs by co-microinjection EGFP-*Ssvas* 3′UTR and mCherry-*Drvasa* 3′UTR mRNAs. Fluorescence first expressed in the blastoderm at the 30–50% epiboly stage **(A1–A3)**; PGCs differentiated from somatic cells and gathered on both sides of the embryonic body at the somite stage **(B1–B3)**; PGCs aggregated under the trunk at the heart beating stage **(C1–C3)** and settled on the dorsal part of the gut at 1 day after hatching **(D1–D3)**. **(E1–F3)** Visualization marine medaka PGCs by co-microinjection of EGFP-*Ssvas* 3′UTR and mCherry-*Omvasa* 3′UTR mRNAs. Fluorescence appeared at the 30% epiboly stage **(E1–E3)** and PGCs aligned on both sides of the trunk at the somite stage **(F1–F3)**. The insets in F2 and F3 were magnification of signal areas. PGCs were indicated by white arrows. Scale bars, 100 μm.

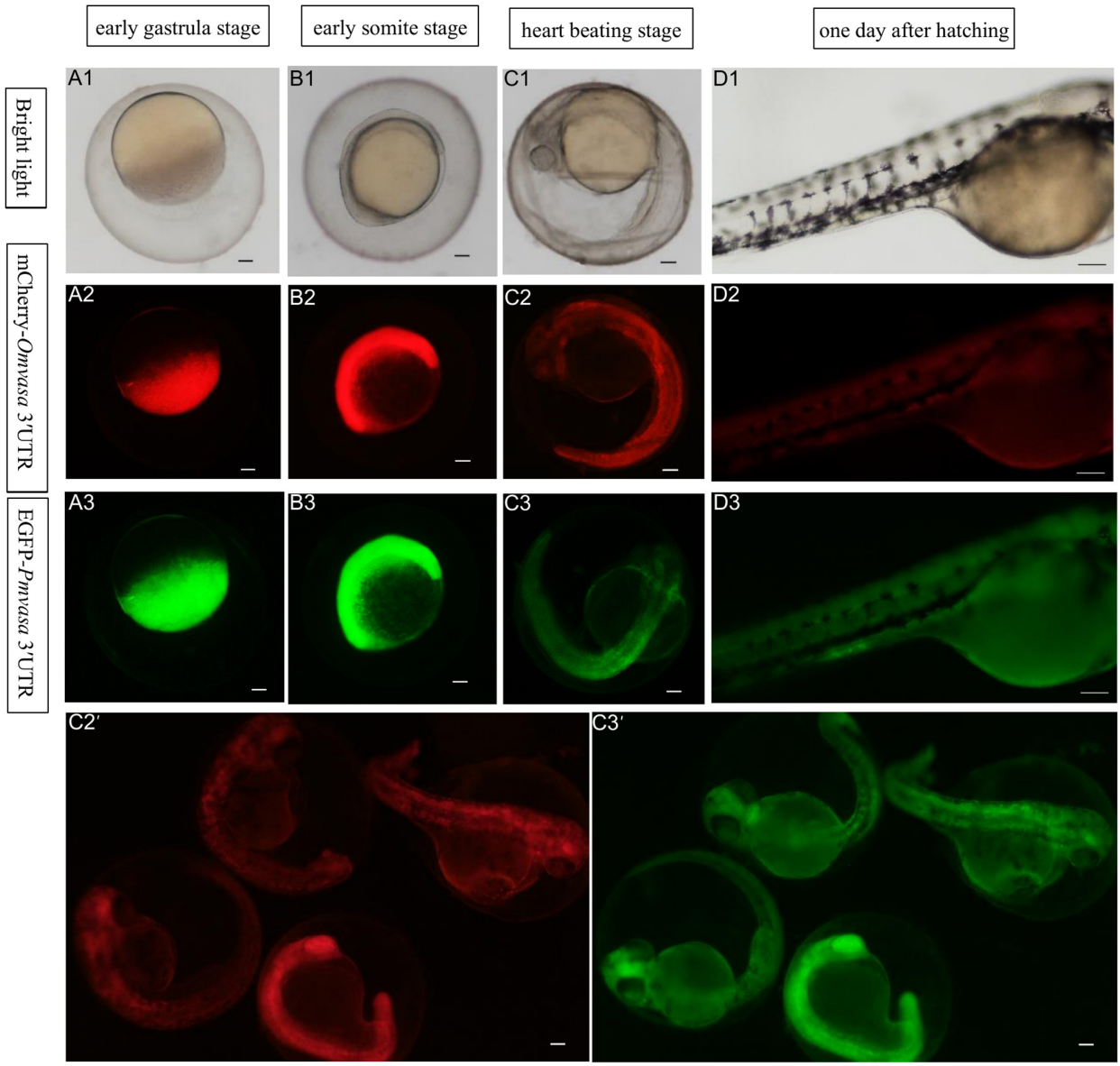

FIGURE 7 | The ability of *Oryzias melastigma* and *Pagrus major vasa* 3′UTRs in labeling zebrafish PGCs. The EGFP-*Pmvasa* 3′UTR and mCherry-*Omvasa* 3′UTR mRNAs were co-microinjection into zebrafish embryos. Fluorescence appeared at the early gastrula stage **(A1–A3)** and highly expressed in the embryonic body at the early somite stage **(B1–B3)**; PGCs did not differentiate from somatic cells at the heart beating stage **(C1–C3)** and 1 day after hatching **(D1–D3)**. View of the embryos of the heart beating stage in a wide range **(C2′,C3′)**. Scale bars, 100 μm.

Phylogenetic Analysis and MEME Motifs Analysis in Teleost *vasa* 3′UTRs

The teleost of *Sebastes schlegelii*, *Pagrus major*, *Oryzias latipes*, *Oryzias melastigma*, and *Danio rerio* were comparative analysis in this study. Phylogenetic analysis showed that *Sebastes schlegelii* and *Pagrus major* were clustered in one clade, while *Oryzias latipes* and *Oryzias melastigma* were clustered in one clade, both of which belonged to Euteleostei species (**Figure 8A**). And *Danio rerio* was grouped into a single branch, belonging to Osteriophysans species (**Figure 8A**).

M1–M20 motifs of *vasa* 3′UTRs were compared among the five teleost species. *Sebastes schlegelii* and *Pagrus major* had more similar conservative elements, while *Oryzias latipes* and *Oryzias melastigma* had more similar motifs (**Figures 8B,C**). Moreover, *Danio rerio* showed obvious different motifs with above species (**Figures 8B,C**). The results of MEME analysis were totally consistent with those of the phylogenetic analysis. However, in comparison with other three species, the motifs of M10, M12, and M19 specifically existed in *Sebastes schlegelii* and *Danio rerio* (**Figures 8B,C**).

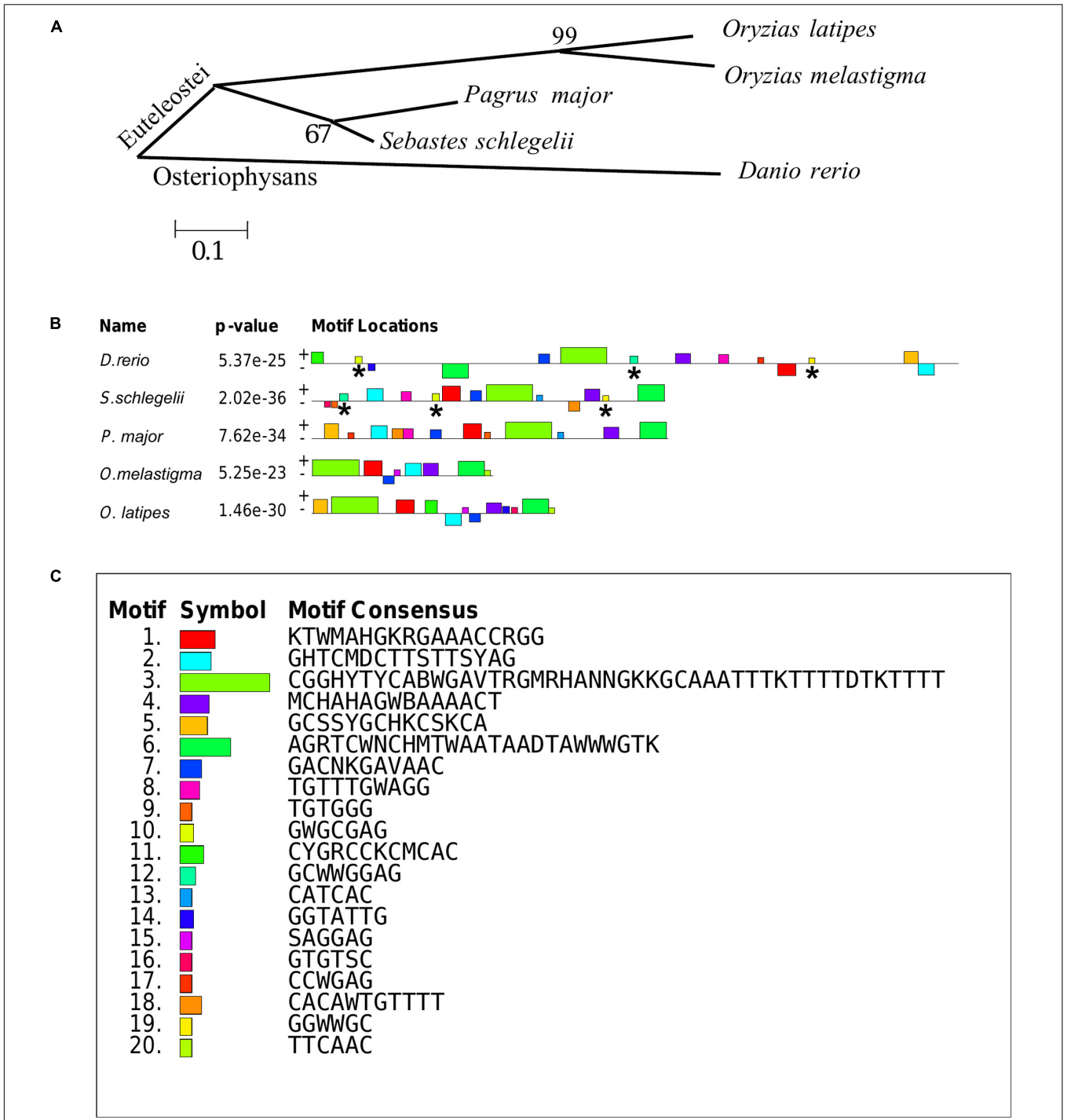

FIGURE 8 | Phylogenetic analysis and MEME motifs analysis in teleost *vasa* 3′UTRs. **(A)** Phylogenetic analysis of teleost *vasa* 3′UTRs by MEGA4. **(B,C)** Conservative functional motifs analysis in teleost *vasa* 3′UTRs by MEME. The twenty motifs designated as M1–M20 were indicated by different color codes **(B)**, and every color code represented motif consensus **(C)**. The motifs of M10, M12, and M19 marked with asterisks were only localized in *Danio rerio* and *Sebastes schlegelii* rather than the other three species.

DISCUSSION

The present study reported that the *vasa* identified the germline in *Sebastes schlegelii*. The *Sebastes schlegelii* Vasa protein possessed typical conserved domains of the DEAD-box protein family. By WISH, the *Ssvas* mRNA distributed uniformly throughout each blastomere at the blastula stage, failing in early localization during the cleavage stage. It was not until the

late gastrula stage that PGCs gradually formed and randomly aligned along the anterior of the body axes. Then, PGCs moved posterior-ward and lined both sides of the embryonic body at the somite stage, and localized at the dorsal sides of the gut and ventral side of notochord at hatching stage. After birth, PGCs localized in the upper part of the body cavity. They were covered by single-layer somatic cells, migrated to the genital ridge, and formed elongated gonadal primordia in the posterior part of the body cavity at 10 days. The migration routes and final location of PGCs during embryogenesis were similar to medaka (Shinomiya et al., 2000). Moreover, the time of primordial gonad formation of the viviparous economic fish after birth was earlier than most of oviparous fish such as turbot, Japanese flounder, and rainbow trout after hatching, which might be related to the long embryonic development time of viviparous fish *in vivo* (Fernandez et al., 2015; Zhao et al., 2017; Yang et al., 2018). This study firstly described the origination and migration pattern of PGCs in viviparous marine economic fish.

Medaka, rainbow trout, and rainbowfish (*Melanotaenia fluviatilis*) belonged to Euteleostei species, in which the *vasa* transcripts failed to localize at the cleavage furrows (Knaut et al., 2002). However, in the other Euteleostei, including turbot (Lin et al., 2012b), ukigori (Saito et al., 2004) and Atlantic cod (Presslauer et al., 2012), *vasa* mRNA is located at the edge of the first two cleavage furrows, which was similar to that reported in Osteriophysans species, such as zebrafish and carp (*Cyprinus carpio*) (Knaut et al., 2002). We found that the black rockfish was another new viviparous species that lacked the early localization ability in Euteleostei. Although black rockfish, medaka, Atlantic cod, and turbot were closely related in phylogeny, the *vasa* RNA early localization modes were totally different. This indicated that early germ plasm distribution and PGCs origination in different species had no direct relationship with evolution.

It has been proven that the 3′UTR of *vasa* plays a critical role for the stabilization of chimeric RNA in PGCs but not in somatic cells (Knaut et al., 2002; Wolke et al., 2002; Kataoka et al., 2006; Mishima et al., 2006). Visualization fish PGCs *in vivo* could be achieved by chimeric RNA fused fluorescent protein coding sequence to *vasa* 3′UTR (Knaut et al., 2002; Lin et al., 2012a; Ye et al., 2016). This labeling function of *vasa* 3′UTR was relatively conservative, and the PGCs of one species could be labeled by 3′UTRs from highly diverged taxonomic groups (Yoshizaki et al., 2005; Saito et al., 2006; Zhou et al., 2019). For example, PGCs of rainbow trout could be visualized by *vasa* 3′UTRs from both Nibe croaker (*Nibea mitsukurii*) and zebrafish (Yoshizaki et al., 2005). Also, the turbot PGCs could be traced by *vasa* 3′UTR from zebrafish (Zhou et al., 2019). However, the chimeric mRNA of the medaka (GFP-*olvasa* 3′UTR mRNA) failed to label the PGCs in zebrafish or loach (*Misgurnus anguillicaudatus*) embryos (Saito et al., 2006). The previous study proved that zebrafish had a 180-nucleotide element that encompassed the second conserved region of the *vasa* 3′UTR, which was sufficient for *vasa* mRNA localization to the germ plasm, while medaka lacked this region (Knaut et al., 2002). In this study, we firstly discovered that the *vasa* 3′UTR of black rockfish could be used to mark both zebrafish with early localization and medaka without early localization, while the *vasa* 3′UTR of red seabream and marine medaka that lacked early localization (article in publishing) failed to trace the PGCs of zebrafish. These results indicated that the *vasa* 3′UTRs of teleost showed a difference in labeling zebrafish PGCs, which may depend on the specific functional motifs in 3′UTR.

Therefore, we compared the twenty most important motifs of *vasa* 3′UTRs between black rockfish and other four typical fish species. We discovered that, although the black rockfish had the further genetic relationship with zebrafish than other four species in phylogeny, besides some basal motifs similar to the other four specie, there were three motifs of M10, M12, and M19 specifically presented in zebrafish which only existed in black rockfish rather than the other three species. These three specific motifs might partially explain why only the *vasa* 3′UTR of black rockfish was able to successfully trace PGCs in zebrafish. All of the above results also indicated that the *vasa* 3′UTR must possess the essential motifs that play an important role in tracing the PGCs instead of phylogenetic relationships.

In conclusion, we described the expression pattern of *Ssvas* during germ cell origination, development, and maturation process. We firstly reported a viviparous marine economic fish species which failed in early localization until the late gastrula stage. Interestingly, the *vasa* 3′UTR of black rockfish could be used to label PGCs of zebrafish and marine medaka, representing two different typical origination and migration patterns. Compared to other three Euteleostei species, we found that besides some basal motifs, black rockfish had three motifs just presented in zebrafish. Therefore, we speculated that these motifs might play an important role in labeling zebrafish PGCs. The results of this study will improve our understanding of the localization of the germplasm component and the origination of PGCs in teleost and facilitate germ cell manipulation.

DATA AVAILABILITY STATEMENT

All datasets presented in this study are included in the article/supplementary material.

ETHICS STATEMENT

The animal study was reviewed and approved by the Institutional Animal Care and Use Committee, Institute of Oceanology, Chinese Academy of Sciences.

AUTHOR CONTRIBUTIONS

LZ, QL, and JL conceived and designed the study. LZ and SD contributed to the experimental work. LZ and QL contributed to the manuscript writing and revision, respectively. XW, HZ, TD, JY, LW, and ZS contributed with the experimental materials. All authors read and approved the final manuscript.

FUNDING

This research was funded by the National Key Research and Development Program (2018YFD0901205 and 2018YFD0901204), Shandong Province Key R&D Projects (2019GHY112013), Shandong Province Major Science and Technology Innovation Project (2018SDKJ0302-4), and China Agriculture Research System (CARS-47).

REFERENCES

Bailey, T. L., and Elkan, C. (1994). Fitting a mixture model by expectation maximization to discover motifs in biopolymers. *Proc. Int. Conf. Intell. Syst. Mol. Biol.* 2, 28–36.

Braat, A. K., Speksnijder, J. E., and Zivkovic, D. (1999). Germ line development in fishes. *Int. J. Dev. Biol.* 43, 745–760. doi: 10.1007/s11626-999-0044-2

Fernandez, J. A., Bubner, E. J., Takeuchi, Y., Yoshizaki, G., Wang, T., Cummins, S. F., et al. (2015). Primordial germ cell migration in the yellowtail kingfish (*Seriola lalandi*) and identification of stromal cell-derived factor 1. *Gen. Comp. Endocrinol.* 213, 16–23. doi: 10.1016/j.ygcen.2015.02.007

Gao, Z., Wang, H. P., Rapp, D., O'Bryant, P., Wallat, G., Wang, W., et al. (2009). Gonadal sex differentiation in the bluegill sunfish *Lepomis crochirus* and its relation to fish size and age. *Aquaculture* 294, 138–146. doi: 10.1016/j.aquaculture.2009.05.024

Goto-Kazeto, R., Saito, T., Takagi, M., Arai, K., and Yamaha, E. (2010). Isolation of teleost primordial germ cells using flow cytometry. *Int. J. Dev. Biol.* 54, 1485–1490. doi: 10.1387/ijdb.092914rg

Hartung, O., Forbes, M. M., and Marlow, F. L. (2014). Zebrafish *vasa* is required for germ-cell differentiation and maintenance. *Mol. Reprod. Dev.* 81, 946–961. doi: 10.1002/mrd.22414

Hong, N., Li, M. Y., Yuan, Y. M., Wang, T. S., Yi, M. S., Xu, H., et al. (2016). Dnd is a critical specifier of primordial germ cells in the medaka fish. *Stem Cell Rep.* 6, 411–421. doi: 10.1016/j.stemcr.2016.01.002

Kai, Y., and Soes, D. M. (2009). A record of *Sebastes schlegelii* Hilgendorf, 1880 from Dutch coastal waters. *Aquat. Invas.* 4, 417–419. doi: 10.3391/ai.2009.4.2.23

Kataoka, K., Yamaguchi, T., Orii, H., Tazaki, A., Watanabe, K., and Mochii, M. (2006). Visualization of the *Xenopus* primordial germ cells using a green fluorescent protein controlled by *cis* elements of the 3′ untranslated region of the *DEADSouth* gene. *Mech. Dev.* 123, 746–760. doi: 10.1016/j.mod.2006.07.006

Knaut, H., Pelegri, F., Bohmann, K., Schwarz, H., and Nüsslein-Volhard, C. (2000). Zebrafish *vasa* RNA but not its protein is a component of the germ plasm and segregates asymmetrically before germline specification. *J. Cell Biol.* 149, 875–888. doi: 10.1083/jcb.149.4.875

Knaut, H., Steinbeisser, H., Schwarz, H., and Nüsslein-Volhard, C. (2002). An evolutionary conserved region in the *vasa* 3′ UTR targets RNA translation to the germ cells in the zebrafish. *Curr. Biol.* 12, 454–466. doi: 10.1016/S0960-9822(02)00723-6

Kobayashi, T., Kajiura-Kobayashi, H., and Nagahama, Y. (2000). Differential expression of *vasa* homologue gene in the germ cells during oogenesis and spermatogenesis in a teleost fish, tilapia. *Oreochromis niloticus*. *Mech. Dev.* 99, 139–142. doi: 10.1016/S0925-4773(00)00464-0

Li, M. Y., Hong, N., Xu, H. Y., Yi, M. S., Li, C. M., Gui, J. F., et al. (2009). Medaka *vasa* is required for migration but not survival of primordial germ cells. *Mech. Dev.* 126, 366–381. doi: 10.1016/j.mod.2009.02.004

Lin, F., Xu, S. H., Ma, D. Y., Xiao, Z. Z., Zhao, C. Y., Xiao, Y. S., et al. (2012b). Germ line specific expression of a *vasa* homologue gene in turbot (*Scophthalmus maximus*): evidence for *vasa* localization at cleavage furrows in euteleostei. *Mol. Reprod. Dev.* 79, 803–813. doi: 10.1002/mrd.22120

Lin, F., Liu, Q. H., Li, M. Y., Li, Z. D., Hong, N., Li, J., et al. (2012a). Transient and stable GFP expression in germ cells by the *vasa* regulatory sequences from the red seabream (*Pagrus major*). *Int. J. Biol. Sci.* 8, 882–890. doi: 10.7150/ijbs.4421

Lindeman, R. E., and Pelegri, F. (2010). Vertebrate maternal-effect genes: insights into fertilization, early cleavage divisions, and germ cell determinant localization from studies in the zebrafish. *Mol. Reprod. Dev.* 77, 299–313. doi: 10.1002/mrd.21128

Liu, Q. H., Wang, X. Y., Xiao, Y. S., Zhao, H. X., Xu, S. H., Wang, Y. F., et al. (2019). Sequencing of the black rockfish chromosomal genome provides insight into sperm storage in the female ovary. *DNA Res.* 26, 453–464. doi: 10.1093/dnares/dsz023

Mishima, Y., Giraldez, A. J., Takeda, Y., Fujiwara, T., Sakamoto, H., Schier, A. F., et al. (2006). Differential regulation of germline mRNAs in soma and germ cells by zebrafish miR-430. *Curr. Biol.* 16, 2135–2142. doi: 10.1016/j.cub.2006.08.086

Mu, W. J., Wen, H. S., He, F., Li, J. F., Liu, M., Ma, R. Q., et al. (2013). Cloning and expression analysis of vasa during the reproductive cycle of Korean rockfish, *Sebastes schlegeli*. *J. Ocean U. China* 12, 115–124. doi: 10.1007/s11802-013-1941-2

Nishimura, T., and Tanaka, M. (2014). Gonadal development in fish. *Sex. Dev.* 8, 252–261. doi: 10.1159/000364924

Okutsu, T., Yano, A., Nagasawa, K., Shikina, S., Kobayashi, T., Takeuchi, Y., et al. (2006). Manipulation of fish germ cell: visualization, cryopreservation and transplantation. *J. Reprod. Dev.* 52, 685–693. doi: 10.1262/jrd.18096

Piferrer, F. (2001). Endocrine sex control strategies for the feminization of teleost fish. *Aquaculture* 197, 229–281. doi: 10.1016/B978-0-444-50913-0.50014-X

Presslauer, C., Nagasawa, K., Fernandes, J. M. O., and Babiak, I. (2012). Expression of *vasa* and *nanos3* during primordial germ cell formation and migration in Atlantic cod (*Gadus morhua* L.). *Theriogenology* 78, 1262–1277. doi: 10.1016/j.theriogenology.2012.05.022

Saito, T., Fujimoto, T., Maegawa, S., Inoue, K., Tanaka, M., Arai, K., et al. (2006). Visualization of primordial germ cells in vivo using GFP-*nos1* 3′UTR mRNA. *Int. J. Dev. Biol.* 50, 691–699. doi: 10.1387/ijdb.062143ts

Saito, T., Otani, S., Fujimoto, T., Suzuki, T., Takako Nakatsuji, T., Arai, K., et al. (2004). The germ line lineage in ukigori, *Gymnogobius* species (Teleostei: Gobiidae) during embryonic development. *Int. J. Dev. Biol.* 48, 1079–1085. doi: 10.1387/ijdb.041912ts

Saitou, N., and Nei, M. (1987). The neighbor-joining method: a new method for reconstructing phylogenetic trees. *Mol. Biol. Evol.* 4, 406–425. doi: 10.1266/jjg.61.559

Shinomiya, A., Tanaka, M., Kobayashi, T., Nagahama, Y., and Hamaguchi, S. (2000). The *vasa*-like gene, *olvas*, identifies the migration path of primordial germ cells during embryonic body formation stage in the medaka, *Oryzias latipes*. *Dev. Growth Differ.* 42, 317–326. doi: 10.1046/j.1440-169x.2000.00521.x

Takeuchi, Y., Yoshizaki, G., and Takeuchi, T. (2004). Biotechnology: surrogate broodstock produces salmonids. *Nature* 430, 629–630. doi: 10.1038/430629a

Wolke, U., Weidinger, G., Köprunner, M., and Raz, E. (2002). Multiple levels of posttranscriptional control lead to germ line-specific gene expression in the zebrafish. *Curr. Biol.* 12, 289–294. doi: 10.1016/s0960-9822(02)00679-6

Xu, H. Y., Li, M. Y., Gui, J. F., and Hong, Y. H. (2007). Cloning and expression of medaka *dazl* during embryogenesis and gametogenesis. *Gene Exp. Patterns* 7, 332–338. doi: 10.1016/j.modgep.2006.08.001

Xu, H. Y., Li, M. Y., Gui, J. F., and Hong, Y. H. (2010). Fish germ cells. *Sci. China Life Sci.* 53, 435–446. doi: 10.1007/s11427-010-0058-8

Yang, Y., Liu, Q. H., Xiao, Y. S., Wang, X. Y., An, H., Song, Z. C., et al. (2018). Germ cell migration, proliferation and differentiation during gonadal morphogenesis in all-female japanese flounder (*paralichthys olivaceus*). *Anat. Rec.* 301, 727–741. doi: 10.1002/ar.23698

Ye, H., Yue, H. M., Yang, X. G., Li, C. J., and Wei, Q. W. (2016). Identification and sexually dimorphic expression of *vasa* isoforms in Dabry' s sturgeon (*Acipenser dabryanus*), and functional analysis of *vasa* 3′-untranslated region. *Cell Tissue Res.* 366, 203–218. doi: 10.1007/s00441-016-2418-6

Yoon, C., Kawakami, K., and Hopkins, N. (1997). Zebrafish *vasa* homologue RNA is localized to the cleavage planes of 2- and 4-cell-stage embryos and is expressed in the primordial germ cells. *Development* 124, 3157–3165. doi: 10.1007/s004290050089

Yoshizaki, G., Sakatani, S., Tominaga, H., and Takeuchi, T. (2010). Cloning and characterization of a *vasa*-like gene in rainbow trout and its expression in the

germ cell lineage. *Mol. Reprod. Dev.* 55, 364–371. doi: 10.1002/(SICI)1098-2795(200004)55:43.0.CO

Yoshizaki, G., Tago, Y., Takeuchi, Y., Sawatari, E., Kobayashi, T., and Takeuchi, T. (2005). Green fluorescent protein labeling of primordial germ cells using a nontransgenic method and its application for germ cell transplantation in salmonidae. *Biol. Reprod.* 73, 88–93. doi: 10.1095/biolreprod.104.034249

Zhao, C. Y., Xu, S. H., Liu, Y. F., Wang, Y. F., Liu, Q. H., and Li, J. (2017). Gonadogenesis analysis and sex differentiation in cultured turbot (*Scophthalmus maximus*). *Fish Physiol. Biochem.* 43, 265–278. doi: 10.1007/s10695-016-0284-5

Zhou, L., Wang, X. Y., Liu, Q. H., Xu, S. H., Zhao, H. X., Han, M. M., et al. (2019). Visualization of turbot (*Scophthalmus maximus*) primordial germ cells in vivo using fluorescent protein mediated by the 3′ untranslated region of *nanos3* or *vasa* gene. *Mar. Biotechnol.* 21, 671–682. doi: 10.1007/s10126-019-09911-z

Conflict of Interest: ZS was employed by the company Weihai Shenghang Aquatic Product Science and Technology Co., Ltd.

The remaining authors declare that the research was conducted in the absence of any commercial or financial relationships that could be construed as a potential conflict of interest.

frontiers in Cell and Developmental Biology

REVIEW
published: 28 January 2021
doi: 10.3389/fcell.2020.593613

Regulatory Mechanisms of Vitellogenesis in Insects

*Zhongxia Wu†, Libin Yang†, Qiongjie He and Shutang Zhou**

State Key Laboratory of Cotton Biology, Key Laboratory of Plant Stress Biology, School of Life Sciences, Henan University, Kaifeng, China

Vitellogenesis is pre-requisite to insect egg production and embryonic development after oviposition. During insect vitellogenesis, the yolk protein precursor vitellogenin (Vg) is mainly synthesized in the fat body, transported by the hemolymph through the intercellular spaces (known as patency) in the follicular epithelium to reach the membrane of maturing oocytes, and sequestered into the maturing oocytes via receptor-mediated endocytosis. Insect vitellogenesis is governed by two critical hormones, the sesquiterpenoid juvenile hormone (JH) and the ecdysteriod 20-hydroxyecdysone (20E). JH acts as the principal gonadotropic hormone to stimulate vitellogenesis in basal hemimetabolous and most holometabolous insects. 20E is critical for vitellogenesis in some hymenopterans, lepidopterans and dipterans. Furthermore, microRNA (miRNA) and nutritional (amino acid/Target of Rapamycin and insulin) pathways interplay with JH and 20E signaling cascades to control insect vitellogenesis. Revealing the regulatory mechanisms underlying insect vitellogenesis is critical for understanding insect reproduction and helpful for developing new strategies of insect pest control. Here, we outline the recent research progress in the molecular action of gonadotropic JH and 20E along with the role of miRNA and nutritional sensor in regulating insect vitellogenesis. We highlight the advancements in the regulatory mechanisms of insect vitellogenesis by the coordination of hormone, miRNA and nutritional signaling pathways.

Keywords: vitellogenin, juvenile hormone, ecdysone, nutrition, insect reproduction

OPEN ACCESS

Edited by:
Graça Soveral,
University of Lisbon, Portugal

Reviewed by:
Kai Lu,
Fujian Agriculture and Forestry University, China
Zilá Luz Paulino Simões,
University of São Paulo, Brazil

***Correspondence:**
Shutang Zhou
szhou@henu.edu.cn

†These authors have contributed equally to this work

Specialty section:
This article was submitted to Cellular Biochemistry, a section of the journal Frontiers in Cell and Developmental Biology

Received: *11 August 2020*
Accepted: *22 December 2020*
Published: *28 January 2021*

Citation:
Wu Z, Yang L, He Q and Zhou S (2021) Regulatory Mechanisms of Vitellogenesis in Insects. Front. Cell Dev. Biol. 8:593613. doi: 10.3389/fcell.2020.593613

INTRODUCTION

A hallmark of female insect reproduction is vitellogenesis, a heterosynthetic process by which vitellogenin (Vg) is mostly synthesized in the fat body and deposited into developing oocytes. In addition to the fat body, Vg synthesis has been reported in follicle cells (Gilbert et al., 1998), nurse cells (Melo et al., 2000; Matsumoto et al., 2008) and hemocytes (Bai et al., 2015; Huo et al., 2018) in several insect species. Vg is critical for egg maturation during adulthood and embryonic growth after oviposition. In the honey bee *Apis mellifera*, Vg also protects the queen and long-lived worker bees from oxidative stress and further extends their life span (Seehuus et al., 2006; Corona et al., 2007; Ihle et al., 2015). Additionally, Vg plays a role in sensing fat body sugars and gustatory perception in the worker bees (Amdam et al., 2006; Wang et al., 2012, 2013). Furthermore, *A. mellifera* Vg acts as a pathogen recognition receptor and transports pathogen-derived molecules into the offspring to achieve trans-generational immunity (Garcia et al., 2010; Salmela et al., 2015; Zhang et al., 2015). In the small brown planthopper *Laodelphax striatellus*, Vg synthesized by hemocytes can facilitate the vertical transmission of rice stripe virus (Huo et al., 2018). The number

of *Vg* genes among different insect species ranges from one to three in general, while the mosquito *Aedes aegypti* and the ant *Linepithema humile* possess up to five *Vg* genes (Corona et al., 2013) (**Supplementary Table 1**). The presence of multiple copies of *Vg* genes and multiple forms of Vg protein in insects is unclear. It is conceivable that two or more copies of *Vg* gene ensure the efficient production of yolk protein precursors required for the maturation of multiple eggs. The variation of *Vg* gene and protein in diverse insect species might reflect the evolutionary selection and the strategy of adaptation to environment (Garcia et al., 2010). Vg protein is a large glycolipophosphoprotein that is often oligomeric in their native state, with monomers consisting of two or more subunits (apoproteins). The molecular weights vary from 150 kDa to 200 kDa for large subunits and from 40 kDa to 65 kDa for small subunits, respectively (Lee et al., 2015). Vg protein sequences are evolutionarily conserved across insect orders except for yolk proteins (YPs) in Diptera. In the fruit fly *Drosophila melanogaster*, YPs form a different family of proteins to nurse maturing oocytes. Vg is generally composed of a lipoprotein N-terminal domain (LPD_N) for lipid binding, a 1943 domain with unknown function (DUF1943), and a von Willebrand factor type D domain (vWFD) in the C-terminus (Morandin et al., 2014). LPD_N has a conserved polyserine tract possessing consensus cleavage motifs ($^{R}/_{K}XX^{R}/_{K}$) (Tufail and Takeda, 2008). Vg proteins are phosphorylated at the polyserine tract, but the function of Vg phosphorylation remains elusive (Tufail and Takeda, 2008).

Cumulative studies have established that insect vitellogenesis is controlled by two classic hormones, the sesquiterpenoid juvenile hormone (JH) and the ecdysteroid 20-hydroxyecdysone (20E, an active form of ecdysone). Both JH and 20E can stimulate various aspects of vitellogenesis but vary across insect orders depending on reproductive traits (Wyatt and Davey, 1996; Raikhel et al., 2005; Roy et al., 2018; Santos et al., 2019; Song and Zhou, 2020). In evolutionarily primitive hemimetabolous insects such as the migratory locust *Locusta migratoria* and the German cockroach *Blattella germanica*, JH acts independently of 20E to stimulate vitellogenesis and oocyte maturation (Wyatt and Davey, 1996; Belles, 2004; Roy et al., 2018; Song and Zhou, 2020). In holometabolous coleopteran like the red flour beetle *Tribolium castaneum*, JH governs Vg synthesis in the fat body while 20E participates in ovarian growth and oocyte maturation (Parthasarathy et al., 2010a,b; Sheng et al., 2011). In many lepidopterans including the tobacco hornworm *Manduca sexta* and the cotton bollworm *Helicoverpa armigera*, in which Vg synthesis is initiated in adults, JH plays a principal role in vitellogenesis (Swevers and Iatrou, 2003; Telfer, 2009). However, in other lepidopterans such as the silkworm *Bombyx mori,* the silk moth *Hyalophora cecropia,* and the armyworm *Spodoptera frugiperda*, in which Vg is synthesized prior to adult ecdysis, 20E appears to have a primary role in vitellogenesis (Swevers and Iatrou, 2003; Telfer, 2009). In the mosquito *Ae. aegypti*, JH promotes fat body becoming competent for Vg synthesis, while 20E stimulates *Vg* expression and oocyte maturation after a blood meal (Raikhel et al., 2002; Shin et al., 2012). In *D. melanogaster*, 20E is responsible for the high rate of Vg synthesis in the fat body and JH controls Vg uptake into oocytes (Bownes, 1990; Carney and Bender, 2000; Berger and Dubrovsky, 2005).

Nutrients play a pivotal role in insect vitellogenesis. As nutritional sensors, the amino acid/Target of Rapamycin (AA/TOR) and insulin (or insulin-like peptide, ILP) are involved in biosynthesis of JH and 20E and crosstalk with JH and 20E pathways, which in turn regulate various aspects of insect vitellogenesis (Badisco et al., 2013; Hansen et al., 2014; Smykal and Raikhel, 2015; Roy et al., 2018). Furthermore, recent studies have revealed an essential role of microRNA (miRNA) in the regulation of insect vitellogenesis (Roy et al., 2018; Song and Zhou, 2020). Hence, this review covers the present status of our understanding in the regulatory mechanisms of insect vitellogenesis including Vg synthesis in the fat body and uptake in the ovary.

REGULATION OF Vg SYNTHESIS IN THE FAT BODY

Insect fat body, analogous to the vertebrate liver and adipose tissue, is the major source for Vg synthesis. Recently, research advancements have been achieved in the molecular mechanisms of Vg synthesis regulated by JH, 20E, miRNA and nutritional pathways. For the regulatory mechanisms of 20E, AA/TOR and peptides in insect vitellogenesis and oogenesis, we refer readers to three recent reviews (Roy et al., 2018; Lenaerts et al., 2019; Swevers, 2019). Here, we outline the recent accomplishments in regulating Vg synthesis in the fat body, with the emphasis on the role of JH, miRNA and ILP pathways (**Figure 1**).

JH Action on Vg Synthesis

The molecular action of JH relies on its intracellular receptor Methoprene-tolerant (Met), a member of basic helix-loop-helix Per-Arnt-Sim (bHLH-PAS) transcription factor family. JH induces the heterodimerization of Met with another bHLH-PAS protein, Taiman (Tai) to form an active JH-receptor complex (Jindra et al., 2013). The JH-Met/Tai receptor complex consequently activates the transcription of JH-responsive genes (Charles et al., 2011; Li et al., 2011; Kayukawa et al., 2012; Guo et al., 2014; Jindra et al., 2015; Wu et al., 2016, 2018; Wang Z. et al., 2017). In adult insects, JH requires the Met/Tai complex to achieve its previtellogenic and vitellogenic effects on fat body competency and Vg synthesis (Zou et al., 2013; Guo et al., 2014; Gujar and Palli, 2016; Wang Z. et al., 2017). RNAi-mediated knockdown of *Met* resulted in significant reduction of *Vg* expression level accompanied by arrested oocyte maturation and blocked egg production in a variety of investigated insects including *T. castaneum*, *L. migratoria*, *H. armigera*, the linden bug *Pyrrhocoris apterus*, the brown planthopper *Nilaparvata lugens*, the oriental fruit fly *Bactrocera dorsalis*, and the white-backed planthopper *Sogatella furcifera* (Parthasarathy et al., 2010b; Shpigler et al., 2014; Smykal et al., 2014; Song et al., 2014; Lin et al., 2015; Ma et al., 2018; Yue et al., 2018; Hu et al., 2019). In *L. migratoria*, *P. apterus*, and *Ae. aegypti*, depletion of *Tai* or its orthologs *FISC* and *p160/SRC* led to significantly declined levels of *Vg* transcripts along with blocked oocyte development

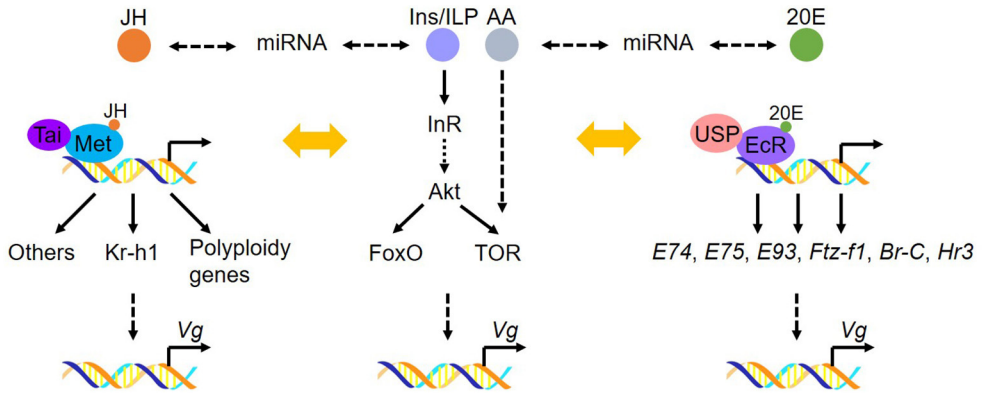

FIGURE 1 | Molecular basis of Vg synthesis in the fat body. JH receptor complex Met/Tai directly regulates the transcription of target genes encoding *Kr-h1* and the polyploidy genes (including DNA replication and cell cycle genes). 20E receptor complex EcR/USP directly activates the expression of 20E-responsive genes. Nutritional signaling is involved in Vg production in the fat body by interplay with JH or 20E. In addition, miRNA participates in JH- or 20E-dominant Vg synthesis in the fat body. These factors directly or indirectly regulate *Vg* transcription and vitellogenesis.

(Smykal et al., 2014; Wang Z. et al., 2017). *Krüppel-homolog 1* (*Kr-h1*), a primary JH early-response gene that codes for a zinc finger transcription factor, transduces JH signaling in regulating adult reproduction (Kayukawa et al., 2012; Shin et al., 2012; Song et al., 2014). The role of Kr-h1 in insect vitellogenesis varies among insect species. In *L. migratoria*, *B. dorsalis*, and the rice stem borer *Chilo suppressalis*, Kr-h1 mediates JH action to promote vitellogenesis and oocyte maturation (Song et al., 2014; Yue et al., 2018; Tang et al., 2020). In *Ae. aegypti*, Kr-h1 transduces JH signaling as both activator and repressor to regulate the expression of JH-responsive genes involved in previtellogenic development, consequently regulating egg production after a blood meal (Shin et al., 2012; Zou et al., 2013; Ojani et al., 2018). In *T. castaneum*, depletion of *Met* caused more than 80% decrease of *Vg* mRNA levels, whereas *Kr-h1* knockdown resulted in about 30% reduction of *Vg* transcripts (Parthasarathy et al., 2010b). In *P. apterus*, knockdown of *Met* or *Tai* but not *Kr-h1* suppressed Vg synthesis in the fat body (Smykal et al., 2014). In the common bed bug *Cimex lectularius*, *Kr-h1* knockdown appeared to have no significant impact on vitellogenesis (Gujar and Palli, 2016).

L. migratoria, a hemimetabolous species bearing the panoistic ovary and synchronously matured oocytes, has been a long-standing model for studying JH-dependent female reproduction (Wyatt and Davey, 1996; Roy et al., 2018). In adult females of *L. migratoria*, JH induces Vg synthesis in the fat body, initiates intercellular space (patency) in the follicular epithelium, and facilitates the uptake of Vg into developing oocytes (Wyatt and Davey, 1996; Song and Zhou, 2020). During the first gonadotrophic cycle, locust fat body undergoes endocycle to produce up to 32C (chromatin copies per cell) polyploid cells required for massive Vg synthesis (Guo et al., 2014). RNA-seq-based gene expression profiling followed by qRT-PCR validation demonstrated that JH upregulated the expression of 16 genes related to DNA replication and 13 genes involved in cell cycle progression, suggesting that JH plays a pivotal role in the onset and progression of polyploidy by promoting endocycle in the fat body (Guo et al., 2014). Of these 29 genes, chromosome maintenance genes 3, 4, 7 (*Mcm3*, *Mcm4*, and *Mcm7*), *cell-division-cycle 6* (*Cdc6*), *cyclin-dependent kinase 6* (*Cdk6*) and *adenovirus E2 factor-1* (*E2f1*) expressed in response to both JH and Met (Guo et al., 2014). Further studies revealed that the JH-Met/Tai receptor complex bound to the consensus sequences with E-box or E-box-like motifs in the promoters of *Mcm4*, *Mcm7*, *Cdc6*, *Cdk6*, and *E2f1* and activated their transcription. Knockdown of *Mcm4*, *Mcm7*, *Cdc6*, *Cdk6*, or *E2f1* in vitellogenic female locusts resulted in significant reduction in fat body cell ploidy, accompanied by markedly reduced *Vg* expression levels, arrested oocyte maturation and impaired egg production (Guo et al., 2014; Wu et al., 2016, 2018). Interestingly, depletion of *Met* had no significant effect on other genes upregulated by JH (Guo et al., 2014), suggesting the involvement of other signaling cascades that interplay with JH. Next, Wu et al. (2020) demonstrated that JH stimulated FoxO dephosphorylation through leucine carboxyl methyltransferase 1 (LCMT1)-mediated activation of protein phosphatase 2A (PP2A). JH-LCMT1-PP2A axis-triggered FoxO dephosphorylation facilitated FoxO translocation in nuclei and activated the transcription of *cell-division-cycle 2* (*Cdc2*) and *origin-recognition-complex subunit 5* (*Orc5*). Knockdown of *LCMT1*, *PP2A*, *FoxO*, *Cdc2*, or *Orc5* in vitellogenic female locusts resulted in lower ploidy and significantly reduced *Vg* expression in the fat body as well as arrested oocyte maturation and suppressed egg development (Wu et al., 2020). Collectively, JH acts via its receptor complex Met/Tai to induce the expression of *Mcm4*/*7*, *Cdc6*, *Cdk6*, and *E2f1*, and through LCMT1-PP2A-FoxO axis to trigger the expression of *Cdc2* and *Orc5* (Guo et al., 2014; Wu et al., 2016, 2018, 2020). These two signaling pathways coordinate to promote fat body cell polyploidization for large-scale Vg synthesis, which meets the requirement of synchronous maturation of multiple eggs in *L. migratoria*.

Ae. aegypti serves as an ideal model for studying JH-dependent posteclosion or previtellogenic development. Besides the JH-Met/Tai complex, JH induces the dimerization of Met with Cycle to upregulate gene transcription for previtellogenic development

in *Ae. aegypti* (Shin et al., 2012). JH acts via Met to induce the expression of *Regulator of Ribosome Synthesis 1* (*RRS1*) and *Ribosomal protein L32* (*RpL32*), consequently enhancing ribosomal biogenesis in the fat body essential for massive Vg synthesis (Wang J. L. et al., 2017). Saha et al. (2019) reported that JH induced the expression of gene coding for Hairy which dimerizes with Groucho to form a transcriptional repressor complex mediating the repressive function of JH. Interestingly, Hairy and Kr-h1 acted synergistically in the JH/Met gene repression hierarchy during previtellogenic development of *Ae. aegypti* (Saha et al., 2019). JH exerts both genomic and non-genomic action. For non-genomic action, JH acts via the RTK-PLC-IP3-CaMKII signaling cascade to trigger Met phosphorylation that enhances its transcriptional activity in previtellogenic development of *Ae. aegypti* (Liu et al., 2015; Ojani et al., 2016). Moreover, JH triggers the RTK-PI3K-Akt signaling pathway to stimulate the phosphorylation of serine/arginine-rich (pre-mRNA) splicing factor (SRSF), which induces the alternative splicing of Tai to produce Tai-A and Tai-B isoforms (Liu et al., 2018). These two isoforms could potentiate the transcriptional activity of 20E-receptor in the fat body of adult female mosquitoes, consequently promoting blood meal-induced vitellogenesis and egg production (Liu et al., 2018).

Nutritional Control of Vg Synthesis

AA/TOR pathway has been demonstrated to play pivotal roles in activating Vg synthesis in divergent orders of insects (Sancak et al., 2008; Carpenter et al., 2012; Koyama et al., 2013; Lu et al., 2016). Suppression of TOR activity by rapamycin treatment or RNA-mediated knockdown inhibited *Vg* expression in *Ae. aegypti* and *N. lugens* (Hansen et al., 2004; Lu et al., 2016). Moreover, TOR tends to have a positive effect on JH biosynthesis and vitellogenesis. In *T. castaneum*, *B. germanica*, and the American cockroach *Periplaneta americana*, TOR and ILP signaling could enhance the expression of *JH methyltransferase* (*JHAMT*), *Met* and *Kr-h1*, further stimulating *Vg* expression and oocyte maturation (Parthasarathy and Palli, 2011; Abrisqueta et al., 2014; Zhu et al., 2020). Moreover, insulin/TOR signaling affects 20E synthesis and secretion as well, further associates with vitellogenesis and egg production in *D. melanogaster* and *Ae. aegypti* (Tu et al., 2002; Dhara et al., 2013).

FoxO plays a vital role in mediating the crosstalk between insulin and JH signaling pathways to coordinate insect vitellogenesis (Koyama et al., 2013; Smykal and Raikhel, 2015; Roy et al., 2018; Santos et al., 2019). In *B. germanica*, depletion of insulin receptor gene (*InR*) or *FoxO* in fed adult females resulted in markedly reduced *Vg* expression along with impaired oocyte maturation (Abrisqueta et al., 2014). Similarly, *FoxO* knockdown led to reduction of *Vg* transcript levels in fed adult females of *T. castaneum*, *Ae. aegypti*, *L. migratoria* and the soybean pod borer *Maruca vitrata* (Hansen et al., 2007; Parthasarathy and Palli, 2011; Abrisqueta et al., 2014; Al Baki et al., 2019; Wu et al., 2020). However, silencing of *FoxO* in the starved adult females of *B. germanica* caused significant increase of *Vg* expression due to elevated biosynthesis of JH (Suren-Castillo et al., 2012; Abrisqueta et al., 2014). In *B. mori*, FoxO suppresses the expression of JH degradation genes *JHE*, *JHDK,* and *JHEH* to protect JH from degradation (Zeng et al., 2017). Interestingly, FoxO binds to *Vg2* gene promoter and inhibits its transcription in *T. castaneum*. After adult emergence, JH induces *ILP* expression and FoxO phosphorylation, which in turn releases FoxO binding and activates *Vg2* transcription (Sheng et al., 2011).

miRNA Regulation of Vg Synthesis

As fine-tuners, miRNAs generally downregulate their target genes by translation inhibition or mRNA degradation in a spatiotemporal manner. Nevertheless, miRNAs can bind the 5′-UTR or CDS of target mRNAs to upregulate gene expression (Vasudevan et al., 2007; Zhou et al., 2009; Yang et al., 2014; He et al., 2016). The role of miRNAs in oogenesis has been extensively studied in *D. melanogaster* (Asgari, 2013; Shcherbata, 2019; Song and Zhou, 2020). Recently, miRNA functions in vitellogenesis and oocyte maturation have been explored in non-model insects like *Ae. aegypti* and *L. migratoria* (Lucas et al., 2015b; Roy et al., 2018; Song and Zhou, 2020). As two previous reviews have covered miRNA regulation in insect reproduction (Roy et al., 2018; Song and Zhou, 2020), we update the recent advances in the role of miRNAs in insect vitellogenesis.

Dicer 1 and Argonaute1 (Ago1) are two key enzymes involved in miRNA biogenesis and functioning. Depletion of *Dicer 1* or *Ago1* in *D. melanogaster*, *B. germanica*, *L. migratoria*, and *N. Lugens* led to defective phenotypes of female reproduction including decreased *Vg* expression and impaired oocyte maturation (Jin and Xie, 2007; Azzam et al., 2012; Tanaka and Piulachs, 2012; Song et al., 2013; Zhang et al., 2013). In adult female locusts, JH upregulated 59 miRNAs and downregulated 23 miRNAs (Song et al., 2013). Of JH-downregulated miRNAs, let-7 and miR-278 bound to *Kr-h1* coding sequence and repressed its expression. Application of let-7 and miR-278 agomiRs resulted in significantly reduced *Kr-h1* expression along with markedly decreased abundance of Vg protein and blocked oocyte maturation (Song et al., 2018). Intriguingly, JH titer increases from the previtellogenic stage to vitellogenic phase, whereas let-7 and miR-278 have the opposite tendency in abundance (Song et al., 2018; Guo et al., 2019). The increased JH titer and declined abundance of let-7 and miR-278, therefore, ensure high levels of Kr-h1 required for vitellogenesis. miR-2/13/71 is clustered miRNAs downregulated by JH in *L. migratoria* (Song et al., 2019). miR-2/13/71 bound to the coding sequence of *Notch* mRNA to inhibit its expression. Injection of miR-2/13/71 agomiRs in adult female locusts also led to reduced *Vg* transcripts and arrested oocyte maturation (Song et al., 2019). Likewise, the increased JH titer and declined abundance of miR-2/13/71 in vitellogenic female locusts contribute to high levels of Notch for successful vitellogenesis and egg development (Song et al., 2019).

In *Ae. aegypti*, lineage-specific miR-1890 targets the 3′UTR of JH-regulated *Chymotrypsin-like serine protease* (*JHA15*). After a blood meal, 20E suppresses miR-1890 expression to prevent adult females from impaired blood digestion in the midgut and Vg synthesis in the fat body (Lucas et al., 2015b). Disruption of miR-275, miR-1174 or miR-8 also caused defects in blood digestion, vitellogenesis and egg production in the vitellogenic females of *Ae. aegypti* (Bryant et al., 2010; Liu et al., 2014; Lucas et al., 2015a).

Moreover, miR-989, most abundant in the fat body and ovary of *Ae. aegypti*, directly targets *Vg* gene during female reproduction (Zhang et al., 2017). In the malaria mosquito *Anopheles gambiae*, miR-309 antagomiR treatment caused impaired vitellogenesis and egg production (Fu et al., 2017). In *N. lugens*, miR-4868b inhibits the expression of *Glutamine synthase* gene. miR-4868b antagomiR treatment resulted in significant decrease of Vg protein levels along with impeded egg development and reduced fecundity (Fu et al., 2015).

Post-translational Regulation of Synthesized Vg

Nascently synthesized Vg in the fat body is properly folded in the endoplasmic reticulum (ER) and assembled into the secretory vesicles via membrane fusion with the Golgi apparatus. The 78-kDa Glucose-regulated protein (Grp78), a heat shock protein 70 kDa family member is one of the most abundant chaperones in fat body ER of *L. migratoria* (Luo et al., 2017). During locust vitellogenesis, JH stimulates two *Grp78* genes, *Grp78-1* and *Grp78-2* via differential signaling pathways, which together accelerate the production of Grp78 chaperone. Grp78 facilitates the proper folding of massively synthesized Vg and avoid ER stress in the fat body (Luo et al., 2017). During the intracellular transportation, Vg stability is threatened by a variety of proteases but protected by protease inhibitors, of which the Kazal-type protease inhibitor is a common subfamily (Van Hoef et al., 2013). Guo et al. (2019) demonstrated that Greglinwas the predominant Kazal-type protease inhibitor in the fat body and ovary of vitellogenic females of *L. migratoria*. During locust vitellogenesis, JH induced high levels of *Greglin* expression to protect Vg from proteolysis (Guo et al., 2019). During the termination of *B. mori* embryonic diapause under low temperature, extracellular signal-regulated kinase (ERK)/mitogen-activated protein kinase (MAPK) signaling is activated in the yolk cells (Iwata et al., 2005). Thereafter, ERK/MAPK increases sorbitol and 20E metabolism by regulating the transcription of downstream genes. The elevated sorbitol-glycogen conversion and 20E secretion promote embryonic development, yolk-cell dispersion as well as yolk protein degradation (Fujiwara et al., 2006).

REGULATION OF Vg UPTAKE BY OVARIES

With the help of hemolymph circulation, Vg is transported into the ovary and absorbed by maturing oocytes. Oocytes are enclosed by the follicle epithelium, which determines the size and shape of oocytes and initiates the intercellular spaces (patency) (Wyatt and Davey, 1996; Raikhel et al., 2005). Vg is transported through patency to the surface of competent oocytes and then internalized via Vg receptor (VgR)-mediated endocytosis (**Figure 2**). JH plays a crucial role in Vg uptake by ovaries in a variety of insects. In adult females of *H. armigera*, depletion of *Met* severely suppressed *Vg* and *VgR* transcription, disrupted yolk protein uptake into oocytes, and eventually led to reduced fecundity (Ma et al., 2018). In *L. migratoria*, knockdown of *Met* or *Kr-h1* caused markedly smaller follicle cells and malfunctional patency (Song et al., 2014). In *B. germanica*, the JH-dependent expression of *SPARC* (*secreted protein, acidic and rich in cysteine*) gene, coding for a calcium-binding glycoprotein that forms part of the extracellular membranes is critical for follicle cell morphological changes and patency induction that facilitate Vg uptake by developing oocytes (Irles et al., 2017).

Role of Na^+/K^+-ATPase in Patency Initiation

Na^+/K^+-ATPase is a heterodimer protein that consists of α- and β-subunits (Lingrel and Kuntzweiler, 1994). The α-subunit, which has 10 transmembrane loops and large cytoplasmic regions, plays a chief function in catalytic action because of its ATP binding site and phosphorylation (Fambrough et al., 1994; Lingrel and Kuntzweiler, 1994). The β-subunit, also known as Nervana, is a nervous system-specific glycoprotein antigen in the adult head of *D. melanogaster*. The β-subunit contains a single transmembrane, a small N-terminal cytoplasmic domain and a large C-terminal extracellular region (Kaplan, 2002). In *B. germanica*, the orthologs of *D. melanogaster* Nervana 1 and Nervana 2 are crucial for oogenesis (Irles et al., 2013). Early study on the kissing bug *Rhodnius prolixus* has demonstrated that JH-stimulated patency is inhibited by application of ouabain, a specific inhibitor of Na^+/K^+-ATPase (Sevala and Davey, 1989), indicating the involvement of Na^+/K^+-ATPase in the regulation of JH-dependent patency initiation and Vg uptake. Subsequently, the role of Na^+/K^+-ATPase in patency initiation has been reported in *L. migratoria*, the beetle *Tenebrio molitor* and the moth *Heliothis virescens* (Sevala and Davey, 1993; Pszczolkowski et al., 2005). In *L. migratoria*, RNAi-mediated knockdown of *Na^+/K^+-ATPase* gene, pharmaceutical inhibition of Na^+/K^+-ATPase phosphorylation or suppression of Na^+/K^+-ATPase activity by inhibitor treatment resulted in the loss of patency along with blocked Vg uptake and impaired egg development (Jing et al., 2018).

As patency is initiated by JH, efforts have been made to elucidate the regulatory mechanisms of Na^+/K^+-ATPase activation by JH. Pharmaceutical approaches with protein kinase C (PKC) activator in *R. prolixus* have shown that PKC activation is required for the induction of JH-dependent Na^+/K^+-ATPase activity (Sevala and Davey, 1989). JH also evokes Na^+/K^+-ATPase-activated patency in *H. virescens* via the signaling pathways including protein kinase A (PKA) and PKC (Pszczolkowski et al., 2005, 2008). Jing et al. (2018) demonstrated that JH triggered a signaling cascade including G protein-coupled receptor (GPCR), receptor tyrosine kinase (RTK), phospholipase C (PLC), inositol trisphosphate (IP3) and PKC to phosphorylate Na^+/K^+-ATPase α-subunit at serine residue 8, leading to activation of Na^+/K^+-ATPase. Activated Na^+/K^+-ATPase is likely to change the ionic balance of follicle cells and cause cell shrinkage, consequently initiating patency for Vg transportation to the surface of maturing oocytes (Jing et al., 2018). However, the specific GPCR or RTK involved in GPCR/RTK-PLC-IP3-PKC signaling cascade remains to be identified. Bai and Palli (2016) reported that Dopamine D2-like receptor (Dop2R) controls Vg uptake by maturing oocytes in *T. castaneum* (Bai and Palli, 2016). In *L. migratoria*, 22 GPCRs were identified in the

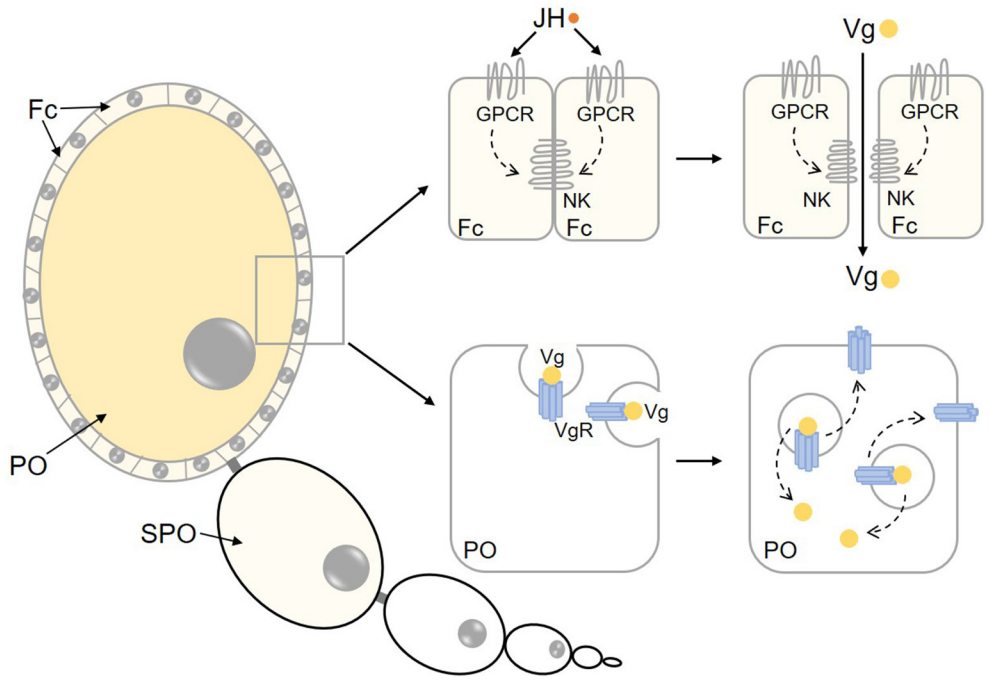

FIGURE 2 | Regulation of Vg uptake by maturing oocytes. Prior to Vg uptake by maturing oocytes, Vg passes through patency among follicle cells, which is regualted by JH action on GPCR and Na^+/K^+-ATPase. Vg is internalized by surrounding oocytes through VgR-mediated endocytosis. Afterwards, Vg is unbound with VgR, then VgR is recycled to the membrane of the oocyte. NK, Na^+/K^+-ATPase; Fc, follicle cells; PO, primary oocyte; SPO, sub-primary oocyte.

ovarian transcriptome of vitellogenic females. RNAi screening revealed that Orphan receptor-A (OR-A1 and OR-A2), C-type muscarinic acetylcholine receptor (mAChR-C) and Cirl-like (CirlL) played key roles in ovarian Vg transportation and uptake (Zheng et al., 2020).

VgR-mediated Vg Endocytosis

Insect VgR belongs to the low-density lipoprotein receptor (LDLR) family (Raikhel and Dhadialla, 1992; Schonbaum et al., 1995; Tufail and Takeda, 2009). Upon binding of Vg to VgR, the Vg/VgR complex clusters in clathrin-coated pits, invaginates into the cytoplasm and pinches off to form intracellular coated vesicles. After transformed into the endosome or transitional yolk body, Vg and VgR are dissociated by ATP-dependent acidification. Subsequently, VgR is recycled back to oocyte membrane surface while Vg is crystallized and stored as vitellin (Vn) in yolk bodies for future embryonic development (Sappington and Raikhel, 1998; Raikhel et al., 2002; Snigirevskaya and Raikhel, 2005; Mitchell and Pérez De León, 2019). In the oriental fruit fly *Bactrocera dorsalis*, depletion of *VgR* blocked Vg uptake and egg development (Cong et al., 2015). Also, knockdown of *VgR* in *N. lugens* and *S. furcifera* caused accumulation of Vg in the hemolymph accompanied by arrested oocyte maturation (Lu et al., 2015; Hu et al., 2019). *VgR* expression is hormonally regulated during reproductive development. In the fire ant *Solenopsis invicta*, JH treatment of cultured ovaries significantly increased *VgR* expression (Chen et al., 2004). Analogously, JH treatment induced *VgR* expression in adult females of *N. lugens* (Lu et al., 2015). Furthermore, JH upregulates *VgR* expression by Met-Kr-h1 pathway in the cabbage beetle *Colaphellus bowringi* (Liu et al., 2019). Interestingly, in *P. americana* whose vitellogenesis is dependent upon JH, the expression of *Vg* and *VgR* is inhibited by additional 20E treatment (Kamruzzaman et al., 2020). Similarly, knockdown of the Halloween genes coding for a group of enzymes involved in 20E synthesis remarkably reduced the levels of *Vg* and *VgR* expression, leading to defective egg development of the diamondback moth *Plutella xylostella* (Peng et al., 2019). In *M. vitrata* and the beet armyworm *Spodoptera exigua*, the expression of *VgR* is regulated by ILP/TOR signaling pathway (Zhao et al., 2018; Al Baki et al., 2019). Notably, two miRNAs, miR-2739 and miR-167 bind directly to the 3′UTR of *B. mori VgR* mRNA and coordinately inhibit *VgR* expression. Overexpression of either miR-2739 or miR-167 using the piggyBac system blocked Vg deposition into oocytes, whereas application of miR-2739 or miR-167 antagomiR resulted in increase of VgR levels and uptake of Vg by oocytes (Chen et al., 2020).

In addition to mediating Vg internalization, VgR is shown to play an important role in vertical transmission of pathogenic microbes and *Wolbachia* symbionts (Guo et al., 2018; Huo et al., 2019; Mitchell and Pérez De León, 2019). In *L. striatellus*, Vg is hitchhiked by the rice stripe virus (RSV), which enters the developing oocytes through VgR-mediated endocytosis (Huo et al., 2018, 2019; He et al., 2019). Also in *L. striatellus*, *Wolbachia* symbionts acquire maternal transmission through the Vg-VgR axis (Guo et al., 2018). It has been demonstrated that a series

of small guanosine triphosphatases (GTPase), whose activities are at peak during vitellogenesis, are involved in the process of Vg vesicular formation, budding, docking and fusion. In *P. americana*, GTPase activity is required for the intracellular trafficking of Vg in the ovary (Elmogy et al., 2014). In *N. lugens*, depletion of *Ran*, a member of GTPase family, brough about markedly reduced *Vg* expression and decreased fecundity (Li et al., 2015).

CONCLUSIONS AND PROSPECTS

Vitellogenesis is one of the most emblematic processes in insect reproduction. Over the past decades, accumulative studies have advanced our understanding of how insect vitellogenesis is governed by hormonal and nutritional pathways. 20E acts through its receptor complex comprised of Ecdysone Receptor (EcR) and Ultraspiracle (USP), leading to transcriptional activation of 20E-response genes including *ecdysone-induced proteins 74* (*E74*), 75 (*E75*), *93F* (*E93*), *Broad-Complex* (*Br-C*), and *Ftz-f1*. The 20E pathway appears to be evolutionarily conserved in vitellogenesis and oogenesis across insect orders (Raikhel et al., 2005; Swevers, 2019). Most recently, relative more research progress has been made on the action of JH, nutrition and miRNA pathways on vitellogenesis in diverse insect species such as *L. migratoria*, *Ae. aegypti*, *T. castaneum*, and *B. germanica* (Roy et al., 2018; Santos et al., 2019; Song and Zhou, 2020). JH acts through its receptor complex or interplays with ILP pathway to stimulate fat body cells undergoing endocycle for polyploidization, which accelerates massive Vg synthesis to meet the requirement for synchronous maturation of multiple eggs in *L. migratoria* (Guo et al., 2014; Wu et al., 2016, 2018, 2020). Moreover, JH acts via Met and intracellular signaling cascades to promote fat body competency ready for Vg synthesis after a blood meal in *Ae. aegypti* (Shin et al., 2012; Ojani et al., 2016; Liu et al., 2018; Saha et al., 2019). The genomic action of JH has been extensively studied since the establishment of Met/Tai as the nuclear JH receptor and the identification of JH-responsive genes. Nevertheless, most studies on JH actions have been conducted in insect molting and metamorphosis. The molecular mechanisms of JH regulation in insect vitellogenesis and oogenesis are largely obscure. The membrane receptor of JH remains to be identified. The roles of JH and 20E in insect reproduction vary across insect orders and even among genera, it is of interest to unveil the evolutionary aspects of hormonal regulation in insect vitellogenesis. In addition, AA/TOR and ILP pathways play pivotal roles in insect vitellogenesis by way of direct regulation or interaction with JH signaling cascade (Parthasarathy and Palli, 2011; Abrisqueta et al., 2014; Roy et al., 2018; Zhu et al., 2020). Moreover, an increasing body of evidence supports the importance of miRNA regulation in insect vitellogenesis. Likewise, miRNAs can interact with JH pathway and modulate JH production, consequently regulating insect vitellogenesis (Roy et al., 2018; Song and Zhou, 2020). Interestingly, JH, miRNAs and cognate genes constitute the regulatory loop and coordinately control Vg synthesis (Song et al., 2018, 2019). Therefore, the molecular basis of JH, miRNA and nutritional pathway crosstalk in regulating insect Vg synthesis and uptake requires further exploration. Furthermore, the involvement of other epigenetic and posttranscriptional regulators in insect vitellogenesis need to be dissected. Currently, studies on Vg secretion from the fat body into the hemolymph and Vg uptake in the ovary are limited. Future discovery of new players in JH-dependent patency initiation in the follicular epithelium and VgR-mediated endocytosis in the oocytes will help construct the regulatory networks controlling insect vitellogenesis and egg production.

AUTHOR CONTRIBUTIONS

ZW, LY, and QH collected the references. ZW, LY and SZ wrote the manuscript. All authors contributed to the article and approved the submitted version.

FUNDING

This work was supported by National Natural Science Foundation of China (NSFC) (31630070 and 31702062).

SUPPLEMENTARY MATERIAL

The Supplementary Material for this article can be found online at: https://www.frontiersin.org/articles/10.3389/fcell.2020.593613/full#supplementary-material

Supplementary Table 1 | Identification of Vg genes in insects.

REFERENCES

Abrisqueta, M., Suren-Castillo, S., and Maestro, J. L. (2014). Insulin receptor-mediated nutritional signalling regulates juvenile hormone biosynthesis and vitellogenin production in the German cockroach. *Insect Biochem. Mol. Biol.* 49, 14–23. doi: 10.1016/j.ibmb.2014.03.005

Al Baki, M. A., Lee, D. W., Jung, J. K., and Kim, Y. (2019). Insulin signaling mediates previtellogenic development and enhances juvenile hormone-mediated vitellogenesis in a lepidopteran insect, *Maruca vitrata*. *BMC Dev. Biol.* 19:14. doi: 10.1186/s12861-019-0194-8

Amdam, G. V., Norberg, K., Page, R. E. Jr., Erber, J., and Scheiner, R. (2006). Downregulation of vitellogenin gene activity increases the gustatory responsiveness of honey bee workers (*Apis mellifera*). *Behav. Brain Res.* 169, 201–205. doi: 10.1016/j.bbr.2006.01.006

Asgari, S. (2013). MicroRNA functions in insects. *Insect Biochem. Mol. Biol.* 43, 388–397. doi: 10.1016/j.ibmb.2012.10.005

Azzam, G., Smibert, P., Lai, E. C., and Liu, J. L. (2012). *Drosophila* Argonaute 1 and its miRNA biogenesis partners are required for oocyte formation and germline cell division. *Dev. Biol.* 365, 384–394. doi: 10.1016/j.ydbio.2012.03.005

Badisco, L., Van Wielendaele, P., and Vanden Broeck, J. (2013). Eat to reproduce: a key role for the insulin signaling pathway in adult insects. *Front. Physiol.* 4:202. doi: 10.3389/fphys.2013.00202

Bai, H., and Palli, S. R. (2016). Identification of G protein-coupled receptors required for vitellogenin uptake into the oocytes of the red flour beetle, *Tribolium castaneum*. *Sci. Rep.* 6:27648. doi: 10.1038/srep27648

Bai, H., Qiao, H., Li, F., Fu, H., Sun, S., Zhang, W., et al. (2015). Molecular characterization and developmental expression of vitellogenin in the oriental river prawn *Macrobrachium nipponense* and the effects of RNA

interference and eyestalk ablation on ovarian maturation. *Gene* 562, 22–31. doi: 10.1016/j.gene.2014.12.008

Belles, X. (2004). "Vitellogenesis directed by juvenile hormone," in *Reproductive Biology of Invertebrates*, ed A. S. Raikhel (Enfield/Plymouth: Science Publisher, Inc.), 157–197.

Berger, E. M., and Dubrovsky, E. B. (2005). Juvenile hormone molecular actions and interactions during development of *Drosophila melanogaster*. *Vitam. Horm*. 73, 175–215. doi: 10.1016/S0083-6729(05)73006-5

Bownes, M. (1990). The yolk proteins and their genes in Drosophila. *Prog. Clin. Biol. Res*. 342, 336–342.

Bryant, B., Macdonald, W., and Raikhel, A. S. (2010). microRNA miR-275 is indispensable for blood digestion and egg development in the mosquito *Aedes aegypti*. *Proc. Natl. Acad. Sci. U. S. A*. 107, 22391–22398. doi: 10.1073/pnas.1016230107

Carney, G. E., and Bender, M. (2000). The *Drosophila ecdysone receptor* (*EcR*) gene is required maternally for normal oogenesis. *Genetics* 154, 1203–1211.

Carpenter, V. K., Drake, L. L., Aguirre, S. E., Price, D. P., Rodriguez, S. D., and Hansen, I. A. (2012). SLC7 amino acid transporters of the yellow fever mosquito *Aedes aegypti* and their role in fat body TOR signaling and reproduction. *J. Insect Physiol*. 58, 513–522. doi: 10.1016/j.jinsphys.2012.01.005

Charles, J. P., Iwema, T., Epa, V. C., Takaki, K., Rynes, J., and Jindra, M. (2011). Ligand-binding properties of a juvenile hormone receptor, Methoprene-tolerant. *Proc. Natl. Acad. Sci. U. S. A*. 108, 21128–21133. doi: 10.1073/pnas.1116123109

Chen, E., Chen, Z., Li, S., Xing, D., Guo, H., Liu, J., et al. (2020). bmo-miR-2739 and the novel microRNA miR-167 coordinately regulate the expression of the vitellogenin receptor in *Bombyx mori* oogenesis. *Development* 147:dev183723. doi: 10.1242/dev.183723

Chen, M. E., Lewis, D. K., Keeley, L. L., and Pietrantonio, P. V. (2004). cDNA cloning and transcriptional regulation of the vitellogenin receptor from the imported fire ant, *Solenopsis invicta* Buren (Hymenoptera: Formicidae). *Insect Mol. Biol*. 13, 195–204. doi: 10.1111/j.0962-1075.2004.00477.x

Cong, L., Yang, W. J., Jiang, X. Z., Niu, J. Z., Shen, G. M., Ran, C., et al. (2015). The essential role of vitellogenin receptor in ovary development and vitellogenin uptake in *Bactrocera dorsalis* (Hendel). *Int. J. Mol. Sci*. 16, 18368–18383. doi: 10.3390/ijms160818368

Corona, M., Libbrecht, R., Wurm, Y., Riba-Grognuz, O., Studer, R. A., and Keller, L. (2013). Vitellogenin underwent subfunctionalization to acquire caste and behavioral specific expression in the harvester ant *Pogonomyrmex barbatus*. *PLoS Genet*. 9:e1003730. doi: 10.1371/journal.pgen.1003730

Corona, M., Velarde, R. A., Remolina, S., Moran-Lauter, A., Wang, Y., Hughes, K. A., et al. (2007). Vitellogenin, juvenile hormone, insulin signaling, and queen honey bee longevity. *Proc. Natl. Acad. Sci. U. S. A*. 104, 7128–7133. doi: 10.1073/pnas.0701909104

Dhara, A., Eum, J. H., Robertson, A., Gulia-Nuss, M., Vogel, K. J., Clark, K. D., et al. (2013). Ovary ecdysteroidogenic hormone functions independently of the insulin receptor in the yellow fever mosquito, *Aedes aegypti*. *Insect Biochem. Mol. Biol*. 43, 1100–1108. doi: 10.1016/j.ibmb.2013.09.004

Elmogy, M., Elgendy, A. M., and Takeda, M. (2014). Detection of small GTP binding proteins showing GTPase and GTP/ATP binding activities in the ovary of the American Cockroach, Periplaneta Americana, during oogenesis. *Am. J. BioSci.* 2:106. doi: 10.11648/j.ajbio.20140203.15

Fambrough, D. M., Lemas, M. V., Hamrick, M., Emerick, M., Renaud, K. J., Inman, E. M., et al. (1994). Analysis of subunit assembly of the Na-K-ATPase. *Am. J. Physiol.-Cell Physiol.* 266:C579-89. doi: 10.1152/ajpcell.1994.266.3.C579

Fu, X., Dimopoulos, G., and Zhu, J. (2017). Association of microRNAs with Argonaute proteins in the malaria mosquito *Anopheles gambiae* after blood ingestion. *Sci. Rep*. 7:6493. doi: 10.1038/s41598-017-07013-1

Fu, X., Li, T., Chen, J., Dong, Y., Qiu, J., Kang, K., et al. (2015). Functional screen for microRNAs of *Nilaparvata lugens* reveals that targeting of glutamine synthase by miR-4868b regulates fecundity. *J. Insect Physiol*. 83, 22–29. doi: 10.1016/j.jinsphys.2015.11.003

Fujiwara, Y., Tanaka, Y., Iwata, K., Rubio, R. O., Yaginuma, T., Yamashita, O., et al. (2006). ERK/MAPK regulates ecdysteroid and sorbitol metabolism for embryonic diapause termination in the silkworm, *Bombyx mori*. *J. Insect Physiol.* 52, 569–575. doi: 10.1016/j.jinsphys.2006.02.004

Garcia, J., Munro, E. S., Monte, M. M., Fourrier, M. C., Whitelaw, J., Smail, D. A., et al. (2010). Atlantic salmon (Salmo salar L.) serum vitellogenin neutralises infectivity of infectious pancreatic necrosis virus (IPNV). *Fish Shellfish Immunol.* 29, 293–297. doi: 10.1016/j.fsi.2010.04.010

Gilbert, L. I., Serafin, R. B., Watkins, N. L., and Richard, D. S. (1998). Ecdysteroids regulate yolk protein uptake by *Drosophila melanogaster* oocytes. *J. Insect Physiol*. 44, 637–644. doi: 10.1016/S0022-1910(98)00020-1

Gujar, H., and Palli, S. R. (2016). Juvenile hormone regulation of female reproduction in the common bed bug, *Cimex lectularius*. *Sci. Rep*. 6:35546. doi: 10.1038/srep35546

Guo, W., Wu, Z., Song, J., Jiang, F., Wang, Z., Deng, S., et al. (2014). Juvenile hormone-receptor complex acts on *mcm4* and *mcm7* to promote polyploidy and vitellogenesis in the migratory locust. *PLoS Genet*. 10:e1004702. doi: 10.1371/journal.pgen.1004702

Guo, W., Wu, Z., Yang, L., Cai, Z., Zhao, L., and Zhou, S. (2019). Juvenile hormone-dependent Kazal-type serine protease inhibitor Greglin safeguards insect vitellogenesis and egg production. *FASEB J*. 33, 917–927. doi: 10.1096/fj.201801068R

Guo, Y., Hoffmann, A. A., Xu, X. Q., Mo, P. W., Huang, H. J., Gong, J. T., et al. (2018). Vertical transmission of *Wolbachia* is associated with host vitellogenin in *Laodelphax striatellus*. *Front. Microbiol*. 9:2016. doi: 10.3389/fmicb.2018.02016

Hansen, I. A., Attardo, G. M., Park, J. H., Peng, Q., and Raikhel, A. S. (2004). Target of rapamycin-mediated amino acid signaling in mosquito anautogeny. *Proc. Natl. Acad. Sci. U. S. A*. 101, 10626–10631. doi: 10.1073/pnas.0403460101

Hansen, I. A., Attardo, G. M., Rodriguez, S. D., and Drake, L. L. (2014). Four-way regulation of mosquito yolk protein precursor genes by juvenile hormone-, ecdysone-, nutrient-, and insulin-like peptide signaling pathways. *Front. Physiol*. 5:103. doi: 10.3389/fphys.2014.00103

Hansen, I. A., Sieglaff, D. H., Munro, J. B., Shiao, S. H., Cruz, J., Lee, I. W., et al. (2007). Forkhead transcription factors regulate mosquito reproduction. *Insect Biochem. Mol. Biol*. 37, 985–997. doi: 10.1016/j.ibmb.2007.05.008

He, J., Chen, Q., Wei, Y., Jiang, F., Yang, M., Hao, S., et al. (2016). MicroRNA-276 promotes egg-hatching synchrony by up-regulating *brm* in locusts. *Proc. Natl. Acad. Sci. U. S. A*. 113, 584–589. doi: 10.1073/pnas.1521098113

He, K., Lin, K., Ding, S., Wang, G., and Li, F. (2019). The vitellogenin receptor has an essential role in vertical transmission of rice stripe virus during oogenesis in the small brown plant hopper. *Pest Manag. Sci*. 75, 1370–1382. doi: 10.1002/ps.5256

Hu, K., Tian, P., Tang, Y., Yang, L., Qiu, L., He, H., et al. (2019). Molecular characterization of vitellogenin and its receptor in *Sogatella furcifera*, and their function in oocyte maturation. *Front. Physiol*. 10:1532. doi: 10.3389/fphys.2019.01532

Huo, Y., Yu, Y., Chen, L., Li, Q., Zhang, M., Song, Z., et al. (2018). Insect tissue-specific vitellogenin facilitates transmission of plant virus. *PLoS Pathog.* 14:e1006909. doi: 10.1371/journal.ppat.1006909

Huo, Y., Yu, Y., Liu, Q., Liu, D., Zhang, M., Liang, J., et al. (2019). Rice stripe virus hitchhikes the vector insect vitellogenin ligand-receptor pathway for ovary entry. *Philos. Trans. R. Soc. Lond. B Biol. Sci*. 374:20180312. doi: 10.1098/rstb.2018.0312

Ihle, K. E., Fondrk, M. K., Page, R. E., and Amdam, G. V. (2015). Genotype effect on lifespan following vitellogenin knockdown. *Exp. Gerontol*. 61, 113–122. doi: 10.1016/j.exger.2014.12.007

Irles, P., Ramos, S., and Piulachs, M. D. (2017). SPARC preserves follicular epithelium integrity in insect ovaries. *Dev. Biol*. 422, 105–114. doi: 10.1016/j.ydbio.2017.01.005

Irles, P., Silva-Torres, F. A., and Piulachs, M. D. (2013). RNAi reveals the key role of Nervana 1 in cockroach oogenesis and embryo development. *Insect Biochem. Mol. Biol*. 43, 178–188. doi: 10.1016/j.ibmb.2012.12.003

Iwata, K., Shindome, C., Kobayashi, Y., Takeda, M., Yamashita, O., Shiomi, K., et al. (2005). Temperature-dependent activation of ERK/MAPK in yolk cells and its role in embryonic diapause termination in the silkworm *Bombyx mori*. *J. Insect Physiol*. 51, 1306–1312. doi: 10.1016/j.jinsphys.2005.07.009

Jin, Z., and Xie, T. (2007). Dcr-1 maintains *Drosophila* ovarian stem cells. *Curr. Biol*. 17, 539–544. doi: 10.1016/j.cub.2007.01.050

Jindra, M., Belles, X., and Shinoda, T. (2015). Molecular basis of juvenile hormone signaling. *Curr. Opin. Insect Sci*. 11, 39–46. doi: 10.1016/j.cois.2015.08.004

Jindra, M., Palli, S. R., and Riddiford, L. M. (2013). The juvenile hormone signaling pathway in insect development. *Annu. Rev. Entomol*. 58, 181–204. doi: 10.1146/annurev-ento-120811-153700

Jing, Y. P., An, H., Zhang, S., Wang, N., and Zhou, S. (2018). Protein kinase C mediates juvenile hormone-dependent phosphorylation of Na(+)/K(+)-ATPase to induce ovarian follicular patency for yolk protein uptake. *J. Biol. Chem*. 293, 20112–20122. doi: 10.1074/jbc.RA118.005692

Kamruzzaman, A. S. M., Mikani, A., Mohamed, A. A., Elgendy, A. M., and Takeda, M. (2020). Crosstalk among indoleamines, neuropeptides and JH/20E in regulation of reproduction in the American Cockroach, *Periplaneta americana*. *Insects* 11:155. doi: 10.3390/insects11030155

Kaplan, J. H. (2002). Biochemistry of Na,K-ATPase. *Annu. Rev. Biochem*. 71, 511–535. doi: 10.1146/annurev.biochem.71.102201.141218

Kayukawa, T., Minakuchi, C., Namiki, T., Togawa, T., Yoshiyama, M., Kamimura, M., et al. (2012). Transcriptional regulation of juvenile hormone-mediated induction of Krüppel homolog 1, a repressor of insect metamorphosis. *Proc. Natl. Acad. Sci. U. S. A*. 109, 11729–11734. doi: 10.1073/pnas.1204951109

Koyama, T., Mendes, C. C., and Mirth, C. K. (2013). Mechanisms regulating nutrition-dependent developmental plasticity through organ-specific effects in insects. *Front. Physiol*. 4:263. doi: 10.3389/fphys.2013.00263

Lee, K. Y., Yoon, H. J., and Jin, B. R. (2015). *Osmia cornifrons* vitellogenin: cDNA cloning, structural analysis and developmental expression. *Entomol. Res*. 45, 94–101. doi: 10.1111/1748-5967.12098

Lenaerts, C., Monjon, E., Van Lommel, J., Verbakel, L., and Vanden Broeck, J. (2019). Peptides in insect oogenesis. *Curr. Opin. Insect Sci*. 31, 58–64. doi: 10.1016/j.cois.2018.08.007

Li, K. L., Wan, P. J., Wang, W. X., Lai, F. X., and Fu, Q. (2015). Ran involved in the development and reproduction is a potential target for rna-interference-based pest management in *Nilaparvata lugens*. *PLoS ONE* 10:e0142142. doi: 10.1371/journal.pone.0142142

Li, M., Mead, E. A., and Zhu, J. (2011). Heterodimer of two bHLH-PAS proteins mediates juvenile hormone-induced gene expression. *Proc. Natl. Acad. Sci. U. S. A*. 108, 638–643. doi: 10.1073/pnas.1013914108

Lin, X., Yao, Y., and Wang, B. (2015). Methoprene-tolerant (Met) and Krüpple-homologue 1 (Kr-h1) are required for ovariole development and egg maturation in the brown plant hopper. *Sci. Rep*. 5:18064. doi: 10.1038/srep18064

Lingrel, J. B., and Kuntzweiler, T. (1994). Na+,K(+)-ATPase. *J. Biol. Chem*. 269, 19659–19662.

Liu, P., Fu, X., and Zhu, J. (2018). Juvenile hormone-regulated alternative splicing of the *taiman* gene primes the ecdysteroid response in adult mosquitoes. *Proc. Natl. Acad. Sci. U. S. A*. 115, E7738–E7747. doi: 10.1073/pnas.1808146115

Liu, P., Peng, H. J., and Zhu, J. (2015). Juvenile hormone-activated phospholipase C pathway enhances transcriptional activation by the methoprene-tolerant protein. *Proc. Natl. Acad. Sci. U. S. A*. 112, E1871–1879. doi: 10.1073/pnas.1423204112

Liu, S., Lucas, K. J., Roy, S., Ha, J., and Raikhel, A. S. (2014). Mosquito-specific microRNA-1174 targets serine hydroxymethyltransferase to control key functions in the gut. *Proc. Natl. Acad. Sci. U. S. A*. 111, 14460–14465. doi: 10.1073/pnas.1416278111

Liu, W., Guo, S., Sun, D., Zhu, L., Zhu, F., Lei, C. L., et al. (2019). Molecular characterization and juvenile hormone-regulated transcription of the vitellogenin receptor in the cabbage beetle *Colaphellus bowringi*. *Comp. Biochem. Physiol. Part A Mol. Integr. Physiol*. 229, 69–75. doi: 10.1016/j.cbpa.2018.12.004

Lu, K., Chen, X., Liu, W. T., and Zhou, Q. (2016). TOR pathway-mediated juvenile hormone synthesis regulates nutrient-dependent female reproduction in *Nilaparvata lugens* (Stål). *Int. J. Mol. Sci*. 17:438. doi: 10.3390/ijms17040438

Lu, K., Shu, Y., Zhou, J., Zhang, X., Zhang, X., Chen, M., et al. (2015). Molecular characterization and RNA interference analysis of vitellogenin receptor from *Nilaparvata lugens* (Stål). *J. Insect Physiol*. 73, 20–29. doi: 10.1016/j.jinsphys.2015.01.007

Lucas, K. J., Roy, S., Ha, J., Gervaise, A. L., Kokoza, V. A., and Raikhel, A. S. (2015a). MicroRNA-8 targets the Wingless signaling pathway in the female mosquito fat body to regulate reproductive processes. *Proc. Natl. Acad. Sci. U. S. A*. 112, 1440–1445. doi: 10.1073/pnas.1424408112

Lucas, K. J., Zhao, B., Roy, S., Gervaise, A. L., and Raikhel, A. S. (2015b). Mosquito-specific microRNA-1890 targets the juvenile hormone-regulated serine protease JHA15 in the female mosquito gut. *RNA Biol*. 12, 1383–1390. doi: 10.1080/15476286.2015.1101525

Luo, M., Li, D., Wang, Z., Guo, W., Kang, L., and Zhou, S. (2017). Juvenile hormone differentially regulates two *Grp78* genes encoding protein chaperones required for insect fat body cell homeostasis and vitellogenesis. *J. Biol. Chem*. 292, 8823–8834. doi: 10.1074/jbc.M117.780957

Ma, L., Zhang, W., Liu, C., Chen, L., Xu, Y., Xiao, H., et al. (2018). Methoprene-tolerant (Met) is indispensable for larval metamorphosis and female reproduction in the cotton bollworm *Helicoverpa armigera*. *Front. Physiol*. 9:1601. doi: 10.3389/fphys.2018.01601

Matsumoto, T., Yamano, K., Kitamura, M., and Hara, A. (2008). Ovarian follicle cells are the site of vitellogenin synthesis in the Pacific abalone *Haliotis discus hannai*. *Comp. Biochem. Physiol. Part A Mol. Integr. Physiol*. 149, 293–298. doi: 10.1016/j.cbpa.2008.01.003

Melo, A. C., Valle, D., Machado, E. A., Salerno, A. P., Paiva-Silva, G. O., Cunha, E. S. N. L., et al. (2000). Synthesis of vitellogenin by the follicle cells of *Rhodnius prolixus*. *Insect Biochem. Mol. Biol*. 30, 549–557. doi: 10.1016/S0965-1748(00)00023-0

Mitchell, R. D. III, Sonenshine, D. E., and Pérez De León, A. A. (2019). Vitellogenin receptor as a target for tick control: a mini-review. *Front. Physiol*. 10:618. doi: 10.3389/fphys.2019.00618

Morandin, C., Havukainen, H., Kulmuni, J., Dhaygude, K., Trontti, K., and Helantera, H. (2014). Not only for egg yolk–functional and evolutionary insights from expression, selection, and structural analyses of Formica ant vitellogenins. *Mol. Biol. Evol*. 31, 2181–2193. doi: 10.1093/molbev/msu171

Ojani, R., Fu, X., Ahmed, T., Liu, P., and Zhu, J. (2018). Krüppel homologue 1 acts as a repressor and an activator in the transcriptional response to juvenile hormone in adult mosquitoes. *Insect Mol. Biol*. 27, 268–278. doi: 10.1111/imb.12370

Ojani, R., Liu, P., Fu, X., and Zhu, J. (2016). Protein kinase C modulates transcriptional activation by the juvenile hormone receptor methoprene-tolerant. *Insect Biochem. Mol. Biol*. 70, 44–52. doi: 10.1016/j.ibmb.2015.12.001

Parthasarathy, R., and Palli, S. R. (2011). Molecular analysis of nutritional and hormonal regulation of female reproduction in the red flour beetle, *Tribolium castaneum*. *Insect Biochem. Mol. Biol*. 41, 294–305. doi: 10.1016/j.ibmb.2011.01.006

Parthasarathy, R., Sheng, Z., Sun, Z., and Palli, S. R. (2010a). Ecdysteroid regulation of ovarian growth and oocyte maturation in the red flour beetle, *Tribolium castaneum*. *Insect Biochem. Mol. Biol*. 40, 429–439. doi: 10.1016/j.ibmb.2010.04.002

Parthasarathy, R., Sun, Z., Bai, H., and Palli, S. R. (2010b). Juvenile hormone regulation of vitellogenin synthesis in the red flour beetle, *Tribolium castaneum*. *Insect Biochem. Mol. Biol*. 40, 405–414. doi: 10.1016/j.ibmb.2010.03.006

Peng, L., Wang, L., Zou, M. M., Vasseur, L., Chu, L. N., Qin, Y. D., et al. (2019). Identification of halloween genes and RNA interference-mediated functional characterization of a halloween gene shadow in *Plutella xylostella*. *Front. Physiol*. 10:1120. doi: 10.3389/fphys.2019.01120

Pszczolkowski, M. A., Olson, E., Rhine, C., and Ramaswamy, S. B. (2008). Role for calcium in the development of ovarial patency in *Heliothis virescens*. *J. Insect Physiol*. 54, 358–366. doi: 10.1016/j.jinsphys.2007.10.005

Pszczolkowski, M. A., Peterson, A., Srinivasan, A., and Ramaswamy, S. B. (2005). Pharmacological analysis of ovarial patency in *Heliothis virescens*. *J. Insect Physiol*. 51, 445–453. doi: 10.1016/j.jinsphys.2005.01.008

Raikhel, A. S., Brown, M. R., and Belles, X. (2005). "Hormonal control of reproductive processes," in *Comprehensive Molecular Insect Science,* eds. L. I. Gilbert, K. Iatrou, and S. S. Gill (Boston: Elsevier), 433–491. doi: 10.1016/B0-44-451924-6/00040-5

Raikhel, A. S., and Dhadialla, T. S. (1992). Accumulation of yolk proteins in insect oocytes. *Annu. Rev. Entomol*. 37, 217–251. doi: 10.1146/annurev.en.37.010192.001245

Raikhel, A. S., Kokoza, V. A., Zhu, J., Martin, D., Wang, S. F., Li, C., et al. (2002). Molecular biology of mosquito vitellogenesis: from basic studies to genetic engineering of antipathogen immunity. *Insect Biochem. Mol. Biol*. 32, 1275–1286. doi: 10.1016/S0965-1748(02)00090-5

Roy, S., Saha, T. T., Zou, Z., and Raikhel, A. S. (2018). Regulatory pathways controlling female insect reproduction. *Annu. Rev. Entomol*. 63, 489–511. doi: 10.1146/annurev-ento-020117-043258

Saha, T. T., Roy, S., Pei, G., Dou, W., Zou, Z., and Raikhel, A. S. (2019). Synergistic action of the transcription factors Krüppel homolog 1 and Hairy in juvenile

hormone/Methoprene-tolerant-mediated gene-repression in the mosquito *Aedes aegypti*. *PLoS Genet*. 15:e1008443. doi: 10.1371/journal.pgen.1008443

Salmela, H., Amdam, G. V., and Freitak, D. (2015). Transfer of immunity from mother to offspring is mediated via egg-yolk protein vitellogenin. *PLoS Pathog*. 11:e1005015. doi: 10.1371/journal.ppat.1005015

Sancak, Y., Peterson, T. R., Shaul, Y. D., Lindquist, R. A., Thoreen, C. C., Bar-Peled, L., et al. (2008). The Rag GTPases bind raptor and mediate amino acid signaling to mTORC1. *Science* 320, 1496–1501. doi: 10.1126/science.1157535

Santos, C. G., Humann, F. C., and Hartfelder, K. (2019). Juvenile hormone signaling in insect oogenesis. *Curr. Opin. Insect Sci*. 31, 43–48. doi: 10.1016/j.cois.2018.07.010

Sappington, T. W., and Raikhel, A. S. (1998). Molecular characteristics of insect vitellogenins and vitellogenin receptors. *Insect Biochem. Mol. Biol*. 28, 277–300. doi: 10.1016/S0965-1748(97)00110-0

Schonbaum, C., Lee, S., and Mahowald, A. P. (1995). The Drosophila yolkless gene encodes a vitellogenin receptor belonging to the low density lipoprotein receptor superfamily. *Proc. Natl. Acad. Sci. U. S. A*. 92, 1485–1489. doi: 10.1073/pnas.92.5.1485

Seehuus, S. C., Norberg, K., Gimsa, U., Krekling, T., and Amdam, G. V. (2006). Reproductive protein protects functionally sterile honey bee workers from oxidative stress. *Proc. Natl. Acad. Sci. U. S. A*. 103, 962–967. doi: 10.1073/pnas.0502681103

Sevala, V. L., and Davey, K. G. (1989). Action of juvenile hormone on the follicle cells of *Rhodnius prolixus*: evidence for a novel regulatory mechanism involving protein kinase C. *Experientia* 45, 355–356. doi: 10.1007/BF01957476

Sevala, V. L., and Davey, K. G. (1993). Juvenile hormone dependent phosphorylation of a 100 kDa polypeptide is mediated by protein kinase C in the follicle cells of *Rhodnius prolixus*. *Invert. Reprod. Dev*. 23, 189–193. doi: 10.1080/07924259.1993.9672314

Shcherbata, H. R. (2019). miRNA functions in stem cells and their niches: lessons from the Drosophila ovary. *Curr. Opin. Insect Sci*. 31, 29–36. doi: 10.1016/j.cois.2018.07.006

Sheng, Z., Xu, J., Bai, H., Zhu, F., and Palli, S. R. (2011). Juvenile hormone regulates vitellogenin gene expression through insulin-like peptide signaling pathway in the red flour beetle, *Tribolium castaneum*. *J. Biol. Chem*. 286, 41924–41936. doi: 10.1074/jbc.M111.269845

Shin, S. W., Zou, Z., Saha, T. T., and Raikhel, A. S. (2012). bHLH-PAS heterodimer of methoprene-tolerant and Cycle mediates circadian expression of juvenile hormone-induced mosquito genes. *Proc. Natl. Acad. Sci. U. S. A*. 109, 16576–16581. doi: 10.1073/pnas.1214209109

Shpigler, H., Amsalem, E., Huang, Z. Y., Cohen, M., Siegel, A. J., Hefetz, A., et al. (2014). Gonadotropic and physiological functions of juvenile hormone in Bumblebee (*Bombus terrestris*) workers. *PLoS ONE* 9:e100650. doi: 10.1371/journal.pone.0100650

Smykal, V., Bajgar, A., Provaznik, J., Fexova, S., Buricova, M., Takaki, K., et al. (2014). Juvenile hormone signaling during reproduction and development of the linden bug, *Pyrrhocoris apterus*. *Insect Biochem. Mol. Biol*. 45, 69–76. doi: 10.1016/j.ibmb.2013.12.003

Smykal, V., and Raikhel, A. S. (2015). Nutritional control of insect reproduction. *Curr. Opin. Insect Sci*. 11, 31–38. doi: 10.1016/j.cois.2015.08.003

Snigirevskaya, E. S., and Raikhel, A. S. (2005). "Receptor-mediated endocytosis of yolkproteins in insect oocytes," in *Progress in Vitellogenesis. Reproductive Biology of Invertebrates*, eds A. S. Raikhel and T. W. Sappington (Enfield; Plymouth: Science Publishers, Inc), 199–228.

Song, J., Guo, W., Jiang, F., Kang, L., and Zhou, S. (2013). Argonaute 1 is indispensable for juvenile hormone mediated oogenesis in the migratory locust, *Locusta migratoria*. *Insect Biochem. Mol. Biol*. 43, 879–887. doi: 10.1016/j.ibmb.2013.06.004

Song, J., Li, W., Zhao, H., Gao, L., Fan, Y., and Zhou, S. (2018). The microRNAs let-7 and miR-278 regulate insect metamorphosis and oogenesis by targeting the juvenile hormone early-response gene Krüppel-homolog 1. *Development* 145:dev170670. doi: 10.1242/dev.170670

Song, J., Li, W., Zhao, H., and Zhou, S. (2019). Clustered miR-2, miR-13a, miR-13b and miR-71 coordinately target *Notch* gene to regulate oogenesis of the migratory locust *Locusta migratoria*. *Insect Biochem. Mol. Biol*. 106, 39–46. doi: 10.1016/j.ibmb.2018.11.004

Song, J., Wu, Z., Wang, Z., Deng, S., and Zhou, S. (2014). Krüppel-homolog 1 mediates juvenile hormone action to promote vitellogenesis and oocyte maturation in the migratory locust. *Insect Biochem. Mol. Biol*. 52, 94–101. doi: 10.1016/j.ibmb.2014.07.001

Song, J., and Zhou, S. (2020). Post-transcriptional regulation of insect metamorphosis and oogenesis. *Cell. Mol. Life Sci*. 77, 1893–1909. doi: 10.1007/s00018-019-03361-5

Suren-Castillo, S., Abrisqueta, M., and Maestro, J. L. (2012). FoxO inhibits juvenile hormone biosynthesis and vitellogenin production in the German cockroach. *Insect Biochem. Mol. Biol*. 42, 491–498. doi: 10.1016/j.ibmb.2012.03.006

Swevers, L. (2019). An update on ecdysone signaling during insect oogenesis. *Curr. Opin. Insect Sci*. 31, 8–13. doi: 10.1016/j.cois.2018.07.003

Swevers, L., and Iatrou, K. (2003). The ecdysone regulatory cascade and ovarian development in lepidopteran insects: insights from the silkmoth paradigm. *Insect Biochem. Mol. Biol*. 33, 1285–1297. doi: 10.1016/j.ibmb.2003.06.012

Tanaka, E. D., and Piulachs, M. D. (2012). Dicer-1 is a key enzyme in the regulation of oogenesis in panoistic ovaries. *Biol. Cell*. 104, 452–461. doi: 10.1111/boc.201100044

Tang, Y., He, H., Qu, X., Cai, Y., Ding, W., Qiu, L., et al. (2020). RNA interference-mediated knockdown of the transcription factor Kruppel homologue 1 suppresses vitellogenesis in *Chilo suppressalis*. *Insect Mol. Biol*. 29, 183–192. doi: 10.1111/imb.12617

Telfer, W. H. (2009). Egg formation in lepidoptera. *J. Insect Sci*. 9, 1–21. doi: 10.1673/031.009.5001

Tu, M. P., Yin, C. M., and Tatar, M. (2002). Impaired ovarian ecdysone synthesis of *Drosophila melanogaster* insulin receptor mutants. *Aging Cell* 1, 158–160. doi: 10.1046/j.1474-9728.2002.00016.x

Tufail, M., and Takeda, M. (2008). Molecular characteristics of insect vitellogenins. *J. Insect Physiol*. 54, 1447–1458. doi: 10.1016/j.jinsphys.2008.08.007

Tufail, M., and Takeda, M. (2009). Insect vitellogenin/lipophorin receptors: molecular structures, role in oogenesis, and regulatory mechanisms. *J. Insect Physiol*. 55, 87–103. doi: 10.1016/j.jinsphys.2008.11.007

Van Hoef, V., Breugelmans, B., Spit, J., Simonet, G., Zels, S., and Vanden Broeck, J. (2013). Phylogenetic distribution of protease inhibitors of the Kazal-family within the Arthropoda. *Peptides* 41, 59–65. doi: 10.1016/j.peptides.2012.10.015

Vasudevan, S., Tong, Y., and Steitz, J. A. (2007). Switching from repression to activation: microRNAs can up-regulate translation. *Science* 318, 1931–1934. doi: 10.1126/science.1149460

Wang, J. L., Saha, T. T., Zhang, Y., Zhang, C., and Raikhel, A. S. (2017). Juvenile hormone and its receptor methoprene-tolerant promote ribosomal biogenesis and vitellogenesis in the *Aedes aegypti* mosquito. *J. Biol. Chem*. 292, 10306–10315. doi: 10.1074/jbc.M116.761387

Wang, Y., Baker, N., and Amdam, G. V. (2013). RNAi-mediated double gene knockdown and gustatory perception measurement in honey bees (*Apis mellifera*). *J. Vis. Exp*. 77:50446. doi: 10.3791/50446

Wang, Y., Brent, C. S., Fennern, E., and Amdam, G. V. (2012). Gustatory perception and fat body energy metabolism are jointly affected by vitellogenin and juvenile hormone in honey bees. *PLoS Genet*. 8:e1002779. doi: 10.1371/journal.pgen.1002779

Wang, Z., Yang, L., Song, J., Kang, L., and Zhou, S. (2017). An isoform of Taiman that contains a PRD-repeat motif is indispensable for transducing the vitellogenic juvenile hormone signal in *Locusta migratoria*. *Insect Biochem. Mol. Biol*. 82, 31–40. doi: 10.1016/j.ibmb.2017.01.009

Wu, Z., Guo, W., Xie, Y., and Zhou, S. (2016). Juvenile hormone activates the transcription of *cell-division-cycle 6* (*Cdc6*) for polyploidy-dependent insect vitellogenesis and oogenesis. *J. Biol. Chem*. 291, 5418–5427. doi: 10.1074/jbc.M115.698936

Wu, Z., Guo, W., Yang, L., He, Q., and Zhou, S. (2018). Juvenile hormone promotes locust fat body cell polyploidization and vitellogenesis by activating the transcription of *Cdk6* and *E2f1*. *Insect Biochem. Mol. Biol*. 102, 1–10. doi: 10.1016/j.ibmb.2018.09.002

Wu, Z., He, Q., Zeng, B., Zhou, H., and Zhou, S. (2020). Juvenile hormone acts through FoxO to promote *Cdc2* and *Orc5* transcription for polyploidy-dependent vitellogenesis. *Development* 147:dev188813. doi: 10.1242/dev.188813

Wyatt, G. R., and Davey, K. G. (1996). Cellular and molecular actions of juvenile hormone II. Roles of juvenile hormone in adult insects. *Adv. In. Insect Phys*. 26, 1–155. doi: 10.1016/S0065-2806(08)60030-2

Yang, M., Wei, Y., Jiang, F., Wang, Y., Guo, X., He, J., et al. (2014). MicroRNA-133 inhibits behavioral aggregation by controlling dopamine

synthesis in locusts. *PLoS Genet*. 10:e1004206. doi: 10.1371/journal.pgen.1004206

Yue, Y., Yang, R. L., Wang, W. P., Zhou, Q. H., Chen, E. H., Yuan, G. R., et al. (2018). Involvement of *Met* and *Kr-h1* in JH-Mediated Reproduction of Female *Bactrocera dorsalis* (Hendel). *Front. Physiol*. 9:482. doi: 10.3389/fphys.2018.00482

Zeng, B., Huang, Y., Xu, J., Shiotsuki, T., Bai, H., Palli, S. R., et al. (2017). The FOXO transcription factor controls insect growth and development by regulating juvenile hormone degradation in the silkworm, *Bombyx mori*. *J. Biol. Chem.* 292, 11659–11669. doi: 10.1074/jbc.M117.777797

Zhang, S., Dong, Y., and Cui, P. (2015). Vitellogenin is an immunocompetent molecule for mother and offspring in fish. *Fish Shellfish Immunol*. 46, 710–715. doi: 10.1016/j.fsi.2015.08.011

Zhang, X., Aksoy, E., Girke, T., Raikhel, A. S., and Karginov, F. V. (2017). Transcriptome-wide microRNA and target dynamics in the fat body during the gonadotrophic cycle of *Aedes aegypti*. *Proc. Natl. Acad. Sci. U. S. A.* 114, E1895–e1903. doi: 10.1073/pnas.1701474114

Zhang, X., Lu, K., and Zhou, Q. (2013). Dicer1 is crucial for the oocyte maturation of telotrophic ovary in *Nilaparvata lugens* (STÅL) (Hemiptera: Geometroidea). *Arch. Insect Biochem. Physiol*. 84, 194–208. doi: 10.1002/arch.21136

Zhao, J., Sun, Y., Xiao, L., Tan, Y., Jiang, Y., and Bai, L. (2018). Vitellogenin and vitellogenin receptor gene expression profiles in *Spodoptera exigua* are related to host plant suitability. *Pest Manag. Sci*. 74, 950–958. doi: 10.1002/ps.4794

Zheng, H., Zeng, B., Shang, T., and Zhou, S. (2020). Identification of G protein-coupled receptors required for vitellogenesis and egg development in an insect with panoistic ovary. *Insect Sci*. doi: 10.1111/1744-7917.12841

Zhou, X., Duan, X., Qian, J., and Li, F. (2009). Abundant conserved microRNA target sites in the 5'-untranslated region and coding sequence. *Genetica* 137, 159–164. doi: 10.1007/s10709-009-9378-7

Zhu, S., Liu, F., Zeng, H., Li, N., Ren, C., Su, Y., et al. (2020). Insulin/IGF signaling and TORC1 promote vitellogenesis via inducing juvenile hormone biosynthesis in the American cockroach. *Development* 147:dev188805. doi: 10.1242/dev.188805

Zou, Z., Saha, T. T., Roy, S., Shin, S. W., Backman, T. W., Girke, T., et al. (2013). Juvenile hormone and its receptor, methoprene-tolerant, control the dynamics of mosquito gene expression. *Proc. Natl. Acad. Sci. U. S. A.* 110, E2173–2181. doi: 10.1073/pnas.1305293110

Conflict of Interest: The authors declare that the research was conducted in the absence of any commercial or financial relationships that could be construed as a potential conflict of interest.

frontiers in Cell and Developmental Biology

ORIGINAL RESEARCH
published: 11 February 2021
doi: 10.3389/fcell.2020.628473

The Inflammasome Contributes to Depletion of the Ovarian Reserve During Aging in Mice

Carolina Lliberos[1], *Seng H. Liew*[1], *Ashley Mansell*[2] *and Karla J. Hutt*[1]*

[1] Department of Anatomy and Developmental Biology, Monash Biomedicine Discovery Institute, Monash University, Clayton, VIC, Australia, [2] Centre for Innate Immunity and Infectious Diseases, Hudson Institute of Medical Research, Clayton, VIC, Australia

Ovarian aging is a natural process characterized by follicular depletion and a reduction in oocyte quality, resulting in loss of ovarian function, cycle irregularity and eventually infertility and menopause. The factors that contribute to ovarian aging have not been fully characterized. Activation of the NLRP3 inflammasome has been implicated in age-associated inflammation and diminished function in several organs. In this study, we used *Asc*$^{-/-}$ and *Nlrp3*$^{-/-}$ mice to investigate the possibility that chronic low-grade systemic inflammation mediated by the inflammasome contributes to diminished ovarian reserves as females age. Pro-inflammatory cytokines, IL-6, IL-18, and TNF-α, were decreased in the serum of aging *Asc*$^{-/-}$ mice compared to WT. Within the ovary of reproductively aged *Asc*$^{-/-}$ mice, mRNA levels of major pro-inflammatory genes Tnfa, Il1a, and Il1b were decreased, and macrophage infiltration was reduced compared to age-matched WT controls. Notably, suppression of the inflammatory phenotype in *Asc*$^{-/-}$ mice was associated with retention of follicular reserves during reproductive aging. Similarly, the expression of intra-ovarian pro-inflammatory cytokines was reduced, and follicle numbers were significantly elevated, in aging *Nlrp3*$^{-/-}$ mice compared to WT controls. These data suggest that inflammasome-dependent inflammation contributes to the age-associated depletion of follicles and raises the possibility that ovarian aging could be delayed, and fertile window prolonged, by suppressing inflammatory processes in the ovary.

Keywords: inflammation, inflammasome, follicle, ovary, ovarian ageing, cytokine, NLRP3, ASC

OPEN ACCESS

Edited by:
Francesca Elizabeth Duncan, Northwestern University, United States

Reviewed by:
Barbara Vanderhyden, University of Ottawa, Canada
Michele Teresa Pritchard, University of Kansas Medical Center, United States
Jennifer Gerton, Stowers Institute for Medical Research, United States

***Correspondence:**
Karla J. Hutt
karla.hutt@monash.edu

Specialty section:
This article was submitted to Cellular Biochemistry, a section of the journal Frontiers in Cell and Developmental Biology

Received: *12 November 2020*
Accepted: *22 December 2020*
Published: *11 February 2021*

Citation:
Lliberos C, Liew SH, Mansell A and Hutt KJ (2021) The Inflammasome Contributes to Depletion of the Ovarian Reserve During Aging in Mice. Front. Cell Dev. Biol. 8:628473. doi: 10.3389/fcell.2020.628473

INTRODUCTION

Female fertility declines dramatically with age, primarily due to the loss of oocyte number and quality (Findlay et al., 2018). A woman's lifetime supply of oocytes is stored in her ovaries in structures called primordial follicles. Most primordial follicles are dormant, but a few at a time become activated to begin folliculogenesis, which is characterized by growth of the oocyte, plus the proliferation, and differentiation of the granulosa cells that support oocyte development. Folliculogenesis results in the cyclic production of female reproductive hormones that have important roles in pregnancy and female health, and ultimately culminates in the ovulation of a mature oocyte. After birth, the number of primordial follicles steadily declines as consequence of follicle recruitment, follicle atresia, and the normal aging process. Eventually the supply of healthy follicles becomes so low that females become infertile and undergo menopause. In addition to natural ovarian aging, follicles can be depleted much earlier than expected, leading to premature

ovarian insufficiency. Loss of ovarian function, as a consequence of either physiological or pathological processes, has serious and widespread health impacts for women, including infertility and increased risk of heart disease and osteoporotic fractures because of reduced hormone production (Broekmans et al., 2009). Despite this significance, the suite of molecular mechanisms underlying the normal age-specific decline in ovarian function, or the early loss of ovarian follicles, remain largely unknown.

Non-infectious chronic, low-grade inflammation, is a hallmark of the normal aging process, that underpins a range of age-related pathologies (Franceschi et al., 2000). It is proposed that damaged cells and macromolecules that accumulate with age act as "danger signals" detected by inflammasomes, multi-protein complexes employed by the innate immune system that proteolytically mature pro-IL-1β and pro-IL-18 into bioactive cytokines that induce sterile inflammation (Goldberg and Dixit, 2015). In addition to their beneficial roles, IL-1β and IL-18 also contribute to functional decline and disease during aging (Goldberg and Dixit, 2015; Xia et al., 2016). Accumulating evidence suggests that low grade chronic inflammation contributes to age-related functional decline. Several studies in mice have shown that disruption of the NLR Family Pyrin Domain Containing 3 (NLRP3) inflammasome reduces inflammation, prolongs the healthy lifespan and delays the aging process (Youm et al., 2013; Marín-Aguilar et al., 2020). NLRP3 is a sensor of molecules released by damaged cells (Danger Associated Molecular Patterns or DAMPs) and cellular stressors, most of which increase and accumulate with age (Franceschi and Campisi, 2014). When NLRP3 recognizes DAMPs, it engages the adaptor protein ASC (apoptosis-associated speck-like protein containing a CARD), which is present in other inflammasomes (e.g., AIM2), and the complex then recruits and matures the protease Caspase 1. This activated inflammasome then processes IL-1β and IL-18 precursors, which leads to secretion of the pro-inflammatory cytokines IL-1β and IL-18 (Goldberg and Dixit, 2015). Similar to *Nlrp3*$^{-/-}$ mice, ASC-deficient mice display dramatically reduced IL-18 and IL-1β levels in serum, and slowed functional aging (Youm et al., 2013). These studies strongly support a link between NLRP3 inflammasome-dependent inflammation and age-related functional decline.

The factors responsible for diminished fertility in older women are likely to be multifactorial and have not been fully elucidated. Intriguingly, a recent study showed that ovaries from reproductively old mice (equivalent to women aged 38–45) are fibrotic with characteristics of chronic inflammation, including the expression of inflammatory genes and proteins (Briley et al., 2016). Inflammasome complexes have been predominately studied in innate immune cells, including macrophages, monocytes, and neutrophils (Goldberg and Dixit, 2015). However, recent studies indicate that epithelial cells of different tissues can express active inflammasome complexes (Santana et al., 2016). In addition, the expression of both NLRP3 protein and the adaptor molecule ASC have been previously detected in the C57BL/6 mouse ovary (Zhang et al., 2019). ASC was detected in oocytes, theca cells, and stroma, whereas NLRP3 was localized to the oocytes, theca cells, follicular fluid, and stroma (Zhang et al., 2019). Furthermore, a recent publication has shown an age-associated accumulation of DAMPs (i.e., lipofuscin) in the ovarian tissue (Urzua et al., 2018). In this publication, Urzua et al. demonstrated an excessive accumulation of incompletely digested cell debris in the form of lipofuscin in reproductively aged mouse ovaries (Urzua et al., 2018). More recently, Rowley et al. reported that age-related DAMPs, such as low molecular weight (LMW) hyaluronan fragments, may be a potential driver of the age-associated inflammation characteristic of ovaries from reproductively old mice (Rowley et al., 2020). However, whether accumulation of LMW hyaluronan fragments occurs in advanced reproductively aged ovaries is still under investigation. Therefore, in this study, we investigated the hypothesis that chronic low-grade systemic and local inflammation mediated by the inflammasome contributes to loss of ovarian follicular reserves as females age. To do this, the systemic and intra-ovarian inflammatory phenotype were investigated, and immune cell populations and ovarian follicles were quantified in ASC- and NLRP3-deficient mice.

MATERIALS AND METHODS

Animals

Female C57BL/6J wild-type (WT), *Asc*$^{-/-}$ and *Nlrp3*$^{-/-}$ mice on a C57BL/6J background were housed in a temperature-controlled high-barrier facility (Monash University ARL) with a 12 h light-dark cycle and free access to mouse chow and water. All animal procedures and experiments were compliant with the NHMRC Australian Code of Practice for the Care and Use of Animals and approved by the Monash Animal Research Platform Animal Ethics Committee. *Asc*$^{-/-}$ and *Nlrp3*$^{-/-}$ mice have been previously described (Kanneganti et al., 2006; Ozoren et al., 2014). Animals were aged to 2 (young sexually mature) (WT $n = 6$, *Asc*$^{-/-}$ $n = 6$, *Nlrp3*$^{-/-}$ $n = 6$), 6 (adult peak fertility) (WT $n = 8$, A*sc*$^{-/-}$ $n = 8$, *Nlrp3*$^{-/-}$ $n = 8$), 12 (reproductively old) (WT $n = 11$, A*sc*$^{-/-}$ $n = 13$, *Nlrp3*$^{-/-}$ $n = 11$), and 18 months (extreme reproductively aged) (WT $n = 8$, A*sc*$^{-/-}$ $n = 6$, *Nlrp3*$^{-/-}$ $n = 4$), and ovaries and blood were collected. Age of mice was chosen based on previous publications (Finch et al., 1984; Kevenaar et al., 2006; Finch, 2014; Liew et al., 2014). Serum was obtained by centrifugation at 5,000 rpm for 5 min, then transferred to a sterile Eppendorf tube, and stored at −80°C. One ovary from each mouse was either fixed in Bouin's solution, frozen at −80°C or directly used for Flow Cytometry. For flow cytometric study, stage of estrous cycle was determined by vaginal cytology immediately after mice being sacrificed at 9 months of age and recorded in **Supplementary Table 1**. Vaginal smears were stained with Rapid Diff Stain Kit (Australian Biostain, ARD.K) and classified based on the different cell types present as previously described (Ora et al., 2015). For Bouin's, tissues were fixed overnight at 4°C, and then washed three times with 70% ethanol.

Gene Expression

One frozen ovary per mouse was homogenized using a Retsch mixer Mill MM 400. Total RNA was extracted using RNeasy

Mini kit (Qiagen, 74104) followed by DNase I treatment (Qiagen, 79254) to ensure the complete removal of any DNA contamination. RNA concentration and purity were measured using the NanoDrop 2000 spectrophotometer (ThermoFisher Scientific). Five hundred nanogram of RNA were subsequently reverse transcribed to cDNA using a SuperScript III First-Strand synthesis kit (ThermoFisher Scientific, 18080051). A Bio-Rad CFX384 machine was used for quantitative real-time PCR using the 2x QuantiNova SYBR Green PCR Master Mix as described by the manufacturer (Qiagen, 208052). GAPDH was used as the endogenous control. Results are expressed as fold change in expression compared to 2-month-old WT mice and were calculated using the $2^{-\Delta\Delta Ct}$ method. The thermal cycling conditions used for 2x QuantiNova SYBR Green PCR Master Mix were 2 min at 95°C, followed by 40 cycles of 5 s at 95°C and 10 s at 60°C. The specificity of the process was controlled by Melting Curve analyses. The primers used in this study are detailed in **Supplementary Table 2**.

Histology

Bouin's-fixed ovaries were embedded and processed in Glycol Methacrylate (GMA) resin and serially sectioned at 20 μm. Every third resin section was collected, stained with Periodic Acid-Schiff (PAS) and counterstained with hematoxylin for follicle quantification and the assessment of ovarian volume.

Quantification of Ovarian Follicles

Primordial and primary follicle numbers were estimated using unbiased stereology, while number of growing and atretic follicles and corpora lutea numbers were quantified by direct counting under a Nikon light microscope, as previously described (Myers et al., 2004; Sarma et al., 2020; Winship et al., 2020).

Ovarian Volume

Ovarian volume was assessed using the Cavalieri Estimator function on the Stereo Investigator version 2018.2.2 software on an Olympus BX50 microscope with a 10x objective. Briefly, a point-counting grid with a density of 200 μm was used to estimate the area of every sixth section through the ovary. Final ovarian volume was calculated using the following equation: $\bigvee_{ov} = a\ (p)\, dt \sum_{i=1}^{n} P_i$, where $a\ (p)$ is the area associated with each grid point, d is the distance between two consecutive sections, t is the section thickness and $\sum_{i=1}^{n} P_i$ is the sum of all points counted in each section.

Quantifying Serum Anti-Müllerian Hormone

Serum anti-Müllerian hormone (AMH) concentration was determined using the commercially available AMH Gen II ELISA assay kit (Beckman Coulter, California, A79766) according to the manufacturer's instructions. AMH levels were measured for serum samples of 12-month-old WT ($n = 6$), $Asc^{-/-}$ ($n = 6$), and $Nlrp3^{-/-}$ mice ($n = 6$). Serum samples were assayed in duplicates and the absorbance was measured using the CLARIOstar microplate reader (BMG Labtechset, Ortenberg, Germany).

Cytokine Measurement

Serum IL-6, TNF-α, and IL-18 concentrations were measured by a specific murine ELISA kit [Biolegend, 431307 (IL-6) and 430907 (TNF-α) and Abcam, ab216165 (IL-18)] according to the manufacturer's instructions. Serum samples were assayed in duplicates and absorbance read using the CLARIOstar microplate reader (BMG Labtechset, Ortenberg, Germany).

Flow Cytometry

Fresh ovaries from 9-month-old WT ($n = 5$) and $Asc^{-/-}$ mice ($n = 3$) were digested in a 37°C shaker at 120 rpm in digestion buffer (Dulbecco's phosphate-buffered saline (DPBS, ThermoFisher Scientific, 14190250) with 0.4% Collagenase IV (Sigma-Aldrich, AC5138), 0.1% Deoxyribonuclease I (Sigma-Aldrich, DN25), 0.2% Dispase II (Sigma-Aldrich, D4693), and 0.2% Hyaluronidase (Sigma-Aldrich, H3506) for 30 min. 1 ml of neutralization buffer (DPBS containing 20% dialyzed FBS (Assay Matrix, ASFBS-U) and 5 mM EDTA) was added to the buffer to stop the digestion. Cell pellet was collected by centrifugation and resuspended in FACS buffer [DPBS containing 0.5% Bovine Serum Albumin (BSA, Sigma-Aldrich, A9418) and 5 mM EDTA]. Cell suspension was then filtrated and counted.

For staining, ovarian cell suspensions were blocked with an Fc blocking agent for 10 min. Isolated cells were then incubated with the antibodies of interest for 30 min and stained with Live/Dead Viability Stain 700 (FVS700, 1:2,000, BD Biosciences, 564997) for 10 min. Finally, stained cells were transferred to round bottom polypropylene FACS tubes (Falcon). All staining protocol was carried out at 4°C and FACS buffer was used as the diluent for each stain unless indicated otherwise. Data was collected on a BD LSRFortessa X-20 cell analyzer (BD Biosciences, NSW, Australia) and analyzed using FlowJo version 10 (Tree Star Inc., Oregon, USA). Antibodies and stains used in this study are detailed in **Supplementary Table 3**.

Stimulation of Ovulation and Oocyte Collection

Ovulation was induced in 12-month-old WT ($n = 3$), $Asc^{-/-}$ ($n = 5$), and $Nlrp3^{-/-}$ mice ($n = 3$) by intraperitoneal injection with pregnant mare serum gonadotropin (15 IU PMSG; Intervet) followed 44–48 h later by human chorionic gonadotropin (15 IU hCG; Intervet). After 12–16 h, cumulus oocyte complexes (COC) were collected from the oviduct and fully mature MII stage oocytes were exposed by digestion in M2 media with 0.3% hyaluronidase (Sigma-Aldrich).

Statistical Analysis

Data are presented as mean ± standard error of the mean (SEM). Statistical analyses were analyzed using GraphPad Prism version 8 (GraphPad Software, California, USA). Data normality was tested using Shapiro-Wilk test. Within each age group, data from $Asc^{-/-}$ or $Nlrp3^{-/-}$ mice were compared with WT. Normally distributed data were analyzed using unpaired Student's t-test. Not normally distributed data were analyzed

by Mann-Whitney test. Differences were considered significant when $p < 0.05$.

RESULTS

Pro-inflammatory Cytokine Levels Are Reduced in the Serum of Aging *Asc*$^{-/-}$ Mice

The NLRP3 inflammasome is a major driver of age-related sterile inflammation in multiple organs (Youm et al., 2013; Goldberg and Dixit, 2015). To determine if loss of ASC or NLRP3 reduces systemic inflammation, pro-inflammatory cytokines were measured in serum from 2, 6, and 12-month-old WT, *Asc*$^{-/-}$, and *Nlrp3*$^{-/-}$ mice and 18-month-old WT and *Asc*$^{-/-}$ mice (**Figure 1**). IL-6, TNF-α, and IL-18 all increased with age in the serum of WT mice. However, while circulating levels of IL-6, TNF-α, and IL-18 were similar between genotypes at 2 and 6 months, their expression was significantly lower in *Asc*$^{-/-}$ mice than WT mice at 12 and 18 months (**Figures 1A–C**). In contrast to *Asc*$^{-/-}$ mice, TNF-α and IL-18 were not significantly different in *Nlrp3*$^{-/-}$ from age-matched WT mice at 12 months ($p > 0.05$) (**Figures 1B,C**). For *Nlrp3*$^{-/-}$ mice, the concentration of TNF-α and IL-18 in serum at 18 months, and IL-6 at all ages, was not determined due to lack of serum availability. These data indicate that deletion of adaptor protein ASC, but not NLRP3, attenuates the levels of systemic inflammatory cytokines observed in mice during reproductive aging.

NLRP3 Inflammasome

To examine the intra-ovarian expression profile of the NLRP3 inflammasome, the mRNA expression levels of Nlrp3 and Asc were determined at 2, 6, 12, and 18-months of age (**Figures 2A,B**). As expected, Nlrp3 and Asc genes were not expressed in *Nlrp3*$^{-/-}$ and *Asc*$^{-/-}$ ovaries at any age, respectively (**Figures 2A,B**). Nlrp3 expression in 2, 6, and 12-month-old *Asc*$^{-/-}$ mice was similar to WT mice and decreased significantly at 18 months of age (**Figure 2A**). Asc mRNA levels in *Nlrp3*$^{-/-}$ mice only showed a significant decrease at 6 months compared to WT mice (**Figure 2B**).

To further investigate the effect of inflammasome ablation on downstream factors of NLRP3 inflammasome, caspase-1 and IL-18, mRNA expression levels of caspase 1 and Il18 were analyzed in ovaries from WT, *Asc*$^{-/-}$, and *Nlrp3*$^{-/-}$ ovaries (**Figures 2C,D**). Casp1 mRNA expression was significantly decreased at 6 and 18 months of age in *Asc*$^{-/-}$ and *Nlrp3*$^{-/-}$ mice compared to WT mice (**Figure 2C**). mRNA levels of Il18 were increased in 12-month-old *Asc*$^{-/-}$ and *Nlrp3*$^{-/-}$ mice and significantly decreased at 18 months of age compared to WT mice (**Figure 2D**).

Taken together, corresponding with Casp1, Nlrp3, Il1b, and Il18 as NF-κB-dependent genes, reduction of these components and substrates of the inflammasome is consistent with a reduction in age-related systemic inflammation.

The Expression of Pro-inflammatory Genes Is Reduced in Ovaries From Aging *Asc*$^{-/-}$ Mice

We next investigated the effect of ASC or NLRP3 deletion on intra-ovarian inflammation. mRNA levels of major pro-inflammatory genes Tnfa, Il1a, Il1b, and Il6 were examined in 2, 6, 12, and 18-month-old WT, *Asc*$^{-/-}$, and *Nlrp3*$^{-/-}$ ovaries (**Figures 3A–D**).

In general, Tnfa, Il1a, Il1b mRNA levels tended to increase gradually with age in WT ovaries, with significantly higher levels observed at 18 months than 2 months (**Figures 3A–D**). In contrast, the expression of Tnfa, Il1a, Il1b did not increase with age in ovaries from *Asc*$^{-/-}$ mice, and mRNA levels were significantly lower than in WT ovaries at 12 and 18 months (**Figures 3A–C**). Similarly, in ovaries from *Nlrp3*$^{-/-}$ mice, Il1a and Il1b were significantly decreased relative to WT mice at 12 months of age, and Tnfa was decreased at 18 months (**Figures 3A–C**). Unexpectedly, significantly higher expression levels of Il6 were observed in *Asc*$^{-/-}$ and *Nlrp3*$^{-/-}$ ovaries compared to WT at 6 months of age, but this increase was transient and not observed at any other age (**Figure 3D**).

Expression levels of anti-inflammatory gene Il10 were also measured (**Figure 3E**). A significant increase in the mRNA levels was observed in ovaries from *Asc*$^{-/-}$ and *Nlrp3*$^{-/-}$ mice relative to WT mice at 6 months, while at 18 months, significantly lower expression levels of Il10 was observed in knock-out mice compared to ovaries from WT mice (**Figure 3E**).

Next, the expression pattern of Csf1 and Csf2 were examined because of their involvement in the regulation of macrophages and granulocytes (**Figures 3F,G**). While Csf1 mRNA showed a small increase at 6 months in *Asc*$^{-/-}$ mice compared to WT, no other changes were evident (**Figure 3F**). However, Csf2 mRNA expression was significantly lower in ovaries from 12 and 18-month-old *Asc*$^{-/-}$ and *Nlrp3*$^{-/-}$ mice compared to WT ovaries (**Figure 3G**). Finally, mRNA levels of Ccl5, a chemokine that mediates recruitment of leukocytes to inflammatory sites, was also measured (**Figure 3H**). Gene expression was significantly decreased in ovaries from 12 and 18-month-old *Asc*$^{-/-}$ and *Nlrp3*$^{-/-}$ mice compared to WT (**Figure 3H**).

Taken together, these data indicate that mRNA expression markers of age-associated inflammatory response in aged *Asc*$^{-/-}$ and *Nlrp3*$^{-/-}$ ovaries are reduced compared to WT ovaries. Expression levels of inflammatory cytokines Tnfa, Il1a, Il1b, and Csf2, as well as Ccl5 chemokine, were significantly lower in reproductively old inflammasome-deficient mice, suggesting that migration to inflammatory sites and subsequent stimulation of immune cells, is impaired in the ovarian tissue due to inflammasome ablation.

Immune Cell Populations in the Mouse Ovary Were Significantly Decreased by ASC Ablation

Since our results indicated that systemic and intra-ovarian pro-inflammatory levels were lower in *Asc*$^{-/-}$ mice than WT mice during reproductive aging, we next examined local immune cell populations in 9-month-old *Asc*$^{-/-}$ ovaries. The

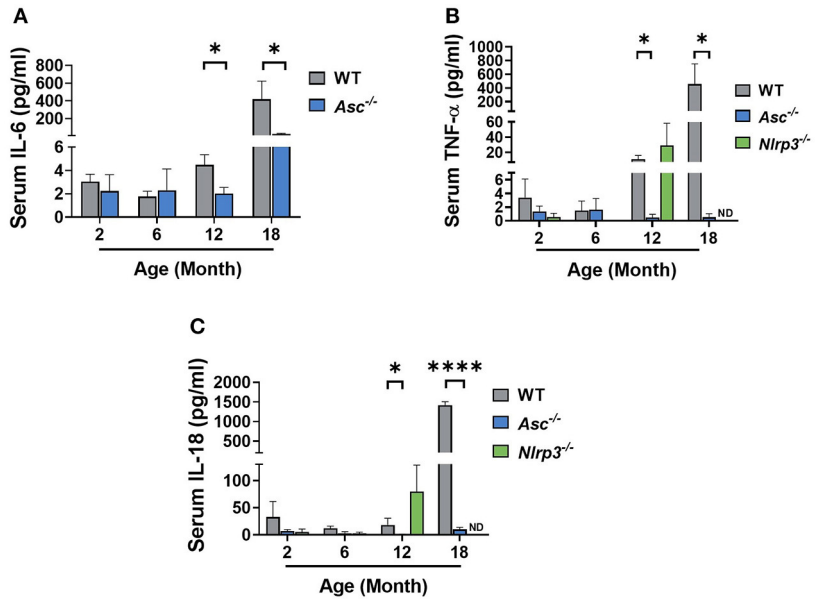

FIGURE 1 | Pro-inflammatory cytokine levels are reduced in the serum of aging *Asc*$^{-/-}$ mice. Serum IL-6 **(A)** concentration measured in 2, 6, 12, and 18-month-old WT and *Asc*$^{-/-}$ mice. Circulating levels of TNF-α **(B)** and IL-18 **(C)** determined in 2, 6, 12, and 18-month-old WT, *Asc*$^{-/-}$, and *Nlrp3*$^{-/-}$ mice. $n = 4$–6 per cohort. ND, Not Determined. Data are presented as mean ± SEM. For each age group, comparisons were made with WT using Student's *t*-test **(A,C)** or Mann-Whitney test **(A–C)** (*$p < 0.05$, ****$p < 0.0001$).

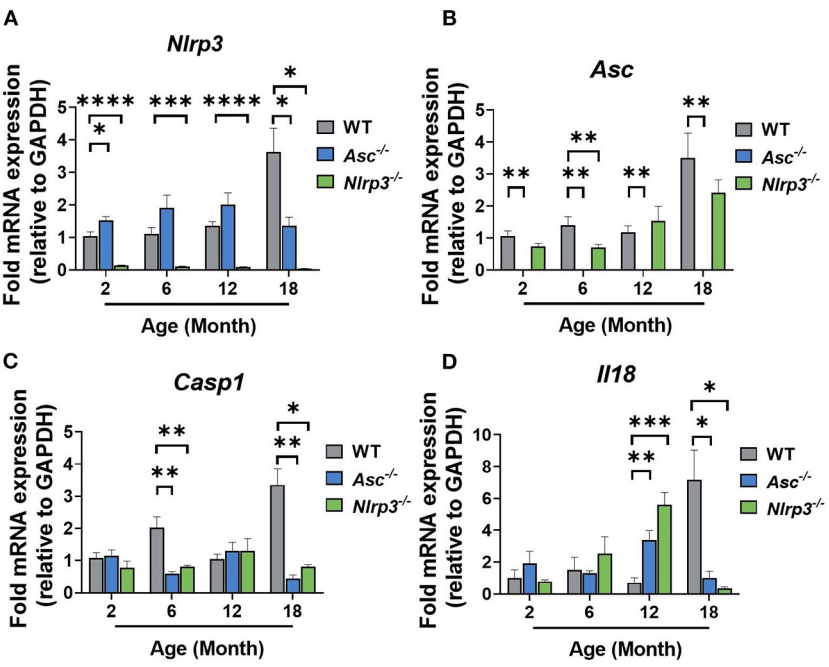

FIGURE 2 | Gene expression levels of inflammasome-related genes Nlrp3 **(A)** and Asc **(B)**, caspase 1 **(C)** and inflammasome-associated cytokine Il18 **(D)** in ovaries from 2, 6, 12, and 18-month-old WT, *Asc*$^{-/-}$, and *Nlrp3*$^{-/-}$ mice. $n = 3$–6 per cohort. Data are presented as mean ± SEM. For each age group, comparisons were made with WT using Student's *t*-test **(A–D)** or Mann-Whitney test **(D)** (*$p < 0.05$, **$p < 0.01$, ***$p < 0.001$, ****$p < 0.0001$).

gating strategy used in this study was conducted as described in **Supplementary Figure 1**. In brief, ovarian cells were first gated for singlets (FSC-H vs. FSC-A) and lymphoid/myeloid populations (SSC-A vs. FSC-A). CD11b, TCRβ, NK1.1, and CD19 expression were used to identify different immune cell populations, analyzing only live cells. NK cells were gated as

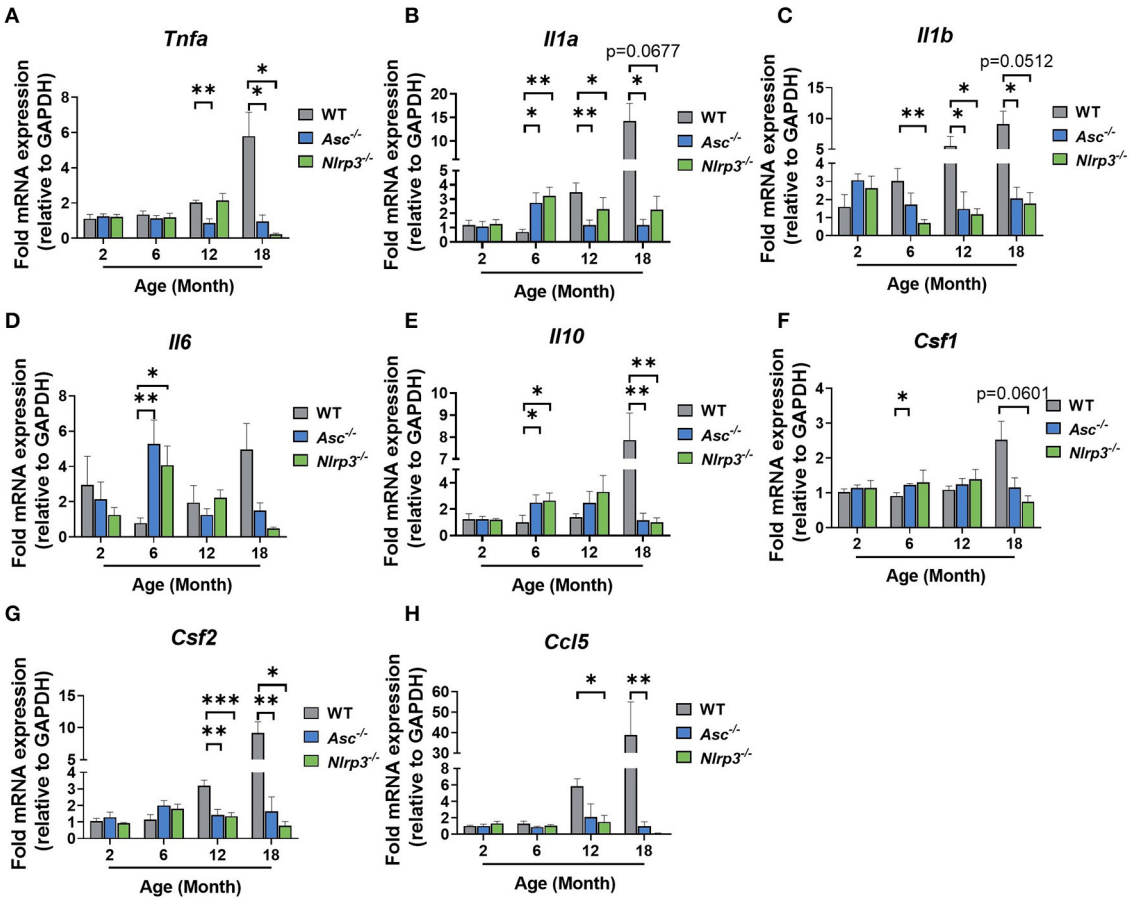

FIGURE 3 | The expression of pro-inflammatory genes is reduced in ovaries from aging $Asc^{-/-}$ mice. Gene expression levels of Tnfa **(A)**, Il1a **(B)**, Il1b **(C)**, Il6 **(D)**, Il10 **(E)**, Csf1 **(F)**, Csf2 **(G)**, and Ccl5 **(H)** in ovaries from 2, 6, 12, and 18-month-old WT, $Asc^{-/-}$, and $Nlrp3^{-/-}$ mice. $n = 3$–6 per cohort. All data are presented as mean ± SEM. For each age group, comparisons were made with WT using Student's *t*-test **(A–H)** or Mann-Whitney test **(A–H)** (*$p < 0.05$, **$p < 0.01$, ***$p < 0.001$).

NK1.1+TCRβ- and B cells as CD19+. T cells were identified based on TCR expression (TCRβ+) and either CD4 or CD8. Finally, F4/80 surface marker was used to identify macrophages within the CD11b+ population (F4/80+CD11b+).

Lymphoid cell populations, including B and T cells, did not show any significant change in $Asc^{-/-}$ ovaries compared to WT, either in the percentage or number of cells ($p > 0.05$) (**Figures 4A–D**). The percentage of NK cells showed a trend toward a decrease in ovaries from $Asc^{-/-}$ mice compared to WT mice ($p = 0.0767$) (**Figures 4E,F**).

Importantly, significant differences were observed in myeloid populations. The proportion and number of ovarian cells comprising the CD11b+ population was significantly decreased in $Asc^{-/-}$ ovaries compared to WT (**Figure 4G**). Consistent with CD11b+ cell population data, a significant decrease was also observed in the percentage of F4/80+CD11b+ macrophages in ovaries from $Asc^{-/-}$ mice relative to WT mice, while the number of macrophages showed a trend toward a decrease in $Asc^{-/-}$ ovaries compared to WT ($p = 0.0683$) (**Figures 4H,I**). Thus, our findings suggest that ablation of ASC attenuate macrophage presence in the mouse ovary, which may lead to the reduction of expression levels of inflammatory genes like Tnfa, Il1a, and Ccl5.

Loss of ASC or NLRP3 Significantly Preserves the Primordial Follicle Pool in Reproductively Old Mice

The ovarian reserve constitutes a finite reservoir of primordial follicles in the ovaries that determines the length of the female fertile lifespan (Findlay et al., 2015, 2018). Some studies have suggested that inflammatory cytokines, such as TNF-α, have an impact on primordial follicle survival (Morrison and Marcinkiewicz, 2002; Greenfeld et al., 2007). Therefore, primordial follicles were examined in ovaries from 2, 6, 12, and 18-month-old WT, $Asc^{-/-}$, and $Nlrp3^{-/-}$ mice in order to investigate the contribution of the inflammasome-dependent inflammation to the age-related follicle depletion (**Figure 5**). At 2 and 6 months of age, primordial follicle numbers in ovaries from $Asc^{-/-}$ and $Nlrp3^{-/-}$ mice were not significantly different from WT ovaries. These data suggest that reproductively young

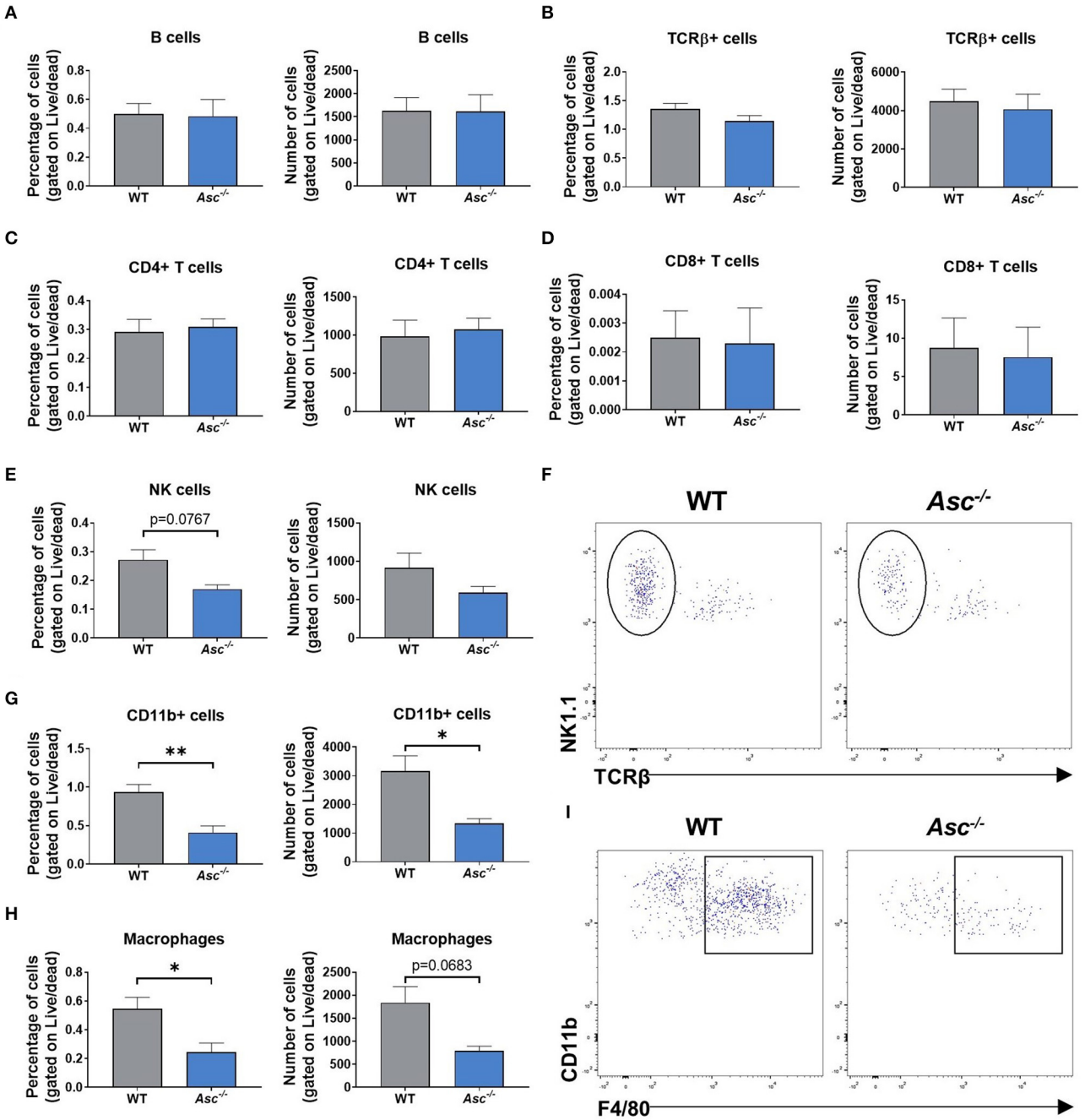

FIGURE 4 | Immune cell populations in the mouse ovary were significantly decreased by ASC ablation. Percentage and number of B cells **(A)**, T cells **(B)**, CD4+ **(C)**, and CD8+ T cells **(D)**, NK1.1+TCRβ- NK cells **(E)**, CD11b+ cells **(G)**, and F4/80+CD11b+ macrophages **(H)** present in ovaries from 9-month-old WT and $Asc^{-/-}$ mice. $n = 3$–5 per cohort. Representative dot plots of NK1.1+TCRβ- NK cells **(F)** and F4/80+CD11b+ macrophages **(I)** in ovaries from 9-month-old WT and $Asc^{-/-}$ mice. Data are presented as mean ± SEM. For each age group, comparisons were made with WT using Student's *t*-test **(A–H)** or Mann-Whitney test **(D)** (*$p < 0.05$, **$p < 0.01$).

inflammasome-deficient mice have normal primordial follicle endowment. Critically, ovaries from 12-month-old $Asc^{-/-}$ and $Nlrp3^{-/-}$ mice contained significantly more primordial follicles than WT mice, consistent with retention of the ovarian reserve during reproductive aging (**Figure 5B**). Even at 18 months of age, when the pool of primordial follicles was severely depleted in WT ovaries, $Asc^{-/-}$ mice still retain elevated primordial follicles (**Figure 5C**). A similar trend was observed for $Nlrp3^{-/-}$ mice at 18 months, though the difference with WT was not statistically significant (**Figure 5C**).

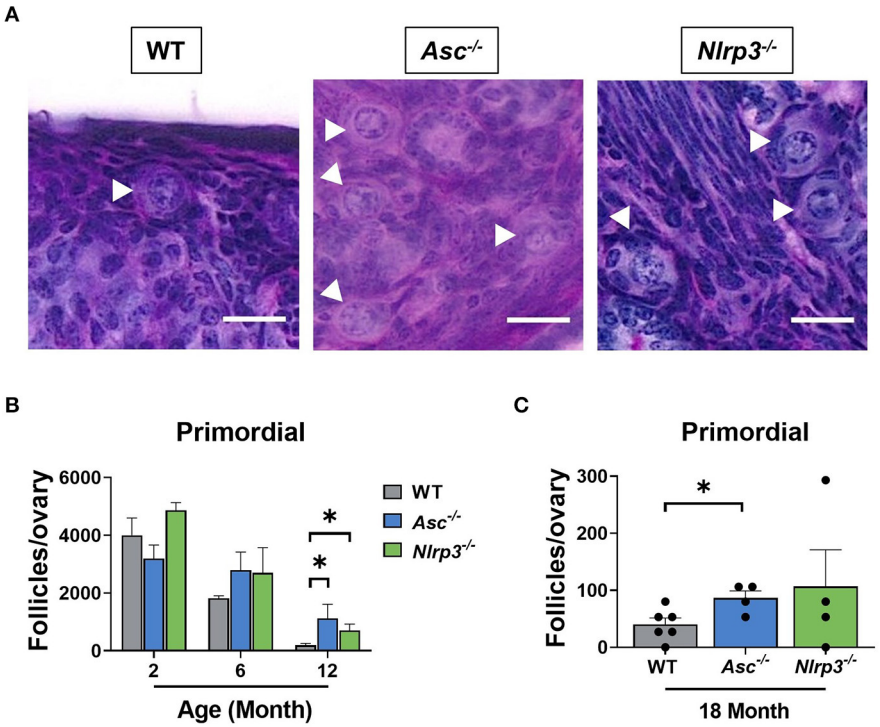

FIGURE 5 | Loss of ASC or NLRP3 significantly preserves the primordial follicle pool in reproductively old mice. **(A)** Representative images of PAS-stained ovaries of 12-month-old WT, *Asc*$^{-/-}$, and *Nlrp3*$^{-/-}$ mice. White head arrows indicate primordial follicles. Scale bars are 20 μm. Primordial **(B)** follicle numbers in ovaries from 2, 6, and 12-month-old WT, *Asc*$^{-/-}$, and *Nlrp3*$^{-/-}$ mice. $n = 3$–6 per cohort. Primordial **(C)** follicle numbers in ovaries from 18-month-old WT, *Asc*$^{-/-}$, and *Nlrp3*$^{-/-}$ mice. $n = 4$–6 per cohort. Each dot represents one animal. Data are presented as mean ± SEM. For each age group, comparisons were made with WT using Student's *t*-test **(A,B)** or Mann-Whitney test **(A)** (*$p < 0.05$).

Loss of ASC or NLRP3 Significantly Preserves the Growing Follicle Pool in Reproductively Old Mice

The number of healthy and atretic growing follicles were determined in ovaries from 2, 6, 12, and 18-month-old WT, *Asc*$^{-/-}$, and *Nlrp3*$^{-/-}$ mice (**Figures 6A–E**). Consistent with our findings for primordial follicles, the number of primary, secondary and antral follicles was similar between WT and *Asc*$^{-/-}$ ovaries at 2 and 6 months. However, a significant increase in the number of growing follicles at each of these three stages was observed in 12-month-old *Asc*$^{-/-}$ ovaries compared to WT ovaries (**Figures 6A–D**). Secondary and antral follicle numbers were also significantly increased in *Nlrp3*$^{-/-}$ mice at 12 months of age compared to WT mice (**Figures 6C,D**). By 18 months of age growing follicle numbers were not statistically significantly different between genotypes, however, there was a trend toward more antral follicles in *Nlrp3*$^{-/-}$ mice. There were no significant changes in the atretic follicle number between groups ($p > 0.05$) (**Figure 6E**).

AMH is produced by granulosa cells in growing follicles, with the highest production from secondary and early antral follicles and is often used as a clinical marker of the ovarian reserve (Kevenaar et al., 2006). To investigate the impact of losing ASC or NLRP3 function on AMH levels, serum was collected from 12-month-old *Asc*$^{-/-}$ and *Nlrp3*$^{-/-}$ mice. A significant increase in the serum AMH concentration was observed in 12-month-old *Asc*$^{-/-}$ mice compared to age-matched WT mice (**Figure 6F**). This finding is consistent with observations that primary, secondary and antral follicle numbers were significantly higher in 12-month-old *Asc*$^{-/-}$ relative to WT mice (**Figures 6B–D**). There were no differences in serum AMH levels between 12-month-old WT and *Nlrp3*$^{-/-}$ mice ($p > 0.05$) (**Figure 6F**), despite increased numbers of secondary and antral follicles.

Overall, these results demonstrate that deletion of NLRP3 or ASC preserves follicle numbers during aging in mice.

Loss of ASC or NLRP3 Increases the Number of Corpora Lutea in Reproductively Aged Mice

Corpora lutea are an indirect marker of recent ovulation. To determine if loss of ASC or NLRP3 function impacts ovulation, corpora lutea were quantified in 2, 6, 12, and 18-month-old WT, *Asc*$^{-/-}$, and *Nlrp3*$^{-/-}$ mice (**Figures 7A,B**). Corpora lutea number was similar between genotypes in reproductively young mice. Older WT mice had few corpora lutea, but a striking increase was observed in ovaries from reproductively aged 12-month-old *Asc*$^{-/-}$ and *Nlrp3*$^{-/-}$ mice relative to age-matched

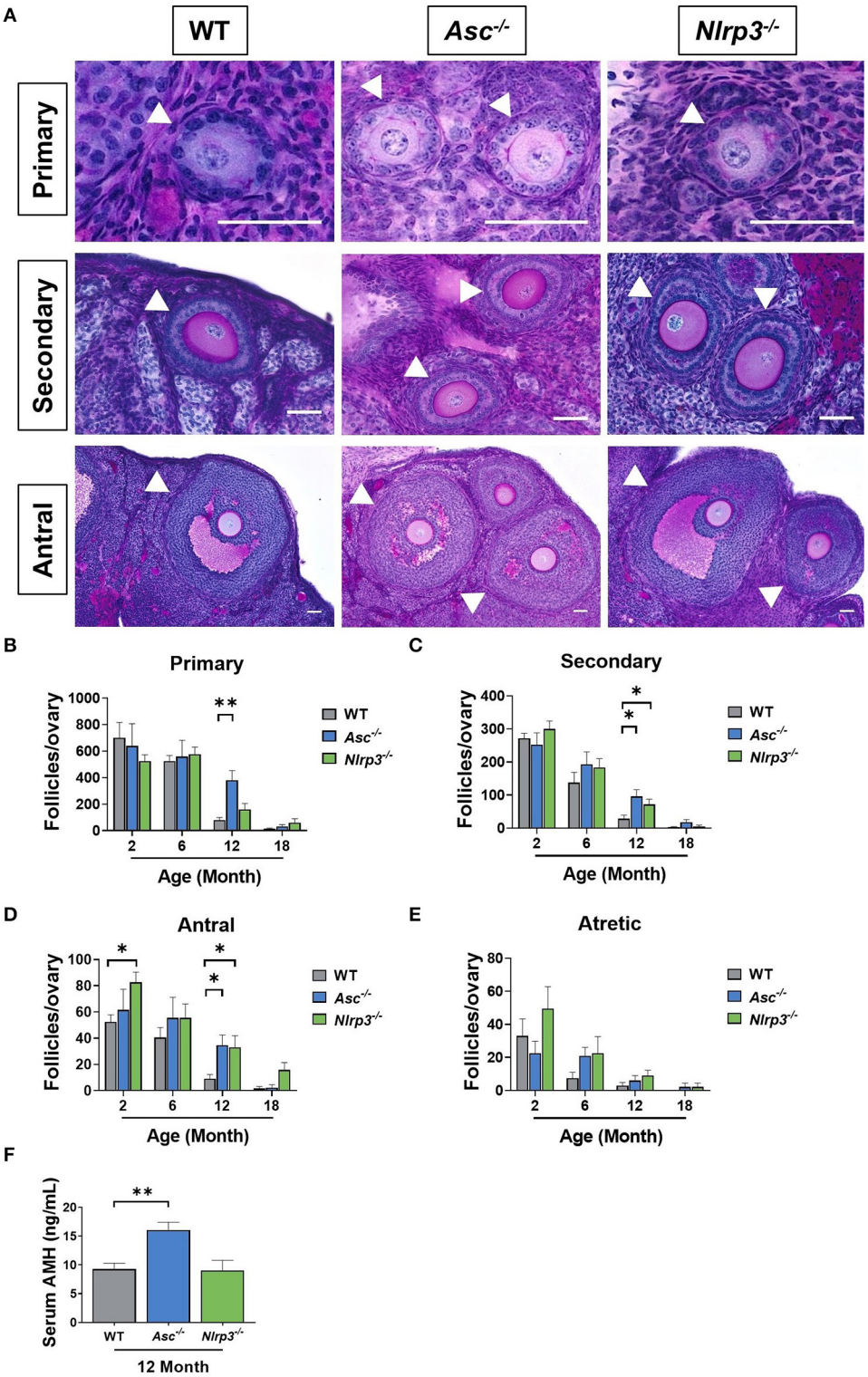

FIGURE 6 | Loss of ASC or NLRP3 significantly preserves the growing follicle pool in reproductively old mice. **(A)** Representative images of PAS-stained ovarian sections showing primary, secondary and antral follicles of 12-month-old WT, *Asc*$^{-/-}$, and *Nlrp3*$^{-/-}$ mice. Scale bars are 50 μm. Primary, secondary and antral follicles are indicated by white head arrows. Primary **(B)**, secondary **(C)**, antral **(D)**, and atretic **(E)** follicle numbers in ovaries from 2, 6, 12, and 18-month-old WT, *Asc*$^{-/-}$, and *Nlrp3*$^{-/-}$ mice. $n = 4$–6 per cohort. Serum AMH **(F)** concentration in 12-month-old WT, *Asc*$^{-/-}$, and *Nlrp3*$^{-/-}$ mice. $n = 6$ per cohort. All data are presented as mean ± SEM. For each age group, comparisons were made with WT using Student's *t*-test **(B–F)** or Mann-Whitney test **(B–F)** (*$p < 0.05$, **$p < 0.01$).

WT mice (**Figures 7A,B**). In particular, it was noted that the number of corpora lutea in 12-month-old *Nlrp3*$^{-/-}$ mice was similar to that observed in 6-month-old WT mice.

Corpora lutea typically grow from 200 to 750 μm in mice (Mircea et al., 2009), making a large contribution to the total ovarian volume. Ovarian volume was assessed in 2, 6, 12, and 18-month-old WT, *Asc*$^{-/-}$, and *Nlrp3*$^{-/-}$ mice (**Figure 7C**). Ovaries from 12-month-old WT mice were significantly smaller compared to age-matched A*sc*$^{-/-}$ and *Nlrp3*$^{-/-}$ ovaries (**Figure 7C**), consistent with corpora lutea data (**Figure 7B**). By 18 months of age, there was no difference in corpora lutea numbers or volume between *Asc*$^{-/-}$ or *Nlrp3*$^{-/-}$ and WT mice ($p > 0.05$), consistent with the end of fertility at advanced reproductive age (**Figure 7B**).

These data suggest that ovaries from both *Asc*$^{-/-}$ and *Nlrp3*$^{-/-}$ mice remain functionally active for longer than WT mice, and indicate that the reproductive lifespan may be prolonged in these animals. To investigate ovulation rate in more detail, we hormonally stimulated 12-month-old mice using standard superovulation protocols and collected oocytes from the oviduct. Interestingly, there was no significant difference in the total number or MII-stage ovulated oocytes collected from *Asc*$^{-/-}$, *Nlrp3*$^{-/-}$, and WT mice (**Supplementary Figure 2**). Indeed, the ovulated oocytes that were not MII were mostly fragmented oocytes. Thus, even though natural ovulation might be improved in inflammasome-deficient mice during aging (as indicated by increased follicles and corpora lutea), artificial induction of ovulation did not result in the maturation of more oocytes in *Asc*$^{-/-}$ or *Nlrp3*$^{-/-}$ female mice.

DISCUSSION

Recent studies have suggested that the NLRP3 inflammasome has a major influence on inflammaging, which is proposed to underlie a range of pathologies associated with the normal aging process (Goldberg and Dixit, 2015; Latz and Duewell, 2018). In this study, we investigated the hypothesis that the inflammasome, and the NLRP3 inflammasome in particular, contributes to age-related follicle depletion. We found that deletion of the inflammasome adaptor protein ASC in mice lowered serum pro-inflammatory cytokine levels, reduced the intra-ovarian expression of pro-inflammatory cytokines and myeloid cell populations, and attenuated the age-related depletion of follicles at all stages of development. Similarly, loss of NLRP3 preserved follicle numbers in older mice compared to WT controls. Loss of ASC or NLRP3 was also associated with increased CL number, which may be indicative of improved ovulatory capacity during aging. Altogether, these studies implicate the inflammasome in follicle depletion during the normal aging process and suggest that ovarian aging could be delayed by blocking the inflammasome, possibly leading to extended fertility. However, it should be noted that additional studies, including an analysis of fertility, are required to confirm the latter.

Similar to earlier studies (Youm et al., 2013), we found that systemic levels of inflammation were significantly lower in reproductively aged *Asc*$^{-/-}$ mice than age-matched WTs. Youm et al. (2013) also reported that 23-month-old *Nlrp3*$^{-/-}$ mice exhibited higher serum IL-18 levels than *Asc*$^{-/-}$ mice, but significantly lower than WT mice, suggesting that *Nlrp3*$^{-/-}$ mice also exhibit reduced inflammation during aging, although possibly to a lesser extent than in *Asc*$^{-/-}$ mice (Youm et al., 2013). In our study, *Nlrp3*$^{-/-}$ mice did not exhibit a decrease in the serum IL18 or TNFα, compared to age matched WT mice, but we did not examine these cytokines in the serum of mice *Nlrp3*$^{-/-}$ mice beyond 12 months of age, which may have been too young for changes to be detected. Overall, our data are consistent with previous publications showing that disruption of the inflammasome attenuates age-associated inflammatory levels (Duewell et al., 2010; Youm et al., 2013).

In our study, inflammasome-deficient mice also exhibited reduced intra-ovarian gene expression levels of Tnfa, Il1a, and Il1b at 12 and 18 months of age, all of which have been associated with the inflammaging in other organs (Goldberg and Dixit, 2015). For example, previous studies have shown that ablation of the inflammasome significantly reduced Il1b expression in aged fat tissue and hippocampus and Tnfa levels in hippocampus and cerebral cortex from 23-month-old mice (Youm et al., 2013). Furthermore, elimination of NLRP3 inflammasome decreased levels of IL-1β cytokine in the pancreas from 12-month-old obese mice compared to age-match WT mice, as revealed by immunofluorescence (Youm et al., 2011). Interestingly, other studies have demonstrated that increased IL-6 expression is strongly associated with chronic inflammation during generalized aging (Maggio et al., 2006). Moreover, increased levels of IL-6 in the culture media from old CB6F1 mouse ovaries compared to young ovaries has been recently reported by Briley et al. (2016). However, in our study no decrease was found in IL-6 mRNA levels in ovaries from reproductively aged *Asc*$^{-/-}$ and *Nlrp3*$^{-/-}$ mice compared to WT mice.

Inflammasome-dependent inflammation is driven by IL-1β and IL-18 cytokines, which are able to activate the inflammatory transcription factor NF-κB (Tsuji-takayama et al., 1999; Liu et al., 2017). In addition, various pro-inflammatory genes, including Il1b and Il18, as well as inflammasome-related genes Nlrp3 and caspase 1, are transcriptionally regulated by NF-κB activation (Lee et al., 2015; Liu et al., 2017). As discussed above, in our study, Il18, Il1b, and caspase 1 mRNA expression was decreased in aged ovaries from *Asc*$^{-/-}$ and *Nlrp3*$^{-/-}$ mice. These data are consistent with disruption of NLRP3 inflammasome and reduced cytokine-mediated stimulation (i.e., IL-1β and TNF-α) of NF-κB, leading to a lower expression of NF-κB-dependent genes Il18, Il1b, and caspase 1. The existence of alternative pathways of IL-1β and IL-18 activation that are independent of the inflammasomes have been described (van de Veerdonk et al., 2011). For example, neutrophils are considered the principal source of proteinase 3, which processes IL-1β, during the acute bacterial and fungal infection. In the later stages of infection, caspase-1, and inflammasome would become more important for the production of mature IL-1β (van de Veerdonk et al., 2011).

The reduction in systemic and local inflammation, and retention of follicle numbers was more subtle in *Nlrp3*$^{-/-}$ mice than *Asc*$^{-/-}$ mice. Since ASC adaptor protein is present in other

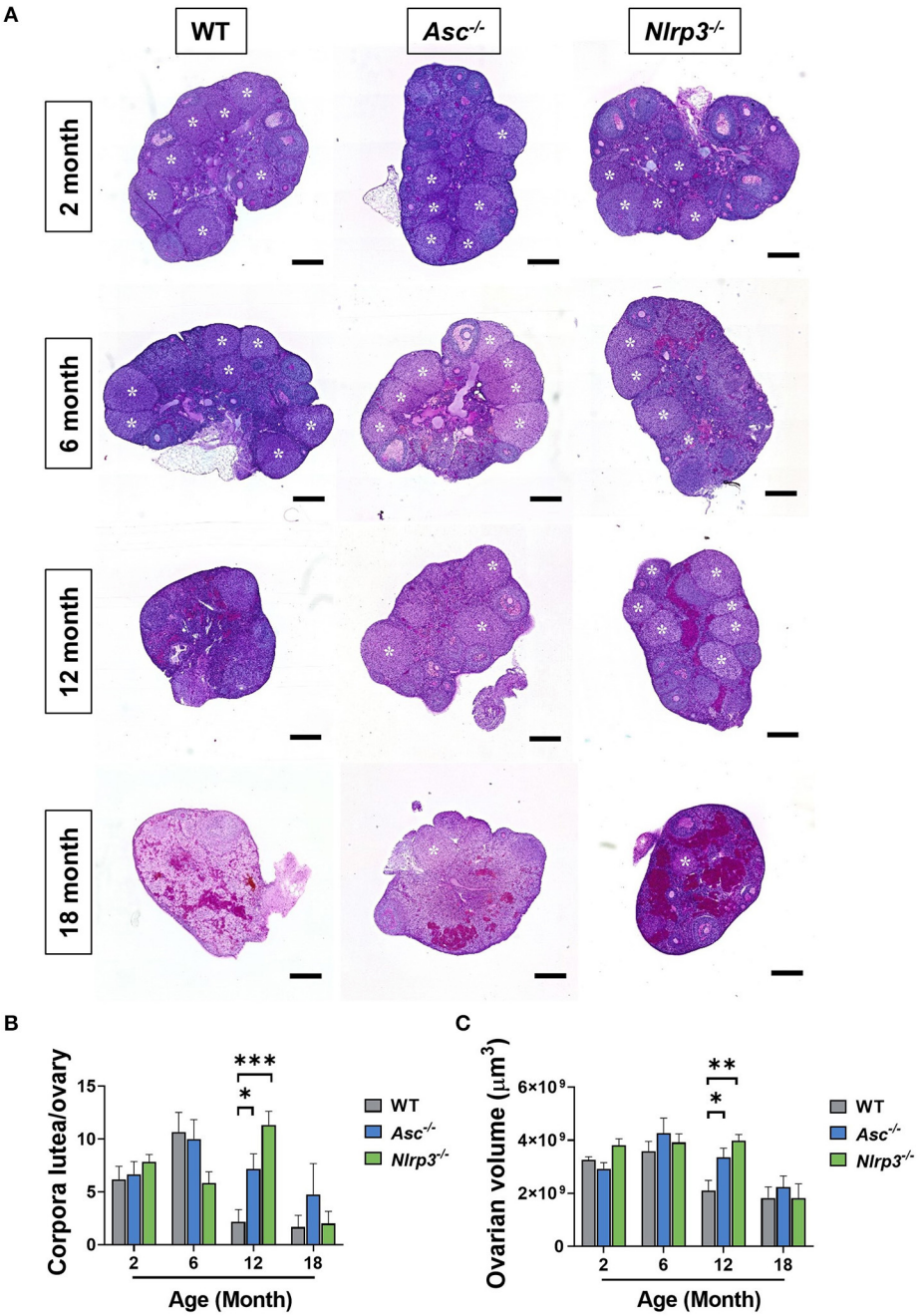

FIGURE 7 | Loss of ASC or NLRP3 increases the number of corpora lutea in reproductively aged mice. **(A)** Representative images of whole ovarian sections of 2, 6, 12, and 18-month-old WT, *Asc*$^{-/-}$, and *Nlrp3*$^{-/-}$ mice. White asterisks indicate corpora lutea. Scale bars are 400 µm. Corpora lutea numbers **(B)** in ovaries from 2, 6, 12, and 18-month-old WT, *Asc*$^{-/-}$, and *Nlrp3*$^{-/-}$ mice. Ovarian volume **(C)** for 2, 6, 12, and 18-month-old WT, *Asc*$^{-/-}$, and *Nlrp3*$^{-/-}$ mice. $n = 4$–6 per cohort. All data are presented as mean ± SEM. For each age group, comparisons were made with WT using Student's *t*-test (*$p < 0.05$, **$p < 0.01$, ***$p < 0.001$).

inflammasomes, such as AIM2 (Schroder and Tschopp, 2010), it is possible that other inflammasomes could also play a role in the age-associated inflammation and follicle depletion. Indeed, the AIM2 inflammasome senses host- and pathogen-associated cytosolic dsDNA, leading to caspase-1 activation and catalytic cleavage of IL-1β and IL-18 pre-forms (Kumari et al., 2020). A recent publication indicated that release of DNA after cumulative cell damage in aging cells leads to activation of cytosolic DNA sensors that trigger an inflammatory response (Lan et al., 2019). Considering these data, future experiments could investigate the possibility that accumulation of cytosolic DNA occurs in ovarian cells with age, promoting activation of AIM2 inflammasome

in the aging ovary. It is also worth mentioning that recent investigations have suggested that ASC and NLRP3 exhibit an inflammasome-independent function under certain conditions. Watanabe et al. (2020) has recently reported that ASC negatively regulates GPVI signaling in platelets and enhances thrombus formation, independent of NLRP3 inflammasome and IL-1β (Watanabe et al., 2020).

Importantly, primordial follicle numbers in *Asc*$^{-/-}$ and *Nlrp3*$^{-/-}$ mice were similar to WT at 2 and 6 months of age, but were elevated compared to controls at 12 months. These data suggest that deletion of ASC or NLRP3 reduces the rate at which primordial follicle depletion occurs as mice age, and rules out the possibility that these mice simply entered adulthood with greater numbers of primordial follicles. Altogether, our observations suggest an association between low-grade chronic inflammation and age-related follicle depletion, as previously proposed (Cui et al., 2011; Uri-Belapolsky et al., 2014; Briley et al., 2016), as well as specifically implicating inflammasome-derived inflammation. Notably, TNF-α can promote oocyte apoptosis (Kaipia et al., 1996; Morrison and Marcinkiewicz, 2002; Greenfeld et al., 2007) *via* TNF receptor 2 located in pre-follicular oocytes, and primordial and growing follicles (Greenfeld et al., 2007; Wang et al., 2020). Thus, lower mRNA levels of Tnfa observed in ovaries from aging *Asc*$^{-/-}$ mice could contribute to a reduction in the normal rate of primordial follicle death. Indeed, oocytes from mice lacking TNF-α exhibited lower levels of Caspase-3, leading to the larger follicle reserve observed in *Tnfa*$^{-/-}$ mice (Cui et al., 2011). Similarly, Youm et al. indicated that obesity-induced increase in pancreatic β-cell death was reduced in *Nlrp3*$^{-/-}$ obese mice as indicated by lower number of TUNEL-positive cells (Youm et al., 2011).

Consistent with the primordial follicle data, antral follicles and corpora lutea were increased in aged *Asc*$^{-/-}$ and *Nlrp3*$^{-/-}$ mice, suggesting increased ovulatory potential. Previous studies have indicated that deletion of cytokines like IL-1α or TNF-α resulted in an increased response to gonadotropins, along with an enhanced pregnancy rate and litter size (Gordon, 1999; Uri-Belapolsky et al., 2014). However, our superovulation study did not show an improved ovulation rate in inflammasome-deficient mice. Zhang et al. (2019) demonstrated that follicular expression of ASC and NLRP3 is induced by exogenous hormonal stimulation (e.g., PMSG), suggesting a possible role of NLRP3 inflammasome in the regulation of the ovulatory process (Zhang et al., 2019). A possible role for the NLRP3 inflammasome in response to hormonal priming during superovulation might explain why we saw no differences in the number of oocytes ovulated between *Asc*$^{-/-}$, *Nlrp3*$^{-/-}$ mice, and WT mice. Furthermore, it has been reported that treatment of female mice with supra-physiological doses of exogenous gonadotropin impacts on female reproductive organs by damaging the reproductive function and maternal environment (Park et al., 2015), which could be also affecting the outcome of the superovulation procedure. Alternatively, it is possible that the increased corpora lutea in inflammasome deficient mice could be the results of impaired corpora lutea regression. Thus, further studies are required to determine if ovulation is enhanced or corpus luteum regression underlies the observed phenotype.

Macrophages are the most abundant innate immune cells present in the ovary and are essential for ovarian function, with roles in regulating follicle growth, tissue remodeling at ovulation and formation and regression of corpus luteum (Wu et al., 2004). Interestingly, during regression of corpora lutea, the number of macrophages increases, indicating the critical role of these immune cells during luteolysis (Wu et al., 2004). Additionally, macrophages are the main source of TNF-α in the corpora lutea of different species, being this cytokine critical in the regulation of luteal angiogenesis (Lu et al., 2019). Our flow cytometry results indicate that fewer percentage of macrophages were present in *Asc*$^{-/-}$ ovaries than in WT ovaries. Therefore, this reduced percentage of macrophages could be delaying corpora lutea regression, as previously mentioned, resulting in higher number of corpora lutea in inflammasome deficient mice.

Lower percentage of ovarian macrophages found in *Asc*$^{-/-}$ mice is consistent with lower Ccl5 expression in the ovary, along with other inflammatory genes (e.g., Tnfa or Il1a), which may suggest that leukocyte recruitment to inflammatory sites is reduced. Zhang et al. (2020) showed that monocyte-derived macrophages were increased in aged ovaries compared to young ovaries, along with an increase in Ccl5 expression (Zhang et al., 2020). Notably, TNF-α plays a central role in activating and maintaining the inflammatory response (Parameswaran and Patial, 2010). Activated macrophages produce TNF-α *via* NF-κB transcription factor, which in turn is able to induce NF-κB activation in a self-regulating manner (Parameswaran and Patial, 2010), leading to persistent, low-grade inflammation which is characteristic of aging process (Franceschi and Campisi, 2014; Goldberg and Dixit, 2015). Within the ovary, TNF-α promotes DNA fragmentation and follicle apoptosis (Kaipia et al., 1996; Morrison and Marcinkiewicz, 2002; Greenfeld et al., 2007), thus the decreased percentage of ovarian macrophages found in *Asc*$^{-/-}$ mice could explain the decreased local inflammatory response, which subsequently would contribute to the elevated oocyte survival. A limitation of our flow cytometry study is that the estrous cycle of mice were not synchronized, which can affect the final results since macrophage number and distribution can change during the estrous cycle (Wu et al., 2004). Furthermore, in this study, cells were firstly gated for singlets and traditional lymphoid/myeloid cell populations. Following this gating strategy, we have probably excluded macrophage multinucleated giant cells, which have been associated with chronic inflammation and ovarian aging (Briley et al., 2016), from the flow cytometry analysis, since these cells are much larger.

While macrophages are known to be important for ovarian function, it is not known what role NK cells play. Recently, Gounder et al. (2018) reported an increase in the circulating human NK cell population and a decrease in the proliferation potential upon aging (Gounder et al., 2018). Activated NK cells secrete a large variety of cytokines, including TNF-α, which, as described earlier, is critical for inflammaging and can promote oocyte-mediated apoptosis (Nersesian et al., 2019). In this study, the proportion of NK cells in the ovary of *Asc*$^{-/-}$ mice tended to be lower than WT mice, potentially highlighting that NK cells may contribute to the ovarian inflammatory environment,

though further studies would be required to investigate this possibility in more detail.

Overall, the data presented in this study indicate that ablation of the inflammasome prevents age-related depletion of the ovarian reserve by reducing the local inflammatory environment, possible mediated by a reduction in the percentage of ovarian macrophages in aged inflammasome-deficient mice. The results observed in this study significantly advance our understanding of the mechanisms responsible for the regulation of oocyte number as female age and provide potential therapeutic targets for the development of new strategies to improve reproductive lifespan for advanced reproductive-aged women.

DATA AVAILABILITY STATEMENT

The raw data supporting the conclusions of this article will be made available by the authors, without undue reservation.

ETHICS STATEMENT

The animal study was reviewed and approved by Monash Animal Ethics Committee.

AUTHOR CONTRIBUTIONS

KH, AM, and CL designed the experiments, analyzed the data, and edited the manuscript. CL and SL performed the experiments. CL and KH wrote the manuscript. All authors contributed to the article and approved the submitted version.

FUNDING

This work was made possible through Victorian State Government Operational Infrastructure Support, Australian Government NHMRC IRIISS, and ARC FT190100265.

ACKNOWLEDGMENTS

The authors would like to acknowledge the Monash Histology Platform.

SUPPLEMENTARY MATERIAL

The Supplementary Material for this article can be found online at: https://www.frontiersin.org/articles/10.3389/fcell.2020.628473/full#supplementary-material

REFERENCES

Briley, S. M., Jasti, S., McCracken, J. M., Hornick, J. E., Fegley, B., Pritchard, M. T., et al. (2016). Reproductive age-associated fibrosis in the stroma of the mammalian ovary. *Reproduction* 152, 245–260. doi: 10.1530/REP-16-0129

Broekmans, F. J., Soules, M. R., and Fauser, B. C. (2009). Ovarian aging: mechanisms and clinical consequences. *Endocr. Rev.* 30, 465–493. doi: 10.1210/er.2009-0006

Cui, L., Yang, G., Pan, J., and Zhang, C. (2011). Tumor necrosis factor alpha knockout increases fertility of mice. *Theriogenology* 75, 867–876. doi: 10.1016/j.theriogenology.2010.10.029

Duewell, P., Kono, H., Rayner, K. J., Sirois, C. M., Bauernfeind, F. G., Abela, G. S., et al. (2010). NLRP3 inflammasomes are required for atherogenesis and activated by cholesterol crystals. *Nature* 464, 1357–1361. doi: 10.1038/nature08938

Finch, C. E. (2014). The menopause and aging, a comparative perspective. *J. Steroid Biochem. Mol. Biol.* 142, 132–141. doi: 10.1016/j.jsbmb.2013.03.010

Finch, C. E., Felicio, L. S., Mobbs, C. V., and Nelson, J. F. (1984). Ovarian and steroidal influences on neuroendocrine aging processes in female rodents*. *Endocrine Rev.* 5, 467–497. doi: 10.1210/edrv-5-4-467

Findlay, J. K., Hutt, K. J., Hickey, M., and Anderson, R. A. (2015). What is the "ovarian reserve?" *Fertil. Steril.* 103, 628–630. doi: 10.1016/j.fertnstert.2014.10.037

Findlay, J. K., Hutt, K. J., Hickey, M., and Anderson, R. A. (2018). How is the number of primordial follicles in the ovarian reserve established? *Biol. Reprod.* 93, 1–7. doi: 10.1095/biolreprod.115.133652

Franceschi, C., Bonafè, M., Valensin, S., Olivieri, F., De Luca, M., Ottaviani, E., et al. (2000). Inflamm-aging: an evolutionary perspective on immunosenescence. *Ann. N.Y. Acad. Sci.* 908, 244–254. doi: 10.1111/j.1749-6632.2000.tb06651.x

Franceschi, C., and Campisi, J. (2014). Chronic inflammation (inflammaging) and its potential contribution to age-associated diseases. *J. Gerontol. Ser. A Biol. Sci. Med. Sci.* 69, S4–S9. doi: 10.1093/gerona/glu057

Goldberg, E. L., and Dixit, V. D. (2015). Drivers of age-related inflammation and strategies for healthspan extension. *Immunol. Rev.* 265, 63–74. doi: 10.1111/imr.12295

Gordon, S. (1999). Macrophage-restricted molecules: role in differentiation and activation. *Immunol. Lett.* 65, 5–8. doi: 10.1016/S0165-2478(98)00116-3

Gounder, S. S., Abdullah, B. J. J., Radzuanb, N. E. I. B. M., Zain, F. D. B. M., Sait, N. B. M., Chua, C., et al. (2018). Effect of aging on NK cell population and their proliferation at *ex vivo* culture condition. *Anal. Cell. Pathol.* 2018:7871814. doi: 10.1155/2018/7871814

Greenfeld, C. R., Roby, K. F., Pepling, M. E., Babus, J. K., Terranova, P. F., and Flaws, J. A. (2007). Tumor necrosis factor (TNF) receptor type 2 is an important mediator of TNF alpha function in the mouse ovary. *Biol. Reprod.* 76, 224–231. doi: 10.1095/biolreprod.106.055509

Kaipia, A., Chun, S., Eisenhauer, K., and Hsueh, A. J. W. (1996). Tumor necrosis factor-a and its second messenger, ceramide, stimulate apoptosis in cultures ovarian follicles. *Endocrinology* 137, 4864–4870. doi: 10.1210/endo.137.11.8895358

Kanneganti, T. D., Özören, N., Body-Malapel, M., Amer, A., Park, J. H., Franchi, L., et al. (2006). Bacterial RNA and small antiviral compounds activate caspase-1 through cryopyrin/Nalp3. *Nature* 440, 233–236. doi: 10.1038/nature04517

Kevenaar, M. E., Meerasahib, M. F., Kramer, P., van de Lang-Born, B. M. N., de Jong, F. H., Groome, N. P., et al. (2006). Serum anti-mÃllerian hormone levels reflect the size of the primordial follicle pool in mice. *Endocrinology* 147, 3228–3234. doi: 10.1210/en.2005-1588

Kumari, P., Russo, A. J., Shivcharan, S., and Rathinam, V. A. (2020). AIM2 in health and disease: inflammasome and beyond. *Immunol. Rev.* 297, 83–95. doi: 10.1111/imr.12903

Lan, Y. Y., Heather, J. M., Eisenhaure, T., Garris, S., Lieb, D., Raychowdhury, R., et al. (2019). Extranuclear DNA accumulates in aged cells and contributes to senescence and inflammation. *Aging Cell* 18, 1–12. doi: 10.1111/acel.12901

Latz, E., and Duewell, P. (2018). NLRP3 inflammasome activation in inflammaging. *Semin. Immunol.* 40, 61–73. doi: 10.1016/j.smim.2018.09.001

Lee, D.-J., Du, F., Chen, S.-W., Nakasaki, M., Rana, I., Shih, V. F. S., et al. (2015). Regulation and function of the caspase-1 in an inflammatory microenvironment. *J. Invest. Dermatol.* 135, 2012–2020. doi: 10.1038/jid.2015.119

Liew, S. H., Vaithiyanathan, K., Cook, M., Bouillet, P., Scott, C. L., Kerr, J. B., et al. (2014). Loss of the proapoptotic BH3-only protein BCL-2 modifying factor prolongs the fertile life span in female mice1. *Biol. Reprod.* 90, 1–9. doi: 10.1095/biolreprod.113.116947

Liu, T., Zhang, L., Joo, D., and Sun, S. (2017). NF-κB signaling in inflammation. *Signal Transduct. Targeted Ther.* 2:17023. doi: 10.1038/sigtrans.2017.23

Lu, E., Li, C., Wang, J., and Zhang, C. (2019). Inflammation and angiogenesis in the corpus luteum. *J. Obstetr. Gynaecol. Res.* 45, 1967–1974. doi: 10.1111/jog.14076

Maggio, M., Guralnik, J. M., Longo, D. L., and Ferrucci, L. (2006). Interleukin-6 in aging and chronic disease:a magnificent pathway. *J. Gerontol. Med. Sci.* 61, 575–584. doi: 10.1093/gerona/61.6.575

Marín-Aguilar, F., Lechuga-Vieco, A. V., Alcocer-Gómez, E., Castejón-Vega, B., Lucas, J., Garrido, C., et al. (2020). NLRP3 inflammasome suppression improves longevity and prevents cardiac aging in male mice. *Aging Cell* 19, 1–14. doi: 10.1111/acel.13050

Mircea, C. N., Lujan, M. E., Jaiswal, R. S., Singh, J., Adams, G. P., and Pierson, R. A. (2009). Ovarian imaging in the mouse using ultrasound biomicroscopy (UBM): a validation study. *Reprod. Fertility Dev.* 21, 579–586. doi: 10.1071/RD08295

Morrison, L. J., and Marcinkiewicz, J. L. (2002). Tumor necrosis factor alpha enhances oocyte/follicle apoptosis in the neonatal rat ovary. *Biol. Reprod.* 66, 450–457. doi: 10.1095/biolreprod66.2.450

Myers, M., Britt, K. L., Wreford, N. G. M., Ebling, F. J. P., and Kerr, J. B. (2004). Methods for quantifying follicular numbers within the mouse ovary. *Reproduction* 127, 569–580. doi: 10.1530/rep.1.00095

Nersesian, S., Glazebrook, H., Toulany, J., Grantham, S. R., and Boudreau, J. E. (2019). Naturally killing the silent killer: NK cell-based immunotherapy for ovarian cancer. *Front. Immunol.* 10:1782. doi: 10.3389/fimmu.2019.01782

Ora, M. I. C. C., Ooistra, L. I. K., and Travlos, G. (2015). Vaginal cytology of the laboratory rat and mouse: review and criteria for the staging of the estrous cycle using stained vaginal smears. *Toxicol. Pathol.* 43, 776–793. doi: 10.1177/0192623315570339

Ozoren, N., Masumoto, J., Franchi, L., Kanneganti, T.-D., Body-Malapel, M., Erturk, I., et al. (2014). Distinct roles of TLR2 and the adaptor ASC in IL-1 /IL-18 secretion in response to listeria monocytogenes. *J. Immunol.* 176, 4337–4342. doi: 10.4049/jimmunol.176.7.4337

Parameswaran, N., and Patial, S. (2010). Tumor necrosis factor-α signaling in macrophages. *Crit. Rev. Eukaryotic Gene Express.* 20, 87–103. doi: 10.1615/CritRevEukarGeneExpr.v20.i2.10

Park, S.-J., Kim, T.-S., Kim, J.-M., Chang, K.-T., Lee, H.-S., and Lee, D.-S. (2015). Repeated superovulation via PMSG/hCG administration induces 2-Cys peroxiredoxins expression and overoxidation in the reproductive tracts of female mice. *Mol. Cells* 38, 1071–1078. doi: 10.14348/molcells.2015.0173

Rowley, J. E., Amargant, F., Zhou, L. T., Galligos, A., Simon, L. E., Pritchard, M. T., et al. (2020). Low molecular weight hyaluronan induces an inflammatory response in ovarian stromal cells and impairs gamete development *in vitro*. *Int. J. Mol. Sci.* 21, 1–24. doi: 10.3390/ijms21031036

Santana, P. T., Martel, J., Lai, H.-C., Perfettini, J.-L., Kanellopoulos, J. M., Young, J. D., et al. (2016). Is the inflammasome relevant for epithelial cell function? *Microbes Infect.* 18, 93–101. doi: 10.1016/j.micinf.2015.10.007

Sarma, U. C., Winship, A. L., and Hutt, K. J. (2020). Comparison of methods for quantifying primordial follicles in the mouse ovary. *J. Ovarian Res.* 13:121. doi: 10.1186/s13048-020-00724-6

Schroder, K., and Tschopp, J. (2010). The inflammasomes. *Cell* 140, 821–832. doi: 10.1016/j.cell.2010.01.040

Tsuji-takayama, K., Aizawa, Y., Okamoto, I., Kojima, H., and Koide, K. (1999). Interleukin-18 induces interferon-gamma production through NF-kB and NFAT activation in murine T helper type 1 cells. *Cell. Immunol.* 50, 41–50. doi: 10.1006/cimm.1999.1542

Uri-Belapolsky, S., Shaish, A., Eliyahu, E., Grossman, H., Levi, M., Chuderland, D., et al. (2014). Interleukin-1 deficiency prolongs ovarian lifespan in mice. *Proc. Natl. Acad. Sci. U.S.A.* 111, 12492–12497. doi: 10.1073/pnas.1323955111

Urzua, U., Chacon, C., Espinoza, R., Martínez, S., and Hernandez, N. (2018). Parity-dependent hemosiderin and lipofuscin accumulation in the reproductively aged mouse ovary. *Anal. Cell. Pathol.* 2018:1289103. doi: 10.1155/2018/1289103

van de Veerdonk, F. L., Netea, M. G., Dinarello, C. A., and Joosten, L. A. B. (2011). Inflammasome activation and IL-1β and IL-18 processing during infection. *Trends Immunol.* 32, 110–116. doi: 10.1016/j.it.2011.01.003

Wang, S., Zheng, Y., Li, J., Yu, Y., Zhang, W., Song, M., et al. (2020). Single-cell transcriptomic atlas of primate ovarian aging. *Cell* 180, 1–16. doi: 10.1016/j.cell.2020.01.009

Watanabe, S., Usui-Kawanishi, F., Komada, T., Karasawa, T., Kamata, R., Yamada, N., et al. (2020). ASC regulates platelet activation and contributes to thrombus formation independent of NLRP3 inflammasome. *Biochem. Biophys. Res. Commun.* 531, 125–132. doi: 10.1016/j.bbrc.2020.07.063

Winship, A., Sarma, U. C., Alesi, L. R., and Hutt, K. J. (2020). Accurate follicle enumeration in adult mouse ovaries. *JoVE*. e61782. doi: 10.3791/61782

Wu, R., Van der Hoek, K. H., Ryan, N. K., Norman, R. J., and Robker, R. L. (2004). Macrophage contributions to ovarian function. *Human Reprod. Update* 10, 119–133. doi: 10.1093/humupd/dmh011

Xia, S., Zhang, X., Zheng, S., Khanabdali, R., Kalionis, B., Wu, J., et al. (2016). An update on inflamm-aging: mechanisms, prevention, and treatment. *J. Immunol. Res.* 2016:8426874. doi: 10.1155/2016/8426874

Youm, Y. H., Adijiang, A., Vandanmagsar, B., Burk, D., Ravussin, A., and Dixit, V. D. (2011). Elimination of the NLRP3-ASC inflammasome protects against chronic obesity-induced pancreatic damage. *Endocrinology* 152, 4039–4045. doi: 10.1210/en.2011-1326

Youm, Y. H., Grant, R. W., McCabe, L. R., Albarado, D. C., Nguyen, K. Y., Ravussin, A., et al. (2013). Canonical Nlrp3 inflammasome links systemic low-grade inflammation to functional decline in aging. *Cell Metab.* 18, 519–532. doi: 10.1016/j.cmet.2013.09.010

Zhang, Z., Schlamp, F., Huang, L., Clark, H., and Brayboy, L. (2020). Inflammaging is associated with shifted macrophage ontogeny and polarization in the aging mouse ovary. *Reproduction* 159, 325–337. doi: 10.1530/REP-19-0330

Zhang, Z., Wang, F., and Zhang, Y. (2019). Expression and contribution of NLRP3 inflammasome during the follicular development induced by PMSG. *Front. Cell Dev. Biol.* 7:256. doi: 10.3389/fcell.2019.00256

Conflict of Interest: The authors declare that the research was conducted in the absence of any commercial or financial relationships that could be construed as a potential conflict of interest.

frontiers in Cell and Developmental Biology

ORIGINAL RESEARCH
published: 23 March 2021
doi: 10.3389/fcell.2021.644135

Tet1 Deficiency Leads to Premature Ovarian Failure

Linlin Liu[1,2†], Huasong Wang[1,2†], Guo_Liang Xu[3,4] and Lin Liu[1,2]*

[1] Department of Cell Biology and Genetics, College of Life Sciences, Nankai University, Tianjin, China, [2] State Key Laboratory of Medicinal Chemical Biology, Nankai University, Tianjin, China, [3] State Key Laboratory of Molecular Biology, Shanghai Institute of Biochemistry and Cell Biology, Chinese Academy of Sciences, Shanghai, China, [4] Key Laboratory of Medical Epigenetics and Metabolism, Institutes of Biomedical Sciences, Medical College of Fudan University, Shanghai, China

Tet enzymes participate in DNA demethylation and play critical roles in stem cell pluripotency and differentiation. DNA methylation alters with age. We find that *Tet1* deficiency reduces fertility and leads to accelerated reproductive failure with age. Noticeably, *Tet1*-deficient mice at young age exhibit dramatically reduced follicle reserve and the follicle reserve further decreases with age, phenomenon consistent with premature ovarian failure (POF) syndrome. Consequently, *Tet1*-deficient mice become infertile by reproductive middle age, while age matched wild-type mice still robustly reproduce. Moreover, by single cell transcriptome analysis of oocytes, *Tet1* deficiency elevates organelle fission, associated with defects in ubiquitination and declined autophagy, and also upregulates signaling pathways for Alzheimer's diseases, but down-regulates X-chromosome linked genes, such as *Fmr1*, which is known to be implicated in POF. Additionally, *Line1* is aberrantly upregulated and endogenous retroviruses also are altered in *Tet1*-deficient oocytes. These molecular changes are consistent with oocyte senescence and follicle atresia and depletion found in premature ovarian failure or insufficiency. Our data suggest that *Tet1* enzyme plays roles in maintaining oocyte quality as well as oocyte number and follicle reserve and its deficiency can lead to POF.

Keywords: *Tet1*, aging, epigenetics, oocyte, premature ovarian failure

OPEN ACCESS

Edited by:
Francesca Elizabeth Duncan, Northwestern University, United States

Reviewed by:
Michael Klutstein, Hebrew University of Jerusalem, Israel
Ivana Celic, Tulane University, United States

***Correspondence:**
Lin Liu
liulin@nankai.edu.cn

† These authors have contributed equally to this work

Specialty section:
This article was submitted to Cellular Biochemistry, a section of the journal Frontiers in Cell and Developmental Biology

Received: *20 December 2020*
Accepted: *26 February 2021*
Published: *23 March 2021*

Citation:
Liu L, Wang H, Xu G_L and Liu L (2021) Tet1 Deficiency Leads to Premature Ovarian Failure. Front. Cell Dev. Biol. 9:644135. doi: 10.3389/fcell.2021.644135

INTRODUCTION

Ten-eleven translocation (Tet) methylcytosine dioxygenases play a major role in shaping DNA methylation patterns through demethylation (Wu and Zhang, 2017). Tet enzymes have been demonstrated to play important roles in ESC pluripotency and differentiation (Ito et al., 2010; Koh et al., 2011). However, *Tet1* or *Tet2* -null mice are viable and overtly normal double *Tet1*/*Tet2*-deficient mice are also obtained (Dawlaty et al., 2011, 2013; Ko et al., 2011), but, some *Tet1*-deficient mice display a smaller body size at birth, which might reflect a developmental delay. Moreover, Tet1-mediated 5 hmC signals play important role in DNA demethylation during primordial germ cell (PGC) development and meiosis (Yamaguchi et al., 2012, 2013a; Hill et al., 2018). *Tet1* deficiency results in meiotic defects of PGCs, including impaired homologous pairing and recombination in meiotic germ cells (meiocytes) during fetal development, probably due to insufficient demethylation and failed activation of meiotic genes (Yamaguchi et al., 2013a), such that *Tet1*-deficient mice at young age already exhibit reduced number of oocytes in the ovary and subfertility (Yamaguchi et al., 2012, 2013a). It also will be interesting to investigate whether *Tet1* deficiency impacts reproductive aging of adult mice.

From the onset of reproductive maturity, organismal aging is characterized by declined fecundity, increased tissue dysfunction, and susceptibility to disease or mortality (Rando and Chang, 2012). The aging process is associated with altered epigenetic regulation, including DNA methylation, histone modification and chromatin remodeling (Zhang et al., 2020). DNA methylation involves in many aspects of cellular and molecular changes in aging (Lopez-Otin et al., 2013). Moreover, change to DNA methylation in aging has been used to predict the chronological age of human somatic tissues and individuals (Hannum et al., 2013; Horvath, 2013). Predictions have been made from heterogeneous samples such as lung, liver, and brain tissues as well as whole blood and peripheral blood mononuclear cells, and isolated CD4 + T cells, monocytes, and B cells (Horvath, 2013). Epigenetic clock sites have been defined also in multiple tissues in mouse (Stubbs et al., 2017) and age-related methylation changes between mouse and human were partially conserved (Maegawa et al., 2010). Deeper understanding of epigenetic alterations in aging and the molecular basis of the DNA methylation clock is of particular interest as epigenetic modifications can be reversed, allowing manipulation to potentially reverse aging and thus therapeutic potential (Rando and Chang, 2012; Cole et al., 2017; Chen and Kerr, 2019; Zhang et al., 2020). Nevertheless, it remains elusive whether *Tet* deficiency can impact aging in the adult.

Ovarian aging is mainly characterized by a sharp decrease in the number of oocyte and follicles and a decrease in oocyte quality (van Rooij et al., 2005; Broekmans et al., 2007, 2009; Tatone et al., 2008). The number of oocytes and follicles stored known as follicle reserve at birth is fixed, which cannot be replenished by germ cells in postnatal ovaries, but with age, periodic ovulation, follicle atresia and apoptosis are the main causes of a sharp decline in the number of follicles (Faddy, 2000; Bristol-Gould et al., 2006; Broekmans et al., 2007; Djahanbakhch et al., 2007; Notarianni, 2011; Zhang et al., 2012). Follicle depletion, in turn, causes lower levels of estrogen secretion in the body, eventually leading to menopause (Lawson et al., 2003).

Recently, we report that *Tet2* deficiency accelerates reproductive aging in the adult female mice (Wang et al., 2020). Here we compared the fertility of mice deficient for *Tet1* from young to reproductive old age. We report roles of *Tet1* in maintaining oocyte quality in addition to oocyte number for preserving fertility with age.

MATERIALS AND METHODS

Tet1 Knockout Mice

Tet1 knockout ($Tet1^{-/-}$) mice were generated from 129 × C57BL/6J mixed genetic background (Zhang et al., 2013). Most of wild-type (WT) and *Tet1* knockout mice were generated from *Tet1* heterozygotes mating. For fertility analysis, $Tet1^{-/-}$ females were crossed with WT male at young age and vaginal plugs were checked daily. All mice in the study were maintained in a mixed 129 × C57BL/6 background. All mouse experiments were carried out in accordance with the guidelines and regulations and approved by the Institutional Animal Care and Use Committee of Nankai University.

Genotyping

Postnatal mice at 2 weeks old were genotyped using DNA extracted from their ears. PCR was carried out at 94°C for 2 min, followed by 35 cycles at 94°C for 30 s, 60°C for 30 s, and 72°C for 1 min. DNA fragments were visualized by agarose gel electrophoresis. The genotyping primers were listed as follows.

Tet1-C	CAGTAGTATTTTGCCTGCCTGCAT
Tet1-R	TTCCCTAAGGAGTTTACTGCAACG
Tet1-F	CATCCTAAATAACCCAACCACCAA

H&E of Ovary and Follicle Count

Ovaries were collected from different group mice ($n > 10$ mice for young and middle-age group and $n = 7$–8 mice for old group) and fixed by immersion in 4% paraformaldehyde (PFA) overnight at 4°C, and tissues were embedded with paraffin wax, based on previous methods (Liu et al., 2013). The follicles were categorized into primordial and primary, secondary and antral, accordingly (Myers et al., 2004). Follicles were classified as primordial and primary if they contained an oocyte surrounded by a single layer of squamous, or, cuboidal granulosa cells. Secondary follicles were identified as having more than one layer of granulosa cells with no visible antrum. Antral follicles possessed one or two small areas of follicular fluid (antrum) or a single large antral space.

Oocyte Collection

For collection of oocytes for RNA-seq, female mice from the different groups were superovulated by intraperitoneal injection of 5 I U pregnant mare's serum gonadotrophin (PMSG), followed 46-48 h later by 5 I U human chorionic gonadotrophin (hCG), to obtain MII oocytes. Granulosa cells attached to oocytes were removed in M2, or HKSOM supplemented with 0.03% hyaluronidase by gently pipetting.

Quantitative Real-Time PCR

RNA was isolated from ovaries using RNeasy mini kit (Qiagen), and subject to cDNA synthesis using Moloney Murine Leukemia Virus Reverse Transcriptase (Invitrogen). PCR reactions were set up in duplicates using the FastStart Universal SYBR Green Master (4913914001, Roche) and run on the Mastercycler® RealPlex2 real time PCR detection system (Eppendorf). The final PCR reaction volume in 20 μl contained 10 μl SYBR Green PCR Master Mix, 1 μl cDNA template, 2 μl primer mixture and 7 μl water. Thermal cycling was carried out with a 10 min denaturation step at 95°C, followed by two-step cycles, 15 s at 95°C and 1 min at 60°C. Each sample was analyzed using GAPDH as the internal control. Primers were designed as follows.

Tet1-Foward	CCTCACAGGCACAGGTTACA
Tet1-Reverse	ATTTGGGGCCATTTACTGGT
Gapdh-Foward	TCAACAGCAACTCCCACTCTTCCA
Gapdh-Reverse	ACCACCCTGTTGCTGTAGCCGTAT

Immunofluorescence of Spreads, Sections, and Oocytes

For paraffin sections, after deparaffinizing, rehydrating and washing in PBS (pH 7.2–7.4), the sections were subjected to high pressure antigen recovery sequentially in citrate buffer (pH 6.0) for 3 min, incubated with blocking solution (5% goat serum and 0.1% BSA in PBS) for 2 h at room temperature, and then incubated with the diluted primary antibodies [anti-5 hmC (39769, Active Motif), anti-Tet1 (MABE1144, Millipore), anti-Oct4 (SC-5279, Santa Cruz)] overnight at 4°C. After washing with PBS, sections were incubated with appropriate secondary antibodies (Alexa Fluor® FITC, 488, or 594). The sections were then stained with 1 μg/ml DAPI for 10 min to reveal nuclei, washed with PBS, and mounted in Vectashield (H-1000, Vector Laboratories, Burlingame, CA, United States). Relative integrated fluorescence intensity for 5 hmC was estimated by Image J software. The threshold was defined using non-specific background fluorescence.

Single-Cell Isolation and Lysis

MII oocytes were collected from young WT ($n = 19$), $Tet1^{-/-}$ ($n = 15$) or from old WT ($n = 19$), $Tet1^{-/-}$ ($n = 14$) mice in two biologically repeated experiments. Single MII oocyte was resuspended in PBS with 0.1% BSA (A3311-10g, Sigma), picked up in 1 μL 0.1% BSA using a micropipette with an epT.I.P.S. pipette tip (0030000838, Eppendorf) under a dissecting microscope, and transferred to the bottom of a 200-μL PCR tube (8-strip, nuclease-free, thin-walled PCR tubes with caps, PCR-0208-C, Axygen) containing oligo (dT) primer, Triton X-100, and Recombinant RNase Inhibitor (RRI, 2313A, Takara). Samples were frozen in liquid nitrogen and stored or used immediately.

Reverse Transcription

Frozen or fresh samples were melted on ice and 1 μL deoxyribonucleoside triphosphate (R0191, Thermo Scientific) was added into the tubes, vortexed gently, and incubated at 37°C for 3 min. The cDNAs were then synthesized using SuperScript™ II Reverse Transcriptase (18064071, Thermo Scientific) by slightly modified Smart-seq2 methods (Picelli et al., 2014), followed by 15 cycles of PCR using KAPA HotStart ReadyMix (KK2602, KAPA Biosystems) and then purified using Agencount AMPure XP beads (A63881, Beckman).

Library Construction and Sequencing

RNA-seq libraries were prepared using Smart-seq2 methods as previously described (Picelli et al., 2014). Briefly, the libraries were prepared by using TruePrep DNA Library Prep Kit V2 for Illumina® (TD503-02, Vazyme Biotech co.,ltd.) according to the manual instruction. Samples were barcoded during library preparation and multiplex sequenced, with a 150-bp pair-end sequencing strategy on a HiSeq 10x (Illumina).

Single-Cell RNA-seq Data Analysis

Raw reads were processed using trim-galore and clean reads were mapped to mm 10 from UCSC genome[1] by Hisat2 (v2.1.0) with default parameters (Kim et al., 2013, 2015). Uniquely mapped reads annotated in Gencode vM17 were calculated by Featurecounts (Liao et al., 2014), with default parameters (featureCounts −T 30 −O −Q 30 −p −a gencode.vM17.annotation.gtf.gz -o v17.txt *.bam). Sum factor normalization was applied with deconvolution of size factors within different batch samples using SCnorm (Bacher et al., 2017). Raw counts were normalized by library size via counts of exon model per million mapped reads (CPM). Gene expression was counted in individual oocyte when the transcript number was >1. Dynamic changes of differentially expressed genes (DEGs) between different groups were analyzed using Deseq2 (Love et al., 2014). DEGs were defined only if p value was <0.05, and a fold change was >1.5. Young $Tet1^{-/-}$ oocytes had 2,013 downregulated and 1,557 upregulated genes, compared with those of young WT oocytes. There were 1,448 downregulated and 1,696 upregulated genes in old $Tet1^{-/-}$ oocytes compared with those of old WT oocytes.

Functional Annotation

Gene ontology (GO) terms were collected from MGI (Bult et al., 2019) and kyoto encyclopedia of genes and genomes (KEGG) pathways from KEGG pathway database (Wixon and Kell, 2000). Enrichment results were obtained using clusterprofiler (Yu et al., 2012) and KOBAS (Xie et al., 2011).

Analysis of Transposable Elements

Reads were mapped to mm 10 from UCSC genome see text footnote 1 by Hisat2 (v2.1.0) with default parameters as above. For estimation of retroelement expression, "repeatMasker" track, was downloaded from UCSC genome browser in GTF, based on the genomic coordination in GTF files. Annotation file of transposable elements was extracted and made as a SAF file, which is uploaded in https://github.com/LianaLiu/single. Reads were counted using featurecounts and only the unique mapped reads with completely overlapping retrotransposon coordinates were counted. Class and family of transposable elements are also provided in the supplementary datasheet **Supplementary Table 1**. Annotation of full-length retrotransposon elements was constructed based on methods described previously (Kaul et al., 2019).

Full length of L1 annotation file was also analyzed according to the previous method (Deininger et al., 2017; Kaul et al., 2019), with slight modifications, and 6,000 bp of L1 sequence were assumed to be the full-length elements. We utilized our paired-end RNA-seq reads aligned by Hisat2 and Samtools to create a sorted bam file and annotated based on our data.

Hormone Assays

Serum anti-Mullerian hormone (AMH) levels were assayed using ELISA kit (CK-E90200, Hangzhou EastBiopharm CO., LTD.). Quality control serum, sterilized distilled water, and five series diluted standard samples for a standard curve were tested for each serum sample. The intra- and inter-assay coefficients of variability for AMH were below 8 and 12%.

[1] http://genome.ucsc.edu/

Statistical Analysis

Data were analyzed by student's *t*-test, χ2 test or fisher's exact test for paired comparison, or by ANOVA and means compared by Fisher's protected least-significant difference (PLSD) for multiple comparisons using the StatView from SAS Institute and the graphs made by GraphPad Prism 7 (GraphPad Software, San Diego, CA, United States). Kruskal-Wallis test was used to compare multiple groups using ggpubr R package. Linear regression analysis was done using GraphPad Prism 7. The data between groups were considered significant when $P < 0.05$ (*), 0.01(**) or 0.001(***).

RESULTS

Tet1 Deficiency Reduces Follicle Reserve and Causes Premature Ovarian Failure and Infertility

To study whether Tet1 regulates fertility with age, we employed *Tet1* deficient mice generated using homologous recombination by deleting exons 11-13 (Zhang et al., 2013). Homozygous *Tet1* knockout mice ($Tet1^{-/-}$) were produced by crossing heterozygous mice (**Supplementary Figure 1A**). However, *Tet1* deficiency resulted in death of a small proportion of embryos (**Supplementary Figure 1B**), consistent with previous study (Yamaguchi et al., 2012). The *Tet1* knockout was evaluated based on genotyping, as well as the minimal mRNA expression level of *Tet1* determined by qPCR (**Supplementary Figure 1C**). Also, Tet1 protein was absent in $Tet1^{-/-}$ blastocysts by immunofluorescence microscopy (**Supplementary Figure 1D**), further validating the successful knockout of the *Tet1* gene. Representative primordial oocytes were shown by enclosed granulosa cells (**Supplementary Figure 1E**). The 5 hmC levels of primordial oocytes from $Tet1^{-/-}$ mice as shown by immunofluorescence were decreased compared to WT oocytes (**Supplementary Figure 1F**).

Wild-type (WT) and $Tet1^{-/-}$ female mice at the reproductive age of 2–4 months (young), 7–9 months (middle-age) and 10–12 months (old), were mated with young WT males, and the successfully mated females judged by the presence of mating plug next morning were allowed to deliver the pups to determine the fertility. WT mice exhibited reduced fertility with age as shown by smaller litter size, as expected for natural reproductive aging in females. Comparatively, $Tet1^{-/-}$ female mice manifested declined fertility and accelerated reproductive failure with age, as they produced smaller litter size than that of age-matched WT mice (**Figure 1A**). By linear regression analysis, WT and $Tet1^{-/-}$ mice with age displayed similar negative slope in the production of the offspring (**Figure 1B**). While WT females at middle-age produced an average of six pups, $Tet1^{-/-}$ deficient age-matched mice or at an older age failed to give birth to a pup (**Figure 1A**). $Tet1^{-/-}$ female mice were infertile at middle-age. This phenomenon is comparable to premature ovarian failure. Consistently, ovaries of $Tet1^{-/-}$ females at three age groups were lighter than those of age-matched WT females from young to old age (**Figure 1C**). By examining the ovarian serial sections by histology, the number of primordial and primary follicles as well as secondary and mature antral follicles was dramatically reduced in $Tet1^{-/-}$ females from the three age groups, compared to WT mice served as control (**Figures 1D,E**). Slope in the declined number of follicles in WT mice with age appeared to be much higher than did $Tet1^{-/-}$ mice, and the decrease of secondary and antral follicles in $Tet1^{-/-}$ mice with age actually was not significant (**Figure 1F**). This likely was because the follicle reserve was already dramatically lower in $Tet1^{-/-}$ than in WT mice at young age. Consistently, lower AMH levels indicative of ovarian reserve were found in serum of $Tet1^{-/-}$ than in WT mice at young age (**Figure 1G**). Therefore, *Tet1* deficiency decreases fecundity particularly with age. The decreased fecundity is largely caused by prominent reduction of follicle reserve and development, and also probably by reduced oocyte quality.

Transcriptome Analysis of *Tet1*-Deficient Oocytes in Comparison With WT Oocytes

To examine potential molecular changes in the oocytes, we performed single-cell RNA-seq detecting an average number of genes more than 15,000 (**Supplementary Figure 2A**) to analyze the oocytes of $Tet1^{-/-}$ ($n = 15$) and WT ($n = 19$) collected from young mice in two biological repeated experiments. $Tet1^{-/-}$ oocytes showed 2,013 downregulated (p value < 0.05, and a fold change <-1.5) and 1,557 upregulated genes (p value < 0.05, and a fold change >1.5), compared with WT oocytes (**Figure 2A**). Significantly downregulated genes in $Tet1^{-/-}$ oocytes included *Fmr1* and *Tet1*, supporting an effective deletion of *Tet1*. Also, we analyzed differential gene expression among chromosomes (**Supplementary Figure 2A**). Notably, gene expression on chromosome X (**Figure 2B**) and in mitochondrial functions (**Figure 2C**) was significantly decreased in $Tet1^{-/-}$ oocytes compared with WT oocytes. About 39 genes located on X-chromosomes such as *Nudf11*, *Tmem47*, and *Fmr1* were down-regulated in $Tet1^{-/-}$ oocytes. Due to the important roles of *Fmr1*, we used metascape to analyzed the potential protein-protein interaction enrichment analysis and found Fmr1 might interact with *Hnrnpu* and *Pabpc1* (**Supplementary Figure 2B**). Moreover, the upregulated genes by *Tet1* deficiency were enriched in homologous recombination, cell cycle, fanconi anemia pathway, Alzheimer's disease, and metabolic pathways, while downregulated genes enriched in Ras signaling pathway, neurotrophin signaling pathway, which can cause premature ovarian failure (Dorfman et al., 2014), and notably autophagy and ubiquitin mediated proteolysis (**Figures 2D–F**). By GO enrichment analysis, downregulated genes after *Tet1* deficiency were enriched in mRNA processing, regulation of mRNA stability, histone modification, negative regulation of apoptotic pathway such as *Uri1*, *Rtkn2*, *Nr4a2, Bcl2l2, Akt1* and *Psme3*, and also protein polyubiquitination (**Figures 2G,H**). Interestingly, genes for DNA repair, nuclear division, chromosome segregation and organelle fission were upregulated in *Tet1*-deficient oocytes (**Figures 2G,I**). Increased apoptosis has been implicated in reduction of germ cell numbers (Yamaguchi et al., 2012). Together, these results suggest that elevated organelle fission and reduced protein polyubiquitination

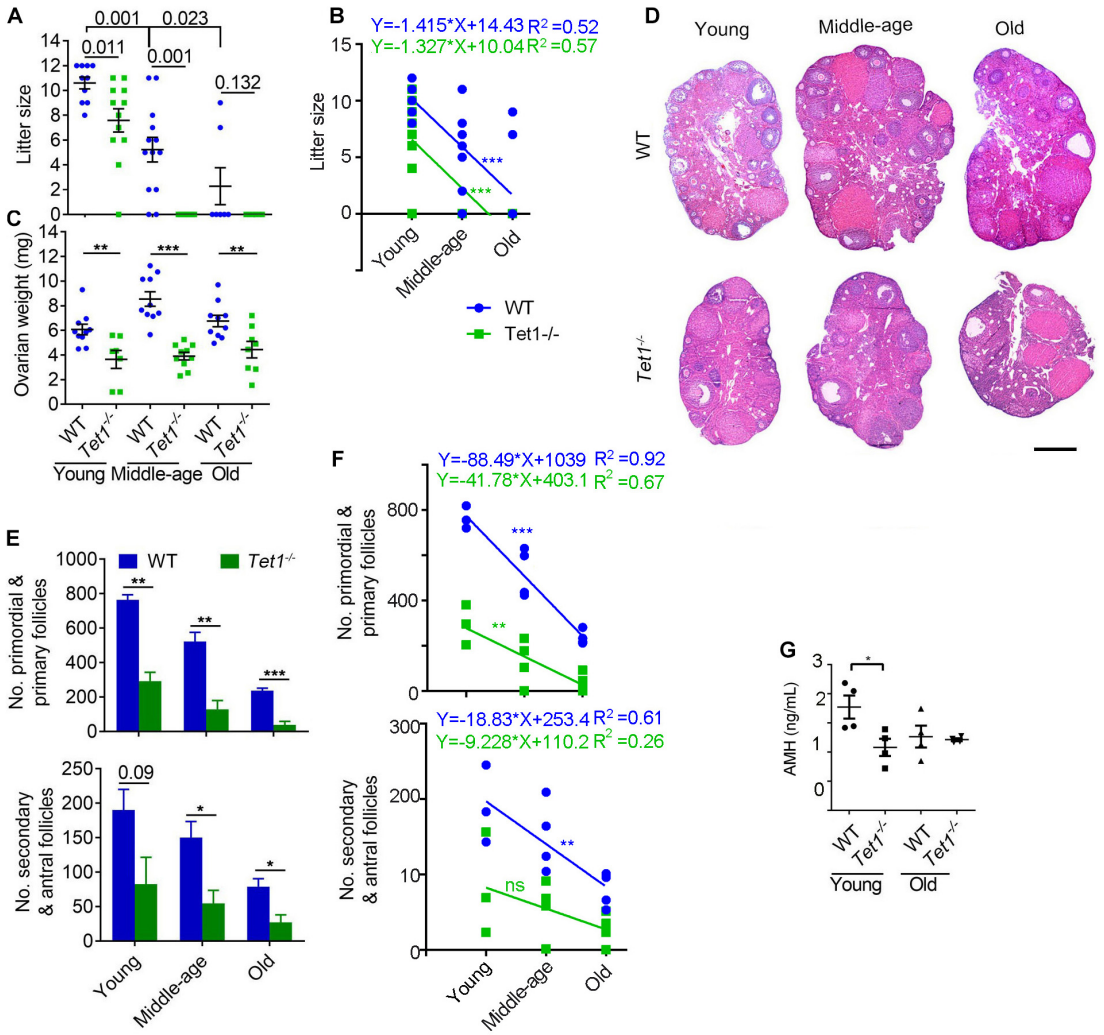

FIGURE 1 | *Tet1* knockout causes subfertility and premature ovarian failure. **(A)** Average litter size of wild-type (WT) and *Tet1* knockout ($Tet1^{-/-}$) female mice at three different reproductive age (young, 2–4 months; middle-age, 7–9 months; old, 10–12 months). $n > 10$ mice for young and middle-age group and $n = 7$–8 mice for old group. **(B)** Linear regression analysis of the age effects on litter size between WT and $Tet1^{-/-}$ mice. $n > 10$ mice for young and middle-age group and $n = 7$–8 mice for old group. **(C)** Average weight per ovary from WT and $Tet1^{-/-}$ mice. $n > 7$. **(D)** Representative images of hematoxylin and eosin (H&E) staining of ovarian sections from young, middle-age and old groups. Scale bar, 500 μm. **(E)** Number of primordial and primary follicles, or secondary and antral follicles from WT and $Tet1^{-/-}$ mice. $n = 4$-6. **(F)** Linear regression analysis of the age effects on the number of follicles between WT and $Tet1^{-/-}$ mice. $n = 3$-4. ns, no significant difference. **(G)** AMH levels in serum of WT and $Tet1^{-/-}$ mice by ELISA assay ($n = 4$). The bars show mean ± SEM. *$P < 0.05$; **$P < 0.01$; ***$P < 0.001$. The P value is labeled if $P > 0.05$ **(A,E)**.

and autophagy might be implicated in reduced oocyte quality resulting from loss of *Tet1*.

Further, we compared our single cell RNA-seq data on oocytes with published data on PGCs (Yamaguchi et al., 2012) and found that 63 genes including *Rnf8*, *Tet3*, *Fmr1nb*, and *Xlr5a/b/c* were commonly downregulated in both *Tet1*-deficient oocytes and PGCs (**Supplementary Figures 3A,B**). We also compared our data using oocytes with the differentially expressed genes (DEG) associated with differential methylated regions (DMR) from published data using PGCs (Yamaguchi et al., 2012). About 20 genes, including *Tet1*, *Sycp3*, *Dazl*, and *Sirt6*, exhibited reduced expression in association with increased methylation after *Tet1* deficiency (**Supplementary Figure 3C**). The analysis shows that Tet1 also plays a role in maturing oocytes in addition to its function in PGCs and meiosis.

Transcriptome Analysis of Old *Tet1*-Deficient Oocytes

We further analyzed differential gene expression between old WT ($n = 19$) and $Tet1^{-/-}$ oocytes ($n = 14$) in two biological repeats. *Tet1*, as expected, and *Dazl* were downregulated in old $Tet1^{-/-}$ oocytes compared with old WT oocytes, while *Dnmt3a* was highly expressed in old $Tet1^{-/-}$ oocytes (**Figure 3A**). Downregulated genes in old $Tet1^{-/-}$ oocytes were enriched in insulin signaling pathway, Parkinson's disease, pathways

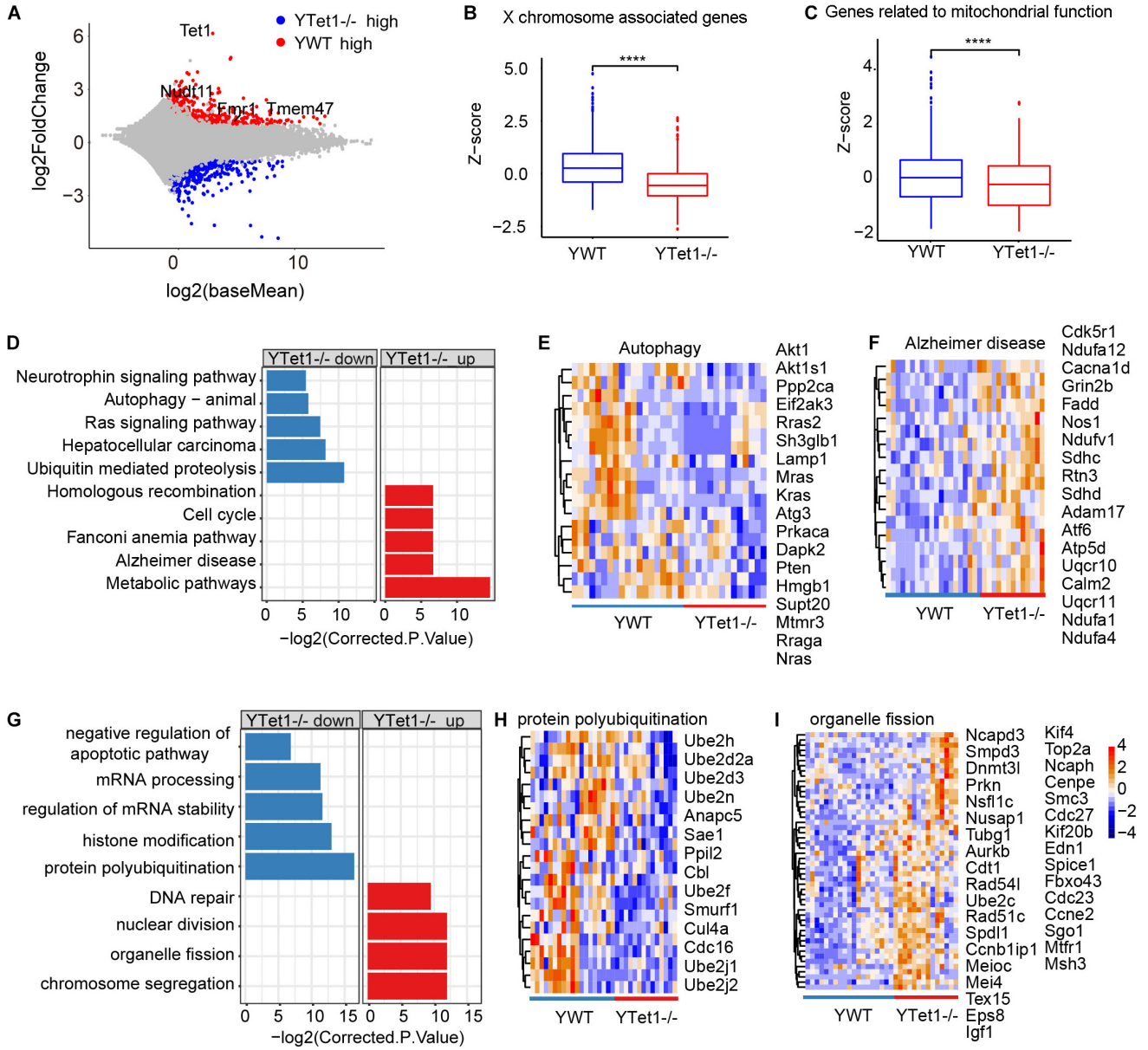

FIGURE 2 | Differential gene expression of *Tet1*$^{-/-}$ and WT oocytes. **(A)** Scatter-plots showing gene expression profile between young *Tet1*$^{-/-}$ ($n = 15$) and WT ($n = 19$) oocytes from two biological repeats. **(B)** Boxplot showing gene expression on chromosome X and downregulated in young *Tet1*$^{-/-}$ oocytes compared with young WT oocytes. ****$P < 0.0001$. **(C)** Boxplot showing expression of genes on mitochondrial function and Downregulated in young Tet1$^{-/-}$ oocytes. **(D)** KEGG enrichment results showing genes downregulated or upregulated after *Tet1* deficiency. *X*-axis represents the corrected *p* value (FDR) using Benjamini and Hochberg. **(E)** Pheatmap showing genes enriched in autophagy signaling pathway down regulated in *Tet1* deficient oocytes. **(F)** Pheatmap showing genes enriched in Alzheimer's disease upregulated in *Tet1* deficient oocytes. **(G)** GO enrichment results showing genes downregulated or upregulated after *Tet1* deficiency. *X*-axis represents the corrected *p* value (FDR) using Benjamini and Hochberg. **(H)** Pheatmap showing genes enriched in protein polyubiquitination in *Tet1* deficient oocytes. **(I)** Pheatmap showing genes enriched in organelle fission upregulated in *Tet1* deficient oocytes.

in cancer and sphingolipid signaling pathway, and genes upregulated in old *Tet1*$^{-/-}$ oocytes enriched in spliceosome, choline metabolism in cancer, and phospholipase D signaling pathway (**Figure 3B**). The expression of genes enriched in insulin signaling pathway (**Figure 3C**), were decreased and genes enriched in spliceosome (**Figure 3D**) were increased in *Tet1*$^{-/-}$ oocytes. By GO enrichment analysis, genes upregulated in old *Tet1*$^{-/-}$ oocytes were enriched in cellular component disassembly, negative regulation of organelle organization, small GTPase mediated signal transduction, DNA repair, regulation of DNA metabolic process and protein localization to Golgi apparatus, whereas genes downregulated enriched in organelle

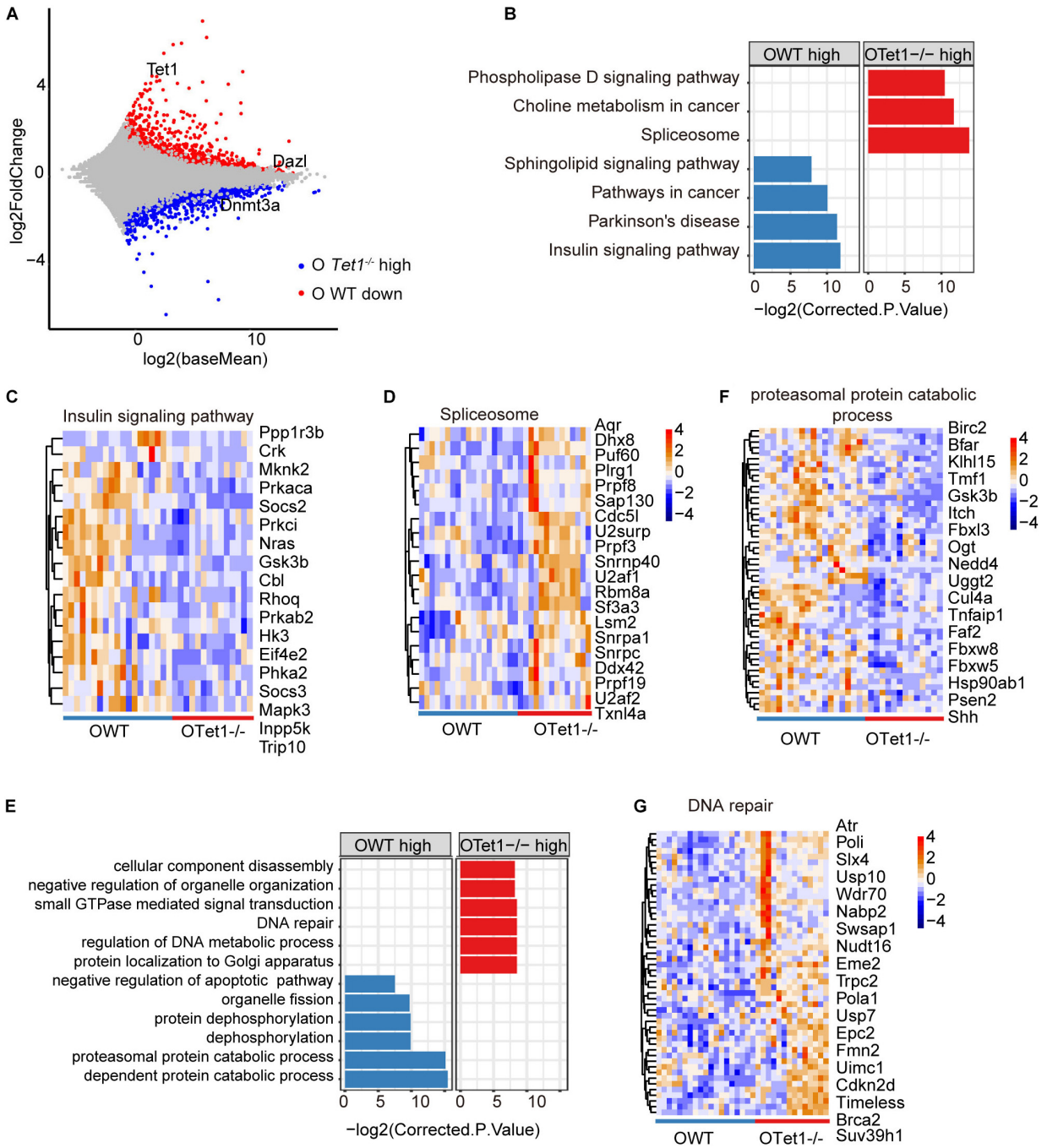

FIGURE 3 | Differential gene expression of old *Tet1*$^{-/-}$ and WT oocytes. **(A)** Scatter-plots showing gene expression profile between old *Tet1*$^{-/-}$ ($n = 14$) and WT ($n = 19$) oocytes from two biological repeats. **(B)** KEGG enrichment results showing genes downregulated or upregulated after *Tet1* deficiency. *X*-axis represents the corrected *p* value (FDR) using Benjamini and Hochberg. **(C)** Pheatmap showing genes enriched in insulin signaling pathway in *Tet1* deficient oocytes. **(D)** Pheatmap showing genes enriched in spliceosome in *Tet1* deficient oocytes. **(E)** GO enrichment results showing genes downregulated or upregulated after *Tet1* deficiency. *X*-axis represents the corrected *p* value (FDR) using Benjamini and Hochberg. **(F)** Pheatmap showing genes enriched in proteasomal protein catabolic process in *Tet1* deficient oocytes. **(G)** Pheatmap showing genes enriched in DNA repair in *Tet1* deficient oocytes.

fission, protein dephosphorylation, proteasomal protein catabolic process and negative regulation of apoptotic pathway including genes including *Akt1*, *Bcl2*, *Nr4a2,* etc (**Figure 3E**). Expression of genes enriched in proteasomal protein catabolic process were decreased (**Figure 3F**), and those in DNA repair were increased (**Figure 3G**). Implication of increased DNA repair is not known, but possibly suggests increased DNA damage stress due to loss of *Tet1*.

Additionally, we analyzed the differential gene expression between young and old $Tet1^{-/-}$ oocytes to explore the aging effect on *Tet1*-deficiency. There were 1,117 upregulated and 1,216 downregulated genes in old $Tet1^{-/-}$ mouse oocytes compared with young $Tet1^{-/-}$ oocytes (**Figure 4A**). Comparatively, more genes were upregulated and downregulated in old WT oocytes (**Figure 4B**). By comparing the differential gene number between WT and $Tet1^{-/-}$ oocytes with mouse age, interestingly, aging affects gene expression more in WT than in $Tet1^{-/-}$ oocytes (**Figure 4C**). However, the mismatch repair was increased in old $Tet1^{-/-}$ oocytes compared with young $Tet1^{-/-}$ oocytes by KEGG enrichment analysis (**Figure 4D**), while apoptotic process was enriched in young $Tet1^{-/-}$ oocytes (**Figure 4E**). These results show that *Tet1* deficiency may overlap some of the aging effect on gene expression. Alternatively, based on complex analysis above, *Tet1* deficiency induces partial aging effects on oocyte function.

Increase of *LINE1* Transcripts in $Tet1^{-/-}$ Oocytes

Transposable elements (TEs) constitute approximately 40% of the mouse genome (Bourc'his and Bestor, 2004) and DNA methylation plays roles in repressing TEs (Wu and Zhang, 2010; Cardelli, 2018). Previously, loss of *Tet1* was associated with increased methylation and reduced transcriptional activation of TEs in PGCs (Hill et al., 2018). We analyzed transcripts of TEs in oocytes of young and old mice based on our single cell RNA-seq data. Proportion of *LINE* and *SINE* was slightly higher in $Tet1^{-/-}$ oocytes compared with young WT oocytes

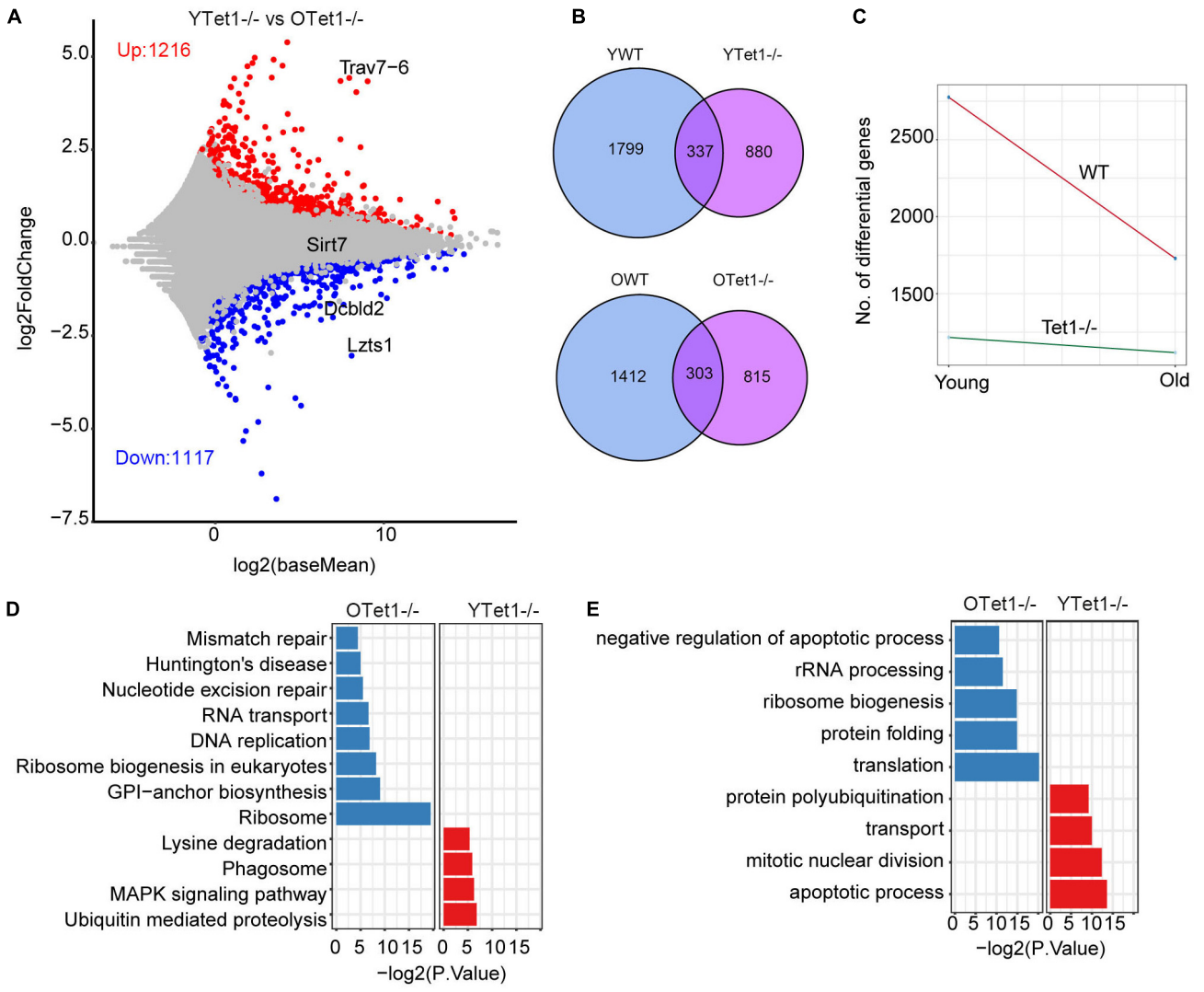

FIGURE 4 | Differential gene expression between young and old $Tet1^{-/-}$ oocytes. **(A)** Scatter plot displaying differential gene expression between young and old $Tet1^{-/-}$ oocytes. **(B)** Venn plot showing the upregulated and downregulated genes between young and old WT oocytes, and young and old $Tet1^{-/-}$ oocytes. **(C)** Slope plot showing the change between WT and $Tet1^{-/-}$ oocytes. **(D)** KEGG enrichment results of differential genes between young and old $Tet1^{-/-}$ oocytes. *X*-axis represents the *p*-value. **(E)** GO enrichment results of differential genes between young and old $Tet1^{-/-}$ oocytes. *X*-axis represents the *p*-value.

(**Figure 5A**). Further analysis of different *ERVs* revealed that the proportion of *ERVL-MaLR* was higher in *Tet1*$^{-/-}$ than that in WT oocytes (**Figure 5B**). Moreover, we used *z*-score to compare the expression of *ERVL-MaLR* belonging to *ERVL-Ma,* and showed that it was increased in *Tet1*$^{-/-}$ oocytes (**Figure 5C**). To further analyze the difference between young *Tet1*$^{-/-}$ and WT oocytes, we performed differential analysis using Deseq2 and found that *L1-mus1* and *L1-mus3* transcripts were increased in young *Tet1*$^{-/-}$ oocytes compared with age-matched WT oocytes (**Figure 5D**). Based on previous study, only 1/10 L1 elements were full-length with lower coding for retrotranspositionally competent L1 elements (Deininger et al., 2017). We further

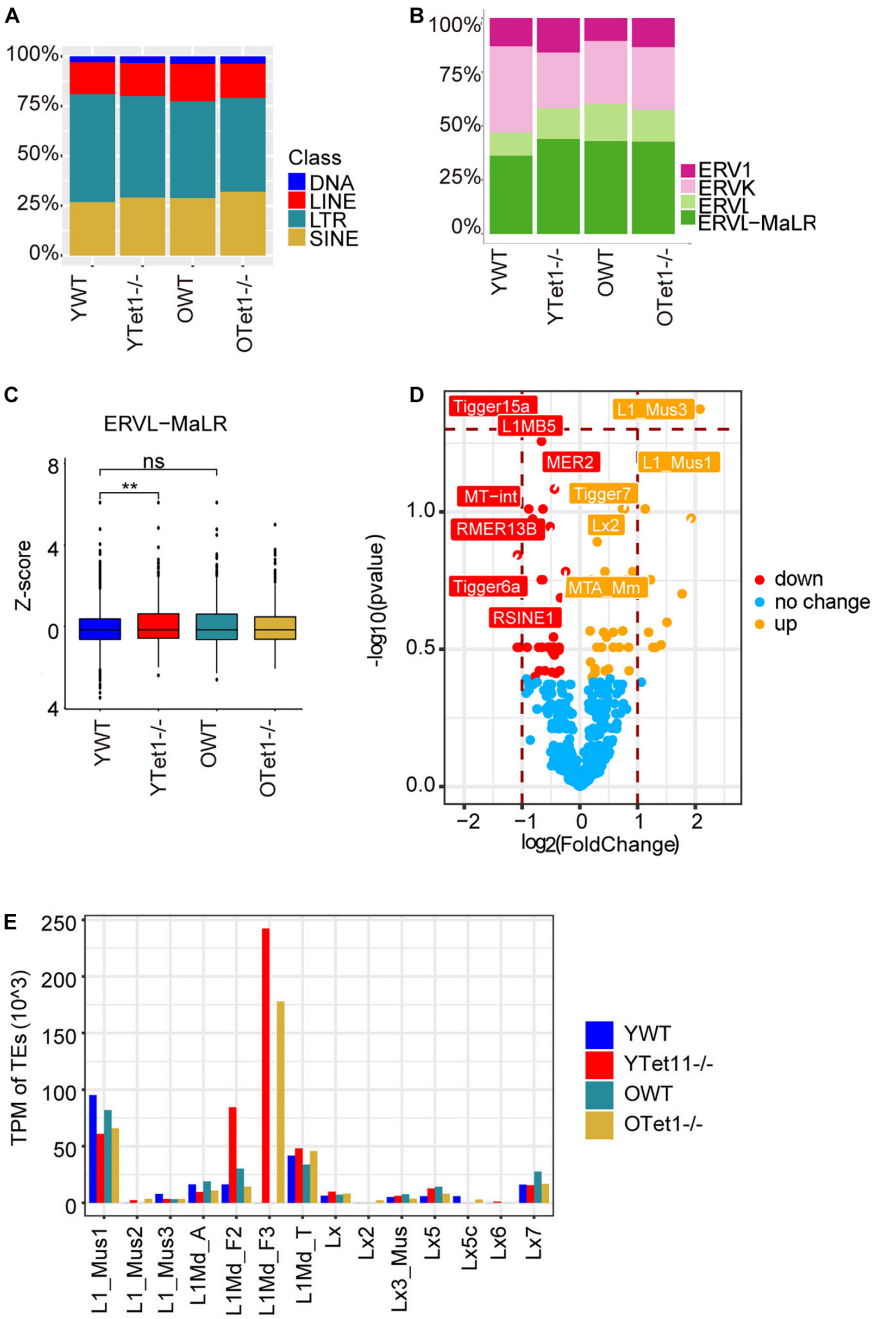

FIGURE 5 | Expression of transposon elements (TEs) of *Tet1*$^{-/-}$ and WT oocytes. **(A)** Barplot showing the proportion of TEs in young *Tet1*$^{-/-}$, WT, old *Tet1*$^{-/-}$, and WT oocytes. **(B)** Barplot displaying the proportion of ERVs in young *Tet1*$^{-/-}$, WT, old *Tet1*$^{-/-}$, and WT oocytes. **(C)** *Z*-score showing expression of ERVL-MaLR between young *Tet1*$^{-/-}$ and WT oocytes. Data are shown as mean ± SEM. $^{**}P < 0.01$. **(D)** Volcano showing the differential TEs between young *Tet1*$^{-/-}$ and WT oocytes. Orange represented upregulated TEs compared with young WT oocytes. **(E)** Expression of Full-length L1 family in young *Tet1*$^{-/-}$ and WT oocytes, and old *Tet1*$^{-/-}$ and WT oocytes.

analyzed the full-length L1 family and found that *L1Md_F3* was notably highly expressed in $Tet1^{-/-}$ deficient oocytes, in contrast to WT oocytes (**Figure 5E**). These results together suggest that *Tet1* deficiency also may alter transcription of TEs in oocytes.

DISCUSSION

Here, we show that *Tet1* deficiency leads to POF by influencing the quality of oocytes, including aberrant X-chromosome inactivation, and increased expression of L1-mus, as well as the oocyte number and follicle reserve. Previous elegant study demonstrated critical role of *Tet1* in meiosis/PGCs during fetal development (Yamaguchi et al., 2012). *Tet1* deficiency leads to aberrant meiosis, increased methylation on meiosis genes and subfertility in young mice (Yamaguchi et al., 2012). We extended the study by evaluating age effects on the fertility and oocytes in adult mice deficient in *Tet1*. We find that *Tet1* deficient mice at reproductive middle-age already are completely infertile, consistent with POF or primary ovarian insufficiency (POI), which is characterized by the premature depletion of ovarian follicles and infertility at mid-reproductive age (Shah and Nagarajan, 2014; Delcour et al., 2019).

We show that *Tet1* deficiency upregulates genes for Alzheimer's diseases, but reduces expression of X-chromosome-linked genes, such as *Fmr1*. These defects might be linked in POF. Women with primary ovarian insufficiency (POI) or POF are at increased risk for non-communicable diseases such as, Alzheimer's disease, cardiovascular disease, and osteoporosis (Harlow and Signorello, 2000; Shah and Nagarajan, 2014). POF has repeatedly been associated to X-chromosome deletions and haploinsufficiency of X-linked genes can be on the basis of POF (Ferreira et al., 2010). X chromosome inactivation could underlie POF linked to cognitive impairment in Alzheimer's disease (Al-Hinti et al., 2007; Bretherick et al., 2007; Davey, 2013), regardless existing discrepancy on X chromosome in POF. Moreover, fragile X mental retardation type 1 (*FMR1*) gene premutation on the X chromosome have been frequently found in POF or POI (Jin et al., 2012; Shamilova et al., 2013; Bouali et al., 2015; Qin et al., 2015; Mila et al., 2018). FMR1 gene premutation allele's carrier women have an increased risk for, or, susceptibility to POF (Ferreira et al., 2010; Pu et al., 2014). *FMR1* gene premutation is the first single-gene cause of primary ovarian failure (Fragile X-associated primary ovarian insufficiency) and one of the most common causes of ataxia (fragile X-associated tremor/ataxia syndrome), and multiple additional phenotypes including neuropathy and neuropsychiatric alterations (Mila et al., 2018).

Moreover, loss of *Tet1* increases DNA methylation as shown by increased expression of Dnmt3a and declined 5hmC levels in oocytes. Tet enzyme can regulate DNA demethylation as well as transcription (Wu and Zhang, 2017; Greenberg and Bourc'his, 2019). DNA methylation is one of the best-characterized epigenetic modifications and has been implicated in numerous biological processes, including transposable element silencing, genomic imprinting and X chromosome inactivation (Wu and Zhang, 2010; Dai et al., 2016). Oxidation of 5-methylcytosine by TET dioxygenases can lead to global demethylation (Dai et al., 2016; Wu and Zhang, 2017). About 60–80% of the CpG sites in the mammalian genome are modified by 5 mC (Smith and Meissner, 2013). TET-mediated oxidation has a locus-specific effect (Yamaguchi et al., 2012, 2013b; Dawlaty et al., 2013; Wu and Zhang, 2017). For instance, integrative Genomics Viewer reveals that the binding of Tet1 and 5 hmC levels on *Fmr1* locus in WT is decreased in *Tet1*-knockdown ESCs by analysis of published data GEO datasets (GSE24841) (Williams et al., 2011), likely reducing expression of *Fmr1*. Indeed, blocking DNA methylation by 5-azacytidine (5-azaC or 5-azadC) has achieved a significant reactivation of *FMR1* gene expression in fragile X syndrome cellular models (Bar-Nur et al., 2012). Also, L1 and ERVL-MaLR are aberrantly expressed in *Tet1*-deficient oocytes. *L1* is highly expressed during mouse oocyte development and embryo cleavage stage (Jachowicz et al., 2017). But, elevated L1 expression correlates with fetal oocyte attrition, oocyte aneuploidy and embryonic lethality (Malki et al., 2014).

Additionally, *Tet1* deficiency results in declined ubiquitination and autophagy but increased organelle fission in oocytes, and these defects presumably can be detrimental to clearance of damaged, or, senescent organelles in the cells. Impaired autophagy can lead to POF (Gawriluk et al., 2014; Delcour et al., 2019). *Tet1* deficiency also decreases Ras signaling pathways. Appropriate activation of RAS signaling is crucial for directing normal follicle development (Fan et al., 2008).

Further experiments are required to investigate the underlying molecular mechanisms of how *Tet1* regulates these signaling pathways associated with POF or POI. Also, the question remains as to whether Tet1 has similar function in human fertility and in POF patients. Nevertheless, our findings that Tet1 may involve in autophagy, X-chromosome activation and Alzheimer's disease provide additional insights into molecular basis of POF.

DATA AVAILABILITY STATEMENT

RNA-seq data have been deposited in the GEO database under the accession number GSE142163.

ETHICS STATEMENT

The animal study was reviewed and approved by the Institutional Animal Care and Use Committee, Nankai University. Written informed consent was obtained from the owners for the participation of their animals in this study.

AUTHOR CONTRIBUTIONS

HW performed the experiments on fertility and histology, and prepared the manuscript. LinlLiu analyzed the RNA-seq data and prepared the manuscript. G_LX provided the materials, advised the project, and revised the manuscript. LinLiu conceived the study, designed experiments, and wrote the manuscript. All authors contributed to the article and approved the submitted version.

FUNDING

This work was supported by the National Natural Science Foundation of China (31571546 and 91749129).

ACKNOWLEDGMENTS

We thank Wei Deng, Qin Xu, Guian Huang, Jiao Yang, and Haiying Wang for help in the experiments.

SUPPLEMENTARY MATERIAL

The Supplementary Material for this article can be found online at: https://www.frontiersin.org/articles/10.3389/fcell.2021.644135/full#supplementary-material

Supplementary Figure 1 | Loss of *Tet1* in female mice reduces 5 hmC levels in oocytes. **(A)** PCR genotyping of *Tet1* mutant mice. Primer sequences are listed in **Supplementary Table 2**. **(B)** Table summarizing the litter size and Mendelian ratio of $Tet1^{-/-}$ mice. **(C)** *Tet1* mRNA expression level in ovaries of young mice by qPCR analysis. **(D)** Tet1 protein expression level in E3.5 blastocysts by immunofluorescence. Scale bar, 10 μm. **(E)** Representative images of primordial follicles from young WT mouse ovary. **(F)** Representative images of primordial follicles stained with 5 hmC antibody. Dashed line indicates the primordial oocyte. Scale bar, 10 μm. Bottom panel, Relative 5 hmC level in primordial oocytes from young mice. $n = 21$ oocytes counted for each group. Data represents mean ± SEM. $^{***}P < 0.001$.

Supplementary Figure 2 | Distribution of differentially expressed genes across chromosomes. **(A)** Scatter plot illustrating the chromosomal distribution of differential genes Between young WT and $Tet1^{-/-}$ oocytes. **(B)** Protein-protein interactome network analysis using Metascape (http://metascape.org/gp/index.html#) showing the potential interaction of Fmr1, Hnrnpu and Pabpc1 and with other proteins.

Supplementary Figure 3 | Coverage of Smart-seq2 of oocytes and comparison with transcriptome data on PGCs from Yamaguchi et al., 2012. **(A)** Boxplot displaying number of genes sequenced in oocytes. **(B)** Venn plot showing the overlapped, downregulated genes between oocytes based on our data and PGCs from Yamaguchi et al., 2012. **(C)** Venn plot showing the overlapped, downregulated genes between oocytes and PGCss associated with DMRs, based on Yamaguchi et al., 2012.

REFERENCES

Al-Hinti, J. T., Nagan, N., and Harik, S. I. (2007). Fragile X premutation in a woman with cognitive impairment, tremor, and history of premature ovarian failure. *Alzheimer Dis. Assoc. Disord.* 21, 262–264. doi: 10.1097/wad.0b013e31811ec130

Bacher, R., Chu, L. F., Leng, N., Gasch, A. P., Thomson, J. A., Stewart, R. M., et al. (2017). SCnorm: robust normalization of single-cell RNA-seq data. *Nat. Methods* 14, 584–586. doi: 10.1038/nmeth.4263

Bar-Nur, O., Caspi, I., and Benvenisty, N. (2012). Molecular analysis of FMR1 reactivation in fragile-X induced pluripotent stem cells and their neuronal derivatives. *J. Mol. Cell. Biol.* 4, 180–183. doi: 10.1093/jmcb/mjs007

Bouali, N., Hmida, D., Mougou, S., Bouligand, J., Lakhal, B., Dimessi, S., et al. (2015). Analysis of FMR1 gene premutation and X chromosome cytogenetic abnormalities in 100 Tunisian patients presenting premature ovarian failure. *Ann. Endocrinol.* 76, 671–678. doi: 10.1016/j.ando.2015.10.001

Bourc'his, D., and Bestor, T. H. (2004). Meiotic catastrophe and retrotransposon reactivation in male germ cells lacking Dnmt3L. *Nature* 431, 96–99. doi: 10.1038/nature02886

Bretherick, K. L., Metzger, D. L., Chanoine, J. P., Panagiotopoulos, C., Watson, S. K., Lam, W. L., et al. (2007). Skewed X-chromosome inactivation is associated with primary but not secondary ovarian failure. *Am. J. Med. Genet. A* 143A, 945–951. doi: 10.1002/ajmg.a.31679

Bristol-Gould, S. K., Kreeger, P. K., Selkirk, C. G., Kilen, S. M., Mayo, K. E., Shea, L. D., et al. (2006). Fate of the initial follicle pool: empirical and mathematical evidence supporting its sufficiency for adult fertility. *Dev. Biol.* 298, 149–154. doi: 10.1016/j.ydbio.2006.06.023

Broekmans, F. J., Knauff, E. A., te Velde, E. R., Macklon, N. S., and Fauser, B. C. (2007). Female reproductive ageing: current knowledge and future trends. *Trends Endocrinol. Metab.* 18, 58–65. doi: 10.1016/j.tem.2007.01.004

Broekmans, F. J., Soules, M. R., and Fauser, B. C. (2009). Ovarian aging: mechanisms and clinical consequences. *Endocr. Rev.* 30, 465–493. doi: 10.1210/er.2009-0006

Bult, C. J., Blake, J. A., Smith, C. L., Kadin, J. A., Richardson, J. E., and Mouse Genome Database Group (2019). Mouse Genome Database (MGD) 2019. *Nucleic Acids Res.* 47, D801–D806.

Cardelli, M. (2018). The epigenetic alterations of endogenous retroelements in aging. *Mech. Ageing Dev.* 174, 30–46. doi: 10.1016/j.mad.2018.02.002

Chen, D., and Kerr, C. (2019). The epigenetics of stem cell aging comes of age. *Trends Cell Biol.* 29, 563–568. doi: 10.1016/j.tcb.2019.03.006

Cole, J. J., Robertson, N. A., Rather, M. I., Thomson, J. P., McBryan, T., Sproul, D., et al. (2017). Diverse interventions that extend mouse lifespan suppress shared age-associated epigenetic changes at critical gene regulatory regions. *Genome Biol.* 18:58.

Dai, H. Q., Wang, B. A., Yang, L., Chen, J. J., Zhu, G. C., Sun, M. L., et al. (2016). TET-mediated DNA demethylation controls gastrulation by regulating Lefty-Nodal signalling. *Nature* 538, 528–532. doi: 10.1038/nature20095

Davey, D. A. (2013). Alzheimer's disease, dementia, mild cognitive impairment and the menopause: a 'window of opportunity'? *Womens Health* 9, 279–290. doi: 10.2217/whe.13.22

Dawlaty, M. M., Breiling, A., Le, T., Raddatz, G., Barrasa, M. I., Cheng, A. W., et al. (2013). Combined deficiency of Tet1 and Tet2 causes epigenetic abnormalities but is compatible with postnatal development. *Dev. Cell* 24, 310–323. doi: 10.1016/j.devcel.2012.12.015

Dawlaty, M. M., Ganz, K., Powell, B. E., Hu, Y. C., Markoulaki, S., Cheng, A. W., et al. (2011). Tet1 is dispensable for maintaining pluripotency and its loss is compatible with embryonic and postnatal development. *Cell Stem Cell* 9, 166–175. doi: 10.1016/j.stem.2011.07.010

Deininger, P., Morales, M. E., White, T. B., Baddoo, M., Hedges, D. J., Servant, G., et al. (2017). A comprehensive approach to expression of L1 loci. *Nucleic Acids Res.* 45:e31. doi: 10.1093/nar/gkw1067

Delcour, C., Amazit, L., Patino, L. C., Magnin, F., Fagart, J., Delemer, B., et al. (2019). ATG7 and ATG9A loss-of-function variants trigger autophagy impairment and ovarian failure. *Genet. Med.* 21, 930–938. doi: 10.1038/s41436-018-0287-y

Djahanbakhch, O., Ezzati, M., and Zosmer, A. (2007). Reproductive ageing in women. *J. Pathol.* 211, 219–231. doi: 10.1002/path.2108

Dorfman, M. D., Garcia-Rudaz, C., Alderman, Z., Kerr, B., Lomniczi, A., Dissen, G. A., et al. (2014). Loss of Ntrk2/Kiss1r signaling in oocytes causes premature ovarian failure. *Endocrinology* 155, 3098–3111. doi: 10.1210/en.2014-1111

Faddy, M. J. (2000). Follicle dynamics during ovarian ageing. *Mol. Cell. Endocrinol.* 163, 43–48. doi: 10.1016/s0303-7207(99)00238-5

Fan, H. Y., Shimada, M., Liu, Z., Cahill, N., Noma, N., Wu, Y., et al. (2008). Selective expression of KrasG12D in granulosa cells of the mouse ovary causes defects in follicle development and ovulation. *Development* 135, 2127–2137. doi: 10.1242/dev.020560

Ferreira, S. I., Matoso, E., Pinto, M., Almeida, J., Liehr, T., Melo, J. B., et al. (2010). X-chromosome terminal deletion in a female with premature ovarian failure: haploinsufficiency of X-linked genes as a possible explanation. *Mol. Cytogenet.* 3:14. doi: 10.1186/1755-8166-3-14

Gawriluk, T. R., Ko, C., Hong, X., and Christenson, L. K. (2014). Beclin-1 deficiency in the murine ovary results in the reduction of progesterone production to promote preterm labor. *Proc. Natl. Acad. Sci. U.S.A.* 111, E4194–E4203.

Greenberg, M. V. C., and Bourc'his, D. (2019). The diverse roles of DNA methylation in mammalian development and disease. *Nat. Rev. Mol. Cell Biol.* 20, 590–607. doi: 10.1038/s41580-019-0159-6

Hannum, G., Guinney, J., Zhao, L., Zhang, L., Hughes, G., Sadda, S., et al. (2013). Genome-wide methylation profiles reveal quantitative views of human aging rates. *Mol. Cell.* 49, 359–367. doi: 10.1016/j.molcel.2012.10.016

Harlow, B. L., and Signorello, L. B. (2000). Factors associated with early menopause. *Maturitas* 35, 3–9. doi: 10.1016/s0378-5122(00)00092-x

Hill, P. W. S., Leitch, H. G., Requena, C. E., Sun, Z., Amouroux, R., Roman-Trufero, M., et al. (2018). Epigenetic reprogramming enables the transition from primordial germ cell to gonocyte. *Nature* 555, 392–396. doi: 10.1038/nature25964

Horvath, S. (2013). DNA methylation age of human tissues and cell types. *Genome Biol.* 14:R115.

Ito, S., D'Alessio, A. C., Taranova, O. V., Hong, K., Sowers, L. C., and Zhang, Y. (2010). Role of Tet proteins in 5mC to 5hmC conversion, ES-cell self-renewal and inner cell mass specification. *Nature* 466, 1129–1133. doi: 10.1038/nature09303

Jachowicz, J. W., Bing, X., Pontabry, J., Boskovic, A., Rando, O. J., and Torres-Padilla, M. E. (2017). LINE-1 activation after fertilization regulates global chromatin accessibility in the early mouse embryo. *Nat. Genet.* 49, 1502–1510. doi: 10.1038/ng.3945

Jin, M., Yu, Y., and Huang, H. (2012). An update on primary ovarian insufficiency. *Sci. China Life Sci.* 55, 677–686.

Kaul, T., Morales, M. E., Smither, E., Baddoo, M., Belancio, V. P., and Deininger, P. (2019). RNA next-generation sequencing and a bioinformatics pipeline to identify expressed LINE-1s at the locus-specific level. *J. Vis. Exp.* 147: 59771.

Kim, D., Langmead, B., and Salzberg, S. L. (2015). HISAT: a fast spliced aligner with low memory requirements. *Nat. Methods* 12, 357–360. doi: 10.1038/nmeth.3317

Kim, D., Pertea, G., Trapnell, C., Pimentel, H., Kelley, R., and Salzberg, S. L. (2013). TopHat2: accurate alignment of transcriptomes in the presence of insertions, deletions and gene fusions. *Genome Biol.* 14:R36.

Ko, M., Bandukwala, H. S., An, J., Lamperti, E. D., Thompson, E. C., Hastie, R., et al. (2011). Ten-Eleven-Translocation 2 (TET2) negatively regulates homeostasis and differentiation of hematopoietic stem cells in mice. *Proc. Natl. Acad. Sci. U.S.A.* 108, 14566–14571. doi: 10.1073/pnas.1112317108

Koh, K. P., Yabuuchi, A., Rao, S., Huang, Y., Cunniff, K., Nardone, J., et al. (2011). Tet1 and Tet2 regulate 5-hydroxymethylcytosine production and cell lineage specification in mouse embryonic stem cells. *Cell Stem Cell* 8, 200–213. doi: 10.1016/j.stem.2011.01.008

Lawson, R., El-Toukhy, T., Kassab, A., Taylor, A., Braude, P., Parsons, J., et al. (2003). Poor response to ovulation induction is a stronger predictor of early menopause than elevated basal FSH: a life table analysis. *Hum. Reprod.* 18, 527–533. doi: 10.1093/humrep/deg101

Liao, Y., Smyth, G. K., and Shi, W. (2014). featureCounts: an efficient general purpose program for assigning sequence reads to genomic features. *Bioinformatics* 30, 923–930. doi: 10.1093/bioinformatics/btt656

Liu, M., Yin, Y., Ye, X., Zeng, M., Zhao, Q., Keefe, D. L., et al. (2013). Resveratrol protects against age-associated infertility in mice. *Hum. Reprod.* 28, 707–717.

Lopez-Otin, C., Blasco, M. A., Partridge, L., Serrano, M., and Kroemer, G. (2013). The hallmarks of aging. *Cell* 153, 1194–1217.

Love, M. I., Huber, W., and Anders, S. (2014). Moderated estimation of fold change and dispersion for RNA-seq data with DESeq2. *Genome Biol.* 15:550.

Maegawa, S., Hinkal, G., Kim, H. S., Shen, L., Zhang, L., Zhang, J., et al. (2010). Widespread and tissue specific age-related DNA methylation changes in mice. *Genome Res.* 20, 332–340. doi: 10.1101/gr.096826.109

Malki, S., van der Heijden, G. W., O'Donnell, K. A., Martin, S. L., and Bortvin, A. (2014). A role for retrotransposon LINE-1 in fetal oocyte attrition in mice. *Dev. Cell* 29, 521–533. doi: 10.1016/j.devcel.2014.04.027

Mila, M., Alvarez-Mora, M. I., Madrigal, I., and Rodriguez-Revenga, L. (2018). Fragile X syndrome: an overview and update of the FMR1 gene. *Clin. Genet.* 93, 197–205. doi: 10.1111/cge.13075

Myers, M., Britt, K. L., Wreford, N. G., Ebling, F. J., and Kerr, J. B. (2004). Methods for quantifying follicular numbers within the mouse ovary. *Reproduction* 127, 569–580. doi: 10.1530/rep.1.00095

Notarianni, E. (2011). Reinterpretation of evidence advanced for neo-oogenesis in mammals, in terms of a finite oocyte reserve. *J. Ovarian Res.* 4:1. doi: 10.1186/1757-2215-4-1

Picelli, S., Faridani, O. R., Bjorklund, A. K., Winberg, G., Sagasser, S., and Sandberg, R. (2014). Full-length RNA-seq from single cells using Smart-seq2. *Nat. Protoc.* 9, 171–181. doi: 10.1038/nprot.2014.006

Pu, D., Xing, Y., Gao, Y., Gu, L., and Wu, J. (2014). Gene variation and premature ovarian failure: a meta-analysis. *Eur. J. Obstet. Gynecol. Reprod. Biol.* 182, 226–237. doi: 10.1016/j.ejogrb.2014.09.036

Qin, Y., Jiao, X., Simpson, J. L., and Chen, Z. J. (2015). Genetics of primary ovarian insufficiency: new developments and opportunities. *Hum. Reprod. Update* 21, 787–808. doi: 10.1093/humupd/dmv036

Rando, T. A., and Chang, H. Y. (2012). Aging, rejuvenation, and epigenetic reprogramming: resetting the aging clock. *Cell* 148, 46–57. doi: 10.1016/j.cell.2012.01.003

Shah, D., and Nagarajan, N. (2014). Premature menopause - meeting the needs. *Post Reprod. Health* 20, 62–68. doi: 10.1177/2053691145319099

Shamilova, N. N., Marchenko, L. A., Dolgushina, N. V., Zaletaev, D. V., and Sukhikh, G. T. (2013). The role of genetic and autoimmune factors in premature ovarian failure. *J. Assist. Reprod. Genet.* 30, 617–622. doi: 10.1007/s10815-013-9974-4

Smith, Z. D., and Meissner, A. (2013). DNA methylation: roles in mammalian development. *Nat. Rev. Genet.* 14, 204–220. doi: 10.1038/nrg3354

Stubbs, T. M., Bonder, M. J., Stark, A. K., Krueger, F., Team, B. I. A. C., von Meyenn, F., et al. (2017). Multi-tissue DNA methylation age predictor in mouse. *Genome Biol.* 18:68.

Tatone, C., Amicarelli, F., Carbone, M. C., Monteleone, P., Caserta, D., Marci, R., et al. (2008). Cellular and molecular aspects of ovarian follicle ageing. *Hum. Reprod. Update* 14, 131–142. doi: 10.1093/humupd/dmm048

van Rooij, I. A., Broekmans, F. J., Scheffer, G. J., Looman, C. W., Habbema, J. D., de Jong, F. H., et al. (2005). Serum antimullerian hormone levels best reflect the reproductive decline with age in normal women with proven fertility: a longitudinal study. *Fertil. Steril.* 83, 979–987. doi: 10.1016/j.fertnstert.2004.11.029

Wang, H., Liu, L., Gou, M., Huang, G., Tian, C., Yang, J., et al. (2020). Roles of Tet2 in meiosis, fertility and reproductive aging. *Protein Cell* [Epub ahead of print].

Williams, K., Christensen, J., Pedersen, M. T., Johansen, J. V., Cloos, P. A., Rappsilber, J., et al. (2011). TET1 and hydroxymethylcytosine in transcription and DNA methylation fidelity. *Nature* 473, 343–348. doi: 10.1038/nature10066

Wixon, J., and Kell, D. (2000). The Kyoto encyclopedia of genes and genomes–KEGG. *Yeast* 17, 48–55.

Wu, S. C., and Zhang, Y. (2010). Active DNA demethylation: many roads lead to Rome. *Nat. Rev. Mol. Cell Biol.* 11, 607–620. doi: 10.1038/nrm2950

Wu, X., and Zhang, Y. (2017). TET-mediated active DNA demethylation: mechanism, function and beyond. *Nat. Rev. Genet.* 18, 517–534. doi: 10.1038/nrg.2017.33

Xie, C., Mao, X., Huang, J., Ding, Y., Wu, J., Dong, S., et al. (2011). KOBAS 2.0: a web server for annotation and identification of enriched pathways and diseases. *Nucleic Acids Res.* 39, W316–W322.

Yamaguchi, S., Hong, K., Liu, R., Inoue, A., Shen, L., Zhang, K., et al. (2013a). Dynamics of 5-methylcytosine and 5-hydroxymethylcytosine during germ cell reprogramming. *Cell Res.* 23, 329–339. doi: 10.1038/cr.2013.22

Yamaguchi, S., Shen, L., Liu, Y., Sendler, D., and Zhang, Y. (2013b). Role of Tet1 in erasure of genomic imprinting. *Nature* 504, 460–464. doi: 10.1038/nature12805

Yamaguchi, S., Hong, K., Liu, R., Shen, L., Inoue, A., Diep, D., et al. (2012). Tet1 controls meiosis by regulating meiotic gene expression. *Nature* 492, 443–447. doi: 10.1038/nature11709

Yu, G., Wang, L. G., Han, Y., and He, Q. Y. (2012). clusterProfiler: an R package for comparing biological themes among gene clusters. *OMICS* 16, 284–287. doi: 10.1089/omi.2011.0118

Zhang, H., Zheng, W., Shen, Y., Adhikari, D., Ueno, H., and Liu, K. (2012). Experimental evidence showing that no mitotically active female germline progenitors exist in postnatal mouse ovaries. *Proc. Natl. Acad. Sci. U.S.A.* 109, 12580–12585. doi: 10.1073/pnas.1206600109

Zhang, R. R., Cui, Q. Y., Murai, K., Lim, Y. C., Smith, Z. D., and Jin, S. (2013). Tet1 regulates adult hippocampal neurogenesis and cognition. *Cell Stem Cell* 13, 237–245. doi: 10.1016/j.stem.2013.05.006

Zhang, W., Qu, J., Liu, G. H., and Belmonte, J. C. I. (2020). The ageing epigenome and its rejuvenation. *Nat. Rev. Mol. Cell Biol.* 21, 137–150. doi: 10.1038/s41580-019-0204-5

Conflict of Interest: The authors declare that the research was conducted in the absence of any commercial or financial relationships that could be construed as a potential conflict of interest.

frontiers in Cell and Developmental Biology

REVIEW
published: 16 April 2021
doi: 10.3389/fcell.2021.660626

Proteostasis in the Male and Female Germline: A New Outlook on the Maintenance of Reproductive Health

*Shenae L. Cafe[1], Brett Nixon[1], Heath Ecroyd[2,3], Jacinta H. Martin[4], David A. Skerrett-Byrne[1] and Elizabeth G. Bromfield[1,5]**

[1] Priority Research Centre for Reproductive Science, Faculty of Science, The University of Newcastle, Callaghan, NSW, Australia, [2] Molecular Horizons, School of Chemistry and Molecular Bioscience, University of Wollongong, Wollongong, NSW, Australia, [3] Illawarra Health and Medical Research Institute, Wollongong, NSW, Australia, [4] Department of Human Genetics, McGill University Health Centre Research Institute, Montreal, QC, Canada, [5] Department of Biochemistry and Cell Biology, Faculty of Veterinary Medicine, Utrecht University, Utrecht, Netherlands

For fully differentiated, long lived cells the maintenance of protein homeostasis (proteostasis) becomes a crucial determinant of cellular function and viability. Neurons are the most well-known example of this phenomenon where the majority of these cells must survive the entire course of life. However, male and female germ cells are also uniquely dependent on the maintenance of proteostasis to achieve successful fertilization. Oocytes, also long-lived cells, are subjected to prolonged periods of arrest and are largely reliant on the translation of stored mRNAs, accumulated during the growth period, to support meiotic maturation and subsequent embryogenesis. Conversely, sperm cells, while relatively ephemeral, are completely reliant on proteostasis due to the absence of both transcription and translation. Despite these remarkable, cell-specific features there has been little focus on understanding protein homeostasis in reproductive cells and how/whether proteostasis is "reset" during embryogenesis. Here, we seek to capture the momentum of this growing field by highlighting novel findings regarding germline proteostasis and how this knowledge can be used to promote reproductive health. In this review we capture proteostasis in the context of both somatic cell and germline aging and discuss the influence of oxidative stress on protein function. In particular, we highlight the contributions of proteostasis changes to oocyte aging and encourage a focus in this area that may complement the extensive analyses of DNA damage and aneuploidy that have long occupied the oocyte aging field. Moreover, we discuss the influence of common non-enzymatic protein modifications on the stability of proteins in the male germline, how these changes affect sperm function, and how they may be prevented to preserve fertility. Through this review we aim to bring to light a new trajectory for our field and highlight the potential to harness the germ cell's natural proteostasis mechanisms to improve reproductive health. This manuscript will be of interest to those in the fields of proteostasis, aging, male and female gamete reproductive biology, embryogenesis, and life course health.

Keywords: protein homeostasis, reproductive aging, oxidative stress, chaperone, germ cell, oocyte, sirtuin, spermatozoa

OPEN ACCESS

Edited by:
Francesca Elizabeth Duncan, Northwestern University, United States

Reviewed by:
Miguel Angel Brieño-Enriquez, Magee-Womens Research Institute, United States
Marco Conti, University of California, San Francisco, United States

****Correspondence:***
Elizabeth G. Bromfield
Elizabeth.bromfield@newcastle.edu.au

Specialty section:
This article was submitted to Cellular Biochemistry, a section of the journal Frontiers in Cell and Developmental Biology

Received: *29 January 2021*
Accepted: *22 March 2021*
Published: *16 April 2021*

Citation:
Cafe SL, Nixon B, Ecroyd H, Martin JH, Skerrett-Byrne DA and Bromfield EG (2021) Proteostasis in the Male and Female Germline: A New Outlook on the Maintenance of Reproductive Health. Front. Cell Dev. Biol. 9:660626. doi: 10.3389/fcell.2021.660626

INTRODUCTION

A functional proteome is essential for the survival of cells and organisms, resulting in a considerable investment of energy into the maintenance of cellular protein homeostasis (proteostasis). As energy demands change in response to the environment, such as during aging and oxidative stress, proteostasis can be compromised leading to a harmful accumulation of damaged or misfolded proteins and the induction of degenerative diseases such as Alzheimer's disease (AD) and Amyotrophic lateral sclerosis (ALS). For the male and female germline, the regulation of proteostasis can be particularly challenging as the male gamete experiences prolonged periods in the relative absence of transcription and translation while the female gamete is similarly transcriptionally inactive prior to fertilization and embryonic genome activation. Consequently, maintaining a functional proteome becomes heavily reliant upon proteostasis machinery, the cellular environment and post-translational protein regulation.

Distinctively, in the case of the gametes, the stakes are extremely high as the maintenance of proteostasis throughout the life of germ cells is critical to ensure the fitness of the next generation. In recent years, a focus on characterizing the proteomes of germ cells has begun to reveal the importance of proteostasis both to cellular and organismal development, as well as for fertilization. Herein, we provide an important update on the contribution of proteostasis disruption to male and female infertility and highlight key areas for future research through the specific lenses of reproductive aging and oxidative stress; two of the most prevalent elements that compromise germ cell function and contribute to infertility in humans. Moreover, we draw on relevant discoveries in somatic cells and model organisms to propose a new trajectory for the field of mammalian reproduction that may lead to better regulation of proteostasis and the improvement of male and female reproductive health.

THE PROTEOSTASIS NETWORK IN HEALTH AND DISEASE

Proteostasis describes the homeostatic relationship between protein production, assembly, and degradation. It is thought that up to 30% of newly synthesized proteins are misfolded as a consequence of the complex intracellular milieu, where macromolecular crowding poses as a major challenge to the delicate state of equilibrium between the native and non-native conformations of proteins (Grune et al., 2004; Houck et al., 2012). Following translation, most nascent polypeptides must correctly fold into their three-dimensional structures prior to fulfilling their functional roles. Disruptions in this process potentiates protein aggregation, in turn, requiring cells to engage a consortium of defense mechanisms in order to mitigate the impact of misfolded protein species (Dobson, 2004; Schaur et al., 2015; Radwan et al., 2017). The proteostasis network (PN) includes elements capable of modulating protein synthesis/translation, trafficking, folding, secretion and degradation; and can be altered transiently or permanently in response to stress and other compounding factors (Koga et al., 2011; Kim et al., 2013).

Protein aggregation can be triggered by numerous cellular challenges including oxidative stress-induced unfolding/misfolding, a compromised proteostasis network, or age-dependent decline in protein folding machinery, diminished quality control, as well as mutations that increase the propensity of a protein to aggregate (Stefani, 2004). Different forms of aggregates can arise from the same protein due to exposure to diverse stress conditions. The term aggregate has broad connotations, referring to composites of misfolded proteins that compromise cellular function (Hohn et al., 2013; Mattoo and Goloubinoff, 2014; Radwan et al., 2017). Similarly, whilst the term amyloid refers to a type of insoluble protein aggregates, these are dominated by β-sheet secondary structures and a fibrillar morphology and often found within inclusion bodies (Stefani, 2004). Concordantly, protein aggregation, and the accumulation of the toxic protein species as a result of this process, is often indicative of a decline in proteostasis (Radwan et al., 2017). The unchecked propagation of protein aggregates often accompanies the onset of severe disease states (Chiti and Dobson, 2006), with notable examples including AD, ALS, type 2 diabetes, and the spongiform encephalopathies (e.g., mad cow disease); all of which are progressive disorders associated with high rates of morbidity and mortality (Rambaran and Serpell, 2008).

Key Components of the Proteostasis Network Relevant to This Review

In view of the deleterious impact of protein aggregation, it is perhaps not surprising that somatic cells are generally endowed with a sophisticated suite of cellular surveillance and defense mechanisms designed to detect, counter and/or repair protein aggregate formation. Such mechanisms include the synergistic action of the heat shock response (HSR), unfolded protein response (UPR^{ER} and UPR^{mt}), ubiquitin-proteasome system (UPS) and autophagic-lysosomal pathways; all of which combine to play crucial roles in the maintenance of cellular homeostasis (**Figure 1**). Whilst each of these mechanisms are undoubtedly important, here we focus only on those elements of the PN summarized in **Figure 1** in order to provide context to proteostasis mechanisms as they relate to male and female fertility. For a comprehensive review of all proteostasis elements and mechanisms see Labbadia and Morimoto, 2015 and Klaips et al., 2018.

Protein Degradation

As a primary line of defense against aggregation-induced cellular toxicity, the proteasome complex is responsible for the catalytic degradation of irreversibly damaged and/or dysfunctional proteins and the recycling of their components. Proteins destined for proteasomal degradation are tagged with polyubiquitin chain(s) consisting of four or more ubiquitin moieties, via the action of one of the more than 600 ubiquitin ligases represented in the human genome (Iconomou and Saunders, 2016; Zheng and Shabek, 2017). The assembly of specific proteasome subunits directs the formation of the 20S proteasome, 26S proteasome (consisting of the 20S core plus 19S regulatory cap) and the

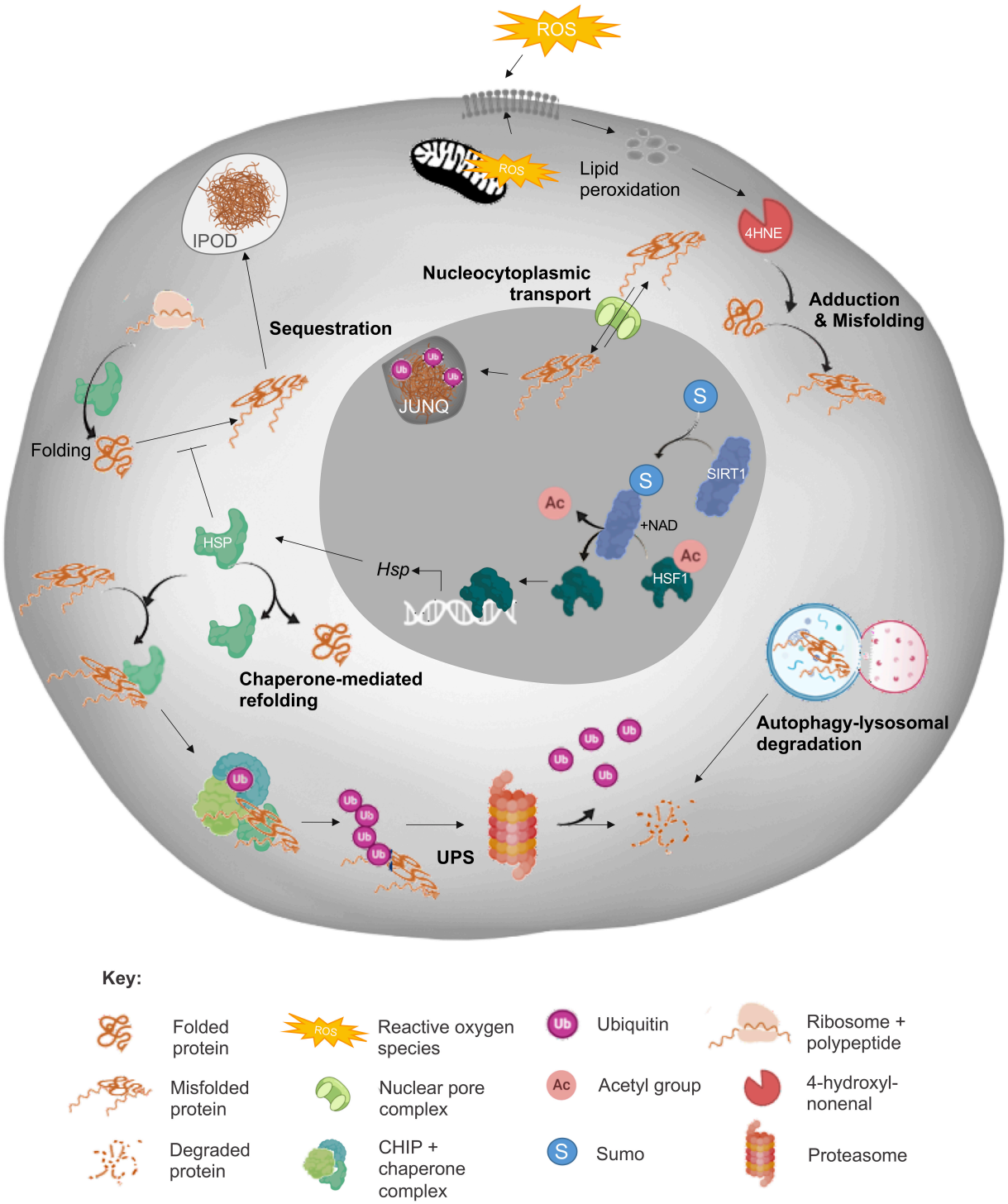

FIGURE 1 | Summary of the cellular proteostasis network. The fate of misfolded proteins arising from oxidative stress (ROS)-induced cascades varies depending on the nature of the protein and extent of damage. As depicted, adduction by reactive carbonyl species (RCS) such as 4-hydroxynonenal (4HNE) can elicit protein misfolding and necessitate the engagement of a panoply of cellular defense mechanisms designed to prevent propagation of protein damage and/or directly eliminate misfolded proteins. Among these mechanisms, the sensing of redox state and subsequent induction of heat shock response (HSR) by sirtuins (SIRT) leads to the upregulation of heat shock protein (Hsp) expression. The HSPs, or chaperone proteins are capable of directing misfolded targets toward pathways of protein refolding or targeted degradation via the ubiquitin-proteasomal pathway (UPS). As a more direct, but less selective route of degradation, misfolded proteins can also be recycled via autophagy/lysosomal machinery. Alternatively, misfolded proteins can be compartmentalized into insoluble protein deposits (IPOD) or sequestered into juxtanuclear quality control compartments (JUNQs) via shuttling between the cytoplasm and nucleus directed by nucleocytoplasmic transport machinery. Elements of this figure were made in BioRender.

immunoproteasome (20S in combination with an 11S regulatory subunit), among other tissue specific forms (Grune et al., 2004; Hohn et al., 2013). In somatic cells, proteasome activity is up-regulated in response to moderate levels of oxidative stress and thereafter it fulfils a key role in the resolution of dysfunctional and misfolded proteins (Ding et al., 2003; Pickering et al., 2010). In contrast, exposure to chronic and/or intense oxidative insults can lead to proteasome inhibition and in extreme situations, complete disassembly (Davies, 2001; Ferrington and Kapphahn, 2004; Aiken et al., 2011). Proteasome activity is also decreased in multiple organs with increased age and, in model species such as *Drosophila*, these insults have contributed to defective 20S and 19S association leading to compromised 26S proteasome assembly (Tonoki et al., 2009). Alternatively, proteasomal dysfunction may also be caused by post-translational modifications (PTMs) and the extent of substrate aggregation (Keller et al., 2000; Im and Chung, 2016), with heavily cross-linked proteins demonstrated to "clog" the proteasome and even cause proteasomal inhibition (Hohn et al., 2013).

Crosstalk between the UPS and the autophagy-lysosomal system is proposed to occur through the conformation of ubiquitin chains as well as the activity of the autophagy receptor p62 (Kocaturk and Gozuacik, 2018). As a compensatory, or alternative, mechanism to the UPS, autophagy is a catabolic process responsible for the degradation of superfluous and dysfunctional organelles, long-lived proteins and protein aggregate structures and can be categorized into three distinct subtypes, macroautophagy, chaperone-mediated autophagy, and mitophagy (Lilienbaum, 2013; Peters et al., 2020). Macroautophagy (hereafter referred to as autophagy) is characterized by the formation of double membrane bound structures, autophagosomes, and is regulated by mammalian target of rapamycin (mTOR). Initially described as a non-selective waste disposal pathway, selective roles for autophagy have since been reported with regards to the removal of protein aggregates or inclusions, a process termed aggrephagy (Mancias and Kimmelman, 2016). As a clearance mechanism for protein aggregates, aggrephagy has been investigated using multimerized fluorescent particles which track the interaction of clusters (mimicking aggregates) with ubiquitin prior to the recruitment of p62 and microtubule-associated protein 1A/1B-light chain 3 (LC3), preceding lysosomal degradation (Janssen et al., 2018). The selective nature of aggrephagy rests with a combination of molecular chaperones such as BAG family molecular chaperone regulator 3 (BAG3) (Gamerdinger et al., 2011; Lamark and Johansen, 2012; Klimek et al., 2017) and autophagy receptors such as p62 and TAX1BP1 (Bjorkoy et al., 2005; Pankiv et al., 2007; Sarraf et al., 2019), the latter of which links cargo to autophagosomes.

Molecular Chaperones

The proteasome and lysosome are by no means the only components of the PN that are dysregulated in response to aging and oxidative stress. Indeed, it has been shown that nearly 50% of molecular chaperones expressed in the human brain are differentially regulated equivalently upon aging or in response to the development of neurodegenerative conditions (Smith et al., 2015). Interestingly, 70% of the human "chaperome," consisting of >332 genes responsible for chaperone and co-chaperone production (Brehme et al., 2014), is dysregulated in opposing directions between cancer and neurodegeneration, corroborating the notion that the collapse of the proteostasis network is responsible for a wide range of pathogenic conditions (Hadizadeh Esfahani et al., 2018).

The proteostasis network is modulated by an armada of chaperones functioning as "holdases" and "foldases" (Hipp et al., 2019). In their capacity as holdases, chaperones temporarily prevent protein aggregation by binding to exposed hydrophobic regions of proteins that would otherwise trigger aggregation (Mattoo and Goloubinoff, 2014; Diaz-Villanueva et al., 2015; Hipp et al., 2019). Alternatively, those chaperones with foldase activity facilitate protein stabilization, folding, disaggregation and refolding. Although some chaperones are constitutively expressed, the ability of some chaperones to be induced by stress enables cells to adapt to changing environmental conditions and intracellular signals (Hohn et al., 2013). The chaperone machinery expressed in mammals, are broadly divided into five main families based on molecular weight, namely the small heat shock proteins (HSPs), HSP40s, HSP60s/CCT chaperonins, HSP70s/110 and HSP90s (Hartl et al., 2011; Dun et al., 2012).

As a reflection of its importance as a protein stabilizer within the PN (Hohn et al., 2013), HSP90 proteins account for approximately 1–2% of all proteins in eukaryotic cells (Niforou et al., 2014). The members belonging to the HSP90 protein family are highly conserved molecules with an approximate molecular weight of 90 kDa. The Human HSP90 family includes five members with the overall structure of HSP90 homologs comprising three conserved domains; N-terminal domain, C-terminal domain and middle domain (Hoter et al., 2018). HSP90 proteins commonly work in concert with HSP70 (Mayer and Bukau, 2005; Labbadia et al., 2012; Radwan et al., 2017) to recruit the C-terminus of HSC70 interacting protein (CHIP), which in turn ubiquitinates misfolded proteins (**Figure 1**) to direct them away from refolding, and toward proteasomal degradation (Shang and Taylor, 2011; Houck et al., 2012; Hipp et al., 2019). Recent work from our laboratory has implicated HSP90 in the mitigation of protein aggregate accumulation in developing male germ cells; such that selective HSP90 inhibition resulted in a significant increase in protein aggregates (Cafe et al., 2020). Such findings imply that the action of the HSP90 chaperone family in aggregate mitigation may be conserved in germ cells and somatic cells. Similarly, the HSP70 chaperone family also fulfils ancillary roles in protein transport, folding, degradation, dissolution of protein complexes and control of regulatory proteins (Daugaard et al., 2007). By way of example, an 8-fold increase in HSP70 abundance has been recorded in neuronal cells harboring mutant huntingtin protein [mHtt; an amyloidogenic mutant that drives the progression of Huntington's disease (HD)] (Tagawa et al., 2007). Such a result may arise as a consequence of the sequestration of HSP70, and its co-chaperone HSP40, into aggregates in HD, thus reducing their availability to participate in refolding (Simoes-Pires et al., 2013). The importance of the HSP40/70 activity is demonstrated by the ability of this complex to reduce

polyglutamine (polyQ) formation, and superoxide dismutase 1 (SOD1; the major protein involved in ALS pathogenesis) aggregation (Wacker et al., 2004; Smith et al., 2015). Additionally, the intercellular transmission of HSP40/70, via exosomes, can fortify the PN defenses of cells containing aggregated proteins (Takeuchi et al., 2015).

The small heat shock protein family (sHSPs) enables cells to respond to stress by stabilizing aggregation-prone proteins. Members such as HSP27 can target damaged proteins for UPS-mediated degradation, while HSP22 promotes autophagy-mediated degradation of targets (Niforou et al., 2014). sHSPs prevent aggregation of SOD1 (Yerbury et al., 2013), and promote autophagic clearance through the interaction of HSP22 with CHIP/HSC70/BAG3 (Crippa et al., 2010). As such, HSP22 and HSP20 are elevated in response to AD, HD, and ALS, and HSP27 is found in tangles of hyperphosphorylated tau in AD (Treweek et al., 2015).

Compartmentalization and Partitioning

A widely conserved mechanism to combat the toxicity of protein aggregates is through the compartmentalization and/or sequestration of misfolded proteins within cells. In several studies it has been shown that cytoplasmic aggregates exhibit higher toxicity than their nuclear counterparts, possibly due to the sequestration of aggregates into intranuclear inclusions (Woerner et al., 2016) and interactions with compartment specific chaperones (Da Cruz and Cleveland, 2016). The three main examples of this compartmentalization include the formation of aggresomes at the microtubule organizing center (Kawaguchi et al., 2003; Simoes-Pires et al., 2013), the sequestration of ubiquitinated misfolded proteins into juxtanuclear quality control compartments (JUNQs) and the direction of terminally aggregated proteins to insoluble protein deposits (IPODs; **Figure 1**; Kaganovich et al., 2008; Radwan et al., 2017) for resolution via autophagy (Hohn et al., 2013). Furthermore, recent research in this field has implicated the nucleocytoplasmic transport machinery in the regulation of proteostasis in somatic cells (Shibata and Morimoto, 2014).

The nuclear envelope enforces spatial separation of the nucleus and cytosol of eukaryotic cells and consequently the segregation of genetic material, transcriptional and translational machinery, and metabolic systems. As such, there is a requirement for transport machinery to recognize and regulate the movement of molecular components across the nuclear envelope (Pemberton and Paschal, 2005; Lange et al., 2007). The intracellular distribution, and hence the mislocalization of proteins, appears to be key to their toxicity (Ferrigno and Silver, 2000; Barmada et al., 2010). Accordingly, mutations in the nuclear localization sequence (NLS) of misfolded proteins (the sequence that targets them for nuclear import) increases their toxicity (Woerner et al., 2016), with their aberrant interactions with the nuclear pore contributing to protein conformational disorders including ALS and tauopathies (Eftekharzadeh et al., 2018). Additionally, the mislocalization of nuclear import machinery (KPNA2 and B1), along with nuclear pore components, has been found in the brains and spinal tissue of ALS patients (Kim and Taylor, 2017). Moreover, cytoplasmic aggregates have the ability to disrupt the transport of other biomolecules through the nuclear pore (Woerner et al., 2016; Radwan et al., 2017), further perpetuating proteostatic imbalance. Such defects can be perpetuated from the host cell onto daughter cells, with protein aggregate inclusions (IPOD and JUNQ) known to be asymmetrically inherited into daughter cells at the cost of mitosis speed and lifespan of the daughter cell (Rujano et al., 2006). Whilst a myriad of karyopherin proteins have also been identified in the male (Loveland et al., 2015) and female germ lines (Mihalas et al., 2015), we are only just beginning to understand the role they may play in mitigating the risk posed by misfolded proteins in these cells (Cafe et al., 2020).

Post-translational Modifications

Owing to their innate ability to alter protein structure and function, PTMs can modulate and disrupt biological processes associated with cellular longevity, reproduction and neurodegeneration (Sambataro and Pennuto, 2017; Santos and Lindner, 2017). There are hundreds of PTMs that proteins can acquire during the life-course of a cell, ultimately giving rise to a dynamic proteome that is vastly more complex than the genome would suggest (Kulkarni and Uversky, 2018). Occurring via both enzymatic and non-enzymatic means, common forms of PTMs include phosphorylation, glycosylation, acetylation, methylation, sumoylation, palmitoylation, biotinylation, ubiquitination, nitration, chlorination, and oxidation/reduction. Illustrative of the extent of PTMs, it has been proposed that as many as 80–90% of proteins may be acetylated in eukaryotic organisms (Arnesen et al., 2009), while approximately 30% are subject to phosphorylation (Cohen, 2000).

Unlike physiological PTMs, carbonylation reactions are generally held to be detrimental and capable of leading to protein misfolding, crosslinking and eventually aggregation (Petersen and Doorn, 2004), that is archetypal of many disease states (Bizzozero et al., 2005; Liu et al., 2005; Reed et al., 2009). Protein carbonylation refers to chemical modification of the primary structure of a protein via the addition of reactive carbonyl species (RCS), a prime example of which is 4-hydroxynonenal (4HNE) adduction. 4HNE exhibits dose-dependent effects on cellular function with lower doses increasing proteasome activity and higher doses being incongruous with cellular function, leading to protein aggregation, proteasomal inhibition and eventually cell death (Aiken et al., 2011; Bromfield et al., 2015, 2017; Nixon et al., 2019a). Elevated concentrations of 4HNE have also been detected in association with various neurodegenerative diseases and causally linked to disease pathologies via adduction and dysregulation of the cellular proteome (Yoritaka et al., 1996; Markesbery and Lovell, 1998; Schaur et al., 2015). Illustrative of this is the tau protein, which is known to be modified by 4HNE resulting in the stabilization of neurofibrillary tangles (Liu et al., 2005). Additionally, as a potential contributor to the propagation of protein aggregation, 4HNE treatment of neurons results in a 2.5-fold increase in the packaging of α-synuclein (the aggregation of which is responsible for Parkinson's disease) oligomers/fibrils

into extracellular vesicles, which can be internalized by untreated neurons, thus disseminating aggregates and enhancing toxicity (Zhang et al., 2018). As discussed in the sections below, 4HNE treatment also elicits pervasive impacts in both the male and female germlines.

Aside from carbonylation, ubiquitination, nitration and phosphorylation modifications have also been linked to the aggregation of proteins such as α-synuclein with downstream consequences including neurotoxicity (Santos and Lindner, 2017). Additionally, as ubiquitination often competes for the same residues as acetylation, this can accentuate protein aggregate accumulation. Indeed, it has been shown that insufficient levels of SIRT1, can preclude proteasome-mediated degradation of substrates since the acetylation of lysine residues effectively prevents access of ubiquitin ligases (Min et al., 2013). In a similar context, hyperphosphorylation of tau can dramatically increase aggregate formation and is associated with tau tangles in AD (Fujiwara et al., 2002; Ren et al., 2014). In addition to the ability of PTMs to modify the activity of individual proteins, at times promoting their aggregation, PTMs have also been shown to decrease proteasome activity through direct adduction. Both the carbonylation and oxidative modification of proteasome subunits has been reported (Ishii et al., 2005; Hohn and Grune, 2014), resulting in destabilization of the proteasome complex and a commensurate inhibition of its catalytic activity. Such modifications reduce proteolytic degradation of misfolded or damaged proteins, leaving them instead to form aggregates (Grune et al., 2004).

Considering the mature sperm cell is transcriptionally and translationally quiescent, it must rely on the cumulative efforts of PN components to maintain the fidelity of intrinsic proteins during post-testicular maturation (Maciel et al., 2019). Fittingly, PTMs are crucial for the acquisition of sperm functional competence, playing key roles in capacitation-associated signaling events that underpin hyperactivated motility and oocyte interactions (Aitken and Nixon, 2013; Nixon and Bromfield, 2018). Whilst they are crucial for normal function, PTMs are interlinked with diverse disease states, extending beyond neurodegeneration to include infertility. Highlighting this, excessive levels of reactive nitrogen species (RNS)-induced modifications have been documented in the defective spermatozoa of asthenozoospermic patients (Lefievre et al., 2007; Martinez-Heredia et al., 2008). Additionally, dysregulated glycosylation, acetylation, ubiquitination, and SUMOylation are linked to abnormal sperm morphology and impaired fertilization and embryo development (Samanta et al., 2016; Maciel et al., 2019). These protein modifications represent important examples of the parallels that exist between germ and somatic cell proteostasis. Indeed, a range of features associated with neurodegenerative conditions, including dysregulation of the PN, are common to the pathologies of both male and female infertility (**Supplementary Table 1**). This information is critical to our understanding of how we may manipulate the PN to prevent fertility loss. Accordingly, in the following sections we consider to the contribution of proteostasis to male and female germ cell development and fertility.

MAINTAINING PROTEOSTASIS DURING MALE GERM CELL DEVELOPMENT

Advanced paternal age has been linked to declines in semen quality with a reduction in volume and sperm motility (Frattarelli et al., 2008), increased morphological abnormalities [most pronounced in men over 50; (Kidd et al., 2001)], increased time to pregnancy (Ford et al., 2000) and an increased mutational load due to DNA damage (Petersen et al., 2018; Yatsenko and Turek, 2018; Pino et al., 2020). Additionally, evidence is mounting in support of a link between advanced paternal age and the incidence of developmental abnormalities in offspring including autism and schizophrenia (Drevet and Aitken, 2020), but the etiologies underpinning reductions in semen quality remain largely unresolved. Notwithstanding this increasing evidence that paternal age does pose concerns in terms of both male fertility and offspring health, the role that proteostasis disruption may play in these issues remains uncharacterized. Despite this, in the context of sperm production and function, protein homeostasis and the PN network are known to be critical for successful sperm production and maturation (Dun et al., 2012) and in the survival and function of mature spermatozoa that carry out fertilization in the relative absence of transcription and translation (Bromfield et al., 2015). Moreover, it is well known that the mature spermatozoon is highly sensitive to oxidative protein damage due to a lack of cytoplasmic antioxidants and functional detoxifying machinery (Drevet and Aitken, 2020). Thus, irreversible protein damage, such as that elicited by RCS and other lipid peroxidation products, can rapidly affect sperm cell motility and viability (Bromfield et al., 2019). Given this, it is not surprising that oxidative stress is one of the major contributing factors to clinical male infertility.

Herein, we discuss what is known regarding protein homeostasis across the specific stages of sperm cell development and how the PN network relates to male fertility, especially in the context of oxidative cellular damage.

Testicular Germ Cells

In mammals, the establishment of a self-populating stem cell niche in the testis occurs during early embryonic development and underpins the ability to produce gametes at sexual maturation. The male gametes, spermatozoa, are produced through a synchronized and highly complex differentiation pathway known as spermatogenesis (**Figure 2**). The stringent regulation of spermatogenesis is enabled by the compartmental organization of the testis; tight junctions between Sertoli cells form a blood-testis barrier that gives rise to an immune-privileged intratubular environment, which is maintained with support from the Sertoli and peritubular myoid cells as well as Leydig cells residing in the interstitium (Hermo et al., 2010; Garcia and Hofmann, 2015). All of these factors are required to act in concert with one another and in response to inter- and intra-cellular signals, with any disruptions to the process of spermatogenesis having the potential to result in subfertility.

Similar to somatic cells, developing male germ cells are protected through the action of the UPS and formation of

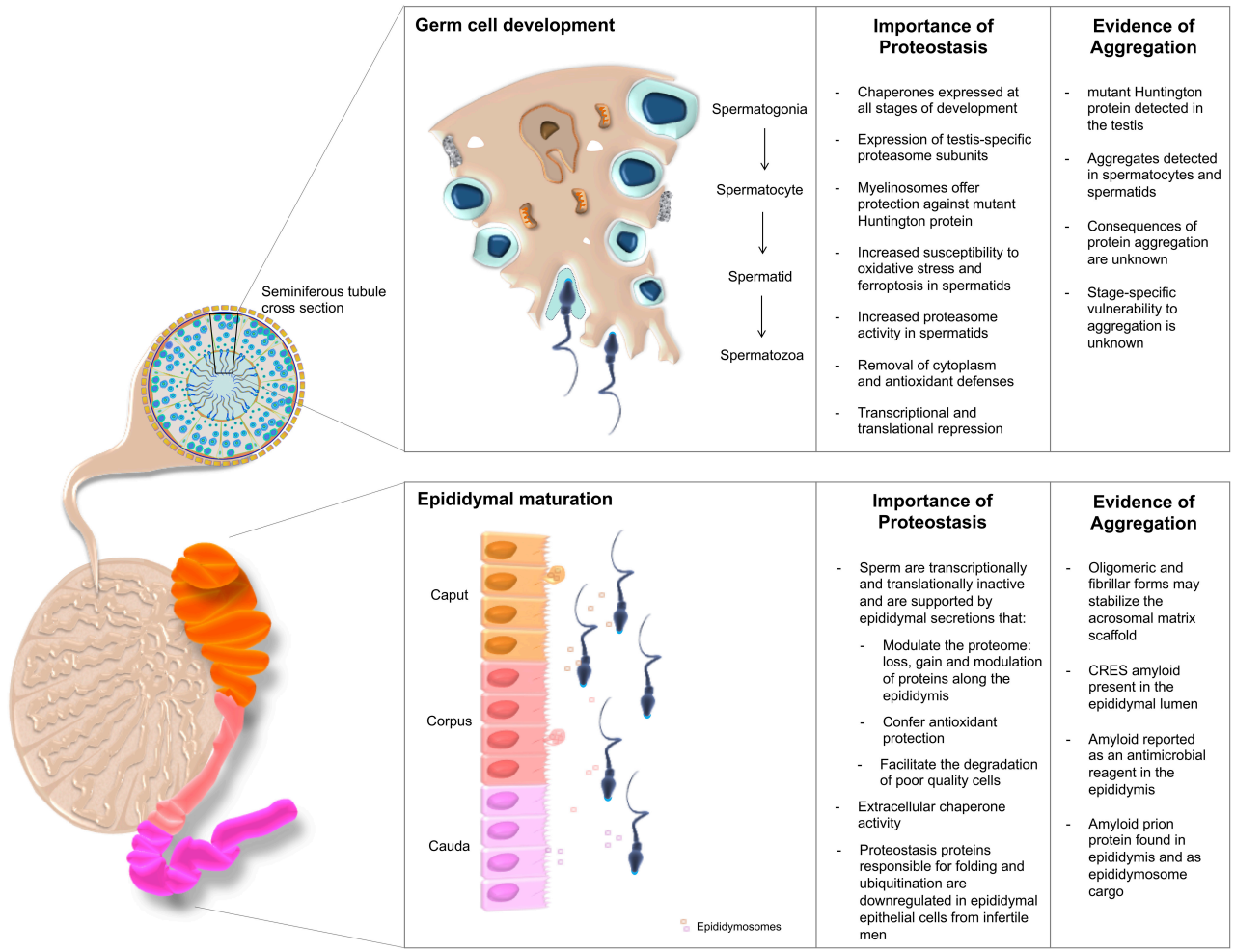

FIGURE 2 | The importance of proteostasis throughout male germ cell development. Male germ cells are produced through successive waves of spermatogenesis occurring within the seminiferous tubules of the testes, yet acquire functional competence during their subsequent transport through the epididymis. The integrity of both maturational phases is intimately regulated by complex proteostasis networks, which work in concert to secure the continuous production of high quality spermatozoa. Despite these quality control measures, the formation of protein aggregates has been documented at various sites within the male reproductive tract. Although their origins remain largely enigmatic, such deposits have been ascribed both pathological and functional roles.

the spermatoproteasome. The testis specific proteasomal subunit PSMA8, which is incorporated into the core "spermatoproteasome" (Uechi et al., 2014), responsible for the degradation of ubiquitinated proteins during spermatogenesis (Gomez et al., 2019), is known to be dysregulated in infertile patients presenting with varicocele (Agarwal et al., 2015). Further, the UPS is responsible for the removal of excess cytoplasm and ubiquitinated histones from developing germ cells (Hou and Yang, 2013). Accordingly, increased ubiquitination profiles and proteasome activity have been recorded in post-meiotic round spermatids compared to their spermatocyte precursors (Tipler et al., 1997). Downstream of testicular development there is also evidence for ubiquitination of proteins on defective spermatozoa, potentially causing a targeting of the whole cell for removal through phagocytosis by the epididymal epithelial cells prior to ejaculation (Sutovsky et al., 2001). Developmental studies in *Drosophila melanogaster* reveal a number of paralogous proteasome subunits that are testis-specific with knockouts resulting in male sterility (Belote and Zhong, 2009). Similarly, mice null for the PA200 proteasome subunit also exhibit reduced fertility (Khor et al., 2006; Qian et al., 2013).

In addition to the quality control imposed by the UPS during spermatogenesis, molecular chaperones constitute a key component of the proteostasis machinery harbored by the male reproductive system (Dun et al., 2012). In fact, a mutation in HSP90A in mice contributes to the establishment of an infertility phenotype attributed to the failure of spermatocytes to progress beyond the pachytene spermatocyte stage and the complete loss of subsequent germ cell populations (Grad et al., 2010). Interestingly, a similar phenotype is observed in HSP70 family member knockouts of both HSPA2 (Dix et al., 1996) and HSBP1 KO mice (Zhu et al., 1997; Rogon et al., 2014), with failure to produce sperm in both KO backgrounds having been linked to defects in synaptonemal complex formation and the

assembly of a CDC2/cyclinB1 complex that is required for G2/M transition (Zhu et al., 1997). Following meiosis, HSPA2 also acts as a regulator of DNA packaging during spermatogenesis (Dun et al., 2012).

During testicular sperm cell development, RCS such as 4HNE and malondialdehyde (MDA) have been shown to modulate germline protein homeostasis and the stability of HSPA2. Evidence for this lies in the treatment of male germ cells with RCS, which triggers protein adduction (Bromfield et al., 2015; Nixon et al., 2019a), protein aggregation (Cafe et al., 2020) and sensitizes spermatids to demise through a ferroptotic cell death pathway (Bromfield et al., 2019). Additionally, the incubation of spermatozoa with low levels of 4HNE is known to result in an increase in proteasome activity and the subsequent proteolytic degradation of HSPA2 (Bromfield et al., 2017). A summary of our current understanding of the contribution of protein homeostasis to sperm cell development and fertility is presented in **Figure 2**.

In addition to the important role that chaperones play in the regulation of proteostasis in the male germline, the contribution of sirtuin proteins to fertility has also received increasing attention in recent years (Bell et al., 2014; Rato et al., 2016; Liu et al., 2017; Tatone et al., 2018; Zhang et al., 2019; Alam et al., 2020). Sirtuins (SIRTs) are a family of class III NAD-dependent deacetylases that have been extensively linked to the regulation of lifespan and the protection of cells against proteotoxicity. Seven mammalian sirtuins have been identified as residing in either the nucleus (SIRT1, 3, 6, and 7), cytoplasm (SIRT2) or mitochondria (SIRT3, 4 and 5) (Yamamoto et al., 2007). In these locations, SIRT activity is coordinated by interactions with nicotinamide adenine dinucleotide (NAD^+). NAD^+ is a central molecule in cellular respiration and additionally has the capacity to act as a signaling molecule and partake in redox reactions. It follows that reduced NAD^+ availability, such as occurs during aging or in response to excessive oxidative stress, leads to a concomitant reduction in SIRT activity and contributes to the pathogenesis of disorders associated with protein misfolding (Imai and Guarente, 2016). Conversely, the deacetylation of heat shock factor 1 (HSF1) and subsequent activation of the HSR by SIRT1 (Westerheide et al., 2009) has been shown to augment protection against aggregation-based diseases. For instance, SIRT1-mediated deacetylation of tau protein, the aggregation of which is associated with the progression of AD, enhances its degradation (Herskovits and Guarente, 2013).

The deletion of sirtuin genes results in the dysregulation of male (and female) germline development (Tatone et al., 2018). As such, conditional ablation of sirtuins from male germ cells leads to reduced fertility including delayed differentiation of pre-meiotic germ cells, decreased sperm number, an increased proportion of abnormal spermatozoa (Bell et al., 2014) and disrupted acrosome biogenesis (Liu et al., 2017). These phenotypes reflect the key role that sirtuins fulfill in sensing imbalances in the metabolic state of cells and thereafter enabling the cell to mount an appropriate stress response.

Epididymal Sperm Maturation

Although spermatozoa are morphologically mature when they exit the testis, functional maturity is not achieved until completion of epididymal transit. Owing to the purported silencing of the cell's transcriptional and translational machinery (Ren et al., 2017), such maturational events are governed by the extrinsic factors they encounter in the epididymis and female reproductive tract (Nixon et al., 2019b). Upon leaving the testis sperm enter the proximal caput segment of the epididymis before being conveyed through the corpus to cauda (distal end) whereupon they are stored until ejaculation. Reflecting its role in the promotion of sperm maturation, defects in epididymal physiology are linked to defective sperm function and a failure to complete events related to fertilization (Yeung et al., 1998; Cooper et al., 2004). This maturation process is governed by the unique luminal microenvironment in which sperm are bathed, comprising of both soluble factors secreted by the lining epididymal epithelium, as well as those packaged into extracellular vesicles known as epididymosomes (Zhou et al., 2018).

One particular curiosity of the epididymal luminal environment is the presence of insoluble extracellular proteinaceous species resembling amyloid. Indeed, the epididymis has been shown to contain amyloidogenic prion protein both contained in epididymosomes and in soluble form (Ecroyd et al., 2004) as well as amyloid forms of the CRES (cystatin-related epididymal spermatogenic subgroup) protein, following its secretion within the proximal caput (Cornwall, 2009). Notably, the amyloid structures formed from prion and CRES proteins have been proposed to fulfill functional rather than pathological roles, including acting as scaffolds (Chau et al., 2008) and facilitating the delivery/uptake of luminal proteins into the maturing sperm cells (Cornwall et al., 2011). Together with exosomes, such interactions drive dramatic changes in the sperm proteome including the loss, gain, modification and/or repositioning of proteins. Illustrative of the scale of this phenomenon, Skerget et al. (2015) identified 732 proteins that are acquired by mouse spermatozoa and a further 1,034 proteins that are reportedly lost from these cells as they transit the epididymis. Among those proteins that display altered abundance, several proteasome subunits become enriched in maturing sperm (Skerget et al., 2015), with purported roles extending to the mediation of downstream sperm-egg interactions. While this dramatic remodeling is thought to happen in the relative absence of protein turnover, upon interrogation using stable isotope incorporation and mass spectrometry, a subset of epididymal sperm proteins (and seminal vesicle proteins) were found to be subject to rapid turnover suggesting there may be some capacity for protein production (Claydon et al., 2012). In Infertile men, alterations in the gene expression profile of epididymal epithelial cells has been observed; with those encoding proteins involved in protein folding, proteolysis, and ubiquitination, all found to be downregulated (Dube et al., 2008; Cornwall, 2009). Similarly, a conserved decrease in CRES expression has been reported in infertile mouse models generated by either ablation of the c-ros tyrosine kinase receptor or the transgenic expression of the glutathione peroxidase 5 gene (GPX5) in all the epididymal segments (Cooper et al., 2003, 2004).

In line with the identification of protein aggregates within the epididymis, this specialized tissue contains functional

elements of the UPS (Baska et al., 2008), which may facilitate the removal of poor quality sperm and collaborate with extracellular chaperones to maintain proteostasis within the luminal environment. Notably, the bulk of the epididymal extracellular chaperone activity appears to rest with the glycoprotein clusterin (Humphreys et al., 1999), which is abundantly secreted into the proximal epididymal segments to account for as much as 41% of all luminal protein content (Dacheux and Dacheux, 2002). Consistent with its identification among protein aggregates in pathological disease states including AD and diabetes (Wyatt et al., 2013; Foster et al., 2019), clusterin also associates with prion protein in the epididymal lumen (Ecroyd et al., 2004). Taken together, these data suggest that clusterin may fine-tune the solubility of this protein within the luminal environment (Cornwall et al., 2011). However, whether such roles extend to regulating the extent of amyloid formation, and hence function, among aggregation-prone proteins such as CRES, remains to be investigated.

Mature Spermatozoa

The importance of proteostasis is not relinquished once the mature spermatozoon is formed, instead the proteostasis network remains crucial for fertilization processes. As such, a myriad of barriers exist to ensure that the "fittest"/best quality sperm cells are preferentially primed for fertilization. Among these quality control measures, it has been shown that, in addition to their role in promoting sperm maturation, epididymosomes may deliver ubiquitin to moribund or poor quality spermatozoa, effectively tagging them for degradation prior to ejaculation (Sutovsky et al., 2001; Baska et al., 2008; Cornwall, 2009). Similarly, proteasome activity also appears to play a role during capacitation and acrosomal exocytosis, the final stages of sperm maturation that occur in the female reproductive tract. Thus, chemical inhibition of the sperm proteasome results in capacitation failure (Morales et al., 2003), an inability of sperm to digest the zona pellucida surrounding the oocyte (Sutovsky et al., 2004; Zimmerman et al., 2011), and an attendant decrease in fertilization rates *in vitro* (Pasten et al., 2005). In accordance with their purported role in sperm-zona interactions, a complex consisting of multiple proteasome subunits has been isolated from the surface of human sperm (Redgrove et al., 2011). Moreover, in boar spermatozoa it has been demonstrated that proteasome co-purifying proteins, such as acrosin binding protein, appear to be processed by the proteasome in a capacitation-dependent manner (Zigo et al., 2019). Furthermore, decreased proteasome activity has been correlated with decreased motility and normal morphology in human spermatozoa (Rosales et al., 2011).

The chaperoning function of heat shock proteins has also been implicated in the regulation of gamete interactions. In one of the most well studied examples, HSPA2 has been implicated in the assembly and presentation of zona pellucida receptor complexes on the surface of mature human sperm cells (Redgrove et al., 2012). In our laboratory, we have shown that the dysregulation of HSPA2 that results from 4HNE adduction under conditions of oxidative stress compromises human sperm-zona interactions and leads to a loss of fertilization potential (Bromfield et al., 2017). The physiological implications of HSPA2 dysregulation are also evident in the under-representation of this protein witnessed in the spermatozoa of infertile men (Cedenho et al., 2006; Redgrove et al., 2012). Additionally, the loss or inhibition of alternative chaperones, such as HSP90A, within the sperm proteome can also result in an infertility phenotype. Specifically, Li K. et al. (2014) have demonstrated that the pharmacological inhibition of HSP90 can prevent Ca^{2+} signaling and hyperactivation; raising the prospect that this chaperone is important for calcium homeostasis associated with sperm capacitation.

Contribution of Somatic Cells to Germline Proteostasis

Sertoli cells are known as the "nurse" cells of the testis and, through structural support and secretory action, are responsible for initiating and regulating spermatogenesis. While their role in the maintenance of testicular proteostasis is largely unknown, analysis of testicular morphology in older men has revealed a reduction in Sertoli cell number and an increased nucleus size within the remaining Sertoli cells, which may be indicative of increased protein turnover (Pohl et al., 2019). Sertoli cells have been shown to contain multilamellar bodies with lysosome-like characteristics termed myelinosomes (Yefimova et al., 2016). Common in lysosomal storage and protein aggregation disorders, myelinosomes act as storage organelles for misfolded proteins and help maintain cellular homeostasis through non-catabolic pathways. Interestingly, myelinosomes have also been identified in Sertoli cells and seminal plasma (Yefimova et al., 2016, 2019, 2020). Huntingtin protein is present at equivalent levels in both the brain and testis, with mutations leading to both neurodegeneration and sterility (late onset) through a loss in post-meiotic cell types and testicular atrophy (Van Raamsdonk et al., 2006, 2007). Although, both pathologies can occur concomitantly at ages >39 years, no aggregated forms of mHtt have thus far been confirmed in the testes of individuals (or in mouse models) affected by HD. This remarkable difference between the brain and the testis was found to be due to myelinosomes within Sertoli cells and their unique capacity to secrete misfolded proteins to avoid aggregation and maintain cell proteostasis. The ability to release the aggregation-prone mutant form of Huntingtin (and also CFTR) but retain the normal Huntingtin protein form is facilitated by the multivesicular bodies (MVBs), whereby inhibition of MVB excretion resulted in the retention of misfolded Huntingtin inside TM4 Sertoli cells (Yefimova et al., 2016, 2019). This represents a newly characterized and remarkable form of germ cell protection afforded by its somatic cell neighbors.

Pathological vs. Functional Protein Aggregation in the Male Germline

The formation of amyloid is not always a toxic event for cells and organisms, as such the stability and resistance provided by the cross-beta sheet structure has been exploited in essentially all phyla, appearing in cellular materials as diverse as biofilms, silk, and melanosomes (Stefani, 2004; Fowler et al., 2007; Maury, 2009; Pham et al., 2014). Functional amyloid, defined

as naturally forming filamentous aggregates, have also been characterized in the context of reproductive tissues and fluid including as key structural components of the acrosomal matrix (Cornwall, 2009), epididymal plasma and the zona pellucida surrounding the oocyte (Egge et al., 2015). It follows that the structural remodeling of amyloids are linked to changes in gamete function, as illustrated by the pH-dependent disassembly of the acrosomal matrix that accompanies the acrosome reaction/release of acrosomal contents in capacitated mouse spermatozoa (Guyonnet et al., 2014). Proteomic analysis of the "amyloid core" of the mouse sperm acrosome has revealed the presence of the cystatins, CRES and cystatin C (Guyonnet et al., 2014). Mice lacking CRES display fertility defects pertaining to the inability of sperm to undergo acrosomal exocytosis *in vitro* (Chau and Cornwall, 2011). Notably, CRES proteins have also been confirmed to co-localize with positively stained amyloid in epididymal lumen (Whelly et al., 2012, 2016) and have been isolated from epididymal plasma using protein aggregation pulldown strategies (Whelly et al., 2016). Consistent with the antimicrobial properties that have been attributed to amyloid formation in other systems (Kagan et al., 2012), the potential for epididymal CRES proteins to confer antimicrobial properties and protect sperm from ascending pathogens has also recently been postulated (Hewetson et al., 2017).

Aside from CRES, cystatin C also co-localizes with amyloid structures in the epididymal fluid and with AD-associated amyloid plaques. A point mutation in human cystatin C (L68Q) triggers cystatin C to become highly unstable and aggregation-prone (Calero et al., 2001) to the point that its' deposition in the affected individual is fatal; findings that substantiate the potential of functional amyloids to become pathological under some conditions (Whelly et al., 2014). Similarly, transgenic mice carrying the L68Q mutation of human cystatin C display reduced fertility associated with a reduction in sperm-zona pellucida binding, increased sperm cell death and agglutination. Furthermore, incubation of wild-type sperm with epididymal fluid from L68Q mutant mice recapitulates the mutant phenotype (Whelly et al., 2014).

Building on the findings of mouse models, two classes of amyloids with divergent primary sequence, but similar biochemical properties, have been isolated from human semen, namely: prostatic acid phosphatase peptides (PAP, also known as Semen-derived Enhancer of Viral Infection or SEVI (Munch et al., 2007; Lee and Ramamoorthy, 2018)) and semenogelin (SEM) amyloid (Roan et al., 2017). Both SEVI (Munch et al., 2007; Rocker et al., 2018) and SEM (Roan et al., 2011) have been associated with increased HIV transmission *in vitro* due to amyloid-enhancement of virion attachment and fusion. Contrasting to the roles of semen amyloid in HIV infection, SEM fibrils are also proposed to promote the removal of apoptotic/dysfunctional or excess sperm through engagement of macrophage clearance (Roan et al., 2017). A mouse model of *Neisseria gonorrhoeae* exposure also indicates that seminal fluid amyloid is capable of preventing infection through increased phagocytosis and stimulation of the immune response (Shamri et al., 2013). With further research into extracellular protein aggregation, the formation of amyloid in fluids of the male reproductive tract may prove to widely contribute to male fertility.

PROTEIN HEALTH DURING REPRODUCTIVE AGING IN WOMEN

Unlike the prolonged period of fertility in men, the reproductive capacity of women begins to decline precipitously in the third decade of life (Silber et al., 2017). Corollary to this, extensive efforts have been made toward defining the mechanisms underpinning the age-dependent reduction in oocyte quality/competence and the diminishing ovarian reserve. This focus has led to a compelling new understanding of the role of meiotic errors, DNA damage and chromosome abnormalities in oocyte aging and early embryo development, areas that have recently been reviewed (Greaney et al., 2018; Winship et al., 2018; Martin et al., 2019).

For reproductive cells, errors in the segregation of the chromosomes have particularly severe consequences as they give rise to aneuploid embryos that often result in miscarriage or suffer congenital abnormalities (Nagaoka et al., 2012; Greaney et al., 2018; Gruhn et al., 2019; Hassold et al., 2020). Meiosis in human oocytes is especially error prone with aneuploidy rates ranging from 15% in younger women to a staggering 30–70% in oocytes from older women and, by comparison, spermatozoa have an average aneuploidy rate of 1–4% (Nagaoka et al., 2012; Hou et al., 2013; Ottolini et al., 2015; Greaney et al., 2018; Gruhn et al., 2019). While elegant studies of DNA damage, spindle abnormalities and meiotic errors have provided unique insight into oocyte aging and meiotic failure (Mihajlović and FitzHarris, 2018; Gruhn et al., 2019; Zielinska et al., 2019; Hassold et al., 2020; Mikwar et al., 2020), advances in the application of proteomic and RNA-sequencing technology to oocytes are beginning to reveal an additional layer of complexity to this process whereby declining proteostasis contributes widely to maternal aging processes (Duncan et al., 2017). Our improved understanding of reproductive failure has been marked by the discovery that proteins critical for meiosis, such as those comprising the cohesion complex, are in fact extremely long-lived with no capacity for renewal during oocyte development (Revenkova et al., 2010; Tachibana-Konwalski et al., 2010; Burkhardt et al., 2016; Lee, 2020). Furthermore, evidence for deleterious PTMs of proteasome subunits coupled with declining proteasome activity in aged oocytes has given rise to novel streams of research into the maintenance of oocyte proteostasis (Mihalas et al., 2018). Herein, we discuss the latest findings on age-related changes to the oocyte proteome, the susceptibility of the mammalian oocyte to declining proteostasis and highlight the merit of a whole ovary approach toward a definitive understanding of reproductive aging in women.

The Contribution of Declining Proteostasis to Oocyte Aging

The female gamete is a long-lived cell that experiences periods of prolonged arrest (of up to decades) and phases of transcriptional quiescence that place immense pressure on protein networks for

cell survival. In humans, folliculogenesis commences *in utero* with the recruitment of pre-granulosa cells to germ cells to form the primordial follicle. Primordial follicles are meiotically arrested here in an extended prophase I, termed the germinal vesicle (GV) arrest (Gosden and Lee, 2010). The majority of oocytes in the ovary exist as primordial follicles constituting the ovarian reservoir. These oocytes are then sequentially recruited to the developing follicle pool at periodic intervals throughout adult life where they undergo a protracted period of maturation and eventually, ovulation (Coticchio et al., 2015). In congruence with the length of time that they are held in meiotic prophase in the ovary, these oocytes accumulate a legacy of exposure to both exogenous and endogenous insults that can lead to DNA and protein damage (Titus et al., 2013; Mihalas et al., 2017).

In understanding the susceptibility of oocytes to changes in proteostasis, it is important to note that transcription ceases when oocytes complete their growth phase prior to reentry into meiosis (Gosden and Lee, 2010; Meneau et al., 2020). During the growth phase, mRNA is synthesized for either immediate translation or storage in repressive complexes (Huarte et al., 1992; Meneau et al., 2020). During the subsequent maturation phase, these repressive complexes are removed and translation is activated (Martin et al., 2019; Meneau et al., 2020; Yang et al., 2020). At this stage the oocyte is one of the most translationally active cells in the body, placing unique pressure on both ribosome biogenesis and accurate protein synthesis to attain competence for fertilization (Gosden and Lee, 2010; Duncan et al., 2017). While the progression through meiosis is dependent upon active translation and protein accumulation (Meneau et al., 2020; Yang et al., 2020), PTMs to existing proteins also play an important role in the final stages of meiosis (Gosden and Lee, 2010; Meneau et al., 2020). This phase represents a critical window for proteostasis (from re-entry into meiosis until embryonic cleavage) whereby phosphorylation changes driven by cell cycle kinases are essential to enact meiotic resumption, maintain metaphase II arrest, and guide early preimplantation development (Kikuchi et al., 2002; Gosden and Lee, 2010; Meneau et al., 2020). Given this, it is not surprising that follicles from older mice, which have less robust protein quality control mechanisms than their younger counterparts (Duncan et al., 2017), suffer severe consequences from any loss of proteostasis during development.

Analogous to the role of Sertoli cells in the support of male germ cell development, the maturing oocytes within the preovulatory follicle, and immediately after ovulation, are enclosed within layers of nurturing cumulus cells (McLaughlin and McIver, 2009), which supply most of the metabolites and signaling molecules essential for oocyte function (Russell et al., 2016; Baena and Terasaki, 2019). While our understanding of the effects of aging on the relationship between cumulus cells and the oocyte is minimal, RNA sequencing of growing mouse ovarian follicles has revealed a marked age-dependent upregulation of oocyte specific genes that encode paracrine factors (namely *Fgf8*, *Gdf9,* and *Bmp15*), which stimulate metabolic cooperativity between the oocyte and granulosa cells. This finding is suggestive of a response to decreased support from the surrounding somatic cells to the oocyte with age, which may have downstream effects on oocyte proteostasis (Duncan et al., 2017). Importantly, this indicates that to understand changes in oocyte proteostasis with age, both the cumulus cell proteome and the oocyte proteome must be considered together.

Although proteomic studies focusing on the specific contributions of the PN to oocyte aging remain to be performed, recent studies have identified a large number of mouse oocyte proteins and transcripts that are dysregulated at key age transitions (Steuerwald et al., 2007; Grøndahl et al., 2010; Schwarzer et al., 2014; Barragán et al., 2017; Duncan et al., 2017; Wang et al., 2020). Utilizing single-follicle RNA sequencing, Duncan et al. (2017) have revealed important signatures of disrupted proteostasis in the growing GV oocytes from mice of advanced reproductive age (14–17 months). Specifically, these aged oocytes were characterized by differential expression of genes related to the nucleolus, endoplasmic reticulum and protein processing, with a significant decrease in proteins involved in: HSP binding, the UPR and misfolded protein response, mannosylation, N-linked glycosylation, and ubiquitination, in the follicles of older mice compared to their younger counterparts (6–12 weeks). This suggests that young oocytes are far more robust with regards to protein quality control than older oocytes. These findings are well supported by transcriptomic and single cell RNA sequencing studies (Grøndahl et al., 2010; Barragán et al., 2017; Wang et al., 2020) that demonstrate the dramatic modulation of mammalian oocyte transcriptomes with age, with the potential for these age-related effects on transcription to result in methylation differences (Castillo-Fernandez et al., 2020). These transcriptomic resources will enhance our understanding of changes in proteostasis that contribute to aging.

An additional resource to help understand how oocyte proteostasis changes with age is the proteomic and transcriptomic analysis performed by Schwarzer et al. (2014) on oocytes from three life stages; pubertal (3 weeks), mature (∼8 weeks), and climacteric (∼58 weeks). Interestingly, quantitative comparison of changes in the transcriptomic and proteomic molecular maps revealed a surprisingly low level of correlation (Schwarzer et al., 2014). This important finding suggests that transcriptomic analysis cannot necessarily be used as a surrogate for proteomic analysis in aged oocytes, highlighting a need for more comprehensive proteomic investigations into oocyte and ovarian aging. Using the publicly available proteomic dataset supplied by these authors (Schwarzer et al., 2014) and other relevant transcriptomic and proteomic studies of oocyte aging (McReynolds et al., 2012; Al-Edani et al., 2014; Duncan et al., 2017), we have assembled a proteostasis-centric resource to more comprehensively and rapidly survey datasets for proteostasis network proteins that are dysregulated with age (**Figure 3** and **Supplementary File 1**). While the proteins presented in **Figure 3** require experimental validation to confirm their directional changes, this *in silico* analysis sheds light on the extent of the dysregulation to proteostasis elements that occurs with age in cumulus cells and oocytes.

Notably, in aged oocytes 172 proteins related to molecular chaperones have been identified as being dysregulated, almost one quarter of which were also dysregulated in cumulus cells.

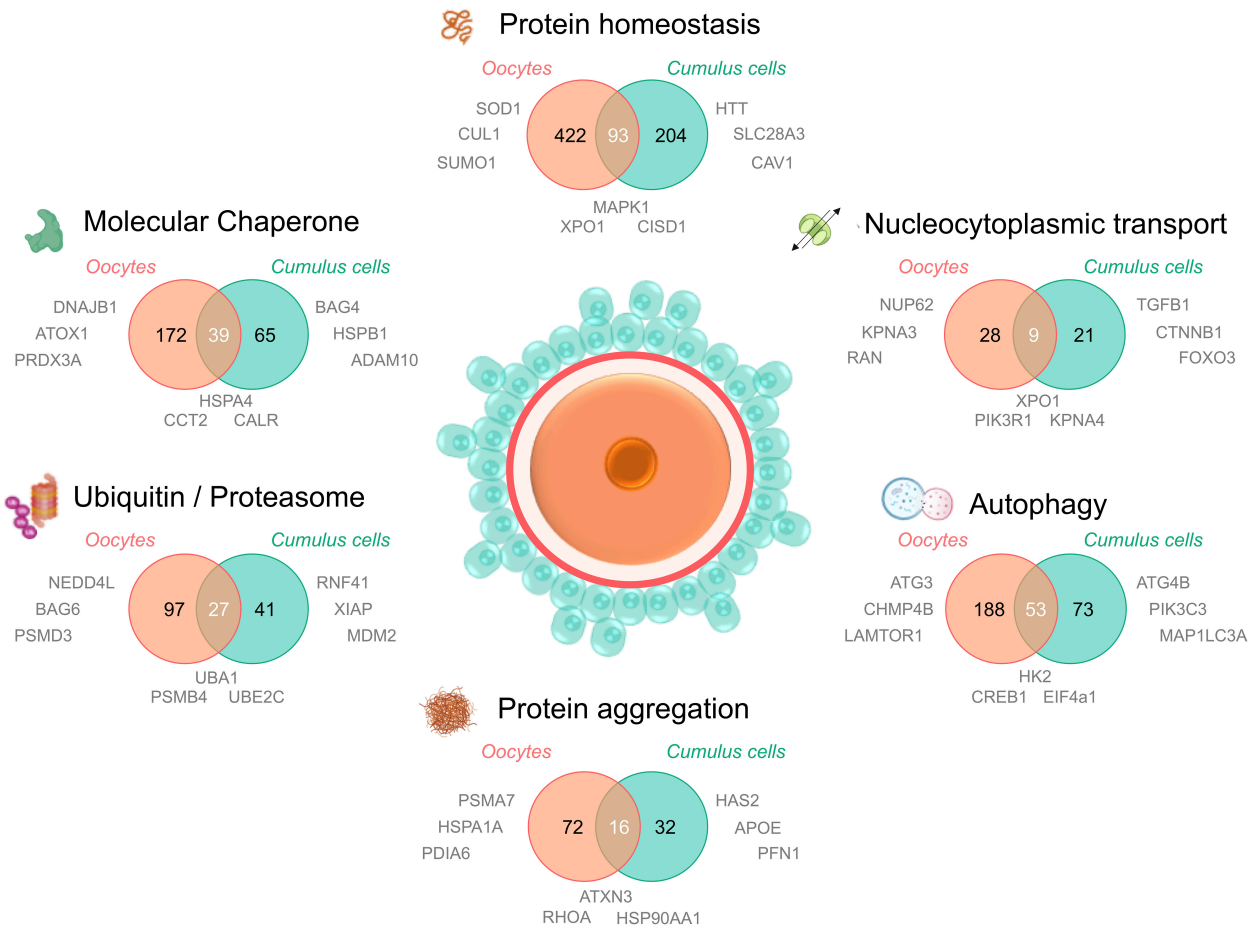

FIGURE 3 | Proteomic/transcriptomic evidence for the dysregulation of the protein homeostasis network in aged oocytes and cumulus cells. To understand the contribution of proteostasis to aging in oocytes and cumulus cells, four recent proteomic and/or transcriptomic datasets of maternally aged oocytes and cumulus cells (Oocytes; Schwarzer et al., 2014; Duncan et al., 2017; Cumulus cells; McReynolds et al., 2012; Al-Edani et al., 2014) were analyzed for dysregulated elements involved in proteostasis. Proteins and transcripts were defined as "age-dysregulated" by individual cut offs (fold change and significance) specified by the authors of each primary research paper. A database of all proteostasis network related proteins was compiled from neXtProt (Zahn-Zabal et al., 2020; v2.27.0; https://www.nextprot.org; neXtProt Data release 17/01/2020) through six individual searches titled "Protein homeostasis, Protein aggregation, Autophagy, Nucleocytoplasmic transport, Ubiquitin/proteasome, and Molecular chaperone." Human neXtProt protein accessions were then mapped to their UniProt mouse homologs to generate both mouse and human proteostasis databases (found in **Supplementary File 1**). Age-dysregulated proteins and transcripts listed in the **Supplementary Material** of the four primary manuscripts were uniformly converted to their corresponding mouse homologs and UniProt protein accessions and used to search for corresponding proteostasis related ID's in the 6 NeXtProt database categories. These data were used to generate Venn diagrams comparing the putative age-dysregulated proteins in oocytes vs. cumulus cells and to supply relevant examples of dysregulated proteins adjacent to the component of interest. Aged oocyte IDs were from CBCF1 mice aged between 14 and 17 months (climacteric) and aged cumulus cell IDs were from cumulus-oocyte complexes from women of equivalent advanced maternal age (37–45 years). Examples included in **Figure 3** were selected from age-dysregulated protein IDs. Full protein names, UniProt accessions, the proteostasis network database used to generate this figure, and lists of oocyte and cumulus cell dysregulated protein accessions can be found in **Supplementary File 1**. The sharing of IDs between aged oocytes and cumulus cells is putative but provides novel candidates for research into the contribution of declining proteostasis to reproductive aging. Elements of this figure were made in BioRender.

Other dysregulated oocyte and cumulus cell proteins include those involved in PTMs such as SUMO1, NEDD4L, and multiple enzymes featured in ubiquitylation pathways (**Supplementary File 1**). Importantly, the ubiquitin encoding gene Ubb is known to be essential for meiotic progression in mouse oocytes (Ryu et al., 2008). Intriguingly, some of the dysregulated proteins mapped to karyopherin family proteins and nuclear pore proteins involved in nucleocytoplasmic transport (**Figure 3**). While the contribution of these proteins to oocyte aging is unknown, it is possible that, analogous to somatic cells, oocytes use nucleocytoplasmic transport to ensure subcellular management of misfolded or aggregating proteins. Recent studies of karyopherin expression has indeed mapped unique expression profiles for many of the members of this family in oocyte and follicle development (Mihalas et al., 2015), citing a possible role for these proteins in meiotic spindle function. Moreover, we have recently demonstrated that the inhibition of karyopherin A2 and B1 (KPNA2/B1) and XPO1 can exacerbate the formation of protein aggregates in male germ cells and contribute to a loss of cellular viability (Cafe et al., 2020). This provides a clear impetus

to study nucleocytoplasmic transport in oocytes and cumulus cells as a potential contributing factor to oocyte aging.

Finally, several proteasomal degradation related proteins were also altered in oocytes and cumulus cells with age (**Figure 3**). This agrees with our findings that proteasome activity declines in aged mouse GV oocytes, which can be modeled *in vitro* through the induction of oxidative stress using 4HNE (Mihalas et al., 2018). Through this model we have also identified several core proteasome subunits that are sensitive to direct modification by 4HNE, a phenomenon that also disrupts proteostasis in somatic cells (Jung et al., 2014). 4HNE also elicits a reduction in kinetochore-microtubule and tubulin polymerization that may contribute to oocyte aging and increases in aneuploidy (Mihalas et al., 2017, 2018). Coupled with the knowledge that cohesin and several centromere-specific histones are long-lived proteins that deteriorate with age in the absence of renewal pathways (Revenkova et al., 2010; Tachibana-Konwalski et al., 2010; Burkhardt et al., 2016; Greaney et al., 2018; Lee, 2020), proteostasis defects either driven by oxidative modifications or the collapse of protein quality control over time, form a compelling explanation to support many aspects of oocyte aging and the loss of meiotic fidelity.

Ovarian Tissue Aging and Reproductive Disorders

While many dysregulated proteins featuring in proteomic and transcriptomic datasets are common to aged cumulus cells and aged oocytes (**Figure 3**), a majority of the proteins mapped in each proteostasis category are in fact unique to each specific cell type. Such findings reinforce the pressing need to thoroughly investigate both the somatic and germ cell contributions to reproductive failure in women. Beyond the follicles themselves, the ovarian stroma also experiences age related changes that contribute to declining fertility. The ovarian stroma is highly heterogeneous and consists of abundant extracellular matrix (ECM) components, fibroblasts, endothelial cells, smooth muscle cells and immune cells (Tingen et al., 2011). This extra-follicular compartment of the ovary is the microenvironment in which follicles develop and provides important signaling and structural support. Although the mechanisms remain uncertain, it is known that an age-dependent increase in stromal inflammation and fibrosis also negatively impacts the quality of the gametes (Rowley et al., 2020).

An important component of the stromal compartment is the ECM and, in particular, its ubiquitous component, hyaluronan; a linear polysaccharide with pleiotropic roles in tissue structure, cell signaling and inflammation (Rowley et al., 2020; Takasugi et al., 2020). In the context of the ovary, recent work has demonstrated that total hyaluronan content in the ovarian stroma decreases with age and is effectively "replaced" by collagen leading to dramatic changes in ovarian biomechanics pertaining to increased stiffness (Amargant et al., 2020). Importantly, these age-associated changes are conserved between the mouse and humans (Amargant et al., 2020) and may be associated with the production of oocytes with compromised morphology, poor meiotic competence, and impaired granulosa cell function (Amargant et al., 2020; Rowley et al., 2020). In pathological states or during tissue aging, it also known that the fragmentation of hyaluronan yields a low molecular weight polymer (<250 kDa) linked to inflammation, fibrotic disease (Takasugi et al., 2020). Conversely, in healthy tissues, high molecular mass hyaluronan (>1 MDa) predominates and promotes tissue hydration, homeostasis and the protection of cells from stress-induced cell cycle arrest and cell death (Takasugi et al., 2020).

These latter discoveries flowed from investigation of the naked mole-rat, the longest lived rodent with a lifespan of up to 30 years; exceeding its predicted lifespan by fivefold (Edrey et al., 2011). Uniquely, the reproductive function of female naked mole-rats also increases with age until the animals reach >20 years old (Buffenstein, 2008). In understanding the remarkable lifespan of this rodent it is important to note that the naked mole-rat produces very high molecular weight hyaluronan (>6 mKD). This high molecular weight hyaluronan greatly exceeds the length of other mammalian species and is synthesized by a form of hyaluronan synthase 2 (HAS2) that differs from that found in mice (Tian et al., 2013; Faulkes et al., 2015). Additionally, naked mole-rat proteins are better at maintaining their structure and function under conditions of oxidative stress (Perez et al., 2009; De Waal et al., 2013), which can partially be explained by high proteasomal (Rodriguez et al., 2012) and autophagic activity (Zhao et al., 2014). This implies that the handling of proteotoxic stress, rather than presence or absence of the damage itself, is likely to influence cell longevity and viability (Takasugi et al., 2020). While the mechanisms promoting hyaluronan fragmentation are not entirely understood, age-dependent increases in hyaluronan degradation enzyme (hyaluronidase) activity and ROS production have been implicated (Monslow et al., 2015). This suggests that the protection of the ovary from oxidative stress and/or the bolstering of high molecular mass hyaluronan in the ovarian stroma may provide novel avenues to prevent the deleterious changes associated with aging.

Providing a Clean Slate for Embryogenesis

Following fertilization, proteostasis has been shown to play a remarkable role in promoting healthy zygote/embryo development as it prevents the transmission of oocyte-harbored aggregates and toxic species to the next generation. In this context, studies in the model organism, *Caenorhabditis elegans*, have demonstrated that proteostatic remodeling events are capable of eliminating protein aggregates within the oocyte. This process is initiated upon mating via the action of sperm-secreted hormones, which activate a switch (VATPase catalytic subunit) to promote lysosomal acidification, effectively preparing a "clean slate" for proteostasis in the zygote (Bohnert and Kenyon, 2017). Acidification of the lysosome under these conditions occurs in concert with altered mitochondrial activity and metabolism within the oocyte, suggesting an important link between metabolism and proteostasis (Bohnert and Kenyon, 2017). Interestingly, it has also been shown that female worms devoid of sperm fail to initiate and clear protein carbonyls,

while conversely, sperm-proximal oocytes in hermaphrodites efficiently remove protein carbonyls and exhibit a marked increase in the capacity to degrade protein aggregates (Goudeau and Aguilaniu, 2010). In addition to these observations in *C. elegans*, novel findings in budding yeast suggest that the process of meiotic differentiation is capable of eliminating the cellular damage induced by aging (Unal et al., 2011; King et al., 2019). This occurs through the sequestering of nuclear senescence factors, including aggregates, away from the chromosomes during meiosis II (King et al., 2019). This remarkable process leads to the elimination of abnormal cellular components such as aggregates, extrachromosomal ribosomal DNA and abnormal nucleolar material, preventing the inheritance of these factors into the newly formed gametes in a form of "meiotic rejuvenation." Conversely, some amyloid-like protein aggregates can play functional rather than pathological roles and are utilized by cells as important regulators of gametogenesis. This was first described for the RNA binding protein Rim4 that is required for translational repression during gametogenesis in yeast (Berchowitz et al., 2015). Whilst equivalent mechanisms of proteostatic remodeling and meiotic rejuvenation have yet to be investigated in mammalian oocytes, the detection of lysosome acidification during *Xenopus* oocyte maturation raises the prospect that at least the former may be a conserved phenomenon (Bohnert and Kenyon, 2017).

Proteostasis and Female Reproductive Health Issues

Beyond the oocyte itself, the broader contributions of proteotoxic stress to pregnancy complications and female reproductive health issues are starting to receive considerable attention. In women with endometriosis, new evidence points to an excess of ROS in the granulosa cells of growing follicles that results in a cascade of adverse sequelae beginning with the activation of ER stress pathways and leading to granulosa cell senescence, impaired cumulus oocyte complex maturation, follicle apoptosis, metabolic disturbance in the oocytes, and ovarian fibrosis; which combined underpin endometriosis-associated infertility (Lin et al., 2020). Furthermore, preeclampsia, a leading cause of pregnancy-associated morbidity and mortality, is now being viewed as a protein misfolding disorder as toxic depositions of misfolded proteins have been found to accumulate in body fluids and in the placenta of preeclamptic women (Cater et al., 2019). Concerningly, these protein aggregates are thought to contribute to the defective trophoblast invasion, placental ischemia and ER stress that are hallmark features of this pregnancy disorder (Gerasimova et al., 2019). The mechanisms behind the induction of protein misfolding in preeclamptic pregnancies are undoubtedly complex, however, the novel discovery of the anti-aggregation chaperone activity of pregnancy zone protein (PZP), a protein that is dramatically increased in maternal blood plasma during pregnancy, may aid our understanding of this phenomenon. PZP has been shown to efficiently inhibit *in vitro* aggregation of several vulnerable proteins (Cater et al., 2019). Thus, PZP upregulation during pregnancy may represent an important maternal adaptation to maintain extracellular proteostasis during gestation and it is possible that it is the disruption, or overwhelming of PZP during pregnancy that underpins the accumulation of misfolded proteins (Cater et al., 2019). Further research will need to be conducted to determine whether the stabilization of PZP throughout pregnancy can reduce the incidence of preeclamptic pregnancies. Given increasing evidence that women who have experienced preeclampsia may be at an increased risk of adverse outcomes in other protein misfolding disorders such as AD (Theilen et al., 2016) and cataract formation later in life (Auger et al., 2017), it will be important to investigate the mechanistic commonalities between germ and somatic cell protein homeostasis.

DISCUSSION AND CONCLUSION

Organismal Proteostasis and the Compromise of Lifespan for Reproduction

Reproduction is a high-cost scenario and, with current reproductive success being preponderant to future reproduction, natural selection often favors genes that mediate survival earlier in life as opposed to after the peak of reproductive activity (Maklakov and Immler, 2016). This causal, inverse relationship between reproduction and lifespan is perhaps best surmised in the "disposable soma theory," which posits that investment into the germline is prioritized over that of the soma (Kirkwood, 1977). Whilst empirical evidence supporting the trade-off between life span and reproduction is limited, pioneering studies in *C. elegans* and *D. melanogaster* have recently given credence to this model.

In *C. elegans*, the ability to maintain somatic cell proteostasis declines dramatically upon the initiation of reproduction (Khodakarami et al., 2015). Remarkably, germline ablation in *C. elegans* (i.e., removal of the germline without an attendant removal of the whole gonad), promotes longevity by triggering a signaling network regulated by both transcription factors and microRNAs (Ermolaeva et al., 2013; Shemesh et al., 2013). This response converges on the FOXO transcription factor, DAF-16, which activates downstream proteasome-related genes, increasing stress resistance and ultimately organismal longevity (Vilchez et al., 2012; Shemesh et al., 2013). Strikingly, *mir-71* expression in neuronal cells is also enough to rescue gonadal longevity, pointing to a cell-non-autonomous relationship between the nervous system and the gonad, a prime example of the importance of organismal proteostasis (Antebi, 2013). Similarly, interconnections between stress response pathways, the reproductive system and metabolism have been linked to the expression of glucagon-like-peptide 1 (*glp1)*. Thus, stress resistance and the maintenance of somatic cell proteostasis, can be promoted in germline ablation models wherein *glp1* mutations prevent germ cell proliferation prior to adulthood transition. Curiously, these mutations also facilitate the suppression of protein aggregation and polyQ disease progression (Shemesh et al., 2013). Germline-less *C. elegans* are more resistant

to proteotoxic stress conditions such as heat stress and are better protected from protein aggregate and polyglutamine-driven toxicity, a phenomenon partially attributed to increased proteasome activity in the somatic cells (Vilchez et al., 2012). These cells also exhibit increased autophagic activity and lipase-4-dependent lipolysis, which may modulate the longevity phenotype through increased lipid clearance or enhanced regulation of lipid-derived signaling molecules such as aldehydes (Folick et al., 2015).

Not unlike *C. elegans*, a dysregulation of PN gene expression and a concomitant decrease in proteasomal catalytic activity have been noted during the aging process in both male and female *Drosophila*. By contrast, proteasome activity is retained within the germ cells of these flies (Tsakiri et al., 2013), with molecular chaperones and proteasome machinery normally elevated 2-8-fold in the abdomen compared to the thorax (Fredriksson et al., 2012)- further highlighting the battle of resource allocation between the germ line and the soma. These unique molecular links between reproduction and lifespan form a growing body of literature on organismal proteostasis that is currently being verified in mammalian model species. Importantly, these findings highlight the importance of the maintenance of proteostasis in the germline for the health and wellbeing of organisms as the remodeling of the organismal stress response associated with the onset of reproduction may render organisms more susceptible to environmental insults. Thus, in depth studies of the mammalian proteostasis network and mechanisms for aggregate clearance are needed to better understand male and female reproductive health throughout life.

Therapeutics Targeted Toward Proteostasis to Promote Reproductive Health

In consideration of the wealth of reproductive and non-reproductive disorders underpinned by protein misfolding and aggregation, it is apparent that there are substantial dividends to be gained from modulation of the proteostasis network in the context of protecting neuronal and germ cells alike. In evaluating appropriate strategies, the framework provided by the FoldEx model is particularly informative (Powers et al., 2009). That is, effective amelioration of a protein-misfolding disorder necessitates that a misfolded protein must shift to within the proteostasis boundary delineated by the stability, misfolding rate and folding rate of the protein. Taking pharmacological chaperones as an example, there are three theoretical ways in which loss-of-function misfolding diseases could be modulated using these reagents. In principle, pharmacological chaperones could function by either increasing the folding rate of a protein, thermodynamic stabilization or decreasing misfolding rate by stabilization of native protein structure; the latter two of which have been experimentally verified (Powers et al., 2009). Thus, proteostasis regulators could be used to alter the composition and concentration of proteostasis network components and hence move the proteostasis boundary, potentially mimicking UPR and HSR including the induction of HSP70 and HSP90 families of chaperones (Westerheide and Morimoto, 2005) and modulation of histone deacetylases (HDACs) (Gan, 2007; Outeiro et al., 2007; Westerheide et al., 2009).

Illustrative of this potential, HDAC modulation through class II histone deacetylases (Sirtuins), has gained considerable interest in the field of neurodegeneration owing to the potential to ameliorate stress responses and protein aggregation and promote healthy aging (Merksamer et al., 2013). Importantly, a role for SIRT proteins in fertility is beginning to emerge following several reports of a defective reproductive phenotype in SIRT1-null animals (McBurney et al., 2003; Coussens et al., 2008). The loss of SIRT1 in both sexes results in infertility phenotypes, characterized in the male by severely disrupted spermatogenesis, reduced spermatogonial stem cell population and DNA damage (Coussens et al., 2008). Despite the promise of SIRT1 activators to reduce stress sensitivity in other tissues, the ability of SIRT1 to protect male germ cells against oxidative stress has yet to be evaluated. Nevertheless, we have recently begun to explore whether SIRT1 activation can modulate levels of protein aggregation in developing male germ cells. Intriguingly, the use of the SIRT1 activator, SRT1720, resulted in a significant decrease in protein aggregation in both pre- and post-meiotic populations of pachytene spermatocytes and round spermatids (Cafe et al., 2020). Moreover, with regards to female fertility the downregulation of SIRT1 is associated with reduction of the ovarian reserve and important roles for both SIRT1 and SIRT3 in the sensing of redox state and energy homeostasis have been reported in oocytes, granulosa cells and early embryos (Tatone et al., 2015, 2018). Indeed, SIRT1 has now been shown to slow the age-related decline in oocyte quality thereby sustaining female fertility (Iljas et al., 2020). However, SIRT3 appears to be dispensable for female fertility (Iljas and Homer, 2020). Several of the SIRT family enzymes are yet to be explicitly explored in relation to reproductive health and this will likely be an important avenue to pursue in relation to the maintenance of proteostasis during reproductive aging in men and women. In addition to the direct modulation of Sirtuins, several recent studies have demonstrated that supplementation with the NAD+ precursor nicotinamide mononucleotide (NMN) improves the quality of maternally aged oocytes through the restoration of both mitochondrial function and meiotic competency (Wu et al., 2019; Bertoldo et al., 2020; Miao et al., 2020). These outcomes could be recapitulated in mice through the overexpression of SIRT2 (Bertoldo et al., 2020). Beyond the oocyte, NMN was also able to improve developmental competency in the embryos produced from aged animals (Bertoldo et al., 2020; Miao et al., 2020). While NMN was not able to protect the ovary from the severe damage caused by chemotherapy (Stringer et al., 2019), the bolstering of NAD+ provides promise for the improvement of reproductive outcomes of women of advanced maternal age.

In many diseases and disorders of proteostasis, recent progress toward therapeutics has been enabled through the targeting of the integrated stress response (ISR). The ISR is an evolutionarily conserved signaling network coupled to the UPR and HSR, operating through the reprogramming of translation (Costa-Mattioli and Walter, 2020). Importantly, this network modulates diverse stress inputs (such as nutrient deprivation, proteostasis defects and redox imbalance) and leads to a central output –

a reduction in the translation of specific mRNAs that promote proteostasis. Evidence linking the ISR to the maintenance of cellular homeostasis and apoptosis in the reproductive organs of men, allied to its contribution to infertility in animal models (Karna et al., 2019), identifies the ISR as a potentially attractive therapeutic target. Additionally, the discovery of PZP as an anti-aggregation factor for proteins involved in preeclampsia (Cater et al., 2019) opens an important window for the regulation of protein misfolding disorders that affect female reproductive health. Our ability to capitalize on these novel proteostasis interventions in the context of infertility research is now predicated on improvements in our fundamental knowledge of aggregation-prone proteins in gametes and the PN in germ cells more broadly.

AUTHOR CONTRIBUTIONS

SC, EB, and BN were responsible for study design, execution, analysis, manuscript drafting, and critical discussion. HE, JM, and DS-B participated in manuscript editing and critical discussion. All authors contributed to the article and approved the submitted version.

FUNDING

This work was supported by the National Health and Medical Research Council of Australia (NHMRC) Project Grant (APP1163319) awarded to BN and EB. SC was supported by The University of Newcastle Research Post-Graduate Scholarship. EB and BN are the recipients of NHMRC Early Career (APP1138701) and Senior Research (APP1154837) Fellowships, respectively.

SUPPLEMENTARY MATERIAL

The Supplementary Material for this article can be found online at: https://www.frontiersin.org/articles/10.3389/fcell.2021.660626/full#supplementary-material

REFERENCES

Agarwal, A., Panner Selvam, M. K., and Baskaran, S. (2020). Proteomic analyses of human sperm cells: understanding the role of proteins and molecular pathways affecting male reproductive health. *Int. J. Mol. Sci.* 21:1621. doi: 10.3390/ijms21051621

Agarwal, A., Sharma, R., Durairajanayagam, D., Ayaz, A., Cui, Z., Willard, B., et al. (2015). Major protein alterations in spermatozoa from infertile men with unilateral varicocele. *Reprod. Biol. Endocrinol.* 13:8.

Aiken, C. T., Kaake, R. M., Wang, X., and Huang, L. (2011). Oxidative stress-mediated regulation of proteasome complexes. *Mol. Cell. Proteomics* 10:R110006924.

Aitken, R. J., and Nixon, B. (2013). Sperm capacitation: a distant landscape glimpsed but unexplored. *Mol. Hum. Reprod.* 19, 785–793. doi: 10.1093/molehr/gat067

Alam, F., Khan, T. A., Ali, R., Tariq, F., and Rehman, R. (2020). SIRTI and cortisol in unexplained infertile females; a cross sectional study, in Karachi Pakistan. *Taiwan J. Obstet. Gynecol.* 59, 189–194.

Al-Edani, T., Assou, S., Ferrieres, A., Bringer Deutsch, S., Gala, A., Lecellier, C. H., et al. (2014). Female aging alters expression of human cumulus cells genes that are essential for oocyte quality. *Biomed. Res. Int.* 2014:964614.

Amargant, F., Manuel, S. L., Tu, Q., Parkes, W. S., Rivas, F., Zhou, L. T., et al. (2020). Ovarian stiffness increases with age in the mammalian ovary and depends on collagen and hyaluronan matrices. *Aging Cell* 19:e13259.

Antebi, A. (2013). Regulation of longevity by the reproductive system. *Exp. Gerontol.* 48, 596–602. doi: 10.1016/j.exger.2012.09.009

Arnesen, T., Van Damme, P., Polevoda, B., Helsens, K., Evjenth, R., Colaert, N., et al. (2009). Proteomics analyses reveal the evolutionary conservation and divergence of N-terminal acetyltransferases from yeast and humans. *Proc. Natl. Acad. Sci. U.S.A.* 106, 8157–8162. doi: 10.1073/pnas.0901931106

Atwal, R. S., Desmond, C. R., Caron, N., Maiuri, T., Xia, J., Sipione, S., et al. (2011). Kinase inhibitors modulate huntingtin cell localization and toxicity. *Nat. Chem. Biol.* 7, 453–460. doi: 10.1038/nchembio.582

Auger, N., Rheaume, M. A., Paradis, G., Healy-Profitos, J., Hsieh, A., and Fraser, W. D. (2017). Preeclampsia and the risk of cataract extraction in life. *Am. J. Obstet. Gynecol.* 216, e411–e417.

Baena, V., and Terasaki, M. (2019). Three-dimensional organization of transzonal projections and other cytoplasmic extensions in the mouse ovarian follicle. *Sci. Rep.* 9:1262.

Barmada, S. J., Skibinski, G., Korb, E., Rao, E. J., Wu, J. Y., and Finkbeiner, S. (2010). Cytoplasmic mislocalization of TDP-43 is toxic to neurons and enhanced by a mutation associated with familial amyotrophic lateral sclerosis. *J. Neurosci.* 30, 639–649. doi: 10.1523/jneurosci.4988-09.2010

Barragán, M., Pons, J., Ferrer-Vaquer, A., Cornet-Bartolome, D., Schweitzer, A., Hubbard, J., et al. (2017). The transcriptome of human oocytes is related to age and ovarian reserve. *Mol. Hum. Reprod.* 23, 535–548. doi: 10.1093/molehr/gax033

Baska, K. M., Manandhar, G., Feng, D., Agca, Y., Tengowski, M. W., Sutovsky, M., et al. (2008). Mechanism of extracellular ubiquitination in the mammalian epididymis. *J. Cell. Physiol.* 215, 684–696. doi: 10.1002/jcp.21349

Bell, E. L., Nagamori, I., Williams, E. O., Del Rosario, A. M., Bryson, B. D., Watson, N., et al. (2014). SirT1 is required in the male germ cell for differentiation and fecundity in mice. *Development* 141, 3495–3504. doi: 10.1242/dev.110627

Belote, J. M., and Zhong, L. (2009). Duplicated proteasome subunit genes in *Drosophila* and their roles in spermatogenesis. *Heredity* 103, 23–31. doi: 10.1038/hdy.2009.23

Berchowitz, L. E., Kabachinski, G., Walker, M. R., Carlile, T. M., Gilbert, W. V., Schwartz, T. U., et al. (2015). Regulated formation of an amyloid-like translational repressor governs gametogenesis. *Cell* 163, 406–418. doi: 10.1016/j.cell.2015.08.060

Bertoldo, M. J., Listijono, D. R., Ho, W. J., Riepsamen, A. H., Goss, D. M., Richani, D., et al. (2020). NAD(+) repletion rescues female fertility during reproductive aging. *Cell Rep.* 30, 1670–1681.e7.

Bizzozero, O. A., DeJesus, G., Callahan, K., and Pastuszyn, A. (2005). Elevated protein carbonylation in the brain white matter and gray matter of patients with multiple sclerosis. *J. Neurosci. Res.* 81, 687–695. doi: 10.1002/jnr.20587

Bjorkoy, G., Lamark, T., Brech, A., Outzen, H., Perander, M., Overvatn, A., et al. (2005). p62/SQSTM1 forms protein aggregates degraded by autophagy and has a protective effect on huntingtin-induced cell death. *J. Cell Biol.* 171, 603–614. doi: 10.1083/jcb.200507002

Bohnert, K. A., and Kenyon, C. (2017). A lysosomal switch triggers proteostasis renewal in the immortal C. elegans germ lineage. *Nature* 551, 629–633. doi: 10.1038/nature24620

Brehme, M., Voisine, C., Rolland, T., Wachi, S., Soper, J. H., Zhu, Y., et al. (2014). A chaperome subnetwork safeguards proteostasis in aging and neurodegenerative disease. *Cell Rep.* 9, 1135–1150. doi: 10.1016/j.celrep.2014.09.042

Bromfield, E. G., Aitken, R. J., Anderson, A. L., McLaughlin, E. A., and Nixon, B. (2015). The impact of oxidative stress on chaperone-mediated human sperm-egg interaction. *Hum. Reprod.* 30, 2597–2613. doi: 10.1093/humrep/dev214

Bromfield, E. G., Aitken, R. J., McLaughlin, E. A., and Nixon, B. (2017). Proteolytic degradation of heat shock protein A2 occurs in response to oxidative stress in male germ cells of the mouse. *Mol. Hum. Reprod.* 23, 91–105.

Bromfield, E. G., McLaughlin, E. A., Aitken, R. J., and Nixon, B. (2016). Heat shock protein member A2 forms a stable complex with angiotensin converting enzyme and protein disulfide isomerase A6 in human spermatozoa. *Mol. Hum. Reprod.* 22, 93–109. doi: 10.1093/molehr/gav073

Bromfield, E. G., Walters, J. L. H., Cafe, S. L., Bernstein, I. R., Stanger, S. J., Anderson, A. L., et al. (2019). Differential cell death decisions in the testis: evidence for an exclusive window of ferroptosis in round spermatids. *Mol. Hum. Reprod.* 25, 241–256. doi: 10.1093/molehr/gaz015

Buffenstein, R. (2008). Negligible senescence in the longest living rodent, the naked mole-rat: insights from a successfully aging species. *J. Comp. Physiol. B* 178, 439–445. doi: 10.1007/s00360-007-0237-5

Burkhardt, S., Borsos, M., Szydlowska, A., Godwin, J., Williams, S. A., Cohen, P. E., et al. (2016). Chromosome cohesion established by Rec8-cohesin in fetal oocytes is maintained without detectable turnover in oocytes arrested for months in mice. *Curr. Biol.* 26, 678–685. doi: 10.1016/j.cub.2015.12.073

Cafe, S. L., Nixon, B., Dun, M. D., Roman, S. D., Bernstein, I. R., and Bromfield, E. G. (2020). Oxidative stress dysregulates protein homeostasis within the male germ line. *Antioxid. Redox Signal.* 32, 487–503. doi: 10.1089/ars.2019.7832

Calero, M., Pawlik, M., Soto, C., Castano, E. M., Sigurdsson, E. M., Kumar, A., et al. (2001). Distinct properties of wild-type and the amyloidogenic human cystatin C variant of hereditary cerebral hemorrhage with amyloidosis, Icelandic type. *J. Neurochem.* 77, 628–637. doi: 10.1046/j.1471-4159.2001.00256.x

Campanella, C., Pace, A., Caruso Bavisotto, C., Marzullo, P., Marino Gammazza, A., Buscemi, S., et al. (2018). Heat shock proteins in Alzheimer's disease: role and targeting. *Int. J. Mol. Sci.* 19:2603.

Castillo-Fernandez, J., Herrera-Puerta, E., Demond, H., Clark, S. J., Hanna, C. W., Hemberger, M., et al. (2020). Increased transcriptome variation and localised DNA methylation changes in oocytes from aged mice revealed by parallel single-cell analysis. *Aging Cell* 19:e13278.

Cater, J. H., Kumita, J. R., Zeineddine Abdallah, R., Zhao, G., Bernardo-Gancedo, A., Henry, A., et al. (2019). Human pregnancy zone protein stabilizes misfolded proteins including preeclampsia- and Alzheimer's-associated amyloid beta peptide. *Proc. Natl. Acad. Sci. U.S.A.* 116, 6101–6110. doi: 10.1073/pnas.1817298116

Cedenho, A. P., Lima, S. B., Cenedeze, M. A., Spaine, D. M., Ortiz, V., and Oehninger, S. (2006). Oligozoospermia and heat-shock protein expression in ejaculated spermatozoa. *Hum. Reprod.* 21, 1791–1794. doi: 10.1093/humrep/del055

Chan, H. C., Ruan, Y. C., He, Q., Chen, M. H., Chen, H., Xu, W. M., et al. (2009). The cystic fibrosis transmembrane conductance regulator in reproductive health and disease. *J. Physiol.* 587, 2187–2195.

Chau, K. M., and Cornwall, G. A. (2011). Reduced fertility in vitro in mice lacking the cystatin CRES (cystatin-related epididymal spermatogenic): rescue by exposure of spermatozoa to dibutyryl cAMP and isobutylmethylxanthine. *Biol. Reprod.* 84, 140–152. doi: 10.1095/biolreprod.110.084855

Chau, K. M., Kaur, G., and Cornwall, G. A. (2008). Sperm lacking cystatin-related epididymal spermatogenic protein (CRES) exhibit impaired capacitation. *Biol. Reprod.* 78(Suppl. 1):167. doi: 10.1093/biolreprod/78.s1.167c

Chiti, F., and Dobson, C. M. (2006). Protein misfolding, functional amyloid, and human disease. *Annu. Rev. Biochem.* 75, 333–366. doi: 10.1146/annurev.biochem.75.101304.123901

Claydon, A. J., Ramm, S. A., Pennington, A., Hurst, J. L., Stockley, P., and Beynon, R. (2012). Heterogenous turnover of sperm and seminal vesicle proteins in the mouse revealed by dynamic metabolic labeling. *Mol. Cell. Proteomics* 11:M111014993.

Cohen, P. (2000). The regulation of protein function by multisite phosphorylation–a 25 year update. *Trends Biochem. Sci.* 25, 596–601. doi: 10.1016/s0968-0004(00)01712-6

Cooper, T. G., Wagenfeld, A., Cornwall, G. A., Hsia, N., Chu, S. T., Orgebin-Crist, M. C., et al. (2003). Gene and protein expression in the epididymis of infertile c-ros receptor tyrosine kinase-deficient mice. *Biol. Reprod.* 69, 1750–1762. doi: 10.1095/biolreprod.103.017566

Cooper, T. G., Yeung, C. H., Wagenfeld, A., Nieschlag, E., Poutanen, M., Huhtaniemi, I., et al. (2004). Mouse models of infertility due to swollen spermatozoa. *Mol. Cell. Endocrinol.* 216, 55–63. doi: 10.1016/j.mce.2003.10.076

Cornwall, G. A. (2009). New insights into epididymal biology and function. *Hum. Reprod. Update* 15, 213–227. doi: 10.1093/humupd/dmn055

Cornwall, G. A., Von Horsten, H. H., and Whelly, S. (2011). Cystatin-related epididymal spermatogenic aggregates in the epididymis. *J. Androl.* 32, 679–685. doi: 10.2164/jandrol.111.012963

Costa-Mattioli, M., and Walter, P. (2020). The integrated stress response: from mechanism to disease. *Science* 368:eaat5314. doi: 10.1126/science.aat5314

Coticchio, G., Dal Canto, M., Mignini Renzini, M., Guglielmo, M. C., Brambillasca, F., Turchi, D., et al. (2015). Oocyte maturation: gamete-somatic cells interactions, meiotic resumption, cytoskeletal dynamics and cytoplasmic reorganization. *Hum. Reprod. Update* 21, 427–454. doi: 10.1093/humupd/dmv011

Coussens, M., Maresh, J. G., Yanagimachi, R., Maeda, G., and Allsopp, R. (2008). Sirt1 deficiency attenuates spermatogenesis and germ cell function. *PLoS One* 3:e1571. doi: 10.1371/journal.pone.0001571

Crippa, V., Sau, D., Rusmini, P., Boncoraglio, A., Onesto, E., Bolzoni, E., et al. (2010). The small heat shock protein B8 (HspB8) promotes autophagic removal of misfolded proteins involved in amyotrophic lateral sclerosis (ALS). *Hum. Mol. Genet.* 19, 3440–3456. doi: 10.1093/hmg/ddq257

Da Cruz, S., and Cleveland, D. W. (2016). CELL BIOLOGY. Disrupted nuclear import-export in neurodegeneration. *Science* 351, 125–126. doi: 10.1126/science.aad9872

Dacheux, J.-L., and Dacheux, F. (2002). "Protein secretion in the epididymis," in *The Epididymis: From Molecules to Clinical Practice: A Comprehensive Survey of the Efferent Ducts, the Epididymis and the Vas Deferens*, eds B. Robaire and B. T. Hinton (Boston, MA: Springer), 151–168. doi: 10.1007/978-1-4615-0679-9_9

Daugaard, M., Rohde, M., and Jaattela, M. (2007). The heat shock protein 70 family: highly homologous proteins with overlapping and distinct functions. *FEBS Lett.* 581, 3702–3710. doi: 10.1016/j.febslet.2007.05.039

Davies, K. J. (2001). Degradation of oxidized proteins by the 20S proteasome. *Biochimie* 83, 301–310. doi: 10.1016/s0300-9084(01)01250-0

De Waal, E. M., Liang, H., Pierce, A., Hamilton, R. T., Buffenstein, R., and Chaudhuri, A. R. (2013). Elevated protein carbonylation and oxidative stress do not affect protein structure and function in the long-living naked-mole rat: a proteomic approach. *Biochem. Biophys. Res. Commun.* 434, 815–819. doi: 10.1016/j.bbrc.2013.04.019

Di Domenico, F., Head, E., Butterfield, D. A., and Perluigi, M. (2014). Oxidative stress and proteostasis network: culprit and casualty of Alzheimer's-like neurodegeneration. *Adv. Geriatr.* 2014:527518.

Dias, T. R., Agarwal, A., Pushparaj, P. N., Ahmad, G., and Sharma, R. (2020). Reduced semen quality in patients with testicular cancer seminoma is associated with alterations in the expression of sperm proteins. *Asian J. Androl.* 22, 88–93. doi: 10.4103/aja.aja_17_19

Diaz-Villanueva, J. F., Diaz-Molina, R., and Garcia-Gonzalez, V. (2015). Protein folding and mechanisms of proteostasis. *Int. J. Mol. Sci.* 16, 17193–17230. doi: 10.3390/ijms160817193

Ding, Q., Reinacker, K., Dimayuga, E., Nukala, V., Drake, J., Butterfield, D. A., et al. (2003). Role of the proteasome in protein oxidation and neural viability following low-level oxidative stress. *FEBS Lett.* 546, 228–232. doi: 10.1016/s0014-5793(03)00582-9

Dix, D. J., Allen, J. W., Collins, B. W., Mori, C., Nakamura, N., Poorman-Allen, P., et al. (1996). Targeted gene disruption of Hsp70-2 results in failed meiosis, germ cell apoptosis, and male infertility. *Proc. Natl. Acad. Sci. U.S.A.* 93, 3264–3268. doi: 10.1073/pnas.93.8.3264

Dobson, C. M. (2004). Principles of protein folding, misfolding and aggregation. *Semin. Cell Dev. Biol.* 15, 3–16. doi: 10.1016/j.semcdb.2003.12.008

Donde, A., Sun, M., Jeong, Y. H., Wen, X., Ling, J., Lin, S., et al. (2020). Upregulation of ATG7 attenuates motor neuron dysfunction associated with depletion of TARDBP/TDP-43. *Autophagy* 16, 672–682. doi: 10.1080/15548627.2019.1635379

Drevet, J. R., and Aitken, R. J. (2020). Oxidation of sperm nucleus in mammals: a physiological necessity to some extent with adverse impacts on oocyte and offspring. *Antioxidants (Basel)* 9:95. doi: 10.3390/antiox9020095

Dube, E., Hermo, L., Chan, P. T., and Cyr, D. G. (2008). Alterations in gene expression in the caput epididymides of nonobstructive azoospermic men. *Biol. Reprod.* 78, 342–351. doi: 10.1095/biolreprod.107.062760

Dun, M. D., Aitken, R. J., and Nixon, B. (2012). The role of molecular chaperones in spermatogenesis and the post-testicular maturation of mammalian spermatozoa. *Hum. Reprod. Update* 18, 420–435. doi: 10.1093/humupd/dms009

Dun, M. D., Smith, N. D., Baker, M. A., Lin, M., Aitken, R. J., and Nixon, B. (2011). The chaperonin containing TCP1 complex (CCT/TRiC) is involved in mediating sperm-oocyte interaction. *J. Biol. Chem.* 286, 36875–36887. doi: 10.1074/jbc.m110.188888

Duncan, F. E., Jasti, S., Paulson, A., Kelsh, J. M., Fegley, B., and Gerton, J. L. (2017). Age-associated dysregulation of protein metabolism in the mammalian oocyte. *Aging Cell* 16, 1381–1393. doi: 10.1111/acel.12676

Ecroyd, H., Sarradin, P., Dacheux, J. L., and Gatti, J. L. (2004). Compartmentalization of prion isoforms within the reproductive tract of the ram. *Biol. Reprod.* 71, 993–1001. doi: 10.1095/biolreprod.104.029801

Edrey, Y. H., Hanes, M., Pinto, M., Mele, J., and Buffenstein, R. (2011). Successful aging and sustained good health in the naked mole rat: a long-lived mammalian model for biogerontology and biomedical research. *ILAR J.* 52, 41–53. doi: 10.1093/ilar.52.1.41

Eftekharzadeh, B., Daigle, J. G., Kapinos, L. E., Coyne, A., Schiantarelli, J., Carlomagno, Y., et al. (2018). Tau protein disrupts nucleocytoplasmic transport in Alzheimer's disease. *Neuron* 99, 925–940.e7.

Egge, N., Muthusubramanian, A., and Cornwall, G. A. (2015). Amyloid properties of the mouse egg zona pellucida. *PLoS One* 10:e0129907. doi: 10.1371/journal.pone.0129907

Ermolaeva, M. A., Segref, A., Dakhovnik, A., Ou, H. L., Schneider, J. I., Utermöhlen, O., et al. (2013). DNA damage in germ cells induces an innate immune response that triggers systemic stress resistance. *Nature* 501, 416–420. doi: 10.1038/nature12452

Farout, L., Mary, J., Vinh, J., Szweda, L. I., and Friguet, B. (2006). Inactivation of the proteasome by 4-hydroxy-2-nonenal is site specific and dependant on 20S proteasome subtypes. *Arch. Biochem. Biophys.* 453, 135–142. doi: 10.1016/j.abb.2006.02.003

Faulkes, C. G., Davies, K. T., Rossiter, S. J., and Bennett, N. C. (2015). Molecular evolution of the hyaluronan synthase 2 gene in mammals: implications for adaptations to the subterranean niche and cancer resistance. *Biol. Lett.* 11:20150185. doi: 10.1098/rsbl.2015.0185

Ferrigno, P., and Silver, P. A. (2000). Polyglutamine expansions: proteolysis, chaperones, and the dangers of promiscuity. *Neuron* 26, 9–12. doi: 10.1016/s0896-6273(00)81132-0

Ferrington, D. A., and Kapphahn, R. J. (2004). Catalytic site-specific inhibition of the 20S proteasome by 4-hydroxynonenal. *FEBS Lett.* 578, 217–223. doi: 10.1016/j.febslet.2004.11.003

Folick, A., Oakley, H. D., Yu, Y., Armstrong, E. H., Kumari, M., Sanor, L., et al. (2015). Aging. Lysosomal signaling molecules regulate longevity in *Caenorhabditis elegans*. *Science* 347, 83–86. doi: 10.1126/science.1258857

Ford, W. C., North, K., Taylor, H., Farrow, A., Hull, M. G., and Golding, J. (2000). Increasing paternal age is associated with delayed conception in a large population of fertile couples: evidence for declining fecundity in older men. The ALSPAC study team (Avon longitudinal study of pregnancy and childhood). *Hum. Reprod.* 15, 1703–1708. doi: 10.1093/humrep/15.8.1703

Foster, E. M., Dangla-Valls, A., Lovestone, S., Ribe, E. M., and Buckley, N. J. (2019). Clusterin in Alzheimer's disease: mechanisms, genetics, and lessons from other pathologies. *Front. Neurosci.* 13:164. doi: 10.1097/00002093-198802030-00012

Fowler, D. M., Koulov, A. V., Balch, W. E., and Kelly, J. W. (2007). Functional amyloid–from bacteria to humans. *Trends Biochem. Sci.* 32, 217–224. doi: 10.1016/j.tibs.2007.03.003

Fraser-Pitt, D., and O'Neil, D. (2015). Cystic fibrosis – a multiorgan protein misfolding disease. *Future Sci. OA* 1:FSO57.

Frattarelli, J. L., Miller, K. A., Miller, B. T., Elkind-Hirsch, K., and Scott, R. T. Jr. (2008). Male age negatively impacts embryo development and reproductive outcome in donor oocyte assisted reproductive technology cycles. *Fertil. Steril.* 90, 97–103. doi: 10.1016/j.fertnstert.2007.06.009

Fredriksson, A., Johansson Krogh, E., Hernebring, M., Pettersson, E., Javadi, A., Almstedt, A., et al. (2012). Effects of aging and reproduction on protein quality control in soma and gametes of *Drosophila melanogaster*. *Aging Cell* 11, 634–643. doi: 10.1111/j.1474-9726.2012.00823.x

Fu, M., Liu, M., Sauve, A. A., Jiao, X., Zhang, X., Wu, X., et al. (2006). Hormonal control of androgen receptor function through SIRT1. *Mol. Cell. Biol.* 26, 8122–8135. doi: 10.1128/mcb.00289-06

Fujiwara, H., Hasegawa, M., Dohmae, N., Kawashima, A., Masliah, E., Goldberg, M. S., et al. (2002). alpha-Synuclein is phosphorylated in synucleinopathy lesions. *Nat. Cell Biol.* 4, 160–164. doi: 10.1038/ncb748

Gan, L. (2007). Therapeutic potential of sirtuin-activating compounds in Alzheimer's disease. *Drug News Perspect.* 20, 233–239. doi: 10.1358/dnp.2007.20.4.1101162

Gamerdinger, M., Kaya, A. M., Wolfrum, U., Clement, A. M., and Behl, C. (2011). BAG3 mediates chaperone-based aggresome-targeting and selective autophagy of misfolded proteins. *EMBO Rep.* 12, 149–156. doi: 10.1038/embor.2010.203

Garcia, T. X., and Hofmann, M. C. (2015). Regulation of germ line stem cell homeostasis. *Anim. Reprod.* 12, 35–45.

Gawriluk, T. R., Hale, A. N., Flaws, J. A., Dillon, C. P., Green, D. R., and Rucker, E. B. III (2011). Autophagy is a cell survival program for female germ cells in the murine ovary. *Reproduction* 141, 759–765. doi: 10.1530/rep-10-0489

Gerasimova, E. M., Fedotov, S. A., Kachkin, D. V., Vashukova, E. S., Glotov, A. S., Chernoff, Y. O., et al. (2019). Protein misfolding during pregnancy: new approaches to preeclampsia diagnostics. *Int. J. Mol. Sci.* 20:6183. doi: 10.3390/ijms20246183

Gioia, L., Festuccia, C., Colapietro, A., Gloria, A., Contri, A., and Valbonetti, L. (2019). Abundances of autophagy-related protein LC3B in granulosa cells, cumulus cells, and oocytes during atresia of pig antral follicles. *Anim. Reprod. Sci.* 211:106225. doi: 10.1016/j.anireprosci.2019.106225

Gomez, H. L., Felipe-Medina, N., Condezo, Y. B., Garcia-Valiente, R., Ramos, I., Suja, J. A., et al. (2019). The PSMA8 subunit of the spermatoproteasome is essential for proper meiotic exit and mouse fertility. *PLoS Genet.* 15:e1008316. doi: 10.1371/journal.pgen.1008316

Gosden, R., and Lee, B. (2010). Portrait of an oocyte: our obscure origin. *J. Clin. Invest.* 120, 973–983. doi: 10.1172/jci41294

Goudeau, J., and Aguilaniu, H. (2010). Carbonylated proteins are eliminated during reproduction in C. elegans. *Aging Cell* 9, 991–1003. doi: 10.1111/j.1474-9726.2010.00625.x

Grad, I., Cederroth, C. R., Walicki, J., Grey, C., Barluenga, S., Winssinger, N., et al. (2010). The molecular chaperone Hsp90alpha is required for meiotic progression of spermatocytes beyond pachytene in the mouse. *PLoS One* 5:e15770. doi: 10.1371/journal.pone.0015770

Greaney, J., Wei, Z., and Homer, H. (2018). Regulation of chromosome segregation in oocytes and the cellular basis for female meiotic errors. *Hum. Reprod. Update* 24, 135–161. doi: 10.1093/humupd/dmx035

Grøndahl, M. L., Andersen, Y. C., Bogstad, J., Nielsen, F. C., Meinertz, H., and Borup, R. (2010). Gene expression profiles of single human mature oocytes in relation to age. *Hum. Reprod.* 25, 957–968. doi: 10.1093/humrep/deq014

Gruhn, J. R., Zielinska, A. P., Shukla, V., Blanshard, R., Capalbo, A., Cimadomo, D., et al. (2019). Chromosome errors in human eggs shape natural fertility over reproductive life span. *Science* 365, 1466–1469. doi: 10.1126/science.aav7321

Grune, T., Jung, T., Merker, K., and Davies, K. J. (2004). Decreased proteolysis caused by protein aggregates, inclusion bodies, plaques, lipofuscin, ceroid, and 'aggresomes' during oxidative stress, aging, and disease. *Int. J. Biochem. Cell Biol.* 36, 2519–2530. doi: 10.1016/j.biocel.2004.04.020

Gupta, S., Fedor, J., Biedenharn, K., and Agarwal, A. (2013). Lifestyle factors and oxidative stress in female infertility: is there an evidence base to support the linkage? *Expert Rev. Obstet. Gynecol.* 8, 607–624. doi: 10.1586/17474108.2013.849418

Guyonnet, B., Egge, N., and Cornwall, G. A. (2014). Functional amyloids in the mouse sperm acrosome. *Mol. Cell. Biol.* 34, 2624–2634. doi: 10.1128/mcb.00073-14

Hadizadeh Esfahani, A., Sverchkova, A., Saez-Rodriguez, J., Schuppert, A. A., and Brehme, M. (2018). A systematic atlas of chaperome deregulation topologies across the human cancer landscape. *PLoS Comput. Biol.* 14:e1005890. doi: 10.1371/journal.pcbi.1005890

Hale, A. N., Ledbetter, D. J., Gawriluk, T. R., and Rucker, E. B. III (2013). Autophagy: regulation and role in development. *Autophagy* 9, 951–972. doi: 10.4161/auto.24273

Hamada, A. J., Esteves, S. C., and Agarwal, A. (2013). A comprehensive review of genetics and genetic testing in azoospermia. *Clinics (Sao Paulo)* 68(Suppl. 1), 39–60. doi: 10.6061/clinics/2013(sup01)06

Hamatani, T., Falco, G., Carter, M. G., Akutsu, H., Stagg, C. A., Sharov, A. A., et al. (2004). Age-associated alteration of gene expression patterns in mouse oocytes. *Hum. Mol. Genet.* 13, 2263–2278. doi: 10.1093/hmg/ddh241

Hartl, F. U., and Hayer-Hartl, M. (2002). Molecular chaperones in the cytosol: from nascent chain to folded protein. *Science* 295, 1852–1858. doi: 10.1126/science.1068408

Hartl, F. U., Bracher, A., and Hayer-Hartl, M. (2011). Molecular chaperones in protein folding and proteostasis. *Nature* 475, 324–332. doi: 10.1038/nature10317

Hassold, T., Maylor-Hagen, H., Wood, A., Gruhn, J., Hoffmann, E., Broman, K. W., et al. (2020). Failure to recombine is a common feature of human oogenesis. *Am. J. Hum. Genet.* 108, 16–24. doi: 10.1016/j.ajhg.2020.11.010

Hermo, L., Pelletier, R. M., Cyr, D. G., and Smith, C. E. (2010). Surfing the wave, cycle, life history, and genes/proteins expressed by testicular germ cells. Part 2: changes in spermatid organelles associated with development of spermatozoa. *Microsc. Res. Tech.* 73, 279–319.

Herskovits, A. Z., and Guarente, L. (2013). Sirtuin deacetylases in neurodegenerative diseases of aging. *Cell Res.* 23, 746–758. doi: 10.1038/cr.2013.70

Hewetson, A., Do, H. Q., Myers, C., Muthusubramanian, A., Sutton, R. B., Wylie, B. J., et al. (2017). Functional amyloids in reproduction. *Biomolecules* 7:46. doi: 10.3390/biom7030046

Hipp, M. S., Kasturi, P., and Hartl, F. U. (2019). The proteostasis network and its decline in ageing. *Nat. Rev. Mol. Cell Biol.* 20, 421–435. doi: 10.1038/s41580-019-0101-y

Ho, Y. S., Gargano, M., Cao, J., Bronson, R. T., Heimler, I., and Hutz, R. J. (1998). Reduced fertility in female mice lacking copper-zinc superoxide dismutase. *J. Biol. Chem.* 273, 7765–7769. doi: 10.1074/jbc.273.13.7765

Hohn, A., Konig, J., and Grune, T. (2013). Protein oxidation in aging and the removal of oxidized proteins. *J. Proteomics* 92, 132–159. doi: 10.1016/j.jprot.2013.01.004

Hohn, T. J., and Grune, T. (2014). The proteasome and the degradation of oxidized proteins: part III-Redox regulation of the proteasomal system. *Redox Biol.* 2, 388–394. doi: 10.1016/j.redox.2013.12.029

Hoter, A., El-Sabban, M. E., and Naim, H. Y. (2018). The HSP90 family: structure, regulation, function, and implications in health and disease. *Int. J. Mol. Sci.* 19:2560. doi: 10.3390/ijms19092560

Hou, C. C., and Yang, W. X. (2013). New insights to the ubiquitin-proteasome pathway (UPP) mechanism during spermatogenesis. *Mol. Biol. Rep.* 40, 3213–3230. doi: 10.1007/s11033-012-2397-y

Hou, Y., Fan, W., Yan, L., Li, R., Lian, Y., Huang, J., et al. (2013). Genome analyses of single human oocytes. *Cell* 155, 1492–1506. doi: 10.1016/j.cell.2013.11.040

Houck, S. A., Singh, S., and Cyr, D. M. (2012). Cellular responses to misfolded proteins and protein aggregates. *Methods Mol. Biol.* 832, 455–461. doi: 10.1007/978-1-61779-474-2_32

Huarte, J., Stutz, A., O'Connell, M. L., Gubler, P., Belin, D., Darrow, A. L., et al. (1992). Transient translational silencing by reversible mRNA deadenylation. *Cell* 69, 1021–1030. doi: 10.1016/0092-8674(92)90620-r

Humphreys, D. T., Carver, J. A., Easterbrook-Smith, S. B., and Wilson, M. R. (1999). Clusterin has chaperone-like activity similar to that of small heat shock proteins. *J. Biol. Chem.* 274, 6875–6881. doi: 10.1074/jbc.274.11.6875

Iconomou, M., and Saunders, D. N. (2016). Systematic approaches to identify E3 ligase substrates. *Biochem. J.* 473, 4083–4101. doi: 10.1042/bcj20160719

Iljas, J. D., and Homer, H. A. (2020). Sirt3 is dispensable for oocyte quality and female fertility in lean and obese mice. *FASEB J.* 34, 6641–6653. doi: 10.1096/fj.202000153r

Iljas, J. D., Wei, Z., and Homer, H. A. (2020). Sirt1 sustains female fertility by slowing age-related decline in oocyte quality required for post-fertilization embryo development. *Aging Cell* 19:e13204.

Im, E., and Chung, K. C. (2016). Precise assembly and regulation of 26S proteasome and correlation between proteasome dysfunction and neurodegenerative diseases. *BMB Rep.* 49, 459–473. doi: 10.5483/bmbrep.2016.49.9.094

Imai, S. I., and Guarente, L. (2016). It takes two to tango: NAD(+) and sirtuins in aging/longevity control. *NPJ Aging Mech. Dis.* 2:16017.

Ishii, T., Sakurai, T., Usami, H., and Uchida, K. (2005). Oxidative modification of proteasome: identification of an oxidation-sensitive subunit in 26 S proteasome. *Biochemistry* 44, 13893–13901. doi: 10.1021/bi051336u

Janssen, A. F. J., Katrukha, E. A., van Straaten, W., Verlhac, P., Reggiori, F., and Kapitein, L. C. (2018). Probing aggrephagy using chemically-induced protein aggregates. *Nat. Commun.* 9:4245.

Jaronen, M., Goldsteins, G., and Koistinaho, J. (2014). ER stress and unfolded protein response in amyotrophic lateral sclerosis-a controversial role of protein disulphide isomerase. *Front. Cell. Neurosci.* 8:402. doi: 10.3389/fncel.2014.00402

Jeon, G. S., Nakamura, T., Lee, J. S., Choi, W. J., Ahn, S. W., Lee, K. W., et al. (2014). Potential effect of S-nitrosylated protein disulfide isomerase on mutant SOD1 aggregation and neuronal cell death in amyotrophic lateral sclerosis. *Mol. Neurobiol.* 49, 796–807. doi: 10.1007/s12035-013-8562-z

Jung, T., Hohn, A., and Grune, T. (2014). The proteasome and the degradation of oxidized proteins: Part II - protein oxidation and proteasomal degradation. *Redox Biol.* 2, 99–104. doi: 10.1016/j.redox.2013.12.008

Kagan, B. L., Jang, H., Capone, R., Teran Arce, F., Ramachandran, S., Lal, R., et al. (2012). Antimicrobial properties of amyloid peptides. *Mol. Pharm.* 9, 708–717. doi: 10.1021/mp200419b

Kaganovich, D., Kopito, R., and Frydman, J. (2008). Misfolded proteins partition between two distinct quality control compartments. *Nature* 454, 1088–1095. doi: 10.1038/nature07195

Karna, K. K., Shin, Y. S., Choi, B. R., Kim, H. K., and Park, J. K. (2019). The role of endoplasmic reticulum stress response in male reproductive physiology and pathology: a review. *World J. Mens Health* 37, 484–494. doi: 10.5534/wjmh.190038

Kawaguchi, Y., Kovacs, J. J., McLaurin, A., Vance, J. M., Ito, A., and Yao, T. P. (2003). The deacetylase HDAC6 regulates aggresome formation and cell viability in response to misfolded protein stress. *Cell* 115, 727–738. doi: 10.1016/s0092-8674(03)00939-5

Keller, J. N., Hanni, K. B., and Markesbery, W. R. (2000). Possible involvement of proteasome inhibition in aging: implications for oxidative stress. *Mech. Ageing Dev.* 113, 61–70. doi: 10.1016/s0047-6374(99)00101-3

Khodakarami, A., Saez, I., Mels, J., and Vilchez, D. (2015). Mediation of organismal aging and somatic proteostasis by the germline. *Front. Mol. Biosci.* 2:3. doi: 10.3389/fmolb.2015.00003

Khor, B., Bredemeyer, A. L., Huang, C. Y., Turnbull, I. R., Evans, R., Maggi, L. B. Jr., et al. (2006). Proteasome activator PA200 is required for normal spermatogenesis. *Mol. Cell. Biol.* 26, 2999–3007. doi: 10.1128/mcb.26.8.2999-3007.2006

Kidd, S. A., Eskenazi, B., and Wyrobek, A. J. (2001). Effects of male age on semen quality and fertility: a review of the literature. *Fertil. Steril.* 75, 237–248. doi: 10.1016/s0015-0282(00)01679-4

Kikuchi, K., Naito, K., Noguchi, J., Kaneko, H., and Tojo, H. (2002). Maturation/M-phase promoting factor regulates aging of porcine oocytes matured in vitro. *Cloning Stem Cells* 4, 211–222. doi: 10.1089/15362300260339494

Kim, D., Nguyen, M. D., Dobbin, M. M., Fischer, A., Sananbenesi, F., Rodgers, J. T., et al. (2007). SIRT1 deacetylase protects against neurodegeneration in models for Alzheimer's disease and amyotrophic lateral sclerosis. *EMBO J.* 26, 3169–3179. doi: 10.1038/sj.emboj.7601758

Kim, H. J., and Taylor, J. P. (2017). Lost in transportation: nucleocytoplasmic transport defects in ALS and other neurodegenerative diseases. *Neuron* 96, 285–297. doi: 10.1016/j.neuron.2017.07.029

Kim, Y. E., Hipp, M. S., Bracher, A., Hayer-Hartl, M., and Hartl, F. U. (2013). Molecular chaperone functions in protein folding and proteostasis. *Annu. Rev. Biochem.* 82, 323–355. doi: 10.1146/annurev-biochem-060208-092442

King, G. A., Goodman, J. S., Schick, J. G., Chetlapalli, K., Jorgens, D. M., McDonald, K. L., et al. (2019). Meiotic cellular rejuvenation is coupled to nuclear remodeling in budding yeast. *Elife* 8:e47156.

Kirkwood, T. B. (1977). Evolution of ageing. *Nature* 270, 301–304.

Klaips, C. L., Jayaraj, G. G., and Hartl, F. U. (2018). Pathways of cellular proteostasis in aging and disease. *J. Cell Biol.* 217, 51–63. doi: 10.1083/jcb.201709072

Klimek, C., Kathage, B., Wordehoff, J., and Hohfeld, J. (2017). BAG3-mediated proteostasis at a glance. *J. Cell Sci.* 130, 2781–2788. doi: 10.1242/jcs.203679

Klucken, J., Shin, Y., Masliah, E., Hyman, B. T., and McLean, P. J. (2004). Hsp70 reduces alpha-synuclein aggregation and toxicity. *J. Biol. Chem.* 279, 25497–25502. doi: 10.1074/jbc.m400255200

Kocaturk, N. M., and Gozuacik, D. (2018). Crosstalk between mammalian autophagy and the ubiquitin-proteasome system. *Front. Cell Dev. Biol.* 6:128. doi: 10.3389/fcell.2018.00128

Koga, H., Kaushik, S., and Cuervo, A. M. (2011). Protein homeostasis and aging: the importance of exquisite quality control. *Ageing Res. Rev.* 10, 205–215. doi: 10.1016/j.arr.2010.02.001

Kohan, L., Tabiee, O., and Sepahi, N. (2019). HSPA1L and HSPA1B gene polymorphisms and haplotypes are associated with idiopathic male infertility in Iranian population. *Eur. J. Obstet. Gynecol. Reprod. Biol.* 240, 57–61. doi: 10.1016/j.ejogrb.2019.06.014

Kulkarni, P., and Uversky, V. N. (2018). Intrinsically disordered proteins: the dark horse of the dark proteome. *Proteomics* 18:e1800061.

Kumar, V., Rahman, S., Choudhry, H., Zamzami, M. A., Sarwar Jamal, M., Islam, A., et al. (2017). Computing disease-linked SOD1 mutations: deciphering protein stability and patient-phenotype relations. *Sci. Rep.* 7:4678.

Kwok, C. T., Morris, A. G., Frampton, J., Smith, B., Shaw, C. E., and de Belleroche, J. (2013). Association studies indicate that protein disulfide isomerase is a risk factor in amyotrophic lateral sclerosis. *Free Radic. Biol. Med.* 58, 81–86. doi: 10.1016/j.freeradbiomed.2013.01.001

Labbadia, J., and Morimoto, R. I. (2015). The biology of proteostasis in aging and disease. *Annu. Rev. Biochem.* 84, 435–464.

Labbadia, J., Novoselov, S. S., Bett, J. S., Weiss, A., Paganetti, P., Bates, G. P., et al. (2012). Suppression of protein aggregation by chaperone modification of high molecular weight complexes. *Brain* 135, 1180–1196. doi: 10.1093/brain/aws022

Lamark, T., and Johansen, T. (2012). Aggrephagy: selective disposal of protein aggregates by macroautophagy. *Int. J. Cell Biol.* 2012:736905.

Lange, A., Mills, R. E., Lange, C. J., Stewart, M., Devine, S. E., and Corbett, A. H. (2007). Classical nuclear localization signals: definition, function, and interaction with importin alpha. *J. Biol. Chem.* 282, 5101–5105. doi: 10.1074/jbc.r600026200

Le Masson, F., Razak, Z., Kaigo, M., Audouard, C., Charry, C., Cooke, H., et al. (2011). Identification of heat shock factor 1 molecular and cellular targets during embryonic and adult female meiosis. *Mol. Cell. Biol.* 31, 3410–3423. doi: 10.1128/mcb.05237-11

Lee, J. (2020). Is age-related increase of chromosome segregation errors in mammalian oocytes caused by cohesin deterioration? *Reprod. Med. Biol.* 19, 32–41. doi: 10.1002/rmb2.12299

Lee, J., Giordano, S., and Zhang, J. (2012). Autophagy, mitochondria and oxidative stress: cross-talk and redox signalling. *Biochem. J.* 441, 523–540. doi: 10.1042/bj20111451

Lee, Y. H., and Ramamoorthy, A. (2018). Semen-derived amyloidogenic peptides-Key players of HIV infection. *Protein Sci.* 27, 1151–1165. doi: 10.1002/pro.3395

Lefievre, L., Chen, Y., Conner, S. J., Scott, J. L., Publicover, S. J., Ford, W. C., et al. (2007). Human spermatozoa contain multiple targets for protein S-nitrosylation: an alternative mechanism of the modulation of sperm function by nitric oxide? *Proteomics* 7, 3066–3084. doi: 10.1002/pmic.200700254

Li, J., Huan, Y., Xie, B., Wang, J., Zhao, Y., Jiao, M., et al. (2014). Identification and characterization of an oocyte factor required for sperm decondensation in pig. *Reproduction* 148, 367–375. doi: 10.1530/rep-14-0264

Li, K., Xue, Y., Chen, A., Jiang, Y., Xie, H., Shi, Q., et al. (2014). Heat shock protein 90 has roles in intracellular calcium homeostasis, protein tyrosine phosphorylation regulation, and progesterone-responsive sperm function in human sperm. *PLoS One* 9:e115841. doi: 10.1371/journal.pone.0115841

Lilienbaum, A. (2013). Relationship between the proteasomal system and autophagy. *Int. J. Biochem. Mol. Biol.* 4, 1–26.

Lin, X., Dai, Y., Tong, X., Xu, W., Huang, Q., Jin, X., et al. (2020). Excessive oxidative stress in cumulus granulosa cells induced cell senescence contributes to endometriosis-associated infertility. *Redox Biol.* 30:101431. doi: 10.1016/j.redox.2020.101431

Liu, C., Song, Z., Wang, L., Yu, H., Liu, W., Shang, Y., et al. (2017). Sirt1 regulates acrosome biogenesis by modulating autophagic flux during spermiogenesis in mice. *Development* 144, 441–451. doi: 10.1242/dev.147074

Liu, Q., Smith, M. A., Avila, J., DeBernardis, J., Kansal, M., Takeda, A., et al. (2005). Alzheimer-specific epitopes of tau represent lipid peroxidation-induced conformations. *Free Radic. Biol. Med.* 38, 746–754. doi: 10.1016/j.freeradbiomed.2004.11.005

Lord, T., Nixon, B., Jones, K. T., and Aitken, R. J. (2013). Melatonin prevents postovulatory oocyte aging in the mouse and extends the window for optimal fertilization in vitro. *Biol. Reprod.* 88:67.

Loveland, K. L., Major, A. T., Butler, R., Young, J. C., Jans, D. A., and Miyamoto, Y. (2015). Putting things in place for fertilization: discovering roles for importin proteins in cell fate and spermatogenesis. *Asian J. Androl.* 17, 537–544. doi: 10.4103/1008-682x.154310

Maciel, V. L., Tamashiro, L. K., and Bertolla, R. P. (2019). Post-translational modifications of seminal proteins and their importance in male fertility potential. *Expert Rev. Proteomics* 16, 941–950. doi: 10.1080/14789450.2019.1693895

Maklakov, A. A., and Immler, S. (2016). The expensive germline and the evolution of ageing. *Curr. Biol.* 26, R577–R586.

Mancias, J. D., and Kimmelman, A. C. (2016). Mechanisms of selective autophagy in normal physiology and cancer. *J. Mol. Biol.* 428, 1659–1680. doi: 10.1016/j.jmb.2016.02.027

Markesbery, W. R., and Lovell, M. A. (1998). Four-hydroxynonenal, a product of lipid peroxidation, is increased in the brain in Alzheimer's disease. *Neurobiol. Aging* 19, 33–36. doi: 10.1016/s0197-4580(98)00009-8

Martin, J. H., Aitken, R. J., Bromfield, E. G., and Nixon, B. (2019). DNA damage and repair in the female germline: contributions to ART. *Hum. Reprod. Update* 25, 180–201. doi: 10.1093/humupd/dmy040

Martinez-Heredia, J., de Mateo, S., Vidal-Taboada, J. M., Ballesca, J. L., and Oliva, R. (2008). Identification of proteomic differences in asthenozoospermic sperm samples. *Hum. Reprod.* 23, 783–791. doi: 10.1093/humrep/den024

Mason, D. A., Fleming, R. J., and Goldfarb, D. S. (2002). Drosophila melanogaster importin alpha1 and alpha3 can replace importin alpha2 during spermatogenesis but not oogenesis. *Genetics* 161, 157–170.

Mattoo, R. U., and Goloubinoff, P. (2014). Molecular chaperones are nanomachines that catalytically unfold misfolded and alternatively folded proteins. *Cell. Mol. Life Sci.* 71, 3311–3325. doi: 10.1007/s00018-014-1627-y

Maury, C. P. (2009). The emerging concept of functional amyloid. *J. Intern. Med.* 265, 329–334. doi: 10.1111/j.1365-2796.2008.02068.x

Mayer, M. P., and Bukau, B. (2005). Hsp70 chaperones: cellular functions and molecular mechanism. *Cell. Mol. Life Sci.* 62, 670–684. doi: 10.1007/s00018-004-4464-6

McBurney, M. W., Yang, X., Jardine, K., Hixon, M., Boekelheide, K., Webb, J. R., et al. (2003). The mammalian SIR2alpha protein has a role in embryogenesis and gametogenesis. *Mol. Cell. Biol.* 23, 38–54. doi: 10.1128/mcb.23.1.38-54.2003

McLaughlin, E. A., and McIver, S. C. (2009). Awakening the oocyte: controlling primordial follicle development. *Reproduction* 137, 1–11. doi: 10.1530/rep-08-0118

McReynolds, S., Dzieciatkowska, M., McCallie, B. R., Mitchell, S. D., Stevens, J., Hansen, K., et al. (2012). Impact of maternal aging on the molecular signature of human cumulus cells. *Fertil. Steril.* 98, 1574–1580.e5.

Meneau, F., Dupre, A., Jessus, C., and Daldello, E. M. (2020). Translational control of *Xenopus* oocyte meiosis: toward the genomic era. *Cells* 9:1502. doi: 10.3390/cells9061502

Merksamer, P. I., Liu, Y., He, W., Hirschey, M. D., Chen, D., and Verdin, E. (2013). The sirtuins, oxidative stress and aging: an emerging link. *Aging (Albany NY)* 5, 144–150. doi: 10.18632/aging.100544

Miao, Y., Cui, Z., Gao, Q., Rui, R., and Xiong, B. (2020). Nicotinamide mononucleotide supplementation reverses the declining quality of maternally aged oocytes. *Cell Rep.* 32:107987. doi: 10.1016/j.celrep.2020.107987

Mihajlović, A. I., and FitzHarris, G. (2018). Segregating chromosomes in the mammalian oocyte. *Curr. Biol.* 28, R895–R907.

Mihalas, B. P., Bromfield, E. G., Sutherland, J. M., De Iuliis, G. N., McLaughlin, E. A., Aitken, R. J., et al. (2018). Oxidative damage in naturally aged mouse oocytes is exacerbated by dysregulation of proteasomal activity. *J. Biol. Chem.* 293, 18944–18964. doi: 10.1074/jbc.ra118.005751

Mihalas, B. P., De Iuliis, G. N., Redgrove, K. A., McLaughlin, E. A., and Nixon, B. (2017). The lipid peroxidation product 4-hydroxynonenal contributes to oxidative stress-mediated deterioration of the ageing oocyte. *Sci. Rep.* 7:6247.

Mihalas, B. P., Western, P. S., Loveland, K. L., McLaughlin, E. A., and Holt, J. E. (2015). Changing expression and subcellular distribution of karyopherins during murine oogenesis. *Reproduction* 150, 485–496. doi: 10.1530/rep-14-0585

Mikwar, M., MacFarlane, A. J., and Marchetti, F. (2020). Mechanisms of oocyte aneuploidy associated with advanced maternal age. *Mutat. Res.* 785:108320. doi: 10.1016/j.mrrev.2020.108320

Min, S. W., Sohn, P. D., Cho, S. H., Swanson, R. A., and Gan, L. (2013). Sirtuins in neurodegenerative diseases: an update on potential mechanisms. *Front. Aging Neurosci.* 5:53. doi: 10.3389/fnagi.2013.00053

Monslow, J., Govindaraju, P., and Pure, E. (2015). Hyaluronan – a functional and structural sweet spot in the tissue microenvironment. *Front. Immunol.* 6:231. doi: 10.3389/fimmu.2015.00231

Morales, P., Kong, M., Pizarro, E., and Pasten, C. (2003). Participation of the sperm proteasome in human fertilization. *Hum. Reprod.* 18, 1010–1017. doi: 10.1093/humrep/deg111

Munch, J., Rucker, E., Standker, L., Adermann, K., Goffinet, C., Schindler, M., et al. (2007). Semen-derived amyloid fibrils drastically enhance HIV infection. *Cell* 131, 1059–1071. doi: 10.1016/j.cell.2007.10.014

Nagaoka, S. I., Hassold, T. J., and Hunt, P. A. (2012). Human aneuploidy: mechanisms and new insights into an age-old problem. *Nat. Rev. Genet.* 13, 493–504. doi: 10.1038/nrg3245

Niforou, K., Cheimonidou, C., and Trougakos, I. P. (2014). Molecular chaperones and proteostasis regulation during redox imbalance. *Redox Biol.* 2, 323–332. doi: 10.1016/j.redox.2014.01.017

Nixon, B., and Bromfield, E. G. (2018). "Sperm capacitation," in *Encyclopedia of Reproduction*, 2nd Edn, ed. M. K. Skinner (Oxford: Academic Press), 272–278. doi: 10.1016/b978-0-12-801238-3.64464-1

Nixon, B., Bernstein, I. R., Cafe, S. L., Delehedde, M., Sergeant, N., Anderson, A. L., et al. (2019a). A kinase anchor protein 4 is vulnerable to oxidative adduction in male germ cells. *Front. Cell Dev. Biol.* 7:319. doi: 10.3389/fcell.2019.00319

Nixon, B., De Iuliis, G. N., Hart, H. M., Zhou, W., Mathe, A., Bernstein, I. R., et al. (2019b). Proteomic profiling of mouse epididymosomes reveals their contributions to post-testicular sperm maturation. *Mol. Cell. Proteomics* 18(Suppl. 1), S91–S108.

Noda, Y., Ota, K., Shirasawa, T., and Shimizu, T. (2012). Copper/zinc superoxide dismutase insufficiency impairs progesterone secretion and fertility in female mice. *Biol. Reprod.* 86, 1–8.

Ottolini, C. S., Newnham, L., Capalbo, A., Natesan, S. A., Joshi, H. A., Cimadomo, D., et al. (2015). Genome-wide maps of recombination and chromosome segregation in human oocytes and embryos show selection for maternal recombination rates. *Nat. Genet.* 47, 727–735. doi: 10.1038/ng.3306

Outeiro, T. F., Kontopoulos, E., Altmann, S. M., Kufareva, I., Strathearn, K. E., Amore, A. M., et al. (2007). Sirtuin 2 inhibitors rescue alpha-synuclein-mediated toxicity in models of Parkinson's disease. *Science* 317, 516–519. doi: 10.1126/science.1143780

Pan, H., Ma, P., Zhu, W., and Schultz, R. M. (2008). Age-associated increase in aneuploidy and changes in gene expression in mouse eggs. *Dev. Biol.* 316, 397–407. doi: 10.1016/j.ydbio.2008.01.048

Pankiv, S., Clausen, T. H., Lamark, T., Brech, A., Bruun, J. A., Outzen, H., et al. (2007). p62/SQSTM1 binds directly to Atg8/LC3 to facilitate degradation of ubiquitinated protein aggregates by autophagy. *J. Biol. Chem.* 282, 24131–24145. doi: 10.1074/jbc.m702824200

Pasten, C., Morales, P., and Kong, M. (2005). Role of the sperm proteasome during fertilization and gamete interaction in the mouse. *Mol. Reprod. Dev.* 71, 209–219. doi: 10.1002/mrd.20280

Pemberton, L. F., and Paschal, B. M. (2005). Mechanisms of receptor-mediated nuclear import and nuclear export. *Traffic* 6, 187–198. doi: 10.1111/j.1600-0854.2005.00270.x

Perez, V. I., Buffenstein, R., Masamsetti, V., Leonard, S., Salmon, A. B., Mele, J., et al. (2009). Protein stability and resistance to oxidative stress are determinants of longevity in the longest-living rodent, the naked mole-rat. *Proc. Natl. Acad. Sci. U.S.A.* 106, 3059–3064. doi: 10.1073/pnas.0809620106

Peters, A. E., Mihalas, B. P., Bromfield, E. G., Roman, S. D., Nixon, B., and Sutherland, J. M. (2020). Autophagy in female fertility: a role in oxidative stress and aging. *Antioxid. Redox Signal.* 32, 550–568. doi: 10.1089/ars.2019.7986

Petersen, C. G., Mauri, A. L., Vagnini, L. D., Renzi, A., Petersen, B., Mattila, M., et al. (2018). The effects of male age on sperm DNA damage: an evaluation of 2,178 semen samples. *JBRA Assist. Reprod.* 22, 323–330.

Petersen, D. R., and Doorn, J. A. (2004). Reactions of 4-hydroxynonenal with proteins and cellular targets. *Free Radic. Biol. Med.* 37, 937–945. doi: 10.1016/j.freeradbiomed.2004.06.012

Pham, C. L., Kwan, A. H., and Sunde, M. (2014). Functional amyloid: widespread in nature, diverse in purpose. *Essays Biochem.* 56, 207–219. doi: 10.1042/bse0560207

Pickering, A. M., Koop, A. L., Teoh, C. Y., Ermak, G., Grune, T., and Davies, K. J. (2010). The immunoproteasome, the 20S proteasome and the PA28alphabeta proteasome regulator are oxidative-stress-adaptive proteolytic complexes. *Biochem. J.* 432, 585–594. doi: 10.1042/bj20100878

Pickford, F., Masliah, E., Britschgi, M., Lucin, K., Narasimhan, R., Jaeger, P. A., et al. (2008). The autophagy-related protein beclin 1 shows reduced expression in early Alzheimer disease and regulates amyloid beta accumulation in mice. *J. Clin. Invest.* 118, 2190–2199.

Pino, V., Sanz, A., Valdes, N., Crosby, J., and Mackenna, A. (2020). The effects of aging on semen parameters and sperm DNA fragmentation. *JBRA Assist. Reprod.* 24, 82–86.

Pohl, E., Hoffken, V., Schlatt, S., Kliesch, S., Gromoll, J., and Wistuba, J. (2019). Ageing in men with normal spermatogenesis alters spermatogonial dynamics and nuclear morphology in Sertoli cells. *Andrology* 7, 827–839. doi: 10.1111/andr.12665

Popa-Wagner, A., Mitran, S., Sivanesan, S., Chang, E., and Buga, A. M. (2013). ROS and brain diseases: the good, the bad, and the ugly. *Oxid. Med. Cell. Longev.* 2013:963520.

Powers, E. T., Morimoto, R. I., Dillin, A., Kelly, J. W., and Balch, W. E. (2009). Biological and chemical approaches to diseases of proteostasis deficiency. *Annu. Rev. Biochem.* 78, 959–991. doi: 10.1146/annurev.biochem.052308.114844

Qi, L., Zhang, X. D., Wu, J. C., Lin, F., Wang, J., DiFiglia, M., et al. (2012). The role of chaperone-mediated autophagy in huntingtin degradation. *PLoS One* 7:e46834. doi: 10.1371/journal.pone.0046834

Qian, M. X., Pang, Y., Liu, C. H., Haratake, K., Du, B. Y., Ji, D. Y., et al. (2013). Acetylation-mediated proteasomal degradation of core histones during DNA repair and spermatogenesis. *Cell* 153, 1012–1024. doi: 10.1016/j.cell.2013.04.032

Radwan, M., Wood, R. J., Sui, X., and Hatters, D. M. (2017). When proteostasis goes bad: protein aggregation in the cell. *IUBMB Life* 69, 49–54. doi: 10.1002/iub.1597

Rambaran, R. N., and Serpell, L. C. (2008). Amyloid fibrils: abnormal protein assembly. *Prion* 2, 112–117. doi: 10.4161/pri.2.3.7488

Ramesh, N., and Pandey, U. B. (2017). Autophagy dysregulation in ALS: when protein aggregates get out of hand. *Front. Mol. Neurosci.* 10:263. doi: 10.3389/fnmol.2017.00263

Rato, L., Alves, M. G., Silva, B. M., Sousa, M., and Oliveira, P. F. (2016). Sirtuins: novel players in male reproductive health. *Curr. Med. Chem.* 23, 1084–1099. doi: 10.2174/0929867323666160229114248

Redgrove, K. A., Anderson, A. L., Dun, M. D., McLaughlin, E. A., O'Bryan, M. K., Aitken, R. J., et al. (2011). Involvement of multimeric protein complexes in mediating the capacitation-dependent binding of human spermatozoa to homologous zonae pellucidae. *Dev. Biol.* 356, 460–474. doi: 10.1016/j.ydbio.2011.05.674

Redgrove, K. A., Nixon, B., Baker, M. A., Hetherington, L., Baker, G., Liu, D. Y., et al. (2012). The molecular chaperone HSPA2 plays a key role in regulating the expression of sperm surface receptors that mediate sperm-egg recognition. *PLoS One* 7:e50851. doi: 10.1371/journal.pone.0050851

Reed, T. T., Pierce, W. M., Markesbery, W. R., and Butterfield, D. A. (2009). Proteomic identification of HNE-bound proteins in early Alzheimer disease: insights into the role of lipid peroxidation in the progression of AD. *Brain Res.* 1274, 66–76. doi: 10.1016/j.brainres.2009.04.009

Ren, R. J., Dammer, E. B., Wang, G., Seyfried, N. T., and Levey, A. I. (2014). Proteomics of protein post-translational modifications implicated in neurodegeneration. *Transl. Neurodegener.* 3:23. doi: 10.1186/2047-9158-3-23

Ren, X., Chen, X., Wang, Z., and Wang, D. (2017). Is transcription in sperm stationary or dynamic? *J. Reprod. Dev.* 63, 439–443. doi: 10.1262/jrd.2016-093

Reveillaud, I., Phillips, J., Duyf, B., Hilliker, A., Kongpachith, A., and Fleming, J. E. (1994). Phenotypic rescue by a bovine transgene in a Cu/Zn superoxide dismutase-null mutant of *Drosophila melanogaster*. *Mol. Cell. Biol.* 14, 1302–1307. doi: 10.1128/mcb.14.2.1302

Revenkova, E., Herrmann, K., Adelfalk, C., and Jessberger, R. (2010). Oocyte cohesin expression restricted to predictyate stages provides full fertility and prevents aneuploidy. *Curr. Biol.* 20, 1529–1533. doi: 10.1016/j.cub.2010.08.024

Roan, N. R., Muller, J. A., Liu, H., Chu, S., Arnold, F., Sturzel, C. M., et al. (2011). Peptides released by physiological cleavage of semen coagulum proteins form amyloids that enhance HIV infection. *Cell Host Microbe* 10, 541–550. doi: 10.1016/j.chom.2011.10.010

Roan, N. R., Sandi-Monroy, N., Kohgadai, N., Usmani, S. M., Hamil, K. G., Neidleman, J., et al. (2017). Semen amyloids participate in spermatozoa selection and clearance. *Elife* 6:e24888.

Rocker, A., Roan, N. R., Yadav, J. K., Fandrich, M., and Munch, J. (2018). Structure, function and antagonism of semen amyloids. *Chem. Commun. (Camb)* 54, 7557–7569. doi: 10.1039/c8cc01491d

Rodriguez, A., Briley, S. M., Patton, B. K., Tripurani, S. K., Rajapakshe, K., Coarfa, C., et al. (2019). Loss of the E2 SUMO-conjugating enzyme Ube2i in oocytes during ovarian folliculogenesis causes infertility in mice. *Development* 146:dev176701. doi: 10.1242/dev.176701

Rodriguez, K. A., Edrey, Y. H., Osmulski, P., Gaczynska, M., and Buffenstein, R. (2012). Altered composition of liver proteasome assemblies contributes to enhanced proteasome activity in the exceptionally long-lived naked mole-rat. *PLoS One* 7:e35890. doi: 10.1371/journal.pone.0035890

Rogon, C., Ulbricht, A., Hesse, M., Alberti, S., Vijayaraj, P., Best, D., et al. (2014). HSP70-binding protein HSPBP1 regulates chaperone expression at a posttranslational level and is essential for spermatogenesis. *Mol. Biol. Cell* 25, 2260–2271. doi: 10.1091/mbc.e14-02-0742

Rosales, O., Opazo, C., Diaz, E. S., Villegas, J. V., Sanchez, R., and Morales, P. (2011). Proteasome activity and proteasome subunit transcripts in human spermatozoa separated by a discontinuous Percoll gradient. *Andrologia* 43, 106–113. doi: 10.1111/j.1439-0272.2009.01029.x

Rowley, J. E., Amargant, F., Zhou, L. T., Galligos, A., Simon, L. E., Pritchard, M. T., et al. (2020). Low molecular weight hyaluronan induces an inflammatory response in ovarian stromal cells and impairs gamete development in vitro. *Int. J. Mol. Sci.* 21:1036. doi: 10.3390/ijms21031036

Rujano, M. A., Bosveld, F., Salomons, F. A., Dijk, F., van Waarde, M. A., van der Want, J. J., et al. (2006). Polarised asymmetric inheritance of accumulated protein damage in higher eukaryotes. *PLoS Biol* 4:e417. doi: 10.1371/journal.pbio.0040417

Russell, D. L., Gilchrist, R. B., Brown, H. M., and Thompson, J. G. (2016). Bidirectional communication between cumulus cells and the oocyte: old hands and new players? *Theriogenology* 86, 62–68. doi: 10.1016/j.theriogenology.2016.04.019

Ryu, K. Y., Sinnar, S. A., Reinholdt, L. G., Vaccari, S., Hall, S., Garcia, M. A., et al. (2008). The mouse polyubiquitin gene Ubb is essential for meiotic progression. *Mol. Cell. Biol.* 28, 1136–1146. doi: 10.1128/mcb.01566-07

Şahin, A., Held, A., Bredvik, K., Major, P., Achilli, T. M., Kerson, A. G., et al. (2017). Human SOD1 ALS mutations in a *Drosophila* knock-in model cause severe phenotypes and reveal dosage-sensitive gain- and loss-of-function components. *Genetics* 205, 707–723. doi: 10.1534/genetics.116.190850

Samanta, L., Sharma, R., Cui, Z., and Agarwal, A. (2019). Proteomic analysis reveals dysregulated cell signaling in ejaculated spermatozoa from infertile men. *Asian J. Androl.* 21, 121–130. doi: 10.4103/aja.aja_56_18

Samanta, L., Swain, N., Ayaz, A., Venugopal, V., and Agarwal, A. (2016). Post-translational modifications in sperm proteome: the chemistry of proteome diversifications in the pathophysiology of male factor infertility. *Biochim. Biophys. Acta* 1860, 1450–1465. doi: 10.1016/j.bbagen.2016.04.001

Sambataro, F., and Pennuto, M. (2017). Post-translational modifications and protein quality control in motor neuron and polyglutamine diseases. *Front. Mol. Neurosci.* 10:82. doi: 10.3389/fnmol.2017.00082

Santos, A. L., and Lindner, A. B. (2017). Protein posttranslational modifications: roles in aging and age-related disease. *Oxid. Med. Cell. Longev.* 2017:5716409.

Sarraf, S., Shah, H., Kanfer, G., Ward, M., and Youle, R. (2019). Selective autophagic clearance of protein aggregates is mediated by the autophagy receptor, TAX1BP1. *bioRxiv* [Preprint] doi: 10.1101/558767

Schaur, R. J., Siems, W., Bresgen, N., and Eckl, P. M. (2015). 4-Hydroxy-nonenal-A bioactive lipid peroxidation product. *Biomolecules* 5, 2247–2337. doi: 10.3390/biom5042247

Schwarzer, C., Siatkowski, M., Pfeiffer, M. J., Baeumer, N., Drexler, H. C., Wang, B., et al. (2014). Maternal age effect on mouse oocytes: new biological insight from proteomic analysis. *Reproduction* 148, 55–72. doi: 10.1530/rep-14-0126

Seleem, A. K., El Refaeey, A. A., Shaalan, D., Sherbiny, Y., and Badawy, A. (2014). Superoxide dismutase in polycystic ovary syndrome patients undergoing intracytoplasmic sperm injection. *J. Assist. Reprod. Genet.* 31, 499–504. doi: 10.1007/s10815-014-0190-7

Shamri, R., Young, K. M., and Weller, P. F. (2013). PI3K, ERK, p38 MAPK and integrins regulate CCR3-mediated secretion of mouse and human eosinophil-associated RNases. *Allergy* 68, 880–889. doi: 10.1111/all.12163

Shang, F., and Taylor, A. (2011). Ubiquitin-proteasome pathway and cellular responses to oxidative stress. *Free Radic. Biol. Med.* 51, 5–16. doi: 10.1016/j.freeradbiomed.2011.03.031

Shang, Y., Wang, H., Jia, P., Zhao, H., Liu, C., Liu, W., et al. (2016). Autophagy regulates spermatid differentiation via degradation of PDLIM1. *Autophagy* 12, 1575–1592. doi: 10.1080/15548627.2016.1192750

Shemesh, N., Shai, N., and Ben-Zvi, A. (2013). Germline stem cell arrest inhibits the collapse of somatic proteostasis early in *Caenorhabditis elegans* adulthood. *Aging Cell* 12, 814–822. doi: 10.1111/acel.12110

Shen, K., and Frydman, J. (2013). "The interplay between the chaperonin TRiC and N-terminal region of Huntintin mediates Huntington's disease aggregation and pathogenesis," in *Protein Quality Control in Neurodegenerative Diseases*, eds R. Morimoto and Y. Christen (Berlin: Springer), 126–127.

Shibata, Y., and Morimoto, R. I. (2014). How the nucleus copes with proteotoxic stress. *Curr. Biol.* 24, R463–R474.

Siegel, S. J., Bieschke, J., Powers, E. T., and Kelly, J. W. (2007). The oxidative stress metabolite 4-hydroxynonenal promotes Alzheimer protofibril formation. *Biochemistry* 46, 1503–1510. doi: 10.1021/bi061853s

Silber, S. J., Kato, K., Aoyama, N., Yabuuchi, A., Skaletsky, H., Fan, Y., et al. (2017). Intrinsic fertility of human oocytes. *Fertil. Steril.* 107, 1232–1237. doi: 10.1016/j.fertnstert.2017.03.014

Simoes-Pires, C., Zwick, V., Nurisso, A., Schenker, E., Carrupt, P. A., and Cuendet, M. (2013). HDAC6 as a target for neurodegenerative diseases: what makes it different from the other HDACs? *Mol. Neurodegener.* 8:7. doi: 10.1186/1750-1326-8-7

Skerget, S., Rosenow, M. A., Petritis, K., and Karr, T. L. (2015). Sperm proteome maturation in the mouse epididymis. *PLoS One* 10:e0140650. doi: 10.1371/journal.pone.0140650

Smith, H. L., Li, W., and Cheetham, M. E. (2015). Molecular chaperones and neuronal proteostasis. *Semin. Cell Dev. Biol.* 40, 142–152. doi: 10.1016/j.semcdb.2015.03.003

Song, Z. H., Yu, H. Y., Wang, P., Mao, G. K., Liu, W. X., Li, M. N., et al. (2015). Germ cell-specific Atg7 knockout results in primary ovarian insufficiency in female mice. *Cell Death Dis.* 6:e1589. doi: 10.1038/cddis.2014.559

Stefani, M. (2004). Protein misfolding and aggregation: new examples in medicine and biology of the dark side of the protein world. *Biochim. Biophys. Acta* 1739, 5–25. doi: 10.1016/j.bbadis.2004.08.004

Steuerwald, N. M., Bermudez, M. G., Wells, D., Munne, S., and Cohen, J. (2007). Maternal age-related differential global expression profiles observed in human oocytes. *Reprod. Biomed. Online* 14, 700–708. doi: 10.1016/s1472-6483(10)60671-2

Stringer, J., Groenewegen, E., Liew, S. H., and Hutt, K. J. (2019). Nicotinamide mononucleotide does not protect the ovarian reserve from cancer treatments. *Reproduction* 159, 105–113.

Sun, Y.-C., Wang, Y.-Y., Sun, X.-F., Cheng, S.-F., Li, L., Zhao, Y., et al. (2018). The role of autophagy during murine primordial follicle assembly. *Aging* 10, 197–211. doi: 10.18632/aging.101376

Sutovsky, P., Manandhar, G., McCauley, T. C., Caamano, J. N., Sutovsky, M., Thompson, W. E., et al. (2004). Proteasomal interference prevents zona pellucida penetration and fertilization in mammals. *Biol. Reprod.* 71, 1625–1637. doi: 10.1095/biolreprod.104.032532

Sutovsky, P., Moreno, R., Ramalho-Santos, J., Dominko, T., Thompson, W. E., and Schatten, G. (2001). A putative, ubiquitin-dependent mechanism for the recognition and elimination of defective spermatozoa in the mammalian epididymis. *J. Cell Sci.* 114, 1665–1675.

Tachibana-Konwalski, K., Godwin, J., van der Weyden, L., Champion, L., Kudo, N. R., Adams, D. J., et al. (2010). Rec8-containing cohesin maintains bivalents without turnover during the growing phase of mouse oocytes. *Genes Dev.* 24, 2505–2516. doi: 10.1101/gad.605910

Tagawa, K., Marubuchi, S., Qi, M. L., Enokido, Y., Tamura, T., Inagaki, R., et al. (2007). The induction levels of heat shock protein 70 differentiate the vulnerabilities to mutant huntingtin among neuronal subtypes. *J. Neurosci.* 27, 868–880. doi: 10.1523/jneurosci.4522-06.2007

Takasugi, M., Firsanov, D., Tombline, G., Ning, H., Ablaeva, J., Seluanov, A., et al. (2020). Naked mole-rat very-high-molecular-mass hyaluronan exhibits superior cytoprotective properties. *Nat. Commun.* 11:2376.

Takeuchi, T., Suzuki, M., Fujikake, N., Popiel, H. A., Kikuchi, H., Futaki, S., et al. (2015). Intercellular chaperone transmission via exosomes contributes to maintenance of protein homeostasis at the organismal level. *Proc. Natl. Acad. Sci. U.S.A.* 112, E2497–E2506.

Tatone, C., Di Emidio, G., Barbonetti, A., Carta, G., Luciano, A. M., Falone, S., et al. (2018). Sirtuins in gamete biology and reproductive physiology: emerging roles and therapeutic potential in female and male infertility. *Hum. Reprod. Update* 24, 267–289. doi: 10.1093/humupd/dmy003

Tatone, C., Di Emidio, G., Vitti, M., Di Carlo, M., Santini, S. Jr., D'Alessandro, A. M., et al. (2015). Sirtuin functions in female fertility: possible role in oxidative stress and aging. *Oxid. Med. Cell. Longev.* 2015:659687.

Theilen, L. H., Fraser, A., Hollingshaus, M. S., Schliep, K. C., Varner, M. W., Smith, K. R., et al. (2016). All-cause and cause-specific mortality after hypertensive disease of pregnancy. *Obstet. Gynecol.* 128, 238–244. doi: 10.1097/aog.0000000000001534

Tingen, C. M., Kiesewetter, S. E., Jozefik, J., Thomas, C., Tagler, D., Shea, L., et al. (2011). A macrophage and theca cell-enriched stromal cell population influences growth and survival of immature murine follicles in vitro. *Reproduction* 141, 809–820. doi: 10.1530/rep-10-0483

Tipler, C. P., Hutchon, S. P., Hendil, K., Tanaka, K., Fishel, S., and Mayer, R. J. (1997). Purification and characterization of 26S proteasomes from human and mouse spermatozoa. *Mol. Hum. Reprod.* 3, 1053–1060. doi: 10.1093/molehr/3.12.1053

Tian, X., Azpurua, J., Hine, C., Vaidya A., Myakishev-Rempel, M., Ablaeva, J., et al. (2013). High-molecular-mass hyaluronan mediates the cancer resistance of the naked mole rat. *Nature* 499, 346–349. doi: 10.1038/nature12234

Titus, S., Li, F., Stobezki, R., Akula, K., Unsal, E., Jeong, K., et al. (2013). Impairment of BRCA1-related DNA double-strand break repair leads to ovarian aging in mice and humans. *Sci. Transl. Med.* 5:172ra121.

Tonoki, A., Kuranaga, E., Tomioka, T., Hamazaki, J., Murata, S., Tanaka, K., et al. (2009). Genetic evidence linking age-dependent attenuation of the 26S proteasome with the aging process. *Mol. Cell. Biol.* 29, 1095–1106. doi: 10.1128/mcb.01227-08

Tremellen, K. (2008). Oxidative stress and male infertility–a clinical perspective. *Hum. Reprod. Update* 14, 243–258. doi: 10.1093/humupd/dmn004

Treweek, T. M., Meehan, S., Ecroyd, H., and Carver, J. A. (2015). Small heat-shock proteins: important players in regulating cellular proteostasis. *Cell. Mol. Life Sci.* 72, 429–451. doi: 10.1007/s00018-014-1754-5

Tsakiri, E. N., Sykiotis, G. P., Papassideri, I. S., Gorgoulis, V. G., Bohmann, D., and Trougakos, I. P. (2013). Differential regulation of proteasome functionality in reproductive vs. somatic tissues of *Drosophila* during aging or oxidative stress. *FASEB J.* 27, 2407–2420. doi: 10.1096/fj.12-221408

Uechi, H., Hamazaki, J., and Murata, S. (2014). Characterization of the testis-specific proteasome subunit alpha4s in mammals. *J. Biol. Chem.* 289, 12365–12374. doi: 10.1074/jbc.m114.558866

Unal, E., Kinde, B., and Amon, A. (2011). Gametogenesis eliminates age-induced cellular damage and resets life span in yeast. *Science* 332, 1554–1557. doi: 10.1126/science.1204349

Van Raamsdonk, J. M., Gibson, W. T., Pearson, J., Murphy, Z., Lu, G., Leavitt, B. R., et al. (2006). Body weight is modulated by levels of full-length huntingtin. *Hum. Mol. Genet.* 15, 1513–1523. doi: 10.1093/hmg/ddl072

Van Raamsdonk, J. M., Murphy, Z., Selva, D. M., Hamidizadeh, R., Pearson, J., Petersen, A., et al. (2007). Testicular degeneration in Huntington disease. *Neurobiol. Dis.* 26, 512–520. doi: 10.1016/j.nbd.2007.01.006

Vilchez, D., Morantte, I., Liu, Z., Douglas, P. M., Merkwirth, C., Rodrigues, A. P., et al. (2012). RPN-6 determines C. elegans longevity under proteotoxic stress conditions. *Nature* 489, 263–268. doi: 10.1038/nature11315

Wacker, J. L., Zareie, M. H., Fong, H., Sarikaya, M., and Muchowski, P. J. (2004). Hsp70 and Hsp40 attenuate formation of spherical and annular polyglutamine oligomers by partitioning monomer. *Nat. Struct. Mol. Biol.* 11, 1215–1222. doi: 10.1038/nsmb860

Wang, H., Wan, H., Li, X., Liu, W., Chen, Q., Wang, Y., et al. (2014). Atg7 is required for acrosome biogenesis during spermatogenesis in mice. *Cell Res.* 24, 852–869. doi: 10.1038/cr.2014.70

Wang, S., Zheng, Y., Li, J., Yu, Y., Zhang, W., Song, M., et al. (2020). Single-cell transcriptomic atlas of primate ovarian aging. *Cell* 180, 585–600.e19.

Wang, T., Gao, H., Li, W., and Liu, C. (2019). Essential role of histone replacement and modifications in male fertility. *Front. Genet.* 10:962. doi: 10.3389/fgene.2019.00962

Westerheide, S. D., Anckar, J., Stevens, S. M. Jr., Sistonen, L., and Morimoto, R. I. (2009). Stress-inducible regulation of heat shock factor 1 by the deacetylase SIRT1. *Science* 323, 1063–1066. doi: 10.1126/science.1165946

Westerheide, S. D., and Morimoto, R. I. (2005). Heat shock response modulators as therapeutic tools for diseases of protein conformation. *J. Biol. Chem.* 280, 33097–33100. doi: 10.1074/jbc.r500010200

Whelly, S., Johnson, S., Powell, J., Borchardt, C., Hastert, M. C., and Cornwall, G. A. (2012). Nonpathological extracellular amyloid is present during normal epididymal sperm maturation. *PLoS One* 7:e36394. doi: 10.1371/journal.pone.0036394

Whelly, S., Muthusubramanian, A., Powell, J., Johnson, S., Hastert, M. C., and Cornwall, G. A. (2016). Cystatin-related epididymal spermatogenic subgroup members are part of an amyloid matrix and associated with extracellular vesicles in the mouse epididymal lumen. *Mol. Hum. Reprod.* 22, 729–744. doi: 10.1093/molehr/gaw049

Whelly, S., Serobian, G., Borchardt, C., Powell, J., Johnson, S., Hakansson, K., et al. (2014). Fertility defects in mice expressing the L68Q variant of human cystatin C: a role for amyloid in male infertility. *J. Biol. Chem.* 289, 7718–7729. doi: 10.1074/jbc.m113.515759

Winship, A. L., Stringer, J. M., Liew, S. H., and Hutt, K. J. (2018). The importance of DNA repair for maintaining oocyte quality in response to anti-cancer treatments, environmental toxins and maternal ageing. *Hum. Reprod. Update* 24, 119–134. doi: 10.1093/humupd/dmy002

Woerner, A. C., Frottin, F., Hornburg, D., Feng, L. R., Meissner, F., Patra, M., et al. (2016). Cytoplasmic protein aggregates interfere with nucleocytoplasmic transport of protein and RNA. *Science* 351, 173–176. doi: 10.1126/science.aad2033

Wu, X., Hu, F., Zeng, J., Han, L., Qiu, D., Wang, H., et al. (2019). NMNAT2-mediated NAD(+) generation is essential for quality control of aged oocytes. *Aging Cell* 18:e12955. doi: 10.1111/acel.12955

Wyatt, A. R., Yerbury, J. J., Ecroyd, H., and Wilson, M. R. (2013). Extracellular chaperones and proteostasis. *Annu. Rev. Biochem.* 82, 295–322. doi: 10.1146/annurev-biochem-072711-163904

Yalcin, G. (2017). Sirtuins and neurodegeneration. *J. Neurol. Neuromed.* 3, 13–20. doi: 10.29245/2572.942x/2017/1.1168

Yamamoto, H., Schoonjans, K., and Auwerx, J. (2007). Sirtuin functions in health and disease. *Mol. Endocrinol.* 21, 1745–1755. doi: 10.1210/me.2007-0079

Yang, F., Wang, W., Cetinbas, M., Sadreyev, R. I., and Blower, M. D. (2020). Genome-wide analysis identifies cis-acting elements regulating mRNA polyadenylation and translation during vertebrate oocyte maturation. *RNA* 26, 324–344. doi: 10.1261/rna.073247.119

Yang, M., Jin, Y., Fan, S., Liang, X., Jia, J., Tan, Z., et al. (2019). Inhibition of neddylation causes meiotic arrest in mouse oocyte. *Cell Cycle* 18, 1254–1267. doi: 10.1080/15384101.2019.1617453

Yatsenko, A. N., and Turek, P. J. (2018). Reproductive genetics and the aging male. *J. Assist. Reprod. Genet.* 35, 933–941. doi: 10.1007/s10815-018-1148-y

Yefimova, M. G., Béré, E., Cantereau-Becq, A., Harnois, T., Meunier, A. C., Messaddeq, N., et al. (2016). Myelinosomes act as natural secretory organelles in Sertoli cells to prevent accumulation of aggregate-prone mutant Huntingtin and CFTR. *Hum. Mol. Genet.* 25, 4170–4185. doi: 10.1093/hmg/ddw251

Yefimova, M. G., Buschiazzo, A., Burel, A., Lavault, M. T., Pimentel, C., Jouve, G., et al. (2019). Autophagy is increased in cryptorchid testis resulting in abnormal spermatozoa. *Asian J. Androl.* 21, 570–576. doi: 10.4103/aja.aja_12_19

Yefimova, M., Bere, E., Neyroud, A. S., Jegou, B., Bourmeyster, N., and Ravel, C. (2020). Myelinosome-like vesicles in human seminal plasma: a cryo-electron microscopy study. *Cryobiology* 92, 15–20.

Yerbury, J. J., Gower, D., Vanags, L., Roberts, K., Lee, J. A., and Ecroyd, H. (2013). The small heat shock proteins alphaB-crystallin and Hsp27 suppress SOD1 aggregation in vitro. *Cell Stress Chaperones* 18, 251–257. doi: 10.1007/s12192-012-0371-1

Yeung, C. H., Sonnenberg-Riethmacher, E., and Cooper, T. G. (1998). Receptor tyrosine kinase c-ros knockout mice as a model for the study of epididymal regulation of sperm function. *J. Reprod. Fertil. Suppl.* 53, 137–147.

Yoritaka, A., Hattori, N., Uchida, K., Tanaka, M., Stadtman, E. R., and Mizuno, Y. (1996). Immunohistochemical detection of 4-hydroxynonenal protein adducts in Parkinson disease. *Proc. Natl. Acad. Sci. U.S.A.* 93, 2696–2701. doi: 10.1073/pnas.93.7.2696

Yuan, Y., Wheeler, M. B., and Krisher, R. L. (2012). Disrupted redox homeostasis and aberrant redox gene expression in porcine oocytes contribute to decreased developmental competence. *Biol. Reprod.* 87:78.

Zahn-Zabal, M., Michel, P. A., Gateau, A., Nikitin, F., Schaeffer, M., Audot, E., et al. (2020). The neXtProt knowledgebase in 2020: data, tools and usability improvements. *Nucleic Acids Res.* 48, D328–D334. doi: 10.1093/nar/gkz995

Zhang, S., Eitan, E., Wu, T. Y., and Mattson, M. P. (2018). Intercellular transfer of pathogenic alpha-synuclein by extracellular vesicles is induced by the lipid peroxidation product 4-hydroxynonenal. *Neurobiol. Aging* 61, 52–65. doi: 10.1016/j.neurobiolaging.2017.09.016

Zhang, T., Du, X., Zhao, L., He, M., Lin, L., Guo, C., et al. (2019). SIRT1 facilitates primordial follicle recruitment independent of deacetylase activity through directly modulating Akt1 and mTOR transcription. *FASEB J.* 33, 14703–14716. doi: 10.1096/fj.201900782r

Zhao, S., Lin, L., Kan, G., Xu, C., Tang, Q., Yu, C., et al. (2014). High autophagy in the naked mole rat may play a significant role in maintaining good health. *Cell. Physiol. Biochem.* 33, 321–332. doi: 10.1159/000356672

Zheng, N., and Shabek, N. (2017). Ubiquitin ligases: structure, function, and regulation. *Annu. Rev. Biochem.* 86, 129–157. doi: 10.1146/annurev-biochem-060815-014922

Zhou, W., De Iuliis, G. N., Dun, M. D., and Nixon, B. (2018). Characteristics of the epididymal luminal environment responsible for sperm maturation and storage. *Front. Endocrinol. (Lausanne)* 9:59. doi: 10.3389/fendo.2018.00059

Zhu, D., Dix, D. J., and Eddy, E. M. (1997). HSP70-2 is required for CDC2 kinase activity in meiosis I of mouse spermatocytes. *Development* 124, 3007–3014.

Zielinska, A. P., Bellou, E., Sharma, N., Frombach, A. S., Seres, K. B., Gruhn, J. R., et al. (2019). Meiotic kinetochores fragment into multiple lobes upon Cohesin loss in aging eggs. *Curr. Bio.* 29, 3749–3765.e7. doi: 10.1016/j.cub.2019.09.006

Zigo, M., Manaskova-Postlerova, P., Jonakova, V., Kerns, K., and Sutovsky, P. (2019). Compartmentalization of the proteasome-interacting proteins during sperm capacitation. *Sci. Rep.* 9:12583.

Zimmerman, S. W., Manandhar, G., Yi, Y. J., Gupta, S. K., Sutovsky, M., Odhiambo, J. F., et al. (2011). Sperm proteasomes degrade sperm receptor on the egg zona pellucida during mammalian fertilization. *PLoS One* 6:e17256. doi: 10.1371/journal.pone.0017256

Conflict of Interest: The authors declare that the research was conducted in the absence of any commercial or financial relationships that could be construed as a potential conflict of interest.

frontiers in Cell and Developmental Biology

MINI REVIEW
published: 19 May 2021
doi: 10.3389/fcell.2021.680471

Understanding Reproductive Aging in Wildlife to Improve Animal Conservation and Human Reproductive Health

Pierre Comizzoli[1]* *and Mary Ann Ottinger*[2]

[1] *Smithsonian Conservation Biology Institute, National Zoological Park, Washington, DC, United States,* [2] *Department of Biology and Biochemistry, University of Houston, Houston, TX, United States*

Similar to humans and laboratory animals, reproductive aging is observed in wild species-from small invertebrates to large mammals. Aging issues are also prevalent in rare and endangered species under human care as their life expectancy is longer than in the wild. The objectives of this review are to (1) present conserved as well as distinctive traits of reproductive aging in different wild animal species (2) highlight the value of comparative studies to address aging issues in conservation breeding as well as in human reproductive medicine, and (3) suggest next steps forward in that research area. From social insects to mega-vertebrates, reproductive aging studies as well as observations in the wild or in breeding centers often remain at the physiological or organismal scale (senescence) rather than at the germ cell level. Overall, multiple traits are conserved across very different species (depletion of the ovarian reserve or no decline in testicular functions), but unique features also exist (endless reproductive life or unaltered quality of germ cells). There is a broad consensus about the need to fill research gaps because many cellular and molecular processes during reproductive aging remain undescribed. More research in male aging is particularly needed across all species. Furthermore, studies on reproductive aging of target species in their natural habitat (sentinel species) are crucial to define more accurate reproductive indicators relevant to other species, including humans, sharing the same environment. Wild species can significantly contribute to our general knowledge of a crucial phenomenon and provide new approaches to extend the reproductive lifespan.

Keywords: wildlife, reproduction, fertility, aging, animal models

OPEN ACCESS

Edited by:
Vittorio Sebastiano, Stanford University, United States

Reviewed by:
Giulia Ricci, University of Campania Luigi Vanvitelli, Italy
Mikael Molin, Chalmers University of Technology, Sweden

***Correspondence:**
Pierre Comizzoli
comizzolip@si.edu

Specialty section:
This article was submitted to Cellular Biochemistry, a section of the journal Frontiers in Cell and Developmental Biology

Received: *14 March 2021*
Accepted: *27 April 2021*
Published: *19 May 2021*

Citation:
Comizzoli P and Ottinger MA (2021) Understanding Reproductive Aging in Wildlife to Improve Animal Conservation and Human Reproductive Health. Front. Cell Dev. Biol. 9:680471. doi: 10.3389/fcell.2021.680471

INTRODUCTION

Reproductive aging is a process involving a combination of multiple intrinsic and extrinsic factors affecting the whole organism and more directly the reproductive organs as well as the quality of germ cells. Reproductive aging in human and laboratory animals has been studied for decades at the physiological, hormonal, cellular, and molecular levels. As gamete quality declines more rapidly

in women than in men, reproductive aging leads to infertility, increased miscarriages, and birth defects (vom Saal et al., 1994; Sharma et al., 2015; Duncan and Gerton, 2018; Marshall and Rivera, 2018; Quesada-Candela et al., 2021). The menopause is the last menstrual cycle in women and other primates, which may or may not be ovulatory. Fertility is typically lost before menopause (vom Saal et al., 1994; Wu et al., 2010). While there is a depletion of ovarian reserve, there is no comparable loss in testicular germ cells. Research in aging has identified key evolutionarily conserved lifespan-mediating genetic pathways (Partridge, 2010). However, mechanisms mediating reproductive senescence and somatic lifespan in males and females remain limited. Aging of the reproductive organs and functions can occur before aging of the entire organism; this can lead to several months or years of post-reproductive life in different species (Ellison and Ottinger, 2014). On the other hand, in addition to the natural aging of the organism, environmental factors (such as, endocrine disruptors, nutrition, or stress) can impact and even accelerate reproductive aging (Ottinger, 2010).

Comparative studies in multiple animal models have been essential to improve our understanding of aging mechanisms and to develop mitigation strategies. Invertebrate and vertebrate models, including worms, birds, and mammals have provided organisms for the study of reproductive aging (Packer et al., 1998; Tatar, 2010; Jones et al., 2014). Interestingly, some processes of reproductive aging are common among species (Ottinger, 2010). For instance, germline aging observed in *Caenorhabditis elegans and Drosophila melanogaster* has conserved properties in the process of mammalian ovarian aging (Tatar, 2010). Recent studies of the mouse epigenome (i.e., global and imprinted DNA methylation, histone modifications, and epigenetic modifiers) have demonstrated its implication in physiological aging of gametes and embryos (Marshall and Rivera, 2018). In addition, maternal age impacts uterine adaptability to pregnancy and reproductive success in laboratory mice (Woods et al., 2017).

In livestock species, similar to humans, decreasing levels of anti-Mullerian hormone (AMH) during aging are associated with declining reproductive performance. This can be used as a predictor of fertility longevity in cattle; however, it still remains largely unexplored in sheep and other farm species (Mossa et al., 2017). Domestic horses can also be considered as good model for reproductive aging processes because mechanisms have been well described in mares and stallions (Turner, 2019; Carnevale et al., 2020).

In laboratory and domestic animal models, some aspects of reproductive aging have received more attention in females than males (especially about hormone levels and germ cell production). For instance, aging in the drosophila model still remains understudied in males. However, recent reports have shown that, not only sperm, but also seminal fluid are both qualitatively and quantitatively affected by age with each component making distinct contributions to declining reproductive performance in older males (Sepil et al., 2020). Studies conducted in Japanese quail (*Coturnix japonica*) males demonstrated that similar to mammals, plasma androgen levels decline gradually, being accompanied by a loss of reproductive behavior (Ottinger, 2010). Interestingly, testosterone treatment can restore reproduction in aging male quail while it is not effective in primates (Ottinger, 2010).

In addition to existing animal models, there is a need for more comparative studies on other species with different sizes, anatomies, physiologies, and life expectancies to improve our understanding of reproductive aging. The huge diversity in anatomy and reproductive physiology observed in wildlife therefore is an untapped resource for aging research (Comizzoli et al., 2018; Comizzoli and Holt, 2019). There are striking differences in reproductive aging going from semelparity (rapid senescence and death after a first breeding season like in salmonids or marsupial mouse, *Antechinus sp.*) to negligible reproductive senescence (naked mole rats, *Heterocephalus glaber*) (Edrey et al., 2011). Even though common species within a given family can often serve as models for the wild counterparts, reproductive traits are sometimes not related to taxonomy, even for closely related species (Cohen, 2018). This is why we need to keep adding many different species to our datasets. Studies in wild species (in their natural habitats or in conservation breeding centers) are invaluable because we can learn about unique adaptations especially in long-lived species, which will not only improve conservation efforts, but also provide new comparative models for other domestic species, and importantly for humans.

The objectives of this review are to (1) present conserved as well as distinctive traits of reproductive aging in different wild animal species (2) highlight the value of comparative studies to address aging issues in conservation breeding as well as in human reproductive medicine, and (3) suggest next steps forward in research.

LESSONS FROM REPRODUCTIVE AGING IN WILD MAMMALIAN SPECIES

The study of reproductive senescence in free-ranging populations is invaluable as it allows to better understand fundamental aspects, such as mate choice, sperm competition, or environmental impact. Furthermore, short- and long-lived wild species exhibit unique characteristics that inform our understanding of aging processes. An overview of the impact of aging on reproductive traits (including some observed in humans) in selected wild mammalian species (from rodents to non-human primates) is presented in **Table 1**. First, it is clear that there is still a research gap to be filled in order to have a better understanding of reproductive aging across mammalian species. However, many existing reports already highlight striking commonalities and differences between species when looking at reproductive traits known to be also affected by aging in humans. The following examples illustrate the diversity among wild mammalian species.

In carnivores like the European badger (*Meles meles*), there is strong evidence for a gradual decline in sex-steroid levels with age in both sexes, which is even followed by over 2 years of post-reproductive life (Sugianto et al., 2020). Interestingly, this hormonal decline is not observed in aging female cheetahs

TABLE 1 | Impact of aging on different reproductive traits (including some observed in humans) and occurrence of post-reproductive lifespan in selected wild mammalian species.

	Lagomorphs and rodents	Artiodactyls	elephants	Marine mammals	Carnivores	Primates
Impact of aging on:						
Hormonal levels (decline in males and females)	None or little data	None or little data	Multiple reports in females	None or little data	Reports in multiple species in females	Reports in multiple species in females
Folliculogenesis (finite number of oocytes in the ovaries)	Reports in multiple species	Reports in multiple species	None or little data	Reports in whales	Reports in multiple species	Reports in multiple species
Success of birth and lactation (decline)	None or little data	None or little data	None or little data	Reports in dolphins	None or little data	None or little data
Male fertility (decline in sperm production and secondary sexual traits)	None or little data	Reports in multiple species	None or little data	None or little data	Reports in red wolf and ferrets	Reports in multiple species
Post-reproductive lifespan in the wild	Reports in multiple species	None or little data	Multiple reports in females	Reports in toothed whales	None or little data	Reports in multiple species

Shading indicates multiple data reports available (darker color) and moderate amount of available data (lighter color).

(*Acinonyx jubatus*) after the age of 9, which is even older than the average life expectancy (Crosier et al., 2011).

Surprisingly, aging red deer (*Cervus elaphus*) stags show a faster decline in annual breeding success than females that went through successive gestations and lactations (Nussey et al., 2009; Bender and Piasecke, 2019). In wild red wolves (*Canis rufus*), reproductive aging in males also is observed while there is no evidence for reproductive aging in wild female wolves (Sparkman et al., 2017).

In bighorn sheep (*Ovis canadensis*), there is no consequence of early life reproduction; however, for a given number of offspring, females that weaned more sons than daughters experience earlier senescence (Douhard et al., 2020). Offspring sex ratio could help explain among-individual variation in senescence rates, perhaps in other species, including humans.

Reproductive senescence in female non-human primates involves the depletion of the ovarian reserves similar to humans (Walker et al., 2009). However, in wild chimpanzees (*Pan troglodytes*), females with high number of years spent gestating and lactating during their reproductive lives have a delayed ovulatory attrition (Atsalis and Videan, 2009). Studies in wild baboons (*Papio* sp.) also suggested that reproductive senescence occurs later in females than males (Altmann et al., 2010).

Advanced maternal age also affects the capacity to provision and rear surviving offspring. In wild populations of bottlenose dolphins (*Tursiops aduncus*), calf survival decreases with maternal age because of less maternal investment (Karniski et al., 2018).

Long-lived species such as elephants, whales and primates exhibit extended post-fertile survival compared to species with shorter lifespans. In wild African elephants (*Loxondonta africana*), although reproduction does not entirely cease until the age of 65 year old, females have a relatively long post-reproductive life (>15 years; Lee et al., 2016). Interestingly, presence of mothers and grandmothers in the group improves daughter's reproduction (Lee et al., 2016). Note that post-reproductive life also is reported in a few species of toothed whales (Ellis et al., 2018); however, this is an uncommon trait in mammalian species compared to humans (Ellison and Ottinger, 2014).

There is no apparent decline in fertility with age in very few mammalian species, such as the tundra vole (*Microtus oeconomus*) (Cohen, 2018) or the famous female naked mole rat (*Heterocephalus glaber*) (Edrey et al., 2011; Place et al., 2021).

Lastly, in terms of extrinsic factors influencing reproductive aging, the environment plays a non-negligible role. Interestingly, in the Eurasian beaver (*Castor fiber*), earlier breeding opportunities lead to earlier senescence through resource-dependent mechanisms (Campbell et al., 2017). This clearly shows that reproductive lifespan is determined by

external factors, including resource availability, in addition to reproductive strategies.

Overall, there are considerable variations among species because the correlation between age and fertility is not linear (Jones et al., 2014). While some species can be used as models for closely related species, there are often exceptions confirming the rule. In humans, reproduction mainly occurs at younger adult ages. Although more spread over the lifespan, it is similar in species like killer whales (*Orcinus orca*), chimpanzees (*Pan troglodytes*), and chamois (*Rupicapra rupicapra*). Notably, some species rather show an increase in fertility as they age (tundra voles, *Microtus oeconomus*) (Jones et al., 2014). As seen above, some patterns of reproductive aging are distinct in human compared to primates. Reproductive senescence in midlife, although apparent in natural-fertility, natural-mortality populations of humans, is generally absent in other primates (Alberts et al., 2013). Lastly, aging in females is more prevalent than in males that have continuous spermatogenesis at advanced ages in many species.

LESSONS FROM REPRODUCTIVE AGING IN WILD NON-MAMMALIAN SPECIES

An overview of the knowledge about the impact of aging on reproductive traits (including some observed in humans) in selected wild non-mammalian species (from corals to birds) is presented in **Table 2**. As observed in mammalian species, there is sometimes no relation between taxonomy and reproductive aging observations. Overall, many knowledge gaps have to be filled regarding the impact of aging on hormonal levels, number of oocytes in the ovaries, male aging (primary and secondary traits), and post-reproductive lifespan (Ellison and Ottinger, 2014). Nevertheless, current reports in non-mammalian species are highly informative and may contribute to our overall understanding of reproductive aging.

While it is not so common in mammalian species, the absence of fertility decline with aging is reported in many different non-mammalian species from corals to birds (Nisbet et al., 1999; Bythell et al., 2018; Cohen, 2018; **Table 2**). Species having a sustained fertility can be very diverse like different species of fresh water mussels (Haag and Staton, 2003), tardigrades (Tsujimoto et al., 2016), queens in social insects like ants and bees (Heinze and Schrempf, 2008), fish (Greenland sharks, *Somniosus microcephalus*), reptiles (freshwater crocodile, *Crocodylus johnsoni*), and some birds (Southern fulmars, *Fulmarus glacialoides*; or Alpine swift, *Tachymarptis melba*) (Cohen, 2018).

As seen above in some wild mammals, insects like field crickets (*Gryllus campestris*) investing more in early reproduction may senesce faster and die younger (Rodríguez-Muñoz et al., 2019). In wild blue-throated warblers (*Setophaga caerulescens*) older males tend to have longer sperm cells, which may be advantageous in post-copulatory sexual selection (Cramer et al., 2020). While male aging is reported in some bird species (Lemaître and Gaillard, 2017), changes in sperm morphology with age are not observed in other birds, though they have been observed in insects and fishes (Cramer et al., 2020).

Post-reproductive lifespan does not appear to be common in non-mammalian species with only few reports in fish (herrings, *Clupea harengus*) (Benoît et al., 2020) or birds (Bali mynahs, *Leucopsar rothschildi*) (Jones et al., 2014).

LESSONS FROM REPRODUCTIVE AGING IN CONSERVATION BREEDING (*EX SITU*)

Zoo animal populations represent an ideal model to study reproductive aging process since lifespan is frequently longer than in the wild, so repeated observations under controlled conditions are possible. Reproductive aging also represents a major issue in conservation breeding, especially for genetically valuable individuals that are too often not reproducing (Hermes et al., 2004; Crosier et al., 2020).

Research on naked mole rat (*Heterocephalus glaber*) colonies has generated intriguing data. Unusually large ovarian reserve in naked-mole rat provides one mechanism to account for this species' protracted fertility. However, whether germ cell nests in adult ovaries contribute to the long reproductive lifespan remains to be determined (Place et al., 2021).

In terms of male aging, the black-footed ferret (*Mustela nigripes*), has revealed that even modest aging decreases sperm production and libido while abnormal sperm number increases (Wolf et al., 2000). This is one of the few examples of rapid reproductive aging in males. In contrast, recent studies in binturong (*Arctictis binturong*) show that males of advanced ages still produce good quality semen (Zainuddin et al., 2021).

Prolonged exposure to endogenous sex steroids and long stretches of non-reproductive periods correlate with early reproductive aging and pathologies in females. For instance, this is observed in nulliparous females in Asian or African elephants (*Elephas maximus*, *Loxodonta africana*) and cheetahs (*Acinonyx jubatus*) (Hermes et al., 2004; Ludwig et al., 2019). As reported in humans and domestic animals as well as in species in the wild (see above), early pregnancy may provide natural protective mechanisms against premature reproductive senescence. Prolonged non-reproductive periods during long-term maintenance of female rhinoceroses (African and Asian species) and elephants in captivity, are associated with an asymmetric reproductive aging process and subsequent development of genital pathology (leiomyoma) as well as premature senescence (Hermes et al., 2004).

Importantly, issues mentioned above can potentially be overcome by species-specific Assisted Reproductive Technologies to ensure early breeding and fertility extension. Furthermore, the extent of the reproductive life in females can be documented opportunistically when the reproductive age limit is not known (which is the case in most species). A good illustration is the recent birth of a giant panda (*Ailuropoda melanoleuca*) cub by artificial insemination with frozen-thawed semen in one of the oldest females in captivity (Comizzoli, 2020). While artificial

TABLE 2 | Impact of aging on different reproductive traits (including some observed in humans) and occurrence of post-reproductive lifespan in selected wild non-mammalian species.

	Corals	Mollusks	Tardigrades	Insects	Fish	Reptiles	Birds
No (or minimal) decline in fertility with age in males and females	Multiple reports	Reports in freshwater mussels	Multiple reports	Reports in social insects	Reports in multiple species	Reports in multiple species	Reports in multiple species
Impact of aging on:							
Hormonal levels (decline in males and females)	Not relevant	Not relevant	Not relevant	None or little data	None or little data	Unlikely	Reports in multiple species
Folliculogenesis (finite number of oocytes in the ovaries)	No data	No data	No data	Reports in drosophila	None or little data	Unlikely	None or little data
Male aging (decline in sperm production and secondary sexual traits)	No data	No data	No data	Reports in drosophila	None or little data	Unlikely	Reports in multiple species
Post-reproductive lifespan	Unlikely	Unlikely	Unlikely	Unlikely	Reports in multiple species	Unlikely	Reports in multiple species

Shading indicates multiple data reports available (darker color) and moderate amount of available data (lighter color).

insemination was primarily used for management purpose, it ended up provided new data about reproductive aging limit in that species.

As in livestock species and humans, recent studies on cheetahs demonstrate that the age-associated decline in AMH is variable but needs to be taken into consideration to optimize fertility management and decisions about assisted reproduction (Place et al., 2017). Interestingly in cheetahs (*Acinonyx jubatus*), uterine environment in aging females is the real issue while oocyte quality is not affected (Crosier et al., 2011). This can be circumvented by performing *in vitro* fertilization (IVF) on oocytes from old donors and transfer the resulting embryos into young recipient females (Crosier et al., 2020).

PENDING QUESTIONS AND NEXT STEPS

As highlighted in **Table 1**, there are many unknowns in wild mammals about the effect of aging on hormonal levels, gamete number and quality, conception, preimplantation embryo, embryo implantation, fetal development, birth, lactation, maternal care, and future fertility of the offspring. Marsupials are not even mentioned in that table because of the absence of data; with the exception being the semelparous marsupial mice (*Antechinus sp.*) that quickly dies after the breeding season (Cohen, 2018). Except for few reports on reproductive aging in rhinoceroses, wild perissodactyls also have not been studied extensively.

As in humans, we need more research in wild species about major cellular processes that are involved in the loss of oocyte quality with advancing age (Quesada-Candela et al., 2021). Except in one study in cheetahs (*Acinonyx jubatus*), nothing is known about the influence of aging in gamete quality (success of fertilization and early embryo development) or uterine environment (Crosier et al., 2011; Ludwig et al., 2019). Even though spermatogenesis or mating behavior does not seem to be impacted by aging in most mammals, there is still a lack of knowledge. There also is no information about reproductive life of offspring born from aging parents (including epigenetic transmissions due to aging).

In non-mammalians species (**Table 2**), even more research gaps to have to be filled regarding the aging effect on hormonal levels, gamete number and quality, conception, embryo development, metamorphosis, hatching, maternal care, fertility of the offspring. For instance, there are no clear data in amphibians (Jones et al., 2014). There also is a need for more investigations in reptiles that seem to be unique because of the apparent lack of decline in fertility (Hoekstra et al., 2019).

Overall, a clear understanding of the evolutionary causes and consequences of reproductive senescence is still lacking and requires new and integrative approaches. Importantly, investigations of the role of environmental conditions on reproductive senescence also are missing. The epigenetics aspect of reproductive aging needs to be expanded to wild species following examples of research in laboratory and domestic models (Ge et al., 2015; Marshall and Rivera, 2018;

Chamani and Keefe, 2019). In addition, the role of miRNAs as marker of reproductive aging (as reported in human ovaries; Battaglia et al., 2020) should also explored.

Although studies in reproductive aging are less advanced in wild species, it can potentially contribute to the general knowledge of a crucial phenomenon and provide new ideas to extend the length and quality of reproductive life in conservation breeding as well as in human reproductive medicine. To fill the current gaps, several options are possible. We first need to better understand the mechanisms behind commonalities and differences observed between species. Findings will then be translatable to other species. There also is the additional value of studying wild species in their natural habitats as sentinel for human populations sharing the same environment. Original aging traits (or non-aging traits) reported above could suggest some research areas or questions in humans, for instance:

- Understanding rapid vs. absence of decline in fertility.
- Exploring sustained oocyte quality in felids (and other species having induced ovulations).
- Examining the influence of parental age on offspring reproductive health (using massive database like the Zoological Management Information System).
- Characterizing the impact of allostatic load (the sum or accumulation of the "burden" due to environment and other stressors like disease, etc. Comizzoli et al., 2019) on reproductive aging.
- Studying more animal models (mammalian and non-mammalian species) known for very long lifespan.
- Using the systems biology approach to better understand and mitigate reproductive aging.

Regarding mitigations and treatments, expanding reproductive life could be achieved through, hormonal treatments (therapies for aging stallions; Turner, 2019), or supplementations during IVF and embryo development for aging donors. Another option would be to increase the ovarian reserve during fetal development (through Bone Morphogenetic Proteins for instance; Regan et al., 2018).

Importantly, lessons learned from human reproductive medicine could also inspire strategies in wildlife. For instance, it would be interesting to explore the impact of aging on reproductive microbiomes (Murphy et al., 2019) since this area is still largely unexplored in wildlife (Comizzoli and Power, 2019). Other examples pertain to the improvement of IVF in aged patients (Gleicher et al., 2016) or the rejuvenation of reproductive tissues through mitochondria biogenesis (Kim et al., 2021).

CONCLUSION

Reproductive aging in wild animal species has been mainly documented at the level of overall reproductive senescence rather than at the germ cell development mechanisms. There is a broad consensus about the need to fill research gaps since a lot of cellular and molecular characterizations behind reproductive aging observations remain to be done. There also is a need for more research in male aging across all species. More studies on reproductive aging of target species in their natural habitat (sentinel species) also are crucial to define more accurate reproductive metrics that are relevant to species, including humans, sharing the same habitats. We must keep building bridges between the ecology of senescence and areas of research in reproductive science. Repeated observations in zoo animals also will remain invaluable sources of information to decipher the mystery of reproductive aging.

In sum, wild species can potentially contribute to the general knowledge of a crucial phenomenon. Comparative models will help to understand the fundamental mechanisms underlying reproductive aging and then develop new approaches to extend the length and the quality of reproductive lifespan, which will ultimately impact overall health.

AUTHOR CONTRIBUTIONS

PC and MA contributed equally to the preparation and the writing of the manuscript. Both authors contributed to the article and approved the submitted version.

REFERENCES

Alberts, S. C., Altmann, J., Brockman, D. K., Cords, M., Fedigan, L. M., Pusey, A., et al. (2013). Reproductive aging patterns in primates reveal that humans are distinct. *Proc. Natl. Acad. Sci. U. S. A.* 110, 13440–13445. doi: 10.1073/pnas.1311857110

Altmann, J., Gesquiere, L., Galbany, J., Onyango, P. O., and Alberts, S. C. (2010). Life history context of reproductive aging in a wild primate model. *Ann. N. Y. Acad. Sci.* 1204, 127–138. doi: 10.1111/j.1749-6632.2010.05531.x

Atsalis, S., and Videan, E. (2009). Reproductive aging in captive and wild common chimpanzees: factors influencing the rate of follicular depletion. *Am. J. Primatol.* 71, 271–282. doi: 10.1002/ajp.20650

Battaglia, R., Musumeci, P., Ragusa, M., Barbagallo, D., Scalia, M., Zimbone, M., et al. (2020). Ovarian aging increases small extracellular vesicle CD81+ release in human follicular fluid and influences miRNA profiles. *Aging* 12, 12324–12341. doi: 10.18632/aging.103441

Bender, L. C., and Piasecke, J. R. (2019). Reproductive senescence in free-ranging North American elk *Cervus elaphus* Cervidae. *Mammalia* 593–600. doi: 10.1515/mammalia-2018-0076

Benoît, H. P., Benhalima, K., and McDermid, J. L. (2020). Histological evidence of reproductive senescence in atlantic herring (Clupea harengus). *Can. J. Zool.* 98, 73–78. doi: 10.1139/cjz-2019-0084

Bythell, J. C., Brown, B. E., and Kirkwood, T. B. L. (2018). Do reef corals age? *Biol. Rev.* 93, 1192–1202. doi: 10.1111/brv.12391

Campbell, R. D., Rosell, F., Newman, C., and Macdonald, D. W. (2017). Age-related changes in somatic condition and reproduction in the Eurasian beaver: resource history influences onset of reproductive senescence. *PLoS One* 12:e0187484. doi: 10.1371/journal.pone.0187484

Carnevale, E. M., Catandi, G. D., and Fresa, K. (2020). Equine Aging and the Oocyte: a Potential Model for Reproductive Aging in Women. *J. Equine Vet. Sci.* 89:103022. doi: 10.1016/j.jevs.2020.103022

Chamani, I. J., and Keefe, D. L. (2019). Epigenetics and Female Reproductive Aging. *Front. Endocrinol.* 10:473. doi: 10.3389/fendo.2019.00473

Cohen, A. A. (2018). Aging across the tree of life: the importance of a comparative perspective for the use of animal models in aging. *Biochim. Biophys. Acta Mol. Basis Dis.* 1864, 2680–2689. doi: 10.1016/j.bbadis.2017.05.028

Comizzoli, P. (2020). Birth of a Giant Panda Cub after Artificial Insemination with Frozen-Thawed Semen: a Powerful Reminder about the Key Role of Biopreservation and Biobanking for Wildlife Conservation. *Biopreserv. Biobank.* 18, 349–350. doi: 10.1089/bio.2020.29076.pjc

Comizzoli, P., Brown, J. L., and Holt, W. V. (2019). Reproductive science as an essential component of conservation biology: new edition. *Adv. Exp. Med. Biol.* 1200, 1–10. doi: 10.1007/978-3-030-23633-5_1

Comizzoli, P., and Holt, W. V. (2019). Breakthroughs and new horizons in reproductive biology of rare and endangered animal species. *Biol. Reprod.* 101, 514–525. doi: 10.1093/biolre/ioz031

Comizzoli, P., Paulson, E. E., and McGinnis, L. K. (2018). The mutual benefits of research in wild animal species and human-assisted reproduction. *J. Assist. Reprod. Genet.* 35, 551–560. doi: 10.1007/s10815-018-1136-2

Comizzoli, P., and Power, M. (2019). Reproductive microbiomes in wild animal species: a new dimension in conservation biology. *Adv. Exp. Med. Biol.* 1200, 225–240. doi: 10.1007/978-3-030-23633-5_8

Cramer, E., Krauss, N., Rowlison, T., and Comizzoli, P. (2020). Sperm morphology and male age in black-throated blue warblers, an ecological model system. *Animals* 10, 1–9. doi: 10.3390/ani10071175

Crosier, A. E., Lamy, J., Bapodra, P., Rapp, S., Maly, M., Junge, R., et al. (2020). First birth of cheetah cubs from in vitro fertilization and embryo transfer. *Animals* 10:1811. doi: 10.3390/ani10101811

Crosier, A. E. A. E., Comizzoli, P., Baker, T., Davidson, A., Munson, L., Howard, J., et al. (2011). Increasing age influences uterine integrity, but not ovarian function or oocyte quality, in the cheetah (Acinonyx jubatus). *Biol. Reprod.* 85, 243–253. doi: 10.1095/biolreprod.110.089417

Douhard, M., Festa-Bianchet, M., and Pelletier, F. (2020). Sons accelerate maternal aging in a wild mammal. *Proc. Natl. Acad. Sci. U. S. A.* 117, 4850–4857. doi: 10.1073/pnas.1914654117

Duncan, F. E., and Gerton, J. L. (2018). Mammalian oogenesis and female reproductive aging. *Aging* 10, 162–163. doi: 10.18632/aging.101381

Edrey, Y. H., Hanes, M., Pinto, M., Mele, J., and Buffenstein, R. (2011). Successful aging and sustained good health in the naked mole rat: a long-lived mammalian model for biogerontology and biomedical research. *ILAR J.* 52, 41–53. doi: 10.1093/ilar.52.1.41

Ellis, S., Franks, D. W., Nattrass, S., Cant, M. A., Bradley, D. L., Giles, D., et al. (2018). Postreproductive lifespans are rare in mammals. *Ecol. Evol.* 8, 2482–2494. doi: 10.1002/ece3.3856

Ellison, P. T., and Ottinger, M. A. (2014). "A comparative perspective on reproductive aging, reproductive cessation, post-reproductive life, and social behavior," in *in Sociality, Hierarchy, Health: Comparative Biodemography: A Collection of Papers*, eds M. Weinstein and M. A. Lane (Washington, DC: The National Academies Press), 315–338. doi: 10.17226/18822

Ge, Z. J., Schatten, H., Zhang, C. L., and Sun, Q. Y. (2015). Oocyte ageing and epigenetics. *Reproduction* 149, R103–R114. doi: 10.1530/REP-14-0242

Gleicher, N., Kushnir, V. A., Albertini, D. F., and Barad, D. H. (2016). Improvements in IVF in women of advanced age. *J. Endocrinol.* 230, F1–F6. doi: 10.1530/JOE-16-0105

Haag, W. R., and Staton, J. L. (2003). Variation in fecundity and other reproductive traits in freshwater mussels. *Freshw. Biol.* 48, 2118–2130. doi: 10.1046/j.1365-2427.2003.01155.x

Heinze, J., and Schrempf, A. (2008). Aging and reproduction in social insects - A mini-review. *Gerontology* 54, 160–167. doi: 10.1159/000122472

Hermes, R., Hildebrandt, T. B., and Göritz, F. (2004). Reproductive problems directly attributable to long-term captivity-asymmetric reproductive aging. *Anim. Reprod. Sci.* 8, 49–60. doi: 10.1016/j.anireprosci.2004.05.015

Hoekstra, L. A., Schwartz, T. S., Sparkman, A. M., Miller, D. A. W., and Bronikowski, A. M. (2019). The untapped potential of reptile biodiversity for understanding how and why animals age. *Funct. Ecol.* 34, 38–54. doi: 10.1111/1365-2435.13450

Jones, O. R., Scheuerlein, A., Salguero-Gómez, R., Camarda, C. G., Schaible, R., Casper, B. B., et al. (2014). Diversity of ageing across the tree of life. *Nature* 505, 169–173. doi: 10.1038/nature12789

Karniski, C., Krzyszczyk, E., and Mann, J. (2018). Senescence impacts reproduction and maternal investment in bottlenose dolphins. *Proc. R. Soc. B Biol. Sci.* 285:20181123. doi: 10.1098/rspb.2018.1123

Kim, T., Vo, C., Tanaka, Y., and Kawamura, K. (2021). Ovarian Rejuvenation Using Autologous Platelet-Rich Plasma. *Endocrines* 2, 15–27. doi: 10.3390/endocrines2010002

Lee, P. C., Fishlock, V., Webber, C. E., and Moss, C. J. (2016). The reproductive advantages of a long life: longevity and senescence in wild female African elephants. *Behav. Ecol. Sociobiol.* 70, 337–345. doi: 10.1007/s00265-015-2051-5

Lemaître, J. F., and Gaillard, J. M. (2017). Reproductive senescence: new perspectives in the wild. *Biol. Rev.* 92, 2182–2199. doi: 10.1111/brv.12328

Ludwig, C., Dehnhard, M., Pribbenow, S., Silinski-mehr, S., Hofer, H., and Wachter, B. (2019). Asymmetric reproductive aging in cheetah (Acinonyx jubatus) females in European zoos. *J. Zoo Aquar. Res.* 7, 87–93.

Marshall, K. L., and Rivera, R. M. (2018). The effects of superovulation and reproductive aging on the epigenome of the oocyte and embryo. *Mol. Reprod. Dev.* 85, 90–105. doi: 10.1002/mrd.22951

Mossa, F., Jimenez-Krassel, F., Scheetz, D., Weber-Nielsen, M., Evans, A. C. O., and Ireland, J. J. (2017). Anti-Müllerian Hormone (AMH) and fertility management in agricultural species. *Reproduction* 154, R1–R11. doi: 10.1530/REP-17-0104

Murphy, K., Keller, M. J., Anastos, K., Sinclair, S., Devlin, J. C., Shi, Q., et al. (2019). Impact of reproductive aging on the vaginal microbiome and soluble immune mediators in women living with and at-risk for HIV infection. *PLoS One* 14:e0216049. doi: 10.1371/journal.pone.0216049

Nisbet, I. C. T., Finch, C. E., Thompson, N., Russek-Cohen, E., Proudman, J. A., and Ottinger, M. A. (1999). Endocrine patterns during aging in the common tern (Sterna hirundo). *Gen. Comp. Endocrinol.* 114, 279–286. doi: 10.1006/gcen.1999.7255

Nussey, D. H., Kruuk, L. E. B., Morris, A., Clements, M. N., Pemberton, J. M., and Clutton-Brock, T. H. (2009). Inter- And intrasexual variation in aging patterns across reproductive traits in a wild red deer population. *Am. Nat.* 174, 342–357. doi: 10.1086/603615

Ottinger, M. A. (2010). Mechanisms of reproductive aging: conserved mechanisms and environmental factors. *Ann. N. Y. Acad. Sci.* 1204, 73–81. doi: 10.1111/j.1749-6632.2010.05653.x

Packer, C., Tatar, M., and Collins, A. (1998). Reproductive cessation in female mammals. *Nature* 392, 807–811. doi: 10.1038/33910

Partridge, L. (2010). The new biology of ageing. *Philos. Trans. R. Soc. Lond. B Biol. Sci.* 365, 147–154. doi: 10.1098/rstb.2009.0222

Place, N. J., Prado, A. M., Faykoo-Martinez, M., Brieño-Enriquez, M. A., Albertini, D. F., and Holmes, M. M. (2021). Germ cell nests in adult ovaries and an unusually large ovarian reserve in the naked mole-rat. *Reproduction* 161, 89–98. doi: 10.1530/REP-20-0304

Place, N. J. N. J., Crosier, A. E. A. E., Comizzoli, P., Nagashima, J. B. J. B., Haefele, H., Schmidt-Küntzel, A., et al. (2017). Age-associated and deslorelin-induced declines in serum anti-Müllerian hormone concentrations in female cheetahs, Acinonyx jubatus. *Gen. Comp. Endocrinol.* 250, 54–57. doi: 10.1016/j.ygcen.2017.06.003

Quesada-Candela, C., Loose, J., Ghazi, A., and Yanowitz, J. L. (2021). Molecular basis of reproductive senescence: insights from model organisms. *J. Assist. Reprod. Genet.* 38, 17–32. doi: 10.1007/s10815-020-01959-4

Regan, S. L. P., Knight, P. G., Yovich, J. L., Leung, Y., Arfuso, F., and Dharmarajan, A. (2018). Involvement of Bone Morphogenetic Proteins (BMP) in the Regulation of Ovarian Function. *Vitam. Horm.* 107, 227–261. doi: 10.1016/bs.vh.2018.01.015

Rodríguez-Muñ;oz, R., Boonekamp, J. J., Liu, X. P., Skicko, I., Fisher, D. N., Hopwood, P., et al. (2019). Testing the effect of early-life reproductive effort on age-related decline in a wild insect. *Evolution* 73, 317–328. doi: 10.1111/evo.13679

Sepil, I., Hopkins, B. R., Dean, R., Bath, E., Friedman, S., Swanson, B., et al. (2020). Male reproductive aging arises via multifaceted mating-dependent sperm and seminal proteome declines, but is postponable in Drosophila. *Proc. Natl. Acad. Sci. U. S. A.* 117, 17094–17103. doi: 10.1073/pnas.2009053117

Sharma, R., Agarwal, A., Rohra, V. K., Assidi, M., Abu-Elmagd, M., and Turki, R. F. (2015). Effects of increased paternal age on sperm quality, reproductive outcome and associated epigenetic risks to offspring. *Reprod. Biol. Endocrinol.* 13:35. doi: 10.1186/s12958-015-0028-x

Sparkman, A. M., Blois, M., Adams, J., Waits, L., Miller, D. A. W., and Murray, D. L. (2017). Evidence for sex-specific reproductive senescence in monogamous cooperatively breeding red wolves. *Behav. Ecol. Sociobiol.* 71:6.

Sugianto, N. A., Newman, C., Macdonald, D. W., and Buesching, C. D. (2020). Reproductive and Somatic Senescence in the European Badger (*Meles meles*): evidence from Lifetime Sex-Steroid Profiles. *Zoology* 141:125803. doi: 10.1016/j.zool.2020.125803

Tatar, M. (2010). Reproductive aging in invertebrate genetic models. *Ann. N. Y. Acad. Sci.* 1204, 149–155. doi: 10.1111/j.1749-6632.2010.05522.x

Tsujimoto, M., Komori, O., and Imura, S. (2016). Effect of lifespan and age on reproductive performance of the tardigrade Acutuncus antarcticus: minimal reproductive senescence. *Hydrobiologia* 772, 93–102. doi: 10.1007/s10750-016-2643-8

Turner, R. M. (2019). Declining testicular function in the aging stallion: management options and future therapies. *Anim. Reprod. Sci.* 207, 171–179. doi: 10.1016/j.anireprosci.2019.06.009

vom Saal, F. S., Finch, C. E., and Nelson, J. F. (1994). Natural History and Mechanisms of Reproductive Aging in Humans, Laboratory Rodents, and Other Selected Vertebrates. *Physiol. Reprod.* 2, 1213–1314.

Walker, M. L., Anderson, D. C., Herndon, J. G., and Walker, L. C. (2009). Ovarian aging in squirrel monkeys (Saimiri sciureus). *Reproduction* 138, 793–799.

Wolf, K. N., Wildt, D. E., Vargas, A., Marinari, P. E., Kreeger, J. S., Ottinger, M. A., et al. (2000). Age-dependent changes in sperm production, semen quality, and testicular volume in the black-footed ferret (*Mustela nigripes*). *Biol. Reprod.* 63, 179–187. doi: 10.1095/biolreprod63.1.179

Woods, L., Perez-Garcia, V., Kieckbusch, J., Wang, X., Demayo, F., Colucci, F., et al. (2017). Decidualisation and placentation defects are a major cause of age-related reproductive decline. *Nat. Commun.* 8:352. doi: 10.1038/s41467-017-00308-x

Wu, J. M., Takahashi, D. L., Ingram, D. K., Mattison, J. A., Roth, G., Ottinger, M. A., et al. (2010). Ovarian reserve tests and their utility in predicting response to controlled ovarian stimulation in rhesus monkeys. *Am. J. Primatol.* 72, 672–680. doi: 10.1002/ajp.20823

Zainuddin, Z. Z., Sipangkui, S., Farqhan Kelana, M., Chee, Y. K., Tarmizi, M. R. M., and Comizzoli, P. (2021). Repeated Evaluations of Testes and Semen Characteristics in Two Binturongs (Arctictis binturong). *Front. Vet. Sci.* 8:658573. doi: 10.3389/fvets.2021.658573

Conflict of Interest: The authors declare that the research was conducted in the absence of any commercial or financial relationships that could be construed as a potential conflict of interest.

frontiers in Cell and Developmental Biology

ORIGINAL RESEARCH
published: 11 June 2021
doi: 10.3389/fcell.2021.690373

Oleic Acid Protects *Caenorhabditis* Mothers From Mating-Induced Death and the Cost of Reproduction

*Leo S. Choi†, Cheng Shi†, Jasmine Ashraf, Salman Sohrabi and Coleen T. Murphy**

Department of Molecular Biology, Lewis-Sigler Institute for Integrative Genomics, Princeton University, Princeton, NJ, United States

Reproduction comes at a cost, including accelerated death. Previous studies of the interconnections between reproduction, lifespan, and fat metabolism in *C. elegans* were predominantly performed in low-reproduction conditions. To understand how increased reproduction affects lifespan and fat metabolism, we examined mated worms; we find that a Δ9 desaturase, FAT-7, is significantly up-regulated. Dietary supplementation of oleic acid (OA), the immediate downstream product of FAT-7 activity, restores fat storage and completely rescues mating-induced death, while other fatty acids cannot. OA-mediated lifespan restoration is also observed in *C. elegans* mutants suffering increased death from short-term mating, and in mated *C. remanei* females, indicating a conserved role of oleic acid in post-mating lifespan regulation. Our results suggest that increased reproduction can be uncoupled from the costs of reproduction from somatic longevity regulation if provided with the limiting lipid, oleic acid.

Keywords: *Caenorhabditis elegans*, longevity, reproduction, oleic acid, mating-induced death, metabolism, cost of reproduction

OPEN ACCESS

Edited by:
Arjumand Ghazi,
University of Pittsburgh, United States

Reviewed by:
Javier Apfeld,
Northeastern University, United States
Eric Greer,
Harvard Medical School, United States

***Correspondence:**
Coleen T. Murphy
ctmurphy@princeton.edu

†These authors share first authorship

Specialty section:
This article was submitted to Cellular Biochemistry, a section of the journal Frontiers in Cell and Developmental Biology

Received: *02 April 2021*
Accepted: *11 May 2021*
Published: *11 June 2021*

Citation:
Choi LS, Shi C, Ashraf J, Sohrabi S and Murphy CT (2021) Oleic Acid Protects Caenorhabditis Mothers From Mating-Induced Death and the Cost of Reproduction. Front. Cell Dev. Biol. 9:690373. doi: 10.3389/fcell.2021.690373

INTRODUCTION

Reproduction is a costly process that depletes energy reserves that may be needed for somatic maintenance and survival (Williams, 1966; Hansen et al., 2013), thus linking reproduction with fat metabolism and lifespan regulation. In many organisms, increased reproduction leads to decreased lifespan, and vice versa (Drori and Folman, 1976; Hansen et al., 2013; Maures et al., 2014; Shi and Murphy, 2014). For example, castrated Korean eunuchs were reported to have lived 15–20 years longer than non-castrated men of similar socio-economic status (Min et al., 2012), while Chinese emperors known for extremely promiscuous behavior lived ∼35% shorter than their counterparts (Shi et al., 2015). *Caenorhabditis elegans* has been established as an outstanding model to investigate these interconnections. In *C. elegans*, removal of germline stem cells leads to a significant increase in lifespan (Hsin and Kenyon, 1999) as well as fat accumulation in the somatic tissues (O'Rourke et al., 2009). By contrast, mating accelerates the proliferation of germline stem cells, increases progeny production, and causes a dramatic fat loss and lifespan decrease (Shi and Murphy, 2014). The genetic analysis of mechanisms underlying the effects of mating or removal of reproductive system on *C. elegans*' fat metabolism and longevity have implicated a network that includes insulin/IGF-1 (Insulin-like Growth Factor-1) signaling, steroid signaling, lipolysis, autophagy, NHR (Nuclear Hormone Receptor) signaling, and fatty acid desaturation (Lapierre and Hansen, 2012). However, the exact relationship between fat loss and lifespan reduction is largely unknown; while fat is

generally regarded as its energy source (Hansen et al., 2013), we do not know whether fat is depleted to enhance reproductive outcome, decreasing somatic maintenance and thus shortening lifespan. It also remains unclear exactly which fatty acids are depleted in mated *C. elegans*, and whether different types of fatty acids contribute to different effects in mating-induced death.

Fatty acids are precursor molecules for all lipid classes, including storage lipids [triacylglycerols (TAGs)], membrane lipids (phospholipids and sphingolipids), and signaling lipids (fatty acyl amides, eicosanoids, and others) (Fahy et al., 2009). Fat metabolism plays a crucial role in regulating the lifespan of germlineless mutants and worms with reduced reproduction. Under nutrient-poor and oxidative stress conditions, omega-3 and omega-6 fatty acids mediate the balance of lipid stores between the soma and germline (Lynn et al., 2015), suggesting a pivotal role of fatty acids in coordinating reproduction and somatic aging.

However, these previous *C. elegans* studies examined fat metabolism in animals with no or very low reproduction: either in germlineless mutants, or under conditions such as nutrient deprivation and oxidative stress where reproduction is very limited, or in self-fertilized hermaphrodites limited by sperm number. It remains unclear how fat metabolism changes when reproduction is *increased*, and whether in this circumstance fatty acids still play a role in coordinating somatic aging and reproduction. To address this question, here we increased worms' reproduction in the most natural way by mating them with males, which typically increases progeny production by 100–200% (Ward and Carrel, 1979; Hodgkin and Barnes, 1991), and examined lifespan, fat levels, transcriptional changes, and supplementation with fatty acids. Remarkably, oleic acid (OA) treatment specifically restores the fat loss induced by mating, and also rescues the lifespan reduction induced by mating, without affecting reproduction. This lifespan rescue by oleic acid supplementation is also pertinent to short-term mating and is conserved in gonochoristic (male and female) *C. remanei* species. Our results suggest that increased reproduction is not associated with inevitable lifespan reduction, and that metabolism of a specific fatty acid is able to uncouple the costs of reproduction from somatic longevity regulation.

RESULTS

Mating Induces a Significant Lifespan Decrease Regardless of the Initial Level of Overall Fat Storage

In *C. elegans,* extended longevity is associated with altered fat metabolism and reduced reproduction, while mating significantly reduces lifespan and induces significant fat loss. However, all previous studies of the links between longevity and fat storage used worms with limited reproduction. While *daf-2* (Insulin signaling) and germlineless *glp-1* mutants are long-lived and store more fat, dietary restricted worms, such as *eat-2*, are long-lived but have less overall fat (Brooks et al., 2009; O'Rourke et al., 2009; Bar et al., 2016), making the relationship between fat levels and longevity less clear. Therefore, examining the relationship between fat metabolism and lifespan regulation in mated worms could provide new insights.

We previously showed that mating shortens lifespan and induces significant fat loss in both wild-type worms and longevity mutants, including those with excessive fat accumulation such as *daf-2* and *glp-1* (**Supplementary Figures 1A-C**, Shi and Murphy, 2014). We wondered whether the lifespan of longevity mutants with reduced fat storage would also be affected by mating. Dietary restriction decreases the overall fat content but robustly extends lifespan across organisms (Walker et al., 2005; Ruetenik and Barrientos, 2015; López-Otín et al., 2016). We tested the lifespan of mated worms under dietary restriction, using two methods of dietary restriction (Greer and Brunet, 2009). *eat-2* mutants have defects in pharyngeal pumping, thus consume less food than wild-type animals (Avery, 1993). Solid plate-based dietary restriction (sDR) takes the colony-forming unit of bacteria into account, using 1×10^{11} cfu/mL for *ad libitum* feeding and 1×10^{8} cfu/mL for dietary restriction (Greer and Brunet, 2009). We found that mating significantly decreases the lifespan of DR worms, just as it does in wild-type animals (**Figure 1A** and **Supplementary Figure 1D**). Similarly, mating also led to a significant fat loss in *eat-2* mutants, as evidenced by Oil Red O staining which stains the major fat stores, TAGs (O'Rourke et al., 2009; **Figure 1B**). Thus, the reduced level of overall fat storage prior to mating in DR-treated animals does not protect the worms from mating-induced death.

Endogenous Oleic Acid Protects Worms Against Mating-Induced Death

To better understand how fat metabolism is altered after mating, we performed transcriptional analysis of mated vs. unmated *glp-1* hermaphrodites (Booth et al., 2020). *glp-1* mothers lack a germline to produce any eggs, which allowed us to disregard transcriptional changes in eggs, and instead focus on somatic changes. The lifespan of *glp-1* animals is decreased by mating and they lose over 40% of their fat stores (Shi and Murphy, 2014). Our transcriptional analysis revealed that genes with significant expressional changes in response to mating were enriched for *organic acid metabolic process* (q-value: $9.8e^{-22}$) and *lipid catabolic process* (q-value: $3e^{-06}$) (**Supplementary Figure 2**), which is consistent with the mating-induced fat loss phenotype. The lipid-regulating gene *fat-7* was significantly induced in mated worms, while *elo-2* was significantly downregulated (**Figure 1C**). Both of the genes are involved in polyunsaturated fatty acids (PUFA) synthesis: *fat-7* encodes a Δ9 desaturase enzyme that converts C18:0 stearic acid into C18:1n-9 oleic acid (OA), while *elo-2* encodes a key enzyme that regulates elongation of C16 and C18 fatty acids (**Figure 1D**). (There are three main types of fatty acids: saturated, monounsaturated, and polyunsaturated, which refers to fat molecules that have none, one, and more than one unsaturated carbon bond, respectively). ELO-2 functions in several different steps of the pathway, and loss of function of *elo-2* causes multiple defects (Kniazeva et al., 2003). Down-regulation of *elo-2* in mated worms likely contributes to mating-induced fat loss. By contrast, the up-regulation of *fat-7,* a fatty acid synthesis

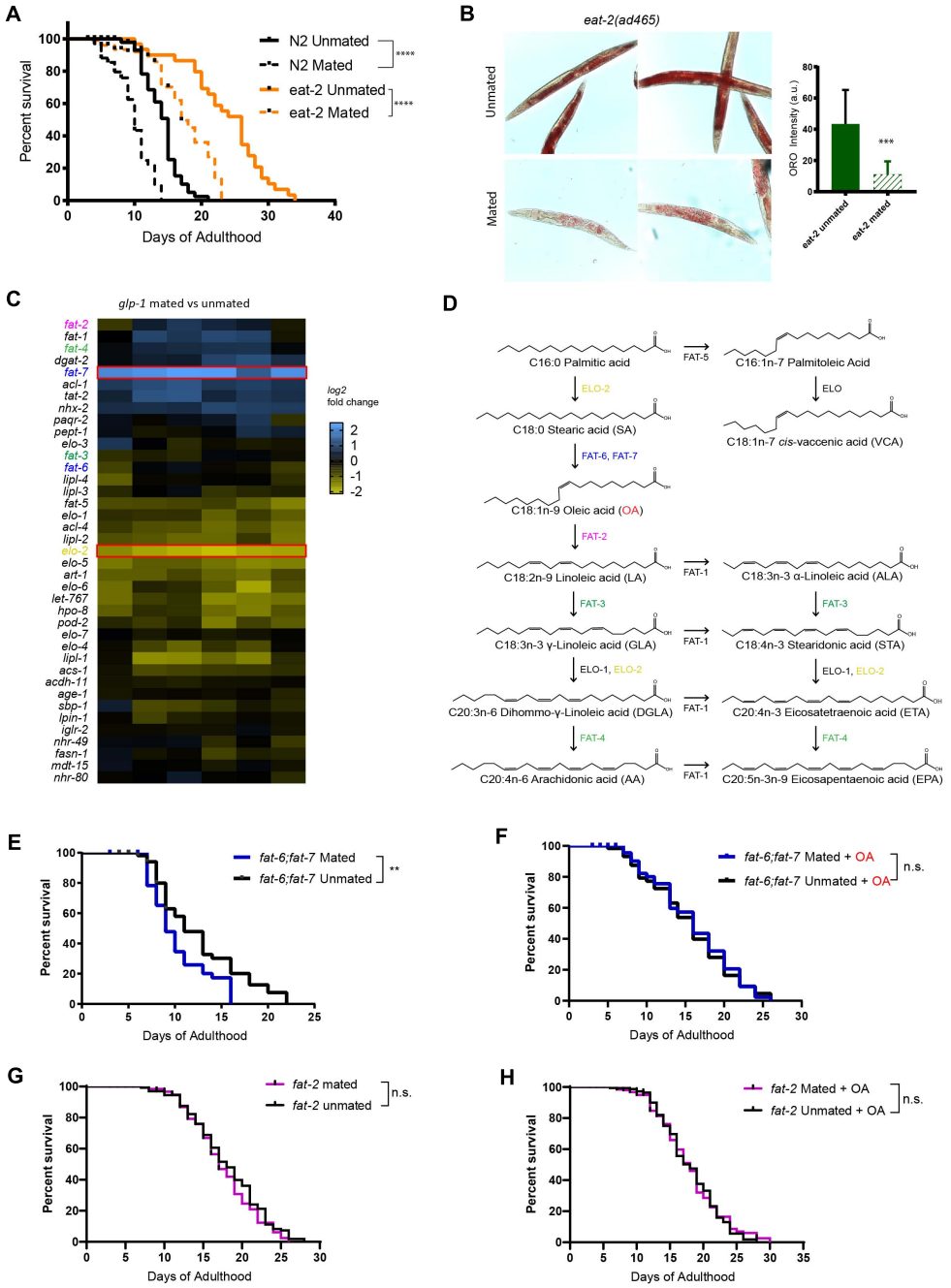

FIGURE 1 | Endogenous oleic acid protects worms from mating-induced death. *t*-test, *$p < 0.05$, **$p < 0.01$, ***$p < 0.001$, ****$p < 0.0001$ for all graphs. For all the lifespan assays performed in this study, Kaplan–Meier analysis with log-rank (Mantel–Cox) test was used to determine statistical significance (lifespan of mated worms was always compared to unmated worms of the same genotype/treatment unless stated otherwise). Error bars represent SEM unless noted. n.s., not significant. a.u., arbitrary units. **(A)** Mated worms under dietary restriction live longer than those *ad libitum* despite extreme depletion of fat. N2 Unmated: 14.0 ± 0.4 days, $n = 50$, N2 mated: 8.8 ± 0.4 days, $n = 100$, $p < 0.0001$; *eat-2(ad465)* unmated: 23.6 ± 1.1 days, $n = 50$, *eat-2(ad465)* mated: 15.1 ± 1.2 days, $n = 100$, $p < 0.0001$. **(B)** Mating induces significant fat loss in *eat-2(ad465)* hermaphrodites. Left: representative Oil Red O staining pictures; Right: quantification of Oil Red O staining. **(C)** Expression heatmap of genes related to fatty acid biosynthesis in mated *C. elegans glp-1(e2141)* hermaphrodites. **(D)** Pathway of *de novo* fatty acid synthesis in *C. elegans*, including molecular structure of each fatty acid. **(E,F)** Mutants that cannot synthesize oleic acid have dramatic lifespan loss after mating, and oleic acid supplementation fully rescues the mating-induced lifespan decrease *fat-6;fat-7* unmated: 12.3 ± 0.7 days, $n = 60$; *fat-6;fat-7* mated: 9.6 ± 0.4 days, $n = 100$, $p = 0.0059$; *fat-6;fat-7* unmated + oleic acid: 15.1 ± 0.8 days, $n = 60$; *fat-6;fat-7* mated + oleic acid: 15.5 ± 0.8 days, $n = 100$, $p = 0.7648$. **(G,H)** Mutants that contain excess endogenous oleic acid are protected from lifespan loss after mating. *fat-2* unmated: 18.1 ± 0.4 days, $n = 175$; *fat-2* mated: 17.1 ± 0.4 days, $n = 193$, $p = 0.2178$; *fat-2* unmated + oleic acid: 18.0 ± 0.4 days, $n = 173$; *fat-2* mated + oleic acid: 18.0 ± 0.4 days, $n = 215$, $p = 0.7598$.

gene, in the mated worms suffering from significant fat loss is counterintuitive, suggesting that its upregulation is more likely to compensate for the severe mating-induced fat loss. FAT-6 and FAT-7 are required to generate oleic acid from its direct upstream precursor stearic acid (**Figure 1D**), and act in a compensatory mechanism in single mutants (Brock et al., 2006). *fat-6;fat-7* double mutants cannot endogenously synthesize oleic acid and downstream PUFAs, and instead rely solely on fatty acids provided by the bacterial diet (Brooks et al., 2009); OA is almost non-existent in the common lab bacteria, OP50 (Deline et al., 2013). *fat-2* encodes the desaturase enzyme that converts oleic acid to its direct downstream product, linoleic acid (**Figure 1D**). In *fat-2* worms, oleic acid accumulates to almost a quarter of all fat, which is nearly 15-fold above the 1.7% found in wild-type animals (Watts and Browse, 2002). Therefore, these two mutants, *fat-6;fat-7* and *fat-2*, represent the effects of lack of OA and accumulation of OA, respectively.

To understand the importance of endogenous oleic acid in mating-induced death, we compared these mutants' mated and unmated lifespans. *fat-6;fat-7* mutants displayed many visible defects, such as slow growth, low brood size, and decreased body size, and have a short lifespan relative to wild-type worms (Brock et al., 2007). Mated *fat-6;fat-7* worms lived shorter than unmated *fat-6;fat-7* worms (**Figure 1E**), indicating that mating-induced death does not require the presence of OA. Supplementation with oleic acid greatly increased the lifespans of mated *fat-6;fat-7* worms, eliminating the difference between mated and unmated animals (**Figure 1F**), suggesting that the addition of exogenous OA both increases lifespan and eliminates mating-induced lifespan reduction.

By contrast with *fat-6;fat-7* mutants, *fat-2* mutants, which accumulate oleic acid, were both long-lived prior to mating (15% increase relative to unmated N2; $p = 0.0002$; pooled results from three biological replicates, **Supplementary Figure 3A** and **Supplementary Table 1**) and resistant to mating-induced lifespan reduction (**Figure 1G**, $p = 0.2187$). Further supplementation of oleic acid had no effect on *fat-2* lifespan (**Figure 1H**, $p = 0.7598$), suggesting that presence of endogenous oleic acid grants *fat-2* mutants protection from mating-induced death.

OA Specifically Increases Mated Lifespan

Since excess endogenous oleic acid (via mutants) protects animals against mating-induced death, we wondered if supplementing mated worms with exogenous oleic acid could also mitigate mating-induced death. Therefore, we supplemented mated wild-type (N2) hermaphrodites with oleic acid or with fatty acids (FA) in the FA synthesis pathway to determine the specificity of fatty acid supplementation. Oleic acid (OA), linoleic acid (LA), *cis*-vaccenic acid (VCA), dihommo-γ-linoleic acid (DGLA), and eicosapentaenoic acid (EPA) were added to the agar media of mated and unmated wild-type *C. elegans* hermaphrodites. Consistent with a previous finding that dietary supplementation of oleic acid, palmitoleic acid, or *cis*-vaccenic acid extends the lifespan of unmated hermaphrodites (Han et al., 2017), the addition of each fatty acid caused a slight increase in the lifespan of unmated wild-type hermaphrodites (**Figures 2A–F** and **Supplementary Table 1**, lifespan increase of individual fatty acid supplementation: OA, 12%; LA, 11%; VCA, 11%; DGLA, 17%; EPA, 16%), demonstrating that these fatty acids are successfully being taken up by the worms. Mated N2 worms without any fatty acid supplementation had a ∼30% shorter lifespan than unmated worms (**Figures 1A**, **2A**). While oleic acid supplementation completely rescued the lifespan loss caused by mating (**Figure 2B**), supplementation with any other fatty acid failed to rescue mating-induced lifespan decrease (**Figures 2C–F**), suggesting that oleic acid is specifically required for post-mating lifespan regulation. We supplemented the plates with various concentrations of oleic acid (OA) and found that OA showed a positive lifespan effect at low concentration (0.8 mM; 10% increase, p-value < 0.001) and completely inhibited mating-induced death at higher concentration (2 mM; 30% increase, $p < 0.001$) (**Supplementary Figure 3B**). While 2 mM is likely to achieve supraphysiological levels of OA, Han et al. (2017) showed that 0.8 mM fatty acid supplementation leads to a 2–3-fold increase in the corresponding FA in the worm.

To understand why only oleic acid is able to rescue mating-induced death, we compared the transcriptomes of mated vs. unmated hermaphrodites raised on normal agar media and on media with oleic acid, linoleic acid, and eicosapentaenoic acid supplementation. In all four conditions, mating led to dramatic transcriptional changes in hermaphrodites (**Supplementary Table 2**; one-class SAM). Principal component analysis separated mating-induced transcriptome changes based on the presence/absence of exogenous fatty acids supplementation (**Supplementary Figure 4A**), and to a lesser degree the specific type of fatty acid added (**Supplementary Figure 4B**). Similarly, supplementation of fatty acids accounted for the vast majority of difference in molecular functions, biological processes, cellular components, and transcription factors underlying mating-induced transcriptional changes revealed by Gene Ontology Enrichment analysis (**Supplementary Figure 5**), among which glycoprotein and peptidoglycan metabolic/catabolic processes (examples include lysozyme genes *lys-4*, *lys-5*, *lys-6*, **Supplementary Figure 5B** and **Supplementary Table 3**), and "pseudopodium" (mostly major sperm protein related genes, **Supplementary Figure 5C** and **Supplementary Table 3**) were enriched for genes that are up-regulated after mating with oleic acid supplementation.

To better understand how oleic acid specifically protects the worms from mating-induced death, we next performed two-class SAM analysis of the mated vs. unmated transcriptomes, and identified genes that were significantly differentially expressed upon mating *only* with oleic acid supplementation (FDR = 5%, $q < 5.92\%$; **Supplementary Table 4** and **Figures 2G,H**). In addition to genes encoding major sperm proteins and lysozymes as previously identified using one-class SAM analysis, we found several longevity genes and genes responsible for lipid metabolism/fatty acid storage that were specifically regulated in mated worms in the presence of oleic acid, including the serpentine receptor *sri-40*, which has recently been shown to regulate hermaphrodite lifespan both with and without males

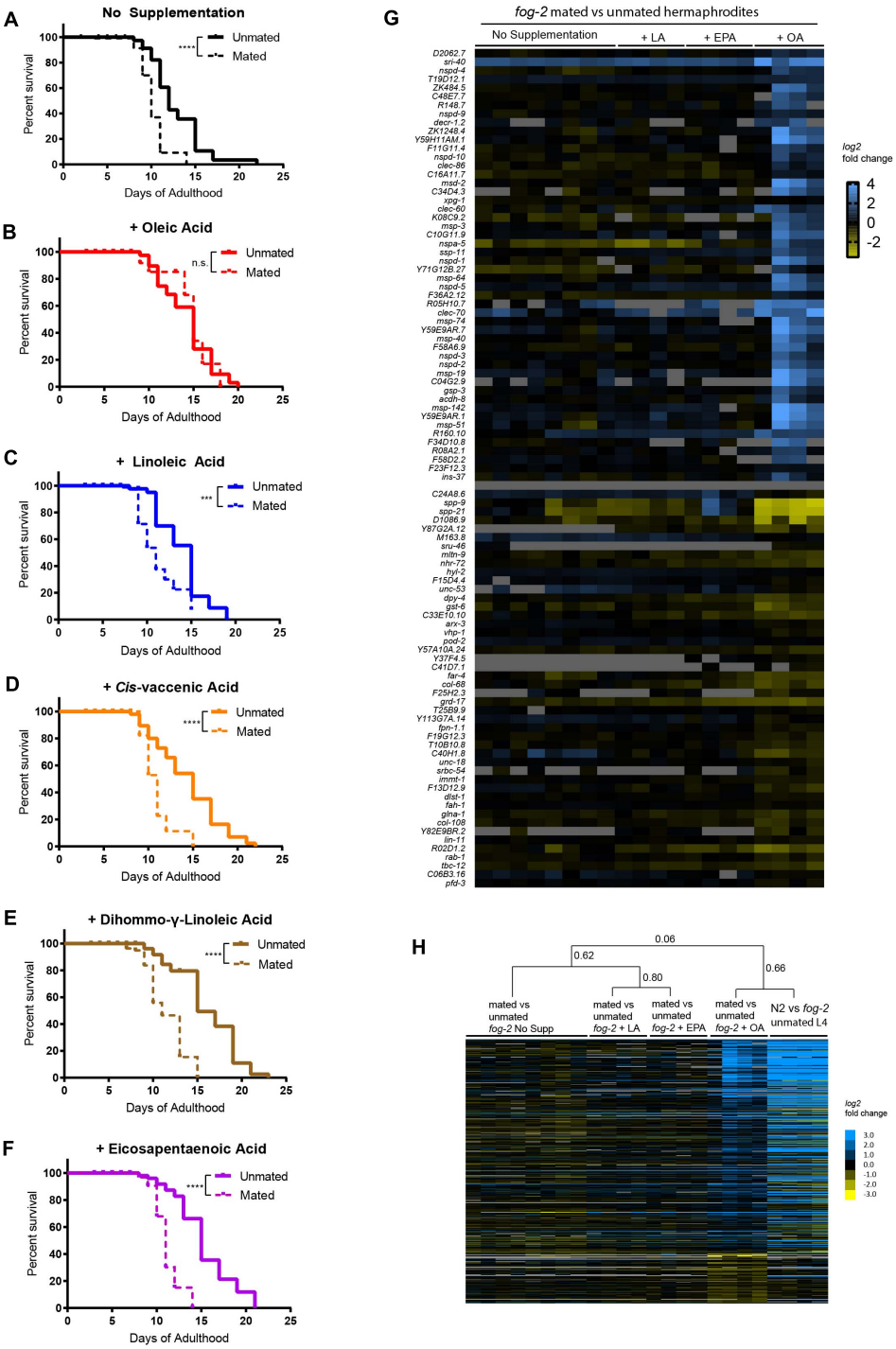

FIGURE 2 | Oleic acid supplementation rescues mating-induced death in wild-type *C. elegans* mothers. **(A–F)** Only oleic acid supplementation rescues lifespan loss induced by mating. N2 unmated: 12.7 ± 0.6 days, $n = 60$; mated: 9.4 ± 0.4 days, $n = 100$, $p < 0.0001$; unmated + OA: 14.2 ± 0.5 days, $n = 60$; mated + OA: 13.3 ± 1.2 days, $n = 100$, $p = 0.8344$; unmated + LA: 14.3 ± 0.6 days, $n = 60$; mated + LA: 10.2 ± 0.4 days, $n = 100$, $p = 0.0007$; unmated + VCA: 14.3 ± 0.6 days, $n = 60$; mated + VCA: 10.5 ± 0.3 days, $n = 100$, $p < 0.0001$; unmated + DGLA: 15.9 ± 0.6 days, $n = 60$; mated + DGLA: 9.8 ± 0.5 days, $n = 100$, $p < 0.0001$; unmated + EPA: 15.2 ± 0.5, $n = 60$; mated + EPA: 10.3 ± 0.4, $n = 100$, $p < 0.0001$. **(G)** Heatmap of top 50 genes that were significantly differentially expressed upon mating with oleic acid supplementation identified by two-class SAM analysis (Tusher et al., 2001). **(H)** Heatmap of differentially expressed genes identified by two-class SAM analysis comparing the transcriptomes of mated vs. unmated worms with oleic acid supplementation to all other conditions. The same list of genes was retrieved from published data (N2 vs. *fog-2* unmated L4 hermaphrodites, Shi et al., 2019) and their heatmap were added on the right to show striking similarity. Hierarchical clustering of the arrays were performed by Cluster 3.0 (de Hoon et al., 2004) using centroid linkage method. Correlation coefficients are listed next to the corresponding branches/nodes.

(Booth et al., 2020). Genes that regulate mitochondrial fatty acid beta oxidation, such as *acdh-8*, *decr-1.2*, and *decr-1.3*, were specifically up-regulated in mated worms with oleic acid supplementation, suggesting that oleic acid's unique ability to modulate lipid homeostasis might contribute to its specificity in regulating the longevity of mated worms. Finally, *ins-37*, which encodes an insulin receptor antagonist (Zheng et al., 2018), was specifically up-regulated in oleic acid treated mated worms. We previously showed that self-sperm-induced overexpression of *ins-37* protects hermaphrodites from short-term mating (Shi et al., 2019). Indeed, the oleic acid-specific mating-induced up-regulated gene expression profile resembles the transcriptional pattern of young hermaphrodites with self-sperm (**Figure 2H**; Pearson correlation = 0.66; Shi et al., 2019). The striking similarity in transcriptional profiles between these two conditions suggests that oleic acid utilizes a similar pathway to that of worms that still contain their own sperm (Booth et al., 2019; Shi et al., 2019), to protect against mating-induced death, to live long. Therefore, oleic acid-mediated sustained up-regulation of *ins-37* may provide long-term protection from mating-induced death.

Oleic Acid Supplementation Restores Lifespan and Fat Loss in Mated Worms Without Affecting Reproductive Health

Because lifespan, reproduction, and fat storage are closely coupled (Hansen et al., 2013), with fat acting at the nexus of longevity-reproduction trade off, we next checked the overall fat storage in wild-type mated and unmated worms in the presence and absence of exogenous oleic acid. Upon mating, animals normally lose a significant fraction of their somatic fat stores (**Figures 3A,B**; Shi and Murphy, 2014), a shift that is necessary for the normal development of progeny (Heimbucher et al., 2020). We found that oleic acid supplementation fully rescued mating-induced somatic fat loss in mated worms, and also increased fat storage in unmated worms by ∼10% (**Figures 3A,B**). However, neither progeny production rates nor total brood sizes are reduced upon OA treatment (**Figures 3C–E**) – that is, animals supplemented with OA are able to produce progeny without any trade-off in lifespan. These results suggest that oleic acid supplementation allows animals to reproduce fully without any loss of lifespan. Therefore, OA is critical for the restoration of longevity that is lost upon mating and progeny production, solving the longevity trade-off that reproduction normally costs.

Lifespan Rescue Through Oleic Acid Supplementation Is Conserved

Caenorhabditis elegans hermaphrodites self-reproduce through internal self-fertilization with their own sperm ("self-sperm") (Ward and Carrel, 1979). The presence of self-sperm protects the hermaphrodites from mating-induced death (Booth et al., 2019; Shi et al., 2019). We next wondered what role self-sperm-mediated protection might play in OA-mediated lifespan rescue. Previously, we found that self-sperm protects and slows down mating-induced death in *C. elegans* hermaphrodites through nuclear localization of HLH-30, the *C. elegans* ortholog of the mammalian transcription factor EB (TFEB), a conserved master regulator of autophagy and key pro-longevity regulator (Lapierre et al., 2013; Shi et al., 2019). We first tested *C. elegans* hermaphrodites with no self-sperm. The protective effect of OA was confirmed in short-term mating of N2 hermaphrodites for 2 h on Day 3 of adulthood when self-sperm is still present (**Figure 4A**); 2 h of mating is sufficient to induce a significant lifespan reduction in worms who lack self-sperm and therefore also lack the protective antagonist insulin (INS-37). Specifically, *fog-2* (feminization of germline) mutants lack self-sperm (Schedl and Kimble, 1988; **Figure 4B**) and are short-lived after mating. Oleic acid supplementation had no effect on lifespan on either unmated or 2 h-mated wild-type hermaphrodites that had self-sperm (**Figure 4C**), but oleic acid supplementation fully rescued the lifespan reduction of mated *fog-2* (self-spermless) mutants (**Figure 4D**). This conserved effect was further validated in *hlh-30* mutants that also suffer from 2 h-mating-induced death even in the presence of self-sperm (**Figure 4E**); oleic acid supplementation rescued *hlh-30's* mated lifespan decrease, as well (**Figure 4F**), suggesting that oleic acid may act downstream of HLH-30/TFEB to regulate lifespan.

Finally, we wondered if oleic acid supplementation is specific for hermaphrodites, or whether it can also rescue the early death of mated gonochoristic species females. We showed previously that *C. remanei* females also have significantly reduced lifespan after mating with *C. remanei* males (Shi and Murphy, 2014). Remarkably, mated females supplemented with oleic acid lived as long as unmated females with and without supplementation (**Figure 4G**), just as in the case of *C. elegans* wild-type hermaphrodites (**Figure 4H**). These results suggest that lifespan rescue through oleic acid supplementation is evolutionarily conserved in mated *Caenorhabditis* mothers.

DISCUSSION

The trade-off between reproduction and lifespan has been observed in a variety of animals (Partridge et al., 2005; Hansen et al., 2013). Fat, as the major means of storing energy, has been shown to be closely involved in both reproduction and lifespan regulation. The same inverse relationship also exists between reproduction and fat storage (Hansen et al., 2013; Lynn et al., 2015; Heimbucher et al., 2020). Germline-less *glp-1* worms upregulate the Δ9 desaturase enzyme FAT-6/SCD1 (Stearoyl-CoA Desaturase 1) (Goudeau et al., 2011) and shift the lipid profile to increase somatic maintenance and longevity (Ratnappan et al., 2014), while deficiency of the H3K4me3 methyltransferase (*ash-2*, *set-2*) upregulates Δ9 desaturases FAT-5 and FAT-7, leading to the accumulation of mono-unsaturated fatty acids and subsequent lifespan extension (Han et al., 2017).

By contrast, mated hermaphrodites demonstrate the inverse relationship between reproduction, longevity, and fat storage: mating increases progeny production by 2–3 fold, reduces fat stores, and significantly shortens lifespan compared to unmated hermaphrodites. Here, we have shown that oleic acid, a product of the Δ9 desaturase enzyme FAT-7 – whether through its endogenous accumulation by loss of FAT-2 activity or through exogenous supplementation – can prevent mating-induced

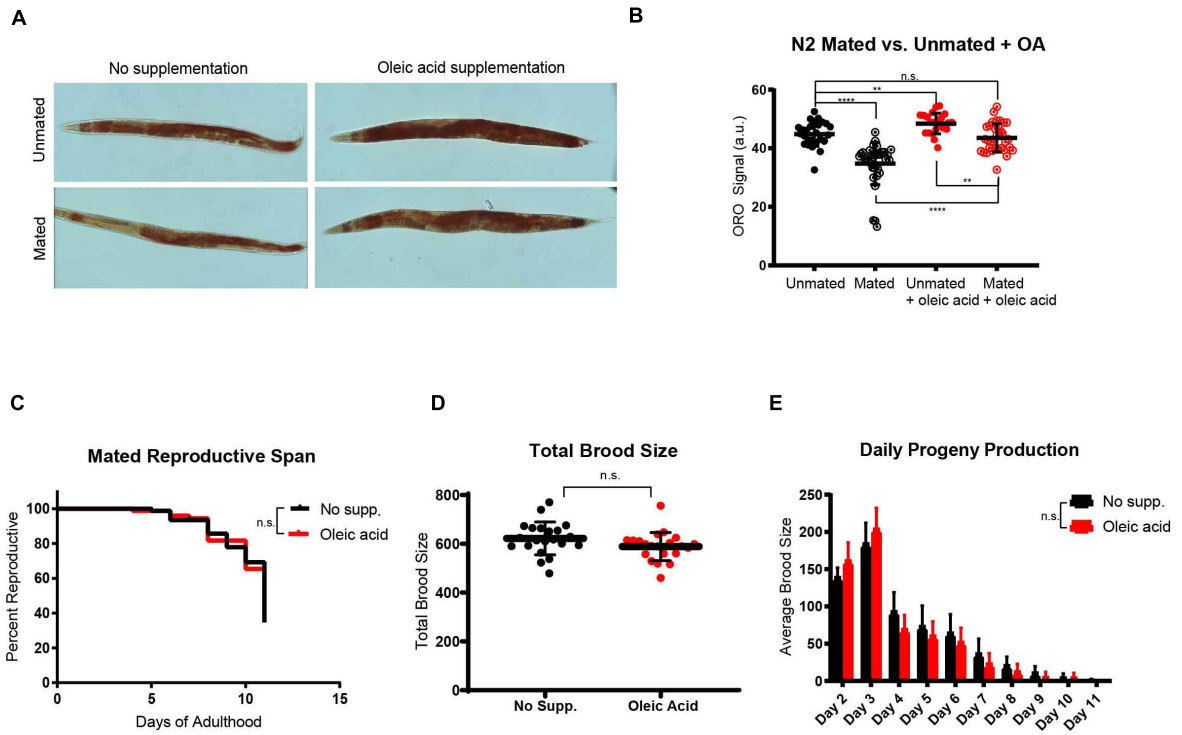

FIGURE 3 | Oleic acid supplementation restores fat storage without changing the reproduction of *C. elegans* mothers. **(A)** Dietary supplementation of oleic acid restores overall fat storage in wild-type hermaphrodites. Representative pictures of Oil red O fat staining are shown. **(B)** Quantification of Oil red O fat staining. Error bars: SD. *t*-test, $^{**}p < 0.01$, $^{****}p < 0.0001$, n.s., not significant. **(C)** The reproductive span of mated worms is not affected by oleic acid supplementation. **(D)** The total brood size of mated worms is not affected by oleic acid supplementation. **(E)** Daily progeny productions of mated worms with and without oleic acid supplementation are not statistically different.

death (**Figure 5**). Furthermore, the lifespan-rescuing effect of oleic acid is evolutionarily conserved in self-spermless hermaphrodites and females of gonochoristic *Caenorhabditis* species. Dietary supplementation of oleic acid as well as a few other monounsaturated fatty acids (MUFAs), including palmitoleic and *cis*-vaccenic acid can extend the lifespan of unmated hermaphrodites (Han et al., 2017). However, supplementing other fatty acids is not able to ameliorate the mating-induced death. Additionally, oleic acid supplementation leads to a much larger lifespan extension in mated worms compared to unmated hermaphrodites (**Supplementary Figure 6**). Taken together, our results demonstrate the specificity of oleic acid in regulating post-mating lifespan, and suggest that it is slightly different from H3K4me3 methyltransferase-mediated transgenerational inheritance of longevity.

Our analysis of mated animals with increased reproduction revealed that overall (total) fat levels play no role in the lifespan regulation of mated worms; that is, mating reduces the lifespan of longevity mutants, whether they exhibit increased or decreased fat levels prior to mating. Our transcriptome analysis of mated and unmated worms revealed mating-induced upregulation of regulators of fatty acid metabolism. Only oleic acid treatment can rescue fat loss induced by mating and lifespan reduction induced by mating, without affecting reproduction. Our additional transcriptome analysis comparing mated vs. unmated worms on media containing different types of fatty acids revealed that only oleic acid supplementation induces self-sperm-like protective transcriptional pattern in mated worms. Specifically, the insulin-like peptide antagonist, INS-37, which we previously found to be expressed at high levels in worms that still contain self-sperm, and which prevents male-sperm mating-induced death (Shi et al., 2019), is expressed at higher levels in oleic acid-treated worms.

Our results suggest that oleic acid depletion in the soma is the ultimate downstream cost of reproduction. Oleic acid might affect the soma through maintenance of membrane fluidity (stearic acid/oleic acid ratio) (Funari et al., 2003) or because of general lipid storage. It is notable that other lipids in the pathway were not able to rescue mating-induced death, suggesting that this specific fatty acid has a unique role in somatic maintenance and growth. The specificity of oleic acid has also been reported in mediating the age-dependent somatic depletion of fat (Asdf) (Lynn et al., 2015), as oleic acid is the only fatty acid that is able to rescue the Asdf phenotype. Even though the Asdf phenotype was examined in unmated worms and under oxidative stress, which differs from the mating-induced death in this study, both phenotypes involve the interaction between the soma and germline. The fact that the specificity of oleic acid is observed in both studies further increases the likelihood of oleic acid as the possible link between germline/reproduction and somatic maintenance/lifespan. Oleic acid, more than other fatty acids that did not affect longevity, regulates the expression of several genes involved in fatty acid storage.

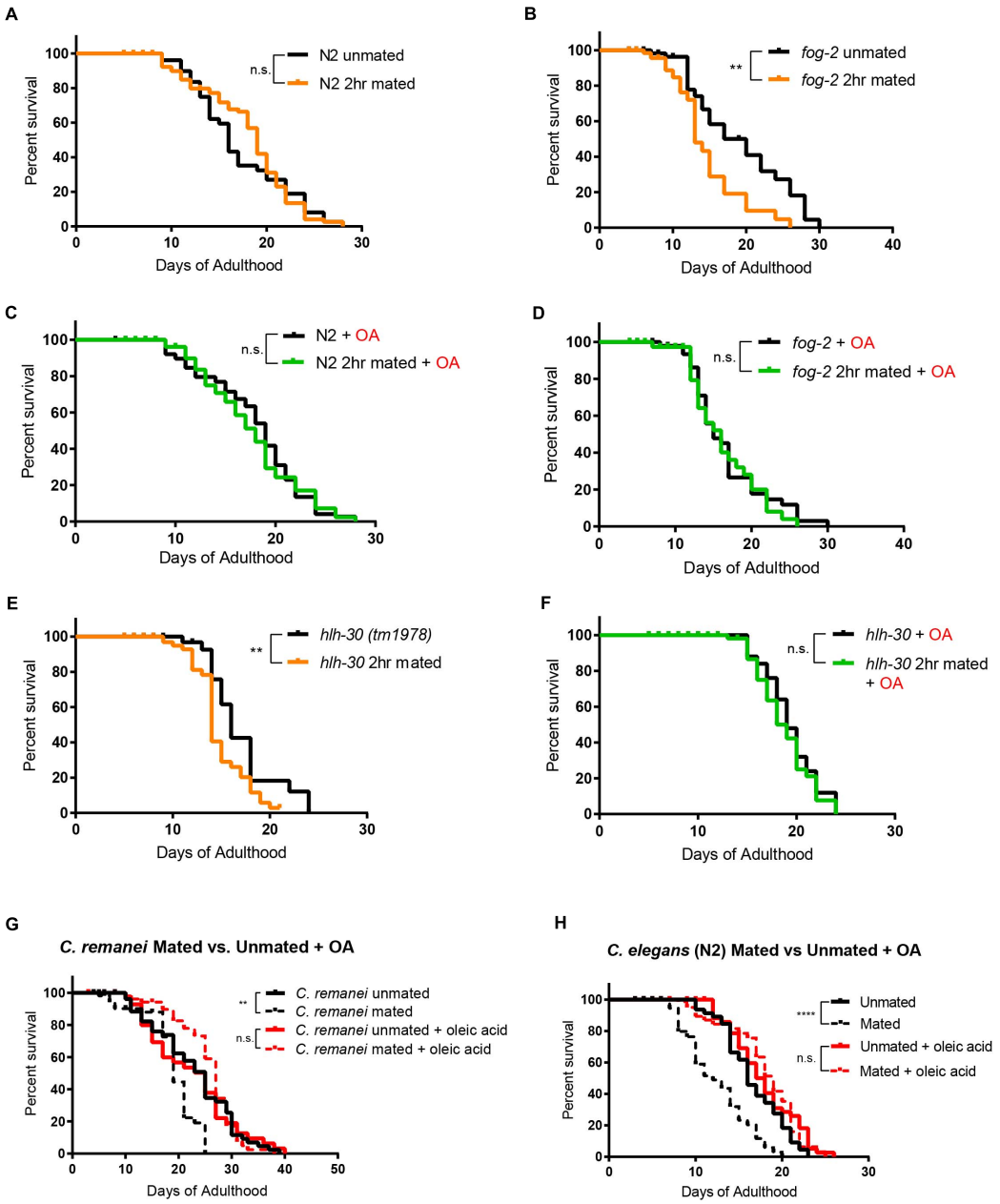

FIGURE 4 | Oleic acid-specific mating-induced death rescue is conserved. Kaplan-Meier analysis with log-rank (Mantel-Cox) test was used to determine statistical significance for all the lifespan assays (lifespan of mated worms was always compared to unmated worms of the same genotype/treatment). $^{**}p < 0.01$, $^{****}p < 0.0001$. **(A–F)** Oleic acid protects worms from short-term mating-induced death. **(A)** Unmated N2: 16.7 ± 0.8 days, $n = 60$; 2 h mated: 17.8 ± 0.5 days, $n = 100$, $p = 0.5900$. **(B)** Unmated *fog-2*: 18.2 ± 1.4 days, $n = 60$; *fog-2* 2 h mated: 14.0 ± 1.0 days, $n = 100$, $p = 0.0044$. **(C)** Unmated N2 + oleic acid: 17.4 ± 0.7 days, $n = 60$; 2 h mated + oleic acid: 17.7 ± 0.6 days, $n = 100$, $p = 0.7676$. **(D)** Unmated *fog-2* + oleic acid: 16.4 ± 0.8 days, $n = 60$; *fog-2* 2 h mated + oleic acid: 16.2 ± 0.9 days, $n = 100$, $p = 0.5910$. **(E)** Unmated *hlh-30*: 16.6 days ± 0.8 days, $n = 60$; *hlh-30* 2 h mated: 14.3 ± 0.4 days, $n = 100$, $p = 0.0117$. **(F)** Unmated *hlh-30* + oleic acid: 19.4 ± 0.5 days, $n = 60$; *hlh-30* 2 h mated + oleic acid: 18.8 ± 0.4 days, $n = 100$, $p = 0.4357$. **(G)** Mated *C. remanei* mothers' lifespans are also rescued by oleic acid supplementation. Unmated: 22.6 ± 1.2 days, $n = 60$; mated: 18.2 ± 0.8 days, $n = 60$, $p = 0.0029$; unmated + oleic acid: 21.9 ± 1.4 days, $n = 60$; mated + oleic acid: 25.3 ± 0.9 days, $n = 60$, $p = 0.3266$. **(H)** Lifespans of unmated and mated N2 hermaphrodites with and without oleic acid supplementation. Unmated: 16.6 ± 0.5 days, $n = 49$; mated: 11.8 ± 0.5 days, $n = 80$, $p < 0.0001$; unmated + oleic acid: 17.9 ± 0.6 days, $n = 50$; mated + oleic acid: 18.1 ± 0.6 days, $n = 80$, $p = 0.9466$.

In addition to dietary supplementation, we also show that endogenous oleic acid is beneficial to mated worms. Genetically blocking FAT-2, the desaturase enzyme that converts oleic acid to linoleic acid, increases endogenous oleic acid levels (Watts and Browse, 2002) as well as the level of total triglyceride (TAG) (Horikawa and Sakamoto, 2010), which we find protects the

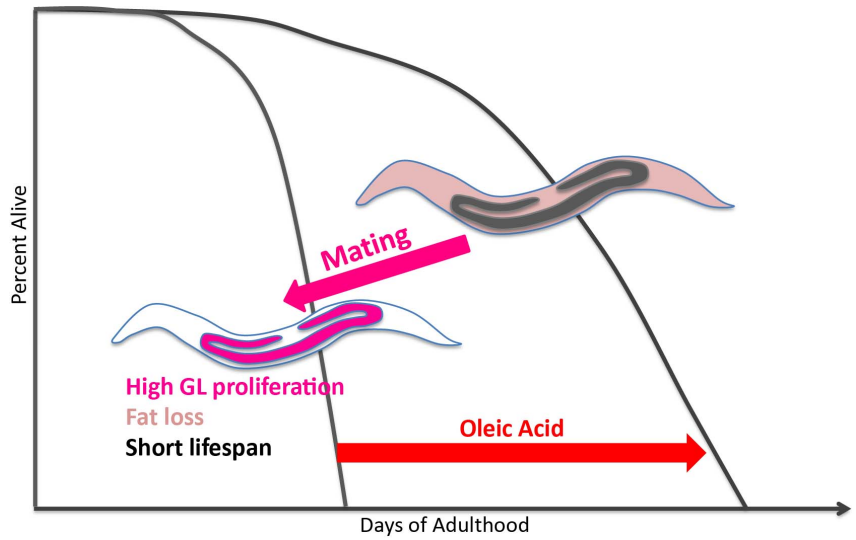

FIGURE 5 | Model of oleic acid-mediated lifespan restoration in mated worms. Mating leads to germline hyperactivity, fat loss, and shortened lifespan in *Caenorhabditis* mothers. Oleic acid addition (whether endogenously or exogenously) is able to restore the lifespan decrease caused by mating.

worms from mating-induced death. FAT-6 and FAT-7 are the stearoyl CoA desaturases (SCD) that convert stearic acid to oleic acid. Interestingly, *fat-6* and *fat-7* are up-regulated in long-lived mutants such as *daf-2* and *glp-1* (Murphy et al., 2003; Goudeau et al., 2011), indicating again that increased endogenous oleic acid is beneficial to worms. It is possible that oleic acid is the somatic energy source that extends lifespan in these mutants. FAT-6/FAT-7/SCD1 desaturase enzyme activity is highly conserved. In mammals including humans, oleic acid is the prime substrate for triglyceride (Chu et al., 2006). Loss of SCD1, which synthesizes oleic acid, was shown to protect against adiposity by preventing the accumulation of triglyceride in mice (Ntambi et al., 2002), just as *fat-6;fat-7* mutant worms have significantly low levels of triglyceride storage (Watts and Browse, 2002). Furthermore, SCD1 is strongly upregulated in response to ovariectomy in mice (Paquette et al., 2008). The biological roles of oleic acid and desaturation are thus conserved in several aspects between *C. elegans* and humans. With regard to reproduction, oleic acid is a major determinant of plasma membrane fluidity in many cells, including follicular cells (Funari et al., 2003). In bovine oocytes, oleic acid plays a key role in membrane fluidity that counteracts the detrimental effects of exposure to saturated fatty acids (Aardema et al., 2011), and acts as a metabolic regulator of oxidative stress and cellular signaling in oocytes, early embryonic development, and female fertility (Fayezi et al., 2018).

Oleic acid is likely to be the linchpin of the reproductive and somatic energy balance. Mating-induced up-regulation of *fat-7,* which converts stearic acid to oleic acid, could be a response of the mated worms to prepare themselves with more endogenous oleic acid for dramatically increased progeny production. At the same time, the somatic reserve of oleic acid is depleted as indicated by the loss of fat storage to fuel the mating-induced elevated reproductive activity. In this case, mated worms prioritize oleic acid for reproduction, and the outcome is increased reproduction at the cost of lifespan. By contrast, in *daf-2* and *glp-1* mutants with reduced or no reproductive activity, more oleic acid accumulates in the somatic tissues and may be utilized for somatic maintenance, leading to an extension of lifespan. Therefore, oleic acid is likely to be the limiting energy source that reproduction and somatic maintenance compete for. Our results suggest that oleic acid depletion is a prime example of the cost of reproduction. Excitingly, it is one that appears to be reversible through dietary supplementation of oleic acid. Oleic acid, along with the evolutionarily conserved enzymes in the pathway, might be therapeutic targets that could help humans improve reproductive and somatic health at the same time without having to sacrifice one for the other.

MATERIALS AND METHODS

Strains and Maintenance

All worm strains used in this study are listed below. All strains were maintained on Nematode Growth Media (NGM) plates at 20°C according to the standard procedure (Brenner, 1974).

Strain	Genotype	Source
N2	Wild-type	CGC
CB4108	*fog-2(q71) V*	CGC
CB4037	*glp-1(e2141) III*	CGC
RB969	*fat-2(ok873) IV*	CGC
BX156	*fat-6(tm331) IV;fat-7(wa36)V*	CGC
JIN1375	*hlh-30(tm1978) IV*	CGC
PB4641	*Caenorhabditis remanei*	CGC

CGC is the Caenorhabditis Genetics Center.

Mating Assays

All assays were performed at 20°C, and all worms were synchronized through bleaching adult worms with a mixture of NaOCl and KOH, leaving only the eggs.

Twenty-Four Hour Group Mating

Ten centimeter NGM plate was seeded with 300 μL of OP50 (Brenner, 1974) to create a ∼3 cm diameter of bacterial lawn. Hundred hermaphrodites and 300 males at late L4 were transferred onto the plate. The ratio of 1 hermaphrodite to 3 males was used to optimize mating. 24 h later, the hermaphrodites were transferred onto newly seeded plates without males. Complete mating means that males transfer enough sperm so that all progeny produced are cross-progeny (half males, half hermaphrodites). Incomplete mating means that males do not transfer enough sperm so that their sperm is used up and hermaphrodites later revert to using their own sperm, evidently seen from the ratio of male: hermaphrodite offspring. The progeny of the mated hermaphrodites was checked every day, and incompletely mated worms were censored.

For *C. remanei*, the same method was used for mating. Since males deposit copulatory plugs onto females' vulva after mating, mated females without the plugs and unmated females with the plugs were both censored.

Two Hour Short-Term Mating

The same setup was used as group mating, but the mating was allowed for only 2 h. Hermaphrodites were transferred first onto seeded plates, and males were moved onto the plates later in an orderly and timely manner, so that each experimental group has exactly 2 h for mating.

Lifespan Assay

Lifespan assays were performed using 3 cm NGM plates seeded with 25 μL of OP50. A maximum of 20 worms were present at each plate. For mated group, $n = 100$ while for unmated group, $n > 50$. Worms were transferred every day to freshly seeded plates during the reproductive period to eliminate confounding progeny, and every other day afterward. Worms were scored dead if they did not respond to repeated prods with a pick. The beginning of Day 1 of adulthood was defined as $t = 0$, and Kaplan–Meier survival analysis was performed with the log-rank (Mantel–Cox) method. Lifespan curves were generated using GraphPad Prism. Bagged (matricide), exploded, or lost worms were censored.

fat-6;fat-7 mutants had suspended growth, so they were considered Day 1 adults when the egg-laying began.

Reproductive Span and Brood Size Assay

Individual hermaphrodites after mating were transferred onto 3 cm NGM plates seeded with 25 μL of OP50 and moved to fresh plates daily until reproduction ceased for at least 2 days. The old plates were left at 20°C for 2 days to allow the offspring to grow into adults, which were manually counted for daily production and total brood size. At least 20 plates of individual worms were counted to account for individual variation. The last day of reproduction was marked as the last day of progeny production, evidenced by no worms on the old plates. When matricide occurred, the worm was censored from the experiment on that day. Kaplan–Meier analysis with log-rank (Mantel–Cox) method was performed to compare the reproductive spans. Reproductive span curves and brood size values were graphed using GraphPad Prism.

Fatty Acid Supplementation

The fatty acid supplementation was adapted from the published protocol (Deline et al., 2013) with minor modifications from a more recent publication (Han et al., 2017). The detergent Tergitol (type NP-40, Sigma-Aldrich) was added to a final concentration of 0.001% in liquid NGM media, and an optimized concentration of 0.8 mM was supplemented for all fatty acids. For our purpose, fatty acids were in ethanol solution and were further dissolved in purified water by shaking for 30 min. The working stock was made fresh every time. The media was stirred for at least 5 min after the working stock was added. The fatty acids were deemed incompletely dissolved if a similar number of oil bubbles can be seen in the media with and without the detergent. Plates were kept inside a dark plastic box with no ventilation, but with sterile lab tissues that were replaced every day to absorb moisture. This method enabled the plates to remain without visible blackening of the fatty acid bubbles for a longer period. Control plates were made using the exact same procedure including the detergent and the ethanol, but not the fatty acid. Correct and consistent application of this procedure was essential for the replicability of the results.

Oil Red O Staining and Quantification

Oil Red O staining was adapted from the published protocol to stain around 100 worms per condition (Wählby et al., 2014). Approximately 10 worms were imaged per slide with Nikon Ti. Oil Red O quantification was performed as published (O'Rourke et al., 2009). Briefly, colored images were split into RGB monochromatic images in Image J. The polygon selection tool was used to outline the boundary of each worm. The Oil Red O staining arbitrary unit (a.u.) was determined by mean gray value within the worm, calculated by the difference between the signals in Blue/Green and Red channel. T-test analysis was performed to compare the fat staining of different groups of worms. Individual intensity values were graphed using GraphPad Prism.

Microarrays

Microarray data of mated and unmated *glp-1(e2141)* was retrieved from the previous publication (Booth et al., 2020). *glp-1(e2141)* hermaphrodites grown at the restrictive temperature (25°C) were mated on day 1 of adulthood for 24 h in a 2:1 male:hermaphrodite ratio. Two hundred hermaphrodites were collected on day 2/3 of adulthood for each biological replicate. In fatty acids supplementation experiments, eggs from bleached *fog-2(q71)* hermaphrodites were grown on NGM plates with various fatty acids supplementation at the final concentration of 1 mM. In mated groups, *fog-2* hermaphrodites were mated with young males for 24 h from day 1 of adulthood to day

2 of adulthood in the presence of fatty acid supplementation. About 200 hermaphrodites were collected on day 3 of adulthood for each biological replicate. RNA was extracted by the heat vortexing method. Two-color Agilent microarrays were used for expression analysis. Significantly differentially expressed gene sets were identified using SAM (Tusher et al., 2001). One class SAM was performed to identify genes that are significantly differentially expressed after mating in each fatty acid supplementation condition (**Supplementary Figure 5**). Two class SAM was performed to identify genes that are significantly differentially expressed after mating specific to oleic acid supplementation (**Figures 2G,H**). Principal component analysis was performed in R using prcomp function based on the genes identified by one class SAM (**Supplementary Figure 4**). Gene ontology enrichment analysis was performed using wormbase enrichment tools (**Supplementary Figure 2B**)[1], and multi-query function of gProfiler (**Supplementary Figure 5**) (Raudvere et al., 2019).

Original microarray dataset can be found in PUMAdb:

Mated and unmated *glp-1(e2141)* hermaphrodites: https://puma.princeton.edu/cgi-bin/exptsets/review.pl?exptset_no=7345.

Mated and unmated *fog-2(q71)* hermaphrodites with different fatty acids supplementation: https://puma.princeton.edu/cgi-bin/exptsets/review.pl?exptset_no=7359.

DATA AVAILABILITY STATEMENT

The datasets presented in this study can be found in online repositories. The names of the repository/repositories and accession number(s) can be found in the article/ **Supplementary Material**.

AUTHOR CONTRIBUTIONS

LSC and CTM designed the research. LSC, CS, JA, and SS performed the research and analyzed the data. LSC, CS, and CTM wrote the paper. All authors listed have made a substantial, direct and intellectual contribution to the work, and approved it for publication.

FUNDING

This work was supported by the HHMI-Simons Faculty Scholar Award to CTM, NIH R01 AG034446, and support from the Susan W. and James C. Blair '61 P87 Endowed Senior thesis fund to LSC.

ACKNOWLEDGMENTS

We thank the *Caenorhabditis Genetics Center* (CGC) for strains, and members of the CTM's laboratory for critically reading the manuscript and valuable feedback.

[1]https://wormbase.org/tools/enrichment/tea/tea.cgi

SUPPLEMENTARY MATERIAL

The Supplementary Material for this article can be found online at: https://www.frontiersin.org/articles/10.3389/fcell.2021.690373/full#supplementary-material

Supplementary Figure 1 | Mating causes dramatic fat loss and lifespan decrease in longevity mutants. **(A)** *daf-2(e1370)* longevity mutants are short-lived post-mating. Unmated *daf-2*: 37.0 ± 1.9 days, $n = 47$, mated *daf-2*: 19.4 ± 2.2 days, $n = 60$, $p < 0.0001$. **(B)** *glp-1(e2141)* mutants live shorter after mating as well. Unmated *glp-1*: 24.1 ± 1.3 days, $n = 48$, mated *glp-1*: 11.6 ± 0.5 days, $n = 60$, $p < 0.0001$. **(C)** Quantification of Oil red O fat staining of mated and unmated wild-type (N2), *daf-2*, and *glp-1* worms. **(D)** Mated worms under solid plate-based dietary restriction (sDR) live longer than those *ad libitum*. N2 Unmated: 14.0 ± 0.4 days, $n = 50$, N2 mated: 8.8 ± 0.4 days, $n = 100$, $p < 0.0001$; unmated + sDR: 23.7 ± 1.4 days, $n = 50$, mated + sDR: 14.1 ± 2.0 days, $n = 100$, $p = 0.0042$.

Supplementary Figure 2 | Genome-wide transcriptional analysis of mated vs. unmated *glp-1* hermaphrodites. **(A)** Heatmap of whole transcriptome comparison between mated and unmated *glp-1(e2141)* hermaphrodites. **(B)** Gene ontology enrichment analysis of significantly differentially expressed genes.

Supplementary Figure 3 | Both endogenous and exogenous oleic acid influence the lifespan of *C. elegans*. **(A)** Worms with excessive endogenous oleic acid are longer-lived. Lifespans: N2 unmated: 15.8 ± 0.4 days, $n = 160$; *fat-2* unmated: 18.1 ± 0.4 days, $n = 173$, $p = 0.0002$. **(B)** Dosage test of oleic acid supplementation. With improved fatty acid dissolution technique, 0.8 mM of supplementation was deemed sufficient for all later experiments. Unmated N2: 14.2 ± 0.5 days, $n = 50$; mated: 9.5 ± 0.3 days, $n = 100$; mated + 0.8 mM oleic acid: 12.2 ± 0.6 days, $n = 100$; mated + 2.0 mM oleic acid: 13.8 ± 0.7 days, $n = 100$.

Supplementary Figure 4 | Transcriptomes of mated vs. unmated hermaphrodites are affected by fatty acids supplementation. **(A)** Principal component analysis of the transcriptomes of mated vs. unmated hermaphrodites raised on agar media with oleic acid (OA), linoleic acid (LA), eicosapentaenoic acid (EPA), and no supplementation (Ctrl). **(B)** Principal component analysis of the transcriptomes of mated vs. unmated hermaphrodites raised on agar media with oleic acid (OA), linoleic acid (LA), and eicosapentaenoic acid (EPA) supplementation.

Supplementary Figure 5 | Gene Ontology analysis of transcriptomes of mated vs. unmated hermaphrodites with different fatty acids supplementation and control. Enrichment of molecular function **(A)**, biological process **(B)**, cellular component **(C)**, and transcription factor **(D)** were compared for all four conditions: worms raised on normal media (ctrl), on media with oleic acid (OA), linoleic acid (LA), and eicosapentaenoic acid (EPA) supplementation.

Supplementary Figure 6 | Oleic acid supplementation increases the lifespan of mated worms more significantly. **(A)** Percent lifespan increase of the mated worms in the presence of oleic acid supplementation (30%; all genotypes included, each dot represents one lifespan replicate) is significantly higher than that of the unmated worms (5%), $p = 0.0159$, unpaired *t*-test. **(B)** Oleic acid supplementation does not affect the lifespans of *fat-2* mutants which have excessive endogenous oleic acid: only about 2% increase. The rest of the mated worms have an average of 40% lifespan increase in the presence of oleic acid supplementation compared to the 6% lifespan increase of the unmated worms, $p = 0.0071$, unpaired *t*-test. **(C)** Percent lifespan increase with the oleic acid treatment of each lifespan experiment with genotypes listed.

Supplementary Table 1 | Lifespan Summary.

Supplementary Table 2 | Mating-induced differentially expressed genes identified by one-class SAM analysis.

Supplementary Table 3 | Gene Ontology Enrichment Analysis of genes in **Supplementary Table 2**.

Supplementary Table 4 | Oleic acid-specific mating-induced differentially expressed genes identified by two-class SAM analysis.

REFERENCES

Aardema, H., Vos, P. L. A. M., Lolicato, F., Roelen, B. A. J., Knijn, H. M., Vaandrager, A. B., et al. (2011). Oleic Acid Prevents Detrimental Effects of Saturated Fatty Acids on Bovine Oocyte Developmental Competence1. *Biol. Reprod.* 85, 62–69. doi: 10.1095/biolreprod.110.088815

Avery, L. (1993). The genetics of feeding in Caenorhabditis elegans. *Genetics* 133, 897–917. doi: 10.1093/genetics/133.4.897

Bar, D. Z., Charar, C., Dorfman, J., Yadid, T., Tafforeau, L., Lafontaine, D. L. J., et al. (2016). Cell size and fat content of dietary-restricted <em>Caenorhabditis elegans<em> are regulated by ATX-2, an mTOR repressor. *Proc. Natl. Acad. Sci.* 113, E4620–E4629.

Booth, L. N., Maures, T. J., Yeo, R. W., Tantilert, C., and Brunet, A. (2019). Self-sperm induce resistance to the detrimental effects of sexual encounters with males in hermaphroditic nematodes. *Elife* 8:e46418.

Booth, L. N., Shi, C., Tantilert, C., Yeo, R. W., Hebestreit, K., Hollenhorst, C. N., et al. (2020). *Males Deploy Multifaceted Strategies and Hijack Longevity Pathways to Induce Premature Demise of the Opposite Sex*. United States: Cold Spring Harbor Laboratory.

Brenner, S. (1974). The genetics of Caenorhabditis elegans. *Genetics* 77, 71–94. doi: 10.1093/genetics/77.1.71

Brock, T. J., Browse, J., and Watts, J. L. (2006). Genetic Regulation of Unsaturated Fatty Acid Composition in C. elegans. *PLoS Genet.* 2:e108. doi: 10.1371/journal.pgen.0020108

Brock, T. J., Browse, J., and Watts, J. L. (2007). Fatty acid desaturation and the regulation of adiposity in Caenorhabditis elegans. *Genetics* 176, 865–875. doi: 10.1534/genetics.107.071860

Brooks, K. K., Liang, B., and Watts, J. L. (2009). The Influence of Bacterial Diet on Fat Storage in C. elegans. *PLoS One* 4:e7545. doi: 10.1371/journal.pone.0007545

Chu, K., Miyazaki, M., Man, W. C., and Ntambi, J. M. (2006). Stearoyl-coenzyme A desaturase 1 deficiency protects against hypertriglyceridemia and increases plasma high-density lipoprotein cholesterol induced by liver X receptor activation. *Mol. Cell. Biol.* 26, 6786–6798. doi: 10.1128/mcb.00077-06

de Hoon, M. J. L., Imoto, S., Nolan, J., and Miyano, S. (2004). Open source clustering software. *Bioinformatics* 20, 1453–1454.

Deline, M. L., Vrablik, T. L., and Watts, J. L. (2013). Dietary supplementation of polyunsaturated fatty acids in Caenorhabditis elegans. *J. Vis. Exp.* 2013:50879.

Drori, D., and Folman, Y. (1976). Environmental effects on longevity in the male rat: exercise, mating, castration and restricted feeding. *Exp. Gerontol.* 11, 25–32. doi: 10.1016/0531-5565(76)90007-3

Fahy, E., Subramaniam, S., Murphy, R. C., Nishijima, M., Raetz, C. R. H., Shimizu, T., et al. (2009). Update of the LIPID MAPS comprehensive classification system for lipids. *J. Lipid Res.* 50, S9–S14.

Fayezi, S., Leroy, J. L. M. R., Ghaffari Novin, M., and Darabi, M. (2018). Oleic acid in the modulation of oocyte and preimplantation embryo development. *Zygote* 26, 1–13. doi: 10.1017/s0967199417000582

Funari, S. S., Barceló, F., and Escribá, P. V. (2003). Effects of oleic acid and its congeners, elaidic and stearic acids, on the structural properties of phosphatidylethanolamine membranes. *J. Lipid Res.* 44, 567–575. doi: 10.1194/jlr.m200356-jlr200

Goudeau, J., Bellemin, S., Toselli-Mollereau, E., Shamalnasab, M., Chen, Y., and Aguilaniu, H. (2011). Fatty acid desaturation links germ cell loss to longevity through NHR-80/HNF4 in C. elegans. *PLoS Biol.* 9:e1000599. doi: 10.1371/journal.pbio.1000599

Greer, E. L., and Brunet, A. (2009). Different dietary restriction regimens extend lifespan by both independent and overlapping genetic pathways in C. elegans. *Aging Cell.* 8, 113–127. doi: 10.1111/j.1474-9726.2009.00459.x

Han, S., Schroeder, E. A., Silva-García, C. G., Hebestreit, K., Mair, W. B., and Brunet, A. (2017). Mono-unsaturated fatty acids link H3K4me3 modifiers to C. elegans lifespan. *Nature* 544, 185–190. doi: 10.1038/nature21686

Hansen, M., Flatt, T., and Aguilaniu, H. (2013). Reproduction, fat metabolism, and life span: what is the connection? *Cell. Metab.* 17, 10–19. doi: 10.1016/j.cmet.2012.12.003

Heimbucher, T., Hog, J., Gupta, P., and Murphy, C. T. (2020). PQM-1 controls hypoxic survival via regulation of lipid metabolism. *Nat. Commun.* 11, 4627–4627.

Hodgkin, J., and Barnes, T. M. (1991). More is not better: brood size and population growth in a self-fertilizing nematode. *Proc. Biol. Sci.* 246, 19–24. doi: 10.1098/rspb.1991.0119

Horikawa, M., and Sakamoto, K. (2010). Polyunsaturated fatty acids are involved in regulatory mechanism of fatty acid homeostasis via daf-2/insulin signaling in Caenorhabditis elegans. *Mol. Cell. Endocrinol.* 323, 183–192. doi: 10.1016/j.mce.2010.03.004

Hsin, H., and Kenyon, C. (1999). Signals from the reproductive system regulate the lifespan of C. elegans. *Nature* 399, 362–366. doi: 10.1038/20694

Kniazeva, M., Sieber, M., McCauley, S., Zhang, K., Watts, J. L., and Han, M. (2003). Suppression of the ELO-2 FA elongation activity results in alterations of the fatty acid composition and multiple physiological defects, including abnormal ultradian rhythms, in Caenorhabditis elegans. *Genetics* 163, 159–169. doi: 10.1093/genetics/163.1.159

Lapierre, L. R., De Magalhaes Filho, C. D., McQuary, P. R., Chu, C.-C., Visvikis, O., Chang, J. T., et al. (2013). The TFEB orthologue HLH-30 regulates autophagy and modulates longevity in Caenorhabditis elegans. *Nat. Commun.* 4, 2267–2267.

Lapierre, L. R., and Hansen, M. (2012). Lessons from C. elegans: signaling pathways for longevity. *Trends Endocrinol. Metab.* 23, 637–644. doi: 10.1016/j.tem.2012.07.007

López-Otín, C., Galluzzi, L., Freije, J. M. P., Madeo, F., and Kroemer, G. (2016). Metabolic Control of Longevity. *Cell* 166, 802–821. doi: 10.1016/j.cell.2016.07.031

Lynn, D. A., Dalton, H. M., Sowa, J. N., Wang, M. C., Soukas, A. A., and Curran, S. P. (2015). Omega-3 and -6 fatty acids allocate somatic and germline lipids to ensure fitness during nutrient and oxidative stress in Caenorhabditis elegans. *Proc. Natl. Acad. Sci. U. S. A.* 112, 15378–15383. doi: 10.1073/pnas.1514012112

Maures, T. J., Booth, L. N., Benayoun, B. A., Izrayelit, Y., Schroeder, F. C., and Brunet, A. (2014). Males shorten the life span of C. elegans hermaphrodites via secreted compounds. *Science* 343, 541–544. doi: 10.1126/science.1244160

Min, K. J., Lee, C. K., and Park, H. N. (2012). The lifespan of Korean eunuchs. *Curr. Biol.* 22, R792–R793.

Murphy, C. T., McCarroll, S. A., Bargmann, C. I., Fraser, A., Kamath, R. S., Ahringer, J., et al. (2003). Genes that act downstream of DAF-16 to influence the lifespan of Caenorhabditis elegans. *Nature* 424, 277–283. doi: 10.1038/nature01789

Ntambi, J. M., Miyazaki, M., Stoehr, J. P., Lan, H., Kendziorski, C. M., Yandell, B. S., et al. (2002). Loss of stearoyl–CoA desaturase-1 function protects mice against adiposity. *Proc. Natl. Acad. Sci.* 99:11482. doi: 10.1073/pnas.132384699

O'Rourke, E. J., Soukas, A. A., Carr, C. E., and Ruvkun, G. (2009). C. elegans major fats are stored in vesicles distinct from lysosome-related organelles. *Cell. Metab.* 10, 430–435. doi: 10.1016/j.cmet.2009.10.002

Paquette, A., Wang, D., Jankowski, M., Gutkowska, J., and Lavoie, J.-M. (2008). Effects of ovariectomy on PPARα, SREBP-1c, and SCD-1 gene expression in the rat liver. *Menopause* 15, 1169–75.

Partridge, L., Gems, D., and Withers, D. J. (2005). Sex and Death: what Is the Connection? *Cell* 120, 461–472. doi: 10.1016/j.cell.2005.01.026

Ratnappan, R., Amrit, F. R. G., Chen, S.-W., Gill, H., Holden, K., Ward, J., et al. (2014). Germline signals deploy NHR-49 to modulate fatty-acid β-oxidation and desaturation in somatic tissues of C. elegans. *PLoS Genet.* 10:e1004829. doi: 10.1371/journal.pgen.1004829

Raudvere, U., Kolberg, L., Kuzmin, I., Arak, T., Adler, P., Peterson, H., et al. (2019). g:Profiler: a web server for functional enrichment analysis and conversions of gene lists (2019 update). *Nucleic Acids Res.* 47, W191–W198.

Ruetenik, A., and Barrientos, A. (2015). Dietary restriction, mitochondrial function and aging: from yeast to humans. *Biochim. Biophys. Acta* 1847, 1434–1447. doi: 10.1016/j.bbabio.2015.05.005

Schedl, T., and Kimble, J. (1988). fog-2, a germ-line-specific sex determination gene required for hermaphrodite spermatogenesis in Caenorhabditis elegans. *Genetics* 119, 43–61. doi: 10.1093/genetics/119.1.43

Shi, C., Booth, L. N., and Murphy, C. T. (2019). Insulin-like peptides and the mTOR-TFEB pathway protect Caenorhabditis elegans hermaphrodites from mating-induced death. *Elife* 8:e46413.

Shi, C., and Murphy, C. T. (2014). Mating induces shrinking and death in Caenorhabditis mothers. *Science* 343, 536–540. doi: 10.1126/science.1242958

Shi, C., Runnels, A. M., and Murphy, C. T. (2015). Mating-induced Male Death and Pheromone Toxin-regulated Androstasis. *bioRxiv*. doi: 10.1101/034181

Tusher, V. G., Tibshirani, R., and Chu, G. (2001). Significance analysis of microarrays applied to the ionizing radiation response. *Proc. Natl. Acad. Sci. U. S. A.* 98, 5116–5121. doi: 10.1073/pnas.091062498

Wählby, C., Conery, A. L., Bray, M.-A., Kamentsky, L., Larkins-Ford, J., Sokolnicki, K. L., et al. (2014). High- and low-throughput scoring of fat mass and body fat distribution in C. elegans. *Methods* 68, 492–499. doi: 10.1016/j.ymeth.2014.04.017

Walker, G., Houthoofd, K., Vanfleteren, J. R., and Gems, D. (2005). Dietary restriction in C. elegans: from rate-of-living effects to nutrient sensing pathways. *Mech. Ageing Dev.* 126, 929–937. doi: 10.1016/j.mad.2005.03.014

Ward, S., and Carrel, J. S. (1979). Fertilization and sperm competition in the nematodeCaenorhabditis elegans. *Dev. Biol.* 73, 304–321. doi: 10.1016/0012-1606(79)90069-1

Watts, J. L., and Browse, J. (2002). Genetic dissection of polyunsaturated fatty acid synthesis in Caenorhabditis elegans. *Proc. Natl. Acad. Sci. U. S. A.* 99, 5854–5859. doi: 10.1073/pnas.092064799

Williams, G. C. (1966). Natural Selection, the Costs of Reproduction, and a Refinement of Lack's Principle. *Am. Nat.* 100, 687–690. doi: 10.1086/282461

Zheng, S., Chiu, H., Boudreau, J., Papanicolaou, T., Bendena, W., and Chin-Sang, I. (2018). A functional study of all 40 Caenorhabditis elegans insulin-like peptides. *J. Biol. Chem.* 293, 16912–16922. doi: 10.1074/jbc.ra118.004542

Conflict of Interest: The authors declare that the research was conducted in the absence of any commercial or financial relationships that could be construed as a potential conflict of interest.

frontiers in Cell and Developmental Biology

ORIGINAL RESEARCH
published: 16 June 2021
doi: 10.3389/fcell.2021.693742

Immature Follicular Origins and Disrupted Oocyte Growth Pathways Contribute to Decreased Gamete Quality During Reproductive Juvenescence in Mice

Atsuko Kusuhara[1†], Elnur Babayev[1†], Luhan T. Zhou[1], Vijay P. Singh[2], Jennifer L. Gerton[2] and Francesca E. Duncan[1]*

[1] Department of Obstetrics and Gynecology, Feinberg School of Medicine, Northwestern University, Chicago, IL, United States, [2] Stowers Institute for Medical Research, Kansas City, MO, United States

OPEN ACCESS

Edited by:
Dolores Busso, University of the Andes, Chile

Reviewed by:
Patrick Hannon, University of Kentucky, United States
Marta Tesone, CONICET Instituto de Biología y Medicina Experimental (IBYME), Argentina

***Correspondence:**
Francesca E. Duncan
f-duncan@northwestern.edu

† These authors have contributed equally to this work and share first authorship

Specialty section:
This article was submitted to Molecular and Cellular Reproduction, a section of the journal Frontiers in Cell and Developmental Biology

Received: *12 April 2021*
Accepted: *24 May 2021*
Published: *16 June 2021*

Citation:
Kusuhara A, Babayev E, Zhou LT, Singh VP, Gerton JL and Duncan FE (2021) Immature Follicular Origins and Disrupted Oocyte Growth Pathways Contribute to Decreased Gamete Quality During Reproductive Juvenescence in Mice. Front. Cell Dev. Biol. 9:693742. doi: 10.3389/fcell.2021.693742

Egg quality dictates fertility outcomes, and although there is a well-documented decline with advanced reproductive age, how it changes during puberty is less understood. Such knowledge is critical, since advances in Assisted Reproductive Technologies are enabling pre- and peri-pubertal patients to preserve fertility in the medical setting. Therefore, we investigated egg quality parameters in a mouse model of the pubertal transition or juvenescence (postnatal day; PND 11–40). Animal weight, vaginal opening, serum inhibin B levels, oocyte yield, oocyte diameter, and zona pellucida thickness increased with age. After PND 15, there was an age-associated ability of oocytes to resume meiosis and reach metaphase of meiosis II (MII) following *in vitro* maturation (IVM). However, eggs from the younger cohort (PND 16–20) had significantly more chromosome configuration abnormalities relative to the older cohorts and many were at telophase I instead of MII, indicative of a cell cycle delay. Oocytes from the youngest mouse cohorts originated from the smallest antral follicles with the fewest cumulus layers per oocyte, suggesting a more developmentally immature state. RNA Seq analysis of oocytes from mice at distinct ages revealed that the genes involved in cellular growth signaling pathways (PI3K, mTOR, and Hippo) were consistently repressed with meiotic competence, whereas genes involved in cellular communication were upregulated in oocytes with age. Taken together, these data demonstrate that gametes harvested during the pubertal transition have low meiotic maturation potential and derive from immature follicular origins.

Keywords: aging, puberty, follicle, meiosis, zona pellucida, cumulus cells, oocyte, spindle

INTRODUCTION

Female reproductive aging is associated with a striking reduction in gamete quantity and quality beginning when women reach their mid-thirties, and this contributes to both loss of fertility and endocrine function (Hassold and Chiu, 1985; Speroff, 1994; Armstrong, 2001; Franasiak et al., 2014). Much less is known about how egg quality is impacted at the other end of the age spectrum

because pregnancy in adolescence is avoided in most cultures and societies. However, this need is rapidly emerging in the medical and particularly pediatric oncology setting. Due to clinical advances in diagnostics and therapeutics, more than 80% of children with a malignancy will achieve a 5-year survival, making approximately 1 in 750 a childhood cancer survivor in the United States (Ward et al., 2014). Despite these life-saving improvements, childhood cancer survivors show accelerated aging phenotypes relative to their cancer-free siblings (Green et al., 2009). With regards to reproductive function, survivors are more likely than their siblings to experience infertility (Green et al., 2009; Nielsen et al., 2013). This has fueled the field of Oncofertility—the merging of oncology and fertility—to explore and expand fertility preservation options for men, women, and children (Gracia and Woodruff, 2012; Woodruff, 2015).

For females, standard fertility preservation options include oocyte and embryo banking, but these techniques are not suitable for prepubertal girls. In these populations, technologies such as ovarian tissue cryopreservation (OTC), as well as *ex vivo in vitro* maturation (IVM) can be used (Anderson and Wallace, 2011; Wang et al., 2016; Algarroba et al., 2018). In OTC, ovarian tissue is removed from the patient and cortical strips containing primordial follicles are cryopreserved to later be used for transplantation to restore endocrine function and/or fertility. While ovarian tissue transplantation has resulted in >130 live births worldwide, the knowledge of its success using tissue isolated from prepubertal and adolescent girls is limited but is increasing as the individuals who have stored ovarian tissue are surviving their cancer and reaching the age where they want to restore their reproductive potential (Duncan et al., 2015; Jensen et al., 2017a,b; Takae et al., 2019). *Ex vivo* IVM is an emerging method that can be coupled with OTC to broaden the fertility preservation options for young girls (Revel et al., 2009; Anderson and Wallace, 2011). In this method, immature oocytes are collected *ex vivo* from small antral follicles at the same time that the harvested ovarian tissue is prepared into cortical strips for OTC (Kristensen et al., 2011). These oocytes are then matured *in vitro,* and mature eggs arrested at metaphase of meiosis II (MII) are cryopreserved for the female's future use (Revel et al., 2009). Fertilization of eggs derived from *ex vivo* IVM has resulted in pregnancies and live birth, and mature eggs have been obtained successfully from premenarchal and adolescent girls alongside frozen ovarian tissue (Revel et al., 2003; Uzelac et al., 2015; Fasano et al., 2017). The use of such methods in young females is increasing, and in the past 5 years more than 70% of the participants who have undergone OTC through the Oncofertility Consortium's National Physicians Cooperative were under the age of 18 (Duncan et al., 2015; Armstrong et al., 2018).

Given these trends in fertility preservation, the eggs that normally would not have contributed to physiologic fertility will in fact be used clinically. Thus, there is a critical need to examine egg quality parameters in young females. In fact, compelling evidence already exists that egg quality may be suboptimal at the youngest ages in addition to advanced reproductive age. Many studies show inferior developmental capacity of oocytes obtained from younger, pre-pubertal mammals (Pinkert et al., 1989; Eppig et al., 1992; Revel et al., 1995; Damiani et al., 1996; Khatir et al., 1996; O'Brien et al., 1996, 1997; Ledda et al., 1997; Izquierdo et al., 1999). In addition, girls experience a one to 3 year period of adolescent sterility or subfecundity following menarche, and this phenomenon is evolutionarily conserved (Hartman, 1931). Moreover, the incidence of egg aneuploidy and trisomies in clinically recognized pregnancies exhibit a u- or j-shaped curve, respectively, where the frequency of these events is the highest at both ends of the reproductive spectrum (Hassold and Chiu, 1985; Gruhn et al., 2019). This pattern was also observed in a comprehensive chromosomal screening study of human embryos demonstrating that the incidence of aneuploidy was >40% for women in the early twenties, compared to 20–25% in mid to late twenties (Franasiak et al., 2014). Puberty involves a complex series of maturational events involving the development of the hypothalamic-pituitary-ovarian axis that drives oogenesis and folliculogenesis. Therefore, we hypothesized that puberty is a particularly sensitive window in the development of a high quality gamete and investigated the determinants of egg quality using a mouse model of the pubertal transition.

RESULTS

Characterization of a Mouse Model of the Pubertal Transition

We used a mouse model of the pubertal transition and an experimental paradigm that mimics how gametes are obtained clinically in the fertility preservation setting for young females, whereby oocytes from antral follicles are isolated from unstimulated ovaries and matured *in vitro* to obtain eggs arrested at metaphase stage of meiosis II (MII) (Revel et al., 2009; Abir et al., 2016). In mice, puberty typically occurs more than 20 days after birth (Vandenbergh, 1967; Smitz and Cortvrindt, 2002). Increased gonadotropin-releasing hormone (GnRH) pulse frequency is an important event that marks puberty. In rodents, GnRH is secreted in a pulsatile fashion beginning at PND 5, and the highest GnRH pulse frequencies are observed between PND 40–45 (Prevot et al., 2003). Therefore, we examined gamete quality endpoints in age cohorts of mice spanning puberty: PND 11–15, 16–20, 21–25, 26–30, 31–35, and 36–40. To confirm that these age cohorts spanned this period of development, we examined animal weights and vaginal opening. Growth patterns are an important factor in assessing pubertal timing, and weight increase is associated with puberty (Kennedy and Mitra, 1963). Animal weight increased significantly over the pubertal transition from 8.6 ± 1.8 g on PND 11–15 to 25.3 ± 1.3 g by PND 36–40 ($p < 0.001$, **Figure 1A**). Vaginal opening is often used as an outward manifestation of puberty (Caligioni, 2009). In fact, significantly fewer GnRH pulse frequencies are observed in animals prior to vaginal opening compared to those that are analyzed after vaginal opening, suggesting a tight link between vaginal opening and pubertal status (Sisk et al., 2001). In our model, vaginal opening was first observed in a subset of mice beginning on PND 18 (**Figure 1B**). The percentage of mice exhibiting vaginal opening increased until PND 27, after which point 100% of animals were positive for this phenotype, suggesting that they had reached puberty (**Figure 1B**).

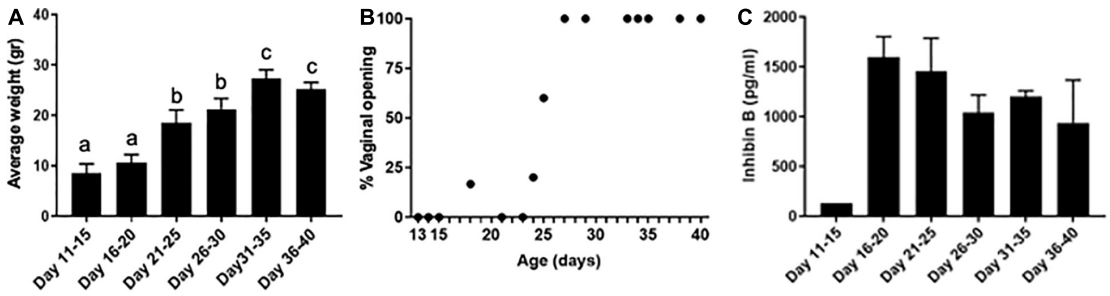

FIGURE 1 | Pubertal transition in mice as characterized by changes in weight, vaginal opening, and inhibin B levels. **(A)** Average mouse weight in different age cohorts was measured across pubertal transition (n = 42, 5—9 mice per age cohort). Error bars represent standard error of the mean (SEM). Columns with different letterheads are significantly different from each other ($p < 0.001$). **(B)** Percent of mice with vaginal opening was tracked at different ages spanning pubertal transition ($n =$ 39). Mice were not tracked longitudinally; instead, mice within each age cohort represented distinct biological replicates and were euthanized immediately following the evaluation of vaginal opening. **(C)** Serum inhibin B levels were measured in mice across pubertal transition ($n = 21$ mice, 3–5 mice per age cohort—one pooled serum sample from 5 mice was tested for PND 11–15, and individual serum samples were used in other age groups).

To further characterize that our age cohorts spanned the pubertal transition, we analyzed serum levels of the gonadal peptide inhibin B (**Figure 1C**). Serum inhibin B levels are a marker of follicular activity which occurs during the pubertal transition, including an increased number of developing follicles and those reaching a later stage of development (Rivier and Vale, 1987; Raivio and Dunkel, 2002). In our model, inhibin B levels were low in PND 11–15 mice (127.3 pg/ml) but increased dramatically in the PND 16–20 cohort (1,595.25 ± 179.32 pg/ml), suggesting that these time points delineate an important transition in the onset of puberty (**Figure 1C**). We also measured estradiol levels and found that they were detectable across the age cohorts. The levels were less than 10 pg/ml and not significantly different across age groups. However, there was a trend of increasing estradiol levels from 3.8 ± 0.5 pg/ml in PND 16–20 mice to 8.2 ± 1.1 pg/ml in PND 26–30 mice.

Oocyte Diameter and Meiotic Competence Increases Across the Pubertal Transition

To determine how the pubertal transition affected oocyte characteristics, we counted the average number of oocytes collected per mouse and measured oocyte diameter and zona pellucida thickness across the age cohorts (**Figure 2A**). Although the pattern was not consistent across all cohorts, there did appear to be a general increase in oocyte yield with increasing age (**Figure 2B**). For example, relative to PND 11–15, significantly more oocytes were collected at PND 21–25 and PND 31–35 (18.3 ± 16.7 oocytes/mouse, 43.7 ± 15.2 oocytes/mouse, and 42.5 ± 11.8 oocytes/mouse, respectively, $p < 0.01$). The ratio of oocytes enclosed in cumulus oocyte complexes to denuded ones upon isolation was similar across cohorts (**Supplementary Figure 1**). There was a clear age-associated increase in oocyte diameter (**Figure 2C**). Average oocyte diameter increased significantly from 65.6 ± 4.7 μm on PND 11–15 to 71.0 ± 4.1 μm on PND 16–20 and 78.4 ± 4.6 μm on PND 21–25 ($p < 0.01$, **Figure 2C**). Oocytes reached maximal diameter on PND 21–25, after which point there was no further increase. To further assess how oogenesis may differ across the pubertal transition, we examined the average thickness of the zona pellucida in oocytes collected from mice in different age cohorts (**Figure 2D**). The zona pellucida is a glycoprotein matrix secreted by the oocyte during its growth phase, and positive correlations between zona thickness and maturation, fertilization, and preimplantation embryo development outcomes have been reported in multiple species (Conner et al., 2005). Zona pellucida thickness increased significantly from 4.4 ± 0.5 μm in oocytes from PND 11–15 mice to approximately 6.0 μm in the cohorts beyond PND 21 (**Figure 2D**, $p < 0.01$).

A key hallmark of gamete quality is the acquisition of meiotic competence or the ability of the oocyte to resume meiosis and reach MII at which stage it can be fertilized. To define the precise time when oocytes achieve meiotic competence, we performed IVM and scored the ability of oocytes isolated from the different age cohorts to progress through meiosis (**Figure 3A**). Oocytes isolated from mice in the PND 11–15 cohort lacked meiotic competence, with only 1.0 ± 2.5% of the cells reaching MII (**Figure 3B** and **Supplementary Figure 2C**). In fact, this age cohort had a significantly higher percentage of cells (54.2 ± 38.5%, $p < 0.05$) arrested in prophase I (GV-intact) relative to the other age cohorts (**Figure 3B** and **Supplementary Figure 2A**). After PND 15, the ability of oocytes to reach MII following IVM increased to between 55.4 and 72.7% in the older age cohorts (**Figure 3B** and **Supplementary Figure 2C**). Although there was no significant difference in meiotic competence among the age cohorts after PND 15, the PND16–20 cohort exhibited the largest variation (**Supplementary Figure 2C**). Therefore, we examined meiotic competence more closely over 2-day intervals during this early period of the pubertal transition. Meiotic competence increased steadily over this period, with 0% of cells reaching MII on PND 14, 39.7 ± 30.5% of cells on PND 16, and 81.5 ± 0.9% on PND 18 (**Figure 3C**). Interestingly, we noted that PND 16 mice naturally segregated into two distinct subgroups by weight, and the heavier group (≥9 g) had more meiotically competent oocytes >50% compared to <10% in mice that weighed <9 g (data not shown).

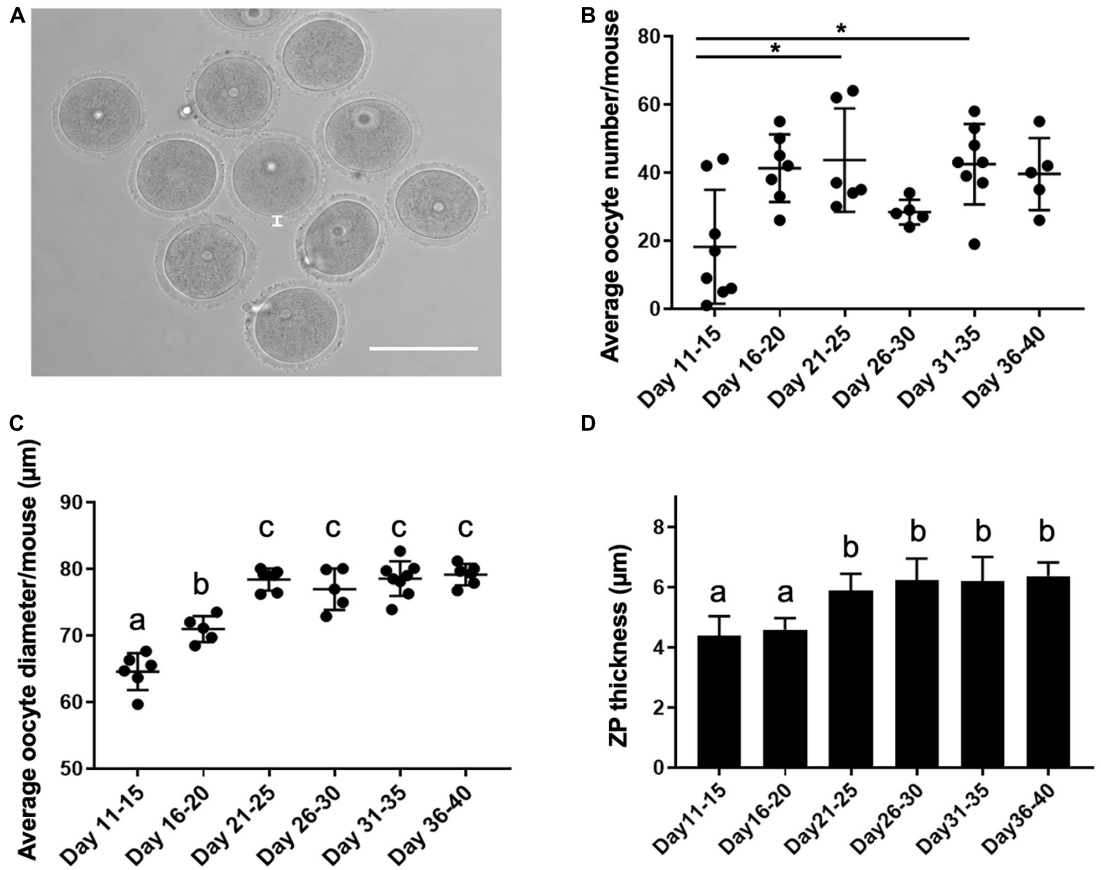

FIGURE 2 | Oocyte characteristics during the pubertal transition as assessed by yield, diameter, and zona pellucida thickness. **(A)** A representative transmitted light image of oocytes isolated from antral follicles. The thickness of the zona pellucida (ZP) is delineated by the white line. The scale bar is 100 μm. **(B)** The average number of oocytes collected per mouse in each age cohort was examined ($n = 36$ mice, 5–8 mice per age cohort). Asterisks denote groups significantly different from each other ($p < 0.01$). **(C)** The average oocyte diameter was calculated for oocytes collected from each mouse in distinct age cohorts ($n = 363$ oocytes, 36 mice, 4–8 mice per age cohort). Groups with different letterheads are significantly different from each other ($p < 0.01$). **(D)** Zona pellucida thickness was measured for a total of 113 oocytes from 7 to 15 mice per age cohort, and the average values are plotted. Error bars represent standard deviation (SD). Column bars with different letterheads are significantly different from each other ($p < 0.01$).

Altered Chromosome Configurations Following IVM Are Highest in Eggs Obtained From Mice During Pubertal Transition Period

Although the majority of cells in mice > PND 15 were able to reach MII following IVM, the quality of the resulting gametes may not be equivalent across the pubertal transition. Chromosome segregation is essential for oocyte meiosis and defects in this process can result in aneuploidy. Therefore, we examined whether chromosome configuration defects were observed in mature eggs across the pubertal transition. To do this, we divided the spindle phenotypes observed in MII eggs into four main categories: (i) normal chromosome alignment along the metaphase plate, (ii) 1 chromosome misaligned on the metaphase plate, (iii) >1 chromosome misaligned on the metaphase plate, and (iv) other configurations such as telophase I (**Figure 4A**). We observed an inverse relationship between the age of mice (PND 15–40) and percentage of eggs with chromosome configuration abnormalities (**Figure 4B**). Although this relationship was weak and not statistically significant ($r = -0.22$, $p = 0.23$), the incidence of overall chromosome abnormalities was significantly higher in the PND 16–20 cohort when compared to the older age cohorts (46.7 ± 30.2% vs. 17.6 ± 14.8%, $p < 0.01$, **Figure 4C**). We further subdivided the types of abnormalities observed and found that the majority of abnormal cells in the PND 16–20 cohort exhibited telophase I configurations, indicative of a cell cycle delay in meiotic progression (**Figure 4D**).

Decreased Egg Quality Parameters Are Associated With Smaller Follicle Diameters and Reduced Cumulus Cell Layers

Coordinated growth between the oocyte and its surrounding somatic cells in the follicle during oogenesis and folliculogenesis is essential for the generation of a high-quality gamete (Hyun et al., 2003; Magalhaes-Padilha et al., 2013). Thus, we wanted to examine whether the differences we observed in egg quality

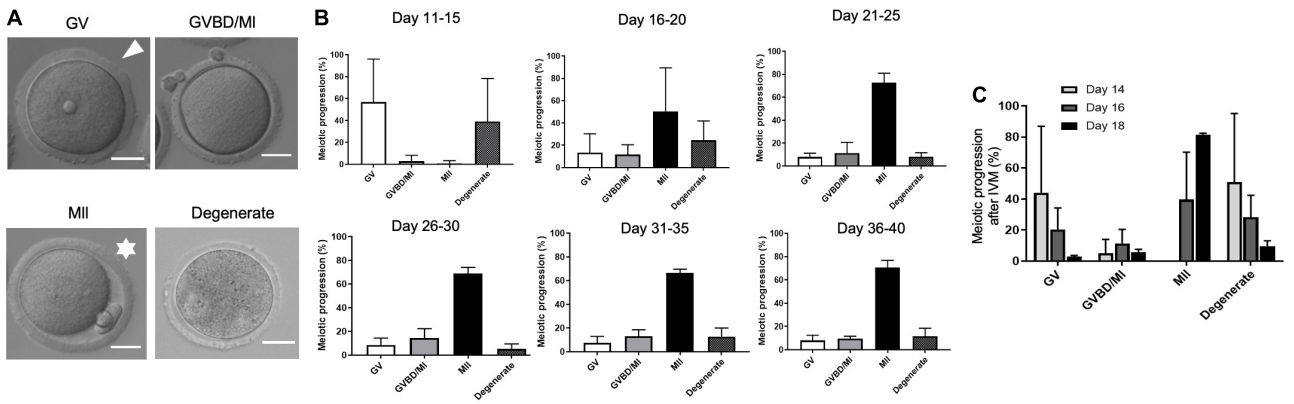

FIGURE 3 | Age-dependent acquisition of oocyte meiotic competence in mice. **(A)** The ability of the oocytes in each age cohort to progress through meiosis following *in vitro* maturation (IVM) was scored according to morphological criteria as visible in the representative transmitted light images. Cells with an intact germinal vesicle (GV; arrowhead) were arrested at prophase I; cells that had extruded a first polar body (asterisks) reached metaphase of meiosis II (MII); cells that lacked a GV or a PB had undergone germinal vesicle breakdown (GVBD) or were at metaphase of meiosis I (MI). Fragmented, lysed, or shrunken cells were classified as degenerated. The scale bars are 25 μm. **(B)** Percentage of oocytes isolated from mice that progressed to specific stages of meiosis following IVM was calculated for each age cohort ($n = 34$ mice, 4–8 mice per age cohort). **(C)** Percentage of oocytes isolated from PND 14, PND 16, and PND 18 mice that progressed to specific stages of meiosis following IVM. MII-arrested eggs are first observed on PND 16. PND, postnatal day.

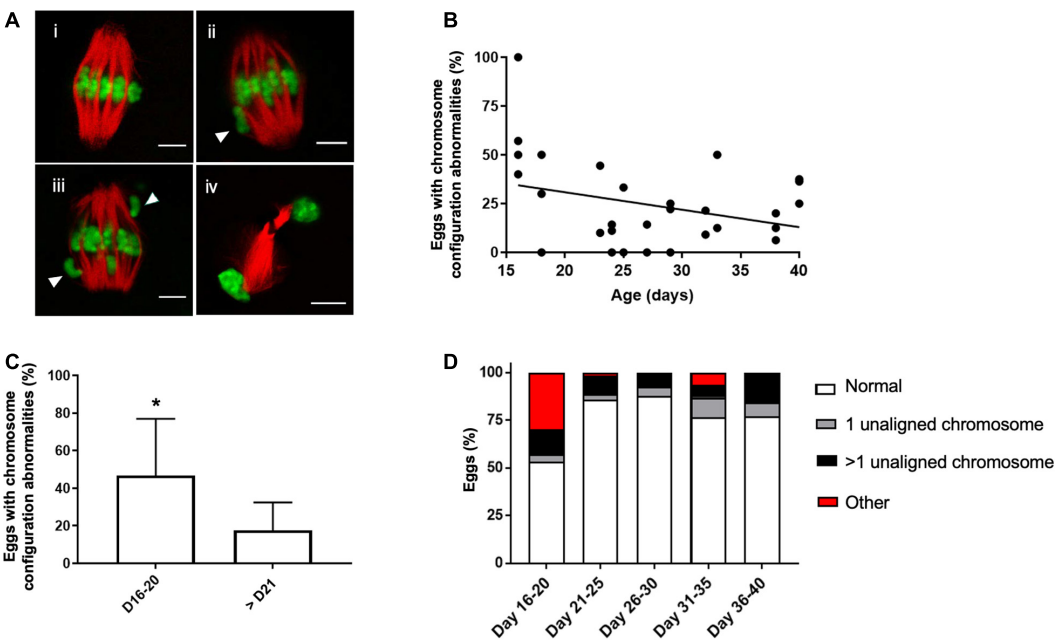

FIGURE 4 | Abnormal meiotic chromosome configurations are more prevalent in the youngest age cohort. **(A)** Representative confocal images of how different chromosome configurations observed in MII eggs were categorized: (i) normal bipolar spindle with chromosomes aligned on the metaphase plate (ii) spindle with 1 misaligned chromosome (arrowhead), (iii) spindle with (>1 misaligned chromosomes (arrowheads), and (iv) a telophase I spindle indicative of cell cycle delay. The scale bar is 5 μm. **(B)** The correlation between mouse age and the percentage of eggs with abnormal chromosome configurations ($n = 244$ eggs from 4 to 8 mice per age cohort). Line was fit to the data ($r = -0.22$, $p = 0.23$). **(C)** The average incidence of chromosomal abnormalities in MII eggs per mouse in the PND 16–20 was plotted relative to the other ages in aggregate. Asterisk denotes significant difference between the groups ($p < 0.01$, $n = 244$ eggs from 4 to 8 mice per age cohort). **(D)** Percentage of MII eggs with specific chromosome configuration abnormalities was plotted in each age cohort according to the criteria established in **(A)**.

across the pubertal transition could have origins at the level of the follicle. Therefore, we examined histological sections of ovarian tissue from mice in each of the age cohorts to identify follicles that contained oocytes with the approximate diameter as those collected directly from ovarian tissue (**Figures 2C, 5A,B**). In formalin fixed paraffin embedded tissue (FFPE) ovarian tissue sections, we observed that oocyte diameter significantly increased from 56.9 ± 3.2 μm on PND 11–15 to 60.8 ± 3.6 μm on PND 16–20 and 70.7 ± 3.8 μm on PND 21–25 ($p < 0.01$). Oocytes reached maximal diameter on PND 21–25,

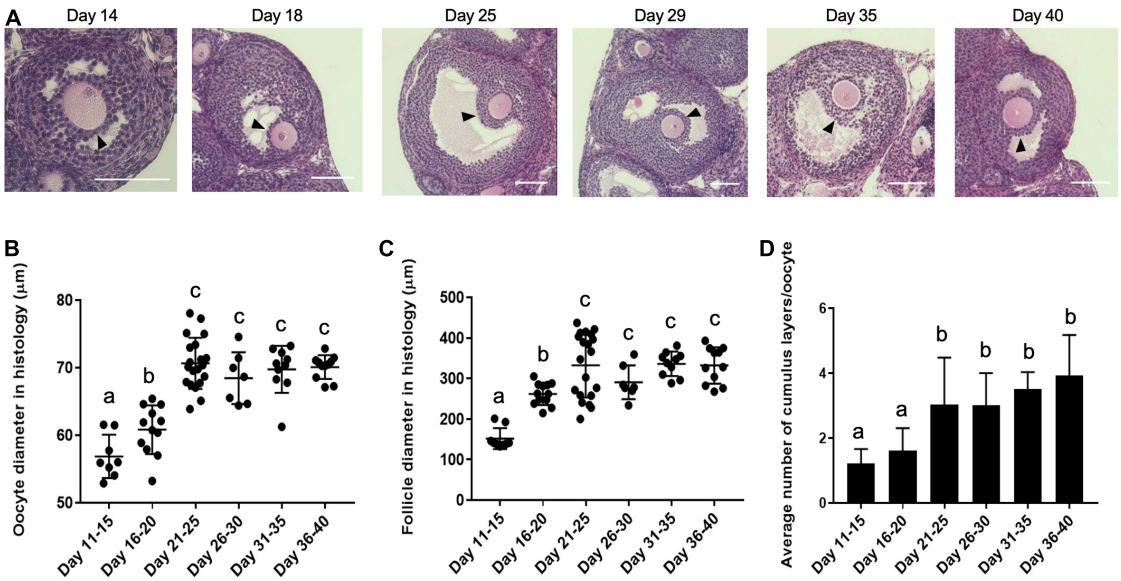

FIGURE 5 | Histological analysis demonstrates that oocytes originate from follicles with increasing diameter and attain more cumulus cell layers as puberty progresses. **(A)** Representative histology sections of antral follicles in mice at different ages across the pubertal transition that contain oocytes of the approximate size as those that were isolated directly from the ovary (**Figure 2C**). The arrowheads highlight the cumulus cell layers. The scale bars are 100 μm. **(B)** The average oocyte diameter in antral follicles in ovarian histological sections in the different age cohorts are shown ($n = 68$ oocytes within ovaries from at least 2 mice per age cohort analyzed, $p < 0.01$). **(C)** The average follicle diameter of the oocytes measured in **(B)** was plotted ($n = 68$ follicles within ovaries from at least 2 mice per age cohort analyzed, $p < 0.01$). **(D)** The average number of cumulus cell layers surrounding the oocytes in the follicles assessed in **(B,C)** were counted in the section containing the oocyte nucleus as shown in **(A)** ($n = 68$ cumulus-oocyte-complexes within ovaries from at least 2 mice per age cohort analyzed). Cohorts with different letterheads are significantly different from each other ($p < 0.01$).

after which point there was no further increase with increasing age (**Figure 5B**). The slight discrepancy in average diameters between freshly isolated oocytes and those observed in FFPE was likely an artifact of tissue fixation and processing. We then measured the corresponding follicle diameter for each oocyte and found that the average follicle diameter increased during the pubertal transition from 152.0 ± 25.8 μm on PND 11–15 to 262.1 ± 27.5 μm on PND 16–20 and 332.7 ± 77.4 μm on PND 21–25 ($p < 0.01$) (**Figure 5C**). The average follicle diameter plateaued after this point. Thus, oocytes from the youngest age cohorts are derived from small antral follicles which likely accounts for their small size.

At the time of antral cavity formation, the somatic component of the follicle differentiates into two cell types—mural granulosa cells and cumulus cells. The cumulus cells directly surround the oocyte and participate in bidirectional communication to support the oocyte's metabolic demands (Tanghe et al., 2002; Kordus and LaVoie, 2017). To investigate whether there were differences in the cumulus cell layers that surrounded oocytes across pubertal transition, we counted the average number of layers in each antral follicle that we measured. An average of 1.61 ± 0.68 layers of cumulus cells surrounded oocytes in follicles from the youngest cohort, whereas this gradually increased to 3.92 ± 1.20 layers of cumulus cells per oocyte in follicles from the oldest cohort ($p < 0.01$) (**Figure 5D**). This histological analysis demonstrates that the increase in oocyte diameter observed across the pubertal transition is associated with a corresponding increase in the average follicle diameter and number of cumulus cell layers surrounding the oocyte. Therefore, the lack of meiotic competence observed in oocytes from PND 11–15 cohort as well as the increase in meiotic defects observed in oocytes from PND 16–20 cohort is likely explained by their origin from small, immature follicles.

Gene Expression Signatures Differentiate Oocytes Based on Meiotic Competence and Quality

To understand the molecular signatures that underlie meiotic competence and egg quality during the pubertal transition, we performed RNA-Seq on oocytes from PND 13, 16, and PND 40 mice (**Figure 6A**). The PND 16 animals were further sub-divided into those that weighed less (<9 g) (PND 16 small) and those that weighed more (≥9 g) (PND 16 large). These ages broadly represent mice with oocytes that lack meiotic competence (PND 13, PND 16 small), oocytes that have meiotic competence but are of suboptimal quality (PND 16 large), and oocytes that have meiotic competence and are of optimal quality (PND 40). Oocytes were collected from 3 mice per condition to create three independent pools for RNA Seq analysis. All samples had a similar number of read counts and tended to have a higher correlation to samples within the same category as compared to between categories (**Supplementary Figures 3A,B**). For each condition, the mean RPKM value for each gene was used for further analysis using DESeq2. Differentially expressed genes from pairwise comparisons between conditions were identified based on two

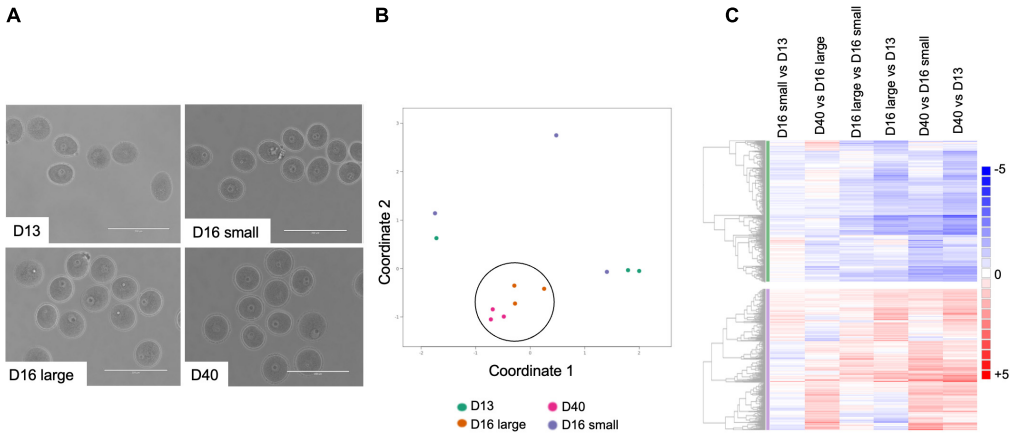

FIGURE 6 | Oocytes collected from mice across the pubertal transition have differential patterns of gene expression. **(A)** Representative transmitted light images of oocytes used for RNASeq analysis from mice at different ages: PND 13, PND 16 small (from small mice), PND 16 large (from large mice), and PND 40. **(B)** Multidimensional scaling (MDS) plot shows oocytes from PND 16 large and PND 40 clustered together (circle) as compared to PND 13 and PND 16 small oocytes. **(C)** Pairwise analysis of differentially expressed genes (fold change +1.5 and −1.5 and adj $p < 0.05$) across different oocyte cohorts shows similar gene expression patterns when comparing PND 16 large with PND 13, PND 40 with PND 16 small and PND 40 with PND 13.

criteria: 1.5-fold change and adjusted *P*-value less than or equal to 0.05. Volcano plots demonstrate that the number of differentially expressed genes becomes more pronounced as the difference in animal age increases, with the greatest number of differentially expressed genes observed between oocytes from PND 40 vs. PND 13 mice (**Supplementary Figures 4A–C** and **Table 1**). The fewest differentially expressed genes were observed when comparing oocytes from PND 16 small vs. PND 13 mice (**Supplementary Figure 4A**) and PND 40 vs. PND 16 large mice (**Supplementary Figure 4E**), suggesting that these groups of oocytes are most similar to each other. Consistent with this, oocytes from PND 16 large and PND 40 mice clustered together relative to PND 13 and PND 16 small mice in a multidimensional scaling (MDS) plot (**Figure 6B**). Pairwise analysis demonstrated similar expression differences between PND 16 large vs. PND 13, PND 40 vs. PND 13, and PND 40 vs. PND 16 small, revealing the gene expression program for maturation (**Figure 6C**). Interestingly, there were differentially expressed genes between oocytes from PND 16 large and PND 16 small mice despite the animals being the same age, presumably reflecting the different maturation of these oocytes (**Figure 6C** and **Supplementary Figure 4D**).

To identify gene expression profiles that underlie meiotic competence, we compared differentially expressed genes between meiotically non-competent (PND 13 and PND 16 small) and competent (PND 16 large and PND 40) oocyte cohorts. These populations are in fact significantly different with respect to their gene expression as evidenced by the volcano plot (**Figure 7A**). Interestingly, when we performed an over representation analysis (ORA), we saw that there is a significant perturbation of several pathways (**Figure 7B**). Based on Gene Ontology analysis, genes involved in phosphatidylinositide 3-kinase, mTOR, and Hippo signaling pathways were predominantly downregulated in the age cohort associated with oocyte meiotic competence (PND 16 large and PND 40) (**Table 2** and **Figure 7C**).

TABLE 1 | Pairwise analysis of differentially expressed genes (fold change +1.5 and −1.5 and adj $p < 0.05$) across different oocyte cohorts.

S. No.	Comparison	Number of upregulated genes	Number of downregulated genes
1	PND16 small vs. PND13	57	138
2	PND16 large vs. PND13	504	1,445
3	PND40 vs. PND13	894	1,861
4	PND16 large vs. PND16 small	178	537
5	PND40 vs. PND16 large	511	252
6	PND40 vs. PND16 small	793	1,313
7	PND 16 large and PND 40 vs. PND 13 and PND 16 small	580	1,603

Oocytes from PND 16 large and PND 40 mice are both meiotically competent, but those from PND 40 mice are of better quality based on their follicular origins, spindle morphology, and chromosome configuration. Thus, comparison of gene expression between these cohorts allows interrogation of pathways required for gamete quality. Gene Ontology analysis revealed that differentially expressed genes involved in cellular communication (i.e., cell periphery, plasma membrane, postsynapse, extracellular region, cell junction, extracellular vesicle, dense core granule) are upregulated in oocytes from PND 40 mice (**Table 3**). Thus, interaction between the oocyte and its surrounding cumulus cells at this stage is fundamental to the development of a high-quality gamete.

DISCUSSION

Advances in pediatric fertility preservation are necessitating a better understanding of egg quality in young girls. Ovarian tissue cryopreservation (OTC) is the mainstay of fertility preservation

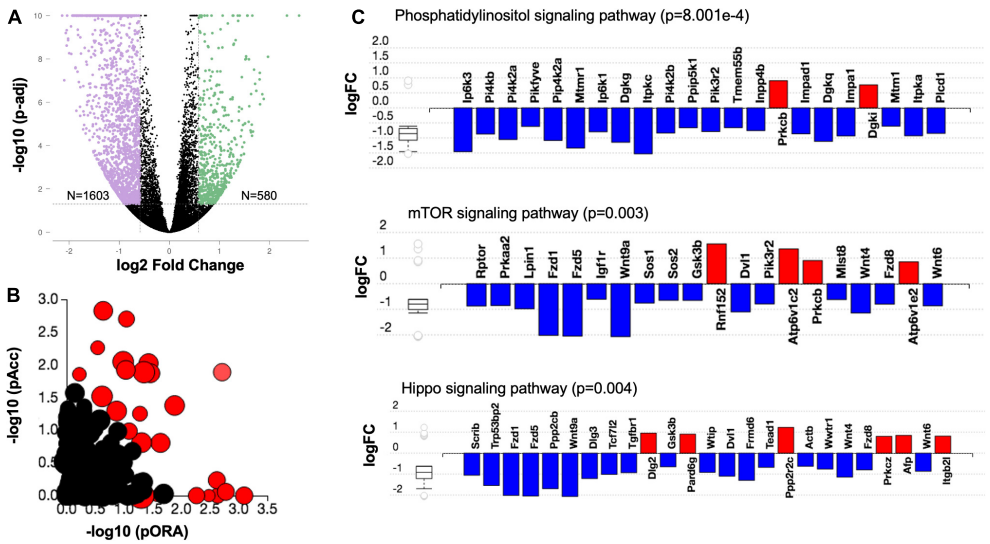

FIGURE 7 | Downregulation of cellular growth pathways in the oocyte is associated with meiotic competence. **(A)** Volcano plot for differentially expressed genes (fold change +1.5 and −1.5 and adjusted $p < 0.05$) between meiotically competent (PND 16 large and PND 40) and non-competent (PND 13 and PND 16 small) oocytes. **(B)** Evidence plot for significantly enriched pathways. Red bubbles represent significant pathways (*p*-value correction factor), and black bubbles represent non-significant pathways. The size of each bubble corresponds to the number of genes affected in that pathway. The horizontal axis shows the inverse log of *p*-value computed using over representation analysis (pORA). The vertical axis shows the inverse log of *p*-value for the accumulated perturbation of the pathway (pAcc). This approach is called the impact analysis and combines the *p*-value into the global *p*-value which is displayed in **Table 1**. **(C)** Differentially expressed genes in Phosphatidylinositol ($p = 8.001e{-}4$), mTOR ($p = 0.003$) and Hippo signaling ($p = 0.004$) pathways in meiotically competent as compared to sub-competent oocytes.

for prepubertal females (Practice Committee of the American Society for Reproductive Medicine, 2019). However, live birth rates following ovarian tissue transplantation are low, and in some cases there is a risk of reseeding malignant cells upon transplantation (Meirow et al., 2008; Donnez et al., 2015; Van der Ven et al., 2016). Therefore, isolation of immature oocytes and follicles from ovarian tissues with subsequent *in vitro* growth and maturation is a vigorous research area. There are also emerging reports of ovarian stimulation, oocyte retrieval, and cryopreservation from pre-pubertal females (Reichman et al., 2012; Azem et al., 2020). Thus, understanding the quality of these gametes is of paramount importance especially because studies in multiple animal species and humans have raised concerns regarding the suboptimal quality of gametes in this population (Franasiak et al., 2014; Duncan, 2017; Gruhn et al., 2019).

Here we report the characterization and use of a mouse model of the pubertal transition to understand egg quality during this period. Our mouse model recapitulated key features of puberty in humans, including increase in weight and rising inhibin B levels (Raivio and Dunkel, 2002). As mice progressed through puberty, there was an increase in the ability of oocytes to undergo meiotic maturation, and there may be a potential association with animal weight as well. This is consistent with previous observations which showed that the developmental competence of *in vitro* matured mouse oocytes is higher in 26-day old compared to 22-day old mice (Eppig et al., 1992). We narrowed down PND 16 as an important developmental switch in the acquisition of meiotic competence in the CD-1 mouse strain. This was an unexpected and interesting finding. There were only 2 mice in each group and thus we chose not to show these data in the current manuscript due to small number of animals. However, it is an important and active area of further investigation. Meiotic competence correlated with the increased size of the follicles and oocytes, and this is consistent with previous studies demonstrating that oocyte and follicular size are important factors in determining oocyte developmental competence during the pubertal transition in mice (Eppig and Schroeder, 1989; Eppig et al., 1992). In pigs, increased follicle size is associated with improved meiotic maturation and developmental competence (Marchal et al., 2002). Interestingly, the size-dependence is also observed *in vitro* because there is an association between increasing size of the antral follicle and improved meiotic and embryo developmental competence in isolated mouse follicles grown in alginate hydrogels (Xiao et al., 2015). Consistent with animal studies, data from humans also show that oocyte diameter needs to reach a certain size, 112 μm in one study (Duncan et al., 2012), before meiotic competence is obtained.

Although the ability of an oocyte to reach MII is a prerequisite to form a gamete that can undergo normal fertilization, just because a gamete extrudes a first polar body does not mean it is of high quality. In fact, we observed a higher incidence of chromosome configuration abnormalities in meiotically competent oocytes from mice early during the pubertal transition compared to older age cohorts. These observations are consistent with what is observed in human where there is an increased incidence of aneuploidy in oocytes and embryos obtained from girls during the pre-pubertal period and in early years of adolescence and the reproductive lifespan (Franasiak et al., 2014; Gruhn et al., 2019). Although chromosome abnormalities are common at both ends of the age spectrum, there are differences in the phenotypes suggesting distinct underlying mechanisms. For example, in the mouse model, our data

TABLE 2 | Top 10 enriched pathways between meiotically competent (PND 16 large and PND 40) and non-competent (PND 16 small and PND 13) oocytes.

Pathway name	*p*-value
Melanogenesis	2.918e–4
Phosphatidylinositol signaling system	8.001e–4
Basal cell carcinoma	0.002
N-Glycan biosynthesis	0.002
mTOR signaling pathway	0.003
Hepatocellular carcinoma	0.003
Glycosaminoglycan biosynthesis—chondroitin sulfate	0.003
Hippo signaling pathway	0.004
Proteoglycans in cancer	0.005
Human papillomavirus infection	0.005

PND, postnatal day.

TABLE 3 | Top 10 GO term summary (cellular components) between PND 40 and PND 16 large oocytes.

Name gene	(DE/All)	*p*-value
Cell periphery	216/3,980	3.700e-5
Plasma membrane	209/3,868	7.000e-5
Plasma membrane part	122/2,073	1.300e–4
Dense core granule	5/16	4.100e–4
Postsynapse	34/445	8.000e–4
Extracellular region	189/3,606	9.100e–4
Synapse part	47/685	9.600e–4
Cell junction	72/1,165	9.800e–4
Synapse	56/859	0.001
Extracellular vesicle	132/2,412	0.001

DE, differential expression, PND, postnatal day.

suggests that cell cycle delays and telophase configurations are predominant abnormalities in oocytes from mice during the pubertal transition. In contrast, loss of chromosome cohesion and premature separation of sister chromatids (PSSC) is the predominant mechanism of aneuploidy associated with advanced reproductive age (Chiang et al., 2010). In humans, meiotic non-disjunction appears to be the predominant mechanism responsible for aneuploidy in women <20 years old compared to PSSC or reverse segregation which increases with advanced age and is the primary mechanism of aneuploidy in older women (Duncan et al., 2012; Gruhn et al., 2019). Thus, while aneuploidy associated with advanced reproductive age appears to be due to a deterioration of pathways related to chromosome segregation (Pan et al., 2008; Duncan et al., 2017), the defects observed in oocytes in juvenescence are likely due to the immature status of the gametes.

In our study, the acquisition of meiotic competence during the pubertal transition was associated with decreased expression of cellular growth pathways, including PI3K, mTOR, and Hippo. The differences in these transcriptomic signatures could be secondary to the antral follicle size differences between age groups, which is not surprising given immaturity of hypothalamic-pituitary-ovarian (HPO) axis in pre-pubertal animals. Although there are many reports highlighting the importance of these signaling pathways in primordial follicle activation (John et al., 2008; Reddy et al., 2008; Kawamura et al., 2013; Sun et al., 2015; Yan et al., 2018), studies examining their role in continued oocyte growth and meiotic maturation are limited. In one study, conditional knockout of mTOR in growing oocytes resulted in severely compromised oocyte developmental competence despite only slight reduction in the number of ovulated oocytes (Guo et al., 2018). Interestingly, the majority of these oocytes demonstrated chromosome configuration defects in meiosis I where telophase I configuration was the predominant abnormality. These findings along with the results of our study point to the role of these growth pathways beyond early folliculogenesis.

In many cells, there is a direct relationship between cell size and cell cycle (Goranov et al., 2009), with growth and cell cycle progression being highly intertwined (Jorgensen and Tyers, 2004). Inhibition of cell growth leads to cell cycle arrest (Temin, 1971; Pardee, 1974; Prescott, 1976; Jorgensen and Tyers, 2004) and activation of growth pathways drives cell cycle progression (Backman et al., 2002; Rupes, 2002; Saucedo and Edgar, 2002). Mitotic cells enforce critical cell size thresholds at G1/S and/or G2/M phase transitions (Shields et al., 1978; Dolznig et al., 2004; Jorgensen and Tyers, 2004). Similar mechanisms might be at play in oocytes. Oocyte growth is associated with the accumulation of cell cycle proteins including Cyclin B, $p34^{CDC2}$ and CDC25 (Chesnel and Eppig, 1995; Kanatsu-Shinohara et al., 2000), and the threshold amount of these proteins is thought to be needed for meiotic progression. There is also an association between the oocyte size and meiotic competence (Duncan et al., 2012). Thus, the observed association of decreased expression of genes involved in growth pathways with oocyte meiotic competence may reflect that this population of oocytes has reached a critical size threshold and has accumulated the necessary molecules to undergo meiosis. Therefore, these growth pathways are downregulated as the oocyte diverts resources from growth to support downstream processes of meiotic maturation, fertilization, and preimplantation embryo development.

Although oocyte meiotic progression was similar across ages following PND 16, the quality of the gametes was not because there were fewer chromosome abnormalities in oocytes from the older age cohorts. There appears to be fundamental biological differences in follicles that occur with age because even in human, the same stage follicles obtained from pre-pubertal girls show compromised *in vitro* growth potential compared to those isolated from adults (Anderson et al., 2014). In our mouse model, we demonstrated that oocytes from younger mice come from smaller antral follicles with fewer cumulus cell layers relative to the older mice. Moreover, genes that regulate cellular communication are differentially expressed when comparing oocytes from PND 16 large and PND 40 cohorts even though oocytes from both populations of mice are meiotically competent. This highlights the potential mechanism of quality difference between gametes obtained during the pubertal transition and from adults.

Communication between the oocyte and cumulus-granulosa cells is pivotal for oocyte growth, metabolism, and maintenance of meiotic arrest (Ackert et al., 2001; Eppig et al., 2005;

Sugiura et al., 2005; Su et al., 2008; Kidder and Vanderhyden, 2010; Wigglesworth et al., 2013; Dumesic et al., 2015; El-Hayek and Clarke, 2015; El-Hayek et al., 2018). Despite having comparably high meiotic maturation rate, oocytes with thicker cumulus cell layers appear to have higher blastocyst development rate in mice (Zhou et al., 2014). We also noted that the ZP was thinner in younger mice and increased throughout the pubertal transition. The ZP is important for mediating bi-directional communication between the oocyte and its surrounding granulosa cells via transzonal projections (TZPs) and associated gap junctions. The increase in zona thickness and increased expression of cellular communication genes that occurs coincidently with animal age across the pubertal transition underscores the potential important role of transzonal projections (TZPs) in determining gamete quality during this period. Thus, impaired bidirectional communication between the oocyte and granulosa cells may be shared mechanisms of reduced gamete quality at both ends of the aging spectrum, since TZP number and function is decreased in reproductively old mice (El-Hayek et al., 2018).

In summary, our work demonstrates that the pubertal transition in female mice is associated with suboptimal gamete quality. In juvenescence, insufficiently activated growth pathways or cellular communication with surrounding somatic cells appear to be the predominant mechanisms responsible for poor gamete quality. This is in contrast to reproductively old mice where advanced age is associated with perturbation of degradation of mRNAs and altered expression of genes important in spindle formation, kinetochore-microtubule attachment, and chromosome segregation (Pan et al., 2008). Our findings have important translational implications. For example, age and/or weight of the pediatric patient undergoing fertility preservation may have prognostic value for future reproduction that may help clinicians better counsel patients and develop appropriate treatment plans. In addition, the non-invasive assessment of meiotic spindles using the PolScope (Moon et al., 2003; Konc et al., 2004; Rama Raju et al., 2007) may aid in selection through distinguishing morphologically mature eggs with polar bodies that have cell cycle abnormalities (i.e., telophase I). We can also use our results to improve clinical IVM strategies. C-type natriuretic peptide (CNP) pretreatment of immature oocytes from PCOS patients before IVM was previously shown to improve maturation rates and embryo development (Sanchez et al., 2019). CNP maintains the oocytes in a protracted period of meiotic arrest via activation of the NPR2 receptor (Gilchrist et al., 2016; Sugimura et al., 2018) and likely improves cytoplasmic maturation by allowing more time for the accumulation of factors necessary to support meiosis and early embryo development. However, stimulation of growth pathways in addition to the maintenance of meiotic arrest may be necessary to further improve IVM outcomes, and this can be combined with the development of oocyte diameter thresholds to assess meiotic competency. Moreover, the elucidation of molecular mechanisms regulating the switch from oocyte growth to the acquisition of meiotic competence and investigating whether there is an active mechanism of suppression of these growth pathways will provide important clues for our understanding of oocyte maturation.

MATERIALS AND METHODS

Animals

Reproductively adult CD-1 male and female mice were obtained from Envigo (Indianapolis, IN) and used to establish an in-house breeding colony. Mice were maintained in a temperature-, humidity-, and light- (14 h light:10 h darkness) controlled barrier facility within Northwestern University's Center of Comparative Medicine. Mice were provided with food and water *ad libitum*. Diet formulated to exclude soybean meal, which minimizes the presence of isoflavones, the primary type of phytoestrogen was used (Teklad Global irradiated 2916 chow: Envigo, Madison, WI). CD-1 female pups in the following aged cohorts that spanned the pubertal transition were obtained from the breeding colony: postnatal day (PND) 11–15, 16–20, 21–25, 26–30, 31–35, and 36–40. A total of 58 mice were used in this study, with between 7 and 15 mice used in each age cohort. Prior to euthanasia, mice were weighed, and the pubertal status of each animal was verified by visual analysis of the vaginal opening as described previously (McLean et al., 2012). All experiments were performed in accordance with the National Institutes of Health Guidelines for Care and Use of Laboratory Animals and under protocols approved by the Northwestern University Institutional Animal Care and Use Committee (IACUC).

Hormone Assays

Serum estradiol (E2) and inhibin B levels were assessed by the University of Virginia's Center for Research in Reproduction—Ligand Assay and Analysis Core. All blood samples were drawn from the inferior vena cava, clotted, and centrifuged. Serum was stored at −80°C until hormone analyses. Estradiol concentrations were determined using Mouse/Rat Estradiol ELISA kit (Calbiotech, El Cajon, CA), and the intraassay coefficient of variation (CV) was 6.8% and the interassay CV was 8.9%. Inhibin B concentrations were determined using an Inhibin B (ELISA) kit (AnschLabs, Webster, TX). The intraassay CV was 4.8%, and the interassay CV was 6.7%. Samples and standards for each gonadal hormone assay were run in duplicate. Blood was taken from between 3 and 5 mice in each age cohort. Samples were run for individual animals except in the PND 11–15 cohort where one pooled sample from 5 mice was run due to insufficient volume of blood that can be collected from animals at these young ages.

Oocyte Collection and Imaging

Ovaries were harvested from unstimulated mice (no exposure to gonadotropins) to mimic *ex vivo* IVM in the fertility preservation setting. Cumulus oocyte complexes (COCs) were isolated from the ovaries by poking antral follicles using 25-gauge needles. Collection media was Leibovitz's L-15 medium (Life Technologies, Grand Island, NY, United States) supplemented with 3 mg/ml polyvinylpyrrolidone (PVP) (Sigma-Aldrich Co., St. Louis, MO, United States) and 0.3% penicillin-streptomycin (PS) (Life Technologies, Grand Island, NY, United States). Ten micrometer milrinone was also added to the media to prevent spontaneous meiotic resumption which is an oocyte-specific

specific phosphodiesterase 3 inhibitor that maintains meiotic arrest by inhibiting cAMP degradation (Jensen et al., 2002). Cumulus cells were mechanically removed from the oocytes by gentle pipetting, and denuded oocytes containing intact germinal vesicles (GV) were transferred into media consisting of α-MEM Glutamax (MEM) (Life Technologies, Grand Island, NY, United States) supplemented with 3 mg/ml Bovine Serum Albumin (BSA), 0.5% PS (MEM/BSA/PS), and 10 μM milrinone for short-term culture in a humidified atmosphere of 5% CO_2 in air at 37°C. Oocytes were imaged by brightfield microscopy using a 20x objective on an EVOS FL Auto live imaging microscope system (Life Technologies, Grand Island, NY, United States). Average oocyte diameter measurements were made using the EVOS FL Auto based on two perpendicular measurements from plasma membrane to plasma membrane of each oocyte. The thickness of the zona pellucida was also measured on images taken on the EVOS FL Auto.

In vitro Maturation and Scoring of Meiotic Progression

To initiate synchronous and spontaneous meiotic resumption, oocytes were rinsed through large droplets of L15/PVP/PS to remove milrinone and placed in 1 ml of MEM/BSA/PS. Oocytes were *in vitro* matured for 14–16 h in a humidified atmosphere of 5% CO_2 in air at 37°C. Following IVM, oocytes were evaluated by brightfield microscopy, and their meiotic stage was assessed using established morphological criteria (Treff et al., 2016). In brief, oocytes with a visible nucleus were arrested at prophase of meiosis I in the germinal vesicle (GV)-intact stage. Oocytes without a nucleus or a polar body were considered to have undergone germinal vesicle breakdown (GVBD) or were at metaphase of meiosis I (MI). If polar bodies were visible in the perivitelline space, the oocytes were considered arrested at metaphase of meiosis II (MII). Fragmented, shrunken, or misshapen oocytes were classified as degenerate (D).

Immunofluorescence, Confocal Microscopy, and Spindle Assessment

To assess spindle morphology, oocytes were fixed in 3.8% paraformaldehyde (Electron Microscopy Science Hatfield, PA) in phosphate buffered saline (PBS) containing 0.1% Triton-X-100 for 1 h at 37°C. After washing three times in blocking buffer containing phosphate buffered saline (PBS) containing 0.3% albumin (BSA), 0.01% Tween-20, and 0.02% sodium azide (NaN_3), oocytes were then permeabilized in PBS containing 0.3% BSA, 0.1% Triton-X-100, and 0.02% NaN_3 for 15 min at room temperature. Samples were then washed twice in blocking buffer and microtubules were stained with an alpha tubulin 488-conjugated anti-rabbit primary antibody (11H10; Cell Signaling Technology, Danvers, MA) (1:100 dilution) for 2 h at room temperature. Oocytes were rinsed three times in blocking buffer and then mounted on glass slides in Vectashield containing 4′,6-diamidino-2-phenylindole (DAPI; Vector Laboratories, Burlingame, CA). Oocytes were imaged on a Leica SP5 inverted laser scanning confocal microscope (Leica Microsystems) using a 63X objective and the 405 and 488 nm lasers. For each oocyte, 0.5 μm optical thick sections were taken through the region of the spindle, and stacks or maximum projections were analyzed. Spindle length was measured from pole-to-pole based on tubulin fluorescence using Image J software (National Institutes of Health, Bethesda, MD). Spindles that were oriented perpendicular to the image plane were excluded from the analysis. Chromosome configuration was analyzed and categorized as follows: normal (no misaligned chromosomes), 1 misaligned chromosome on the metaphase plate, >1 misaligned chromosome on the metaphase plate, and other. The other category included cells that were at the incorrect cell cycle stage such as anaphase or telophase.

Histological Analysis

Ovaries were harvested from mice across age cohorts, and the bursa and excess fat were removed. Ovaries were fixed in Modified Davidson's fixative, a combination of 14% ethyl alcohol, 37.5% formalin, 37–39% glacial acetic acid in deionized water (Electron Microscopy Sciences, Hatfield, PA). Ovaries were fixed at room temperature for 6 h with gentle agitation and then transferred to 4°C overnight (∼15 h). Samples were washed and stored in 70% ethanol. Each ovary was processed and dehydrated using an automated tissue processor (Leica Biosystems, Buffalo Grove, IL) and embedded in paraffin wax (Leica EG1160, Leica Biosystems). Ovaries were serial sectioned at a 5 μm thickness, and every fifth section of a ribbon was placed on a separate slide designated for Hematoxylin and Eosin (H&E) staining. Slides were H&E stained using the AutostainerXL (Leica Biosystems) and then imaged using the EVOS FLUO Auto microscope. All sections were examined. Average follicle and corresponding diameter measurements were made within histological images using the EVOS FL Auto software. Only follicles with an oocyte nucleus visible in the center were used for measurements as this represented the mid-point of the follicle. Follicle measurements were based on two perpendicular measurements from basement membrane-to-basement membrane, and oocyte measurements were based off of two perpendicular measurements from plasma membrane-to-plasma membrane. The number of cumulus cell layers surrounding each oocyte in antral follicles were also counted.

RNASeq in Oocytes

Oocytes were collected from four cohorts of mice: PND 13, PND 16 small (mice < 9 g), PND 16 large (mice ≥ 9 g), and PND 40 mice. For each cohort, pooled oocytes were snap frozen in three replicates. Each replicate had 18–45 oocytes. RNA was isolated using RNeasy Plus mini kit (Qiagen, Germany, 74134). cDNA synthesis was performed using NEB Next Ultra II directional RNA library prep kit (New England Biolabs, Ipswich, MA, E7760S) after rRNA depletion (NEB Next rRNA depletion kit, E6310S) for Illumina next generation sequencing (HiSeq-50 bp). Data were analyzed by Rosalind[1], with a Hyper Scale architecture developed by OnRamp BioInformatics, Inc. (San Diego, CA). Additional gene enrichment is available from the following partner institutions: Advaita[2].

[1]https://rosalind.onramp.bio/

[2]http://www.advaitabio.com/ipathwayguide

Statistical Analysis

Statistical analysis was performed using GraphPad Prism software (version 9.0.1 for Mac, GraphPad Software, San Diego, California United States). Categorical and numerical variables were analyzed using one-way ANOVA, Kruskal-Wallis, *t*-test, chi-square, Fisher's exact or Spearmen correlation tests where relevant following normality tests where necessary. $P < 0.05$ was considered statistically significant. Tukey test was used for multiple comparisons following one-way ANOVA.

DATA AVAILABILITY STATEMENT

The data was deposited in Gene Expression Omnibus—GEO accession number is GSE171858 (https://www.ncbi.nlm.nih.gov/geo/query/acc.cgi?acc=GSE171858). Original data underlying this manuscript can also be accessed from the Stowers Original Data Repository at http://www.stowers.org/research/publications/libpb-1617.

ETHICS STATEMENT

The animal study was reviewed and approved by the Northwestern University Institutional Animal Care and Use Committee.

AUTHOR CONTRIBUTIONS

FD, JG, and AK: conceptualization, funding, resources, supervision, and methodology. FD: project administration. AK, VS, FD, and EB: writing. All authors: investigation, formal analysis, validation, visualization, and final approval.

FUNDING

This work was supported by the MS-RSM Program and the Center for Reproductive Health After Disease (P50 HD076188) from the National Centers for Translational Research in Reproduction and Infertility (NCTRI) and the Stowers Institute for Medical Research.

ACKNOWLEDGMENTS

We acknowledge Drs. Eve Feinberg and Teresa Woodruff for insightful discussions concerning this study. We also thank Sarah Wagner for assistance with animal husbandry and Allison Grover for histological processing and sectioning. We acknowledge the Molecular Biology Core at the Stowers Institute for technical assistance with RNASeq.

SUPPLEMENTARY MATERIAL

The Supplementary Material for this article can be found online at: https://www.frontiersin.org/articles/10.3389/fcell.2021.693742/full#supplementary-material

REFERENCES

Abir, R., Ben-Aharon, I., Garor, R., Yaniv, I., Ash, S., Stemmer, S. M., et al. (2016). Cryopreservation of in vitro matured oocytes in addition to ovarian tissue freezing for fertility preservation in paediatric female cancer patients before and after cancer therapy. *Hum. Reprod.* 31, 750–762. doi: 10.1093/humrep/dew007

Ackert, C. L., Gittens, J. E., O'Brien, M. J., Eppig, J. J., and Kidder, G. M. (2001). Intercellular communication via connexin43 gap junctions is required for ovarian folliculogenesis in the mouse. *Dev. Biol.* 233, 258–270. doi: 10.1006/dbio.2001.0216

Algarroba, G. N., Sanfilippo, J. S., and Valli-Pulaski, H. (2018). Female fertility preservation in the pediatric and adolescent cancer patient population. *Best Pract. Res. Clin. Obstet. Gynaecol.* 48, 147–157. doi: 10.1016/j.bpobgyn.2017.10.009

Anderson, R. A., McLaughlin, M., Wallace, W. H., Albertini, D. F., and Telfer, E. E. (2014). The immature human ovary shows loss of abnormal follicles and increasing follicle developmental competence through childhood and adolescence. *Hum. Reprod.* 29, 97–106. doi: 10.1093/humrep/det388

Anderson, R. A., and Wallace, W. H. (2011). Fertility preservation in girls and young women. *Clin. Endocrinol.* 75, 409–419. doi: 10.1111/j.1365-2265.2011.04100.x

Armstrong, A. G., Kimler, B. F., Smith, B. M., Woodruff, T. K., Pavone, M. E., and Duncan, F. E. (2018). Ovarian tissue cryopreservation in young females through the Oncofertility Consortium's National Physicians Cooperative. *Future Oncol.* 14, 363–378. doi: 10.2217/fon-2017-0410

Armstrong, D. T. (2001). Effects of maternal age on oocyte developmental competence. *Theriogenology* 55, 1303–1322.

Azem, F., Brener, A., Malinger, G., Reches, A., Many, A., Yogev, Y., et al. (2020). Bypassing physiological puberty, a novel procedure of oocyte cryopreservation at age 7: a case report and review of the literature. *Fertil. Steril.* 114, 374–378. doi: 10.1016/j.fertnstert.2020.03.009

Backman, S., Stambolic, V., and Mak, T. (2002). PTEN function in mammalian cell size regulation. *Curr. Opin. Neurobiol.* 12, 516–522. doi: 10.1016/s0959-4388(02)00354-9

Caligioni, C. S. (2009). Assessing reproductive status/stages in mice. *Curr. Protoc. Neurosci.* 4:4I. doi: 10.1002/0471142301.nsa04is48

Chesnel, F., and Eppig, J. J. (1995). Synthesis and accumulation of p34cdc2 and cyclin B in mouse oocytes during acquisition of competence to resume meiosis. *Mol. Reprod. Dev.* 40, 503–508. doi: 10.1002/mrd.1080400414

Chiang, T., Duncan, F. E., Schindler, K., Schultz, R. M., and Lampson, M. A. (2010). Evidence that weakened centromere cohesion is a leading cause of age-related aneuploidy in oocytes. *Curr. Biol.* 20, 1522–1528. doi: 10.1016/j.cub.2010.06.069

Conner, S. J., Lefievre, L., Hughes, D. C., and Barratt, C. L. (2005). Cracking the egg: increased complexity in the zona pellucida. *Hum. Reprod.* 20, 1148–1152. doi: 10.1093/humrep/deh835

Damiani, P., Fissore, R. A., Cibelli, J. B., Long, C. R., Balise, J. J., Robl, J. M., et al. (1996). Evaluation of developmental competence, nuclear and ooplasmic maturation of calf oocytes. *Mol. Reprod. Dev.* 45, 521–534. doi: 10.1002/(SICI)1098-2795(199612)45:4<521::AID-MRD15<3.0.CO;2-Z

Dolznig, H., Grebien, F., Sauer, T., Beug, H., and Mullner, E. W. (2004). Evidence for a size-sensing mechanism in animal cells. *Nat. Cell Biol.* 6, 899–905. doi: 10.1038/ncb1166

Donnez, J., Dolmans, M. M., Diaz, C., and Pellicer, A. (2015). Ovarian cortex transplantation: time to move on from experimental studies to open

clinical application. *Fertil. Steril.* 104, 1097–1098. doi: 10.1016/j.fertnstert.2015.08.005

Dumesic, D. A., Meldrum, D. R., Katz-Jaffe, M. G., Krisher, R. L., and Schoolcraft, W. B. (2015). Oocyte environment: follicular fluid and cumulus cells are critical for oocyte health. *Fertil. Steril.* 103, 303–316. doi: 10.1016/j.fertnstert.2014.11.015

Duncan, F. E. (2017). Egg Quality during the Pubertal Transition-Is Youth All It's Cracked Up to Be? *Front. Endocrinol.* 8:226. doi: 10.3389/fendo.2017.00226

Duncan, F. E., Hornick, J. E., Lampson, M. A., Schultz, R. M., Shea, L. D., and Woodruff, T. K. (2012). Chromosome cohesion decreases in human eggs with advanced maternal age. *Aging Cell* 11, 1121–1124. doi: 10.1111/j.1474-9726.2012.00866.x

Duncan, F. E., Jasti, S., Paulson, A., Kelsh, J. M., Fegley, B., and Gerton, J. L. (2017). Age-associated dysregulation of protein metabolism in the mammalian oocyte. *Aging Cell* 16, 1381–1393. doi: 10.1111/acel.12676

Duncan, F. E., Pavone, M. E., Gunn, A. H., Badawy, S., Gracia, C., Ginsberg, J. P., et al. (2015). Pediatric and Teen Ovarian Tissue Removed for Cryopreservation Contains Follicles Irrespective of Age, Disease Diagnosis, Treatment History, and Specimen Processing Methods. *J. Adolesc. Young Adult Oncol.* 4, 174–183. doi: 10.1089/jayao.2015.0032

El-Hayek, S., and Clarke, H. J. (2015). Follicle-Stimulating Hormone Increases Gap Junctional Communication Between Somatic and Germ-Line Follicular Compartments During Murine Oogenesis. *Biol. Reprod.* 93:47. doi: 10.1095/biolreprod.115.129569

El-Hayek, S., Yang, Q., Abbassi, L., FitzHarris, G., and Clarke, H. J. (2018). Mammalian Oocytes Locally Remodel Follicular Architecture to Provide the Foundation for Germline-Soma Communication. *Curr. Biol.* 28:e1123. doi: 10.1016/j.cub.2018.02.039

Eppig, J. J., Pendola, F. L., Wigglesworth, K., and Pendola, J. K. (2005). Mouse oocytes regulate metabolic cooperativity between granulosa cells and oocytes: amino acid transport. *Biol. Reprod.* 73, 351–357. doi: 10.1095/biolreprod.105.041798

Eppig, J. J., and Schroeder, A. C. (1989). Capacity of mouse oocytes from preantral follicles to undergo embryogenesis and development to live young after growth, maturation, and fertilization in vitro. *Biol. Reprod.* 41, 268–276. doi: 10.1095/biolreprod41.2.268

Eppig, J. J., Schroeder, A. C., and O'Brien, M. J. (1992). Developmental capacity of mouse oocytes matured in vitro: effects of gonadotrophic stimulation, follicular origin and oocyte size. *J. Reprod. Fertil.* 95, 119–127.

Fasano, G., Dechene, J., Antonacci, R., Biramane, J., Vannin, A. S., Van Langendonckt, A., et al. (2017). Outcomes of immature oocytes collected from ovarian tissue for cryopreservation in adult and prepubertal patients. *Reprod. Biomed. Online* 34, 575–582. doi: 10.1016/j.rbmo.2017.03.007

Franasiak, J. M., Forman, E. J., Hong, K. H., Werner, M. D., Upham, K. M., Treff, N. R., et al. (2014). The nature of aneuploidy with increasing age of the female partner: a review of 15,169 consecutive trophectoderm biopsies evaluated with comprehensive chromosomal screening. *Fertil. Steril.* 101, 656–663.e1. doi: 10.1016/j.fertnstert.2013.11.004

Gilchrist, R. B., Luciano, A. M., Richani, D., Zeng, H. T., Wang, X., Vos, M. D., et al. (2016). Oocyte maturation and quality: role of cyclic nucleotides. *Reproduction* 152, R143–57. doi: 10.1530/REP-15-0606

Goranov, A. I., Cook, M., Ricicova, M., Ben-Ari, G., Gonzalez, C., Hansen, C., et al. (2009). The rate of cell growth is governed by cell cycle stage. *Genes Dev.* 23, 1408–1422. doi: 10.1101/gad.1777309

Gracia, C., and Woodruff, T. K. (eds). (2012). *Oncofertility Medical Practice*. New York: Springer.

Green, D. M., Kawashima, T., Stovall, M., Leisenring, W., Sklar, C. A., Mertens, A. C., et al. (2009). Fertility of female survivors of childhood cancer: a report from the childhood cancer survivor study. *J. Clin. Oncol.* 27, 2677–2685. doi: 10.1200/jco.2008.20.1541

Gruhn, J. R., Zielinska, A. P., Shukla, V., Blanshard, R., Capalbo, A., Cimadomo, D., et al. (2019). Chromosome errors in human eggs shape natural fertility over reproductive life span. *Science* 365, 1466–1469. doi: 10.1126/science.aav7321

Guo, J., Zhang, T., Guo, Y., Sun, T., Li, H., Zhang, X., et al. (2018). Oocyte stage-specific effects of MTOR determine granulosa cell fate and oocyte quality in mice. *Proc. Natl. Acad. Sci. U. S. A.* 115, E5326–E5333. doi: 10.1073/pnas.1800352115

Hartman, C. G. (1931). ON THE RELATIVE STERILITY OF THE ADOLESCENT ORGANISM. *Science* 74, 226–227. doi: 10.1126/science.74.1913.226

Hassold, T., and Chiu, D. (1985). Maternal age-specific rates of numerical chromosome abnormalities with special reference to trisomy. *Hum. Genet.* 70, 11–17.

Hyun, S. H., Lee, G. S., Kim, D. Y., Kim, H. S., Lee, S. H., Kim, S., et al. (2003). Effect of maturation media and oocytes derived from sows or gilts on the development of cloned pig embryos. *Theriogenology* 59, 1641–1649.

Izquierdo, D., Villamediana, P., and Paramio, M. T. (1999). Effect of culture media on embryo development from prepubertal goat IVM-IVF oocytes. *Theriogenology* 52, 847–861. doi: 10.1016/S0093-691X(99)00177-6

Jensen, A. K., Macklon, K. T., Fedder, J., Ernst, E., Humaidan, P., and Andersen, C. Y. (2017a). 86 successful births and 9 ongoing pregnancies worldwide in women transplanted with frozen-thawed ovarian tissue: focus on birth and perinatal outcome in 40 of these children. *J. Assist. Reprod. Genet.* 34, 325–336. doi: 10.1007/s10815-016-0843-9

Jensen, A. K., Rechnitzer, C., Macklon, K. T., Ifversen, M. R., Birkebaek, N., Clausen, N., et al. (2017b). Cryopreservation of ovarian tissue for fertility preservation in a large cohort of young girls: focus on pubertal development. *Hum. Reprod.* 32, 154–164. doi: 10.1093/humrep/dew273

Jensen, J. T., Schwinof, K. M., Zelinski-Wooten, M. B., Conti, M., DePaolo, L. V., and Stouffer, R. L. (2002). Phosphodiesterase 3 inhibitors selectively block the spontaneous resumption of meiosis by macaque oocytes in vitro. *Hum. Reprod.* 17, 2079–2084. doi: 10.1093/humrep/17.8.2079

John, G. B., Gallardo, T. D., Shirley, L. J., and Castrillon, D. H. (2008). Foxo3 is a PI3K-dependent molecular switch controlling the initiation of oocyte growth. *Dev. Biol.* 321, 197–204. doi: 10.1016/j.ydbio.2008.06.017

Jorgensen, P., and Tyers, M. (2004). How cells coordinate growth and division. *Curr. Biol.* 14, R1014–R1027. doi: 10.1016/j.cub.2004.11.027

Kanatsu-Shinohara, M., Schultz, R. M., and Kopf, G. S. (2000). Acquisition of meiotic competence in mouse oocytes: absolute amounts of p34(cdc2), cyclin B1, cdc25C, and wee1 in meiotically incompetent and competent oocytes. *Biol. Reprod.* 63, 1610–1616. doi: 10.1095/biolreprod63.6.1610

Kawamura, K., Cheng, Y., Suzuki, N., Deguchi, M., Sato, Y., Takae, S., et al. (2013). Hippo signaling disruption and Akt stimulation of ovarian follicles for infertility treatment. *Proc. Natl. Acad. Sci. U. S. A.* 110, 17474–17479. doi: 10.1073/pnas.1312830110

Kennedy, G. C., and Mitra, J. (1963). Body weight and food intake as initiating factors for puberty in the rat. *J. Physiol.* 166, 408–418.

Khatir, H., Lonergan, P., Carolan, C., and Mermillod, P. (1996). Prepubertal bovine oocyte: a negative model for studying oocyte developmental competence. *Mol. Reprod. Dev.* 45, 231–239. doi: 10.1002/(SICI)1098-2795(199610)45:2<231::AID-MRD17<3.0.CO;2-3

Kidder, G. M., and Vanderhyden, B. C. (2010). Bidirectional communication between oocytes and follicle cells: ensuring oocyte developmental competence. *Can. J. Physiol. Pharmacol.* 88, 399–413. doi: 10.1139/y10-009

Konc, J., Kanyo, K., and Cseh, S. (2004). Visualization and examination of the meiotic spindle in human oocytes with polscope. *J. Assist. Reprod. Genet.* 21, 349–353. doi: 10.1023/b:jarg.0000046202.00570.1d

Kordus, R. J., and LaVoie, H. A. (2017). Granulosa cell biomarkers to predict pregnancy in ART: pieces to solve the puzzle. *Reproduction* 153, R69–R83. doi: 10.1530/rep-16-0500

Kristensen, S. G., Rasmussen, A., Byskov, A. G., and Andersen, C. Y. (2011). Isolation of pre-antral follicles from human ovarian medulla tissue. *Hum. Reprod.* 26, 157–166. doi: 10.1093/humrep/deq318

Ledda, S., Bogliolo, L., Calvia, P., Leoni, G., and Naitana, S. (1997). Meiotic progression and developmental competence of oocytes collected from juvenile and adult ewes. *J. Reprod. Fertil.* 109, 73–78. doi: 10.1530/jrf.0.1090073

Magalhaes-Padilha, D. M., Geisler-Lee, J., Wischral, A., Gastal, M. O., Fonseca, G. R., Eloy, Y. R., et al. (2013). Gene Expression During Early Folliculogenesis in Goats Using Microarray Analysis. *Biol. Reprod.* 89:19. doi: 10.1095/biolreprod.112.106096

Marchal, R., Vigneron, C., Perreau, C., Bali-Papp, A., and Mermillod, P. (2002). Effect of follicular size on meiotic and developmental competence of porcine oocytes. *Theriogenology* 57, 1523–1532.

McLean, A. C., Valenzuela, N., Fai, S., and Bennett, S. A. (2012). Performing vaginal lavage, crystal violet staining, and vaginal cytological evaluation for mouse estrous cycle staging identification. *J. Vis. Exp.* 67:e4389. doi: 10.3791/4389

Meirow, D., Hardan, I., Dor, J., Fridman, E., Elizur, S., Ra'anani, H., et al. (2008). Searching for evidence of disease and malignant cell contamination in ovarian tissue stored from hematologic cancer patients. *Hum. Reprod.* 23, 1007–1013. doi: 10.1093/humrep/den055

Moon, J. H., Hyun, C. S., Lee, S. W., Son, W. Y., Yoon, S. H., and Lim, J. H. (2003). Visualization of the metaphase II meiotic spindle in living human oocytes using the Polscope enables the prediction of embryonic developmental competence after ICSI. *Hum. Reprod.* 18, 817–820. doi: 10.1093/humrep/deg165

Nielsen, S. N., Andersen, A. N., Schmidt, K. T., Rechnitzer, C., Schmiegelow, K., Bentzen, J. G., et al. (2013). A 10-year follow up of reproductive function in women treated for childhood cancer. *Reprod. Biomed. Online* 27, 192–200. doi: 10.1016/j.rbmo.2013.04.003

O'Brien, J. K., Catt, S. L., Ireland, K. A., Maxwell, W. M., and Evans, G. (1997). In vitro and in vivo developmental capacity of oocytes from prepubertal and adult sheep. *Theriogenology* 47, 1433–1443. doi: 10.1016/s0093-691x(97)00134-9

O'Brien, J. K., Dwarte, D., Ryan, J. P., Maxwell, W. M., and Evans, G. (1996). Developmental capacity, energy metabolism and ultrastructure of mature oocytes from prepubertal and adult sheep. *Reprod. Fertil. Dev.* 8, 1029–1037. doi: 10.1071/rd9961029

Pan, H., Ma, P., Zhu, W., and Schultz, R. M. (2008). Age-associated increase in aneuploidy and changes in gene expression in mouse eggs. *Dev. Biol.* 316, 397–407. doi: 10.1016/j.ydbio.2008.01.048

Pardee, A. B. (1974). A restriction point for control of normal animal cell proliferation. *Proc. Natl. Acad. Sci. U. S. A.* 71, 1286–1290. doi: 10.1073/pnas.71.4.1286

Pinkert, C. A., Kooyman, D. L., Baumgartner, A., and Keisler, D. H. (1989). In-vitro development of zygotes from superovulated prepubertal and mature gilts. *J. Reprod. Fertil.* 87, 63–66. doi: 10.1530/jrf.0.0870063

Practice Committee of the American Society for Reproductive Medicine. (2019). Fertility preservation in patients undergoing gonadotoxic therapy or gonadectomy: a committee opinion. *Fertil. Steril.* 112, 1022–1033. doi: 10.1016/j.fertnstert.2019.09.013

Prescott, D. M. (1976). The cell cycle and the control of cellular reproduction. *Adv. Genet.* 18, 99–177. doi: 10.1016/s0065-2660(08)60438-1

Prevot, V., Rio, C., Cho, G. J., Lomniczi, A., Heger, S., Neville, C. M., et al. (2003). Normal female sexual development requires neuregulin-erbB receptor signaling in hypothalamic astrocytes. *J. Neurosci.* 23, 230–239.

Raivio, T., and Dunkel, L. (2002). Inhibins in childhood and puberty. *Best Pract. Res. Clin. Endocrinol. Metab.* 16, 43–52. doi: 10.1053/beem.2001.0179

Rama Raju, G. A., Prakash, G. J., Krishna, K. M., and Madan, K. (2007). Meiotic spindle and zona pellucida characteristics as predictors of embryonic development: a preliminary study using PolScope imaging. *Reprod. Biomed. Online* 14, 166–174. doi: 10.1016/s1472-6483(10)60784-5

Reddy, P., Liu, L., Adhikari, D., Jagarlamudi, K., Rajareddy, S., Shen, Y., et al. (2008). Oocyte-specific deletion of Pten causes premature activation of the primordial follicle pool. *Science* 319, 611–613. doi: 10.1126/science.1152257

Reichman, D. E., Davis, O. K., Zaninovic, N., Rosenwaks, Z., and Goldschlag, D. E. (2012). Fertility preservation using controlled ovarian hyperstimulation and oocyte cryopreservation in a premenarcheal female with myelodysplastic syndrome. *Fertil. Steril.* 98, 1225–1228. doi: 10.1016/j.fertnstert.2012.07.1056

Revel, A., Koler, M., Simon, A., Lewin, A., Laufer, N., and Safran, A. (2003). Oocyte collection during cryopreservation of the ovarian cortex. *Fertil. Steril.* 79, 1237–1239. doi: 10.1016/s0015-0282(02)04963-4

Revel, A., Revel-Vilk, S., Aizenman, E., Porat-Katz, A., Safran, A., Ben-Meir, A., et al. (2009). At what age can human oocytes be obtained?. *Fertil. Steril.* 92, 458–463. doi: 10.1016/j.fertnstert.2008.07.013

Revel, F., Mermillod, P., Peynot, N., Renard, J. P., and Heyman, Y. (1995). Low developmental capacity of in vitro matured and fertilized oocytes from calves compared with that of cows. *J. Reprod. Fertil.* 103, 115–120. doi: 10.1530/jrf.0.1030115

Rivier, C., and Vale, W. (1987). Inhibin: measurement and role in the immature female rat. *Endocrinology* 120, 1688–1690. doi: 10.1210/endo-120-4-1688

Rupes, I. (2002). Checking cell size in yeast. *Trends Genet.* 18, 479–485. doi: 10.1016/s0168-9525(02)02745-2

Sanchez, F., Le, A. H., Ho, V. N. A., Romero, S., Van Ranst, H., De Vos, M., et al. (2019). Biphasic in vitro maturation (CAPA-IVM) specifically improves the developmental capacity of oocytes from small antral follicles. *J. Assist. Reprod. Genet.* 36, 2135–2144. doi: 10.1007/s10815-019-01551-5

Saucedo, L. J., and Edgar, B. A. (2002). Why size matters: altering cell size. *Curr. Opin. Genet. Dev.* 12, 565–571. doi: 10.1016/s0959-437x(02)00341-6

Shields, R., Brooks, R. F., Riddle, P. N., Capellaro, D. F., and Delia, D. (1978). Cell size, cell cycle and transition probability in mouse fibroblasts. *Cell* 15, 469–474. doi: 10.1016/0092-8674(78)90016-8

Sisk, C. L., Richardson, H. N., Chappell, P. E., and Levine, J. E. (2001). In vivo gonadotropin-releasing hormone secretion in female rats during peripubertal development and on proestrus. *Endocrinology* 142, 2929–2936. doi: 10.1210/endo.142.7.8239

Smitz, J. E., and Cortvrindt, R. G. (2002). The earliest stages of folliculogenesis in vitro. *Reproduction* 123, 185–202.

Speroff, L. (1994). The effect of aging on fertility. *Curr. Opin. Obstet. Gynecol.* 6, 115–120.

Su, Y. Q., Sugiura, K., Wigglesworth, K., O'Brien, M. J., Affourtit, J. P., Pangas, S. A., et al. (2008). Oocyte regulation of metabolic cooperativity between mouse cumulus cells and oocytes: BMP15 and GDF9 control cholesterol biosynthesis in cumulus cells. *Development* 135, 111–121. doi: 10.1242/dev.009068

Sugimura, S., Yamanouchi, T., Palmerini, M. G., Hashiyada, Y., Imai, K., and Gilchrist, R. B. (2018). Effect of pre-in vitro maturation with cAMP modulators on the acquisition of oocyte developmental competence in cattle. *J. Reprod. Dev.* 64, 233–241. doi: 10.1262/jrd.2018-009

Sugiura, K., Pendola, F. L., and Eppig, J. J. (2005). Oocyte control of metabolic cooperativity between oocytes and companion granulosa cells: energy metabolism. *Dev. Biol.* 279, 20–30. doi: 10.1016/j.ydbio.2004.11.027

Sun, X., Su, Y., He, Y., Zhang, J., Liu, W., Zhang, H., et al. (2015). New strategy for in vitro activation of primordial follicles with mTOR and PI3K stimulators. *Cell Cycle* 14, 721–731. doi: 10.1080/15384101.2014.995496

Takae, S., Lee, J. R., Mahajan, N., Wiweko, B., Sukcharoen, N., Novero, V., et al. (2019). Fertility Preservation for Child and Adolescent Cancer Patients in Asian Countries. *Front. Endocrinol.* 10:655. doi: 10.3389/fendo.2019.00655

Tanghe, S., Van Soom, A., Nauwynck, H., Coryn, M., and de Kruif, A. (2002). Minireview: functions of the cumulus oophorus during oocyte maturation, ovulation, and fertilization. *Mol. Reprod. Dev.* 61, 414–424. doi: 10.1002/mrd.10102

Temin, H. M. (1971). Stimulation by serum of multiplication of stationary chicken cells. *J. Cell Physiol.* 78, 161–170. doi: 10.1002/jcp.1040780202

Treff, N. R., Krisher, R. L., Tao, X., Garnsey, H., Bohrer, C., Silva, E., et al. (2016). Next Generation Sequencing-Based Comprehensive Chromosome Screening in Mouse Polar Bodies, Oocytes, and Embryos. *Biol. Reprod.* 94:76. doi: 10.1095/biolreprod.115.135483

Uzelac, P. S., Delaney, A. A., Christensen, G. L., Bohler, H. C., and Nakajima, S. T. (2015). Live birth following in vitro maturation of oocytes retrieved from extracorporeal ovarian tissue aspiration and embryo cryopreservation for 5 years. *Fertil. Steril.* 104, 1258–1260. doi: 10.1016/j.fertnstert.2015.07.1148

Van der Ven, H., Liebenthron, J., Beckmann, M., Toth, B., Korell, M., Krussel, J., et al. (2016). Ninety-five orthotopic transplantations in 74 women of ovarian tissue after cytotoxic treatment in a fertility preservation network: tissue activity, pregnancy and delivery rates. *Hum. Reprod.* 31, 2031–2041. doi: 10.1093/humrep/dew165

Vandenbergh, J. G. (1967). Effect of the presence of a male on the sexual maturation of female mice. *Endocrinology* 81, 345–349. doi: 10.1210/endo-81-2-345

Wang, X., Gook, D. A., Walters, K. A., Anazodo, A., Ledger, W. L., and Gilchrist, R. B. (2016). Improving fertility preservation for girls and women by coupling oocyte in vitro maturation with existing strategies. *Womens Health* 12, 275–278. doi: 10.2217/whe-2016-0019

Ward, E., DeSantis, C., Robbins, A., Kohler, B., and Jemal, A. (2014). Childhood and adolescent cancer statistics, 2014. *CA Cancer J. Clin.* 64, 83–103. doi: 10.3322/caac.21219

Wigglesworth, K., Lee, K. B., O'Brien, M. J., Peng, J., Matzuk, M. M., and Eppig, J. J. (2013). Bidirectional communication between oocytes and ovarian follicular somatic cells is required for meiotic arrest of mammalian oocytes. *Proc. Natl. Acad. Sci. U. S. A.* 110, E3723–E3729. doi: 10.1073/pnas.1314829110

Woodruff, T. K. (2015). Oncofertility: a grand collaboration between reproductive medicine and oncology. *Reproduction* 150, S1–S10. doi: 10.1530/rep-15-0163

Xiao, S., Duncan, F. E., Bai, L., Nguyen, C. T., Shea, L. D., and Woodruff, T. K. (2015). Size-specific follicle selection improves mouse oocyte reproductive outcomes. *Reproduction* 150, 183–192. doi: 10.1530/rep-15-0175

Yan, H., Zhang, J., Wen, J., Wang, Y., Niu, W., Teng, Z., et al. (2018). CDC42 controls the activation of primordial follicles by regulating PI3K signaling in mouse oocytes. *BMC Biol.* 16:73. doi: 10.1186/s12915-018-0541-4

Zhou, H. X., Ma, Y. Z., Liu, Y. L., Chen, Y., Zhou, C. J., Wu, S. N., et al. (2014). Assessment of mouse germinal vesicle stage oocyte quality by evaluating the cumulus layer, zona pellucida, and perivitelline space. *PLoS One* 9:e105812. doi: 10.1371/journal.pone.0105812

Conflict of Interest: The authors declare that the research was conducted in the absence of any commercial or financial relationships that could be construed as a potential conflict of interest.

frontiers in Cell and Developmental Biology

ORIGINAL RESEARCH
published: 18 June 2021
doi: 10.3389/fcell.2021.667682

Age-Dependent *in vitro* Maturation Efficacy of Human Oocytes – Is There an Optimal Age?

Gilad Karavani[1†], Peera Wasserzug-Pash[2†], Talya Mordechai-Daniel[1], Dvora Bauman[1], Michael Klutstein[2‡] and Tal Imbar[1‡]*

[1] Fertility Preservation Service, Department of Obstetrics and Gynecology, Hadassah Ein Kerem Medical Center and Faculty of Medicine, The Hebrew University of Jerusalem, Jerusalem, Israel, [2] Institute of Biomedical and Oral Research, Faculty of Dental Medicine, The Hebrew University of Jerusalem, Jerusalem, Israel

OPEN ACCESS

Edited by:
Eleonora Napoli,
University of California, Davis,
United States

Reviewed by:
Raquel L. Bernardino,
University of Porto, Portugal
Volker Doetsch,
Goethe Business School, Germany

***Correspondence:**
Tal Imbar
talim@hadassah.org.il

[†] These authors share first authorship

[‡] These authors share last authorship

Specialty section:
This article was submitted to Cellular Biochemistry, a section of the journal Frontiers in Cell and Developmental Biology

Received: 14 February 2021
Accepted: 31 May 2021
Published: 18 June 2021

Citation:
Karavani G, Wasserzug-Pash P, Mordechai-Daniel T, Bauman D, Klutstein M and Imbar T (2021) Age-Dependent in vitro Maturation Efficacy of Human Oocytes – Is There an Optimal Age? Front. Cell Dev. Biol. 9:667682. doi: 10.3389/fcell.2021.667682

In vitro maturation of oocytes from antral follicles seen during tissue harvesting is a fertility preservation technique with potential advantages over ovarian tissue cryopreservation (OTC), as mature frozen and later thawed oocyte used for fertilization poses decreased risk of malignant cells re-seeding, as compared to ovarian tissue implantation. We previously demonstrated that *in vitro* maturation (IVM) performed following OTC in fertility preservation patients, even in pre-menarche girls, yields a fair amount of oocytes available for IVM and freezing for future use. We conducted a retrospective cohort study, evaluating IVM outcomes in chemotherapy naïve patients referred for fertility preservation by OTC that had oocyte collected from the medium with attempted IVM. A total of 133 chemotherapy naïve patients aged 1–35 years were included in the study. The primary outcome was IVM rate in the different age groups – pre-menarche (1–5 and ≥6 years), post-menarche (menarche-17 years), young adults (18–24 years) and adults (25–29 and 30–35 years). We demonstrate a gradual increase in mean IVM rate in the age groups from 1 to 25 years [4.6% (1–5 years), 23.8% (6 years to menarche), and 28.4% (menarche to 17 years)], with a peak of 38.3% in the 18–24 years group, followed by a decrease in the 25–29 years group (19.3%), down to a very low IVM rate (8.9%) in the 30–35 years group. A significant difference in IVM rates was noted between the age extremes – the very young (1–5 years) and the oldest (30–35 years) groups, as compared with the 18–24-year group ($p < 0.001$). Importantly, number of oocytes matured, percent of patients with matured oocytes, and overall maturation rate differed significantly ($p < 0.001$). Our finding of extremely low success rates in those very young (under 6 years) and older (≥30 years) patients suggests that oocytes retrieved during OTC prior to chemotherapy have an optimal window of age that shows higher success rates, suggesting that oocytes may have an inherent tendency toward better maturation in those age groups.

Keywords: *in vitro* maturation, ovarian tissue cryopreservation, fertility preservation, women age, oocyte

INTRODUCTION

Cryopreservation of ovarian cortical tissue followed by auto-transplantation has emerged as a promising fertility preservation option (Feigin et al., 2007). Immature oocytes, usually in the germinal vesicle (GV) stage can be found during ovarian tissue handling (Revel et al., 2009; Gruhn et al., 2018) and the ability for maturation *in vitro* and cryopreservation as mature oocytes, provides an additional option for fertility preservation (Chian et al., 2013).

In vitro maturation (IVM) of oocytes from antral follicles seen during tissue harvesting is a fertility preservation technique with potential advantages over ovarian tissue cryopreservation (OTC). Although not well established, IVM is believed to be feasible even in the pediatric age group. A mature frozen and later thawed oocyte used for fertilization might serve as a safer option than re-implantation of ovarian cortex tissue, posing decreased risk of malignant cells re-seeding. In our previously published work, we demonstrated that IVM performed following OTC in fertility preservation patients, even in pre-menarche girls, yields a fair amount of oocytes available for IVM and freezing for future use. However, in the very young age group (under 6 years) there are substantially decreased maturation rates, making this procedure invaluable in this age group (Karavani et al., 2019).

The human age-specific fertility rate follows an inverted u shape curve: beginning to rise with puberty (usually marked by the occurrence of menarche), reaching a peak around the age of 30 years, followed by a decline, beginning around the age of 35 toward significant low maturity and fertility rate in the early 40s and later (Hawkes and Smith, 2010). A similar trend was observed for euploid oocyte rate across reproductive lifespan with a peak of euploid oocyte rate around the age of 25 (Gruhn et al., 2019). However, the rate of oocyte maturation capability as related to age has yet to be analyzed. Of important note is the fact that oocyte maturation capability is not necessarily linked to aneuploidy, and aneuploid oocytes can still mature.

As resources are limited and patients and their families are often required to fund the fertility preservation process, it is of need to optimize and personalize consultation regarding the success rate of IVM attempt in oocytes retrieved during OTC, especially considering the fact that an ovarian tissue with potential future use has already been preserved during the process.

Herein, we aimed to study the human age-specific oocytes maturation ability in naïve human oocytes collected from media of ovarian cortex pieces during fertility preservation procedures in order to define the age groups in which IVM should be attempted following OTC.

MATERIALS AND METHODS

Study Population

Our study cohort consisted of female patients aged 1–35 years, referred to our fertility preservation clinic between 2003 and 2020. Patients for whom data regarding cancer diagnosis, chemotherapy, and OTC related data was available were included in the study. While those chemotherapy and radiotherapy exposed patients, and patients for which oocytes were not found in the medium following OTC (and therefore IVM was not performed) were excluded. Counseling regarding fertility preservation was done in a multidisciplinary consultation that included an oncologist, pediatric hematologist and reproductive specialist, as well as a coordinating nurse and social worker. Female patients under 18 years of age were consulted with parental presence. After obtaining informed consent, patients who decided to freeze ovarian tissue underwent partial/complete laparoscopic oophorectomy. In our country, OTC is reimbursed by the national health insurance and therefore does not require out of pocket coverage. The primary outcome were the overall and mean IVM rates in each age group.

Data Collection

Data was collected from patients' electronic medical records and from the IVF laboratory database. Parameters retrieved included: demographic and clinical data; cancer diagnosis; age at diagnosis; treatment with chemotherapy and its timing with regard to OTC; OTC procedure related information (partial or complete oophorectomy) and IVF laboratory data – including OTC (number of ovarian tissue ampules cryopreserved); oocytes retrieval and the IVM process and outcomes with emphasis given to the assessment of number of matured oocytes following IVM, overall and per patient IVM rate according to age groups and percent of patient with at least one matured oocyte following IVM.

Ovarian Tissue Cryopreservation Procedure

The OTC procedure done in our center includes the removal of the entire (complete oophorectomy) or most of the ovary (partial oophorectomy) in a laparoscopic procedure. The tissue is then placed on ice in Leibovitz L-15 medium (GIBCO-BRL, Paisley, United Kingdom) and transferred immediately to the adjacent IVF laboratory for tissue examination and processing. In some cases, predominantly younger patients, insertion of a venous access device (port-a-cath) or bone-marrow aspiration is performed following the oophorectomy. In the case of normal post-operative course, discharge is customarily 24 h post procedure. Freezing of ovarian tissue has previously been described in the literature (Meirow et al., 1999) and performed in a similar fashion in our medical center. Briefly, ovarian cortex is carefully separated from the medulla in a specific media using sterile scissors. The tissue is then cut into 5-mm^3 stripes, that are transferred to pre-cooled freezing medium containing 1.5 M dimethyl sulfoxide (DMSO) and 0.1 M sucrose. Each fragment is then placed in a 2 ml cryovial containing a cryoprotectant medium (sucrose, ethylene glycol, and serum substitute supplement) and processed using a slow freezing protocol in a programmable freezing machine (Kryo 360, Planer, United Kingdom). The frozen vials, each containing five cortex slices, are then stored in liquid nitrogen.

Cumulus Oocyte Complexes Collection From the Media and Cortex

Following the cortex dissection and cryopreservation, the remaining medium is scanned for the presence of follicles and oocytes prior to disposal. Additionally, aspiration of antral follicles observed on the ovarian surface is performed under a dissecting microscope using a 1-mL syringe and a 19-gage needle prior to cryopreservation. Follicles found in the media and aspirated follicles are flushed with HEPES-buffered human tubal fluid (HTF) medium (Irvine Scientific, Santa Ana, CA, United States) containing 10% synthetic serum supplement (SSS; Irvine Scientific). All cumulus oocyte complexes collected are incubated in P1 medium (Irvine Scientific) supplemented with 10% SSS, at 37°C in 90% N_2, 5% CO_2, and 5% O_2.

In vitro Maturation

The IVM technique in our medical center has been previously reported (Karavani et al., 2019) and will be briefly described. IVM was performed on GV oocytes using Sage medium (Al-rad medical, Nes Ziona, Israel) supplemented with 0.075 IU/mL luteinizing hormone (LH) and 0.075 IU/mL follicle stimulating hormone (FSH) overnight. SAGE IVM culture media was used for the incubation of Cumulus-oocyte complexes, and 24-h later denudation of oocytes was performed. Additional 24 h incubation with fresh SAGE IVM culture media was applied for those oocytes which did not reach maturity. Finally, Matured MII oocytes were vitrified using Sage protocol.

Study Age Groups

Patients included in the study (1–35 years) were divided into six groups, according to age at OTC. The pre-menarche patients were allocated to one of two groups – those under 6 years and those 6 years or older, as previous studies (Karavani et al., 2019; Fouks et al., 2020) found differences in IVM efficacy between these age groups. Post-menarche patients were divided into groups using 5-year intervals. Hence, the six age groups for this study were: (1) 1–5 years; (2) 6 years to menarche; (3) menarche to 17 years; (4) 18–24 years; (5) 25–29 years; (6) 30–35 years. The OTC and IVM outcomes were compared between each group. Additionally, statistical analysis was performed on the entire study cohort to evaluate possible parameters associated with the number of oocytes matured and the mean IVM rate per patient.

The Institutional ethical review board approval was received for this study (IRB 0288-16-HMO) by the Human Research Ethics Committees of the Hadassah Hebrew University Medical Center, Jerusalem, Israel.

Statistical Analysis

Patient characteristics were described as proportions for categorical variables and the significance between groups was tested using the Fisher's exact test. For quantitative variables [presented as mean ± standard deviation (SD)], the comparison between independent variables of the six study groups was performed using the Kruskall–Wallis test. Comparison between paired groups for significant difference in the IVM rate parameter was done using the Tukey's Studentized Range (HSD) test. Association of the patients' age and the *in vitro* maturation rate was tested using the Pearson correlation coefficient ("*r*") for the 1–17 years and the 18–35 years age groups separately.

The ANCOVA analyses were applied to assess the effect of several parameters on the continuous dependent variables of mean IVM rate and number of oocytes matured using IVM. All tests applied were two-tailed, with a p-value of <0.05 considered statistically significant. SAS Version 9.4 (SAS Institute, Cary, NC, United States) software was used for statistical analysis.

RESULTS

Study Population

A total of 202 patients were referred for fertility preservation by OTC in our fertility preservation unit, with planned attempted IVM process in cases of oocytes retrieved from the medium or the ovarian tissue. Following OTC, oocytes were retrieved and IVM was performed for 170 of 202 patients (87.0%), for which oocytes were available following retrieval from the medium. Thirty-seven patients received chemotherapy prior to OTC (21.8%) and were subsequently excluded, with a total of 133 patients (78.2%) being eligible and included in the final analysis. Age range was between 1 and 35 years, with a mean age of 17.15 ± 7.8 years [median 17 (IQR 10.5) years]. The most common indication for fertility preservation was diagnosis of hematologic conditions (34.6%), followed by sarcoma (30.8%), carcinoma and other solid tumors (24.1%), and non-oncological conditions (10.5%) (genetic, autoimmune, etc.). The mean age of menarche was 12.9 years. Oocytes were successfully matured in 68.4% (91/133) of patients, with an overall IVM rate for the entire study cohort being 25.0% (342/1370).

Comparison of OTC Indication and Data According to Age Groups

The types of diagnoses leading to OTC in the patients included in the study are presented in **Table 1**. Solid tumors and sarcomas were the common cause for fertility preservation in the younger age group, prior to menarche (65%). This trend changes toward sarcomas and hematologic cancers from the age of menarche through 25 years of age (79.4%). Hematologic cancers are still common until the age of 30 (50%), but decline thereafter leaving solid tumors, mainly breast cancer, as the leading cause of fertility preservation in the over 30 years age group.

Throughout all age groups, nearly seventy percent of the patients underwent total unilateral oophorectomy, with different rates of partial oophorectomy ($p = 0.002$), the lowest being in the age extremes [1–5 years (23.1%) and 25–35 years (4%)].

OTC Results and IVM Outcomes in the Different Age Groups

Ovarian tissue cryopreservation procedure results in each age group are presented in **Table 2**. The number of ampules with ovarian cortex tissue preserved per patient differed significantly with age ($p < 0.001$), showing an increased number of ampules

TABLE 1 | Comparison of basic characteristics of the study population according to age groups (n = 133).

	1–5 years (n = 13)	6 years-menarche (n = 27)	Menarche-17 years (n = 35)	18–24 years (n = 33)	25–29 years (n = 14)	30–35 years (n = 11)	p-value
Age (years)	4.2 ± 1.4	10.3 ± 1.6	15.5 ± 1.4	20.4 ± 2.0	26.9 ± 1.2	32.5 ± 1.8	
Type of malignancy							<0.05[a]
Hematologic	0	7 (25.9%)	15 (42.9%)	15 (45.5%)	7 (50.0%)	2 (18.2%)	
Solid/carcinoma	7 (53.8%)	4 (14.8%)	6 (17.1%)	4 (12.1%)	4 (28.6%)	7 (63.6%)	
Sarcoma	3 (23.1%)	12 (44.4%)	13 (37.1%)	11(33.3%)	1 (7.1%)	1 (9.1%)	
Vascular/neurologic/other	3 (23.1%)	4 (14.8%)	1 (2.9%)	3 (9.1%)	2 (14.3%)	1 (9.1%)	
Partial oophorectomy	3 (23.1%)	15 (55.6%)	13 (37.1%)	8 (24.2%)	1 (7.1%)[b]	0[b]	0.002

Data are given as mean ± SD, n (%) or n/N (%).
[a] *Tukey's Studentized Range test showed a significant difference only between the 1–5 years and the menarche-17 years groups.*
[b] *Tukey's Studentized Range test showed a significant difference when compared to the 6 years-menarche group.*

TABLE 2 | Comparison of ovarian tissue cryopreservation and *in vitro* maturation results according to age groups (n = 133).

	1–5 years (n = 13)	6 years-menarche (n = 27)	Menarche-17 years (n = 35)	18–24 years (n = 33)	25–29 years (n = 14)	30–35 years (n = 11)	p-value
No. of ampules preserved[a]	8.2 ± 1.9[b]	10.4 ± 2.6[c]	12.9 ± 2.6	14.2 ± 3.0	14.0 ± 2.8	12.3 ± 3.4	<0.001
No. of oocytes retrieved per patient	9.0 ± 7.0	11.2 ± 6.2	11.4 ± 8.5	10.5 ± 7.4	9.9 ± 11.7	6.0 ± 6.4	0.073
No. of oocytes matured per patient	0.4 ± 0.7[d,e]	2.4 ± 2.4	3.4 ± 3.3	3.6 ± 3.3	2.1 ± 3.5	0.5 ± 0.9[d]	<0.001
No. of patients with matured oocytes	4 (30.8%)[e]	20 (74.1%)	30 (85.7%)	26 (78.8%)	7 (50.0%)	4 (33.3%)	<0.001
Maturation rate per patient (%)	4.6 ± 0.1[d]	23.8 ± 22.2	28.4 ± 21.5	38.3 ± 26.8	19.3 ± 19.3	8.9 ± 12.3[d]	<0.001
Overall maturation rate	5/117 (4.3%)[f]	65/302 (21.5%)	118/398 (29.7%)	118/348 (32.9%)	30/139 (21.6%)	6/66 (9.1%)[g]	<0.001

Data are given as mean ± SD, n (%) or n/N (%).
[a] *Reflecting tissue volume. Each ampule contains 10 slivers of ovarian tissue for grafting.*
[b] *Tukey's Studentized Range test showed a significant difference ($p < 0.001$) when compared to the menarche – 35 years age groups.*
[c] *Tukey's Studentized Range test showed a significant difference ($p < 0.001$) when compared to the menarche – 29 years age groups.*
[d] *Tukey's Studentized Range test showed a significant difference ($p < 0.001$) when compared to the 18–24 years group.*
[e] *Tukey's Studentized Range test showed a significant difference ($p < 0.001$) when compared to the menarche-17 years group.*
[f] *Tukey's Studentized Range test showed a significant difference ($p < 0.001$) when compared to the 6–29 years age groups.*
[g] *Tukey's Studentized Range test showed a significant difference ($p < 0.001$) when compared to the menarche-17 and 18–24 years age groups.*

preserved at advanced patient age, with a significantly lower yield of cortical stripes in the very young (under the age of 6) age group. Interestingly, the number of oocytes found per patient during the procedure is similar throughout all the different age groups (p = 0.073). However, the similar oocytes harvest was not reflected in the total number of oocytes eventually matured and frozen. The oocytes from the youngest age group (1–5 years) demonstrated a low maturation rate, with the mean number of oocytes matured in patients under the age of 6 being only 0.4 with and an overall IVM rate of only 4.6%. The number of mature oocytes and total IVM rate increased with patient age, reaching its peak in the 18–24 age group (3.6 oocytes matured and 38.1% IVM rate). This peak was followed by an abrupt decrease in mean IVM rates in the 25–29 years group (19.3%), down to an extremely low mean IVM rate of 8.9% in the 30–35 years group (**Table 2** and **Figure 1**). In a paired group analysis, corrected to multiple comparisons [Tukey's Studentized Range (HSD) test], a significant difference in IVM rates was noted between the age extremes – the very young (1–5 years) and the oldest (30–35 years) groups as compared with the 18–24 years ($p < 0.001$). Number of oocytes matured, percent of patients with at least one matured oocyte and the overall maturation rate showed a similar pattern with a significant difference between the age groups ($p < 0.001$ for all three parameters) (**Table 2**).

Figures 2A–C presents a cross-sectional association of patient age with the number of oocytes retrieved, matured, and *in vitro* maturation rates. The number of oocytes retrieved showed no significant trend with age (**Figure 2A**), a result consistent with the data presented in **Table 2**. Quadric fit was calculated for the number of mature oocytes retrieved from each patient, presenting negative orientation, with peak at the age of 18.5 (**Figure 2B**). The same process was applied to maturation rates, with the percent of mature oocytes retrieved from total oocytes pool per patient. The quadric equation presented negative orientation for the maturation rates as well, with a peak detected at the age of 18 (**Figure 2C**). To further asses the presence of the increase and subsequent decline of maturation potential, linear correlation between age and number of mature oocytes retrieved and IVM rate was performed for patients aged 1–17 years and aged 18–35 years separately (according to the trend demonstrated throughout the age groups). This analysis showed a significant positive linear correlation between patients aged 1–17 years for both parameters – (r = 0.36 and r = 0.31, p = 0.017 and p = 0.006; respectively), while demonstrating an inverse, negative correlation between age and number of mature oocytes in older patients – the 18–35 year group (r = −0.33 and r = −0.38, p = 0.012 and, p = 0.004; respectively).

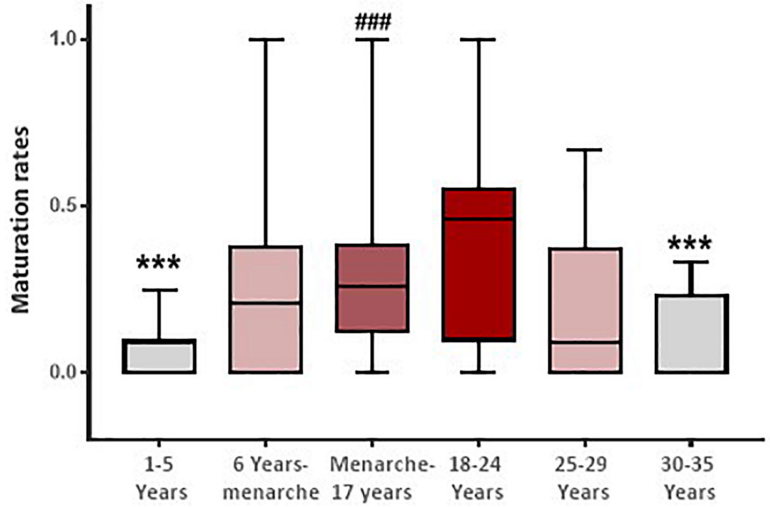

FIGURE 1 | Patient *in vitro* maturation rate following ovarian tissue cryopreservation according to six age groups – (1) 1–5 years; (2) 6 years to menarche; (3) menarche to 17 years; (4) 18–24 years; (5) 25–29 years; and (6) 30–35 years. $^{***}p < 0.001$ when compared to the 18–24 years age group. $^{###}p < 0.001$ when compared to the 1–5 years age group.

Performing ANCOVA analyses, we did not find that type of malignancy, type of oophorectomy (partial/complete), age at diagnosis (as a continuous parameter) or number of oocytes retrieved to be significantly associated with the IVM rate.

DISCUSSION

This study aimed to evaluate the efficacy of *in vitro* maturation following OTC in a large cohort of patients of different ages from infancy to adulthood. The main outcome was the average IVM rate and the overall IVM rate according to age at OTC, using 5-year intervals and consideration of menarche status.

Our results show that while the number of oocytes retrieved during OTC without any prior external gonadotropin priming is similar in the different age groups, the ability to mature these oocytes *in vitro*, is related to patient age. We found that the optimal age for maximal IVM efficacy – represented by the highest IVM rates – is between menarche to 25 years (29–38% maturation rate), while young pre-menarche girls (under 6 years) and women 30 years or older achieve extremely low (<10%) IVM rates This trend was also seen in other parameters, such as the number of matured oocytes, percent of patients with matured oocytes and the overall maturation rate within each age group.

Interestingly, our findings suggest that the potential of immature oocytes to mature *in vitro* continuously improves during childhood, even prior to menarche. Later in life, the loss of *in vitro* maturation potential begins as early the as the mid-twenties with a sharp decline during the first half of the 4th decade of life. These findings imply that ovarian aging as expressed by the ability to mature unstimulated oocytes starts earlier than we know from our clinical results in the IVF settings, whereas pregnancies and live birth rates tend to dramatically drop along the fifth decade of life (Broekmans et al., 2007). These maturation defects can stem from many different biological pathways and processes, which may include: a change in maturation-related ovarian processes that are altered with age (Mara et al., 2020); changes in the composition and behavior of the ovarian tissue with age (Amargant et al., 2020); epigenetic changes that occur in oocytes with age (Wasserzug-Pash and Klutstein, 2019; Wasserzug-Pash et al., 2020) and enhanced ROS (Di Emidio et al., 2014; Babayev et al., 2016) and DNA damage (Marangos et al., 2015; Wasserzug-Pash and Klutstein, 2019) in older oocytes. The results shown here emphasize that aged oocytes begin to deteriorate even before the onset of significant aneuploidy, as demonstrated in mouse oocytes (Merriman et al., 2012).

These results also show that young oocytes have a reduced maturation capacity before the onset of menarche. The improvement of oocyte maturation and quality in the younger age groups may also stem from several possible mechanisms. Although the specific reasons for this phenomenon are unknown, such mechanisms may include epigenetic changes occurring in oocytes with age (Wasserzug-Pash and Klutstein, 2019), and differential gene expression with age (Reyes et al., 2017). These finding may also imply that handling and culturing of oocytes from infants and older women should be managed through a different IVM technique and not the standard, widely used laboratory IVM protocol, with consideration of the different physiology and mechanisms involved in oocyte maturation in these age groups. It should be mentioned that the properties and behavior of oocytes in very young ages are an under-studied subject that merits more attention.

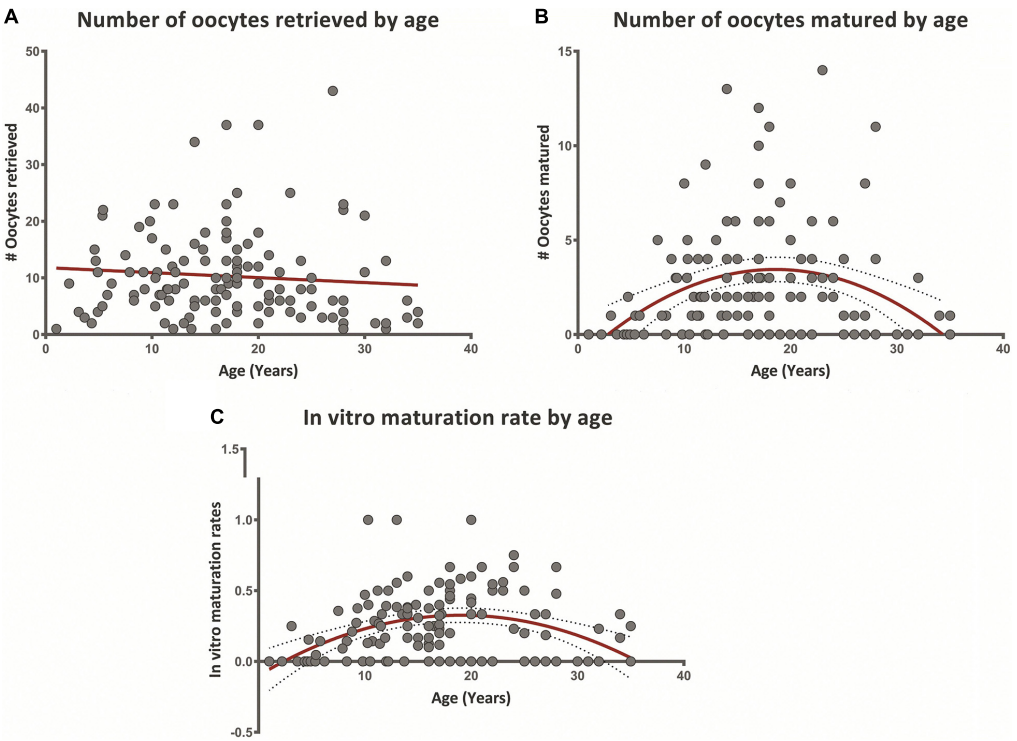

FIGURE 2 | (A–C) Oocyte retrieval following ovarian tissue cryopreservation and *in vitro* maturation outcomes according to patient age (1–35 years). **(A)** Number of oocytes retrieved following ovarian tissue cryopreservation according to patient age. Linear regression trend is observed in red. **(B)** Number of oocytes matured by *in vitro* maturation according to patient age. Quadric fit line presented in red, with confidence interval of 95% (dotted lines). **(C)** Average rate of mature oocytes/total oocytes retrieved (*in vitro* maturation rate) per patient according to age. Quadric fit line presented in red, with confidence interval of 95% (dotted lines).

Previous studies evaluating the effect of patient age on oocyte maturation and fertilization ability had demonstrated that natural fertility in humans follows an inverse U-curve, where young females (≥13 to early 20s) and women of advancing maternal age (mid-30s and above) show reduced rates of pregnancy and live births (Hawkes and Smith, 2010; Fouks et al., 2020). This inverted U phenomena was recently attributed to chromosome segregation in human oocytes causing increased rates of oocyte aneuploidy in both ends of the fertility life span. The authors suggested that chromosome-based mechanisms in oocytes determines the curve of natural fertility in humans, and that the reasons for aneuploidy differ between young and old oocytes (7). While our findings agree with the presence of an inverted U-curve in human fertility, in our fertility preservation patients the peak of the curve is shifted to the left, toward the younger age where naïve oocytes have the ability for IVM. In our study, we found a peak of maturation is achieved around the 18–24-year age group, as compared to a peak age of 28 for euploid oocytes as demonstrated by Gruhn et al. (2019). These clinical findings may imply that other factors aside from chromosome number influences natural fertility span as suggested above.

This study has several limitations, the main being its retrospective design. Moreover, data regarding ovarian reserve evaluation was not available for most of the patients, due to our pre-op OTC procedures protocol. Up to date, none of our patients have used their frozen *in vitro* matured oocytes, and as such, further implications of age on *in vitro* matured oocytes quality and implantation potential have yet to be evaluated. As far as we know, this study is the largest cohort that evaluated patients that underwent IVM in the context of fertility preservation.

The strengths of this study include the cohort's wide age range (1–35 years), enabling us to compare IVM efficacy in a single center according to different age groups. Patients were not exposed to any external gonadotropins prior to searching and handling the oocytes, thereby enabling us to study the unperturbed IVM rate of oocytes for each patient naturally. In addition, all oocytes were evaluated and treated in the same center using a single IVM protocol, performed by the same trained staff of embryologists, thereby minimizing the laboratory technique effect on the general results.

CONCLUSION

To conclude, the ability to mature *in vitro* oocytes retrieved during OTC is associated with patient age. The optimal IVM efficacy is prior to menarche until 25 years of age. Young pre-menarche girls and women over age 30 demonstrated extremely low (<10%) IVM success rates. IVM of oocyte retrieved from patients in these age groups should be considered carefully, with regard to its potential efficacy and possible alternative laboratory approach should be investigated. Our results show that oocyte maturation has an optimal age window in which the

success rate is much higher-demonstrating higher competence of oocytes in this window.

DATA AVAILABILITY STATEMENT

The original contributions presented in the study are included in the article/supplementary material, further inquiries can be directed to the corresponding author/s.

ETHICS STATEMENT

The studies involving human participants were reviewed and approved by The Institutional Ethical Review Board approval was received for this study (IRB 0288-16-HMO) by the Human Research Ethics Committees of the Hadassah Hebrew University Medical Center, Jerusalem, Israel. Written informed consent to participate in this study was provided by the participants' legal guardian/next of kin.

AUTHOR CONTRIBUTIONS

GK and PW-P contributed to the conception and design of the study, analysis and interpretation of the data, and drafting of the manuscript. TM-D contributed to the acquisition, analysis, and interpretation of data and drafting and revision of the manuscript. DB contributed to the interpretation of the data and drafting and revision of the manuscript. MK and TI contributed to the conception and design of the study, acquisition, analysis, and interpretation of the data, and drafting and revision of the manuscript. All authors have approved the final version of the study.

FUNDING

The Hebrew University and Hadassah Joint Research Fund 2018 (TI and MK). STEP-GTP fellowship and an Arianne De-Rothschild fellowship to PW-P.

REFERENCES

Amargant, F., Manuel, S. L., Tu, Q., Parkes, W. S., Rivas, F., Zhou, L. T., et al. (2020). Ovarian stiffness increases with age in the mammalian ovary and depends on collagen and hyaluronan matrices. *Aging Cell* 19:e13259. doi: 10.1111/acel.13259

Babayev, E., Wang, T., Szigeti-Buck, K., Lowther, K., Taylor, H. S., Horvath, T., et al. (2016). Reproductive aging is associated with changes in oocyte mitochondrial dynamics, function, and mtDNA quantity. *Maturitas* 93, 121–130. doi: 10.1016/j.maturitas.2016.06.015

Broekmans, F. J., Knauff, E. A., te Velde, E. R., Macklon, N. S., and Fauser, B. C. (2007). Female reproductive ageing: current knowledge and future trends. *Trends. Endocrinol. Metabol.* 18, 58–65. doi: 10.1016/j.tem.2007.01.004

Chian, R. C., Uzelac, P. S., and Nargund, G. (2013). *In vitro* maturation of human immature oocytes for fertility preservation. *Fertil. Steril.* 99, 1173–1181. doi: 10.1016/j.fertnstert.2013.01.141

Di Emidio, G., Falone, S., Vitti, M., D'Alessandro, A. M., Vento, M., Di Pietro, C., et al. (2014). SIRT1 signalling protects mouse oocytes against oxidative stress and is deregulated during aging. *Hum. Reprod.* 29, 2006–2017. doi: 10.1093/humrep/deu160

Feigin, E., Abir, R., Fisch, B., Kravarusic, D., Steinberg, R., Nitke, S., et al. (2007). Laparoscopic ovarian tissue preservation in young patients at risk for ovarian failure as a result of chemotherapy/irradiation for primary malignancy. *J. Pediatr. Surg.* 42, 862–864. doi: 10.1016/j.jpedsurg.2006.12.041

Fouks, Y., Hamilton, E., Cohen, Y., Hasson, J., Kalma, Y., and Azem, F. (2020). *In-vitro* maturation of oocytes recovered during cryopreservation of pre-pubertal girls undergoing fertility preservation. *Reprod. Biomed. Online* 41, 869–873. doi: 10.1016/j.rbmo.2020.07.015

Gruhn, J. R., Kristensen, S. G., Andersen, C. Y., and Hoffmann, E. R. (2018). *In vitro* maturation and culture of human oocytes. *Methods Mol. Biol.* 1818, 23–30. doi: 10.1007/978-1-4939-8603-3_3

Gruhn, J. R., Zielinska, A. P., Shukla, V., Blanshard, R., Capalbo, A., Cimadomo, D., et al. (2019). Chromosome errors in human eggs shape natural fertility over reproductive life span. *Science* 365, 1466–1469. doi: 10.1126/science.aav7321

Hawkes, K., and Smith, K. R. (2010). Do women stop early? Similarities in fertility decline in humans and chimpanzees. *Ann. N. Y. Acad. Sci.* 1204, 43–53. doi: 10.1111/j.1749-6632.2010.05527.x

Karavani, G., Schachter-Safrai, N., Revel, A., Mordechai-Daniel, T., Bauman, D., and Imbar, T. (2019). *In vitro* maturation rates in young premenarche patients. *Fertil. Steril.* 112, 315–322. doi: 10.1016/j.fertnstert.2019.03.026

Mara, J. N., Zhou, L. T., Larmore, M., Johnson, B., Ayiku, R., Amargant, F., et al. (2020). Ovulation and ovarian wound healing are impaired with advanced reproductive age. *Aging* 12, 9686–9713. doi: 10.18632/aging.103237

Marangos, P., Stevense, M., Niaka, K., Lagoudaki, M., Nabti, I., Jessberger, R., et al. (2015). DNA damage-induced metaphase I arrest is mediated by the spindle assembly checkpoint and maternal age. *Nat. Commun.* 6:8706. doi: 10.1038/ncomms9706

Meirow, D., Fasouliotis, S. J., Nugent, D., Schenker, J. G., Gosden, R. G., and Rutherford, A. J. (1999). A laparoscopic technique for obtaining ovarian cortical biopsy specimens for fertility conservation in patients with cancer. *Fertil. Steril.* 71, 948–951. doi: 10.1016/s0015-0282(99)00067-9

Merriman, J. A., Jennings, P. C., McLaughlin, E. A., and Jones, K. T. (2012). Effect of aging on superovulation efficiency, aneuploidy rates, and sister chromatid cohesion in mice aged up to 15 months. *Biol. Reprod.* 86:49. doi: 10.1095/biolreprod.111.095711

Revel, A., Revel-Vilk, S., Aizenman, E., Porat-Katz, A., Safran, A., Ben-Meir, A., et al. (2009). At what age can human oocytes be obtained? *Fertil. Steril.* 92, 458–463. doi: 10.1016/j.fertnstert.2008.07.013

Reyes, J. M., Silva, E., Chitwood, J. L., Schoolcraft, W. B., Krisher, R. L., and Ross, P. J. (2017). Differing molecular response of young and advanced maternal age human oocytes to IVM. *Hum. Reprod.* 32, 2199–2208. doi: 10.1093/humrep/dex284

Wasserzug-Pash, P., and Klutstein, M. (2019). Epigenetic changes in mammalian gametes throughout their lifetime: the four seasons metaphor. *Chromosoma* 128, 423–441. doi: 10.1007/s00412-019-00704-w

Wasserzug-Pash, P., Rothman, R., Reich, E., Schonberger, O., Weiss, Y., Srebnik, N., et al. (2020). Loss of heterochromatin and retrotransposon silencing constitute an early phase in oocyte aging. *bioRxiv* [Preprint]. doi: 10.1101/2020.10.28.358440

Conflict of Interest: The authors declare that the research was conducted in the absence of any commercial or financial relationships that could be construed as a potential conflict of interest.

frontiers in Cell and Developmental Biology

REVIEW
published: 08 July 2021
doi: 10.3389/fcell.2021.699671

Germline Stem and Progenitor Cell Aging in *C. elegans*

*Theadora Tolkin and E. Jane Albert Hubbard**

Department of Cell Biology, Skirball Institute of Biomolecular Medicine, NYU Grossman School of Medicine, New York, NY, United States

Like many animals and humans, reproduction in the nematode *C. elegans* declines with age. This decline is the cumulative result of age-related changes in several steps of germline function, many of which are highly accessible for experimental investigation in this short-lived model organism. Here we review recent work showing that a very early and major contributing step to reproductive decline is the depletion of the germline stem and progenitor cell pool. Since many cellular and molecular aspects of stem cell biology and aging are conserved across animals, understanding mechanisms of age-related decline of germline stem and progenitor cells in *C. elegans* has broad implications for aging stem cells, germline stem cells, and reproductive aging.

Keywords: reproductive aging, germline flux, stem cell aging, insulin/IGF-like signal transduction pathway, Notch pathway

OPEN ACCESS

Edited by:
Miguel Angel Brieño-Enriquez, Magee-Womens Research Institute, United States

Reviewed by:
David Gems, University College London, United Kingdom
Ilya Ruvinsky, Northwestern University, United States
Maria Olmedo, Seville University, Spain

***Correspondence:**
E. Jane Albert Hubbard
jane.hubbard@med.nyu.edu

Specialty section:
This article was submitted to Cellular Biochemistry, a section of the journal Frontiers in Cell and Developmental Biology

Received: *23 April 2021*
Accepted: *07 June 2021*
Published: *08 July 2021*

Citation:
Tolkin T and Hubbard EJA (2021) Germline Stem and Progenitor Cell Aging in C. elegans. Front. Cell Dev. Biol. 9:699671. doi: 10.3389/fcell.2021.699671

INTRODUCTION

C. elegans is a well-established model for germline development and for aging. Several interesting related areas of study include how the *C. elegans* germ line regulates longevity (see Antebi, 2012, for review) and how reproductive cessation may relate to population success in the wild (see Hughes et al., 2007; Galimov and Gems, 2021). These will not be discussed here. Instead, we focus on the comparatively young field investigating how the *C. elegans* germ line itself ages.

In typical laboratory growth conditions, *C. elegans* hermaphrodites cease reproducing long before they die, roughly mid-way through their average 2-3 week lifespan; the average times for reproductive cessation and lifespan both depend on whether the hermaphrodites have mated (Hughes et al., 2007; Pickett et al., 2013). Among several age-related changes in the germ line, the loss of germline stem and progenitor cells is emerging as a key driver of reproductive cessation, as detailed below.

Several important aspects of *C. elegans* reproductive biology shape how reproductive aging, also referred to as reproductive senescence, is studied in this system. Therefore, prior to discussing the recent literature pertaining to the aging stem and progenitor pool, we briefly introduce the adult hermaphrodite reproductive system, Notch-mediated signaling and stem cells, and we address the effects of sperm availability in limiting reproduction. In these three introductory sections we provide only a brief overview and, at the end of each section, we direct the reader to recent reviews for additional details.

The remainder of this review covers recent work addressing the age-related decline of the germline stem and progenitor cell pool, its regulation by longevity pathways, its cellular and molecular underpinnings, and its effect on progeny production. Finally, we discuss related open questions of stem cell aging for which this model system is particularly amenable to address experimentally.

ASPECTS OF *C. ELEGANS* REPRODUCTIVE BIOLOGY RELEVANT TO REPRODUCTIVE AGING STUDIES

Adult Hermaphrodite Reproductive System

Most *C. elegans* aging studies have been conducted in the hermaphrodite, a morphological "female" that produces sperm for a short time at the end of larval life before switching solely to oocyte production. The tube-shaped adult hermaphrodite gonad is closed at the distal end, and opens to the uterus at the proximal end (**Figure 1A**). Hermaphrodites bear two gonad "arms" (one anterior and one posterior) that open to a single uterus. A pool of proliferating germ cells resides at each distal (closed) end, in a region dubbed the progenitor zone (PZ). The PZ pool of cells accumulates during larval stages and reaches a maximum number of cells in early adulthood. The PZ contains germline stem cells, their proliferating progeny, and cells in meiotic S phase. Cells enter prophase of meiosis I as they leave this zone.

Each germ cell nucleus is surrounded by its own plasma membrane, including nuclei in the distal zone, but germ cells retain an opening to a core (the rachis) into which contents flow proximally to supply growing oocytes. As many as 85% of adult germ cells that enter prophase of meiosis I have been estimated to later undergo apoptosis in late pachytene. This cell death is thought to constitute a nurse cell function providing material for growing oocytes via the core.

Adult germ cells that do not undergo programmed cell death continue to mature as oocytes, arresting in diakinesis while awaiting their "turn" to reach the proximal-most position in the oviduct (**Figure 1**). In response to hormone signals from sperm residing in the spermatheca (located just proximal to the oviduct), oocytes escape arrest, undergo meiotic maturation, and are ovulated into the spermatheca where they are fertilized. Each zygote then moves into the uterus and begins embryonic development. For details on germline development and oocyte maturation, the reader is directed to recent reviews and additional references therein (Das and Arur, 2017; Hillers et al., 2017; Huelgas-Morales and Greenstein, 2018; Hubbard and Schedl, 2019).

Notch Signaling and Germline Stem Cells

Maintenance of *C. elegans* germline stem cell identity depends on canonical Notch signaling. Each distal end of the hermaphrodite gonad is capped by single somatic cell called the distal tip cell (DTC; **Figure 1A**). The DTC produces Delta-like ligands that activate a Notch family receptor, GLP-1, that is present on the surface of germ cells in the PZ. GLP-1 activity in the distal germ cells activates the transcription of two genes, *sygl-1* and *lst-1,* the products of which act largely redundantly to prevent differentiation. SYGL-1-positive cells therefore can be considered stem cells, as distinct from SYGL-1-negative cells in the PZ that cycle through a last mitosis before entering meiotic S phase. Since SYGL-1 and LST-1 were relatively recently discovered and characterized as the sole early response to GLP-1 signaling

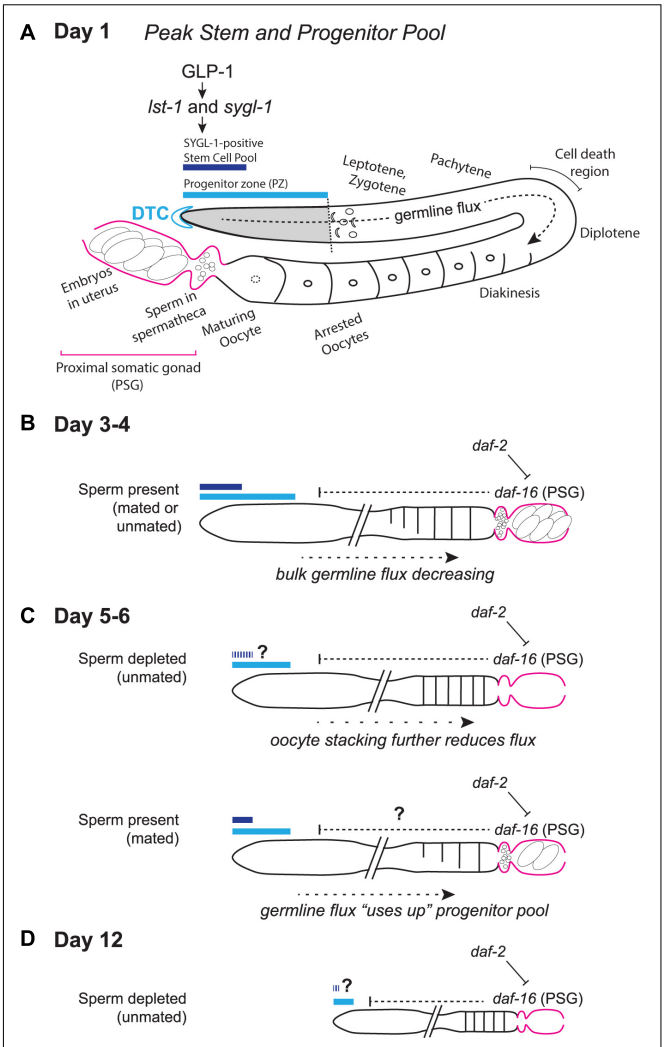

FIGURE 1 | Schematic representation of the aging *C. elegans* adult hermaphrodite reproductive system. **(A)** Early adult gonad anatomy. The germline progenitor zone is located at the distal end of the gonad. As progenitors proliferate, they are displaced and move proximally ("germline flux"), progressing through oogenic prophase of meiosis I until they become arrested in diakinesis at the proximal end of the oviduct, awaiting maturation-inducing signals from sperm in the spermatheca. **(B)** Simplified schematic of a days 3–4 adult gonad, depicting distal stem/progenitor pool and proximal arrested oocytes, sperm in the spermatheca and embryos in the uterus. **(C)** Schematics representing aged (days 5–6) sperm-depleted and sperm-replete conditions. **(D)** Schematic representing a post-reproductive day 12 gonad. Regardless of sperm availability, reproduction has ceased, and the progenitor zone is severely reduced. Diagrams in **(A–D)** represent wild-type worms. Additional notes: The progenitor zone of aged hermaphrodites contains fewer cells than at adult day 1 peak; in mated hermaphrodites (as yet untested in the other conditions) SYGL-1- and LST-1- positive pools also decline. Sperm-depleted hermaphrodites accumulate unfertilized oocytes in the oviduct, whereas sperm-replete hermaphrodites do not. The PZ mitotic cell cycle also slows, as does the rate of meiotic entry and the rate of progression through prophase of meiosis I. These age-related changes in bulk germline flux contribute to the reduction in progeny production with age. The numbers of oocytes are schematized here to emphasize flux vs. stacking; Kocsisova et al. (2019) report an average of ~14 oocytes are in diplotene and diakinesis at days 1 and 3 and an average of ~9 at day 5 in mated hermaphrodites. See text for details and additional references.

(Kershner et al., 2014; Shin et al., 2017; Haupt et al., 2019; Chen et al., 2020), and since techniques (such as those for single-copy insertions necessary for transgene expression in the germ line and for CRISPR/Cas9-mediated tagging) have only relatively recently gained widespread use in the field, only one aging study (Kocsisova et al., 2019) has thus far distinguished stem vs. non-stem pools within the aging PZ. For details on GLP-1 Notch signaling in the germ line and additional details of the *C. elegans* stem cell system, the reader is directed to recent reviews and additional references therein (Greenwald and Kovall, 2013; Kershner et al., 2013; Hubbard and Schedl, 2019).

Sperm Limitation and Oocyte Maturation

Two additional features of *C. elegans* reproductive biology are that sperm are limiting for self-progeny production, and that sperm are required to stimulate oocyte maturation (see Huelgas-Morales and Greenstein, 2018). Self-sperm that are generated in the last larval stage of hermaphrodite development fertilize oocytes one by one as oocytes are ovulated into the spermatheca. Sperm are thereby depleted over time, and unmated hermaphrodites will produce effectively the same number of self-progeny as they have self-sperm. Unmated hermaphrodites cease reproduction after ∼4–5 days having produced ∼300 self-progeny. Thereafter, oocytes arrested in diakinesis stack up in the oviduct. These oocytes are occasionally ovulated into the uterus and can be expelled from the animal through the vulva. Unfertilized oocytes that remain in the uterus can also become endomitotic. Thus, the cessation of reproduction in unmated hermaphrodites in the lab is mainly driven by sperm depletion, not reproductive or germ cell aging *per se*.

The limit to self-progeny production can be circumvented if a hermaphrodite mates with a male. In this scenario, abundant sperm are present and arrested oocytes do not stack up in the oviduct. Rather, oocytes are continuously matured and ovulated in response to sperm signals. The two different scenarios—one in which oocytes remain arrested in the absence of sperm, and one in which oocytes are continuously maturing and ovulating—represent different scenarios for worm biology and for reproductive aging as defined by progeny production (Pickett et al., 2013).

THE GERMLINE STEM AND PROGENITOR POOLS DECLINE WITH AGE

Given the complex biology of sperm limitation and oocyte maturation, a major finding that has emerged from recent studies is that the number of germ cells in the progenitor zone (PZ) declines with age. This occurs in both unmated and mated hermaphrodites despite the profound gene expression changes that accompany sperm depletion (Angeles-Albores et al., 2017). In both scenarios, this PZ decline begins early in adulthood, during peak reproduction, and before somatic aging becomes apparent (Garigan et al., 2002; Killian and Hubbard, 2005; Hughes et al., 2007; Luo et al., 2010; Narbonne et al., 2015; Qin and Hubbard, 2015; Kocsisova et al., 2019). Discrepancies regarding exact PZ numbers (see a summary in Materials and Methods of Kocsisova et al., 2019), likely reflect different laboratory conditions and strains, as well as different analysis and imaging techniques. For example, dissected gonads from very old worms are fragile, possibly unintentionally biasing results from such preparations to gonads from less fragile worms in an aging population. Nevertheless, the studies discussed below confirm that PZ decline is a hallmark feature of aging, and that depletion of the stem/progenitor pool is a major driver of the age-related decline in reproductive output.

Insulin/IGF-Like Receptor Signaling (IIS) and Decline of the Germline Progenitor Pool With Age

Not long after the groundbreaking discovery that *daf-2*, which encodes the sole insulin/IGF-like receptor in *C. elegans*, promotes aging, a role was postulated for this gene and its signaling pathway (hereafter abbreviated as IIS) in reproductive aging. Reduction-of-function (*rf)* mutations in *daf-2* extend lifespan in a manner dependent upon the transcription factor DAF-16 FOXO (see Kenyon, 2010 for review). That *daf-2* influences germ cell aging was suggested by a qualitative examination and rating of germ cell morphology in *daf-2* and *daf-16* mutants (Garigan et al., 2002). A quantitative measure associated with germline aging, a decline in the number of PZ cells in wild-type adult hermaphrodites over time, was subsequently documented in fixed whole-mount preparations (Killian and Hubbard, 2005), and this observation has been confirmed by studies in several different labs (Luo et al., 2010; Narbonne et al., 2015; Qin and Hubbard, 2015; Kocsisova et al., 2019). Reducing IIS slows the age-related decline in the number of cells in the PZ, and this slower depletion of the PZ pool in *daf-2* mutants is dependent on *daf-16* (Luo et al., 2010; Qin and Hubbard, 2015).

One hypothesis that was considered for why germline progenitor pool depletion might be delayed in the *daf-2* long-lived mutant is that whatever mechanisms extend lifespan might slow germline aging as measured by PZ depletion. However, this explanation proved unlikely since the tissues that require wild-type *daf-16* activity to promote longevity downstream of *daf-2* are not the same as those that require wild-type *daf-16* activity to affect depletion of the PZ. That is, tissue-specific expression of *daf-16*(+) in the intestine of the worm partially reverses the effects of *daf-16* loss on lifespan of the *daf-16; daf-2* double mutant, making it more similar to *daf-2* alone (Libina et al., 2003). However, animals carrying the same transgene showed a PZ pool similar to the *daf-16; daf-2* double mutant rather than to the *daf-2* mutant alone at day 12 of adulthood. Nor does transgenic expression of *daf-16*(+) in muscle or neurons influence age-related PZ loss in the *daf-16; daf-2* double mutant (Qin and Hubbard, 2015).

Instead, unexpectedly, *daf-16*(+) is required in certain cells of the proximal somatic gonad (PSG), a source of DAF-16 not previously linked to longevity nor to PZ regulation. Specifically, expression of *daf-16*(+) in a subset of (*fos-1a*-positive) PSG cells of the spermatheca and uterine lineage completely reversed the effect of the *daf-16* mutant such that the double mutant *daf-16;*

daf-2 expressing *daf-16*(+) in PSG cells maintained a larger PZ pool with age, similar to the *daf-2* mutant alone. Consistent with this finding, tissue-specific RNAi depletion of *daf-16* in the same PSG cells mimicked loss of *daf-16,* while depletion of *daf-16* in the germ line did not (Qin and Hubbard, 2015). This last result was also somewhat surprising since the *daf-2* signaling pathway is required germline-autonomously to promote accumulation of the PZ pool during larval stages (Michaelson et al., 2010). One possible explanation for these results was that these PSG cells represented an undiscovered source of *daf-16*(+) activity in promoting longevity. However, this possibility was ruled out since lifespan is unaffected in *daf-16; daf-2* double mutant worms bearing the PSG-expressed *daf-16*(+) transgene. Thus, age-related germline progenitor pool decline and organismal lifespan can be modulated by the same IIS signaling pathway, but from anatomically distinct activities of *daf-16* in the worm (Qin and Hubbard, 2015).

The Progenitor Zone Is "Used Up" by Germline Flux

The unexpected role for DAF-16 in PSG cells opened a number of questions regarding the mechanism by which the PZ is depleted with age. In short, the results support a model in which the progenitor pool is "used up" over time. An analysis of mutants that interfere with sperm production, ovulation, or fertilization suggested that the rate at which germ cells leave the system by oocyte ovulation influences the rate of PZ loss. That is, preventing ovulation slows the PZ pool decline. This effect is seen in sperm-less mutants in which oocytes stack up in the oviduct, and the effect can be partially reversed by reintroducing sperm. Importantly, the maintenance of the PZ over time that occurs in the absence of sperm is partially dependent on *daf-16* in the PSGs (Qin and Hubbard, 2015). In addition, local germline-autonomous feedback slows cell cycle progression in the PZ pool in response to accumulating oocytes, in a manner dependent on *daf-18,* which encodes the *C. elegan*s ortholog of human tumor suppressor PTEN (Narbonne et al., 2015; see also below).

Time-Course and Cellular Mechanisms of Progenitor Pool Decline

The decline in the number of PZ cells begins early, by day 3 of adulthood, coincident with peak reproductive output and before various measures of somatic decline are evident (Killian and Hubbard, 2005; Pickett et al., 2013; Kocsisova et al., 2019). While estimates vary in terms of exact cell number, in both unmated and mated hermaphrodites, the PZ declines from ∼200 to 250 cells at day 1 of adulthood to ∼100 to 150 cells by day 6. PZ cell numbers continue to decline during adulthood, such that an average of ∼50 PZ cells remain on adult day 12 in unmated hermaphrodites (Qin and Hubbard, 2015). The time-course of progeny production, in both unmated and mated hermaphrodites shows an early peak and then steep decline: in either case, an average of ∼150 progeny are produced on adult day 2, while very few progeny are produced after day 5 in unmated and after day 8 in mated hermaphrodites (Pickett et al., 2013; Kocsisova et al., 2019).

The number of cells in the PZ at any given time is a function of several factors, the interdependence of which is not fully resolved. These factors include the starting number of stem cells and non-stem cells in early adulthood, the rate of proliferation of each of these pools within the PZ, the rate of entry of cells into the meiotic pathway by commitment to meiotic S phase, the duration of meiotic S phase, and entry into prophase of meiosis I. Each of these factors may or may not change in concert over time. The rate of particular phases of mitotic cell cycle progress is, in particular, difficult to measure, requiring arduous pulse-chase time-course analysis (e.g., Fox et al., 2011; Kocsisova et al., 2019; see below). Mitotic index—the number of cells in metaphase divided by the number of proliferation-competent cells in a pool—is a proxy for the rate of cell cycle progression since, in theory, a higher mitotic index in a population of cells would reflect a faster average rate of cell cycle progression. However, compensatory alterations of other cell cycle phases or cell populations that are not uniform can potentially confound the interpretation of mitotic index alone. In addition, the length of time that *C. elegans* germ cells express a common mitotic marker (phospho-histone H3) is itself subject to nutritional state (Gerhold et al., 2015). Another mitotic index measure that gives a lower but perhaps more reliable index is the proportion of cells in metaphase or anaphase of mitosis. These concerns notwithstanding, by either measure, cells in the PZ of self-fertile hermaphrodites display a reduction in mitotic index as sperm become depleted (Narbonne et al., 2015; Qin and Hubbard, 2015).

While GLP-1 is not thought to regulate cell cycle, stem cell identity and cell cycle dynamics are not completely independent. As germ cells are displaced away from the distal end, they lose contact with the DTC and lose GLP-1 activity. Since germ cells spend the majority of time in S and G2, after these cells lose GLP-1 activity they must usually cycle through M phase before entering meiotic S (Fox and Schedl, 2015). As a result, a prolonged G2 of an aged germ cell cycle may appear to inhibit meiotic entry. An extreme example is seen in germ cells such as those in adult reproductive diapause (ARD) that are essentially arrested (Angelo and Van Gilst, 2009; Seidel and Kimble, 2011). These cells do not enter meiotic prophase even in the absence of GLP-1 Notch signaling (Seidel and Kimble, 2015), likely because they cannot progress to meiotic S.

What forestalls the age-related decline in the PZ pool when *daf-2* is reduced or when germline flux is decreased upon sperm depletion? One factor is likely to be slower cell cycle progression. Introducing sperm to sperm-depleted hermaphrodites can accelerate the decline of PZ cells (Qin and Hubbard, 2015) and elevate mitotic index (Narbonne et al., 2015). Together, these results suggest that the rate of cell proliferation is an important factor dictating the number of PZ cells at a given time. Reduced *daf-2* and slowed oocyte flux both correlate with lower mitotic index in early adulthood (Narbonne et al., 2015). Day 1 mitotic index is lower in conditional *daf-2* mutants at the restrictive temperature regardless of mating status, while sperm-less mutants display reduced mitotic index that is partially reversed by mating. In both cases, loss of DAF-18 PTEN, a

phosphatase that can oppose the PI3 kinase activity downstream of DAF-2, restores mitotic index. Based on manipulations that selectively allow or block flux in one gonad arm or the other within the same hermaphrodite, Narbonne et al. (2015) postulate that accumulated oocytes themselves locally antagonize DAF-2-mediated signaling via DAF-18 PTEN to slow the cell cycle in the same gonad arm. Interpretation of some of these experiments is complicated, however, especially those that use tumor-forming mutants in which the propensity to form tumors and the rate of proliferation within tumors are not necessarily correlated (see Hubbard and Schedl, 2019, for a discussion of tumorous mutants). Based on genetic analysis, DAF-18 is proposed to act upstream of AMPK and MAP kinase signaling (Narbonne et al., 2017). In this model, the logjam of arrested, un-ovulated oocytes in the proximal oviduct would signal either directly or indirectly to the distal germ line to slow the cell cycle and/or modulate progression into meiosis I prophase (see also Discussion).

Decline of the Progenitor Pool Is a Main Contributor to Reproductive Decline With Age

To understand how changes to the progenitor pool ultimately relate to progeny production, it is necessary to analyze hermaphrodite reproductive aging in sperm-replete conditions. This is because sperm depletion limits progeny production and introduces confounding effects due to the build-up of arrested oocytes upon sperm depletion. Therefore, Kocsisova et al. (2019) examined reproductive aging in mated worms. This comprehensive study demonstrated that PZ depletion does indeed occur in sperm-replete conditions, that it includes a depletion of the SYGL-1-positive stem cell pool, that it begins early relative to somatic aging, and that it is a primary contributor to reduced progeny production with age. Although oocyte quality is controlled by multiple mechanisms (e.g., Nadarajan et al., 2009; Luo et al., 2010; Templeman et al., 2018; see also below; Bhargava et al., 2020; Templeman et al., 2020), oocyte quantity, and hence the number of progeny, is tightly correlated with output from the PZ pool (Agarwal et al., 2018; Kocsisova et al., 2019).

Overall, a 14-fold reduction in progeny production occurs in mated worms by adult day 7 compared to adult day 1, and the reduction in progeny production follows PZ depletion with a delay of ∼2.5 days, the time required for cells to go from PZ to oocyte (Kocsisova et al., 2019). The observation that the PZ in worms with reduced *glp-1* activity declines faster suggested that loss of the GLP-1-responding stem cell pool contributes to PZ decline (as opposed to, for example, only a loss of non-stem progenitors) (Qin and Hubbard, 2015). A *bona fide* stem cell decline was demonstrated by Kocsisova et al. (2019) using CRISPR/Cas9-generated tagged SYGL-1 and LST-1 proteins. A reduced SYGL-1-positive stem cell pool was seen as a shortening of the proximal extent of SYGL-1 protein detection, and that the decline was due to reduced GLP-1 signaling was indicated by a decreased proximal extent of LST-1 protein. Together, stem cell decline is ∼2-fold by adult day 5 (Kocsisova et al., 2019).

Cell cycle analysis in mated hermaphrodites, measuring M and S phase index as well as G2 duration and total non-S duration, indicated that between days 1 and 3 of adulthood, the duration of the G2 is extended ∼2 fold (2.5–4.9 h), as is the entire non-S portion of the cell cycle (G2 + M + G1; 3.4–7.4 h). Interestingly, neither the M-phase index nor S-phase index change over this timeframe in mated worms. One possible explanation is that pro-metaphase may be lengthened as well, as these studies used anti-phospho-histone H3 to measure mitotic index. Taking all these data into account, the average speed of the cell cycle is reduced ∼2-fold by day 3 (Kocsisova et al., 2019).

In addition to PZ cells lengthening certain cell cycle stages in aging mated worms, the rate at which they enter meiosis is also reduced, as indicated by pulse-chase analysis of EdU-labeled germ cells (Kocsisova et al., 2019). In general, how the rate of meiotic entry is controlled is unknown. However, regulation could occur at several different levels since multiple pathways control the decision to enter the meiotic pathway upon loss of GLP-1 signaling (see Hubbard and Schedl, 2019). Taken together, the change in the total output of the PZ, including stem cell depletion, reduced cell cycle, and reduced meiotic entry, is estimated as ∼4.5-fold by day 5 and ∼11-fold by day 7, relative to peak (Kocsisova et al., 2019).

In addition to a slower rate of entry into prophase of meiosis I, progress through meiotic prophase also slows with age. Aging extends time spent in leptotene/zygotene as well as pachytene (Jaramillo-Lambert et al., 2007; Kocsisova et al., 2019). However, the same proportion of cells were estimated to undergo physiological apoptosis at day 1 as at day 5. Thus, an additional delay in progression through the various stages of prophase of meiosis I, rather than an increase in the proportion of cells that die, likely contributes to the mid-life reduction in progeny production (Kocsisova et al., 2019).

Among a number of germline aging phenotypes, the age-related reduction of the PZ pool occurs in essentially all individuals within the aging population, both mated and unmated hermaphrodites (Luo et al., 2010; Narbonne et al., 2015; Qin and Hubbard, 2015; Kocsisova et al., 2019). In addition, this age-related phenotype occurs similarly in both gonad arms within individuals, arguing for a systemic rather than a local effect (Kocsisova et al., 2019). In contrast, two additional sporadic low-frequency aging phenotypes are observed in mated hermaphrodites: a shift of the DTC nucleus position and endomitotic oocytes in the oviduct (as distinct from endomitotic oocytes in the uterus which accumulate in hermaphrodites that have exhausted their sperm supply). Longitudinal studies of hermaphrodites displaying these two infrequently-observed defects indicate that the two are not correlated and, while a shifted DTC nucleus does not strongly correlate with reproductive decline, the presence of endomitotic oocytes in the oviduct of mated worms negatively impacts reproduction. In addition, the DTC phenotype was often restricted to one gonad arm and not the other within individuals, while the presence of endomitotic oocytes in one gonad arm in an individual was correlated with an increased probability of observing an endomitotic oocyte in the other gonad arm of the same individual, suggesting a local mechanism for the former and a possible systemic effect for the latter (Kocsisova et al., 2019).

DISCUSSION AND OPEN QUESTIONS

Many open questions remain regarding germline stem and progenitor cell aging, and many of these open questions are experimentally accessible in *C. elegans* (Corsi et al., 2015). The system is both fast-reproducing and fast-aging. It is amenable to unbiased genetic screening and single-cell omics. Moreover, cell and tissue autonomy can be rigorously established, developmental vs. aging effects can be separated using conditional alleles or other conditional manipulations, and longitudinal studies of individual worms using live markers are feasible since the worms are transparent. Most important, many cellular and molecular aspects of aging and stem cells are conserved between *C. elegans* and mammals (see Hubbard and Schedl, 2019). Therefore, studying the aging germ line in this system is likely to further our understanding of stem cell aging in general and reproductive aging in particular. Below we discuss some of these open questions and associated hypotheses.

How Is the Germ Cell Cycle Regulated During Aging?

Like germ cells of other organisms (Hsu et al., 2008; Ables and Drummond-Barbosa, 2013; Kao et al., 2015) and like mammalian embryonic stem cells (White and Dalton, 2005), *C. elegans* germ cells display unusual cell cycle control, including a very short to no G1 (Fox et al., 2011; Lara-Gonzalez et al., 2019). Although CDK-2/CYE-1 Cyclin E is required for cell cycle progression, in contrast to somatic cells where CDK2/Cyclin E is typically limited to late G1 and early S phase, the complex is present in germ cells at high levels throughout the mitotic germ cell cycle, where it also has a role in promoting the proliferative fate (Fox et al., 2011). Interestingly, a similar situation exists in *Drosophila* for Cyclin E (Hsu et al., 2008; Ables and Drummond-Barbosa, 2013), where S phase delay occurs in aging germline stem cells (Kao et al., 2015). In *C. elegans* germ cells, GSK-3 glycogen synthase kinase is required to maintain high levels of *cdk-2* transcription throughout the cell cycle to promote a high rate of cell cycle progression (Furuta et al., 2018). The unusual nature of the germline cell cycle necessitates careful characterization of cell cycle markers. For example, a well-characterized marker for S-phase, PCNA or PCN-1 in *C. elegans*, can accumulate in all PZ nuclei throughout the cell cycle, when only about half are in active S-phase as measured by EdU labeling (Kocsisova et al., 2018). A deeper understanding of the mechanism of stem cell cycle regulation in the germ line, together with well-characterized markers for cell cycle stages, will facilitate experiments needed for a more thorough understanding of how the germ cell cycle changes with advancing age.

The negligible G1 necessitates germ cell cycle regulation in other phases of the cycle. In germ cells, G2 arrest occurs in nutrient-poor conditions in several developmental scenarios, including the first larval stage, dauer and ARD (e.g., Fukuyama et al., 2006; Seidel and Kimble, 2015; Tenen and Greenwald, 2019), and the G2 is extended in older mated hermaphrodites (Kocsisova et al., 2019). One question is whether IIS, which promotes PZ mitotic index in larval and adult germ cells (Michaelson et al., 2010; Narbonne et al., 2015; Roy et al., 2016), is involved in the extension of G2 with age. If so, does it share mechanisms of IIS-mediated G2 regulation that occur in *Drosophila* neural stem cells (Otsuki and Brand, 2018)? Which of the many *C. elegans* insulin/IGF-like ligands are responsible, and how are they regulated by age? If not IIS, what mechanisms cause the extension of G2 with age?

Even though the average rate of cell cycle progression, which reduces the number of cells born over time, and the average rate of meiotic entry are both slowed with age, the number of cells in the PZ declines with age in either sperm-depleted or sperm-replete conditions. This suggests that the two rates of change are unequal; that is, either they start or progress differently over time. The rate of change in the cell cycle within the stem cell vs. non-stem progenitor pools may also differ. Nevertheless, stem cell depletion is likely a major factor in overall PZ decline since fewer stem cells results in fewer progenitors that can enter meiosis. The stem vs. progenitor state and cell cycle status of cells that remain in the PZ in oldest worms is also unresolved.

How Is Stem Cell Fate and Function Altered With Age?

The age-related decline in the pool of germ line stem cells is defined by the reduced number of the GLP-1 Notch responsive (SYGL-1-positive) cells in the distal germ line. One possibility is that this conserved Notch signaling pathway is affected by age-related cellular and tissue-level changes. Since Notch activity regulates stem cell fate in several different mammalian organ contexts, worm studies may inform our understanding of stem cell aging in higher organisms as well. Even in cases where other (non-Notch) signaling pathways control stem cell fate, features of stem cell signaling in the context of aging tissues may well be conserved.

Notch activation in the *C. elegans* germ line occurs via membrane-bound ligand expression in the somatic niche cell and the GLP-1 receptor on the surface of germ cells. Why does the number of SYGL-1-expressing stem cells decrease as animals age? Are the levels of Notch signaling in the stem cells reduced? If so, at what step of the signaling pathway? Is the post-transcriptional regulation of Notch pathway components or effectors different in old worms than in young ones? How do changes in Notch signaling interface with the changes in the germ cell cycle? To what extent is the reduction in Notch signaling due to general age-related changes to cell membranes or signaling centers? Is the efficacy of signal reception or transmission affected by age-related alterations in receptor membrane localization or receptor processing? Is the reduction in Notch signaling due to aging in the soma or in the germ line? Do age-related changes in nuclear transport or germ cell chromatin interface with transcriptional activation downstream of receptor signaling? Do changes to Notch pathway signaling reflect interactions with other age-related signals that impinge on the germ line? If so, how?

Equally interesting will be an understanding of how specific aspects of cell biological aging, such as changes to the basement membrane, to mitochondrial function, or to proteostasis, contribute to the decline in stem cell fate and function. It is

possible, for example, that some aspects of cellular aging impact cell cycle while others impact cell fate decisions via effects on specific signal transduction pathways.

How Does IIS Regulate the PZ? Do Other Aging Pathways Prevent PZ Decline?

With respect to IIS, organismal lifespan and the germline progenitor pool are regulated in anatomically distinct ways. How does *daf-16* expression in a subset of proximal somatic gonadal cells regulate the rate of decline of the PZ pool? One hypothesis is that a *daf-16*-dependent secreted factor signals directly to the germ line. Alternatively, PSG-to-germline communication could occur through intermediate tissues. The relevant targets of *daf-16* in the PSG will also be important to identify. To what extent does this pathway act at the level of germline stem cell identity, cell cycle, or both? It will also be of interest to determine how other age-defying conditions and genetic manipulations influence PZ aging, and, if so, whether they act by mechanisms similar to or distinct from the *daf-2* pathway.

Interfering with germ cell flux also delays the decline of PZ cell numbers with age. This effect appears to be linked to ovulation of oocytes and is partially dependent on *daf-16* in the proximal somatic gonad (Qin and Hubbard, 2015) as well as *daf-18*, AMPK and MAP kinase (Narbonne et al., 2015, 2017). Whether these pathways act directly or indirectly on the PZ requires further investigation.

How Is PZ Decline Related to Oocyte Quality?

By about day 5 of adulthood, oocytes show overt signs of deterioration (Garigan et al., 2002; Luo et al., 2010). They become morphologically disordered, and the progeny they give rise to show a higher incidence of chromosome non-disjunction and embryonic lethality, even if the old hermaphrodite is provided with sperm from a young male (Killian and Hubbard, 2001; Luo et al., 2010; Templeman et al., 2018; Imakubo et al., 2021). Though never fully avoided, defects in late life reproductive quality are delayed in long-lived mutants. However, the rate of egg-laying is also reduced throughout the life-span of long-lived mutants (Pickett et al., 2013), so one possibility is that oocyte deterioration will always occur after a certain number of oocytes have been produced, rather than at a particular biological age of the worm. Given the long journey a germ cell makes from stem cell to oocyte, it is also likely that age-dependent oocyte defects result from age-related changes in multiple factors and processes distributed throughout the course of ongoing germ cell maturation, starting from the stem cells themselves.

An interesting and potentially relevant observation is that reducing GLP-1 signaling in the distal germ line regulates the size of oocytes: reducing *glp-1* activity results in large oocytes, while elevating *glp-1* activity results in small oocytes (Nadarajan et al., 2009). This effect of *glp-1* on oocyte size is dependent on DTC-mediated GLP-1 activation, gap junctions, and cell death. It is mediated by alterations in the rate of actomyosin streaming to oocytes as well as the timing of oocyte cellularization. These observations demonstrate that the effects of GLP-1 signaling activity in the PZ, in addition to regulation of stem cell numbers, may have downstream effects on oocytes relevant to oocyte quality in aging.

A related question is: does PZ decline affect subsequent progression through prophase of meiosis I? Or are these independently regulated processes? Although age does not appear to affect physiological cell death during prophase, it does influence the rate of progression through prophase (Kocsisova et al., 2019). Progression through several distinct points of prophase of meiosis I is regulated by DAF-2 and RAS/MPK signaling (see Das and Arur, 2017 for a review). That oocytes arrested in late prophase may feed back on the PZ via DAF-18 PTEN, via AMPK and MAPK has been proposed (Narbonne et al., 2015, 2017), however, it is at present difficult to untangle the causal links between these pathways vis-à-vis the PZ and meiotic prophase progression, since *daf-2*, *daf-18*, and *mpk-1* all act at multiple steps in both processes. Additional questions concern how reducing the progenitor pool or slowing meiotic prophase affects the quality and quantity of material that eventually accumulates in oocytes.

How Is PZ Decline and Reproductive Aging Affected by the Worm's Environment?

C. elegans is a powerful model for understanding how an organism's environment, physiology and genetics together dictate phenotype. *C. elegans* research continues to advance genetic understanding of virtually every aspect of development and cell biology, largely under highly controlled laboratory conditions using a mono-species abundant food source. However, the worm's environment—microbial (both quality and quantity), pheromone, and temperature—impacts many aspects of development. A well-understood example is the regulation of dauer, an alternate pre-reproductive larval stage that is resistant to poor environmental conditions (see Fielenbach and Antebi, 2008 for a review). Interestingly, molecular pathways that regulate dauer such as IIS, TGFβ, and nuclear hormone signaling pathways, also affect both aging and the germ line, even when worms have not experienced dauer (e.g., Michaelson et al., 2010; Dalfó et al., 2012; Thondamal et al., 2015; Pekar et al., 2017), and IIS regulates meiotic progression in response to nutrient availably (Lopez et al., 2013).

Aging and reproduction are particularly sensitive to environmental manipulation in *C. elegans*. Under extreme conditions of starvation in late larval stages, reproductive adults can arrest germline stem cell divisions and slow the rate of oocyte production from the usual ∼3 oocytes ovulated per hour per gonad arm in peak times to fewer than one every 8 h (Angelo and Van Gilst, 2009; Seidel and Kimble, 2011). Remarkably, worms can remain in this condition far longer than their normal lifespan and rebound to become reproductively competent adults with a functional, albeit reduced, PZ (Roy et al., 2016). Responses to other stressors such as oxidative and heat stress are also altered with age, but it is unclear how they affect germline aging.

Slowing the germline progenitor cell cycle during environmentally unfavorable conditions or after sperm depletion

may be an evolutionary strategy to allow sperm-depleted hermaphrodites to temporarily retain germline progenitors despite advancing age, such that PZ cell proliferation, entry into and through meiotic prophase, and oocyte production can resume quickly upon locating new food sources and/or males with which to mate.

CONCLUDING REMARKS

The quirks of *C. elegans* life history and reproductive strategies have been sculpted by evolution to ensure its success in the wild. Nevertheless, together with its advantages as a laboratory model organism, these quirks offer rich opportunities for experimental analysis of reproductive and stem cell aging. Given the conservation of cellular and molecular processes from worms to mammals, and given the history of what model organism research has contributed to fundamental biology relevant to human health, studies on germline stem cell aging should offer broad implications beyond the worm.

AUTHOR CONTRIBUTIONS

Both authors contributed to the article and approved the submitted version.

FUNDING

This work was supported by NIH R01AG065672 to EJAH and American Cancer Society Postdoctoral Fellowship PF-19-231-01-CSM to TT.

REFERENCES

Ables, E. T., and Drummond-Barbosa, D. (2013). Cyclin E controls Drosophila female germline stem cell maintenance independently of its role in proliferation by modulating responsiveness to niche signals. *Development* 140, 530–540. doi: 10.1242/dev.088583

Agarwal, I., Farnow, C., Jiang, J., Kim, K. S., Leet, D. E., Solomon, R. Z., et al. (2018). HOP-1 presenilin deficiency causes a late-onset notch signaling phenotype that affects adult germline function in *Caenorhabditis elegans*. *Genetics* 208, 745–762. doi: 10.1534/genetics.117.300605

Angeles-Albores, D., Leighton, D. H. W., Tsou, T., Khaw, T. H., Antoshechkin, I., and Sternberg, P. W. (2017). The *Caenorhabditis elegans* female-like state: decoupling the transcriptomic effects of aging and sperm status. *G3* 7, 2969–2977. doi: 10.1534/g3.117.300080

Angelo, G., and Van Gilst, M. R. (2009). Starvation protects germline stem cells and extends reproductive longevity in C. elegans. *Science* 326, 954–958. doi: 10.1126/science.1178343

Antebi, A. (2012). Regulation of longevity by the reproductive system. *Exp. Gerontol.* 48, 596–602. doi: 10.1016/j.exger.2012.09.009

Bhargava, V., Goldstein, C. D., Russell, L., Xu, L., Ahmed, M., Li, W., et al. (2020). GCNA preserves genome integrity and fertility across species. *Dev. Cell* 52, 38–52 e10.

Chen, J., Mohammad, A., Pazdernik, N., Huang, H., Bowman, B., Tycksen, E., et al. (2020). GLP-1 Notch-LAG-1 CSL control of the germline stem cell fate is mediated by transcriptional targets lst-1 and sygl-1. *PLoS Genet.* 16:e1008650. doi: 10.1371/journal.pgen.1008650

Corsi, A. K., Wightman, B., and Chalfie, M. (2015). A transparent window into biology: a primer on *Caenorhabditis elegans*. *Genetics* 200, 387–407. doi: 10.1534/genetics.115.176099

Dalfó, D., Michaelson, D., and Hubbard, E. J. A. (2012). Sensory regulation of the C. elegans germline through TGF-β-dependent signaling in the Niche. *Curr. Biol.* 22, 712–719. doi: 10.1016/j.cub.2012.02.064

Das, D., and Arur, S. (2017). Conserved insulin signaling in the regulation of oocyte growth, development, and maturation. *Mol. Reprod. Dev.* 84, 444–459. doi: 10.1002/mrd.22806

Fielenbach, N., and Antebi, A. (2008). C. elegans dauer formation and the molecular basis of plasticity. *Genes Dev.* 22, 2149–2165. doi: 10.1101/gad.1701508

Fox, P. M., and Schedl, T. (2015). Analysis of germline stem cell differentiation following loss of GLP-1 notch activity in *Caenorhabditis elegans*. *Genetics* 201, 167–184. doi: 10.1534/genetics.115.178061

Fox, P. M., Vought, V. E., Hanazawa, M., Lee, M.-H., Maine, E. M., and Schedl, T. (2011). Cyclin E and CDK-2 regulate proliferative cell fate and cell cycle progression in the C. elegans germline. *Development* 138, 2223–2234. doi: 10.1242/dev.059535

Fukuyama, M., Rougvie, A. E., and Rothman, J. H. (2006). C. elegans DAF-18/PTEN mediates nutrient-dependent arrest of cell cycle and growth in the germline. *Curr. Biol.* 16, 773–779. doi: 10.1016/j.cub.2006.02.073

Furuta, T., Joo, H. J., Trimmer, K. A., Chen, S. Y., and Arur, S. (2018). GSK-3 promotes S-phase entry and progression in C. elegans germline stem cells to maintain tissue output. *Development* 145:dev161042.

Galimov, E. R., and Gems, D. (2021). Death happy: adaptive ageing and its evolution by kin selection in organisms with colonial ecology. *Philos. Trans. R. Soc. Lond. B Biol. Sci.* 376:20190730. doi: 10.1098/rstb.2019.0730

Garigan, D., Hsu, A.-L., Fraser, A. G., Kamath, R. S., Ahringer, J., and Kenyon, C. (2002). Genetic analysis of tissue aging in *Caenorhabditis elegans*: a role for heat-shock factor and bacterial proliferation. *Genetics* 161, 1101–1112. doi: 10.1093/genetics/161.3.1101

Gerhold, A. R., Ryan, J., Vallee-Trudeau, J. N., Dorn, J. F., Labbe, J. C., and Maddox, P. S. (2015). Investigating the regulation of stem and progenitor cell mitotic progression by in situ imaging. *Curr. Biol.* 25, 1123–1134. doi: 10.1016/j.cub.2015.02.054

Greenwald, I., and Kovall, R. (2013). Notch signaling: genetics and structure. *WormBook* 17, 1–28. doi: 10.1895/wormbook.1.10.2

Haupt, K. A., Enright, A. L., Ferdous, A. S., Kershner, A. M., Shin, H., Wickens, M., et al. (2019). The molecular basis of LST-1 self-renewal activity and its control of stem cell pool size. *Development* 146:dev181644.

Hillers, K. J., Jantsch, V., Martinez-Perez, E., and Yanowitz, J. L. (2017). Meiosis. *WormBook* 2017, 1–43.

Hsu, H.-J., LaFever, L., and Drummond-Barbosa, D. (2008). Diet controls normal and tumorous germline stem cells via insulin-dependent and -independent mechanisms in Drosophila. *Dev. Biol.* 313, 700–712. doi: 10.1016/j.ydbio.2007.11.006

Hubbard, E. J. A., and Schedl, T. (2019). Biology of the *Caenorhabditis elegans* germline stem cell system. *Genetics* 213, 1145–1188. doi: 10.1534/genetics.119.300238

Huelgas-Morales, G., and Greenstein, D. (2018). Control of oocyte meiotic maturation in C. elegans. *Semin. Cell Dev. Biol.* 84, 90–99. doi: 10.1016/j.semcdb.2017.12.005

Hughes, S. E., Evason, K., Xiong, C., and Kornfeld, K. (2007). Genetic and pharmacological factors that influence reproductive aging in nematodes. *PLoS Genet.* 3:e25. doi: 10.1371/journal.pgen.0030025.eor

Imakubo, M., Takayama, J., Okada, H., and Onami, S. (2021). Statistical image processing quantifies the changes in cytoplasmic texture associated with aging in *Caenorhabditis elegans* oocytes. *BMC Bioinform.* 22:73.

Jaramillo-Lambert, A., Ellefson, M., Villeneuve, A. M., and Engebrecht, J. (2007). Differential timing of S phases, X chromosome replication, and meiotic prophase in the C. elegans germ line. *Dev. Biol.* 308, 206–221. doi: 10.1016/j.ydbio.2007.05.019

Kao, S. H., Tseng, C. Y., Wan, C. L., Su, Y. H., Hsieh, C. C., Pi, H., et al. (2015). Aging and insulin signaling differentially control normal and tumorous germline stem cells. *Aging Cell* 14, 25–34. doi: 10.1111/acel.12288

Kenyon, C. J. (2010). The genetics of ageing. *Nature* 464, 504–512.

Kershner, A. M., Shin, H., Hansen, T. J., and Kimble, J. (2014). Discovery of two GLP-1/Notch target genes that account for the role of GLP-1/Notch signaling in stem cell maintenance. *Proc. Natl. Acad. Sci.* 111, 3739–3744. doi: 10.1073/pnas.1401861111

Kershner, A., Crittenden, S. L., Friend, K., Sorensen, E. B., Porter, D. F., and Kimble, J. (2013). *Germline Stem Cells and their Regulation in the Nematode Caenorhabditis elegans*. Dordrecht: Springer.

Killian, D. J., and Hubbard, E. J. A. (2001). RNAi feeding to produce males. *Worm Breeder's Gazette* 17:32.

Killian, D. J., and Hubbard, E. J. A. (2005). Caenorhabditis elegans germline patterning requires coordinated development of the somatic gonadal sheath and the germ line. *Dev. Biol.* 279, 322–335. doi: 10.1016/j.ydbio.2004.12.021

Kocsisova, Z., Kornfeld, K., and Schedl, T. (2018). Cell cycle accumulation of the proliferating cell nuclear antigen PCN-1 transitions from continuous in the adult germline to intermittent in the early embryo of C. elegans. *BMC Dev. Biol.* 18:12.

Kocsisova, Z., Kornfeld, K., and Schedl, T. (2019). Rapid population-wide declines in stem cell number and activity during reproductive aging in C. elegans. *Development* 146:dev.173195.

Lara-Gonzalez, P., Moyle, M. W., Budrewicz, J., Mendoza-Lopez, J., Oegema, K., and Desai, A. (2019). The G2-to-M transition is ensured by a dual mechanism that protects cyclin B from degradation by Cdc20-activated APC/C. *Dev. Cell* 51, 313–325. doi: 10.1016/j.devcel.2019.09.005

Libina, N., Berman, J. R., and Kenyon, C. (2003). Tissue-specific activities of C. elegans DAF-16 in the regulation of lifespan. *Cell* 115, 489–502. doi: 10.1016/s0092-8674(03)00889-4

Lopez, A. L., Chen, J., Joo, H. J., Drake, M., Shidate, M., Kseib, C., et al. (2013). DAF-2 and ERK couple nutrient availability to meiotic progression during *Caenorhabditis elegans* oogenesis. *Dev. Cell* 27, 227–240. doi: 10.1016/j.devcel.2013.09.008

Luo, S., Kleemann, G. A., Ashraf, J. M., Shaw, W. M., and Murphy, C. T. (2010). TGF-β and insulin signaling regulate reproductive aging via oocyte and germline quality maintenance. *Cell* 143, 299–312. doi: 10.1016/j.cell.2010.09.013

Michaelson, D., Korta, D. Z., Capua, Y., and Hubbard, E. J. A. (2010). Insulin signaling promotes germline proliferation in C. elegans. *Development* 137, 671–680. doi: 10.1242/dev.042523

Nadarajan, S., Govindan, J. A., McGovern, M., Hubbard, E. J. A., and Greenstein, D. (2009). MSP and GLP-1/Notch signaling coordinately regulate actomyosin-dependent cytoplasmic streaming and oocyte growth in C. elegans. *Development* 136, 2223–2234. doi: 10.1242/dev.034603

Narbonne, P., Maddox, P. S., and Labbe, J. C. (2015). DAF-18/PTEN locally antagonizes insulin signalling to couple germline stem cell proliferation to oocyte needs in C. elegans. *Development* 142, 4230–4241.

Narbonne, P., Maddox, P. S., and Labbe, J. C. (2017). DAF-18/PTEN signals through AAK-1/AMPK to inhibit MPK-1/MAPK in feedback control of germline stem cell proliferation. *PLoS Genet.* 13:e1006738. doi: 10.1371/journal.pgen.1006738

Otsuki, L., and Brand, A. H. (2018). Cell cycle heterogeneity directs the timing of neural stem cell activation from quiescence. *Science* 360, 99–102. doi: 10.1126/science.aan8795

Pekar, O., Ow, M. C., Hui, K. Y., Noyes, M. B., Hall, S. E., and Hubbard, E. J. A. (2017). Linking the environment, DAF-7/TGFbeta signaling and LAG-2/DSL ligand expression in the germline stem cell niche. *Development* 144, 2896–2906. doi: 10.1242/dev.147660

Pickett, C. L., Dietrich, N., Chen, J., Xiong, C., and Kornfeld, K. (2013). Mated progeny production is a biomarker of aging in *Caenorhabditis elegans*. *G3* 3, 2219–2232. doi: 10.1534/g3.113.008664

Qin, Z., and Hubbard, E. J. A. (2015). Non-autonomous DAF-16/FOXO activity antagonizes age-related loss of C. elegans germline stem/progenitor cells. *Nat. Commun.* 6:7107.

Roy, D., Michaelson, D., Hochman, T., Santella, A., Bao, Z., Goldberg, J. D., et al. (2016). Cell cycle features of C. elegans germline stem/progenitor cells vary temporally and spatially. *Dev. Biol.* 409, 261–271. doi: 10.1016/j.ydbio.2015.10.031

Seidel, H. S., and Kimble, J. (2011). The oogenic germline starvation response in C. elegans. *PLoS One* 6:e28074. doi: 10.1371/journal.pone.0028074

Seidel, H. S., and Kimble, J. (2015). Cell-cycle quiescence maintains Caenorhabditis elegans germline stem cells independent of GLP-1/Notch. *eLife* 4:e10832.

Shin, H., Haupt, K. A., Kershner, A. M., Kroll-Conner, P., Wickens, M., and Kimble, J. (2017). SYGL-1 and LST-1 link niche signaling to PUF RNA repression for stem cell maintenance in *Caenorhabditis elegans*. *PLoS Genet.* 13:e1007121. doi: 10.1371/journal.pgen.1007121

Templeman, N. M., Cota, V., Keyes, W., Kaletsky, R., and Murphy, C. T. (2020). CREB non-autonomously controls reproductive aging through hedgehog/patched signaling. *Dev. Cell* 54, 92–105. doi: 10.1016/j.devcel.2020.05.023

Templeman, N. M., Luo, S., Kaletsky, R., Shi, C., Ashraf, J., Keyes, W., et al. (2018). Insulin signaling regulates oocyte quality maintenance with age via cathepsin B activity. *Curr. Biol.* 753–760 e754.

Tenen, C. C., and Greenwald, I. (2019). Cell non-autonomous function of daf-18/PTEN in the somatic gonad coordinates somatic gonad and germline development in C. elegans Dauer Larvae. *Curr. Biol.* 29, 1064–1072 e1068.

Thondamal, M., Witting, M., Schmitt-Kopplin, P., and Aguilaniu, H. (2015). Steroid hormone signalling links reproduction to lifespan in dietary-restricted *Caenorhabditis elegans*. *Nat. Commun.* 5:4879.

White, J., and Dalton, S. (2005). Cell cycle control of embryonic stem cells. *Stem. Cell Rev.* 1, 131–138. doi: 10.1385/scr:1:2:131

Conflict of Interest: The authors declare that the research was conducted in the absence of any commercial or financial relationships that could be construed as a potential conflict of interest.

frontiers in Cell and Developmental Biology

ORIGINAL RESEARCH
published: 16 July 2021
doi: 10.3389/fcell.2021.652809

Comparative Proteomics and Phosphoproteomics Analysis Reveal the Possible Breed Difference in Yorkshire and Duroc Boar Spermatozoa

Yongjie Xu[1,2†], Qiu Han[1†], Chaofeng Ma[3†], Yaling Wang[1], Pengpeng Zhang[1,2], Cencen Li[1,2], Xiaofang Cheng[1,2] and Haixia Xu[1,2]*

[1] College of Life Science, Xinyang Normal University, Xinyang, China, [2] Institute for Conservation and Utilization of Agro-Bioresources in Dabie Mountains, Xinyang Normal University, Xinyang, China, [3] Xinyang Animal Disease Control and Prevention Center, Xinyang, China

OPEN ACCESS

Edited by:
Vittorio Sebastiano, Stanford University, United States

Reviewed by:
Ning Li, Hong Kong University of Science and Technology, Hong Kong
Qiangzhen Yang, Shanghai Jiao Tong University, China

***Correspondence:**
Haixia Xu
hxxu214@126.com

† These authors have contributed equally to this work

Specialty section:
This article was submitted to Cellular Biochemistry, a section of the journal Frontiers in Cell and Developmental Biology

Received: *13 January 2021*
Accepted: *18 June 2021*
Published: *16 July 2021*

Citation:
Xu Y, Han Q, Ma C, Wang Y, Zhang P, Li C, Cheng X and Xu H (2021) Comparative Proteomics and Phosphoproteomics Analysis Reveal the Possible Breed Difference in Yorkshire and Duroc Boar Spermatozoa. Front. Cell Dev. Biol. 9:652809. doi: 10.3389/fcell.2021.652809

Sperm cells are of unique elongated structure and function, the development of which is tightly regulated by the existing proteins and the posttranslational modifications (PTM) of these proteins. Based on the phylogenetic relationships of various swine breeds, Yorkshire boar is believed to be distinctly different from Duroc boar. The comprehensive differential proteomics and phosphoproteomics profilings were performed on spermatozoa from both Yorkshire and Duroc boars. By both peptide and PTM peptide quantification followed by statistical analyses, 167 differentially expressed proteins were identified from 1,745 proteins, and 283 differentially expressed phosphopeptides corresponding to 102 unique differentially phosphorylated proteins were measured from 1,140 identified phosphopeptides derived from 363 phosphorylated proteins. The representative results were validated by Western blots. Pathway enrichment analyses revealed that majority of differential expression proteins and differential phosphorylation proteins were primarily concerned with spermatogenesis, male gamete generation, sperm motility, energy metabolism, cilium morphogenesis, axonemal dynein complex assembly, sperm–egg recognition, and capacitation. Remarkably, axonemal dynein complex assembly related proteins, such as SMCP, SUN5, ODF1, AKAP3, and AKAP4 that play a key regulatory role in the sperm physiological functions, were significantly higher in Duroc spermatozoa than that of Yorkshire. Furthermore, phosphorylation of sperm-specific proteins, such as CABYR, ROPN1, CALM1, PRKAR2A, and PRKAR1A, participates in regulation of the boar sperm motility mainly through the cAMP/PKA signal pathway in different breeds, demonstrating that protein phosphorylation may be an important mechanism underlying the sperm diversity. Protein–protein interaction analysis revealed that the 14 overlapped proteins between differential expression proteins and differential phosphorylation proteins potentially played a key role in sperm development and motility of the flagellum,

including the proteins ODF1, SMCP, AKAP4, FSIP2, and SUN5. Taken together, these physiologically and functionally differentially expressed proteins (DEPs) and differentially expressed phosphorylated proteins (DPPs) may constitute the proteomic backgrounds between the two different boar breeds. The validation will be performed to delineate the roles of these PTM proteins as modulators of Yorkshire and Duroc boar spermatozoa.

Keywords: spermatozoa, breed, sperm motility, proteomics, phosphoproteomics, iTRAQ labeling

INTRODUCTION

In the modern swine production, artificial insemination (AI) is one of the most critical technologies in the genetic improvement of porcine herds. Sperm quality, as an important boar reproductive trait with moderate to low heritability, is crucial for insuring the success of AI, which is influenced by both environmental and genetic factors (Marques et al., 2017; Gao et al., 2019). Duroc, Yorkshire, and Landrace are the most frequently used pigs in commercial production and have favorable growth performance. Due to the various origins, these breeds not only are significantly different in the aspect of meat productive traits but also have great differences in reproductive traits, such as male fertility traits, including sperm number, sperm-fertilizing capacity, sperm motility, concentration, and vitality, and semen volume (Koh et al., 1976; Kasimanickam and Kastelic, 2016; Shanmugam et al., 2016). For instance, Large White and Landrace boars had higher total sperm number and ejaculate volume, but less sperm motility and concentration than Duroc breeds (Ciereszko et al., 2000; Smital, 2009). Although it is known that there are differences in semen traits among the different porcine breeds, the diversity in the molecular mechanism of the genetic background has not been well characterized. Thereby, providing the impetus to understanding the genetic background associated with sperm quality traits in different breeds is of great benefit to improve the genetic selection for these traits and accelerate genetic progress.

Mature mammalian sperm are highly differentiated haploid cells which almost silenced at the level of transcriptional and translational regulation. As the carrier of patrilineal genes, sperm cells are unique in elongated structure and function and are tightly regulated by the existing proteins and the posttranslational modifications (PTM), which have served as a resource pool for screening of key targets involved in sperm motility regulation (Samanta et al., 2016; Dai et al., 2019b; Gadadhar et al., 2021). Owing to this essential role in sperm cells, the study of sperm protein is of great significance for clarifying the physiological process of mammalian spermatogenesis and conception. Due to the extensive application of "omics" technology for system biology, tremendous progress has been made in recent years on protein function research through global proteome analysis and its complex interaction in response to specific disturbance (Larance and Lamond, 2015; Dai et al., 2019a). Proteomics has also been widely used in the study of human and other animal sperm, which can reflect the protein composition, distribution, and function of sperm cells from a macro perspective, and indicated that sperm proteins play essential functional roles and contribute to vital biological processes such as spermatogenesis, sperm motility, sperm capacitation, fertilization, and male infertility (Chalmel and Rolland, 2015; Baker, 2016; Maciel et al., 2019; Agarwal et al., 2020; Martin-Hidalgo et al., 2020). Therefore, quantitative proteomics analysis is a potent tool for understanding the quality variation in sperm functions.

On a genome analysis of cumulative nucleotide differences, Yorkshire pigs differed significantly from Duroc, consistent with being the two breeds with a rather distant relationship based on phylogenetic analyses (Kim et al., 2015). The semen trait differences in sperm motility and capacitation, fertility, and semen volume among the porcine breeds were studied in the previous experiments (Ciereszko et al., 2000; Smital et al., 2004; Flowers, 2008; Smital, 2009). The protein function of sperm-fertilizing and its relationship with different boar breeds have been increasingly a focus in these years, and the identification of differentially expressed proteins in spermatozoa can help to clarify the molecular mechanisms of the genetic background from different boar breeds. Xinhong et al. (2018) firstly showed an iTRAQ-based proteomics analysis of sperm proteins in Meishan and Duroc boar species and provided significant information for elucidating the molecular basis responsible for variety-specific differences in pig reproductive efficiency. Despite that protein regulation at the phosphorylation level plays crucial functions in sperm, very few studies have reported the diversities in phosphoproteins associated with sperm motility between different porcine breeds. The precise genetic mechanisms behind the sperm vitality and motility in different breeds remain unclear, and there was no comprehensive analysis of the proteome or phosphoproteome determining breed differences in boar sperm. In this research, we used a global analysis of iTRAQ-based quantitative proteome coupled with phosphopeptide-enrichment strategies to reveal the boar spermatozoa proteome and find the PTMs associated with the breed differences using Yorkshire and Duroc boar spermatozoa. Our results show that the porcine sperm protein phosphorylation status relates exclusively to sperm structure and motility in different breeds, thus supporting its importance for phosphorylation status changes in distinguishing breed specificity. Moreover, this research will provide a new insight to understanding the molecular basis of the differences in pig reproductive efficiency between Duroc and Yorkshire breeds.

MATERIALS AND METHODS

Semen Sources and Preparation

Fresh boar semen was obtained from Hongzhan Pig Breeding Farm (Xinyang, Henan, China). All boars were fed similar

amounts of a common ration, with management and nutrition in accordance with good industry practices. Semen was collected concurrently from Duroc and Yorkshire boars (four boars per breed), with all boars 18–24 months old at the time of semen collection. Semen was treated according to the method as described by Kasimanickam and Kastelic (2016). Briefly, initial post-collection motility was consistently $\geq$ 80%, the minimum content of sperm with normal morphology was 80%, and the sperm density was 2.0∼3.5 $\times$ 10^8/ml. The sperm-rich fraction was diluted in Beltsville thawing solution (BTS) buffer (1:1 volume) and transported to the laboratory at 37°C within 1 h. Upon arrival, diluted semen was placed in 50-ml Falcon tubes and centrifuged at 1,000 *g* for 20 min (4°C) to separate seminal plasma. Sperm were washed twice using BTS at 1,000 *g* for 20 min (4°C). The sperm pellet was resuspended in BTS, then aliquoted into microcentrifuge tubes, and centrifuged at 16,000 *g* for 10 min (4°C). The supernatant was completely discarded, and the sperm precipitate was fast frozen in liquid nitrogen and stored in the refrigerator at –80°C until used. All procedures were carried out in accordance with the Animal Ethical Treatment Guidelines and were approved by the Animal Care Commission of the College of Life Science, Xinyang Normal University, China.

Sperm Protein Extraction

Immediately after collection, 15-ml tubes were fully filled from each ejaculation/segment and were centrifuged twice at 1,500 *g* for 10 min. Sperm pellets were lysed in STD buffer (1 mM DTT, 4% SDS, 150 mM Tris–HCl pH 8.0) containing a 1% protease inhibitor cocktail (Roche). The sample was homogenized on ice by sonication with an ultrasonic cell crusher (DH92-IIN, Toshiba) 10 times (10-s pulse on/15-s pulse off). Samples were centrifuged at 16,000 *g* for 45 min at 4°C, and the supernatants were collected. The protein concentration was quantified by the BCA assay (Beyotime, P0012S, Shanghai, China) with BSA protein as standard.

Protein Digestion, iTRAQ Labeling, and Peptide Fractionation

Protein digestion was performed according to the previously filter-aided sample preparation (FASP) procedure (Wisniewski et al., 2009). Briefly, 200 μg of each protein sample was mixed with 200 μl UA buffer (8 M urea, 150 mM Tris–HCl pH 8.0) and concentrated for 15 min at 14,000 *g* using 10-kDa ultrafiltration centrifuge tubes. The retentates were resuspended in 200 μl UA buffer and concentrated for another 15 min at 14,000 *g* at room temperature. Then, 100 μl of 0.05 M IAA in UA buffer was added to inhibit reduced cysteine residues, and the samples were incubated for 30 min in darkness and concentrated for 10 min at 14,000 *g*. Subsequently, the filters were washed with 100 μl of UA buffer twice and spun for 10 min at 14,000 g, and then washed twice with 100 μl of DS buffer (50 mM trimethylammonium bicarbonate at pH 8.5) and spun for 10 min at 14,000 *g*. Finally, the protein suspensions were digested with 40 μl 50 ng/μl sequencing-grade trypsin (Roche, IN, United States) (2 μg trypsin in 40 μl DS buffer) overnight at 37°C, and the resulting peptides were collected as a filtrate. The peptide content was estimated by UV light spectral density at 280 nm (Wisniewski et al., 2009).

For proteome analysis, the resulting peptide mixture was labeled using the iTRAQ Reagent-8Plex Multiplex kit (AB SCIEX, Foster City, CA, United States) according to the manufacturer's instructions. In detail, each iTRAQ reagent was dissolved in 70 μl of ethanol and added to different peptide mixtures. The 80-μg digested peptides from each sample were incubated with specific iTRAQ reagents (iTRAQ reagents 113, 114, 115, and 116 used for four Duroc sperm samples, and iTRAQ reagents 117, 118, 119, and 121 for four Yorkshire sperm samples, respectively) for 1 h at room temperature. The digested peptides used for proteomic and phosphoproteomic analysis were labeled separately. After labeling, samples were multiplexed and concentrated in a vacuum concentrator for further identification and quantification by LC-MS/MS. Proteins showing different abundances between the Yorkshire and Duroc groups, as shown in **Figure 1**, were subjected to bioinformatics analysis, and quantification was validated by Western blot.

Additionally, to identify more proteins for proteome analysis, Strong cation exchange (SCX) was applied to separate the mixed peptides using AKTA Purifier 100 (GE Healthcare, Fairfield, CT, United States) as previously described (Dong et al., 2017). In brief, the vacuum-dried iTRAQ-labeled peptide mixture was reconstituted in 2 ml buffer A (25% CAN and 10 mM KH_2PO_4 pH 3.0), loaded onto a Polysulfoethyl 4.6 mm $\times$ 100 mm column (5 μm, 200 Å) (PolyLC Inc., Columbia, MD, United States), and eluted at 0.7 ml/min with the following concentrations of buffer B (25% CAN, 500 mM KCl, and 10 mM KH_2PO_4 pH 3.0) successively: 0% buffer B from 0 to 25 min; 10% buffer B for 32 min; 20% buffer B for 42 min; 45% buffer B for 47 min; 100% to 0% buffer B from 52 to 60 min; and 0% buffer B for 75 min. After separation, the 33 fractions collected were combined to 10 fractions according to SCX chromatogram, then desalted on standard density Empore SPE C_{18} cartridges (Sigma, St. Louis, MO, United States) with inner diameter 7 mm and volume 3 ml, concentrated by vacuum centrifugation.

Phosphopeptide Enrichment

Phosphopeptide enrichment was done as described previously (Du et al., 2017). Briefly, the vacuum-dried peptide mixture was resuspended in 500 μl loading buffer (2% glutamic acid/2% TFA/65% ACN). TiO_2 beads were added, and the samples were agitated by end-over-end rotation at 20°C for 40 min. The phosphopeptide-bound beads were collected by brief centrifugation, washed three times with 50 μl of buffer I (3% TFA/30% ACN), and then washed three times with 50 μl of buffer II (0.3% TFA/80% ACN) to remove any non-adsorbed material. Phosphopeptides were finally eluted with 50 μl of elution buffer (15% NH_4OH/40% ACN), dried, and stored at –80°C until further analysis.

LC-MS/MS Analysis Based on Q Exactive Mass Spectrometry

LC-MS/MS analyses were performed on a Q Exactive mass spectrometer coupled to an EASY-nLC 1000 nano-HPLC system

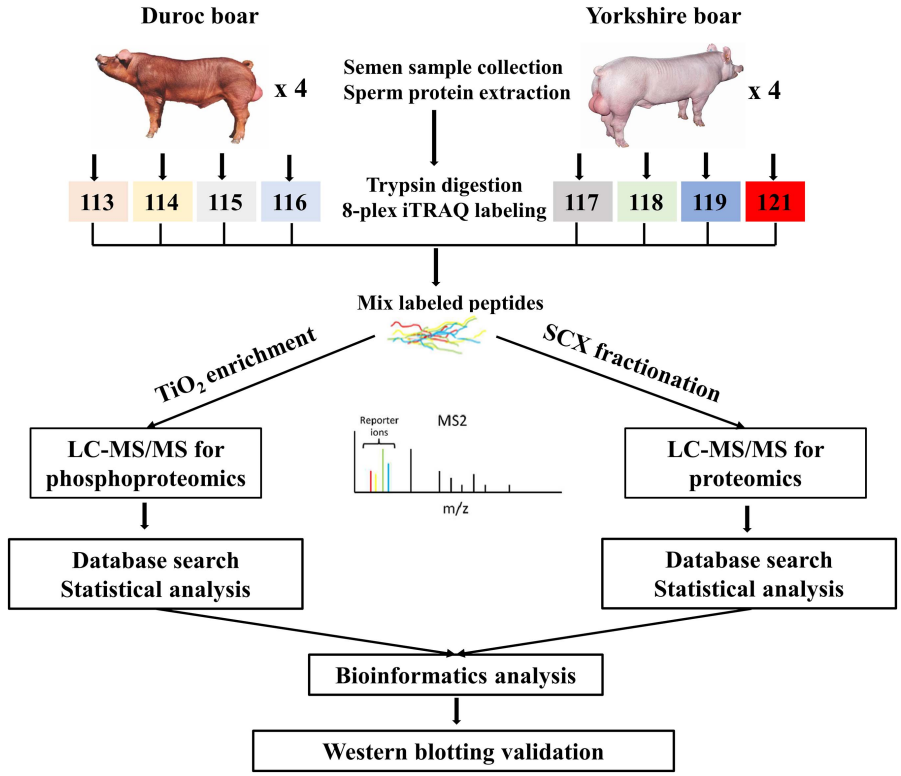

FIGURE 1 | Experimental design and schematic diagram of the workflow. Boar sperm was chosen for analysis of the differential proteomes between the Duroc and Yorkshire pig breeds. A total of eight boars were analyzed by iTRAQ 8Plex-based parallel quantitative proteomics and phosphoproteomics, using the LC-MS/MS workflow. After thorough statistical analyses of the proteomics data, the differentially expressed proteins and phosphoproteins/sites were conducted for the subsequent bioinformatics analysis and some of the important differentially expressed proteins were selected for validation of the discovery results by western blotting.

(Proxeon Biosystems, Thermo Fisher Scientific, Waltham, MA, United States) as described previously (Wei et al., 2018). Briefly, each dried peptide fraction or dried TiO_2-enriched phosphopeptides were reconstituted in 20 μl of 0.1% formic acid and loaded on a Thermo Scientific EASY column (2 cm × 100 μm, 5 μm C18 resin) equilibrated with 95% Buffer A (0.1% formic acid), and then the peptides were loaded and separated on a C18 column (25 cm × 75 μm, 3 μm C18 resin) at a flow rate of 250 nl/min. Peptide and phosphopeptide mixtures were eluted using buffer A (0.1% formic acid) and buffer B (100% acetonitrile and 0.1% formic acid) under a 170-min gradient with a flow rate of 250 nl/min (0–30% buffer B for 120 min, 30–50% buffer B for 25 min, 50–100% buffer B for 15 min, and finally 100% buffer B for 10 min).

For MS data acquisition, the eluted peptides and phosphopeptides were analyzed in positive ion mode on a Q Exactive mass spectrometer (Thermo Finnigan, San Jose, CA, United States) using data-dependent acquisition. The full mass scan was acquired by the Orbitrap mass analyzer from m/z 300 to 1800 with a resolution of 70,000 at m/z 200, and the AGC target was set to 3×10^6 with a max injection time of 20 ms. The 10 most intense parent ions were fragmented by higher-energy collisional dissociation (HCD). The MS/MS scans were also acquired by the Orbitrap with 17,500 resolution at m/z 200, and the AGC target was set to 2×10^4 with a max injection time of 60 ms. System control and data collection were performed by Xcalibur software (Thermo Fisher Scientific, United States). The mass spectrometry raw data have been deposited to the ProteomeXchange Consortium[1] *via* the iProX partner repository with the dataset identifier PXD025607 (Ma et al., 2019). The raw MS data files contain 15 files. P230-01.msf and P230-PH-3.msf are the search engine output files for proteome and phosphoproteome analysis, respectively. P230-1.raw, P230-2.raw, P230-3.raw, P230-4.raw, P230-5.raw, P230-6.raw, P230-7.raw, P230-8.raw, and P230-9.raw are the mass spectrometer output files of the proteome. P230-PH-1.raw, P230-PH-2.raw, and P230-PH-3.raw are the mass spectrometer output files of the phosphoproteome.

Mass Spectrometry Data Analysis

The raw MS/MS files were processed with Proteome Discoverer version 1.4 (Thermo Fisher Scientific, United States) and subjected to an in-house UniProt Sus scrofa (pig) protein database (UniProt 2018_01_27; 50,008 sequences; updated on 1-27-2018) searching using Mascot Server Version 2.2 (Matrix Science, London, United Kingdom). For proteome

[1]http://proteomecentral.proteomexchange.org

analysis, the parameters for database searching were set as follows: enzyme, trypsin; iTRAQ 8Plex labels, the N-terminal and lysine residues; maximum missed cleavages, 2; fixed modification, carbamidomethylation of cysteine residues; peptide mass tolerance, ±20 ppm; MS/MS tolerance, 0.1 Da; variable modifications, oxidation of methionine. For the phosphoproteome, parameters for protein identification were set as follows: enzyme, trypsin; mass values, monoisotopic; peptide mass tolerance, ±20 ppm; MS/MS tolerance, 0.1 Da; maximum missed cleavage, 2; iTRAQ 8Plex labels, the N-terminal and lysine residues; fixed modification, carbamidomethylation of cysteine residues; variable modifications, oxidation of methionine and phosphorylation of threonine/serine/tyrosine; instrument type, ESI-TRAP. The decoy database pattern was set as the reverse of the target database. Trypsin with full enzyme specificity and only peptides with a minimum length of six amino acids were selected. Protein identification was succeeded by at least one unique peptide identification. The minimum MaxQuant score of phosphorylation sites was 40. All reported data were based on 99% confidence for protein, peptide, and phosphorylation site identifications as determined by an FDR of ≤0.01 (Sandberg et al., 2012). Protein identification was supported by at least one unique peptide identification. PhosphoRS score >50 and PhosphoRS site probability >75% indicate that a site is truly phosphorylated (Olsen et al., 2006).

Peptides with different amino acid sequences or modifications were identified as unique peptides. For quantification, only unique peptides were considered, and it was performed simultaneously with protein identification using Proteome Discoverer software. The $\log_2$ values of the measured precursor intensities were normalized by the median values across an entire labeling experiment to correct for protein abundance variation (Unwin et al., 2010). A two-sample *t*-test was carried out within SPSS 18.0. Proteins or phosphopeptides with $p < 0.05$ after Benjamini and Hochberg adjustment and fold-change ratios ≥1.3 or ≤0.77 were considered as differentially expressed proteins (DEPs) or differentially expressed phosphopeptides (DEPPs).

Bioinformatics Analysis

The biological functions of identified DEPs and differential phosphorylation proteins (DPPs) were annotated using GO enrichment[2] and the KEGG pathway[3]. To understand these DEPs and DPPs in terms of the published literature, interactions among them in relation to function and biological pathways were determined using the IPA tool. Interactions among all the related DEPs and DPPs were constructed using the program STRING[4]. The STRING program was set to show no more than 10 interactions and medium confidence.

Western Blotting

Sperm lysates were run on SDS-PAGE gels, and immunoblotting was performed according to our previous procedure (Xu et al., 2012). The primary antibodies used were as follows: mouse anti-HNRNPK (ab39975, Abcam, Cambridge, MA, United States), rabbit anti-AKAP3 (13907-1-AP, Proteintech, Wuhan, China), rabbit anti-ODF1 (24736-1-AP, Proteintech), rabbit anti-PTGDS (10754-2-AP, Proteintech), rabbit anti-AKAP4 (24986-1-AP, Proteintech), rabbit anti-GK (13360-1-AP, Proteintech), and mouse anti-GAPDH (AF5009, Beyotime). Immunoblots were repeated at least three times for each sample from four Duroc and Yorkshire pigs, respectively. Detection of proteins was performed using enhanced chemiluminescence (ECL). Finally, the blot was imaged using a FluorChem M multicolor fluorescence Western blot imaging system (ProteinSimple, San Jose, CA, United States).

RESULTS

Proteomic and Phosphoproteomic Profiles of Porcine Spermatozoa

In this study, the global protein expression and phosphorylation events were compared between Duroc and Yorkshire boar spermatozoa using 8Plex iTRAQ-based quantitative proteomics. Four independent biological replicates were performed for each sperm protein sample for iTRAQ labeling. We identified 10,876 unique peptides from 187,889 spectra corresponding to 1,745 protein species (**Supplementary Data 1, 2**, <1% FDR). The 1,745 identified proteins were annotated with UniProtKB (ENSEMBL) databases, corresponding to 1,697 (97.2%) full protein and 48 (2.8%) protein fragment annotations. However, 384 identified proteins were cataloged as uncharacterized protein isoforms due to the scarcity of porcine protein databases. Among these proteins, 1,738 were successfully quantified, of which 150 proteins were detected as DEPs between the two groups as a cutoff of 1.3-fold change (**Figure 2A**). The predicted molecular weights (MW) of the identified proteins vary widely with a range from 1.7 to 763.6 kDa with a mean of 57.3 kDa (**Figure 3A**). The sequence coverage of peptides (**Figure 3B**) and the distribution of the peptide number (**Figure 3C**) and peptide length (**Figure 3D**) were also provided. More than 67.9% of the identified peptides were detected from at least two unique peptides. In addition, the protein sequence coverage with >50, 40–50%, 30–40%, 20–30%, 10–20%, 5–10%, and under 5% variation accounted for 7.51, 6.70, 9.17, 14.10, 20.34 18.85, and 23.32%, respectively, of the total identified proteins (**Figure 3B**).

Using PhosphoRS probability cutoff >75%, 1,140 phosphosites were identified from 1,064 unique phosphopeptides mapping to 363 proteins of porcine sperm (**Supplementary Data 3**), of which 283 unique phosphopeptides were detected to be differentially expressed between the two breeds as a cutoff of 1.3-fold change (**Figure 2B**). Amid these phosphopeptides, 705 peptides only showed one phosphorylation site, 274 peptides showed two, and 49 peptides showed three or more. On analysis of phosphosites of the phosphorylated proteins, 208 proteins were identified to be phosphorylated at a single site on the protein sequence, and 155 proteins were phosphorylated at two or more. AKAP4, as the most prominent

[2]http://www.geneontology.org

[3]http://www.kegg.jp

[4]http://string-db.org

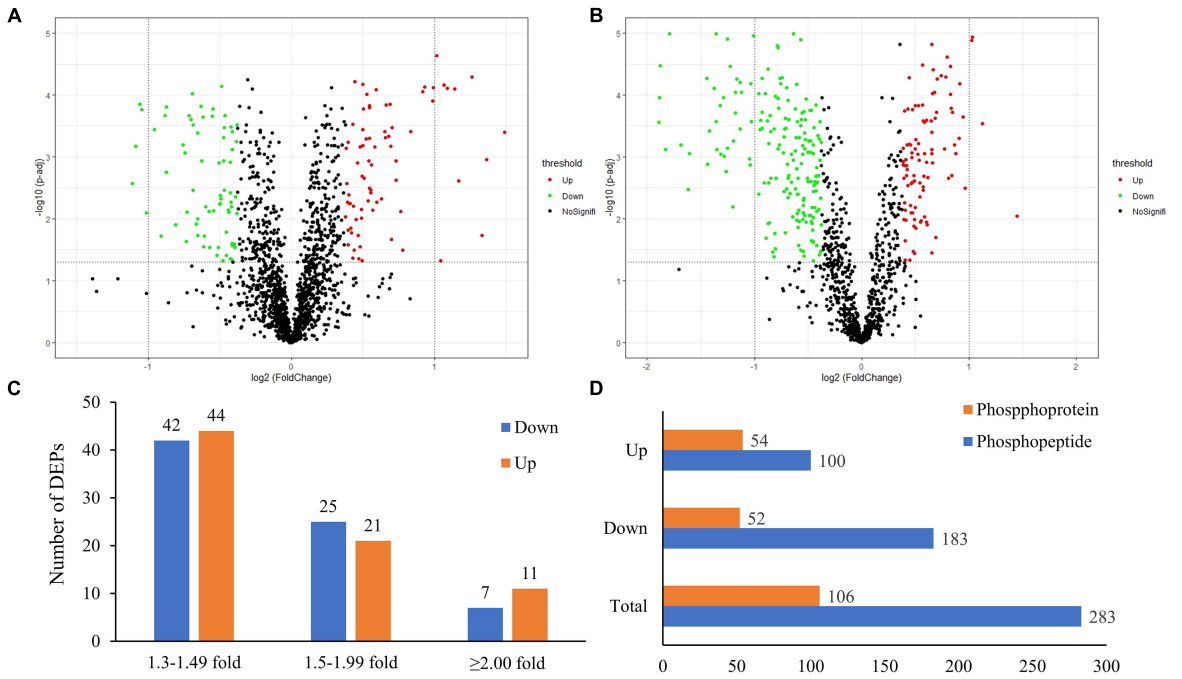

FIGURE 2 | The global proteome and phosphoproteome analysis of Yorkshire and Duroc boar spermatozoa. **(A)** Volcano plot of the quantified proteins in all biological replicates (the significant downregulated and upregulated protein shown in the green and red plots, respectively). **(B)** Volcano plot of the quantified phosphorylated sites in all biological replicates after TiO_2 enrichment (the significant downregulated and upregulated phosphorylated sites shown in the green and red plots, respectively). **(C)** The fold-change distribution of DEPs. **(D)** Summary of the DEPPs and DPPs between Yorkshire and Duroc boar spermatozoa.

example, is identified as being targeted for 45 phosphorylated sites including 55 phosphopeptides (**Supplementary Figure 1**). As would be expected, consistent with previous published reports, the 1,140 assigned sites included 990 phosphorylated serine (pS), 140 phosphorylated threonine (pT), and 10 phosphorylated tyrosine (pY) residues (ratios of 86.8, 12.3, and 0.9%), respectively, indicated in **Figure 4A**. These results can tremendously contribute to the porcine sperm protein phosphorylation database for future study.

Comparing the number of identified proteins and phosphorylated proteins, all the proteins identified in proteomics (1,745) and phosphoproteomics (363) sets were demonstrated in the Venn diagram (**Figure 5A**). Only 274 proteins (75.5%) were overlapped between non-modified proteins and phosphoproteins, while ∼24.5% of the total phosphoproteins were not detected in the global proteomics analysis. The explanation for this result was that most of the identified phosphorylated proteins are expressed in relatively low abundance in porcine sperm and identified mainly depending on the specificity of the enrichment strategy for phosphopeptides. In unenriched fractions, there are more redundant peptides mainly derived from a very small number of highly abundant proteins, such as sperm structure proteins (e.g., PRM-1, several tubulin family members, FN1, and ODF1) and sperm–egg interaction proteins (e.g., SPACA1, SPESP1, PSP-I/II, and AQN-3), which decrease the probability of low-abundance-protein identification. This comparison also demonstrated that the extensive biochemical heterogeneity of sperm proteins led to the technical challenge and complexity of sperm proteome for its high dynamicity and diversity.

To obtain a global view of the biological function of the identified proteins and phosphoproteins, enriched GO terms were performed using the Panther classification system[5]. The cutoff of the *p*-value is set to 0.05, and terms of the same category are ordered by *p*-values. Analysis indicated that this global porcine sperm proteome returned dominant terms of cytoplasm, membrane, mitochondrion, cell periphery, and cell projection among the top GO cellular compartment categories when ranked based on number of annotated proteins (**Supplementary Figure 2A**). The notable enrichment GO biological processes were metabolic process, biological regulation, regulation of cellular process, stimulus response, regulation of metabolic process, cellular component assembly, and reproduction (**Supplementary Figure 2B**). Additional categories of direct relevance to sperm physiology/function included reproductive process, cell communication, and spermatogenesis. The dominant GO molecular functions represented in the porcine sperm proteome included that of catalytic activity, hydrolase activity, small molecule binding, nucleotide binding, and oxidoreductase activity, with some 313, 164, 159, 143, and 72 proteins mapping to each of these respective categories (**Supplementary Figure 2C**). Phosphoproteins were overrepresented from cell organelles, such as integral component of membrane, intrinsic component of

[5]http://www.pantherdb.org/

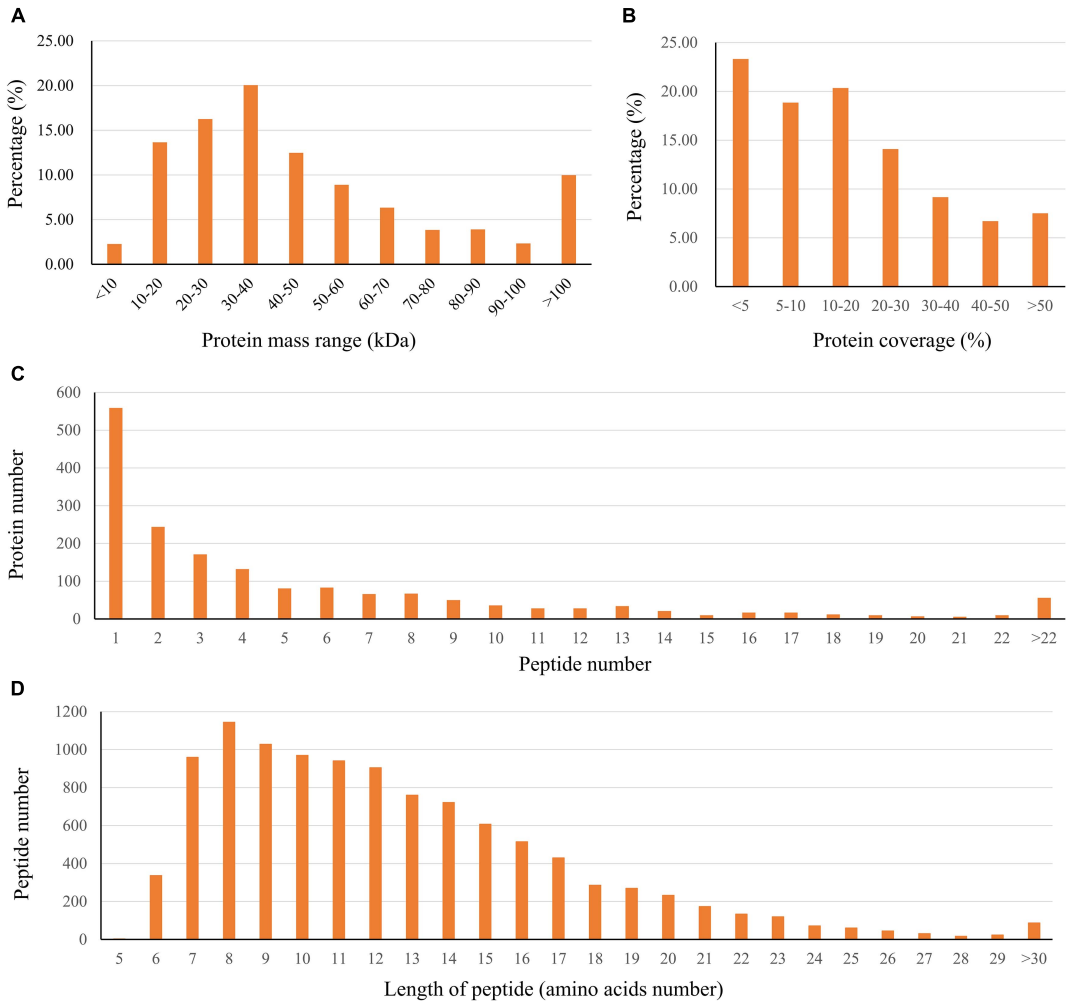

FIGURE 3 | Characteristics of the identified unique peptides in boar sperm samples. **(A)** The protein mass distribution. **(B)** The protein coverage. **(C)** The distribution of unique peptide number. **(D)** The distribution of peptides based on their length.

membrane, cytoskeletal part, cell projection, and microtubule cytoskeleton, and more involved in biological regulation, stimulus response, reproductive process, regulation of biological process, and spermatogenesis, and with the function of catalytic activity, hydrolase activity, small molecule binding, and anion binding.

To gain insight into the potential categorization of mycobacterial kinase substrates, the Motif-X algorithm was used to analyze the phosphorylation motifs with a relative occurrence rate threshold of 3% and a possibility threshold of $p < 10^{-6}$ (Chou and Schwartz, 2011). Due to lack of a specialized annotated kinase/phosphatase motif database in pigs, the generated motifs were matched against the Human Protein Reference Database[6]. We identified predominantly three phospho-motifs, KXXpS for PKCs and AKT (Ren et al., 2018), pSP/pTP for GSK-3, CDK, and MAPK families (**Figure 4C**). Thirty-seven substrates shared the KXXpS motif, of which three phosphopeptides (two proteins, AKAP4 and VAPA) were lowly phosphorylated in Yorkshire boar spermatozoa. In this category, the two AKAP4 phosphopeptides (AVSKIASEMAHDA and AAEKGYSVGDLLQ) involved in sperm motility and regulation of signal transduction pathways were found to be 1.33-fold and 3.03-fold, respectively, more highly phosphorylated in Duroc boar spermatozoa. Furthermore, 36 substrates shared the pSP motif, of which five phosphopeptides (four proteins, SPATA18, SPACA1, AKAP4, and SPATA31D1) were lowly phosphorylated in Yorkshire boar spermatozoa and four proteins (NT5C1B, CABYR-1, CFAP45, and TMEM202) were lowly phosphorylated in Duroc boar spermatozoa. Interestingly, 11 kinase substrates shared pTP, of which four (three proteins, DNAH8, St6galnac2, and NT5C1B) were highly phosphorylated in Yorkshire boar spermatozoa and three proteins (ODF2, PRDX5, and AKAP4) were highly phosphorylated in Duroc boar spermatozoa. Most of these proteins belonged to the motile cilium, sperm flagellum, or sperm fibrous sheath components. For example, AKAPs are related to sperm fertility

[6]http://www.hprd.org

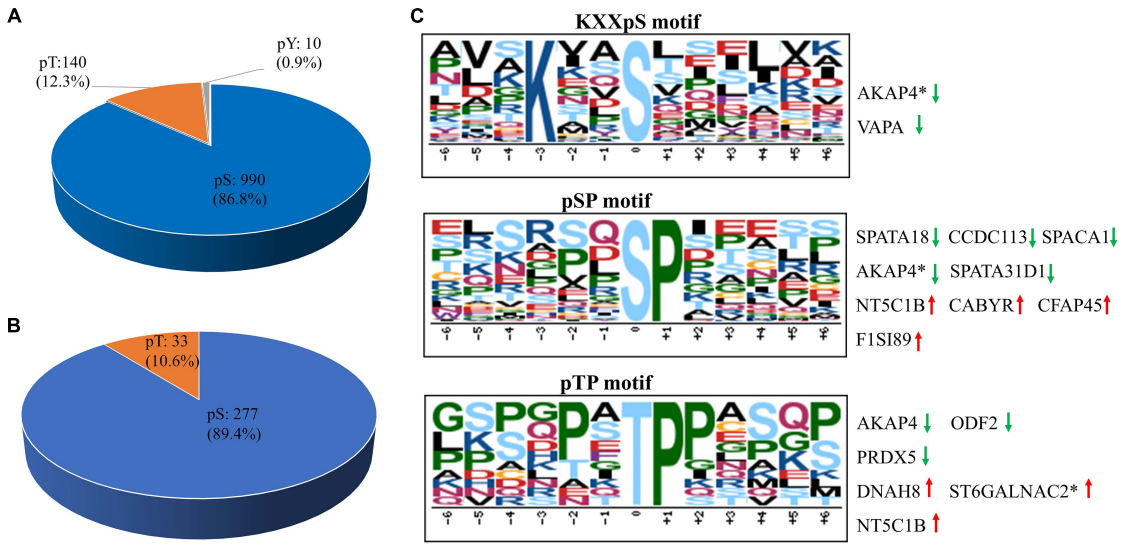

FIGURE 4 | The distribution and phosphorylation motif enrichment of the identified phosphorylation events. **(A)** The distribution of the phosphorylated serine (pS), threonine (pT), and tyrosine (pY) among the identified phosphorylation events. **(B)** The distribution of pS and pT sites of the differentially expressed phosphopeptides in boar sperm. **(C)** The Significantly enriched phosphorylation motif from all phosphorylation events. The height and color of the residues represent the frequency occurring at the respective positions and their physicochemical properties, respectively. Red arrow represents upregulated phosphosites, green arrow represents downregulated phosphosites, and asterisk represents that two or more phosphosites own the same the phosphorylation motif in the same protein.

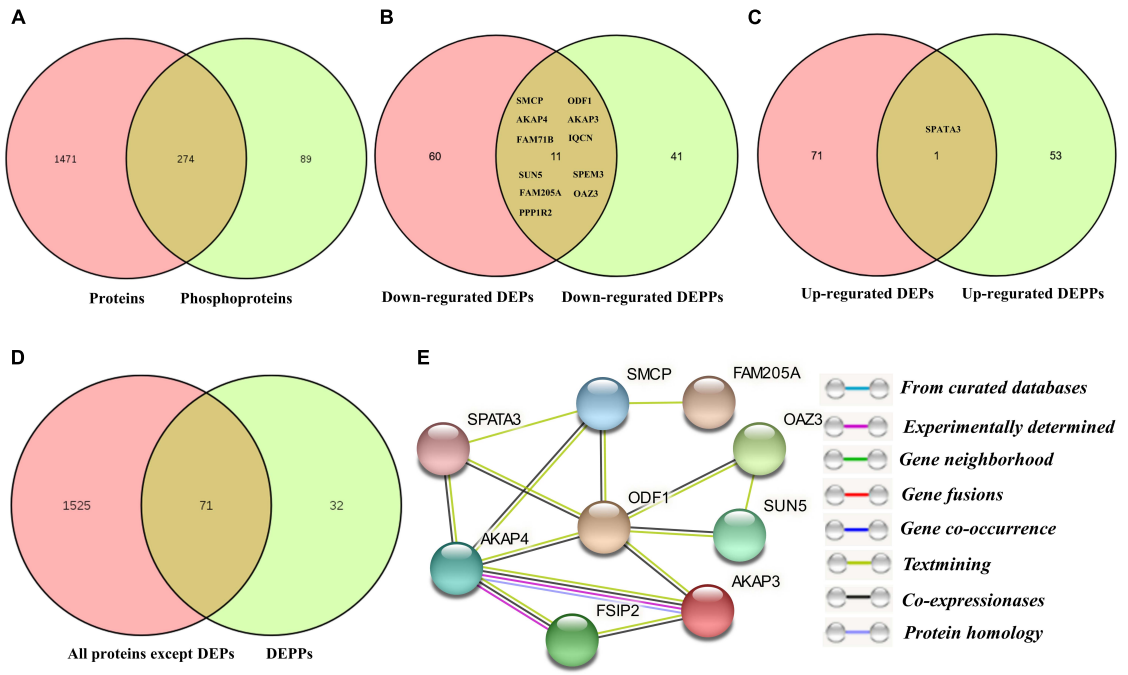

FIGURE 5 | The correlation analysis between DEPs and DEPPs. **(A)** Venn diagram of the correlation numbers between quantified proteins and phosphoproteins. **(B)** Venn diagram of the correlation numbers between downregulated DEPs and downregulated DEPPs. **(C)** Venn diagram of the correlation numbers between upregulated DEPs and upregulated DEPPs. **(D)** Venn diagram of the intersection numbers between total identified porcine boar sperm proteins and DEPPs. **(E)** The protein–protein interaction network of the 14 overlapped proteins between DEPs and DEPPs.

as a platform to integrate the cAMP signaling pathway and others through the binding with ion channels, protein kinases, and small GTP-binding proteins (Skroblin et al., 2010). The phosphorylation motif analysis demonstrated that AKAP4 is the potential substrate of MAPK and PKC protein kinases. This is consistent with the fact that AKAP4 can act as an important

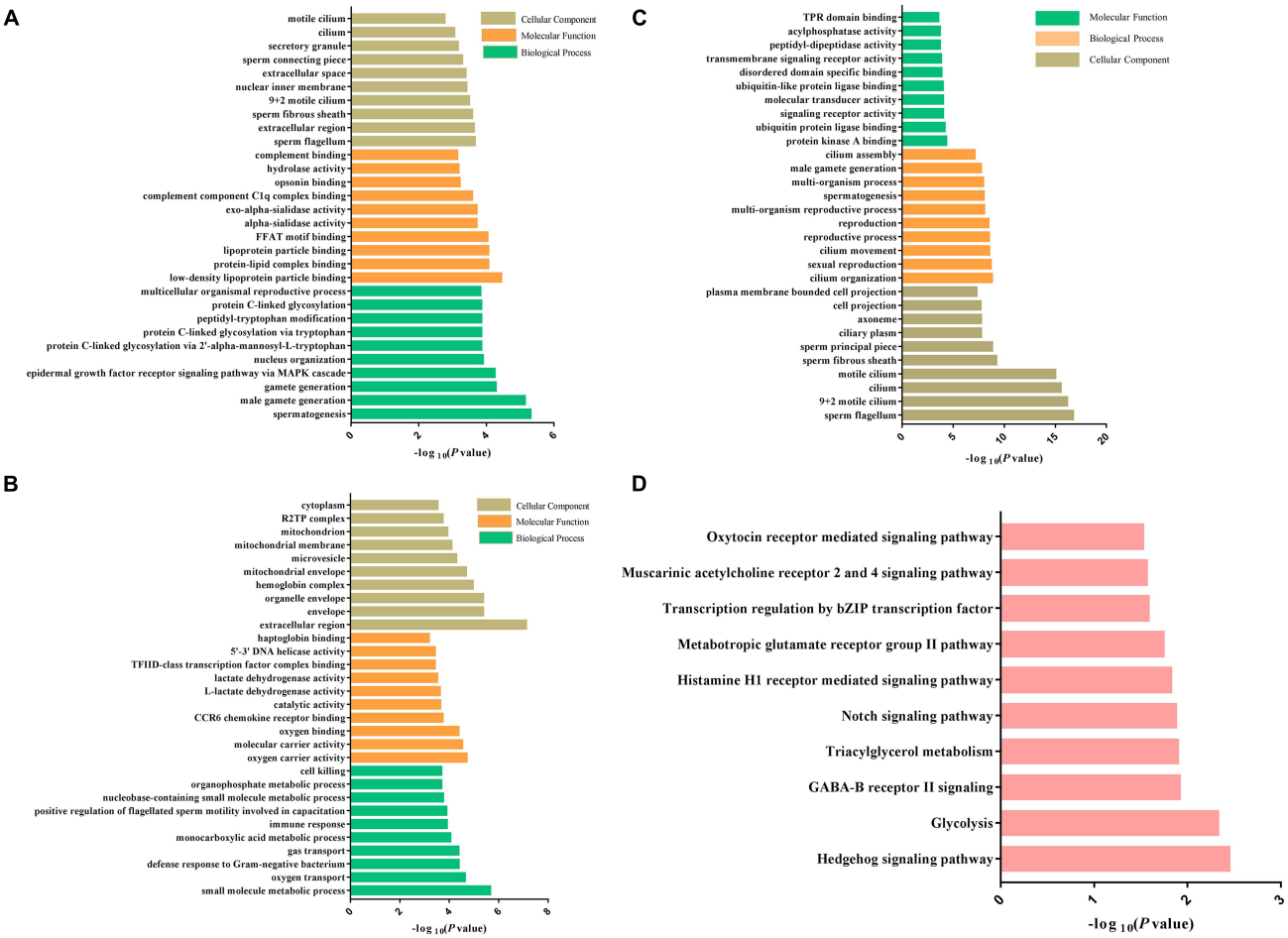

FIGURE 6 | Bioinformatics analysis of the DEPs and DPPs between Yorkshire and Duroc boar Spermatozoa. **(A)** Downregulated DEP GO terms. **(B)** Upregulated DEP GO terms. **(C)** GO enrichment analysis of the DEPs between Yorkshire and Duroc boar spermatozoa. **(D)** The top 12 KEGG pathways in the DPPs between Yorkshire and Duroc boar spermatozoa.

regulator between the cAMP/PKA and PKC/ERK1/2 signal pathways in spermatozoa to regulate acrosome reaction and sperm capacitation (Rahamim Ben-Navi et al., 2016). These data confirmed that variation in phosphorylation between Duroc and Yorkshire boar spermatozoa may play a crucial role in the difference in sperm motion and capacitation of two breeds *via* the phosphorylation-mediated signal pathway.

Classification of Proteins Identified From the DEPs in Duroc and Yorkshire Spermatozoa

At the total protein level, 150/1,697 (∼8.83%) DEPs were identified between Yorkshire versus Duroc pig spermatozoa (fold change ≥ 1.3 and $p < 0.05$) (**Supplementary Data 4**). Furthermore, the change in expression of most identified protein species (86/150, 57.33%) in the Yorkshire versus Duroc spermatozoa was ±1.30- to ±1.49-fold, whereas only 46 and 18 protein species showed fold change between ±1.50 and ±1.99 and ≥2.00- or ≤2.00-fold in these two breeds, respectively (**Figure 2C**). As a result, 150 DEPs containing 74 downregulated proteins and 76 upregulated proteins were found in Yorkshire pigs and used for subsequent function analysis and selected validation experiments. The protein with the strongest downregulation in Yorkshire boar sperm was ATP synthase ATP8 (UniProt Accession No. B6EDV3) (**Supplementary Data 4**). The proteins with the strongest decrease in Yorkshire boar sperm further include signaling and sperm motility proteins (AKAP4, ODF1, WGA16) implicated in fertility regulation, and adhesive glycoprotein (THBS1). On the other hand, the most increased proteins in Yorkshire boar sperm (**Supplementary Data 4**) also surprisingly comprised the mitochondrial membrane ATP synthase ATP8 (UniProt Accession No. A0A076EBU5) but had a different UniProt accession. The extreme expression difference of the same protein between the two breeds is probably due to the mutation of ATP8. Further analysis of the unique peptide segment of identification ATP8 also found that there were two amino acid differences between B6EDV3 (IYLPLLLPPR, high expression in Duroc boar sperm) and A0A076EBU5 (IYLPLSLPLR, high expression in Yorkshire boar sperm). The

list of upregulated proteins also comprises proteins involved in glycometabolism (GK, LDHC); and proteins implicated in ATP binding (RUVBL1, RUVBL2).

The DEPs between Duroc and Yorkshire spermatozoa were functionally annotated against the UniProt databases and then grouped based on GO enrichment: biological process, biological functions, and cellular component. Between the two breeds, GO analysis revealed that downregulated proteins were enriched in the biological process categories of the reproduction process, such as spermatogenesis, male gamete generation, and multicellular organism reproduction. For the molecular function, most groups were related to the oxygen activity, molecular carrier activity, oxygen binding, catalytic activity, and L-lactate dehydrogenase activity. For the cellular component, the downregulated proteins were enriched in sperm fibrous sheath, sperm flagellum, sperm-connecting piece, motile cilium, and secretory granule (**Figure 6A**). However, for the upregulated proteins, most of the groups were enriched in the cellular component of the extracellular region, organelle envelope, hemoglobin complex and mitochondrial membrane, no-sperm fibrous, and motile cilium. For the biological process and molecular function, most of the enrichment terms were transport process and binding activity, respectively, which were different from the downregulated proteins (**Figure 6B**). Additionally, it was noted that terms of defense response to fertilization, bacterium, and detoxification enriched in the biological process only for the upregulated proteins. These results suggested that the DEPs might play roles in spermatozoa motility.

Differentially Accumulated Phosphopeptides in Duroc and Yorkshire Spermatozoa

We analyzed the phosphopeptide distribution of the fold-change ratio (Yorkshire vs. Duroc), and the cutoff used for identification of the DEPPs was set at 1.3-fold change. In total, we identified 283/1,140 (∼24.82%) phosphopeptides that experienced differential phosphorylation in the two breeds ($p < 0.05$). Among these peptides, 100 increased and 183 decreased in the Yorkshire group, respectively (**Figure 2D** and **Supplementary Data 5**). In addition, 310 phosphorylation events were identified from the 283 phosphopeptides, and of these phosphorylation residues, 277 (89.4%) were serine and 33 (10.6%) were threonine (**Figure 4B**). Among these phosphorylated events, a remarkable bias was identified for the serine residue with a high percentage of ∼89% for all differentially phosphorylated sites. Subsequently, the threonine residue was the second common phosphorylated target, with no phosphotyrosine site being identified as differential phosphorylation in our analysis. In general, we showed a trend for proportionally more peptides undergoing increased, as opposed to reduced, phosphorylation in Duroc versus Yorkshire boar spermatozoa (183 vs. 100, respectively; **Table 1**).

The 283 phosphopeptides came from 102 phosphoproteins; thus, these phosphoproteins were regarded as DPPs. Of these DPPs, 65 held only one DEPP, 12 held two DEPPs, and 25 held three or more DEPPs (**Supplementary Data 5**). Thus, 39 DPPs were identified as being targeted for multiple phosphorylated sites, with 10 most prominent examples being AKAP4, FSIP2, SPATA18, NT5C1B, ACTL11, AKAP3, ST6GALNAC2, FAM71B, ODF2, and SPACA1, each with as many as 41, 18, 15, 15, 11, 11, 8, 8, 6, and 6 DEPPs, respectively (**Supplementary Data 5**). The DPPs of the top 10 DEPPs with multiple phosphorylation events accounted for almost half of all DPPs. The greatest differences among the regulated events were seen for the Ser513 and Ser517 of CCDC136, the Ser2378 of FN1, the Ser1441 of FSIP2, the Ser206, Ser348, Ser543, and Ser826 of AKAP4, the Ser300 and Ser302 of SPATA18, the Ser126 of FAM205A, and the Ser117 of TXNDC presenting fold changes > 3. Based on the expression pattern of the phosphorylated peptides, 100 increased phosphopeptides belong to 54 phosphoproteins and 183 decreased phosphopeptides belong to 52 phosphoproteins (**Figure 2D**). Four phosphoproteins (e.g., CCDC151, ALMS1, PROCA1, and ST6GALNAC2) containing both upregulated and downregulated unique phosphopeptides (**Supplementary Data 5**) were counted as both increased and decreased proteins for the subsequent GO analysis. To compare the number of DEPs and DPPs, 11 downregulated proteins (e.g., SMCP, ODF1, AKAP4, AKAP3, FAM714D, SPEM3, SUN5) and 1 upregulated protein (SPATA3) were overlapped respectively (**Figures 5B,C**). However, 71 out of a total 110 DPPs (∼69.1%) were not found in the DEPs but found in other proteins with no significant difference changes (**Figure 5D**). For example, ROPN1, involved in fibrous sheath integrity and sperm motility (Fiedler et al., 2013), was found to have ∼2 times higher phosphorylation expression in Duroc spermatozoa in the Ser62 site, while there was no significant change in the protein level between the two breeds of sperm. SPACA1, a testis-specific expression gene, is localized in sperm acrosomes and is found to be important for sperm–egg binding and fusion (Fujihara et al., 2012; Yamatoya et al., 2019), which had multiple higher phosphorylation sites (e.g., Ser291, Ser278, Ser256, Thr273/Ser278) in Yorkshire boar sperm. These results suggested that a high percentage of phosphorylated proteins in boar spermatozoa are probably associated with a breed difference in regulating sperm function.

To understand the biological roles of differential protein phosphorylation in different genetic backgrounds in boar spermatozoa, the DPPs were annotated by the GO term enrichment and KEGG pathway analysis. First, GO enrichment for all DPPs was conducted, and 48 GO categories were enriched. As shown in **Figure 6C**, the DPPs were clustered into top GO terms depending on their biological processes, including cilium organization, sexual reproduction, cilium movement, spermatogenesis, cilium assembly, and multiorganism process. The DPPs were classified into top groups based on their cell component, and these GO terms contained sperm flagellum, motile cilium, sperm fibrous sheath, sperm principal piece, and ciliary plasm, and axoneme. Based on their molecular function, the DPPs were classified into 10 groups including protein kinase A binding, ubiquitin protein ligase binding, TPR domain binding, transmembrane signaling receptor activity, molecular transducer activity, acylphosphatase activity. These data of GO term enrichment dramatically suggest that genetic

TABLE 1 | The list of the differentially expressed phosphoproteins involving the sperm fertility.

No.	Protein accessions	Gene name	Protein description	Phosphorylation site	Abundance alteration	Putative reproduction-related function
1	K7GRU7	ACE	Angiotensin I converting enzyme (peptidyl-dipeptidase A) 1	Ser607, Ser607	Up	Fertilization
2	A0A0B8RW53	ACLY	ATP-citrate synthase	Ser455	Up	Energy production
3	A0A286ZKT4	ALMS1	Alstrom syndrome protein 1	Ser56/Thr57, Ser1969	Up	Sperm motility
4	F1SP29	ACTL7A	Actin-like protein 7A	Ser54	Up	Fertilization
5	P24540	ACYP1	Acylphosphatase-1	Ser95	Up	Unknown
6	F1S498/ A0A286ZYY7	ADAM20	Disintegrin and metalloproteinase domain-containing protein 20-like	Thr739/Ser742	Up	Sperm maturation and fertilization
7	F1SPH1	PA2G4	Proliferation-associated protein 2G4	Thr328	Up	Signaling
8	F1RNX2	PDCD5	Programmed cell death protein 5	Ser119	Up	Sperm apoptosis
9	I3LN27	PDZD9	PDZ domain-containing protein 9	Thr142/Ser143/Ser145	Up	Unknown
10	F1SBB1	CABYR-1	Calcium-binding tyrosine phosphorylation-regulated transcript variant 1	Ser125/Ser132/Thr138, Ser125/Ser132, Ser336/Ser340, Ser353/Ser356/Ser358	Up	Sperm motility
11	I3LK18	PKD2L2	Polycystic kidney disease 2-like 2	Ser518	Up	Spermatogenesis
12	B4DCU2	CALM1	Calmodulin 1	Ser10	Up	Sperm capacitation
13	I3LCU9	CARHSP1	Calcium regulated heat stable protein 1	Ser29/Ser31	Up	Unknown
14	I3LGU2	CCDC114	Coiled-coil domain-containing protein 114	Ser553/Ser556	Up	Sperm motility
15	F1SQY0	PPP1R2	Protein phosphatase inhibitor 2	Ser89, Ser89/Ser90	Up	Sperm motility
16	F1SI09	PPP1R7	Protein phosphatase 1 regulatory subunit 7	Ser44/Ser48	Up	Sperm motility
17	F1S598	CCDC151	Coiled-coil domain-containing protein 151	Ser586,	Up	Sperm motility
18	A0A286ZWC2	CCDC7	Coiled-coil domain-containing protein 7	Ser297	Up	Sperm motility
19	C1PIG4	PRKAR2A	cAMP-dependent protein kinase regulatory subunit type II alpha	Ser56/Ser58	Up	Sperm motility
20	A0A287AF38	PROCA1	Protein PROCA1	Ser349, Ser340/Ser349, Ser99	Up	Unknown
21	F1RJW3	CFAP45	Cilia- and flagella-associated protein 45	Ser40, Ser59	Up	Unknown
22	F1SSL6	PSMA3	Proteasome subunit alpha type 3	Ser250	Up	Protein degradation
23	F1S227	PTRH2	Peptidyl-tRNA hydrolase 2, mitochondrial	Ser46	Up	Sperm apoptosis
24	A0A287AR56	QSOX2	Sulfhydryl oxidase 2	Ser596	Up	Sperm maturation
25	I3LC61	CYCL2	Cylicin-2	Thr213/Ser215	Up	Spermatogenesis
26	F1S1R1	CYLC1	Cylicin 1	Ser374/Thr375/Ser379, Ser275	Up	Spermatogenesis
27	I3LNF2	DNAH1	Dynein heavy chain 1, axonemal	Ser66/Thr71	Up	Sperm motility
28	A0A287ASX5	RSPH3	Radial spoke head protein 3	Ser344, Ser288	Up	Sperm motility
29	A0A287AGL6	RSPH6A	Radial spoke head protein 4 homolog A	Ser186	Up	Sperm motility
30	A0A287AL46	SLC26A8	Testis anion transporter 1	Ser617/Ser619	Up	Detoxification
31	F1SJU0	EFCAB6	EF-hand calcium-binding domain-containing protein 6	Ser58/Ser61/Ser62, Ser58/Ser62, Ser48, Ser48/Ser53	Up	Fertilization
32	A0A287AHI3	PPP6R3	Serine/threonine-protein phosphatase 6 regulatory subunit 3	Ser455	Up	Unknown
33	A0A286ZY74	TMEM159	Transmembrane protein 159	Ser21	Up	Fertilization
34	A0A287B7U4	TMEM190	Transmembrane protein 190	Ser127, Ser123/Ser127, Ser123/Thr125/Ser127	Up	Fertilization
35	F1SI89	TMEM202	Transmembrane protein 202	Ser111, Ser107, Ser107/Ser111, Ser98/Ser107/Ser111	Up	Fertilization
36	F1S7B1	SPA17	Sperm surface protein Sp17	Ser141	Up	Spermatogenesis, sperm–egg interaction, sperm capacitation, acrosome reaction
37	D5K8A9	SPACA1	Sperm acrosome membrane-associated protein 1	Thr273/Ser278, Ser291, Ser256, Ser278, Ser256/Thr257, Ser272/Thr273/Ser291	Up	Fertilization

(Continued)

TABLE 1 | Continued

No.	Protein accessions	Gene name	Protein description	Phosphorylation site	Abundance alteration	Putative reproduction-related function
38	A0A287AW88	SPAG9	Sperm associated antigen 9	Ser725/Ser728	Up	Fertilization
39	F1SB33	SYPL1	Synaptophysin-like protein 1	Ser2	Up	Unknown
40	F1SUB4	TBATA	Thymus, brain and testes-associated protein	Ser332/Ser333	Up	Unknown
41	O02705	HSP90AA1	Heat shock protein HSP 90-alpha	Ser263	Up	Protein folding
42	D5K8A4	SPATA3	Spermatogenesis associated 3	Ser148, Ser102/Thr105, Ser199	Up	Spermiogenesis
43	F1RG35	STUB1	STIP1 homology and U-box containing protein 1	Ser25	Up	Protein degradation
44	F2Z5I8	RAB8A	Ras-related protein rab-8a	Ser214	Up	Signaling
45	F1RR24	SPATA32	Spermatogenesis-associated protein 32	Ser136/Ser139, Ser136	Up	Spermiogenesis
46	F1S0P1	RGS22	Regulator of G-protein signaling 22	Ser1250	Up	Signaling
47	A0A286ZJB1	St6galnac2	Alpha-*N*-acetylgalactosaminide alpha-2,6-sialyltransferase 2	Ser43/Thr47, Ser43/Thr47/Ser49, Thr76, Ser95/Ser9, Thr76/Thr79/Ser80, Thr76/Thr79, Ser846	Up	Unknown
48	I3LL86	LRRC37AB	LRRC37AB_C domain-containing protein	Ser513, Ser516, Ser516/Ser518	Up	Unknown
49	F1S2N5	LRRC74A	Leucine-rich repeat-containing protein 74A	Ser73/Thr76	up	Unknown
50	F1RQ56	TSBP1	Testis expressed basic protein 1	Thr317Ser323	Up	Unknown
51	I3LD34	MS4A14	Membrane spanning 4-domains A14	Ser442/Ser451, Ser302/Thr305	Up	Signaling
52	A0A287A852	N/A	Uncharacterized protein	Ser32	Up	Unknown
53	F1S2Q4	NEK9	Serine/threonine-protein kinase Nek9	Ser682	Up	Spermiogenesis
54	F1SAE4	NME8	Thioredoxin domain-containing protein 3	Ser162/Ser166	Up	Sperm tail maturation
55	F1SCU0	NT5C1B	Cytosolic 5'-nucleotidase 1B	Ser67/Ser69/Ser71, Thr66/Ser67/Ser69, Ser69, Ser44, Thr41/Ser44, Ser54, Ser153, Ser19/Ser22, Ser228, Ser40/Ser44, Ser117/Thr120/Ser125, Ser149/Ser153, Ser64/Ser67, Thr72/Ser76, Ser76	Up	Sperm capacitation
56	A0A2C9F3G2	UBC	Polyubiquitin-C	Thr133	Up	Protein degradation
57	A0A287B7D9	EFCAB5	EF-hand calcium-binding domain-containing protein 5	Ser266	Up	Fertilization
58	I3LJA4	ACTL11	Actin-like 11	Ser481, Ser822, Ser85/Ser93, Ser171, Ser263, Ser528, Ser399/Ser402, Ser152, Ser402, Ser528/Thr633, Ser85	Down	
59	A0A286ZQX0	AKAP3	A-kinase anchor protein 3	Thr205/Ser216, Ser186, Ser33, Ser449/Ser457, Ser636, Ser817, Ser449, Ser186, Ser826, Ser700, Ser770	Down	Sperm motility
60	F1RW21/ A0A286ZWH7	AKAP4	A-kinase anchor protein 4	Ser206, Ser543, Ser348, Ser815, Ser461, Ser326, Ser386, Ser634, Ser710, Ser470, Ser111, Ser232, Ser526, Ser599, Ser451, Thr199/Ser206, Ser102, Ser136/Ser198/Thr199, Ser250, Ser213, Ser313, Ser136/Ser140, Ser278, Thr199, Ser751/Ser778, Ser451/Ser453, Ser756, Ser336, Ser54, Ser278/Ser289, Ser36, Ser188,	Down	Sperm motility

(Continued)

TABLE 1 | Continued

No.	Protein accessions	Gene name	Protein description	Phosphorylation site	Abundance alteration	Putative reproduction-related function
				Ser198/Thr199/Ser204, Ser136, Ser138, Thr188/Thr199, Ser136/Ser140/Ser141, Ser543/Ser546, Ser213/Ser219, Thr186, Ser274/Ser278		
61	F1SMN4	CCDC136	Coiled-coil domain-containing protein 136	Ser642, Ser454/Ser461, Thr537, Ser517, Ser513	Down	Sperm motility
62	F1RR82	ODF2	Outer dense fiber protein 2	Ser139, Ser95/Ser96, Thr92/Ser95, Ser37, Ser632, Ser129, Ser74	Down	Sperm motility
63	I6R469	CABYR-3	Calcium binding tyrosine-(Y)-phosphorylation regulated transcript variant 3	Thr246	Down	Sperm motility
64	F1S598	CCDC151	Coiled-coil domain-containing protein 151	Ser330	Down	Sperm motility
65	I3LQX1	CCDC96	Coiled-coil domain-containing protein 96	Ser32, Ser36	Down	Sperm motility
66	F1ST87	CCIN	Calicin	Ser229	Down	Spermiogenesis
67	F1SKP4	PLA2G6	85/88 kDa calcium-independent phospholipase A2	Ser12/Ser13	Down	Sperm motility
68	F1SQZ0	PLCZ1	Phosphoinositide phospholipase C	Ser376	Down	Spermiogenesis
69	C3VMK5	CLDN8	Claudin	Thr86, Thr97	Down	Unknown
70	F1RPZ6	CRISP2	Cysteine-rich secretory protein 2	Ser53	Down	Sperm-egg fusion
71	I3LTK6	OAZ3	Ornithine decarboxylase antizyme 3	Ser9/Ser12	Down	Spermiogenesis
72	F1RQP0	PRDX5	Peroxiredoxin 5	Thr45/Thr51	Down	Detoxification
73	A0A287AKY1	PRKAR1A	cAMP-dependent protein kinase type I-alpha regulatory subunit	Ser374	Down	Sperm motility
74	F1RHJ8	DBIL5	Diazepam-binding inhibitor-like 5	Ser46	Down	Sperm motility
75	F1S3K9	PSEN2	Presenilin	Ser365/Ser367	Down	Signaling
76	A0A287AHL5	DNAH7	Dynein heavy chain 7, axonemal	Ser135	Down	Sperm motility
77	A0A286ZTR0	DRC1	Dynein regulatory complex protein 1	Ser454	Down	Sperm motility
78	F1S8J6	RAB2B	Ras-related protein Rab-2B	Ser194/Ser202	Down	Signaling
79	Q29077	ODF1	Outer dense fiber protein 1	Ser32, Ser122/Ser123, Ser194, Ser122, Ser167, Ser86	Down	Sperm motility
80	A0A287BEZ2	RANBP17	RAN binding protein 17	Ser40	Down	Spermatogenesis
81	I3LT05	ROPN1	Ropporin-1	Ser62	Down	Spermatogenesis, sperm motility
82	I3L912	FAM205A	Protein FAM205A	Ser173, Ser80, Ser93, Ser126	Down	RNA biogenesis
83	A0A287AEH4	FAM205C	Family with sequence similarity 205 member C	Ser28, Ser22	Down	RNA biogenesis
84	F1S2W0	FAM71A	Family with sequence similarity 71, member A	Thr115, Ser399/Ser405, Ser182, Ser405	Down	RNA biogenesis
85	F1RQD7	FAM71B	Family with sequence similarity 71, member B	Ser184, Ser518, Ser494, Ser181/Ser183/Ser184, Ser494/Ser495, Ser183/Ser184, Ser24	Down	RNA biogenesis
86	A0A286ZY95	FN1	Fibronectin	Ser2378	Down	Sperm maturation
87	F1RYK8	FSIP2	Fibrous sheath-interacting protein 2	Ser5985/Ser5989, Ser5378, Ser6144/Ser6157, Ser6324, Ser6608, Ser6305, Ser5577, Ser6223, Ser5780, Ser1320, Ser5770, Ser6069/Ser6075, Ser3603, Ser6159, Ser4611, Ser1504/Ser1505, Ser4769, Ser6069, Ser1441	Down	Spermatogenesis, sperm motility
88	F1S605	GSTM3	Glutathione *S*-transferase	Ser204, Ser6, Ser77	Down	Detoxification
89	A0A287A1G6	HK1	Hexokinase-1	Ser871	Down	Energy production

(Continued)

TABLE 1 | Continued

No.	Protein accessions	Gene name	Protein description	Phosphorylation site	Abundance alteration	Putative reproduction-related function
90	Q5S233	SMCP	Mitochondrial associated cysteine-rich protein	Ser87, Ser92, Thr81/Ser87	Down	Sperm motility
91	I3LFS9	IQCF5	IQ domain-containing protein F5	Ser10	Down	Unknown
92	A0A287AI93	IQCN	IQ motif containing N	Ser344, Ser189/Thr191	Down	Unknown
93	F1SGA5	KLHL24	Kelch-like family member 24	Ser88	Down	Protein degradation
94	A0A287BDE3	LIPE	Hormone-sensitive lipase	Ser647	Down	Energy production
95	I3LC15	LOC100515049	Angiotensin-converting enzyme-like	Ser673, Ser688	Down	Spermatogenesis
96	A0A286ZK47	LOC100626097	Fibrous sheath-interacting protein 2-like	Ser912, Thr6543/Ser6544, Ser727, Ser1594/Ser1596, Ser1366	Down	Sperm motility
97	F1SE68	SPATA18	Spermatogenesis associated 18	Ser101, Ser532, Ser10, Ser159, Ser244, Ser13, Ser312, Ser10/Ser13, Ser552/Ser554/Ser556, Ser259/Ser261, Ser296/Ser298/ Ser300/Ser302, Ser534, Ser302, Ser300/Ser302, Ser534/Ser536	Down	Spermatogenesis
98	I3LDJ2	SPATA19	Spermatogenesis associated 19	Ser116	Down	Spermatogenesis
99	A0A286ZU97	MTCH2	Mitochondrial carrier 2	Ser106, Ser114	Down	Energy production
100	A0A287BJP9	SPATA31D1	Spermatogenesis-associated protein 31D1-like	Thr329, Thr329/Ser333	Down	Spermatogenesis
101	F1S6E2	SPATA6	Spermatogenesis-associated protein 6	Ser238	Down	Spermatogenesis
102	A0A2K6ANY4	SPEM3	Spem1 domain-containing protein	Ser783, Ser648, Ser1105	Down	Unknown
103	A0A286ZZH0	SSMEM1	Serine-rich single-pass membrane protein 1	Ser54	Down	Sperm motility
104	F1SIC8	TBC1D21	TBC1 domain family member 21	Ser15	Down	Sperm motility
105	A0A286ZJB1	St6galnac2	Alpha-*N*-acetylgalactosaminide alpha-2,6-sialyltransferase 2	Thr146	Down	Unknown
106	A0A288CFT0	TPI1	Triosephosphate isomerase 1	Ser35	Down	Energy production
107	A0A288CG60	SUN5	SUN domain-containing protein 5	Ser46	Down	Fertilization
108	A0A286ZM55	MROH1	Maestro heat-like repeat family member 1	Ser7	Down	Unknown
109	F1STE2	TSGA10	Testis-specific protein 10 protein	Ser687	Down	Fertilization
110	I3L5F8	TXNDC15	Thioredoxin domain-containing protein 15	Ser117	Down	Sperm motility
111	A0A287BBB5	VAPA	Vesicle-associated membrane protein-associated protein A	Ser209/Ser211	Down	Unknown
112	F1S2F6	VDAC2	Voltage-dependent anion-selective channel protein 2	Ser115	Down	Energy production
113	A0A286ZKT4	ALMS1	Alstrom syndrome protein 1	Ser756/Ser765	Down	Unknown
114	A0A287AF38	PROCA1	Protein PROCA1	Ser99	Down	Unknown

background interrelated with changes in the phosphorylation levels of different sperm-specific proteins primarily involved in sperm fertility regulation (**Figure 7**). Among them, we saw both upregulated and downregulated DPPs related to sperm motility, sperm capacitation, and acrosome reaction such as AKAP3, AKAP4, ODF1, FSIP2, and ODF2, the proteins of the coiled-coil domain-containing protein family (CCDC136, CCDC114, CCDC7, and CCDC151), SPACA1, DNAH1, SPA17, and CABYR-1. These results suggested that regulation of boar sperm activity is tightly coupled with the opposing action of cellular kinases and phosphatases.

The 110 DPPs were further analyzed using the KEGG database. In total, we found 10 enriched KEGG pathways in different breeds. As illustrated in **Figure 6D**, many fundamental biological pathways were overrepresented by phosphoproteins identified in this study, including hedgehog signaling pathway, glycolysis, triacylglycerol metabolism, Notch signaling pathway, and oxytocin receptor-mediated signaling pathway.

Phosphoproteome Integration in a Molecular Network

To further investigate the relationships among these phosphoproteins, the STRING database (see footnote 4) was used to identify protein–protein interactions (PPI) and to construct a network of interactions based on a variety of sources including various interaction databases, genetic interactions, text mining, and shared pathway interactions. The DPPs were uploaded for the PPI network construction using MCL clustering (inflation parameter = 3), and interactions with at least medium

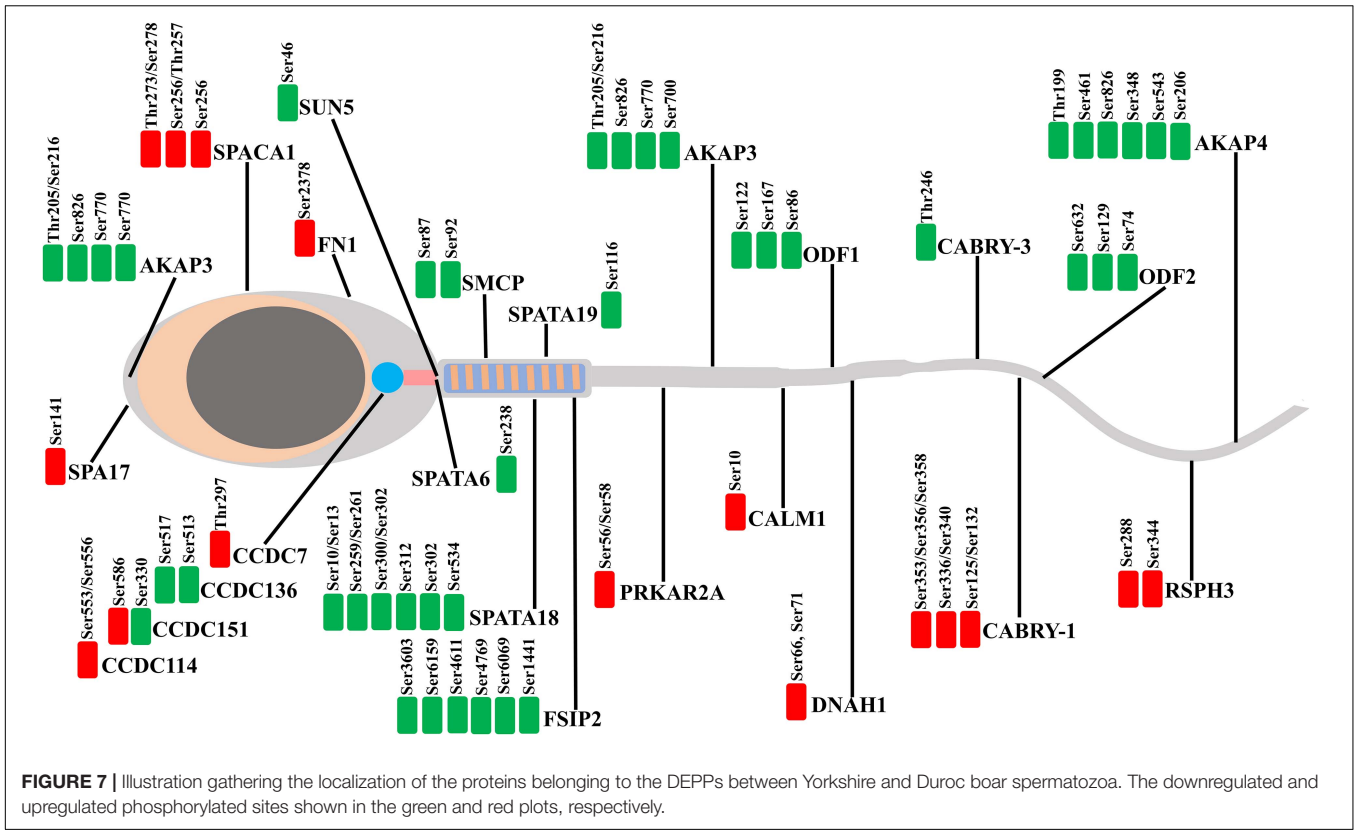

FIGURE 7 | Illustration gathering the localization of the proteins belonging to the DEPPs between Yorkshire and Duroc boar spermatozoa. The downregulated and upregulated phosphorylated sites shown in the green and red plots, respectively.

confidence were set by default (interaction score >0.4). As shown in **Figure 8**, **51** proteins relate to 184 paired relationships. At a glance, the network is organized around several strongly connected subnetworks, the majority of which are directly associated with sperm capacitation and sperm motility. Firstly, we identified a spermatogenesis-related subnetwork, which is composed mainly of upregulated proteins in Duroc boar sperms (e.g., SPATA18, SPATA6, SPATA19, SMCP, ODF1, OAZ3, and SUN5) (**Figure 8**). It contains SPATA18, multiply hyper-phosphorylated in Duroc boar sperm, which is a crucial regulator of mitochondrial quality that participates in repair or degradation of the injured mitochondria (Kitamura et al., 2011). Indeed, it was shown that as a testis-associated p53 target gene, SPATA18 can serve as a monitor of sperm cell differentiation and play a crucial role in the maturation of spermatids into spermatozoa, and proposed to be a structural component of the sperm flagella (Bornstein et al., 2011). Recently, a research in humans demonstrated that the attenuated levels of SPATA18 reduce fertility caused by defects in sperm development (Bornstein et al., 2011). To date, there is no report concerning SPATA18 phosphorylation in boar sperm. Another interesting member of this subnetwork is SPATA3, of which protein products might be involved in spermatogenesis regulation, mainly in spermatogenesis cell apoptosis or spermatogenesis (Ota et al., 2004; Rolland et al., 2014). Seven calcium assembly related DPPs form another subnet including SPA17, FSIP, CABYR, AKAP3, AKAP4, TBATA, and ROPN1. AKAP4, a major sperm fibrous sheath protein that localizes to the entire length of the flagellum in rodent and mammal spermatozoa, is playing multiple roles in flagellar structure, chemotaxis, capacitation, sperm motility, and regulation of signal transduction pathways (Jumeau et al., 2018; Blommaert et al., 2019). AKAP4 is annotated to interact with six other proteins, SPA17, FSIP, CABYR, AKAP3, TBATA, and ROPN1. Intriguingly, we found that CABYR was both hyper- and hypo-phosphorylated with different protein isoforms in Yorkshire boar sperms. This protein is a testis-specific phosphoprotein located in the sperm flagella and regulated by phosphorylation during sperm capacitation (Pelloni et al., 2018). In addition, CABYR can interact with AKAPs in the fibrous sheath of the sperm flagella by its RIIα domain and serve as scaffold and calcium carrier for the enzyme complexes, which mediate energy production leading to hyperactivation of the sperm (Naaby-Hansen et al., 2002; Li et al., 2011; Young et al., 2016). The third largest subnet is composed of five DPPs involved in sperm flagellum motility, including CCDC114, CCDC151, DRC1, NME8, and DNAH1. The other subnets in this PPI network were associated with carbon metabolism, sperm capacitation, and cAMP signaling.

Furthermore, A STRING protein network consisting of 12 overlapped proteins between DEPs and DEPPs of interest in this study is shown in **Figure 5E**. The results indicated that the proteins, such as ODF1 and SMCP, interacted with six other proteins. Among these interactions, ODF1, as the molecular focus, is involved in sperm motility and flagellum development (Mariappa et al., 2010; Hetherington et al., 2017). In this network, only STAPA3 was upregulated in Yorkshire boar sperm.

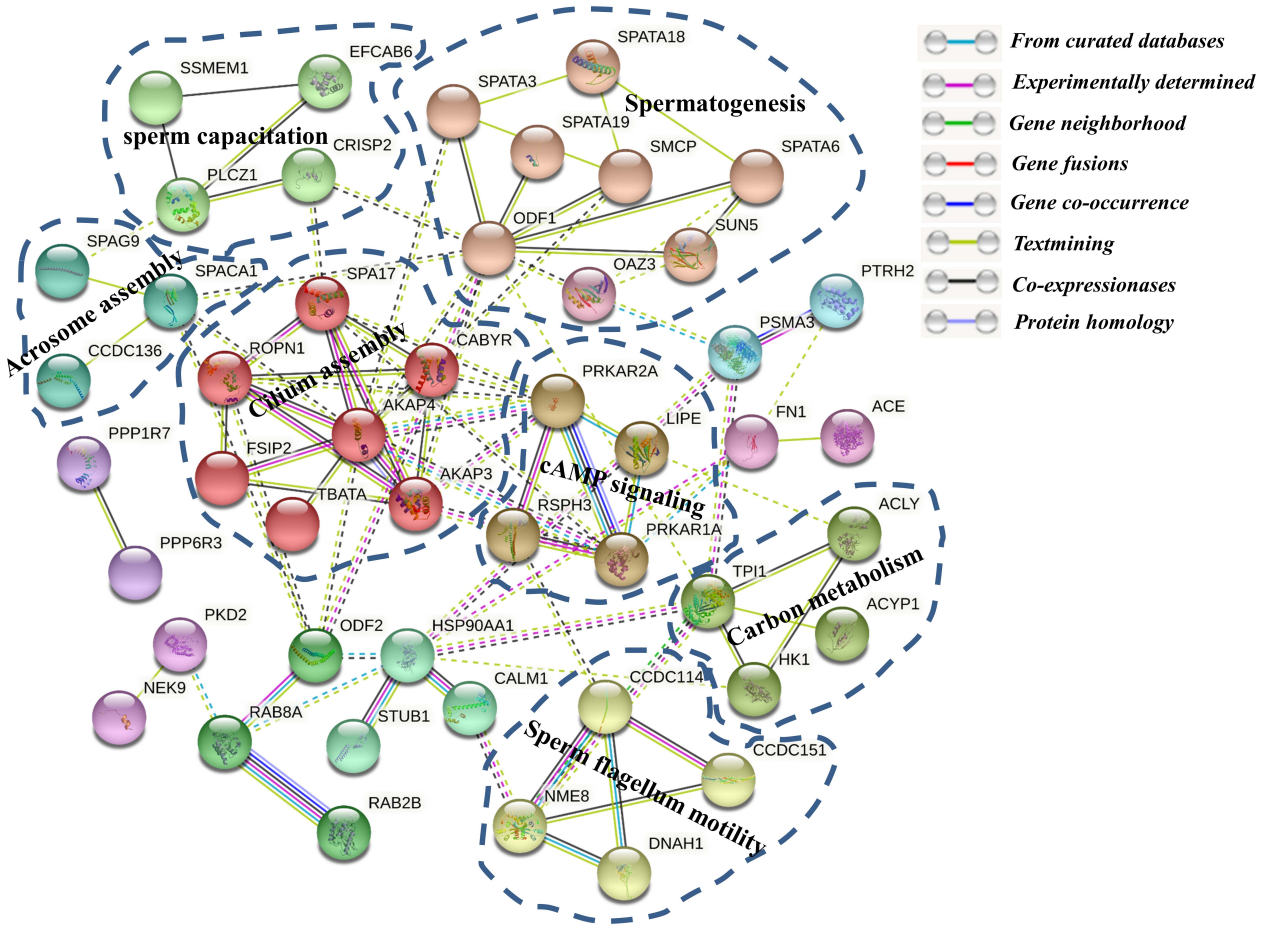

FIGURE 8 | The protein–protein interaction (PPI) network of the differentially phosphorylated phosphoproteins between Yorkshire and Duroc boar spermatozoa. The functional classification of the DPP group is shown in bold.

Confirmation of DEPs by Western Blot Analysis

Proteins with significant fold change and of interest based on their biological function were validated by Western blot analysis. This analysis also included proteins exhibiting the consistent trend of upregulating expression in Yorkshire breed (e.g., HNRNPK, PTGDS, and GK), as well as those that had a higher abundance in Duroc spermatozoa (e.g., AKPK4, AKAP3, and ODF1). All Western blot experiments were performed in triplicate using pooled biological samples ($n = 4$ sample) differing from those employed for iTRAQ proteome analyses and, in each experiment, GAPDH (glyceraldehyde-3-phosphate dehydrogenase) acted as an endogenous control to normalize the targeted proteins (**Figures 9A,B** and **Supplementary Figure 3**). The results confirmed the differential expression of the seven spermatozoa proteins between two breeds, with each of these proteins' expression closely paralleling the trends identified by MS analyses (**Figure 8B**). Accordingly, a linear regression comparing the fold changes recorded for each of these targets revealed a significant correlation ($R^2 = 0.98$; $p < 0.01$) between the quantification data obtained *via* immunoblotting analyses. Taken together, such findings support the accuracy of our data in reflecting the spatial patterns of porcine spermatozoa proteomic signatures.

DISCUSSION

In this study, we provide a first comprehensive quantitative analysis of the protein and protein phosphorylation differences in sperm between Yorkshire and Duroc boar. The iTRAQ-based proteomics and phosphoproteomics strategy is the most powerful technique for the global analysis of signaling networks in defined biological systems (Macek et al., 2009; Deracinois et al., 2013). In the field of livestock reproduction, proteomics has been used to illuminate the molecular basis of sperm freezability, sperm motility, or fertility (He et al., 2016, 2019; Maciel et al., 2018; Pini et al., 2018; Kasimanickam et al., 2019; Perez-Patino et al., 2019a,b; Peris-Frau et al., 2019). However, an in-depth study of proteome-combined phosphoproteome determining breed differences in boar sperm was not conducted so far. Here, we have performed a global analysis of quantitative proteomics coupled with phosphopeptide-enrichment strategies to unravel

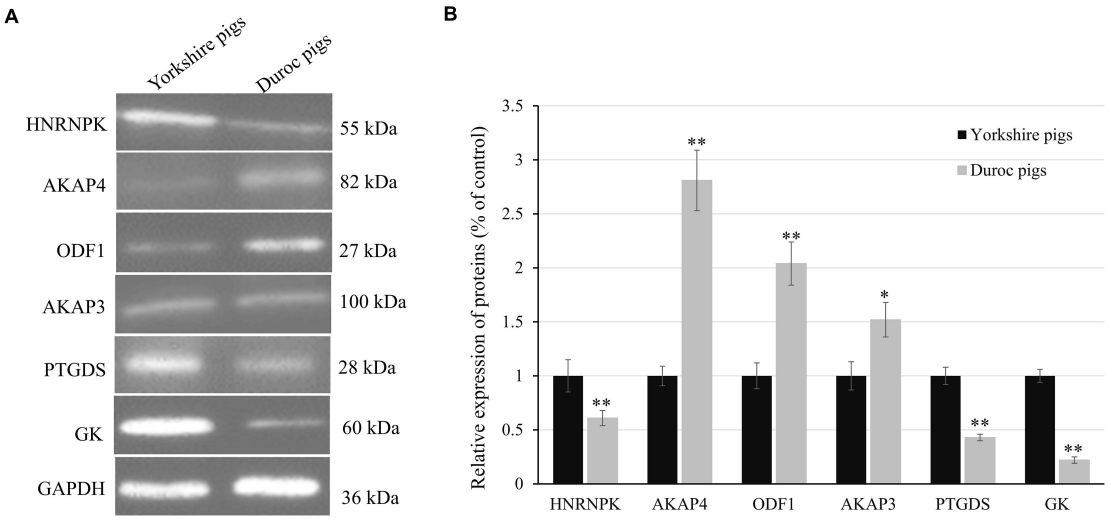

FIGURE 9 | Confirmation of differential expression of proteins between Yorkshire and Duroc boar spermatozoa. **(A)** Expression levels of HNRNPK, AKAP4, ODF1, AKAP3, PTGDS, and GK in Yorkshire and Duroc boar spermatozoa were confirmed by Western blotting. GAPDH served as a loading control. **(B)** Quantified relative band intensity ratio of **(A)**. $^{*}p < 0.05$, $^{**}p < 0.01$.

the boar spermatozoa proteome and identify signatures of PTM associated with the breed differences. The current workflow led us to identify 150 sperm proteins and 283 sperm phosphosites with a dramatically altered abundance in sperm because of the breed difference with sperm motility and capacitation, fertility.

Sperm Proteome Differences Between Yorkshire and Duroc Boar

In the present study, an updated proteome of porcine spermatozoa was generated using iTRAQ combined with LC-MS, which identified 1,745 proteins, and 1,738 of them quantified, most of them encoded in the Sus scrofa taxonomy. The total number of identified proteins was similar to the 1,723 proteins and 1,597 proteins identified recently by Xinhong et al. (2018) and Perez-Patino et al. (2019c), respectively, using iTRAQ technology, which was more than 1,157 proteins identified by Perez-Patino et al. (2019b) using the LC-ESI-MS/MS-based SWATH approach but was substantially lower than 2,728 proteins identified by Feugang et al. (2018) using a shotgun strategy. The difference in the number of identified proteins among the iTRAQ, SWATH, and shotgun approaches may be related to the methodological differences used for peptide enrichment detection, and data processing for protein identification and validation. For example, iTRAQ requires high collision energy, resulting in the loss of fragments of sequence information, which is more restrictive in protein identification than the shotgun strategy (Wiese et al., 2007). In addition, ∼2,000 identified proteins of porcine sperm proteome are far less than the ∼7,500-protein pf human spermatozoa proteome (Amaral et al., 2014), which demonstrates the yet incomplete functional and structural annotation of the porcine protein-coding genes, and many proteins still have no function assigned to them.

The distribution of total identified proteins into the GO enrichment showed a similar pattern to that observed in the human, mouse, or bovine sperm proteome (Martinez-Heredia et al., 2006; Chauvin et al., 2012; Kasvandik et al., 2015). The most enriched functions of sperm proteins were related to the metabolic processes, protein and tRNA transport, nuclear organization, or processes related to sperm function, which demonstrates that the central proteomic architecture of sperm is broadly comparable from these mammalian species. Among the proteins, the GO distribution of DEPs differed from the totality of identified proteins, particularly in biological processes and cellular components. Compared to the total identified proteins, the proportion of DEPs related to reproductive processes involved in sperm motility, sperm capacitation, sperm–oocyte binding, and fusion were significantly higher in Duroc boar sperm. Particularly, the cytoskeletal part proteins of sperm, such as SMCP, AKAP3, AKAP4, SUN5, and ODF1, play an important role in sperm function regulations. Because all boars used in the study were produced and raised in the same environment and fed the same ration, differences between the two breeds in sperm proteins were mainly attributed to their genetic background effect. This identification therefore dramatically indicated that the differences in protein abundance between the two breeds with different genetic backgrounds affected the sperm functionality. In general, the cytoskeletal part proteins in Duroc spermatozoa were superior to those of the Yorkshire spermatozoa and supplied a better condition for the physiological characteristics and structure stability of Duroc boar sperm.

The DEPs resulting from the two different breeds of sperm could help us understand the proteins influencing sperm functionality of genetic factors and provide further insight into their functions. A total of 150 proteins exhibited significantly different expression patterns between the two groups, and 145

proteins were successfully identified as characterized proteins. We determined that most of these proteins were involved in regulation of the reproductive process by bioinformatics analysis. More importantly, 20–25 of these proteins were increased in the Duroc boar spermatozoa, which were suggested to participate in the pathway of spermatogenesis, fertilization, or sperm motility and capacitation, based on their changing expression patterns in Duroc sperm compared to Yorkshire sperm. The changed expression of the above proteins might contribute to the sperm activity, capacitation, and sperm–egg interaction in Duroc boars.

Sperm proteins directly related to the reproductive function play a key role in the fertilization process. For instance, AKAPs are a group of evolutionarily conserved regulators, necessary for sperm motility, sperm capacitation, and acrosome reaction, which have the widespread function of binding to the regulatory subunit of cAMP-PKA and directing the kinase holoenzyme to particular subcellular compartments (Vizel et al., 2015; Autenrieth et al., 2016). AKAP4 binds with AKAP3; they are two major components of the sperm sheath responding to the regulation of the metabolic pathways and signal transduction that maintain sperm function (Brown et al., 2003; Nixon et al., 2019a). AKAP4 plays a key role in completing fibrous sheath assembly, whereas AKAP3 is involved in organizing the basic structure of the fibrous sheath. Previous studies have shown that absence or weak expression of AKAP3 and AKAP4 has been described over the years as being related to sperm dysfunctions with motility impairments (Miki et al., 2002; Hillman et al., 2013; Xu et al., 2020). In contrast, the upregulation of either AKAP4 or AKAP3 in frozen-thawed boar sperm might be associated with their premature capacitation (Chen et al., 2014; Perez-Patino et al., 2019b). A higher expression of AKAP3 and AKAP4 in Duroc boar sperm might promote the sperm function; they play a crucial role in sperm motility. We also observed many DEPs such as ODF1 (Zhao et al., 2018), SMCP (Nayernia et al., 2002), SUN5 (Shang et al., 2017), PRM2 (Zalata et al., 2016), RAB10 (Lin et al., 2017), and OAZ3 (Tokuhiro et al., 2009), which were more abundant in Duroc sperm than in Yorkshire sperm and have previously been associated with the reproductive efficiency of sperm. ODF1 is the major protein of the outer dense fibers in the mammalian sperm tail, taking part in sperm motility and flagellum development. In ODF1 knockout mice, sperm show a weakness in the connecting piece and a disorganized mitochondrial sheath and are also easily decapitated (Yang et al., 2012). Further studies have shown that the lack of ODF1 is observably reduced within infertile men, correlating a weakness between the head and neck regions of sperm (Hetherington et al., 2016). SMCP is a component of the keratinous capsule surrounding sperm mitochondria and play a key role in the stabilization and organization of the helical structure of sperm sheath (Nayernia et al., 2002). Deletion or reduction of SMCP impaired sperm motility, leading to spermatozoa failing to swim in the female reproductive tract and piercing the egg membranes during fertilization (Nayernia et al., 2002; Huang et al., 2016). A decreased expression of these proteins could indicate a weakening in the tail and/or the mitochondrial sheath of sperm, which would explain why Yorkshire spermatozoa have relatively low motility parameters than Duroc. Similarly, the higher abundance of the other four proteins could also clarify the improved functionality of Duroc sperm. In contrast, PSP-I, PSP-II, AQN3, SERPINE2, and TIMP-2, which were negatively related to sperm reproductive efficiency, were decreased in Duroc sperm compared to Yorkshire. PSP-I, PSP-II, and AQN3 are three major members of the sperm adhesin family that are low-molecular-weight glycoproteins and primarily secreted by the seminal vesicles (Topfer-Petersen et al., 1998; Centurion et al., 2003; Feugang et al., 2018). Once bound to the sperm plasma membrane, sperm adhesins are involved in regulating some of the most relevant sperm functions, such as sperm motility, sperm capacitation, acrosome reaction, or sperm-zona pellucida binding. However, if these proteins are overexpressed in sperm, they may also be harmful to sperm function. For example, the high expression of PSP-I/PSP-II dipolymer demonstrated decapacitating effects in boar sperm, which shows a significantly negative correlation with sperm functionality in liquid-preserved pig AI-semen doses (Caballero et al., 2009; Dyck et al., 2011). Furthermore, sperm adhesins increase with the decrease in sperm concentration, resulting in an increase in sperm adhesion concentration in the semen-poor fraction (Garcia et al., 2009). The higher expression of these sperm adhesins in Yorkshire spermatozoa may be closely related to the lower sperm activity and sperm concentration in Yorkshire boar. In addition, SERPINE2, also known as glia-derived nexin or protease nexin-1, has a wide range of serine protease-specific anti-protease activity that inhibits sperm capacitation by preventing the cholesterol from flowing out of the sperm plasma membranes and inhibiting the increase of sperm protein tyrosine phosphorylation (Lu et al., 2011; Li et al., 2018). Previous studies have also demonstrated that a higher abundance of SERPINE2 was related to lower fertility in modern artificially inseminated sows (Perez-Patino et al., 2019a). TIMP-2 is a specific natural inhibitor for MMP-2 which is a member of matrix metalloproteinases (MMPs) and thought to be associated with sperm motility, sperm capacitation, and fertilization (Robert and Gagnon, 1999; Belardin et al., 2019). Thus, the content and activity of TIMP-2 in sperm showed a significantly negative correlation with fertility. The changed expression pattern of these proteins in the Yorkshire spermatozoa can both impact the reproductive efficiency of Yorkshire boars. Therefore, we suggest that the differences in the expression levels of reproductive efficiency-related proteins may be one of the important reasons for reproductive differentiation between Yorkshire and Duroc sperm.

Sperm Phosphoproteome Differences Between Yorkshire and Duroc Boar

It is worth noting that since mature sperm are silent in both transcription and translation, their function is highly dependent on the addition of exogenous proteins (e.g., new sperm proteins during epididymal transit) or PTMs to their existing protein complement (Diez-Sanchez et al., 2003; Dun et al., 2012; Porambo et al., 2012). Phosphorylation, as the most important PTM, allows rapid control of the activity of

signaling and regulatory proteins, which is essential in the regulation of sperm function (Parte et al., 2012; Porambo et al., 2012; Dacheux and Dacheux, 2014). In recent years, the phosphoproteomics strategy has been widely used to uncover the molecular mechanisms of capacitation, sperm maturation, sperm motility, and infertility in human, mice, or other animals (Ficarro et al., 2003; Wang et al., 2015; Gazo et al., 2017; Castillo et al., 2019; Nixon et al., 2019b; Urizar-Arenaza et al., 2019; Martin-Hidalgo et al., 2020). However, a much deeper analysis of the phospho-regulation in the porcine sperm has not been conducted yet. In this study, we show the first global comprehensive analysis of the phosphoproteome of the porcine sperm with different breeds. Using TiO_2-based phosphopeptide enrichment combined with LC-MS/MS analysis, we have identified 1,064 phosphopeptides coming from 363 proteins, resulting in the most complete research of the porcine sperm phosphoproteins to date. According to the results reported in this study, phosphorylated proteins represent 19.8% of the porcine sperm proteome and are primarily involved in nuclear pore organization, sperm–egg recognition, cilium- and flagellum-dependent movement, and metabolism. Lately, Urizar-Arenaza et al. (2019) reported the largest description of the human sperm phosphoproteome with 3,500 identified phosphosites belonging to 1,332 proteins. Compared to the number of identified phosphorylated proteins in the human sperm proteome, the number of porcine sperm phosphoproteins is much smaller, which may be related to the incomplete annotation of the pig proteome. In addition, more than 51.5% porcine-phosphorylated proteins were found in human phosphorylated proteomes, and the most prominent phosphoproteins with multiple phosphorylation events were similar. For example, the five most prominent examples in human sperm are FSIP2 (145), AKAP4 (102), AKAP3 (71), CABYR (45), and ODF2 (37) (Urizar-Arenaza et al., 2019), while the five most prominent examples in porcine sperm are AKAP4 (55), FSIP2 (34), ODF2 (33), AKAP3 (34), and ACTL11 (27). Compared to the humans and mice, data on porcine phosphorylation sites are very scarce so far. Therefore, most of the phosphorylation sites identified in the present study are novel protein phosphorylation sites with uncharacterized or unknown functions in porcine sperm. Thus, the investigation of novel phosphorylation events to elucidate the functions of these sperm phosphoproteins will undoubtedly be of great interest for uncovering the complex regulatory mechanisms involved in porcine sperm function and contribute to the functional categorization of poorly annotated porcine proteins.

Analysis of phosphorylated residue distribution in porcine sperm phosphoproteome demonstrates that the proportion of pS, pT, and pY (86.8, 12.3, and 0.9%, respectively) is more closely in approximate with those experienced in vertebrate cells showing that pS, pT, and pY occur at an estimated ratio of 1,000:100:1 (Raggiaschi et al., 2005). However, only 10 tyrosine phosphorylation sites were identified in this study, which are relatively few. It could be interpreted by the fact that we separated the boar semen fractions under non-capacitated conditions. In general, capacitation seems to be a phenomenon specific to mammals, and accumulating evidence indicates that it generally involves a burst of protein-tyrosine phosphorylation (Ijiri et al., 2012). Therefore, tyrosine phosphorylation is usually minimal in uncapable sperm. The proportion of tyrosine phosphorylation in previous studies of uncapable sperm phosphorylation in humans was also roughly equivalent to our results (Urizar-Arenaza et al., 2019; Martin-Hidalgo et al., 2020).

Motif analysis of regulated phosphorylation sites identified through phosphoproteomic datasets is usually used to predict the protein kinases that respond to the phosphorylation. Consistent with previous research (Huang et al., 2018; Yang et al., 2018), our phosphoproteomics results also demonstrated that some crucial spermatogenesis-related proteins (e.g., SPACA1, SPATA18, and SPATA31D1) and sperm motility-related proteins (e.g., AKAP4, CFAP45, ODF2, CABYR, and CDC96) were respectively phosphorylated at PKCs, AKT, GSK-3, CDK, and MAPK motifs, demonstrating that these proteins are potential targets of the corresponding kinases. Considering the identified phosphorylation motifs, combined with the known consensus on phosphorylation site specificity of serine/threonine kinases, we can predict some important target proteins of upstream kinases involved in the spermatogenesis and sperm motility-related pathways that have different regulations in Yorkshire and Duroc boar sperm. For example, the phosphopeptides identified in porcine AKAP4 at Ser136 sites (YALGFQHALSPSASSCK) contain a specific motif pSP for ERK1/2 that enhances the effect of AKAP4 to bind to the type II regulatory subunit of PKA (Miki and Eddy, 1999). Thus, possible AKAP4 activation by ERK1/2 allows us to concatenate ERK1/2 to the upstream cAMP/PKA signal pathway which plays a key role in human sperm activity, sperm capacitation, and acrosome reaction (Rahamim Ben-Navi et al., 2016).

Phosphoproteomic research shows that 283 DEPPs belonging to a total of 102 proteins of porcine sperm are identified at differential amounts between Yorkshire and Duroc boar. Among them, 54 phosphorylated proteins are more abundant in the Yorkshire spermatozoa, whereas 52 phosphorylated proteins have a higher expression in Duroc sperm (**Table 1**). Significantly, this study showed that the phosphoproteins of Duroc spermatozoa are mainly involved in sperm function and spermatogenesis, such as sperm motility, sperm–egg binding and recognition, and capacitation. These sperm processes are crucial to the fertilization potential in porcine sperm. This is in line with the fact that Duroc sperm also show the best-quality characteristics, being used as a terminal parent in the modern pig industry. Our findings suggest a differential phosphorylated regulation of boar spermatozoa proteins manipulating sperm motility between the different breeds. In particular, the DPPs are primarily involved in crucial requirements of the flagellum for the sperm movement and control of axoneme mechanical components. These results were compared with a similar research in human that the differential regulation of phosphoproteins between high and low motility spermatozoa is mainly associated with cytoskeletal, metabolic, and fibrous sheath proteins (Martin-Hidalgo et al., 2020). In reality, we have identified several more abundant phosphoproteins in Duroc boar sperm which play a role in flagellum assembly and sperm motility (**Figure 7**), such as FSIP2, ODF2, ODF1, CABRY, SMCP, SPATA18, SPATAT19, SUN5, SLC26A8, DNAH1, AKAP3, AKAP4, coiled-coil

domain-containing proteins (CCD7, CCD151, CCD136, CCD114), and cilia- and flagella-associated protein CFAP45. Also, we detected HSP90AA1 which is differentially phosphorylated between Yorkshire and Duroc spermatozoa, sustaining the function of HSPs in porcine male fertility.

In the process of fertilization, sperm not only need to swim to the sites that bind to the egg in the female reproductive tract but also acquire the ability to fertilize with the egg. Therefore, sperm motility is a key factor affecting the fertilization. Usually, sperm motility is mainly formed by the swing of long flagella in the tail of sperm, which is not only affected by the external environment but also regulated by several internal signal pathways (Vernon and Woolley, 2004). The cAMP/PKA signal pathway and Ca^{2+} signal pathway are the two most important signal pathways to regulate mammalian sperm motility (Dey et al., 2019). It is common knowledge that cAMP works directly on PKA, and the specificity and function of PKA in cells are attributed to its localization through anchoring protein AKAPs in response to cAMP signaling. AKAPs take an active part in PKA-dependent protein tyrosine phosphorylation, two members of which also increased the phosphorylation in Duroc boar spermatozoa. As mentioned before, AKAPs serve as scaffolding proteins for integrating the cAMP-PKA pathway and Ca^{2+} signals, and the increased phosphorylation of AKAP3 and AKAP4 could be the connectors between different transduction cascades in sperm motility regulation (Skroblin et al., 2010; Urizar-Arenaza et al., 2019), which strongly supports our research. Similarly, we also detected relative phosphorylation alterations in other proteins known to participate in PKA-dependent pathways including CABYR, ROPN1, CALM1, PRKAR2A, and PRKAR1A. CABYR serves as a key ingredient belonging to the Ca^{2+} signal pathway during the capacitation and acrosome reaction, which performs putative motifs for self-assembly and for binding PRKAR2A (type II regulatory subunit of PKA R-subunit), AKAP3 and AKAP4 (Li et al., 2011; Young et al., 2016). Interestingly, the dephosphorylation of CABYR inhibits its binding capacity with calcium. ROPN1, a capacitation-related protein, is an important ingredient of the fibrous sheath in mammalian sperm, and it resides in the primary piece and the terminal piece of sperm flagella, which is also an important PKA regulator and is active in sperm motility regulation (Chen et al., 2011; Li et al., 2011; Kwon et al., 2014). Another study showed that ROPN1 interacts with AKAP3, and this interaction depends on AKAP3 phosphorylation (Fiedler et al., 2013). These evidences were consistent with our observation of an increased phosphorylation of AKAP3 and AKAP4 in Duroc, indicating that an upregulation of AKAP3 and AKAP4 probably leads to activation of cAMP-mediated PKA signaling. The increased phosphorylation of these proteins suggests an effect on PKA signaling. In addition, PRKAR2A and PRKAR1A are two regulatory subunits of PKA, and PRKAR2A was expressed primarily in the axonemal region of the mammal sperm flagellum, while PRKAR1A was present in connection with sperm's outer dense fibers and fibrous sheath (Fiedler et al., 2008; D'Amours et al., 2018). PRKAR2A contains a phosphorylation site in the inhibitory domain, whereas PRKAR1A subunits do not; this may result in an altered binding affinity for the catalytic subunits, and both of them dimerize by their N-terminal domains and bind to AKAPs (Wu et al., 2007). In the present study, the upregulated phosphorylation of PRKAR1A (Ser374) and downregulated phosphorylation of PRKAR2A (Ser56/Ser58) were detected in Duroc spermatozoa, respectively, indicating that the different phosphorylation of the two PKA regulatory subunits has different functions in sperm motility. Meanwhile, both of the proteins tend to co-express or interact with AKAP3, AKAP4, and other cytoskeletal proteins such as CABYR, ROPN1, FSIP2, ODF1, ODF2, or SMCP. Therefore, we suggested that the phosphorylation of sperm-specific proteins is involved in the regulation of boar sperm motility mainly through the cAMP/PKA signal pathway in different breeds.

On the other side of the coin, the phosphoproteins abundant in Duroc boar sperm are principally involved in sperm energy metabolism, such as TPI1, HK1, and LIPE, and particularly related to regulation of glycolysis pathway and lipolysis. Generally, sperm motility is directly controlled by energy resources, including glycolysis, lipid metabolism, and oxidative phosphorylation (Williams and Ford, 2001). Previous research showed that phosphorylation of these proteins can promote the energy generation *via* catabolic pathways in all kinds of cells. Given these data, the results showed that the sperm potential fertility in Duroc boar was significantly higher than in Yorkshire pigs. This is broadly in line with the higher sperm motility of Duroc boar. In addition, our phosphoproteomics data also found more phosphorylated abundance of ATP-citrate synthase ACLY that links energy metabolism provided by catabolic pathways to biosynthesis in the Yorkshire sperm fraction. These results are consistent with those from the previous phosphoproteome research of human sperm, which showed that carbohydrate metabolic pathways altered in human sperm with the low-motility group (Martin-Hidalgo et al., 2020). In a word, these results supply a valuable insight into the molecular basis of differences in reproductive efficiency between Duroc and Yorkshire boar spermatozoa.

CONCLUSION AND PERSPECTIVES

In summary, the results of this study fully reveal the multiple changes in the protein levels and phosphorylation status between Yorkshire and Duroc sperm and discussed the relationship between pig reproductive efficiency and fertility ability. Through the parallel and large-scale quantitative analyses of porcine spermatozoa proteome and phosphoproteome, a variety of new molecular mechanisms that may help to understand spermatogenesis, sperm motility, fibrous sheath and cytoskeleton, sperm–egg recognition, and energy metabolism were identified. Investigations of possible phosphokinase interactions have revealed that several regulatory kinases may be responsible for the observed variations in protein phosphorylation, including PKCs, MAPK, and PKA. This research provides the foundation of breeding techniques for the rapid dissemination of key genes to improve livestock quality and clarifies the usefulness of proteomic methods in diagnosing reproductive potential in the livestock industry. As far as we

know, this is the first research that shows a parallel quantitative proteomics and phosphoproteomics-based study of porcine sperm global proteins in different breeds, and these data may supply significant information for understanding the molecular mechanisms underlying the differences in reproductive efficiency among different varieties.

DATA AVAILABILITY STATEMENT

The datasets presented in this study can be found in online repositories. The names of the repositories and accession numbers can be found below: ProteomeXchange, http://www.proteomexchange.org/, PXD025607 and iProX, https://www.iprox.org/, IPX0003000002.

ETHICS STATEMENT

The animal study was reviewed and approved by Animal Care Commission of the College of Life Science, Xinyang Normal University, China.

AUTHOR CONTRIBUTIONS

YX and HX designed the study. YX, QH, and CM performed the research. YW and PZ performed the proteomic technology. YX, PZ, CL, and XC analyzed the data. YX, QH, and HX interpreted the data. YX, QH, CM, and HX drafted the manuscript. All authors critically reviewed and approved the final version of the manuscript.

FUNDING

This work was financially supported by the NSFC (31972537), the Central Plains Technological Innovation Leading Talents Project of Henan Province, China (194200510022), and the Nanhu Scholars Program of Xinyang Normal University.

SUPPLEMENTARY MATERIAL

The Supplementary Material for this article can be found online at: https://www.frontiersin.org/articles/10.3389/fcell.2021.652809/full#supplementary-material

Supplementary Figure 1 | Map of AKAP4 phosphorylation sites identified from porcine boar Spermatozoa. The down-regulated phosphorylated sites are represented in green while the up-regulated ones are colorized in red. Black box represents the phosphorylation motif.

Supplementary Figure 2 | GO enrichment analysis of the total identified porcine boar sperm proteins. **(A)** GO cellular compartments categories; **(B)** GO biological process categories; **(C)** GO molecular functions.

Supplementary Figure 3 | Western blot result of the selected proteins.

REFERENCES

Agarwal, A., Panner Selvam, M. K., and Baskaran, S. (2020). Proteomic analyses of human sperm cells: understanding the role of proteins and molecular pathways affecting male reproductive health. *Int. J. Mol. Sci.* 21:1621. doi: 10.3390/ijms21051621

Amaral, A., Castillo, J., Ramalho-Santos, J., and Oliva, R. (2014). The combined human sperm proteome: cellular pathways and implications for basic and clinical science. *Hum. Reprod. Update* 20, 40–62. doi: 10.1093/humupd/dmt046

Autenrieth, K., Bendzunas, N. G., Bertinetti, D. D., Herberg, F. W. P. D., and Kennedy, E. J. P. D. (2016). Defining A-Kinase anchoring protein (AKAP) specificity for the protein kinase a subunit RI (PKA-RI). *Chembiochem* 17, 693–697. doi: 10.1002/cbic.201500632

Baker, M. A. (2016). Proteomics of post-translational modifications of mammalian spermatozoa. *Cell Tissue Res.* 363, 279–287. doi: 10.1007/s00441-015-2249-x

Belardin, L. B., Antoniassi, M. P., Camargo, M., Intasqui, P., Fraietta, R., and Bertolla, R. P. (2019). Semen levels of matrix metalloproteinase (MMP) and tissue inhibitor of metallorproteinases (TIMP) protein families members in men with high and low sperm DNA fragmentation. *Sci. Rep.* 9:903. doi: 10.1038/s41598-018-37122-4

Blommaert, D., Sergeant, N., Delehedde, M., Jouy, N., Mitchell, V., Franck, T., et al. (2019). Expression, localization, and concentration of A-kinase anchor protein 4 (AKAP4) and its precursor (proAKAP4) in equine semen: Promising marker correlated to the total and progressive motility in thawed spermatozoa. *Theriogenology* 131, 52–60. doi: 10.1016/j.theriogenology.2019.03.011

Bornstein, C., Brosh, R., Molchadsky, A., Madar, S., Kogan-Sakin, I., Goldstein, I., et al. (2011). SPATA18, a spermatogenesis-associated gene, is a novel transcriptional target of p53 and p63. *Mol. Cell. Biol.* 31, 1679–1689. doi: 10.1128/MCB.01072-10

Brown, P. R., Miki, K., Harper, D. B., and Eddy, E. M. (2003). A-kinase anchoring protein 4 binding proteins in the fibrous sheath of the sperm flagellum. *Biol. Reprod.* 68, 2241–2248. doi: 10.1095/biolreprod.102.013466

Caballero, I., Vazquez, J. M., Mayor, G. M., Alminana, C., Calvete, J. J., Sanz, L., et al. (2009). PSP-I/PSP-II spermadhesin exert a decapacitation effect on highly extended boar spermatozoa. *Int. J. Androl.* 32, 505–513. doi: 10.1111/j.1365-2605.2008.00887.x

Castillo, J., Bogle, O. A., Jodar, M., Torabi, F., Delgado-Duenas, D., Estanyol, J. M., et al. (2019). Proteomic changes in human sperm during sequential *in vitro* capacitation and acrosome reaction. *Front. Cell. Dev. Biol.* 7:295. doi: 10.3389/fcell.2019.00295

Centurion, F., Vazquez, J. M., Calvete, J. J., Roca, J., Sanz, L., Parrilla, I., et al. (2003). Influence of porcine spermadhesins on the susceptibility of boar spermatozoa to high dilution. *Biol. Reprod.* 69, 640–646. doi: 10.1095/biolreprod.103.016527

Chalmel, F., and Rolland, A. D. (2015). Linking transcriptomics and proteomics in spermatogenesis. *Reproduction* 150, R149–R157. doi: 10.1530/REP-15-0073

Chauvin, T., Xie, F., Liu, T., Nicora, C. D., Yang, F., Camp, D. G., et al. (2012). A systematic analysis of a deep mouse epididymal sperm proteome. *Biol. Reprod.* 87:141. doi: 10.1095/biolreprod.112.104208

Chen, J., Wang, Y., Wei, B., Lai, Y., Yan, Q., Gui, Y., et al. (2011). Functional expression of ropporin in human testis and ejaculated spermatozoa. *J. Androl.* 32, 26–32. doi: 10.2164/jandrol.109.009662

Chen, X., Zhu, H., Hu, C., Hao, H., Zhang, J., Li, K., et al. (2014). Identification of differentially expressed proteins in fresh and frozen-thawed boar spermatozoa by iTRAQ-coupled 2D LC-MS/MS. *Reproduction* 147, 321–330. doi: 10.1530/REP-13-0313

Chou, M. F., and Schwartz, D. (2011). Biological sequence motif discovery using motif-x. *Curr. Protoc. Bioinformatics* Chapter 13, Unit 1315–24. doi: 10.1002/0471250953.bi1315s35

Ciereszko, A., Ottobre, J. S., and Glogowski, J. (2000). Effects of season and breed on sperm acrosin activity and semen quality of boars. *Anim. Reprod. Sci.* 64, 89–96. doi: 10.1016/s0378-4320(00)00194-9

Dacheux, J. L., and Dacheux, F. (2014). New insights into epididymal function in relation to sperm maturation. *Reproduction* 147, R27–R42. doi: 10.1530/REP-13-0420

Dai, L., Prabhu, N., Yu, L. Y., Bacanu, S., Ramos, A. D., and Nordlund, P. (2019a). Horizontal cell biology: monitoring global changes of protein interaction states with the proteome-wide cellular thermal shift assay (CETSA). *Annu. Rev. Biochem.* 88, 383–408. doi: 10.1146/annurev-biochem-062917-012837

Dai, P., Wang, X., Gou, L. T., Li, Z. T., Wen, Z., Chen, Z. G., et al. (2019b). A translation-activating function of MIWI/piRNA during Mouse Spermiogenesis. *Cell* 179, 1566–1581e1516. doi: 10.1016/j.cell.2019.11.022

D'Amours, O., Frenette, G., Bourassa, S., Calvo, E., Blondin, P., and Sullivan, R. (2018). Proteomic markers of functional sperm population in bovines: comparison of low- and high-density spermatozoa following cryopreservation. *J. Proteome Res.* 17, 177–188. doi: 10.1021/acs.jproteome.7b00493

Deracinois, B., Flahaut, C., Duban-Deweer, S., and Karamanos, Y. (2013). Comparative and quantitative global proteomics approaches: an overview. *Proteomes* 1, 180–218. doi: 10.3390/proteomes1030180

Dey, S., Brothag, C., and Vijayaraghavan, S. (2019). Signaling enzymes required for sperm maturation and fertilization in mammals. *Front. Cell. Dev. Biol.* 7:341. doi: 10.3389/fcell.2019.00341

Diez-Sanchez, C., Ruiz-Pesini, E., Montoya, J., Perez-Martos, A., Enriquez, J. A., and Lopez-Perez, M. J. (2003). Mitochondria from ejaculated human spermatozoa do not synthesize proteins. *FEBS Lett.* 553, 205–208. doi: 10.1016/s0014-5793(03)01013-5

Dong, W. T., Xiao, L. F., Hu, J. J., Zhao, X. X., Liu, J. X., and Zhang, Y. (2017). iTRAQ proteomic analysis of the interactions between Bombyx mori nuclear polyhedrosis virus and silkworm. *J. Proteomics* 166, 138–145. doi: 10.1016/j.jprot.2017.07.013

Du, M., Liu, X., Ma, N., Liu, X., Wei, J., Yin, X., et al. (2017). Calcineurin-mediated Dephosphorylation of Acetyl-coA Carboxylase is Required for Pheromone Biosynthesis Activating Neuropeptide (PBAN)-induced Sex Pheromone Biosynthesis in Helicoverpa armigera. *Mol. Cell. Proteomics* 16, 2138–2152. doi: 10.1074/mcp.RA117.000065

Dun, M. D., Aitken, R. J., and Nixon, B. (2012). The role of molecular chaperones in spermatogenesis and the post-testicular maturation of mammalian spermatozoa. *Hum. Reprod. Update* 18, 420–435. doi: 10.1093/humupd/dms009

Dyck, M. K., Foxcroft, G. R., Novak, S., Ruiz-Sanchez, A., Patterson, J., and Dixon, W. T. (2011). Biological markers of boar fertility. *Reprod. Domest. Anim.* 46(Suppl. 2), 55–58. doi: 10.1111/j.1439-0531.2011.01837.x

Feugang, J. M., Liao, S. F., Willard, S. T., and Ryan, P. L. (2018). In-depth proteomic analysis of boar spermatozoa through shotgun and gel-based methods. *BMC Genomics* 19:62. doi: 10.1186/s12864-018-4442-2

Ficarro, S., Chertihin, O., Westbrook, V. A., White, F., Jayes, F., Kalab, P., et al. (2003). Phosphoproteome analysis of capacitated human sperm. Evidence of tyrosine phosphorylation of a kinase-anchoring protein 3 and valosin-containing protein/p97 during capacitation. *J. Biol. Chem.* 278, 11579–11589. doi: 10.1074/jbc.M202325200

Fiedler, S. E., Bajpai, M., and Carr, D. W. (2008). Identification and characterization of RHOA-interacting proteins in bovine spermatozoa. *Biol. Reprod.* 78, 184–192. doi: 10.1095/biolreprod.107.062943

Fiedler, S. E., Dudiki, T., Vijayaraghavan, S., and Carr, D. W. (2013). Loss of R2D2 proteins ROPN1 and ROPN1L causes defects in murine sperm motility, phosphorylation, and fibrous sheath integrity. *Biol. Reprod.* 88:41. doi: 10.1095/biolreprod.112.105262

Flowers, W. L. (2008). Genetic and phenotypic variation in reproductive traits of AI boars. *Theriogenology* 70, 1297–1303. doi: 10.1016/j.theriogenology.2008.06.016

Fujihara, Y., Satouh, Y., Inoue, N., Isotani, A., Ikawa, M., and Okabe, M. (2012). SPACA1-deficient male mice are infertile with abnormally shaped sperm heads reminiscent of globozoospermia. *Development* 139, 3583–3589. doi: 10.1242/dev.081778

Gadadhar, S., Alvarez Viar, G., Hansen, J. N., Gong, A., Kostarev, A., Ialy-Radio, C., et al. (2021). Tubulin glycylation controls axonemal dynein activity, flagellar beat, and male fertility. *Science* 371:eabd4914. doi: 10.1126/science.abd4914

Gao, N., Chen, Y., Liu, X., Zhao, Y., Zhu, L., Liu, A., et al. (2019). Weighted single-step GWAS identified candidate genes associated with semen traits in a Duroc boar population. *BMC Genomics* 20:797. doi: 10.1186/s12864-019-6164-5

Garcia, E. M., Calvete, J. J., Sanz, L., Roca, J., Martinez, E. A., and Vazquez, J. M. (2009). Distinct effects of boar seminal plasma fractions exhibiting different protein profiles on the functionality of highly diluted boar spermatozoa. *Reprod. Domest. Anim.* 44, 200–205. doi: 10.1111/j.1439-0531.2007.01028.x

Gazo, I., Dietrich, M. A., Pruliere, G., Shaliutina-Kolesova, A., Shaliutina, O., Cosson, J., et al. (2017). Protein phosphorylation in spermatozoa motility of Acipenser ruthenus and Cyprinus carpio. *Reproduction* 154, 653–673. doi: 10.1530/REP-16-0662

He, Y., Li, H., Zhang, Y., Hu, J., Shen, Y., Feng, J., et al. (2019). Comparative analysis of mitochondrial proteome reveals the mechanism of enhanced ram sperm motility induced by carbon ion radiation after *in vitro* liquid storage. *Dose Response* 17:1559325818823998. doi: 10.1177/1559325818823998

He, Y., Wang, K., Zhao, X., Zhang, Y., Ma, Y., and Hu, J. (2016). Differential proteome association study of freeze-thaw damage in ram sperm. *Cryobiology* 72, 60–68. doi: 10.1016/j.cryobiol.2015.11.003

Hetherington, L., Schneider, E. K., Scott, C., DeKretser, D., Muller, C. H., Hondermarck, H., et al. (2016). Deficiency in Outer Dense Fiber 1 is a marker and potential driver of idiopathic male infertility. *Mol. Cell. Proteomics* 15, 3685–3693. doi: 10.1074/mcp.M116.060343

Hetherington, L., Schneider, E. K., Scott, C., DeKretser, D., Muller, C. H., Hondermarck, H., et al. (2017). Deficiency in outer dense fiber 1 is a marker and potential driver of idiopathic male infertility. *Mol. Cell. Proteomics* 16, 1172. doi: 10.1074/mcp.A116.060343

Hillman, P., Ickowicz, D., Vizel, R., and Breitbart, H. (2013). Dissociation between AKAP3 and PKARII promotes AKAP3 degradation in sperm capacitation. *PLoS One* 8:e68873. doi: 10.1371/journal.pone.0068873

Huang, H., Scheffler, T. L., Gerrard, D. E., Larsen, M. R., and Lametsch, R. (2018). Quantitative proteomics and phosphoproteomics analysis revealed different regulatory mechanisms of halothane and rendement napole genes in porcine muscle metabolism. *J. Proteome Res.* 17, 2834–2849. doi: 10.1021/acs.jproteome.8b00294

Huang, Q., Luo, L., Alamdar, A., Zhang, J., Liu, L., Tian, M., et al. (2016). Integrated proteomics and metabolomics analysis of rat testis: mechanism of arsenic-induced male reproductive toxicity. *Sci. Rep.* 6:32518. doi: 10.1038/srep32518

Ijiri, T. W., Mahbub Hasan, A. K., and Sato, K. (2012). Protein-tyrosine kinase signaling in the biological functions associated with sperm. *J. Signal. Transduct.* 2012:181560. doi: 10.1155/2012/181560

Jumeau, F., Sigala, J., Dossou-Gbete, F., Frimat, K., Barbotin, A. L., Buee, L., et al. (2018). A-kinase anchor protein 4 precursor (pro-AKAP4) in human spermatozoa. *Andrology* 6, 854–859. doi: 10.1111/andr.12524

Kasimanickam, R. K., Kasimanickam, V. R., Arangasamy, A., and Kastelic, J. P. (2019). Sperm and seminal plasma proteomics of high- versus low-fertility Holstein bulls. *Theriogenology* 126, 41–48. doi: 10.1016/j.theriogenology.2018.11.032

Kasimanickam, V., and Kastelic, J. (2016). MicroRNA in sperm from Duroc, Landrace and Yorkshire boars. *Sci. Rep.* 6:32954. doi: 10.1038/srep32954

Kasvandik, S., Sillaste, G., Velthut-Meikas, A., Mikelsaar, A. V., Hallap, T., Padrik, P., et al. (2015). Bovine sperm plasma membrane proteomics through biotinylation and subcellular enrichment. *Proteomics* 15, 1906–1920. doi: 10.1002/pmic.201400297

Kim, H., Song, K. D., Kim, H. J., Park, W., Kim, J., Lee, T., et al. (2015). Exploring the genetic signature of body size in Yucatan miniature pig. *PLoS One* 10:e0121732. doi: 10.1371/journal.pone.0121732

Kitamura, N., Nakamura, Y., Miyamoto, Y., Miyamoto, T., Kabu, K., Yoshida, M., et al. (2011). Mieap, a p53-inducible protein, controls mitochondrial quality by repairing or eliminating unhealthy mitochondria. *PLoS One* 6:e16060. doi: 10.1371/journal.pone.0016060

Koh, T. J., Crabo, B. G., Tsou, H. L., and Graham, E. F. (1976). Fertility of liquid boar semen as influenced by breed and season. *J. Anim. Sci.* 42, 138–144. doi: 10.2527/jas1976.421138x

Kwon, W. S., Rahman, M. S., Lee, J. S., Kim, J., Yoon, S. J., Park, Y. J., et al. (2014). A comprehensive proteomic approach to identifying capacitation related proteins in boar spermatozoa. *BMC Genomics* 15:897. doi: 10.1186/1471-2164-15-897

Larance, M., and Lamond, A. I. (2015). Multidimensional proteomics for cell biology. *Nat. Rev. Mol. Cell. Biol.* 16, 269–280. doi: 10.1038/nrm3970

Li, S. H., Hwu, Y. M., Lu, C. H., Lin, M. H., Yeh, L. Y., and Lee, R. K. (2018). Serine Protease Inhibitor SERPINE2 Reversibly modulates murine sperm capacitation. *Int. J. Mol. Sci.* 19:1520. doi: 10.3390/ijms19051520

Li, Y. F., He, W., Mandal, A., Kim, Y. H., Digilio, L., Klotz, K., et al. (2011). CABYR binds to AKAP3 and Ropporin in the human sperm fibrous sheath. *Asian J. Androl.* 13, 266–274. doi: 10.1038/aja.2010.149

Lin, Y. H., Ke, C. C., Wang, Y. Y., Chen, M. F., Chen, T. M., Ku, W. C., et al. (2017). RAB10 interacts with the male germ cell-specific GTPase-activating protein during mammalian spermiogenesis. *Int. J. Mol. Sci.* 18:97. doi: 10.3390/ijms18010097

Lu, C. H., Lee, R. K., Hwu, Y. M., Chu, S. L., Chen, Y. J., Chang, W. C., et al. (2011). SERPINE2, a serine protease inhibitor extensively expressed in adult male mouse reproductive tissues, may serve as a murine sperm decapacitation factor. *Biol. Reprod.* 84, 514–525. doi: 10.1095/biolreprod.110.085100

Ma, J., Chen, T., Wu, S., Yang, C., Bai, M., Shu, K., et al. (2019). iProX: an integrated proteome resource. *Nucleic Acids Res.* 47, D1211–D1217. doi: 10.1093/nar/gky869

Macek, B., Mann, M., and Olsen, J. V. (2009). Global and site-specific quantitative phosphoproteomics: principles and applications. *Annu. Rev. Pharmacol. Toxicol.* 49, 199–221. doi: 10.1146/annurev.pharmtox.011008.145606

Maciel, V. L. Jr., Caldas-Bussiere, M. C., Silveira, V., Reis, R. S., Rios, A. F. L., and Paes de Carvalho, C. S. (2018). l-arginine alters the proteome of frozen-thawed bovine sperm during in vitro capacitation. *Theriogenology* 119, 1–9. doi: 10.1016/j.theriogenology.2018.06.018

Maciel, V. L. Jr., Tamashiro, L. K., and Bertolla, R. P. (2019). Post-translational modifications of seminal proteins and their importance in male fertility potential. *Expert Rev. Proteomics* 16, 941–950. doi: 10.1080/14789450.2019.1693895

Mariappa, D., Aladakatti, R. H., Dasari, S. K., Sreekumar, A., Wolkowicz, M., van der Hoorn, F., et al. (2010). Inhibition of tyrosine phosphorylation of sperm flagellar proteins, outer dense fiber protein-2 and tektin-2, is associated with impaired motility during capacitation of hamster spermatozoa. *Mol. Reprod. Dev.* 77, 182–193. doi: 10.1002/mrd.21131

Marques, D. B. D., Lopes, M. S., Broekhuijse, M., Guimaraes, S. E. F., Knol, E. F., Bastiaansen, J. W. M., et al. (2017). Genetic parameters for semen quality and quantity traits in five pig lines. *J. Anim. Sci.* 95, 4251–4259. doi: 10.2527/jas2017.1683

Martinez-Heredia, J., Estanyol, J. M., Ballesca, J. L., and Oliva, R. (2006). Proteomic identification of human sperm proteins. *Proteomics* 6, 4356–4369. doi: 10.1002/pmic.200600094

Martin-Hidalgo, D., Serrano, R., Zaragoza, C., Garcia-Marin, L. J., and Bragado, M. J. (2020). Human sperm phosphoproteome reveals differential phosphoprotein signatures that regulate human sperm motility. *J. Proteomics* 215:103654. doi: 10.1016/j.jprot.2020.103654

Miki, K., and Eddy, E. M. (1999). Single amino acids determine specificity of binding of protein kinase A regulatory subunits by protein kinase A anchoring proteins. *J. Biol. Chem.* 274, 29057–29062. doi: 10.1074/jbc.274.41.29057

Miki, K., Willis, W. D., Brown, P. R., Goulding, E. H., Fulcher, K. D., and Eddy, E. M. (2002). Targeted disruption of the Akap4 gene causes defects in sperm flagellum and motility. *Dev. Biol.* 248, 331–342. doi: 10.1006/dbio.2002.0728

Naaby-Hansen, S., Mandal, A., Wolkowicz, M. J., Sen, B., Westbrook, V. A., Shetty, J., et al. (2002). CABYR, a novel calcium-binding tyrosine phosphorylation-regulated fibrous sheath protein involved in capacitation. *Dev. Biol.* 242, 236–254. doi: 10.1006/dbio.2001.0527

Nayernia, K., Adham, I. M., Burkhardt-Gottges, E., Neesen, J., Rieche, M., Wolf, S., et al. (2002). Asthenozoospermia in mice with targeted deletion of the sperm mitochondrion-associated cysteine-rich protein (Smcp) gene. *Mol. Cell. Biol.* 22, 3046–3052. doi: 10.1128/mcb.22.9.3046-3052.2002

Nixon, B., Bernstein, I. R., Cafe, S. L., Delehedde, M., Sergeant, N., Anderson, A. L., et al. (2019a). A kinase anchor protein 4 is vulnerable to oxidative adduction in male germ cells. *Front. Cell. Dev. Biol.* 7:319. doi: 10.3389/fcell.2019.00319

Nixon, B., Johnston, S. D., Skerrett-Byrne, D. A., Anderson, A. L., Stanger, S. J., Bromfield, E. G., et al. (2019b). Modification of crocodile spermatozoa refutes the tenet that post-testicular sperm maturation is restricted to mammals. *Mol. Cell. Proteomics* 18, S59–S76. doi: 10.1074/mcp.RA118.000904

Olsen, J. V., Blagoev, B., Gnad, F., Macek, B., Kumar, C., Mortensen, P., et al. (2006). Global, *in vivo*, and site-specific phosphorylation dynamics in signaling networks. *Cell* 127, 635–648. doi: 10.1016/j.cell.2006.09.026

Ota, T., Suzuki, Y., Nishikawa, T., Otsuki, T., Sugiyama, T., Irie, R., et al. (2004). Complete sequencing and characterization of 21,243 full-length human cDNAs. *Nat. Genet.* 36, 40–45. doi: 10.1038/ng1285

Parte, P. P., Rao, P., Redij, S., Lobo, V., D'Souza, S. J., Gajbhiye, R., et al. (2012). Sperm phosphoproteome profiling by ultra performance liquid chromatography followed by data independent analysis (LC-MS(E)) reveals altered proteomic signatures in asthenozoospermia. *J. Proteomics* 75, 5861–5871. doi: 10.1016/j.jprot.2012.07.003

Pelloni, M., Paoli, D., Majoli, M., Pallotti, F., Carlini, T., Lenzi, A., et al. (2018). Molecular study of human sperm RNA: Ropporin and CABYR in asthenozoospermia. *J. Endocrinol. Invest.* 41, 781–787. doi: 10.1007/s40618-017-0804-x

Perez-Patino, C., Barranco, I., Li, J., Padilla, L., Martinez, E. A., Rodriguez-Martinez, H., et al. (2019a). Cryopreservation differentially alters the proteome of epididymal and ejaculated pig spermatozoa. *Int. J. Mol. Sci.* 20:1791. doi: 10.3390/ijms20071791

Perez-Patino, C., Li, J., Barranco, I., Martinez, E. A., Rodriguez-Martinez, H., Roca, J., et al. (2019b). The proteome of frozen-thawed pig spermatozoa is dependent on the ejaculate fraction source. *Sci. Rep.* 9:705. doi: 10.1038/s41598-018-36624-5

Perez-Patino, C., Parrilla, I., Li, J., Barranco, I., Martinez, E. A., Rodriguez-Martinez, H., et al. (2019c). The proteome of pig spermatozoa is remodeled during ejaculation. *Mol. Cell. Proteomics* 18, 41–50. doi: 10.1074/mcp.RA118.000840

Peris-Frau, P., Martin-Maestro, A., Iniesta-Cuerda, M., Sanchez-Ajofrin, I., Mateos-Hernandez, L., Garde, J. J., et al. (2019). Freezing-Thawing procedures remodel the proteome of ram sperm before and after *in vitro* capacitation. *Int. J. Mol. Sci.* 20:4596. doi: 10.3390/ijms20184596

Pini, T., Rickard, J. P., Leahy, T., Crossett, B., Druart, X., and de Graaf, S. P. (2018). Cryopreservation and egg yolk medium alter the proteome of ram spermatozoa. *J. Proteomics* 181, 73–82. doi: 10.1016/j.jprot.2018.04.001

Porambo, J. R., Salicioni, A. M., Visconti, P. E., and Platt, M. D. (2012). Sperm phosphoproteomics: historical perspectives and current methodologies. *Expert. Rev. Proteomics* 9, 533–548. doi: 10.1586/epr.12.41

Raggiaschi, R., Gotta, S., and Terstappen, G. C. (2005). Phosphoproteome analysis. *Biosci. Rep.* 25, 33–44. doi: 10.1007/s10540-005-2846-0

Rahamim Ben-Navi, L., Almog, T., Yao, Z., Seger, R., and Naor, Z. (2016). A-Kinase Anchoring Protein 4 (AKAP4) is an ERK1/2 substrate and a switch molecule between cAMP/PKA and PKC/ERK1/2 in human spermatozoa. *Sci. Rep.* 6:37922. doi: 10.1038/srep37922

Ren, L., Li, C., Wang, Y., Teng, Y., Sun, H., Xing, B., et al. (2018). *In Vivo* phosphoproteome analysis reveals kinome reprogramming in hepatocellular carcinoma. *Mol. Cell. Proteomics* 17, 1067–1083. doi: 10.1074/mcp.RA117.000421

Robert, M., and Gagnon, C. (1999). Semenogelin I: a coagulum forming, multifunctional seminal vesicle protein. *Cell. Mol. Life Sci.* 55, 944–960. doi: 10.1007/s000180050346

Rolland, T., Tasan, M., Charloteaux, B., Pevzner, S. J., Zhong, Q., Sahni, N., et al. (2014). A proteome-scale map of the human interactome network. *Cell* 159, 1212–1226. doi: 10.1016/j.cell.2014.10.050

Samanta, L., Swain, N., Ayaz, A., Venugopal, V., and Agarwal, A. (2016). Post-Translational modifications in sperm proteome: the chemistry of proteome diversifications in the pathophysiology of male factor infertility. *Biochim. Biophys. Acta* 1860, 1450–1465. doi: 10.1016/j.bbagen.2016.04.001

Sandberg, A., Lindell, G., Kallstrom, B. N., Branca, R. M., Danielsson, K. G., Dahlberg, M., et al. (2012). Tumor proteomics by multivariate analysis on individual pathway data for characterization of vulvar cancer phenotypes. *Mol. Cell. Proteomics* 11:M112016998. doi: 10.1074/mcp.M112.016998

Shang, Y., Zhu, F., Wang, L., Ouyang, Y. C., Dong, M. Z., Liu, C., et al. (2017). Essential role for SUN5 in anchoring sperm head to the tail. *Elife* 6:e28199. doi: 10.7554/eLife.28199

Shanmugam, M., Kannaki, T. R., and Vinoth, A. (2016). Comparison of semen variables, sperm DNA damage and sperm membrane proteins in two male layer breeder lines. *Anim. Reprod. Sci.* 172, 131–136. doi: 10.1016/j.anireprosci.2016.07.010

Skroblin, P., Grossmann, S., Schafer, G., Rosenthal, W., and Klussmann, E. (2010). Mechanisms of protein kinase A anchoring. *Int. Rev. Cell. Mol. Biol.* 283, 235–330. doi: 10.1016/S1937-6448(10)83005-9

Smital, J. (2009). Effects influencing boar semen. *Anim. Reprod. Sci.* 110, 335–346. doi: 10.1016/j.anireprosci.2008.01.024

Smital, J., De Sousa, L. L., and Mohsen, A. (2004). Differences among breeds and manifestation of heterosis in AI boar sperm output. *Anim. Reprod. Sci.* 80, 121–130. doi: 10.1016/S0378-4320(03)00142-8

Tokuhiro, K., Isotani, A., Yokota, S., Yano, Y., Oshio, S., Hirose, M., et al. (2009). OAZ-t/OAZ3 is essential for rigid connection of sperm tails to heads in mouse. *PLoS Genet.* 5:e1000712. doi: 10.1371/journal.pgen.1000712

Topfer-Petersen, E., Romero, A., Varela, P. F., Ekhlasi-Hundrieser, M., Dostalova, Z., Sanz, L., et al. (1998). Spermadhesins: a new protein family. Facts, hypotheses and perspectives. *Andrologia* 30, 217–224. doi: 10.1111/j.1439-0272.1998.tb01163.x

Unwin, R. D., Griffiths, J. R., and Whetton, A. D. (2010). Simultaneous analysis of relative protein expression levels across multiple samples using iTRAQ isobaric tags with 2D nano LC-MS/MS. *Nat. Protoc.* 5, 1574–1582. doi: 10.1038/nprot.2010.123

Urizar-Arenaza, I., Osinalde, N., Akimov, V., Puglia, M., Candenas, L., Pinto, F. M., et al. (2019). Phosphoproteomic and functional analyses reveal sperm-specific protein changes downstream of kappa opioid receptor in human spermatozoa. *Mol. Cell. Proteomics* 18, S118–S131. doi: 10.1074/mcp.RA118.001133

Vernon, G. G., and Woolley, D. M. (2004). Basal sliding and the mechanics of oscillation in a mammalian sperm flagellum. *Biophys. J.* 87, 3934–3944. doi: 10.1529/biophysj.104.042648

Vizel, R., Hillman, P., Ickowicz, D., and Breitbart, H. (2015). AKAP3 degradation in sperm capacitation is regulated by its tyrosine phosphorylation. *Biochim. Biophys. Acta* 1850, 1912–1920. doi: 10.1016/j.bbagen.2015.06.005

Wang, J., Qi, L., Huang, S., Zhou, T., Guo, Y., Wang, G., et al. (2015). Quantitative phosphoproteomics analysis reveals a key role of insulin growth factor 1 receptor (IGF1R) tyrosine kinase in human sperm capacitation. *Mol. Cell. Proteomics* 14, 1104–1112. doi: 10.1074/mcp.M114.045468

Wei, Y., Gao, Q., Niu, P., Xu, K., Qiu, Y., Hu, Y., et al. (2018). Integrative proteomic and phosphoproteomic profiling of testis from wip1 phosphatase-knockout mice: insights into mechanisms of reduced fertility. *Mol. Cell. Proteomics.* 18, 216–230. doi: 10.1074/mcp.RA117.000479

Wiese, S., Reidegeld, K. A., Meyer, H. E., and Warscheid, B. (2007). Protein labeling by iTRAQ: a new tool for quantitative mass spectrometry in proteome research. *Proteomics* 7, 340–350. doi: 10.1002/pmic.200600422

Williams, A. C., and Ford, W. C. (2001). The role of glucose in supporting motility and capacitation in human spermatozoa. *J. Androl.* 22, 680–695.

Wisniewski, J. R., Zougman, A., Nagaraj, N., and Mann, M. (2009). Universal sample preparation method for proteome analysis. *Nat. Methods* 6, 359–362. doi: 10.1038/nmeth.1322

Wu, J., Brown, S. H., von Daake, S., and Taylor, S. S. (2007). PKA type IIalpha holoenzyme reveals a combinatorial strategy for isoform diversity. *Science* 318, 274–279. doi: 10.1126/science.1146447

Xinhong, L., Zhen, L., Fu, J., Wang, L., Yang, Q., Li, P., et al. (2018). Quantitative proteomic profiling indicates the difference in reproductive efficiency between Meishan and Duroc boar spermatozoa. *Theriogenology* 116, 71–82. doi: 10.1016/j.theriogenology.2018.04.025

Xu, K., Yang, L., Zhang, L., and Qi, H. (2020). Lack of AKAP3 disrupts integrity of the subcellular structure and proteome of mouse sperm and causes male sterility. *Development* 147:dev181057. doi: 10.1242/dev.181057

Xu, Y., Qian, H., Feng, X., Xiong, Y., Lei, M., Ren, Z., et al. (2012). Differential proteome and transcriptome analysis of porcine skeletal muscle during development. *J. Proteomics* 75, 2093–2108. doi: 10.1016/j.jprot.2012.01.013

Yamatoya, K., Kousaka, M., Ito, C., Nakata, K., Hatano, M., Araki, Y., et al. (2019). Cleavage of SPACA1 regulates assembly of sperm-egg membrane fusion machinery in mature spermatozoa. *Biol. Reprod.* 102, 750–757. doi: 10.1093/biolre/ioz223

Yang, K., Meinhardt, A., Zhang, B., Grzmil, P., Adham, I. M., and Hoyer-Fender, S. (2012). The small heat shock protein ODF1/HSPB10 is essential for tight linkage of sperm head to tail and male fertility in mice. *Mol. Cell. Biol.* 32, 216–225. doi: 10.1128/MCB.06158-11

Yang, S., Li, X., Liu, X., Ding, X., Xin, X., Jin, C., et al. (2018). Parallel comparative proteomics and phosphoproteomics reveal that cattle myostatin regulates phosphorylation of key enzymes in glycogen metabolism and glycolysis pathway. *Oncotarget* 9, 11352–11370. doi: 10.18632/oncotarget.24250

Young, S. A., Miyata, H., Satouh, Y., Aitken, R. J., Baker, M. A., and Ikawa, M. (2016). CABYR is essential for fibrous sheath integrity and progressive motility in mouse spermatozoa. *J. Cell. Sci.* 129, 4379–4387. doi: 10.1242/jcs.193151

Zalata, A. A., Mokhtar, N., Atwa, A., Khaled, M., and Shaker, O. G. (2016). The role of protamine 2 gene expression and caspase 9 activity in male infertility. *J. Urol.* 195, 796–800. doi: 10.1016/j.juro.2015.08.101

Zhao, W., Li, Z., Ping, P., Wang, G., Yuan, X., and Sun, F. (2018). Outer dense fibers stabilize the axoneme to maintain sperm motility. *J. Cell. Mol. Med.* 22, 1755–1768. doi: 10.1111/jcmm.13457

Conflict of Interest: The authors declare that the research was conducted in the absence of any commercial or financial relationships that could be construed as a potential conflict of interest.

frontiers in Cell and Developmental Biology

REVIEW
published: 02 August 2021
doi: 10.3389/fcell.2021.710033

Meiotic Cohesin and Variants Associated With Human Reproductive Aging and Disease

*Rachel Beverley[1], Meredith L. Snook[1] and Miguel Angel Brieño-Enríquez[2]**

[1] Division of Reproductive Endocrinology and Infertility, Department of Obstetrics, Gynecology, and Reproductive Sciences, University of Pittsburgh, Pittsburgh, PA, United States, [2] Magee-Womens Research Institute, Department of Obstetrics, Gynecology, and Reproductive Sciences, University of Pittsburgh, Pittsburgh, PA, United States

Successful human reproduction relies on the well-orchestrated development of competent gametes through the process of meiosis. The loading of cohesin, a multi-protein complex, is a key event in the initiation of mammalian meiosis. Establishment of sister chromatid cohesion via cohesin rings is essential for ensuring homologous recombination-mediated DNA repair and future proper chromosome segregation. Cohesin proteins loaded during female fetal life are not replenished over time, and therefore are a potential etiology of age-related aneuploidy in oocytes resulting in decreased fecundity and increased infertility and miscarriage rates with advancing maternal age. Herein, we provide a brief overview of meiotic cohesin and summarize the human genetic studies which have identified genetic variants of cohesin proteins and the associated reproductive phenotypes including primary ovarian insufficiency, trisomy in offspring, and non-obstructive azoospermia. The association of cohesion defects with cancer predisposition and potential impact on aging are also described. Expansion of genetic testing within clinical medicine, with a focus on cohesin protein-related genes, may provide additional insight to previously unknown etiologies of disorders contributing to gamete exhaustion in females, and infertility and reproductive aging in both men and women.

Keywords: cohesin, aging, reproduction, human, primary ovarian insufficiency, meiosis

OPEN ACCESS

Edited by:
Karen Schindler, Rutgers, The State University of New Jersey, United States

Reviewed by:
Diana Libuda, University of Oregon, United States
Sarah Moorey, The University of Tennessee, Knoxville, United States

****Correspondence:***
Miguel Angel Brieño-Enríquez
brienoenriquezma@mwri.magee.edu

Specialty section:
This article was submitted to Molecular and Cellular Reproduction, a section of the journal Frontiers in Cell and Developmental Biology

Received: *17 May 2021*
Accepted: *13 July 2021*
Published: *02 August 2021*

Citation:
Beverley R, Snook ML and Brieño-Enríquez MA (2021) Meiotic Cohesin and Variants Associated With Human Reproductive Aging and Disease. Front. Cell Dev. Biol. 9:710033. doi: 10.3389/fcell.2021.710033

INTRODUCTION

Infertility, a disease defined by the failure to achieve a successful pregnancy after 12 or more months of regular, unprotected intercourse or due to an impairment of a person's capacity to reproduce (Practice Committee of the American Society for Reproductive Medicine, 2020), is estimated to affect approximately 15% of the reproductive age population. A woman's age is the single most important factor determining her ability to conceive as the quantity and quality of oocytes decrease progressively with advancing age (American College of Obstetricians and Gynecologists Committee on Gynecologic Practice and Practice Committee, 2014; Steiner and Jukic, 2016). The number of primordial germ cells, or oogonia, peaks at approximately 6–7 million during mid-gestation, followed by progressive atresia with approximately 1–2 million oocytes present at birth (Motta et al., 1997; Pereda et al., 2006; Mamsen et al., 2012). By puberty, there is estimated to be 300,000–500,000 oocytes remaining, and approximately 25,000 at age 37 years (Forabosco and Sforza, 2007;

Albamonte et al., 2019). Menopause occurs when the number of remaining oocytes falls below a critical threshold of about 1000, regardless of age (American College of Obstetricians and Gynecologists Committee on Gynecologic Practice and Practice Committee, 2014).

Intentional delays in childbearing until later maternal age has been an increasing phenomenon over several decades. In the United States, between 1970 and 2006, the proportion of first births to women age 35 or over increased nearly eight times (Matthews and Hamilton, 2014). This trend has been attributed to multiple factors including women's educational and professional pursuits as well as increasing availability of contraception (Simoni et al., 2017; Kavanaugh et al., 2021). Additionally, surveys of older women have demonstrated misperceptions about the magnitude of fertility decline with age. Reasons for this include recollections of messaging about pregnancy prevention starting in adolescence, healthy lifestyle and family history of normal fertility, as well as incorrect information from media reports of pregnancies in older celebrity women (Mac Dougall et al., 2013).

With later maternal age, women experience a gradual decrease in fecundity and increased rates of miscarriage (American College of Obstetricians and Gynecologists Committee on Gynecologic Practice and Practice Committee, 2014). These poor outcomes with advancing age reflect a decline in oocyte quality which can be associated with no or abnormal fertilization, no implantation, or aneuploidy (notably trisomy) of conceived embryos (Balasch and Gratacos, 2012). This manifests clinically as a higher incidence of infertility, early pregnancy loss, or developmental defects in ongoing pregnancies with increasing maternal age.

Throughout a woman's reproductive life, successful meiosis requires homologous recombination-mediated DNA repair and proper segregation of chromosomes and sister chromatids to yield haploid oocytes. Sister chromatid cohesion, mediated by cohesin rings which tether the two sister chromatids of replicated chromosomes, is essential to ensure that these processes are carried out correctly. Loss or weakening of chromosome cohesion with advancing maternal age has been proposed as a leading cause of age-related aneuploidy in oocytes (Chiang et al., 2010, 2011; Jessberger, 2012; Herbert et al., 2015; Gruhn et al., 2019). Therefore, it is likely that deterioration of the complex of proteins involved in chromosome cohesion, referred to as cohesin proteins, or genetic variants affecting these proteins are potential drivers of age-related infertility and aneuploidy. This review provides an overview of meiotic cohesin and summarizes the human genetic studies that have identified genetic variants of cohesin proteins and the associated reproductive phenotypes.

MEIOSIS AND COHESIN

Understanding the etiology of aneuploidy with advancing maternal age requires an understanding of female mammalian meiosis. Mammalian meiosis is a specialized form of cell division characterized by a single round of DNA replication, followed by two rounds of chromosome segregation resulting in haploid gametes. Segregation of homologous chromosomes occurs during meiosis I (MI) and segregation of sister chromatids occurs during meiosis II (MII) (Zickler and Kleckner, 2015; Bolcun-Filas and Handel, 2018). Female mammalian meiosis commences during fetal life. Chromosomes within oocytes undergo replication and subsequently enter meiotic prophase I, and arrest in this stage for decades until future ovulation or atresia.

Meiotic prophase is the first and longest stage of mammalian meiosis in which the homologous chromosomes must pair, synapse, and undergo meiotic recombination to generate a crossover event. Meiotic prophase I include unique processes which are distinct from mitotic prophase. Following pre-meiotic DNA replication, meiotic prophase I initiates and progresses through various stages including leptonema, zygonema, pachynema, diplonema, and diakinesis (Zickler and Kleckner, 1999, 2015; **Figure 1**). Pairing-synapsis and recombination are hallmarks of prophase I, and are both essential for ensuring homolog interactions leading to the formation of at least one crossover event per chromosome pair. In fact, the number of crossovers and their location is critical for ensuring appropriate disjunction at metaphase I and for maintaining genomic stability. Pairing of homologous chromosomes occurs through the formation of a proteinaceous structure called the synaptonemal complex that forms between homologous chromosomes, while crossover recombination occurs at the DNA level, between two non-sister chromatids (Svetlanov and Cohen, 2004; Holloway and Cohen, 2015; Gray and Cohen, 2016). During leptonema, synaptonemal complex proteins (e.g., SYCP2/3) begin to form a proteinaceous scaffold (axial elements) along each homologous chromosome (Dietrich et al., 1992; Page and Hawley, 2004; Fraune et al., 2012; Cahoon et al., 2019). During zygonema, central element proteins (e.g., SYCP1, TEX12), begin to localize between the lateral elements allowing for continued pairing and synapsis between homologous chromosomes, essentially providing a proteinaceous structure physically tethering them by the end of this stage. At pachynema, lateral elements are completely formed, and the homologous chromosomes are completely synapsed (Zickler and Kleckner, 2015; Cahoon and Hawley, 2016; Gao and Colaiacovo, 2018). During diplonema, the central element of the synaptonemal complex breaks down and the chromosomes begin to repel each other. By diakinesis, homologous chromosomes are only tethered at the sites of crossovers and sister chromatids at sites of centromeres (**Figure 1**).

Recombination during prophase I occurs at the DNA level, between two non-sister chromatids (Svetlanov and Cohen, 2004; Holloway and Cohen, 2015; Gray and Cohen, 2016). Programmed double strand breaks (DSBs) are generated by the protein SPO11 throughout the genome in a very controlled and specific fashion. After creating hundreds of DSBs, they are repaired either as crossovers (COs), non-crossovers (NCO) (Keeney and Kleckner, 1995; Keeney, 2008; Massy, 2016; Robert et al., 2016) or can undergo inter-sister repair as well (Garcia-Muse et al., 2019; Almanzar et al., 2021; Toraason et al., 2021). Generation of COs of homologs is required for proper segregation of homologous chromosomes during MI. The resulting bivalent chromosomes are linked at chiasmata which

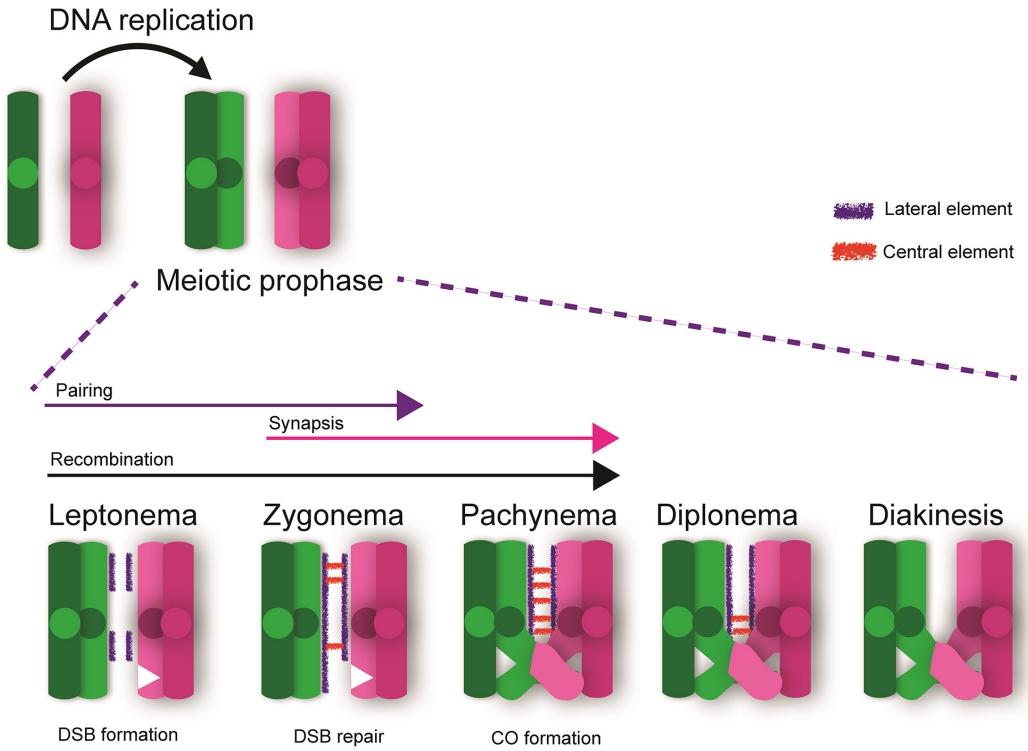

FIGURE 1 | Meiotic Prophase I. Following DNA replication, meiotic prophase initiates. DNA double strand breaks (DSBs) are created during leptonema and the chromosomes initiate the processes of pairing and recombination. These processes progress into zygonema with DSB repair mechanisms ensuring proper homologous recombination. By pachynema, the chromosomes are fully synapsed and sites of crossovers (CO) are apparent. Sites of CO tether the homologous chromosomes together until anaphase I, allowing for proper segregation of homologous chromosomes and reducing the risk of aneuploidy in future gametes. Diplonema is marked by breakdown of the central element of the synaptonemal complex and chromosomes begin to repel each other. By diakinesis, homologous chromosomes are only tethered at the sites of crossovers and sister chromatids at the centromeres.

correspond to sites of crossovers. COs are stabilized by cohesin rings encompassing the sister chromatids distal to these sites on the chromosome arms (Petronczki et al., 2003). Full literature reviews about these processes have been described (Handel and Schimenti, 2010; Hunter, 2015; Gray and Cohen, 2016; Pereira et al., 2020).

Chromosome cohesion is established during pre-meiotic S phase and early prophase I via loading of cohesin rings/complexes. While mitotic and meiotic cohesin subunits are widely conserved in diverse species (Ishiguro, 2019), three types of meiotic cohesin complexes exist in mammalian cells. The subunits of STAG3, SMC1β, and SMC3 are shared in most of these complexes while the kleisin component (REC8, RAD21L, or RAD21) can vary (Herran et al., 2011; McNicoll et al., 2013; Ishiguro, 2019; **Figure 2A**). REC8 and RAD21L are meiosis-specific cohesin components while RAD21 is seen in both mitosis and meiosis. During meiotic prophase, REC8-containing cohesin begins to localize along the chromosomes prior to and during replication of DNA. Alternatively, RAD21L-containing cohesin rings are localized on chromosomes during leptonema and zygonema stages of prophase I and dissociates following late pachynema. The early loading of cohesin during meiosis provides a cohesin axis which serves as a structural core for chromosome organization during meiosis (Ishiguro, 2019). Thus, the cohesin complex is essential for maintaining sister chromatid cohesion and for ensuring correct chromosome segregation (Nasmyth and Haering, 2009). While mitotic and meiotic cohesion events are largely conserved, there are specific differences that exist, specifically, the unique and sequential chromosome segregation profiles during meiosis.

The most well-defined mechanism of cohesin removal during meiosis involves Separase-induced proteolytic cleavage (Verni et al., 2000; Waizenegger et al., 2000; Losada et al., 2002; Buheitel and Stemmann, 2013; Wassmann, 2013; Haarhuis et al., 2014; Hirano, 2015). During meiosis, cleavage of REC8 by Separase is initially restricted to the chromosome arms, and it is not until anaphase II that centromeric REC8 cleavage is initiated (Buonomo et al., 2000; Kitajima et al., 2003; Kudo et al., 2009; Ishiguro et al., 2010; Katis et al., 2010; **Figure 3A**). Centromeric cohesin is essential to maintain sister chromatid cohesion until the second meiotic division. These functions of cohesin ensure future proper chromosome segregation upon resumption of meiosis in sexually mature females at the time of ovulation and later during fertilization. The cohesin rings at the centromeric region are protected by the interaction of Shugoshin 2 (SGO2) and protein phosphatase 2A (PP2A) which keeps REC8 in a hypo-phosphorylated state (Kitajima et al., 2006; Riedel et al., 2006). Maintenance of centromeric cohesin rings during MI protects

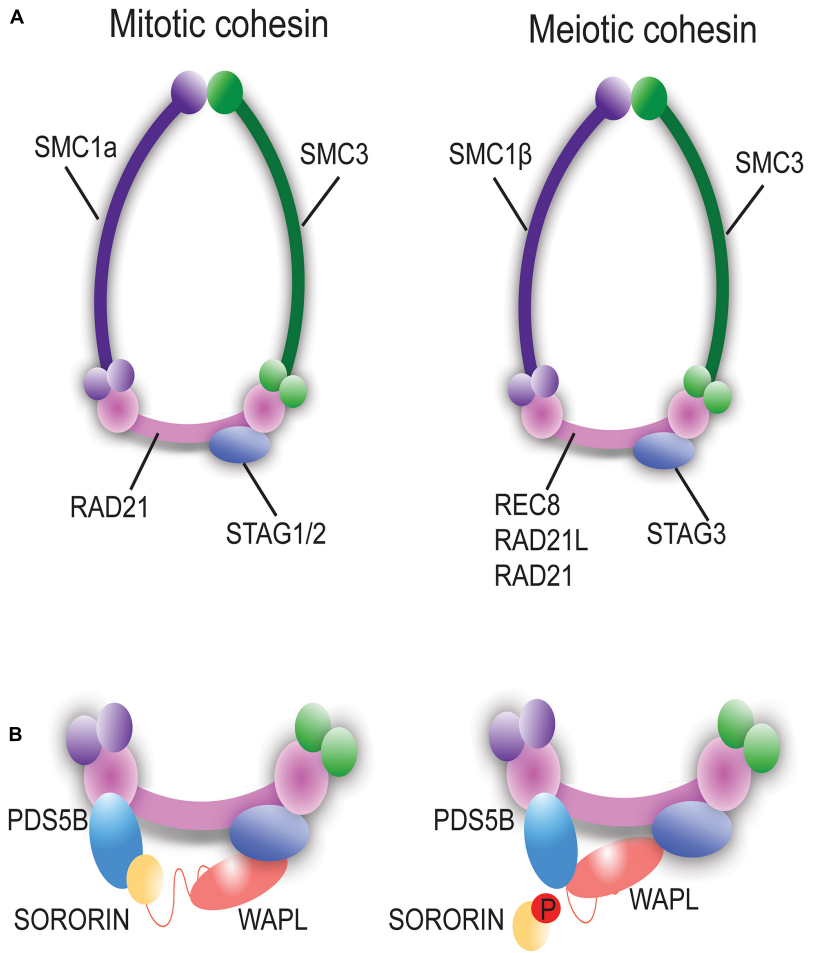

FIGURE 2 | Mitotic vs. Meiotic Cohesin ring components and associated proteins. **(A)** Schematic representation of mitotic and meiotic cohesin complexes. The meiosis-specific cohesin ring proteins are SMC1β, RAD21L, REC8, and STAG3. **(B)** PDS5B, WAPL, and Sororin are associated with the cohesin complex and regulate the dynamic interaction of cohesin with chromatin. Phosphorylation of Sororin dissociates it from the cohesin ring permitting interaction of WAPL with PDS5B to open the of the cohesin ring via the prophase pathway.

from premature segregation of sister chromatids (PSSC). During MII, dissociation of SGO2/PP2A at the centromeres results in phosphorylation of REC8, thus allowing the action of Separase to cleave centromeric cohesin rings which permits segregation of sister chromatids (Lee et al., 2008; Xu et al., 2009; **Figure 3A**).

Cohesin removal also depends on a non-proteolytic mechanism known as the prophase pathway, which precedes the action of Separase. The prophase pathway is orchestrated by an interaction between PDS5B, Sororin and wings apart-like (WAPL) protein (Verni et al., 2000; Nishiyama et al., 2013; Tedeschi et al., 2013). WAPL facilitates unloading of cohesin during prophase through an antagonistic mechanism mediated by competition between WAPL and Sororin for binding to PDS5B (**Figure 2B**; Kitajima et al., 2003; Kudo et al., 2009; Shintomi and Hirano, 2009; Ishiguro et al., 2010; Katis et al., 2010; Nishiyama et al., 2010; Carretero et al., 2013). In meiosis, this pathway has been described in yeast, worms, and mice (Brieno-Enriquez et al., 2016; Crawley et al., 2016; Wolf et al., 2018; Challa et al., 2019).

The proper step-wise removal of the cohesin rings is essential to ensure correct chromosome segregation during MI and MII. In sexually mature females, follicle-stimulating hormone (FSH) promotes growth of a dominant follicle in the ovary. Proliferation of granulosa cells surrounding the follicle leads to estrogen production which ultimately triggers the pre-ovulatory luteinizing hormone (LH) surge (McGee and Hsueh, 2000; Edson et al., 2009; Grive, 2020). The LH surge induces a decline in oocyte cAMP levels which then activates cyclin-dependent kinase 1 (CDK1) driving the transition of the oocyte out of prophase I arrest (Mehlmann et al., 2002; Mehlmann, 2005; Norris et al., 2010; Li et al., 2019). Removal of cohesin from the chromosome arms leads to the resolution of chiasmata and allows homologous chromosomes to segregate during anaphase I. If the first chromosome segregation commences correctly, the daughter cell receives a complete set of chromatids and the other set of chromatids are encompassed in the first polar body. Sister chromatids are maintained together via cohesin rings located at the centromere region. Mammalian oocyte meiosis then arrests

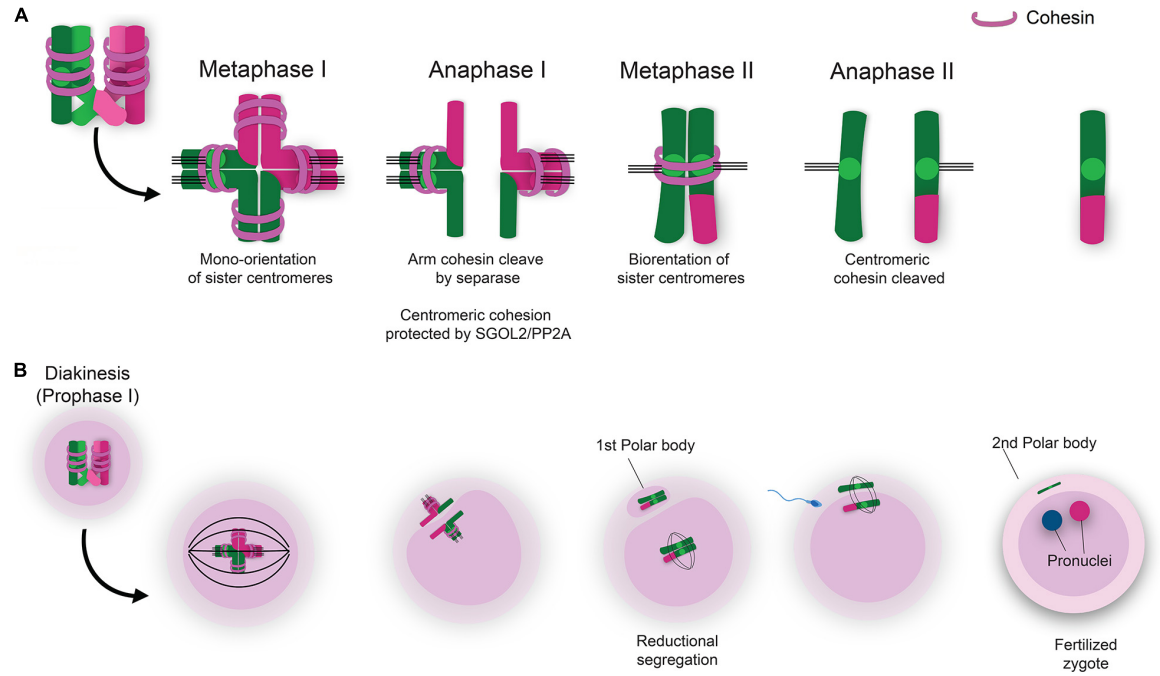

FIGURE 3 | Sequential removal of cohesin ensures proper chromosome segregation and completion of meiosis. **(A)** Removal of cohesin rings from the chromosome arms during MI permits segregation of homologous chromosomes during anaphase I. Cleavage of centromeric cohesin during MII allows for segregation of sister chromatids and formation of haploid gametes. **(B)** The LH surge induces the transition of the oocyte from meiotic prophase I to complete the first meiotic division of homologous chromosomes resulting the extrusion of the first polar body and arrest at metaphase II. Fertilization is the subsequent trigger for the second meiotic division with segregation of sister chromatids and extrusion of the second polar body.

at metaphase II until fertilization, as this event is the trigger for resumption and completion of MII. Resolution of centromeric cohesin rings during MII then allows for the segregation of sister chromatids. These events culminate in the formation of the haploid gamete and the second polar body (**Figure 3B**).

COHESIN AND AGING

Cohesin established in females during fetal life is not replenished over time during postnatal development. Oocyte cohesin expression is restricted to pre- and early meiotic prophase stages and allows for complete fertility and prevents aneuploidy (Revenkova et al., 2010). Additionally, mouse models have shown that no or very little cohesin loading occurs postnatally (Burkhardt et al., 2016). Therefore, it appears that the cohesin established during fetal life provides chromosome cohesion throughout the reproductive lifespan and the loss or weakening of chromosome cohesin may underpin the issue of declining oocyte quality and aneuploidy of aging females. Specifically, cohesin loss appears to occur while oocytes age during the time they are arrested in prophase I (Lister et al., 2010). Long-lived mouse strains as well as humans show an increased interkinetochore distance (IKD) with increasing female age (Chiang et al., 2010; Lister et al., 2010; Gruhn et al., 2019) which is thought to be a surrogate marker for loss of centromeric cohesion. Studies in human females have demonstrated that PSSC is the most common segregation error leading to aneuploidy (Pellestor et al., 2003; Garcia-Cruz et al., 2010; Ottolini et al., 2015; Gruhn et al., 2019). Therefore, weakening of centromeric cohesion is likely a major contributor to aneuploidy seen in women of advanced age. Additionally, studies of human oocytes and embryos have found higher rates of recombination and therefore sites of crossovers in euploid as opposed to aneuploid oocytes (Ottolini et al., 2015; Wang et al., 2017; Gruhn et al., 2019; Hassold et al., 2021). Given the presence of cohesin rings along the chromosome arms adjacent to the sites of crossovers, this data provides another link for the lack or loss of cohesin being a driver of aneuploidy in older women.

COHESIN DEFECTS AND FEMALE REPRODUCTIVE PHENOTYPES

Primary Ovarian Insufficiency

Primary ovarian insufficiency (POI) is defined by oligomenorrhea or amenorrhea prior to age 40 in conjunction with elevated serum FSH levels in the menopausal range, as defined by the reporting laboratory, drawn on two separate occasions at least 1 month apart (Nelson, 2009). Affecting approximately 1% of reproductive-aged women, POI is a heterogeneous disorder with a spectrum of etiologies including cytogenetic abnormalities, autoimmune factors, or various genetic causes. Additionally, POI may result from iatrogenic

factors such as gonadotoxic cancer treatments (Nelson, 2009; Kort et al., 2014; Anderson et al., 2015; Hoekman et al., 2018) or ovarian surgeries. More recent advancements in clinical genetics have uncovered significant genetic contributions to POI, though the etiology in most spontaneous cases remains to be elucidated. Additionally, POI exhibits a spectrum of patient presentations including young girls who present with primary amenorrhea already qualifying for the diagnosis, compared to women in their thirties with subfertility/infertility and/or diminished ovarian reserve who subsequently go on to be formally diagnosed with POI once criteria are met.

Recent studies of families with POI from various ethnic backgrounds have identified several variants in the gene encoding the meiosis-specific cohesin protein STAG3 as a potential etiology for their diagnosis (**Table 1**; Caburet et al., 2014; Le Quesne Stabej et al., 2016; Colombo et al., 2017; He et al., 2018; Franca et al., 2019; Heddar et al., 2019). Interestingly, in all studies which have identified variants in *STAG3*, the index patient case(s) have presented with primary amenorrhea, elevated FSH levels in menopausal range, and streak gonads on ultrasound. These findings are consistent with early gonadal dysgenesis in young girls with otherwise normal 46XX karyotypes.

The first report of mutant cohesin leading to POI was reported by Caburet et al. (2014), in a Palestinian family with four affected sisters and one affected maternal aunt. Whole exome sequencing (WES) was performed on one affected sister and one unaffected sister which identified a deleterious 1 bp deletion (c.968delC) in *STAG3* resulting in a frameshift mutation and subsequent premature stop codon (Caburet et al., 2014). Ultimately, the four affected sisters were found to be homozygous for the mutation while unaffected family members were either heterozygous or homozygous for the non-mutant allele. These authors created a *Stag3*$^{-/-}$ mouse model which had no overt phenotype beyond sterility in both male and female mice. Histologic analysis of ovaries from these mice revealed a lack of oocytes and ovarian follicles as well as dense stroma indicating severe and early ovarian dysgenesis. Fetal oocyte meiotic chromosome spreads also demonstrated that oocytes from the *Stag3*$^{-/-}$ mouse model had loss of centromeric sister chromatid cohesion and axial elements did not progress beyond the leptonema stage of meiotic prophase. Additionally, findings from a different *Stag3*$^{-/-}$ mouse model demonstrated disruption in other meiosis-specific cohesin localization to the chromosome cores which led to disruption in DNA repair processes, synapsis of chromosomes, and pericentromeric heterochromatin clustering. This culminated in disruption of centromeric cohesion during meiotic prophase I with early prophase I arrest and apoptosis of both male and female germ cells (Hopkins et al., 2014). Therefore, studies in mice support the finding that this family (and others in which *STAG3* variants have been identified) has POI on the more severe end of the spectrum with diagnosis at a young age with primary amenorrhea, elevated FSH levels, and streak gonads on ultrasound consistent with a clinical picture of gonadal dysgenesis.

The second report of a *STAG3* variant identified in a family with POI was by Le Quesne Stabej et al. (2016) in a consanguineous Lebanese family with two affected sisters who presented with primary amenorrhea and absent pubertal development. Linkage analysis and WES found a homozygous 2 bp duplication (c.1947_48dupCT) which resulted in a transcript encoding a truncated protein in the *STAG3* gene. Furthermore, Colombo et al. (2017) reported on a consanguineous family of Asian origin with two sisters affected by POI. WES identified a C to G transversion at nucleotide c.677 (c.677C > G) in *STAG3*–both affected sisters were homozygous for this mutation which resulted in a premature stop codon and thus, predicted a truncated protein (p.[Ser227*]). Interestingly, the 87-year-old paternal grandmother and 48-year-old maternal aunt of the sisters were both carriers of this mutation and did not suffer from amenorrhea or infertility, though they did go through premature menopause at age 40 and 37 years old, respectively.

In addition, two sisters affected with POI from a Han Chinese family were found to have a homozygous donor splice site mutation in *STAG3* (c.1573 + 5G > A) which was predicted to result in a frameshift mutation and premature stop codon. The unaffected parents and brother in this family were heterozygous carriers for the mutation (He et al., 2018). Additionally, more recent reports have shown the impact of compound heterozygous *STAG3* variants on families with POI. Heddar et al. (2019) reported on two Caucasian sisters with non-syndromic POI. WES of the proband and unaffected mother identified two novel pathogenic variants including a 1 bp deletion in exon 28 of *STAG3* (c.305delC) which yielded a premature stop codon predicting a truncated protein. The second variant was a T to G substitution in exon 7 (c.659T > G) which led to a missense mutation. Interestingly, this variant was also identified in the unaffected mother who proceeded through menopause at age 51. Franca et al. (2019) identified two rare loss-of function variants in *STAG3* (c.291dupC and c1950C > A) leading to POI in a 21-year-old Brazilian woman. Compound heterozygosity for these variants was felt to be the mode of inheritance given the rarity of both variants and their impact on the transcript and protein; however, the affected patient was adopted and therefore parental DNA was not available to confirm this assumption.

Additional cohesin-ring components have also been implicated in human POI, specifically, SMC1β and REC8 (Bouilly et al., 2016). Bouilly et al. (2016) used multiplex sequencing technology to screen 100 patients with unexplained POI for 19 different candidate genes either known or suspected to play a role in POI pathogenesis. Four patients were identified to harbor variants in genes encoding cohesin-associated proteins. Three of these patients presented with primary amenorrhea and two of them were also siblings. These sisters were diagnosed with POI at age 14 and 17, respectively. They had inherited a *REC8* variant (c.641A > G; Q154R) from their mother and a variant in *GDF9* (c.1360C > T; R54C) from their father. Both variants were predicted to be damaging by the Polyphen2 database (prediction of functional effects of human nsSNPs), a tool which predicts the potential impact of amino acid changes on the structure and function of a protein. The other patient who presented with primary amenorrhea was diagnosed with POI at age 13 and was found to have a variant in *SMC1*β (c.3530A > T; Q1177L) as well

TABLE 1 | Human Cohesin Variants and Reproductive Phenotypes.

Gene	Location	Case(s)	Ethnicity	Reproductive Phenotype	Sequence Variation	Amino Acid Change	Mechanism	References
STAG3	Exons 8–34 omitted	4 affected sisters	Palestinian	PA[a], POI[b]	1bp deletion c.968delC	p.Phe187fs*7	Frameshift mutation and premature stop codon	Caburet et al., 2014
STAG3	Exons 19–32 omitted	2 affected sisters	Lebanese	PA, POI	2bp duplication c.1947_48dupCT	p.Tyr650Serfs*22	Frameshift mutation and premature stop codon	Le Quesne Stabej et al., 2016
STAG3	Skipped exon 15, out-of-frame fusion of exon 14–16	2 affected sisters	Han Chinese	PA, POI	Homozygous donor splice site mutation c.1573 + 5G > A	p.Leu490Thrfs*10	Aberrant splicing results in frameshift mutation and premature stop condon	He et al., 2018
STAG3	Exon 7	2 affected sisters	Asian	PA, POI	c.677C > G	p.Ser227*	Missense mutation and premature stop codon	Colombo et al., 2017
STAG3		1 affected woman	Brazilian	PA, POI	1bp duplication c.291dupC Nucleotide substitution c.1950C > A	p.Asn98Glnfs*2 p.Tyr650*	Frameshift mutation and premature stop codon Change Tyr to Premature stop codon	Franca et al., 2019
STAG3	Truncating mutation in exon 28 Exon 7 substitution	2 affected sisters	Caucasian	PA, POI	c.3052delC c.659T > G	p.Arg1018Aspfs*14 p.Leu220Arg	Frameshift mutation and premature stop codon	Heddar et al., 2019
STAG3	Protein lacks armadillo-type domain Exon 23	1 affected male	–	MA[c], NOA[d]	c.1762dupG c.2394 + IG > A	p.Ala588GlyfsTer9	Frameshift insertion and premature stop codon Splicing variant	Riera-Escamilla et al., 2019
STAG3	Exon 13	1 affected male	German	MA, NOA	c.1262T > G c.1312C > T	p.Leu421Arg p.Arg438Ter	Missense variant changes a conserved amino acid Nonsense substitution and premature stop codon	van der Bijl et al., 2019
STAG3	Splicing variant in intron 2 Frameshift deletion in exon 16	1 affected male	–	MA, NOA	g.100180673del c.1645_1657del	p.His549AlafsTer9	Splicing variant Frameshift deletion leads to premature stop codon at amino acid 558	Krausz et al., 2020
RAD21L				Maternal non-disjunction of Chromosome 21	rs450739		Missense	Chernus et al., 2019
RAD21L	Exon 10 Exon 14	NOA patients vs. fertile controls	Japanese	MA, SCOS[e], NOA	c.1268A > C c.1610G > A	p.His423Pro p.Ser537Asn	Non-synonomous substitutions	Minase et al., 2017
RAD21L	Removal of last 41 amino acids of the protein	1 affected male	–	MA, NOA	c.1543C > T;	p.Arg515Ter	Stopgain homozygous variant	Krausz et al., 2020
SMC1B		2 unrelated patients		SA[f], POI[g] PA, POI[h]	c.662T > C c.3530A > T	p.Ile221Thr p.Gln1177Leu		Bouilly et al., 2016
REC8		2 affected sisters		PA, POI[i]	c.461A > G c.899G > T	p.Gln154Arg p.Arg300Leu		Bouilly et al., 2016

[a] *PA: primary amenorrhea.*
[b] *POI: primary ovarian insufficiency.*
[c] *MA: meiotic arrest.*
[d] *NOA: non-obstructive azoospermia.*
[e] *SCOS: Sertoli cell-only syndrome.*
[f] *Secondary amenorrhea.*
[g] *This patient was also noted to have 2 variants in NOBOX.*
[h] *This patient was also noted to have variant in BMP15.*
[i] *These sisters were also noted to have variant in GDF9.*
**indicates translation stop.*

as *BMP15* (c.13A > C; S5R), both of which were predicted to be damaging by the Polyphen2 database. An additional *SMC1β* variant (c.662T > C; I221T) was identified in one patient with secondary amenorrhea and POI diagnosed at age 22, yet she was also found to have two variants in the oocyte-specific gene, NOBOX. The findings of these studies demonstrate that variants in genes encoding cohesin-associated proteins may play a role in POI pathogenesis. Moreover, digenic and perhaps polygenic inheritance likely plays a role in the timing of onset of POI as well. Future studies of patients with POI, and their evaluation for potential etiologies, may need to consider these candidate genes, and specifically *STAG3*, given multiple affected families across various ethnic backgrounds have been identified to harbor these variants.

Trisomies

The vast majority of meiotic errors detected in human pregnancies result from errors in female meiosis and are a leading cause of pregnancy loss (Hassold and Hunt, 2001; Nagaoka et al., 2012). Meiosis in females is prone to segregation errors such as non-disjunction of homologous chromosomes as well as PSSC resulting in aneuploidy, with trisomy being the most common aneuploidy. While all autosomal chromosomes are susceptible to missegregation (Handyside et al., 2012), most autosomal aneuploidy is not compatible with embryogenesis or implantation. Therefore, autosomal aneuploidy manifests clinically as infertility or subfertility, especially in women at advanced ages. Some pregnancies affected by trisomy can progress to later stages, but most commonly result in miscarriage. Trisomy 13, 18, or 21 can result in live births with children being affected by Patau Syndrome, Edwards Syndrome, or Down Syndrome, respectively. Of these, Trisomy 21 is the most common and the incidence has been increasing in recent decades, which is likely related to women having children later in the reproductive lifespan (Morris and Alberman, 2009; Loane et al., 2013). Given that Trisomy 21 is one of the few chromosomal aneuploidies which may survive to a live birth, studying families (parents and affected child) is a resource to further understand mechanisms of meiotic segregation errors in humans.

Regarding trisomy 21, both increased maternal age as well as altered recombination events, regardless of age, have been associated with meiotic errors (Lamb et al., 1997; Oliver et al., 2008; Ray et al., 2018). The absence of recombination or the presence of a single peri-telomeric recombination event on the long arm of chromosome 21 have been associated with errors during MI and appear to be age-independent, and thus, the more common etiology of trisomy 21 in younger women (Lamb et al., 1997; Oliver et al., 2008; Ray et al., 2018). Errors during MII are associated with increasing maternal age and a peri-centromeric recombinant event on chromosome 21 (Lamb et al., 1997; Oliver et al., 2008, 2012; Ray et al., 2018). This peri-centromeric recombination pattern may lead to a suboptimal configuration which could compromise proteins involved in centromeric cohesin, exacerbating the normal degradation of this complex with age. Alternatively, the peri-centromeric recombinant event may in fact stabilize the tetrad through MI, leading to enrichment in errors during MII in older oocytes (Oliver et al., 2008).

A recent study by Chernus et al. (2019) was undertaken to discover genetic variants which may increase the risk for maternal non-disjunction of chromosome 21 using a candidate gene approach as well as a genome-wide association study (GWAS). The study sample included 749 liveborn offspring with a free, maternally derived, trisomy 21, as well as their available biological parents (n = 1,437 parents). DNA samples were genotyped on the HumanOmniExpressExome-8v1-2 array. These genotypes were then used to determine (1) if the non-disjunction error was maternally derived and (2) if this occurred during MI or MII. Subgroup analyses of mothers vs. fathers, MI mothers vs. fathers, MII mothers vs. fathers, and MI mothers vs. MII mothers were performed. Given that defects in cohesin proteins may play a role in PSSC and aneuploidy, the authors chose to assess candidate genes for meiosis-specific cohesin [*SMC1β*, *REC8*, *RAD21L* (SNP rs450739), and *STAG3*] within the subgroup analyses. Of the analyzed genes involved in the meiotic cohesin complex in this GWAS, there was a statistically significant association with a missense variant in *RAD21L* in the all mothers vs. fathers (OR 0.67) and MI mothers vs. fathers (OR 0.67) subgroup analyses, suggesting variants in this gene may be a risk factor for non-disjunction, more commonly in MI. None of the other candidate genes for cohesin-associated proteins demonstrated significance.

RAD21L is a part of the cohesin complex, which is an important regulator of chromosome dynamics and structure during mitosis and meiosis. Gene disruption of *RAD21L* in male mice leads to infertility whereas in female mice there is apparent age-related infertility (Herran et al., 2011). Additionally, RAD21L has been associated with recombination in males, but less so in females (Kong et al., 2014). Therefore, disruption of *RAD21L* seems to have sexually dimorphic phenotypes–possibly playing a larger role in recombination events in males and potentially a role related to chromosome segregation in females. The *RAD21L* variant association with trisomy 21 seen by Chernus et al. (2019) was more commonly seen in maternal MI errors which would be consistent with prior studies relating errors during MI to aberrations of recombination (Lamb et al., 1997; Oliver et al., 2008; Ray et al., 2018). Interestingly, the *RAD21L* variant association was not significant for MII errors despite RAD21L being a member of the cohesin complex. We would have hypothesized seeing an association with MII errors given their association with maternal age. The authors noted, however, that their sample size was limited and they did not see any unique age-associated variants. Therefore, further studies are needed to investigate alternative genetic variants which may be associated with trisomy 21 as well as how they relate to the timing of the meiotic error and maternal age at conception.

COHESIN DEFECTS AND MALE REPRODUCTIVE PHENOTYPES

Non-obstructive Azoospermia

The most severe form of male factor infertility is non-obstructive azoospermia (NOA). This occurs in approximately 1% of men

of reproductive age (Tournaye et al., 2017). Approximately, 14% of those patients are found to have karyotype abnormalities (Van Assche et al., 1996) while approximately 8–10% have identified Y chromosome microdeletions [azoospermia factor (AZF) deletions] (Ferlin et al., 2007). When NOA is "idiopathic" the assumption is that there is likely a genetic factor involved that is yet to be determined. In recent years, sequencing approaches in families with members affected by azoospermia or severe oligospermia have identified candidate genes using a discovery-oriented approach. This method has not yet identified a cohesin-associated variant.

An alternative approach, utilizing information known from mouse models, has recently identified *STAG3* variants in a cohort of men with azoospermia. Riera-Escamilla et al. (2019) designed a "mouse azoospermia" gene panel consisting of 175 genes and subsequently analyzed those candidate genes via next-generation sequencing in a highly selected cohort of men with idiopathic NOA (n = 33). This cohort included 31 unrelated men and two brothers from a consanguineous family. After sequencing data was filtered, one patient was found to harbor two variants in *STAG3* (compound heterozygote). The *STAG3* variants included a frameshift insertion which generated a premature stop gain in the 597 amino acid; this is predicted to result in a protein lacking the entire armadillo-type domain of *STAG3* which is involved in DNA and protein interactions. The other *STAG3* variant identified was a novel splicing variant located on exon 23, an indispensable site for normal splicing. The patient's unaffected fertile brother was only a heterozygous carrier for the frameshift mutation. Upon histologic analysis of testis biopsies including immunohistochemistry, the authors concluded that meiotic entry occurred with normal frequency, however, meiosis was noted to arrest as there was evidence of DSB formation, but failure to complete chromosome pairing. Therefore, it appears that *STAG3* mutations in this patient resulted in complete bilateral meiotic arrest (MA) of spermatogenesis resulting in NOA.

In similar fashion, van der Bijl et al. (2019) took a candidate gene approach to assessing sequence variants in *STAG3* in a different cohort of men with idiopathic NOA with MA (n = 28). In this analysis, the full coding region of *STAG3* was sequenced directly. These authors identified two compound heterozygous variants in *STAG3* (c.1262T > G; 1312C > T) in exon 13 leading to complete bilateral MA in an otherwise healthy human male. The c.1262T > G variant was paternally inherited and is a missense variant that changes a highly conserved neutral amino acid (Leucine) to a basic amino acid (Arginine) likely affecting protein folding and post-translational modifications. This variant is predicted to be disease-causing by all utilized prediction programs. The c.1312C > T variant was maternally inherited and is a nonsense substitution which introduces a premature stop codon (p.Arg438Ter). The index patient had bilateral small testis volumes (12–13 mL) and normal testosterone levels. The most developed germ cell type in any seminiferous tubule was the primary spermatocyte and a microdissection testicular sperm extraction (microTESE) procedure did not yield any sperm from this patient. Analysis of meiotic chromosome spreads from the spermatocytes of the affected patient found that no meiotic cells progressed through the zygonema stage of meiotic prophase I, which is consistent with MA. Additionally, compound heterozygosity was confirmed by Sanger sequencing of the patient's parents. His brother inherited the c.1262T > G variant and spontaneously conceived two children.

In another recent study by Krausz et al. (2020) performed exome sequencing on 17 men with NOA due to MA who had a negative microTESE procedure. Interestingly, a plausible genetic cause of NOA was identified in 14 of these 17 patients. One patient with complete MA and normal sized testis was found to carry two novel heterozygous loss of function variants in *STAG3*– one splicing variant and one frameshift deletion in exon 16 which led to a premature stop codon at the 558th amino acid affecting the armadillo-type domain.

These studies are the first to demonstrate *STAG3* variants negatively impact protein function and lead to human male infertility due to MA. Similar to observations in females harboring variants in *STAG3* have been shown to be associated with POI as previously described. With further evidence of the important role of cohesin-associated *STAG3* in meiotic events in both males and females, consideration can be made for analysis of *STAG3* in men and women with otherwise "idiopathic" NOA or POI, respectively.

RAD21L is another meiosis-specific cohesin protein which interacts with structural maintenance of chromosome proteins SMC3 and SMC1α/β as well as STAG3 (Gutierrez-Caballero et al., 2011; Ishiguro et al., 2011; Lee and Hirano, 2011). *RAD21L* is transcribed abundantly in testis and localized to the lateral and axial elements of the synaptonemal complex playing an essential role in homologous chromosome synapsis during meiotic prophase I. Male mice deficient in *RAD21L* are defective in homologous chromosome synapsis which in turn leads to zygonema arrest and subsequent azoospermia with male sterility in mice (Herran et al., 2011). Interestingly, age-dependent sterility is seen in female mice lacking *RAD21L* (Gutierrez-Caballero et al., 2011; Herran et al., 2011).

In the study by Krausz et al. (2020) described above, one patient with NOA was noted to have a homozygous stop gain variant in *RAD21L* (c.1543C > T; p.Arg515Ter), which resulted in the removal of the final 41 amino acids of the protein. His fertile brother was found to be a heterozygous carrier. The affected patient had bilaterally small testis and histology demonstrated complete MA. In a targeted gene approach, Minase et al. (2017) evaluated the *RAD21L* coding region in a Japanese cohort with 38 men with NOA due to MA and 140 men with NOA due to Sertoli cell-only syndrome (SCOS) and compared these men to 200 fertile controls. The *RAD21L* coding region was sequenced, and three variants were found (c.454C > A; c.1268A > C; and c.1610G > A). The distribution of two of the variants (c.1268A > C, His423Pro; and c.1610G > A, Ser537Asn) was significantly different between the NOA patients with either MA or SCOS compared with the fertile controls. The authors postulated that these amino acid substitutions may play a role in disruption of spermatogenesis in Japanese patients, however, the function of the SNPs in those positions were predicted to be benign via the PolyPhen2 database. Therefore, the relationship

between these identified SNPs and a mechanistic cause of NOA has yet to be determined.

CANCER PREDISPOSITION AND COHESIN DEFECTS

In addition to its role in sister chromatid cohesion and chromosome segregation, cohesin has been implicated in genome stability owing to its role in DNA repair and recombination. DNA damage arises continuously by various endogenous and exogenous factors and cells must possess mechanisms to repair these lesions. One mechanism is via homologous recombination (HR). In this process, BRCA2 (BRCA2 DNA repair associated) and PALB2 (Partner and Localizer of BRCA2) are key regulators and promote RAD51 activity which is essential for HR. Failure to repair DNA properly may lead to cell apoptosis or cancer (Hoeijmakers, 2001; Prakash et al., 2015). Cohesin subunits have been demonstrated to undergo various mutations in cancer (Losada, 2014; Waldman, 2020). Somatic mutations in cohesin ring components have been observed in colorectal cancer (Sasaki et al., 2021), bladder cancer (Aquila et al., 2018), and hematologic malignancies and germline mutations in cohesin or its regulators are found in cohesinopathies (Horsfield et al., 2012; Cancer Genome Atlas Research Network et al., 2013).

The cohesin-associated protein PDS5B has been shown to be a mediator of homologous recombination *in vitro*. PDS5B associates with BRCA2 in early S-phase and depletion of PDS5B compromises the localization of both RAD51 and BRCA2 to the nucleus essentially disturbing HR and leading to increased cell sensitivity to DNA damaging agents (Brough et al., 2012). Based upon these findings, Couturier et al. (2016) sought to elucidate the role of PDS5B in HR and ovarian cancer prediction. In their analysis, tumor samples were obtained from chemotherapy naïve patients undergoing surgery for ovarian cancer between 1992 and 2012. The authors found that low levels of PDS5B expression correlated with improved survival in these patients. Similarly, Brough et al. (2012) assessed the expression of PDS5B in a panel of 160 invasive breast tumors and found that levels were associated with both histological grade of the breast cancer as well as outcome in patients treated with chemotherapy. In general, lower expression of PDS5B was associated with higher grade tumors and triple negative (estrogen receptor, progesterone receptor, Her2/Neu negative) tumors. Additionally, tumors with lower expression of PDS5B had a favorable response to chemotherapy.

Regarding the meiosis-specific cohesin components, loss of heterozygosity in *STAG3* has been noted in epithelial ovarian carcinomas (Notaridou et al., 2011). In the review of the literature outlined above for women with POI and associated *STAG3* variants, there was one patient noted to have bilateral ovarian tumors diagnosed at age 19 which consisted of a gonadoblastoma on the right ovary and a complex tumor of the left ovary consisting of embryonal carcinoma, choriocarcinoma, and dysgerminoma (Caburet et al., 2014). With this finding and the knowledge that cohesin plays a role in DNA repair and genome stability, additional investigation is needed to determine if women with POI related to cohesin defects are at risk for ovarian cancer and specifically, germ cell tumors.

COHESIN IMPACT ON AGING AND OVERALL HEALTH

As described above, loss or weakening of cohesin has been implicated in reproductive aging and aneuploidy. The end result of reproductive aging is POI/menopause in females or NOA in males and human genetic variants in cohesin-protein components have been implicated in both diagnoses. It is well characterized that POI/early menopause is associated with age-related diseases such as osteoporosis, cardiovascular disease (CVD), and all-cause mortality (Qiu et al., 2013; Tao et al., 2016; Quinn and Cedars, 2018). Regarding CVD pathogenesis, estrogen is felt to be cardioprotective due to effects on vascular endothelium (Mori et al., 2000; Chandrasekar et al., 2001), hence the increase in CVD risk in patients with early menopause. An alternative hypothesis is that premenopausal CVD may have effects on ovarian microvasculature predisposing to ovarian aging (Kok et al., 2006). A recent study by Wang et al. (2021) utilizing prospective data from the Nurses Health Study II found that spontaneous abortion (SAB) was associated with a greater risk of premature death, particularly from CVD. Whether or not SAB was related to microvascular changes or genetic changes was not determined, however, the authors postulated that SAB could be an early marker for future health risk in women, though the underlying mechanisms linking SAB with premature death from CVD still need to be elucidated. Therefore, the question remains if ovarian aging leads to CVD or if general aging in the individual patient is a common underlying risk factor for both CVD and ovarian aging (Cedars, 2013). For example, Hanson et al. (2020) studied young women with poor ovarian response to stimulation in assisted reproductive technology cycles and correlated oocyte yield with DNA methylation profiles in white blood cell (WBC) samples according to the "epigenetic clock" age prediction model (Horvath, 2013, 2015). Interestingly, the authors found that poor ovarian response was associated with epigenetic age acceleration in patient WBC samples.

More recent reports have also implicated male factor infertility in diseases of aging and mortality (Glazer et al., 2017; Francesco et al., 2021). Eisenberg (2016) and Eisenberg et al. (2016) reported that men with oligospermia and azoospermia have higher risks of incident diabetes, kidney disease, and ischemic heart disease in the years following their infertility evaluation. Additionally, men with infertility are at increased risk of various malignancies including testicular, prostate, bladder, and thyroid cancers; melanoma; and hematologic malignancies (Eisenberg et al., 2015). A recent systematic review by Francesco et al. (2021), found that infertile men (as compared to fertile men) have an increased risk of death, with the highest risk being associated with azoospermia.

An underlying link connecting male and female infertility with overall health and lifespan remains uncertain due to the multifactorial pathogenesis of infertility and aging as well as heterogeneity of the literature. However, the use of

infertility, specifically the most extreme versions including POI in females and NOA in males, may provide a biomarker for further counseling on genetic implications for current attempts at conception as well as the future health of patients and their offspring.

CONCLUSION AND PROSPECTS

Expansion of genetic testing within clinical medicine, and specifically reproductive medicine, may offer additional insight into previously unknown etiologies of disease. Specifically focusing on cohesin protein-related genes may inform the diagnosis of disorders contributing to gamete exhaustion in females, as well as infertility and reproductive aging in both men and women. The regulation of cohesin loading and removal requires the coordination of various kinases and phosphatases and further studies are needed to gain a better understanding of these mechanisms. Given that protein kinases are an emerging class of drug targets, identification of genetic defects in cohesin-related genes or regulators may serve as potential targets for future therapeutic studies of reproductive aging.

AUTHOR CONTRIBUTIONS

RB, MS, and MB-E collected the references and wrote the manuscript. All authors contributed to the article and approved the submitted version.

FUNDING

This study was supported by Eunice Kennedy Shriver National Institute of Child Health and Human Development (R00HD090289) and the Magee Auxiliary Research Scholar (MARS) endowment.

REFERENCES

Albamonte, M. I., Albamonte, M. S., Bou-Khair, R. M., Zuccardi, L., and Vitullo, A. D. (2019). The ovarian germinal reserve and apoptosis-related proteins in the infant and adolescent human ovary. *J. Ovarian Res.* 12:22.

Almanzar, D. E., Gordon, S. G., and Rog, O. (2021). Meiotic sister chromatid exchanges are rare in *C. elegans*. *Curr. Biol.* 31, 1499–1507.e3.

American College of Obstetricians and Gynecologists Committee on Gynecologic Practice and Practice Committee (2014). Female age-related fertility decline. Committee Opinion No. 589. *Fertil. Steril.* 101, 633–634. doi: 10.1016/j.fertnstert.2013.12.032

Anderson, R. A., Mitchell, R. T., Kelsey, T. W., Spears, N., Telfer, E. E., and Wallace, W. H. (2015). Cancer treatment and gonadal function: experimental and established strategies for fertility preservation in children and young adults. *Lancet Diabetes Endocrinol.* 3, 556–567. doi: 10.1016/s2213-8587(15)00039-x

Aquila, L., Ohm, J., and Woloszynska-Read, A. (2018). The role of STAG2 in bladder cancer. *Pharmacol. Res.* 131, 143–149. doi: 10.1016/j.phrs.2018.02.025

Balasch, J., and Gratacos, E. (2012). Delayed childbearing: effects on fertility and the outcome of pregnancy. *Curr. Opin. Obstet. Gynecol.* 24, 187–193. doi: 10.1097/gco.0b013e3283517908

Bolcun-Filas, E., and Handel, M. A. (2018). Meiosis: the chromosomal foundation of reproduction. *Biol. Reprod.* 99, 112–126. doi: 10.1093/biolre/ioy021

Bouilly, J., Beau, I., Barraud, S., Bernard, V., Azibi, K., Fagart, J., et al. (2016). Identification of multiple gene mutations accounts for a new genetic architecture of primary ovarian insufficiency. *J. Clin. Endocrinol. Metab.* 101, 4541–4550. doi: 10.1210/jc.2016-2152

Brieno-Enriquez, M. A., Moak, S. L., Toledo, M., Filter, J. J., Gray, S., Barbero, J. L., et al. (2016). Cohesin removal along the chromosome arms during the first meiotic division depends on a NEK1-PP1gamma-WAPL axis in the mouse. *Cell Rep.* 17, 977–986. doi: 10.1016/j.celrep.2016.09.059

Brough, R., Bajrami, I., Vatcheva, R., Natrajan, R., Reis-Filho, J. S., Lord, C. J., et al. (2012). APRIN is a cell cycle specific BRCA2-interacting protein required for genome integrity and a predictor of outcome after chemotherapy in breast cancer. *EMBO J.* 31, 1160–1176. doi: 10.1038/emboj.2011.490

Buheitel, J., and Stemmann, O. (2013). Prophase pathway-dependent removal of cohesin from human chromosomes requires opening of the Smc3-Scc1 gate. *EMBO J.* 32, 666–676. doi: 10.1038/emboj.2013.7

Buonomo, S. B., Clyne, R. K., Fuchs, J., Loidl, J., Uhlmann, F., and Nasmyth, K. (2000). Disjunction of homologous chromosomes in meiosis I depends on proteolytic cleavage of the meiotic cohesin Rec8 by separin. *Cell* 103, 387–398. doi: 10.1016/s0092-8674(00)00131-8

Burkhardt, S., Borsos, M., Szydlowska, A., Godwin, J., Williams, S. A., Cohen, P. E., et al. (2016). Chromosome cohesion established by Rec8-cohesin in fetal oocytes is maintained without detectable turnover in oocytes arrested for months in mice. *Curr. Biol.* 26, 678–685. doi: 10.1016/j.cub.2015.12.073

Caburet, S., Arboleda, V. A., Llano, E., Overbeek, P. A., Barbero, J. L., Oka, K., et al. (2014). Mutant cohesin in premature ovarian failure. *N. Engl. J. Med.* 370, 943–949. doi: 10.1056/nejmoa1309635

Cahoon, C. K., and Hawley, R. S. (2016). Regulating the construction and demolition of the synaptonemal complex. *Nat. Struct. Mol. Biol.* 23, 369–377. doi: 10.1038/nsmb.3208

Cahoon, C. K., Helm, J. M., and Libuda, D. E. (2019). Synaptonemal complex central region proteins promote localization of pro-crossover factors to recombination events during *Caenorhabditis elegans* Meiosis. *Genetics* 213, 395–409. doi: 10.1534/genetics.119.302625

Cancer Genome Atlas Research Network, Ley, T. J., Miller, C., Ding, L., Raphael, B. J., Mungall, A. J., et al. (2013). Genomic and epigenomic landscapes of adult de novo acute myeloid leukemia. *N. Engl. J. Med.* 368, 2059–2074. doi: 10.1056/nejmoa1301689

Carretero, M., Ruiz-Torres, M., Rodriguez-Corsino, M., Barthelemy, I., and Losada, A. (2013). Pds5B is required for cohesion establishment and Aurora B accumulation at centromeres. *EMBO J.* 32, 2938–2949. doi: 10.1038/emboj.2013.230

Cedars, M. I. (2013). Biomarkers of ovarian reserve–do they predict somatic aging? *Semin. Reprod. Med.* 31, 443–451. doi: 10.1055/s-0033-1356480

Challa, K., Shinohara, M., and Shinohara, A. (2019). Meiotic prophase-like pathway for cleavage-independent removal of cohesin for chromosome morphogenesis. *Curr. Genet.* 65, 817–827. doi: 10.1007/s00294-019-00959-x

Chandrasekar, B., Nattel, S., and Tanguay, J. F. (2001). Coronary artery endothelial protection after local delivery of 17beta-estradiol during balloon angioplasty in a porcine model: a potential new pharmacologic approach to improve endothelial function. *J. Am. Coll. Cardiol.* 38, 1570–1576. doi: 10.1016/s0735-1097(01)01552-2

Chernus, J. M., Allen, E. G., Zeng, Z., Hoffman, E. R., Hassold, T. J., Feingold, E., et al. (2019). A candidate gene analysis and GWAS for genes associated with maternal nondisjunction of chromosome 21. *PLoS Genet.* 15:e1008414. doi: 10.1371/journal.pgen.1008414

Chiang, T., Duncan, F. E., Schindler, K., Schultz, R. M., and Lampson, M. A. (2010). Evidence that weakened centromere cohesion is a leading cause of age-related aneuploidy in oocytes. *Curr. Biol.* 20, 1522–1528. doi: 10.1016/j.cub.2010.06.069

Chiang, T., Schultz, R. M., and Lampson, M. A. (2011). Age-dependent susceptibility of chromosome cohesion to premature separase activation in mouse oocytes. *Biol. Reprod.* 85, 1279–1283. doi: 10.1095/biolreprod.111.094094

Colombo, R., Pontoglio, A., and Bini, M. (2017). A STAG3 missense mutation in two sisters with primary ovarian insufficiency. *Eur. J. Obstet. Gynecol. Reprod. Biol.* 216, 269–271. doi: 10.1016/j.ejogrb.2017.08.005

Couturier, A. M., Fleury, H., Patenaude, A. M., Bentley, V. L., Rodrigue, A., Coulombe, Y., et al. (2016). Roles for APRIN (PDS5B) in homologous recombination and in ovarian cancer prediction. *Nucleic Acids Res.* 44, 10879–10897. doi: 10.1093/nar/gkw921

Crawley, O., Barroso, C., Testori, S., Ferrandiz, N., Silva, N., Castellano-Pozo, M., et al. (2016). Cohesin-interacting protein WAPL-1 regulates meiotic chromosome structure and cohesion by antagonizing specific cohesin complexes. *Elife* 5:e10851.

Dietrich, A. J., van Marle, J., Heyting, C., and Vink, A. C. (1992). Ultrastructural evidence for a triple structure of the lateral element of the synaptonemal complex. *J. Struct. Biol.* 109, 196–200. doi: 10.1016/1047-8477(92)90031-5

Edson, M. A., Nagaraja, A. K., and Matzuk, M. M. (2009). The mammalian ovary from genesis to revelation. *Endocr. Rev.* 30, 624–712. doi: 10.1210/er.2009-0012

Eisenberg, M. L. (2016). Risks beyond reproduction for infertile men. *Fertil. Steril.* 105, 300–301. doi: 10.1016/j.fertnstert.2015.11.040

Eisenberg, M. L., Li, S., Brooks, J. D., Cullen, M. R., and Baker, L. C. (2015). Increased risk of cancer in infertile men: analysis of U.S. claims data. *J. Urol.* 193, 1596–1601. doi: 10.1016/j.juro.2014.11.080

Eisenberg, M. L., Li, S., Cullen, M. R., and Baker, L. C. (2016). Increased risk of incident chronic medical conditions in infertile men: analysis of United States claims data. *Fertil. Steril.* 105, 629–636. doi: 10.1016/j.fertnstert.2015.11.011

Ferlin, A., Arredi, B., Speltra, E., Cazzadore, C., Selice, R., Garolla, A., et al. (2007). Molecular and clinical characterization of Y chromosome microdeletions in infertile men: a 10-year experience in Italy. *J. Clin. Endocrinol. Metab.* 92, 762–770. doi: 10.1210/jc.2006-1981

Forabosco, A., and Sforza, C. (2007). Establishment of ovarian reserve: a quantitative morphometric study of the developing human ovary. *Fertil. Steril.* 88, 675–683. doi: 10.1016/j.fertnstert.2006.11.191

Franca, M. M., Nishi, M. Y., Funari, M. F. A., Lerario, A. M., Baracat, E. C., Hayashida, S. A. Y., et al. (2019). Two rare loss-of-function variants in the STAG3 gene leading to primary ovarian insufficiency. *Eur. J. Med. Genet.* 62, 186–189. doi: 10.1016/j.ejmg.2018.07.008

Francesco, D. G., Alex, M. K., Tony, C., Ettore, B., Maria, B. G., Alessandro, S., et al. (2021). The association between mortality and male infertility: systematic review and meta-analysis. *Urology* S0090-4295(21)00287-9. doi: 10.1016/j.urology.2021.02.041

Fraune, J., Schramm, S., Alsheimer, M., and Benavente, R. (2012). The mammalian synaptonemal complex: protein components, assembly and role in meiotic recombination. *Exp. Cell Res.* 318, 1340–1346. doi: 10.1016/j.yexcr.2012.02.018

Gao, J., and Colaiacovo, M. P. (2018). Zipping and unzipping: protein modifications regulating synaptonemal complex dynamics. *Trends Genet.* 34, 232–245. doi: 10.1016/j.tig.2017.12.001

Garcia-Cruz, R., Casanovas, A., Brieno-Enriquez, M., Robles, P., Roig, I., Pujol, A., et al. (2010). Cytogenetic analyses of human oocytes provide new data on non-disjunction mechanisms and the origin of trisomy 16. *Hum. Reprod.* 25, 179–191. doi: 10.1093/humrep/dep347

Garcia-Muse, T., Galindo-Diaz, U., Garcia-Rubio, M., Martin, J. S., Polanowska, J., O'Reilly, N., et al. (2019). A meiotic checkpoint alters repair partner bias to permit inter-sister repair of persistent DSBs. *Cell Rep.* 26, 775–787.e5.

Glazer, C. H., Bonde, J. P., Eisenberg, M. L., Giwercman, A., Haervig, K. K., Rimborg, S., et al. (2017). Male infertility and risk of nonmalignant chronic diseases: a systematic review of the epidemiological evidence. *Semin. Reprod. Med.* 35, 282–290. doi: 10.1055/s-0037-1603568

Gray, S., and Cohen, P. E. (2016). Control of meiotic crossovers: from double-strand break formation to designation. *Annu. Rev. Genet.* 50, 175–210. doi: 10.1146/annurev-genet-120215-035111

Grive, K. J. (2020). Pathways coordinating oocyte attrition and abundance during mammalian ovarian reserve establishment. *Mol. Reprod. Dev.* 87, 843–856. doi: 10.1002/mrd.23401

Gruhn, J. R., Zielinska, A. P., Shukla, V., Blanshard, R., Capalbo, A., Cimadomo, D., et al. (2019). Chromosome errors in human eggs shape natural fertility over reproductive life span. *Science* 365, 1466–1469. doi: 10.1126/science.aav7321

Gutierrez-Caballero, C., Herran, Y., Sanchez-Martin, M., Suja, J. A., Barbero, J. L., Llano, E., et al. (2011). Identification and molecular characterization of the mammalian alpha-kleisin RAD21L. *Cell Cycle* 10, 1477–1487. doi: 10.4161/cc.10.9.15515

Haarhuis, J. H., Elbatsh, A. M., and Rowland, B. D. (2014). Cohesin and its regulation: on the logic of X-shaped chromosomes. *Dev Cell* 31, 7–18. doi: 10.1016/j.devcel.2014.09.010

Handel, M. A., and Schimenti, J. C. (2010). Genetics of mammalian meiosis: regulation, dynamics and impact on fertility. *Nat. Rev. Genet.* 11, 124–136. doi: 10.1038/nrg2723

Handyside, A. H., Montag, M., Magli, M. C., Repping, S., Harper, J., Schmutzler, A., et al. (2012). Multiple meiotic errors caused by predivision of chromatids in women of advanced maternal age undergoing in vitro fertilisation. *Eur. J. Hum. Genet.* 20, 742–747. doi: 10.1038/ejhg.2011.272

Hanson, B. M., Tao, X., Zhan, Y., Jenkins, T. G., Morin, S. J., Scott, R. T., et al. (2020). Young women with poor ovarian response exhibit epigenetic age acceleration based on evaluation of white blood cells using a DNA methylation-derived age prediction model. *Hum. Reprod.* 35, 2579–2588. doi: 10.1093/humrep/deaa206

Hassold, T., and Hunt, P. (2001). To err (meiotically) is human: the genesis of human aneuploidy. *Nat. Rev. Genet.* 2, 280–291. doi: 10.1038/35066065

Hassold, T., Maylor-Hagen, H., Wood, A., Gruhn, J., Hoffmann, E., Broman, K. W., et al. (2021). Failure to recombine is a common feature of human oogenesis. *Am. J. Hum. Genet.* 108, 16–24. doi: 10.1016/j.ajhg.2020.11.010

He, W. B., Banerjee, S., Meng, L. L., Du, J., Gong, F., Huang, H., et al. (2018). Whole-exome sequencing identifies a homozygous donor splice-site mutation in STAG3 that causes primary ovarian insufficiency. *Clin. Genet.* 93, 340–344. doi: 10.1111/cge.13034

Heddar, A., Dessen, P., Flatters, D., and Misrahi, M. (2019). Novel STAG3 mutations in a Caucasian family with primary ovarian insufficiency. *Mol. Genet. Genomics* 294, 1527–1534. doi: 10.1007/s00438-019-01594-4

Herbert, M., Kalleas, D., Cooney, D., Lamb, M., and Lister, L. (2015). Meiosis and maternal aging: insights from aneuploid oocytes and trisomy births. *Cold Spring Harb. Perspect. Biol.* 7:a017970. doi: 10.1101/cshperspect.a017970

Herran, Y., Gutierrez-Caballero, C., Sanchez-Martin, M., Hernandez, T., Viera, A., Barbero, J. L., et al. (2011). The cohesin subunit RAD21L functions in meiotic synapsis and exhibits sexual dimorphism in fertility. *EMBO J.* 30, 3091–3105. doi: 10.1038/emboj.2011.222

Hirano, T. (2015). Chromosome dynamics during mitosis. *Cold Spring Harb. Perspect. Biol.* 7:a015792. doi: 10.1101/cshperspect.a015792

Hoeijmakers, J. H. (2001). Genome maintenance mechanisms for preventing cancer. *Nature* 411, 366–374. doi: 10.1038/35077232

Hoekman, E. J., Knoester, D., Peters, A. A. W., Jansen, F. W., de Kroon, C. D., and Hilders, C. (2018). Ovarian survival after pelvic radiation: transposition until the age of 35 years. *Arch. Gynecol. Obstet.* 298, 1001–1007. doi: 10.1007/s00404-018-4883-5

Holloway, J. K., and Cohen, P. E. (2015). "Mammalian meiosis," in *Knobil and Neill's Physiology of Reproduction*, Vol. 1, eds T. M. Plant and A. J. Zeleznik (Boston, MA: Academic Press), 5–57. doi: 10.1016/b978-0-12-397175-3.00001-6

Hopkins, J., Hwang, G., Jacob, J., Sapp, N., Bedigian, R., Oka, K., et al. (2014). Meiosis-specific cohesin component, Stag3 is essential for maintaining centromere chromatid cohesion, and required for DNA repair and synapsis between homologous chromosomes. *PLoS Genet.* 10:e1004413. doi: 10.1371/journal.pgen.1004413

Horsfield, J. A., Print, C. G., and Monnich, M. (2012). Diverse developmental disorders from the one ring: distinct molecular pathways underlie the cohesinopathies. *Front. Genet.* 3:171. doi: 10.3389/fgene.2012.00171

Horvath, S. (2013). DNA methylation age of human tissues and cell types. *Genome Biol.* 14:R115.

Horvath, S. (2015). Erratum to: DNA methylation age of human tissues and cell types. *Genome Biol.* 16, 96.

Hunter, N. (2015). Meiotic recombination: the essence of heredity. *Cold Spring Harb. Perspect. Biol.* 7:a016618. doi: 10.1101/cshperspect.a016618

Ishiguro, K. I. (2019). The cohesin complex in mammalian meiosis. *Genes Cells* 24, 6–30. doi: 10.1111/gtc.12652

Ishiguro, K., Kim, J., Fujiyama-Nakamura, S., Kato, S., and Watanabe, Y. (2011). A new meiosis-specific cohesin complex implicated in the cohesin code for homologous pairing. *EMBO Rep.* 12, 267–275. doi: 10.1038/embor.2011.2

Ishiguro, T., Tanaka, K., Sakuno, T., and Watanabe, Y. (2010). Shugoshin-PP2A counteracts casein-kinase-1-dependent cleavage of Rec8 by separase. *Nat. Cell Biol.* 12, 500–U201.

Jessberger, R. (2012). Age-related aneuploidy through cohesion exhaustion. *EMBO Rep.* 13, 539–546. doi: 10.1038/embor.2012.54

Katis, V. L., Lipp, J. J., Imre, R., Bogdanova, A., Okaz, E., Habermann, B., et al. (2010). Rec8 Phosphorylation by casein kinase 1 and Cdc7-Dbf4 kinase regulates cohesin cleavage by separase during meiosis. *Dev. Cell* 18, 397–409. doi: 10.1016/j.devcel.2010.01.014

Kavanaugh, M. L., Pliskin, E., and Jerman, J. (2021). Use of concurrent multiple methods of contraception in the United States, 2008 to 2015. *Contracept X* 3:100060. doi: 10.1016/j.conx.2021.100060

Keeney, S. (2008). Spo11 and the formation of DNA double-strand breaks in meiosis. *Genome Dyn. Stab.* 2, 81–123. doi: 10.1007/7050_2007_026

Keeney, S., and Kleckner, N. (1995). Covalent protein-DNA complexes at the 5' strand termini of meiosis-specific double-strand breaks in yeast. *Proc. Natl. Acad. Sci. U.S.A.* 92, 11274–11278. doi: 10.1073/pnas.92.24.11274

Kitajima, T. S., Miyazaki, Y., Yamamoto, M., and Watanabe, Y. (2003). Rec8 cleavage by separase is required for meiotic nuclear divisions in fission yeast. *EMBO J.* 22, 5643–5653. doi: 10.1093/emboj/cdg527

Kitajima, T. S., Sakuno, T., Ishiguro, K., Iemura, S., Natsume, T., Kawashima, S. A., et al. (2006). Shugoshin collaborates with protein phosphatase 2A to protect cohesin. *Nature* 441, 46–52. doi: 10.1038/nature04663

Kok, H. S., van Asselt, K. M., van der Schouw, Y. T., van der Tweel, I., Peeters, P. H., Wilson, P. W., et al. (2006). Heart disease risk determines menopausal age rather than the reverse. *J. Am. Coll. Cardiol.* 47, 1976–1983. doi: 10.1016/j.jacc.2005.12.066

Kong, A., Thorleifsson, G., Frigge, M. L., Masson, G., Gudbjartsson, D. F., Villemoes, R., et al. (2014). Common and low-frequency variants associated with genome-wide recombination rate. *Nat. Genet.* 46, 11–16. doi: 10.1038/ng.2833

Kort, J. D., Eisenberg, M. L., Millheiser, L. S., and Westphal, L. M. (2014). Fertility issues in cancer survivorship. *CA Cancer J. Clin.* 64, 118–134. doi: 10.3322/caac.21205

Krausz, C., Riera-Escamilla, A., Moreno-Mendoza, D., Holleman, K., Cioppi, F., Algaba, F., et al. (2020). Genetic dissection of spermatogenic arrest through exome analysis: clinical implications for the management of azoospermic men. *Genet. Med.* 22, 1956–1966. doi: 10.1038/s41436-020-0907-1

Kudo, N. R., Anger, M., Peters, A. H. F. M., Stemmann, O., Theussl, H. C., Helmhart, W., et al. (2009). Role of cleavage by separase of the Rec8 kleisin subunit of cohesin during mammalian meiosis I. *J. Cell Sci.* 122, 2686–2698. doi: 10.1242/jcs.035287

Lamb, N. E., Feingold, E., Savage, A., Avramopoulos, D., Freeman, S., Gu, Y., et al. (1997). Characterization of susceptible chiasma configurations that increase the risk for maternal nondisjunction of chromosome 21. *Hum. Mol. Genet.* 6, 1391–1399. doi: 10.1093/hmg/6.9.1391

Le Quesne Stabej, P., Williams, H. J., James, C., Tekman, M., Stanescu, H. C., Kleta, R., et al. (2016). STAG3 truncating variant as the cause of primary ovarian insufficiency. *Eur. J. Hum. Genet.* 24, 135–138. doi: 10.1038/ejhg.2015.107

Lee, J., and Hirano, T. (2011). RAD21L, a novel cohesin subunit implicated in linking homologous chromosomes in mammalian meiosis. *J. Cell Biol.* 192, 263–276. doi: 10.1083/jcb.201008005

Lee, J., Kitajima, T. S., Tanno, Y., Yoshida, K., Morita, T., Miyano, T., et al. (2008). Unified mode of centromeric protection by shugoshin in mammalian oocytes and somatic cells. *Nat. Cell Biol.* 10, 42–52. doi: 10.1038/ncb1667

Li, J., Qian, W. P., and Sun, Q. Y. (2019). Cyclins regulating oocyte meiotic cell cycle progressiondagger. *Biol. Reprod.* 101, 878–881. doi: 10.1093/biolre/ioz143

Lister, L. M., Kouznetsova, A., Hyslop, L. A., Kalleas, D., Pace, S. L., Barel, J. C., et al. (2010). Age-related meiotic segregation errors in mammalian oocytes are preceded by depletion of cohesin and Sgo2. *Curr. Biol.* 20, 1511–1521. doi: 10.1016/j.cub.2010.08.023

Loane, M., Morris, J. K., Addor, M. C., Arriola, L., Budd, J., Doray, B., et al. (2013). Twenty-year trends in the prevalence of Down syndrome and other trisomies in Europe: impact of maternal age and prenatal screening. *Eur. J. Hum. Genet.* 21, 27–33. doi: 10.1038/ejhg.2012.94

Losada, A. (2014). Cohesin in cancer: chromosome segregation and beyond. *Nat. Rev. Cancer* 14, 389–393. doi: 10.1038/nrc3743

Losada, A., Hirano, M., and Hirano, T. (2002). Cohesin release is required for sister chromatid resolution, but not for condensin-mediated compaction, at the onset of mitosis. *Genes Dev.* 16, 3004–3016. doi: 10.1101/gad.249202

Mac Dougall, K., Beyene, Y., and Nachtigall, R. D. (2013). Age shock: misperceptions of the impact of age on fertility before and after IVF in women who conceived after age 40. *Hum. Reprod.* 28, 350–356. doi: 10.1093/humrep/des409

Mamsen, L. S., Brochner, C. B., Byskov, A. G., and Mollgard, K. (2012). The migration and loss of human primordial germ stem cells from the hind gut epithelium towards the gonadal ridge. *Int. J. Dev. Biol.* 56, 771–778. doi: 10.1387/ijdb.120202lm

Massy, B. (2016). Meiosis: to pair and recombine, a sophisticated chromosome dance. *Semin. Cell Dev. Biol.* 54, 104–105. doi: 10.1016/j.semcdb.2016.04.016

Matthews, T. J., and Hamilton, B. E. (2014). First births to older women continue to rise. *NCHS Data Brief.* 152, 1–8.

McGee, E. A., and Hsueh, A. J. (2000). Initial and cyclic recruitment of ovarian follicles. *Endocr. Rev.* 21, 200–214. doi: 10.1210/er.21.2.200

McNicoll, F., Stevense, M., and Jessberger, R. (2013). Cohesin in gametogenesis. *Curr. Top. Dev. Biol.* 102, 1–34. doi: 10.1016/b978-0-12-416024-8.00001-5

Mehlmann, L. M. (2005). Stops and starts in mammalian oocytes: recent advances in understanding the regulation of meiotic arrest and oocyte maturation. *Reproduction* 130, 791–799. doi: 10.1530/rep.1.00793

Mehlmann, L. M., Jones, T. L., and Jaffe, L. A. (2002). Meiotic arrest in the mouse follicle maintained by a Gs protein in the oocyte. *Science* 297, 1343–1345. doi: 10.1126/science.1073978

Minase, G., Miyamoto, T., Miyagawa, Y., Iijima, M., Ueda, H., Saijo, Y., et al. (2017). Single-nucleotide polymorphisms in the human RAD21L gene may be a genetic risk factor for Japanese patients with azoospermia caused by meiotic arrest and Sertoli cell-only syndrome. *Hum. Fertil. (Camb.)* 20, 217–220. doi: 10.1080/14647273.2017.1292004

Mori, T., Durand, J., Chen, Y., Thompson, J. A., Bakir, S., and Oparil, S. (2000). Effects of short-term estrogen treatment on the neointimal response to balloon injury of rat carotid artery. *Am. J. Cardiol.* 85, 1276–1279. doi: 10.1016/s0002-9149(00)00748-7

Morris, J. K., and Alberman, E. (2009). Trends in Down's syndrome live births and antenatal diagnoses in England and Wales from 1989 to 2008: analysis of data from the National Down syndrome cytogenetic register. *BMJ* 339:b3794. doi: 10.1136/bmj.b3794

Motta, P. M., Makabe, S., and Nottola, S. A. (1997). The ultrastructure of human reproduction. I. The natural history of the female germ cell: origin, migration and differentiation inside the developing ovary. *Hum. Reprod. Update* 3, 281–295. doi: 10.1093/humupd/3.3.281

Nagaoka, S. I., Hassold, T. J., and Hunt, P. A. (2012). Human aneuploidy: mechanisms and new insights into an age-old problem. *Nat. Rev. Genet.* 13, 493–504. doi: 10.1038/nrg3245

Nasmyth, K., and Haering, C. H. (2009). Cohesin: its roles and mechanisms. *Annu. Rev. Genet.* 43, 525–558. doi: 10.1146/annurev-genet-102108-134233

Nelson, L. M. (2009). Clinical practice. Primary ovarian insufficiency. *N. Engl. J. Med.* 360, 606–614.

Nishiyama, T., Ladurner, R., Schmitz, J., Kreidl, E., Schleiffer, A., Bhaskara, V., et al. (2010). Sororin mediates sister chromatid cohesion by antagonizing Wapl. *Cell* 143, 737–749. doi: 10.1016/j.cell.2010.10.031

Nishiyama, T., Sykora, M. M., Huis in 't Veld, P. J., Mechtler, K., and Peters, J. M. (2013). Aurora B and Cdk1 mediate Wapl activation and release of acetylated cohesin from chromosomes by phosphorylating Sororin. *Proc. Natl. Acad. Sci. U.S.A.* 110, 13404–13409. doi: 10.1073/pnas.1305020110

Norris, R. P., Freudzon, M., Nikolaev, V. O., and Jaffe, L. A. (2010). Epidermal growth factor receptor kinase activity is required for gap junction closure and for part of the decrease in ovarian follicle cGMP in response to LH. *Reproduction* 140, 655–662. doi: 10.1530/rep-10-0288

Notaridou, M., Quaye, L., Dafou, D., Jones, C., Song, H., Hogdall, E., et al. (2011). Common alleles in candidate susceptibility genes associated with risk and development of epithelial ovarian cancer. *Int. J. Cancer* 128, 2063–2074.

Oliver, T. R., Feingold, E., Yu, K., Cheung, V., Tinker, S., Yadav-Shah, M., et al. (2008). New insights into human nondisjunction of chromosome 21 in oocytes. *PLoS Genet.* 4:e1000033. doi: 10.1371/journal.pgen.1000033

Oliver, T. R., Tinker, S. W., Allen, E. G., Hollis, N., Locke, A. E., Bean, L. J., et al. (2012). Altered patterns of multiple recombinant events are associated with nondisjunction of chromosome 21. *Hum Genet* 131, 1039–1046. doi: 10.1007/s00439-011-1121-7

Ottolini, C. S., Newnham, L., Capalbo, A., Natesan, S. A., Joshi, H. A., Cimadomo, D., et al. (2015). Genome-wide maps of recombination and chromosome segregation in human oocytes and embryos show selection for maternal recombination rates. *Nat. Genet.* 47, 727–735. doi: 10.1038/ng.3306

Page, S. L., and Hawley, R. S. (2004). The genetics and molecular biology of the synaptonemal complex. *Annu. Rev. Cell Dev. Biol.* 20, 525–558. doi: 10.1146/annurev.cellbio.19.111301.155141

Pellestor, F., Andreo, B., Arnal, F., Humeau, C., and Demaille, J. (2003). Maternal aging and chromosomal abnormalities: new data drawn from in vitro unfertilized human oocytes. *Hum. Genet.* 112, 195–203. doi: 10.1007/s00439-002-0852-x

Pereda, J., Zorn, T., and Soto-Suazo, M. (2006). Migration of human and mouse primordial germ cells and colonization of the developing ovary: an ultrastructural and cytochemical study. *Microsc. Res. Tech.* 69, 386–395. doi: 10.1002/jemt.20298

Pereira, C., Smolka, M. B., Weiss, R. S., and Brieno-Enriquez, M. A. (2020). ATR signaling in mammalian meiosis: from upstream scaffolds to downstream signaling. *Environ. Mol. Mutagen.* 61, 752–766. doi: 10.1002/em.22401

Petronczki, M., Siomos, M. F., and Nasmyth, K. (2003). Un menage a quatre: the molecular biology of chromosome segregation in meiosis. *Cell* 112, 423–440. doi: 10.1016/s0092-8674(03)00083-7

Practice Committee of the American Society for Reproductive Medicine (2020). Definitions of infertility and recurrent pregnancy loss: a committee opinion. *Fertil. Steril.* 113, 533–535. doi: 10.1016/j.fertnstert.2019.11.025

Prakash, R., Zhang, Y., Feng, W., and Jasin, M. (2015). Homologous recombination and human health: the roles of BRCA1, BRCA2, and associated proteins. *Cold Spring Harb. Perspect. Biol.* 7:a016600. doi: 10.1101/cshperspect.a016600

Qiu, C., Chen, H., Wen, J., Zhu, P., Lin, F., Huang, B., et al. (2013). Associations between age at menarche and menopause with cardiovascular disease, diabetes, and osteoporosis in Chinese women. *J. Clin. Endocrinol. Metab.* 98, 1612–1621. doi: 10.1210/jc.2012-2919

Quinn, M. M., and Cedars, M. I. (2018). Cardiovascular health and ovarian aging. *Fertil. Steril.* 110, 790–793. doi: 10.1016/j.fertnstert.2018.07.1152

Ray, A., Oliver, T. R., Halder, P., Pal, U., Sarkar, S., Dutta, S., et al. (2018). Risk of Down syndrome birth: consanguineous marriage is associated with maternal meiosis-II nondisjunction at younger age and without any detectable recombination error. *Am. J. Med. Genet. A* 176, 2342–2349. doi: 10.1002/ajmg.a.40511

Revenkova, E., Herrmann, K., Adelfalk, C., and Jessberger, R. (2010). Oocyte cohesin expression restricted to predictyate stages provides full fertility and prevents aneuploidy. *Curr. Biol.* 20, 1529–1533. doi: 10.1016/j.cub.2010.08.024

Riedel, C. G., Katis, V. L., Katou, Y., Mori, S., Itoh, T., Helmhart, W., et al. (2006). Protein phosphatase 2A protects centromeric sister chromatid cohesion during meiosis I. *Nature* 441, 53–61. doi: 10.1038/nature04664

Riera-Escamilla, A., Enguita-Marruedo, A., Moreno-Mendoza, D., Chianese, C., Sleddens-Linkels, E., Contini, E., et al. (2019). Sequencing of a 'mouse azoospermia' gene panel in azoospermic men: identification of RNF212 and STAG3 mutations as novel genetic causes of meiotic arrest. *Hum. Reprod.* 34, 978–988. doi: 10.1093/humrep/dez042

Robert, T., Nore, A., Brun, C., Maffre, C., Crimi, B., Bourbon, H. M., et al. (2016). The TopoVIB-like protein family is required for meiotic DNA double-strand break formation. *Science* 351, 943–949. doi: 10.1126/science.aad5309

Sasaki, M., Miyoshi, N., Fujino, S., Saso, K., Ogino, T., Takahashi, H., et al. (2021). The meiosis-specific cohesin component stromal antigen 3 promotes cell migration and chemotherapeutic resistance in colorectal cancer. *Cancer Lett.* 497, 112–122. doi: 10.1016/j.canlet.2020.10.006

Shintomi, K., and Hirano, T. (2009). Releasing cohesin from chromosome arms in early mitosis: opposing actions of Wapl-Pds5 and Sgo1. *Genes Dev.* 23, 2224–2236. doi: 10.1101/gad.1844309

Simoni, M. K., Mu, L., and Collins, S. C. (2017). Women's career priority is associated with attitudes towards family planning and ethical acceptance of reproductive technologies. *Hum. Reprod.* 32, 2069–2075. doi: 10.1093/humrep/dex275

Steiner, A. Z., and Jukic, A. M. (2016). Impact of female age and nulligravidity on fecundity in an older reproductive age cohort. *Fertil. Steril.* 105, 1584–1588.e1.

Svetlanov, A., and Cohen, P. E. (2004). Mismatch repair proteins, meiosis, and mice: understanding the complexities of mammalian meiosis. *Exp. Cell Res.* 296, 71–79. doi: 10.1016/j.yexcr.2004.03.020

Tao, X. Y., Zuo, A. Z., Wang, J. Q., and Tao, F. B. (2016). Effect of primary ovarian insufficiency and early natural menopause on mortality: a meta-analysis. *Climacteric* 19, 27–36. doi: 10.3109/13697137.2015.1094784

Tedeschi, A., Wutz, G., Huet, S., Jaritz, M., Wuensche, A., Schirghuber, E. I, et al. (2013). Wapl is an essential regulator of chromatin structure and chromosome segregation. *Nature* 501, 564–568. doi: 10.1038/nature12471

Toraason, E., Horacek, A., Clark, C., Glover, M. L., Adler, V. L., Premkumar, T., et al. (2021). Meiotic DNA break repair can utilize homolog-independent chromatid templates in *C. elegans*. *Curr. Biol.* 31, 1508–1514.e5.

Tournaye, H., Krausz, C., and Oates, R. D. (2017). Novel concepts in the aetiology of male reproductive impairment. *Lancet Diabetes Endocrinol.* 5, 544–553. doi: 10.1016/s2213-8587(16)30040-7

Van Assche, E., Bonduelle, M., Tournaye, H., Joris, H., Verheyen, G., Devroey, P., et al. (1996). Cytogenetics of infertile men. *Hum. Reprod.* 11(Suppl 4), 1–24; discussion 25–26.

van der Bijl, N., Ropke, A., Biswas, U., Woste, M., Jessberger, R., Kliesch, S., et al. (2019). Mutations in the stromal antigen 3 (STAG3) gene cause male infertility due to meiotic arrest. *Hum. Reprod.* 34, 2112–2119.

Verni, F., Gandhi, R., Goldberg, M. L., and Gatti, M. (2000). Genetic and molecular analysis of wings apart-like (wapl), a gene controlling heterochromatin organization in Drosophila melanogaster. *Genetics* 154, 1693–1710. doi: 10.1093/genetics/154.4.1693

Waizenegger, I. C., Hauf, S., Meinke, A., and Peters, J. M. (2000). Two distinct pathways remove mammalian cohesin from chromosome arms in prophase and from centromeres in anaphase. *Cell* 103, 399–410. doi: 10.1016/s0092-8674(00)00132-x

Waldman, T. (2020). Emerging themes in cohesin cancer biology. *Nat. Rev. Cancer* 20, 504–515. doi: 10.1038/s41568-020-0270-1

Wang, S., Hassold, T., Hunt, P., White, M. A., Zickler, D., Kleckner, N., et al. (2017). Inefficient crossover maturation underlies elevated aneuploidy in human female meiosis. *Cell* 168, 977–989.e17.

Wang, Y. X., Minguez-Alarcon, L., Gaskins, A. J., Missmer, S. A., Rich-Edwards, J. W., Manson, J. E., et al. (2021). Association of spontaneous abortion with all cause and cause specific premature mortality: prospective cohort study. *BMJ* 372:n530. doi: 10.1136/bmj.n530

Wassmann, K. (2013). Sister chromatid segregation in meiosis II: deprotection through phosphorylation. *Cell Cycle* 12, 1352–1359. doi: 10.4161/cc.24600

Wolf, P. G., Cuba Ramos, A., Kenzel, J., Neumann, B., and Stemmann, O. (2018). Studying meiotic cohesin in somatic cells reveals that Rec8-containing cohesin requires Stag3 to function and is regulated by Wapl and sororin. *J. Cell Sci.* 131:jcs212100.

Xu, Z., Cetin, B., Anger, M., Cho, U. S., Helmhart, W., Nasmyth, K., et al. (2009). Structure and function of the PP2A-shugoshin interaction. *Mol. Cell* 35, 426–441. doi: 10.1016/j.molcel.2009.06.031

Zickler, D., and Kleckner, N. (1999). Meiotic chromosomes: integrating structure and function. *Annu. Rev. Genet.* 33, 603–754. doi: 10.1146/annurev.genet.33.1.603

Zickler, D., and Kleckner, N. (2015). Recombination, pairing, and synapsis of homologs during meiosis. *Cold Spring Harb. Perspect. Biol.* 7:a016626. doi: 10.1101/cshperspect.a016626

Conflict of Interest: The authors declare that the research was conducted in the absence of any commercial or financial relationships that could be construed as a potential conflict of interest.

Publisher's Note: All claims expressed in this article are solely those of the authors and do not necessarily represent those of their affiliated organizations, or those of the publisher, the editors and the reviewers. Any product that may be evaluated in this article, or claim that may be made by its manufacturer, is not guaranteed or endorsed by the publisher.

frontiers in Cell and Developmental Biology

ORIGINAL RESEARCH
published: 04 August 2021
doi: 10.3389/fcell.2021.695333

Aging Negatively Impacts DNA Repair and Bivalent Formation in the *C. elegans* Germ Line

*Marilina Raices[1], Richard Bowman[2], Sarit Smolikove[2] and Judith L. Yanowitz[1,3]**

[1] Department of Obstetrics, Gynecology and Reproductive Sciences, Magee-Womens Research Institute, University of Pittsburgh School of Medicine, Pittsburgh, PA, United States, [2] Department of Biology, The University of Iowa, Iowa City, IA, United States, [3] Department of Developmental Biology, Microbiology and Molecular Genetics, Hillman Cancer Center, University of Pittsburgh School of Medicine, Pittsburgh, PA, United States

Defects in crossover (CO) formation during meiosis are a leading cause of birth defects, embryonic lethality, and infertility. In a wide range of species, maternal aging increases aneuploidy and decreases oocyte quality. In *C. elegans* which produce oocytes throughout the first half of adulthood, aging both decreases oocytes quality and increases meiotic errors. Phenotypes of mutations in genes encoding double-strand break (DSB)-associated proteins get more severe with maternal age suggesting that early meiosis reflects a particularly sensitive node during reproductive aging in the worm. We observed that aging has a direct effect on the integrity of *C. elegans* meiotic CO formation, as observed by an increase of univalent chromosomes and fusions at diakinesis, with a considerable increase starting at 4 days. We also characterize the possible causes for the age-related changes in CO formation by analyzing both steady-state levels and kinetics of the ssDNA binding proteins RPA-1 and RAD-51. Profound reductions in numbers of both RPA-1 and RAD-51 foci suggests that both DSB formation and early meiotic repair are compromised in aging worms. Using laser microirradiation and γ-irradiation to induce exogenous damage, we show specifically that recruitment of these homologous recombination proteins is altered. Repair defects can be seen in two-and-one-half day-old adults making the loss of germline repair capacity among the earliest aging phenotypes in the worm.

Keywords: DSB repair, *C. elegans*, germline, RAD51, RPA, aging, meiosis

OPEN ACCESS

Edited by:
Michael Klutstein, Hebrew University of Jerusalem, Israel

Reviewed by:
Alexander Lorenz, University of Aberdeen, United Kingdom
Verena Jantsch, Max F. Perutz Laboratories GmbH, Austria

***Correspondence:**
Judith L. Yanowitz
yanowitzjl@mwri.magee.edu

Specialty section:
This article was submitted to Cellular Biochemistry, a section of the journal Frontiers in Cell and Developmental Biology

Received: *14 April 2021*
Accepted: *12 July 2021*
Published: *04 August 2021*

Citation:
Raices M, Bowman R, Smolikove S and Yanowitz JL (2021) Aging Negatively Impacts DNA Repair and Bivalent Formation in the C. elegans Germ Line. Front. Cell Dev. Biol. 9:695333. doi: 10.3389/fcell.2021.695333

INTRODUCTION

It has been shown that maternal age negatively impacts fertility across species. Particularly in humans, female reproductive capacity declines dramatically after the mid-30 s making it the earliest age-related decline that humans experience (Hassold and Hunt, 2001). A major cause of this reproductive decline is the increasing incidence of oocytes with chromosomal abnormalities, which leads to miscarriage and congenital defects. As more women opt to have children later in life, addressing the issue of female reproductive aging has become increasingly important. Recently, the nematode *Caenorhabditis elegans* has been developed as a model to study reproductive capacity decline with age (Hughes et al., 2007; Andux and Ellis, 2008; Luo et al., 2010; Quesada-Candela et al., 2021).

During meiosis, crossovers (COs), the physical exchange of genetic material between homologs, together with the action of cohesin proteins, ensure proper alignment and segregation of the chromosomes at meiosis I. Across species, age-related loss of cohesin is associated with increased chromosomal non-disjunction (Hodges et al., 2005; Subramanian and Bickel, 2008). In addition, specific CO configurations, specifically those with too few, too many, or misplaced COs (near centromeres and telomeres), are acutely sensitive to maternal age, although they can be segregated appropriately in younger animals (Hodges et al., 2005; Lamb et al., 2005). Historically, numerous studies documented changes in recombination rates in response to external factors, including maternal age (for example, Stern, 1926; Rose and Baillie, 1979; Hussin et al., 2011). As more chromosome-wide techniques have evolved, changes in crossover positioning have also been reported (Lim et al., 2008; Saini et al., 2020). Nevertheless, our understanding of the factors that drive these age-related changes in CO distribution and frequency is still limited.

In species which produce oocytes throughout adult life, defects in DSB induction and CO repair may further impair oocyte quality in older animals. COs are induced by the formation of meiotic double-strand breaks (DSBs) which are repaired by homologous recombination (HR) with specializations for meiosis. DSBs are induced by the evolutionarily conserved topoisomerase VI-like Spo11 (Keeney et al., 1997) in concert with accessory factors that influence the timing, placement, and extent of break formation. Endonucleolytic cleavage by the MRX/N complex releases Spo11 bound to short oligonucleotides and generates 3′ single-stranded DNA (ssDNA) tails (Neale et al., 2005) that are rapidly resected and bound by the ssDNA binding protein complex RPA, protecting them from degradation. RPA is replaced by RAD51 and/or DMC1 which form (Gasior et al., 1998) filaments then can invade the homologous double stranded-DNA of either the sister chromatid or homologous chromosome. This single end-invasion can go on to form double Holliday Junctions (dHJ) (Shinohara et al., 1992; Sung, 1994), a subset of which are resolved to form COs (Schwacha and Kleckner, 1995). COs, together with cohesion, connect the homologous chromosomes, enabling their biorientation toward opposite spindle poles in metaphase I (reviewed in Sansam and Pezza, 2015).

The events of meiosis are tightly regulated to ensure both that each chromosome attains a crossover and that excessive DSBs are repaired and not passed along to offspring. Accordingly, non-HR pathways can step to repair DSBs if HR is ineffective. These include the classical non-homologous end joining (cNHEJ) pathway, microhomology-mediated end jointing (MMEJ), and single-strand annealing (SSA) (Macaisne et al., 2018). In *C. elegans,* DSB-promoting factors HIM-5 and CEP-1/p53 actively repress NHEJ functions allowing preferential use of HR (Mateo et al., 2016), intimating that alternative pathways can be available for DSB repair in early meiosis and are not simply late-acting salvage pathways that eliminate residual breaks.

Aging has a direct effect on the integrity of *C. elegans* meiotic CO formation as an increase in achiasmate chromosomes at diakinesis was observed at day 5 of adulthood, half-way through the worm's reproductive span (Luo et al., 2010; Meneely et al., 2012; Stamper et al., 2013; Achache et al., 2020). Also, it has been reported that maternal age exacerbates CO defects associated with mutations in SPO-11 accessory factors including *dsb-2* and *him-5* (Meneely et al., 2012; Stamper et al., 2013). This suggests that either the DSB break formation or repair machineries (or both) might be inherently sensitive to maternal age. However, the underlying cause(s) of this aging phenotype is not understood. In this study we tested the hypotheses that DSB formation and repair are impaired in aging. We analyzed the effect of maternal age on the recruitment of different HR proteins. To address this, we utilized two irradiation techniques (laser microirradiation and γ-irradiation) to induce exogenous damage in meiotic nuclei of young and aged worms (Harrell et al., 2018; Koury et al., 2018; Mahadevan et al., 2019). We observed that the total numbers of RPA-1 and RAD-51 foci were reduced by maternal age which results from both a decrease in HR-proficient DSBs and attenuated capability to recruit RPA-1 and RAD-51.

MATERIALS AND METHODS

Strains and Genetics

All strains were derived from the wild-type Bristol strain N2 and were cultivated at 20°C under standard conditions. Abbreviated names and full genotypes of the strains used in this study are listed in **Table 1**.

Chromosome Morphology Analysis of Diakinesis Oocytes

The numbers of DNA bodies present in diakinesis oocytes were assessed in intact adult hermaphrodites at days 1 through 10 of adulthood. Animals were picked as L4 larval and transferred each day until the cessation of egg-laying. Adults were fixed in Carnoy's fixative solution (60% ethanol, 30% chloroform, and 10% glacial acetic acid) and stained with 4′,6-diamidino-2-phenylindole (DAPI) (10 mg/ml stock diluted 1:50,000 in 1X Phosphate-buffered saline (PBS) for 15 min. in a humidity chamber. Stain was removed and worms were mounted in Prolong Gold with DAPI, cured overnight at room temperature, and stored at 4°C prior to imaging on a Nikon A1r confocal microscope. Diakinesis images were procured as 0.2μm per plain Z-stacks and visualized using Volocity 3-D Imaging Software (PerkinElmer Corp, now owned by QuorumTechnologies).

Immunostaining and Analysis of RAD-51 Foci

Gonads were dissected from 1-1 and 4-days adults in 1X sperm salts (50 mM PIPES pH 7.0, 25 mM KCl, 1 mM $MgSO_4$, 45 mM NaCl, and 2 mM $CaCl_2$) with 1 mM levamisole and fixed in 1% paraformaldehyde diluted in 1X sperm salts for 5 min in a humid chamber. Slides were then frozen on a metal block on dry ice for at least 10 min prior to flicking off the cover slip and immersing in methanol at −20° C for 2 min followed by 5 s in acetone at 4°C. Slides were then washed in PBSTB [1XPBS with 0.1% Tween and 0.1% bovine serum albumin (BSA)], and incubated

TABLE 1 | *C. elegans* stocks used in this study.

Stock name	Genotype	Abbreviated name in manuscript
N2	*C. elegans* var Bristol (N2).	Wild type
VC531	*rad-54(ok615) VhT2 [bli-4(e937) let-?(q782) qIs48]* (I;III)	*rad-54*
SSM476	*rpa-1(iow92[OLLAS::rpa-1])* II	*OLLAS::rpa-1*
SSM473	*iowSi8[pie-1p::gfp1-10::him-3 3UTR + Cbr-unc119(+)], rpa-1(iow89[gfp11::rpa-1])* II*; unc-119(ed3)**	*gfp::rpa-1*
QP1118	*mels8[unc-119(+) pie-1*^{promoter}*::gfp::cosa-1]* II	*gfp-1::cosa-1*
SSM639	*iowSi8[pie-1p::gfp1-10::him-3 3UTR + Cbr-unc119(+)], rpa-1(iow89[gfp11::rpa-1])* II*; unc-119(ed3)* III*;; spo-11(ok79)* IV*/nT1 [unc-?(n754) let-?]* (IV;V)	*gfp::rpa-1; spo-11*
QP1266	*mels8[unc-119(+) pie-1*^{promoter}*::gfp::cosa-1]* II*; spo-11(me44)* IV*/nT1 [unc-?(n754) let-? qIs50]* (IV;V)*	*gfp::cosa-1; spo-11*
TG2228	*polq-1(tm2026)* III	*polq-1*
FX1524	*cku-70(tm1524)* III	*cku-70*
AV106	*spo-11(ok79)* IV*/nT1 [unc-?(n754) let-?]* (IV;V)	*spo-11*

**The unc-119 gene is used as a selection marker for the transgenes. Prior studies of the cosa-1 strain suggest it does not appear to interfere with crossover formation (Yokoo et al., 2012).*

overnight at 4°C with primary antibody: rabbit anti-RAD-51 generated against peptide ASRQKKSDQEQRAA by Genscript for the Smolikove lab (Alleva et al., 2019), 1:30,000 in PBSTB). The next day, slides were washed 3X in PBSTB for 10 min and incubated with secondary antibody (goat anti-rabbit Alexa 568, 1:2,000 in PBSTB) for 2 h at room temperature in the dark. Slides were then washed 2 X 10 min in PBSTB, and 1 X 10 min with DAPI (10 mg/ml stock diluted 1:50,000 in 1X PBS). Slides were mounted in Prolong Gold with DAPI and put in the dark to cure overnight before imaging.

Three-dimensional (3D) images of the whole germ lines were taken using a Nikon A1r confocal microscope with 0.2 μm step size and analyzed using Volocity 3D software (PerkinElmer). For wild-type worms, we divided the leptotene, zygotene, and pachytene regions into six zones and counted RAD-51 foci in every nucleus for a minimum of three germ lines/age. For *rad-54* mutants, we counted RAD-51 foci in late pachytene nuclei for at least three germ lines/age. For irradiated worms, 15 mid-pachytene nuclei were analyzed.

Analysis of RPA-1 Foci

Gonads of *gfp::rpa-1; spo-11* worms were dissected from 1– to 4-days adults in M9 with 1 mM levamisole. Slides were then freeze-cracked and immersed in cold 100% EtOH for 2 min followed by 20 min in 4% paraformaldehyde/M9 in a humidity chamber. Slides were then washed in PBSTB 1×10 min, incubated with DAPI 1×10 min and washed again. After a quick dry, slides were mounted in Prolong Gold with DAPI.

Analysis of GFP::COSA-1 Foci

gfp::cosa-1 and irradiated *gfp::cosa-1; spo-11* worms were dissected in 1X sperm salts as described above. Slides were immediately freeze-cracked and immersed in 100% cold ethanol for 1 min, and fixed in 4% paraformaldehyde/1X sperm salts again for 10 min. Slides were washed 2X10 min in PBSTB, stained with DAPI in 1XPBS for 10 min followed by one wash with PBSTB for 10 min. Slides were mounted in Prolong Gold with DAPI. Images were acquired and analyzed as described above. GFP::COSA-1 foci in late pachytene nuclei (4 rows of nuclei before diplotene) were counted in at least five germ lines/age.

Western Blotting

For each age, 300 worms were transferred into a glass conical tube and washed thrice with 1X M9 buffer (22 mM KH_2PO_4, 42 mM Na_2HPO_4, 85.5 mM NaCl, 1 mM $MgSO_4$). The remaining liquid was removed, and the worm pellet was transferred to a 1.5 ml tube and flash frozen in liquid nitrogen. Pellets were thawed on ice, mixed with an equal volume of Laemmli Sample Buffer (Bio-Rad #161-0737) with 5% b-mercaptoethanol (Amresco M131), sonicated in a water bath for 2 min, heated at 95°C for 10 min, then spun in a tabletop centrifuge for 5 min at maximum speed. Samples were resolved by 12% PAGE (TGX FastCast, Bio-Rad) and transferred to nitrocellulose in 20% ethanol. The membrane was blocked in 5% non-fat milk/TBST (50 mM Tris-HCl pH 7.4, 150 mM NaCl, and 0.1%Tween-20) for 1 h at RT and incubated in OLLAS-tag antibody, pAb, rabbit (GenScript, A01658, 1μg/ml in 5% milk/TBST) or mouse α-E7 (tubulin, Developmental Studies Hybridoma Bank, 1:2,000 in 5% milk/TBST) ON at 4°C. The next day the membranes were washed in TBST and incubated in α-rabbit-HRP or α-mouse-HRP (1:2,000 in 5% milk/TBST) for 2 h at room temperature. Products were visualized by enhanced chemiluminescence (ECL) according to the manufacturer's instructions.

γ-Irradiation

1– and 4– days adult worms were exposed to 10Gy of γ-irradiation using a ^{137}Cs source (Gammacell1000 Elite; Nordion International). RAD-51 immunostaining was performed as described above on gonads dissected and fixed at 25 min, 4 and 8 h post-IR. RPA-1 detection was assessed at 25 min and 4 h post-IR and GFP::COSA-1 analysis were performed at 8 h post-IR.

Laser Microirradiation, Live Imaging, and Fixation

We followed the protocol outlined in Harrell et al. (2018) with the following modifications: for the live imaging experiments, five worms were imaged at a time at 2 min intervals for 45 min. Z stacks of 10 images at 1μm stages were taken at each interval. For the fixed sample experiments five worms were placed on a

live imaging slide, microirradiated, recovered to an NGM plate until each specified time point, then placed in M9 on frosted microscope slides. The M9 was removed and the worms were fixed in 100% EtOH and mounted with VectaShield.

Endogenous RPA-1 Intensity Measurements

gfp::rpa-1 adult worms were grown to 1, 2, 3, and 4 days old. Their gonads were dissected on charged slides, frozen at −80°C, and placed in −20°C EtOH for 1 min then mounted with 10 μl M9-DAPI and VectaShield. Whole intact gonads were imaged on the DeltaVision wide-field fluorescence microscope (GE Lifesciences) in seven 512 × 512 pixel zones with 100x/1.4 NA oil Olympus objective from the proximal pre-meiotic tip to the distal late pachytene phase of prophase I. Each image was the center slice of the nuclei in the upper section of the syncytial tube in both the DAPI (blue) and FITC (GFP) fluorescent channels. Measurement of the intensity of each nucleus was taken in FIJI in each zone in the FITC channel and corrected to cytoplasmic background.

Counting Recruitment Regions

Recruitment regions were counted in FIJI by visual inspection of each Z-slice of each time interval. A recruitment region was determined to be in response to microirradiation if it appeared in a location that did not contain a localization of RPA-1 fluorescence in the initial control image. Clusters were differentiated from foci when more than one distinct point of fluorescence was present but not separate from each other.

Statistical Analyses

All statistics were performed using GraphPad Prism 9. For all pairwise comparisons presented, the Mann-Whitney *U*-test was performed. For all binary data comparisons, the Fisher's Exact test of independence was used.

Ethics Statement

No studies in this paper required approval by institutional review boards.

RESULTS

Aging Increases Meiotic Defects in *C. elegans*

Multiple lines of evidence indicate that fertility in *C. elegans* declines with maternal age (Hughes et al., 2007; Luo et al., 2010). In both unmated and mated hermaphrodites, days 4–5 of adulthood marks a decline in reproductive capacity that is accelerated in the unmated animals due to lack of sperm (Luo et al., 2010). This timepoint is marked by increases in both inviable eggs and male offspring (Hughes et al., 2007; Luo et al., 2010) which can both be explained by the concomitant increase in CO errors seen in diakinesis oocytes. In order to determine when CO defects are first observed, we analyzed the integrity of chromosomes in N2 diakinesis nuclei throughout adulthood. In young adult animals (day 1), six bivalents were detected at diakinesis by fluorescence microscopy, corresponding to the six pairs of homologous chromosomes each held together by a chiasma (**Figures 1A,B**). A small fraction of nuclei (4%) showed 4 bivalents and 1 larger mass of DNA (**Figure 1D**), a configuration that arises in repair mutants and corresponds to a chromosomal fusion (Martin et al., 2005) but may result from two closely apposed chromosomes (for simplicity, we refer to these as fusions). Since *C. elegans* chromosomes are holocentric, fusion chromosomes would be stably transmitted during meiosis and the subsequent mitotic embryonic divisions, explaining the near 100% hatching rates of eggs. The small fraction of fusions was maintained in 2- and 3-days-old adults. However, after this timepoint, nuclei with five bivalents and two univalents were also apparent, indicating that one pair of chromosomes failed to achieve a CO. As the worms aged, meiotic defects worsened. In 4-day-old adults, ∼15% of the analyzed diakinesis showed nuclei with achiasmate chromosomes and ∼14% exhibited fusions. Since day 4 of adulthood corresponds to the time when meiotic errors increase substantially (**Figure 1A**) and when egg production begins to decrease (Hughes et al., 2007; Luo et al., 2010), we chose this timepoint as the "aged worms" for the remainder of the experiments described herein.

After day 4, meiotic errors continue to increase until reproductive senescence sets in at day 10. Curiously, older animals (>6-days-old) showed some irregular bivalents where the homologous chromosomes appeared to a be separating from one another (**Figure 1C**). Similar separating bivalents were recently reported for aged worms grown at 25°C, and the distinct univalent masses each contained the crossover marker, COSA-1 (Achache et al., 2020). At timepoints after egg-laying has ceased, days 10 and day 13, there remain a surprisingly large fraction of diakinesis oocytes with 6 DAPI bodies meaning that chromosomal abnormalities are not driving reproductive senescence.

To corroborate the impact of age on CO formation, we also examined GFP::COSA-1 foci, a cytological marker of CO commitment (Yokoo et al., 2012). As shown in **Figure 1D**, in 1 day-old adults, 5–6 COSA-1 foci are seen in the last 4 rows of nuclei prior to diplotene, consistent with prior studies (Yokoo et al., 2012; Machovina et al., 2016; Woglar and Villeneuve, 2018). By contrast, in day 4 adults, nearly 20% of nuclei had only 3 or 4 COSA-1 foci indicative of an impairment in CO formation. This decrease in COSA-1 foci could result from the combined effects of fewer DSBs, altered repair kinetics, as well as impaired recruitment of CO designation and commitment factors. Overall, these data support the conclusion that fewer COs are observed in older animals.

The Levels of Homologous Recombination Competent Double-Strand Breaks Decrease With Maternal Age

The increase in univalent (non-CO chromosomes) with maternal age could be explained by the decrease of meiotic-specific DSB

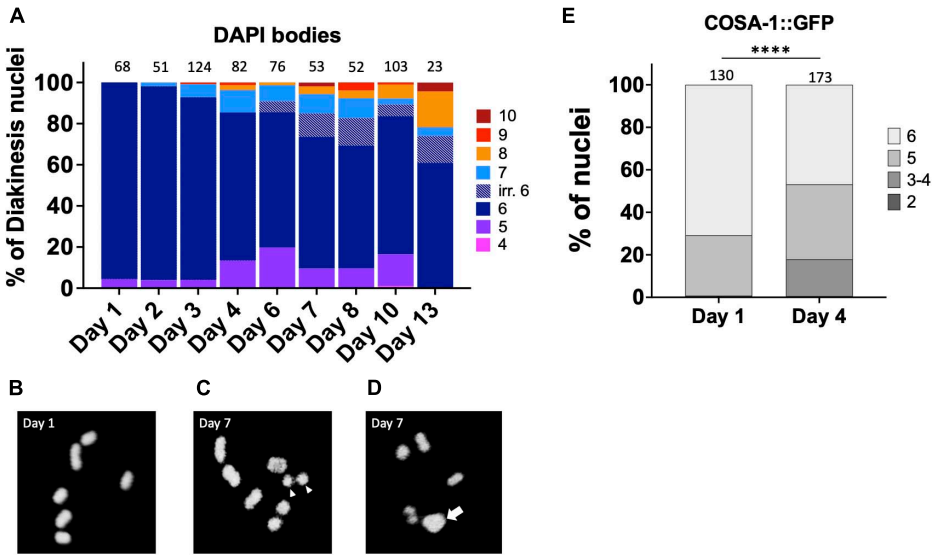

FIGURE 1 | Chiasmata formation is compromised in aging germ lines. Crossover formation is assessed by the number of DAPI-staining bodies at diakinesis. **(A)** Quantification of DAPI-bodies in N2 diakinesis nuclei from the indicated ages. **(B–D)** Representative DAPI-stained images of young **(B)** and aged **(C,D)** N2 worms showing bivalents (day 1), "separated bivalents" (arrowheads) and fusion (arrow). **(E)** Percent of late pachytene-stage nuclei containing the indicated number of COSA-1 foci in *gfp::cosa-1* worms. Numbers on top of bars indicate the total number of nuclei analyzed per age. Statistical significance was determined using Chi-square test. ****$p < 0.0001$.

formation. Therefore, to determine if DSB formation is itself age-sensitive, we took advantage of RAD-51 immunostaining which marks early intermediates of homologous recombination repair, forming foci. Prior studies had shown that greater than 95% of meiotic DSBs can be marked with RAD-51 (Mets and Meyer, 2009). In day 1 adults, we observed the RAD-51 localization pattern expected for wild type *C. elegans* meiosis: RAD-51 foci began to appear during leptotene/zygotene, became numerous by mid- pachytene, and disappeared by late pachytene (**Figures 2A,B**), indicative of efficient DSB repair (Alpi et al., 2003; Mateo et al., 2016). On day 4 of adulthood, the same relative pattern was observed, although the total number of foci was reduced in each region of the early prophase germ line (**Figure 2B**). This was seen most strikingly by the increase in the number of nuclei in the mid-pachytene regions that have zero RAD-51 and the decrease in nuclei with > 6 RAD-51 foci. A decrease in steady-state RAD-51 levels was also reported (Achache et al., 2020). In *spo-11* mutant animals where meiotic DSBs are not made, few to no breaks are seen in Day 1 animals whereas a single RAD-51 focus can be seen in up to half of pachytene nuclei (**Supplementary Figure 1**), suggesting that if anything, the RAD-51 observed in wild-type 4 day-old adults is an over-representation of meiotically-induced breaks. These results suggest either that DSB numbers decrease with age, or that DNA repair kinetics change with age, or both.

Because DSBs are not made simultaneously and because RAD-51 is removed from the break sites as DSBs mature into COs, a static snapshot of the germ line cannot report the total number of DSBs that are made and undergo CO recombination. To assess total DSB numbers, we took advantage of the *rad-54* mutant in which HR is stalled at a step after the recruitment of RAD-51 to resected DSBs, effectively trapping RAD-51 at all of the sites undergoing HR repair (Meneely et al., 2012). Consistent with prior studies, we observed that nearly 50% of day 1 nuclei accumulated between 20 and 40 RAD-51 foci, more than enough DSBs to ensure a CO on each chromosome (**Figure 2C**). In contrast, on day 4 of adulthood, > 95% of the nuclei analyzed showed fewer than 20 RAD-51 foci, indicating that the total number of HR-competent breaks decreased with maternal age (**Figure 2C**). We previously showed that the *him-5(ok1896)* null mutant which fails to achieve COs on the X chromosome contains an average of 9.9 RAD-51 foci/nucleus (Meneely et al., 2012). By inference, the nuclei in older animals with fewer than 10 foci are likely to experience deficits in CO formation.

Homologous Recombination Is Less Efficient in Older Adult Germ Cells

Since the studies above suggest that DSB levels are decreased in older animals and/or may be repaired by non-HR mechanisms, we wanted to directly analyze HR efficiency in meiotic germ cells. To do this, we took advantage of a previously reported assay to examine repair kinetics after γ-radiation (IR)-induced DSBs (Li and Yanowitz, 2019). Post-IR, we assayed the dynamics of RPA-1 and RAD-51. RPA-1 is the ssDNA-binding protein that is the first to coat the resected DNA (Caldwell and Spies, 2020). Importantly, RPA-1 levels do not decrease with maternal age (**Supplementary Figure 2B**). Like RAD-51, RPA-1 is observed as chromatin-associated foci in fixed samples. These studies were performed in the *spo-11* mutant background to eliminate the signal from endogenous meiotic breaks. Previous work determined that 10Gy IR is able to produce ∼20 DSBs per meiotic

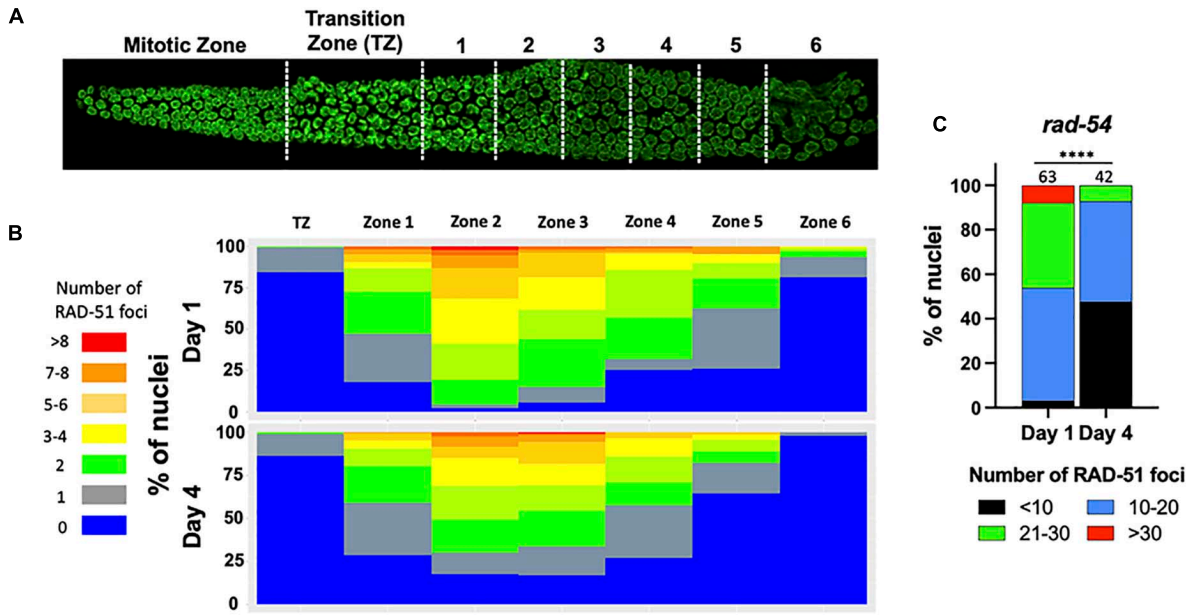

FIGURE 2 | Fewer RAD-51 foci in meiotic nuclei from aged mothers. **(A)** DAPI-stained *C. elegans* germ line showing the regions in which RAD-51 foci were quantified. Each zone corresponds to a particular meiotic stage: Transition zone (TZ) corresponds to leptotene and zygotene, Zones 1 and 2 to early pachytene, Zones 4 and 5 to middle pachytene and Zones 5 and 6 to late pachytene. **(B)** The percentage of nuclei in each zone containing the indicated number of RAD-51 foci. Four gonads per age in N2 worms were quantified. **(C)** Quantification of RAD-51 foci in the *rad-54(ok615)* mutant background. Shown is the percentage of nuclei in late pachytene nuclei containing the indicated number of RAD-51 foci. Numbers on top of bars indicate the total number of nuclei analyzed per age. Statistical significance was determined using Chi-square test. ****$p < 0.0001$.

nucleus, which is sufficient to ensure a CO on each chromosome and is near the endogenous number of meiotic DSBs per nucleus (Mets and Meyer, 2009).

At the earliest time point post-IR (25 min), 99% of the day 1-adult, pachytene nuclei recruited RPA-1 to at least one site, with an average of ∼4.3 foci/nucleus. In contrast, 64% of day 4-adult nuclei failed to recruit RPA-1. Although at 4 h post-irradiation both groups of worms showed elevated numbers of RPA-1 foci, the recruitment of RPA-1 was significantly lower in older animals (**Figure 3A** and **Supplementary Figure 3**). To verify that the expression of GFP::RPA-1 is not reduced over time, thus leading to the reduction on RPA-1 recruitment, we performed measurements of the intensity of the nuclear GFP signal in young adults and 2, 3, and 4 day adults. These experiments were performed on fixed samples to allow analysis at higher resolution. We observed no decrease in overall GFP signal throughout aging (**Supplementary Figure 2**). Together these results suggest that aged animals are defective in recruitment of RPA-1 to DSB sites.

Similar defects in initial recruitment to DNA lesions are observed for RAD-51. At 25 min post-IR, significantly fewer RAD-51 foci are seen in day 4 compared to day 1 adults. RAD-51 foci are diminished in both groups at 4 and 8 h post-IR (**Figure 3B**). However, RAD-51 loss appears slower in 4-day-old adults, as more foci were observed at 8 h post-IR in the day 4 compared to the day 1 adults. While we do not understand the basis for the differences in the patterns of RPA-1 and RAD-51, both sets of data point to altered kinetics of HR repair in older animals.

We also quantified the ability of IR-induced breaks to be converted to CO-committed intermediates by quantifying the recruitment of the COSA-1 to chromosomal foci in late pachytene nuclei (Yokoo et al., 2012). As shown in **Figure 3C**, we observed a remarkable reduction in GFP::COSA-1 foci in the aged animals 8 h post-IR. At this timepoint, nearly half of day 1 nuclei achieved 6 CO- competent foci, whereas almost no day 4 nuclei experienced full COSA-1 levels (**Figure 3C**). Together with our observations that fewer early HR-intermediates are observed in the older animals, these results suggest that the ability to undergo CO recombination is compromised in older animals.

In addition to HR-mediated repair pathways, DSBs can also be repaired by other mechanisms including classical non-homologous end joining (cNHEJ), micro-homology mediated end joining (MMEJ), single-strand annealing (SSA). Break-induced replication (BIR) has not been shown to work in meiosis. We previously showed that in the absence of RAD-51 proteins, SSA, NHEJ, and MMEJ all contribute to repair in the meiotic germ line and that HIM-5 biases use of SSA over NHEJ and MMEJ, suggesting that active mechanisms inhibit use of these alternative DSB repair pathways (Macaisne et al., 2018). We therefore hypothesized that some of the abnormal chromosomal patterns that we observe in diakinesis oocytes from older animals might be explained if these non-HR pathways were to be used more frequently. To test this, we examined the diakinesis figures in *cku-70* and *polq-1* mutant animals that are impaired in NHEJ and MMEJ, respectively. As shown in **Supplementary Figure 4**, impairing NHEJ or MMEJ functions has little to no effect in

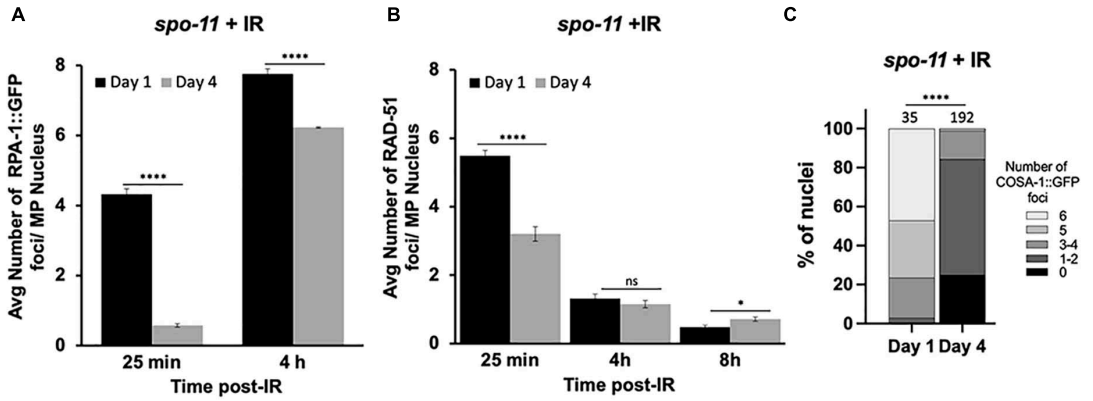

FIGURE 3 | Dynamics of RPA-1 and RAD-51 are altered in aging, meiotic germ cells. *spo*-11 mutant worms at day 1 and day 4 of adulthood were exposed to 10Gy of γ-irradiation. **(A)** Average number of GFP::RPA-1 or **B**) or RAD-51 in mid-pachytene nuclei at indicated timepoints post-exposure. A total of 10 worms per age/timepoint were analyzed in *gfp::rpa-1; spo-11* **(A)** or *spo-11* **(B)** worms. **(C)** Percent of late pachytene nuclei containing the indicated number of COSA-1 foci in *gfp::cosa-1, spo-11* worms at 8 h post-exposure. Statistical significance was determined using Chi-square test. ns $p > 0.1$, *$p < 0.05$, ****$p < 0.0001$.

young animals. In contrast, in older animals loss of *cku-70* or *polq-1* increases the number of nuclei with 6 DAPI bodies. Thus, at least a subset of the chromosome morphology defects observed in diakinesis of older animals is explained by the aberrant activation of NHEJ or MMEJ.

Repair of Complex DSBs Is Severely Impaired in the Aging *C.elegans* Germ Line

Next, we tested whether the age-dependent defects in recruitment of RPA-1 could be aggravated when the DNA damage formed is more complex. Clustered DSBs are forms of complex DNA damage that are more challenging to repair (Nickoloff et al., 2020). Laser microirradiation induces targeted and complex DNA damage that recruits HR proteins and forms characteristic, clustered DSBs (Koury et al., 2018). To examine RPA-1 localization to DSBs in live worms, we utilized the GFP11 tagged RPA-1 strain (Hefel and Smolikove, 2019) described above. In this strain endogenous RPA-1 foci are dim and can be clearly separated during analysis from microirradiation induced foci (Hefel et al., 2021).

To test if RPA-1 recruitment to complex DSBs is impaired with aging we exposed worms to microirradiation at days 1, 2, 2.5, 3, and 4 of adulthood and imaged mid-pachytene (MP) nuclei for 45 min (at 2 min intervals) post-exposure. This time frame was determined in our previous studies where we showed that most RPA-1 foci are recruited within the first 30 min in this strain (Hefel et al., 2021). RPA-1 is recruited to microirradiation induced breaks in a pattern of clusters and foci that cannot be resolved by live imaging (Koury et al., 2018) and is collectively referred to here as recruitment regions. Although the number of recruitment regions was no different between 1– and 2-day-old adults, recruitment in the 45 min window was impaired in 2.5-day-old adults and completely abrogated in 3– and 4-day-old adults (**Figure 4**). To examine if the defects in RPA-1 recruitment were unique to the MP region of the germ line, we performed microirradiation experiments in the other germline regions. We observed similar reductions in RPA-1 recruitment throughout the germ line of aged animals (**Figure 4C**). These data altogether indicated that despite accumulating in the nucleus, RPA-1 fails to assemble on clustered DNA damage in the same kinetics in aged and non-aged worms.

Defects in recruitment of proteins following microirradiation can reflect an abrogation of RPA-1 recruitment or a delay in RPA-1 recruitment to clustered DSBs. Since live imaging data can only be acquired in a limited time window (due to expiration of the worms), analysis in large time scales can only be performed on fixed samples. For this analysis, we microirradiated worms, and then performed gonad dissections at 12 and 25 min, and 4 h timepoints post-microirradiation. We first quantified the percent of nuclei with RPA-1 recruitment regions out of the total number of microirradiated nuclei. 1– and 2-day old adults exhibited maximal recruitment of RPA-1 at the 25 min time point which declined slightly at 4 h (**Figures 5A–C**). In agreement with our live-imaging data, RPA-1 recruitment to microirradiated nuclei was severally impaired in 3-day-old adults and completely abrogated in 4-day-old adults. These data indicate that aged worms fail to recruit RPA-1 to complex DSBs. Aged worms also exhibited an increase in the proportion of foci over clusters (**Figures 5D–F**) which is consistent with inhibition of RPA-1 accumulation on microirradiation-induced DNA damage. Aged worms showed a small increase in number of foci per nucleus in later timepoints (**Figure 5I**, compared to 5G,H). Since for this analysis only nuclei with RPA recruitment regions were scored, this indicates that in the few nuclei in which RPA-1 succeeded in loading to DSBs RPA-1 did not unload in a timely manner.

Altogether our data indicated that, as observed with γ-irradiated worms, microirradiated worms also exhibit defects in RPA-1 recruitment. These defects were more severe in the microirradiated worms, likely due to the complexity of microirradiation induced damage that is more challenging to repair.

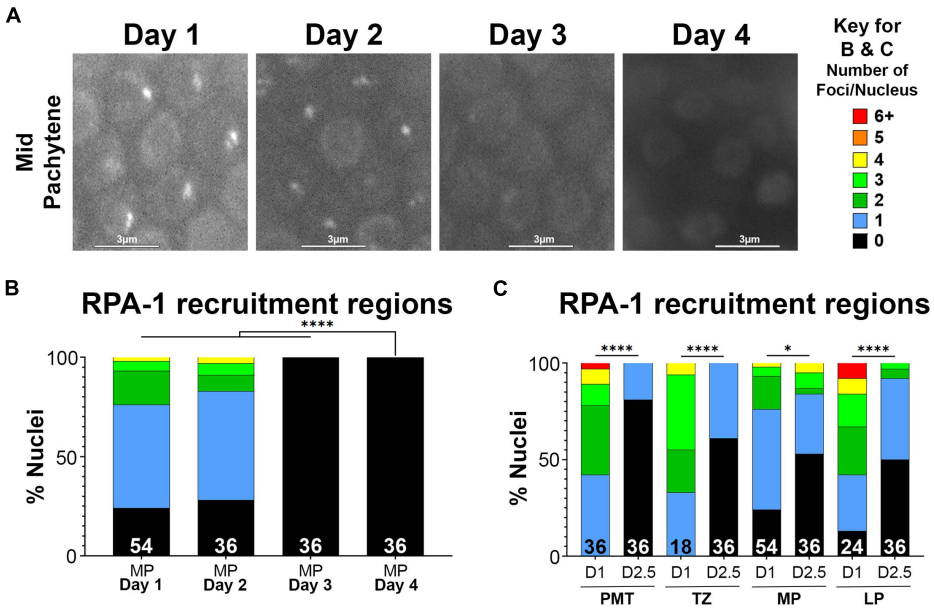

FIGURE 4 | Recruitment of RPA-1 to complex DNA damage decreases with maternal age upon DSB formation. Live imaging of mid-pachytene nuclei post-exposure to microirradiation. **(A)** Left: Representative images from each age of worms examined showing GFP::RPA-1 fluorescence in 20 min post- microirradiation. Images are extracted from the 45-min live-imaging sequence. Scale bars are 3μm. Right: Key for number of recruitment regions represented by each color in panels **(B,C)**. **(B)** Percent of mid-pachytene (MP) nuclei for each age of worm (days post-L4) with the indicated number of GFP::RPA-1 recruitment regions. **(C)** Percent of nuclei in 1-day- and 2.5-day-old adults with the indicated number of GFP::RPA-1 recruitment regions (PMT, pre-meiotic tip; TZ, transition zone; MP, mid-pachytene; LP, late pachytene). Statistical significance was determined using the Fisher's Exact test and *p*-values are indicated as follows: ns ≥ 0.1234, 0.0332–0.1233 = *, ≤ 0.0001 = ****. Nuclei *n*-values as indicated for each condition.

DISCUSSION

While it has been appreciated for decades that oocyte quality diminishes with maternal age, our understanding of the underlying deficits that arise in aged germ cells is still incomplete. We show here that the meiotic processes that control DNA repair and crossover formation deteriorate progressively with maternal age in *C. elegans*. As early as two and one-half days into adult life, just less than one-third of the way through its maximum reproductive period, wild-type worms have profound changes in their ability to recruit DSB-repair proteins to DNA lesions. These defects are the among the earliest harbingers of adult aging in the worm, preceding morphological and physiological somatic changes by several days (Son et al., 2019). In this regard, the oogenic germ line of the adult hermaphrodite may be similar to a human ovary, which also undergoes aging before the rest of the tissues in the body (Hassold and Hunt, 2001).

Since oocytes are made continuously in the worm, we were able to examine how meiotic processes changes in response to age. Using RAD-51 as a surrogate for DSBs, we observed a substantial decrease in HR-competent DSBs in aged germ lines. Since RAD-51 is downstream of resection, a decrease in focus formation could be explained by a *bona fide* decrease in DSB numbers and/or may reflect that DSBs are steered into non-HR (non-CO) pathways in older animals. Our data support defects in both DSB formation and in repair pathway choice.

We reasoned that if DSB efficiency did not decrease with age and DSB levels remained high, then to explain the observed decrease in RAD-51 foci, increasing numbers of chromosomes would be expected undergo non-HR repair. In fact, since most nuclei in day 4 adults have fewer than 10 RAD-51 foci (**Figure 2B**), this would mean that 10-20 DSBs would need to be repaired by alternative pathways. Not only would fewer bivalents be observed, but many larger fusions (and possibly fragments as well) would be seen at diakinesis. This is not what we observed. It was not until the cessation of reproductive life, that more than one fusion chromosome was observed (**Figure 1A**). Instead, > 90% of nuclei appear to repair DSBs as intact, bivalent-like or univalent-like chromosomes throughout the reproductive span. Thus, we infer that substantially fewer DSBs are made as the animal ages. In support of this conclusion, when we trapped RAD-51 protein on the ssDNA filaments with the *rad-54* mutation, RAD-51 levels were significantly reduced. Additionally, the preponderance of bivalent-like chromosomes in the older animals suggests that most chromosomes received a crossover despite low DSB levels, consistent with our previous data on CO distribution in aging animals (Lim et al., 2008). This data suggests that crossover homeostasis mechanisms (Martini et al., 2006) remain proficient in older animals. The reduction in DSBs that we observe either could be a result of an abrogation of SPO-11 activity or could reflect impairments in crossover feedback control mechanisms. The ATM-1 and ATR/ATL-1 kinases are activated by DSBs and downstream ssDNA intermediates and function in a regulatory feedback loop to retain DSB competency until a CO competent intermediate is achieved on all chromosomes

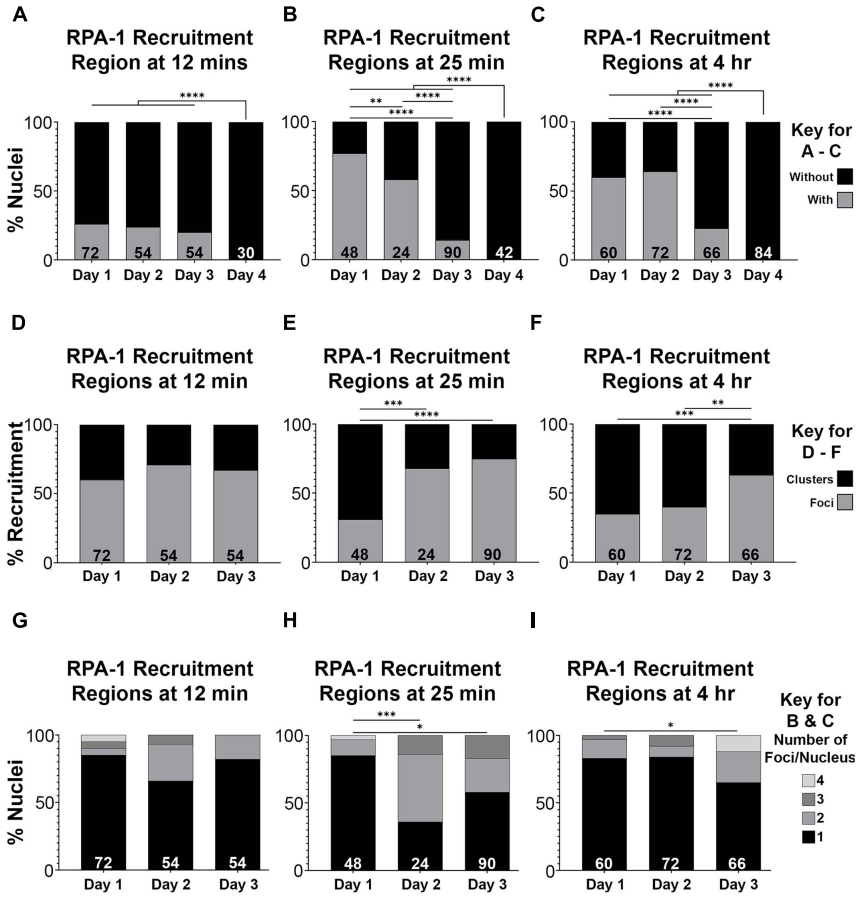

FIGURE 5 | RPA-1 dynamics complex DNA damage attenuates with age. **(A–C)** Percent of mid-pachytene nuclei with RPA-1 recruitment regions out of total number of nuclei 12 min **(A)**, 25 min **(B)** and 4 h **(C)** after microirradiation, in worms at 1, 2, 3, and 4 days post-L4. **(D–F)** Percent RPA-1 recruitment regions appearing as individual foci or as clustered foci per nucleus at 12 min **(D)**, 25 min **(E)** and 4 h **(F)** after microirradiation, in worms at 1, 2, and 3 days post-L4. **(G–I)** Percent of nuclei with the indicated number of RPA-1 recruitment regions per nucleus 12 min **(A)**, 25 min **(B)** and 4 h **(C)** after microirradiation, in worms at 1, 2, and 3 days post L4. Statistical significance was determined using the Fisher's Exact test and *p*-values are indicated as follows: ns ≥ 0.1234, 0.0332–0.1233 = *0.0021–0.0331 = **0.0002–0.0020 = ***, ≤ 0.0001 = ****. *N* values as indicated for each condition.

(Stamper et al., 2013; Lukaszewicz et al., 2018; Li and Yanowitz, 2019). One possibility is that these signaling pathways could be impaired in aging animals to prevent the maintenance of DSB competency.

The increase in fusion chromosomes in aged diakinesis nuclei supports the notion that breaks are being diverted into non-HR repair pathways (**Figure 1A**). The impairment in recruitment of both RPA-1 and RAD-51 after IR and microirradiation also supports the notion that very early events in DSB repair are affected by age. In particular, these studies point to resection as the likely step in repair that is age-sensitive, as processing of the DSB ends regulates both the competition between repair pathways and the ability to recruit RPA-1 (Marini et al., 2019). Chromosome fusions result from repair through NHEJ, MMEJ, or SSA. On day 1 of adulthood, HIM-5 and CEP-1/p53 proteins redundantly inhibit NHEJ during meiosis (Meneely et al., 2012). Although the CO defects of *him-5* worsen with maternal age (Meneely et al., 2012), chromosome fusions were not observed, suggesting that the CEP-1 dependent block to NHEJ is still intact in older animals. The proteins that prevent repair via MMEJ and SSA are currently unknown, so we can only postulate that one or both of these pathways may be accessed to induce the fusions see in aged nuclei.

HR-mediated repair is also severely compromised in aged germ cell nuclei. Using both γ-irradiation and microirradiation, we see significant deficits in the recruitment, accumulation, and turnover of both RPA-1 and RAD-51 at DSB sites (**Figures 3–5**). One caveat to these studies is that we do not know whether old and young worms' chromosomes are equally responsive to irradiation. However, since the nuclear envelope integrity deteriorates (Haithcock et al., 2005; D'Angelo et al., 2009) and chromatin decompacts in older animals (reviewed in Purohit and Chaturvedi, 2017; Sławińska and Krupa, 2021), we would anticipate that DNA damage would increase rather than decrease in older nuclei (Hernández et al., 2015). Further studies on the accessibility of chromatin to DNA damage and developing assay to directly monitor breaks in this system are an avenue of future studies. This impairment is seen in nuclei from the mitotic tip through late pachytene suggesting it reflects

an overall loss of germ line capabilities with age. While this study has been focused on meiotic DNA repair, we note that the effects observed in the mitotic tip of the worm germ line may elucidate how aging impacts repair in replicative cells, including but not limited to the mammalian male germ cells which are maintained by continuous mitotic divisions. Although the general trends between IR and microirradiation are remarkably similar, there are notable differences particularly in regard to RPA-1 accumulation and turnover (**Figures 3**, **5A**). This suggests that the source of DNA damage can dramatically change the persistence of repair intermediates and possibly the outcomes of repair. Microirradiation results in more complex form of DNA damage (clustered DSBs) that are more challenging to repair than dispersed DSBs, like the ones formed by γ-irradiation (Nickoloff et al., 2020). If repair processes are more challenging in older worms, microirradiation may result in more severe effects on recruitment of repair proteins to DSBs, compared to γ-irradiation. Further studies will be required to understand the molecular differences between these repair pathways and how they deteriorate with maternal age.

In the oldest oocytes (>day 6), we observed a novel appearance of some bivalents where the distance between univalents was increased. This separation of the bivalent might occur if, like in mammals and flies, cohesion between exchange homologs is lost with maternal age (Hodges et al., 2005; Subramanian and Bickel, 2008). Additional studies will be required to determine whether cohesin proteins expression or turnover is indeed impacted by maternal age in *C. elegans* and whether there is a functional consequence for the proper segregation of these bivalents.

DATA AVAILABILITY STATEMENT

The raw data supporting the conclusions of this article will be made available by the authors, without undue reservation.

AUTHOR CONTRIBUTIONS

MR performed the studies in **Figures 1–3**, **Supplementary Figures 1**, **3, 4** with some assistance by JY. RB performed the studies in **Figures 4**, **5**, and **Supplementary Figure 2**. All authors contributed to design and interpretation of experiments and the writing and editing of the manuscript.

FUNDING

This work was supported by the NIH grants R01GM104007 to JY and R01GM112657 to SS.

SUPPLEMENTARY MATERIAL

The Supplementary Material for this article can be found online at: https://www.frontiersin.org/articles/10.3389/fcell.2021.695333/full#supplementary-material

Supplementary Figure 1 | RAD-51 staining in dissected germ lines from *spo-11(ok79)* mutants at 1 and 4 days post-L4. DNA is visualized with DAPI (green); RAD-51 with anti-RAD-51 antibodies (Magenta). Shown are maximum projection images through half of the germ line. Almost no RAD-51 foci were observed in germ lines from day 1 adults; approximately half of day 4 adult germ line pachytene nuclei had a single RAD-51 focus.

Supplementary Figure 2 | GFP::RPA-1 levels are not diminished in aging *C. elegans* germline nuclei. **(A)** Representative images of pachytene nuclei from each age of worms examined expressing the endogenously- tagged GFP::RPA-1 fusion protein. Scale bars are 3 μm. **(B)** Western blot analysis of RPA-1 protein in 1 day-old and 4 day-old adults. OLLAS::RPA-1 fusion proteins were detected with anti-OLLAS antibodies. Tubulin serves as loading control. **(C–E)** Average intensity of GFP::RPA-1 in meiotic nuclei, corrected for cytoplasmic background. Each point indicates a single nucleus, error bars indicate the Standard Error of the Mean. **(C)** Pre-meiotic phase nuclei. **(D)** Transition zone (polarized chromatin, leptotene/zygotene phases) nuclei. **(E)** Mid- and late-pachytene phase nuclei. Statistical significance was determined using the Mann-Whitney *U*-test and *p*-values are indicated as follows: ns ≥ 0.1234, 0.0332–0.1233 = *0.0021–0.0331 = **0.0002–0.0020 = *** ≤ 0.0001 = ****. Nuclei *n*-values as indicated for each condition.

Supplementary Figure 3 | Percentage of middle pachytene (MP) nuclei containing the indicated number (key at far right) of GFP::RPA-1 foci (left) or RAD-51 foci (right) in *spo-11* at timepoints post-10Gy of γ-irradiation. Numbers on top of bars indicate the total number of nuclei analyzed per age. A total of 10 worms per age/timepoint were analyzed. Statistical significance was determined using Chi-square test. ns $p > 0.1$, *$p < 0.05$, ****$p < 0.0001$.

Supplementary Figure 4 | Quantification of DAPI-bodies in *cku-70* and *polq-1* diakinesis nuclei from the indicated ages. Data analyzed in **Figure 3** for N2 worms of the same ages was added to allow the comparison with the mutants. Numbers on top of bars indicate the total number of nuclei analyzed per age.

REFERENCES

Achache, H., Falk, R., Lerner, N., Beatus, T., and Tzur, Y. B. (2020). Oocyte aging is controlled by mitogen activated protein kinase signaling. *bioRxiv* [Preprint]. doi: 10.36684/33-2020-1-680-686

Alleva, B., Clausen, S., Koury, E., Hefel, A., and Smolikove, S. (2019). CRL4 regulates recombination and synaptonemal complex aggregation in the *Caenorhabditis elegans* germline. *PLoS Genet.* 15:e1008486. doi: 10.1371/journal.pgen.1008486

Alpi, A., Pasierbek, P., Gartner, A., and Loidl, J. (2003). Genetic and cytological characterization of the recombination protein RAD-51 in *Caenorhabditis elegans*. *Chromosoma* 112, 6–16. doi: 10.1007/s00412-003-0237-5

Andux, S., and Ellis, R. E. (2008). Apoptosis maintains oocyte quality in aging *Caenorhabditis elegans* females. *PLoS Genet.* 4:e1000295. doi: 10.1371/journal.pgen.1000295

Caldwell, C. C., and Spies, M. (2020). Dynamic elements of replication protein A at the crossroads of DNA replication, recombination, and repair. *Crit. Rev. Biochem. Mol. Biol.* 55, 482–507. doi: 10.1080/10409238.2020.1813070

D'Angelo, M. A., Raices, M., Panowski, S. H., and Hetzer, M. W. (2009). Age-dependent deterioration of nuclear pore complexes causes a loss of nuclear integrity in postmitotic cells. *Cell* 136, 284–295. doi: 10.1016/j.cell.2008.11.037

Gasior, S. L., Wong A. K., Yoshiteru, K., Shinohara A., and Bishop, D. K. (1998). Rad52 associates with RPA and functions with Rad55 and Rad57 to assemble meiotic recombination complexes. *Genes Dev.* 12, 2208–2221. doi: 10.1101/gad.12.14.2208

Haithcock, E., Dayani, Y., Neufeld, E., Zahand, A. J., Feinstein, N., Mattout, A., et al. (2005). Age-related changes of nuclear architecture in *Caenorhabditis elegans*. *Proc. Natl. Acad. Sci.U.S.A.* 102, 16690–16695. doi: 10.1073/pnas.0506955102

Harrell, K., Koury, E., and Smolikove, S. (2018). Microirradiation for precise, double-strand break induction in vivo in *Caenorhabditis elegans*. *Bio Protoc.* 8:e3130. doi: 10.21769/bioprotoc.3130

Hassold, T., and Hunt, P. (2001). To err (meiotically) is human: the genesis of human aneuploidy. *Nat. Rev. Genet.* 2:280. doi: 10.1038/35066065

Hefel, A., and Smolikove, S. (2019). Tissue-specific split sfGFP system for streamlined expression of GFP tagged proteins in the *Caenorhabditis elegans* germline. *G3* 9, 1933–1943. doi: 10.1534/g3.119.400162

Hefel, A., Honda, M., Cronin, N., Harrell, K., Patel, P., Spies, M., et al. (2021). RPA complexes in *Caenorhabditis elegans* meiosis; unique roles in replication, meiotic recombination and apoptosis. *Nucleic Acids Res.* 49, 2005–2026. doi: 10.1093/nar/gkaa1293

Hernández, L., Terradas, M., Camps, J., Martin, M., Tusell, L., and Genesca, A. (2015). Aging and radiation: bad companions. *Aging Cell* 14, 153–161. doi: 10.1111/acel.12306

Hodges, C. A., Revenkova, E., Jessberger, R., Hassold, T. J., and Hunt, P. A. (2005). SMC1B-deficient female mice provide evidence that cohesins are a missing link in age-related nondisjunction. *Nat. Genet.* 37, 1351–1355. doi: 10.1038/ng1672

Hughes, S. E., Evason, K., Xiong, C., and Kornfeld, K. (2007). Genetic and pharmacological factors that influence reproductive aging in nematodes. *PLoS Genet.* 3:e25. doi: 10.1371/journal.pgen.0030025

Hussin, J., Roy-Gagnon, M.-H., Gendron, R., Andelfinger, G., and Awadalla, P. (2011). Age-dependent recombination rates in human pedigrees. *PLoS Genet.* 7:e1002251. doi: 10.1371/journal.pgen.1002251

Keeney, S., Giroux, C. N., and Kleckner, N. (1997). Meiosis-specific DNA double-strand breaks are catalyzed by Spo11, a member of a widely conserved protein family. *Cell* 88, 375–384. doi: 10.1016/S0092-8674(00)81876-0

Koury, E., Harrell, K., and Smolikove, S. (2018). Differential RPA-1 and RAD-51 recruitment in vivo throughout the *C. elegans* germline, as revealed by laser microirradiation. *Nucleic Acids Res.* 46, 748–764. doi: 10.1093/nar/gkx1243

Lamb, N. E., Sherman, S. L., and Hassold, T. J. (2005). Effect of meiotic recombination on the production of aneuploid gametes in humans. *Cytogenet. Genome Res.* 111, 250–255. doi: 10.1159/000086896

Li, W., and Yanowitz, J. L. (2019). ATM and ATR influence meiotic crossover formation through antagonistic and overlapping functions in *Caenorhabditis elegans*. *Genetics* 212, 431–443. doi: 10.1534/genetics.119.302193

Lim, J. G. Y., Stine, R. R. W., and Yanowitz, J. L. (2008). Domain-specific regulation of recombination in *Caenorhabditis elegans* in response to temperature, age and sex. *Genetics* 180, 715–726. doi: 10.1534/genetics.108.090142

Lukaszewicz, A., Lange, J., Keeney, S., and Jasin, M. (2018). Control of meiotic double-strand-break formation by ATM: local and global views. *Cell Cycle* 17, 1155–1172. doi: 10.1080/15384101.2018.1464847

Luo, S., Kleemann, G. A., Ashraf, J. M., Shaw, W. M., and Murphy, C. T. (2010). TGF-β and Insulin signaling regulate reproductive aging via oocyte and germline quality maintenance. *Cell* 143, 299–312. doi: 10.1016/j.cell.2010.09.013.TGF-

Macaisne, N., Kessler, Z., and Yanowitz, J. L. (2018). Meiotic double-strand break proteins influence repair pathway utilization. *Genetics* 210, 843–856. doi: 10.1534/genetics.118.301402

Machovina, T. S., Mainpal, R., Daryabeigi, A., McGovern, O., Paouneskou, D., Labella, S., et al. (2016). A surveillance system ensures crossover formation in *C. elegans*. *Curr. Biol.* 26, 2873–2884. doi: 10.1016/j.cub.2016.09.007

Mahadevan, J., Bowerman, S., and Luger, K. (2019). Quantitating repair protein accumulation at DNA lesions: past, present, and future. *DNA Repair* 81:102650. doi: 10.1016/j.dnarep.2019.102650

Marini, F., Rawal, C. C., Liberi, G., and Pellicioli, A. (2019). Regulation of DNA double strand breaks processing: focus on barriers. *Front. Mol. Biosci.* 6:55.

Martin, J. S., Winkelmann, N., Petalcorin, M. I. R., Mcilwraith, M. J., and Boulton, S. J. (2005). RAD-51-dependent and Independent roles of a *Caenorhabditis elegans* BRCA2-Related Protein during DNA double-strand break repair. *Society* 25, 3127–3139. doi: 10.1128/MCB.25.8.3127

Martini, E., Diaz, R. L., Hunter, N., and Keeney, S. (2006). Crossover homeostasis in yeast meiosis. *Cell* 126, 285–295. doi: 10.1016/j.cell.2006.05.044

Mateo, A. R. F., Kessler, Z., Jolliffe, A. K., McGovern, O., Yu, B., Nicolucci, A., et al. (2016). The p53-like protein CEP-1 is required for meiotic fidelity in C. *Elegans*. *Curr. Biol.* 26, 1148–1158. doi: 10.1016/j.cub.2016.03.036

Meneely, P. M., McGovern, O. L., Heinis, F. I., and Yanowitz, J. L. (2012). Crossover distribution and frequency are regulated by him-5 in *Caenorhabditis elegans*. *Genetics* 190, 1251–1266. doi: 10.1534/genetics.111.137463

Mets, D. G., and Meyer, B. J. (2009). Condensins regulate meiotic DNA break distribution, thus crossover frequency, by controlling chromosome structure. *Cell* 139, 73–86. doi: 10.1016/j.cell.2009.07.035

Neale, M. J., Pan, J., and Keeney, S. (2005). Endonucleolytic processing of covalent protein-linked double-strand breaks. *Nature* 436, 1053–1057. doi: 10.1038/jid.2014.371

Nickoloff, J. A., Sharma, N., and Taylor, L. (2020). Clustered DNA double-strand breaks: Biological effects and relevance to cancer radiotherapy. *Genes* 11, 99. doi: 10.3390/genes11010099

Purohit, J. S., and Chaturvedi, M. M. (2017). "Chromatin and aging," in *Topics in Biomedical Gerontology*, eds P. Rath, R. Sharma, and S. Prasad (Singapore: Springer), 205–241.

Quesada-Candela, C., Loose, J., Ghazi, A., and Yanowitz, J. L. (2021). Molecular basis of reproductive senescence: insights from model organisms. *J. Assist. Reprod. Genet.* 38, 17–32. doi: 10.1007/s10815-020-01959-4

Rose, A. M., and Baillie, D. L. (1979). The effect of temperature and parental age on recombination and nondisjunction in *Caenorhabditis elegans*. *Genetics* 92, 409–418. doi: 10.1093/genetics/92.2.409

Saini, R., Singh, A. K., Hyde, G. J., and Baskar, R. (2020). Levels of Heterochiasmy During *Arabidopsis* Development as Reported by Fluorescent Tagged Lines. *G3* 10, 2103–2110. doi: 10.1534/g3.120.401296

Sansam, C. L., and Pezza, R. J. (2015). Connecting by breaking and repairing mechanisms of DNA strand exchange in meiotic recombination. *FEBS J.* 282, 2444–2457. doi: 10.1111/febs.13317

Schwacha, A., and Kleckner, N. (1995). Identification of double Holliday junctions as intermediates in meiotic recombination. *Cell* 83, 783–791. doi: 10.1016/0092-8674(95)90191-4

Shinohara, A., Ogawa, H., and Ogawa, T. (1992). Rad51 protein involved in repair and recombination in *S. cerevisiae* is a RecA-like protein. *Cell* 69, 457–470. doi: 10.1016/0092-8674(92)90447-K

Sławińska, N., and Krupa, R. (2021). Molecular aspects of senescence and organismal ageing—DNA damage response, telomeres, inflammation and chromatin. *Int. J. Mol. Sci.* 22:590. doi: 10.3390/ijms22020590

Son, H. G., Altintas, O., Kim, E. J. E., Kwon, S., and Lee, S. J. V. (2019). Age-dependent changes and biomarkers of aging in *Caenorhabditis elegans*. *Aging Cell* 18, 1–11. doi: 10.1111/acel.12853

Stamper, E. L., Rodenbusch, S. E., Rosu, S., Ahringer, J., Villeneuve, A. M., and Dernburg, A. F. (2013). Identification of DSB-1, a protein required for initiation of meiotic recombination in *Caenorhabditis elegans*, illuminates a crossover assurance checkpoint. *PLoS Genet.* 9:e1003679. doi: 10.1371/journal.pgen.1003679

Stern, C. (1926). An effect of temperature and age on crossing-over in the first chromosome of *Drosophila* melanogaster. *Proc. Natl. Acad. Sci.U.S.A.* 12:530. doi: 10.1073/pnas.12.8.530

Subramanian, V. V., and Bickel, S. E. (2008). Aging predisposes oocytes to meiotic nondisjunction when the cohesin subunit SMC1 is reduced. *PLoS Genet.* 4:e1000263. doi: 10.1371/journal.pgen.1000263

Sung, P. (1994). Catalysis of ATP-dependent homologous DNA pairing and strand exchange by yeast RAD51 protein. *Am. Assoc. Adv. Sci.* 265, 1241–1243. doi: 10.1126/science.8066464

Woglar, A., and Villeneuve, A. M. (2018). Dynamic architecture of DNA repair complexes and the synaptonemal complex at sites of meiotic recombination. *Cell* 173, 1678–1691. doi: 10.1016/j.cell.2018.03.066

Yokoo, R., Zawadzki, K. A., Nabeshima, K., Drake, M., Arur, S., and Villeneuve, A. M. (2012). COSA-1 reveals robust homeostasis and separable licensing and reinforcement steps governing meiotic crossovers. *Cell* 149, 75–87. doi: 10.1016/j.cell.2012.01.052

Conflict of Interest: The authors declare that the research was conducted in the absence of any commercial or financial relationships that could be construed as a potential conflict of interest.

Publisher's Note: All claims expressed in this article are solely those of the authors and do not necessarily represent those of their affiliated organizations, or those of the publisher, the editors and the reviewers. Any product that may be evaluated in this article, or claim that may be made by its manufacturer, is not guaranteed or endorsed by the publisher.

frontiers in Cell and Developmental Biology

ORIGINAL RESEARCH
published: 06 August 2021
doi: 10.3389/fcell.2021.695545

TCF3 Regulates the Proliferation and Apoptosis of Human Spermatogonial Stem Cells by Targeting PODXL

Dai Zhou[1,2,3,4,5], Jingyu Fan[6], Zhizhong Liu[1,7], Ruiling Tang[1,2], Xingming Wang[1,2], Hao Bo[1,2], Fang Zhu[1,2], Xueheng Zhao[1,2], Zenghui Huang[1,2], Liu Xing[1,2], Ke Tao[1,2,8], Han Zhang[1,2], Hongchuan Nie[1,2], Huan Zhang[1,2], Wenbing Zhu[1,2], Zuping He[8] and Liqing Fan[1,2,4,5]**

[1] Institute of Reproduction and Stem Cell Engineering, School of Basic Medicine Science, Central South University, Changsha, China, [2] Reproductive & Genetic Hospital of CITIC-Xiangya, Changsha, China, [3] College of Life Sciences, Hunan Normal University, Changsha, China, [4] Clinical Research Center for Reproduction and Genetics in Hunan Province, Changsha, China, [5] NHC Key Laboratory of Human Stem Cell and Reproductive Engineering, Central South University, Changsha, China, [6] Department of Chemistry and Biochemistry, University of South Carolina, Columbia, SC, United States, [7] Department of Urology, Hunan Cancer Hospital, Changsha, China, [8] The Key Laboratory of Model Animals and Stem Cell Biology in Hunan Province, Hunan Normal University School of Medicine, Changsha, China

OPEN ACCESS

Edited by:
Miguel Angel Brieño-Enriquez, Magee-Womens Research Institute, United States

Reviewed by:
Hanna Pulaski, University of Pittsburgh, United States
Fei Sun, Tongji Medical College, China
Fei Sun, Shanghai Jiao Tong University, China

***Correspondence:**
Liqing Fan
801646@csu.edu.cn
Zuping He
zupinghe@hunnu.edu.cn

Specialty section:
This article was submitted to Molecular and Cellular Reproduction, a section of the journal Frontiers in Cell and Developmental Biology

Received: *15 April 2021*
Accepted: *19 July 2021*
Published: *06 August 2021*

Citation:
Zhou D, Fan J, Liu Z, Tang R, Wang X, Bo H, Zhu F, Zhao X, Huang Z, Xing L, Tao K, Zhang H, Nie H, Zhang H, Zhu W, He Z and Fan L (2021) TCF3 Regulates the Proliferation and Apoptosis of Human Spermatogonial Stem Cells by Targeting PODXL. Front. Cell Dev. Biol. 9:695545. doi: 10.3389/fcell.2021.695545

Spermatogonial stem cells (SSCs) are the initial cells for the spermatogenesis. Although much progress has been made on uncovering a number of modulators for the SSC fate decisions in rodents, the genes mediating human SSCs remain largely unclear. Here we report, for the first time, that TCF3, a member of the basic helix-loop-helix family of transcriptional modulator proteins, can stimulate proliferation and suppress the apoptosis of human SSCs through targeting podocalyxin-like protein (PODXL). TCF3 was expressed primarily in GFRA1-positive spermatogonia, and EGF (epidermal growth factor) elevated TCF3 expression level. Notably, TCF3 enhanced the growth and DNA synthesis of human SSCs, whereas it repressed the apoptosis of human SSCs. RNA sequencing and chromatin immunoprecipitation (ChIP) assays revealed that TCF3 protein regulated the transcription of several genes, including *WNT2B*, *TGFB3*, *CCN4*, *MEGF6*, and *PODXL*, while PODXL silencing compromised the stem cell activity of SSCs. Moreover, the level of TCF3 protein was remarkably lower in patients with spermatogenesis failure when compared to individuals with obstructive azoospermia with normal spermatogenesis. Collectively, these results implicate that TCF3 modulates human SSC proliferation and apoptosis through PODXL. This study is of great significance since it would provide a novel molecular mechanism underlying the fate determinations of human SSCs and it could offer new targets for gene therapy of male infertility.

Keywords: TCF3, human spermatogonial stem cells, proliferation, apoptosis, PODXL

INTRODUCTION

Spermatogonial stem cells (SSCs) reside along the basement membrane of the testicular seminiferous tubules, and they self-renew to maintain the stem cell pool of the testis and differentiate for the continuous production of spermatozoa (Kanatsushinohara et al., 2003; Yeh et al., 2011). In both rodents and primates, SSCs are restricted to A-type undifferentiated

spermatogonia (A_{undiff}). In rodents, A_{undiff} are found as single (A_s) or as syncytia of 2 (A-paired, A_{pr}), 4, 8, and up to 16 (A-aligned, A_{al4-16}) cells interconnected by cytoplasmic bridges (Mäkelä and Toppari, 2018). SSCs are generally considered to be present in A_s spermatogonia (Lord and Oatley, 2017), however, many data indicate that A_{pr} and A_{al} syncytium can re-enter A_s state by breaking the cytoplasmic bridge in an appropriate environment (Hara et al., 2014; Carrieri et al., 2017). In primates, A_{undiff} can be divided into Adark (A_d) and Apale (A_p) according to the degree of nuclei staining. The traditional models propose that A_d spermatogonia are the reserve stem cells, and they steadily generate A_p spermatogonia with adequate self-renewal potential to sustain the stem cell pool (Clermont, 1966), but there are still many controversies about the function of A_d and A_p (Hermann et al., 2009, 2010; Di Persio et al., 2017).

Using testis material from rodents, molecular mechanisms of mouse SSC self-renewal and differentiation have been analyzed. It is now considered that the intricate molecular and cellular interactions form the niche or microenvironment for SSC development (He et al., 2008; Makela and Hobbs, 2019). GFRA1-positive SSCs respond to GDNF and other factors through elevating expression of genes required to sustain the self-renewing state of mouse SSCs, including Etv5 (Oatley et al., 2006), Lhx1 (Oatley et al., 2006), Bcl6b (Oatley et al., 2006), Nanos2 (Sada et al., 2012), and Id4 (Oatley et al., 2011). The secretion of GDNF is under endocrine modulation in FSH by Sertoli cells as well as PMCs (peritubular myoid cells) through the LH-mediated synthesis of testosterone in Leydig cells (Sakai et al., 2018). FGF2 and GDNF synergistically function to promote the robust growth of the undifferentiated spermatogonia *in vitro*, while the role of FGF2 in sustaining the stemness of SSCs *in vivo* remain poorly understood (Takashima et al., 2015). Shisa6, a WNT suppressor, renders SSCs resistant to differentiation induced by WNT. The progenitor spermatogonia primed for the differentiation are originated from the GFRA1-positive SSCs in response to WNT induction (Tokue et al., 2017). They have adopted the *Ngn3* and *Sox3* gene signatures, which separates them clearly from the self-renewing cells and enables them to be responsive to retinoic acid (RA) through expressing RARγ (retinoic acid receptor gamma) (Sugimoto et al., 2012; Hara et al., 2014; Ikami et al., 2015). The RA induction elicits a differentiation commitment in these cells, resulting in the up-regulation of Stra8, Sohlh1 and Kit as well as the down-regulation of Plzf (Ghyselinck et al., 2006; Anderson et al., 2008; Zhou et al., 2008). Besides, RA acts on Sertoli cells, which enhances the expression level of Bmp4 and decreases the transcription of *Gdnf* (Pellegrini et al., 2008; Carlomagno et al., 2010; Yang et al., 2013).

Although much progress has been achieved on unveiling the molecular mechanisms underlying the self-renewal and the differentiation of SSCs in rodents, these rodent SSC mechanisms cannot be repeated in human SSCs. The cell types, as well as the biochemical phenotypes of SSCs are distinct in SSCs between rodents and humans. It is worth noting that human SSCs share some but not all phenotypes with rodent SSCs. As an example, OCT4 (also known as POU5F1) is a hallmark for rodent SSCs; however, OCT4 is not expressed in human SSCs (He et al., 2010; Guo et al., 2017). Moreover, the mouse seminiferous epithelium cycle is usually subdivided into 12 stages, while there are generally only 6 spermatogenic cycle phases in human (Muciaccia et al., 2013). Consequently, the regulatory mechanisms of SSCs have significant differences between humans and rodents. As such, it is of great significance for us to identify the novel molecular regulators modulating the fate determinations of human SSCs.

TCF3 belongs to the E-protein family, the highly conserved bHLH (basic helix-loop-helix) family members of transcriptional modulator proteins (Slattery et al., 2008). TCF3 participates in diverse developmental processes through working with other HLH family proteins (Imayoshi and Kageyama, 2014). It has been reported that TCF3 plays pivotal roles in the stem cell maintenance and differentiation, including the embryonic stem cells, neural stem cells, and hematopoietic stem cells. The alternative splicing of TCF3 regulated by hnRNP H/F modulates the expression of E-cadherin and pluripotency of human embryonic stem cells (Yamazaki et al., 2018). TCF3 maintains the hematopoietic stem cell arsenal and enhances the maturation of myeloerythroid and myelo lymphoid progenitors (Semerad et al., 2009), while TCF3 controls the differentiation of neural stem cells into astrocytes (Bohrer et al., 2015). Moreover, TCF3 proteins trigger and suppress transcription so as to enhance a B cell fate in progenitor cells (Lin et al., 2010). These studies imply that TCF3 is associated with cell fate decisions on various kinds of stem cells.

In the current study, we revealed that TCF3 was mainly expressed in the human SSCs ($GFRA1^+/PCNA^+/KIT^-$) by using immunohistochemistry. We used RNA interference to explore the function of TCF3 in human SSCs, and we demonstrated that TCF3 promoted the proliferation and DNA synthesis but inhibited the apoptosis of human SSC line. In order to identify the targets ofTCF3, RNA sequencing and chromatin immunoprecipitation (ChIP) approaches were employed. TCF3 could directly docks to the promoter region and enhanced the expression levels of podocalyxin-like protein (PODXL), TGFB3, CCN4, and MEGF6. Defective PODXL expression inhibited the proliferation and DNA synthesis but promoted apoptosis of human SSC line. In addition, we revealed that TCF3 levels were remarkably decreased in NOA patients compared to individuals with obstructive azoospermia (OA) with normal spermatogenesis, particularly in the NOA patients with spermatogonial or spermatocytes maturation arrest (Spc MA). Therefore, our study provides novel insights into the molecular mechanisms responsible for the proliferation and the apoptosis of human SSCs, and it provides new clues for the etiology, molecular diagnosis, as well as the treatment of male infertility.

MATERIALS AND METHODS

Human Testis Tissues

This study was approved by the Ethics Committee of the Reproductive & Genetic Hospital of CITIC-Xiangya, Basic Medical Science School, Central South University (LL-SC-2017-015), and the participants signed an informed consent. Adult testicular tissues retrieved for this research were obtained from 12 patients (3 OA and 9 NOA) undergoing conventional testicular

sperm extraction (TESE) or microdissection testicular sperm extraction (m-TESE) aged between 25 and 38 years old, and about 50 mg testicular tissues were acquired. Normal fetal testes for this research were obtained from two donors (19 and 24 weeks). All the samples were washed three times by PBS with 1% penicillin and streptomycin and then fixed with 4% paraformaldehyde (PFA) or stored in liquid nitrogen.

Human SSC Line Culture

The human SSC line was established by overexpressing human SV40 large T antigen in human primary GPR125-positive undifferentiated spermatogonia in our lab (Hou et al., 2015), the cell line was positive for a series of SSC markers including GPR125, GFRA1, PLZF, UCHL1, and THY1, and it can be expanded *in vitro* for a long time.

The human SSC line cells were cultured in DMEM/F12 (Gibco, Grand Island, NY, United States) with 10% FBS (Gibco) and 100 unit/mL streptomycin/penicillin (Invitrogen, CA, United States) at 34°C in 5% CO_2 incubator. The cells were passaged every 4 days using 0.05% trypsin and 0.53 mM EDTA (Invitrogen). In order to seek which growth factor mediates TCF3, the cells were incubated in the DMEM/F12 with the addition of 10 ng/mL GDNF (R&D Systems, MN, United States), 10 ng/mL FGF2 (R&D Systems), 10 ng/mL epidermal growth factor (EGF) (Sigma, MO, United States), or 1,000 IU/mL LIF (Cyagen, Suzhou, China).

RNA Isolation, RT-PCR, and qPCR

The RNAiso Plus reagent (Takara, Kusatsu, Japan) was employed to isolate total RNA from the cells pursuant to the instruction of the manufacturer. The quality and concentrations of total RNA were determined using the Nanodrop (Thermo Scientific, MA, United States), and cDNA was generated from total RNA by using Transcriptor First Strand cDNA Synthesis Kit (Roche, Mannheim, Germany).

Real-time PCR (RT-PCR) was performed in terms of the method as documented previously (Zhou et al., 2020). The PCR reactions were conducted as follows: 95°C for 5 min, denaturation at 95°C for 30 s, annealing at 52–60°C for 45 s as indicated in **Supplementary Table 1**, and elongation at 72°C for 45 s for 32 cycles. RNA without room temperature (RT) was employed as the negative control (NC). Electrophoresis of the PCR amplicons on a 2% agarose gel was performed and ethidium bromide was employed to stain the amplicons. The chemiluminescence imaging system (Chemi-Doc XRS, Bio-Rad, CA, United States) was employed to acquire the images of the bands.

The SYBR Premix Ex Taq II (Takara) was employed to perform qPCR on the Applied Biosystems ABI Prism 7700 system (Applied Biosystems, Foster City, CA, United States) pursuant to the manual of the manufacturer. *ACTB* served as the normalization standard. The $2^{-\Delta\Delta}$ cycle threshold (Ct) approach was utilized to determine relative mRNA expression. Each sample was replicated three times. Primer sequences of the chosen genes for RT-PCR and qPCR were designed and shown in **Supplementary Table 1**.

Immunocytochemistry, Immunohistochemistry, and Immunofluorescence

For the immunocytochemistry, the cells were washed three times with cold PBS (Gibco), and they were fixed with 4% PFA for 15 min. After washing three times in cold PBS, 0.25% Triton X-100 (Sigma) was employed to permeabilize the cells for 10 min. Blocking was performed by 5% BSA at RT for 1 h, and the cells were incubated with the primary antibodies at 4°C overnight. The sources and dilutions of the antibodies were shown in **Supplementary Table 2**. Next, the cells were rinsed with PBS and then incubated with Alexa Fluor 488 labeled IgG or Alexa Fluor 594 labeled IgG secondary antibodies. Thereafter, DAPI staining was used to stain the nucleus of the cells. A fluorescence microscope (Carl Zeiss, Oberkochen, Germany) was employed to capture image of the cells.

For the immunohistochemistry, deparaffinization of the testis sections was conducted with xylene and rehydrated with the graded ethanol. Heat-induced antigen retrieval (HIER) was done in 0.01M sodium citrate buffer in a beaker at 98°C for 18 min, and 3% H_2O_2 (Zsbio, Beijing, China) was utilized to block the endogenous peroxidase activity. Thereafter, 0.25% Triton X-100 (Sigma) was used to permeabilize the cell sections for 15 min, and 5% BSA was employed to block these sections for 1 h at RT. Subsequently, the sections were incubated with primary antibodies at 4°C overnight and followed by rinsing in PBS. Next, the sections were incubated with HRP-labeled secondary antibody for 1 h at RT, and chromogen was detected with the 3,3′-diaminobenzidine (DAB) chromogen kit (Dako, Glostrup, Denmark). The sections were finally stained with hematoxylin. For immunofluorescence, the sections were incubated with Alexa Fluor conjugated second antibody for 1 h at RT, and the cell nuclei were stained with DAPI. The images were acquired using a Zeiss microscope.

Western Blots

Testis tissues and human SSC line were lysed with the RIPA lysis buffer (Thermo Scientific) on ice for about 30 min, and cell lysates were removed by spinning at 12,000 × *g*. The BCA kit (Thermo Scientific) was employed to determine concentration of the proteins. For every sample, 30 μg of total protein extracts were fractionated on the SDS-PAGE Gel (Bio-Rad), and western blotting was performed in terms of the method as documented previously (Zhou et al., 2020). The antibodies and the dilution ratios for the western blotting were shown in **Supplementary Table 2**. The chemiluminescence (Bio-Rad) was employed to visualize the protein bands.

siRNA Transfection

The siRNA sequences targeting human TCF3 and PODXL mRNA were synthesized by Ribobio (Guangzhou, China) and were listed in **Supplementary Table 3**. The siRNA without targeting sequences were used as NCs. Cells were transfected with 100 nM siRNA or NC-siRNA using the Lipofectamine 3000 transfection system (Cat No, Life Technologies, CA, United States) according to the manual of the manufacturer. Cells were harvested after

transfection for 48 h to assess the alterations of gene and protein expression.

CCK-8 Assay

After transfection with siRNAs, human SSC proliferation potential was explored with the CCK-8 assay Kit (Dojindo, Kumamoto, Japan) as described by the manufacturer. Concisely, cell growth medium was replaced with 10% CCK-8 reagents and incubated for 3 h, and the OD values were read at 450 nm on a microplate reader (Thermo Scientific).

EdU Incorporation Assay

In total, 5,000 human SSC line/well were seeded to 96-well plate in DMEM/F12 medium with addition of 50 μm EdU (RiboBio) for 12 h. The cells were rinsed with DMEM and fixed with 4% PFA. Thereafter, 2 mg/mL glycine was employed to neutralize the cells and then permeabilization was performed for 10 min using 0.5% Triton X-100 at RT. Apollo staining reaction buffer was employed for EdU immunostaining, and Hoechst 33342 was used to stain the cell nuclei. The images were captured using a fluorescence microscope (Zeiss), and at least 500 cells were counted to assess the percentages of EdU-positive cells.

Flow Cytometry With Annexin V-APC/PI Staining

To assess the apoptosis of the human SSC line affected by TCF3 siRNAs, cells were digested and rinsed twice in ice-cold PBS. Afterward, 10^6 cells were re-suspended in Annexin V Binding Buffer (BD Biosciences, NJ, United States) in terms of the methods of the manufacturer. The cells were incubated with 5 μl of Annexin V labeled APC and 10 μl of PI solution for 15 min at RT in dark. A C6 flow cytometry instrument (BD Biosciences) was employed to analyze the cells.

TUNEL Assay

The *In Situ* Cell Death Detection Kit (Roche) was further employed to assess the apoptosis of the human SSC line affected by TCF3 siRNAs pursuant to the manual of the manufacturer. The cells were treated with 20 mg/mL proteinase K for 15 min at RT, and they were incubated with dUTP labeling/terminal deoxynucleotidyl transferase (TdT) enzyme buffer for 1 h in the dark. DAPI was used to stain the cell nuclei. The cells with PBS but without the TdT enzyme was employed as the NC. At least 500 cells were evaluated per sample in a Zeiss fluorescence microscope.

RNA Sequencing

The Trizol reagent kit (Invitrogen) was employed to isolate total RNA, and the Agilent 2100 Bioanalyzer (Agilent Technologies, CA, United States) was used to measure RNA quality and checked by RNase free agarose gel electrophoresis. The Oligo (dT) beads were utilized to enrich the eukaryotic mRNA, while the Ribo-ZeroTM Magnetic Kit (Epicentre, WI, United States) was employed to remove rRNA to enrich prokaryotic mRNA. Next, the fragmentation of the enriched mRNA into short fragments was conducted with the fragmentation buffer and followed by reverse transcription into cDNA using random hexamers. DNA polymerase I, dNTP, buffer, and RNase H were employed to synthesize the second strand DNA. Subsequently, the QiaQuick PCR extraction kit (Qiagen, Venlo, Netherlands) was sued to purify the cDNA fragments, followed by their end repair, poly(A) introduction, and ligation with Illumina sequencing adapters. Thereafter, agarose gel electrophoresis was performed to select the ligation products, which were enriched *via* PCR, and sequenced on the Illumina HiSeq2500 system by Gene *Denovo* Biotechnology Co. (Guangzhou, China). Reads obtained from the sequencing machine were filtered by fastp (Chen et al., 2018) (version 0.18.0). The rRNA mapped reads were removed by using a short reads alignment tool Bowtie2 (Langmead and Salzberg, 2012) (version 2.2.8). The remaining clean reads were further employed in assembly and the gene abundance determination. The THISAT (Kim et al., 2015) with "-rna-strandness RF" and other parameters set as a default was employed to map the paired-end clean reads to the reference genome. The StringTie v1.3.1 (Pertea et al., 2015, 2016) was used to assemble the mapped reads in a reference-based strategy. RNA differential expression assessment was conducted by DESeq2 (Love et al., 2014) software, and FDR <0.05 along with absolute fold change ≥ 2 indicated the differentially expressed genes (DEGs) (**Supplementary Data Sheet 1**). The Gene Ontology (GO) (Ashburner et al., 2000) and Kyoto Encyclopedia of Genes and Genomes (KEGG) pathway enrichment analyses (Kanehisa and Goto, 2000) were implemented on the DEGs in human SSC line between TCF3-siRNA 3 and the NC-siRNA.

ChIP Assay and Real-Time PCR

The SimpleChIP® Plus Sonication Chromatin IP Kit (Cell Signaling Technology, MA, United States) was employed to perform ChIP assay. In brief, about 1×10^7 cells were fixed with 1% formaldehyde, then ice-cold 1.25 M glycine was used to quench the cells, which were re-suspended and lysed. The pellets of cells were re-suspended in 400 μl of shearing buffer enriched with Protease/Phosphatase Inhibitor Cocktail (Cell Signaling Technology). Thereafter, sonication was done to shear cross-linked DNA to an optimal fragment of 200–1,000 bp. The sonicated chromatins were confirmed by assessing size distribution on a 1.5% agarose gel. Immunoprecipitation, de-cross linking, and DNA purification steps were performed in terms of the instruction of the manufacturer. In total, 10 μg of sheared chromatin was incubated with TCF3 antibody (2 μg, Santacruz, sc-133075) and normal mouse IgG (2 μg, Cell Signaling Technology, 5873). After being incubated with antibodies at 4°C overnight, ChIP-Grade Protein G Magnetic Beads was added for 2 h. The Protein G Magnetic Beads were filtered through placing the tubes in a magnetic separation rack for 2 min for the solution to clear. The cross-links were reversed by addition of 6 μl 5 M NaCl and 2 μl Proteinase K and incubated for 2 h at 65°C. The DNA purification spin columns (Cell Signaling Technology) were employed to purify the DNA. The enrichment of particular DNA sequences during immunoprecipitation was subjected to RT-PCR with

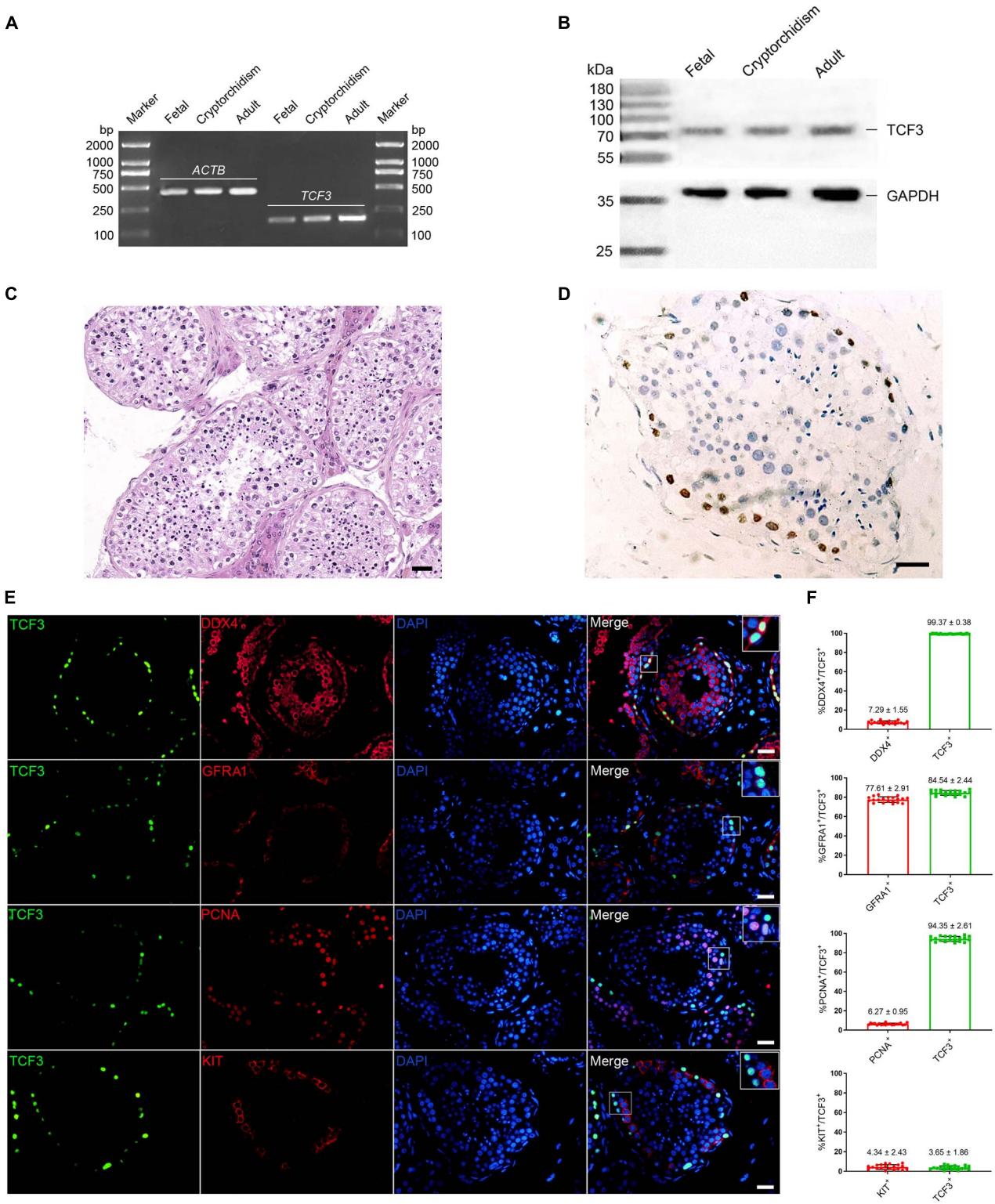

FIGURE 1 | The expression of TCF3 in human testes. **(A)** RT-PCR showed *TCF3* mRNA in human fetal, cryptorchidism, and adult testes. *ACTB* served as the loading control of total RNA. **(B)** Western blotting illustrated the expression of TCF3 protein in human fetal, cryptorchidism, and adult testes. GAPDH was used as the loading control of total protein. **(C,D)** Immunohistochemistry revealed cellular localization of TCF3 in human testis with normal spermatogenesis. **(E)** Double immunostaining showing the co-expression of TCF3 with DDX4, GFRA1, KIT, and PCNA in human testis with normal spermatogenesis. At least 20 seminiferous tubules were counted. **(F)** Percentages of $TCF3^{+}$ cells with DDX4, GFRA1, PCNA, and KIT expression. Scale bars: **(C–E)**, 50 μm.

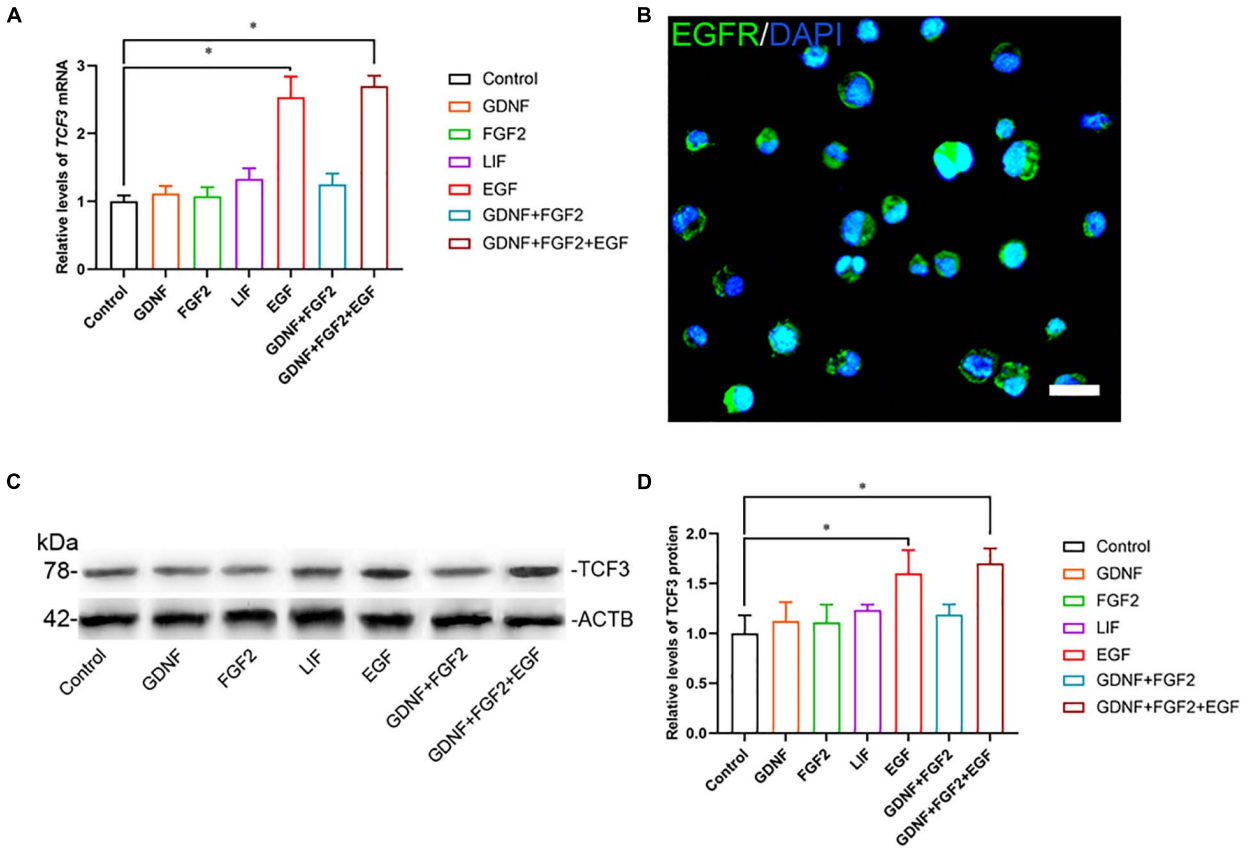

FIGURE 2 | The effect of growth factors GDNF, FGF2, LIF, and EGF on TCF3 expression. **(A)** qPCR assessment of mRNA levels of *TCF3* by growth factors GDNF, FGF2, LIF, and EGF in human SSC line. **(B)** Immunofluorescence showed the presence of EGFR in human SSC line. **(C,D)** Western blotting displayed TCF3 levels by several growth factors. Scale bar: **(B)**, 20 μm. *$p < 0.05$ indicated the significant differences between the growth factor and the control.

ChIP PCR primers. The sequences of the primers are shown in **Supplementary Table 4**.

Statistical Analysis

Descriptive and statistical analyses were implemented in the GraphPad Prism 8.0 (GraphPad software, CA, United States). Each experiment was replicated three times, and all values are presented as the mean ± SD. The *t*-test was employed to calculate the statistical difference between two groups, and the $p < 0.05$ was considered the statistical significance.

RESULTS

TCF3 Is Primarily Expressed in Human Spermatogonial Stem Cells

We first examined TCF3 expression in human fetal and adult testes. RT-PCR and western blots revealed that *TCF3* transcript (**Figure 1A**) and TCF3 protein (**Figure 1B**) were detected in both fetal and adult testes. In fetal testes, most of the gonocytes (precursors of spermatogonia) expressed TCF3. TCF3 expression was more frequently found in DDX4-positive cells than KIT-positive cells, and only 24.19% of TCF3-expressing cells have proliferation ability, as evidenced by the $PCNA^+$ cells (**Supplementary Figure 1**). In normal adult human testes (**Figure 1C**), TCF3 was expressed in the nuclei of spermatogonia along the basement membrane of the seminiferous tubules (**Figure 1D**). Immunofluorescence further showed that 99.37% of TCF3-expressing cells were DDX4-positive germ cells and 84.5% of TCF3-expressing cells were GFRA1-positive spermatogonia. TCF3 was barely found in the KIT-expressing cells. Interestingly, PCNA was found in 94.35% of TCF3-expressing cells (**Figures 1E,F**), which suggests that TCF3 may be involved in cell proliferation in human adult testes. Together, these data implicate that TCF3 is primarily expressed in human SSCs with proliferation potential.

To explore the function and mechanism of TCF3 protein, the human SSC line was utilized. We checked the identity of the human SSC line, and it expressed numerous markers for human primary SSCs, including GFRA1, PLZF, VASA, GPR125, UCHL1, RET, and THY1 (**Supplementary Figures 2A–C**). Additionally, some hallmarks for human Sertoli cells, including GATA4 and SOX9, were not detected in this cell line (**Supplementary Figures 2A–C**). To ascertain which growth factors regulate TCF3, GDNF, FGF2, EGF, or LIF was added to the culture medium of human SSC line. RT-PCR (**Figure 2A**) and western blots (**Figures 2C,D**) showed that EGF elevated the levels of TCF3 in human SSC line,

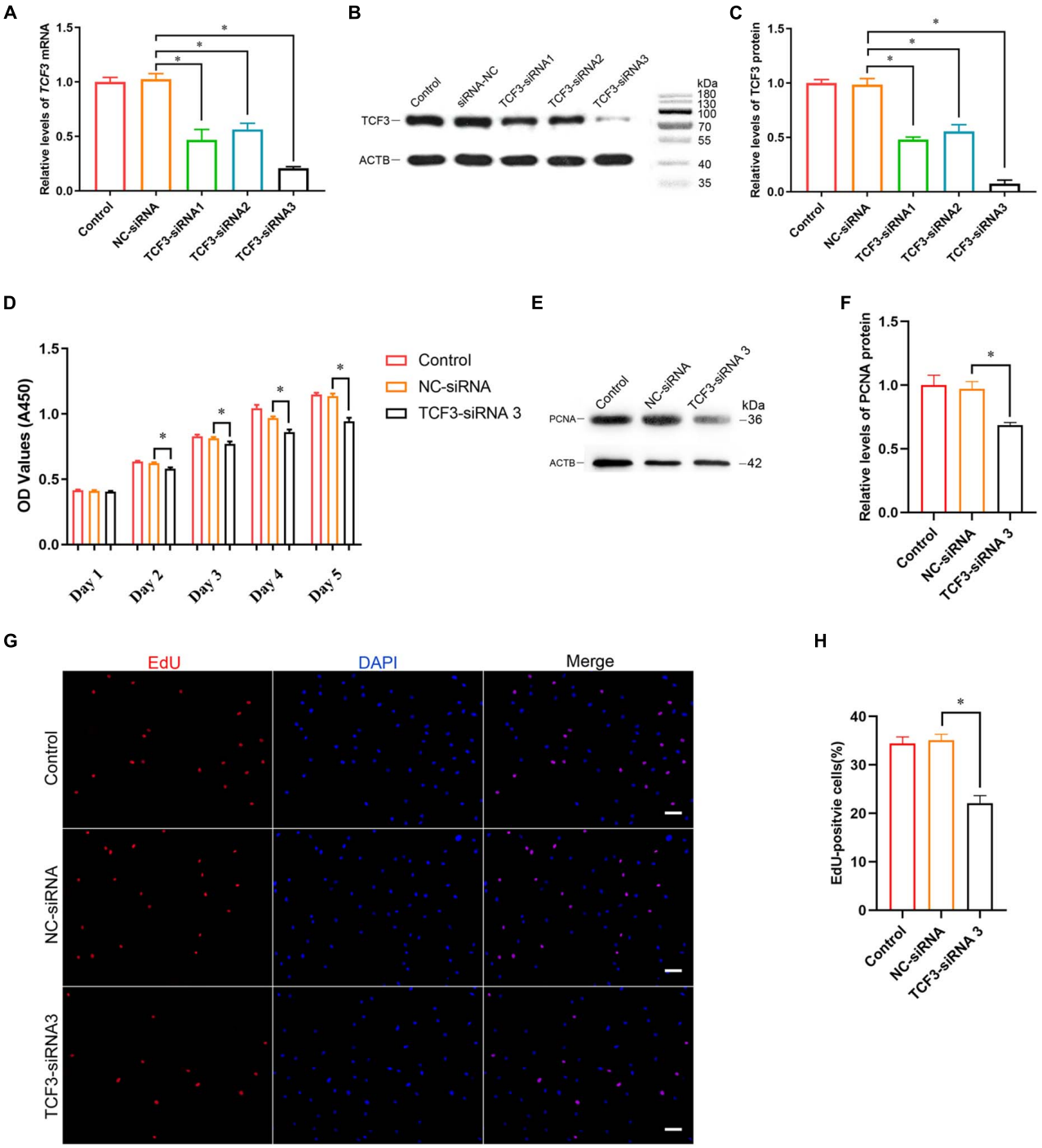

FIGURE 3 | The influence of TCF3 knockdown on human SSC line proliferation. **(A)** qPCR revealed *TCF3* mRNA expression changes in human SSC line by the TCF3-siRNA 1-, 2-, and 3. **(B,C)** Western blotting displayed TCF3 protein expression alterations in human SSC line after the transfection of TCF3-siRNA 1-, 2-, and 3. ACTB was used as the loading control of total protein. **(D)** CCK-8 assay illustrated the proliferation of human SSC line by the (NC-siRNA and TCF3-siRNA 3. **(E,F)** The relative levels of PCNA protein in human SSC line after transfection of NC-siRNA and TCF3-siRNA 3. **(G,H)** The percentages of EdU-positive cells in human SSC line influenced by NC-siRNA and TCF3-siRNA 3. Scale bars: **(G)**, 50 μm. $*p < 0.05$ denoted the significant differences between TCF3-siRNA 3 and NC-siRNA.

whereas there was no obvious difference in the levels of TCF3 by GDNF, FGF2, or LIF (**Figures 2A,C,D**). We also found the expression of EGFR in human SSC line by using immunofluorescence (**Figure 2B**). These results suggest that TCF3 was modulated by EGF rather than by LIF, FGF2, or GDNF in the human SSC line.

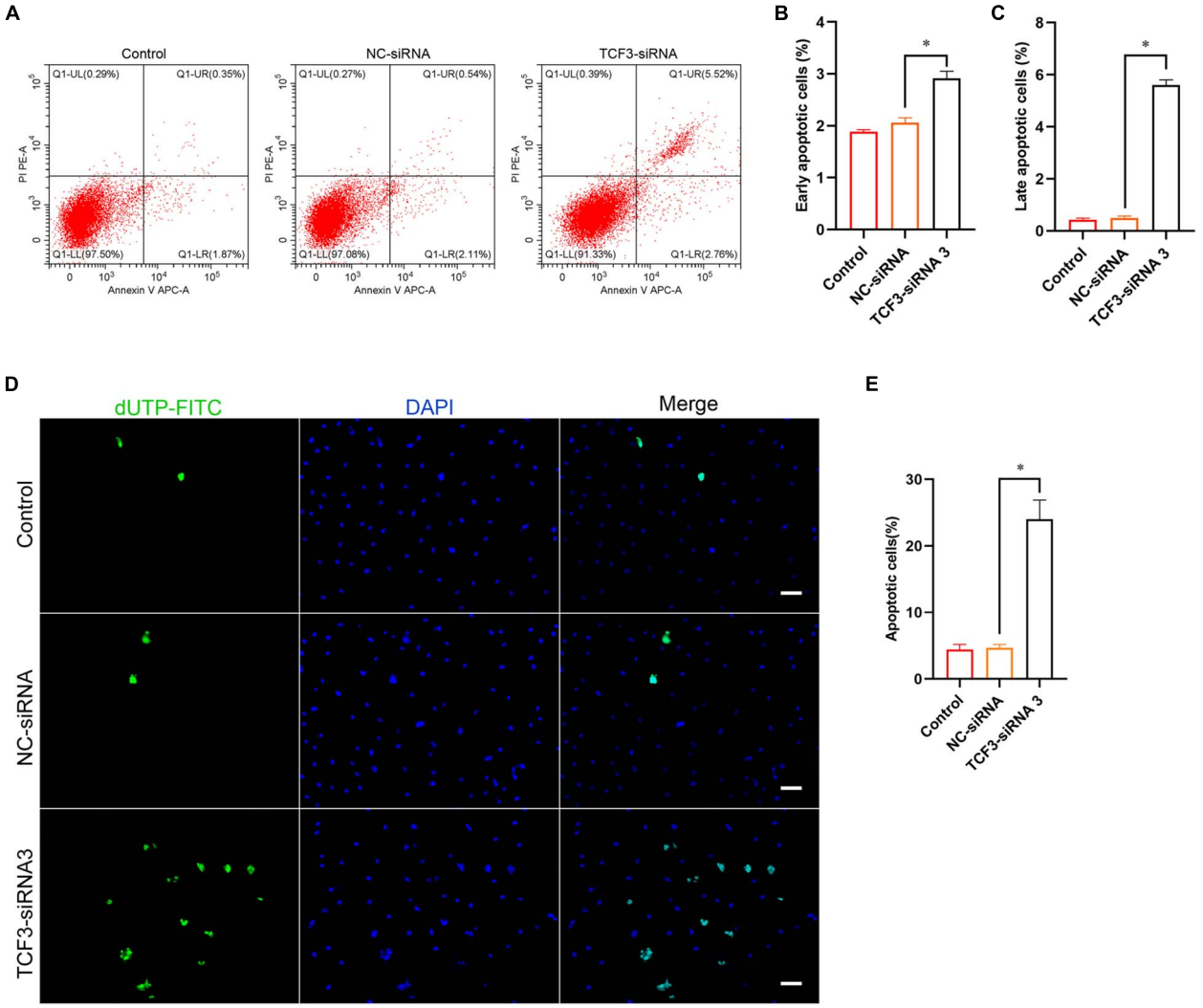

FIGURE 4 | The influence of TCF3 knockdown on the apoptosis of the human SSC cells. **(A–C)** Flow cytometric and APC Annexin V analysis of the percentages of early and late apoptosis in the human SSC line with transfection of NC-siRNA and TCF3-siRNA 3. **(D,E)** TUNEL assays of the percentages of TUNEL$^+$ cells in the human SSC line with transfection of NC-siRNA and TCF3-siRNA 3. Scale bars: **(D)**, 50 μm. *$p < 0.05$ illustrated the significant differences between TCF3-siRNA 3 and NC-siRNA.

TCF3 Knockdown Suppresses the Proliferation and Promotes the Apoptosis of Human SSC Line

To explore the effect of TCF3 knockdown on SSCs, siRNA-triggered silencing of TCF3 was carried out. RT-PCR and western blotting illustrated that the levels of TCF3 were remarkably reduced by TCF3-siRNA 1, 2, and 3, while TCF3-siRNA 3 had the best silencing effect (**Figures 3A–C**). The CCK-8 assay displayed that TCF3-siRNA 3 inhibited the proliferation of human SSC line at day 2 to 5 after siRNA transfection (**Figure 3D**). Western blotting demonstrated that PCNA (cell proliferation hallmark) level was decreased by TCF3-siRNA 3 (**Figures 3E,F**). Likewise, after transfection for 48 h, the percentages of EdU-positive cells were decreased by TCF3-siRNA 3 compared to the NC-siRNA (35.10 ± 1.21 vs. 22.12 ± 1.54%, $p < 0.05$) (**Figures 3G,H**). Considered together, these data indicate that TCF3 promotes the proliferation and DNA synthesis of human SSCs.

Furthermore, Annexin V/PI staining and flow cytometry was used to elucidate the influence of TCF3 on regulating human SSC apoptosis. The percentages of early and late apoptosis in human SSC line were enhanced by TCF3-siRNA 3 compared with the NC-siRNA (**Figures 4A–C**). Similarly, TUNEL assay showed that the percentages of TUNEL-positive cells were elevated by TCF3-siRNA 3 than NC-siRNA (**Figures 4D,E**). Taken together, these results reflect that TCF3 knockdown promotes the apoptosis of human SSC line.

Screening of TCF3 Target Genes

To seek the targeting genes of the TCF3 in human SSCs, RNA sequencing was conducted to screen the alterations in

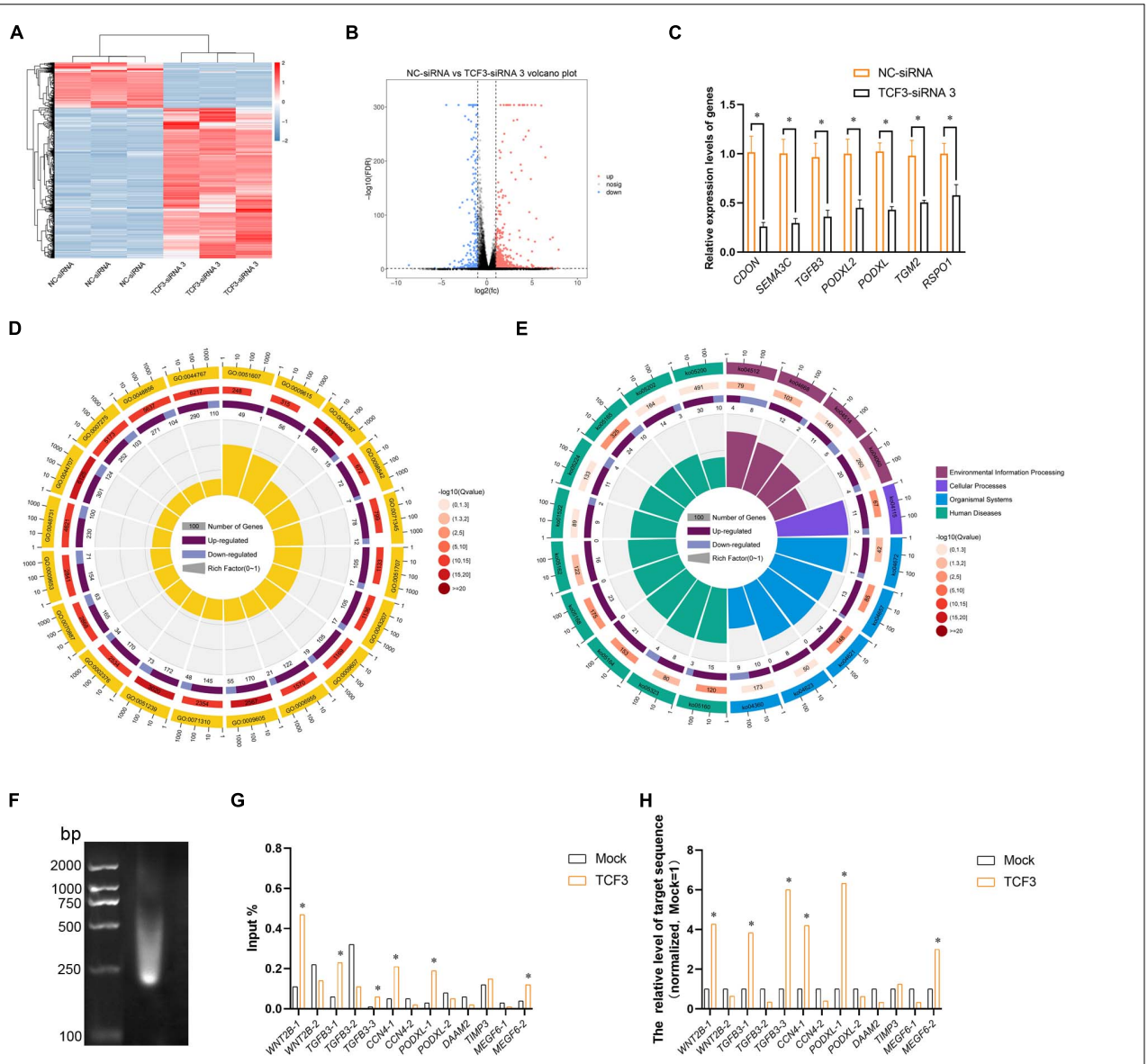

FIGURE 5 | Identification of the target genes of TCF3. **(A)** hierarchical clustering demonstrated the differentially expressed genes (DEGs) in the human SSC line between NC-siRNA and TCF3-siRNA 3. **(B)** Volcano plot illustrated the differentially expressed mRNAs. **(C)** qPCR evaluated the changes in *CDON*, *SEMA3C*, *TGFB3*, *PODXL2*, *PODXL*, *TGM2,* and *RSPO1* mRNA in the human SSC line by TCF3-siRNA 3 and the NC-siRNA. *$p < 0.05$ indicated the significant differences between TCF3-siRNA 3 and NC-siRNA. **(D)** GO circle plot illustrated the top 20 enrichment terms. First circle: GO terms of the top 20 enrichments, and outside circle was the sitting scale of the number of genes. Different colors denoted the different ontologies; the second circle: the number of DEGs was enriched in this GO term and the *Q*-value. The more genes, the longer the bar, the smaller the *Q*-value, and the red the color; the third circle: the bar chart of the proportion of DEGs, and dark purple denoted the fraction of up-regulated genes. Light purple signified the proportion of down-regulated genes, and the specific value was indicated below; the fourth circle: Rich Factor value of each GO term (the number of differences in this GO term was divided by all the numbers), background grid line, each grid indicated 0.1. **(E)** KEGG circle plot for top 20 enrichment pathways. The first circle: top 20 enriched pathways, outside circle was the coordinate scale of gene number, and different colors signified different A classes; the second circle: the number of DEGs enriched in this GO term and the *Q*-value. The more genes, the longer the bar, the smaller the *Q*-value, and the red the color; the third circle: the bar chart of the proportion of DEGs, while dark purple indicated the fraction of up-regulated genes, while light purple represented the proportion of down-regulated genes, the specific value was indicated below; the fourth circle: Rich Factor value of each pathway (the number of differences in this pathway was divided by all the numbers), background grid line, each grid denoted 0.1. **(F)** Gel electrophoresis of DNA after ultrasonication. **(G,H)** qPCR evaluation of the ChIP enriched DNA samples using specified promoter or enhancer primers. Mock, negative mouse IgG control. *$p < 0.05$ indicated the significant difference from Mock.

transcription profiles of human SSC line by TCF3-siRNA 3 or NC-siRNA. About 19,000 genes were detected in human SSC line, and the volcano plot and heat map illustrated that 680 genes were up-regulated and 207 genes were down-regulated by TCF3-siRNA 3 (**Figures 5A,B**). To verify the results of RNA sequencing, a number of randomly chosen genes, including

CDON, *SEMA3C*, *TGFB3*, *PODXL2*, *PODXL*, *TGM2*, and *RSPO1*, were determined by RT-PCR (**Figure 5C**), showing that and the results of these genes was consistent with RNA sequencing. GO and KEGG analyses (**Figures 5D,E**) demonstrated that the DEGs, including *MEGF6*, *SEMA3C*, *WNT2B*, *RPP25*, *TGFB3*, and *PODXL* (**Table 1**), were involved in numerous types of biological process and signaling pathways, which are critical for cell proliferation and survival.

TCF3 is a transcription factor of bHLH family, which can directly bind to promoter regions to regulate gene transcription. In order to identify the targeting genes which are directly regulated by TCF3, ChIP assay, and RT-PCR were performed. We predicted the binding sites of the genes, including *MEGF6*, *WNT2B*, *TGFB3*, *CCN4*, *PODXL*, *DAAM2*, and *TIMP3*, whose expression levels were down-regulated by TCF3-siRNA 3, using JasparDatabase (Fornes et al., 2020), and we designed primers of these genes (**Supplementary Table 4**) for the DNA sequences near the binding sites. We found that the promoter sequence of *WNT2B*, *TGFB3*, *CCN4*, *MEGF6*, and *PODXL* were significantly enriched (**Figures 5F–H**), and TCF3 protein can directly bind to the promoter regions of those genes to regulate their transcription.

PODXL Is a Direct Target of TCF3 in Human SSCs

Podocalyxin-like protein is a member of CD34 family proteins, which carries numerous post-translational epitopes responsible for various kinds of pluripotent surface biomarkers, including TRA-1-60, mAb84, TRA-1-81, GP200, and GCTM2 (Kang et al., 2016). It is also associated with more than 10 human malignancies (Kang et al., 2016; He et al., 2020). These studies suggest that PODXL may be responsible for the impaired proliferative activity of SSC by TCF3 silencing. To confirm this hypothesis, siRNA-mediated knockdown of PODXL was performed. RT-PCR and western blotting illustrated that *PODXL* mRNA and PODXL protein were reduced by all three types of PODXL-siRNA in the human SSC line, and PODXL-siRNA 3 had the most silencing effect (**Figures 6A–C**). CCK8 assay and EdU assay revealed that PODXL-siRNA 3 repressed human SSC proliferation, and the level of PCNA protein was reduced by PODXL-siRNA 3 (**Figures 6D–H**). Furthermore, flow cytometry and TUNEL assay demonstrated that the apoptosis was reduced by PODXL silencing in human SSC line (**Figures 6I–M**). Collectively, these data imply that PODXL knockdown represses the proliferation and DNA synthesis and promotes the apoptosis in human SSCs and that PODXL is a direct downstream target of TCF3 in human SSCs.

TABLE 1 | Top 20 down-regulated genes by TCF3-siRNA 3.

Ensembl gene ID	Genes	NC-siRNA	TCF3-siRNA3	Fold changes
ENSG00000099958	*DERL3*	19.63	2.49	5.94
ENSG00000162591	*MEGF6*	12.41	2.92	4.17
ENSG00000075223	*SEMA3C*	19.46	4.84	4.01
ENSG00000134245	*WNT2B*	26.27	8.75	3.17
ENSG00000075213	*SEMA3A*	62.45	21.27	3.11
ENSG00000178718	*RPP25*	22.39	7.69	3.08
ENSG00000152284	*TCF3*	111.92	38.94	3.04
ENSG00000119699	*TGFB3*	29.04	10.22	3.01
ENSG00000153993	*SEMA3D*	21.96	7.82	2.98
ENSG00000131389	*SLC6A6*	160.08	57.07	2.98
ENSG00000064309	*CDON*	28.51	10.44	2.90
ENSG00000154832	*SPP1*	65.32	24.14	2.87
ENSG00000104415	*WISP1*	99.80	37.16	2.85
ENSG00000128567	*PODXL*	162.11	62.09	2.77
ENSG00000146122	*DAAM2*	28.23	11.10	2.69
ENSG00000168743	*NPNT*	11.36	4.64	2.59
ENSG00000129128	*SPCS3*	49.48	20.23	2.58
ENSG00000149573	*MPZL2*	15.18	6.32	2.53
ENSG00000100234	*TIMP3*	239.50	100.71	2.50
ENSG00000147883	*CDKN2B*	46.95	19.82	2.49

Gene expression values were represented by FPKM.

TCF3 Aberrant Expression Is Associated With Spermatogenesis Failure

NOA is a serious condition affecting male fertility. NOA with spermatogenesis failure can be classified into numerous subtypes, namely Std MA (spermatids maturation arrest), Spc MA, Spg MA (spermatogonia maturation arrest), SCOS (Sertoli cell only syndrome), and HS (hypo-spermatogenesis). To investigate the relation of TCF3 expression and spermatogenesis failure, testis tissues from 12 patients were subjected to histopathological analysis (**Supplementary Figures 3A–L**). We examined TCF3 expression in all testis samples, and western blotting illustrated that the level of TCF3 protein was significant lower in human testis tissues of Spg MA and Spc MA than OA patients, while the level of TCF3 was not significantly decreased in patients with Std MA and HS compared to OA patients (**Figures 7A,B**). Double immunohistochemistry demonstrated that the frequency of TCF3-expressing cells in UCHL1-positive SSCs was decreased in Spg MA and Spc MA (**Figures 7C,D**) when compared to OA patients with normal spermatogenesis. Together, these data reflect that TCF3 aberrant expression is related to maturation arrest at spermatocyte and spermatogonial stages of spermatogenesis.

DISCUSSION

Due to the limited availability of human testicular tissues and no effective approach of culturing and expanding human primary human SSCs, the research on human SSCs is seriously hindered. Human SSC line established by us can solve these problems, since it has an unlimited proliferation potential and the high safety, and thus this cell line is suitable for uncovering the molecular mechanism in modulating the fate decisions of human SSCs (Hou et al., 2015). It has been reported that TCF3 plays vital roles in the regulation of numerous stem cells or progenitors (Semerad et al., 2009; Pfurr et al., 2017; Yamazaki et al., 2018). Most of the phenotypes of TCF3 deficiency are linked to cell proliferation, differentiation, or death. Nevertheless, the impact of TCF3 on

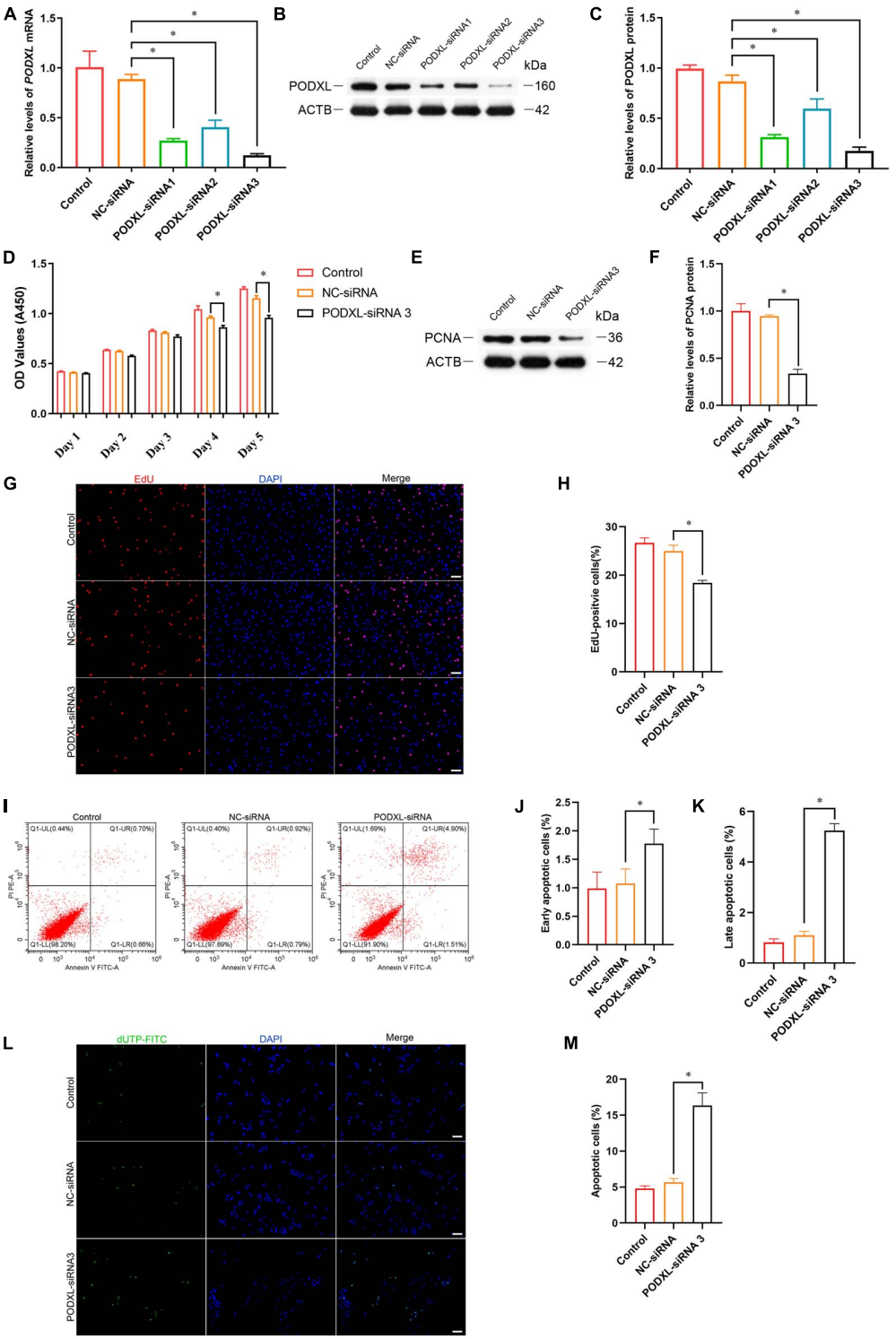

FIGURE 6 | The effect of PODXL knockdown on the proliferation and apoptosis of the human SSC line. **(A)** qPCR assessment of *PODXL* mRNA in the human SSC line transfection with TCF3-siRNA 1-, 2-, and 3. *ACTB* was used for the normalization. **(B,C)** Western blotting showed PODXL proteins in the human SSC line by the PODXL-siRNA 1-, 2-, and 3 treatment. **(D)** CCK-8 assay illustrated the proliferation of in the human SSC line by NC-siRNA and PDOXL-siRNA3 treatment. **(E,F)** Western blotting revealed the PCNA protein levels in the human SSC line by the PODXL-siRNA 3 and NC-siRNA transfection. **(G,H)** EdU assays of DNA synthesis in the human SSC line with the NC-siRNA and PODXL-siRNA3 transfection. **(I–K)** Flow cytometric and APC Annexin V analysis of the proportions of early and late apoptosis in the human SSC line with the NC-siRNA and PODXL-siRNA3 transfection. **(L,M)** TUNEL assay of the fractions of TUNEL$^+$ cells in the human SSC line affected by the NC-siRNA and PODXL-siRNA3. Scale bars: **(G,L)**, 50 μm. *$p < 0.05$ denoted the significant differences between PODXL-siRNA 3 and NC-siRNA.

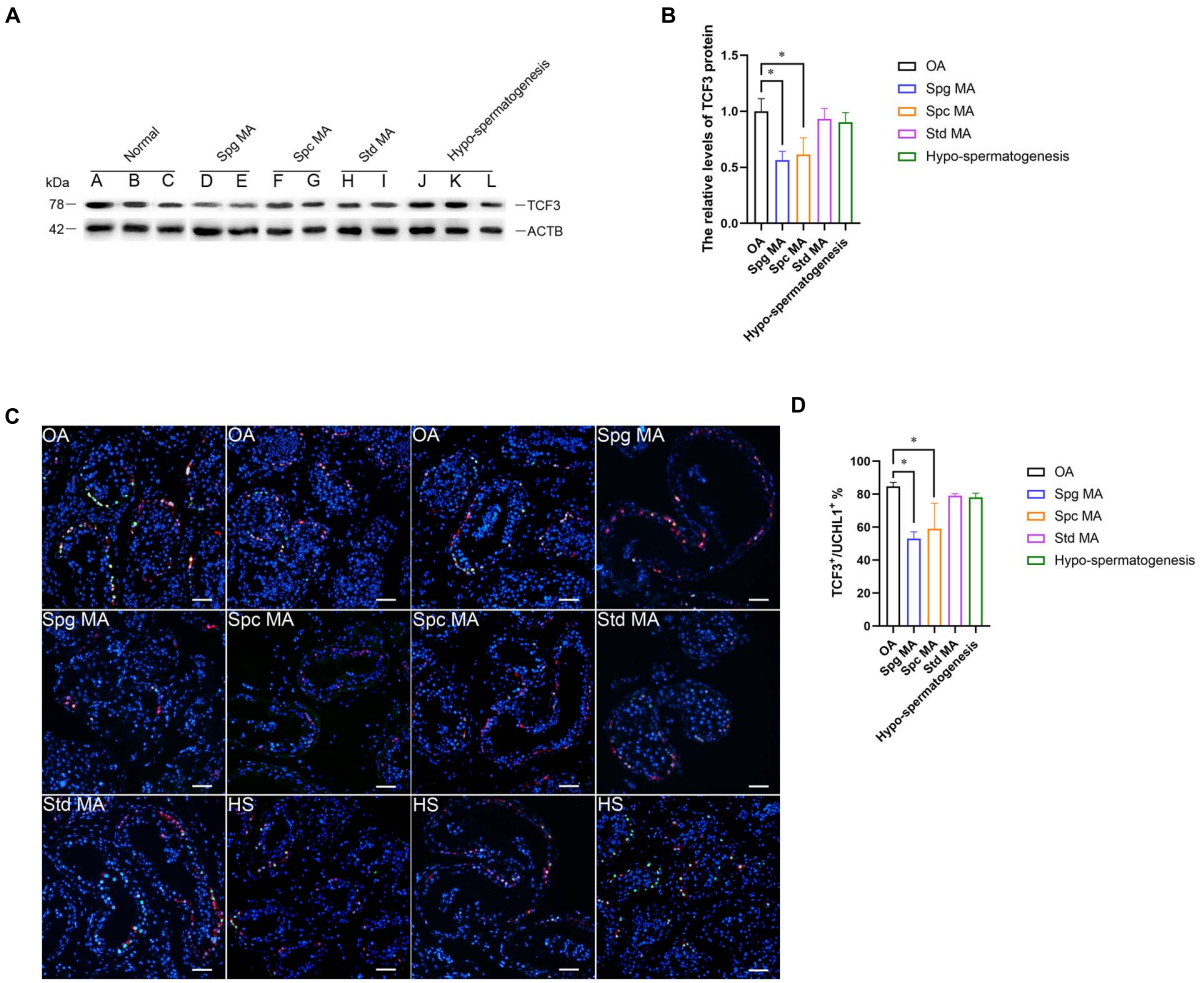

FIGURE 7 | The expression of TCF3 in the testis of OA patients and NOA patients. **(A,B)** Western blotting compared the levels of TCF3 protein between OA and NOA patients. Notes in **(A)**: sample A, B, and C were individuals with OA with normal spermatogenesis; sample D and E were NOA patients with Spg MA; sample F and G were NOA patients with Spc MA; sample H and I were NOA patients with Std MA; and sample J, K, and L were NOA patients with HS. **(C,D)** The percentages of UCHL-positive SSCs with TCF3 expression between OA and various kinds of NOA patients. Scale bars: **(C)**, 100 μm. *$p < 0.05$ indicated the significant differences between OA patients with normal spermatogenesis and NOA patients.

stem cell self-renewal seems to depend on the cell types. In human testes, we revealed that TCF3 was primarily or specifically expressed in self-renewing SSCs ($GFRA1^+/KIT^-$), which was consistent with the finding, by the single cell sequencing, that TCF3 is expressed in cells at States 0 and 1 with a high similarity to infant SSCs or SSEA4-positive adult SSCs, respectively (Guo et al., 2018). We also found that *TCF3* mRNA was up-regulated by EGF, EGF promotes cell proliferation *via* RAS or PI3K pathway (Margolis and Skolnik, 1994; Sabbah et al., 2020), which are key pathways regulating the self-renewal of SSCs in rodents (Kanatsu-Shinohara and Shinohara, 2013), but the precise functions and mechanisms in human spermatogonia are yet to be defined. The leydig cells are the principal source of EGF in the testis, germ cells also produce EGF at the onset of sexual maturation and spermatogenesis (Wald, 2005). Our work will help to explain how the microenvironment support SSC self-renewal and the importance of the cell crosstalk.

Significantly, we demonstrated that TCF3 stimulated the proliferation and DNA synthesis of human SSCs, whereas it inhibited the apoptosis of human SSCs, which would be helpful to expand human SSCs *in vitro* to obtain sufficient cells for basic research and translational application of human SSCs. By RNA sequencing and ChIP assays, we revealed that TCF3 protein regulated the transcription of several genes, including *WNT2B*, *TGFB3*, *CCN4*, *MEGF6*, and *PODXL*. Interestingly, CDH1, which is a target of TCF3 in ESCs (Yamazaki et al., 2018) and it can regulate the self-renewal through cell adhesion of mouse SSCs (Tokuda et al., 2007), was not significantly decreased by TCF3 siRNA in human SSC line, which indicates that CDH1 is not a target for TCF3 in human SSCs. Other genes involved in cell adhesion, including *CDH3*, *PCDH7*, *TGM2*, and *PODXL*, were significantly reduced by TCF3 siRNA in human SSC line. Those data suggest that TCF3 may influence the adhesion of human SSCs *via* different downstream targets

compared to ESCs. It has been shown that PODXL is a pluripotent surface marker and enriched in many cancer cells (He et al., 2020), PODXL positive hematopoietic stem cells can reconstitute myeloid and lymphoid lineages in recipients with lethal radiation (Doyonnas et al., 2005). PODXL promotes cancer development and aggressiveness by activating MAPK and PIK3 pathways. Those evidences indicates that PODXL may be related to stemness and cell proliferation. E- and L-selectin were reported as functional ligands in cancer cells, but we are not sure whether L- or E-selectin can promote SSC proliferation through PODXL. We observed that PODXL silencing compromised the stem cell activity of human SSCs, the roles of other candidate target genes of TCF3 need to be further explored. TGFB3 is a TGF-β (transforming growth factor-beta) family member. TGF-β members are multifunctional cytokines, which participate in the modulation of numerous biological processes, namely cell proliferation, survival, and differentiation (Young et al., 2015). TGFB3 is believed to modulate BTB (blood-testis barrier) dynamics by promoting the endocytosis of integral membrane proteins and their intracellular degradation (Wong et al., 2010), which may be associated with male infertility (Drożdzik et al., 2015). Given that TGFB3 stimulates adipocyte progenitor proliferation (Petrus et al., 2018), it is possible that TGFB3 may also affect spermatogenesis by regulating the proliferation of SSCs. Interestingly, it has been shown that the suppression of the TGFB1 receptor enhances spermatogonial proliferation and spermatogenesis (Moraveji et al., 2019). WNT2B is a ligand of the frizzled family and functions in the canonical Wnt/beta-catenin signaling pathway (Goss et al., 2009), the effect of WNT2B deletion was not as obvious as that of PODXL (data not shown). Although Wnt/β-catenin signaling pathway has been proved to promote the differentiation of in mouse SSCs (Tokue et al., 2017), as a secretory protein, WNT2B may help for our understanding of crosstalk between spermatogonia. SLC6A6 is a transporter of taurine and beta-alanine, which is critical for material transport and energy metabolism (Han et al., 2006), although we did not find evidence that TCF3 could bind to the promoter region of SLC6A6, we are interested in the functions of SLC6A6 in spermatogenesis, it may provide cues to understand the energy metabolism of SSCs.

The TCF3 protein was initially discovered in B-cells as immunoglobulin enhancer binding proteins (Rutherford and LeBrun, 1998); it has a core role in the transcriptional modulator networks that the enhance commitment and differentiation of the B and T cell lineages, and their role in these lineages is regulated by inhibitor of DNA binding (ID) proteins. TCF3 protein can dimerize with any of the four ID proteins (ID1-ID4) (Kee, 2009), and the stimulation of ID3 expression in T cells antagonizes the DNA binding activity of TCF3. Moreover, it is suggested that ID4 is a distinguishing marker of SSCs in the mammalian germline and it modulates the self-renewal of SSCs (Oatley et al., 2011; Chan et al., 2014). Given that TCF3 proteins can dimerize with ID4, and both TCF3 and ID4 are expressed selectively by SSCs, it is possible that TCF3 and ID4 orchestrate the SSCs fate determination and maintain the stem cell pool. Nevertheless, the interactions between TCF3 and ID proteins in SSCs remain to be explored further, while our results provide clues for understanding the functions of ID4 and TCF3.

We have also illustrated that the expression level of TCF3 was reduced in NOA patients, especially in patients with maturation arrest at spermatogonial and spermatocyte stages. Consistent with our observations, a transcription profiling data of human spermatogenic failure also reveals that *TCF3* is down-regulated in spermatogonial maturation arrest and SCOS patients (Spiess et al., 2007); but there is no significant difference in spermatocyte arrest patients (Spiess et al., 2007). We found that there might be the correlation between TCF3 low level and spermatogenic failure. Thus, it would be interesting to establish animal models to further determine whether the deficiency of TCF3 will cause spermatogenesis failure and male infertility.

CONCLUSION

In summary, we have demonstrated, for the first time, that TCF3 is primarily expressed in human SSCs and that it mediates the proliferation, DNA synthesis, and apoptosis of human SSCs. We also unveil an association between TCF3 expression and spermatogenesis failure. Furthermore, we reveal that TCF3 is regulated by EGF and PODXL is a target of TCF3 in human SSCs. Therefore, this study provides novel genes and regulators in modulating the fate determinations of human SSCs. This study is of particular significance since it could offer new targets for gene therapy of male infertility.

DATA AVAILABILITY STATEMENT

The original contributions presented in the study are included in the article/**Supplementary Material**, further inquiries can be directed to the corresponding authors.

ETHICS STATEMENT

This study was approved by the Ethics Committee of the Reproductive & Genetic Hospital of CITIC-Xiangya, Basic Medical Science School, Central South University (LL-SC-2017-015). The patients/participants provided their written informed consent to participate in this study.

AUTHOR CONTRIBUTIONS

LF and ZuH designed the study and supervised the laboratory experiments. DZ conducted the experiments and drafted the manuscript. JF, ZL, RT, XW, HB, FZ, XZ, ZeH, LX, and KT assisted with the experiments and sample collection. HN, HaZ, HuZ, and WZ performed the analysis with constructive discussion and

contributed analysis tools. All authors contributed to the article and approved the submitted version.

FUNDING

This work was supported by the grants from the National Key Research and Development Program of China (2016YFC1000600), Major Scientific and Technological Projects for Collaborative Prevention and Control of Birth Defect in Hunan Province (2019SK1012), Hunan Provincial Grant for Innovative Province Construction (2019SK4012), and Key Grant of Research and Development in Hunan Province (2020DK2002).

SUPPLEMENTARY MATERIAL

The Supplementary Material for this article can be found online at: https://www.frontiersin.org/articles/10.3389/fcell.2021.695545/full#supplementary-material

REFERENCES

Anderson, E. L., Baltus, A. E., Roepers-Gajadien, H. L., Hassold, T. J., de Rooij, D. G., van Pelt, A. M. M., et al. (2008). Stra8 and its inducer, retinoic acid, regulate meiotic initiation in both spermatogenesis and oogenesis in mice. *Proc. Natl. Acad. Sci. U.S.A.* 105, 14976–14980. doi: 10.1073/pnas.0807297105

Ashburner, M., Ball, C. A., Blake, J. A., Botstein, D., Butler, H., Cherry, J. M., et al. (2000). Gene ontology: tool for the unification of biology. The gene ontology consortium. *Nat. Genet.* 25, 25–29.

Bohrer, C., Pfurr, S., Mammadzada, K., Schildge, S., Plappert, L., Hils, M., et al. (2015). The balance of Id3 and E47 determines neural stem/precursor cell differentiation into astrocytes. *EMBO J.* 34, 2804–2819. doi: 10.15252/embj.201591118

Carlomagno, G., van Bragt, M. P. A., Korver, C. M., Repping, S., de Rooij, D. G., and van Pelt, A. M. M. (2010). BMP4-induced differentiation of a rat spermatogonial stem cell line causes changes in its cell adhesion properties. *Biol. Reprod.* 83, 742–749. doi: 10.1095/biolreprod.110.085456

Carrieri, C., Comazzetto, S., Grover, A., Morgan, M., Buness, A., Nerlov, C., et al. (2017). A transit-amplifying population underpins the efficient regenerative capacity of the testis. *J. Exp. Med.* 214:1631.

Chan, F., Oatley, M. J., Kaucher, A. V., Yang, Q. E., Bieberich, C. J., Shashikant, C. S., et al. (2014). Functional and molecular features of the Id4+ germline stem cell population in mouse testes. *Genes Dev.* 28, 1351–1362. doi: 10.1101/gad.240465.114

Chen, S., Zhou, Y., Chen, Y., and Gu, J. (2018). fastp: an ultra-fast all-in-one FASTQ preprocessor. *Bioinformatics* 34, i884–i890. doi: 10.1093/bioinformatics/bty560

Clermont, Y. (1966). Spermatogenesis in man. A study of the spermatogonial population. *Fertil Steril* 17, 705–721.

Di Persio, S., Saracino, R., Fera, S., Muciaccia, B., Esposito, V., Boitani, C., et al. (2017). Spermatogonial kinetics in humans. *Development* 144, 3430–3439. doi: 10.1242/dev.150284

Doyonnas, R., Nielsen, J. S., Chelliah, S., Drew, E., Hara, T., Miyajima, A., et al. (2005). Podocalyxin is a CD34-related marker of murine hematopoietic stem cells and embryonic erythroid cells. *Blood* 105, 4170–4178.

Droździk, M., Kaczmarek, M., Malinowski, D., Broś, U., Kazienko, A., Kurzawa, R., et al. (2015). TGFβ3 (TGFB3) polymorphism is associated with male infertility. *Sci. Rep.* 5:17151. doi: 10.1038/srep17151

Fornes, O., Castro-Mondragon, J. A., Khan, A., van der Lee, R., Zhang, X., Richmond, P. A., et al. (2020). JASPAR 2020: update of the open-access database of transcription factor binding profiles. *Nucleic Acids Res.* 48, D87–D92. doi: 10.1093/nar/gkz1001

Ghyselinck, N. B., Vernet, N., Dennefeld, C., Giese, N., Nau, H., Chambon, P., et al. (2006). Retinoids and spermatogenesis: lessons from mutant mice lacking the plasma retinol binding protein. *Dev. Dyn.* 235, 1608–1622.

Goss, A. M., Tian, Y., Tsukiyama, T., Cohen, E. D., Zhou, D., Lu, M. M., et al. (2009). Wnt2/2b and beta-catenin signaling are necessary and sufficient to specify lung progenitors in the foregut. *Dev. Cell* 17, 290–298. doi: 10.1016/j.devcel.2009.06.005

Guo, J., Grow, E. J., Mlcochova, H., Maher, G. J., Lindskog, C., Nie, X., et al. (2018). The adult human testis transcriptional cell atlas. *Cell Res.* 28, 1141–1157. doi: 10.1038/s41422-018-0099-2

Guo, J., Grow, E. J., Yi, C., Mlcochova, H., Maher, G. J., Lindskog, C., et al. (2017). Chromatin and single-cell RNA-seq profiling reveal dynamic signaling and metabolic transitions during human spermatogonial stem cell development. *Cell Stem Cell* 21, 533–546e536. doi: 10.1016/j.stem.2017.09.003

Han, X., Patters, A. B., Jones, D. P., Zelikovic, I., and Chesney, R. W. (2006). The taurine transporter: mechanisms of regulation. *Acta Physiol.* 87, 61–73.

Hara, K., Nakagawa, T., Enomoto, H., Suzuki, M., Yamamoto, M., Simons, B. D., et al. (2014). Mouse spermatogenic stem cells continually interconvert between equipotent singly isolated and syncytial states. *Cell Stem Cell* 14, 658–672. doi: 10.1016/j.stem.2014.01.019

He, S., Du, W., Li, M., Yan, M., and Zheng, F. (2020). PODXL might be a new prognostic biomarker in various cancers: a meta-analysis and sequential verification with TCGA datasets. *BMC Cancer* 20:620. doi: 10.1186/s12885-020-07108-5

He, Z., Jiang, J., Kokkinaki, M., Golestaneh, N., Hofmann, M. C., and Dym, M. (2008). GDNF Induces CREB-1, ATF-1, and CREM-1 phosphorylation and up-regulates c-fos transcription via the Ras/ERK1/2 pathway to promote mouse spermatogonial stem cell proliferation. *Stem Cells* 26:266.

He, Z., Kokkinaki, M., Jiang, J., Dobrinski, I., and Dym, M. (2010). Isolation, characterization, and culture of human spermatogonia. *Biol. Reprod.* 82, 363–372. doi: 10.1095/biolreprod.109.078550

Hermann, B. P., Sukhwani, M., Hansel, M. C., and Orwig, K. E. (2010). Spermatogonial stem cells in higher primates: are there differences to those in rodents? *Reproduction* 139:479.

Hermann, B. P., Sukhwani, M., Simorangkir, D. R., Chu, T., Plant, T. M., and Orwig, K. E. (2009). Molecular dissection of the male germ cell lineage identifies putative spermatogonial stem cells in rhesus macaques. *Hum. Reprod.* 24, 1704–1716.

Hou, J., Niu, M., Liu, L., Zhu, Z., Wang, X., Sun, M., et al. (2015). Establishment and characterization of human germline stem cell line with unlimited proliferation potentials and no tumor formation. *Sci. Rep.* 5:16922. doi: 10.1038/srep16922

Ikami, K., Tokue, M., Sugimoto, R., Noda, C., Kobayashi, S., Hara, K., et al. (2015). Hierarchical differentiation competence in response to retinoic acid ensures stem cell maintenance during mouse spermatogenesis. *Development* 142, 1582–1592. doi: 10.1242/dev.118695

Imayoshi, I., and Kageyama, R. (2014). bHLH factors in self-renewal, multipotency, and fate choice of neural progenitor cells. *Neuron* 82, 9–23. doi: 10.1016/j.neuron.2014.03.018

Kanatsushinohara, M., Ogonuki, N., Inoue, K., Miki, H., Ogura, A., Toyokuni, S., et al. (2003). Long-term proliferation in culture and germline transmission of mouse male germline stem cells1. *Biol. Reprod.* 69:612.

Kanatsu-Shinohara, M., and Shinohara, T. (2013). Spermatogonial stem cell self-renewal and development. *Annu. Rev. Cell Dev. Biol.* 29, 163–187. doi: 10.1146/annurev-cellbio-101512-122353

Kanehisa, M., and Goto, S. (2000). KEGG: kyoto encyclopedia of genes and genomes. *Nucleic Acids Res.* 28, 27–30.

Kang, L., Yao, C., Khodadadi-Jamayran, A., Xu, W., Zhang, R., Banerjee, N. S., et al. (2016). The universal 3D3 antibody of human PODXL is pluripotent cytotoxic, and identifies a residual population after extended differentiation of pluripotent stem cells. *Stem Cells Dev.* 25, 556–568. doi: 10.1089/scd.2015.0321

Kee, B. L. (2009). E and ID proteins branch out. *Nat. Rev. Immunol.* 9, 175–184. doi: 10.1038/nri2507

Kim, D., Langmead, B., and Salzberg, S. L. (2015). HISAT: a fast spliced aligner with low memory requirements. *Nat. Methods* 12, 357–360. doi: 10.1038/nmeth.3317

Langmead, B., and Salzberg, S. L. (2012). Fast gapped-read alignment with Bowtie 2. *Nat. Methods* 9, 357–359. doi: 10.1038/nmeth.1923

Lin, Y. C., Jhunjhunwala, S., Benner, C., Heinz, S., Welinder, E., Mansson, R., et al. (2010). A global network of transcription factors, involving E2A, EBF1 and Foxo1, that orchestrates B cell fate. *Nat. Immunol.* 11, 635–643. doi: 10.1038/ni.1891

Lord, T., and Oatley, J. M. (2017). A revised Asingle model to explain stem cell dynamics in the mouse male germline. *Reproduction* 154, R55–R64. doi: 10.1530/REP-17-0034

Love, M. I., Huber, W., and Anders, S. (2014). Moderated estimation of fold change and dispersion for RNA-seq data with DESeq2. *Genome Biol.* 15:550.

Makela, J. A., and Hobbs, R. M. (2019). Molecular regulation of spermatogonial stem cell renewal and differentiation. *Reproduction* 158, R169–R187. doi: 10.1530/REP-18-0476

Mäkelä, J.-A., and Toppari, J. (2018). "Spermatogenic cell syncytium," in *Encyclopedia of Reproduction (Second Edition)*, ed. M. K. Skinner (Oxford: Academic Press), 124–133.

Margolis, B., and Skolnik, E. Y. (1994). Activation of Ras by receptor tyrosine kinases. *J. Am. Soc. Nephrol. JASN* 5, 1288–1299.

Moraveji, S.-F., Esfandiari, F., Taleahmad, S., Nikeghbalian, S., Sayahpour, F.-A., Masoudi, N.-S., et al. (2019). Suppression of transforming growth factor-beta signaling enhances spermatogonial proliferation and spermatogenesis recovery following chemotherapy. *Hum. Reprod.* 34, 2430–2442. doi: 10.1093/humrep/dez196

Muciaccia, B., Boitani, C., Berloco, B. P., Nudo, F., Spadetta, G., Stefanini, M., et al. (2013). Novel stage classification of human spermatogenesis based on acrosome development. *Biol. Reprod.* 89:60. doi: 10.1095/biolreprod.113.111682

Oatley, J. M., Avarbock, M. R., Telaranta, A. I., Fearon, D. T., and Brinster, R. L. (2006). Identifying genes important for spermatogonial stem cell self-renewal and survival. *Proc. Natl. Acad. Sci. U.S.A.* 103, 9524–9529.

Oatley, M. J., Kaucher, A. V., Racicot, K. E., and Oatley, J. M. (2011). Inhibitor of DNA binding 4 is expressed selectively by single spermatogonia in the male germline and regulates the self-renewal of spermatogonial stem cells in mice. *Biol. Reprod.* 85, 347–356.

Pellegrini, M., Filipponi, D., Gori, M., Barrios, F., Lolicato, F., Grimaldi, P., et al. (2008). ATRA and KL promote differentiation toward the meiotic program of male germ cells. *Cell Cycle* 7, 3878–3888.

Pertea, M., Kim, D., Pertea, G. M., Leek, J. T., and Salzberg, S. L. (2016). Transcript-level expression analysis of RNA-seq experiments with HISAT, StringTie and Ballgown. *Nat. Protoc.* 11, 1650–1667. doi: 10.1038/nprot.2016.095

Pertea, M., Pertea, G. M., Antonescu, C. M., Chang, T.-C., Mendell, J. T., and Salzberg, S. L. (2015). StringTie enables improved reconstruction of a transcriptome from RNA-seq reads. *Nat. Biotechnol.* 33, 290–295. doi: 10.1038/nbt.3122

Petrus, P., Mejhert, N., Corrales, P., Lecoutre, S., Li, Q., Maldonado, E., et al. (2018). Transforming growth factor-β3 regulates adipocyte number in subcutaneous white adipose tissue. *Cell Rep.* 25, 551–560.e5. doi: 10.1016/j.celrep.2018.09.069

Pfurr, S., Chu, Y.-H., Bohrer, C., Greulich, F., Beattie, R., Mammadzada, K., et al. (2017). The E2A splice variant E47 regulates the differentiation of projection neurons via p57(KIP2) during cortical development. *Development* 144, 3917–3931. doi: 10.1242/dev.145698

Rutherford, M. N., and LeBrun, D. P. (1998). Restricted expression of E2A protein in primary human tissues correlates with proliferation and differentiation. *Am. J. Pathol.* 153, 165–173.

Sabbah, D. A., Hajjo, R., and Sweidan, K. (2020). Review on epidermal growth factor receptor (EGFR) structure, signaling pathways, interactions, and recent updates of EGFR inhibitors. *Curr. Top. Med. Chem.* 20, 815–834. doi: 10.2174/1568026620666200303123102

Sada, A., Hasegawa, K., Pin, P. H., and Saga, Y. (2012). NANOS2 acts downstream of glial cell line-derived neurotrophic factor signaling to suppress differentiation of spermatogonial stem cells. *Stem Cells* 30, 280–291. doi: 10.1002/stem.790

Sakai, M., Masaki, K., Aiba, S., Tone, M., and Takashima, S. (2018). Expression dynamics of self-renewal factors for spermatogonial stem cells in the mouse testis. *J. Reprod. Dev.* 64, 267–275.

Semerad, C. L., Mercer, E. M., Inlay, M. A., Weissman, I. L., and Murre, C. (2009). E2A proteins maintain the hematopoietic stem cell pool and promote the maturation of myelolymphoid and myeloerythroid progenitors. *Proc. Natl. Acad. Sci. U.S.A.* 106, 1930–1935. doi: 10.1073/pnas.0808866106

Slattery, C., Ryan, M. P., and McMorrow, T. (2008). E2A proteins: regulators of cell phenotype in normal physiology and disease. *Int. J. Biochem. Cell Biol.* 40, 1431–1436.

Spiess, A.-N., Feig, C., Schulze, W., Chalmel, F., Cappallo-Obermann, H., Primig, M., et al. (2007). Cross-platform gene expression signature of human spermatogenic failure reveals inflammatory-like response. *Hum. Reprod.* 22, 2936–2946.

Sugimoto, R., Nabeshima, Y.-i, and Yoshida, S. (2012). Retinoic acid metabolism links the periodical differentiation of germ cells with the cycle of Sertoli cells in mouse seminiferous epithelium. *Mech. Dev.* 128, 610–624. doi: 10.1016/j.mod.2011.12.003

Takashima, S., Kanatsu-Shinohara, M., Tanaka, T., Morimoto, H., Inoue, K., Ogonuki, N., et al. (2015). Functional differences between GDNF-dependent and FGF2-dependent mouse spermatogonial stem cell self-renewal. *Stem Cell Rep.* 4, 489–502.

Tokuda, M., Kadokawa, Y., Kurahashi, H., and Marunouchi, T. (2007). CDH1 is a specific marker for undifferentiated spermatogonia in mouse testes. *Biol. Reprod.* 76, 130–141.

Tokue, M., Ikami, K., Mizuno, S., Takagi, C., Miyagi, A., Takada, R., et al. (2017). SHISA6 confers resistance to differentiation-promoting Wnt/beta-catenin signaling in mouse spermatogenic stem cells. *Stem Cell Rep.* 8, 561–575. doi: 10.1016/j.stemcr.2017.01.006

Wald, M. (2005). Epidermal growth factor and spermatogenesis. *J. Urol.* 174, 2089–2090.

Wong, E. W. P., Mruk, D. D., Lee, W. M., and Cheng, C. Y. (2010). Regulation of blood-testis barrier dynamics by TGF-beta3 is a Cdc42-dependent protein trafficking event. *Proc. Natl. Acad. Sci. U.S.A.* 107, 11399–11404. doi: 10.1073/pnas.1001077107

Yamazaki, T., Liu, L., Lazarev, D., Al-Zain, A., Fomin, V., Yeung, P. L., et al. (2018). TCF3 alternative splicing controlled by hnRNP H/F regulates E-cadherin expression and hESC pluripotency. *Genes Dev.* 32, 1161–1174. doi: 10.1101/gad.316984.118

Yang, Q.-E., Racicot, K. E., Kaucher, A. V., Oatley, M. J., and Oatley, J. M. (2013). MicroRNAs 221 and 222 regulate the undifferentiated state in mammalian male germ cells. *Development* 140, 280–290. doi: 10.1242/dev.087403

Yeh, J. R., Zhang, X., and Nagano, M. C. (2011). Wnt5a is a cell-extrinsic factor that supports self-renewal of mouse spermatogonial stem cells. *J. Cell Sci.* 124(Pt 14), 2357–2366. doi: 10.1242/jcs.080903

Young, J. C., Wakitani, S., and Loveland, K. L. (2015). TGF-β superfamily signaling in testis formation and early male germline development. *Semin. Cell Dev. Biol.* 45, 94–103. doi: 10.1016/j.semcdb.2015.10.029

Zhou, D., Wang, X., Liu, Z., Huang, Z., Nie, H., Zhu, W., et al. (2020). The expression characteristics of FBXW7 in human testis suggest its function is different from that in mice. *Tissue Cell* 62:101315. doi: 10.1016/j.tice.2019.101315

Zhou, Q., Nie, R., Li, Y., Friel, P., Mitchell, D., Hess, R. A., et al. (2008). Expression of stimulated by retinoic acid gene 8 (Stra8) in spermatogenic cells induced by retinoic acid: an in vivo study in vitamin A-sufficient postnatal murine testes. *Biol. Reprod.* 79, 35–42. doi: 10.1095/biolreprod.107.066795

Conflict of Interest: The authors declare that the research was conducted in the absence of any commercial or financial relationships that could be construed as a potential conflict of interest.

Publisher's Note: All claims expressed in this article are solely those of the authors and do not necessarily represent those of their affiliated organizations, or those of the publisher, the editors and the reviewers. Any product that may be evaluated in this article, or claim that may be made by its manufacturer, is not guaranteed or endorsed by the publisher.

frontiers in Cell and Developmental Biology

REVIEW
published: 30 August 2021
doi: 10.3389/fcell.2021.710292

Oocyte Competence Biomarkers Associated With Oocyte Maturation: A Review

Batara Sirait[1,2], Budi Wiweko[3,4,5], Ahmad Aulia Jusuf[6], Dein Iftitah[5] and R. Muharam[3,4,5]*

[1] Department of Obstetrics and Gynecology, Faculty of Medicine, Universitas Kristen Indonesia, Jakarta, Indonesia, [2] Morula IVF Jakarta Clinic, Jakarta, Indonesia, [3] Division of Reproductive Endocrinology and Infertility, Department of Obstetrics and Gynecology, Faculty of Medicine, Universitas Indonesia, Jakarta, Indonesia, [4] Yasmin IVF Clinic, Dr. Cipto Mangunkusumo General Hospital, Jakarta, Indonesia, [5] Human Reproductive, Infertility, and Family Planning Research Cluster, Indonesia Medical Education and Research Institute (IMERI), Faculty of Medicine, Universitas Indonesia, Jakarta, Indonesia, [6] Department of Histology, Faculty of Medicine, Universitas Indonesia, Jakarta, Indonesia

Oocyte developmental competence is one of the determining factors that influence the outcomes of an IVF cycle regarding the ability of a female gamete to reach maturation, be fertilized, and uphold an embryonic development up until the blastocyst stage. The current approach of assessing the competency of an oocyte is confined to an ambiguous and subjective oocyte morphological evaluation. Over the years, a myriad of biomarkers in the cumulus-oocyte-complex has been identified that could potentially function as molecular predictors for IVF program prognosis. This review aims to describe the predictive significance of several cumulus-oocyte complex (COC) biomarkers in evaluating oocyte developmental competence. A total of eight acclaimed cumulus biomarkers are examined in the study. RT-PCR and microarray analysis were extensively used to assess the significance of these biomarkers in foreseeing oocyte developmental competence. Notably, these biomarkers regulate vital processes associated with oocyte maturation and were found to be differentially expressed in COC encapsulating oocytes of different maturity. The biomarkers were reviewed according to the respective oocyte maturation events namely: nuclear maturation, apoptosis, and extracellular matrix remodeling, and steroid metabolism. Although substantial *in vitro* evidence was presented to justify the potential use of cumulus biomarkers in predicting oocyte competency and IVF outcomes, the feasibility of assessing these biomarkers as an add-on prognostic procedure in IVF is still restricted due to study challenges.

Keywords: oocyte competence, oocyte maturation, cumulus-oocyte complex (COC), biomarker, *in-vitro* fertilization

OPEN ACCESS

Edited by:
Francesca Elizabeth Duncan, Northwestern University, United States

Reviewed by:
Lynda K. McGinnis, University of Southern California, United States
Xiongbo Peng, Wuhan University, China

****Correspondence:***
Batara Sirait
batarasirait@gmail.com

Specialty section:
This article was submitted to Molecular and Cellular Reproduction, a section of the journal Frontiers in Cell and Developmental Biology

Received: *15 May 2021*
Accepted: *10 August 2021*
Published: *30 August 2021*

Citation:
Sirait B, Wiweko B, Jusuf AA, Iftitah D and Muharam R (2021) Oocyte Competence Biomarkers Associated With Oocyte Maturation: A Review. Front. Cell Dev. Biol. 9:710292. doi: 10.3389/fcell.2021.710292

INTRODUCTION

Controlled ovarian stimulation is a critical step of a successful IVF cycle conducted to stimulate the development of multiple follicles in the ovaries, thereby increasing the chances of harvesting viable eggs that could potentially become viable blastocysts. Depending on the patients' ovarian response status, there are a number of available ovarian stimulation protocols offered by IVF clinics. The protocols generally comprise of administering a combination of gonadotrophin analogs namely gonadotropins-releasing hormone (GnRH) agonist or antagonist, estradiol inhibitors, recombinant follicle-stimulating hormone (FSH), and luteinizing hormone (LH)

(Gallos et al., 2017). While the drug regimens hold paramount importance for IVF and have been established and refined through years of clinical practice and research, the incidence of asynchronous ovarian response persists (Braga et al., 2020). This is evident in the miscellaneous yield of abnormal, immature, and poor-quality oocytes at retrieval. Furthermore, a portion of the immature oocytes would not progress to maturity during *in vitro* culture and could not be subjected to sperm injections while the poor-quality oocytes are at risk of forming aneuploid embryos (Figueira et al., 2010; Bosch et al., 2016). Hence, oocyte quality assessment is carried out prior to syngamy as a predictive marker of oocyte competence and IVF outcomes.

To date, the oocytes quality assessment is mostly based on morphology (Wang and Sun, 2007). The morphological grading system is mainly based on extra-cytoplasmic and cytoplasmic observations, which may give insight into the nuclear and cytoplasmic maturity state (Balaban et al., 2012). A spectrum of publications has supported the relevancy of one or more of the oocyte morphological characteristics in predicting the quality of the subsequent stages of embryo development. Tilia et al. (2020) inferred that oocyte meiotic spindle morphology is correlated to embryo developmental stages and embryo ploidy and that the oocyte morphology scoring system could be useful in determining embryos competent to achieve successful pregnancy (Lazzaroni-Tealdi et al., 2015). However, the accuracy of this morphological grading method in predicting IVF outcomes is still unconvincing due to its subjectivity and the lack of correlation to the quality or competence of the oocytes (Ruvolo et al., 2013). This has led to the current trend of research which attempts to utilize more definitive molecular parameters, such as biomarkers, in outlining the predictive models for IVF outcomes.

A few studies on the transcriptomes of COC have become prominent over the years due to the ease of deriving cumulus cells without jeopardizing the conditions of the oocytes (Wyse et al., 2020). Through methodologies for genotyping and gene expression analysis mainly DNA microarray, RT-qPCR (Reverse-Transcription quantitative Polymerase Chain Reaction), and Next Generation Sequencing (NGS), a large number of vital biomarkers and their roles were unveiled. Correspondingly, complex signal transduction pathways involved in oocyte maturation were gradually assembled, heightening our understanding of the pathophysiology of immature oocytes obtained during a controlled ovarian stimulation in IVF (Chronowska, 2014). The implementation of COC biomarker analysis as an effective IVF predictor could ultimately safeguard patients' assurance throughout the program as they prepare for the next step. These biomarkers were not only anticipated to revolutionize oocyte selection in IVF but also pave attainable approaches that could improve *in vitro* maturation of oocytes, thus possibly increasing the success rate of IVF.

Findings on a total of eight biomarkers were dissected in this study (**Table 1**). These biomarkers are mainly regulatory RNA, proteins, receptors, growth factors, gap junctions, and proteases that are involved in the complex process of oocyte maturation. Most prospective studies are selected with subjects of discussion being the evidence-based breakthroughs of these biomarkers as possible prognostic indicators for an IVF cycle (**Figure 1**). Notably, some biomarkers have different or interconnected modes of action in regulating oocyte maturation and are hereby assorted based on the processes that they associate with during oocyte maturation.

OOCYTE NUCLEAR MATURATION

Nuclear maturation that is characterized by germinal vesicle breakdown denotes the continuation of meiosis I division from prophase I to metaphase II. The majority of intra-ovarian oocytes are arrested at prophase I due to the low activity of maturation promoting factors (MFP), which consist of two sub-unit proteins namely cyclin-dependent kinase 1 (CDK1) and Cyclin B1. Physiologically, low activity of intra-oocyte MPF is instigated by the presence of adenosine monophosphate (cAMP) produced by intra-follicular somatic cells or the oocytes itself (Edry et al., 2006), and cyclic guanosine monophosphate (cGMP) produced by follicular somatic cells (Norris et al., 2009). Both of these molecules are transported into the oocyte via gap junctions. cAMP prevents the activation of CDK1 through the protein kinase A (PKA) signaling pathway, while a high concentration of cGMP inhibits the degradation of cAMP by phosphodiesterase PDE3A enzyme. The inhibitory actions of the signaling molecules altogether ensue the low MPF activity that in turn leads to maturation arrest (Adhikari and Liu, 2014). Luteinizing hormone (LH) plays a significant role in counteracting the inhibitory signaling molecules by restricting the translation of Cx-43 protein, which is an essential backbone protein for the construction of gap-junction (Kalma et al., 2004). Diminished expression of Cx-43 protein alters cell-to-cell communication between intrafollicular somatic cells leading to the low levels of intra-oocyte cAMP and cGMP; thus, inducing the continuation of meiosis prophase I up till the metaphase II arrest. At this stage, oocyte nuclear maturity is discernible by the presence of the first polar body and the emergence of a meiotic spindle that is otherwise not observed in immature oocytes.

LH is engaged in regulating the expression of specific genes that concern the EGF (Epidermal Growth Network) and gap junction permeability to achieve nuclear maturation and finally oocyte competency prior to fertilization (Conti et al., 2012). LH receptor (LHR) plays a central role in the stimulating mechanism of the hormone and the availability of the G-protein coupled LH receptors in human granulosa cells make it a valuable biomarker for oocytes nuclear maturation. Findings by Maman et al. (2012) describe that LHR mRNA is expressed higher in granulosa cells of mature oocytes than granulosa cells of immature oocytes, metaphase 1, and germinal vesicle oocytes, but higher expression of LHR mRNA was found to be associated with decreased fertilization rate. Moreover, Wiweko et al. (2019) investigated the expression of LHR mRNA on oocyte maturation and fertilization rate of two groups of IVF patients, namely poor responders, and non-poor responders. The results indicated that the LHR mRNA relative value was higher but not significant in poor responders compared to non-poor responders. Furthermore, the expression of LHR mRNA had a positive correlation with oocyte maturity and fertilization

TABLE 1 | Summary table of eight cumulus biomarkers and their significance in assessing oocyte development competency and/or IVF outcomes.

Authors	Biomarkers	Oocyte maturation event	Detection method	Sample size	Key findings
Maman et al. (2012)	LHR	Nuclear maturation	RT-PCR	Granulosa cells from 70 IVF patients and 20 IVM (*in vitro* Maturation) patients	Expression of LHR is higher in metaphase II oocytes than in metaphase I and germinal vesicle oocytes ($P < 0.05$), but overexpression is associated with low fertilization capacity ($P < 0.05$)
Wiweko et al. (2019)	LHR		RT-PCR	Granulosa cells from 10 poor responder IVF patients and 20 non-poor responder patients	In poor responders: Positive correlation of LHR expression with oocyte maturity ($r = 0.267$), oocyte morphology ($r = 0.267$), and fertilization rate ($r = 0.430$) In non-poor responders: Negative correlation of LHR expression with oocyte maturity ($r = -0.552$), morphology ($r = -0.164$), and fertilization rate ($r = -0.340$)
Gode et al. (2011)	BMP15, GDF9		Western blot	81 individually derived cumulus-oocyte complexes (COCs) and follicular fluids collected from the first retrieved follicle of 81 IVF/ICSI patients	Nuclear maturation of oocytes ($P < 0.05$) and quality of embryos ($P < 0.05$) are significantly correlated with the level of mature GDF9 in follicular fluid
Li et al. (2014)	BMP15, GDF9		qPCR.	2,426 COCs from 196 IVF/ICSI patients	Expression of GDF9 and BMP15 mRNAs in cumulus granulosa cells were highly correlated with oocyte maturation, fertilization, and embryo quality ($P < 0.05$). Pregnancy predicting capacity is evident (GDF9 with 4.82 cut-off value, 82% sensitivity, and 64% capacity; BMP15 with 2.60 cut-off value, 78% sensitivity, and 52% capacity)
Hasegawa et al. (2007)	Cx43	Apoptosis	RT-PCR	105 CC samples from 29 IVF/ICSI patients	No relationship of Cx43 with fertilization and cleavage rate. Cx43 expression was significantly lower in good morphology cleavage-stage embryos compared to other groups ($P = 0.035$)
Wang et al. (2009)	Cx43		RT-PCR, Immunofluorescence microscopy, Western blot, gap junctional coupling assay	Cumulus cell (CC) samples from 115 patients	A positive correlation ($P < 0.05$) of Cx43 level with embryo quality (cleavage rate and morphology). Cx43 level is significantly higher in patients who became pregnant ($P < 0.01$)
Salehi et al. (2017)	Pro apoptosis proteins (Caspase-3, Caspase-7)		RT-PCR	100 CC from 20 PCOS IVF patients and 100 cumulus cells from 20 normal IVF patients (control group)	Caspase-3 and Caspase-7 expression were higher in PCOS patients. Significant correlation of embryo quality with Caspase-3 ($P = 0.0016$) and Caspase-7 ($P = 0.084$) expression in PCOS patients
Devjak et al. (2012)	SERPINE2	Extracellular matrix remodeling	Microarray, Quantitative real-time PCR (qPCR)	46 CC samples from 21 patients	Positive correlation between microarray and qPCR data ($r = 0.98$, $P = 0.02$) indicating lower expression of SERPINE2 mRNA in cumulus cells of mature oocytes than in immature oocytes
Li et al. (2015)	SERPINE2		RT-PCR	308 COC samples from 40 IVF patients (53 immature oocytes and 255 mature oocytes)	Expression of SERPINE2 was significantly lower in cumulus cells of mature oocytes than in immature oocytes ($P = 0.0002$)

(Continued)

TABLE 1 | Continued

Authors	Biomarkers	Oocyte maturation event	Detection method	Sample size	Key findings
Yung et al. (2010)	ADAMTS-1		Quantitative real-time PCR (qRT-PCR), Western blot	CC from 25 patients	ADAMTS-1 is associated with larger and more mature follicles and is positively correlated with oocyte fertilization capacity
Kordus et al. (2019)	PAPPA	Steroid metabolism	RT-PCR	163 CC samples from 15 patients	PAPPA expression level is significantly higher in CC of oocytes that led to euploid embryos resulting in a live birth ($P < 0.05$, $OR = 4.591$)
Wyse et al. (2020)	42 potential oocyte maturation biomarkers	Transcriptomics of cumulus cells	RNA sequencing, differential expression, pathway analysis, Quantitative real-time PCR (qPCR)	22 COCs from 11 patients	Differentially expressed genes identified between oocytes of different maturity

rate in the poor responders, while a negative correlation was observed in the non-poor responders. Nonetheless, the studies have implied that the expression of LHR is indeed associated with promoting oocyte nuclear maturation. However, there are some limitations in utilizing LHR as biomarkers. Overexpression of LHR has been presumed to give adverse impacts such as low fertilization rate hence expression thresholds of LHR that signify pro-maturation need to be determined. Moreover, as stated by Jeppesen et al. (2012), LHR protein expression might be too low in the granulosa cells for proper detection through RT-qPCR resulting in a tentative conclusion. There are some other notable findings that aim to evaluate prospective biomarkers and could be the alternative or complementary biomarkers. A G protein-coupled receptor, GPR3, that was mainly described and assessed in rodents was associated with meiotic arrest in human oocytes (DiLuigi et al., 2008).

Known as oocyte secreted factors (OSF) that belong to the transforming growth factor-β (TGF-β) family, growth differentiation factor-9 (GDF-9), and bone morphogenetic protein 15 (BMP-15), are proposed to have a potential value as non-invasive markers for determining oocyte developmental potential. In the ovary, GDF-9 and BMP-15 play pivotal roles during folliculogenesis, oocyte maturation, and ovulation (Gilchrist et al., 2004). Although OSFs are mainly secreted by the oocytes, granulosa cells are also known to express the GDF-9 and BMP-15. During the initial discovery, it was believed that GDF-9 and BMP-15 exist as homodimers formed through non-covalent linkage. However, a recent study has proven that both proteins could prevail as heterodimers (GDF-9/BMP-15), later known as cumulin, which possess a higher capability in inducing the proliferation of granulosa cells compared to the respective homodimer forms (Mottershead et al., 2015).

The clinical value of GDF-9 in the follicular fluid has been shown in a study conducted by Gode et al. (2011), in which mature forms of GDF-9 protein were significant in association with oocyte nuclear maturation. Similarly, a study that involved 196 infertile couples undergoing IVF, revealed that the COCs of women who achieved pregnancy expressed higher GDF-9 and BMP-15 mRNA concentrations than those who did not achieve pregnancy (Li et al., 2014). Furthermore, the study has also successfully formulated the cut-off values of both markers (4.82 and 2.60, respectively, for GDF-9 and BMP-15) for predicting pregnancy with sufficient sensitivity (78and 82%, respectively, for GDF-9 and BMP-15). Both studies have provided essential information on the expression of GDF-9 and BMP-15 in infertile couples undergoing IVF and the promising clinical use of the OSF as non-invasive markers to predict oocyte competence.

APOPTOSIS IN OOCYTE MATURATION

Apoptosis or programmed cell death has been known to play a role in influencing the oocyte maturation process. Apoptotic events in granulosa cells cause interference of the granulosa cells-oocytes communication, limiting the maturation-inducing factors (hormones, proteins, and metabolites) supply that are necessary for oocytes to reach meiotic competency (Chaube et al.,

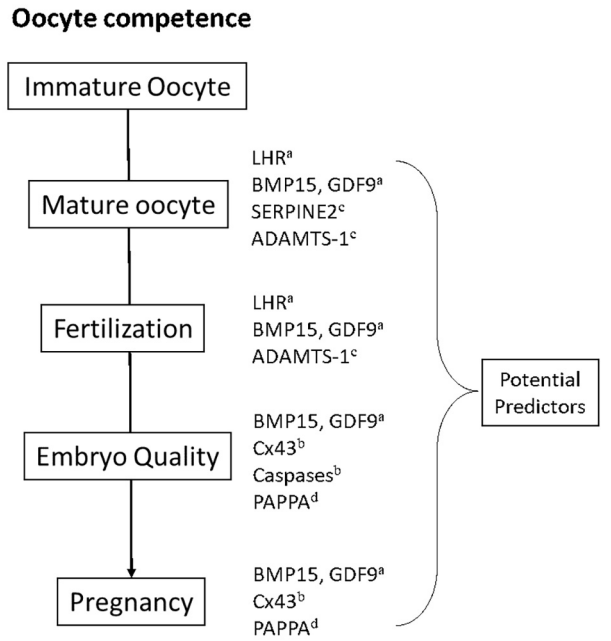

FIGURE 1 | Oocyte competence in IVF could be defined as the ability of an oocyte to achieve the mature oocyte stage, fertilization, embryo stage, and ultimately pregnancy. Expression of the COC-derived genes discussed in this study have exhibited significant predictive values toward the respective IVF stages. [a,b,c,d] refers to the occyte maturation process that the gene regulate: [a]Nuclear maturation, [b]Apoptosis, [c]Extracellular matrix remodeling, [d]Steroid metabolism.

2014). Granulosa cells that do not have the access to all the necessary metabolites would gradually promote the autophagy mechanism before eventually inducing apoptosis mechanism (Altman and Rathmell, 2012). Gap junctions that act as channels for these necessary metabolites play an important role in regulating cell death, survival, and nutrients uptake.

Gap junctions, which allow cell-to-cell communication is found among intrafollicular cells, i.e., mural granulosa cells, cumulus granulosa cells, and oocytes (Anderson and Albertini, 1976; Gilula et al., 1978). Connexins are essential in forming intercellular membrane channels of gap junctions. Connexin (Cx43), particularly, is expressed in granulosa cells and is associated with cell death and survival, and oocyte maturation in model animals (Vozzi et al., 2001; Krysko et al., 2004), making it a potential biomarker for human oocyte quality.

Wang et al. (2009) found that Cx43 expression level had a positive correlation to embryo quality as in morphology and pregnancy rate. It was presumed that low expression of Cx43 is also followed by low availability of fundamental nutrients, creating a metabolic shortage in oocytes that would impact the oocytes in the later developmental stages. This discovery is contradictory to findings by Hasegawa et al. (2007), whereby Cx43 expression was found to be lower in the good-morphology embryo group compared to other groups. This evidence is supported by the fact that LH surge, which is central in meiotic resumption inhibits the translation of gap junction proteins (Kalma et al., 2004). The inhibition of gap junction protein is presumably to limit the transfer of meiotic maturation arresting factor, cAMP and cGMP, from the cumulus cells to oocytes (Norris et al., 2008). In summary, the limitation of Cx43 as a biomarker prevails in the uncertainty as to whether the decreased or increased expression of Cx43 is related to favorable oocyte quality.

Caspase is one of the other pro-apoptotic factors expressed in granulosa cells that could become potential biomarkers. Caspase, a cysteine protease, causes the inactivation of components for physiological processes and morphological changes during apoptosis. Caspase-3 and caspase-7 expressions were found to be higher especially in polycystic ovary syndrome (PCOS) and have a negative correlation to embryo quality (Salehi et al., 2017). Evidently, caspase-3 is the main factor in apoptosis through its association with chromatin condensation, DNA fragmentation, nuclear breakdown, and plasma membrane protrusion, while caspase-7 mainly contributes to the reactive oxygen species (ROS) accumulation and detachment of cells from the extracellular matrix (ECM) (Brentnall et al., 2013). FOXO3 is another gene that is highly expressed during apoptosis and correlated positively with poor quality oocytes in PCOS patients (Mikaeili et al., 2016).

OOCYTE EXTRACELLULAR MATRIX REMODELING

The integrity of the COC extracellular matrix is vital for the bidirectional intercellular communication between oocytes and their surrounding cumulus cells. During oocyte maturation, the dynamic surge of gonadotropins and oocyte-secreted paracrine factors stimulate several genes that participate in a process known as cumulus expansion. The expressed proteins acquire different functions including gap junctions and proteases which predominantly regulate the remodeling of tissues during folliculogenesis; all acting within the intercellular spaces of cumulus cells to promote oocyte maturation (Robker et al., 2018).

SERPINE2 encodes for the serine protease inhibitor E2 that is not only indirectly associated with tissue plasminogen activator in degrading matrix proteins but also plays a role as sperm decapacitation factor. Li et al. (2015) highlighted the considerable difference in *SERPINE2* gene expression between immature and mature oocytes in which RT-qPCR of RNA extracted from 308 COCs revealed a significantly lower expression of *SERPINE2* mRNA in a cumulus of mature oocytes compared to the immature cohort (p = 0.0002). This corroborated a previous study that indicated *SERPINE2* as one of the 116 genes to be differentially expressed in the DNA microarray analysis of cumulus samples between mature and immature oocytes (p = 0.02) (Devjak et al., 2012). Furthermore, the study particularly disclosed no substantial difference in cumulus cell gene expression with regard to the ovarian stimulation protocols. Recent experimentation which managed to construct an NGS library to discern the transcriptomics of cumulus cells also displayed a fourfold decrease in *SERPINE2* expression in

the immature oocyte cohort (Wyse et al., 2020). Concurrently, Wyse et al. (2020) also identified a higher expression of cumulus expansion-associated ADAM-metallopeptidase with thrombospondin type 1 motifs-1 (*ADAMTS-1)* in COC of mature oocytes. This was previously exhibited in a study that specified its essential role in the follicular rupture process. *ADAMTS-1* expression was found to be correlated with oocyte fertilization capacity in which oocytes that underwent successful fertilization acquired a threefold higher expression of cumulus *ADAMTS-1* compared to those that failed to fertilize (Yung et al., 2010).

While these studies might have proven the competency of *SERPINE2* and *ADAMTS-1* as biomarkers for oocyte competency, they are limited to the small immature oocyte sample sizes within the same cycles (controlled ovarian stimulation in IVF typically produces more mature oocytes) hence a larger prospective study is still mandatory. A study on bovine follicles demonstrated the influence of gonadotropins on *SERPINE2* expression in which FSH was found to manifest in the increased *SERPINE2* expression while LH surge before ovulation decreased its expression (Bédard et al., 2003). However, further research is still required to unveil the pathology that leads to the turnarounds in the expression of *SERPINE2* and *ADAMTS−1* in the cumulus of immature oocytes so that the appropriate intervention could be formulated to improve *in vitro* maturation.

OOCYTE STEROID METABOLISM

Steroidogenesis in animal models has been shown to directly impact the meiosis of oocytes and contribute to spontaneous mammalian oocyte maturation (Jamnongjit and Hammes, 2005). While their exact regulatory mechanisms are still rather bleak, steroids secreted by theca and granulosa cells in response to growth factors have been established to act as secondary messengers in pathways that lead to cumulus expansion and thus oocyte maturation. Of utmost interest, studies that explore the metabolomics of cumulus cells have unveiled pappalysin-1 (*PAPPA*) mRNA as a potential predictor of oocyte maturation status and, to a certain degree, the euploidy status of embryos and pregnancy outcomes in IVF (Kordus et al., 2019). *PAPPA* is responsible for the expression of metalloproteinases which actively cleaves insulin-like growth factor binding proteins (IGFB4) to provide the supply of intrafollicular IGF peptides that in turn function as co-gonadotropin for the stimulation of steroidogenesis. Kordus et al. (2019) noted higher *PAPPA* expression levels in cumulus cells of mature oocytes that ultimately developed to become euploid embryos compared to the group of immature oocytes that culminated in arrested embryos. Findings of the study also suggested a computable interplay between the expression of *PAPPA* and other oocyte maturation-associated mRNAs such as *AREG* (amphiregulin) and *LHCGR* (luteinizing hormone/choriogonadotropin receptor) which is a valuable steppingstone toward constructing an ideal predictive model that could gauge the prognosis of IVF.

Another steroidogenesis-associated gene that is also adversely expressed differentially between mature and immature oocytes is *HSD17B1* which encodes Hydroxysteroid (17beta) dehydrogenase 1 (Järvensivu et al., 2015). The enzyme, in the presence of cofactors, regulates the reversible catalytic reaction of converting estrone to estradiol which possesses a higher estrogenic activity. *HSD17B1* has been extensively evaluated in animal models and the recent transcriptomic analysis of human COC samples corroborates the significantly reduced expression of *HSD17B1* in mature oocytes (Wyse et al., 2020), commencing possible research in the mechanism and roles of the gene in promoting the maturation process. Likewise, further research worth investigating would be on the affiliation of *PAPPA,* and *HSD17B1* mRNA expression level in mature oocytes with their respective pregnancy outcomes. Such studies, however, encounter inevitable challenges that demand a large sample of single embryo transfer procedures while still minimizing the clinical and physiological heterogeneity among the samples.

DISCUSSION

Oocyte maturation is a complex process consisting of inter- and intra-connected signaling pathways that are regulated by a series of genes traceable within the COC. Gene expression analyses of RNA samples extracted from COC have revealed that certain genes were particularly expressed differently in oocytes of different maturity hence extending their potential purpose as biomarkers capable of predicting IVF outcomes. The most promising biomarkers thus far are GDF-9 and BMP-15 with proven sensitivity and specificity of predicting pregnancy in a study with the largest sample size among others included here. Furthermore, addition of these growth factors has shown to increase the efficiency of *in vitro* maturation, suggesting their significant roles in promoting oocyte maturation. The potency of other biomarkers such as SERPINE2 and Cx43 require additional investigations due to the relatively small sample size and contradicting results with previously established findings. Meanwhile, recognizing confounding variables are imperative to identify underlying conditions in IVF patients which may affect the expression of these biomarkers such as the significantly higher expression of Caspase proteins in PCOS patients. Although substantial *in vitro* evidence was presented to justify the potential functions of these biomarkers, the clinical practice of examining non-invasive oocyte biomarkers as IVF prognostic measures is still far from achievable. Ideally, such approaches would demand the acquisition of transcriptomic profiles of every oocyte retrieved during ovum pick up, enumerating the expression levels of all the genes mentioned above, in addition to many more.

A large number of COC biomarkers are regulated by FSH and/or LH stimulation. Poor response toward the gonadotrophins have been shown to downregulate genes which, in turn, are associated with the increased p53-pathway for apoptosis, resulting in a restricted maturation process, as observed in immature COCs (Wyse et al., 2020). Contrarily, adequate gonadotrophinresponses characterized by the upregulation of genes for the biosynthesis of estrogen and androgen are displayed in mature oocytes (Wyse et al., 2020). While these findings have collectively added knowledge to the understanding of oocyte maturation process, correlating the

expression level of these genes with the tracking of individual oocyte outcome throughout the IVF program is required before the genes could be denoted as potential IVF predictors. In that note, in the transcriptomic profiling of COCs, there are several novel discoveries on the differential expression of other explored genes between the cohorts of mature and immature oocytes such as genes encoding for Epiregulin (EREG) in cumulus expansion and Phosphodiesterase 3A (PDE3A) in cytoplasmic maturation (Wyse et al., 2020). Nonetheless, the exact mechanism and significance of these genes as indicators for assessing oocyte competence and thus the IVF outcomes are still rather bleak.

While plenty of other biomarkers were not discussed here, this review provides insights on the current progress of studies pertaining to the evaluation of cumulus biomarkers. Common challenges such as the difficulty in obtaining homogeneous study subjects were highlighted, including the imbalance number of mature and immature oocytes retrieved during ovum pick-up, which understandably led to the resultant small sample sizes. Additionally, in the attempts to correlate these biomarkers with IVF outcomes, a large assortment of confounding variables and appropriate statistical methodologies need to be recognized to provide convincing results and evade contradictory findings. It is also imperative to expedite the identification of factors that culminate to the shift in gene expression levels between mature and immature oocytes, bringing about another limitation specifically in the selection of the appropriate model organisms. Other routes of research worth investigating would be to classify metabolite analogs affiliated with the biomarkers and evaluate their effects during *in vitro* maturation process, with hopes for the possibility to boost the competency of oocytes within laboratory settings.

CONCLUSION

In conclusion, the roles of eight cumulus biomarkers in promoting oocyte maturation and their expression profiles in oocytes of different maturity have been well-established to possess statistical values in predicting an IVF cycle. However, the feasibility of assessing these biomarkers as an add-on prognostic procedure in IVF is still restricted due to sampling challenges. Indispensable investigations on the disputable molecular mechanisms are also still necessary for the realization of IVF predictive models that are based on the above-mentioned biomarkers.

AUTHOR CONTRIBUTIONS

BS drafted the early version of this manuscript. BW, AAJ, DI, and RM critically reviewed and revised the content. All authors contributed to the article and approved the submitted version.

FUNDING

This review was funded by an international research publication (PUTI) grant from Universitas Indonesia (contract number: NKB-1320/UN2.RST/HKP.05.00/2020).

REFERENCES

Adhikari, D., and Liu, K. (2014). The regulation of maturation promoting factor during prophase I arrest and meiotic entry in mammalian oocytes. *Mol. Cell. Endocrinol.* 382, 480–487. doi: 10.1016/j.mce.2013.07.027

Altman, B. J., and Rathmell, J. C. (2012). Metabolic stress in autophagy and cell death pathways. *Cold Spring Harb. Perspect. Biol.* 4:a008763. doi: 10.1101/cshperspect.a008763

Anderson, E., and Albertini, D. F. (1976). Gap junctions between the oocyte and companion follicle cells in the mammalian ovary. *J. Cell. Biol.* 71, 680–686. doi: 10.1083/jcb.71.2.680

Balaban, B., Barut, T., and Urman, B. (2012). "Assessment of oocyte quality," in *Practical Manual of in Vitro Fertilization*, eds Z. Peter Nagy, A. C. Varghese, and A. Agarwal (New York, NY: Springer), 105–119.

Bédard, J., Brûlé, S., Price, C. A., Silversides, D. W., and Lussier, J. G. (2003). Serine protease inhibitor-E2 (SERPINE2) is differentially expressed in granulosa cells of dominant follicle in cattle. *Mol. Reprod. Dev.* 64, 152–165. doi: 10.1002/mrd.10239

Bosch, E., Labarta, E., Kolibianakis, E., Rosen, M., and Meldrum, D. (2016). Regimen of ovarian stimulation affects oocyte and therefore embryo quality. *Fertil. Steril.* 105, 560–570. doi: 10.1016/j.fertnstert.2016.01.022

Braga, D. P. A. F., Zanetti, B. F., Setti, A. S., Iaconelli, A. J., and Borges, E. J. (2020). Immature oocyte incidence: contributing factors and effects on mature sibling oocytes in intracytoplasmic sperm injection cycles. *JBRA Assist. Reprod.* 24, 70–76.

Brentnall, M., Rodriguez-Menocal, L., De Guevara, R. L., Cepero, E., and Boise, L. H. (2013). Caspase-9, caspase-3 and caspase-7 have distinct roles during intrinsic apoptosis. *BMC Cell Biol.* 14:32. doi: 10.1186/1471-2121-14-32

Chaube, S. K., Shrivastav, T. G., Prasad, S., Tiwari, M., Tripathi, A., Pandey, A. N., et al. (2014). Clomiphene citrate induces ROS-mediated apoptosis in mammalian oocytes. *Open J. Apoptosis* 3, 52–58. doi: 10.4236/ojapo.2014.33006

Chronowska, E. (2014). High-throughput analysis of ovarian granulosa cell transcriptome. *Biomed Res. Int.* 2014:213570.

Conti, M., Hsieh, M., Musa Zamah, A., and Oh, J. S. (2012). Novel signaling mechanisms in the ovary during oocyte maturation and ovulation. *Mol. Cell. Endocrinol.* 356, 65–73. doi: 10.1016/j.mce.2011.11.002

Devjak, R., Fon Tacer, K., Juvan, P., Virant Klun, I., Rozman, D., and Vrtačnik Bokal, E. (2012). Cumulus cells gene expression profiling in terms of oocyte maturity in controlled ovarian hyperstimulation using GnRH agonist or GnRH antagonist. *PLoS One* 7:e47106. doi: 10.1371/journal.pone.0047106

DiLuigi, A., Weitzman, V. N., Pace, M. C., Siano, L. J., Maier, D., and Mehlmann, L. M. (2008). Meiotic arrest in human oocytes is maintained by a Gs signaling pathway. *Biol. Reprod.* 78, 667–672. doi: 10.1095/biolreprod.107.066019

Edry, I., Sela-Abramovich, S., and Dekel, N. (2006). Meiotic arrest of oocytes depends on cell-to-cell communication in the ovarian follicle. *Mol. Cell. Endocrinol.* 252, 102–106. doi: 10.1016/j.mce.2006.03.009

Figueira, R. D. C. S., de Almeida Ferreira Braga, D. P., Semião-Francisco, L., Madaschi, C., Iaconelli, A., and Borges, E. (2010). Metaphase II human oocyte morphology: contributing factors and effects on fertilization potential and embryo developmental ability in ICSI cycles. *Fertil. Steril.* 94, 1115–1117.

Gallos, I. D., Eapen, A., Price, M. J., Sunkara, S. K., Macklon, N. S., Bhattacharya, S., et al. (2017). Controlled ovarian stimulation protocols for assisted reproduction: a network meta-analysis. *Cochrane Database Syst. Rev.* 2017:CD012586.

Gilchrist, R. B., Ritter, L. J., and Armstrong, D. T. (2004). Oocyte-somatic cell interactions during follicle development in mammals. *Anim. Reprod. Sci.* 8, 431–446. doi: 10.1016/j.anireprosci.2004.05.017

Gilula, N. B., Epstein, M. L., and Beers, W. H. (1978). Cell-to-cell communication and ovulation. A study of the cumulus-oocyte complex. *J. Cell Biol.* 78, 58–75. doi: 10.1083/jcb.78.1.58

Gode, F., Gulekli, B., Dogan, E., Korhan, P., Dogan, S., Bige, O., et al. (2011). Influence of follicular fluid GDF9 and BMP15 on embryo quality. *Fertil. Steril.* 95, 2274–2278. doi: 10.1016/j.fertnstert.2011.03.045

Hasegawa, J., Yanaihara, A., Iwasaki, S., Mitsukawa, K., Negishi, M., and Okai, T. (2007). Reduction of connexin 43 in human cumulus cells yields good embryo competence during ICSI. *J. Assist. Reprod. Genet.* 24, 463–466. doi: 10.1007/s10815-007-9155-4

Jamnongjit, M., and Hammes, S. R. (2005). Oocyte maturation: the coming of age of a germ cell. *Semin. Reprod. Med.* 23, 234–241. doi: 10.1055/s-2005-872451

Järvensivu, P., Saloniemi-Heinonen, T., Awosanya, M., Koskimies, P., Saarinen, N., and Poutanen, M. (2015). HSD17B1 expression enhances estrogen signaling stimulated by the low active estrone, evidenced by an estrogen responsive element-driven reporter gene in vivo. *Chem. Biol. Interact.* 234, 126–134. doi: 10.1016/j.cbi.2015.01.008

Jeppesen, J. V., Kristensen, S. G., Nielsen, M. E., Humaidan, P., Dal Canto, M., Fadini, R., et al. (2012). LH-receptor gene expression in human granulosa and cumulus cells from antral and preovulatory follicles. *J. Clin. Endocrinol. Metab.* 97, E1524–E1531.

Kalma, Y., Granot, I., Galiani, D., Barash, A., and Dekel, N. (2004). Luteinizing hormone-induced connexin 43 down-regulation: inhibition of translation. *Endocrinology* 145, 1617–1624. doi: 10.1210/en.2003-1051

Kordus, R. J., Hossain, A., Corso, M. C., Chakraborty, H., Whitman-Elia, G. F., and LaVoie, H. A. (2019). Cumulus cell pappalysin-1, luteinizing hormone/choriogonadotropin receptor, amphiregulin and hydroxy-delta-5-steroid dehydrogenase, 3 beta- and steroid delta-isomerase 1 mRNA levels associate with oocyte developmental competence and embryo outcomes. *J. Assist. Reprod. Genet.* 36, 1457–1469. doi: 10.1007/s10815-019-01489-8

Krysko, D. V., Mussche, S., Leybaert, L., and D'Herde, K. (2004). Gap junctional communication and connexin43 expression in relation to apoptotic cell death and survival of granulosa cells. *J. Histochem. Cytochem.* 52, 1199–1207. doi: 10.1369/jhc.3a6227.2004

Lazzaroni-Tealdi, E., Barad, D. H., Albertini, D. F., Yu, Y., Kushnir, V. A., Russell, H., et al. (2015). Oocyte scoring enhances embryo-scoring in predicting pregnancy chances with IVF where it counts most. *PLoS One* 10:e0143632. doi: 10.1371/journal.pone.0143632

Li, S. H., Lin, M. H., Hwu, Y. M., Lu, C. H., Yeh, L. Y., Chen, Y. J., et al. (2015). Correlation of cumulus gene expression of GJA1, PRSS35, PTX3, and SERPINE2 with oocyte maturation, fertilization, and embryo development. *Reprod. Biol. Endocrinol.* 13:93. doi: 10.1186/s12958-015-0091-3

Li, Y., Li, R. Q., Ou, S. B., Zhang, N. F., Ren, L., Wei, L. N., et al. (2014). Increased GDF9 and BMP15 mRNA levels in cumulus granulosa cells correlate with oocyte maturation, fertilization, and embryo quality in humans. *Reprod. Biol. Endocrinol.* 12:81. doi: 10.1186/1477-7827-12-81

Maman, E., Yung, Y., Kedem, A., Yerushalmi, G. M., Konopnicki, S., Cohen, B., et al. (2012). High expression of luteinizing hormone receptors messenger RNA by human cumulus granulosa cells is in correlation with decreased fertilization. *Fertil. Steril.* 97, 592–598. doi: 10.1016/j.fertnstert.2011.12.027

Mikaeili, S., Rashidi, B. H., Safa, M., Najafi, A., Sobhani, A., Asadi, E., et al. (2016). Altered FoxO3 expression and apoptosis in granulosa cells of women with polycystic ovary syndrome. *Arch. Gynecol. Obstet.* 294, 185–192. doi: 10.1007/s00404-016-4068-z

Mottershead, D. G., Sugimura, S., Al-Musawi, S. L., Li, J. J., Richani, D., White, M. A., et al. (2015). Cumulin, an oocyte-secreted heterodimer of the transforming growth factor-β family, is a potent activator of granulosa cells and improves oocyte quality. *J. Biol. Chem.* 290, 24007–24020. doi: 10.1074/jbc.m115.671487

Norris, R. P., Freudzon, M., Mehlmann, L. M., Cowan, A. E., Simon, A. M., Paul, D. L., et al. (2008). Luteinizing hormone causes MAP kinase-dependent phosphorylation and closure of connexin 43 gap junctions in mouse ovarian follicles: one of two paths to meiotic resumption. *Development* 135, 3229–3238. doi: 10.1242/dev.025494

Norris, R. P., Ratzan, W. J., Freudzon, M., Mehlmann, L. M., Krall, J., Movsesian, M. A., et al. (2009). Cyclic GMP from the surrounding somatic cells regulates cyclic AMP and meiosis in the mouse oocyte. *Development* 136, 1869–1878. doi: 10.1242/dev.035238

Robker, R. L., Hennebold, J. D., and Russell, D. L. (2018). Coordination of ovulation and oocyte maturation: a good egg at the right time. *Endocrinology* 159, 3209–3218. doi: 10.1210/en.2018-00485

Ruvolo, G., Fattouh, R. R., Bosco, L., Brucculeri, A. M., and Cittadini, E. (2013). New molecular markers for the evaluation of gamete quality. *J. Assist. Reprod. Genet.* 30, 207–212. doi: 10.1007/s10815-013-9943-y

Salehi, E., Aflatoonian, R., Moeini, A., Yamini, N., Asadi, E., Khosravizadeh, Z., et al. (2017). Apoptotic biomarkers in cumulus cells in relation to embryo quality in polycystic ovary syndrome. *Arch. Gynecol. Obstet.* 296, 1219–1227. doi: 10.1007/s00404-017-4523-5

Tilia, L., Chapman, M., Kilani, S., Cooke, S., and Venetis, C. (2020). Oocyte meiotic spindle morphology is a predictive marker of blastocyst ploidy—a prospective cohort study. *Fertil. Steril.* 113, 105–113. doi: 10.1016/j.fertnstert.2019.08.070

Vozzi, C., Formenton, A., Chanson, A., Senn, A., Sahli, R., Shaw, P., et al. (2001). Involvement of connexin 43 in meiotic maturation of bovine oocytes. *Reproduction* 122, 619–628. doi: 10.1530/reprod/122.4.619

Wang, H. X., Tong, D., El-Gehani, F., Tekpetey, F. R., and Kidder, G. M. (2009). Connexin expression and gap junctional coupling in human cumulus cells: contribution to embryo quality. *J. Cell. Mol. Med.* 13, 972–984. doi: 10.1111/j.1582-4934.2008.00373.x

Wang, Q., and Sun, Q. Y. (2007). Evaluation of oocyte quality: morphological, cellular and molecular predictors. *Reprod. Fertil. Dev.* 19, 1–12. doi: 10.1071/rd06103

Wiweko, B., Satria, M. L., Mutia, K., Iffanolida, P. A., Harzif, A. K., Pratama, G., et al. (2019). Correlation between luteinizing hormone receptor gene expression in human granulosa cells with oocyte quality in poor responder patients undergoing in vitro fertilization: a cross-sectional study. *F1000Res.* 8:16. doi: 10.12688/f1000research.17036.1

Wyse, B. A., Fuchs Weizman, N., Kadish, S., Balakier, H., Sangaralingam, M., and Librach, C. L. (2020). Transcriptomics of cumulus cells–a window into oocyte maturation in humans. *J. Ovarian Res.* 13:93.

Yung, Y., Maman, E., Konopnicki, S., Cohen, B., Brengauz, M., Lojkin, I., et al. (2010). ADAMTS-1: a new human ovulatory gene and a cumulus marker for fertilization capacity. *Mol. Cell. Endocrinol.* 328, 104–108. doi: 10.1016/j.mce.2010.07.019

Conflict of Interest: The authors declare that the research was conducted in the absence of any commercial or financial relationships that could be construed as a potential conflict of interest.

Publisher's Note: All claims expressed in this article are solely those of the authors and do not necessarily represent those of their affiliated organizations, or those of the publisher, the editors and the reviewers. Any product that may be evaluated in this article, or claim that may be made by its manufacturer, is not guaranteed or endorsed by the publisher.

frontiers in Cell and Developmental Biology

ORIGINAL RESEARCH
published: 08 September 2021
doi: 10.3389/fcell.2021.710864

Alpha/Beta Hydrolase Domain-Containing Protein 2 Regulates the Rhythm of Follicular Maturation and Estrous Stages of the Female Reproductive Cycle

Ida Björkgren[1], Dong Hwa Chung[1], Sarah Mendoza[1], Liliya Gabelev-Khasin[1], Natalie T. Petersen[1], Andrew Modzelewski[1], Lin He[1] and Polina V. Lishko[1,2]**

[1] Department of Molecular and Cell Biology, University of California, Berkeley, Berkeley, CA, United States, [2] The Center for Reproductive Longevity and Equality at the Buck Institute for Research on Aging, Novato, CA, United States

OPEN ACCESS

Edited by:
Francesca Elizabeth Duncan, Northwestern University, United States

Reviewed by:
Ricardo Daniel Moreno, Pontificia Universidad Católica de Chile, Chile
Lynda K. McGinnis, University of Southern California, United States

***Correspondence:**
Polina V. Lishko
lishko@berkeley.edu
Ida Björkgren
ida.bjorkgren@ucr.uu.se

Specialty section:
This article was submitted to Molecular and Cellular Reproduction, a section of the journal Frontiers in Cell and Developmental Biology

Received: 17 May 2021
Accepted: 09 August 2021
Published: 08 September 2021

Citation:
Björkgren I, Chung DH, Mendoza S, Gabelev-Khasin L, Petersen NT, Modzelewski A, He L and Lishko PV (2021) Alpha/Beta Hydrolase Domain-Containing Protein 2 Regulates the Rhythm of Follicular Maturation and Estrous Stages of the Female Reproductive Cycle. Front. Cell Dev. Biol. 9:710864. doi: 10.3389/fcell.2021.710864

Mammalian female fertility is defined by a successful and strictly periodic ovarian cycle, which is under the control of gonadotropins and steroid hormones, particularly progesterone and estrogen. The latter two are produced by the ovaries that are engaged in controlled follicular growth, maturation, and release of the eggs, i.e., ovulation. The steroid hormones regulate ovarian cycles *via* genomic signaling, by altering gene transcription and protein synthesis. However, despite this well-studied mechanism, steroid hormones can also signal *via* direct, non-genomic action, by binding to their membrane receptors. Here we show, that the recently discovered membrane progesterone receptor α/β hydrolase domain-containing protein 2 (ABHD2) is highly expressed in mammalian ovaries where the protein plays a novel regulatory role in follicle maturation and the sexual cycle of females. Ablation of *Abhd2* caused a dysregulation of the estrous cycle rhythm with females showing shortened luteal stages while remaining in the estrus stage for a longer time. Interestingly, the ovaries of *Abhd2* knockout (KO) females resemble polycystic ovary morphology (PCOM) with a high number of atretic antral follicles that could be rescued with injection of gonadotropins. Such a procedure also allowed *Abhd2* KO females to ovulate a significantly increased number of mature and fertile eggs in comparison with their wild-type littermates. These results suggest a novel regulatory role of ABHD2 as an important factor in non-genomic steroid regulation of the female reproductive cycle.

Keywords: estrous cycle, steroid signaling, alpha/beta hydrolase domain-containing protein 2, ABHD2, female reproductive cycle, PCOM, ovary, ovulation

INTRODUCTION

Female fertility is highly regulated by the hypothalamic–pituitary–gonadal axis of hormone secretion, which results in a balanced estrogen to progesterone signaling and, in turn, produces the cyclic nature of ovarian follicle development. In many placental mammals, this cycle is known as the estrous cycle, with the exception of primates which have a menstrual cycle. The

estrous cycle is generally subdivided into four phases: proestrus, estrus, metestrus, and diestrus (**Supplementary Figure 1**). The first phase, proestrus, begins with the rapid growth of several ovarian follicles and can, in mice, last about 1 day. During this phase, the old corpus luteum (CL) degenerates, while the vaginal epithelium proliferates. Proestrus can be easily identified by the large number of non-cornified nucleated epithelial cells found in smears collected by vaginal lavage (**Supplementary Figure 1**). Steadily increasing levels of estrogen stimulate preovulatory follicles that undergo their final growth phase. The second phase, estrus, follows proestrus and is the stage that experiences the peak of gonadotropin secretion by the pituitary gland, resulting in maximal secretion of estrogens by the ovaries. Dominant follicles produce high levels of estradiol to inhibit the development of smaller antral follicles (Roy and Greenwald, 1987) and simultaneously promote ovulation through expression of the nuclear progesterone receptor and induction of progesterone secretion (Lydon et al., 1995; Hashimoto-Partyka et al., 2006). Ovulation occurs during the estrus stage, which together with proestrus comprise the follicular phase. The estrus stage can also be easily identified using vaginal smears that show presence of larger cornified epithelial cells (**Supplementary Figure 1**). Progesterone and its receptors are primarily needed during the subsequent luteal phase (metestrus and diestrus), which occurs immediately after ovulation, and results in the consequent development of CL from the ovulated follicle (**Supplementary Figure 1**). CL is the main producer of progesterone, which peaks during diestrus (Walmer et al., 1992), and if pregnancy is not obtained, the CL goes through luteolysis, which leads to reduced progesterone secretion and stimulates development of the immature follicles.

Progesterone is a powerful regulator of the ovarian cycle that occurs *via* genomic signaling mechanisms and results from progesterone binding to its nuclear receptors inside the cell, which leads to changes in gene transcription and protein synthesis. However, it has been known that progesterone may also signal *via* a non-genomic or direct pathway, by binding to its membrane receptors. The latter signaling pathway is required for frog oocyte maturation (Revelli et al., 1998), human sperm cell activation (Blackmore et al., 1990, 1991; Baldi et al., 1991), and likely triggers anesthesia in rodents (Poisbeau et al., 2014). Recently, by using transcriptionally silent spermatozoa as a model, we have identified the novel membrane progesterone receptor, the α/β hydrolase domain-containing protein 2 (ABHD2) as well as described the signaling pathway that is initiated by progesterone association with ABHD2 (Miller et al., 2016). Monoacylglycerol lipase ABHD2 is the first evolutionary conserved steroid-activating enzyme that hydrolyzes endocannabinoid 2-arachidonoylglycerol (Miller et al., 2016). Here, we show that ABHD2 is not only expressed in sperm but also displays high expression in ovaries, particularly in CL and stromal cells. To study this further, we have generated an *Abhd2* KO mouse by using the highly efficient CRISPR Ribonucleoprotein Electroporation of Zygotes (CRISPR-EZ) technique (Chen et al., 2016; Modzelewski et al., 2018) and evaluated its fertility phenotype. We show that ABHD2 is needed to regulate the cyclic maturation of follicles, where ablation of *Abhd2* gives rise to a phenotype similar to that of polycystic ovary morphology (PCOM) with irregular menstrual cycles and an increased number of atretic follicles, but without the fertility issues associated with polycystic ovary syndrome (PCOS).

RESULTS

Abhd2 Expression in Ovarian Stromal Cells and Corpora Lutea

While ABHD2 has been described as an important regulator of sperm function (Miller et al., 2016), the function of ABHD2 in female reproduction was not known. Interestingly, unlike the male reproductive tissues, we found that ABHD2 is not detected in the female gametes but is predominantly expressed in the stromal cells surrounding the developing follicles (**Figure 1a**). The presence of both ABHD2 protein and mRNA was observed in pre-pubertal mouse ovaries, as shown here by immunohistochemical (IHC) staining and reverse transcriptase quantitative PCR (RT-qPCR; **Figures 1b,c**). Around 1 month after birth, when the ovulatory cycle begins, ABHD2 expression is further found in the lutein cells of CL (**Figure 1a**). In correlation with this, qPCR studies showed highest *Abhd2* mRNA presence right after ovulation during the estrus stage (**Figure 1c**), and the expression levels are even further increased after induction of superovulation by gonadotropin injection (**Figure 1c**).

Generation of the *Abhd2* Knockout Mouse Line

To study the role of ABHD2 in female reproduction, we have generated an *Abhd2* KO mouse line by utilizing the CRISPR-EZ technique (Chen et al., 2016), where single guide RNA (sgRNA)/Cas9 complexes are delivered into mouse zygotes by electroporation. Cas9-mediated deletion of *Abhd2* exon 6 was performed through intron-specific binding of two sgRNAs (**Figure 2a**). The deletion resulted in the removal of a serine (S208), the amino acid important for the catalytic function of ABHD2, and resulted in a frameshift and a premature stop codon in exon 7 (**Supplementary Figure 2**). Complete ablation of *Abhd2* was further confirmed by genotyping PCR (**Figure 2b**), qPCR (**Figure 2c**), Western blotting (**Figure 2d**), and IHC analysis of the mouse ovary (**Figures 2e,f**). The KO mice were born at a Mendelian ratio when breeding heterozygous males with females. No obvious morphological or health phenotypes have been observed, and both homozygous and heterozygous females appeared fertile and healthy with similar body weight as their wild-type littermates (**Supplementary Figure 3A**).

Superovulation of *Abhd2*$^{+/-}$ and *Abhd2*$^{-/-}$ Females Gives Rise to an Increased Number of Ovulated Eggs

Both the litter size and birth rate of *Abhd2*$^{+/-}$ and *Abhd2*$^{-/-}$ females were not significantly different from that of wild-type mice (**Table 1**). In addition, spontaneous ovulation gave rise to similar numbers of eggs for all genotypes (**Figure 3A**). However, when injected with gonadotropins,

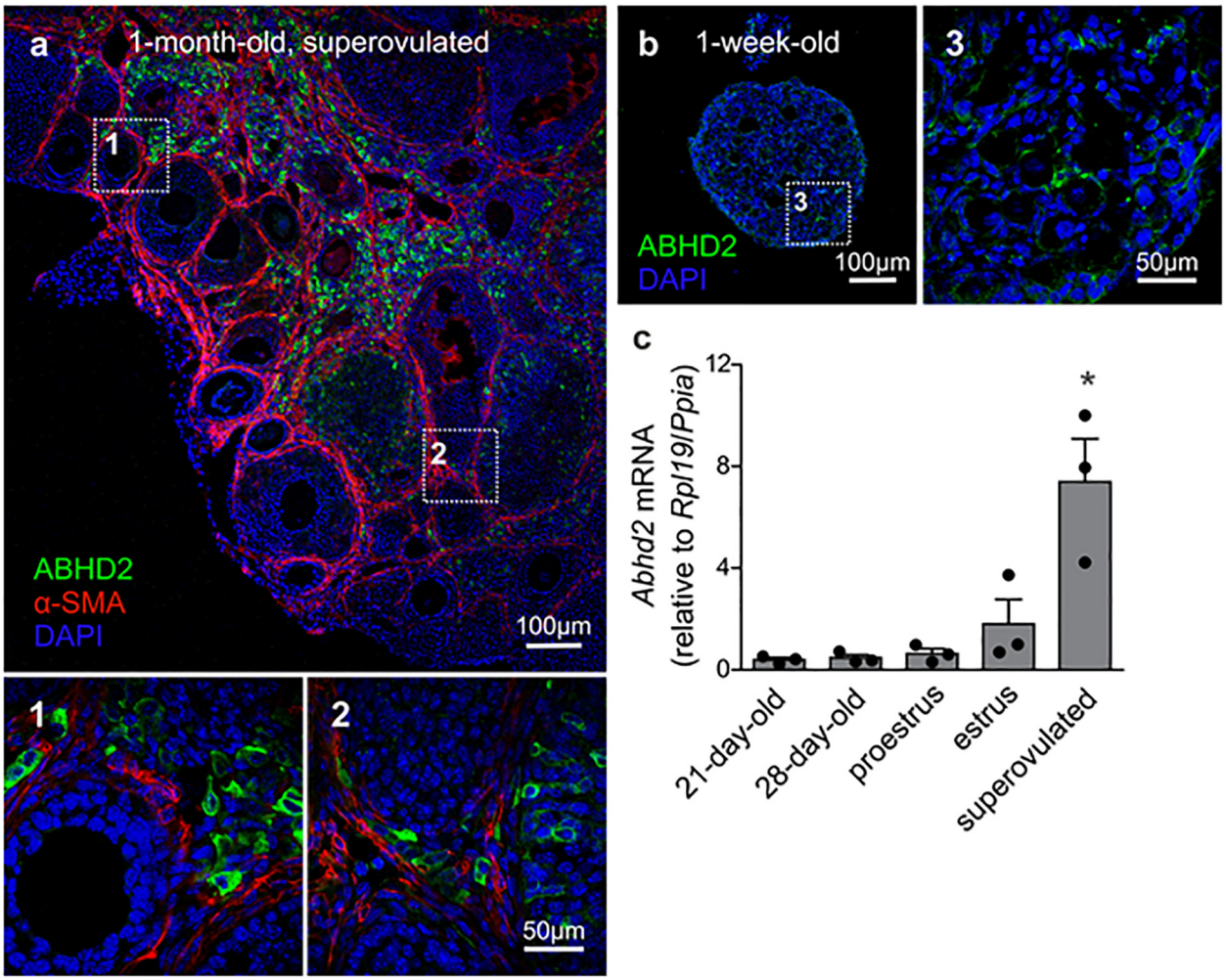

FIGURE 1 | Expression of alpha/beta hydrolase domain-containing protein 2 (ABHD2) in the mouse ovary. **(a)** Immunohistochemical (IHC) staining of a 1-month-old superovulated wild-type mouse ovary shows ABHD2 in the stromal cells (1) and in cells of the corpus luteum (CL) (2), while the protein is not present in the granulosa cells and oocytes of developing follicles, demarcated by staining of the surrounding smooth muscle layer **(b)**, and (3) Stromal cells of 1-week-old pre-pubertal mouse ovaries also display ABHD2 staining while **(c)** shows similar expression levels of *Abhd2* before and after the first round of ovulation, as detected in 21- and 28-day-old mice ovaries. The expression levels increase after ovulation, as seen in ovaries at estrus and after superovulation. Samples (n = 3 for each timepoint) were collected from 3-month-old females in proestrus and estrus and 1-month-old superovulated females. Expression levels measured by qPCR were normalized to the expression of ribosomal protein L19 (*Rpl19*) and peptidylprolyl isomerase A (*Ppia*). Statistical significance was calculated using the unpaired t-test, and the significance of changes is indicated as follows: $^*p \leq 0.05$.

pregnant mare serum gonadotropin (PMSG) and human chorionic gonadotropin (hCG)—a standard method to induce superovulation (Christenson and Eleftheriou, 1972), both the *Abhd2*$^{+/-}$ and *Abhd2*$^{-/-}$ females produced significantly higher numbers of ovulated eggs (**Figure 3B**). The phenotype was not a result of prematurely ovulated follicles, as *in vitro* fertilization (IVF) studies led to a similar success rate in formation of blastulae as when using eggs from wild-type females (*Abhd2*$^{+/+}$: 72.4% ± 11.3% n = 3, *Abhd2*$^{+/-}$: 81.5% ± 9.1%, *Abhd2*$^{-/-}$: 75.0% ± 8.3% fertilized eggs, n = 4 for both genotypes). The fertility of 7- to 8-month-old *Abhd2*$^{+/-}$ and *Abhd2*$^{-/-}$ females in normal breeding was similar to that of wild-type mice (**Table 1**). Superovulation of the older animals up to 15-month old resulted in a similar decline in the number of ovulated eggs, although some heterozygous and homozygous mice still showed numbers comparable with that of the much younger animals (**Figure 3C**).

Abhd2 Ablation Results in a Dysregulated Estrous Cycle

Interestingly, when following the estrous cycle of virgin females for 1 month, the *Abhd2*$^{-/-}$ females presented with a significantly higher percentage of days in estrus, while proestrus and diestrus were shortened compared with the wild-type females (**Figures 3D-F** and **Supplementary Figure 4**). Although the *Abhd2*$^{-/-}$ mice showed a prolonged estrus, they cycled in a regular fashion (*Abhd2*$^{+/+}$: 4.75 ± 0.33 days/cycle, *Abhd2*$^{+/-}$: 4.8 ± 0.53 days/cycle, *Abhd2*$^{-/-}$: 4.43 ± 0.29 days/cycle) and

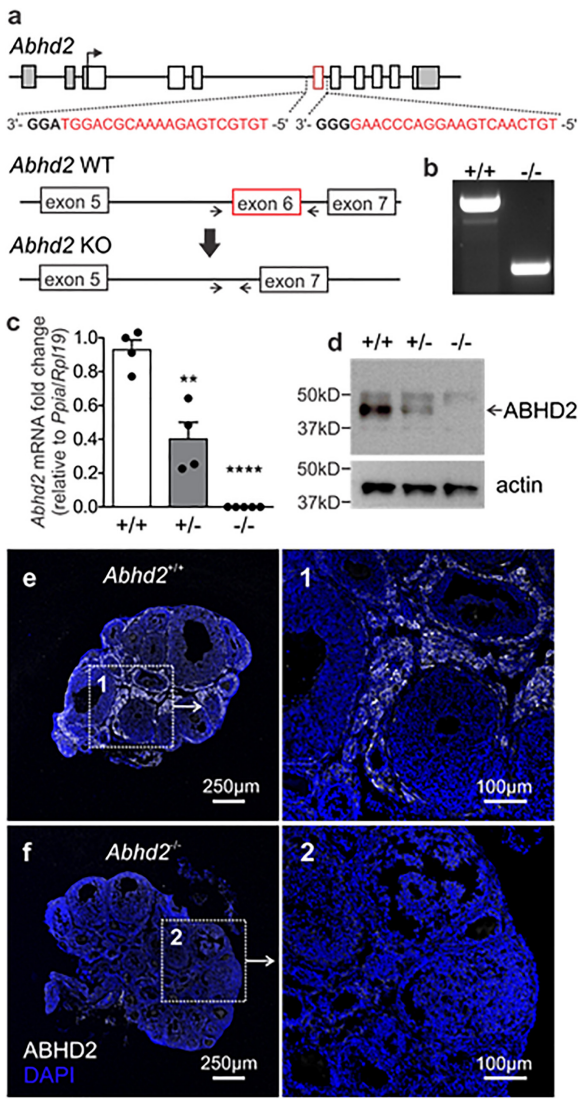

FIGURE 2 | Generation of the Abhd2 KO mouse line. **(a)** Schematic picture of the *Mus musculus Abhd2* gene with untranslated regions marked in gray. Deletion of exon 6 (in red) was performed by CRISPR/Cas9, targeting sequences in the surrounding introns. The sequences of the two sgRNAs are labeled in red and the PAM sequence in bold. **(b)** Genotyping of mice was performed using primers that bind outside the deleted sequence (arrows). The PCR product from a wild-type mouse (+/+) contains the exon 6 sequence while the full KO (-/-) lacks *Abhd2* exon 6. $Abhd2^{+/-}$ mice show a significant reduction of *Abhd2* expression in both **(c)** qPCR and **(d)** western blot studies while the full KO $Abhd2^{-/-}$ completely lacks expression of exon 6 and the protein. Expression levels detected by qPCR were normalized to the expression of ribosomal protein L19 (*Rpl19*) and peptidylprolyl isomerase A (*Ppia*). Statistical significance was calculated using the unpaired *t*-test and the significance of changes is indicated as follows: $^{**}p \leq 0.01$; $^{****}p \leq 0.0001$. $Abhd2^{+/+}$ $n = 4$, $Abhd2^{+/-}$ $n = 4$, and $Abhd2^{-/-}$ $n = 5$. **(e)** The $Abhd2^{+/+}$ mouse ovary shows ABHD2 in the stromal cells surrounding the follicles. **(f)** No protein staining was detected in the $Abhd2^{-/-}$ ovary.

gave rise to litters at a similar rate as $Abhd2^{+/+}$ females (**Table 1**). Previous studies have shown that altered estrogen and androgen levels during pregnancy can affect the estrous cycle of female pups (Abbott et al., 2006). To determine whether or not the maternal genotype influenced the observed phenotype, the estrous cycle of $Abhd2^{+/-}$ females born from wild-type mothers who were mated with homozygous males or homozygous mothers mated with heterozygous males were compared. The month-long measurements showed a similar prolonged estrus in all females ($Abhd2^{+/-}$ females born from $Abhd2^{+/+}$ mothers: 47.2% ± 3.7%; $Abhd2^{+/-}$ mothers: 46.5% ± 6.1%; $Abhd2^{-/-}$ mothers: 46.7% ± 1.9% of days in estrus), while wild-types had only 35.6% ± 5.6% of days in estrus. These results indicate that the observed phenotype was mainly due to the genotype of the pups and not due to epigenetic influence.

Increased Number of Atretic Antral Follicles in $Abhd2^{+/-}$ and $Abhd2^{-/-}$ Ovaries

To determine whether or not the increased number of ovulated eggs produced during superovulation was due to an altered follicular development, early antral and antral follicles and the corpora lutea of ovaries from $Abhd2^{+/+}$, $Abhd2^{+/-}$, and $Abhd2^{-/-}$ littermate females in proestrus were counted. There was a significant decrease in the number of early antral follicles of both $Abhd2^{+/-}$ and $Abhd2^{-/-}$ ovaries compared with those of $Abhd2^{+/+}$ mice (**Figure 4a**). Instead, the females showed an increased number of antral, pre-ovulatory, follicles, and, in the case of $Abhd2^{+/-}$ females, a higher number of corpora lutea (**Figure 4a**). However, these differences did not lead to an altered weight of the ovaries when comparing the different genotypes (**Supplementary Figure 3B**). Hematoxylin staining of the ovary showed a difference in atretic versus healthy, living follicles, with a larger number of atretic follicles present in $Abhd2^{+/-}$ and $Abhd2^{-/-}$ ovaries compared with those of $Abhd2^{+/+}$ mice (**Figures 4b,c**). This was further confirmed by terminal deoxynucleotidyl transferase dUTP nick-end labeling (TUNEL) staining, where follicles going through atresia showed increased labeling of granulosa cells (**Figures 4d,e**). When counting only the healthy antral follicles, no genotype-specific difference in follicle number was observed. Although the $Abhd2^{+/-}$ mice displayed increased follicle atresia compared with the wild-type mice, the number of healthy antral follicles was comparable with that of $Abhd2^{+/+}$ ovaries (**Figure 4b**).

Alpha/Beta Hydrolase Domain-Containing Protein 2 Is Dispensable for *in vitro* Follicle Culture and Ovulation

The increased transition from early antral to antral follicles after *Abhd2* ablation could account for the observed phenotype of superovulated $Abhd2^{+/-}$ and $Abhd2^{-/-}$ females. However, as progesterone is needed to initiate the signaling pathways leading to ovulation, *in vitro* follicle culture was performed to determine the role of ABHD2 in this process. Follicles from immature mice were collected and cultured for 4 days, after which ovulation was induced by the addition of hCG to the culture media (**Figures 5A–C**). The percentage of ovulated follicles was similar between $Abhd2^{+/+}$ and $Abhd2^{-/-}$ females (**Figure 5A**).

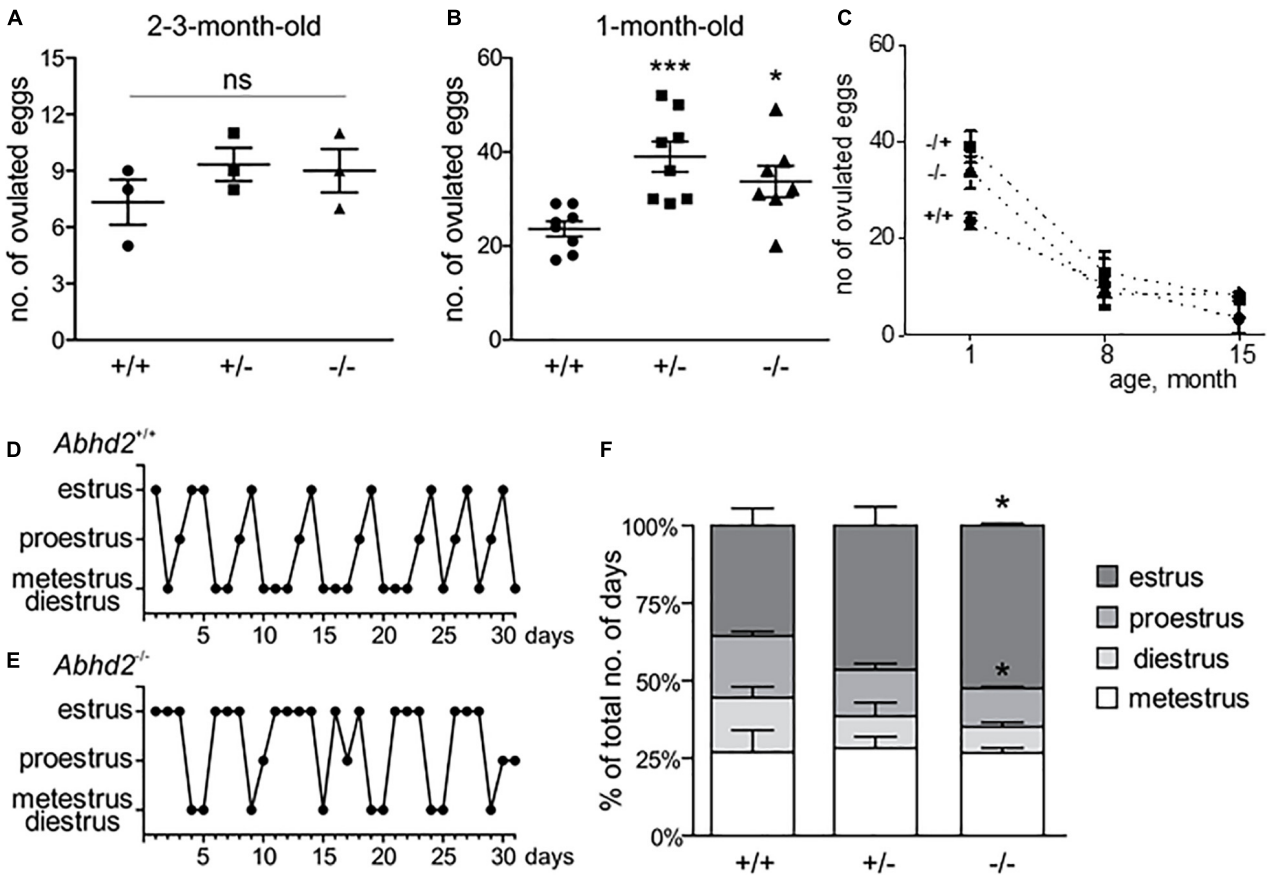

FIGURE 3 | Abhd2$^{-/-}$ female ovulation and estrous cycle. **(A)** Spontaneous ovulation gave rise to similar numbers of eggs for all genotypes (n = 3 for each genotype). **(B)** *Abhd2* ablation caused significantly increased numbers of ovulated eggs after induction of superovulation, in both 1-month-old *Abhd2*$^{+/-}$ (n = 8) and *Abhd2*$^{-/-}$ (n = 7) females compared with *Abhd2*$^{+/+}$ mice (n = 8). Statistical significance was calculated using the unpaired t-test, and the significance of changes is indicated as follows: $^{*}p \leq 0.05$; $^{***}p \leq 0.001$. **(C)** Age-dependent decline in the number of eggs obtained after superovulation of 1-month-old females [data from panel **(B)**], as well as 7- to 8-month-old (*Abhd2*$^{+/+}$ n = 5, *Abhd2*$^{+/-}$ n = 7, and *Abhd2*$^{-/-}$ n = 6) and 15-month-old females (n = 3 per genotype). Representative graphs of the estrous cycle of a **(D)** *Abhd2*$^{+/+}$ and **(E)** *Abhd2*$^{-/-}$ female mouse where the *Abhd2* KO female shows prolonged stages in estrus although displaying cyclical changes throughout the month. **(F)** The combined measurements of three mice of each genotype also showed a significantly altered distribution of days in the different estrous stages, in particular, the increased percentage of days in estrus and decreased percentage of days in proestrus of *Abhd2*$^{-/-}$ females compared with *Abhd2*$^{+/+}$ mice (n = 3 for each genotype).

However, as the initial number of large follicles (240 ± 10 μm in diameter) collected from the *Abhd2*$^{-/-}$ ovaries was higher than that from the wild-type ovaries, the total number of ovulated follicles was increased in cultures from the *Abhd2*$^{-/-}$ females (**Figure 5B**). These results are similar to the higher number of ovulated eggs observed after superovulation of *Abhd2*$^{-/-}$ mice. In conclusion, *Abhd2* ablation does not appear to affect the ovulation process directly but rather gives rise to an increased number of mature follicles, possibly by shortening the timing of diestrus and proestrus.

TABLE 1 | Breeding efficiency of *Abhd2*$^{-/-}$ females.

Female genotype	+/+	+/–	–/–	–/–
Male genotype	+/+	+/–	+/+	+/–
No. of breeding pairs	3	9	2	5
Pups/litter	5.92 ± 0.72	6.46 ± 0.25	6.73 ± 0.68	5.88 ± 0.57
Days between litters	32.4 ± 3.27	31.6 ± 2.03	31.3 ± 3.00	26.1 ± 1.91

Changes in Ovarian Gene Expression After *Abhd2* Ablation

The observed changes in follicle development and estrous cycle of *Abhd2*$^{-/-}$ females might not only result from an altered progesterone signaling but could also be influenced by a change in hormone synthesis. Ovarian hormone production is mainly governed by gonadotropins released by the pituitary gland. Although mRNA of *Abhd2* has been detected in different brain regions, we have not been able to show the presence of the ABHD2 protein in areas other than the epithelial cells of the choroid plexus (**Supplementary Figure 5**), thus, making it unlikely that the observed ovarian phenotype would be

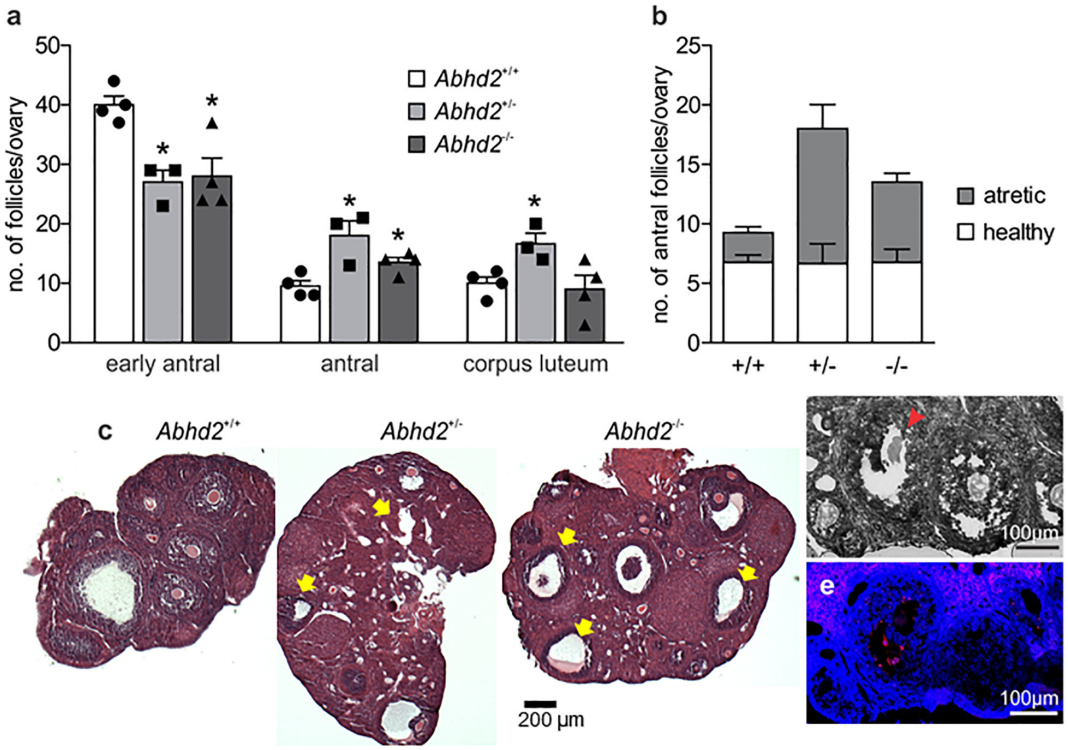

FIGURE 4 | Follicle count of the proestrus ovary. **(a)** Ovaries of 3.5-month-old *Abhd2*$^{+/-}$ (n = 3) and *Abhd2*$^{-/-}$ (n = 4) mice showed significantly lower numbers of early antral follicles, while the antral follicle number was increased compared with the *Abhd2*$^{+/+}$ females (n = 4). **(b)** However, although hematoxylin staining of *Abhd2*$^{+/-}$ and *Abhd2*$^{-/-}$ ovaries displayed a higher number of atretic antral follicles compared with the wild-type ovaries, the total number of healthy follicles was similar between genotypes. **(c)** Representative images of *Abhd2*$^{+/+}$, *Abhd2*$^{+/-}$, and *Abhd2*$^{-/-}$ ovaries with apoptotic antral follicles marked by arrows. **(d,e)** TUNEL staining confirmed the follicles as apoptotic by labeling the granulosa cells of the atretic follicles. Statistical significance was calculated using the unpaired t-test and the significance of changes is indicated as follows: $^{*}p \leq 0.05$. *Abhd2*$^{+/+}$ n = 4, *Abhd2*$^{+/-}$ n = 3, and *Abhd2*$^{-/-}$ n = 4, for all analyses.

caused by changes in neuronal function. To study the effect of *Abhd2* ablation on steroidogenesis in the ovaries, qPCR was performed to detect expression levels of enzymes involved in hormone synthesis. Ovaries of superovulated *Abhd2*$^{-/-}$ females showed no difference in expression of the follicle-stimulating hormone receptor (*Fshr*), a protein vital for follicle development and hormone synthesis, compared with ovaries of *Abhd2*$^{+/+}$ mice (**Figure 6A**). Neither was there a difference in the expression of cytochrome P450 family members (*Cyp11a1*, *Cyp17a1*, or *Cyp19a1*), the enzymes required for synthesis of progesterone, androgens, and estrogens, respectively. Since increased vascularization of the ovary precedes ovulation, the expression of vascular endothelial growth factor A (*Vegfa*), the factor required for vascular endothelial proliferation was also determined. However, no difference in expression between *Abhd2*$^{-/-}$ and *Abhd2*$^{+/+}$ was detected (**Figure 6A**). The expression of nerve growth factor (*Ngf*) and its receptor [nerve growth factor receptor (*Ngfr*)] that are involved in ovulation and in the estrous cycle, were not different between *Abhd2*$^{-/-}$ and *Abhd*$^{+/+}$ females. However, the expression of the NGF receptor neurotrophic receptor tyrosine kinase 1 [*Ntrk1*, previously known as tropomyosin receptor kinase A (*TrkA*)] was significantly increased in KO ovaries compared with those of wild-type mice (**Figure 6B**). It is interesting to note that the expression of NGF in stromal cells of the rodent ovary resembles that of ABHD2 (Dissen et al., 1996). Furthermore, increased NGF levels caused the mice to remain in the estrus stage even though they are still cycling (Dissen et al., 2009; Wilson et al., 2014). NGF signaling is also elevated in women with PCOS (Dissen et al., 2009; Gulino et al., 2016), while increased NGF signaling causes mice to show signs of PCOM, with a higher number of atretic antral follicles, without displaying cyst formation—the phenotype we also observed in *Abhd2*$^{-/-}$ females.

DISCUSSION

The data presented here show a novel regulatory role for the membrane progesterone receptor ABHD2 in follicle development and the sexual cycle of females. ABHD2 is already present in pre-pubertal ovaries, and the expression remains high in older animals, with localization of the protein to stromal cells surrounding the developing follicles and in corpora lutea. *Abhd2* ablation caused a dysregulation of the estrous cycle rhythm with females remaining in the estrus stage for a longer time while also displaying an increased transition of early antral follicles into pre-ovulatory antral follicles. Injection of

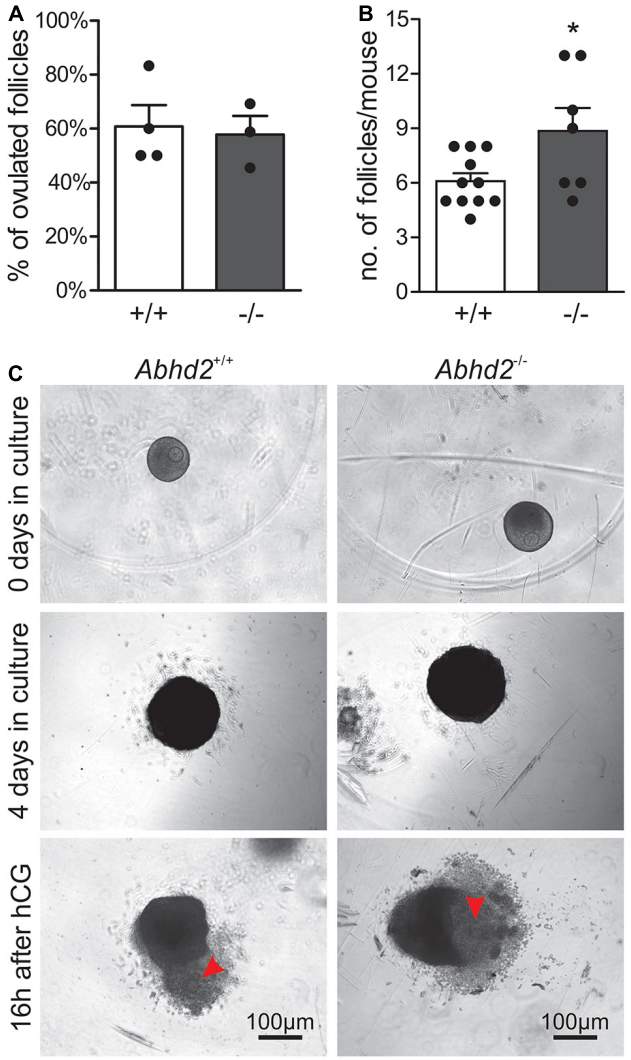

FIGURE 5 | *In vitro* ovulation. Follicles collected from immature mouse ovaries ($Abhd2^{+/+}$ $n = 11$ and $Abhd2^{-/-}$ $n = 7$) were cultured to antral stage, after which ovulation was induced by incubation with hCG. **(A)** No difference in ovulation efficiency was observed between $Abhd2^{+/+}$ and $Abhd2^{-/-}$ mice although **(B)** the ovaries of $Abhd2^{-/-}$ mice contained a higher number of large follicles. **(C)** Representative image of *in vitro* ovulation of an $Abhd2^{+/+}$ and an $Abhd2^{-/-}$ follicle. Statistical significance was calculated using the unpaired *t*-test and the significance of changes is indicated as follows: $*p \leq 0.05$. Using 2–3 mice each time, *in vitro* ovulation was performed four times for $Abhd2^{+/+}$ follicles and three times for follicles collected from $Abhd2^{-/-}$ mice.

PMSG and hCG [which function in a similar manner as the endogenously produced follicle-stimulating hormone (FSH) and luteinizing hormone (LH), respectively, (Engmann et al., 1999)] allowed the follicles to develop fully and resulted in the $Abhd2^{-/-}$ mice ovulating a high number of mature eggs. However, in the native state, the antral follicles displayed signs of atresia, and the $Abhd2^{-/-}$ females ovulated a similar number of eggs as their wild-type littermates. ABHD2 was further shown to only regulate follicle maturation and not influence ovulation directly, by *in vitro* culture, where follicles from $Abhd2^{-/-}$ ovaries responded to hormones in a similar way as those from $Abhd2^{+/+}$ mice.

Interestingly, the phenotype of $Abhd2^{-/-}$ mice resembled that of women with PCOM, where the increased number of anovulatory antral follicles can be rescued through administration of FSH (Engmann et al., 1999; Swanton et al., 2010). Although PCOS is associated with ovarian PCOM, many women display cyst formation without the fertility issues of PCOS. Women who are diagnosed with PCOM may have irregular menstrual cycles with higher numbers of atretic follicles, but can still be fertile (Rosenfield, 2015). The hormone serum concentrations of these women also lie in between those of healthy women and women with PCOS, the latter having significantly higher androgen levels (Rosenfield et al., 2012). Several animal models have been developed to explain the mechanism behind PCOS, for example, administration of high levels of androgens to female mice gives rise to a similar, although more severe, dysregulation of ovarian functions as that observed in $Abhd2^{-/-}$ females. Injection of dehydroepiandrosterone (DHEA) to BALBc females for 20 days caused increased serum levels of both estrogen and progesterone that resulted in the animals remaining in a constant stage of estrus while being unable to ovulate (Luchetti et al., 2004; Sander et al., 2006). Other mouse models with PCOS also showed anovulation but with the mice estrous cycle remaining in diestrus instead of estrus. Injection of dihydrotestosterone (DHT) to C57Bl/6J females for 90 days led to significantly lower levels of progesterone and a fixed cycle at a so-called pseudo-diestrus stage (Caldwell et al., 2014). Balanced steroid secretion and signaling is, thus, what causes the transition from one stage of the estrous cycle to the next and would implicate a lack in hormone balance of $Abhd2^{-/-}$ mice. However, the $Abhd2^{-/-}$ mice did not display a fully developed PCOS, but rather a PCOM phenotype as they were able to ovulate, showed similar fertility as wild-type mice in normal mating, but had an increased number of atretic follicles. Furthermore, the fertility rate would indicate that there were no major changes in luteal function or progesterone levels, as the developing embryos were able to implant and mature to full-term. In addition, $Abhd2^{-/-}$ females still showed estrous cycles with the only differences being a prolonged estrus, and shortened diestrus and proestrus. Excess androgen exposure during fetal development can also lead to a PCOS phenotype in rodents and results in disrupted estrous cycles of the pups (Sullivan and Moenter, 2004). However, we could not detect any difference in estrous cycles when comparing heterozygous mice born from $Abhd2^{+/+}$, $Abhd2^{+/-}$, or $Abhd2^{-/-}$ females, further indicating that the hormone levels of the $Abhd2^{-/-}$ mothers would not be altered in such a way that it could affect the fertility of their offspring. In both rodents and humans, PCOS is often accompanied by a change in insulin resistance and increased body mass index (Sirmans and Pate, 2013; van Houten and Visser, 2014). However, $Abhd2^{-/-}$ females showed regular reduction in glucose levels in glucose tolerance tests, and their body weight was not increased compared with the $Abhd2^{+/+}$ females (**Supplementary Figures 3A,C,D**). In regard to hormone production, there was no significant increase

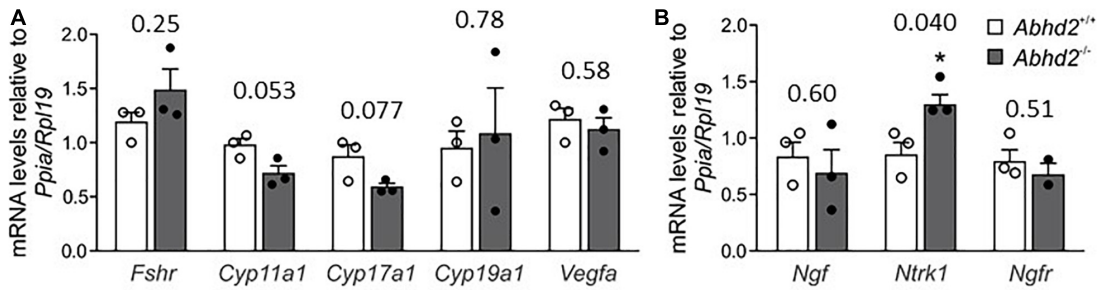

FIGURE 6 | Ovarian gene expression. Relative expression levels of genes involved in steroid synthesis, follicle development and ovulation were measured by qPCR using ovaries of three *Abhd2*$^{+/+}$ and three *Abhd2*$^{-/-}$ 1-month old superovulated mice. **(A)** Expression levels were normalized to the expression of ribosomal protein L19 (*Rpl19*) and peptidylprolyl isomerase A (*Ppia*). Follicle stimulating hormone receptor (*Fshr*), cytochrome P450 family 11 subfamily A member 1 (*Cyp11a1*), cytochrome P450 family 17 subfamily A member 1 (*Cyp17a1*), cytochrome P450 family 19 subfamily A member 1 (*Cyp19a1*), vascular endothelial growth factor A (*Vegfa*), and **(B)** nerve growth factor (*Ngf*), neurotrophic receptor tyrosine kinase 1 (*Ntrk1*), and nerve growth factor receptor (*Ngfr*). Statistical significance was calculated using the unpaired *t*-test, with *p*-values above columns and the significance of changes indicated as: $^{*}p \leq 0.05$.

or decrease in the expression of enzymes regulating steroid production in *Abhd2*$^{-/-}$ ovaries after superovulation, which further supports a PCOM phenotype of mildly altered or normal steroid levels in *Abhd2*$^{-/-}$ mice.

The only detected difference in gene expression after superovulation of wild-type and *Abhd2*$^{-/-}$ mice was an increased expression of the NGF receptor *Ntrk1*. As previously mentioned, the expression of NGF in stromal cells of the rodent ovary resembles that of ABHD2 (Dissen et al., 1996). However, similar to ABHD2, NGF signaling does not only regulate the function of the interstitial cells but can also affect the maturation of granulosa cells, as seen in a mouse model with excess expression of *Ngf*. The *Ngf* overexpressors present with increased antral formation and apoptosis of granulosa cells, which leads to a PCOM phenotype without the formation of ovarian cysts (Dissen et al., 2009; Wilson et al., 2014). However, an additional, mild increase in LH levels caused cysts to form, which would indicate that increased NGF signaling could promote the formation of PCOS (Dissen et al., 2009). Thus, further studies are needed to determine if a change in pituitary hormone secretion could lead to a more prominent phenotype of *Abhd2*$^{-/-}$ mice.

The estrous cycle of mice also changes during aging, with fertile animals spending more time in estrus than older animals who usually become acyclic and remain in diestrus (Nelson et al., 1982). This was shown in a mouse model of premature ovarian failure where the tumor necrosis receptor type I (*Tnfr1*) was ablated. Younger *Tnfr1* KO females, similar to the *Abhd2*$^{-/-}$ mice, displayed a stronger ovulatory response to hormone injections than wild-type females. Young animals also showed a longer period in estrus, which was similar to estrous cycles of 6-month-old females (Roby et al., 1999). The phenotype was caused by a premature sexual maturity, which led to an early onset of senescence at 6 months of age with lower number of litters produced and a disruption in estrous cyclicity (Roby et al., 1999). Similarly, a mouse model with granulosa cell-specific ablation of neuregulin 1 (*Nrg1*) showed signs of early ovarian failure where the estrous cycle stayed in a continuous, so-called, weak estrus (Umehara et al., 2017). These mice also displayed increased fibrosis of ovarian stroma and lower numbers of progeny, a phenotype similar to that of older animals (Umehara et al., 2017). The premature ovarian aging of both *Nrg1* and *Tnfr1* KO females is related to a reduced response to FSH and LH (Roby et al., 1999; Umehara et al., 2017). Although *Abhd2*$^{-/-}$ females show a prolonged estrus at around 3 months of age, this did not lead to a premature decline in fertility at 8 months of age, as was determined by breeding data from *Abhd2*$^{+/-}$ and *Abhd2*$^{-/-}$ females. In addition, there was no observed early depletion in ovulated follicles due to the increased number of antral follicles of *Abhd2* KO females. This was shown after superovulation of older *Abhd2*$^{+/-}$ and *Abhd2*$^{-/-}$ females which still produced similar number of eggs compared with wild-type mice of similar age. It is more likely that the transition from early antral to antral follicle differentiation was altered, as the higher number of antral follicles correlated with a similar decrease in number of early antral follicles. Such a transition might not be enough to give rise to depletion of the ovarian follicular reserve. Instead, we propose that the increased number of anovulatory antral follicles at proestrus could cause the prolonged estrus stage observed in *Abhd2*$^{-/-}$ females. The mice would remain in estrus until the follicles have gone through apoptosis and would thereafter proceed toward the next stage of the estrous cycle. The lack of membrane progesterone receptor (ABHD2) in stromal cells at diestrus, the stage with highest progesterone production (MacDonald et al., 2014), could then cause the cycle to move rapidly into the follicular phase.

In humans, downregulation of *ABHD2* expression resulted in anoikis resistance in high-grade serous ovarian cancer (Yamanoi et al., 2016). The phenotype was attributed to an increased phosphorylation of p38MAPK and MAPK3/1, the signaling pathways which have previously been shown to regulate anoikis resistance (Carduner et al., 2014; Cai et al., 2015; Yamanoi et al., 2016). In healthy ovaries, MAPK3/1 (also known as ERK1/2) signaling is needed for multiple steps in follicle maturation. In early antral follicles, MAPK3/1 phosphorylation inhibits proliferation and induces differentiation of granulosa cells, while in antral follicles, it stimulates cumulus cell expansion and ovulation (Fan et al., 2009). Considering the phenotype of *Abhd2*$^{-/-}$ mice, an increased MAPK3/1 signaling could cause the

observed increase in antral follicle differentiation while further activation through LH signaling could give rise to ovulation of the mature follicles.

In conclusion, *Abhd2* ablation caused an altered follicle maturation, which led to a higher number of antral follicles with an atretic phenotype. In addition, a change in estrous cyclicity was observed with mice spending longer times in estrus. Future studies will focus on the functional role of ABHD2 in this process, which could affect several progesterone signaling pathways in the ovary, including phosphorylation of MAPK/ERK. Furthermore, because of a phenotype resembling PCOM and the known expression of ABHD2 in human ovaries, continued studies of the role of ABHD2 in human follicle maturation and the menstrual cycle could be vital to explain the process of PCOM.

MATERIALS AND METHODS

Generation of *Abhd2* KO Mice Using CRISPR Ribonucleoprotein Electroporation of Zygotes

The CRISPR-EZ method, where single guide RNA (sgRNA)/Cas9 complexes are delivered into mouse zygotes by electroporation, was developed by Chen et al. (2016) and Modzelewski et al. (2018).

SgRNAs to target the introns flanking *Abhd2* exon 6 were designed as previously described. Briefly, we utilized the Gene Perturbation Platform (Doench et al., 2016), Chop-Chop (Montague et al., 2014), and CRISPR Design (Hsu et al., 2013) algorithms to design sgRNAs for the target sequence. The obtained 20-nt sequences were incorporated into a DNA oligonucleotide template containing a T7 promoter and a sgRNA scaffold by overlapping PCR using Phusion high fidelity DNA polymerase (New England Biolabs, M0530). The primer sequences for overlapping PCR were as previously described (Chen et al., 2016) including the designed sgRNA sequences; sgRNA1: 5′-TGTGCTGAGAAAACGCAGGT-3′ and sgRNA2: 5′-TGTCAACTGAAGGACCCAAG-3′) The template sequence was transcribed into RNA using a T7 RNA polymerase (New England Biolabs, E2040S) after which the DNA template was removed by treatment with RNase-Free DNaseI (New England Biolabs, M0303S). The produced sgRNAs were further purified by allowing them to bind to SeraMeg Speedbeads magnetic carboxylate-modified particles (GE Healthcare, 65152105050250). After washing the bead/RNA pellets with 80% ethanol the sgRNAs were eluted in nuclease-free water (Ambion, AM9937) and stored at −80°C until use.

To form a ribonucleoprotein complex, the Cas9 protein (QB3 Macrolab, University of California at Berkeley) was incubated with the two sgRNAs in a solution containing 20 mM HEPES (Sigma, H7523), pH 7.5, 150 mM KCl (Fisher Chemical, P217), 1 mM $MgCl_2$ (Sigma, 68475), 10% glycerol, (Sigma, G2025), and 1 mM reducing agent DL-dithiothreitol (Sigma, D0632), to a final molar ratio of 1:2. The ribonucleoprotein mixture was prepared at 37°C for 10 min immediately before electroporation. To obtain zygotes, 4-week-old C57Bl/6N (Charles River) female mice were superovulated by intraperitoneal injection (i.p.) of 5 IU (PMSG, Sigma, G4877), and 48 h later, 5 IU (hCG, Millipore, 230734), after which they were immediately put in mating with fertile 2- to 4-month-old C57Bl/6N males. Twelve hours post coitum, females with a plug were euthanized, and the one-cell zygotes were collected from the ampulla of the oviduct. The cumulus cells surrounding the fertilized eggs were removed by hyaluronidase treatment (Life Global Group, LGHY-010), and the zona pellucida was weakened by incubation in acidic Tyrode's solution (Sigma, T1788) as previously described (Chen et al., 2016). For delivery of the sgRNA/Cas9 complex, ∼40 zygotes were pooled in Opti-MEM reduced serum media (Gibco, 31985-070) containing the preformed Cas9/sgRNA ribonucleoproteins and loaded into a 1-mm electroporation cuvette (BioRad, 165-2089). Electroporation was performed using the GenePulser Xcell (BioRad, 1652660) with six pulses at 30 V for 3 ms, separated by a 100-ms interval. Immediately after electroporation, the zygotes were washed in KSOM + AA media (KCl-enriched simplex optimization medium with amino acid supplement, Zenith Biotech, ZEKS-050) supplemented with 4 mg/ml bovine serum albumin (BSA, Sigma, A9647), and cultured overnight in KSOM/BSA at 37°C, 5% CO_2. The following day, the embryos that had developed into two-cell stage were implanted into pseudopregnant CD-1 females (Envigo) at ∼10 embryos per oviduct by the UC Berkeley Cancer Research Laboratory, Gene Targeting Facility. The resulting progeny was genotyped using EmeraldAmp GT PCR Master Mix (Takara, RR310) and primers flanking the deleted region of *Abhd2*, Abhd2 Fw: 5′-AGGGCTTAACTCTTGCTGGT-3′, Abhd2 Rev: 5′-ACTCAGACACGATCCGAGAC-3′, Tm: 56°C. Each mouse, positive for the deleted region of *Abhd2*, was placed in breeding with a C57Bl/6N mouse of the opposite gender. The heterozygous progeny of these matings were further bred to produce $Abhd2^{-/-}$ mice and the control $Abhd2^{+/+}$ littermates. All mice were kept in the Animal Facility of the University of California, Berkeley, fed with standard chow diet (PicoLab Rodent diet 20, #5053, LabDiet) and hyper-chlorinated water *ad libitum* in a room with controlled light (14-h light, 10-h darkness) and temperature (23 ± 0.5°C).

Breeding Efficiency and Spontaneous Ovulation

To determine the breeding efficiency of $Abhd2^{+/+}$, $Abhd2^{+/-}$, and $Abhd2^{-/-}$ female mice, 2-month-old females of each genotype were placed in breeding with either $Abhd2^{+/+}$ males ($Abhd2^{+/+}$ and $Abhd2^{-/-}$ females) or $Abhd2^{+/-}$ males ($Abhd2^{+/-}$ and $Abhd2^{-/-}$ females) for ∼6 months. Two or more breeding pairs of each genotype combination were used to determine the average number of offspring per litter and the birth rate of female mice. Furthermore, to detect the number of spontaneously ovulated eggs, 2- to 3-month-old females in proestrus were placed in breeding with fertile $Abhd2^{+/+}$ male mice. When a copulatory plug was detected, the females were euthanized, and the fertilized zygotes were collected from the oviduct ampulla in Dulbecco's phosphate-buffered saline (DPBS, Gibco, 14190-144) and counted.

Superovulation and *in vitro* Fertilization

Sperm from the cauda epididymides of 2-month-old C57Bl/6N male mice were allowed to swim out in Embryomax Human Tubal Fluid medium (HTF, Millipore, MR-070-D) and incubated for capacitation, 1 h at 37°C, 5% CO_2. To collect eggs from seven *Abhd2*$^{+/+}$, eight *Abhd2*$^{+/-}$, and seven *Abhd2*$^{-/-}$ females, superovulation of 3.5- to 4-week-old mice was performed using i.p. injection of PMSG and hCG as described above. Thirteen hours after hCG injection, the females were euthanized, and the cumulus–oocyte complexes were collected from the oviduct ampulla in HTF medium and counted. IVF was performed as previously described (Navarrete et al., 2015) using 300,000 sperm/ml HTF medium. After fertilization, the zygotes were washed in KSOM + AA media, supplemented with 4 μl of BSA and divided into ∼15 zygotes/10 μl of KSOM/BSA for culture at 37°C, 5% CO_2. Three and a half days following IVF, the number of fertilized eggs was determined as the percentage of embryos that had reached morula or blastula stage.

Evaluation of the Mouse Estrous Cycle

Each stage of the mouse estrous cycle was determined in the afternoon by cytological assessment of vaginal smear samples. Samples were collected from 2.5-month-old *Abhd2*$^{+/+}$, *Abhd2*$^{+/-}$, and *Abhd2*$^{-/-}$ mice, three females of each genotype, every day for 1 month. DPBS was used to collect samples of each mouse, using the methods previously described (McLean et al., 2012). Samples were separately placed on glass slides and examined under an Olympus IX-75 inverted light microscope for cellular contents. Visual representation of each estrous cycle phase indicated by Zenclussen et al. (2014) was used as a reference.

Ovarian Follicle Count

To count the total number of follicles in *Abhd2*$^{+/+}$, *Abhd2*$^{+/-}$, and *Abhd2*$^{-/-}$ ovaries, 3- to 4 3.5-month-old female mice of each genotype were euthanized at proestrus stage, and the ovaries were dissected out and weighed. The larger of the two ovaries was fixed in 4% paraformaldehyde (Electron Microscopy Sciences, 15714), embedded in optimal cutting temperature compound (OCT, Sakura, 4583), frozen on dry ice, and stored at −80°C until use. The ovaries were sectioned through, and every fifth section of 8 μm was mounted on glass slides and stained with hematoxylin 1 (Fisher HealthCare, 220-101) using standard procedures. Images of each ovarian section were taken at ×50 magnification and organized sequentially for follicle counting. Using this method, we were able to only count each follicle once, even though the larger follicles were present in several sections. Each follicle was categorized as early antral, antral, or CL based on their morphology. Early antral follicles were identified by the presence of segmented cavities between multiple layers of granulosa cells surrounding the oocyte. Antral follicles were identified by the presence of a large continuous antral cavity, and CL by the absence of oocytes. Atretic antral follicles were defined by a thinning of the granulosa cell layer, which displayed many pyknotic cells, and the additional lack of a clear cumulus cell layer surrounding the oocyte. The morphology of the atretic antral follicles were further confirmed by comparing hematoxylin and TUNEL stainings.

In vitro Ovulation

Ovaries were retrieved from 11 20- to 21-day-old wild-type (C57Bl/6N) and seven *Abhd2*$^{-/-}$ female mice as described previously (Xu et al., 2006; Skory et al., 2015). Briefly, ovaries were placed in dissection media [L15 media (Gibco, 11415-064), 0.5% PenStrep (Fisher Scientific, 15140-122), and 1% fetal bovine serum (FBS, X&Y Cell Culture, FBS-500-HI)], and the bursal sac and any excess material were removed. Each ovary was halved and incubated in collagenase media [Minimum essential medium alpha (αMEM, Gibco, 12561-056), 0.5% PenStrep, 0.8% type I collagenase (Worthington, LS004194), and 1% DNase I (Fisher Scientific, EN0521)] at 37°C and 5% CO_2 for 40 min. Preantral follicles were mechanically isolated using 28-gauge insulin needles in dissection media. Only intact follicles that were 240 ± 10 μm in diameter were isolated and incubated at 37°C and 5% CO_2 in maintenance media (αMEM, 0.5% PenStrep, and 1% FBS) for 2 h before encapsulation. Follicles were encapsulated in 0.7% alginate and cultured as previously described (Xu et al., 2006; Skory et al., 2015), with slight modifications. The encapsulated follicles were placed individually in a 96-well plate (Fisher Scientific, 08-772-53) and cultured for 4 days in 100 μl of growth media [αMEM, 3 mg/ml of BSA, 1 mg/ml of bovine fetuin (Sigma, F3385), 0.01 IU/ml of recombinant human FSH (NHPP, Dr. Parlow), 5 μg/ml of insulin, 5 μg/ml of transferrin, and 5 ng/ml of selenium (Sigma, I1884)]. At day 2 of culture, half of the growth media were exchanged. After 4 days in culture, the alginate was removed by incubating the follicles in alginate lyase media [αMEM, 0.5% PenStrep, 1% FBS, and 1 mg/ml of alginate lyase (Sigma, A1603)] at 37°C and 5% CO_2 for 30 min. Thereafter, antral follicles larger than 330 ± 15 μm in diameter were washed in ovulation media [αMEM, 10% FBS, 5 ng/ml of EGF (Sigma, E4127), 1.5 IU/ml of hCG, 5 μg/ml of insulin, 5 μg/ml of transferrin, and 5 ng/ml of selenium] and placed individually in a 96-well plate containing 100 μl of ovulation media per well. After 16 h at 37°C and 5% CO_2, the percentage of successful ovulation was calculated as the number of follicles with a clear visual evidence of follicle rupture and oocyte extrusion compared with the total follicle number.

Western Blotting

To detect ABHD2 protein in ovaries and different brain regions, 3.5- to 4-week-old *Abhd2*$^{+/+}$, *Abhd2*$^{+/-}$, and *Abhd2*$^{-/-}$ superovulated mice and a 2.5-month-old *Abhd2*$^{+/+}$ female, respectively, were euthanized, the tissue dissected and snap frozen, and protein was isolated using standard procedures. The samples were analyzed by Western blotting, using a rabbit polyclonal anti-ABHD2 antibody (1:10,000 dilution, Proteintech Group, 14039-1-AP) and a peroxidase-conjugated anti-rabbit secondary antibody (1:15,000 dilution, Abcam, ab6721). To ensure equal sample loading, the membrane was stripped by incubation with 1 Min Plus Strip (GM Biosciences, GM6011) according to the instructions of the manufacturer. Thereafter, the membrane was re-hybridized with a mouse monoclonal anti-actin antibody (1:5,000 dilution, Abcam, ab3280-500) and

a peroxidase-conjugated goat anti-mouse secondary antibody (1:15,000 dilution, EMD-Millipore, AP181P).

Immunohistochemistry

Ovaries of superovulated 3.5- to 4-week-old *Abhd2*$^{+/+}$ and *Abhd2*$^{-/-}$ mice were fixed overnight at 4°C in 4% PFA, and the ovary of a 1-week-old *Abhd2*$^{+/+}$ female was fixed for 4 h after which they went through a sucrose gradient (10—20—30% sucrose/PBS) and were frozen in OCT. To detect localization of ABHD2 in the ovary, 8-μm sections were placed on charged slides and immediately used for staining, according to standard procedures. In brief, for antigen retrieval, the sections were incubated in 1% SDS solution for 5 min, blocked in 5% BSA for 1 h at room temperature, and incubated overnight at 4°C with rabbit polyclonal anti-ABHD2 (1:300) and mouse monoclonal anti-α-actin (1:500, sc-32251, Santa Cruz Biotechnology). The antibody–antigen complexes were visualized by incubation for 1 h at room temperature with 1:2,000 Alexa Fluor 488-conjugated goat anti-rabbit (Molecular Probes A11008/Jackson ImmunoResearch, 111-485-144) and Cy5-conjugated donkey anti-mouse (Jackson ImmunoResearch, 715-175-150) or anti-rabbit (Jackson ImmunoResearch, 711-015-152) antibodies. The sections were mounted using ProLong Gold antifade reagent with DAPI (Invitrogen, P36935) and imaged using confocal laser scanning microscopy (Olympus Fluoview FV1000).

Reverse Transcriptase and Quantitative RT-PCR

For analysis of gene expression, 21- and 28-day-old *Abhd2*$^{+/+}$ mice were euthanized, and the ovaries were dissected out and snap frozen. Samples from superovulated 1- to 2-month-old mice at proestrus and estrus were similarly collected and frozen. Total RNA was isolated from the tissues using TRIzol reagent according to the instructions of the manufacturer (Ambion, 15596018). For reverse transcription, 1 μg of total RNA was treated with DNaseI and reverse-transcribed by using the RevertAid H Minus RT enzyme (Fisher Scientific, EP0451). The cDNA was diluted 1:50–1:100 for qPCR. qPCR was performed using the DyNAmo HS SYBR Green qPCR Master Mix (Fisher Scientific, F-410). All samples were run in triplicate reactions. For analysis of *Abhd2* expression at different time points in wild-type mice ovaries primers binding to exon 3 and exon 4 were used (*Abhd2* e3 Fw and *Abhd2* e4 Re). To determine expression of the deleted exon 6 in *Abhd2*, KO mice primers binding in exon 5 and exon 6 were used (*Abhd2* e5 Fw and *Abhd2* e6 Re). Ribosomal protein L19 (*Rpl19*) and peptidylprolyl isomerase A (*Ppia*) were used as endogenous controls to equalize for the amounts of RNA in the ovaries. Primer sequences for *Rpl19*, *Ppia*, and cytochrome P450 family 19 subfamily A member 1 (*Cyp19a1*) were as previously described (Björkgren et al., 2012; Hakkarainen et al., 2015). Primer sequences and qPCR conditions for analyzing the expression of *Abhd2*, *Fshr*, cytochrome P450 family 11 subfamily A member 1 (*Cyp11a1*), cytochrome P450 family 17 subfamily A member 1 (*Cyp17a1*), *Vegfa*, *Ngf*, *Ntrk1*, and *Ngfr* are described in **Supplementary Table 1**.

Intraperitoneal Glucose Tolerance Test

To detect the effect of *Abhd2* ablation on glucose uptake, 2.5-month-old *Abhd2*$^{+/+}$ (n = 5), *Abhd2*$^{+/-}$ (n = 7), and *Abhd2*$^{-/-}$ (n = 6) female mice were fasted overnight (16 h). Blood glucose levels were measured as mmol/L by tail vein sampling using Contour Next ONE meter (Ascensia Diabetes Care) and Contour Next blood glucose test strips (Ascensia Diabetes Care). Immediately after baseline measurement (0 min), the mice were given an i.p. injection of 2 g/kg glucose (20% solution), and blood glucose levels were measured at 15, 30, 60, and 120 min after injection.

Statistical Analyses

For statistical analyses of fertility efficiency, ovulation number, days in estrus, follicle numbers, and gene expression levels, the GraphPad Prism 5 software (GraphPad Software, Inc., La Jolla, CA, United States) was used. Unpaired t-test was used to determine statistical significance, assigning $p \leq 0.05$ as the limit. All results are shown with standard error of mean.

DATA AVAILABILITY STATEMENT

The original contributions presented in the study are included in the article/**Supplementary Material**, further inquiries can be directed to the corresponding authors.

ETHICS STATEMENT

The animal study was reviewed and approved by the Animals were humanely killed according to ACUC guidelines with every effort made to minimize suffering. All experiments were performed in accordance with NIH Guidelines for Animal Research and approved by the UC Berkeley Animal Care and Use Committee (AUP 2015-07-7742).

AUTHOR CONTRIBUTIONS

IB and PL conceived the project, designed the experiments, and wrote the manuscript. IB performed or assisted in the completion of all studies, data acquisition, and analysis for the manuscript. DHC collected the samples for estrous stage analysis, determined the follicle count, and performed *in vitro* follicle culture. SM and NP assisted in the maintenance of the mouse colony and performing molecular biology analysis. LG-K and NP assisted in performing the *in vitro* fertilization studies. AM provided assistance in designing the sgRNAs and assisted with performing the zygote electroporation. LH helped with CRISPR-EZ by providing essential reagents and support. All authors discussed the results and commented on the manuscript.

FUNDING

This work was supported by R01GM111802, the Pew Biomedical Scholars Award, and the Packer Wentz Endowment Will and

the GCRLE grant from Global Consortium for Reproductive Longevity and Equality at the Buck Institute, made possible by the Bia-Echo Foundation (to PL). Publication made possible in part by support from the Berkeley Research Impact Initiative (BRII) sponsored by the UC Berkeley Library.

ACKNOWLEDGMENTS

We thank S. Chen (Department of Molecular and Cell Biology, University of California, Berkeley) for preparation of the SeraMeg SpeedBeads for sgRNA purification and A. Shikanov (Department of Biomedical Engineering, University of Michigan) for providing the protocol for *in vitro* follicle culture.

SUPPLEMENTARY MATERIAL

The Supplementary Material for this article can be found online at: https://www.frontiersin.org/articles/10.3389/fcell.2021.710864/full#supplementary-material

Supplementary Figure 1 | Estrous cycle of mice. Smears from vaginal lavage of mice show the distinct cell types of different estrous stages. Proestrus shows multiple nucleated cells (arrows) while the estrus sample only displays cornified epithelial cells. When the mouse enters the luteal phase, leukocytes start to appear and at diestrus they are the dominant cell type in the smear. At proestrus the antral follicle is formed, as depicted in the drawing. The mature oocyte is ovulated at estrus after which the remaining follicle goes through luteinization and forms corpus luteum (CL). Active secretion of progesterone from CL peaks at diestrus followed by luteolysis of the CL cells and resumption of proestrus.

Supplementary Figure 2 | CRISPR-EZ results. **(A)** Genotyping of the 17 mice born after implantation of 78 CRISPR-EZ treated 2-cell stage embryos showed seven pups with a deletion of *Abhd2* exon 6. Two of the mice, marked in red, were chosen for further phenotypic analysis. **(B,D)** Sequencing of the shorter *Abhd2* KO product, obtained after genotyping PCR of the founder mice, showed a deletion of exon 6 starting in the surrounding introns. The chromatograms correspond to the sequence marked in red, with arrows pointing to the ligation site of the two introns. **(C,E)** Superovulation results from pups born from the two founder mouse lines display similar increase in number of ovulated eggs.

Supplementary Figure 3 | *Abhd2* ablation does not alter the weight or the glucose uptake of mice. **(A,B)** The weight of 2-4-month-old female mice and ovaries from 3 to 4-month-old mice in proestrus did not differ between genotypes. **(C)** Average values of glucose tolerance test of 2.5-month-old female mice, fasted overnight and thereafter given an intraperitoneal injection of 2 g/kg glucose. **(D)** The individual measurements of the mice used for the glucose tolerance test in panel **(C)**. No statistical difference was detected in glucose uptake when comparing *Abhd2*$^{+/+}$, *Abhd2*$^{+/-}$, and *Abhd2*$^{-/-}$ mice.

Supplementary Figure 4 | Estrous cycle of *Abhd2*$^{-/-}$ mice. The estrous cycle measured for 1 month in mice used for the analysis in **Figure 3F**.

Supplementary Figure 5 | *ABHD2* in different brain regions of mice. ABHD2 was detected in lateral (LCP) and 4th ventricle choroid plexus (4thCP) by Western blot, while the main olfactory bulb (OB), the cerebral cortex (CTX), the hippocampus (HIP) and the cerebellum (CB) of female mice only show background staining. Samples were collected from a 2.5-month-old *Abhd2*$^{+/+}$ female mouse.

REFERENCES

Abbott, D. H., Padmanabhan, V., and Dumesic, D. A. (2006). Contributions of androgen and estrogen to fetal programming of ovarian dysfunction. *Reprod. Biol. Endocrinol.* 4:17. doi: 10.1186/1477-7827-4-17

Baldi, E., Casano, R., Falsetti, C., Krausz, C., Maggi, M., and Forti, G. (1991). Intracellular calcium accumulation and responsiveness to progesterone in capacitating human spermatozoa. *J. Androl.* 12, 323–330.

Björkgren, I., Saastamoinen, L., Krutskikh, A., Huhtaniemi, I., Poutanen, M., and Sipilä, P. (2012). Dicer1 ablation in the mouse epididymis causes dedifferentiation of the epithelium and imbalance in sex steroid signaling. *PLoS One* 7:e38457. doi: 10.1371/journal.pone.0038457

Blackmore, P. F., Beebe, S. J., Danforth, D. R., and Alexander, N. (1990). Progesterone and 17 alpha-hydroxyprogesterone. Novel stimulators of calcium influx in human sperm. *J. Biol. Chem.* 265, 1376–1380. doi: 10.1016/s0021-9258(19)40024-0

Blackmore, P. F., Neulen, J., Lattanzio, F., and Beebe, S. J. (1991). Cell surface-binding sites for progesterone mediate calcium uptake in human sperm. *J. Biol. Chem.* 266, 18655–18659. doi: 10.1016/s0021-9258(18)55113-9

Cai, Q., Yan, L., and Xu, Y. (2015). Anoikis resistance is a critical feature of highly aggressive ovarian cancer cells. *Oncogene* 34, 3315–3324. doi: 10.1038/onc.2014.264

Caldwell, A. S., Middleton, L. J., Jimenez, M., Desai, R., McMahon, A. C., Allan, C. M., et al. (2014). Characterization of reproductive, metabolic, and endocrine features of polycystic ovary syndrome in female hyperandrogenic mouse models. *Endocrinology* 155, 3146–3159. doi: 10.1210/en.2014-1196

Carduner, L., Picot, C. R., Leroy-Dudal, J., Blay, L., Kellouche, S., and Carreiras, F. (2014). Cell cycle arrest or survival signaling through alphav integrins, activation of PKC and ERK1/2 lead to anoikis resistance of ovarian cancer spheroids. *Exp. Cell Res.* 320, 329–342. doi: 10.1016/j.yexcr.2013.11.011

Chen, S., Lee, B., Lee, A. Y., Modzelewski, A. J., and He, L. (2016). Highly efficient mouse genome editing by CRISPR ribonucleoprotein electroporation of zygotes. *J. Biol. Chem.* 291, 14457–14467. doi: 10.1074/jbc.M116.733154

Christenson, C. M., and Eleftheriou, B. E. (1972). Dose-dependence of superovulation response in mice to two injections of PMSG. *J. Reprod. Fertil.* 29, 287–289. doi: 10.1530/jrf.0.0290287

Dissen, G. A., Garcia-Rudaz, C., Paredes, A., Mayer, C., Mayerhofer, A., and Ojeda, S. R. (2009). Excessive ovarian production of nerve growth factor facilitates development of cystic ovarian morphology in mice and is a feature of polycystic ovarian syndrome in humans. *Endocrinology* 150, 2906–2914. doi: 10.1210/en.2008-1575

Dissen, G. A., Hill, D. F., Costa, M. E., Les Dees, C. W., Lara, H. E., and Ojeda, S. R. (1996). A role for trkA nerve growth factor receptors in mammalian ovulation. *Endocrinology* 137, 198–209. doi: 10.1210/endo.137.1.8536613

Doench, J. G., Fusi, N., Sullender, M., Hegde, M., Vaimberg, E. W., Donovan, K. F., et al. (2016). Optimized sgRNA design to maximize activity and minimize off-target effects of CRISPR-Cas9. *Nat. Biotechnol.* 34, 184–191. doi: 10.1038/nbt.3437

Engmann, L., Maconochie, N., Sladkevicius, P., Bekir, J., Campbell, S., and Tan, S. L. (1999). The outcome of in-vitro fertilization treatment in women with sonographic evidence of polycystic ovarian morphology. *Hum. Reprod.* 14, 167–171. doi: 10.1093/humrep/14.1.167

Fan, H. Y., Liu, Z., Shimada, M., Sterneck, E., Johnson, P. F., Hedrick, S. M., et al. (2009). MAPK3/1 (ERK1/2) in ovarian granulosa cells are essential for female fertility. *Science* 324, 938–941. doi: 10.1126/science.1171396

Gulino, F. A., Giuffrida, E., Leonardi, E., Marilli, I., and Palumbo, M. A. (2016). Intrafollicular nerve growth factor concentration in patients with polycystic ovary syndrome: a case-control study. *Minerva Ginecol.* 68, 110–116.

Hakkarainen, J., Jokela, H., Pakarinen, P., Heikelä, H., Kätkänaho, L., Vandenput, L., et al. (2015). Hydroxysteroid (17beta)-dehydrogenase 1-deficient female mice present with normal puberty onset but are severely subfertile due to a defect in luteinization and progesterone production. *FASEB J.* 29, 3806–3816. doi: 10.1096/fj.14-269035

Hashimoto-Partyka, M. K., Lydon, J. P., and Iruela-Arispe, M. L. (2006). Generation of a mouse for conditional excision of progesterone receptor. *Genesis* 44, 391–395. doi: 10.1002/dvg.20227

Hsu, P. D., Scott, D. A., Weinstein, J. A., Ran, F. A., Konermann, S., Agarwala, V., et al. (2013). DNA targeting specificity of RNA-guided Cas9 nucleases. *Nat. Biotechnol.* 31, 827–832. doi: 10.1038/nbt.2647

Luchetti, C. G., Solano, M. E., Sander, V., Arcos, M. L., Gonzalez, C., Di Girolamo, G., et al. (2004). Effects of dehydroepiandrosterone on ovarian cystogenesis and immune function. *J. Reprod. Immunol.* 64, 59–74. doi: 10.1016/j.jri.2004.04.002

Lydon, J. P., DeMayo, F. J., Funk, C. R., Mani, S. K., Hughes, A. R., Montgomery, C. A. Jr., et al. (1995). Mice lacking progesterone receptor exhibit pleiotropic reproductive abnormalities. *Genes Dev.* 9, 2266–2278. doi: 10.1101/gad.9.18.2266

MacDonald, J. K., Pyle, W. G., Reitz, C. J., and Howlett, S. E. (2014). Cardiac contraction, calcium transients, and myofilament calcium sensitivity fluctuate with the estrous cycle in young adult female mice. *Am. J. Physiol. Heart Circ. Physiol.* 306, H938–H953. doi: 10.1152/ajpheart.00730.2013

McLean, A. C., Valenzuela, N., Fai, S., and Bennett, S. A. (2012). Performing vaginal lavage, crystal violet staining, and vaginal cytological evaluation for mouse estrous cycle staging identification. *J. Vis. Exp.* e4389. doi: 10.3791/4389

Miller, M. R., Mannowetz, N., Iavarone, A. T., Safavi, R., Gracheva, E. O., Smith, J. F., et al. (2016). Unconventional endocannabinoid signaling governs sperm activation via the sex hormone progesterone. *Science* 352, 555–559. doi: 10.1126/science.aad6887

Modzelewski, A. J., Chen, S., Willis, B. J., Lloyd, K. C. K., Wood, J. A., and He, L. (2018). Efficient mouse genome engineering by CRISPR-EZ technology. *Nat. Protoc.* 13, 1253–1274. doi: 10.1038/nprot.2018.012

Montague, T. G., Cruz, J. M., Gagnon, J. A., Church, G. M., and Valen, E. (2014). CHOPCHOP: a CRISPR/Cas9 and TALEN web tool for genome editing. *Nucleic Acids Res.* 42, W401–W407. doi: 10.1093/nar/gku410

Navarrete, F. A., García-Vázquez, F. A., Alvau, A., Escoffier, J., Krapf, D., Sánchez-Cárdenas, C., et al. (2015). Biphasic role of calcium in mouse sperm capacitation signaling pathways. *J. Cell Physiol.* 230, 1758–1769. doi: 10.1002/jcp.24873

Nelson, J. F., Felicio, L. S., Randall, P. K., Sims, C., and Finch, C. E. (1982). A longitudinal study of estrous cyclicity in aging C57BL/6J mice: i. cycle frequency, length and vaginal cytology. *Biol. Reprod.* 27, 327–339. doi: 10.1095/biolreprod27.2.327

Poisbeau, P., Keller, A. F., Aouad, M., Kamoun, N., Groyer, G., and Schumacher, M. (2014). Analgesic strategies aimed at stimulating the endogenous production of allopregnanolone. *Front. Cell Neurosci.* 8:174. doi: 10.3389/fncel.2014.00174

Revelli, A., Massobrio, M., and Tesarik, J. (1998). Nongenomic actions of steroid hormones in reproductive tissues. *Endocr. Rev.* 19, 3–17. doi: 10.1210/edrv.19.1.0322

Roby, K. F., Son, D. S., and Terranova, P. F. (1999). Alterations of events related to ovarian function in tumor necrosis factor receptor type I knockout mice. *Biol. Reprod.* 61, 1616–1621. doi: 10.1095/biolreprod61.6.1616

Rosenfield, R. L. (2015). The polycystic ovary morphology-polycystic ovary syndrome spectrum. *J. Pediatr. Adolesc. Gynecol.* 28, 412–419. doi: 10.1016/j.jpag.2014.07.016

Rosenfield, R. L., Wroblewski, K., Padmanabhan, V., Littlejohn, E., Mortensen, M., and Ehrmann, D. A. (2012). Antimüllerian hormone levels are independently related to ovarian hyperandrogenism and polycystic ovaries. *Fertil. Steril.* 98, 242–249. doi: 10.1016/j.fertnstert.2012.03.059

Roy, S. K., and Greenwald, G. S. (1987). In vitro steroidogenesis by primary to antral follicles in the hamster during the periovulatory period: effects of follicle-stimulating hormone, luteinizing hormone, and prolactin. *Biol. Reprod.* 37, 39–46. doi: 10.1095/biolreprod37.1.39

Sander, V., Luchetti, C. G., Solano, M. E., Elia, E., Di Girolamo, G., Gonzalez, C., et al. (2006). Role of the N, N'-dimethylbiguanide metformin in the treatment of female prepuberal BALB/c mice hyperandrogenized with dehydroepiandrosterone. *Reproduction* 131, 591–602. doi: 10.1530/rep.1.00941

Sirmans, S. M., and Pate, K. A. (2013). Epidemiology, diagnosis, and management of polycystic ovary syndrome. *Clin. Epidemiol.* 6, 1–13. doi: 10.2147/CLEP.S37559

Skory, R. M., Xu, Y., Shea, L. D., and Woodruff, T. K. (2015). Engineering the ovarian cycle using in vitro follicle culture. *Hum. Reprod.* 30, 1386–1395. doi: 10.1093/humrep/dev052

Sullivan, S. D., and Moenter, S. M. (2004). Prenatal androgens alter GABAergic drive to gonadotropin-releasing hormone neurons: implications for a common fertility disorder. *Proc. Natl. Acad. Sci. U.S.A.* 101, 7129–7134. doi: 10.1073/pnas.0308058101

Swanton, A., Storey, L., McVeigh, E., and Child, T. (2010). IVF outcome in women with PCOS, PCO and normal ovarian morphology. *Eur. J. Obstet. Gynecol. Reprod. Biol.* 149, 68–71. doi: 10.1016/j.ejogrb.2009.11.017

Umehara, T., Kawai, T., Kawashima, I., Tanaka, K., Okuda, S., Kitasaka, H., et al. (2017). The acceleration of reproductive aging in Nrg1(flox/flox);Cyp19-Cre female mice. *Aging Cell* 16, 1288–1299. doi: 10.1111/acel.12662

van Houten, E. L., and Visser, J. A. (2014). Mouse models to study polycystic ovary syndrome: a possible link between metabolism and ovarian function? *Reprod. Biol.* 14, 32–43. doi: 10.1016/j.repbio.2013.09.007

Walmer, D. K., Wrona, M. A., Hughes, C. L., and Nelson, K. G. (1992). Lactoferrin expression in the mouse reproductive tract during the natural estrous cycle: correlation with circulating estradiol and progesterone. *Endocrinology* 131, 1458–1466. doi: 10.1210/endo.131.3.1505477

Wilson, J. L., Chen, W., Dissen, G. A., Ojeda, S. R., Cowley, M. A., Garcia-Rudaz, C., et al. (2014). Excess of nerve growth factor in the ovary causes a polycystic ovary-like syndrome in mice, which closely resembles both reproductive and metabolic aspects of the human syndrome. *Endocrinology* 155, 4494–4506. doi: 10.1210/en.2014-1368

Xu, M., Kreeger, P. K., Shea, L. D., and Woodruff, T. K. (2006). Tissue-engineered follicles produce live, fertile offspring. *Tissue Eng.* 12, 2739–2746. doi: 10.1089/ten.2006.12.2739

Yamanoi, K., Matsumura, N., Murphy, S. K., Baba, T., Abiko, K., Hamanishi, J., et al. (2016). Suppression of ABHD2, identified through a functional genomics screen, causes anoikis resistance, chemoresistance and poor prognosis in ovarian cancer. *Oncotarget* 7, 47620–47636. doi: 10.18632/oncotarget.9951

Zenclussen, M. L., Casalis, P. A., Jensen, F., Woidacki, K., and Zenclussen, A. C. (2014). Hormonal fluctuations during the estrous cycle modulate heme Oxygenase-1 expression in the uterus. *Front. Endocrinol.* 5:32. doi: 10.3389/fendo.2014.00032

Conflict of Interest: LH is an inventor on patents of an electroporation-based CRISPR technology for mouse genome engineering and is a co-founder of a company to further develop this technology for mammalian genome editing.

The remaining authors declare that the research was conducted in the absence of any commercial or financial relationships that could be construed as a potential conflict of interest.

Publisher's Note: All claims expressed in this article are solely those of the authors and do not necessarily represent those of their affiliated organizations, or those of the publisher, the editors and the reviewers. Any product that may be evaluated in this article, or claim that may be made by its manufacturer, is not guaranteed or endorsed by the publisher.

frontiers in Cell and Developmental Biology

REVIEW
published: 16 September 2021
doi: 10.3389/fcell.2021.718522

Reproductive Aging in *Caenorhabditis elegans*: From Molecules to Ecology

*Andrea Scharf[1], Franziska Pohl[1,2], Brian M. Egan[1], Zuzana Kocsisova[1] and Kerry Kornfeld[1]**

[1] Department of Developmental Biology, Washington University School of Medicine, St. Louis, MO, United States,
[2] Department of Medicine, Washington University School of Medicine, St. Louis, MO, United States

Aging animals display a broad range of progressive degenerative changes, and one of the most fascinating is the decline of female reproductive function. In the model organism *Caenorhabditis elegans*, hermaphrodites reach a peak of progeny production on day 2 of adulthood and then display a rapid decline; progeny production typically ends by day 8 of adulthood. Since animals typically survive until day 15 of adulthood, there is a substantial post reproductive lifespan. Here we review the molecular and cellular changes that occur during reproductive aging, including reductions in stem cell number and activity, slowing meiotic progression, diminished Notch signaling, and deterioration of germ line and oocyte morphology. Several interventions have been identified that delay reproductive aging, including mutations, drugs and environmental factors such as temperature. The detailed description of reproductive aging coupled with interventions that delay this process have made *C. elegans* a leading model system to understand the mechanisms that drive reproductive aging. While reproductive aging has dramatic consequences for individual fertility, it also has consequences for the ecology of the population. Population dynamics are driven by birth and death, and reproductive aging is one important factor that influences birth rate. A variety of theories have been advanced to explain why reproductive aging occurs and how it has been sculpted during evolution. Here we summarize these theories and discuss the utility of *C. elegans* for testing mechanistic and evolutionary models of reproductive aging.

Keywords: reproduction, germ line, aging, evolution, matricidal hatching, egg-laying, oocyte quality, menopause

OPEN ACCESS

Edited by:
Michael Klutstein, The Hebrew University of Jerusalem, Israel

Reviewed by:
E. Jane Albert Hubbard, NYU Grossman School of Medicine, United States
Yoanatan Tzur, The Hebrew University of Jerusalem, Israel

***Correspondence:**
Kerry Kornfeld
kornfeld@wustl.edu

Specialty section:
This article was submitted to Molecular and Cellular Reproduction, a section of the journal Frontiers in Cell and Developmental Biology

Received: *01 June 2021*
Accepted: *04 August 2021*
Published: *16 September 2021*

Citation:
Scharf A, Pohl F, Egan BM, Kocsisova Z and Kornfeld K (2021) Reproductive Aging in Caenorhabditis elegans: From Molecules to Ecology. Front. Cell Dev. Biol. 9:718522. doi: 10.3389/fcell.2021.718522

INTRODUCTION

Aging can be defined as the progressive decline of tissue morphology and function with increasing chronological age that eventually results in death of the organism. Since the discovery of single gene mutations that delay age-related decline and extend lifespan, *Caenorhabditis elegans* has become one of the leading model organisms to study aging (Friedman and Johnson, 1988; Kenyon et al., 1993; Tissenbaum, 2015). This non-parasitic, 1 mm nematode species lives on rotten plant material in the wild and can be easily cultivated on agar dishes or liquid medium in the laboratory (Corsi et al., 2015). *C. elegans* is well suited for aging research due to its short average lifespan of approximately 15 days and well characterized progressive, degenerative changes that are also observed in many larger animals with much longer lifespans, such as mammals (Collins et al., 2007). Interestingly, the nematode also experiences a loss of reproductive capacity

in mid-life and a substantial post reproductive lifespan, similar to human females that undergo menopause around 50 years of age and typically survive until 80 years of age. In addition, oocyte quality decreases during hermaphrodite aging, which parallels the increasing likelihood of birth defects with increasing maternal age in humans (Nagaoka et al., 2012). These similarities between nematodes and humans indicate that *C. elegans* is a relevant model system to investigate the process of reproductive aging. The major advantage of *C. elegans* is that it is an experimentally powerful model organism: the animals are easy to cultivate, they are transparent which makes it easy to analyze morphological changes, and they are amenable to sophisticated genetic approaches due to their androdioecy (Morsci et al., 2011; Corsi et al., 2015). Populations consist of mostly hermaphrodites with few males, and they can be kept as clonal populations. The experimental advantages of studying this animal have led to systematic descriptions of age-related changes in its germ line, investigations of the underlying mechanisms, and the discovery of interventions that prolong the reproductive period and conserve oocyte quality later in life.

In this review, we focus on reproductive aging of the *C. elegans* hermaphrodite. Although males are of interest, it is much more difficult to analyze the age-related decline of male reproduction and little information is available. The germline of *C. elegans* hermaphrodites is regulated by sperm, and in hermaphrodites that lack sperm the oocytes display time-dependent loss of viability (Andux and Ellis, 2008; Adam Bohnert and Kenyon, 2017; Achache et al., 2021). We do not focus on this process because the regulatory circuit appears to function in young and old animals and thus is distinct from age-related degeneration. More specifically, we discuss observational studies that document the age-related decline of reproductive function in unmated and mated wild-type hermaphrodites, matricidal death as a reproductive aging phenotype, and morphological and molecular age-related changes of the reproductive organs. We then describe interventions that delay reproductive aging and provide evidence regarding mechanistic drivers, including single gene mutations, drugs, and environmental factors. Finally, we consider the ecological consequences of reproductive aging in light of evolutionary theory. Many other fine reviews cover the development and function of the germ line in young animals (Lints and Hall, 2009b; Hubbard and Schedl, 2019), the age-related decline of oocyte quality (Luo and Murphy, 2011), germ line soma interaction in aging (Antebi, 2013), and the comparison of reproductive aging in different model organisms including humans (Quesada-Candela et al., 2021).

Caenorhabditis elegans develops from a fertilized egg into a mature egg-laying hermaphrodite in about 65 h at 20°C (Byerly et al., 1976). The reproductive organs are organized into two U-shaped symmetric gonad arms, through which developing eggs proceed in an assembly line fashion (**Figure 1A**). Each arm is comprised of the somatic gonad and the germ line, including the spermatheca. They unite in a shared uterus with the egg-laying apparatus. The function of the reproductive organs is to produce mature gametes, fertilize oocytes, and deposit the eggs into the environment. The stem cells reside in the progenitor zone of the distal syncytial germ line. The progenitor zone is about 20-cell-diameters long and harbors the only stem cells of adult *C. elegans*, the mitotic cycling germline stem cells. This region also includes the progenitor cells and the meiotic S-phase cells. Proliferation of germline stem cells is initiated and maintained by Notch ligand from the somatic distal tip cell. Germline stem cells that receive Notch signal remain in mitosis, but as they migrate proximally and lose contact with the distal tip cell, the stem cell nuclei enter the meiotic prophase with an average duration of 48 h including cellularization and growth (Hubbard and Schedl, 2019). It is challenging to precisely define these stem cells experimentally and conceptually, since they transition from the stem cell fate to a non-stem cell fate as they progress along the germ line. If stem cells are defined using molecular markers as SYGL-1 positive, then these cells do not proceed directly into meiotic S phase but rather they usually divide after losing SYGL-1 expression. In contrast to the early blastoderm in *Drosophila*, *C. elegans* stem cell nuclei are surrounded by cell membranes and behave like cells (Lints and Hall, 2009b). The number of germ cells that enter prophase of meiosis I is larger than the number that complete prophase of meiosis I as a result of apoptosis that occurs in late pachytene. The surviving germ cells then require an activation signal from the sperm in the form of the major sperm protein, which induces the completion of meiosis and the ovulation into the spermatheca, where fertilization occurs (Luo and Murphy, 2011; Pazdernik and Schedl, 2013; Huelgas-Morales and Greenstein, 2018; Hubbard and Schedl, 2019). After fertilization, the oocyte moves through the uterus and is pushed into the environment via the vulva. Production of fertilized eggs follows a time schedule that results in a characteristic progeny production curve (**Figures 1C,D**). After the hermaphrodite sexually matures, progeny production increases until it reaches a peak on adult day 2 (adult day 1 is defined as the 24-h period after the hermaphrodite laid its first egg, adult day 2 is defined as the subsequent 24-h period, etc.). At peak production, oocytes are ovulated every ∼23 min (McCarter et al., 1999), resulting in an average of ∼150 progeny per day. Progeny production rapidly decreases over the following days until it ceases around adult day 6–9. Summary statistics are useful to compare progeny production curves including timing of egg production (reproductive span to peak, reproductive span after peak, total reproductive span) and number of eggs produced (peak progeny number, total progeny number, progeny produced on day 7 and beyond) (**Figures 1D,E**).

REPRODUCTIVE DECLINE IN SELF-FERTILE VERSUS MATED HERMAPHRODITES

Early studies by Klass (1977) and Croll et al. (1977) documented that there is an age-related peak and decline in fertilized eggs deposited into the environment that corresponds to the depletion of sperm in self-fertile hermaphrodites (**Figures 1B,C**). This is consistent with the findings of Ward and Carrel (1979) that there is an age-related decrease in the number of sperm in or near the spermatheca. As a result of sperm depletion, hermaphrodites begin to deposit unfertilized oocytes, resulting in

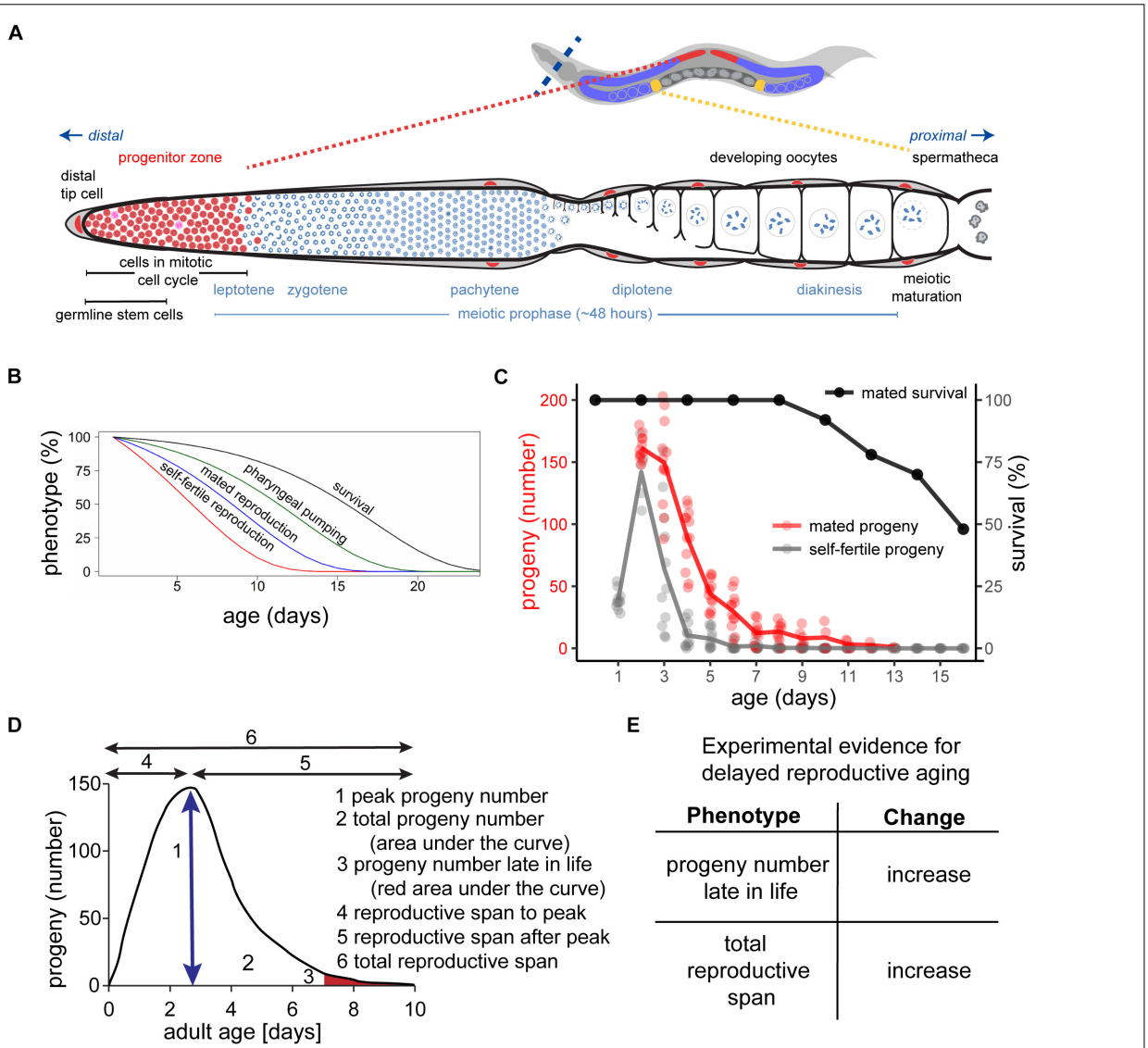

FIGURE 1 | Somatic and reproductive aging in *Caenorhabditis elegans*. **(A)** Architecture of one of the two gonad arms of a young adult hermaphrodite. At the distal end of the gonad, the somatic distal tip cell (red) is embedded in other somatic gonad cells (gray) and maintains the germline stem cell fate via GLP-1/Notch signaling. The germline stem cells (SYGL-1 positive cells) progress from the distal end of the gonad to the proximal end. During this journey, they undergo mitosis in the progenitor zone (red), progress through the meiotic prophase and meiotic maturation. Finally, they are ready to be fertilized by sperm in the spermathecal (yellow). In adults, the progenitor zone and the early prophase of meiosis I overlap. Adapted from Kocsisova et al. (2019). **(B)** *C. elegans* exhibits age-related degenerative changes of the soma and the germ line. Self-fertile reproduction (red) and mated reproduction (blue) decreases before somatic functions such as pharyngeal pumping (green), and survival (black). Adapted from Kumar et al. (2014). **(C)** Progeny production curves of unmated/self-fertile (gray) versus mated (red) hermaphrodites. Mated hermaphrodites survive beyond their reproductive span (black). Note that hermaphrodites that died by matricidal hatching were censored. Adapted from Kocsisova et al. (2019). **(D)** Summary statistics for analysis of the progeny production curve: peak egg number (arrow under the curve); total egg number (area under total curve), egg number late in life (red area under tail of curve), reproductive span to the peak, reproductive span after the peak, and total reproductive span (black arrows). **(E)** Experimental evidence for delayed reproductive aging in mated hermaphrodites – an increase in the total reproductive span and/or an increase in the number of eggs laid late in life.

a delayed, slightly overlapping, and much smaller peak compared to fertilized oocytes. Because the germ line responds to sperm depletion by arresting oocyte development, a phenotype called oocyte "stacking," only a relatively small number of unfertilized oocytes are deposited. The term oocyte "stacking" refers to the columnar shape displayed by oocytes under these conditions. These age-related changes can be modulated by temperature, and the self-fertile reproductive span is extended by cold temperatures (Klass, 1977; Huang et al., 2004).

It is important to differentiate between self-fertile and mated reproduction. In self-fertile hermaphrodites, the first ~300 germ cells differentiate as sperm, and the remaining germ cells differentiate as oocytes. As a consequence, the production of fertilized oocytes is limited by the number of self-sperm,

and no additional self-sperm can be produced. Thus, the age-related decline of egg production displayed by self-fertile hermaphrodites is primarily a result of sperm depletion, and it is not necessarily an accurate indication of reproductive aging. Hermaphrodites can also mate with males, which are rare in the wild, but can be easily enriched under laboratory conditions (Lints and Hall, 2009a). Mating provides the hermaphrodites with excess sperm and removes the limitations of sperm depletion (Ward and Carrel, 1979; Hodgkin and Barnes, 1991). The difference between self-fertile and mated reproduction manifests in different reproductive spans and progeny numbers (**Figures 1B,C**). Wild-type hermaphrodites that are self-fertile display a total reproductive span of 4.6 days at 20°C on standard nematode growth medium seeded with live *E. coli* OP50. By contrast, a brief period of mating (24–48 h exposure to males) extends the total reproductive span to 8.8 days (Pickett et al., 2013). The total progeny number increases from ∼330 progeny in self-fertile hermaphrodites to ∼710 progeny in mated hermaphrodites (Pickett et al., 2013).

The decline in self-fertile or mated reproductive capacity occurs relatively early in life, before age-related declines of somatic tissues required for neuromuscular activity and life support systems required for survival (**Figures 1B,C**, **2**; Huang et al., 2004; Pickett et al., 2013). More specifically, mated progeny production declines from a peak of ∼150 progeny/day on adult day 2 to ∼40 progeny/day on adult day 5 and to ∼12 progeny/day on adult day 7, while day 7 adults are still feeding, moving, and alive (Kocsisova et al., 2019). This suggests that the age-related decline in reproductive function may not be primarily caused by a decline in the somatic functions that maintain survival.

To explicitly investigate the relationship between reproductive aging and somatic aging, investigators have used the approach of longitudinal analysis. By making serial measurements of age-related declines in a single individual, it is possible to determine if two age-related declines are correlated. Huang et al. (2004) showed that the total reproductive span is not correlated with measures of somatic aging such as movement span and lifespan in self-fertile hermaphrodites, consistent with the model that the reproductive span in these animals is controlled by the number of self-sperm and the rate of self-sperm utilization; the number of self-sperm is established in larvae and is not related to aging. By contrast, Pickett et al. (2013) showed that there is a positive correlation between the total reproductive span and measures of somatic aging such as lifespan in mated hermaphrodites. In other words, individual worms that produced progeny for an extended period also lived for an extended period. These results indicate that reproductive and somatic aging are controlled by similar processes, and highlight the importance of measuring reproductive aging in mated hermaphrodites.

Males can have multiple effects on hermaphrodites, including transfer of sperm, transfer of seminal fluid, and physical trauma. Thus, the results of mating experiments depend on the duration and intensity of mating, including the number of males and ratio of males to hermaphrodites. For studies of reproductive aging, the strategy is to minimize male exposure by using a small number of males for a brief duration. Hughes et al. (2007) showed that it is typically sufficient to expose hermaphrodites for 24–48 h with

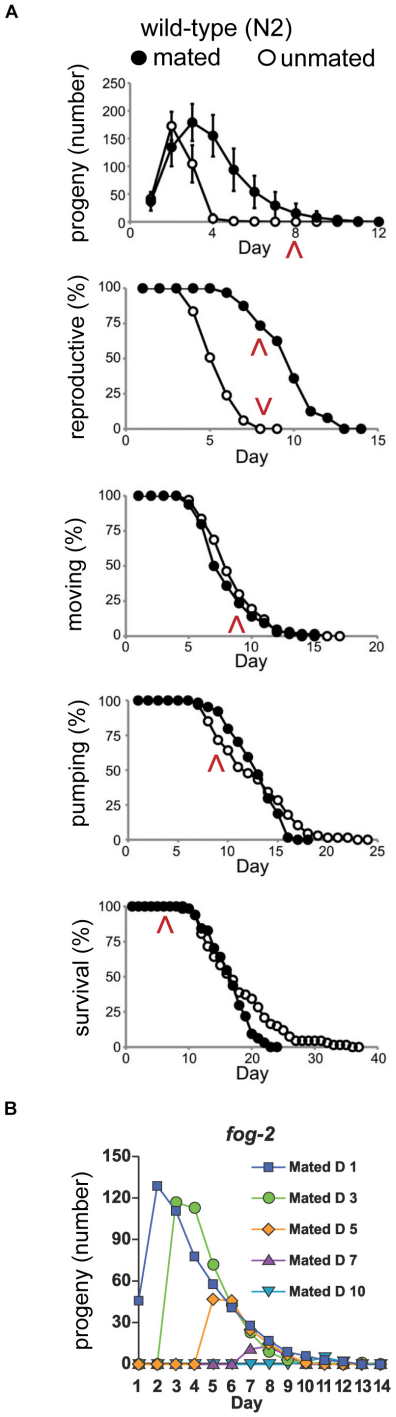

FIGURE 2 | Somatic and reproductive aging are independent of progeny production. **(A)** Progeny production, reproductive span, body movement span, pharyngeal pumping span, and lifespan of mated and unmated wild-type hermaphrodites. The increase in amount and duration of progeny production caused by male mating does not accelerate somatic aging. Red arrowheads highlight day 8 in each span. Adapted from Pickett et al. (2013). **(B)** Feminized *fog-2(q71)* mutants were mated to wild-type males for 24–48 h at different ages. Progeny curves show that late progeny production and reproductive span after peak were independent of early progeny production. Adapted from Hughes et al. (2007).

males to provide a lifetime supply of sperm. To ensure sperm are not depleted late in life, the investigator can monitor the sex ratio of progeny. Hermaphrodites that cease producing male progeny late in life are inferred to have run out of male sperm and can be censored from the analysis.

Early studies reported contradictory results of the effect of mating on hermaphrodites: Van Voorhies (1992) found minimal effects of mating on hermaphrodites, whereas Gems and Riddle (1996) reported dramatic effects with lifespans of mated hermaphrodites reduced ∼40% due to an increase in stress. Both groups used a 1.5 male to hermaphrodite ratio and retained the males for the duration of the lifespan. Pickett et al. (2013) systematically measured how brief, 24–48 h mating affects somatic aging. There was a minimal effect on somatic aging - the mean body movement span decreased 8%, the pharyngeal pumping span decreased 3%, and the mean lifespan decreased by 9% in mated compared to self-fertile hermaphrodites (**Figure 2A**). In contrast, Shi and Murphy (2014) described a shrinking phenotype for hermaphrodites mated for a period of 24 h and a more than 40% decrease in lifespan. Shi and Murphy (2014) concluded that seminal fluid transferred by males to hermaphrodites contributes to this effect. Other investigators concluded that males release pheromones that cause the decrease in the lifespan of mated hermaphrodites (Maures et al., 2014; Shi et al., 2017). In addition, the small molecule nacq#1 that is predominantly produced by males reduces the lifespan of hermaphrodites in picomolar concentrations (Ludewig et al., 2019). By contrast, self-sperm protects hermaphrodites against male toxicity (Booth et al., 2019; Shi et al., 2019). These studies highlight one of the challenges of analyzing female reproductive aging – the ability of females to produce fertilized progeny is the gold standard measure of reproduction and the typical endpoint in studies of reproductive aging. However, fertilized progeny require male sperm, and the acquision of male sperm inevitably involves confounding variables that must be considered and controlled.

USING THE GERM LINE TO MAKE EGGS DOES NOT ACCELERATE REPRODUCTIVE AGING

Many theories have suggested that aging is a use-dependent degenerative decline. In other words, the more a system is used, the more rapidly it will decline. The alternative model is that age-related degeneration is controlled by a "clock," and degenerative change will occur whether or not the system is used. *C. elegans* reproductive aging provides a powerful system to test these concepts. In particular, by using self-sterile mutants, it is possible to fully control progeny production by controlling the time when hermaphrodites mate with males. Hughes et al. (2007) showed that the shape of the curve describing the decline in egg-laying was essentially the same for animals mated on day 1 or mated on later days (**Figure 2B**). Thus, making progeny early in life did not accelerate or delay reproductive decline, indicating that this process is regulated by a timing mechanism.

Theoretical work has also proposed that there is a tradeoff between reproduction and somatic maintenance, which appears to predict that high levels of early reproduction will cause an acceleration of somatic aging. Pickett et al. (2013) examined somatic aging in self-fertile and mated hermaphrodites. Although mated hermaphrodites produced many more progeny, there was very little difference between the declines of movement, pharynx pumping and survival probability (**Figure 2A**). Thus, progeny production does not shorten lifespan or accelerate somatic aging (Pickett et al., 2013). Furthermore, Pickett et al. (2013) performed longitudinal studies and discovered that in mated hermaphrodites, high levels of progeny are positively correlated with long lifespan. In other words, individuals that made the most progeny for the longest period also tended to live the longest. This provides further evidence that making eggs does not cause the somatic tissues to degenerate – if anything, it appears that making a large number of eggs is evidence of a robust individual that is likely to live an extended period.

AGE-RELATED CHANGES IN MEIOTIC RECOMBINATION, PROGENY VIABILITY AND MORPHOLOGY

Mated hermaphrodites display a decrease in recombination frequencies, whereas older hermaphrodites display a higher rate of X-chromosome nondisjunction that results in the production of more males late in life (Rose and Baillie, 1979). In contrast to this early study, Lim et al. (2008) could not detect a difference in crossover frequency by analyzing chromosome III. However, they discovered that adult day 1 mated hermaphrodites exhibit different crossover positions compared to adult day 6/7 animals (Lim et al., 2008). A direct consequence of this age-related change in the location of crossovers is that early progeny clearly differ from late progeny.

Self-fertile hermaphrodites produce embryos that have a high rate of viability; more than 99% of embryos laid will hatch (Andux and Ellis, 2008). Andux and Ellis (2008) also reported that lethality increased up to ∼20% in embryos that developed from stacked oocytes. Mated hermaphrodites have a larger reservoir of sperm, allowing them to continue producing progeny later in life. Embryos laid by mated and self-fertile hermaphrodites display a similar rate of lethality early in the reproductive span (adult day 1–4) that is lower than 1%. However, lethality among embryos that developed from non-stacked oocytes produced by older mothers was ∼3% (Andux and Ellis, 2008; Luo et al., 2010; Luo and Murphy, 2011). Andux and Ellis (2008) used sperm-defective *fog-2* "female" mutants to examine the effect of maternal age on embryonic viability. Until adult day ∼6.5, there is very little embryonic lethality. However, embryonic lethality displayed an age-related increase from adult days 6.5–9, culminating in about 20% lethality (**Figure 3A**). This suggests that maternal age has a negative effect on embryo viability, but it is important to consider the caveat that the *fog-2* mutation may affect germline aging beyond feminization. A practical limitation of these studies is the difficulty of obtaining large numbers of eggs produced by older hermaphrodites, since day 9 adults lay only a few

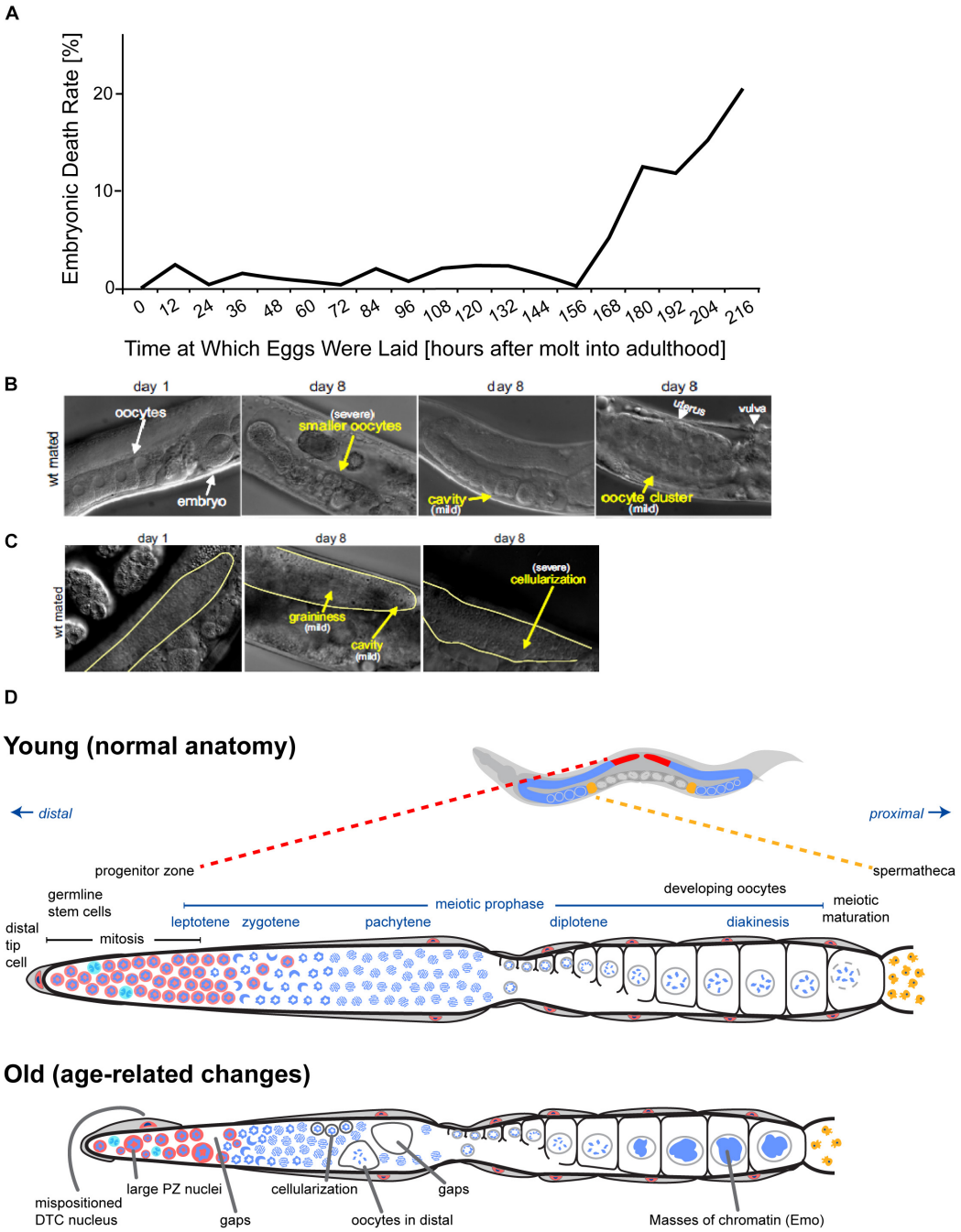

FIGURE 3 | Age-related declines of oocyte and germline quality. **(A)** *fog-2(q71)* mutant animals that do not produce self-sperm were mated to males (start: 0 h), and the percentage of unhatched embryos was determined every 12 h. The embryonic death rate displays an age-related increase to ~20% by day 9. Adapted from Andux and Ellis (2008). **(B)** Oocytes of adult day 8 mated wild-type hermaphrodites display morphological defects visible using differential interference contrast microscopy (DIC). Compared to adult day 1 mated wild-type hermaphrodites, oocytes in adult day 8 hermaphrodites can be smaller, clustered, or contain cavities (yellow arrows). Reprinted from Luo et al. (2010) with permission from Elsevier. **(C)** The distal germ line of adult day 8 mated wild-type hermaphrodites displays morphological defects visible using DIC microscopy. Compared to adult day 1 mated wild-type hermaphrodites, the distal germ line loses its smoothness in adult day 8 hermaphrodites and can appear grainy with cavities or exhibit severe cellularization (yellow arrows). The morphological defects are defined according Garigan et al. (2002). Reprinted from Luo et al. (2010) with permission from Elsevier. **(D)** Anatomy of *C. elegans* germ line in young versus old hermaphrodites. Top: *C. elegans* hermaphrodites have two U-shaped germ lines (red and blue). The spermatheca is shown in yellow, and the uterus with developing embryos is shown in dark gray. Middle: Diagram of one unfolded young *C. elegans* hermaphrodite germ line. Nuclear morphology can be visualized by staining DNA with DAPI (blue). The distal progenitor zone (red) contains mitotically cycling stem and progenitor cells. The distal tip cell (DTC) provides the GLP-1/Notch ligand to maintain the stem cell fate of these cells. As cells migrate away from the DTC, they exit the progenitor zone and enter meiotic prophase. Bottom: Diagram of one unfolded old *C. elegans* hermaphrodite germ line. Numerous age-related changes in the germ line have been reported. Several are illustrated here. Adapted from Kocsisova et al. (2019).

eggs. Thus, it has been difficult to identify interventions that influence this phenotype.

Consistent with this functional analysis, morphological analysis of age-related changes in the germ line reveals smaller oocytes and oocyte clusters in wild-type hermaphrodites (**Figures 3B,C**; Luo et al., 2010). Hibshman et al. (2016) examined the effect of maternal age on hatched embryos. Younger mothers (day 0 of adulthood) produced larval progeny that were ∼205 μm in length; progeny length peaked at day 1 at ∼215 μm before declining slightly at day 2 (Hibshman et al., 2016). In contrast, Perez et al. (2017) reported that progeny from adult day 1 self-fertile hermaphrodites were significantly shorter than progeny from adult day 2 and 3 self-fertile hermaphrodites. The length of larvae from adult day 1 hermaphrodites was ∼250 μm at hatching and ∼860 μm 42 h post hatching; for adult day 2 hermaphrodites, larval length was ∼260 μm at hatching and ∼910 μm 42 h post hatching; for adult day 3 hermaphrodites, larval length was ∼270 μm at hatching and ∼940 μm 42 h post hatching (Perez et al., 2017). In addition, the brood size of adult day 1 progeny was ∼250 progeny, which is less than the brood size of adult day 2 or 3 progeny (∼320 progeny) (Perez et al., 2017).

MATRICIDAL HATCHING

If a hermaphrodite stops laying eggs into the environment, then fertilized eggs inside the uterus continue developing and hatch internally after about 12.5 h. The hatched larvae consume the biomass of the hermaphrodite, resulting in maternal death (**Figures 4A–C**). The maturing larvae leave the maternal body, often as dauer stage larvae. This phenotype is known as matricidal hatching, endotokia matricida, facultative viviparity, or "bag-of-worms" (Luc et al., 1979; Pickett and Kornfeld, 2013). This phenotype is not unique to *C. elegans*; it can be observed in other Rhabditia species as well as non-nematode species (Johnigk and Ehlers, 1999; Luong et al., 1999). In *C. elegans*, matricidal hatching is caused by genetic defects, adaptive signals, or age-related degeneration of the egg-laying system: (1) Mutant animals with developmental defects in the egg-laying system cannot lay eggs and reproduce via matricidal hatching (Trent et al., 1983). This phenotype was the basis for genetic screens that identified a wide range of genes important for development of the vulva, vulval muscles, and HSN neurons that innervate the vulval muscles. In addition, these studies were also the basis for the discovery of many components of important highly-conserved regulatory pathways such as EGFR, Rb, and Notch. (2) Egg retention and matricidal hatching can also be triggered by food deprivation. Starving hermaphrodites stop laying eggs, probably as a strategy to ensure that fertilized eggs can survive (Chen and Caswell-Chen, 2004). The next generation, born as dauer larvae through matricidal hatching, is optimized to survive the deprivation conditions. (3) Hermaphrodites stop laying eggs as they get older due to age-related degeneration of the egg-laying apparatus (Pickett and Kornfeld, 2013). This age-related change is not caused by use-dependent damage. With increasing age, hermaphrodites lose the ability to respond to exogenous serotonin, which triggers egg-laying in young adults with a functional egg-laying system. Consequently, mated wild-type hermaphrodites with an extended reproductive span display an increase of 70% in the frequency of matricidal hatching compared to self-fertile hermaphrodites that cease progeny production several days earlier due to sperm depletion (**Figures 4D,E**; Pickett and Kornfeld, 2013). In a sense, there is a "race" between the age-related decline in egg production and the age-related decline in the system that deposits eggs into the environment. If the egg production system declines first, as is typical in self-fertile hermaphrodites, then animals display an extended post reproductive lifespan. However, if the age-related decline in the somatic systems that deposit eggs occurs first, as is typical in mated hermaphrodites, then death is caused by matricidal hatching and there is no post reproductive lifespan. Interestingly, the percentage of hermaphrodites that display matricidal hatching increases in strains with mutations that induce longevity and extend the reproductive span when mated to males: *daf-2*, *age-1*, *clk-1*, *isp-1*, *sma-2*, and *sma-3* (Pickett and Kornfeld, 2013). In some *daf-2(lf)* mutants, essentially 100% of mated hermaphrodites die from matricidal hatching.

Vigne et al. (2021) identified wild-type strains that display premature loss of sensitivity to exogenous serotonin. These strains develop normally and have the ability to lay eggs in the first hours of adulthood. However, in contrast to the standard wild-type strain N2, these strains start to retain eggs in the uterus on adult day 1 due to a lack of responsiveness to food availability. Thus, they exhibit near-constitutive matricidal hatching (Vigne et al., 2021).

AGE-RELATED MORPHOLOGICAL, MOLECULAR AND FUNCTIONAL DETERIORATION OF THE GERM LINE

To ultimately understand mechanisms of reproductive aging, it is first necessary to have a detailed description of how the reproductive system functions in young animals and how it changes during aging. While these observational studies do not directly test the functional consequence of age-related changes, they are important for establishing hypotheses, and these phenotypes are the basis for evaluating interventions that influence reproductive aging. The germ line, somatic gonad, and more distant somatic tissues all contribute to reproduction, and it is important to understand how age-related changes in the reproductive tract and somatic tissues affect reproductive function. One important distinction when considering age-related changes is whether the change is observed at a low frequency in only a subset of animals or at a high frequency in all animals. Low frequency changes can be described as sporadic (**Figure 5A**), and this pattern suggests the cause may be stochastic events. By contrast, high frequency changes can be described as population-wide, and this pattern suggests the cause may be a genetic program or an environmental influence that is experienced by every animal.

Low frequency, sporadic changes during reproductive aging: If meiotic maturation and ovulation are miscoordinated,

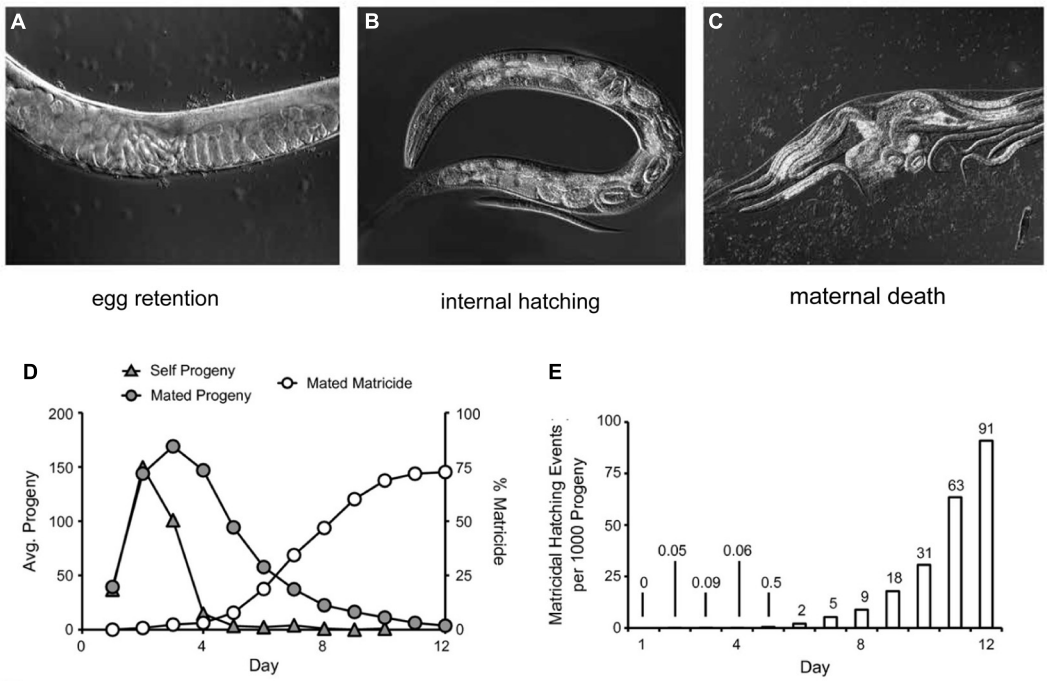

FIGURE 4 | Matricidal hatching. Wild strain JU751 hermaphrodites exhibit nearly constitutive matricidal hatching. DIC microscopic micrographs depict the progression: **(A)** Eggs are retained in the uterus, showing a "stacking of embryos" phenotype. **(B)** Retained embryos will continue to develop and hatch inside the uterus. **(C)** Hatched larvae grow inside the hermaphrodite and feed on the maternal tissue. Finally, the hermaphrodite bursts and releases the progeny in dauer stage. **(A–C)** Adapted from Vigne et al. (2021). **(D)** The cumulative percentage of matricidal hatching in mated wild-type hermaphrodite in comparison to progeny production curves of unmated/self-fertile and mated wild-type hermaphrodites. Adapted from Pickett and Kornfeld (2013). **(E)** Incidence number of matricidal hatchings per 1,000 progeny laid by mated wild-type hermaphrodites. Until day 6, progeny production carries a small risk of matricidal hatching, but after day 6 the risk increases exponentially. Adapted from Pickett and Kornfeld (2013).

endomitotic oocytes occur, which then also disturb future successful coordination of these processes. Mutants with a high frequency of endomitotic oocytes (the Emo phenotype) have reduced fertility, indicating that this defect has functional consequences. Kocsisova et al. (2019) observed a small fraction of day 5 mated hermaphrodites that display endomitotic oocytes in the proximal gonad arm (**Figures 3D**, **5B,C**). A longitudinal study demonstrated that this phenotype is positively correlated with reduced progeny production, indicating that in a subset of animals, endomitotic oocytes are a cause of age-related decline in fertility.

The distal tip cell (DTC) is a somatic cell positioned at the distal end of each gonad arm; the DTC provides the niche for germline stem cells and expresses Notch ligands that promote stem cell fate (**Figure 1A**). Kocsisova et al. (2019) reported that the DTC may mislocalize away from the distal tip of the gonad in day 5 mated adult hermaphrodites (**Figure 3D**). While severe defects in DTC position can cause obvious abnormalities in the gonad, severe defects are a low frequency, sporadic event that is not likely to explain the population-wide declines in egg production.

High frequency, population-wide changes during reproductive aging: The structure of the gonad undergoes visible deterioration as the animal ages (**Figures 3C,D**). It is challenging to quantify these morphological changes, and several investigators have established approaches using high magnification DIC optics. In a pioneering study, Garigan et al. (2002) defined five morphological categories based on the degree of disorganization, allowing a numeric score for each individual. Within the gonad, changes in the process of oocyte maturation and ovulation occur with age. In unmated hermaphrodites, sperm depletion results in an arrest of oocyte maturation, resulting in unfertilized oocytes "stacking" in the proximal gonad (Luo et al., 2010; Hughes et al., 2011). Hermaphrodites older than 8 days display a disorganization of the distal germ line with cavities, contraction into clumps, vacuoles, debris, graininess and cellularization (**Figures 3C,D**; Luo et al., 2010; Hughes et al., 2011). Hughes et al. (2011) established approaches to quantify deterioration and showed that mutations that delay reproductive aging can also delay age-related changes in morphology. While this type of evidence is suggestive that the morphological changes cause the functional decline, this correlation does not rigorously establish cause.

To gain insight beyond the morphological changes observable with DIC optics, investigators began using sophisticated assays developed to measure germ line function in young animals, including antibody staining to identify regions of the germ line and phases of the cell cycle. Furthermore, by using the nucleotide analog EdU that is incorporated into newly synthesized DNA, it is possible to observe the dynamics of DNA replication, duration

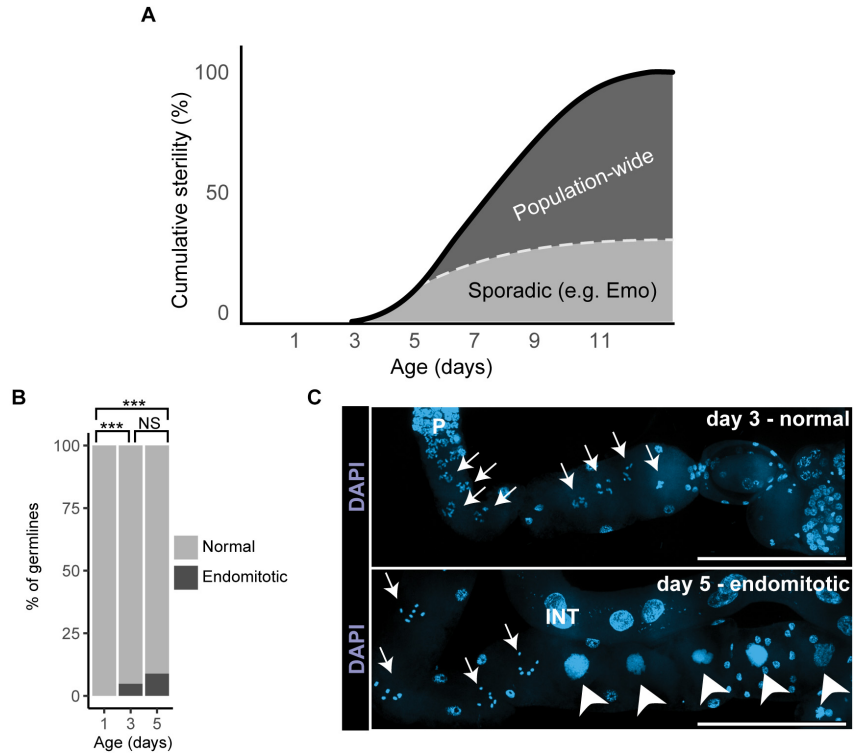

FIGURE 5 | Sporadic degenerative changes in the aging germ line. **(A)** The graph illustrates how sporadic and population-wide changes contribute to cumulative age-related sterility in mated wild-type hermaphrodites. Endomitotic oocytes or shifted distal tip cells are sporadic degenerative changes and account for less than half of age-related sterility (the dotted line indicates a model of the relative contribution of sporadic defects). Declines in stem cell number and activity, PZ and germ line shrinking, as well as slower cell cycles are population-wide changes that appear to be the main drivers of reproductive aging. Adapted from Kocsisova et al. (2019). **(B)** Analysis of sporadic changes in day 1, 3, and 5 mated wild-type hermaphrodites: Percentage of dissected germ lines with (black) or without (gray) endomitotic oocytes (black). Adapted from Kocsisova et al. (2019). **(C)** Representative fluorescence micrographs of wild-type mated hermaphrodites stained with the DNA-dye DAPI. Oocytes of a day 3 adult show normal chromosomes in diakinesis (arrows in top panel) in contrast to endomitotic oocytes (arrowheads in lower panel) of a day 5 adult. P, pachytene; INT, intestine. Scale bars: 100 μm. Adapted from Kocsisova et al. (2019).

of the cell cycle, and the rate of germ cell progression through the gonad. In young adult hermaphrodites, the germline stem cells of the progenitor zone (PZ) take 6.5–8 h to go through one complete round of the cell cycle (Fox et al., 2011). The M-phase index (percent of cells in M-phase at a moment in time) decreases with age in unmated hermaphrodites, suggesting an arrest in the germ cell cycle (Narbonne et al., 2015; Qin and Hubbard, 2015); mating to males delays this decline (Narbonne et al., 2015). Kocsisova et al. (2019) reported an age-related increase in the time necessary to complete the cell cycle, increasing to ∼12 h in day 3 and 5 adult mated hermaphrodites (**Figures 6A,B**). Notably, this increase in cell cycle duration was measured on adult day 3, about 2 days before there is a substantial decline in progeny production, indicating that declines in the distal germ line may be the first changes during reproductive aging.

In the distal most end of the germ line near the DTC, germ cells undergo mitotic division in the PZ. In young adult self-fertile hermaphrodites, there are ∼200–250 mitotically dividing cells in this region (there is some variation in this value determined by different laboratories) (Killian and Hubbard, 2005; Crittenden et al., 2006; Luo et al., 2010; Narbonne et al., 2015; Qin and Hubbard, 2015). Some laboratories observed changes in the number of cells in the PZ in older hermaphrodites: Luo et al. (2010) reported a decrease to ∼150 cells at day 6; Killian and Hubbard (2005) as well as Qin and Hubbard (2015) observed ∼150 cells at day 3, ∼100 cells at day 6, and ∼50 cells at day 12; Narbonne et al. (2015) observed ∼80 cells at day 7. Variation in the PZ cell number has been observed between self-fertile and mated hermaphrodites – several laboratories reported a more rapid decline in PZ cell number in mated animals, suggesting that the PZ may become more rapidly depleted in mated animals (**Figure 6C**; Shi and Murphy, 2014; Narbonne et al., 2015; Qin and Hubbard, 2015; Kocsisova et al., 2019). Apoptosis plays an important functional role in reducing the number of germ cells in late pachytene during early adulthood, and a possible explanation for the age-related reduction in stem cell number is "apoptotic run on" (de la Guardia et al., 2016). The discovery of age-related increases in apoptotic germ cells and the ratio of apoptotic cells/germ cells supports the hypothesis that excess apoptosis causes the age-related reduction in stem cell number, which may be an example of an unproductive run-on program (de la Guardia et al., 2016).

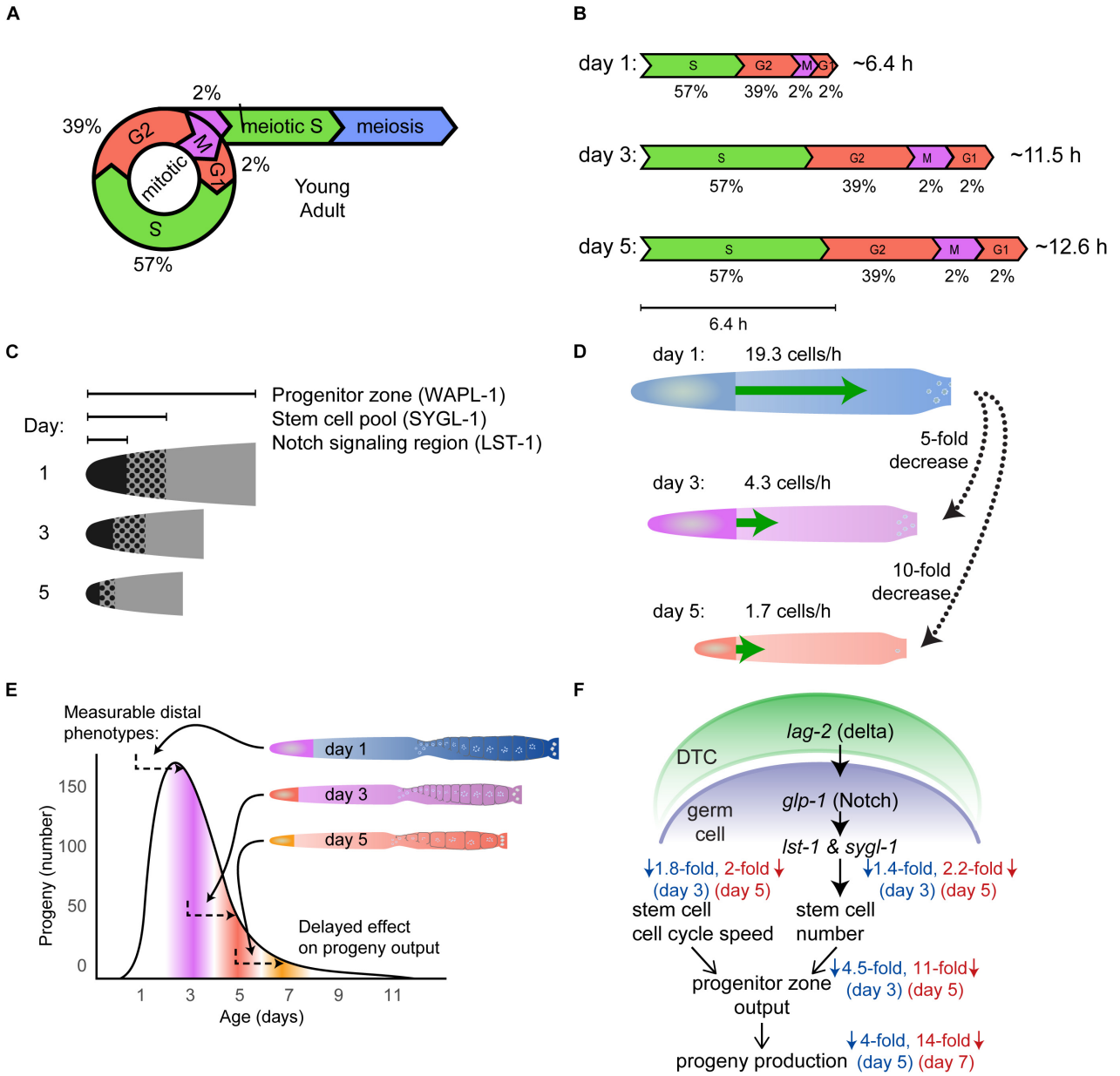

FIGURE 6 | Population-wide, age-related degenerative changes in the germ line. **(A)** Schematic of the mitotic cell cycle and meiotic entry of young adult wild-type germ cells, including duration of time in each phase expressed as a percent (Fox et al., 2011). Adapted from Kocsisova et al. (2019). **(B)** The duration of the cell cycle increases with age in mated wild-type hermaphrodites. The scale diagram summarizes the duration of different phases of the cell cycle in day 3 and 5 animals compared to day 1 animals. The values below indicate the percentage of time in each phase, whereas the values on the right indicate the total cell cycle duration time. Adapted from Kocsisova et al. (2019). **(C)** The schematic shows that the size of the Notch signaling region, stem cell pool, and the progenitor zone (PZ) shrinks with age. Notch signaling was visualized by LST-1 labeling, the stem cell pool was visualized by SYGL-1 labeling, and the progenitor zone was labeled with WAPL-1 antibodies in day 1, 3, and 5 germ lines. Adapted from Kocsisova et al. (2019). **(D)** The schematic displays the age-related decrease in the rate of meiotic entry (green arrow) in the germ line of mated wild-type hermaphrodites. Day 5 and 3 germ lines show a 10-fold and 5-fold decrease, respectively, compared to day 1 germ lines. Adapted from Kocsisova et al. (2019). **(E)** The schematic shows that changes in the distal germ line correlate with changes in the progeny production curve about 2 days later (arrows). The size of the germ line and the progenitor zone (PZ) decreases before the progeny production declines. The PZ cells need two or more days to become oocytes and be laid as eggs. Therefore, age-related changes such as the shrinking of the germ line and PZ affect progeny production with a delay. Adapted from Kocsisova et al. (2019). **(F)** Summary and model of reproductive aging in *C. elegans*. Adapted from Kocsisova et al. (2019).

Moving proximally down the germ line, in the meiotic entry region, germ cells begin entering meiotic prophase. In young adults, the process of meiotic prophase progression and oogenesis takes ~2 days, and has been observed to slow in day 1.5 adults (Jaramillo-Lambert et al., 2007). Schisa et al. (2001) reported an increase in perinuclear staining of RNA-rich "P granules" in

the germ line of old adult hermaphrodites compared to young hermaphrodites. Kocsisova et al. (2019) used EdU labeling to measure the movement rate of cells exiting the PZ. The rate of movement declined from ∼19.3 cells/hours on adult day 1 to ∼4.3 cells/hours on adult day 3 to ∼1.7 cells/hour on adult day 5 (**Figure 6D**). This is a remarkable and early change that strongly points to the distal germ line as the origin of reproductive aging (**Figure 6E**).

The DTC signals the germ line to specify stem cell fate via the GLP-1 Notch pathway. As germ cells move proximally away from the distal tip of the gonad, they lose Notch signaling and transition from mitotic cell cycling into meiotic S-phase (Fox and Schedl, 2015). *lst-1* and *sygl-1,* two germline transcriptional targets of GLP-1 signaling, are known to be redundantly necessary and individually sufficient for promoting stem cell fate (Kershner et al., 2014; Lee et al., 2016; Shin et al., 2017). Observing the number of cells that express these proteins provides information about the extent of Notch signaling. The number of cells expressing LST-1 and SYGL-1 in day 1 adult mated hermaphrodites is ∼38 for LST-1 and ∼81 for SYGL-1; this number is reduced by half by day 5 (**Figures 6C,F**; Shin et al., 2017; Kocsisova et al., 2019). This is an example of a molecular read out – the pattern and level of protein expression - that displays an age-related change and indicates that there is a progressive reduction of the Notch-mediated signaling system that maintains germline stem cells.

PHARMACOLOGICAL COMPOUNDS THAT INFLUENCE REPRODUCTIVE AGING

To move beyond descriptions of age-related changes to an understanding of mechanism, it is necessary to identify interventions that can influence reproductive aging. *C. elegans* is a powerful model to screen for such interventions, and it has been a leading system for innovative discovery in this area. Here we consider three categories of interventions that have been demonstrated to delay reproductive aging: drugs, single gene mutations, and environmental factors (**Figure 7**, **Tables 1**, **2** and **Supplementary Table 1**). We focus on delayed reproductive aging rather than accelerated reproductive aging because there are many ways to reduce reproduction, and only a small number of these are likely to be relevant to aging. By contrast, it is relatively rare to find interventions that extend reproduction, and these are more likely to modulate the aging process. An important issue is what assays or measurements constitute strong evidence for delayed reproductive aging? As illustrated in **Figure 1E**, the most stringent and reliable are (1) increases in the total reproductive span, which is conceptually similar to extended lifespan for studies of somatic aging, and (2) increases in the number of viable progeny produced late in life, which is conceptually similar to extended healthspan for studies of somatic aging. *C. elegans* has long been used as a model to examine the effects of pharmacological compounds on aging. To date, many compounds have been shown to extend nematode lifespan (Lucanic et al., 2013, 2017); however, only a few of these compounds have been shown to delay reproductive aging (**Table 1**).

Ethosuximide is an anticonvulsant medication commonly used to treat seizures in humans. Evason et al. (2005) discovered that exposure to ethosuximide at 4 mg/mL in the medium resulted in a 17% increase in mean adult lifespan, as well as an increase in the amount of time that animals displayed fast body movement and pharyngeal pumping, indicating that ethosuximide also delays age-related physiological decline (Evason et al., 2005). Ethosuximide treatment does not affect self-fertile reproductive span, but mated hermaphrodites displayed an increase in the reproductive span of 12% (Evason et al., 2005; Hughes et al., 2007). Notably, ethosuximide did not reduce progeny production early in life (**Figure 7A** and **Table 1**). In addition, ethosuximide protects against matricidal hatching (Scharf et al., 2016). Ethosuximide is likely to function by inhibiting the activity of amphid neurons (Collins et al., 2008). These results suggest that it is possible to increase the reproductive span without affecting early reproduction, and that sensory perception by amphid neurons accelerates somatic and reproductive aging.

Trehalose is a dissacharide used as a human food additive. Honda et al. (2010) observed that trehalose at a concentration of 5mM in the medium extended mean lifespan by ∼30%. In addition, trehalose treatment extended the maximum reproductive span of wild-type (N2) self-fertile hermaphrodites: untreated animals stopped producing progeny at day 11 of adulthood, while trehalose treated animals continued producing progeny to day 15 (**Table 1**; Honda et al., 2010). Furthermore, trehalose treatment increased the mean reproductive span from 7.9 days to 11.0 days (Honda et al., 2010).

Resveratrol is a stilbenoid, naturally occurring phenolic compound found in foods such as grapes/red wine that has been demonstrated to affect aging in several organisms (Akinwumi, 2018). In *C. elegans*, resveratrol treatment at 50 μM in the medium extended mean lifespan by 64% and maximum lifespan by 30% (Gruber et al., 2007). Resveratrol treatment reduced the number of progeny produced early in life (defined as day 0–4 of adulthood) while increasing the number of progeny produced later in life (day 5–9); the total number of progeny produced was unaffected (**Table 1**; Gruber et al., 2007).

Dimethyl sulfoxide (DMSO) and dimethyl formamide (DMF) are amphipathic solvents commonly used in the chemical and biological sciences. Due to their ability to dissolve both polar and nonpolar compounds, they are often used to deliver pharmacological compounds in drug screens. Interestingly, treating nematodes with these solvents alone was reported to extend lifespan by 20 and 50% for DMSO (0.8% v/v) and DMF (0.75% v/v), respectively (Frankowski et al., 2013). These compounds also significantly reduced brood size and delayed the onset of egg-laying, while also extending the egg-laying period (**Table 1**; Frankowski et al., 2013).

Vitamin E has long been known to extend lifespan in many animals (Zuckerman and Geist, 1983). In *C. elegans*, vitamin E administration at 400-800μg/mL in the medium increased mean lifespan by 17–23% (Harrington and Harley, 1988). Vitamin

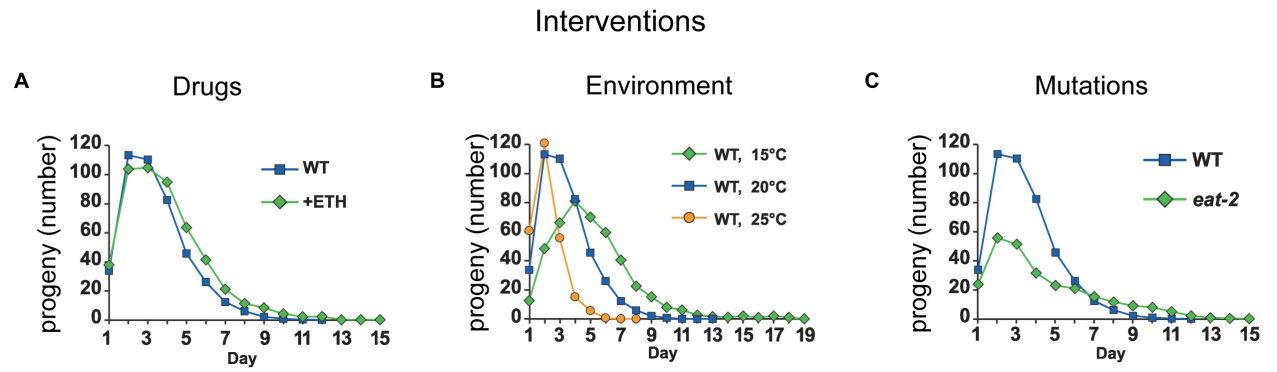

FIGURE 7 | Environmental, genetic, and pharmacological factors can delay reproductive aging. Representative interventions that prolong the reproductive span and increase late progeny production in short (24 h) mated *C. elegans* hermaphrodites. **(A)** Ethosuximide-treatment increases mid-life and late progeny production and prolongs the reproductive span in mated wild-type *C. elegans*. Adapted from Hughes et al. (2007). **(B)** Increasing the culture temperature from 20°C (blue curve) to 25°C (yellow curve) decreases late progeny production and reduces the reproductive span after peak in mated wild-type *C. elegans*. By contrast, reducing the culture temperature to 15°C (green curve) decreases early progeny production, increases late progeny production, increases reproductive span to peak, and extends the reproductive span after peak in mated wild-type *C. elegans*. Adapted from Hughes et al. (2007). **(C)** Mated *C. elegans* hermaphrodites with a mutation in *eat-2* (green) display decreased early progeny production, decreased peak progeny number, increased late progeny production, and an extended total reproductive span compared to wild type. Adapted from Hughes et al. (2007).

E treatment reduces total progeny production (Zuckerman and Geist, 1983; Harrington and Harley, 1988); however, it also increases the mean days of reproduction (**Table 1**; Harrington and Harley, 1988).

Folic acid is a naturally occurring compound found in leafy vegetables, beans, and fruits. Treatment with folic acid at 25μM in the medium extends mean worm lifespan by 26% (Rathor et al., 2015). The final day of progeny production increases from day 10 of adulthood to day 12, and total progeny production was reduced (**Table 1**; Rathor et al., 2015).

Metformin is a drug commonly used to treat type-2 diabetes in humans; it extends lifespan in non-diabetic mice, as well as reducing all-cause mortality in non-diabetic humans (Scarpello, 2003; Anisimov et al., 2011). Onken and Driscoll (2010) observed that metformin treatment at 10 or 50 μM in the medium increased median lifespan by 40%. Metformin treatment reduced the number of eggs laid early in the reproductive period, while also extending the total reproductive period by 1 day (**Table 1**; Onken and Driscoll, 2010). Notably, this phenotype is similar to the effects caused by dietary restriction (DR). Cabreiro et al. (2013) also analyzed metformin and observed that lifespan extension depends on the bacterial food source; they concluded that metformin extended worm lifespan by interrupting bacterial methionine and folate metabolism, inducing a DR phenotype in worms via methionine restriction, rather than working directly on *C. elegans* metabolism (Cabreiro et al., 2013). These findings are an important cautionary tale regarding the complexity of interpreting drug studies in *C. elegans* when worms are feeding on live bacteria, and the bacteria may also be influenced by the drug.

3-dihydro-2-phenyl-sulfanylenebenzo[d] [1,3,2]-oxa-zaphosphole or FW1256, is an **H_2S donor compound** initially prepared by Feng et al. (2015). Treatment with 500 μM FW1256 in the medium extends lifespan and health span of wild-type hermaphrodites and also shifts the peak of progeny production from day 5 to day 7 (Ng et al., 2020). The total number of progeny on day 4 and 5 are decreased, while the number of eggs on day 6–9 are increased, shifting the progeny curve to the right. The total number of eggs per hermaphrodite is slightly (not significant) increased. Even taking a slight developmental delay of a little less than one day (about 20 h) into consideration, this treatment still delays reproductive aging (**Table 1**).

An important observation in aging biology is that mutations in genes involved in distinct aging regulatory pathways can additively influence lifespan. In a similar fashion, pharmacological inhibition of targets that affect disparate longevity pathways can sometimes have additive effects on aging. Admasu et al. (2018) discovered that drugs targeting different pathways can further extend lifespan compared to animals treated with single drugs alone; notably, the combination of rapamycin (an mTORC1 inhibitor), allantoin (a DR mimetic), and either psora-4 (a K-channel blocker) or rifampicin (a JNK inhibitor) can extend the reproductive span of adult hermaphrodites while not reducing overall brood size (Admasu et al., 2018).

GENETIC PATHWAYS THAT INFLUENCE REPRODUCTIVE AGING

Insulin/IGF-1 Signaling Pathway

The **Insulin/IGF-1 signaling pathway** (**Figure 8A**) is the most prominent pathway in *C. elegans* aging research, as the first mutations discovered to extend lifespan affected genes encoding Insulin/IGF-1 signaling pathway components (Friedman and Johnson, 1988; Kenyon et al., 1993). The heart of this pathway is DAF-2, the only insulin-like receptor in *C. elegans*. In contrast, *C. elegans* can express about 40 insulin-like molecules that could in principle bind DAF-2; however, the peptides

TABLE 1 | Compounds that modulate reproductive aging in *Caenorhabditis elegans*.

Intervention[1]	Longitudinal experiments[2]/ Male mated[3]	Reproductive span to peak (days)[4]	Reproductive span after peak (days)[5]	Total reproductive span (days)[6]	Peak progeny number[7]	Total progeny number[8]	Matricidal hatching[9]	References
H_2S by means of FW1256 (500 μM)	yes/no	↑	↓	↓	↑	+/−	ND	Ng et al., 2020
Ethosuximide (4 mg/ml)	yes/yes day1	+/−	↑	↑	+/−	+/−	reduced	Hughes et al., 2007
Trehalose (5 mM)	yes/no	+/−	↑	↑	+/−	+/−	ND	Honda et al., 2010
Resveratrol (50 μM)	yes/no	↑	+/−	↑	↓	+/−	ND	Gruber et al., 2007
DMSO (0.8% v/v)	yes/no	↑	↓	↑	↓	↓	ND	Frankowski et al., 2013
DMF (0.75% v/v)	yes/no	↑	↑	↑	↓	↓	ND	Frankowski et al., 2013
Vitamin E (400, 800 μg/mL)	yes/no	↑	↑	↑	↓	↓	ND	Zuckerman and Geist, 1983; Harrington and Harley, 1988
Folic acid (25 μM)	yes/no	+/−	↑	↑	↓	↓	ND	Rathor et al., 2015
Metformin (10, 50 μM)	yes/no	↑	↑	↑	↓	↓	ND	Onken and Driscoll, 2010; Cabreiro et al., 2013

[1] *Intervention: pharmacological compounds (concentration in medium).*
[2] *Longitudinal experiment: the same individual animal is observed at sequential time points. yes: measured in a longitudinal experiment, no: measured in a cross-sectional experiment.*
[3] *Male mated: yes – hermaphrodites were exposed to males, with adult day of exposure specified, no: self-fertile hermaphrodites.*
[4] *Reproductive span to peak: time from adult day 0 until day of peak egg-laying (**Figure 1**).*
[5] *Reproductive span after peak: time from day of peak egg-laying until last day of egg-laying (**Figure 1**).*
[6] *Total reproductive span: time from adult day 0 until last day of egg-laying (**Figure 1**).*
[7] *Peak progeny number: Number of eggs laid on day of peak progeny production (**Figure 1**).*
[8] *Total progeny number: Total number of eggs laid (**Figure 1**).*
[9] *Matricidal hatching: If mature hermaphrodites cannot deposit eggs into the environment, then eggs hatch inside the hermaphrodite, and larvae feed on the parent resulting in death.*
[4−9] *↑: increase; ↓: decrease; +/−: no change; reduced: lower frequency; ND: not determined.*

that bind DAF-2 during different processes is an active area of research and much remains unknown. Activated DAF-2 initiates a kinase cascade that results in phosphorylation of DAF-16, a FoxO transcription factor. Phosphorylated DAF-16 does not accumulate in the nucleus, and therefore cannot regulate transcription of its target genes. The Insulin/IGF-1 pathway is conserved in all eukaryotes. It connects the control of growth, reproduction, metabolism, and aging to nutrient status (Murphy and Hu, 2013).

Loss-of-function mutations in the *daf-2* gene result in lifespan extensions, because DAF-16 accumulates in the nucleus and constitutively regulates target genes that promote longevity. In contrast, loss-of-function mutations in the *daf-16* gene shorten lifespan. The Insulin/IGF-1 signaling pathway also impacts reproductive aging (**Figures 8B,C** and **Supplementary Table 1**). Loss-of-function mutations in the *daf-2* and *age-1* genes extend the reproductive span in mated *C. elegans (*Hughes et al., 2007; Luo et al., 2009); these mutant hermaphrodites display decreased early reproduction, increased late reproduction, and an increase in the percentage of reproductively active hermaphrodites (**Figures 8B,C** and **Supplementary Table 1**). Consistent with these observations from candidate gene approaches, *daf-2* and other insulin/IGF-1 signaling pathway genes were identified in an unbiased screen for reproductive span extension (Wang et al., 2014). The reproductive aging delay in *daf-2* mutants is dependent on *daf-16*, similar to the lifespan extension (Hughes et al., 2007; Luo et al., 2009). Morphological analysis revealed that the germ line in *daf-2* mutants remains intact for longer and displays delayed age-related deterioration (Garigan et al., 2002; Luo et al., 2010). By contrast, hermaphrodites with *daf-16* mutations display an accelerated age-related deterioration of the germ line (Garigan et al., 2002). Qin and Hubbard (2015) showed that the age-related depletion of the progenitor zone is *daf-2* dependent. *daf-2* mutants displayed a longer period of maintenance of the progenitor zone that is dependent on *daf-16*, but in a manner that is largely non-autonomous and has a different anatomical focus from lifespan extension (Qin and Hubbard, 2015). Loss-of-function mutations in *daf-16* reduce the number of reproductively active hermaphrodites prematurely, reduce total and peak progeny number, and cause a shorter reproductive span (**Figures 8B,C** and **Supplementary Table 1**; Hughes et al., 2011).

TABLE 2 | Environmental interventions that modulate reproductive aging in *Caenorhabditis elegans*.

Intervention[1]		Longitudinal experiments[2]/ Male mated[3]	Reproductive span to peak (days)[4]	Reproductive span after peak (days)[5]	Total reproductive span (days)[6]	Peak progeny number[7]	Total progeny number[8]	Matricidal hatching[9]	References
Temperature	WT 15°C	yes/yes day1	↑	ND	↑	↓	+/−	ND	Hughes et al., 2007
	WT 25°C	yes/yes day1	+/−	ND	↓	+/−	↓	ND	Hughes et al., 2007
Bacterial/food source in comparison to *E. coli* OP50	Staphylococcus epidermidis	yes/no	↑	↑	↑	ND	+/−	ND	Madhu et al., 2019
	E. coli K-12 HT115"	yes/no	+/−	↓	↓	↑	+/−	ND	Stuhr and Curran, 2020
	E. coli B&*K-12* HB101"	yes/no	+/−	↓	↓	↑	+/−	ND	Stuhr and Curran, 2020
	Sphingomonas aquatilis "Yellow"	yes/no	+/−	↓	↓	+/−	↓	ND	Stuhr and Curran, 2020
	Xanthomonas citri "Orange"	yes/no	+/−	↓	↓	↑	+/−	ND	Stuhr and Curran, 2020
	Methylobacterium braciatum "Red"	yes/both	+/−	↓	↓	+/−	↓	ND	Stuhr and Curran, 2020
Fungi	Yeast *Candida albicans*	yes/no	+/−	+	+	↓	+/−	ND	Feistel et al., 2019

[1]*Intervention: Temperature or bacterial food source.*
[2]*Longitudinal experiment: the same individual animal is observed at sequential time points. yes: measured in a longitudinal experiment, no: measured in a cross-sectional experiment.*
[3]*Male mated: yes – hermaphrodites were exposed to males, with adult day of exposure specified, no: self-fertile hermaphrodites.*
[4]*Reproductive span to peak: time from adult day 0 until day of peak egg-laying (**Figure 1**).*
[5]*Reproductive span after peak: time from day of peak egg-laying until last day of egg-laying (**Figure 1**).*
[6]*Total reproductive span: time from adult day 0 until last day of egg-laying (**Figure 1**).*
[7]*Peak progeny number: Number of eggs laid on day of peak progeny production (**Figure 1**).*
[8]*Total progeny number: Total number of eggs laid (**Figure 1**).*
[9]*Matricidal hatching: If mature hermaphrodites cannot deposit eggs into the environment, then eggs hatch inside the hermaphrodite, and larvae feed on the parent resulting in death.*
[4−9] *↑: increase; ↓: decrease; +/−: no change; ND: not determined.*

TGF-β Dauer Pathway and TGF-β Sma/Mab Pathway

In *C. elegans,* two partially related Transforming Growth Factor-β (TGF-β) pathways, the TGF-β (*daf-7)* dauer and the TGF-β (*dbl-1*) Sma/Mab pathways (Savage-Dunn, 2005; Gumienny and Savage-Dunn, 2013), have been implicated in aging (Shaw et al., 2007; Kaplan et al., 2015; Tissenbaum, 2015; Tominaga and Suzuki, 2019). Both pathways act through *daf-4* (**Figures 8D,E**) (Luo et al., 2009). These pathways are highly conserved at the molecular and functional level in many species, including *Drosophila* and humans (Gumienny and Savage-Dunn, 2013; Monsivais et al., 2017). Not only are these pathways associated with somatic aging, they are also associated with reproductive aging. In particular, loss-of-function caused by chromosomal mutations or RNA interference (RNAi) of genes in the TGF-β Sma/Mab pathways, including the type-II receptor gene *daf-4*, R-Smad genes *sma-2* and *-3*, Co-Smad genes *sma-4* and *sma-9* (*C. elegans* homolog of Schnurri (Foehr et al., 2006)), and the ligand gene *dbl-1*, all significantly affect the fraction of animals that are reproductive at an older age and produce progeny curves of varying shapes (**Figures 8F–I** and **Supplementary Table 1**). Although genes in the TGF-β dauer pathway extend the reproductive span (e.g., the ligand *daf-7* and *crh-1*, a *C. elegans* homolog of mammalian CREB (Templeman et al., 2020), antagonistic Co-Smad *daf-3*, type-I receptor *daf-1* and R-Smad *daf-14*), their effects are less robust compared to the TGF-β Sma/Mab pathway (Luo et al., 2009, 2010; Gumienny and Savage-Dunn, 2013). The type-II receptor gene *daf-4*, which is also involved in the TGF- β dauer pathway, causes a greater effect on reproduction (**Figure 8H**; Luo et al., 2009). The TGF-β Sma/Mab pathway was found to delay reproductive aging by maintaining oocyte and germline quality cell non-autonomously by acting in the hypodermis (Luo et al., 2010; Templeman et al., 2020). A genome-wide RNAi screen by Wang et al. (2014) for extended reproduction identified many genes associated with these two pathways, in addition to several genes related to sodium homeostasis (*nhx-2* and *sgk-1*) (**Supplementary Table 1**).

Dietary Restriction

Dietary Restriction (DR) has long been established to extend lifespan in many species of animals, including mice, fruit flies, and nematodes (McCay et al., 1935; Kapahi et al., 2017;

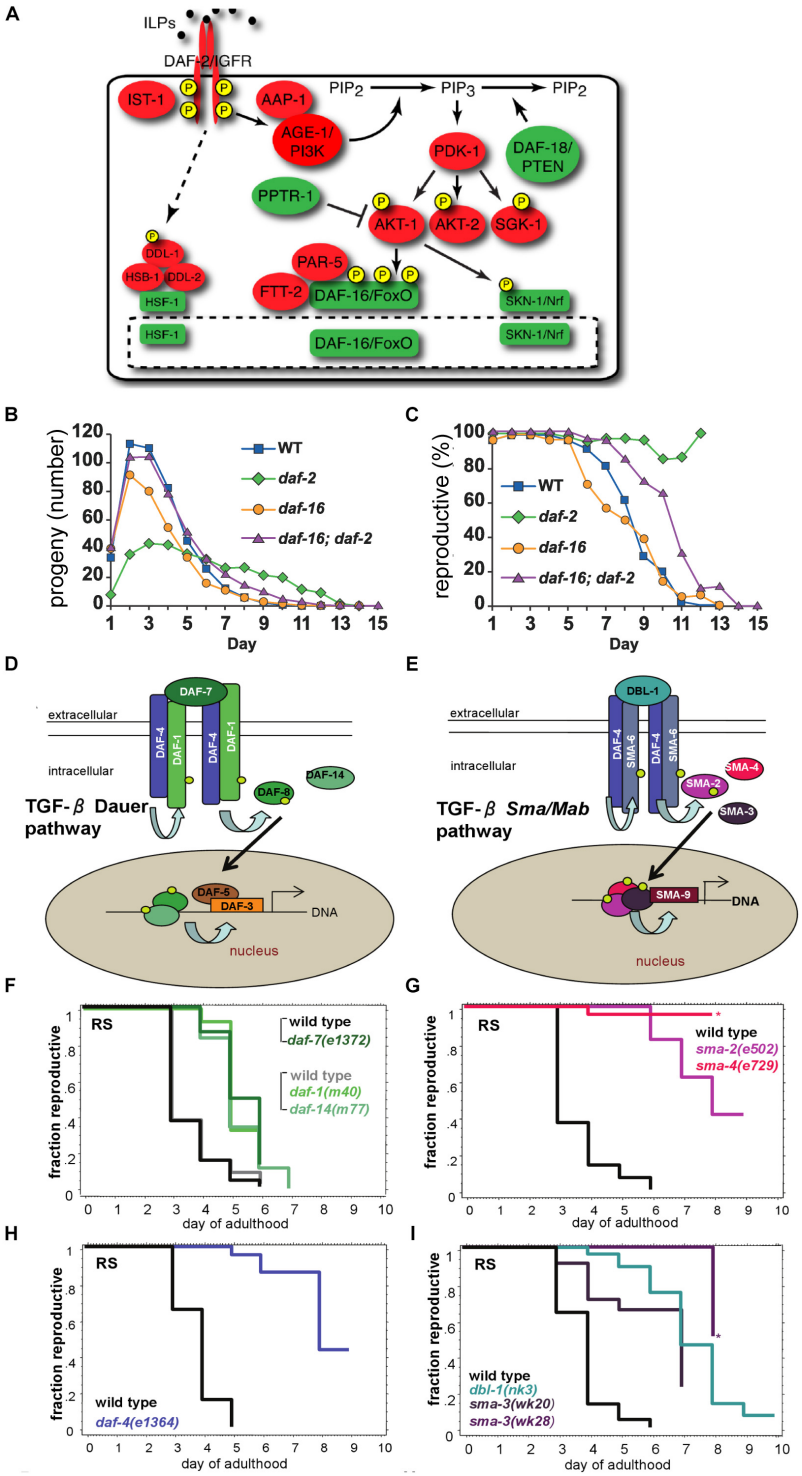

FIGURE 8 | Mutations in the TGF-β and the Insulin/IGF-1 signaling pathways increase reproductive capacity. **(A)** The schematic depicts the Insulin/IGF-1 signaling pathway. Adapted from Murphy and Hu (2013). **(B)** Mated hermaphrodites with a mutation in the *daf-2* gene (green) display reduced peak progeny number, increased late progeny production, and an extended total reproductive span. By contrast, mated *daf-16* mutant hermaphrodites display a reduced peak progeny number, a reduced total progeny number, and a reduced total reproductive span. Adapted from Hughes et al. (2007). **(C)** Mated *daf-2* mutants show a higher percentage of live hermaphrodites producing progeny late in life compared to mated *daf-2;daf-16* double mutants, mated *daf-16* mutants or mated wild-type animals. Adapted from Hughes et al. (2007). **(D,E)** The schematics depict the TGF-β Dauer pathway and the TGF-β *Sma/Mab* pathway. Adapted from Luo et al. (2009). **(F–I)** *C. elegans* hermaphrodites with mutations in the TGF-β Dauer pathway **(F,H)** or TGF-β *Sma/Mab* **(G,I)** display an extended reproductive span compared to wild type. Adapted from Luo et al. (2009).

Krittika and Yadav, 2019). This intervention has been of particular interest in the field of aging due in part to its highly conserved nature.

Several genetic mutations have been identified in *C. elegans* that can lead to DR. Mutations in the *eat-2* and *phm-2* genes extend mean adult lifespan, reduce adult body size, reduce total brood size, and extend the reproductive period (**Figure 7C** and **Supplementary Table 1**; Lakowski and Hekimi, 1998; Hughes et al., 2007; Kumar et al., 2019). These mutations alter the structure or function of the pharynx, thereby reducing the pumping rate or altering the pumping motion (Lakowski and Hekimi, 1998; Hughes et al., 2011; Kumar et al., 2019). Indeed, the *phm-2(am117)* mutation was first identified in a screen for delayed reproductive aging, prior to being molecularly identified (Hughes et al., 2011). However, recent studies by Kumar et al. (2019) indicate that the interpretation of these mutations is more complicated than anticipated. Coordinated pharyngeal pumping brings bacterial food into the organism and also grinds the bacteria so that they cannot colonize the intestine. Mutations in *eat-2* and *phm-2* cause pharyngeal defects that impair bacterial grinding, which allows live bacteria to enter and colonize the intestine of young adults. Thus, these mutants are immunocompromised. Because the standard bacterial food source, *E. coli* OP50, is mildly pathogenic, intestinal colonization provokes the innate immune response, which includes bacterial avoidance behavior. The bacterial avoidance behavior appears to cause dietary restriction in these mutants rather than an inability to ingest enough bacteria. Because these mutations lead to bacterial pathogenesis, an innate immune response, and bacterial avoidance behavior that leads to DR, any or all of these problems might contribute to the effect on reproductive aging.

Several non-genetic methods have been used to induce DR in worms, including dilution of the bacterial food source or interruption of food availability via intermittent fasting (Kaeberlein et al., 2006; Lee et al., 2006; Bishop and Guarente, 2007; Panowski et al., 2007; Chen et al., 2009; Greer and Brunet, 2009). Bishop and Guarente (2007) demonstrated that hermaphrodites grown in liquid medium with restricted bacterial concentration display reduced brood size and an extended reproductive period, ceasing reproduction on adult day 14 compared to day 8 in ad-libitum fed animals (Bishop and Guarente, 2007). Chen et al. (2009) demonstrated that a reduction in bacterial concentration was correlated with reduced fecundity (Chen et al., 2009). A change from 1.0×10^{12} cfu/mL to 1.0×10^{8} cfu/mL resulted in a reduction in brood size from ∼200 to ∼50, but with no observable change in the length of the reproductive period. Houthoofd et al. (2002) observed that culture in axenic liquid media reduced brood size and extended the reproductive period. Szewczyk et al. (2006) used the chemically defined growth medium CeMM and observed a reduction in brood size from ∼240 to ∼81, as well as an extension of the reproductive period from adult days 2–4 to days 7–14.

It has long been theorized that the effect of DR on lifespan is the result of a trade-off in caloric investment between reproduction and maintenance of somatic tissues (Holliday, 1989). However, studies in nematodes have shown that reduction in reproductive capacity is not necessary for lifespan extension by DR (Kaeberlein et al., 2006). Additionally, many studies have shown that various methods of DR still extend lifespan in nematodes treated with 5-fluorodeoxyuridine (FUDR, an inhibitor of nematode reproduction), suggesting that lifespan extension is independent of reproduction with respect to DR (Kaeberlein et al., 2006; Panowski et al., 2007; Greer and Brunet, 2009). We discuss this issue further in the section below regarding reproductive aging and evolutionary theories of aging.

GABAergic Signaling

Cermak et al. (2020) recently reported the importance of GABAergic signaling for dopamine-induced egg-laying. The GABAergic-signaling-defective *unc-25(lf)* mutations delay egg-laying by one day. Compared to wild-type worms, which display an egg-laying peak on adult day 2, *unc-25* mutants display a peak on adult day 3; *unc-25* mutants display higher progeny numbers on days 4-6, but produced slightly fewer total progeny. *unc-25* encodes a neuronal-specific glutamic acid decarboxylase, which is required for GABA synthesis. These results indicate that GABergic signaling regulates egg-laying; this is in agreement with previous observations by Tanis et al. (2009) that muscimol, a selective agonist for $GABA_A$ receptors, inhibits egg-laying similar to a mutation of the inhibitory *unc-49* $GABA_A$ receptor. This is likely due to the fact that *C. elegans* vulval muscles receive synaptic input from a number of different neurons, including GABAergic VD neurons, and muscle contractions are required for egg-laying (Cermak et al., 2020).

ENVIRONMENT: TEMPERATURE AND FOOD SOURCE

Reproduction and reproductive aging in *C. elegans* are influenced by the environment. Standard laboratory conditions for culturing *C. elegans* and measuring reproduction are nematode growth medium (NGM) agar dishes with a lawn of *E. coli* bacteria as a food source at 20°C. Reducing the temperature to 15°C delays reproductive aging (**Figure 7B** and **Table 2**), whereas increasing the temperature to 25°C accelerates reproductive aging (Hughes et al., 2007). There are two main theories for these temperature effects: (1) Both heat and cold are perceived as stresses, and the activation of stress response pathways modifies the reproductive schedule. (2) *C. elegans* are poikilotherm animals, and the rate of metabolic reactions responds to temperature, resulting in changes to the reproductive schedule. Both of these theories may be true, and it is difficult to distinguish these effects.

The most common *E. coli* strains used as a food source for *C. elegans* are OP50 or HT115 for classic developmental biology assays or RNAi experiments, respectively (Conte et al., 2015). Culturing *C. elegans* on different bacterial strains or species as a food source has been reported to cause a number of effects, which have been previously reviewed (Darby, 2005; Kim, 2013; Kim and Flavell, 2020; Poupet et al., 2020). The effect of different bacterial species on reproductive aging, however, is limited to a

small number of recent studies (**Table 2**). Madhu et al. (2019) reported that wild-type *C. elegans* egg-laying curves changed when cultured on *S. marcescens* or *S. epidermidisi*. *S. marcescens* decreased the number of eggs laid at the peak and did not affect reproductive aging. By contrast, *S. epidermidis* extended the reproductive span significantly, with more eggs laid on days 5–11. The total brood size was slightly, but not significantly, decreased from ∼215 to ∼175 on average (Madhu et al., 2019).

In self-fertile hermaphrodites, changing the *E. coli* food source from OP50 to IAI1 or F11 increased the peak progeny number, while the total progeny number remained unchanged (Baeriswyl et al., 2010). Self-fertile hermaphrodites cultured on *Comamonas* sp., *Bacillus megaterium* or *E. coli* strains HB101, HT115, or MG1655 showed reduced reproductive lifespans compared to OP50 (Sowa et al., 2015). Furthermore, culturing hermaphrodites on HB101 reduces their reproductive success after exposure to males late in life (day 10/11) (Sowa et al., 2015). The authors suggest links between olfactory sensation, neuroendocrine signaling, and reproductive timing. Stuhr and Curran (2020) also reported that hermaphrodites cultured on *E. coli* OP50, HT115, and HB101 have the same number of total progeny. However, they found the shape of the progeny production curves is slightly altered. For example, HT115 and HB101 increase peak progeny numbers on day 2 and decrease progeny number on day 3 compared to OP50. By contrast, culture on *Methylobacterium braciatum* and *Sphingomonas aquatilis* significantly decreased total progeny number. While changing the bacterial diet can have striking effects, these experiments can be difficult to interpret because bacteria influence *C. elegans* in at least two ways. First, the bacteria are a complex set of chemical nutrients, and different bacterial strains and species change the amount and ratio of many nutrients at the same time. Second, bacteria have a spectrum of pathogenicity for *C. elegans*, and the standard *E. coli* OP50 strain is mildly pathogenic. Thus, changing bacteria can simultaneously affect pathogenesis, immune response, bacterial avoidance behavior, and nutrition.

ECOLOGICAL AND EVOLUTIONARY CONSEQUENCES OF REPRODUCTIVE AGING

A large amount of thought and theory have been expended to understand why animals age, and in particular why the reproductive system ages. Because reproductive aging limits individual progeny production, it is often considered a negative trait. Many have argued that evolution will select for animals that make more progeny for a longer period of time, and that animals that make less progeny for a shorter period of time will not compete successfully and will not pass on their genes. Self-fertile hermaphrodites such as *C. elegans* add additional complexity to these questions. Hodgkin and Barnes (1991) analyzed a mutant hermaphrodite that produces more male sperm before switching to oocyte production. These hermpahrodites can make a larger number of self-progeny than wild-type hermaphrodites, but they are delayed in generating the first egg compared to wild type. Thus, *C. elegans* hermaphrodites confront a tradeoff between time to first self-fertile egg laid and the total number of self-fertile eggs it can eventually lay. While observational and interventional studies of *C. elegans* cannot directly answer these teleological or "why" questions, the experimental power of the system makes it well suited to testing some of the predictions of these theories. Here we describe some prominent theories of why somatic and reproductive aging occurs, and consider how the results of studying *C. elegans* bear on these ideas.

To begin, it is worth considering a central conundrum of reproductive aging – if reproduction is the purpose of animal life, and evolution selects for greater levels of reproduction, then the intuitive prediction is that animals would reproduce up until the time they die – that reproduction would be the last system to fail, so that an individual could make as many progeny as possible while it still survived. *C. elegans* is ideal for testing this prediction, and the answer is clear. As a result of reproductive aging, germline function and reproductive capacity decline before somatic aging compromises life support systems (**Figures 1B,C**). Therefore, many hermaphrodites spend more than a third of the lifespan as post reproductive adults (Pickett et al., 2013). This is not simply a trait of worms – human females and many other animals display substantial post reproductive life spans. While it has been argued that humans may have a post reproductive lifespan to serve as grandparents, this does not apply to *C. elegans* or many other species that do not provide maternal care. Thus, to explain the pattern of reproductive aging observed in *C. elegans*, a theory should explain why reproduction fails before life support systems.

The theory of aging proposed by Medawar in a lecture delivered in 1952 has a prominent role in the field. Medawar proposed that the evolution of aging is driven by extrinsic death that gradually reduces the number of animals in a birth cohort. As the number of animals decreases, evolution by natural selection cannot effectively select for greater longevity. This is undoubtedly true in the limiting case – evolution by natural selection cannot promote additional longevity after all the animals in a cohort have died from extrinsic mortality. Because "the force of natural selection weakens with increasing age" (Medawar, 1952), deleterious traits or harmful alleles can accumulate, resulting in age-related pathologies or, simply, aging. According to this theory, reproductive aging developed in the "shadow of selection" of extrinsic mortality. In other words, reproductive aging is a deleterious trait, and high levels of progeny production with life-long reproductive capacity would be the favorable trait, but extrinsic death prevents natural selection from promoting further reproductive longevity.

A few years later, Williams extended this theory by proposing that selective forces favor early reproduction with the byproduct being antagonistically pleiotropic genes that result in the decline of reproduction later in life (Williams, 1957). Here Williams recognized the centrality of reproductive aging, which is why studies of reproductive aging are the key to evaluating these evolutionary theories. In addition, Williams postulated that "there should be little or no post reproductive period" (Gaillard and Lemaître, 2017). This prediction of the antagonistic pleiotropy theory is clearly not supported by studies of *C. elegans*

or many other species. Both theories were founded on the assumption that age-related declines are a result of protected life in captivity, and that animals in the wild die only of extrinsic factors. Over the last decades, field studies reported many different species that experience age-related declines in the wild (Nussey et al., 2013). Thus, this assumption of these theories is not supported. The antagonistic pleiotropy theory is widely discussed because it predicts that decreasing early reproduction can cause an extension of the reproductive span. This pattern has frequently been observed in *C. elegans*. For example, mutations of *daf-2* and dietary restriction both reduce early progeny production and increase late progeny production. While these observations conform to a prediction of the antagonistic pleiotropy theory, they are also consistent with other theories. At this time, the most concerning aspect of these theories is that they do not appear to make predictions that enable the theories to be critically tested and falsified. Both Medawar and Williams were theorists, and they provided no data to evaluate these ideas. While experimental observations have been made that are consistent with these theories, there are also data that are not consistent, and these "flies in the ointment" are often addressed by theory defense. For example, if mutation #1 causes a decrease in early progeny production and an increase in late progeny production, then it supports the theory. If mutation #2 does not cause a decrease in early progeny production and yet still causes an increase in late progeny production, then it does not support the theory. However, theory defense could argue that mutation #2 may reduce early progeny production under some alternative environmental condition, and the fact that it was not observed in one or more conditions that were tested does not rule out the possibility that it would be observed in some condition. Thus, these data would not be accepted as falsifying the theory. It begins to appear that these theories have left the realm of hypothesis and entered the realm of belief.

Kirkwood's disposable soma theory of aging, a modification of William's antagonistic pleiotropy theory, builds on the assumption that "natural selection trades late survival for enhanced early fecundity" (Kirkwood and Rose, 1991) and explains aging by allocation of resources to reproduction earlier in life (Kirkwood et al., 2017). The occurrence of aging in the wild is in agreements with this theory- it would be the result of an optimal distribution key that only allocates a certain amount of energy to maintenance with the consequence of an optimal aging rate and lifespan (Kowald and Kirkwood, 2015). While this theory can explain somatic aging and lifespan, it is more complicated to apply to the data of reproductive aging in *C. elegans*. Is the early functional decline of the germ line followed by the reproductive capacity decline a result of misallocation of resources to maintenance of the reproductive system? While increased progeny production has clear trade-offs in many species due to intensive maternal care and limited resources, the trade-offs for reproductive longevity in *C. elegans* are less obvious. It also seems difficult to find the connection between resource allocation and the heterogeneous reproductive aging pattern that were reviewed here (**Tables 2**, **3** and **Supplementary Table 1**). Furthermore,

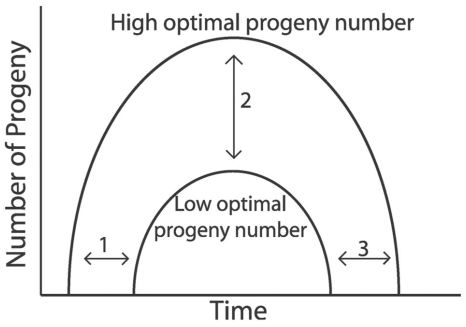

FIGURE 9 | Optimal progeny number theory. The schematic of hypothetical progeny production curves display how progeny number can be controlled: (1) timing of onset of reproduction, (2) quantity of progeny, and (3) timing of cessation of reproduction or reproductive aging. Thus, reproductive aging is one of the critical inputs that controls progeny number. According to the theory, there is an optimal progeny number that stabilizes population dynamics and support long-term survival of populations. Therefore, reproductive aging can be an advantageous trait that might be sculpted by evolution. Adapted from Hughes et al. (2007).

Hsin and Kenyon (2009) showed that ablation of the entire gonad (germ line and somatic gonad) does not extend lifespan in *C. elegans*. Taken at face value, this result directly contradicts the disposable soma theory.

All of these theories are based on the assumption that reproductive aging is a deleterious trait. By contrast, Hughes et al. (2007) proposed the optimal progeny number theory based on the assumption that reproductive aging is an advantageous trait (**Figure 9**; Hughes et al., 2007). According to this theory, reproductive aging is an adaptive trait that promotes reproductive success in the context of populations and their long-term survival in ecosystems with finite resources. An optimal progeny number can limit the population from growing too large in times of rich food availability and exceeding the carrying capacity of the environment. Populations that exceed carrying capacity enter a phase of starvation and instability characterized by boom and bust cycles and the threat of extinction. In contrast, reproductive restraint can stabilize population fluctuations and be advantageous for population survival in the long-term. The optimal progeny theory explains why reproductive aging declines before somatic aging – the central conundrum of this field. To achieve the optimal progeny production curve, the somatic tissues were selected for durability so they do not become the rate limiting step in reproduction. The optimal progeny number theory predicts the existence of mutations that decrease early reproduction and extend late reproduction. According to this theory, such genes promote early reproduction, which is adaptive, and they promote the age-related decline of reproduction, which is also adaptive. Thus, this theory explains the same observations that support the antagonistic pleiotropy theory without invoking genetic tradeoffs.

The key prediction of the optimal progeny number theory is that hermaphrodites that produce fewer progeny can be selected for by evolution because they stabilize population dynamics. Thus, to test this theory requires a new level of

analysis -determining how the traits of individuals interact with population dynamics. In practice, this will require analyzing reproductive aging in the context of populations and ecosystems in the laboratory. Such an approach would make it possible to directly measure how different progeny production curves and progeny numbers affect population fluctuations over many generations in different environments. Most importantly, it would bridge the gap between the scarce data available from *C. elegans* in the wild with widespread data from individual animal measurements in the laboratory. This is an important future goal for the field, and advances in computational modeling make it seem achievable. Recently, Galimov and Gems (2020) reported a computational simulation that examined the role of aging during the population dynamics of a *C. elegans* colony. Future work in this area is likely to deliver important answers to fundamental questions in the field.

CONCLUSION

(1) Detailed descriptions of age-related morphological changes in the *C. elegans* germ line are now available. They began with gross morphology determined by DIC optics, and have now been extended to measurements of the number, cell cycle duration, and rate of meiotic progression of the germ-line stem cells. These studies point to the distal germ line as the source of early degenerative change, which results in reduced egg-laying with a two-day delay (**Figure 6E**). The major challenge for future studies will be to elucidate the mechanism that controls this rapid and early decline. Because this decline occurs rapidly and in every animal, it seems unlikely to be caused by stochastic damage from the environment, which would be expected to be variable between animals. Rather, it appears to be caused by processes encoded in the genomes or environmental factors that affect every individual. Deciphering the mechanism of this population-wide decline would be a major achievement.

(2) Many genetic, pharmacological, and environmental factors that delay reproductive aging have now been identified. The challenge is to understand the chain of events that leads from the intervention to extended reproductive function. In most cases, little is currently known. One limitation of these studies is that the reported data are difficult to compare due to heterogeneity in methods and selective reporting of time points. Some studies only provided cross sectional data and reported progeny numbers for only a single day. To achieve a more standard and unified analysis, we suggest that future studies of reproductive aging interventions in *C. elegans* incorporate the following approaches: (1) hermaphrodites should be briefly mated with males (24–48 h) to avoid sperm depletion; (2) a complete progeny production curve should be presented, so that it is possible to determine total reproductive span, reproductive span after peak, peak progeny number, and total progeny number. An example is provided by Hughes et al. (2007). This unified protocol would help to compare data and to gain a deeper understanding of reproductive aging plasticity.

(3) It is still unclear why reproduction declines before the soma deteriorates in *C. elegans*. Future studies are needed to address this essential question and the related question of why *C. elegans* has a long post reproductive lifespan.

(4) Reproductive aging in *C. elegans* has only been studied in laboratory conditions where animals are relatively isolated and provided with an excess of bacterial food. While field studies in the wild are difficult to conduct due to the small size and subterranean lifestyle of these worms, experiments are needed to understand reproductive aging in the context of populations. A population-level approach can answer important questions such as (i) Is the post reproductive lifespan observed under optimal food conditions also present when worms are cultured in a population? (ii) How frequent is matricidal hatching in a population, and how does it affect population dynamics, (iii) Is there an optimal progeny number that can stabilize population dynamics, and how can reproductive restraint be maintained if mutants arise that make additional progeny? (iv) Can reproductive aging be adaptive, and if so in which conditions?

(5) Although *C. elegans* and humans have obvious differences, they also share striking similarities. In the case of reproductive aging, more information about the process in both worms and humans is necessary to fully evaluate the relevance of *C. elegans* as a model system. Several interesting parallels have emerged thus far: (1) *C. elegans* hermaphrodites and human females both display a substantial post-reproductive lifespan. (2) Oocyte quality displays age-related declines in both systems. (3) The same molecular pathways can control the rate of somatic aging in both systems, such as insulin/IGF-1 pathway and dietary restriction, and these similarities might extend to reproductive aging. If the systems share an underlying biology, then the experimental power of *C. elegans* is likely to accelerate the understanding of human reproductive aging.

AUTHOR CONTRIBUTIONS

AS, FP, BME, ZK, and KK provided scientific input and wrote the manuscript. All authors contributed to the article and approved the submitted version.

FUNDING

The work was supported by the NIH grants RO1 AG02656106A1, R21 AG058037, and RO1 AG057748 to KK, the Irving Boime Graduate Student Fellowship to BME, and by a postdoctoral fellowship from the National Ataxia Foundation to FP.

ACKNOWLEDGMENTS

We thank the Caenorhabditis Genetics Center [funded by NIH Office of Research Infrastructure Programs (P40 OD010440)] for providing strains.

SUPPLEMENTARY MATERIAL

The Supplementary Material for this article can be found online at: https://www.frontiersin.org/articles/10.3389/fcell.2021.718522/full#supplementary-material

REFERENCES

Achache, H., Falk, R., Lerner, N., Beatus, T., and Tzur, Y. B. (2021). Oocyte aging is controlled by mitogen-activated protein kinase signaling. *Aging Cell* 20:e13386. doi: 10.1111/acel.13386

Adam Bohnert, K., and Kenyon, C. (2017). A lysosomal switch triggers proteostasis renewal in the immortal *C. elegans* germ lineage. *Nature* 551, 629–633. doi: 10.1038/nature24620

Admasu, T. D., Chaithanya Batchu, K., Barardo, D., Ng, L. F., Lam, V. Y. M., Xiao, L., et al. (2018). Drug synergy slows aging and improves healthspan through igf and srebp lipid signaling. *Dev. Cell* 47, 67–79.e5. doi: 10.1016/j.devcel.2018.09.001

Akinwumi, B. C. (2018). Biological activities of stilbenoids. *Int. J. Mol. Sci.* 19:792. doi: 10.3390/ijms19030792

Andux, S., and Ellis, R. E. (2008). Apoptosis maintains oocyte quality in aging *Caenorhabditis elegans* females. *PLoS Genet.* 4:e1000295. doi: 10.1371/journal.pgen.1000295

Anisimov, V. N., Berstein, L. M., Popovich, I. G., Zabezhinski, M. A., Egormin, P. A., Piskunova, T. S., et al. (2011). If started early in life, metformin treatment increases life span and postpones tumors in female SHR mice. *Aging (Albany. NY)* 3, 148–157. doi: 10.18632/aging.100273

Antebi, A. (2013). Regulation of longevity by the reproductive system. *Exp. Gerontol.* 48, 596–602. doi: 10.1016/j.exger.2012.09.009

Baeriswyl, S., Diard, M., Mosser, T., Leroy, M., Manière, X., Taddei, F., et al. (2010). Modulation of aging profiles in isogenic populations of *Caenorhabditis elegans* by bacteria causing different extrinsic mortality rates. *Biogerontology* 11, 53–65. doi: 10.1007/s10522-009-9228-0

Bishop, N. A., and Guarente, L. (2007). Two neurons mediate diet-restriction-induced longevity in *C. elegans*. *Nature* 447, 545–549. doi: 10.1038/nature05904

Booth, L. N., Maures, T. J., Yeo, R. W., Tantilert, C., and Brunet, A. (2019). Self-sperm induce resistance to the detrimental effects of sexual encounters with males in hermaphroditic nematodes. *eLife* 8:e46418. doi: 10.7554/eLife.46418

Byerly, L., Cassada, R. C., and Russell, R. L. (1976). The life cycle of the nematode *Caenorhabditis elegans*: I. Wild-type growth and reproduction. *Dev. Biol.* 51, 23–33. doi: 10.1016/0012-1606(76)90119-6

Cabreiro, F., Au, C., Leung, K. Y., Vergara-Irigaray, N., Cochemé, H. M., Noori, T., et al. (2013). Metformin retards aging in *C. elegans* by altering microbial folate and methionine metabolism. *Cell* 153, 228–239. doi: 10.1016/j.cell.2013.02.035

Cermak, N., Yu, S. K., Clark, R., Huang, Y. C., Baskoylu, S. N., and Flavell, S. W. (2020). Whole-organism behavioral profiling reveals a role for dopamine in statedependent motor program coupling in *C. elegans*. *Elife* 9:e57093. doi: 10.7554/eLife.57093

Chen, D., Thomas, E. L., and Kapahi, P. (2009). HIF-1 modulates dietary restriction-mediated lifespan extension via IRE-1 in *Caenorhabditis elegans*. *PLoS Genet.* 5:e1000486. doi: 10.1371/journal.pgen.1000486

Chen, J., and Caswell-Chen, E. P. (2004). Facultative vivipary is a life-history trait in *Caenorhabditis elegans*. *J. Nematol.* 36, 107–113.

Collins, J. J., Evason, K., Pickett, C. L., Schneider, D. L., and Kornfeld, K. (2008). The anticonvulsant ethosuximide disrupts sensory function to extend *C. elegans* lifespan. *PLoS Genet.* 4:e1000230. doi: 10.1371/journal.pgen.1000230

Collins, J. J., Huang, C., Hughes, S., and Kornfeld, K. (2007). The measurement and analysis of age-related changes in *Caenorhabditis elegans*. *WormBook* 1–21. doi: 10.1895/wormbook.1.137.1

Conte, D., MacNei, L. T., Walhout, A. J. M., and Mello, C. C. (2015). RNA interference in *Caenorhabditis elegans*. *Curr. Protoc. Mol. Biol.* 2015, 26.3.1–26.3.30. doi: 10.1002/0471142727.mb2603s109

Corsi, A. K., Wightman, B., and Chalfie, M. (2015). A transparent window into biology: a primer on *Caenorhabditis elegans*. *Genetics* 2, 387–407. doi: 10.1534/genetics.115.176099

Crittenden, S. L., Leonhard, K. A., Byrd, D. T., and Kimble, J. (2006). Cellular analyses of the mitotic region in the *Caenorhabditis elegans* adult germ line. *Mol. Biol. Cell* 17, 3051–3061. doi: 10.1091/mbc.E06-03-0170

Croll, N. A., Smith, J. M., and Zuckerman, B. M. (1977). The aging process of the nematode *Caenorhabditis elegans* in bacterial and axenic culture. *Exp. Aging Res.* 3, 175–189. doi: 10.1080/03610737708257101

Darby C. (2005). Interactions with microbial pathogens. *WormBook* 1–15. doi: 10.1895/wormbook.1.21.1

de la Guardia, Y., Gilliat, A. F., Hellberg, J., Rennert, P., Cabreiro, F., and Gems, D. (2016). Run-on of germline apoptosis promotes gonad senescence in *C. elegans*. *Oncotarget* 7, 39082–39096. doi: 10.18632/oncotarget.9681

Evason, K., Huang, C., Yamben, I., Covey, D. F., and Kornfeld, K. (2005). Anticonvulsant medications extend worm life-span. *Science* 307, 258–262. doi: 10.1126/science.1105299

Feistel, D. J., Elmostafa, R., Nguyen, N., Penley, M., Morran, L., and Hickman, M. A. (2019). a novel virulence phenotype rapidly assesses candida fungal pathogenesis in healthy and immunocompromised *Caenorhabditis elegans* hosts. *mSphere* 4, e00697-18. doi: 10.1128/msphere.00697-18

Feng, W., Teo, X. Y., Novera, W., Ramanujulu, P. M., Liang, D., Huang, D., et al. (2015). Discovery of new H2S releasing phosphordithioates and 2,3-dihydro-2-PHENYL-2-sulfanylenebenzo[d][1,3,2]oxazaphospholes with improved antiproliferative activity. *J. Med. Chem.* 58, 6456–6480. doi: 10.1021/acs.jmedchem.5b00848

Foehr, M. L., Lindy, A. S., Fairbank, R. C., Amin, N. M., Xu, M., Yanowitz, J., et al. (2006). An antagonistic role for the *C. elegans* Schnurri homolog SMA-9 in modulating TGFβ signaling during mesodermal patterning. *Development* 133, 2887–2896. doi: 10.1242/dev.02476

Fox, P. M., and Schedl, T. (2015). Analysis of germline stem cell differentiation following loss of GLP-1 notch activity in *Caenorhabditis elegans*. *Genetics* 201, 167–184. doi: 10.1534/genetics.115.178061

Fox, P. M., Vought, V. E., Hanazawa, M., Lee, M. H., Maine, E. M., and Sched, T. (2011). Cyclin e and CDK-2 regulate proliferative cell fate and cell cycle progression in the *C. elegans* germline. *Development* 138, 2223–2234. doi: 10.1242/dev.059535

Frankowski, H., Alavez, S., Spilman, P., Mark, K. A., Nelson, J. D., Mollahan, P., et al. (2013). Dimethyl sulfoxide and dimethyl formamide increase lifespan of *C. elegans* in liquid. *Mech. Ageing Dev.* 134, 69–78. doi: 10.1016/j.mad.2012.10.002

Friedman, D. B., and Johnson, T. E. (1988). A mutation in the age-1 gene in *Caenorhabditis elegans* lengthens life and reduces hermaphrodite fertility. *Genetics* 118, 75–86.

Gaillard, J. M., and Lemaître, J. F. (2017). The Williams' legacy: a critical reappraisal of his nine predictions about the evolution of senescence. *Evolution (N. Y.)* 71, 2768–2785. doi: 10.1111/evo.13379

Galimov, E. R., and Gems, D. (2020). Shorter life and reduced fecundity can increase colony fitness in virtual *Caenorhabditis elegans*. *Aging Cell* 19:e13141. doi: 10.1111/acel.13141

Garigan, D., Hsu, A. L., Fraser, A. G., Kamath, R. S., Abringet, J., and Kenyon, C. (2002). Genetic analysis of tissue aging in *Caenorhabditis elegans*: a role for heat-shock factor and bacterial proliferation. *Genetics* 161, 1101–1112.

Gems, D., and Riddle, D. L. (1996). Longevity in *Caenorhabditis elegans* reduced by mating but not gamete production. *Nature* 379, 723–725. doi: 10.1038/379723a0

Greer, E. L., and Brunet, A. (2009). Different dietary restriction regimens extend lifespan by both independent and overlapping genetic pathways in *C. elegans*. *Aging Cell* 8, 113–127. doi: 10.1111/j.1474-9726.2009.00459.x

Gruber, J., Tang, S. Y., and Halliwell, B. (2007). Evidence for a trade-off between survival and fitness caused by resveratrol treatment of *Caenorhabditis elegans*. *Ann. N. Y. Acad. Sci.* 1100, 530–542. doi: 10.1196/annals.1395.059

Gumienny T. L., and Savage-Dunn C. (2013). TGF-β signaling in *C. elegans*. *WormBook* 1–34. doi: oi:10.1895/wormbook

Harrington, L. A., and Harley, C. B. (1988). Effect of vitamin E on lifespan and reproduction in *Caenorhabditis elegans*. *Mech. Ageing Dev.* 43, 71–78. doi: 10.1016/0047-6374(88)90098-X

Hibshman, J. D., Hung, A., and Baugh, L. R. (2016). Maternal diet and insulin-like signaling control intergenerational plasticity of progeny size and starvation resistance. *PLoS Genet.* 12:e1007639. doi: 10.1371/journal.pgen.1006396

Hodgkin, J., and Barnes, T. M. (1991). More is not better: brood size and population growth in a self-fertilizing nematode. *Proc. R. Soc. Lond. B Biol. Sci.* 246, 19–24. doi: 10.1098/rspb.1991.0119

Holliday, R. (1989). Food, reproduction and longevity: is the extended lifespan of calorie-restricted animals an evolutionary adaptation? *Bioessays* 10, 125–127. doi: 10.1002/bies.950100408

Honda, Y., Tanaka, M., and Honda, S. (2010). Trehalose extends longevity in the nematode *Caenorhabditis elegans*. *Aging Cell* 9, 558–569. doi: 10.1111/j.1474-9726.2010.00582.x

Houthoofd, K., Braeckman, B. P., Lenaerts, I., Brys, K., De Vreese, A., Van Eygen, S., et al. (2002). Axenic growth up-regulates mass-specific metabolic rate, stress resistance, and extends life span in *Caenorhabditis elegans*. *Exp. Gerontol.* 37, 1371–1378. doi: 10.1016/S0531-5565(02)00173-0

Hsin, H., and Kenyon, C. (2009). Signals from the reproductive system regulate the lifespan of *C. elegans*. *Nature* 399, 362–366.

Huang, C., Xiong, C., and Kornfeld, K. (2004). Measurements of age-related changes of physiological processes that predict lifespan of *Caenorhabditis elegans*. *Proc. Natl. Acad. Sci. U.S.A.* 101, 8084–8089. doi: 10.1073/pnas.0400848101

Hubbard, E. J. A., and Schedl, T. (2019). Biology of the *Caenorhabditis elegans* germline stem cell system. *Genetics* 213, 1145–1188.

Huelgas-Morales, G., and Greenstein, D. (2018). Control of oocyte meiotic maturation in *C. elegans*. *Semin. Cell Dev. Biol.* 84, 90–99. doi: 10.1016/j.semcdb.2017.12.005

Hughes, S. E., Evason, K., Xiong, C., and Kornfeld, K. (2007). Genetic and pharmacological factors that influence reproductive aging in nematodes. *PLoS Genet.* 3:e25. doi: 10.1371/journal.pgen.0030025

Hughes, S. E., Huang, C., and Kornfeld, K. (2011). Identification of mutations that delay somatic or reproductive aging of *Caenorhabditis elegans*. *Genetics* 189, 341–356. doi: 10.1534/genetics.111.130450

Jaramillo-Lambert, A., Ellefson, M., Villeneuve, A. M., and Engebrecht, J. A. (2007). Differential timing of S phases, X chromosome replication, and meiotic prophase in the *C. elegans* germ line. *Dev. Biol.* 308, 206–221. doi: 10.1016/j.ydbio.2007.05.019

Johnigk, S. A., and Ehlers, R. U. (1999). Endotokia matricida in hermaphrodites of Heterorhabditis spp. and the effect of the food supply. *Nematology* 1, 717–726. doi: 10.1163/156854199508748

Kaeberlein, T. L., Smith, E. D., Tsuchiya, M., Welton, K. L., Thomas, J. H., Fields, S., et al. (2006). Lifespan extension in *Caenorhabditis elegans* by complete removal of food. *Aging Cell* 5, 487–494. doi: 10.1111/j.1474-9726.2006.00238.x

Kapahi, P., Kaeberlein, M., and Hansen, M. (2017). Dietary restriction and lifespan: lessons from invertebrate models. *Ageing Res. Rev.* 39, 3–14. doi: 10.1016/j.arr.2016.12.005

Kaplan, R. E. W., Chen, Y., Moore, B. T., Jordan, J. M., Maxwell, C. S., Schindler, A. J., et al. (2015). dbl-1/TGF-β and daf-12/NHR signaling mediate cell-nonautonomous effects of daf-16/FOXO on starvation-induced developmental arrest. *PLoS Genet.* 11:e1005731. doi: 10.1371/journal.pgen.1005731

Kenyon, C., Chang, J., and Gensch, E. (1993). A *C. elegans* mutant that lives twice as long as wild type. *Nature* 366, 461–464.

Kershner, A. M., Shin, H., Hansen, T. J., and Kimble, J. (2014). Discovery of two GLP-1/Notch target genes that account for the role of GLP-1/Notch signaling in stem cell maintenance. *Proc. Natl. Acad. Sci. U.S.A.* 111, 3739–3744. doi: 10.1073/pnas.1401861111

Killian, D. J., and Hubbard, E. J. A. (2005). *Caenorhabditis elegans* germline patterning requires coordinated development of the somatic gonadal sheath and the germ line. *Dev. Biol.* 279, 322–335. doi: 10.1016/j.ydbio.2004.12.021

Kim, D. H. (2013). Bacteria and the aging and longevity of *Caenorhabditis elegans*. *Annu. Rev. Genet.* 47, 233–246. doi: 10.1146/annurev-genet-111212-133352

Kim, D. H., and Flavell, S. W. (2020). Host-microbe interactions and the behavior of *Caenorhabditis elegans*. *J. Neurogenet.* 34, 500–509. doi: 10.1080/01677063.2020.1802724

Kirkwood, T. B. L., and Rose, M. R. (1991). Evolution of senescence: late survival sacrificed for reproduction. *Philos. Trans. R. Soc. Lond. B* 332, 15–24. doi: 10.1098/rstb.1991.0028

Kirkwood, T. B. L., Zandveld, J., Zwaan, B. J., Kirkwood, T. B. L., and Shanley, D. P. (2017). Growing more positive with age: the relationship between reproduction and survival in aging flies. *Exp. Gerontol.* 90, 34–42. doi: 10.1016/j.exger.2017.01.016

Klass, M. R. (1977). Aging in the nematode *Caenorhabditis elegans*: major biological and environmental factors influencing life span. *Mech. Ageing Dev.* 6, 413–429. doi: 10.1016/0047-6374(77)90043-4

Kocsisova, Z., Kornfeld, K., and Schedl, T. (2019). Rapid population-wide declines in stem cell number and activity during reproductive aging in *C. elegans*. *Development* 146:dev173195. doi: 10.1242/dev.173195

Kowald, A., and Kirkwood, T. B. L. (2015). Evolutionary significance of ageing in the wild. *Exp. Gerontol.* 71, 89–94. doi: 10.1016/j.exger.2015.08.006

Krittika, S., and Yadav, P. (2019). An overview of two decades of diet restriction studies using *Drosophila*. *Biogerontology* 20, 723–740. doi: 10.1007/s10522-019-09827-0

Kumar, S., Egan, B. M., Kocsisova, Z., Schneider, D. L., Murphy, J. T., Diwan, A., et al. (2019). Lifespan extension in *C. elegans* caused by bacterial colonization of the intestine and subsequent activation of an innate immune response. *Dev. Cell* 49, 100–117.e6. doi: 10.1016/j.devcel.2019.03.010

Kumar, S., Kocsisova, Z., and Kornfeld, K. (2014). Keep on laying eggs mama, RNAi my reproductive aging blues away. *PLoS Genet.* 10:e1004808. doi: 10.1371/journal.pgen.1004808

Lakowski, B., and Hekimi, S. (1998). The genetics of caloric restriction in *Caenorhabditis elegans*. *Proc. Natl. Acad. Sci. U.S.A.* 95, 13091–13096. doi: 10.1073/pnas.95.22.13091

Lee, C. H., Sorensen, E. B., Lynch, T. R., and Kimble, J. (2016). *C. elegans* GLP-1/notch activates transcription in a probability gradient across the germline stem cell pool. *eLife* 5, 269–282. doi: 10.7554/eLife.18370

Lee, G. D., Wilson, M. A., Zhu, M., Wolkow, C. A., De Cabo, R., Ingram, D. K., et al. (2006). Dietary deprivation extends lifespan in *Caenorhabditis elegans*. *Aging Cell* 5, 515–524. doi: 10.1111/j.1474-9726.2006.00241.x

Lim, J. G. Y., Stine, R. R. W., and Yanowitz, J. L. (2008). Domain-specific regulation of recombination in *Caenorhabditis elegans* in response to temperature, age and sex. *Genetics* 180, 715–726. doi: 10.1534/genetics.108.090142

Lints, R. and Hall, D. H. (2009a). "Male introduction," in *WormAtlas*. doi: 10.3908/wormatlas.2.1

Lints, R. and Hall, D. H. (2009b). "Reproductive system, overview," in *WormAtlas*. doi: 10.3908/wormatlas.1.21

Luc, M., Danold, P., and Taylor, C. N. (1979). On endotokia matricida and intra-uterine developement and hatching in nematodes. *Nematology* 25, 268–274.

Lucanic, M., Lithgow, G. J., and Alavez, S. (2013). Pharmacological lifespan extension of invertebrates. *Ageing Res. Rev.* 12, 445–458. doi: 10.1016/j.arr.2012.06.006

Lucanic, M., Plummer, W. T., Chen, E., Harke, J., Foulger, A. C., Onken, B., et al. (2017). Impact of genetic background and experimental reproducibility on identifying chemical compounds with robust longevity effects. *Nat. Commun.* 8:14256. doi: 10.1038/ncomms14256

Ludewig, A. H., Artyukhin, A. B., Aprison, E. Z., Rodrigues, P. R., Pulido, D. C., Burkhardt, R. N., et al. (2019). An excreted small molecule promotes *C. elegans* reproductive development and aging. *Nat. Chem. Biol.* 15, 838–845. doi: 10.1038/s41589-019-0321-7

Luo, S., and Murphy, C. T. (2011). *Caenorhabditis elegans* reproductive aging: regulation and underlying mechanisms. *Genesis* 49, 53–65. doi: 10.1002/dvg.20694

Luo, S., Kleemann, G. A., Ashraf, J. M., Shaw, W. M., and Murphy, C. T. (2010). TGF-β and insulin signaling regulate reproductive aging via oocyte and germline quality maintenance. *Cell* 143, 299–312. doi: 10.1016/j.cell.2010.09.013

Luo, S., Shaw, W. M., Ashraf, J., and Murphy, C. T. (2009). TGF-ß Sma/Mab signaling mutations uncouple reproductive aging from somatic aging. *PLoS Genet.* 5:e1000789. doi: 10.1371/journal.pgen.1000789

Luong, L. T., Platzer, E. G., De Ley, P., Thomas, W. K., Luong, L. T., Platzer, E. G., et al. (1999). Morphological, molecular, and biological characterization of Mehdinema alii (Nematoda: Diplogasterida) from the decorated cricket (*Gryllodes sigillatus*). *J. Parasitol.* 85, 1053–1064.

Madhu, B., Salazar, A., and Gumienny, T. (2019). *Caenorhabditis elegans* egg-laying and brood-size changes upon exposure to *Serratia marcescens* and Staphylococcus epidermidis are independent of DBL-1 signaling. *MicroPublication Biol.* 2019. doi: 10.17912/2r51-b476

Maures, T. J., Booth, L. N., Benayoun, B. A., Izrayelit, Y., Schroeder, F. C., and Brunet, A. (2014). Males shorten the life span of *C. elegans* hermaphrodites via secreted compounds. *Science* 343, 541–544. doi: 10.1126/science.1244160

McCarter, J., Bartlett, B., Dang, T., and Schedl, T. (1999). On the control of oocyte meiotic maturation and ovulation in *Caenorhabditis elegans*. *Dev. Biol.* 205, 111–128. doi: 10.1006/dbio.1998.9109

McCay, C. M., Crowell, M. F., and Maynard, L. A. (1935). The effect of retarded growth upon the length of life span and upon the ultimate body size. *Nutrition* 5, 155–171; discussion 172. doi: 10.1093/jn/10.1.63

Medawar, P. (1952). *An Unsolved Problem of Biology*. London: H. K. Lewis.

Monsivais, D., Matzuk, M. M., and Pangas, S. A. (2017). The TGF-β family in the reproductive tract. *Cold Spring Harb. Perspect. Biol.* 9:a022251. doi: 10.1101/cshperspect.a022251

Morsci, N. S., Haas, L. A., and Barr, M. M. (2011). Sperm status regulates sexual attraction in *Caenorhabditis elegans*. *Genetics* 189, 1341–1346. doi: 10.1534/genetics.111.133603

Murphy, C. T., and Hu, P. J. (2013). Insulin/insulin-like growth factor signaling in *C. elegans*. *WormBook* 1–43. doi: 10.1895/wormbook.1.164.1 PMID: 24395814

Nagaoka, S. I., Hassold, T. J., and Hunt, P. A. (2012). Human aneuploidy: mechanisms and new insights into an age-old problem. *Nat. Rev. Genet.* 13, 493–504. doi: 10.1038/nrg3245

Narbonne, P., Maddox, P. S., and Labbé, J. C. (2015). DAF-18/PTEN locally antagonizes insulin signalling to couple germline stem cell proliferation to oocyte needs in *C. elegans*. *Development* 142, 4230–4241. doi: 10.1242/dev.130252

Ng, L. T., Ng, L. F., Tang, R. M. Y., Barardo, D., Halliwell, B., Moore, P. K., et al. (2020). Lifespan and healthspan benefits of exogenous H2S in *C. elegans* are independent from effects downstream of eat-2 mutation. *NPJ Aging Mech. Dis.* 6:6. doi: 10.1038/s41514-020-0044-8

Nussey, D. H., Froy, H., Lemaitre, J. F., Gaillard, J. M., and Austad, S. N. (2013). Senescence in natural populations of animals: widespread evidence and its implications for bio-gerontology. *Ageing Res. Rev.* 12, 214–225. doi: 10.1016/j.arr.2012.07.004

Onken, B., and Driscoll, M. (2010). Metformin Induces a dietary restriction-like state and the oxidative stress response to extend *C. elegans* healthspan via AMPK, LKB1, and SKN-1. *PLoS One* 5:e8758. doi: 10.1371/journal.pone.0008758

Panowski, S. H., Wolff, S., Aguilaniu, H., Durieux, J., and Dillin, A. (2007). PHA-4/Foxa mediates diet-restriction-induced longevity of *C. elegans*. *Nature* 447, 550–555. doi: 10.1038/nature05837

Pazdernik, N., and Schedl, T. (2013). "Introduction to germ cell development in *Caenorhabditis elegans*," in *Germ Cell Development in C. elegans, Advances in Experimental Medicine and Biology*, ed. T. Schedl (New York, NY: Springer), doi: 10.1007/978-1-4614-4015-4

Perez, M. F., Francesconi, M., Hidalgo-Carcedo, C., and Lehner, B. (2017). Maternal age generates phenotypic variation in *Caenorhabditis elegans*. *Nature* 552, 106–109. doi: 10.1038/nature25012

Pickett, C. L., and Kornfeld, K. (2013). Age-related degeneration of the egg-laying system promotes matricidal hatching in *Caenorhabditis elegans*. *Aging Cell* 12, 544–553. doi: 10.1111/acel.12079

Pickett, C. L., Dietrich, N., Chen, J., Xiong, C., and Kornfeld, K. (2013). Mated progeny production is a biomarker of aging in caenorhabditis elegans. *G3* 3, 2219–2232. doi: 10.1534/g3.113.008664

Poupet, C., Chassard, C., Nivoliez, A., and Bornes, S. (2020). *Caenorhabditis elegans*, a host to investigate the probiotic properties of beneficial microorganisms. *Front. Nutr.* 7:135. doi: 10.3389/fnut.2020.00135

Qin, Z., and Hubbard, E. J. A. (2015). Non-autonomous DAF-16/FOXO activity antagonizes age-related loss of *C. elegans* germline stem/progenitor cells. *Nat. Commun.* 6:7107. doi: 10.1038/ncomms8107

Quesada-Candela, C., Loose, J., Ghazi, A., and Yanowitz, J. L. (2021). Molecular basis of reproductive senescence: insights from model organisms. *J. Assist. Reprod. Genet.* 38, 17–32.

Rathor, L., Akhlaq, A. B., Pandey, S., Srivastava, S., and Pandey, R. (2015). Folic acid supplementation at lower doses increases oxidative stress resistance and longevity in *Caenorhabditis elegans*. *Age (Dordr.)* 37:113. doi: 10.1007/s11357-015-9850-5

Rose, A. M., and Baillie, D. L. (1979). The effect of temperature and parental age on recombination and nondisjunction in *Caenorhabditis elegans*. *Genetics* 92, 409–418. doi: 10.1093/genetics/92.2.409

Savage-Dunn, C. (2005). TGF-β signaling. *WormBook* 9, 1–12. doi: 10.1895/wormbook.1.22.1

Scarpello, J. H. B. (2003). Improving survival with metformin: the evidence base today. *Diabet. Metab.* 29, S36–S36. doi: 10.1016/s1262-3636(03)72786-4

Scharf, A., Gührs, K. H., and Von Mikecz, A. (2016). Anti-amyloid compounds protect from silica nanoparticle-induced neurotoxicity in the nematode *C. elegans*. *Nanotoxicology* 10, 426–435. doi: 10.3109/17435390.2015.1073399

Schisa, J. A., Pitt, J. N., and Priess, J. R. (2001). Analysis of RNA associated with P granules in germ cells of *C. elegans* adults. *Development* 128, 1287–1298.

Shaw, W. M., Luo, S., Landis, J., Ashraf, J., and Murphy, C. T. (2007). The *C. elegans* TGF-β dauer pathway regulates longevity via insulin signaling. *Curr. Biol.* 17, 1635–1645. doi: 10.1016/j.cub.2007.08.058

Shi, C., and Murphy, C. T. (2014). Mating induces shrinking and death in *Caenorhabditis* mothers. *Science* 343, 536–540. doi: 10.1126/science.1242958

Shi, C., Booth, L. N., and Murphy, C. T. (2019). Insulin-like peptides and the mTOR-TFEB pathway protect *Caenorhabditis elegans* hermaphrodites from mating-induced death. *eLife* 8:e46413. doi: 10.7554/eLife.46413

Shi, C., Runnels, A. M., and Murphy, C. T. (2017). Mating and male pheromone kill *Caenorhabditis* males through distinct mechanisms. *eLife* 6:e23493. doi: 10.7554/eLife.23493

Shin, H., Haupt, K. A., Kershner, A. M., Kroll-Conner, P., Wickens, M., and Kimble, J. (2017). SYGL-1 and LST-1 link niche signaling to PUF RNA repression for stem cell maintenance in *Caenorhabditis elegans*. *PLoS Genet.* 13:e1007121. doi: 10.1371/journal.pgen.1007121

Sowa, J. N., Mutlu, A. S., Xia, F., and Wang, M. C. (2015). Olfaction modulates reproductive plasticity through neuroendocrine signaling in *Caenorhabditis elegans*. *Curr. Biol.* 25, 2284–2289. doi: 10.1016/j.cub.2015.07.023

Stuhr, N. L., and Curran, S. P. (2020). Bacterial diets differentially alter lifespan and healthspan trajectories in *C. elegans*. *Commun. Biol.* 3:653. doi: 10.1038/s42003-020-01379-1

Szewczyk, N. J., Udranszky, I. A., Kozak, E., Sunga, J., Kim, S. K., Jacobson, L. A., et al. (2006). Delayed development and lifespan extension as features of metabolic lifestyle alteration in *C. elegans* under dietary restriction. *J. Exp. Biol.* 209, 4129–4139. doi: 10.1242/jeb.02492

Tanis, J. E., Bellemer, A., Moresco, J. J., Forbush, B., and Koelle, M. R. (2009). The potassium chloride cotransporter KCC-2 coordinates development of inhibitory neurotransmission and synapse structure in *Caenorhabditis elegans*. *J. Neurosci.* 29, 9943–9954. doi: 10.1523/JNEUROSCI.1989-09.2009

Templeman, N. M., Cota, V., Keyes, W., Kaletsky, R., and Murphy, C. T. (2020). CREB Non-autonomously controls reproductive aging through hedgehog/patched signaling. *Dev. Cell* 54, 92–105.e5. doi: 10.1016/j.devcel.2020.05.023

Tissenbaum, H. A. (2015). Using *C. elegans* for aging research. *Invertebr. Reprod. Dev.* 59, 59–63. doi: 10.1080/07924259.2014.940470

Tominaga, K., and Suzuki, H. I. (2019). TGF-β signaling in cellular senescence and aging-related pathology. *Int. J. Mol. Sci.* 20:5002. doi: 10.3390/ijms20205002

Trent, C., Tsuing, N., and Horvitz, H. R. (1983). Egg-laying defective mutants of the nematode *Caenorhabditis elegans*. *Genetics* 104, 619–647. doi: 10.1093/genetics/104.4.619

Van Voorhies, W. A. (1992). Production of sperm reduces nematode lifespan. *Nature* 360, 456–458. doi: 10.1038/360456a0

Vigne, P., Gimond, C., Ferrari, C., Vielle, A., Hallin, J., Pino-Querido, A., et al. (2021). A single-nucleotide change underlies the genetic assimilation of a plastic trait. *Sci. Adv.* 7:eabd9941. doi: 10.1126/sciadv.abd9941

Wang, M. C., Oakley, H. D., Carr, C. E., Sowa, J. N., and Ruvkun, G. (2014). Gene pathways that delay caenorhabditis elegans reproductive senescence. *PLoS Genet.* 10:e1004752. doi: 10.1371/journal.pgen.1004752

Ward, S., and Carrel, J. S. (1979). Fertilization and sperm competition in the nematode *Caenorhabditis elegans*. *Dev. Biol.* 73, 304–321. doi: 10.1016/0012-1606(79)90069-1

Williams, G. C. (1957). Pleiotropy, natural selection, and the evolution of senescence. *Evolution* 11, 398–411.

Zuckerman, B. M., and Geist, M. A. (1983). Effects of vitamin E on the nematode *Caenorhabditis elegans*. *Age* 6, 1–4. doi: 10.1007/BF02431837

Conflict of Interest: The authors declare that the research was conducted in the absence of any commercial or financial relationships that could be construed as a potential conflict of interest.

Publisher's Note: All claims expressed in this article are solely those of the authors and do not necessarily represent those of their affiliated organizations, or those of the publisher, the editors and the reviewers. Any product that may be evaluated in this article, or claim that may be made by its manufacturer, is not guaranteed or endorsed by the publisher.

frontiers in Cell and Developmental Biology

REVIEW
published: 03 November 2021
doi: 10.3389/fcell.2021.710186

The Dynamic Regulation of mRNA Translation and Ribosome Biogenesis During Germ Cell Development and Reproductive Aging

*Marianne Mercer, Seoyeon Jang, Chunyang Ni and Michael Buszczak**

Department of Molecular Biology, The University of Texas Southwestern Medical Center, Dallas, TX, United States

OPEN ACCESS

Edited by:
Miguel Angel Brieño-Enriquez, Magee-Womens Research Institute & Foundation, United States

Reviewed by:
Andrej Susor, Institute of Animal Physiology and Genetics, Academy of Sciences of the Czech Republic (ASCR), Czechia
Prashanth Rangan, University at Albany, United States
Elizabeth Snyder, Rutgers, The State University of New Jersey, United States

***Correspondence:**
Michael Buszczak
michael.buszczak@utsouthwestern.edu

Specialty section:
This article was submitted to Cellular Biochemistry, a section of the journal Frontiers in Cell and Developmental Biology

Received: *15 May 2021*
Accepted: *07 October 2021*
Published: *03 November 2021*

Citation:
Mercer M, Jang S, Ni C and Buszczak M (2021) The Dynamic Regulation of mRNA Translation and Ribosome Biogenesis During Germ Cell Development and Reproductive Aging. Front. Cell Dev. Biol. 9:710186. doi: 10.3389/fcell.2021.710186

The regulation of mRNA translation, both globally and at the level of individual transcripts, plays a central role in the development and function of germ cells across species. Genetic studies using flies, worms, zebrafish and mice have highlighted the importance of specific RNA binding proteins in driving various aspects of germ cell formation and function. Many of these mRNA binding proteins, including Pumilio, Nanos, Vasa and Dazl have been conserved through evolution, specifically mark germ cells, and carry out similar functions across species. These proteins typically influence mRNA translation by binding to specific elements within the 3′ untranslated region (UTR) of target messages. Emerging evidence indicates that the global regulation of mRNA translation also plays an important role in germ cell development. For example, ribosome biogenesis is often regulated in a stage specific manner during gametogenesis. Moreover, oocytes need to produce and store a sufficient number of ribosomes to support the development of the early embryo until the initiation of zygotic transcription. Accumulating evidence indicates that disruption of mRNA translation regulatory mechanisms likely contributes to infertility and reproductive aging in humans. These findings highlight the importance of gaining further insights into the mechanisms that control mRNA translation within germ cells. Future work in this area will likely have important impacts beyond germ cell biology.

Keywords: mRNA translation, ribosome, germline, aging, development, ribosome biogenesis

INTRODUCTION

Germ cells are essential for the propagation of multicellular species and share many features that have long fascinated biologists. They undergo extensive epigenetic reprogramming back to a state that supports totipotency in the fertilized zygote, they are exceptionally good at repairing DNA damage, they are the only cells in our bodies that undergo meiosis, and they protect against the invasion and proliferation of transposable elements. Germ cells also spend portions of their life in a transcriptionally quiescent state, necessitating the use of translation-based mechanisms to achieve changes in their gene expression programs. Indeed, genetic studies in *Drosophila*, *Caenorhabditis elegans*, zebrafish, and mice have demonstrated that stage-specific regulation of mRNA translation,

both at the level of individual transcripts and on a global scale, plays a central role in the formation, differentiation, and function of germ cells across species. This review will be divided into two main sections. The first will focus on how RNA binding proteins influence the translation of key regulators of germ cell formation and female germ cell differentiation. Many of these RNA binding proteins bind to elements within the 3′UTR of target transcripts and directly or indirectly interfere with cap dependent translation initiation. Through the course of this first section, we will also touch upon emerging models of *in trans* regulation between mRNAs and how condensate formation may influence translation of individual transcripts. The second section will be devoted to discussing how ribosome biogenesis, ribosomal protein paralogs, global regulation of translation, and ribosome storage impact germ cell function. The dynamic regulation of ribosome biogenesis and global protein synthesis represents a relatively new and underexplored theme in the context of germ cell development. As such, we will highlight key questions that remain in this area.

RNA BINDING PROTEINS AND THE REGULATED TRANSLATION OF mRNAs DURING GERM CELL FORMATION

Genetic studies in a variety of model systems (**Figure 1**) have led the way in establishing our current understanding of how RNA binding proteins and the regulated translation of individual mRNAs drive various aspects of germ cell development and early embryogenesis. Many of these proteins, including Nanos, Pumilio, Vasa, and Dazl, have long served as useful markers of germ cell identity across different species (Lesch and Page, 2012) (**Table 1**). These proteins play central roles in establishing germ cell identity, regulating germ cell differentiation, preparing germ cells for entry into meiosis and controlling other aspects of germ cell function. In the interest of space, we will primarily focus on how the regulated translation of individual mRNAs controls the specification and differentiation of *Drosophila* female germ cells. Importantly, many excellent recent reviews describe important findings from other model systems (Voronina et al., 2011; Lai and King, 2013; Susor et al., 2016; Jamieson-Lucy and Mullins, 2019; Huggins and Keiper, 2020). We will touch upon commonalities in the regulation of translation between these different species.

Germ Plasm Formation in *Drosophila*

Characterization of *Drosophila* germ cell formation has served as a useful platform for understanding how the regulation of mRNA translation initiation (**Figure 2**) impacts cell fate decisions [reviewed in Lehmann (2016)]. While we have gained substantial knowledge regarding many of the RNA binding proteins involved in controlling germ cell specification and development, several important questions remain: how do different regulatory mechanisms coordinate with one another, how is the translation of specific messages turned on and off in a temporally specific manner, and to what extent does condensate formation and phase transitions allow for the translation of specific messages to be toggled back and forth between an active and repressed state? Reviewing the current knowledge will provide context for discussing these and other open questions in the field.

Early *Drosophila* embryos initially develop as a syncytium in which nuclei undergo mitotic divisions in a common cytoplasm. This cytoplasm is patterned, with RNAs and proteins localized to specific regions within the embryo. Nuclei move to the periphery of the embryo and are eventually surrounded by plasm membrane to form individual cells, through a process known as cellularization. Primordial germ cells form during cellularization in the posterior pole of the embryo through uptake of specialized cytoplasm referred to as germ plasm (**Figure 1**). Germ plasm formation depends on Oskar protein, which contains two RNA-binding domains: the OSK RNA-binding domain and the OST-HTH/LOTUS domain (Markussen et al., 1995; Rongo et al., 1995; Lehmann, 2016). Oskar mRNA and protein are first localized to the posterior pole of the oocyte during oogenesis. To begin to understand the mechanisms that control *Drosophila* germ plasm formation, we must first consider the process of oogenesis.

Drosophila ovaries are composed of tube-like structures called ovarioles, which house sequentially developing egg chambers (**Figure 1**). Each developing egg chamber contains 16 interconnected germ cells (15 nurse cells and 1 oocyte), surrounded by a layer of somatically derived follicle cells (Spradling, 1993). During most of oogenesis, the oocyte is transcriptionally quiescent. The synthesis of RNAs and many proteins occurs in the nurse cells and these molecules are then actively transported to the oocyte, often in a microtubule dependent manner. The transport of *oskar* mRNA from nurse cells to the oocyte, and its repression during this transport, depends on several proteins including Staufen, components of the Exon Junction Complex and Bruno (Kim-Ha et al., 1991; St Johnston et al., 1991; Hachet and Ephrussi, 2004). Importantly, the translation of *oskar* mRNA is repressed until it localizes to the posterior pole in the oocyte, and then only at a developmentally appropriate time. This repression depends on the mRNA binding protein Bruno. Sequencing the *Drosophila* genome revealed 3 Bruno paralogs: Bruno1, 2, and 3. Bruno1 binds to Bruno Response elements (BREs) within the 3′UTR of *oskar* mRNA through its RNA recognition motifs (Snee et al., 2008). BREs and other regulatory elements cluster within two regions at opposite ends of the *oskar* 3′UTR: the AB region and the C region (Reveal et al., 2010). All three participate in the translational repression of *oskar* mRNA and region C has an additional role in promoting *oskar* translation once the mRNA reaches the posterior pole of the oocyte. Bruno binding to these regions serves to recruit a second protein, Cup (Nakamura et al., 2004) (**Figure 3**). Cup was originally characterized based on its female sterile phenotype and regulation of nurse cell chromosome morphology (Keyes and Spradling, 1997). Cup resides in the cytoplasm (Keyes and Spradling, 1997), and a collection of studies found that this protein plays an important role in regulating the translation of key transcripts during oogenesis (Verrotti and Wharton, 2000; Wilhelm et al., 2003, 2005; Macdonald, 2004; Nakamura et al., 2004; Nelson et al., 2004; Zappavigna et al., 2004; Piccioni et al., 2005, 2009; Chekulaeva et al., 2006; Clouse et al., 2008; Igreja and Izaurralde, 2011; Wong and Schedl, 2011; Kinkelin et al., 2012; Gotze et al., 2017). Cup contains a

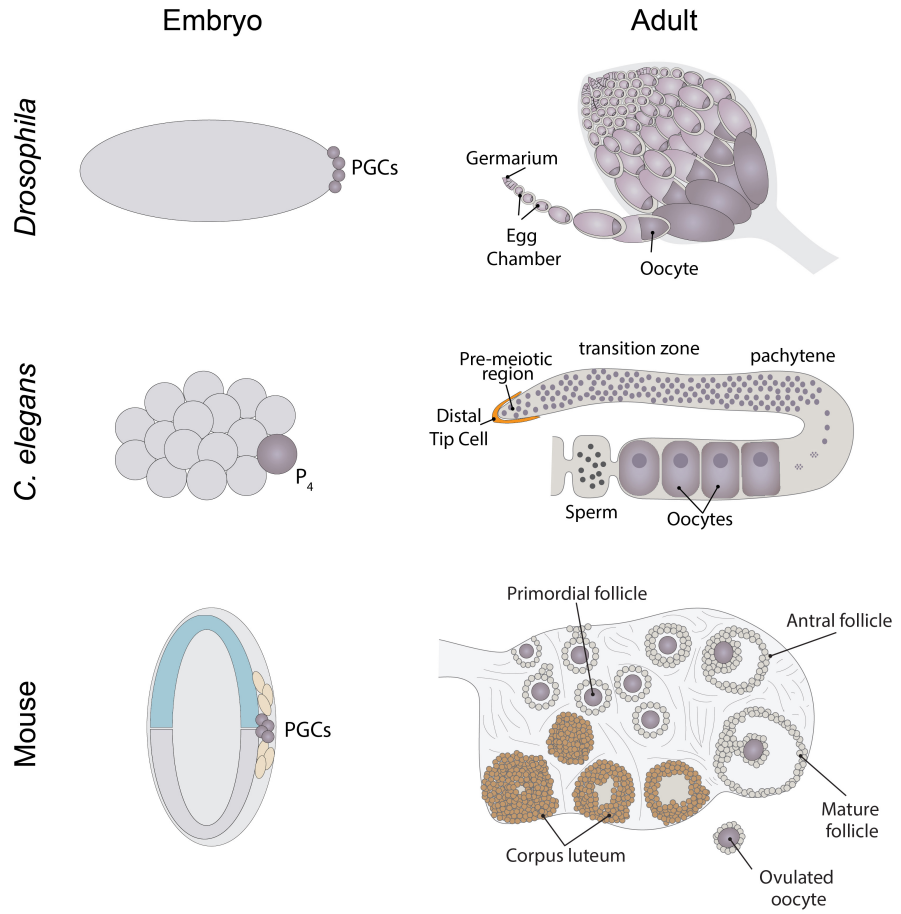

FIGURE 1 | Schematics of where *Drosophila*, *Caenorhabditis elegans*, and mouse PGCs originate from and adult ovary structures.

TABLE 1 | Germ cell enriched genes across species.

	Caenorhabditis elegans	***Drosophila***	**Zebrafish**	**Mammals**	**Function**
Vasa	GLH-1, GLH-2, GLH-3, GLH-4	Vasa	DDX4	DDX4	RNA helicase; Polar granule component; Positive regulation of mRNA translation
Nanos	NOS-1, NOS-2	Nanos	NANOS-1 NANOS-2 NANOS-3	NANOS-1 NANOS-2 NANOS-3	Zinc finger RNA binding protein; Negative regulation of mRNA translation
Pumilio	FBF-1, FBF-2, PUF-3, PUF-5, PUF-6, PUF-7, PUF-9, PUF-11	Pumilio	PUM1, PUM2	PUM1, PUM2	RNA binding protein; Negative regulation of mRNA translation; Linked with inhibition of meiosis
Dazl	DAZ-1	Boule	DAZL	DAZ, DAZL, BOULE	RNA binding protein; Negative and positive regulation of mRNA translation; Promotes progression through meiosis

YxxxxLφ (where x is any amino acid and φ is a hydrophobic amino acid) motif found in several eIF4E binding proteins, including the translation initiation factor eIF4G (**Figure 3**). Cup binding to eIF4E associated with the 7-methylguanosine cap blocks eIF4G binding and thus prevents translation initiation (Wilhelm et al., 2003; Nakamura et al., 2004; Nelson et al., 2004; Kinkelin et al., 2012). Packaging of *oskar* mRNA into silencing particles, which prevent mRNAs from engaging with ribosomes may also contribute to the spatial and temporal regulation of *oskar* mRNA translation (Chekulaeva et al., 2006). Traditionally, Bruno and Cup are typically modeled as acting *in cis*. Intriguingly, expression of an *oskar* mRNA engineered to not produce a protein but carrying all the endogenous regulatory elements can rescue the correct regulation of *oskar* mRNAs which have had all their BREs mutated (Reveal et al., 2010). This observation suggests the possibility of additional *in*

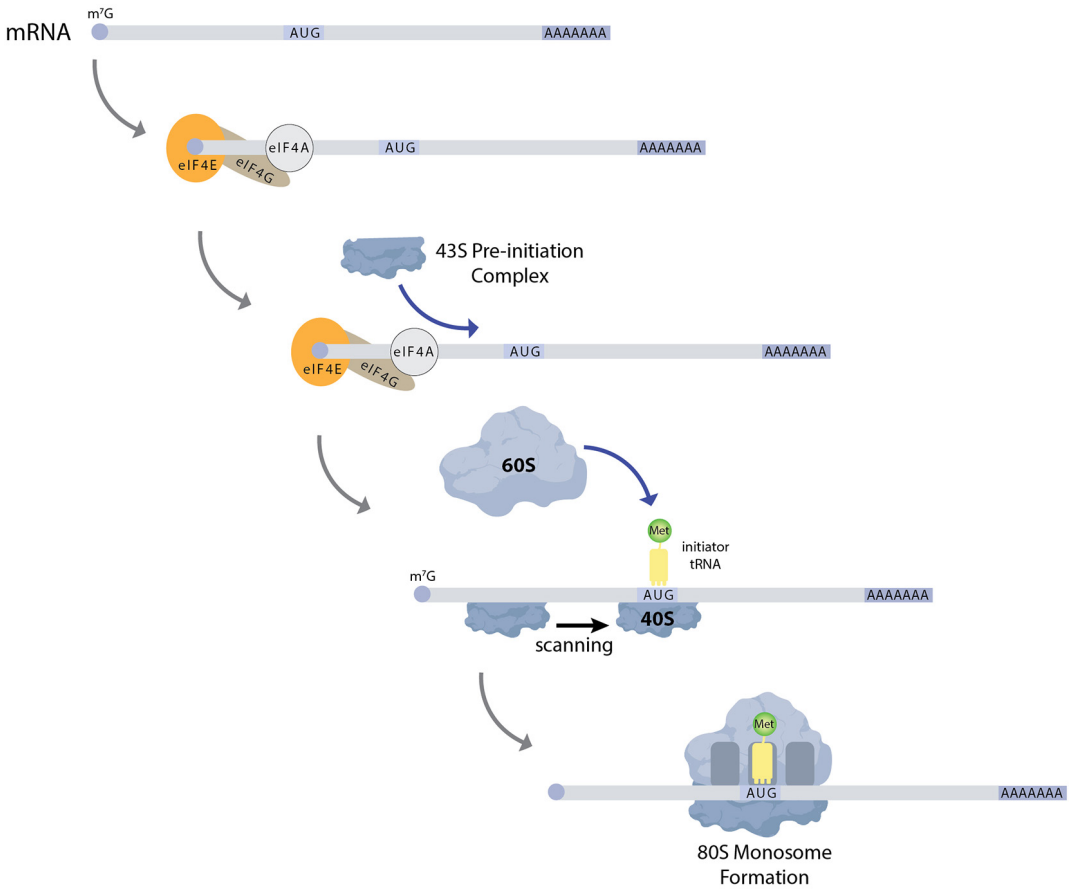

FIGURE 2 | Schematic of general translation initiation. mRNAs generally have a 7-methylguanosine cap and a poly-A tail. The cap serves to recruit the translation initiation factor eIF4E to mRNAs. eIF4E then recruits the scaffold protein eIF4G, which in turn brings the RNA helicase eIF4A to mRNA. eIF4A serves to unwind secondary structure within the 5′UTR of mRNAs, which allows for the recruitment of the 43S pre-initiation complex. This complex then scans the mRNA for a start codon, typically AUG. Next the 60S subunit is recruited to the mRNA to form a 80S monosome. Multiple ribosomes can associate with mRNAs to form polysomes.

trans regulation, whereby Bruno binding to one *oskar* transcript influences the regulation of other *oskar* transcripts. In a follow-up study, Macdonald et al. (2016) presented additional transgenic rescue experiments and molecular modeling to provide further support the model of *in trans* regulation of *oskar* mRNA regulation. Importantly, this regulation likely takes place in the context of higher order ribonucleoprotein particles (RNPs). RNPs belong to a group of structures collectively referred to as biomolecular condensates, which represent a local concentration of molecules in membrane-less foci. While liquid-liquid phase separation, defined as process by which liquid phases form to minimize free energy, underlies the formation of many condensates, this is not always the case [reviewed in Lyon et al. (2021)]. How phase separation and condensate formation contributes to the regulation of mRNA translation is an ongoing area of study. An intriguing possibility is that the in *trans* regulation of *oskar* translation reflects the association of co-regulated *oskar* mRNAs with specific condensates. In light of growing evidence that RNAs and RNA binding proteins accumulate in discrete compartments within cells, the further study of *in trans* regulation of mRNA translation and the control of condensate formation will have important implications beyond germ cell specification.

Once *oskar* mRNA localizes to the posterior pole of the oocyte, repression of its translation is relieved. The mechanisms that regulate this switch from a repressed to an active state are coming into focus. For example, over-expression of *oskar* 3′UTR promotes *oskar* translation, suggesting that repressors such as Bruno are expressed at limited levels and may be titrated away from *oskar* mRNA under the right circumstances (Smith et al., 1992; Kanke and Macdonald, 2015). In addition, several factors including the poly-A-binding proteins Orb and PABP are needed for *oskar* translation (Castagnetti and Ephrussi, 2003; Vazquez-Pianzola et al., 2011). More recent results indicate that a member of the Makorin family of proteins, which contain C3H-type zinc fingers and a RING E3 ubiquitin ligase domain, helps to regulate *oskar* translational activation (Dold et al., 2020). *Drosophila* Makorin 1(Mkrn1) has previously been linked with embryonic patterning (Liu and Lasko, 2015), and new results from the Lasko lab provide evidence that this protein promotes pole plasm formation in the oocyte (Dold et al., 2020). Mkrn1 mutants exhibit proper localization of *oskar* mRNA to

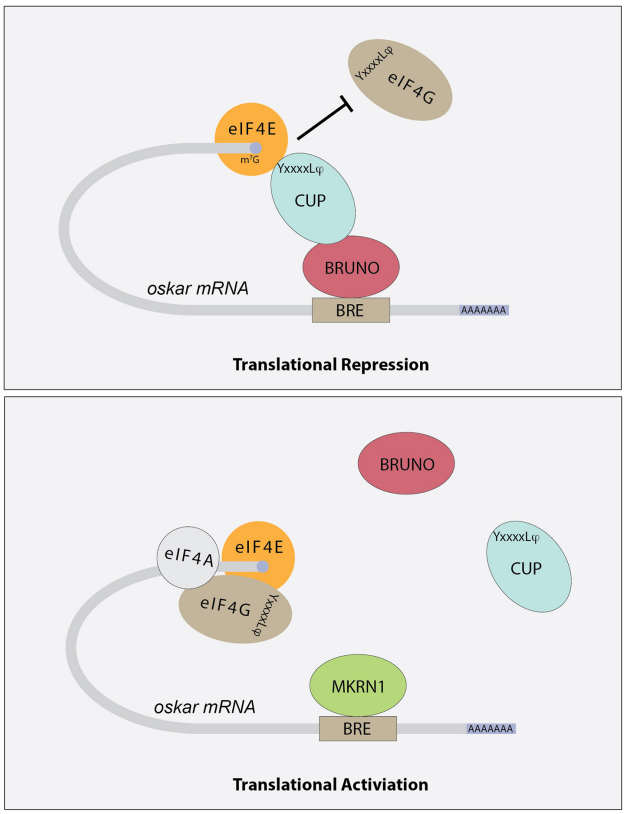

FIGURE 3 | Schematic showing how different factors contribute to the regulation of *oskar* mRNA translation. Bruno binds to Bruno Response Elements (BREs) in the 3′UTR of target mRNAs, including *oskar*. Bruno associates with Cup protein, which in turns binds to eIF4E, preventing the recruitment of eIF4G and effectively blocking translation initiation. The YxxxxLφ (where *x* is any amino acid and φ is a hydrophobic amino acid) motif is indicated. Other mRNA binding proteins, including Mkrn1, compete with Bruno for binding. Once these proteins displace Bruno and Cup, translation initiation can proceed.

the posterior pole but do not produce Oskar protein. Mkrn1 itself localizes to the pole plasm and associates with BREs within *oskar* mRNA. More Bruno1 appears to associate with *oskar* mRNA in *Mkrn1* mutants and the Oskar protein defect in *Mkrn1* mutants is partially suppressed by Bruno1 mutations. Together these data support a model whereby Mkrn1 and Bruno1 compete for binding to *oskar* mRNA (**Figure 3**). Whether the E3 ligase activity of Mrkn1 is needed to promote Oskar protein expression remains an open question. In other contexts, Mrkn1 has also been associated with ribosome-associated translation quality control of polyadenylated transcripts (Hildebrandt et al., 2019). Whether this activity impacts *oskar* translation also remains unknown.

The *oskar* gene encodes short and long protein isoforms (Markussen et al., 1995; Rongo et al., 1995), which serve to recruit a number of other RNA binding proteins to the pole plasm including Vasa (Breitwieser et al., 1996; Jeske et al., 2015). *Drosophila vasa* was originally discovered in a maternal effect lethal screen (Lasko and Ashburner, 1988). *vasa* mutants lack primordial germ cells and have disrupted posterior segments, resulting in embryonic lethality. Vasa is expressed in the germ cells of ovaries and testes, but its function is not required in the testes as male *vasa* mutants are fertile. Several excellent reviews describing Vasa function have been written (Yajima and Wessel, 2011; Lasko, 2013; Wessel, 2016; Dehghani and Lasko, 2017). Briefly, Vasa is a DEAD-box RNA helicase that marks germ cells across species. Vasa activates translation of several mRNAs including *nanos* in the pole plasm of the *Drosophila* embryo (Gavis and Lehmann, 1994). This activity appears to depend on its association with the general translation factor eIF5B (Johnstone and Lasko, 2004), which promotes recruitment of the 60S subunit and formation of 80S monosomes. Thus, Vasa is critical for the translational activation of both components of the pole plasm that help to specify PGCs within developing embryos and for proteins needed for the continued development of germ cells. Beyond regulating translation, Vasa also has additional functions including interacting with components of small RNA surveillance pathways (Xiol et al., 2014).

The Regulation of *Drosophila* Germ Cell Differentiation by mRNA Translation Based Mechanisms

In addition to germ cell formation, translation regulators are necessary for *Drosophila* germline stem cell (GSC) maintenance and differentiation [reviewed in Slaidina and Lehmann (2014)] (**Figure 4**). For example, in GSCs, Nanos and Pumilio repress the translation of transcripts that promote differentiation. Nanos belongs to a super family of proteins defined by tandem CCHC zinc fingers (Irish et al., 1989; Wang and Lehmann, 1991; Curtis et al., 1995; Kugler and Lasko, 2009). These zinc fingers interact with RNA. Pumilio is another highly conserved RNA binding protein and is a founding member of the PUF protein family, named for *Drosophila* Pumilio and *C. elegans* fem-3 binding factor (FBF) (Barker et al., 1992; Zamore et al., 1997; Forbes and Lehmann, 1998). Pumilio proteins act to repress mRNA translation and promote the degradation of transcripts. Nanos and Pumilio work together to repress transcripts necessary for differentiation, including *mei-P26* and *brat* (Harris et al., 2011; Joly et al., 2013). It is interesting that while Nanos and Pumilio repress *brat* translation in GSCs, Brat aids Nanos and Pumilio in repressing *hunchback* mRNA in the *Drosophila* embryo (Loedige et al., 2014). These translation repression networks are complex and likely involve many different cofactors. While *mei-P26* and *brat* are known targets, many targets of Nanos and Pumilio have yet to be identified. Target mRNAs of Nanos typically contain Nanos response elements (NREs), which represent the minimal sequence necessary for Nanos mediated repression. Each NRE contains a Pumilio response element (PRE) and is necessary for Nanos and Pumilio to interact (Sonoda and Wharton, 1999). Nanos binds to the three bases upstream of the PRE and acts a clamp, stabilizing the interaction of Pumilio with less favorable PREs (Weidmann et al., 2016). The Nanos N terminus recruits and directly interacts with the CCR4-NOT complex to promote the deadenylation of mRNAs. Target mRNAs are decapped in a deadenylation dependent manner. Nanos can also repress the translation of mRNAs independent of

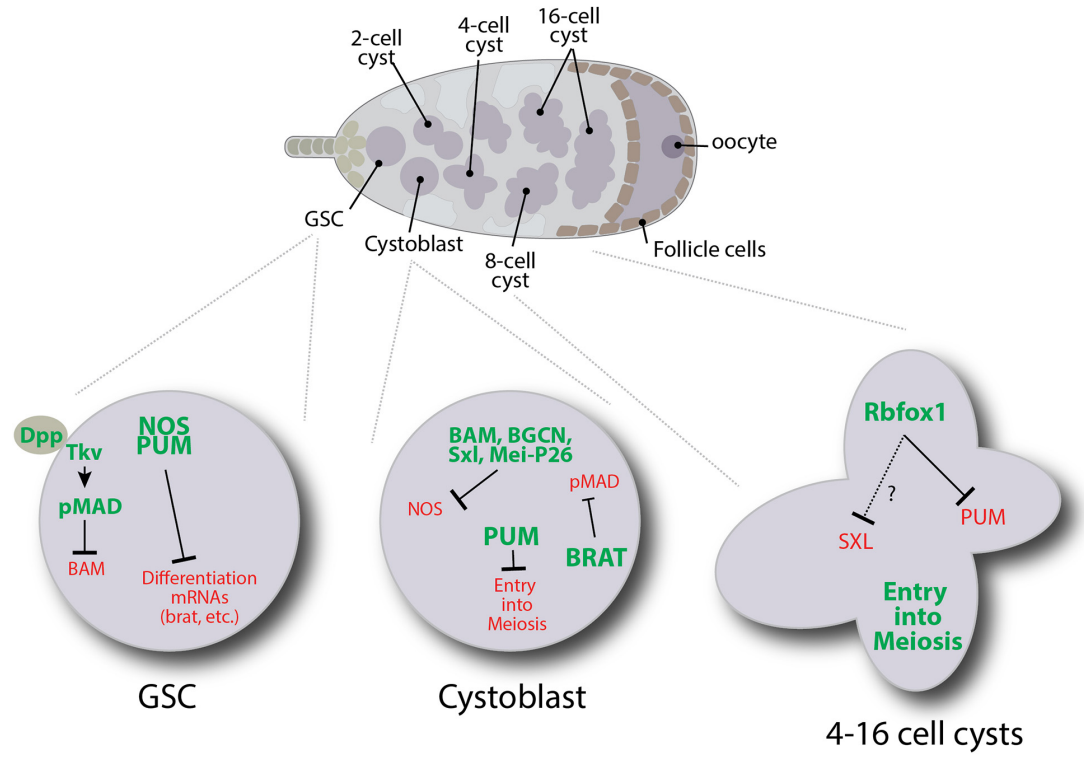

FIGURE 4 | Schematic illustrating some of the translation regulatory pathways that control specific events during the early stages of *Drosophila* female germ cell development.

deadenylation, decapping and degradation (Raisch et al., 2016), but the molecular mechanisms that underlie this activity remain uncharacterized.

When GSCs divide, they produce GSCs and cystoblast daughter cells. In GSCs, transcription of the differentiation factor *bam* is repressed by the BMP signaling pathway (Chen and McKearin, 2003a,b; Song et al., 2004; Chen and McKearin, 2005). Any GSC daughter displaced out of the niche no longer receives BMP signals resulting in *bam* expression. Bam is both necessary and sufficient for *Drosophila* germ cell differentiation (McKearin and Spradling, 1990; Ohlstein and McKearin, 1997). Bam works together with Bgcn, Mei-P26 and Sxl to target *nanos* mRNA for repression through a 3′UTR-dependent mechanism (Li et al., 2009). Bam, Bgcn, Mei-P26, and Sxl physically interact, and both Mei-P26 and Sxl interact with *nanos* mRNA (Chau et al., 2012; Li et al., 2012, 2013). Deleting the one Sxl binding site within the 3′UTR of *nanos* prevents its repression (Chau et al., 2012). Yet Sxl alone is not sufficient to repress *nanos* translation as both Sxl and Nanos are expressed in GSCs. In other contexts, Sxl represses translation by interacting with the corepressor Unr, which interacts with PABP to prevent the recruitment of ribosomal preinitiation complexes to 5′UTRs [reviewed in Moschall et al. (2017)]. *nanos* mRNA does not have a clear Unr binding site, suggesting that an alternative mechanism may be at play. Along these lines, Bam appears to recruit the CCR4-NOT complex to promote the decapping and deadenylation of *nanos* and other target mRNAs (Sgromo et al., 2018). Further work will be needed to fully understand the specific roles of Sxl, Bgcn, and Mei-P26 in regulating the decay of target messages.

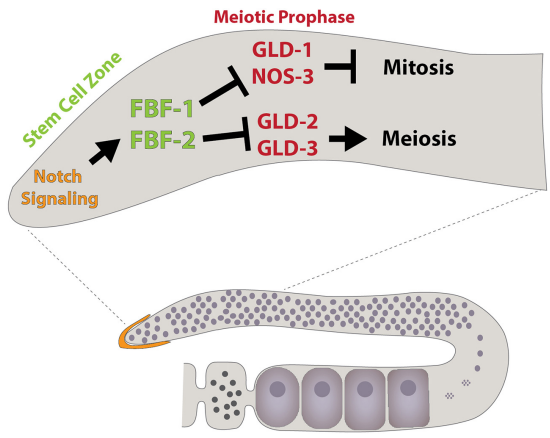

FIGURE 5 | Schematic illustrating some components that regulate *C. elegans* germline development, including the Puf family members FBF-1 and FBF-2. Modeled after Ellenbecker et al. (2019).

Unlike Nanos, Pumilio exhibits expression in cystoblasts and two-cell cysts. Pumilio has been shown to form a tertiary complex with Bam and Bgcn through its N terminal domain

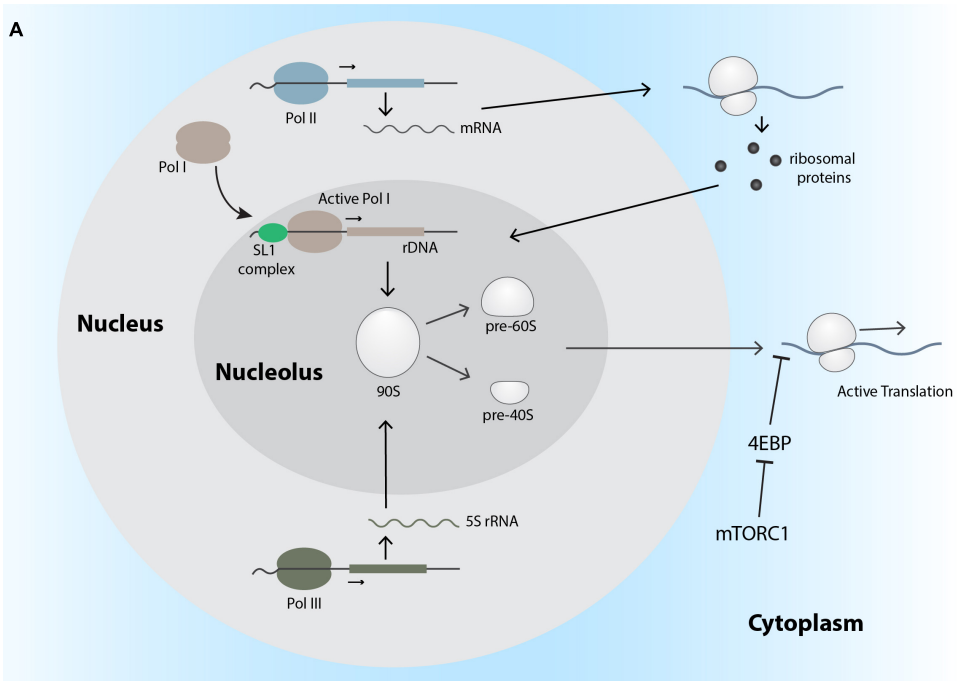

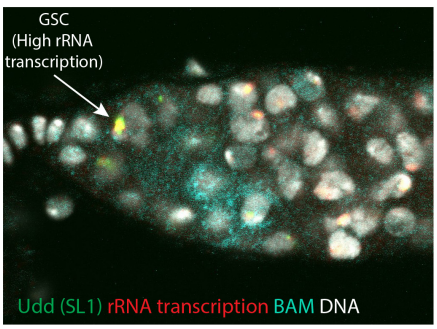

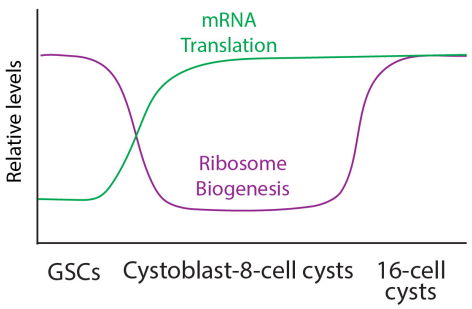

FIGURE 6 | Stage specific regulation of rRNA transcription, ribosome biogenesis, and global protein translation. **(A)** Schematic describing the process of ribosome biogenesis. **(B)** A wildtype *Drosophila* germarium pulse-labeled with Br-UTP to mark nascent rRNA (red) and stained for Udd (green), Bam (cyan), and DNA (gray). The arrow points to a GSC with relatively high rRNA transcription and Udd levels. **(C)** A graph showing the relative levels of ribosome biogenesis and mRNA translation based on published work.

(Kim et al., 2010). Pumilio also interacts with Brat to repress *mad*, *dMyc*, and components of the BMP signaling pathway (Harris et al., 2011). In addition, Brat associates with Mei-P26 and Ago1 through the NHL domain of Mei-P26 (Neumüller et al., 2008), suggesting these proteins work together to repress factors required for GSC maintenance.

Starting in 4-cell cysts, *pumilio* mRNA translation is repressed by Rbfox1. Loss of Rbfox1 and the continued expression of Pumilio result in developmental arrest (Tastan et al., 2010; Carreira-Rosario et al., 2016). Prolonged expression of Pumilio causes germ cells to dedifferentiate back into a mitotically active state. Rbfox1 belongs to a family of RNA binding proteins that regulate alternative splicing and translation (Conboy, 2017). In *Drosophila* female germ cells, cytoplasmic isoforms of Rbfox1 bind to (U)CGAUG elements in the 3′UTR of *pumilio* transcripts. Interestingly, Rbfox1 does not appear to promote the deadenylation of *pumilio*, and *pumilio* mRNA levels remain unchanged in *Rbfox1* mutants (Carreira-Rosario et al., 2016). The molecular mechanism by which Rbfox1 represses the translation of *pumilio* and its other targets in the germline remains unclear. However, Rbfox1 protein has two intrinsically disordered regions (IDRs) which typically mediate low valency interactions that can promote phase separation (Uversky et al., 2015). Moreover, Rbfox1 colocalizes with several RNP granules suggesting it may promote the sequestration of mRNAs away from translation initiation factors and ribosomes (Kucherenko and Shcherbata, 2018). All together, these various studies indicate that translational regulation represents the major

mechanism for regulating gene expression in the *Drosophila* adult female germline. Many RNA binding proteins involved in controlling germ cell differentiation have different binding partners at different stages, adding to the complexity of the regulatory networks. Additional work is needed to understand these networks more fully.

The Function of *C. elegans* Vasa, Nanos, and Pumilio Homologs

Like *Drosophila*, germ cell formation in *C. elegans* also occurs through a preformation mechanism [reviewed in Wang and Seydoux (2013)]. mRNA-protein complexes called P granules, which are analogous to *Drosophila* germ granules, are distributed throughout the cytoplasm of the one cell embryo (P_0). The P-granules segregate into cells of the P lineage during the next four divisions. The P_4 cell then divides to give rise to the germline founder cells called Z2 and Z3, which give rise to the adult germline. P granules continue to be protected from degradation in Z2 and Z3 during subsequent development through to adulthood. Eventually these cells give rise to the adult germline.

C. elegans adults can exist as either hermaphrodites or males. The gonad of hermaphrodites has long served as a powerful model for identifying and characterizing factors needed for germline maintenance and function. *C. elegans* adults contain two symmetric U-shaped gonads, which house the germline (**Figure 1**). Most of the germline exists as a syncytium. Notch signaling from the distal tip cell keeps germline cells in an undifferentiated and proliferative state. As these cells move away from the distal tip, they begin to differentiate and enter meiosis.

Much attention has been given to the characterization of P granules within the *C. elegans* embryonic and adult germline (Wang and Seydoux, 2014). The majority of the protein components of P granules are RNA binding proteins including the Vasa homologs GLH-1, GLH-2, GLH-3, and GLH-4, the P granule assembly factors PGL-1, PGL-2 and PGL-3, and OMA-1 and OMA-2. GLH-1 and GLH-4 function to promote the perinuclear localization of P granules. P granules do not appear to be needed for germ cell specification, but proteins that localize to these structures are needed for fertility. Interestingly, compromising multiple P granule nucleation factors along with GLH-1 and GLH-4 results in the ectopic expression of somatic-specific genes, including factors normally associated with neurons and muscle, within the germline (Updike et al., 2014; Knutson et al., 2017). Recent work has begun to characterize the biophysical properties of P granules (Forman-Kay et al., 2018; Seydoux, 2018; Cable et al., 2019; Lee and Seydoux, 2019; Ouyang et al., 2019; Putnam et al., 2019; Lee et al., 2020; Putnam and Seydoux, 2021). These structures likely represent privileged environments in which resident mRNAs are shielded from engaging with the translation machinery. For example, protein-RNA tethering assays reveal that the translation of reporter mRNAs is repressed upon recruitment to P granules (Aoki et al., 2021). In addition, recent detailed genetic characterization of GLH-1 suggests that Vasa homologs likely serve as "solvents," which play a variety of important roles within germ cells including promoting the activity of small RNA surveillance pathways and enabling the trafficking of mRNAs out of P granules (Marnik and Updike, 2019; Marnik et al., 2019).

The worm genome also encodes 10 Pumilio-like proteins including FBF-1, FBF-2, PUF-8, and PUF-11 [reviewed in Wang and Voronina (2020)]. Half of these genes exhibit enriched expression in germ cells and promote the maintenance of the germline. Initial characterization of FBF-1 and FBF-2 revealed these proteins promote mitotic germline stem cell proliferation (**Figure 5**). Within this context, both proteins repress the expression of *gld-1*, which drives the commitment to the meiotic cell cycle (Crittenden et al., 2002). Subsequent studies showed the FBF-1 and FBF-2 also repress the expression of multiple components of the synaptonemal complex, the formation of which is a critical step in meiosis and germline differentiation, through a 3′UTR dependent mechanism (Merritt and Seydoux, 2010). The binding of FBF-1 and FBF-2, along with other family members, typically regulate gene expression by deadenylating target mRNAs, resulting in translational repression or RNA decay. In addition, other studies hint at the possibility that worm and mammalian PUF proteins can coordinate with Argonaute miRNA-binding proteins and inhibit translation elongation (Friend et al., 2012).

While earlier work provides evidence that FBF-1 and FBF-2 exhibit functional redundancy (Crittenden et al., 2002; Lamont et al., 2004; Bernstein et al., 2005; Merritt and Seydoux, 2010), significant differences in their mutant phenotypes and subcellular localization have remained poorly understood. Recent papers have begun to resolve this conundrum. FBF-1 appears to restrict the rate at which germline cells enter meiosis, whereas FBF-2 promotes both cell proliferation and entry into meiosis (Wang et al., 2020). Both proteins directly target a common set of mRNAs, including the *Cyclin B* homolog *cyb-2.1*. Mutating FBF binding sites within *cyb-2.1* mRNA and additional loss-of-function experiments provide evidence that the germline coordinates regulation of the cell cycle and meiotic entry through the differential activity of FBF-1 and FBF-2 on specific sets of target genes. Moreover, FBF-1 requires the CCR4-NOT deadenylase complex, while FBF-2 appears to protect messages from deadenylation. These different activities are mediated by regions of the protein outside of the RNA-binding domain.

Additional PUF domain proteins may also contribute to the regulation of the cell cycle and entry into meiosis. Disruption of signaling between the distal tip cell and the germline results in a more severe germline stem cell phenotype than the combined loss of *fbf-1* and *fbf-2* (Austin and Kimble, 1987; Crittenden et al., 2002; Merritt and Seydoux, 2010; Kershner et al., 2014; Shin et al., 2017). Two additional PUF domain proteins, PUF-3 and PUF-11, which play a role in regulating germline maintenance and differentiation have been identified. Genetic analysis reveals that the phenotype of quadruple *fbf-1, fbf-2, puf-3,* and *puf-11* mutants is strikingly similar to glp-1/Notch mutants, revealing new aspects of the complex regulatory PUF protein networks that control germline behavior (Haupt et al., 2020). Further work will be needed to fully delineate how these four *C. elegans* RNA binding proteins coordinate with one another to achieve a balance between germline stem cell divisions and differentiation.

Caenorhabditis elegans also express three orthologs of *nanos*, and two of them, *nos-1* and *nos-2*, function in germline development (Subramaniam and Seydoux, 1999). Simultaneous loss of *nos-1* and *nos-2* causes a premature proliferation phenotype in PGCs, resulting in their eventual loss during larval development. Like *Drosophila nanos*, these worm orthologs encode cytoplasmic proteins that target mRNAs for translational silencing or degradation. Nanos-3 physically interacts with the Pumilio homolog FBF-1, and together help to control sperm-oocyte cell fate decisions during development by targeting *fem-3* for post-transcriptional silencing (Kraemer et al., 1999). Subsequent work has focused on defining additional endogenous targets mRNA targets of these three Nanos proteins. The Seydoux lab has shown that loss of *nos-1* and *nos-2* results in both the upregulation of oocyte transcripts and the inappropriate upregulation of other transcripts that are normally kept silent in PGCs (Lee et al., 2017). Interestingly, *nos-1* and *nos-2* appear to repress the expression of LIN-15B, a synMuvB class transcription factor known to antagonize transcriptional silencing. Moreover, disruption of *lin-15b* suppresses both the sterility and the observed changes in the gene expression programs of *nos-1 nos-2* double mutants.

Work in *C. elegans* has also pioneered our understanding of the relationship between translational repression and P granules. Recent work has highlighted the importance of a group of genes called *m*aternal-*e*ffect *g*erm-cell defective (MEG) in controlling P granule formation and activity (Leacock and Reinke, 2008; Kapelle and Reinke, 2011; Smith et al., 2016; Dodson and Kennedy, 2019; Ouyang et al., 2019; Putnam et al., 2019; Lee et al., 2020). For example, proteins that contain intrinsically disordered regions including MEG-2 and MEG-3, promote phase separation (Dodson and Kennedy, 2019; Ouyang et al., 2019; Putnam et al., 2019; Lee et al., 2020). Various mRNAs localize to these condensates, including *nos-2* (Lee et al., 2020). One challenge in the field has been determining whether mRNAs are first recruited to P granules for silencing or whether they accumulate to these granules as a consequence of their repression. Recent experiments examining the regulation of *nos-2* mRNA provide evidence for the latter (Lee et al., 2020). This study found that RNA localization tended to trend with translational status and that accumulation of mRNAs to P granules depended on the activity of translational repressors. Lastly, subjecting worms to heat shock, which disrupts translation initiation, results in a shift of diffusely localized transcripts to P granules (Lee et al., 2020), providing further evidence of links between translational state and localization to P granules.

Regulation of mRNA Translation by Vasa, Pumilio, and Nanos Homologs in Vertebrate Germ Cells

Multiple studies have identified clear Vasa homologs in zebrafish, *Xenopus*, mice, rats, monkeys and humans (Leroy et al., 1989; Komiya and Tanigawa, 1995; Olsen et al., 1997; Castrillon et al., 2000; Toyooka et al., 2000; Hermann et al., 2007; Mitchell et al., 2008; Encinas et al., 2012; Gassei et al., 2017). These genes have retained their enriched expression in germ cells, and continue to serve as valuable markers of germ cell fate in various contexts [reviewed in Lasko (2013)], including the generation and differentiation of primordial germ cell like cells (Saitou and Miyauchi, 2016; Tang et al., 2016; Kobayashi et al., 2017). The temporal and stage specific expression pattern of Vasa varies from species to species. For example, in mice the expression of DDX4 (the typically used name for Vasa in mammals; also known as Mvh) is first observed in germ cells after they have populated the genital ridge, while in rats DDX4 expression is detectable much earlier in migrating PGCs (Fujiwara et al., 1994; Encinas et al., 2012). In both rodents, DDX4 expression continues in post-meiotic sperm and oocytes. Interestingly, mutations in rodent *DDX4* only appear to disrupt the fertility of males but not females. DDX4 localizes to the chromatoid body, a germ cell specific perinuclear RNA granule, in developing spermatids. Similar to Vasa homologs in *Drosophila* and *C. elegans*, immunoprecipitation experiments show that DDX4 associates with a large number of potential target mRNAs. Some of these mRNAs encode for proteins that play important roles in the translational regulation within the germline, including DDX25 and eIF4B (Tsai-Morris et al., 2004; Nagamori et al., 2011; Yamaguchi et al., 2013).

Homologs of Pumilio and Nanos also contribute to formation, maintenance and development of vertebrate germ cells. Mice and humans have two clear Pumilio homologs, PUM1 and PUM2, and two divergent PUM homologs, PUM3/Puf-A and NOP9 (Goldstrohm et al., 2018). *Pum2* does not appear needed for male or female fertility, although a gene trap within the locus results in morphologically smaller testes (Xu et al., 2007). Deletion of *Pum1* in mice results in reduced male fertility, marked by increased apoptosis in germ cells (Chen et al., 2012). Loss of *Pum1* also leads to subfertility in female mice (Mak et al., 2016), and defects in the maternal phase of embryogenesis (Mak et al., 2018). Subsequent work shows that simultaneous deletion of both *Pum1* and *Pum2* results reduced body size and cell proliferation, partially through mis-regulation of *Cdkn1b* (Lin et al., 2019). Loss of both *Pum1* and *Pum2* also disrupts neurogenesis in mice (Zhang et al., 2017). Like its fly and worm counterparts, PUM1 and PUM2 bind to thousands of transcripts, with significant overlap between the two proteins, in both the testis and nervous system. Similar to other species, these PUM binding sites are enriched for the UGUA(A/C/U)AUA motif. PUM binding to mRNAs typically results in transcript destabilization and/or translational repression. For example, recent work shows that PUM1 forms highly clustered aggregates around *Mad2* and *cyclin B1* RNA granules in mouse oocytes (Takei et al., 2020). This localization correlates with translational repression of these two RNAs. In turn, the breakdown of these PUM1 aggregates correlates with the activation of *Mad2* and *Cyclin B1* translation. Importantly, stabilization of PUM1 aggregates blocks oocyte differentiation, indicating that the dissolution of these aggregates at a particular point in oocyte differentiation is important for their continued maturation.

In related findings, mammalian PUM proteins may also play important roles in the proliferation and differentiation of embryonic stem cells (Uyhazi et al., 2020). Loss of *Pum1* in ESCs results in increased expression of pluripotency genes. By

contrast, *Pum2* mutant ESCs display decreased pluripotency and accelerated differentiation. Again, the target mRNAs for both proteins show significant overlap, but within the context of ESCs, PUM1, and PUM2 appear to regulate different subsets of target mRNAs in both a positive and negative manner. In addition, PUM1 and PUM2 regulate the expression of one another, forming regulatory feedback loops.

In addition to co-regulation through 3′UTR-dependent mechanisms, mammals have evolved additional mechanisms for controlling the availability of PUM1 and PUM2. For example, recent work shows that the long non-coding RNA NORAD, which contains a series of PUM binding sites, acts to sequester PUM protein (Lee et al., 2016). Over-expression and increased availability of PUM1 and PUM2 leads to genomic instability in somatic cells, and loss of NORAD in mice results in a striking premature aging phenotype (Kopp et al., 2019). NORAD serves to titrate the amount of available PUM protein to a level that accommodates a cell's specific needs. New work provides insights into the ability of NORAD to regulate phase transitions through multivalent interactions. Importantly, the formation of NORAD dependent condensates allows for the super-stoichiometric retention of PUM proteins (Elguindy and Mendell, 2021). While *Norad* mutant mice do not appear to have any overt fertility problems, future work will be needed to more thoroughly assay how loss of this and other long non-coding RNAs impact germ cell development and reproductive aging by interacting with translation regulatory machinery. In addition, it will be interesting to test whether germ granules also promote the super-stoichiometric retention of specific mRNAs and their binding proteins.

Mammalian genomes contain three nanos orthologs: *nanos1, nanos2,* and *nanos3* (De Keuckelaere et al., 2018). *nanos1* is expressed in the nervous system and does not appear to function in germ cell development (Haraguchi et al., 2003). By contrast, NANOS2 and NANOS3 play important roles in germ cell maintenance and differentiation (Tsuda et al., 2003; Suzuki et al., 2007). NANOS3 is expressed in primordial germ cells and has served as an important marker in several studies that describe the formation and differentiation of iPS cell and embryonic stem cell derived primordial germ cell-like cells (PGCLCs) (Irie et al., 2015; Irie and Surani, 2017; Chen et al., 2019). *nanos2* is expressed in a male specific manner in spermatogonial stem cells. NANOS2 interacts with Dead end 1 (DND1), another RNA binding protein that promotes the survival of PGCs, and the CCR4-NOT deadenylation complex (Suzuki et al., 2016). Loss of *nanos2* results in reduced expression of DNMT3L, a methyltransferase that functions in establishing male specific DNA methylation patterns. Interestingly, while NANOS2 expression can rescue the germ cell defects caused by disruption of NANOS3, the reverse is not true (Tsuda et al., 2003). A recent study has shed new light on the roles of NANOS2 and NANOS3 in germ cell development (Wright et al., 2021). Double *nanos2* and *nanos3* mutants exhibit a rapid loss of germ cells. NANOS3 serves to prevent apoptosis in germ cells upon loss of *nanos2*. Further analysis shows that while NANOS2 and NANOS3 are structurally similar, the unique amino acid sequence within a zinc finger of NANOS2 is required for its specific interaction with DND1. These biochemical experiments provide a reasonable explanation for why NANOS3 expression cannot rescue *nanos2* mutant phenotypes.

Accumulating evidence shows that orthologs of *vasa, nanos,* and *pumilio* play important roles in the regulation of germ cell formation and function in humans (Jaruzelska et al., 2003; Moore et al., 2003; Lasko, 2013). For example, Pumilio-Nanos complexes function in human germ cells and mutations in *nanos3* have been linked with ovarian insufficiency (Wu et al., 2013; Santos et al., 2014). Interestingly, despite lack of *nanos1* expression in mouse germ cells, mutations in the gene have been linked with human male infertility, marked by oligo-astheno-teratozoospermia or complete germ cell loss (Kusz-Zamelczyk et al., 2013). Human PUM2 protein interacts with two other RNA binding proteins called Deleted in Azoospermia (DAZ) and DAZ-Like (DAZL) (Moore et al., 2003). Encoded by a gene on the Y-chromosome, DAZ has been linked with a number of different defects in human spermatogenesis. The expression of DAZL marks commitment to a germ cell fate and helps to regulate germ cell development and entry into meiosis in mice. A recent paper from the Conti lab provides evidence that DAZL functions to both repress and activate translation of different transcripts within maturing oocytes (Yang et al., 2020). Global analysis shows that ribosome loading onto maternal RNAs is disrupted upon depletion of DAZL. This effect is mediated, in part, through elements found within the 3′UTRs of these transcripts. DAZL directly interacts with these RNAs and phenotypes associated with DAZL loss can be rescued by injection of wildtype DAZL protein. Interestingly, the translation of several transcripts, including *Akap10*, *Cenpe*, *Nsf*, *Ywhaz,* and *Nin*, appears upregulated in the absence of DAZL. Further work shows the directionality of DAZL-dependent regulation depends on other elements found within the 3′UTRs of target mRNAs. This co-regulation was also hinted at in a previous study by the same group (Sousa Martins et al., 2016). The theme of multiple mRNA binding proteins influencing context specific regulation of translation is important across species. Further work will be needed to more fully understand how the presence of multiple factors on individual transcripts is integrated to ensure the proper regulation of translation in space and time. Whether allelic variants of DAZL impact human infertility also requires additional investigation (Rosario et al., 2016).

REGULATION OF TRANSLATION MACHINERY DURING GERM CELL DEVELOPMENT

Although previously considered as a house-keeping function, emerging evidence is now showing that protein synthesis can be heterogeneous across different cell-types and developmental stages [reviewed in Buszczak et al. (2014)]. mRNA translation depends on ribosomes, which are composed of about 80 different ribosomal proteins (RPs) and 4 rRNAs. Ribosomes are initially assembled as two distinct subunits, a small 40S subunit and a large 60S subunit within a subdomain of the nucleus called the nucleolus (Klinge and Woolford, 2019)

(**Figure 6A**). Each subunit is independently exported out of the nucleus and into the cytoplasm. Emerging evidence indicates that female germ cells may dynamically regulate ribosome biogenesis during their differentiation as they develop into fertilizable oocytes. Not only is ribosome biogenesis regulated, but specific translation initiation and elongation factors are also enriched and regulated in the germline. Much work still needs to be done to understand how ribosomes and the translation machinery work in concert during the development of the oocyte. Furthermore, oocytes store large numbers of ribosomes for use upon fertilization. Understanding this storage process and how it may deteriorate over time can give us insights into reproductive aging.

rDNA Repeat Amplification in Germ Cells

rDNA has a direct influence on the total number of ribosomes that can be generated at any point in time. rDNA is commonly organized as tandem repeats, the number of which can vary across species. For example, *Saccharomyces cerevisiae* has ∼150 copies of rDNA on chromosome XII, *Drosophila* has 200–250 repeats on the X and Y chromosomes, and humans have hundreds of rDNA copies in clusters located on multiple chromosomes. rDNA copy number can vary across different mouse strains. In addition, not all repeats are transcribed at any point in time, and we are just beginning to understand the regulatory factors that control the activity of any particular rDNA gene.

Recombination rates within rDNA loci can be relatively high compared to other regions of the genome due to their repetitive nature, leading to increases and decreases in rDNA repeat number (Nelson et al., 2019; Warmerdam and Wolthuis, 2019). rDNA instability increases with age in a range of organisms ranging from yeast to *Drosophila* and rDNA copy number can vary in cancer cells (Wang and Lemos, 2017). Any changes in rDNA repeat number within germ cells will be passed to the next generation and could have a significant impact on the viability and reproductive success of progeny. A recent study adds to the evidence that organisms have evolved mechanisms for maintaining rDNA copy number over multiple generations. Lu et al. (2018) found that aging *Drosophila* males experience a decline in rDNA copy number, which is subsequentially inherited by their offspring. Strikingly, however, germline stem cells from young flies, which initially received a reduced number of rDNA repeats, are able to recover rDNA copy number back to a level more in line with the rest of the population. Thus, it appears that germ cells can "sense" and adjust rDNA copy number, so it is maintained within a species-specific range. What sets this range across species and the mechanisms that underlie this germ cell phenomenon remain unknown, but a recent study using yeast may provide some potential hints (Iida and Kobayashi, 2019). Upstream Activating Factor (UAF) serves to drive Pol I transcription of rRNA. Reduction of rDNA repeats decreases the number of UAF binding sites, in turn leading to increased levels of "free" UAF. UAF, unbound to rDNA, moves to directly repress the histone deacetylase SIR2. SIR2 negatively regulates a number of genes which control recombination rates within the rDNA locus. Reduced expression of these factors results in rDNA amplification. Thus, the movement of UAF from rDNA to the SIR2 gene upon reduction in rDNA copy number, and back to rDNA once copy number has been restored to a level that matches the availability of UAF, represents a simple but elegant feedback loop through which cells can control repeat numbers within this locus. This model predicts that over-expression of UAF may limit viability through multiple cell divisions, as rDNA copy number decreases. Indeed, expressing UAF in yeast strains that already have reduced rDNA copy number results in cell growth defects. Further experiments will be needed to test whether similar mechanisms act within germ cells of multiple cellular organisms to set rDNA copy number within a species-specific range.

In addition to regulating chromosomal rDNA copy number, the oocytes of certain amphibians and fish exhibit the remarkable ability to amplify rDNA by producing extra-chromosomal copies of these repeats. Cytological studies of amphibian oocytes provided the first hints that oocytes may have extra copies of rDNA. Brown and Dawid (1968) extended these earlier studies and found that *Xenopus* germinal vesicles contained hundreds of cresyl violet labeled nucleoli (Brown and Dawid, 1968). Subsequent experiments using equilibrium density gradient centrifugation in CsCl and comparative hybridization between germinal vesicle and somatic cell DNA definitively showed that the oocytes of *Sedum mexicanum* and *Necturus maculosus* contained extra-chromosomal copies of rDNA. Others went on to show that extra-chromosomal rDNA can be found in the oocytes produced by a variety of organisms (Gall, 1968, 1969; Gall et al., 1969; Macgregor, 1972; Gall and Rochaix, 1974; Davidian et al., 2021). Despite their occurrence across several vertebrate species, prevailing evidence indicates that placental mammals do not amplify rDNA within their oocytes using this mechanism (Bachvarova, 1985; Tian et al., 2001).

What is the functional significance of this amplification? Oocytes are often large cells and need a high level of ribosomes to support ongoing mRNA translation over variable periods of storage in the absence of transcription (and hence in the absence of ribosome biogenesis). Many species store massive numbers of ribosomes. Cellular components stored within the oocyte need to accumulate at a sufficient level to support early embryogenesis until the onset of zygotic transcription and the restarting of the ribosome assembly process. In many species, zygotic transcription does not start until after many cell divisions. Thus, changes in gene expression during early differentiation typically occur at the level of mRNA translation. Increased rDNA levels may simply be needed to support the enhanced levels of ribosome biogenesis that occurs in the oocytes of many species. Of note, zygotic transcription in mice and human starts within 1–2 cell divisions after fertilization, perhaps obviating the need for large-scale rDNA amplification.

Knowledge regarding the formation of extra-chromosomal nucleoli comes mostly from the study of amphibian oocytes. A recent paper by Davidian et al. (2021) provides a thoughtful description of the current state of the field. Briefly, the extra synthesis of rDNA begins at the pachytene stage of meiotic prophase, through a gene amplification process. Later, as these oocytes enter the diplotene stage, the rDNA dissociates to form

a large number of extra-chromosomal nucleoli. More recent work has characterized the liquid-like properties of these extra-chromosomal nucleoli (Brangwynne et al., 2011; Feric et al., 2016). These findings have paved the way for the further characterization of the biophysical properties of nucleoli and other nuclear bodies from different cell types. Previous studies using electron microscopy suggested that extrachromosomal rDNA may form from rolling circle intermediates (Hourcade et al., 1973, 1974). But what triggers this oocyte-specific gene amplification process during meiosis and how the overall copy number is regulated remains largely unknown. In the future, genetic and biochemical approaches may begin to reveal new insights into this interesting phenomenon.

Other organisms have evolved oocyte specific rRNA genes. For example, *Xenopus* and zebrafish both have oocyte specific 5S rRNAs, the sequence of which differs from their somatic cell counterparts (Wegnez and Monier, 1972; Ford and Southern, 1973; Wakefield and Gurdon, 1983; Locati et al., 2017a). These maternal rRNAs are entirely replaced by a somatic 5S during embryonic development (Wormington and Brown, 1983). This specificity in germline and somatic rRNAs appears to extend to 45S rRNA, the pre-cursor to 5.8S, 18S and 28S rRNAs (Locati et al., 2017b). *In silico* analysis suggests the expansion segments in 18S rRNA may preferentially drive the translation of specific mRNAs in the germline and the soma. More recent experiments, focused on characterizing DNA methylation within the zebrafish germline, uncovered oocyte specific amplification of a 11.5 kb region within the genome that contains 45S rRNA (Ortega-Recalde et al., 2019). Interestingly, the demethylation and amplification of this locus correlates with the expansion of "1B" oocytes. These 1B oocytes contain multiple nucleoli and provide signals that drive the feminization of the gonad. Thus, these results suggest modification of rDNA is linked with sex determination in this species.

Stage-Specific Regulation of Ribosome Biogenesis During Germ Cell Development

In *Drosophila*, well-conserved growth regulators, such as Myc, modulate female germline growth potential (Maines et al., 2004; Neumüller et al., 2008; Rhiner et al., 2009; Harris et al., 2011). Some studies further suggest that the rate of ribosome production may be different between GSCs and cells within differentiating cysts (Neumüller et al., 2008). For example, during the mitotic divisions of GSCs, Wicked, the *Drosophila* homolog of the U3 snoRNP protein UTP18, becomes enriched in cytoplasmic particles, which asymmetrically segregate to GSCs (Fichelson et al., 2009). snoRNPs contain snoRNAs which serve to guide modification enzymes to specific sites on rRNA, as ribosomes are being assembled in the nucleolus. The asymmetric localization of Wicked suggests that ribosome assembly factors become enriched in GSCs, which in turn support higher levels of ribosome biogenesis in stem cells relative to their differentiating daughters.

This model is also supported by observations that Pol I activity differs between *Drosophila* GSCs and their differentiating progeny (**Figure 6B**). Across eukaryotes, two functionally distinct Pol I complexes exist: Pol I α and Pol I β. Only Pol I β, which associates with TIF-IA and represents a relatively small fraction of the total soluble Pol I pool, is initiation-competent and capable of productive assembly at the rRNA gene promoter (Miller et al., 2001). In mammalian cells, the selectivity factor 1 (SL1) complex, which consists of TATA-box-binding protein (TBP) and several TBP-associated factors (TAFs), including TAF1B and TAF1C, binds to the core promoter of rDNA genes (Beckmann et al., 1995; Russell and Zomerdijk, 2005; Knutson and Hahn, 2011; Naidu et al., 2011). Once bound, the SL1 complex recruits the TIF-IA-containing Pol I complex to the rDNA promoter (Russell and Zomerdijk, 2005). Components of the *Drosophila* SL1 complex were identified based on the study of a female sterile mutation in a gene called *under-developed* (*udd*). Udd localizes to the nucleolus and is broadly expressed in both germline and somatic cells. Co-staining with various markers revealed that Udd always tightly localizes to a central region within nucleoli of non-dividing cells. Mass spectrometry and co-immunoprecipitation showed that Udd associates with *Drosophila* homologs of the TAF1B and TAF1C Pol I transcription factors. Further genetic experiments show that all three proteins are involved with promoting Pol I transcriptional activity. Pulse-labeling nascent rRNA reveals GSCs exhibit higher levels of rRNA transcription relative to their immediate progeny (Zhang et al., 2014) (**Figure 6B**). Like Wicked, Udd protein becomes enriched in GSCs immediately after the completion of GSC mitosis, again suggesting that GSCs employ mechanisms to ensure high levels of ribosome production. However, enhanced levels of ribosome biogenesis do not necessarily correlate with high levels of mRNA translation within germ cells. OP-Puro pulse labeling and RNAi knockdown of ribosomal proteins showed that rRNA transcription and protein synthesis are uncoupled during early germ cell differentiation (Sanchez et al., 2016) (**Figure 6C**). Moreover, ribosome assembly appears to regulate the final steps of mitosis in GSCs. A RNAi knockdown screen in the male germline also revealed a requirement for ribosomal proteins in driving the expression of mitotic factors in GSCs (Liu et al., 2016). These combined results indicate the regulation of ribosome biogenesis and global translation likely influence germ cell development in both males and females.

The developmental potential of vertebrate oocytes may also be closely linked with ribosome biogenesis. Transcriptome analysis of rainbow trout embryo viability indicates that the dynamic regulation of ribosome assembly factors plays a critical role in ensuring egg quality in this species (Ma et al., 2019). In mammals, the nucleolus and the dynamic regulation of rDNA activity plays an essential role in producing fertilizable oocytes [reviewed in Kresoja-Rakic and Santoro (2019)]. During their growth phase, mammalian oocytes produce a large number of ribosomes along with other material needed to support their rapid growth. Once they reach their full size, oocytes can progress into meiosis. However, full sized oocytes display two distinct nuclear morphologies marked by a "surrounded nucleolus" (SN) or a "non-surrounded nucleolus" (NSN). Both types of oocytes can undergo meiosis and undergo fertilization, but NSN type oocytes are transcriptionally active whereas SN type oocytes are not. The nucleoli of SN oocytes undergo a distinct

morphological change to form structures known as nucleolus-like bodies (NLBs). As oocytes undergo meiosis, the nuclear envelop breaks down resulting in the release of NLB components into the cytoplasm. More recent work has shown that NSN and SN oocytes can be easily distinguished from one another through use of a Fibrillarin (FBL) GFP reporter (Wang and Na, 2021). In addition, NSN oocytes appear to experience more DNA damage compared to their SN counterparts based on γH2AX staining (Wang and Na, 2021). Further experiments will be needed to more fully characterize these differences. Strikingly, NSN oocyte derived embryos arrest at the two-cell stage of embryogenesis, whereas SN oocyte derived oocytes maintain a greater competence to complete embryogenesis. Together, these findings indicate that the regulation of the nucleolar morphology and activity are essential for the generation of competent oocytes.

Ribosomal Protein Heterogeneity in Germ Cells

Accumulating evidence suggests that ribosomes within a given cell may be heterogeneous (Xue and Barna, 2012; Barna, 2015; Shi and Barna, 2015; Shi et al., 2017; Genuth and Barna, 2018; Leppek and Barna, 2019; Leppek et al., 2020). This heterogeneity can take on many forms including the differential post-translational modification of ribosome proteins and/or rRNA and differential ribosome protein composition. Differences in ribosomes have been hypothesized to promote distinct mRNA translation programs during development and in times of stress. However, the functional significance of ribosome heterogeneity within any one context should be carefully evaluated in light of findings that changes in overall ribosome levels can have differential effects on mRNAs that experience high or low rates in translation initiation (Mills and Green, 2017).

The *Drosophila* genome encodes several ribosomal protein paralogs (Marygold et al., 2007), which exhibit different expression patterns, providing a potential experimental platform for studying ribosome heterogeneity. Microarray analysis (Kai et al., 2005) and later RNA-seq experiments (Graveley et al., 2011), showed that several of ribosomal protein paralogs, including *RpS5b*, *RpS19b,* and *RpS10a*, display enriched expression in gonads. Most of the ubiquitously expressed RP paralogs are on the X chromosome, while the paralogous genes that exhibit tissue specific expression are on an autosome. These ribosomal protein paralogs may carry-out tissue specific functions. For example, mutations in *RpS5a* result in a minute phenotype and lethality, while deletion of *RpS5b* leads to female sterility (Kong et al., 2019; Jang et al., 2021). Transgenic rescue experiments suggest that *RpS5a* and *RpS5b* may serve partially redundant functions in the germline (Kong et al., 2019; Jang et al., 2021), but pulldown experiments suggest that RpS5b containing ribosomes may show a preference for engaging with mRNAs encoding factors in mitochondrial electron transport (Kong et al., 2019).

RpL22-like encodes alternative protein isoforms (L22-like and L22-like short), both of which are expressed in the gonad and incorporated into polysomes (Kearse et al., 2010). RpL22, but not RpL22-like, is SUMOylated, especially in testis and sumoylated RpL22 does not associate with ribosomes (Kearse et al., 2013). This suggests that RpL22 protein may function outside the context of translation, similar to how phosphorylation of RPL13a controls whether this protein associates with the ribosome or negatively regulates translation in an extra-ribosomal manner (Mazumder et al., 2003). The functional role of SUMOylated RpL22 biological function should be investigated more thoroughly during germ cell development. Like RpS5a and RpS5b, RpL22 and RpL22-like appear functionally redundant within germ cells. Interestingly, expression of RpL22 results in decreased levels of RpL22-like, and vice versa, suggesting both proteins regulate the expression of one another to achieve a specific level of RpL22/RpL22-like within germ cells (Mageeney et al., 2018).

In contrast to *Drosophila* and several other model systems, few ribosome protein paralogs exist in mammals. However, some of these may carryout germline specific functions. For example, RpS4 paralogs have been shown to be differentially expressed in male and females. *RpS4X* and *RpS4Y* genes are located on X and Y chromosomes, respectively, and their dysfunction is linked with Turner syndrome (Fisher et al., 1990). RpS4X and RpS4Y differ by 19 amino acids, and both proteins appear interchangeable based on the complementation of temperature sensitive *RpS4X* mutant cells (Watanabe et al., 1993). Furthermore, proteomic analysis of cells from the liver, mammary gland, and testis revealed that paralogs of RpL10 and RpL39, referred to as RpL10-like and RpL39-like, exhibit specific expression in the testis (Sugihara et al., 2010). Future work will be needed to assess the extent to which these gonad specific ribosome protein paralogs function in a tissue specific manner.

Germ Cell Specific Translation Initiation and Elongation Factors

Germ cells also express specific paralogs of broadly used translation factors. For example, the *Drosophila* genome contains eight eIF4E paralogs (Hernández et al., 2005), some of which exhibit specific enriched expression within gonads. The expansion of the number of eIF4 complex members and the germline-specific expression of individual paralogs may provide a sophisticated network of interactions for controlling mRNA translation in space and time within developing germ cells. Along these lines, the *Drosophila* testis expresses relatively high levels of eIF4E-3 and eIF-4 gamma and low eIF5B (Graveley et al., 2011). eIF4E-3 and eIF4G2 are both essential in male fertility and eIF4G2 is needed to drive the germline expression of CycB and Cdc25, both of which are important in meiosis (Hernández et al., 2005; Baker et al., 2015; Ghosh and Lasko, 2015). In addition, a mutation in eIF4G3 also results in male infertility in mice, marked by a failure of spermatocytes to exit meiotic prophase (Sun et al., 2010). Loss of the CDC2A kinase chaperone HSPA2 leads to strikingly similar phenotypes. Further experiments showed the eIF4G3 mutants failed to express HSPA2 protein despite the presence of *Hspa2* mRNA within these cells. These observations indicate that eIF4G3 mediates the translation of specific messages needed

for meiotic exit. Interestingly, a subsequent study showed that eIF4G3 and several other components of the translation machinery localize to the XY body, a chromatin domain formed by transcriptionally inactive sex chromosomes (Hu et al., 2018). These observations suggest that spermatocytes may employ different germ cell-specific mechanisms for regulating the availability of translation factors needed for progression through meiosis.

The *C. elegans* genome also encodes at least five eIF4E-like genes, the function of which have recently been reviewed by Huggins and Keiper (2020). A number of these eIF4E isoforms play important roles in germline maintenance and development (Huggins et al., 2020). For example, IFE-1 exhibits enriched expression in germ cells and the protein associates with P granules. Mutations in IFE-1 result in fertility problems, including both reduced translation of specific maternally deposited mRNAs and defects in sperm development. Mutations in another eIF4E gene, IFE-3, result in defects in growth and germline sex determination. More specifically, the transition from spermatogenesis to oogenesis appears disrupted in IFE-3 mutant hermaphrodites. This defect can be suppressed by disrupting a key masculinizing gene, *fem-3*. IFE-3, along with its binding partner IFET-1, regulates the translation of several germline sex determination factors. By contrast, IFE-1 associates with PGL-1 and appears to regulate the expression of an independent set of mRNAs. The specificity of IFE-1 and IFE-3 function is mediated, at least in part, by association with their respective binding partners.

In addition to tissue specific initiation factors playing key roles in germ cell development and function, additional studies suggest germ cells in specific species may also employ specialized elongation machinery. *Xenopus* have three eEF1A genes. eEF-1S is expressed in the soma but not in germ cells, eEF-1O is expressed during oogenesis and in some adult tissues, and 42Sp50 is only expressed during oogenesis (Abdallah et al., 1991). Understanding the significance of this specialization amongst eEF1A paralogs and whether they drive different rates of elongation and/or influence overall translation fidelity will require further genetic interrogation. Interestingly, more recent work indicates that limiting eEF1A levels is likely an important control point in regulating the activity of germ cells. Work from the Wessel lab shows that protein synthesis rates within sea urchin PGCs is maintained at very low levels relative to neighboring somatic cells (Oulhen et al., 2017). This quiescent state in sea urchin PGCs is dependent on Nanos-2, which excludes eEF1A from PGCs (Oulhen et al., 2017). In addition, cytoplasmic pH has a marked effect on translation rates within PGCs. Similarly, *Drosophila* oocytes undergo extended periods of metabolic quiescence (Sieber et al., 2016). While much effort has gone into understanding the regulation of translation initiation in various contexts, germ cells may employ multiple modes of modulating mRNA translation, including cell-specific mechanisms for controlling elongation rates, to achieve a quiescent state. Further work will be required to determine whether the dynamic regulation of translation elongation represents a commonly used mechanism to control germ cell activity and quiescence.

Communication Between Somatic Cells and Germ Cells Influences mRNA Translation

The maintenance and development of germ cells depends on local communication with their somatic cell neighbors. Long-range and systemic signals also influence germ cell activity. Work in *Drosophila* has illustrated how signals from fat tissue can modulate mTOR signaling within germline stem cells (Armstrong et al., 2014). Subsequent studies from the Drummond-Barbosa lab have continued to characterize how interorgan communication influences germ cell development in flies (Matsuoka et al., 2017; Armstrong and Drummond-Barbosa, 2018; Weaver and Drummond-Barbosa, 2018, 2019, 2020, 2021). Work from the Conti and Eppig labs, among others, shows that bidirectional communication between developing oocytes and their somatic cell neighbors also plays an important role in mammalian germ cell development (Chen et al., 2013; Wigglesworth et al., 2013). This signaling often converges on mRNA translation and the translation of maternal messages is enhanced in the presence of specific somatic cells (Chen et al., 2013). Additional studies show that FSH regulates mRNA translation in mouse oocytes, through indirect mechanisms involving EGF signaling within follicular cells (Franciosi et al., 2016; Tetkova et al., 2019). Signaling through the mTOR pathway acts as a key regulator of mouse germ cell development. For example, the survival of cumulus-oocyte complexes (COCs) depends on mTOR activation (Guo et al., 2016). Paracrine signaling from the oocyte suppresses a negative regulator of mTOR activity within the cumulus cells. In turn, mTOR activation within these cells controls the survival and differentiation of COCs. Conditional loss of *mTOR* in primordial or growing oocytes also causes infertility (Guo et al., 2018), marked by reduced translation of various mRNAs including *protein regulator of cytokinesis 1* and disruption of the first meiotic division. Interestingly, a population of transcripts, many of which play roles in meiotic progression, remain stored within the nuclei of oocytes during their early development (Susor et al., 2015). Upon nuclear envelope breakdown during the first meiotic division, these transcripts, which remain closely associated with chromatin, are translated in an mTOR and eIF4F dependent manner. mTOR activation leads to the phosphorylation and inactivation of 4E-BP1, a well-characterized inhibitor of cap-dependent translation. Work from other groups show that the temporally regulated translation of cell cycle genes, including *Cyclin B2*, helps to drive the progression of meiosis in mouse oocytes (Daldello et al., 2019). Experiments designed to further characterize how intercellular signaling influences mTOR activity, and global and transcript-specific translation represent important work in the coming years. Further insights into this regulation will likely yield improved methods for promoting germ cell differentiation and extended oocyte culture *in vitro*.

Ribosome Accumulation and Storage in Oocytes

Studies dating back to the 1960's observed that protein synthesis in mammalian embryos starts before zygotic transcription is

initiated, indicating that maternally loaded and stored ribosomes are essential for early embryonic development. Indeed, work using *C. elegans* shows that maternally loaded ribosomes can support embryonic development from fertilization until the first larval stage, a time encompassing many cell divisions and tissue diversification (Cenik et al., 2019). The ability of oocytes to store vast quantities of active ribosomes may be a common feature across species. Previous electron microscopy studies revealed that mammalian oocytes store the majority of their ribosomes in cytoplasmic lattice-like (CPL) structures (Burkholder et al., 1971; Bachvarova et al., 1981). Whether similar structures exist in other species remains unexplored. More recent work indicates that the CPL also helps to coordinate organelle dynamics and the microtubule cytoskeleton within oocytes (Kan et al., 2011). Biochemical experiments suggest that the vast majority of ribosomes do not engage in translation during ovulation (Bachvarova and De Leon, 1977), further supporting the model that ribosome association with the CPL stores them in an inactive state. Genetic approaches are beginning to provide insights into the functional significance of CPLs. The ability of ribosomes to associate with the oocyte CPL is regulated by peptidylarginine deiminase 6 (PADI6) (Esposito et al., 2007; Yurttas et al., 2008). Loss of PADI6 results in infertility, marked by defects in protein synthesis and defective embryonic gene activation at the two-cell stage. The CPL cannot be visualized in PADI6 mutants. These results suggest that ribosome association with the CPL is critical for normal mRNA translation during early embryogenesis. Further biochemical studies identified components of the subcortical maternal complex (SCMC) including FLOPED, MATER, FILIA, and TLE6. FLOPED, MATER, and TLE6 are maternally deposited and interact with one another, while FILIA only interacts with MATER (Li et al., 2008). MATER co-localizes with PADI6 within the CPL of mouse oocytes, and loss of MATER results in infertility, marked by developmental arrest in two-cell embryos, similar in many ways to the phenotype caused by loss of maternal PADI6. Loss of MATER also disrupts the distribution of the endoplasmic reticulum and Ca^{2+} homeostasis (Kim et al., 2014), indicating that the protein has functions beyond ribosome storage. The similarity in the developmental arrest phenotypes of NSN oocyte derived embryos with those derived from PADI6 and MATER mutant oocytes is striking. While most antral oocytes from wild-type controls exhibit an SN morphology, 84% of oocytes from a MATER homozygous hypomorphic mutant display a NSN phenotype, suggesting a close connection between oocyte nucleoli, CPLs, and ribosome activity with developmental competence (Monti et al., 2013). However, more recent work suggests that cytoplasmic lattices are not linked with the developmental arrest of two-cell embryos (Longo et al., 2018).

Breakdown of mRNA Translation in Reproductive Aging

Female mammals are born with a finite complement of oocytes. Thus, the female reproductive system begins to age before most other organs. In humans, female reproductive aging is marked by a decline in egg quality, starting late in the third decade of life, and progresses to complete loss of fertility by the time of menopause (Broekmans et al., 2009). Advanced reproductive age is marked by an increase of miscarriages and birth defects (Jones and Lane, 2013). These problems are most readily attributable to gametes: the majority of maternal age effects normally observed in older females are negated when eggs from young healthy donors are used in IVF procedures (Check et al., 2011).

The quality of eggs depends on maternally produced components including mRNAs, proteins, and organelles needed for the completion of early embryogenesis. Human oocytes can remain quiescent for over 40 years, and emerging evidence indicates that older eggs experience a decline in their ability to carry out mRNA translation (Duncan et al., 2017; Duncan and Gerton, 2018). Similar observations have been made in a broad range of species, including mice and *Drosophila* (Duncan et al., 2017; Greenblatt and Spradling, 2018; Greenblatt et al., 2019). Despite these observations across the animal kingdom, we still do not understand the basis for this decline in mRNA translation. Potential causes include, but are not limited to, reduced levels of ribosomes, reduced levels of tRNAs, reduced levels of initiation factors, and/or reduced levels of elongation factors. In addition, several recent papers using worms and flies have shown protein aggregation negatively impacts gamete production (Burn et al., 2015; Bohnert and Kenyon, 2017).

Drosophila has emerged as a useful model for studying the changes in mRNA translation that occur with age. Recent results have shown that the quality of *Drosophila* eggs declines the longer they remain stored and unfertilized within females (Greenblatt and Spradling, 2018; Greenblatt et al., 2019), mimicking what happens in other species such as mammals. Using Ribo-seq, Greenblatt and Spradling (2018) found that stored *Drosophila* eggs experience a decrease in mRNA translation. This decrease is accompanied by a loss of meiotic spindle components and a failure to support viable embryos, again consistent with what has been described in mammals (Duncan et al., 2017; Duncan and Gerton, 2018).

The underlying basis of the decline in mRNA translation in stored eggs across species remains poorly characterized. One possibility is that ribosome levels and function decline with age. The half-life of a typical ribosome within somatic cells is on the order of days. By contrast, eggs, which are stored in a transcriptionally quiescent state and therefore do not produce new rRNA, must maintain the same pool of ribosomes over the course of weeks, months, years, or even decades, depending on the species. Perhaps the ability of "old" ribosomes, which have potentially participated in multiple rounds of translation, to efficiently translate mRNAs of genes involved with regulating the meiotic spindle declines with age. It will also be interesting to evaluate whether the CPL breaks down over long periods of storage in mammalian oocytes.

Common Themes and Unanswered Questions

Germ cells across species rely on a complex network of mRNA binding proteins to regulate translation in space and time. These networks extend beyond Vasa, Nanos, and Pumilio, and

our knowledge regarding how RNA binding proteins regulate germ cell formation and function remains far from complete. The comprehensive characterization of these networks and understanding how they interact with each other and with germ cell specific translation machinery, at a systems level, remains critical work for the future. Perhaps more significantly, we are just beginning to understand how RNA binding proteins that carry intrinsically disordered regions govern germ granule formation. Moreover, recent work has revealed spatial organization within germ granules, adding to the complexity of the system (Trcek et al., 2015, 2020). Understanding the biophysical properties of these condensates, what governs their formation and dissolution, how the movement of different RNAs and proteins in and out of these structures is controlled, and how these granules contribute to and depend on both *cis*- and *trans* regulation of mRNA translation all represent important goals for the field in the coming years. This work will have a broad impact across multiple fields.

In addition, observations made across multiple species indicate that germ cells regulate ribosome biogenesis in a stage specific manner. Typically, robust positive correlations between ribosome levels and mRNA translation levels exist in somatic cells. However, this correlation does not always hold true in germ cells, whether in the context of early germ cell differentiation in *Drosophila* ovaries or quiescent vertebrate oocytes that store an enormous number of ribosomes. Germ cells across species often express germ cell specific paralogs of key translation factors, including ribosomal proteins. Whether these paralogs simply serve to increase overall levels of a general activity or carry out a highly specialized function largely remains an open question. For example, do ribosomes that carry germ cell specific ribosome protein paralogs target specific messages for translation or exhibit different behaviors such as different rates of translation elongation or fidelity? Recent work in *Drosophila* has failed to detect clear functional differences between RpS5A and RpS5B paralogs. However, these experiments were carried out in a lab setting and not out in the wild. Perhaps, functional differences between general and germ cell enriched translation factors will only become apparent under the appropriate environmental conditions. Lastly, the mechanisms that control ribosome activity and storage within the germline are also just coming into focus. How are ribosomes stored for long periods of time? Are there functional differences between maternal and zygotically produced ribosomes? Can manipulating ribosome levels or activity prolong reproductive aging? Further insights into these areas will enhance our understanding of reproductive biology. Thus, the study of mRNA translation within germ cells promises to remain an important area of study for the foreseeable future.

AUTHOR CONTRIBUTIONS

MB, MM, SJ, and CN contributed to the writing and editing of the review. All authors contributed to the article and approved the submitted version.

FUNDING

Work in the Buszczak lab is supported by the National Institute of General Medical Sciences (GM125812 and GM127569).

ACKNOWLEDGMENTS

We wish to apologize to members of the field whose work we were not able to discuss. We would like to thank Odelia Cheng for help with making the figures.

REFERENCES

Abdallah, B., Hourdry, J., Krieg, P. A., Denis, H., and Mazabraud, A. (1991). Germ cell-specific expression of a gene encoding eukaryotic translation elongation factor 1 alpha (eEF-1 alpha) and generation of eEF-1 alpha retropseudogenes in *Xenopus laevis*. *Proc. Natl. Acad. Sci. U.S.A.* 88, 9277–9281. doi: 10.1073/pnas.88.20.9277

Aoki, S. T., Lynch, T. R., Crittenden, S. L., Bingman, C. A., Wickens, M., and Kimble, J. (2021). C. elegans germ granules require both assembly and localized regulators for mRNA repression. *Nat. Commun.* 12:996. doi: 10.1038/s41467-021-21278-1

Armstrong, A. R., and Drummond-Barbosa, D. (2018). Insulin signaling acts in adult adipocytes via GSK-3beta and independently of FOXO to control *Drosophila* female germline stem cell numbers. *Dev. Biol.* 440, 31–39. doi: 10.1016/j.ydbio.2018.04.028

Armstrong, A. R., Laws, K. M., and Drummond-Barbosa, D. (2014). Adipocyte amino acid sensing controls adult germline stem cell number via the amino acid response pathway and independently of Target of *Rapamycin* signaling in *Drosophila*. *Development* 141, 4479–4488. doi: 10.1242/dev.116467

Austin, J., and Kimble, J. (1987). glp-1 is required in the germ line for regulation of the decision between mitosis and meiosis in *C. elegans*. *Cell* 51, 589–599. doi: 10.1016/0092-8674(87)90128-0

Bachvarova, R. (1985). Gene expression during oogenesis and oocyte development in mammals. *Dev. Biol. (N. Y. 1985)* 1, 453–524. doi: 10.1007/978-1-4615-6814-8_11

Bachvarova, R., and De Leon, V. (1977). Stored and polysomal ribosomes of mouse ova. *Dev. Biol.* 58, 248–254. doi: 10.1016/0012-1606(77)90090-2

Bachvarova, R., De Leon, V., and Spiegelman, I. (1981). Mouse egg ribosomes: evidence for storage in lattices. *J. Embryol. Exp. Morphol.* 62, 153–164.

Baker, C. C., Gim, B. S., and Fuller, M. T. (2015). Cell type-specific translational repression of Cyclin B during meiosis in males. *Development* 142, 3394–3402. doi: 10.1242/dev.122341

Barker, D. D., Wang, C., Moore, J., Dickinson, L. K., and Lehmann, R. (1992). Pumilio is essential for function but not for distribution of the *Drosophila* abdominal determinant Nanos. *Genes Dev.* 6, 2312–2326. doi: 10.1101/gad.6.12a.2312

Barna, M. (2015). The ribosome prophecy. *Nat. Rev. Mol. Cell Biol.* 16:268. doi: 10.1038/nrm3993

Beckmann, H., Chen, J. L., O'Brien, T., and Tjian, R. (1995). Coactivator and promoter-selective properties of RNA polymerase I TAFs. *Science* 270, 1506–1509.

Bernstein, D., Hook, B., Hajarnavis, A., Opperman, L., and Wickens, M. (2005). Binding specificity and mRNA targets of a C. elegans PUF protein, FBF-1. *RNA* 11, 447–458. doi: 10.1261/rna.7255805

Bohnert, K. A., and Kenyon, C. (2017). A lysosomal switch triggers proteostasis renewal in the immortal C. elegans germ lineage. *Nature* 551, 629–633. doi: 10.1038/nature24620

Brangwynne, C. P., Mitchison, T. J., and Hyman, A. A. (2011). Active liquid-like behavior of nucleoli determines their size and shape in *Xenopus laevis* oocytes. *Proc. Natl. Acad. Sci.* 108:4334. doi: 10.1073/pnas.1017150108

Breitwieser, W., Markussen, F. H., Horstmann, H., and Ephrussi, A. (1996). Oskar protein interaction with Vasa represents an essential step in polar granule assembly. *Genes Dev.* 10, 2179–2188. doi: 10.1101/gad.10.17.2179

Broekmans, F. J., Soules, M. R., and Fauser, B. C. (2009). Ovarian aging: mechanisms and clinical consequences. *Endocr. Rev.* 30, 465–493. doi: 10.1210/er.2009-0006

Brown, D. D., and Dawid, I. B. (1968). Specific gene amplification in oocytes. Oocyte nuclei contain extrachromosomal replicas of the genes for ribosomal RNA. *Science* 160, 272–280. doi: 10.1126/science.160.3825.272

Burkholder, G. D., Comings, D. E., and Okada, T. A. (1971). A storage form of ribosomes in mouse oocytes. *Exp. Cell Res.* 69, 361–371. doi: 10.1016/0014-4827(71)90236-9

Burn, K. M., Shimada, Y., Ayers, K., Lu, F. Y., Hudson, A. M., and Cooley, L. (2015). Somatic insulin signaling regulates a germline starvation response in *Drosophila* egg chambers (vol 398, pg 206, 2015). *Dev. Biol.* 405, 340–340. doi: 10.1016/j.ydbio.2015.07.016

Buszczak, M., Signer, R. A., and Morrison, S. J. (2014). Cellular differences in protein synthesis regulate tissue homeostasis. *Cell* 159, 242–251. doi: 10.1016/j.cell.2014.09.016

Cable, J., Brangwynne, C., Seydoux, G., Cowburn, D., Pappu, R. V., Castaneda, C. A., et al. (2019). Phase separation in biology and disease-a symposium report. *Ann. N. Y. Acad. Sci.* 1452, 3–11. doi: 10.1111/nyas.14126

Carreira-Rosario, A., Bhargava, V., Hillebrand, J., Kollipara, R. K., Ramaswami, M., and Buszczak, M. (2016). Repression of pumilio protein expression by rbfox1 promotes germ cell differentiation. *Dev. Cell* 36, 562–571. doi: 10.1016/j.devcel.2016.02.010

Castagnetti, S., and Ephrussi, A. (2003). Orb and a long poly(A) tail are required for efficient oskar translation at the posterior pole of the *Drosophila* oocyte. *Development* 130, 835–843. doi: 10.1242/dev.00309

Castrillon, D. H., Quade, B. J., Wang, T., Quigley, C., and Crum, C. P. (2000). The human VASA gene is specifically expressed in the germ cell lineage. *Proc. Natl. Acad. Sci. U.S.A.* 97, 9585–9590.

Cenik, E. S., Meng, X., Tang, N. H., Hall, R. N., Arribere, J. A., Cenik, C., et al. (2019). Maternal ribosomes are sufficient for tissue diversification during embryonic development in C. elegans. *Dev. Cell* 48, 811–826.e816. doi: 10.1016/j.devcel.2019.01.019

Chau, J., Kulnane, L. S., and Salz, H. K. (2012). Sex-lethal enables germline stem cell differentiation by down-regulating Nanos protein levels during *Drosophila* oogenesis. *Proc. Natl. Acad. Sci. U.S.A.* 109, 9465–9470. doi: 10.1073/pnas.1120473109

Check, J. H., Jamison, T., Check, D., Choe, J. K., Brasile, D., and Cohen, R. (2011). Live delivery and implantation rates of donor oocyte recipients in their late forties are similar to younger recipients. *J. Reprod. Med.* 56, 149–152.

Chekulaeva, M., Hentze, M. W., and Ephrussi, A. (2006). Bruno acts as a dual repressor of oskar translation, promoting mRNA oligomerization and formation of silencing particles. *Cell* 124, 521–533. doi: 10.1016/j.cell.2006.01.031

Chen, D., and McKearin, D. (2003a). Dpp signaling silences bam transcription directly to establish asymmetric divisions of germline stem cells. *Curr. Biol.* 13, 1786–1791. doi: 10.1016/j.cub.2003.09.033

Chen, D., and McKearin, D. (2005). Gene circuitry controlling a stem cell niche. *Curr. Biol.* 15, 179–184. doi: 10.1016/j.cub.2005.01.004

Chen, D., and McKearin, D. M. (2003b). A discrete transcriptional silencer in the bam gene determines asymmetric division of the *Drosophila germline* stem cell. *Development* 130, 1159–1170. doi: 10.1242/dev.00325

Chen, D., Sun, N., Hou, L., Kim, R., Faith, J., Aslanyan, M., et al. (2019). Human primordial germ cells are specified from lineage-primed progenitors. *Cell Rep.* 29, 4568–4582 e4565. doi: 10.1016/j.celrep.2019.11.083

Chen, D., Zheng, W., Lin, A., Uyhazi, K., Zhao, H., and Lin, H. (2012). Pumilio 1 suppresses multiple activators of p53 to safeguard spermatogenesis. *Curr. Biol.* 22, 420–425. doi: 10.1016/j.cub.2012.01.039

Chen, J., Torcia, S., Xie, F., Lin, C. J., Cakmak, H., Franciosi, F., et al. (2013). Somatic cells regulate maternal mRNA translation and developmental competence of mouse oocytes. *Nat. Cell Biol.* 15, 1415–1423. doi: 10.1038/ncb2873

Clouse, K. N., Ferguson, S. B., and Schupbach, T. (2008). Squid, Cup, and PABP55B function together to regulate gurken translation in *Drosophila*. *Dev. Biol.* 313, 713–724. doi: 10.1016/j.ydbio.2007.11.008

Conboy, J. G. (2017). Developmental regulation of RNA processing by Rbfox proteins. *Wiley Interdiscip Rev. RNA* 8:e1398. doi: 10.1002/wrna.1398

Crittenden, S. L., Bernstein, D. S., Bachorik, J. L., Thompson, B. E., Gallegos, M., Petcherski, A. G., et al. (2002). A conserved RNA-binding protein controls germline stem cells in *Caenorhabditis elegans*. *Nature* 417, 660–663. doi: 10.1038/nature754

Curtis, D., Apfeld, J., and Lehmann, R. (1995). nanos is an evolutionarily conserved organizer of anterior-posterior polarity. *Development* 121, 1899–1910.

Daldello, E. M., Luong, X. G., Yang, C. R., Kuhn, J., and Conti, M. (2019). Cyclin B2 is required for progression through meiosis in mouse oocytes. *Development* 146:dev172734. doi: 10.1242/dev.172734

Davidian, A., Koshel, E., Dyomin, A., Galkina, S., Saifitdinova, A., and Gaginskaya, E. (2021). On some structural and evolutionary aspects of rDNA amplification in oogenesis of *Trachemys scripta* turtles. *Cell Tissue Res.* 383, 853–864. doi: 10.1007/s00441-020-03282-x

De Keuckelaere, E., Hulpiau, P., Saeys, Y., Berx, G., and van Roy, F. (2018). Nanos genes and their role in development and beyond. *Cell Mol. Life Sci.* 75, 1929–1946. doi: 10.1007/s00018-018-2766-3

Dehghani, M., and Lasko, P. (2017). Multiple functions of the DEAD-Box helicase vasa in drosophila oogenesis. *Results Probl. Cell Differ.* 63, 127–147. doi: 10.1007/978-3-319-60855-6_6

Dodson, A. E., and Kennedy, S. (2019). Germ granules coordinate RNA-based epigenetic inheritance pathways. *Dev. Cell* 50, 704–715 e704. doi: 10.1016/j.devcel.2019.07.025

Dold, A., Han, H., Liu, N., Hildebrandt, A., Bruggemann, M., Ruckle, C., et al. (2020). Makorin 1 controls embryonic patterning by alleviating Bruno1-mediated repression of oskar translation. *PLoS Genet.* 16:e1008581. doi: 10.1371/journal.pgen.1008581

Duncan, F. E., and Gerton, J. L. (2018). Mammalian oogenesis and female reproductive aging. *Aging (Albany NY)* 10, 162–163. doi: 10.18632/aging.101381

Duncan, F. E., Jasti, S., Paulson, A., Kelsh, J. M., Fegley, B., and Gerton, J. L. (2017). Age-associated dysregulation of protein metabolism in the mammalian oocyte. *Aging Cell* 16, 1381–1393. doi: 10.1111/acel.12676

Elguindy, M. M., and Mendell, J. T. (2021). NORAD-induced Pumilio phase separation is required for genome stability. *Nature* 595, 303–308. doi: 10.1038/s41586-021-03633-w

Ellenbecker, M., Osterli, E., Wang, X., Day, N. J., Baumgarten, E., Hickey, B., et al. (2019). Dynein light chain DLC-1 facilitates the function of the germline cell fate regulator GLD-1 in *Caenorhabditis elegans*. *Genetics* 211, 665–681. doi: 10.1534/genetics.118.301617

Encinas, G., Zogbi, C., and Stumpp, T. (2012). Detection of four germ cell markers in rats during testis morphogenesis: differences and similarities with mice. *Cells Tissues Organs* 195, 443–455. doi: 10.1159/000329245

Esposito, G., Vitale, A. M., Leijten, F. P., Strik, A. M., Koonen-Reemst, A. M., Yurttas, P., et al. (2007). Peptidylarginine deiminase (PAD) 6 is essential for oocyte cytoskeletal sheet formation and female fertility. *Mol. Cell Endocrinol.* 273, 25–31. doi: 10.1016/j.mce.2007.05.005

Feric, M., Vaidya, N., Harmon, T. S., Mitrea, D. M., Zhu, L., Richardson, T. M., et al. (2016). Coexisting liquid phases underlie nucleolar subcompartments. *Cell* 165, 1686–1697. doi: 10.1016/j.cell.2016.04.047

Fichelson, P., Moch, C., Ivanovitch, K., Martin, C., Sidor, C. M., Lepesant, J. A., et al. (2009). Live-imaging of single stem cells within their niche reveals that a U3snoRNP component segregates asymmetrically and is required for self-renewal in *Drosophila*. *Nat. Cell Biol.* 11, 685–693. doi: 10.1038/ncb1874

Fisher, E. M. C., Beer-Romero, P., Brown, L. G., Ridley, A., McNeil, J. A., Lawrence, J. B., et al. (1990). Homologous ribosomal protein genes on the human X and Y chromosomes: escape from X inactivation and possible implications for turner syndrome. *Cell* 63, 1205–1218. doi: 10.1016/0092-8674(90)90416-C

Forbes, A., and Lehmann, R. (1998). Nanos and Pumilio have critical roles in the development and function of *Drosophila germline* stem cells. *Development* 125, 679–690.

Ford, P. J., and Southern, E. M. (1973). Different sequences for 5S RNA in kidney cells and ovaries of *Xenopus laevis*. *Nat. New Biol.* 241, 7–12. doi: 10.1038/newbio241007a0

Forman-Kay, J. D., Kriwacki, R. W., and Seydoux, G. (2018). Phase separation in biology and disease. *J. Mol. Biol.* 430, 4603–4606. doi: 10.1016/j.jmb.2018.09.006

Franciosi, F., Manandhar, S., and Conti, M. (2016). FSH regulates mRNA translation in mouse oocytes and promotes developmental competence. *Endocrinology* 157, 872–882. doi: 10.1210/en.2015-1727

Friend, K., Campbell, Z. T., Cooke, A., Kroll-Conner, P., Wickens, M. P., and Kimble, J. (2012). A conserved PUF-Ago-eEF1A complex attenuates translation elongation. *Nat. Struct. Mol. Biol.* 19, 176–183. doi: 10.1038/nsmb.2214

Fujiwara, Y., Komiya, T., Kawabata, H., Sato, M., Fujimoto, H., Furusawa, M., et al. (1994). Isolation of a DEAD-family protein gene that encodes a murine homolog of Drosophila vasa and its specific expression in germ cell lineage. *Proc. Natl. Acad. Sci. U.S.A.* 91, 12258–12262.

Gall, J. G. (1968). Differential synthesis of the genes for ribosomal RNA during amphibian oogenesis. *Proc. Natl. Acad. Sci. U.S.A* 60, 553–560. doi: 10.1073/pnas.60.2.553

Gall, J. G. (1969). The genes for ribosomal RNA during oogenesis. *Genetics* 61 Suppl, 121–132.

Gall, J. G., and Rochaix, J. D. (1974). The amplified ribosomal DNA of dytiscid beetles. *Proc. Natl. Acad. Sci. U.S.A.* 71, 1819–1823. doi: 10.1073/pnas.71.5.1819

Gall, J. G., Macgregor, H. C., and Kidston, M. E. (1969). Gene amplification in the oocytes of *Dytiscid* water beetles. *Chromosoma* 26, 169–187. doi: 10.1007/BF00326453

Gassei, K., Sheng, Y., Fayomi, A., Mital, P., Sukhwani, M., Lin, C. C., et al. (2017). DDX4-EGFP transgenic rat model for the study of germline development and spermatogenesis. *Biol. Reprod.* 96, 707–719. doi: 10.1095/biolreprod.116.142828

Gavis, E. R., and Lehmann, R. (1994). Translational regulation of nanos by RNA localization. *Nature* 369, 315–318. doi: 10.1038/369315a0

Genuth, N. R., and Barna, M. (2018). Heterogeneity and specialized functions of translation machinery: from genes to organisms. *Nat. Rev. Genet.* 19, 431–452. doi: 10.1038/s41576-018-0008-z

Ghosh, S., and Lasko, P. (2015). Loss-of-function analysis reveals distinct requirements of the translation initiation factors eIF4E, eIF4E-3, eIF4G and eIF4G2 in *Drosophila* spermatogenesis. *PLoS One* 10:e0122519. doi: 10.1371/journal.pone.0122519

Goldstrohm, A. C., Hall, T. M. T., and McKenney, K. M. (2018). Post-transcriptional regulatory functions of mammalian pumilio proteins. *Trends Genet.* 34, 972–990. doi: 10.1016/j.tig.2018.09.006

Gotze, M., Dufourt, J., Ihling, C., Rammelt, C., Pierson, S., Sambrani, N., et al. (2017). Translational repression of the *Drosophila* nanos mRNA involves the RNA helicase Belle and RNA coating by Me31B and Trailer hitch. *RNA* 23, 1552–1568. doi: 10.1261/rna.062208.117

Graveley, B. R., Brooks, A. N., Carlson, J. W., Duff, M. O., Landolin, J. M., Yang, L., et al. (2011). The developmental transcriptome of *Drosophila* melanogaster. *Nature* 471, 473–479. doi: 10.1038/nature09715

Greenblatt, E. J., and Spradling, A. C. (2018). Fragile X mental retardation 1 gene enhances the translation of large autism-related proteins. *Science* 361, 709–712. doi: 10.1126/science.aas9963

Greenblatt, E. J., Obniski, R., Mical, C., and Spradling, A. C. (2019). Prolonged ovarian storage of mature Drosophila oocytes dramatically increases meiotic spindle instability. *eLife* 8:e49455. doi: 10.7554/eLife.49455

Guo, J., Shi, L., Gong, X., Jiang, M., Yin, Y., Zhang, X., et al. (2016). Oocyte-dependent activation of MTOR in cumulus cells controls the development and survival of cumulus-oocyte complexes. *J. Cell Sci.* 129, 3091–3103. doi: 10.1242/jcs.182642

Guo, J., Zhang, T., Guo, Y., Sun, T., Li, H., Zhang, X., et al. (2018). Oocyte stage-specific effects of MTOR determine granulosa cell fate and oocyte quality in mice. *Proc. Natl. Acad. Sci. U.S.A.* 115, E5326–E5333. doi: 10.1073/pnas.1800352115

Hachet, O., and Ephrussi, A. (2004). Splicing of oskar RNA in the nucleus is coupled to its cytoplasmic localization. *Nature* 428, 959–963. doi: 10.1038/nature02521

Haraguchi, S., Tsuda, M., Kitajima, S., Sasaoka, Y., Nomura-Kitabayashid, A., Kurokawa, K., et al. (2003). nanos1: a mouse nanos gene expressed in the central nervous system is dispensable for normal development. *Mech. Dev.* 120, 721–731. doi: 10.1016/s0925-4773(03)00043-1

Harris, R. E., Pargett, M., Sutcliffe, C., Umulis, D., and Ashe, H. L. (2011). Brat promotes stem cell differentiation via control of a bistable switch that restricts BMP signaling. *Dev. Cell* 20, 72–83. doi: 10.1016/j.devcel.2010.11.019

Haupt, K. A., Law, K. T., Enright, A. L., Kanzler, C. R., Shin, H., Wickens, M., et al. (2020). A PUF hub drives self-renewal in *Caenorhabditis elegans* germline stem cells. *Genetics* 214, 147–161. doi: 10.1534/genetics.119.302772

Hermann, B. P., Sukhwani, M., Lin, C. C., Sheng, Y., Tomko, J., Rodriguez, M., et al. (2007). Characterization, cryopreservation, and ablation of spermatogonial stem cells in adult rhesus macaques. *Stem Cells* 25, 2330–2338. doi: 10.1634/stemcells.2007-0143

Hernández, G., Altmann, M., Sierra, J. M., Urlaub, H., Diez del Corral, R., Schwartz, P., et al. (2005). Functional analysis of seven genes encoding eight translation initiation factor 4E (eIF4E) isoforms in *Drosophila*. *Mech. Dev.* 122, 529–543. doi: 10.1016/j.mod.2004.11.011

Hildebrandt, A., Brüggemann, M., Rücklé, C., Boerner, S., Heidelberger, J. B., Busch, A., et al. (2019). The RNA-binding ubiquitin ligase MKRN1 functions in ribosome-associated quality control of poly(A) translation. *Genome Biol.* 20, 216. doi: 10.1186/s13059-019-1814-0

Hourcade, D., Dressler, D., and Wolfson, J. (1973). The amplification of ribosomal RNA genes involves a rolling circle intermediate. *Proc. Natl. Acad. Sci. U.S.A.* 70, 2926–2930. doi: 10.1073/pnas.70.10.2926

Hourcade, D., Dressler, D., and Wolfson, J. (1974). The nucleolus and the rolling circle. *Cold Spring Harb. Symp. Quant. Biol.* 38, 537–550. doi: 10.1101/sqb.1974.038.01.058

Hu, J., Sun, F., and Handel, M. A. (2018). Nuclear localization of EIF4G3 suggests a role for the XY body in translational regulation during spermatogenesis in mice. *Biol. Reprod.* 98, 102–114. doi: 10.1093/biolre/iox150

Huggins, H. P., and Keiper, B. D. (2020). Regulation of germ cell mRNPs by eIF4E:4EIP complexes: multiple mechanisms, one goal. *Front. Cell Dev. Biol.* 8:562. doi: 10.3389/fcell.2020.00562

Huggins, H. P., Subash, J. S., Stoffel, H., Henderson, M. A., Hoffman, J. L., Buckner, D. S., et al. (2020). Distinct roles of two eIF4E isoforms in the germline of *Caenorhabditis elegans*. *J Cell Sci* 133, jcs237990. doi: 10.1242/jcs.237990

Igreja, C., and Izaurralde, E. (2011). CUP promotes deadenylation and inhibits decapping of mRNA targets. *Genes Dev.* 25, 1955–1967. doi: 10.1101/gad.17136311

Iida, T., and Kobayashi, T. (2019). RNA polymerase I activators count and adjust ribosomal RNA gene copy number. *Mol. Cell* 73, 645–654 e613. doi: 10.1016/j.molcel.2018.11.029

Irie, N., and Surani, M. A. (2017). Efficient induction and isolation of human primordial germ cell-like cells from competent human pluripotent stem cells. *Methods Mol. Biol.* 1463, 217–226. doi: 10.1007/978-1-4939-4017-2_16

Irie, N., Weinberger, L., Tang, W. W., Kobayashi, T., Viukov, S., Manor, Y. S., et al. (2015). SOX17 is a critical specifier of human primordial germ cell fate. *Cell* 160, 253–268. doi: 10.1016/j.cell.2014.12.013

Irish, V., Lehmann, R., and Akam, M. (1989). The *Drosophila* posterior-group gene nanos functions by repressing hunchback activity. *Nature* 338, 646–648. doi: 10.1038/338646a0

Jamieson-Lucy, A., and Mullins, M. C. (2019). The vertebrate Balbiani body, germ plasm, and oocyte polarity. *Curr. Top. Dev. Biol.* 135, 1–34. doi: 10.1016/bs.ctdb.2019.04.003

Jang, S., Lee, J., Mathews, J., Ruess, H., Williford, A. O., Rangan, P., et al. (2021). The Drosophila ribosome protein S5 paralog RpS5b promotes germ cell and follicle cell differentiation during oogenesis. *Development* 148:dev199511. doi: 10.1242/dev.199511

Jaruzelska, J., Kotecki, M., Kusz, K., Spik, A., Firpo, M., and Reijo Pera, R. A. (2003). Conservation of a Pumilio-Nanos complex from *Drosophila* germ plasm to human germ cells. *Dev. Genes Evol.* 213, 120–126. doi: 10.1007/s00427-003-0303-2

Jeske, M., Bordi, M., Glatt, S., Müller, S., Rybin, V., Müller, C. W., et al. (2015). The crystal structure of the drosophila germline inducer oskar identifies two domains with distinct vasa helicase- and RNA-binding activities. *Cell Rep.* 12, 587–598. doi: 10.1016/j.celrep.2015.06.055

Johnstone, O., and Lasko, P. (2004). Interaction with eIF5B is essential for Vasa function during development. *Development* 131, 4167–4178. doi: 10.1242/dev.01286

Joly, W., Chartier, A., Rojas-Rios, P., Busseau, I., and Simonelig, M. (2013). The CCR4 deadenylase acts with Nanos and Pumilio in the fine-tuning of Mei-P26 expression to promote germline stem cell self-renewal. *Stem Cell Rep.* 1, 411–424. doi: 10.1016/j.stemcr.2013.09.007

Jones, K. T., and Lane, S. I. (2013). Molecular causes of aneuploidy in mammalian eggs. *Development* 140, 3719–3730. doi: 10.1242/dev.090589

Kai, T., Williams, D., and Spradling, A. C. (2005). The expression profile of purified *Drosophila germline* stem cells. *Dev. Biol.* 283, 486–502. doi: 10.1016/j.ydbio.2005.04.018

Kan, R., Yurttas, P., Kim, B., Jin, M., Wo, L., Lee, B., et al. (2011). Regulation of mouse oocyte microtubule and organelle dynamics by PADI6 and the cytoplasmic lattices. *Dev. Biol.* 350, 311–322. doi: 10.1016/j.ydbio.2010.11.033

Kanke, M., and Macdonald, P. M. (2015). Translational activation of oskar mRNA: reevaluation of the role and importance of a 5′ regulatory element [corrected]. *PLoS One* 10:e0125849. doi: 10.1371/journal.pone.0125849

Kapelle, W. S., and Reinke, V. (2011). C. elegans meg-1 and meg-2 differentially interact with nanos family members to either promote or inhibit germ cell proliferation and survival. *Genesis* 49, 380–391. doi: 10.1002/dvg.20726

Kearse, M. G., Chen, A. S., and Ware, V. C. (2010). Expression of ribosomal protein L22e family members in *Drosophila* melanogaster: rpL22-like is differentially expressed and alternatively spliced. *Nucleic Acids Res.* 39, 2701–2716. doi: 10.1093/nar/gkq1218

Kearse, M. G., Ireland, J. A., Prem, S. M., Chen, A. S., and Ware, V. C. (2013). RpL22e, but not RpL22e-like-PA, is SUMOylated and localizes to the nucleoplasm of *Drosophila* meiotic spermatocytes. *Nucleus* 4, 241–258. doi: 10.4161/nucl.25261

Kershner, A. M., Shin, H., Hansen, T. J., and Kimble, J. (2014). Discovery of two GLP-1/Notch target genes that account for the role of GLP-1/Notch signaling in stem cell maintenance. *Proc. Natl. Acad. Sci. U.S.A.* 111, 3739–3744.

Keyes, L. N., and Spradling, A. C. (1997). The Drosophila gene fs(2)cup interacts with otu to define a cytoplasmic pathway required for the structure and function of germ-line chromosomes. *Development* 124, 1419–1431.

Kim, B., Zhang, X., Kan, R., Cohen, R., Mukai, C., Travis, A. J., et al. (2014). The role of MATER in endoplasmic reticulum distribution and calcium homeostasis in mouse oocytes. *Dev. Biol.* 386, 331–339. doi: 10.1016/j.ydbio.2013.12.025

Kim, J. Y., Lee, Y. C., and Kim, C. (2010). Direct inhibition of pumilo activity by Bam and Bgcn in *Drosophila* germ line stem cell differentiation. *J. Biol. Chem.* 285, 4741–4746. doi: 10.1074/jbc.M109.002014

Kim-Ha, J., Smith, J. L., and Macdonald, P. M. (1991). oskar mRNA is localized to the posterior pole of the *Drosophila* oocyte. *Cell* 66, 23–35. doi: 10.1016/0092-8674(91)90136-m

Kinkelin, K., Veith, K., Grunwald, M., and Bono, F. (2012). Crystal structure of a minimal eIF4E-Cup complex reveals a general mechanism of eIF4E regulation in translational repression. *RNA* 18, 1624–1634. doi: 10.1261/rna.033639.112

Klinge, S., and Woolford, J. L. Jr. (2019). Ribosome assembly coming into focus. *Nat. Rev. Mol. Cell Biol.* 20, 116–131. doi: 10.1038/s41580-018-0078-y

Knutson, A. K., Egelhofer, T., Rechtsteiner, A., and Strome, S. (2017). Germ granules prevent accumulation of somatic transcripts in the adult *Caenorhabditis elegans* germline. *Genetics* 206, 163–178. doi: 10.1534/genetics.116.198549

Knutson, B. A., and Hahn, S. (2011). Yeast Rrn7 and human TAF1B are TFIIB-related RNA polymerase I general transcription factors. *Science* 333, 1637–1640. doi: 10.1126/science.1207699

Kobayashi, T., Zhang, H., Tang, W. W. C., Irie, N., Withey, S., Klisch, D., et al. (2017). Principles of early human development and germ cell program from conserved model systems. *Nature* 546, 416–420. doi: 10.1038/nature22812

Komiya, T., and Tanigawa, Y. (1995). Cloning of a gene of the DEAD box protein family which is specifically expressed in germ cells in rats. *Biochem. Biophys. Res. Commun.* 207, 405–410. doi: 10.1006/bbrc.1995.1202

Kong, J., Han, H., Bergalet, J., Bouvrette, L. P. B., Hernandez, G., Moon, N. S., et al. (2019). A ribosomal protein S5 isoform is essential for oogenesis and interacts with distinct RNAs in *Drosophila* melanogaster. *Sci. Rep.* 9:13779. doi: 10.1038/s41598-019-50357-z

Kopp, F., Elguindy, M. M., Yalvac, M. E., Zhang, H., Chen, B., Gillett, F. A., et al. (2019). PUMILIO hyperactivity drives premature aging of Norad-deficient mice. *eLife* 8:e42650. doi: 10.7554/eLife.42650

Kraemer, B., Crittenden, S., Gallegos, M., Moulder, G., Barstead, R., Kimble, J., et al. (1999). NANOS-3 and FBF proteins physically interact to control the sperm-oocyte switch in *Caenorhabditis elegans*. *Curr. Biol.* 9, 1009–1018. doi: 10.1016/s0960-9822(99)80449-7

Kresoja-Rakic, J., and Santoro, R. (2019). Nucleolus and rRNA gene chromatin in early embryo development. *Trends Genet.* 35, 868–879. doi: 10.1016/j.tig.2019.06.005

Kucherenko, M. M., and Shcherbata, H. R. (2018). Stress-dependent miR-980 regulation of Rbfox1/A2bp1 promotes ribonucleoprotein granule formation and cell survival. *Nat. Commun.* 9, 312–312. doi: 10.1038/s41467-017-02757-w

Kugler, J. M., and Lasko, P. (2009). Localization, anchoring and translational control of oskar, gurken, bicoid and nanos mRNA during *Drosophila oogenesis*. *Fly (Austin)* 3, 15–28. doi: 10.4161/fly.3.1.7751

Kusz-Zamelczyk, K., Sajek, M., Spik, A., Glazar, R., Jedrzejczak, P., Latos-Bielenska, A., et al. (2013). Mutations of NANOS1, a human homologue of the *Drosophila morphogen*, are associated with a lack of germ cells in testes or severe oligo-astheno-teratozoospermia. *J. Med. Genet.* 50, 187–193. doi: 10.1136/jmedgenet-2012-101230

Lai, F., and King, M. L. (2013). Repressive translational control in germ cells. *Mol. Reprod. Dev.* 80, 665–676. doi: 10.1002/mrd.22161

Lamont, L. B., Crittenden, S. L., Bernstein, D., Wickens, M., and Kimble, J. (2004). FBF-1 and FBF-2 regulate the size of the mitotic region in the *C. elegans* germline. *Dev. Cell* 7, 697–707. doi: 10.1016/j.devcel.2004.09.013

Lasko, P. (2013). The DEAD-box helicase Vasa: evidence for a multiplicity of functions in RNA processes and developmental biology. *Biochim. Biophys. Acta* 1829, 810–816. doi: 10.1016/j.bbagrm.2013.04.005

Lasko, P. F., and Ashburner, M. (1988). The product of the *Drosophila* gene vasa is very similar to eukaryotic initiation factor-4A. *Nature* 335, 611–617. doi: 10.1038/335611a0

Leacock, S. W., and Reinke, V. (2008). MEG-1 and MEG-2 are embryo-specific P-granule components required for germline development in *Caenorhabditis elegans*. *Genetics* 178, 295–306. doi: 10.1534/genetics.107.080218

Lee, C. S., Lu, T., and Seydoux, G. (2017). Nanos promotes epigenetic reprograming of the germline by down-regulation of the THAP transcription factor LIN-15B. *eLife* 6:e30201. doi: 10.7554/eLife.30201

Lee, C. S., Putnam, A., Lu, T., He, S., Ouyang, J. P. T., and Seydoux, G. (2020). Recruitment of mRNAs to P granules by condensation with intrinsically-disordered proteins. *eLife* 9:e52896. doi: 10.7554/eLife.52896

Lee, C. Y., and Seydoux, G. (2019). Dynamics of mRNA entry into stress granules. *Nat. Cell Biol.* 21, 116–117. doi: 10.1038/s41556-019-0278-5

Lee, S., Kopp, F., Chang, T. C., Sataluri, A., Chen, B., Sivakumar, S., et al. (2016). Noncoding RNA norad regulates genomic stability by sequestering pumilio proteins. *Cell* 164, 69–80. doi: 10.1016/j.cell.2015.12.017

Lehmann, R. (2016). Germ plasm biogenesis–an oskar-centric perspective. *Curr. Top. Dev. Biol.* 116, 679–707. doi: 10.1016/bs.ctdb.2015.11.024

Leppek, K., and Barna, M. (2019). An rRNA variant to deal with stress. *Nat. Microbiol.* 4, 382–383. doi: 10.1038/s41564-019-0396-7

Leppek, K., Fujii, K., Quade, N., Susanto, T. T., Boehringer, D., Lenarcic, T., et al. (2020). Gene- and species-specific hox mrna translation by ribosome expansion segments. *Mol. Cell* 80, 980–995 e913. doi: 10.1016/j.molcel.2020.10.023

Leroy, P., Alzari, P., Sassoon, D., Wolgemuth, D., and Fellous, M. (1989). The protein encoded by a murine male germ cell-specific transcript is a putative ATP-dependent RNA helicase. *Cell* 57, 549–559. doi: 10.1016/0092-8674(89)90125-6

Lesch, B. J., and Page, D. C. (2012). Genetics of germ cell development. *Nat. Rev. Genet.* 13, 781–794. doi: 10.1038/nrg3294

Li, L., Baibakov, B., and Dean, J. (2008). A subcortical maternal complex essential for preimplantation mouse embryogenesis. *Dev. Cell* 15, 416–425. doi: 10.1016/j.devcel.2008.07.010

Li, Y., Maines, J. Z., Tastan, O. Y., McKearin, D. M., and Buszczak, M. (2012). Mei-P26 regulates the maintenance of ovarian germline stem cells by promoting BMP signaling. *Development* 139, 1547–1556. doi: 10.1242/dev.077412

Li, Y., Minor, N. T., Park, J. K., McKearin, D. M., and Maines, J. Z. (2009). Bam and Bgcn antagonize Nanos-dependent germ-line stem cell maintenance. *Proc. Natl. Acad. Sci. U.S.A.* 106, 9304–9309. doi: 10.1073/pnas.0901452106

Li, Y., Zhang, Q., Carreira-Rosario, A., Maines, J. Z., McKearin, D. M., and Buszczak, M. (2013). Mei-p26 cooperates with Bam, Bgcn and Sxl to promote early germline development in the Drosophila ovary. *PLoS One* 8:e58301. doi: 10.1371/journal.pone.0058301

Lin, K., Qiang, W., Zhu, M., Ding, Y., Shi, Q., Chen, X., et al. (2019). Mammalian Pum1 and Pum2 control body size via translational regulation of the cell cycle inhibitor CDKN1B. *Cell Rep.* 26, 2434–2450 e2436. doi: 10.1016/j.celrep.2019.01.111

Liu, N., and Lasko, P. (2015). Analysis of RNA interference lines identifies new functions of maternally-expressed genes involved in embryonic patterning in *Drosophila melanogaster*. *G3 (Bethesda)* 5, 1025–1034. doi: 10.1534/g3.115.017517

Liu, Y., Ge, Q., Chan, B., Liu, H., Singh, S. R., Manley, J., et al. (2016). Whole-animal genome-wide RNAi screen identifies networks regulating male germline stem cells in *Drosophila*. *Nat. Commun.* 7:12149. doi: 10.1038/ncomms12149

Locati, M. D., Pagano, J. F. B., Ensink, W. A., van Olst, M., van Leeuwen, S., Nehrdich, U., et al. (2017a). Linking maternal and somatic 5S rRNA types with different sequence-specific non-LTR retrotransposons. *RNA* 23, 446–456. doi: 10.1261/rna.059642.116

Locati, M. D., Pagano, J. F. B., Girard, G., Ensink, W. A., van Olst, M., van Leeuwen, S., et al. (2017b). Expression of distinct maternal and somatic 5.8S, 18S, and 28S rRNA types during zebrafish development. *RNA* 23, 1188–1199. doi: 10.1261/rna.061515.117

Loedige, I., Stotz, M., Qamar, S., Kramer, K., Hennig, J., Schubert, T., et al. (2014). The NHL domain of BRAT is an RNA-binding domain that directly contacts the hunchback mRNA for regulation. *Genes Dev.* 28, 749–764. doi: 10.1101/gad.236513.113

Longo, M., Boiani, M., Redi, C., and Monti, M. (2018). Cytoplasmic lattices are not linked to mouse 2-cell embryos developmental arrest. *Eur. J. Histochem.* 62:2972. doi: 10.4081/ejh.2018.2972

Lu, K. L., Nelson, J. O., Watase, G. J., Warsinger-Pepe, N., and Yamashita, Y. M. (2018). Transgenerational dynamics of rDNA copy number in *Drosophila* male germline stem cells. *eLife* 7:e32421. doi: 10.7554/eLife.32421

Lyon, A. S., Peeples, W. B., and Rosen, M. K. (2021). A framework for understanding the functions of biomolecular condensates across scales. *Nat. Rev. Mol. Cell Biol.* 22, 215–235. doi: 10.1038/s41580-020-00303-z

Ma, H., Martin, K., Dixon, D., Hernandez, A. G., and Weber, G. M. (2019). Transcriptome analysis of egg viability in rainbow trout, *Oncorhynchus mykiss*. *BMC Genomics* 20:319. doi: 10.1186/s12864-019-5690-5

Macdonald, P. M. (2004). Translational control: a cup half full. *Curr. Biol.* 14, R282–R283. doi: 10.1016/j.cub.2004.03.025

Macdonald, P. M., Kanke, M., and Kenny, A. (2016). Community effects in regulation of translation. *eLife* 5:e10965. doi: 10.7554/eLife.10965

Macgregor, H. C. (1972). The nucleolus and its genes in amphibian oogenesis. *Biol. Rev. Camb. Philos. Soc.* 47, 177–210. doi: 10.1111/j.1469-185x.1972.tb00972.x

Mageeney, C. M., Kearse, M. G., Gershman, B. W., Pritchard, C. E., Colquhoun, J. M., and Ware, V. C. (2018). Functional interplay between ribosomal protein paralogues in the eRpL22 family in *Drosophila melanogaster*. *Fly (Austin)* 12, 143–163. doi: 10.1080/19336934.2018.1549419

Maines, J. Z., Stevens, L. M., Tong, X., and Stein, D. (2004). Drosophila dMyc is required for ovary cell growth and endoreplication. *Development* 131, 775–786. doi: 10.1242/dev.00932

Mak, W., Fang, C., Holden, T., Dratver, M. B., and Lin, H. (2016). An important role of pumilio 1 in regulating the development of the mammalian female germline. *Biol. Reprod.* 94:134. doi: 10.1095/biolreprod.115.137497

Mak, W., Xia, J., Cheng, E. C., Lowther, K., and Lin, H. (2018). A role of Pumilio 1 in mammalian oocyte maturation and maternal phase of embryogenesis. *Cell Biosci.* 8:54. doi: 10.1186/s13578-018-0251-1

Markussen, F. H., Michon, A. M., Breitwieser, W., and Ephrussi, A. (1995). Translational control of oskar generates short OSK, the isoform that induces pole plasma assembly. *Development* 121, 3723–3732.

Marnik, E. A., and Updike, D. L. (2019). Membraneless organelles: P granules in *Caenorhabditis elegans*. *Traffic* 20, 373–379. doi: 10.1111/tra.12644

Marnik, E. A., Fuqua, J. H., Sharp, C. S., Rochester, J. D., Xu, E. L., Holbrook, S. E., et al. (2019). Germline maintenance through the multifaceted activities of GLH/Vasa in *Caenorhabditis elegans* P Granules. *Genetics* 213, 923–939. doi: 10.1534/genetics.119.302670

Marygold, S. J., Roote, J., Reuter, G., Lambertsson, A., Ashburner, M., Millburn, G. H., et al. (2007). The ribosomal protein genes and *Minute loci* of *Drosophila melanogaster*. *Genome Biol.* 8:R216. doi: 10.1186/gb-2007-8-10-r216

Matsuoka, S., Armstrong, A. R., Sampson, L. L., Laws, K. M., and Drummond-Barbosa, D. (2017). Adipocyte metabolic pathways regulated by diet control the female germline stem cell lineage in *Drosophila melanogaster*. *Genetics* 206, 953–971. doi: 10.1534/genetics.117.201921

Mazumder, B., Sampath, P., Seshadri, V., Maitra, R. K., DiCorleto, P. E., and Fox, P. L. (2003). Regulated release of L13a from the 60S ribosomal subunit as a mechanism of transcript-specific translational control. *Cell* 115, 187–198. doi: 10.1016/s0092-8674(03)00773-6

McKearin, D. M., and Spradling, A. C. (1990). bag-of-marbles: a *Drosophila* gene required to initiate both male and female gametogenesis. *Genes Dev.* 4, 2242–2251. doi: 10.1101/gad.4.12b.2242

Merritt, C., and Seydoux, G. (2010). The Puf RNA-binding proteins FBF-1 and FBF-2 inhibit the expression of synaptonemal complex proteins in germline stem cells. *Development* 137, 1787–1798. doi: 10.1242/dev.050799

Miller, G., Panov, K. I., Friedrich, J. K., Trinkle-Mulcahy, L., Lamond, A. I., and Zomerdijk, J. C. B. M. (2001). hRRN3 is essential in the SL1-mediated recruitment of RNA polymerase I to rRNA gene promoters. *EMBO J.* 20, 1373–1382. doi: 10.1093/emboj/20.6.1373

Mills, E. W., and Green, R. (2017). Ribosomopathies: there's strength in numbers. *Science* 358:eaan2755. doi: 10.1126/science.aan2755

Mitchell, R. T., Cowan, G., Morris, K. D., Anderson, R. A., Fraser, H. M., McKenzie, K. J., et al. (2008). Germ cell differentiation in the marmoset (*Callithrix jacchus*) during fetal and neonatal life closely parallels that in the human. *Hum. Reprod.* 23, 2755–2765. doi: 10.1093/humrep/den295

Monti, M., Zanoni, M., Calligaro, A., Ko, M. S., Mauri, P., and Redi, C. A. (2013). Developmental arrest and mouse antral not-surrounded nucleolus oocytes. *Biol. Reprod.* 88:2. doi: 10.1095/biolreprod.112.103887

Moore, F. L., Jaruzelska, J., Fox, M. S., Urano, J., Firpo, M. T., Turek, P. J., et al. (2003). Human Pumilio-2 is expressed in embryonic stem cells and germ cells and interacts with DAZ (Deleted in AZoospermia) and DAZ-like proteins. *Proc. Natl. Acad. Sci. U.S.A.* 100, 538–543. doi: 10.1073/pnas.0234478100

Moschall, R., Gaik, M., and Medenbach, J. (2017). Promiscuity in post-transcriptional control of gene expression: *Drosophila* sex-lethal and its regulatory partnerships. *FEBS Lett.* 591, 1471–1488. doi: 10.1002/1873-3468.12652

Nagamori, I., Cruickshank, V. A., and Sassone-Corsi, P. (2011). Regulation of an RNA granule during spermatogenesis: acetylation of MVH in the chromatoid body of germ cells. *J. Cell Sci.* 124(Pt 24), 4346–4355. doi: 10.1242/jcs.096461

Naidu, S., Friedrich, J. K., Russell, J., and Zomerdijk, J. C. (2011). TAF1B is a TFIIB-like component of the basal transcription machinery for RNA polymerase I. *Science* 333, 1640–1642. doi: 10.1126/science.1207656

Nakamura, A., Sato, K., and Hanyu-Nakamura, K. (2004). Drosophila cup is an eIF4E binding protein that associates with Bruno and regulates oskar mRNA translation in oogenesis. *Dev. Cell* 6, 69–78. doi: 10.1016/s1534-5807(03)00400-3

Nelson, J. O., Watase, G. J., Warsinger-Pepe, N., and Yamashita, Y. M. (2019). Mechanisms of rDNA Copy number maintenance. *Trends Genet.* 35, 734–742. doi: 10.1016/j.tig.2019.07.006

Nelson, M. R., Leidal, A. M., and Smibert, C. A. (2004). Drosophila Cup is an eIF4E-binding protein that functions in Smaug-mediated translational repression. *EMBO J.* 23, 150–159. doi: 10.1038/sj.emboj.7600026

Neumüller, R. A., Betschinger, J., Fischer, A., Bushati, N., Poernbacher, I., Mechtler, K., et al. (2008). Mei-P26 regulates microRNAs and cell growth in the *Drosophila ovarian* stem cell lineage. *Nature* 454, 241–245. doi: 10.1038/nature07014

Ohlstein, B., and McKearin, D. (1997). Ectopic expression of the *Drosophila Bam* protein eliminates oogenic germline stem cells. *Development* 124, 3651–3662.

Olsen, L. C., Aasland, R., and Fjose, A. (1997). A vasa-like gene in zebrafish identifies putative primordial germ cells. *Mech. Dev.* 66, 95–105.

Ortega-Recalde, O., Day, R. C., Gemmell, N. J., and Hore, T. A. (2019). Zebrafish preserve global germline DNA methylation while sex-linked rDNA is amplified and demethylated during feminisation. *Nat. Commun.* 10:3053. doi: 10.1038/s41467-019-10894-7

Oulhen, N., Swartz, S. Z., Laird, J., Mascaro, A., and Wessel, G. M. (2017). Transient translational quiescence in primordial germ cells. *Development* 144, 1201–1210. doi: 10.1242/dev.144170

Ouyang, J. P. T., Folkmann, A., Bernard, L., Lee, C. Y., Seroussi, U., Charlesworth, A. G., et al. (2019). P Granules protect RNA interference genes from silencing by piRNAs. *Dev. Cell* 50, 716–728 e716. doi: 10.1016/j.devcel.2019.07.026

Piccioni, F., Ottone, C., Brescia, P., Pisa, V., Siciliano, G., Galasso, A., et al. (2009). The translational repressor Cup associates with the adaptor protein Miranda and the mRNA carrier Staufen at multiple time-points during *Drosophila oogenesis*. *Gene* 428, 47–52. doi: 10.1016/j.gene.2008.09.019

Piccioni, F., Zappavigna, V., and Verrotti, A. C. (2005). A cup full of functions. *RNA Biol.* 2, 125–128. doi: 10.4161/rna.2.4.2416

Putnam, A., and Seydoux, G. (2021). Cell-free reconstitution of multi-condensate assemblies. *Methods Enzymol.* 646, 83–113. doi: 10.1016/bs.mie.2020.07.004

Putnam, A., Cassani, M., Smith, J., and Seydoux, G. (2019). A gel phase promotes condensation of liquid P granules in *Caenorhabditis elegans* embryos. *Nat. Struct. Mol. Biol.* 26, 220–226. doi: 10.1038/s41594-019-0193-2

Raisch, T., Bhandari, D., Sabath, K., Helms, S., Valkov, E., Weichenrieder, O., et al. (2016). Distinct modes of recruitment of the CCR4-NOT complex by *Drosophila* and vertebrate Nanos. *EMBO J.* 35, 974–990. doi: 10.15252/embj.201593634

Reveal, B., Yan, N., Snee, M. J., Pai, C. I., Gim, Y., and Macdonald, P. M. (2010). BREs mediate both repression and activation of oskar mRNA translation and act in trans. *Dev. Cell* 18, 496–502. doi: 10.1016/j.devcel.2009.12.021

Rhiner, C., Diaz, B., Portela, M., Poyatos, J. F., Fernandez-Ruiz, I., Lopez-Gay, J. M., et al. (2009). Persistent competition among stem cells and their daughters in the *Drosophila ovary* germline niche. *Development* 136, 995–1006. doi: 10.1242/dev.033340

Rongo, C., Gavis, E. R., and Lehmann, R. (1995). Localization of oskar RNA regulates oskar translation and requires Oskar protein. *Development* 121, 2737–2746.

Rosario, R., Adams, I. R., and Anderson, R. A. (2016). Is there a role for DAZL in human female fertility? *Mol. Hum. Reprod.* 22, 377–383. doi: 10.1093/molehr/gaw024

Russell, J., and Zomerdijk, J. C. (2005). RNA-polymerase-I-directed rDNA transcription, life and works. *Trends Biochem. Sci.* 30, 87–96.

Saitou, M., and Miyauchi, H. (2016). Gametogenesis from pluripotent stem cells. *Cell Stem Cell* 18, 721–735. doi: 10.1016/j.stem.2016.05.001

Sanchez, C. G., Teixeira, F. K., Czech, B., Preall, J. B., Zamparini, A. L., Seifert, J. R., et al. (2016). Regulation of ribosome biogenesis and protein synthesis controls germline stem cell differentiation. *Cell Stem Cell* 18, 276–290. doi: 10.1016/j.stem.2015.11.004

Santos, M. G., Machado, A. Z., Martins, C. N., Domenice, S., Costa, E. M., Nishi, M. Y., et al. (2014). Homozygous inactivating mutation in NANOS3 in two sisters with primary ovarian insufficiency. *Biomed. Res. Int.* 2014:787465. doi: 10.1155/2014/787465

Seydoux, G. (2018). The P Granules of *C. elegans*: a genetic model for the study of RNA-protein condensates. *J. Mol. Biol.* 430, 4702–4710. doi: 10.1016/j.jmb.2018.08.007

Sgromo, A., Raisch, T., Backhaus, C., Keskeny, C., Alva, V., Weichenrieder, O., et al. (2018). Drosophila Bag-of-marbles directly interacts with the CAF40 subunit of the CCR4-NOT complex to elicit repression of mRNA targets. *RNA (New York, N.Y.)* 24, 381–395. doi: 10.1261/rna.064584.117

Shi, Z., and Barna, M. (2015). Translating the genome in time and space: specialized ribosomes, RNA regulons, and RNA-binding proteins. *Annu. Rev. Cell Dev. Biol.* 31, 31–54. doi: 10.1146/annurev-cellbio-100814-125346

Shi, Z., Fujii, K., Kovary, K. M., Genuth, N. R., Rost, H. L., Teruel, M. N., et al. (2017). Heterogeneous ribosomes preferentially translate distinct subpools of mRNAs genome-wide. *Mol. Cell* 67, 71–83 e77. doi: 10.1016/j.molcel.2017.05.021

Shin, H., Haupt, K. A., Kershner, A. M., Kroll-Conner, P., Wickens, M., and Kimble, J. (2017). SYGL-1 and LST-1 link niche signaling to PUF RNA repression for stem cell maintenance in *Caenorhabditis elegans*. *PLoS Genet.* 13:e1007121. doi: 10.1371/journal.pgen.1007121

Sieber, M. H., Thomsen, M. B., and Spradling, A. C. (2016). Electron transport chain remodeling by GSK3 during oogenesis connects nutrient state to reproduction. *Cell* 164, 420–432. doi: 10.1016/j.cell.2015.12.020

Slaidina, M., and Lehmann, R. (2014). Translational control in germline stem cell development. *J. Cell Biol.* 207, 13–21. doi: 10.1083/jcb.201407102

Smith, J. L., Wilson, J. E., and Macdonald, P. M. (1992). Overexpression of oskar directs ectopic activation of nanos and presumptive pole cell formation in *Drosophila embryos*. *Cell* 70, 849–859. doi: 10.1016/0092-8674(92)90318-7

Smith, J., Calidas, D., Schmidt, H., Lu, T., Rasoloson, D., and Seydoux, G. (2016). Spatial patterning of P granules by RNA-induced phase separation of the intrinsically-disordered protein MEG-3. *eLife* 5:e21337. doi: 10.7554/eLife.21337

Snee, M., Benz, D., Jen, J., and Macdonald, P. M. (2008). Two distinct domains of Bruno bind specifically to the oskar mRNA. *RNA Biol.* 5, 1–9.

Song, X., Wong, M. D., Kawase, E., Xi, R., Ding, B. C., McCarthy, J. J., et al. (2004). Bmp signals from niche cells directly repress transcription of a differentiation-promoting gene, bag of marbles, in germline stem cells in the *Drosophila ovary*. *Development* 131, 1353–1364. doi: 10.1242/dev.01026

Sonoda, J., and Wharton, R. P. (1999). Recruitment of nanos to hunchback mRNA by pumilio. *Genes Dev.* 13, 2704–2712. doi: 10.1101/gad.13.20.2704

Sousa Martins, J. P., Liu, X., Oke, A., Arora, R., Franciosi, F., Viville, S., et al. (2016). DAZL and CPEB1 regulate mRNA translation synergistically during oocyte maturation. *J. Cell Sci.* 129, 1271–1282. doi: 10.1242/jcs.179218

Spradling, A. C. (1993). "Developmental genetics of oogenesis," in *Development of Drosophila Melanogaster*, ed. M. Bate (Cold Spring Harbor, NY: Cold Spring Harbor Press), 1–70.

St Johnston, D., Beuchle, D., and Nusslein-Volhard, C. (1991). Staufen, a gene required to localize maternal RNAs in the *Drosophila* egg. *Cell* 66, 51–63. doi: 10.1016/0092-8674(91)90138-o

Subramaniam, K., and Seydoux, G. (1999). nos-1 and nos-2, two genes related to *Drosophila* nanos, regulate primordial germ cell development and survival in *Caenorhabditis elegans*. *Development* 126, 4861–4871.

Sugihara, Y., Honda, H., Iida, T., Morinaga, T., Hino, S., Okajima, T., et al. (2010). Proteomic analysis of rodent ribosomes revealed heterogeneity including ribosomal proteins L10-like, L22-like 1, and L39-like. *J. Proteome Res.* 9, 1351–1366. doi: 10.1021/pr9008964

Sun, F., Palmer, K., and Handel, M. A. (2010). Mutation of Eif4g3, encoding a eukaryotic translation initiation factor, causes male infertility and meiotic arrest of mouse spermatocytes. *Development* 137, 1699–1707. doi: 10.1242/dev.043125

Susor, A., Jansova, D., Anger, M., and Kubelka, M. (2016). Translation in the mammalian oocyte in space and time. *Cell Tissue Res.* 363, 69–84. doi: 10.1007/s00441-015-2269-6

Susor, A., Jansova, D., Cerna, R., Danylevska, A., Anger, M., Toralova, T., et al. (2015). Temporal and spatial regulation of translation in the mammalian oocyte via the mTOR-eIF4F pathway. *Nat. Commun.* 6:6078. doi: 10.1038/ncomms7078

Suzuki, A., Niimi, Y., Shinmyozu, K., Zhou, Z., Kiso, M., and Saga, Y. (2016). Dead end1 is an essential partner of NANOS2 for selective binding of target RNAs in male germ cell development. *EMBO Rep.* 17, 37–46. doi: 10.15252/embr.201540828

Suzuki, A., Tsuda, M., and Saga, Y. (2007). Functional redundancy among Nanos proteins and a distinct role of Nanos2 during male germ cell development. *Development* 134, 77–83. doi: 10.1242/dev.02697

Takei, N., Takada, Y., Kawamura, S., Sato, K., Saitoh, A., Bormann, J., et al. (2020). Changes in subcellular structures and states of pumilio 1 regulate the translation of target Mad2 and cyclin B1 mRNAs. *J. Cell Sci.* 133, jcs249128. doi: 10.1242/jcs.249128

Tang, W. W., Kobayashi, T., Irie, N., Dietmann, S., and Surani, M. A. (2016). Specification and epigenetic programming of the human germ line. *Nat. Rev. Genet.* 17, 585–600. doi: 10.1038/nrg.2016.88

Tastan, O. Y., Maines, J. Z., Li, Y., McKearin, D. M., and Buszczak, M. (2010). Drosophila ataxin 2-binding protein 1 marks an intermediate step in the

molecular differentiation of female germline cysts. *Development* 137, 3167–3176. doi: 10.1242/dev.050575

Tetkova, A., Susor, A., Kubelka, M., Nemcova, L., Jansova, D., Dvoran, M., et al. (2019). Follicle-stimulating hormone administration affects amino acid metabolism in mammalian oocytesdagger. *Biol. Reprod.* 101, 719–732. doi: 10.1093/biolre/ioz117

Tian, Q., Kopf, G. S., Brown, R. S., and Tseng, H. (2001). Function of basonuclin in increasing transcription of the ribosomal RNA genes during mouse oogenesis. *Development* 128, 407–416.

Toyooka, Y., Tsunekawa, N., Takahashi, Y., Matsui, Y., Satoh, M., and Noce, T. (2000). Expression and intracellular localization of mouse Vasa-homologue protein during germ cell development. *Mech. Dev.* 93, 139–149. doi: 10.1016/s0925-4773(00)00283-5

Trcek, T., Douglas, T. E., Grosch, M., Yin, Y., Eagle, W. V. I., Gavis, E. R., et al. (2020). Sequence-independent self-assembly of germ granule mRNAs into homotypic clusters. *Mol. Cell* 78, 941–950 e912. doi: 10.1016/j.molcel.2020.05.008

Trcek, T., Grosch, M., York, A., Shroff, H., Lionnet, T., and Lehmann, R. (2015). *Drosophila* germ granules are structured and contain homotypic mRNA clusters. *Nat. Commun.* 6:7962. doi: 10.1038/ncomms8962

Tsai-Morris, C. H., Sheng, Y., Lee, E., Lei, K. J., and Dufau, M. L. (2004). Gonadotropin-regulated testicular RNA helicase (GRTH/Ddx25) is essential for spermatid development and completion of spermatogenesis. *Proc. Natl. Acad. Sci. U.S.A.* 101, 6373–6378. doi: 10.1073/pnas.0401855101

Tsuda, M., Sasaoka, Y., Kiso, M., Abe, K., Haraguchi, S., Kobayashi, S., et al. (2003). Conserved role of nanos proteins in germ cell development. *Science* 301, 1239–1241. doi: 10.1126/science.1085222

Updike, D. L., Knutson, A. K., Egelhofer, T. A., Campbell, A. C., and Strome, S. (2014). Germ-granule components prevent somatic development in the *C. elegans* germline. *Curr. Biol.* 24, 970–975. doi: 10.1016/j.cub.2014.03.015

Uversky, V. N., Kuznetsova, I. M., Turoverov, K. K., and Zaslavsky, B. (2015). Intrinsically disordered proteins as crucial constituents of cellular aqueous two phase systems and coacervates. *FEBS Lett.* 589, 15–22. doi: 10.1016j.febslet.2014.11.028

Uyhazi, K. E., Yang, Y., Liu, N., Qi, H., Huang, X. A., Mak, W., et al. (2020). Pumilio proteins utilize distinct regulatory mechanisms to achieve complementary functions required for pluripotency and embryogenesis. *Proc. Natl. Acad. Sci. U.S.A.* 117, 7851–7862. doi: 10.1073/pnas.1916471117

Vazquez-Pianzola, P., Urlaub, H., and Suter, B. (2011). Pabp binds to the osk 3′UTR and specifically contributes to osk mRNA stability and oocyte accumulation. *Dev. Biol.* 357, 404–418. doi: 10.1016/j.ydbio.2011.07.009

Verrotti, A. C., and Wharton, R. P. (2000). Nanos interacts with cup in the female germline of *Drosophila*. *Development* 127, 5225–5232.

Voronina, E., Seydoux, G., Sassone-Corsi, P., and Nagamori, I. (2011). RNA granules in germ cells. *Cold Spring Harb. Perspect. Biol.* 3:a002774. doi: 10.1101/cshperspect.a002774

Wakefield, L., and Gurdon, J. B. (1983). Cytoplasmic regulation of 5S RNA genes in nuclear-transplant embryos. *EMBO J.* 2, 1613–1619.

Wang, C., and Lehmann, R. (1991). Nanos is the localized posterior determinant in *Drosophila*. *Cell* 66, 637–647. doi: 10.1016/0092-8674(91)90110-k

Wang, J. T., and Seydoux, G. (2013). Germ cell specification. *Adv. Exp. Med. Biol.* 757, 17–39. doi: 10.1007/978-1-4614-4015-4_2

Wang, J. T., and Seydoux, G. (2014). P granules. *Curr. Biol.* 24, R637–R638. doi: 10.1016/j.cub.2014.06.018

Wang, M., and Lemos, B. (2017). Ribosomal DNA copy number amplification and loss in human cancers is linked to tumor genetic context, nucleolus activity, and proliferation. *PLoS Genet.* 13:e1006994. doi: 10.1371/journal.pgen.1006994

Wang, T., and Na, J. (2021). Fibrillarin-GFP facilitates the identification of meiotic competent oocytes. *Front. Cell Dev. Biol.* 9:648331. doi: 10.3389/fcell.2021.648331

Wang, X., and Voronina, E. (2020). Diverse roles of PUF proteins in germline stem and progenitor cell development in *C. elegans*. *Front. Cell Dev. Biol.* 8:29. doi: 10.3389/fcell.2020.00029

Wang, X., Ellenbecker, M., Hickey, B., Day, N. J., Osterli, E., Terzo, M., et al. (2020). Antagonistic control of *Caenorhabditis elegans* germline stem cell proliferation and differentiation by PUF proteins FBF-1 and FBF-2. *eLife* 9:e52788. doi: 10.7554/eLife.52788

Warmerdam, D. O., and Wolthuis, R. M. F. (2019). Keeping ribosomal DNA intact: a repeating challenge. *Chromosome Res.* 27, 57–72. doi: 10.1007/s10577-018-9594-z

Watanabe, M., Zinn, A. R., Page, D. C., and Nishimoto, T. (1993). Functional equivalence of human X- and Y-encoded isoforms of ribosomal protein S4 consistent with a role in Turner syndrome. *Nat. Genet.* 4, 268–271. doi: 10.1038/ng0793-268

Weaver, L. N., and Drummond-Barbosa, D. (2018). Maintenance of proper germline stem cell number requires adipocyte collagen in adult *Drosophila* females. *Genetics* 209, 1155–1166. doi: 10.1534/genetics.118.301137

Weaver, L. N., and Drummond-Barbosa, D. (2019). The nuclear receptor seven up functions in adipocytes and oenocytes to control distinct steps of *Drosophila oogenesis*. *Dev. Biol.* 456, 179–189. doi: 10.1016/j.ydbio.2019.08.015

Weaver, L. N., and Drummond-Barbosa, D. (2020). The nuclear receptor seven up regulates genes involved in immunity and xenobiotic response in the adult drosophila female fat body. *G3 (Bethesda)* 10, 4625–4635. doi: 10.1534/g3.120.401745

Weaver, L. N., and Drummond-Barbosa, D. (2021). Hormone receptor 4 is required in muscles and distinct ovarian cell types to regulate specific steps of *Drosophila oogenesis*. *Development* 148:dev198663. doi: 10.1242/dev.198663

Wegnez, M., and Monier, R. (1972). Sequence heterogeneity of 5 S RNA in *Xenopus laevis*. *FEBS Lett.* 25, 13–20. doi: 10.1016/0014-5793(72)80443-5

Weidmann, C. A., Qiu, C., Arvola, R. M., Lou, T.-F., Killingsworth, J., Campbell, Z. T., et al. (2016). *Drosophila* Nanos acts as a molecular clamp that modulates the RNA-binding and repression activities of *Pumilio*. *eLife* 5:e17096. doi: 10.7554/eLife.17096

Wessel, G. M. (2016). Germ line mechanics–and unfinished business. *Curr. Top. Dev. Biol.* 117, 553–566. doi: 10.1016/bs.ctdb.2015.11.030

Wigglesworth, K., Lee, K. B., O'Brien, M. J., Peng, J., Matzuk, M. M., and Eppig, J. J. (2013). Bidirectional communication between oocytes and ovarian follicular somatic cells is required for meiotic arrest of mammalian oocytes. *Proc. Natl. Acad. Sci. U.S.A.* 110, E3723–E3729. doi: 10.1073/pnas.1314829110

Wilhelm, J. E., Buszczak, M., and Sayles, S. (2005). Efficient protein trafficking requires trailer hitch, a component of a ribonucleoprotein complex localized to the ER in *Drosophila*. *Dev. Cell* 9, 675–685. doi: 10.1016/j.devcel.2005.09.015

Wilhelm, J. E., Hilton, M., Amos, Q., and Henzel, W. J. (2003). Cup is an eIF4E binding protein required for both the translational repression of oskar and the recruitment of Barentsz. *J. Cell Biol.* 163, 1197–1204. doi: 10.1083/jcb.200309088

Wong, L. C., and Schedl, P. (2011). Cup blocks the precocious activation of the orb autoregulatory loop. *PLoS One* 6:e28261. doi: 10.1371/journal.pone.0028261

Wormington, W. M., and Brown, D. D. (1983). Onset of 5 S RNA gene regulation during *Xenopus* embryogenesis. *Dev. Biol.* 99, 248–257. doi: 10.1016/0012-1606(83)90273-7

Wright, D., Kiso, M., and Saga, Y. (2021). Genetic and structural analysis of the in vivo functional redundancy between murine NANOS2 and NANOS3. *Development* 148:dev191916. doi: 10.1242/dev.191916

Wu, X., Wang, B., Dong, Z., Zhou, S., Liu, Z., Shi, G., et al. (2013). A NANOS3 mutation linked to protein degradation causes premature ovarian insufficiency. *Cell Death Dis.* 4:e825. doi: 10.1038/cddis.2013.368

Xiol, J., Spinelli, P., Laussmann, M. A., Homolka, D., Yang, Z., Cora, E., et al. (2014). RNA clamping by Vasa assembles a piRNA amplifier complex on transposon transcripts. *Cell* 157, 1698–1711. doi: 10.1016/j.cell.2014.05.018

Xu, E. Y., Chang, R., Salmon, N. A., and Reijo Pera, R. A. (2007). A gene trap mutation of a murine homolog of the *Drosophila* stem cell factor *Pumilio* results in smaller testes but does not affect litter size or fertility. *Mol. Reprod. Dev.* 74, 912–921. doi: 10.1002/mrd.20687

Xue, S., and Barna, M. (2012). Specialized ribosomes: a new frontier in gene regulation and organismal biology. *Nat. Rev. Mol. Cell Biol.* 13, 355–369. doi: 10.1038/nrm3359

Yajima, M., and Wessel, G. M. (2011). The multiple hats of Vasa: its functions in the germline and in cell cycle progression. *Mol. Reprod. Dev.* 78, 861–867. doi: 10.1002/mrd.21363

Yamaguchi, T., Taguchi, A., Watanabe, K., and Orii, H. (2013). DEADSouth protein localizes to germ plasm and is required for the development of primordial germ cells in *Xenopus laevis*. *Biol. Open* 2, 191–199. doi: 10.1242/bio.20123111

Yang, C. R., Rajkovic, G., Daldello, E. M., Luong, X. G., Chen, J., and Conti, M. (2020). The RNA-binding protein DAZL functions as repressor and activator

of mRNA translation during oocyte maturation. *Nat. Commun.* 11:1399. doi: 10.1038/s41467-020-15209-9

Yurttas, P., Vitale, A. M., Fitzhenry, R. J., Cohen-Gould, L., Wu, W., Gossen, J. A., et al. (2008). Role for PADI6 and the cytoplasmic lattices in ribosomal storage in oocytes and translational control in the early mouse embryo. *Development* 135, 2627–2636. doi: 10.1242/dev.016329

Zamore, P. D., Williamson, J. R., and Lehmann, R. (1997). The Pumilio protein binds RNA through a conserved domain that defines a new class of RNA-binding proteins. *RNA* 3, 1421–1433.

Zappavigna, V., Piccioni, F., Villaescusa, J. C., and Verrotti, A. C. (2004). Cup is a nucleocytoplasmic shuttling protein that interacts with the eukaryotic translation initiation factor 4E to modulate *Drosophila* ovary development. *Proc. Natl. Acad. Sci. U.S.A.* 101, 14800–14805. doi: 10.1073/pnas.0406451101

Zhang, M., Chen, D., Xia, J., Han, W., Cui, X., Neuenkirchen, N., et al. (2017). Post-transcriptional regulation of mouse neurogenesis by *Pumilio* proteins. *Genes Dev.* 31, 1354–1369. doi: 10.1101/gad.298752.117

Zhang, Q., Shalaby, N. A., and Buszczak, M. (2014). Changes in rRNA transcription influence proliferation and cell fate within a stem cell lineage. *Science* 343, 298–301. doi: 10.1126/science.1246384

Conflict of Interest: The authors declare that the research was conducted in the absence of any commercial or financial relationships that could be construed as a potential conflict of interest.

The reviewer PR declared a past co-authorship with the author MB to the handling editor.

frontiers | Frontiers in Cell and Developmental Biology

MINI REVIEW
published: 26 April 2022
doi: 10.3389/fcell.2022.713650

The Role of T Cells in Ovarian Physiology and Infertility

*Laura O. Knapik[1], Shubangi Paresh[2], Dalileh Nabi[3] and Lynae M. Brayboy[3,4]**

[1]University of New England, Biddeford, ME, United States, [2]Crimson Global Academy, Queen Creek, AZ, United States, [3]Department of Neuropediatrics Charité-Universitätsmedizin Berlin, Freie Universität Berlin, Humboldt-Universität zu Berlin, and Berlin Institute of Health, Berlin, Germany, [4]Department of Reproductive Biology, Bedford Research Foundation, Bedford, MA, United States

Infertility affects one in six couples worldwide, with more than 48 million couples affected internationally. The prevalence of infertility is increasing which is thought to be attributed to delayed child-bearing due to socioeconomic factors. Since women are more prone to autoimmune diseases, we sought to describe the correlation between ovarian-mediated infertility and autoimmunity, and more specifically, the role of T cells in infertility. T cells prevent autoimmune diseases and allow maternal immune tolerance of the semi-allogeneic fetus during pregnancy. However, the role of T cells in ovarian physiology has yet to be fully understood.

Keywords: T cells, ovary, female infertility, autoimmune disease, aging

OPEN ACCESS

Edited by:
Miguel Angel Brieño-Enriquez, Magee-Womens Research Institute, United States

Reviewed by:
Srinivasa Reddy Bonam, Institut National de la Santé et de la Recherche Médicale (INSERM), France
Joshua Johnson, University of Colorado Denver, United States

****Correspondence:***
Lynae M. Brayboy
lynae.brayboy@charite.de

Specialty section:
This article was submitted to Cellular Biochemistry, a section of the journal Frontiers in Cell and Developmental Biology

Received: *23 May 2021*
Accepted: *29 March 2022*
Published: *26 April 2022*

Citation:
Knapik LO, Paresh S, Nabi D and Brayboy LM (2022) The Role of T Cells in Ovarian Physiology and Infertility. Front. Cell Dev. Biol. 10:713650. doi: 10.3389/fcell.2022.713650

INTRODUCTION

Age-Related Infertility

Infertility is a disease that impacts one in six couples worldwide. Approximately 48 million couples and 186 million individuals are affected by infertility globally (WHO, 2021). Although prevalent, little is known about the underlying contribution of age-related infertility. This topic is becoming increasingly important as many people opt to delay childbearing due to cultural and socioeconomic factors (Balasch and Gratacós, 2012). While there are some clinical interventions to circumvent age-related infertility, assisted reproductive technologies (ART) are largely inaccessible to much of the global population due to need for specially trained physicians, excessive cost, and extensive laboratory equipment with trained embryologists (Fleetwood et al., 2010; SART, 2021). Age-related decline in oocyte quantity and quality is observed in ovarian physiology, which can lead to infertility as women approach the climacteric. Some women may become prematurely infertile due to diminished ovarian reserve (DOR), which describes a decline in oocyte quantity earlier than physiologically expected (Pastore et al., 2018). The definition of DOR is varied and a precise etiology has yet to be identified. Patients diagnosed with DOR are sometimes unable to utilize ART to overcome infertility, as the disease is known to have a reduced response to ovarian stimulation (Ata et al., 2019). However, young women (<35 years old) with DOR have a better chance of pregnancy compared to aged counterparts, as the quality of the oocyte is not compromised, even though the quantity is. Therefore, age plays a quintessential role in infertility (Pastore et al., 2018). Despite technological advancements, the basic mechanisms of ovarian aging are still not fully understood, and even less is known about the interplay between the immune system and ovarian aging.

Chronic Inflammation in Infertility

There are multiple theories suggesting a mechanism of decreased oocyte quality in relation to age (Ge et al., 2015). One widely held theory, the limited pool theory, states that oocyte quality is affected by an altered hormonal environment, which is thought to be caused in part by DOR. In the limited pool theory there is a smaller pool of oocytes and an altered hormonal environment, which may alter cellular function.

For example increased levels of FSH in DOR might rescue defective oocytes and allow them to resume meiosis. Otherwise, these gametes would undergo apoptosis. However, because of FSH's effects on microtubules, a higher FSH may enhance aneuploidy in oocytes (Dursun et al., 2006; Xu et al., 2011). Taken together, increased FSH allows oogenesis to progress in DOR, but at the cost of chromosomally abnormal oocytes. An alternate theory clashes with the limited pool theory, and states that oocyte quality is affected as physical damage accumulates over time (Zhang et al., 2020).

A less studied theory is the inflammatory theory of aging, dubbed "inflammaging" which has emerging data linking aging with significant immune cell populations in the ovary (Franceschi and Campisi, 2014; Briley et al., 2016). Inflammaging is human aging characterized by low-grade, chronic inflammation (Franceschi and Campisi, 2014). It can be explained using the free radical theory of aging, which illustrates the negative impact of aging on the body (Fulop et al., 2014). Free radical theory of aging states that free radicals, from the environment as well as internal metabolism, cause oxidative damage to cellular elements which, over time, results in an accumulation of structural and functional errors in the body (Pomatto and Davies, 2018). The ovaries are not excluded from this process, and are susceptible to inflammatory damage.

There is emerging evidence regarding resident immune cell populations within the ovary (Briley et al., 2016; Zhang et al., 2020). Previous study has hypothesized early development of a limited pool of ovary-committed bone marrow cells during embryogenesis (Bukovsky and Caudle, 2012). Once depleted, a process that can occur physiologically through aging or pathologically (ie following induction of chemotherapies), oogenesis and follicular restoration are unable to proceed. This demonstrates a fundamental link between ovarian health and the immune system. In addition to aging other examples of chronic inflammation, such as obesity-related inflammation, affect ovarian function as well as oocyte quality (Snider and Wood, 2019). Autoimmune diseases, which by definition are highly inflammatory processes, have been linked to DOR (Sharif et al., 2019). An estimated 10–40% of women with ovarian insufficiency are also diagnosed with an autoimmune disease (Sharif et al., 2019). An astounding 40% of patients diagnosed with autoimmune polyglandular syndrome type 1 (APS-1) are also diagnosed with DOR. APS-1 is a multi-organ, autosomal recessive mutation of the autoimmune regulator gene (AIRE) that directly dysregulates T cell function. Given this link between immunity, specifically T cell failure, and DOR, it is critical to further elucidate the role of T cell biology in the ovary.

T Cells in the Ovary

T cells are resident white blood cells present in the body and the ovary, but very little has been reported about their physiologic role in normal ovarian function. T cells are derived from the bone marrow and are further developed in the thymus to supply the periphery with mature, self-replicating T cells (Hong, 2001). Specifically, the thymus provides a location for antigen presenting cells (APCs) to present antigenic material to naïve T cells, thus promoting T cell maturation and the cell's ability to distinguish between self and non-self antigens, a process known as tolerance (Krueger et al., 2017; Verma and Kelleher, 2017). There are three subsets of T cells: T helper cells, cytotoxic cells and regulatory T cells (Tregs), that all function as critical effectors of the immune response (Gagliani et al., 2017).

Immune cells, particularly Tregs, play a crucial role in the tolerance of allogeneic pregnancy- related tissues and autologous oocytes (Guerin et al., 2009). Maternal immune tolerance of paternal MHCs is important for pregnancy success and fetal survival, as there is evidence of activation against male gametes by the maternal system (Guerin et al., 2009). Therefore, Treg cells may prevent miscarriages that are caused by maternal rejection in humans (Saito et al., 2007). There is evidence demonstrating Tregs in the ovaries are more potent suppressors of autoimmunity than in Tregs in males (Hong, 2001). In a mouse model, when the thymus was removed shortly after birth, spontaneous ovarian autoimmune disease occurred (Samy et al., 2006). Dysregulation of Tregs is thought to be the basis of autoimmune disease establishment and advancement. Autoimmune diseases tend to be more prevalent in women compared to men, and approximately 80% of patients diagnosed with autoimmune diseases identify as female (Ngo et al., 2014; Angum et al., 2020). In thyroidectomized female mice, $CD4^+$ and $CD25^+$ T cell rescue effectively inhibited autoimmune ovarian disease progression compared to thyroidectomized controls (Alard et al., 2001). Clinically, autoantibodies in the ovary are commonly associated with unexplained infertility (Luborsky, 2002). The ovaries are not an immunologically privileged organ and so, a slight variation in tolerogenic, ovary-specific, antigens can have significant negative effects on fertility (Warren et al., 2014). Interestingly, there is a conspicuous population of T cells within the ovary. In a previous study, ovarian cortex samples from 21 healthy, human patients of reproductive age (20–37 years of age) were analyzed via single cell mRNA sequencing for markers selected to identify distinct cell populations (Wagner et al., 2020). Within the study, a small population of immunologic cells were identified, including markers specific to T cells. This finding demonstrates the presence of immunologic cells, such as T cells, within the physiologically competent ovary. An additional study using tissue samples from the medulla of five human ovaries identified a significant cluster of T cells, which constitute approximately 6.2% of the ovary, through single cell RNA sequencing (Wagner et al., 2020; UCSC, 2022). A recent elegant body of work by Ma et al. extrapolated the ovarian gene expression of young (5–6 months) and aged (21–22 months) mice to further identify markers of ovarian aging. Within this study, a significant proportion of differentially expressed genes between the two populations were related to immune function, and aged mice had significantly lower values of naïve $CD4^+$ T cells compared to their younger counterparts. This provides further evidence that naïve $CD4^+$ T cells play a fundamental role in ovarian aging, and decreased presence may represent decreased ability to mount an immune response, perhaps contributing to diminished fertility associated with age (Ma et al., 2020). Taken together, these studies indicate an exigent need to understand the mechanism of T cell regulation in the ovary, as there are potential implications for ovarian disease and fertility outcomes.

T CELLS IN OVARIAN DISEASE

There is a paucity of data regarding the normal, physiologic mechanism of T cell activity in the ovary. However, there is evidence that T cells are involved in the pathogenesis of several

chronic ovarian diseases. It is important to note that it is difficult to distinguish the T cells presence as causal or reactive in both autoimmune processes or metabolic disorders that impact the ovary. Herein we describe some of these disorders:

Autoimmune Oophoritis

Autoimmune oophoritis is a rare, autoimmune disorder resulting in destruction of the ovary that clinically presents with amenorrhea and infertility (Jacob and Koc, 2015). Approximately 5% of people diagnosed with DOR are suspected to carry an autoimmune oophoritis diagnosis (Silva et al., 2014). Diagnosis is made by detecting antibodies in the serum that act against ovarian tissues, in part because the ovaries are difficult to access without surgical intervention (Warren et al., 2014). Very little has been elucidated regarding the mechanism, and specific antigenic target of autoimmune oophoritis. In an animal model, transgenic expression of maternal antigen that embryos require (MATER) was unable to completely prevent autoimmune oophoritis disease progression, suggesting multiple antigenic targets are at play (Otsuka et al., 2011). Histological study has revealed T cells are present in the inflammatory infiltrate of inflicted ovaries (Silva et al., 2014). This demonstrates a need to further understand normal T cell biology, and how this process may go awry resulting in autoimmune oophoritis.

Polycystic Ovary Syndrome

Despite polycystic ovary syndrome (PCOS) being the most common endocrine disorder in women, with a prevalence ranging from 6 to 15% depending on the diagnostic criteria employed, a clear etiology for this heterogeneous disease has yet to be determined (Fauser et al., 2012). The diagnosis of PCOS is a diagnosis of exclusion that must have two out of three consensus criteria including: hyperandrogenism, anovulation or oligovulation, or characteristic ovarian morphology on ultrasound (Legro et al., 2013). PCOS is associated with infertility, 70–80% of individuals diagnosed with the disease struggle with diminished fertility (Ata et al., 2019). However, many organ systems are also impacted, and the overall health of a person with PCOS is compromised throughout their reproductive lifespan. Therefore, PCOS may represent a model for how an ovarian manifestation of a disease may foreshadow somatic disease and long-term non-reproductive clinical sequelae. There have been some reports associated with T cells in the ovaries of patients that suffer from polycystic ovarian syndrome. Specifically, reports of abnormal T cell activation and cytokine production were detected in the follicular fluid of patients diagnosed with PCOS compared to non-PCOS healthy controls (Li et al., 2019).

Ovarian Cancer

Ovarian cancer is the most lethal gynecologic malignancy and is defined as an immunogenic tumor that triggers a natural antitumor immune response against it (Wang et al., 2018). Numerous papers have published a relationship between the ovary and T cells in ovarian cancer, specifically implying that T cells are heavily implicated in ovarian dysgenesis. However, few, if any papers address how T cells could be involved in the molecular mechanism of carcinogenesis of the ovary. One suggested mechanism is that tumor-specific antigens, processed via antigen presenting cells, are presented to T-cells which then activate $CD8^+$ cytotoxic T-cells and $CD4^+$ helper T-cells, which then infiltrate in the tumor. $CD8^+$ cytotoxic T-cells directly target tumor cells whereas, $CD4^+$ helper T-cells regulate an immune response by secreting cytokines that stimulate other immune cells (Westergaard et al., 2019). Thus, tumor-infiltrating T-cells, particularly $CD4^+$ and $CD8^+$ T cells are important predictors of ovarian cancer.

DISCUSSION

Given the burgeoning data suggesting the role of T cells in the ovary, it seems increased discussion and collaboration are needed to understand the complexity of the ovarian immunologic microenvironment. While *in vitro* fertilization (IVF) has afforded relief for many individuals with involuntary childlessness, it must be said that IVF, by all intents and purposes, is a primitive remedy in that it is unable to remediate previously damaged oocytes, potentially including oocytes that may be altered after residing in an immunologically compromised ovary. Further, immunological maladies impacting the ovary lead not only to infertility, but long-term health sequelae that impact women. Therefore, further funding and study is needed to examine the role of T cells in the normal ovarian physiology so that we can manipulate these processes to improve not only reproductive outcomes, but also improve the health of people with ovaries.

AUTHOR CONTRIBUTIONS

SP: literature review and manuscript writing LK: manuscript writing, checking references and editing DN: manuscript writing, checking references and editing LB: literature review and manuscript writing.

FUNDING

Global Consortium for Reproductive Longevity and Equality Junior Scholar Award to LB.

REFERENCES

Alard, P., Thompson, C., Agersborg, S. S., Thatte, J., Setiady, Y., Samy, E., et al. (2001). Endogenous Oocyte Antigens Are Required for Rapid Induction and Progression of Autoimmune Ovarian Disease Following Day-3 Thymectomy. *J. Immunol.* 166, 4363–4369. doi:10.4049/jimmunol.166.7.4363

Angum, F., Khan, T., Kaler, J., Siddiqui, L., and Hussain, A. (2020). The Prevalence of Autoimmune Disorders in Women: A Narrative Review. *Cureus* 12 (5), e8094. doi:10.7759/cureus.8094

Ata, B., Seyhan, A., and Seli, E. (2019). Diminished Ovarian reserve versus Ovarian Aging: Overlaps and Differences. *Curr. Opin. Obstet. Gynecol.* 31, 139–147. doi:10.1097/gco.0000000000000536

Balasch, J., and Gratacós, E. (2012). Delayed Childbearing. *Curr. Opin. Obstet. Gynecol.* 24, 187–193. doi:10.1097/gco.0b013e3283517908

Briley, S. M., Jasti, S., McCracken, J. M., Hornick, J. E., Fegley, B., Pritchard, M. T., et al. (2016). Reproductive Age-Associated Fibrosis in the Stroma of the Mammalian Ovary. *Reproduction* 52 (3), 245–260. doi:10.1530/rep-16-0129

Bukovsky, A., and Caudle, M. R. (2012). Immunoregulation of Follicular Renewal, Selection, POF, and Menopause *In Vivo*, vs. Neo-Oogenesis *In Vitro*, POF and Ovarian Infertility Treatment, and a Clinical Trial. *Reprod. Biol. Endocrinol.* 10, 97. doi:10.1186/1477-7827-10-97

Dursun, P., Gultekin, M., Yuce, K., and Ayhan, A. (2006). What Is the Underlying Cause of Aneuploidy Associated with Increasing Maternal Age? Is it Associated with Elevated Levels of Gonadotropins? *Med. Hypotheses* 66 (1), 143–147. doi:10.1016/j.mehy.2004.10.022

Fauser, B. C. J. M., Tarlatzis, B. C., Rebar, R. W., Legro, R. S., Balen, A. H., Lobo, R., et al. (2012). Consensus on Women's Health Aspects of Polycystic Ovary Syndrome (PCOS): the Amsterdam ESHRE/ASRM-Sponsored 3rd PCOS Consensus Workshop Group. *Fertil. Sterility* 97, 28–38. e25. doi:10.1016/j.fertnstert.2011.09.024

Fleetwood, A., and Campo-Engelstein, L. (2010). "The Impact of Infertility: Why ART Should Be a Higher Priority for Women in the Global South," in *Oncofertility*. Editors T. K. Woodruff, L. Zoloth, L. Campo-Engelstein, and S. Rodriguez (Springer US), 156 237–248. doi:10.1007/978-1-4419-6518-9_18

Franceschi, C., and Campisi, J. (2014). Chronic Inflammation (Inflammaging) and its Potential Contribution to Age-Associated Diseases. *J. Gerontol. A. Biol. Sci. Med. Sci.* 69, S4–S9. doi:10.1093/gerona/glu057(

Fulop, T., Witkowski, J. M., Pawelec, G., Alan, C., and Larbi, A. (2014). "On the Immunological Theory of Aging," in *Interdisciplinary Topics in Gerontology*. Editors L. Robert and T. Fulop (Karger), 163–176. vol. 39. doi:10.1159/000358904

Gagliani, N., and Huber, S. (2017). "Basic Aspects of T Helper Cell Differentiation," in *T-cell Differentiation*. Editor E. Lugli (New York: Springer), 1514, 19–30. doi:10.1007/978-1-4939-6548-9_2

Ge, Z.-J., Schatten, H., Zhang, C.-L., and Sun, Q.-Y. (2015). Oocyte Ageing and Epigenetics. *REPRODUCTION* 149, R103–R114. doi:10.1530/rep-14-0242

Guerin, L. R., Prins, J. R., and Robertson, S. A. (2009). Regulatory T-Cells and Immune Tolerance in Pregnancy: a New Target for Infertility Treatment? *Hum. Reprod. Update* 15, 517–535. doi:10.1093/humupd/dmp004

Hong, R. (2001). The Thymus. Finally Getting Some Respect. *Chest Surg. Clin. N. Am.* 11, 295–310.

Jacob, S., and Koc, M. (2015). Autoimmune Oophoritis: A Rarely Encountered Ovarian Lesion. *Indian J. Pathol. Microbiol.* 58, 249–251. doi:10.4103/0377-4929.155335

Krueger, A., Ziętara, N., and Łyszkiewicz, M. (2017). T Cell Development by the Numbers. *Trends Immunol.* 38, 128–139. doi:10.1016/j.it.2016.10.007

Legro, R. S., Arslanian, S. A., Ehrmann, D. A., Hoeger, K. M., Murad, M. H., Pasquali, R., et al. and Endocrine Society (2013). Diagnosis and Treatment of Polycystic Ovary Syndrome: An Endocrine Society Clinical Practice Guideline. *J. Clin. Endocrinol. Metab.* 98, 4565–4592. doi:10.1210/jc.2013-2350

Li, Z., Peng, A., Feng, Y., Zhang, X., Liu, F., Chen, C., et al. (2019). Detection of T Lymphocyte Subsets and Related Functional Molecules in Follicular Fluid of Patients with Polycystic Ovary Syndrome. *Sci. Rep.* 9, 6040. doi:10.1038/s41598-019-42631-x

Luborsky, J. (2002). Ovarian Autoimmune Disease and Ovarian Autoantibodies. *J. Women's Health Gender-Based Med.* 11, 585–599. doi:10.1089/152460902760360540

Ma, L., Lu, H., Chen, R., Wu, M., Jin, Y., Zhang, J., et al. (2020). Identification of Key Genes and Potential New Biomarkers for Ovarian Aging: A Study Based on RNA-Sequencing Data. *Front. Genet.* 11, 590660. doi:10.3389/fgene.2020.590660

Ngo, S. T., Steyn, F. J., and McCombe, P. A. (2014). Gender Differences in Autoimmune Disease. *Front. Neuroendocrinology* 35, 347–369. doi:10.1016/j.yfrne.2014.04.004

Otsuka, N., Tong, Z.-B., Vanevski, K., Tu, W., Cheng, M. H., and Nelson, L. M. (2011). Autoimmune Oophoritis with Multiple Molecular Targets Mitigated by Transgenic Expression of Mater. *Endocrinology* 152, 2465–2473. doi:10.1210/en.2011-0022

Pastore, L. M., Christianson, M. S., Stelling, J., Kearns, W. G., and Segars, J. H. (2018). Reproductive Ovarian Testing and the Alphabet Soup of Diagnoses: DOR, POI, POF, POR, and FOR. *J. Assist. Reprod. Genet.* 35, 17–23. doi:10.1007/s10815-017-1058-4

Pomatto, L. C. D., and Davies, K. J. A. (2018). Adaptive Homeostasis and the Free Radical Theory of Ageing. *Free Radic. Biol. Med.* 124, 420–430. doi:10.1016/j.freeradbiomed.2018.06.016

Saito, S., Shima, T., Nakashima, A., Shiozaki, A., Ito, M., and Sasaki, Y. (2007). What Is the Role of Regulatory T Cells in the success of Implantation and Early Pregnancy? *J. Assist. Reprod. Genet.* 24, 379–386. doi:10.1007/s10815-007-9140-y

Samy, E. T., Setiady, Y. Y., Ohno, K., Pramoonjago, P., Sharp, C., and Tung, K. S. K. (2006). The Role of Physiological Self-Antigen in the Acquisition and Maintenance of Regulatory T-Cell Function. *Immunol. Rev.* 212, 170–184. doi:10.1111/j.0105-2896.2006.00404.x

SART (2021). Frequently Asked Questions. Available at: https://www.sart.org/patients/frequently-asked-questions/.

Sharif, K., Watad, A., Bridgewood, C., Kanduc, D., Amital, H., and Shoenfeld, Y. (2019). Insights into the Autoimmune Aspect of Premature Ovarian Insufficiency. *Best Pract. Res. Clin. Endocrinol. Metab.* 33, 101323. doi:10.1016/j.beem.2019.101323

Silva, C. A., Yamakami, L. Y., Aikawa, N. E., Araujo, D. B., Carvalho, J. F., and Bonfá, E. (2014). Autoimmune Primary Ovarian Insufficiency. *Autoimmun. Rev.* 13 (4-5), 427–430. doi:10.1016/j.autrev.2014.01.003

Snider, A. P., and Wood, J. R. (2019). Obesity Induces Ovarian Inflammation and Reduces Oocyte Quality. *Reproduction* 158, R79–R90. doi:10.1530/rep-18-0583

UCSC (2022). UCSC Cell Browser. Available at: https://cells.ucsc.edu/?ds=scarface+adult_ovary#.

Verma, N. K., and Kelleher, D. (2017). Not Just an Adhesion Molecule: LFA-1 Contact Tunes the T Lymphocyte Program. *J.I.* 199, 1213–1221. doi:10.4049/jimmunol.1700495

Wagner, M., Yoshihara, M., Douagi, I., Damdimopoulos, A., Panula, S., Petropoulos, S., et al. (2020). Single-cell Analysis of Human Ovarian Cortex Identifies Distinct Cell Populations but No Oogonial Stem Cells. *Nat. Commun.* 11, 1147. doi:10.1038/s41467-020-14936-3

Wang, W., Zou, W., and Liu, J. R. (2018). Tumor-infiltrating T Cells in Epithelial Ovarian Cancer: Predictors of Prognosis and Biological Basis of Immunotherapy. *Gynecol. Oncol.* 151, 1–3. doi:10.1016/j.ygyno.2018.09.005

Warren, B. D., Kinsey, W. K., McGinnis, L. K., Christenson, L. K., Jasti, S., Stevens, A. M., et al. (2014). Ovarian Autoimmune Disease: Clinical Concepts and Animal Models. *Cell. Mol. Immunol.* 11, 510–521. doi:10.1038/cmi.2014.97

Westergaard, M. C. W., Andersen, R., Chong, C., Kjeldsen, J. W., Pedersen, M., Friese, C., et al. (2019). Tumour-reactive T Cell Subsets in the Microenvironment of Ovarian Cancer. *Br. J. Cancer* 120, 424–434. doi:10.1038/s41416-019-0384-y

WHO (2021). Infertility. Available at: https://www.who.int/westernpacific/health-topics/infertility.

Xu, Y.-W., Peng, Y.-T., Wang, B., Zeng, Y.-H., Zhuang, G.-L., and Zhou, C.-Q. (2011). High Follicle-Stimulating Hormone Increases Aneuploidy in Human Oocytes Matured *In Vitro*. *Fertil. Sterility* 95 (1), 99–104. doi:10.1016/j.fertnstert.2010.04.037

Zhang, Z., Schlamp, F., Huang, L., Clark, H., and Brayboy, L. (2020). Inflammaging Is Associated with Shifted Macrophage Ontogeny and Polarization in the Aging Mouse Ovary. *Reproduction* 159, 325–337. doi:10.1530/rep-19-0330

Conflict of Interest: LB works as Chief Medical Officer for Clue by BioWink GmbH.

The remaining authors declare that the research was conducted in the absence of any commercial or financial relationships that could be construed as a potential conflict of interest.

Publisher's Note: All claims expressed in this article are solely those of the authors and do not necessarily represent those of their affiliated organizations, or those of the publisher, the editors, and the reviewers. Any product that may be evaluated in this article, or claim that may be made by its manufacturer, is not guaranteed or endorsed by the publisher.

Advantages of publishing in Frontiers

OPEN ACCESS
Articles are free to read for greatest visibility and readership

FAST PUBLICATION
Around 90 days from submission to decision

HIGH QUALITY PEER-REVIEW
Rigorous, collaborative, and constructive peer-review

TRANSPARENT PEER-REVIEW
Editors and reviewers acknowledged by name on published articles

Frontiers
Avenue du Tribunal-Fédéral 34
1005 Lausanne | Switzerland

Visit us: www.frontiersin.org
Contact us: frontiersin.org/about/contact

REPRODUCIBILITY OF RESEARCH
Support open data and methods to enhance research reproducibility

DIGITAL PUBLISHING
Articles designed for optimal readership across devices

FOLLOW US
@frontiersin

IMPACT METRICS
Advanced article metrics track visibility across digital media

EXTENSIVE PROMOTION
Marketing and promotion of impactful research

LOOP RESEARCH NETWORK
Our network increases your article's readership